



PALACKÝ UNIVERSITY OLMOUC

FACULTY OF SCIENCE

Department of Chemical Biology

**(Un)Natural product synthesis: From phenolics
and nitro fatty acids to unnatural α -amino acids**

A Thesis Submitted for the Degree of Doctor of Sciences

Daniel Chrenko

2024

Bibliografická identifikace

Jméno a příjmení autora	Mgr. Daniel Chrenko
Název práce	Syntéza (ne)přírodních látek: Od fenolických látek a nitro mastných kyselin k nepřírozeným α -aminokyselinám.
Typ práce	Disertační práce
Pracoviště	Katedra Chemické biologie Přírodovědecká fakulta, Univerzita Palackého v Olomouci
Vedoucí práce	doc. RNDr. Jiří Pospíšil, Ph.D.
Abstrakt	Předložená doktorská práce se primárně zabývá syntézou přírodních látek, zejména pak sekundárních metabolitů rostlin, látek přírodním látkám obdobných, studiem jejich biologické aktivity a v neposlední řadě také vývojem syntetických metod jež by přípravu těchto látek umožnily. Konkrétně se v práci zabýváme přípravou fenolických sekundárních metabolitů a jejich derivátů s neolignanovým benzofuranovým skeletem u kterých je očekávána anthelmintická a antiparkinsonová aktivita. Následně se zabýváme syntézou nitro mastných kyselin a vývojem syntetických metod umožňujících jejich stereoselektivní přípravu. Ve třetí části se zabýváme přípravou heteroarylsulfonamidů a z nich následně odvozených heteroaryl alkyl amino kyselin. Tato příprava je založena na konceptu paměti chiralidy.
Klíčová slova	sekundární metabolity; přírodní produkty; syntetické metody; paměť chiralidy; olefinální metody; neolignany; nitrované mastné kyseliny; aminokyseliny
Počet stran	286
Počet příloh	4
Jazyk	English

Bibliographical identification

Author's first name and surname	Mgr. Daniel Chrenko
The title	(Un)Natural product synthesis: From phenolics and nitro fatty acids to unnatural α -amino acids
Type of thesis	Doctoral thesis
Department	Department of Chemical Biology Faculty of Science, Palacký University in Olomouc
Supervisor	assoc. prof. Jiří Pospíšil, Ph.D.
Abstract	<p>The submitted thesis is primarily concerned with the synthesis of natural products, especially secondary metabolites of plants, substances similar to natural substances, the study of their biological activity and last but not least the development of synthetic methods that would enable the synthesis of these substances. Namely, we are concerned with the preparation of phenolic secondary metabolites and their derivatives with a neolignane benzofuran skeleton, which are expected to have anthelmintic and antiparkinsonian activity. Subsequently, we focus on the synthesis of nitro fatty acids and the development of synthetic methods that enable their stereoselective preparation. In the third part, we deal with the preparation of heteroaryl sulfonamides and the heteroaryl alkyl amino acids derived from them. This preparation of heteroaryl alkyl amino acids is based on the concept of memory of chirality.</p>
Keywords	secondary metabolites; natural products; synthetic methods; memory of chirality; olefination methods; neolignans; nitro fatty acids; amino acids
Number of pages	286
Number of appendixes	4
Language	English

I hereby declare that I have written this Thesis independently and listed all literature sources.

In Olomouc,

Daniel Chrenko

„I have no special talent. I am only passionately curious.“

Albert Einstein

Acknowledgement

It would never have been possible to complete this thesis without the help and support of numerous people. First and foremost, I would like to express my heartfelt gratitude to Jiří Pospíšil for offering me the opportunity to join his research group four years ago. He has been an exceptional supervisor, always available when needed the most. Over these four years, he dedicated significant time to help, advise, and teach me, not only in chemistry but also on a personal level. He never said no to my crazy ideas, and for that, I am immensely grateful. I would also like to extend my sincere thanks to Tomáš Pospíšil for his invaluable assistance with NMR problem-solving and for being great company in the laboratory.

I am deeply thankful to all people I have met on this long journey. This includes especially people from the Department of Chemical Biology and Department of Organic Chemistry, especially Jozef, Markét, Darnad, Denča, Magda, Pája and Franta and of course all the members of wonderful Pospisil²ab.

I am profoundly grateful to prof. Mario Waser for accepting me into his group at JKU Linz, where I spent three months at the beginning of 2022 working on development of new phase-transfer catalysts. His guidance and the excellent working environment he provided were invaluable. I also deeply thankful to prof. Cristina Nevado for welcoming me into her research group at UZH Zurich where I spent three months at the end of 2023, gaining new knowledge in photochemistry. I am also grateful to the members of both research group for providing a great and fun working environment. Especially I would like to thank to Paul, David N., Magda, Kathi, Lotte, David W., Ivan, Jaime, Masha, Xiaoyong, Debora, Eleen, Georgia, Loélie, Marc, Michal, Sergio, Wen-Di, Xia, Yawen, Cedric, and Jorge. You made my research stays in Austria and Switzerland unforgettable.

I am also grateful for the financial support provided by the Palacký University Internal Grant Agency (IGA_PrF_2024_007) and Grant Agency of the Czech Republic (no.23-06051S), Mobility UP, Erasmus+, and the Endowment fund of UPOL for generous support.

I am grateful to the most important person in my life, my partner Eva for her constant support and never-ending encouragement throughout my PhD journey. Her belief in me, especially during the most challenging times, has been invaluable.

Nakonec bych chtěl poděkovat mým rodičům a bratrovi Míšovi za nikdy nekončící podporu (nejen) při mém nekonečném studiu. Za to že se mě nebáli pustit do světa a že tu pro mě vždy byli, když jsem je potřeboval. Bez nich bych nebyl tam, kde dnes jsem.

Table of contents

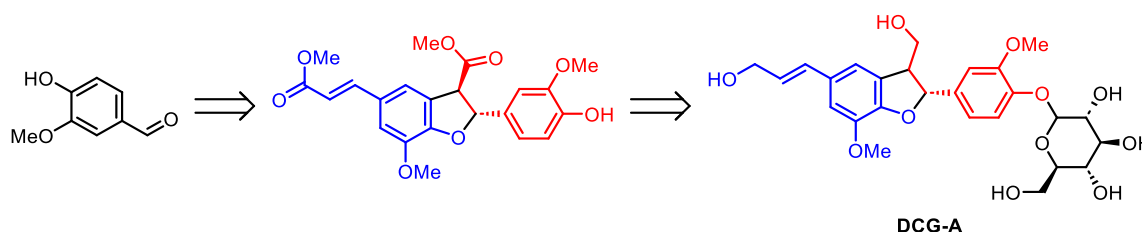
Aims of the Thesis	10
Abbreviations	12
1. Secondary metabolites	16
1.1. Introduction	16
1.2. Phenylpropanoids	18
1.2.1. Introduction of phenylpropanoids	18
1.2.2. Biosynthesis	19
1.2.3. Dimerization of phenylpropanoids	20
1.2.4. Biological activity of neolignans	21
1.3. Synthesis of benzofurans	28
1.3.1. Synthesis based on enzymes and transitional metals	28
1.3.2. Non-biomimetic approaches to dihydrofuran neolignans	29
1.4. Results and discussion	34
1.4.1. Introduction	34
1.4.2. Retrosynthesis plan	34
1.4.3. Towards DCG-A: Formation of monomer units of phenylpropanoids	36
1.4.4. Homocoupling dimerization	36
1.4.5. Introduction of the phenolic protecting group	37
1.4.6. Reduction step	38
1.4.7. Hydroxy Group Protection - Step Five	39
1.4.8. Selective phenolic protecting group removal	40
1.4.9. Introduction of glucose	42
1.4.10. Final step – selective acetyl groups	44
1.4.11. Further reactivity of 8,5' dimers	45
1.4.12. Toward quiquesetinerviusin A	47
1.5. Biological activity evaluation results	51
1.5.1. Anthelmintic activity	51
1.5.2. Cytokinin activity	53
1.6. Conclusions	56
1.7. Experimental section	57
1.7.1. Synthesis of DCG-A and related compounds	58
1.7.2. Synthesis of dehydroquiquesetinerviusin A and related compounds	95
2. Nitro fatty acids	108
2.1. Nitro Fatty Acids: An Introduction	108
2.1.1. Biological activity	109
2.1.2. Synthesis of NO ₂ FAs	113
2.2. Results and discussion	114
2.2.1. Introduction	114
2.2.2. 10-NO ₂ oleic acid	116
2.2.3. 9-NO ₂ oleic acid	119
2.2.4. 10-NO ₂ linoleic acid	121

2.2.5.	10- NO ₂ stearic acids	125
2.2.6.	9-NO ₂ conjugated linoleic acid	126
2.2.7.	14-NO ₂ arachidonic acid	129
2.2.8.	14-NO ₂ anandamide	139
2.3.	Biological evaluation	142
2.4.	Conclusion	143
2.5.	Experimental section	144
2.5.1.	10-NO ₂ OA	146
2.5.2.	9-NO ₂ OA	150
2.5.3.	10-NO ₂ LA	153
2.5.4.	10-NO ₂ SA	160
2.5.5.	9-NO ₂ cLA	162
2.5.6.	14-NO ₂ ARA	168
2.5.7.	oleic acid synthesis using modified Julia-Kocienski method	184
2.5.8.	linoleic acid synthesis using modified Julia-Kocienski method	187
3.	Sulfonamides	194
3.1.	Introduction to Sulfonamides	194
3.1.1.	Biological activity of sulfonamides	194
3.2.	General approaches towards sulfonamides	196
3.3.	Amino acids	198
3.4.	α,α -disubstituted- α -amino-acids	199
3.4.1.	Biological activity of α,α -disubstituted α -AAs	200
3.4.2.	Known methodologies of α,α -disubstituted α AA and their derivatives synthesis	201
3.5.	α -heteroaryl α -substituted α -AAs	204
3.5.1.	Synthesis of α -heteroaryl α -substituted α -amino acid derivatives	204
3.6.	Truce Smiles rearrangement	206
3.7.	Memory of chirality	208
3.8.	Results and discussion	209
3.8.1.	Introduction to sulfonamides synthesis	209
3.8.2.	Introduction to α -heteroaryl α -substituted α -AAs synthesis	218
3.9.	Conclusion	233
3.10.	Experimental section	234
4.	Global conclusion	285
5.	Literature	287
6.	NMR and HPLC	295

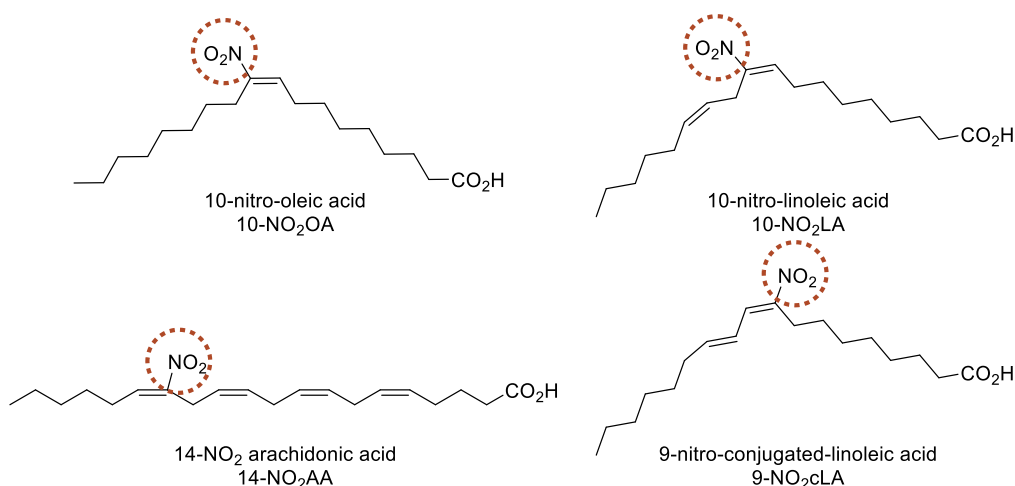
Aims of the Thesis

My thesis focuses on two main fields, natural product synthesis and synthetic method development. Throughout the work, the two themes are intertwined and constantly refer to each other and one inspires the other... And now it is up to me to attempt the almost impossible: to retell the story of my Ph.D.

My first interest was in the synthesis of a well-established class of plant secondary metabolites, phenolic compounds with a phenylpropanoid-dimer skeleton, more precisely, the compounds inspired by dehydrodiconiferyl alcohol glucoside (**DCG-A**). Compounds that contain a benzofuran core in its structure and that are well known for their biological activities that range from anthelmintic, anticancer, and antiviral.

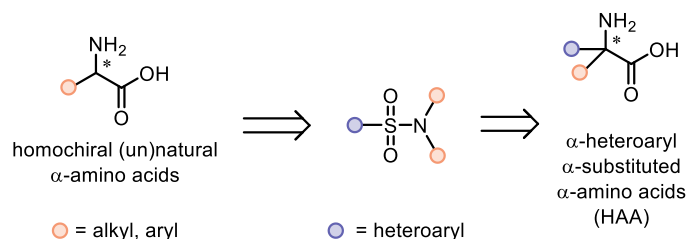


My second interest was in the synthesis of novel classes of natural products (nitro fatty acids) that presented a new synthetic challenge, stereodefined synthesis of multiple 1,2-di and trisubstituted alkenes. To achieve such a goal, a new synthetic pathway toward NO_2 fatty acids (NO_2FA) and 1,2-disubstituted alkenes had to be developed. We succeeded and as “the imaginary cherry on top of the cake,” we capitalized on the gathered experience in the first total synthesis total synthesis of 14- NO_2 arachidonic acid.



Aims

Finally, our attention focused on the development of novel methodologies designed to prepared previously inaccessible heteroarylsulfenamides, structural motive that is commonly exploited in the medicinal chemistry field. For us the class of heteroaryl sulfones was dare for different reasons, we wished to apply it in the context of the concept of 'memory of chirality' to prepare a novel class of amino acids (α -heteroaryl α -substituted α -aminoacids).



In short, my thesis led me from phenylpropanoids based secondary metabolites synthesis, to the synthesis of nitro fatty acids, potential nuclear factor erythroid 2-related factor 2 (Nrf2) activators; and at the same time, the synthetic endeavors connected with stereoselective olefin synthesis, a topic so dear to my supervisor, led me *via* heteroarylsulfonamide synthesis to a new type of unnatural amino acids that could be used in the future as organocatalysts or be incorporated in DNA to form a novel Xeno nucleic acids.

This 'development' of my research then obviously predetermines the content of my thesis that, as a consequence, is divided into three separate parts. **1)** Neolignans, **2)** Nitro fatty acids, **3)** Sulfonamides and novel amino acids.

Abbreviations

°C = degree Celsius	<i>e.r.</i> = enantiomeric ratio
2,6-lutidine = 2,6,-dimethylpyridine	equiv. = equivalent
AA – amino acids	Et ₂ O = diethylether
Ac = acetyl	EtOAc = ethyl acetate
AcCN = acetonitrile	EtOH = ethanol
Ag ₂ O = silver oxide	EWG = electron withdrawing group
AgCO ₃ = silver nitrate	FAs = fatty acids
AgNO ₂ = silver nitrite	FeCl ₃ = Iron trichloride
AgOTf = silver trifluoromethanesulfonate	GC = Gas chromatography
Ar = aryl	h = hour
ARA = arachidonic acid	H ₂ O ₂ = hydrogen peroxide
BBr ₃ = boron tribromide	HAA = α-heteroaryl α-substituted α-amino acids
BCl ₃ = boron trichloride	HCl = hydrochloric acid
BF ₃ = boron trifluoride	HMPA = hexamethylphosphoramide
Bn = benzyl	HPLC = high-performance liquid chromatography
BT = benzo[<i>d</i>]thiazol	HRMS = high resolution mass spectroscopy
Bz = benzoyl	HRP = horseradish peroxidase
CAL-B = <i>Candida antartica</i> lipase B	iPrOH = isopropanol
cat. = catalytic	J = coupling constant
CBr ₄ = carbon tetrabromide	K ₂ CO ₃ = potassium carbonate
CuOTf = Copper(I) trifluoromethanesulfonate	KHMDS = potassium bis(trimethylsilyl)amide
d = doublet	LA = linoleic acid
<i>d.r.</i> = diastereomeric ratio	LC-MS = Liquid chromatography–mass spectroscopy
DBU = 1,8-diazabicyclo[5.4.0]undec-7-ene	LDA = lithium diisopropylamide
DCC = N,N'-dicyclohexylcarbodiimid	LiHMDS = lithium bis(trimethylsilyl)amide
DCE = 1,2-dichloroethane	LiOH = Lithium hydroxide
DCG-A = dehydrodiconiferyl alcohol glucoside	m = multiplet
DCM = dichloromethane	Me = methyl
DFT = density functional theory	MeCN = acetonitrile
DHB = 2,3-dihydrobenzofuran	MeOH = methanol
DIAD = diisopropyl azodicarboxylate	MgBr ₂ = magnesium bromide
DIBAL-H = diisobutyl aluminium hydride	MgSO ₄ = magnesium sulfate
DIC = N,N'-diisopropylcarbodiimide	min. = minute
DIPEA = N,N-diisopropylethylamine	MOM = methoxymethyl
DMAP = 4-dimethyl aminopyridine	MS = mass spectroscopy
DMB = 2,4-dimethoxybenzyl	MTBE = methyl <i>t</i> -butyl ether
DMF = dimethylformamide	n.r. = no reaction
DMP = Dess-Martin reagent	Na ₂ SO ₄ = sodium sulfate
DMSO = dimethylsulfoxide	

Part I: Introduction: Secondary metabolites

NaHMDS = sodium bis(trimethylsilyl)amide	rpm = rotations per minute
NaI = sodium iodide	RT = room temperature
NaOH = sodium hydroxide	s = singlet
NaOMe = sodium methoxide	S.M. = Starting material
NCS = N-chlorosuccinimide	SA = stearic acid
NF- κ B = nuclear factor kappa-light-chain-enhancer of activated B cells	SAR = structure-activity relationship
NH ₃ = ammonia	SEM = 2-(Trimethylsilyl)ethoxymethyl
NMR = Nuclear magnetic resonance spectroscopy	SiO ₂ = Silica (silicon dioxide)
NSAID = Nonsteroidal anti-inflammatory drug	SnCl ₄ = tin chloride
Nrf2 = nuclear factor erythroid 2-related factor 2	t = triplet
OA = oleic acid	TBAF = tetrabutylammonium fluoride
PE = petroleum ether	TBS = <i>t</i> -butyldimethylsilyl
PG = protecting group	TEA = triethylamine
Ph = phenyl	TES = triethylsilyl
PPh ₃ = triphenylphosphine	TFA = trifluoroacetic acid
ppm = parts per million	THF = tetrahydrofuran
<i>p</i> TSA = <i>p</i> -toluenesulfonic acid	TIPS = triisopropylsilyl
py = pyridine	TLC = thin layer chromatography
q = quartet	TMS = trimethylsilyl
QM = quinone methide	OTf = trifluoromethane sulfonate
	UFAs = unsaturated fatty acids
	ZnBr ₂ = zinc bromide

CHAPTER I

1. Secondary metabolites

1.1. Introduction

Plant secondary metabolites are a diverse group of organic compounds produced by plants and other living organisms, such as bacteria, fungi, and plants, which are not strictly necessary for their survival. In other words, they are not included in elemental processes such as growth, development, and reproduction. Such compounds are not essential for survival of the organism, but they play a key role in the organism's interactions with its environment (e.g. defense against herbivores, pathogens, and competitors, as well as communication with other organisms, etc.). And even though such function is not essential to the organism, it greatly increases quality of life, chances of reproduction, or chances of survival when facing to hostile environment pollinators and/or symbiotic partners.¹

In general, secondary metabolites are divided, based on metabolic origin, into three large groups, alkaloids, terpenoids, and phenolic compounds.

1) Alkaloids: Nitrogen-containing compounds, often with a strong physiological effect on mammals. The most known alkaloids are caffeine, morphine, and nicotine (**Figure 1**). Alkaloids often function as defense compounds, deterring herbivores and pathogens due to their bitter taste and, in the extreme case, can even be lethal to the attacker due to their (neuro)toxic properties.²

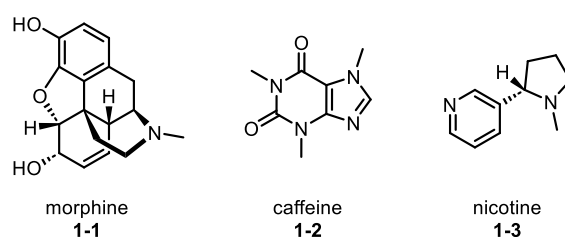


Figure 1: Structure of most known alkaloids.

2) Terpenoids (or isoprenoids): Compounds that originate from the five-carbon subunits of isoprene. Terpenoids participate in various functions, such as plant protection, signaling, or pollination. Examples of those include essential oils (limonene and menthol), carotenoids (β -carotene) and plant hormones (gibberellins and abscisic acid) (**Figure 2**).³

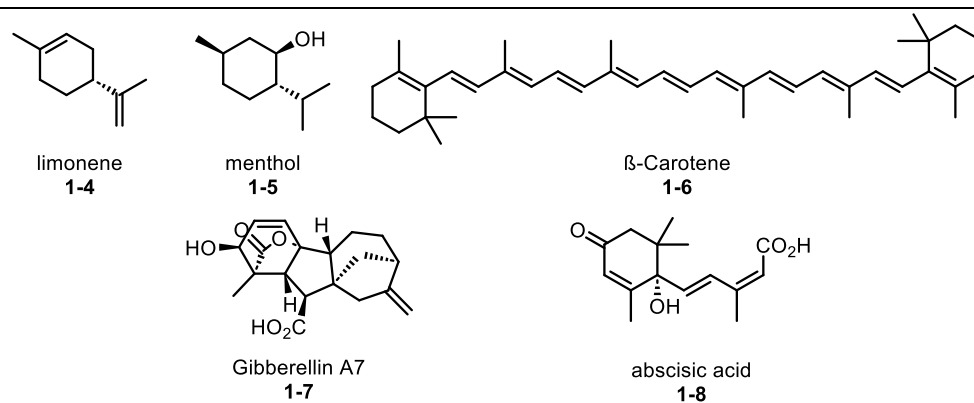


Figure 2: Structure of most known terpenoids.

3) Phenolic compounds: Group of compounds that include one- or more-phenyl subunit with one or more hydroxy groups. Phenolic compounds play a role in plant defense, signaling, and protection against ultraviolet light. Examples include flavonoids (anthocyanins and quercetin), lignans (sanguinolignan A) and neolignans (dehydrodiconiferyl alcohol 4-O- β -D-glucopyranoside), and most importantly lignin, a structural component of plant cell walls (**Figure 3**).^{4,5}

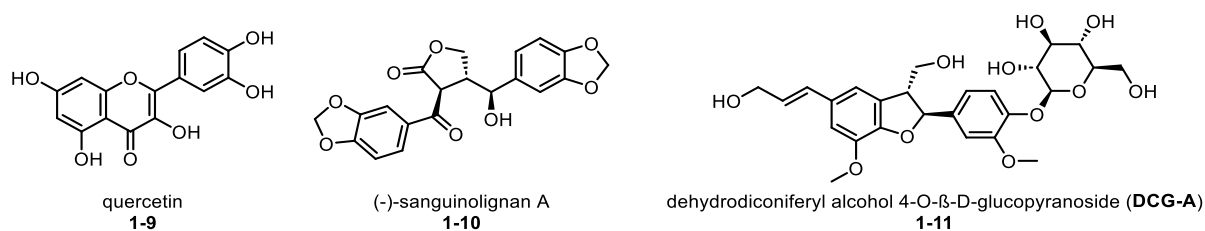


Figure 3: Structure of phenolic compounds.

At this point, I would like to emphasize that (mostly) plant secondary metabolites were extensively used by humans for various purposes mostly related to the healing processes over the past few thousand years, as can be demonstrated, e.g., on the use of salicylic acid (aspirin) to treat the fever.⁶ They are also often the basis for traditional medicines, and still now a days they serve as a key starting point during the development of new drugs.⁵

1.2. Phenylpropanoids

1.2.1. Introduction of phenylpropanoids

In plants, lignans and neolignans are formed by oxidative coupling of the hydroxycinnamic acid derivatives, these structures are formed by a β,β' -linkage between two units of phenylpropanoid. These units can have different side chains (C7-C9) in different oxidation states and vary in the substitution of the aromatic ring (C1-C6). For nomenclature purposes, phenylpropanoid monomers are typically numbered C1-C6 for the aromatic ring and C7-C9 for the propyl chain, with C1 and C7 atoms attached by covalent bond. In the second phenylpropanoid monomer, the numbering follows the same pattern, but with primed numbers (notated with a prime symbol, '). In the context of lignans and neolignans, the numbers mentioned (e.g., C8-C5' or C5-C5') represent the types of carbon-carbon (C-C) bonds formed during the oxidative coupling of two phenylpropanoid units. These numbers correspond to the positions on the aromatic rings where the coupling occurs. The dimerization proceeds *via* the oxidative radical pathway and the generated radical undergoes a further dimerization process. Based on the substitution pattern of the phenylpropanoid unit, the homocoupling occurs at different positions, and various types of dimers are formed. When the word **lignan** is used, a dimer generated by the C8-C8' dimerization process is described and the homodimerization that occurs *via* the C8 positions of both phenylpropanoid units is involved. Products of any other type of dimerization, for example, C8-C5', C5-C5' and C8-C4', are referred to as **neolignans**. The types of dimerization mentioned previously that produce a neolignan skeleton are only a few out of many possibilities, since additional substitution on the aromatic ring of the phenylpropanoid can lead to other possibilities such as, for example, the C8-C5'-dimers (**1-15b**) which are the target dimers of my thesis (**Figure 4**).^{5,7}

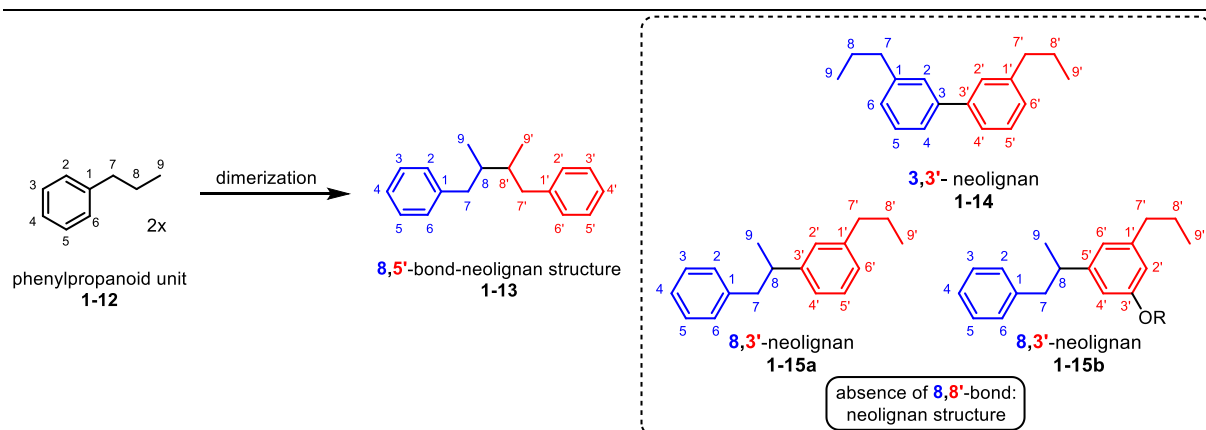
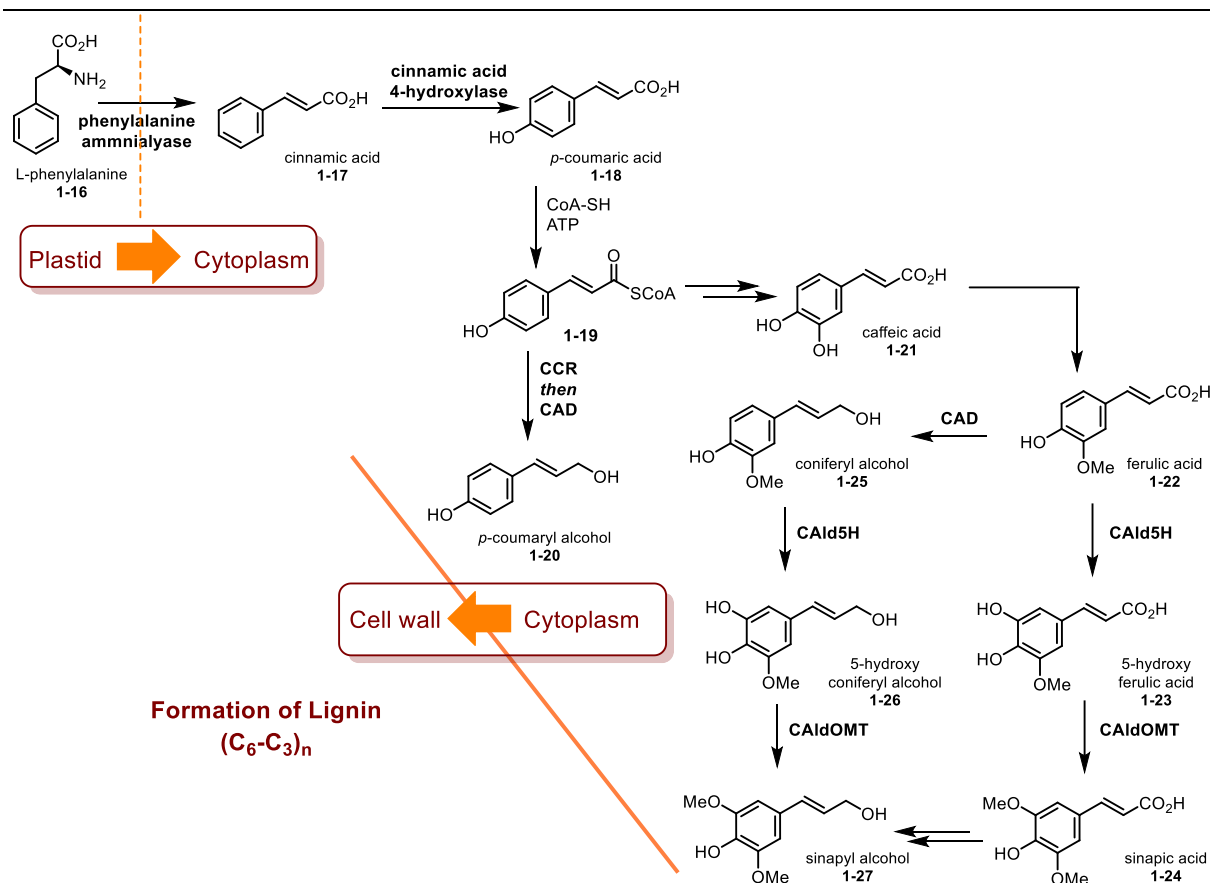


Figure 4: General scheme of neolignan dimerization. Only selected examples of neolignan dimers are shown.⁵

1.2.2. Biosynthesis

Phenolic compounds are plant secondary metabolites that originate in the shikimic acid biosynthesis pathway.^{8,9} From a structural point of view, neolignans are homodimers of phenylpropanoids that originate from the metabolism of L-phenylalanine and with the help of enzymes such as phenylalanine ammonia-lyase L-phenylalanine is transformed to cinnamic acid which is then further hydroxylated with the help of cinnamic acid 4-hydroxylase and cytochrome P450 to *p*-coumaric acid (**Scheme 1**).⁸ The biosynthesis of neolignans itself is an amazing process since one phenylpropanoid-based building block (*p*-coumaric or ferulic acid) undergoes *O*-methyltransferase-mediated methylation to yield cinnamic acid derivative which can further undergo lactase or peroxidase-triggered homodimerization that can yield only up to three products. However, countless (non)enzymatic transformations such as acid-catalysed cyclization, methylation, and/or oxidation literally open the doors to the world of structurally diverse phenolic secondary metabolites. Consequently, the structure and distribution of neolignans differ from plant to plant, biotope to biotope, and depend on the soil, climate, or exposure of the plants to stress.^{5,10}



Scheme 1: Biosynthesis of phenylpropanoid monomers from L-phenylalanine (adapted from⁵).

1.2.3. Dimerization of phenylpropanoids

As demonstrated in the previous chapter, phenylpropanoid dimers (lignans and neolignans) are in plants generated during the oxidative radical dimerization step. This dimerization is mediated by laccases and peroxidases.^{5,11,12} During the process configurationally unstable radical species are generated (as an example, the case of the C8-C5'-dimer is shown in **Figure 5**) and final product of the addition/post-addition transformations, the targeted neolignan **1-34** is formed as a racemic mixture of all possible stereoisomers (**Scheme 2**).

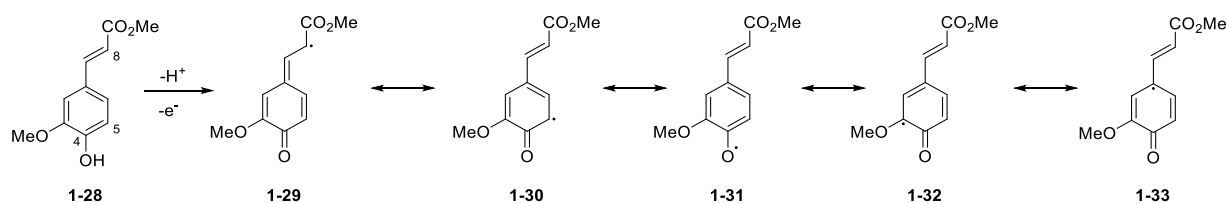
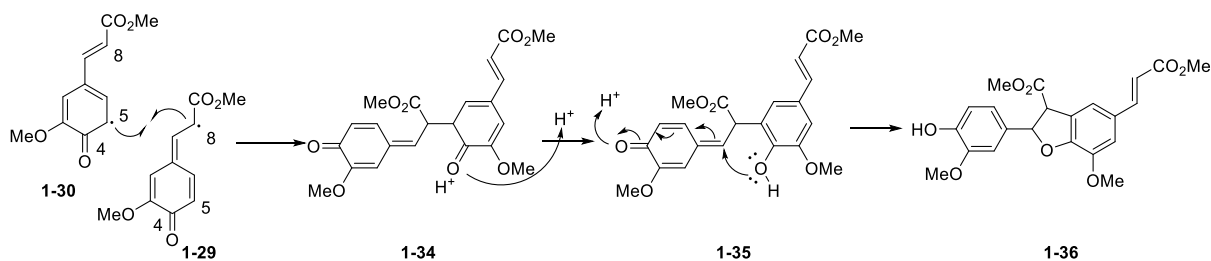


Figure 5: Dehydrogenation of methyl *p*-coumarate to show formation of phenoxy radical.¹³

The stereochemical outcome of plant-based enzymatic oxidative dimerization (many naturally occurring ligands and neolignans are isolated in enantiomerically enriched form) is then influenced by so-called dirigent proteins – proteins that are responsible for the stereoisomeric outcome of the dimerization processes (**Scheme 2**).¹⁴



Scheme 2: 8-5' bimolecular phenoxy radical coupling of a methyl *p*-coumarate to neolignane structure.^{15–17}

As mentioned previously, dimerization itself is *in planta* promoted by metalloenzymes containing peroxidases and lactases, iron and copper centered metalloenzymes. Such information triggered the attention of various synthetic chemists and led to the development of various synthetic methodologies based on the use of Ag(I), Fe(III) or Cu(II) salts (Ag₂O¹⁸, FeCl₃¹⁹, K₃[Fe(CN)₆]²⁰). The utilization of these salts has certain drawbacks, namely their high cost, limited reproducibility, and low reaction yields, accompanied by the formation of various side products. Moreover, the reactions themselves lack regio and stereocontrol that results in low yields of desired adducts and an obvious formation of dimers as racemic mixtures.¹⁶ An alternative way, which is based on the use of oxidizing agents such as H₂O₂ in combination with isolated peroxidases such as horseradish peroxidase (HRP), also brings unsatisfactory results.²¹ However, it was demonstrated that the choice of catalyst or oxidizing agent, as well as the reaction conditions (e.g. temperature, solvent, and concentration), can significantly influence the chemical selectivity (e.g., preference of C8-C8' over C8-C5' dimerization) and the yield of the dimerization process. Through careful optimization of these parameters, researchers could not only control the formation of lignan (C8-C8') or neolignane (C8-C5') structures, but also the stereochemistry of the consequent post-coupling reactions.^{16,17,21}

1.2.4. Biological activity of neolignans

As mentioned in chapter 1.2., neolignans are a subclass of phenolic compounds originating from other than C8-C8' dimerization homocoupling of phenylpropanoid subunits. In total, plants produce virtually thousands of various structurally different neolignans (15 subtypes)

with a wide range of biological activity.^{5,22} They exhibit antimicrobial activity against various bacteria, fungi, and viruses. Their mode of action can involve disrupting the microbial cell membrane, inhibiting the synthesis or function of essential enzymes, or interfere with the synthesis of cellular components, such as proteins or nucleic acids.²³ In some cases, antitumor activity⁵ can be attributed to the ability of neolignan to induce apoptosis (programmed cell death), inhibit cell proliferation, and suppress tumor invasion and metastasis.²⁴ The whole class of such compounds displays a wide range of biological activities that goes far beyond the scope of this Thesis, therefore, I would like to pay attention only to those with the benzofurane-like core skeleton **1-39** (Figure 6).⁵

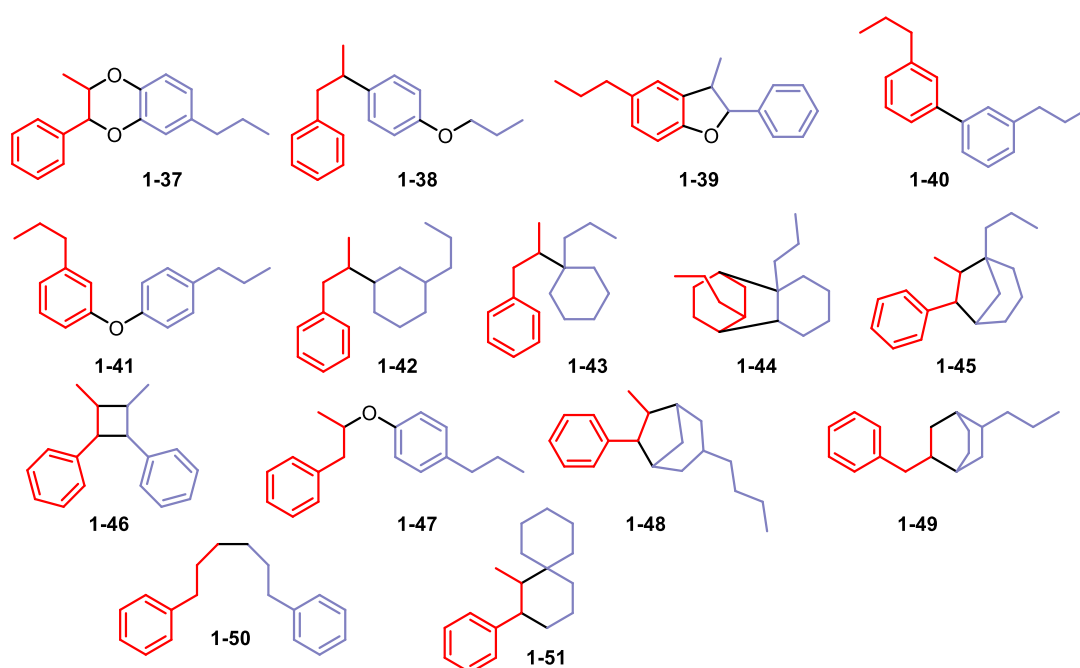


Figure 6: Most accepted structural subtypes of neolignans (adapted from ⁵).

Most neolignans are non-toxic and in many cases presumably even have a positive effect on human bodies. The diverse biological activities of these phenolic compounds range from antiparasitic, anticancer, anti-inflammatory, neuroprotective, antibacterial, antifungal, and antiallergenic.⁵

Licarin A (1-52) isolated from *Nectandra glabrescens Benth* and **burchellin (1-53)** isolated from *Ocotea cymbarum Kunth* exhibit antitrypanosomal activity by interfering with essential biochemical processes in the parasite, leading to its inhibition and death (Figure 7). **Licarin A** caused inhibition of *in vitro* growth of the epimastigote form of *T. cruzi* (Dm28 strain), four

days ($48.5 \pm 2.6 \mu\text{M}$) and seven days ($77.2 \pm 4.9 \mu\text{M}$) after treatment with a dose of $310 \mu\text{M}$, compared to the respective control groups ($81 \pm 6.1 \mu\text{M}$ and $141 \pm 6.2 \mu\text{M}$). The $\text{IC}_{50/96 \text{ h}}$ was $462.7 \mu\text{M}$. **Burchellin** caused partial inhibition *in vitro*, four days ($10.8 \pm 0.6 \mu\text{M}$) and seven days (12.7 ± 1.1) after treating the developing parasites at a dose of $100 \mu\text{g/mL}$ ($294 \mu\text{M}$), compared to the respective control groups ($15.0 \pm 1.7 \mu\text{M}$ and $16.0 \pm 1.5 \mu\text{M}$). $\text{IC}_{50/96 \text{ h}}$ for **burchellin** was of $756 \mu\text{M}$. Each value represents the mean number of parasites ($\times 10^6$) from six individual samples. Both compounds show effectiveness against epimastigote and trypomastigote forms.²⁵

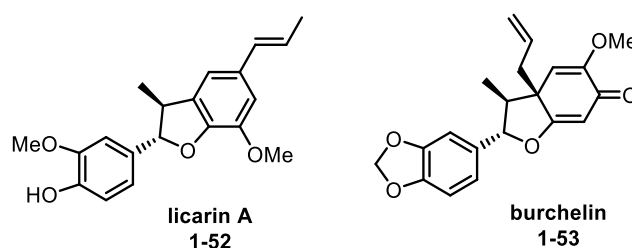


Figure 7: Structure of the licarin A (1-52) and burchellin (1-53).

Some neolignans found in Chinese olives, such as **cinnassin D (1-54)** or **picrasmalignan (1-55)**, have been shown to modulate the inflammatory response by inhibiting the production of pro-inflammatory mediators, such as cytokines and prostaglandins. For **cinnassin D** IC_{50} values ranging from 18.1 to $30.2 \mu\text{M}$ based on its configuration. For **picrasmalignan**, the IC_{50} values ranged from 6.0 to $18.8 \mu\text{M}$. Both compounds exhibited pronounced inhibitory effects on lipopolysaccharide-induced nitric oxide production in RAW 264.7 macrophages. This activity could be beneficial in the management of chronic inflammatory diseases, including arthritis, asthma, and inflammatory bowel diseases (**Figure 8**).²⁶

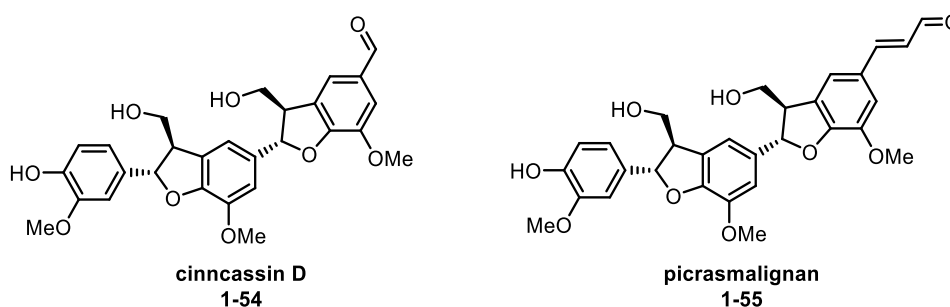


Figure 8: Structure of the cinnassin D (1-54) and picrasmalignan (1-55).

On the other hand **(-)-licarin A (1-52)** and **eupomatenoid-7 (1-56)** have demonstrated neuroprotective activity and protect neuronal cells from damage caused by numerous factors, such as oxidative stress, excitotoxicity, and inflammation. At the same time, **licarin A**

was not toxic at the concentration tested (10 μM). This property could be beneficial in the prevention or treatment of neurodegenerative diseases, such as Alzheimer's and Parkinson's disease (**Figure 9**).²⁷

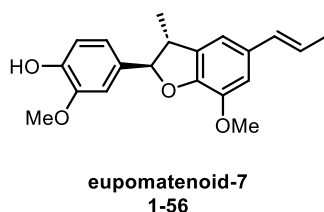


Figure 9: Structure of the eupomatenoid-7 (1-56).

Acuminatin (1-57) and **denudatin B (1-58)** (**Figure 10**) isolated from *Piper betle* showed antibacterial activity by inhibiting the multidrug antibiotic efflux pump NorA. In a study involving cotreatment with antibiotic norfloxacin in a strain of *S. aureus* that overexpresses the efflux pump, the compounds synergistically displayed MIC values of 2 mg/L each and fractional inhibition concentration indices of 0.13-0.25.²⁸

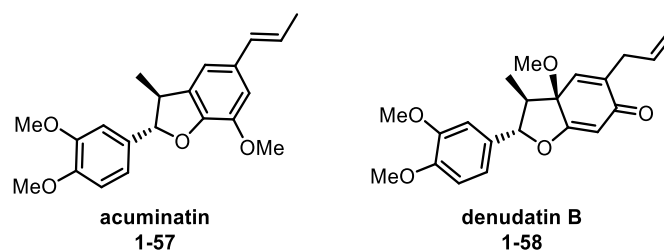


Figure 10: Structure of the acuminatin (1-57) and denudatin B (1-58).

Interestingly, in the study where three sialidase isoforms (NanA–C) were evaluated, **licarin B (1-59)** (**Figure 11**) showed significant activity against NanA with $\text{IC}_{50} = 1.5 \pm 0.4 \mu\text{M}$, NanB with $\text{IC}_{50} = 14.0 \pm 1.6 \mu\text{M}$ and NanC with $\text{IC}_{50} = 30.7 \pm 5.6 \mu\text{M}$.²³

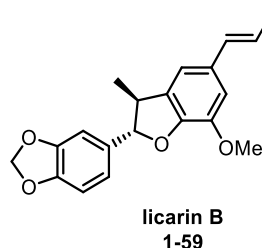


Figure 11: Structure of the licarin B (1-59).

Some neolignans also exhibit antifungal activity. An example is **conocarpan (1-60)** (**Figure 12**) isolated from *piper rivinoides* that displayed antifungal activity against *candida albicans* strains (PRI, $\text{IC}_{50} = 9.20 \pm 1.20 \mu\text{g/mL}$; ATCC 10231 = $19.60 \pm 2.30 \mu\text{g/mL}$) however they were also found to be cytotoxic to mammalian cells.²⁹

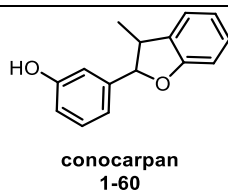


Figure 12: Structure of the conocarpan (1-60).

Lyciumnan (1-61) (Figure 13), an epoxide containing benzofuran neolignan found in *Lycium barbarum L* (used in traditional Chinese medicine) displayed moderate cytotoxic activities against cell lines A549 ($IC_{50} = 37.1 \pm 3.3 \mu M$) HeLa ($IC_{50} = 54.1 \pm 3.9 \mu M$) and PC-3 ($IC_{50} = 51.7 \pm 3.6 \mu M$).²⁴

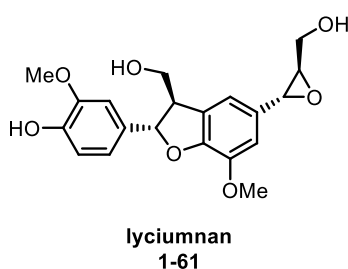


Figure 13: Structure of the lyciumnan (1-61).

Gardenofolin D (1-62) (Figure 14) also showed activity against HeLa cell lines with $IC_{50} = 21.0 \mu M$. The compound was further studied for its effects on cell morphology and apoptosis. Morphological experiments indicated that it induces apoptosis of HeLa cells at $25 \mu M$.³⁰

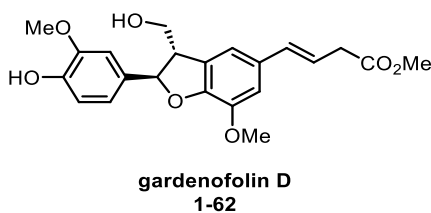


Figure 14: Structure of the gardenofolin D (1-62).

Three new dehydrobenzofuran neolignans, **mappiodoinins A-C (1-63 to 1-65) (Figure 15)**, together with nine known analogues, were isolated from the stems and leaves of *M. iodoies*. Cytotoxicity against several human cancer cell lines of were investigated. For HL-60, IC_{50} ranged from 0.78 to 2.16 μM , for the SMMC-7721 cell line, IC_{50} ranged from 1.06 to 5.32 μM , for A-549, IC_{50} ranged from 2.19 to 5.03 μM , for MCF-7, IC_{50} ranged from 1.28 to 3.69 μM and for the SW-480 cell line, IC_{50} ranged from 0.16 to 1.89 μM . This may be the reason *M. iodoies* had been used to treat tumors in China traditional medicine.³¹

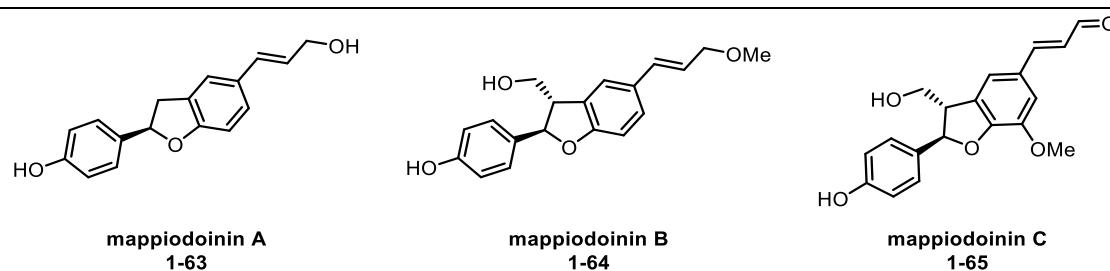


Figure 15: Structure of the mappiodoinin A-C (1-63 to 1-65).

Illiciumlignan D (1-66) (Figure 16) isolated from the branches and leaves of *Illicium wardii* was tested on the ovarian cancer cell line SKOV3, with the $IC_{50} = 8.67 \mu M$.³²

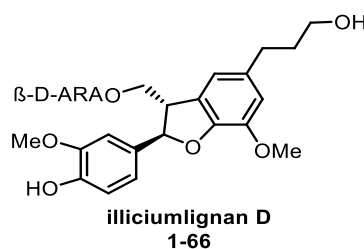
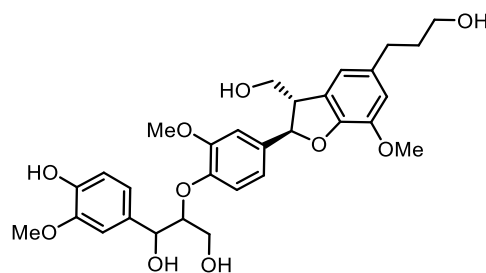


Figure 16: Structure of the illiciumlignan D (1-66).

Sambucasinol A-C (1-67 to 1-69) (Figure 17) were isolated from *S. williamsii* twigs and all showed a potent inhibitory effect on NO production in LPS-stimulated BV-2 cells and NGF secretion in C6 cells with IC_{50} values ranging from 6.82 to 14.70 μM . Compounds also showed consistent cytotoxic activity against cancer cell lines A549, SKOV3, SK-MEL-2 and XF498 with IC_{50} values ranging from 11.07 to 19.62 μM . Therefore, **sambucasinol A-C** are compounds that could be useful for the development of new anti-inflammatory, neuroprotective and anticancer agents.³¹



1-67, sambucasinol A, 7''- α \pm 8''- β R = *trans*-feruloyl
1-68, sambucasinol B, 7''- α 8''- β R = *trans*-feruloyl
1-69, sambucasinol C, 7''- α 8''- β R = *cis*-feruloyl

Figure 17: Structure of the sambucasinol A-C (1-67 to 1-69).

Neolignans also exhibit antiallergic activities – **Maceneolignan (1-70)** (Figure 18) isolated from the aril of *Myristica fragrans* (*Myristicaceae*) inhibited antigen-stimulated tumor

necrosis factor- α production, an important process in the late phase of type I allergic reactions with the TNF- α inhibitor, $IC_{50} = 48.40 \mu M$.³³

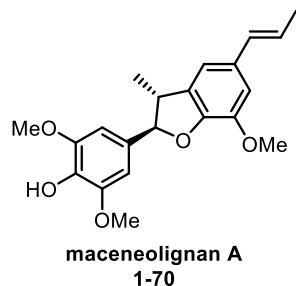


Figure 18: Structure of the maceneolignan A (1-70).

Dehydrodiconiferyl alcohol (1-71) (Figure 19), a compound originally isolated from *Cucurbita moschata*, inhibits osteoclast differentiation and promotes bone morphogenetic protein-2 (BMV-2)–induced osteoblastogenesis acting as an estrogen receptors agonist. This estrogenic effect may serve as a treatment for postmenopausal and ovariectomy-induced bone loss.^{34,35}

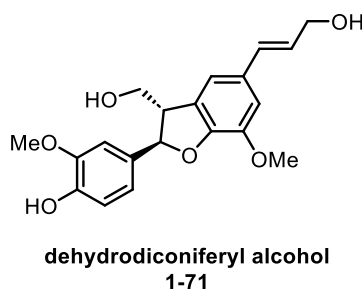


Figure 19: Dehydrodiconiferyl alcohol (1-71).

Lithospermic acid (1-72) and **salviaonolic acid B (1-73)**, compounds isolated from *Salvia miltiorrhiza*, are nontoxic and active against HIV by inhibiting HIV-1 integrase, with the IC_{50} of $0.83 \mu M$ and $0.48 \mu M$, respectively. These two compounds hold promise as novel therapeutic agents against AIDS due to their high potency and absence of cytotoxicity.^{36,37}

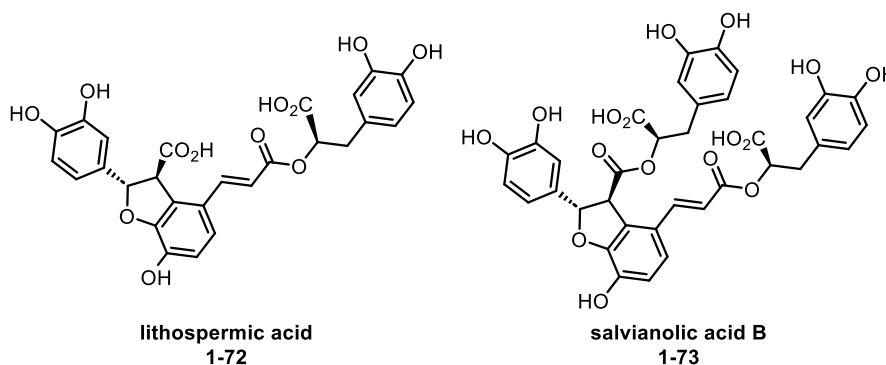


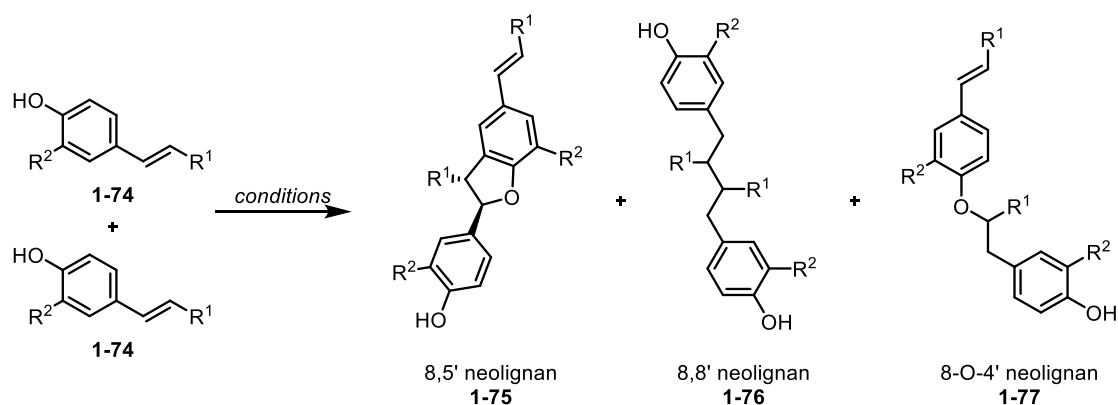
Figure 20: Structure of the lithospermic acid (1-72) and salviaonolic acid B (1-73).

1.3. Synthesis of benzofurans

1.3.1. Synthesis based on enzymes and transitional metals

Several synthetic approaches to **1-39** neolignan (C8-C5') core are based on a biomimetic approach that proceeds *via* transition metal or enzyme (disguised transition metal) mediated oxidative homocoupling of appropriate phenylpropanoid precursors. As was demonstrated in **Figure 5** (homocoupling intermediates), in such a case, the selected substrate must possess the phenolic OH group in *para* position to the attached phenylpropanoid C3 subunit. Therefore, only a few phenolic monomers can undergo dimerization (ferulic, coumaric, and caffeic acid). The key disadvantage of such biomimetic approach lies in the narrow scope of the substrates available for the coupling, reliability of the protocols that lacks general reproducibility, low reaction yields accompanied with various side reaction formation (most common side products are products of 8-O-4' and 8,8' dimerization), and lack in the stereochemistry of the post-coupling steps. The overview of products that are produced by various homodimerization methods is shown in **Table 1**.

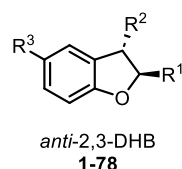
These results play major roles in suggesting that the reaction solvent and water content in the reaction system affect the reaction products obtained from the oxidation either by enzymes or by transitional metals.

Table 1: Different dimerization conditions.

Entry	Conditions	R ¹	R ²	Yield 8,5'	Yield 8,8'	Yield 8-O-4'	Ref.
1	FeCl ₃ , EtOH/water	CH ₃	OCH ₃	30 %	-	-	38
2	FeCl ₃ , acetone/water	CH ₃	OCH ₃	53 %	2 %	-	19
3	Ag ₂ O, DCM	CH ₂ OH	OCH ₃	50 %	-	-	7
4	Ag ₂ O, dioxane	CH ₂ OH	OCH ₃	14 %	-	70 %	
5	Ag ₂ O, benzene/acetone	COOCH ₃	OCH ₃	42-50 %	-	-	18,39
6	Ag ₂ O, benzene/acetone	COOCH ₃	H	35 %	-	-	18
7	K ₃ [Fe(CN) ₆]	COOCH ₃	OCH ₃	19 %	-	-	20
8	K ₃ [Fe(CN) ₆]	COOCH ₃	H	57 %	-	-	20
9	HRP/H ₂ O ₂	CH ₃	OCH ₃	56 %	13 %	22 %	40
10	HRP/H ₂ O ₂	COOCH ₃	H		16 %	-	41
11	Laccase (<i>Rhus vernicifera</i>)	CH ₃	OCH ₃	43 %	-	22 %	42

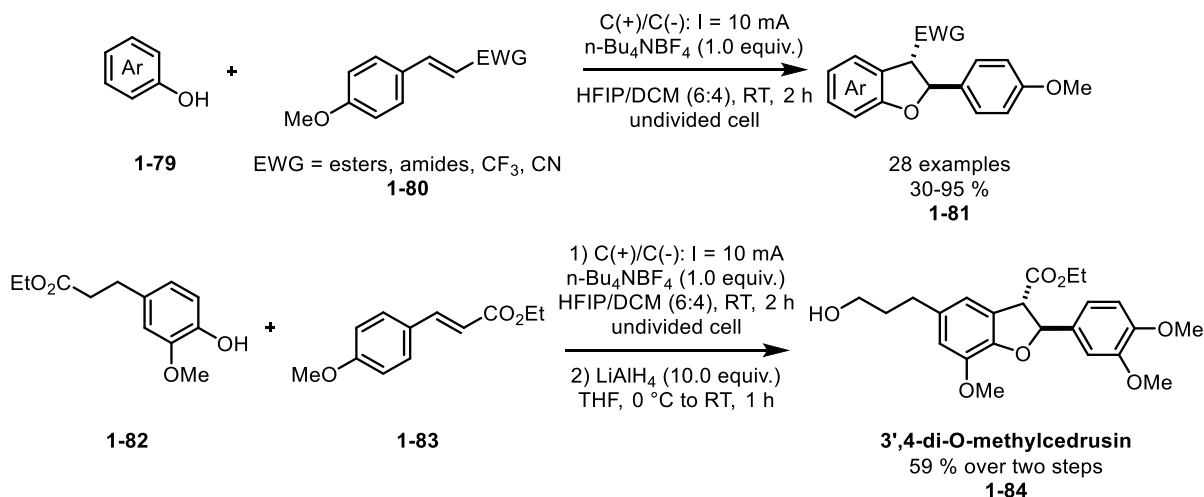
1.3.2. Non-biomimetic approaches to dihydrofuran neolignans

2,3-Dehydrobenzofuran (**DHB**) belongs to the class of organic compounds with the coumaran skeleton, which entails a benzene ring fused to a 2,3-DHB ring (**Figure 21**). Not many methods have been described for the synthesis of *anti* 2,3-disubstituted DHBs, but there are a vast number of developed methods for formation of the benzofuran skeleton.

**Figure 21:** Structure of the *anti*-2,3-DHB (**1-78**).

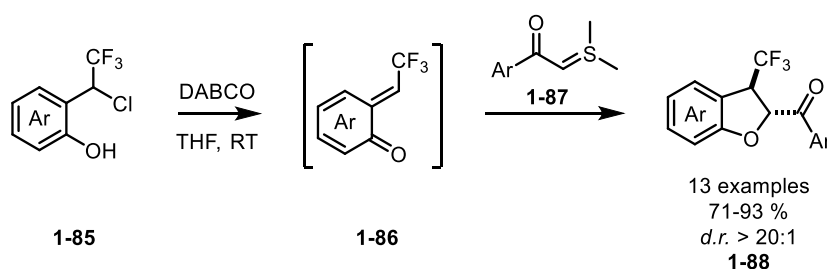
The aim of this chapter is to briefly summarize the most important and recent methods in the synthesis of analogues of *anti*-2,3-disubstituted C8-C5' neolignans.

In 2020, Wang and his coworkers reported an electro-oxidative [3+2] annulation reaction of phenols **1-79** and electron-deficient alkenes **1-80** for the synthesis of various chiral derivatives of 2,3-dehydrobenzofuran-3-ol **1-81**. The reaction might be used to synthesize alkyl amino, trifluoromethyl, and cyano substituted products. The natural product 3',4-di-O-methylcedrusin **1-84** was synthesized using this approach (**Scheme 3**).⁴³



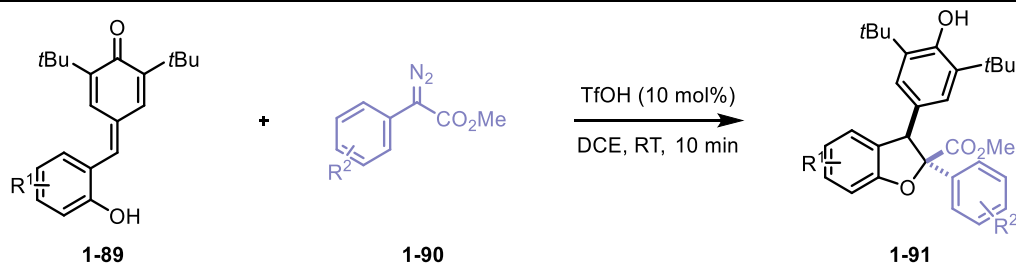
Scheme 3: Cu(I)-catalysed asymmetric synthesis of 2,3-dehydrobenzofuran-3-ol derivatives **1-81** and synthesis of 3',4-di-O-methylcedrusin **1-84**.⁴³

In 2020 Srivari Chandrasekhar and co-workers described an effective synthesis of CF₃ functionalized DHBs **1-88** by annulation of *ortho*-hydroxy-CF₃-benzyl chlorides **1-85** with sulfur ylides **1-87** under basic conditions in a highly diastereoselective manner (**Scheme 4**).⁴⁴



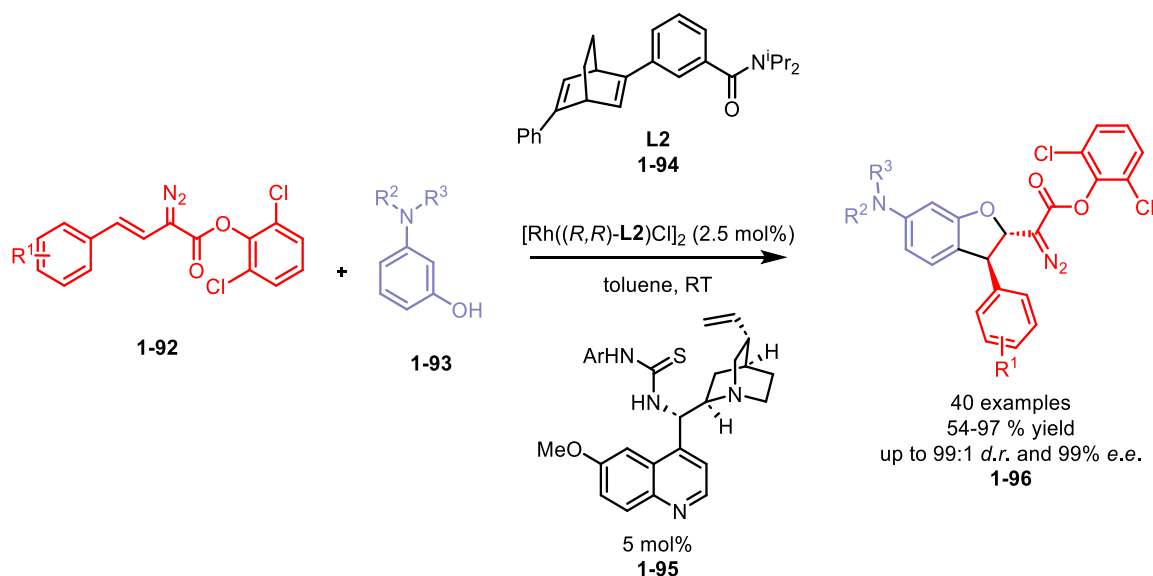
Scheme 4: Diastereoselective synthesis of CF₃-dehydrobenzofurans **1-88** by [4+1] annulation of *in situ*-generated CF₃-*o*-quinone methides **1-86** and sulfur ylides **1-87**.⁴⁴

In 2021, Fener Chen and co-workers developed a methodology for the construction of 2,3-DHB scaffolds containing a quaternary carbon center at the position C2 in **1-91** by the [4+1] annulation reaction of *p*-quinone methides (QM) **1-89** and α -aryl diazoacetates **1-90** (C1 synthon) using a catalytic amount of TfOH (**Scheme 5**).⁴⁵



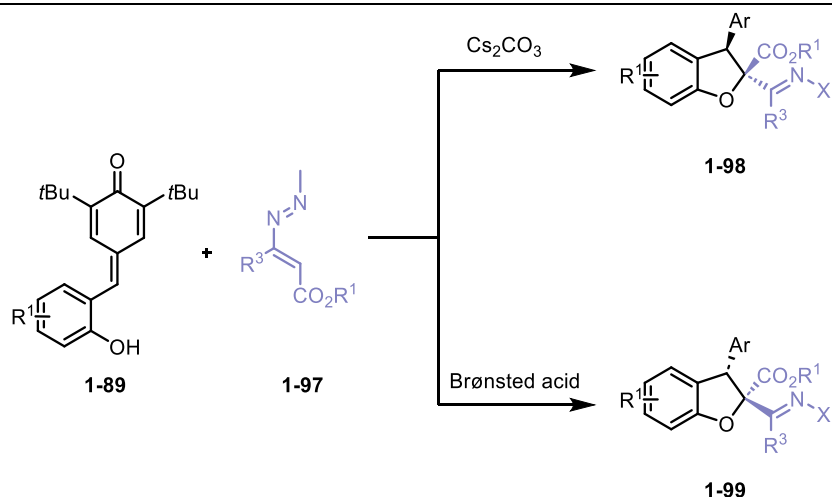
Scheme 5: TfOH-catalysed [4+1] annulation of *p*-QMs **1-89** with α -Aryl Diazoacetates **1-90**.⁴⁵

Ming-Hua Xu and co-workers in 2021 achieved the synthesis of enantioenriched 2,3-disubstituted dihydrobenzofurans **1-94** utilizing arylvinyl diazoacetates **1-92** and aminophenons **1-93** using a chiral rhodium catalyst and organocatalyst **1-95** which independently control the formation of two stereogenic centers through one-pot C-H functionalization/oxa-Michael addition cascade reaction with excellent diastereomeric ratio up to 99 % and excellent yields (**Scheme 6**).⁴⁶



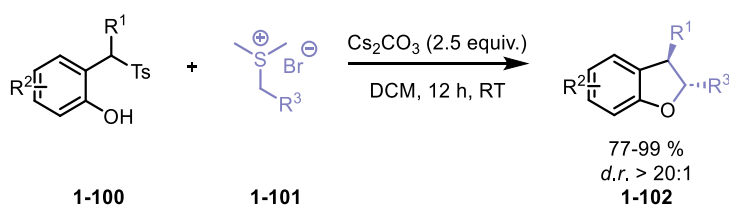
Scheme 6: Stereodivergent synthesis of enantioenriched 2,3-disubstituted dihydrobenzofurans **1-96** via a one-pot C–H functionalization/oxa-Michael addition cascade.⁴⁶

In 2023, Mei group developed a diastereodivergent formal [4+1] cycloaddition of *p*-QMs **1-89** with azoalkenes **1-98** via the domino oxa-1,4-addition/1,6-addition process in good yields and with reversible diastereoselectivities (**Scheme 7**).⁴⁷



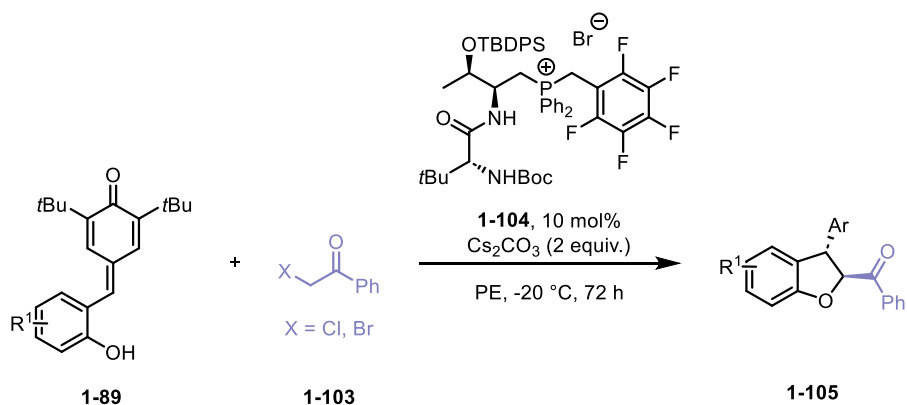
Scheme 7: Diastereodivergent formal [4+1] cycloaddition of azoalkenes **1-97** as one-carbon synthons.⁴⁷

In 2013, a group of Zhou developed a mild method for the generation of *o*-QMs intermediates from 2-tosylalkylphenols **1-100** under basic conditions and their reaction with sulfur ylides **1-101** resulted in the selective synthesis of anti-2,3-DHBs (**Scheme 8**).⁴⁸



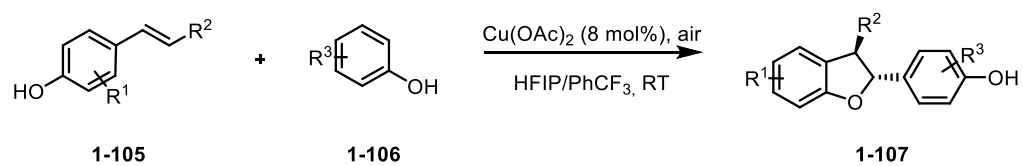
Scheme 8: A mild method for generation of *o*-quinone methides under basic conditions. The facile synthesis of *trans*-2,3-dihydrobenzofurans **1-102**.⁴⁸

In 2019, a group of Wang developed enantioselective [4+1] annulation reaction between hydroxyl-substituted *p*-QMs with α -halogenated ketones by a dipeptide based bifunctional phosphonium salt catalyst (**Scheme 9**).⁴⁹



Scheme 9: Bifunctional phosphonium salt directed enantioselective formal [4+1] annulation of hydroxyl-substituted *p*-QMs with α -halogenated ketones **1-103**.

In 2021, the Liu group developed a biomimetic selective methodology of using copper acetate as a catalyst and air as the terminal oxidant (oxidative cross coupling) (**Scheme 10**).⁷



Scheme 10: Biomimetic selective synthesis of 8,5' neolignan analogues **1-107**.⁷

1.4. Results and discussion*

1.4.1. Introduction

Our research group has a long-standing interest in exploring the biological activities associated with plant secondary metabolites – more specifically, our focus lies in the synthesis of neolignan derivatives with the benzofuran structure (**1-39**) and biological evaluation of prepared library against nematodes in a model *Caenorhabditis elegans* and biological evaluation of antiparkinson activity. This part of the Thesis builds on previous gained knowledge in the synthesis and application of lignans and neolignans within our group.^{5,50–52} Our long-standing goal is to develop a straightforward general synthetic route to dehydrodiconiferyl alcohol glucoside (**DCG-A, 1-108, Figure 22**).

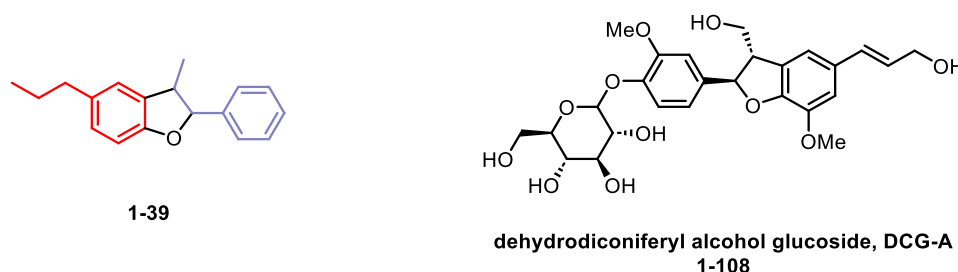


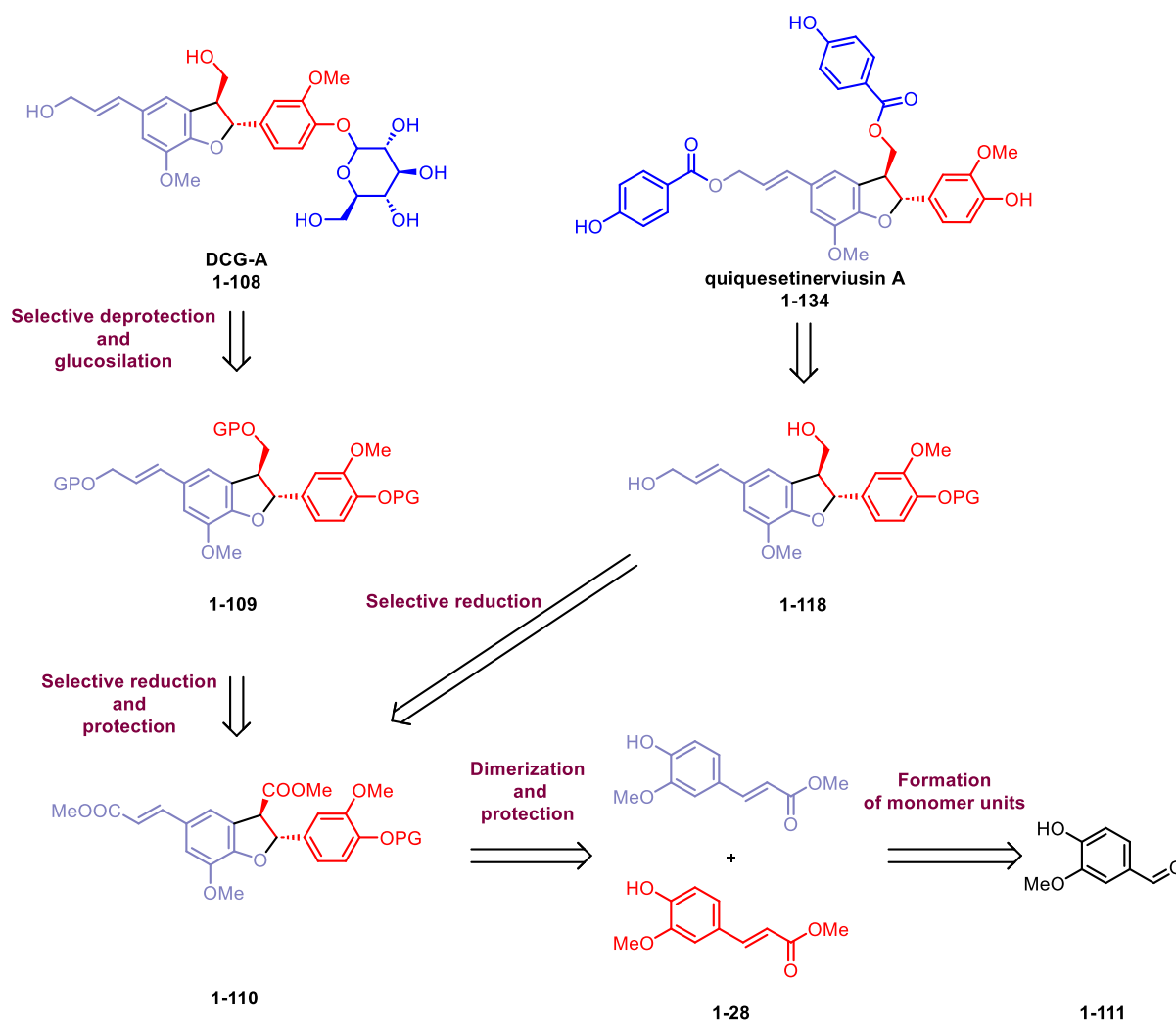
Figure 22: Structure of the general dihydrobenzofuran neolignan core **1-39** and **DCG-A**.

1.4.2. Retrosynthesis plan

Our strategy in achieving the goal of this project was to design a synthesis that would start from a simple and commercially available building block and allow us to prepare not only the **DCG-A** molecule but also analogues of other naturally occurring molecules that would allow us to constitute the whole neolignan-based chemical library suitable for further evaluation of their biological activity. An overview of our retrosynthetic analysis that was supposed to bring us to the **DCG-A** synthesis is outlined in **Scheme 11**.

* This work was supported by the European Regional Development Fund-Project 'Centre for Experimental Plant Biology' (no. CZ.02.1.01/0.0/0.0/16_019/0000738) and by the Palacký University Internal Grant Agency (IGA_PrF_2021_011, IGA_PrF_2021_024, IGA_PrF_2022_012, IGA_PrF_2022_016, IGA_PrF_2022_022). The research presented in this chapter were in part published in the Bachelor theses of Sylvie Lévyová (for details see further) and the manuscript is currently under preparation. The work was done in collaboration with Dr. Alena Kadlecová (anthelmintic activity evaluation), Dr. Hana Vylíčilová (cytokinin essays) and Dr. Gabriel Gonzalez (antiparkinson activity evaluation). As a primary researcher in the project, I was responsible for designing and conducting experimental procedures and measurements, analyzing the data, and interpreting the results. Additionally, I am writing a first draft of the manuscript.

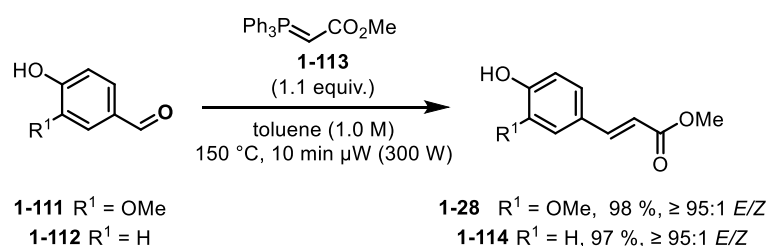
From a retrosynthetic point of view, the plan was divided into three parts and was based on the first (and only) total synthesis of **DCG-A** published in 1998 by Wong group⁵³ where DCG-A was prepared from the diol-protected neolignan dimer **1-109** by a synthetic sequence that comprised selective deprotection of the phenolic -OH group followed by glycosylation of **1-109**. Therefore, we decided to base our retrosynthetic proposal on the exploitation of the same diol **1-109**, which could be prepared by selective reduction of methyl esters to alcohols followed by introduction of a protecting group of **1-110**. This dimer **1-110** could be prepared by dimerization of the neolignan monomers **1-28** and introduction of the protective group in the phenolic hydroxy group. Compound **1-110** could further allow us the synthesis of few more natural products with the same molecular scaffold as in **DCG-A** as demonstrated on the quiquesetinerviusin A (**1-134**) (**Scheme 11**).



Scheme 11: Retrosynthetic plan towards **DCG-A** and **quiquesetinerviusin A**.

1.4.3. Towards DCG-A: Formation of monomer units of phenylpropanoids

Based on our proposal, the synthesis of the **DCG-A** should take 8 steps. We have started our investigation with the first step of the 8-step reaction sequence with the formation of monomer units of methyl ferulate **1-28** together with methyl coumarate **1-114**. We utilized method developed in our group⁵¹ that explore microwave-initiated preparation of phenylpropanoids *via* Wittig reaction and allowed us to obtain both desired monomers in excellent yield and *E* selectivity. The values of selectivity and the reaction yields corresponded to those mentioned in the original protocol; therefore, no optimization of the reaction was required (**Scheme 12**).

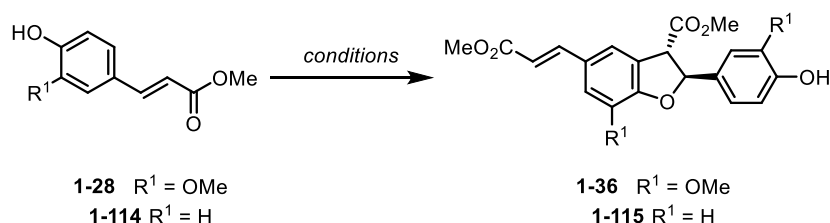


Scheme 12: Microwave-Assisted Synthesis of monomers **1-28** and **1-114**.⁵¹

1.4.4. Homocoupling dimerization

The next step was the homocoupling dimerization of the two monomers **1-28** and **1-114**. The dimerization reaction is an oxidative radical reaction that is well described in the literature^{21,38–41}, hence we screened the best conditions in the literature. Due to the low yields, we have performed optimization of the homocoupling reaction ourselves. Products **1-36** and **1-115** were isolated as white solids in 32 % and 48 % optimized yields, respectively. The conditions and results obtained are summarized in **Table 2**.

Table 2: Dimerization reaction optimization.



Entry	Conditions	R^1	Yields [%] ^a
1	$\text{K}_3[\text{Fe}(\text{CN})_6]$ (2.1 equiv.), DCM/ CHCl_3 1:9 (V/V), RT	CH_3	22
2	$\text{K}_3[\text{Fe}(\text{CN})_6]$ (2.1 equiv.), DCM/ CHCl_3 1:9 (V/V), RT	H	17
3	Ag_2O (2.1 equiv.), acetone/benzene 2:1 (V/V), RT	CH_3	28

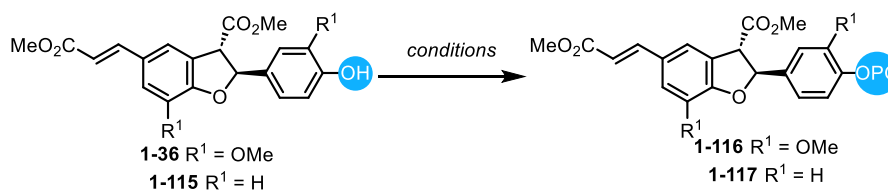
Entry	Conditions	R ¹	Yields [%] ^a
4	Ag ₂ O (1.0 equiv.), benzene/acetone 2:1 (V/V), RT	H	32
5	Ag ₂ O (1.0 equiv.), toluene/acetone 2:1 (V/V), RT	CH ₃	48

a) Refers to isolated yield after the column chromatography on silica gel.

1.4.5. Introduction of the phenolic protecting group

The third step was the introduction of a suitable protection group. We have decided to introduce various protecting groups, which would be orthogonal in reactivity to a reductive condition employed in the next step and could be removed using various reaction mechanisms and under various reaction conditions. Our starting materials **1-36** and **1-115** were selectively protected by dihydropyran (**DHP**), 2-(trimethylsilyl)ethoxymethyl (**SEM**), 2,4-dimethoxybenzyl, triisopropylsilyl (**TIPS**), methoxymethyl (**MOM**) and *tert*-butyldimethylsilyl (**TBS**) in good to excellent yields. The results are shown in **Table 3** below.

Table 3: Conditions for introduction of different protecting groups.



Entry	Conditions	R ¹	OPG	Yields [%] ^a	
1	DHP (4.0 equiv.), <i>p</i> TSA (cat.), RT, 18 h	H	1-117a	DHP	65
2	DIPEA (4.0 equiv.), SEMCl (2.0 equiv.) DCM (0.2 M), 0 °C to RT, 18 h	H	1-117b	SEM	70
3	2,4-dimethoxybenzyl 2,2,2-trichloroacetimidate (1.2 equiv.), <i>p</i> TSA (cat.), DCM (0.25 M), RT, 18 h	H	1-117c		95
4	TEA (3.0 equiv.), TIPSCl (1.3 equiv.) DCM (0.4 M), 0 °C to RT, 18 h	H	1-117d	TIPS	78
5	MOMCl (3.0 equiv., 3.5 M sol. in toluene), DIPEA (2.0 equiv.), DCM (0.5 M), 0 °C to RT, 18 h	H	1-117e	MOM	95
6	MOMCl (3.0 equiv., 3.5 M sol. in toluene), DIPEA (2.0 equiv.), DCM (0.5 M), 0 °C to RT, 18 h	CH ₃	1-116a	MOM	94
7	TEA (3.0 equiv.), TBSCl (1.25 equiv.) DCM (0.5 M), 0 °C to RT, 18 h	H	1-117f	TBS	96
8	TEA (3.0 equiv.), TBSCl (1.25 equiv.) DCM (0.5 M), 0 °C to RT, 18 h	CH ₃	1-116b	TBS	94

a) Refers to isolated yield after the column chromatography on silica gel.

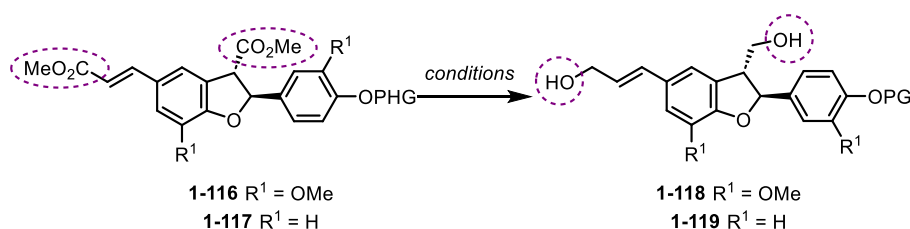
1.4.6. Reduction step

The fourth step of the sequence was the reduction of both ester groups in **1-116** and **1-117** to the corresponding alcohols **1-118** and **1-119**. At this point, our precious experience in the neolignan-core bearing compounds⁵⁰ was used, and DIBAL-H was selected as the most convenient reducing agent. The results are summarized in

Table 4.

We have decided to continue in the synthesis only with the **TBS** protected dimers **1-118b** and **1-119f** and **MOM** protected dimers **1-118a** and **1-118e**, **2,4-dimethoxybenzyl** and **TIPS** protecting groups (unstable under reaction conditions or reaction work-up), and the **DHP** or **SEM** protecting groups (low yielding protocols), were discarded. It should be also noted, that when TBS protected dimers **1-116** and **1-117** were reduced, the reducing agent, DIBAL-H, had to be used in large excess (from 6 equiv. to 11 equiv.) to drive the reaction to completion, otherwise partially reduced products **1-120** and **1-121** were isolated (**Scheme 13**).

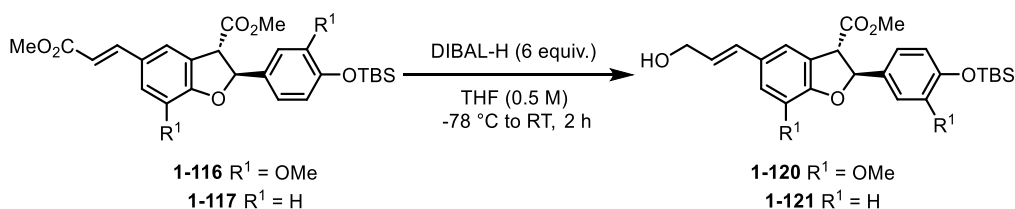
Table 4: Optimization of the reduction of esters to alcohols.



Entry	Conditions	R ¹	product	OPG	Yields [%] ^a
1	DIBAL-H (4.5 equiv., 1 M in THF) DCM (0.5 M), -78 °C to RT, 3 h	H	1-119e	MOM	34
2	DIBAL-H (4.5 equiv., 1 M in THF) THF (0.5 M), -78 °C to RT, 3 h	H	1-119e	MOM	89
3	DIBAL-H (4.5 equiv., 1 M in THF) THF (0.5 M), -78 °C to RT, 3 h	CH ₃	1-118a	MOM	72
4	DIBAL-H (4.5 equiv., 1 M in THF) THF (0.5 M), -78 °C to RT, 3 h	H	1-119a	DHP	15
5	DIBAL-H (4.5 equiv., 1 M in THF) THF (0.5 M), -78 °C to RT, 3 h	H	1-119b	SEM	21
6	DIBAL-H (4.5 equiv., 1 M in THF) THF (0.5 M), -78 °C to RT, 3 h	H	1-119c		N.D. ^b
7	DIBAL-H (4.5 equiv., 1 M in THF)	H	1-119d	TIPS	N.D. ^b

Entry	Conditions	R ¹	product	OPG	Yields [%] ^a
8	THF (0.5 M), -78 °C to RT, 3 h	CH ₃	1-118b	TBS	39 ^c
	DIBAL-H (4.5 equiv., 1 M in THF) DCM (0.5 M), -78 °C to RT, 3 h				
9	DIBAL-H (5 equiv., 1 M in THF) THF (0.5 M), -78 °C to RT, 3 h	H	1-119f	TBS	54 ^c
	DIBAL-H (5 equiv., 1 M in THF) THF (0.5 M), -78 °C to RT, 3 h				
10	DIBAL-H (5 equiv., 1 M in THF) THF (0.5 M), -78 °C to RT, 3 h	CH ₃	1-118b	TBS	51 ^c
	DIBAL-H (5 equiv., 1 M in THF) THF (0.5 M), -78 °C to RT, 3 h				
11	DIBAL-H (6 equiv., 1 M in THF) THF (0.5 M), -78 °C to RT, 4 h	CH ₃	1-118b	TBS	60 ^c
	DIBAL-H (6 equiv., 1 M in THF) THF (0.5 M), -78 °C to RT, 4 h				
12	1) DIBAL-H (6 equiv., 1 M in THF), THF (0.5 M), -78 °C to RT, 2 h	H	1-119f	TBS	90
	2) DIBAL-H (5 equiv., 1 M in THF), THF (0.5 M), RT, 2 h				
13	1) DIBAL-H (6 equiv., 1 M in THF), THF (0.5 M), -78 °C to RT, 2 h	CH ₃	1-118b	TBS	86
	2) DIBAL-H (5 equiv., 1 M in THF), THF (0.5 M), RT, 2 h				

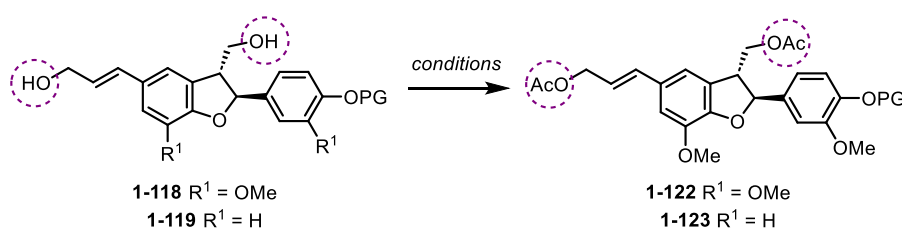
- a) Refers to isolated yield after the column chromatography on silica gel.
 b) Yield not determined, product decomposition.
 c) Incomplete reduction, product(s) of partial reduction of at least of the ester group observed.



Scheme 13: Partial reduction of TBS-containing starting materials.

1.4.7. Hydroxy Group Protection - Step Five

The fifth step was the introduction of an acetyl protecting group on both primary alcohols presented on side chains of TBS and MOM protected benzofuran cores. This was achieved with acetyl chloride in excellent yields for MOM and TBS protected derivatives and the desired products **1-122** and **1-123** were isolated in excellent yields (**Table 5**).

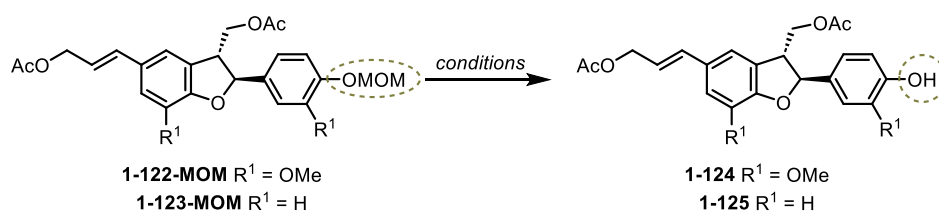
Table 5: Introduction of acetyl protecting group.

Entry	Conditions	R ¹	product	OPG	Yields [%] ^a
1	AcCl (2.2 equiv.), TEA (3.0 equiv.) DCM (0.25 M), 0 °C to RT, 18 h	H	1-123a	MOM	95
2	AcCl (2.2 equiv.), TEA (3.0 equiv.) DCM (0.25 M), 0 °C to RT, 18 h	CH ₃	1-122a	MOM	99
3	AcCl (2.2 equiv.), TEA (3.0 equiv.) DCM (0.25 M), 0 °C to RT, 18 h	H	1-123b	TBS	94
4	AcCl (2.2 equiv.), TEA (3.0 equiv.) DCM (0.25 M), 0 °C to RT, 18 h	CH ₃	1-122b	TBS	98

a) Refers to isolated yield after the column chromatography on silica gel.

1.4.8. Selective phenolic protecting group removal

The sixth step of the sequence was the selective removal of the phenolic protecting group, a simple step that proved to be more than difficult. The removal of the MOM protecting group will first be discussed (**Table 6**). Various reaction conditions were evaluated; however, only **entries 13** and **14** resulted in partial conversion of the starting material. Only when *in situ* generated strong Lewis acid TMSI was used (TMSCl/NaI system, **entry 17**), the conversion of the starting material was quantitative; however, the desired product was isolated only with a 20% yield. Unfortunately, when the reaction was carried out on a larger semipreparative scale (0.5 mmol), only decomposition of the starting material/product was observed. Therefore, we concluded that the MOM protecting group is not suitable to be further exploration in this synthetic scheme.

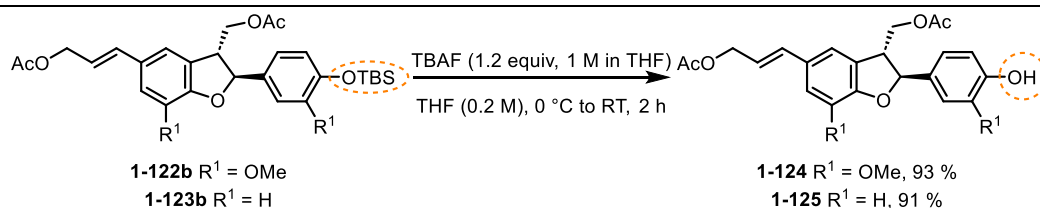
Table 6: Attempted deprotection of the MOM protected group from compounds **1-122** and **1-123**.

Entry	Conditions	R ¹	Comments
1	ZnBr ₂ (3.0 equiv.), Et ₂ O (0.05 M), 0 °C to RT, 18 h	H	decomposition ^b
2	<i>p</i> TSA (1.1 equiv.), MeOH (0.05 M), 30 °C, 2 h ⁵⁴	H	decomposition ^b
3	ZnBr ₂ (1.0 equiv.), lithium thioethoxide (2.0 equiv.) DCM (0.05 M), 0 °C to RT, 18 h ⁵⁵	H	decomposition ^b
4	ZnI ₂ (4.0 equiv.), Et ₂ O (0.05 M), 0 °C to RT, 18 h	CH ₃	decomposition ^b
5	HCl (1.0 equiv., 1 M), MeOH (0.05 M), RT, 1 h ⁵⁶	H	decomposition ^b
6	HCl (20.0 equiv., 4 M in dioxane), THF (0.05 M), 0 °C, 20 min ⁵³	H	decomposition ^b
7	AcCl (2.0 equiv., 1 M), MeOH (0.1 M), RT, 1 h ⁵⁷	H	decomposition ^b
8	TFA (2.0 equiv., 0.0375 M), MeOH (0.1 M), RT, 1 h ⁵⁸	H	decomposition ^b
9	CBr ₄ (0.1 equiv.), <i>i</i> PrOH (0.2 M), 85 °C, 2h ⁵⁹	H	decomposition ^b
10	CBr ₄ (0.2 equiv.), PPh ₃ (0.2 equiv.), DCM (0.2 M), 40 °C, 2 h ⁶⁰	H	decomposition ^b
11	SnCl ₄ (0.1 equiv.), DCM (0.2 M), 0 °C, 1 h ⁶¹	H	decomposition ^b
12	MgBr ₂ ·Et ₂ O complex (5.0 equiv.), DCM (0.5 M), 0 °C, 1 h	H	decomposition ^b
13	TMSOTf (2.0 equiv.), 2,2'-dipyridyl (3.0 equiv.) AcCN (0.1 M), 0 °C, 8 h	H	1-124 (traces) and decomposition ^b
14	TMSOTf (2.0 equiv.), 2,2'-dipyridyl (3.0 equiv.) AcCN (0.1 M), 0 °C, 8 h	CH ₃	1-124 (traces) and decomposition ^b
15	BF ₃ ·Et ₂ O complex (5.0 equiv.), DCM (0.05 M), 0 °C, 2 h	CH ₃	decomposition ^b
16	BF ₃ ·Et ₂ O complex (0.5 equiv.), DCM (0.05 M), 0 °C, 1 h	CH ₃	decomposition ^b
17	NaI (5.0 equiv.), TMSCl (1.5 equiv.), AcCN (0.02 M), RT, 4 h ⁶²	CH ₃	20 % ^a
18	NaI (5.0 equiv.), TMSCl (5.0 equiv.), AcCN (0.04 M) DCM (0.04 M), RT, 4 h ⁶³	CH ₃	decomposition ^b

a) Isolated yield after column chromatography on silica gel.

b) Based on the analysis of the ¹H NMR spectra of the crude reaction mixture.

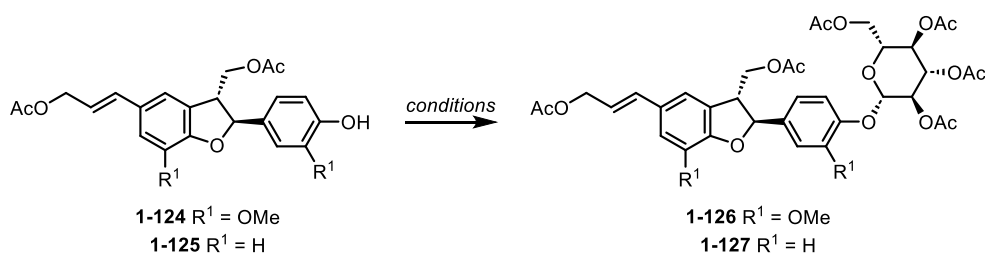
The removal of the TBS group from compounds **1-122b** and **1-123b** was quite straightforward, since both compounds provided by treatment with TBAF in THF the desired desilylated products **1-124** and **1-125** in excellent yields of 93 % and 91 %, respectively. Accidentally, it was also observed that the reaction could also be carried out at -40°C without any observable decrease in the reaction yields. (**Scheme 14**).



Scheme 14: Deprotection of TBS group.

1.4.9. Introduction of glucose

Having a coupling partner available for glucose introduction, a glycosylation reaction could be attempted (Table 7). Our first attempts at the reunion of the glucose derivative with the phenolic compounds started with well-known protocols in the literature that exploit the use of AgCO₃⁶⁴ and Ag₂O⁶⁵ salts as a coupling promoters. However, in all attempted cases, the desired products **1-126** and **1-127** were not formed since either no conversion of the starting phenols **1-124** or **1-125** was observed or the conversion was very low, and no traces of products were detected (entry **1-8**). The use of stronger Lewis acids such as AgOTf⁶⁶ or BF₃.Et₂O led to substrate decomposition (entries **9-11**), and even the change in the glucose mode of activation (from bromide to imidate⁶⁷) did not result in the product formation (entry **12-14**). Finally, the Mitsunobu protocol saved the day and allowed us to isolate the desired **1-126** in 52 % yield. By slight modifications in the reaction conditions (reaction time and temperature), the desired product **1-126** was isolated in 91 % (entry **17**). Those optimized reaction conditions were not attempted on phenol **1-125** for two reasons: (1) at that moment we have run out of the starting material and (2) before it could be rebuilt, the results of the biological evaluation of **DCG-A** for its cytokinin-like properties were obtained and the project was cancelled.

Table 7: Coupling of the phenolic intermediates **1-124** and **1-125** with glucose derivatives.

Entry	Conditions	R ¹	Yields [%] ^a /comments
1	2,3,4,6-tetra-O-acetyl-alpha-D-glucopyranosyl bromide (2.25 equiv.), py (0.05 M), AgCO ₃ (4.0 equiv.), RT, 48 h	H	No conversion ^b
2	2,3,4,6-tetra-O-acetyl-alpha-D-glucopyranosyl bromide (1.1 equiv.), py (0.05 M), K ₂ CO ₃ (10.0 equiv.), AgCO ₃ (4.0 equiv.), RT, 24 h	CH ₃	Low conversion ^b
3	2,3,4,6-tetra-O-acetyl-alpha-D-glucopyranosyl bromide (1.1 equiv.), acetone (0.03 M), K ₂ CO ₃ (10.0 equiv.), AgCO ₃ (4.0 equiv.), RT, 24 h	H	No conversion ^b
4	2,3,4,6-tetra-O-acetyl-alpha-D-glucopyranosyl bromide (1.1 equiv.), DCM (0.05 M), 2,6-lutidine (4.0 equiv.), AgCO ₃ (4.0 equiv.), RT, 18 h	CH ₃	Low conversion ^b
5	2,3,4,6-tetra-O-acetyl-alpha-D-glucopyranosyl bromide (1.2 equiv.), DCM (0.05 M), K ₂ CO ₃ (10.0 equiv.), AgCO ₃ (4.0 equiv.), RT, 24 h	CH ₃	Low conversion ^b
6	2,3,4,6-tetra-O-acetyl-alpha-D-glucopyranosyl bromide (1.2 equiv.), 2,6-lutidine (4.0 equiv.), Ag ₂ O (4.0 equiv.), DCM (0.05 M), RT, 18 h	CH ₃	decomposition ^b
7	2,3,4,6-tetra-O-acetyl-alpha-D-glucopyranosyl bromide (1.2 equiv.), Ag ₂ O (4.0 equiv.), py (0.05 M), RT, 18 h	CH ₃	decomposition ^b
8	2,3,4,6-tetra-O-acetyl-alpha-D-glucopyranosyl bromide (1.2 equiv.), Ag ₂ O (4.0 equiv.), AcCN (0.05 M), RT, 18 h	CH ₃	Low conversion ^b
9	2,3,4,6-tetra-O-acetyl-alpha-D-glucopyranosyl bromide (1.2 equiv.), AgOTf (4.0 equiv.), AcCN (0.09 M), RT, 18 h	CH ₃	decomposition ^b
10	2,3,4,6-tetra-O-acetyl-alpha-D-glucopyranosyl bromide (1.2 equiv.), AgOTf (4.0 equiv.), py (0.05 M), RT, 18 h	CH ₃	decomposition ^b
11	2,3,4,6-tetra-O-acetyl-alpha-D-glucopyranosyl bromide (1.0 equiv.), BF ₃ ·Et ₂ O complex (1.1 equiv.), DCM (0.3 M), 0 °C to RT, 8 h	CH ₃	decomposition ^b
12	(2 <i>R</i> ,3 <i>R</i> ,4 <i>S</i> ,5 <i>R</i> ,6 <i>R</i>)-2-(acetoxymethyl)-6-(2,2,2-trichloro-1- iminoethoxy)tetrahydro-2 <i>H</i> -pyran-3,4,5-triyl triacetate (0.7 equiv.), TMSOTf (0.2 equiv.), DCM (0.3 M), 0 °C to RT, 18 h ⁶⁷	H	decomposition ^b

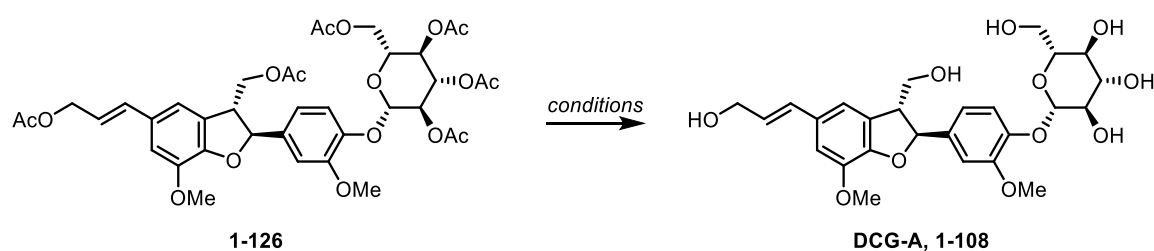
Entry	Conditions	R ¹	Yields [%] ^a /comments
13	(2 <i>R</i> ,3 <i>R</i> ,4 <i>S</i> ,5 <i>R</i> ,6 <i>R</i>)-2-(acetoxymethyl)-6-(2,2,2-trichloro-1-iminoethoxy) tetrahydro-2 <i>H</i> -pyran-3,4,5-triyl triacetate (0.7 equiv.), TMSOTf (0.2 equiv.), DCM (0.3 M), 0 °C to RT, 18 h ⁶⁷	H	decomposition ^b
14	(2 <i>R</i> ,3 <i>R</i> ,4 <i>S</i> ,5 <i>R</i> ,6 <i>R</i>)-2-(acetoxymethyl)-6-(2,2,2-trichloro-1-iminoethoxy) tetrahydro-2 <i>H</i> -pyran-3,4,5-triyl triacetate (1.0 equiv.), TMSOTf (0.1 equiv.), TEA (1.0 equiv.) DCM (0.1 M), -30 °C to RT, 18 h ⁶⁸	H	decomposition ^b
15	2,3,4,6-Tetra-O-acetyl-D-glucopyranose (1.5 equiv.), PPh ₃ (1.5 equiv.), DIAD (1.5 equiv.), THF (0.02 M), 30 °C, 30 min μW (300 W)	CH ₃	52 ^a
16	2,3,4,6-Tetra-O-acetyl-D-glucopyranose (2. equiv.), PPh ₃ (1.5 equiv.), DIAD (1.5 equiv.), THF (0.02 M), 40 °C, 30 min μW (300 W)	CH ₃	74 ^a
17	2,3,4,6-Tetra-O-acetyl-D-glucopyranose (2.0 equiv.), PPh ₃ (1.5 equiv.), DIAD (1.5 equiv.), THF (0.02 M), 50 °C, 45 min μW (300 W)	CH ₃	91 ^a

a) Isolated yield after column chromatography on silica gel.

b) Based on the ¹H NMR spectra of the crude reaction mixture analysis.

1.4.10. Final step – selective acetyl groups

The last step of the sequence was the deprotection of the six acetyl groups of **1-126** (Table 8). First, a simplest reaction protocol based on the use of MeONa⁶⁹ was attempted; however, decomposition of the starting material or product was observed (entry 1 and 2). The change in reaction protocols (temperature, concentration, solvents, MeONa equivalents) furnished the desired conjugate **1-108** (DCG-A) only in low yields (entry 3 to 5). Thus, we moved our attention to the use of K₂CO₃⁷⁰, where the use of excess base (entry 6) led to complete decomposition while when 0.4 equivalents of K₂CO₃ were used, the desired product was isolated with a yield of 28 % (entry 7). The use of mild base TEA in a solvent mixture of MeOH/THF/H₂O resulted in the product DCG-A formation in 37 % yield. The best yield of compound **1-108** was achieved by employing 7*N* NH₃ in MeOH (entry 8). Under such reaction conditions, the desired product was finally obtained in 61 % isolated yield.

Table 8: Final step of the synthesis – acetyl group removal.

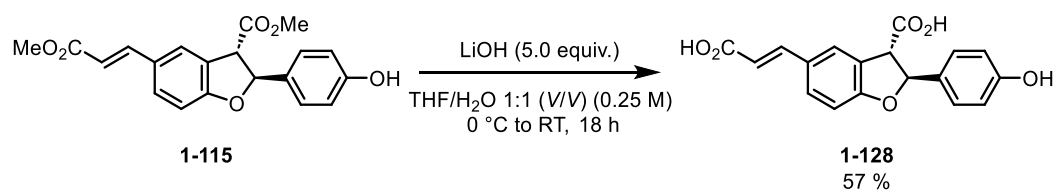
Entry	Conditions	Yields [%] ^a /comments
1	NaOMe (1.0 equiv., 0.1 M), AcCN (1 M), 0 °C to RT, 8 h ^c	decomposition ^b
2	NaOMe (1.0 equiv., 0.1 M), MeOH (0.1 M), 0 °C to RT, 8 h ^c	decomposition ^b
3	NaOMe (0.3 equiv., 0.1 M), MeOH (0.02 M), 0 °C to RT, 1 h ^c	20
4	NaOMe (1.0 equiv., 0.1 M), AcCN (0.1 M), 0 °C to RT, 4 h ^c	33
5	NaOMe (1.0 equiv., 0.1 M), MeOH (0.1 M), 0 °C to RT, 3 h ^d	41
6	K ₂ CO ₃ (7.0 equiv.), MeOH (0.1 M), 0 °C to RT, 1 h	decomposition ^b
7	K ₂ CO ₃ (0.4 equiv.), MeOH (0.04 M), 0 °C to RT, 2 h	28
8	TEA (0.08 M), MeOH (0.08 M), THF (0.08 M), H ₂ O (0.08 M), RT, 18 h ⁷¹	37
9	7N NH ₃ in MeOH (0.05 M), RT, 24 h	61

- a) Isolated yield after column chromatography on silica gel.
 b) Based on the ¹H NMR spectra of the crude reaction mixture analysis.
 c) Commercially available MeONa was used.
 d) Freshly prepared MeONa generated by dissolving Na in MeOH was used.

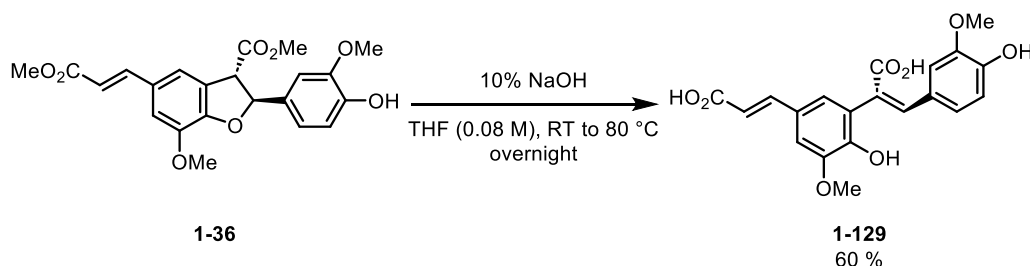
1.4.11. Further reactivity of 8,5' dimers

As mentioned in the introduction, our goal of the project was to constitute a library of the desired neolignan core containing compounds that would be structurally related to **DCG-A**. Thus, various modifications of already prepared compounds were introduced with the aim of broadening the functional group and structural variety. Our attempts towards this goal are summarized within this chapter.

Carboxylic diacid 1-128. One of our goals was to prepare the dicarboxylic acid derivative **1-128**. To do so, we have tried NaOH in H₂O which resulted in decomposition. However, LiOH in the mixture of THF/H₂O resulted in a 57 % isolated yield (**Scheme 15**).

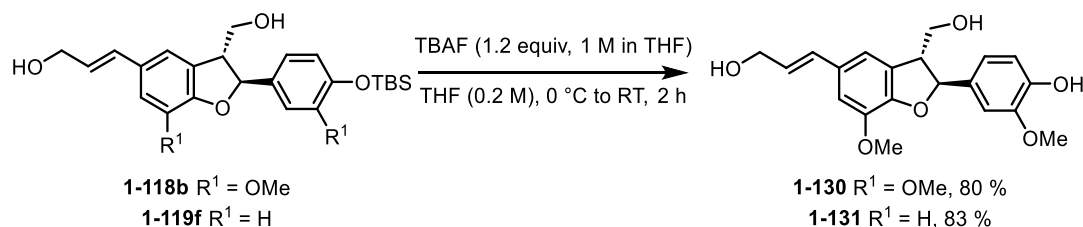
**Scheme 15:** Ester groups hydrolysis that led to diacid **1-128**.

Opened diacid. Interestingly, if NaOH in THF was used to promote carboxylic acid hydrolysis, along with ester hydrolysis, the benzofuran motive also undergoes the base-initiated opening and generates compound **1-129** with a yield of 60 % (**Scheme 16**).



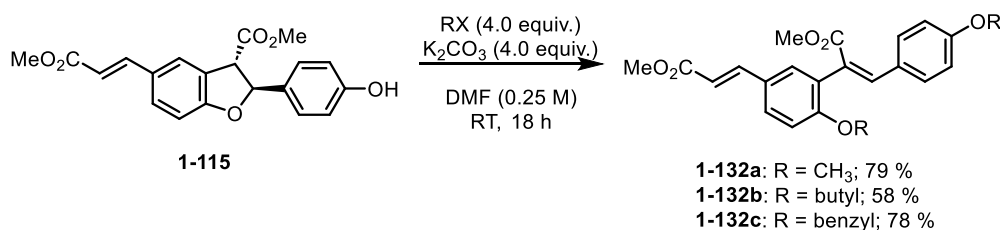
Scheme 16: Formation of 8,5'-diferulic acid **1-129**.

Diol. Dehydrodi-*p*-coumaryl alcohol **1-131** and dehydrodiconiferyl alcohol **1-130** were prepared by TBAF-triggered TBS group removal in **1-118b** and **1-119f** (**Scheme 17**).



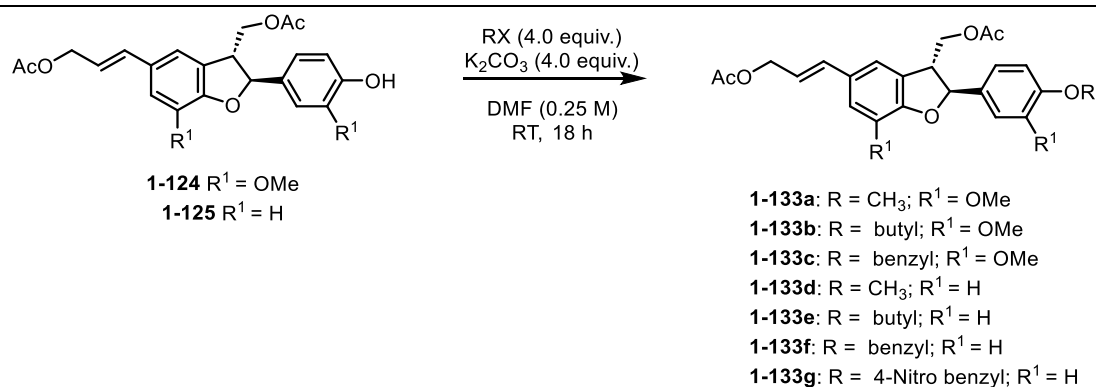
Scheme 17: Deprotection of the TBS group.

Opened diesters. It was observed that if phenol **1-115** is reacted with the mild base in the presence of alkylating reagents, instead of the phenolic group alkylation product, the reaction yields the product of the benzofuran opening where both *in situ* generated phenolic groups are alkylated (**Scheme 18**). Using such a protocol, three different products, all of which vary in the alkylating agent used, were prepared in good to very good yields.



Scheme 18: Ring opening under basic alkylating conditions.

Alkylated phenol. Interestingly, when the same reaction conditions were applied to the reduced and acylated form of the same starting material, no product of the benzofurane skeleton was observed (**Scheme 19**).



Scheme 19: Alkylation of **1-124** with various alkylating agents.

1.4.12. Toward quiquesetinerviusin A[†]

Quiquesetinerviusin A **1-134** is a natural product with a scaffold similar to **DCG-A (1-108)** (**Figure 23**). It was isolated from the *Calamus quiquesetinervius* stem in 2010 and its antioxidant activity was determined to be $\text{IC}_{50} = 23.4 \pm 3.7 \mu\text{M}$.⁷² Quiquesetinerviusin A (**1-134**) was first isolated from a terrestrial plant, however, later it was discovered that the **1-134** type compound can be found more commonly in marine plants, more specifically in the *Posidonia oceanica* family (first identification in 2012).⁷³

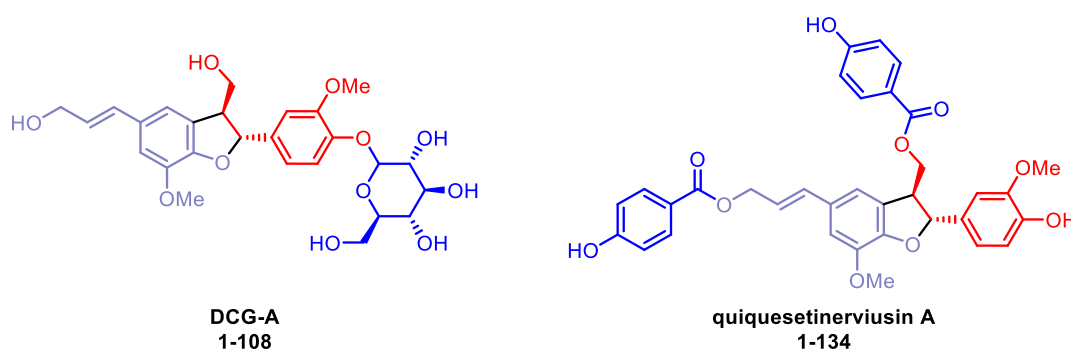


Figure 23: Structure of DCG-A (**1-108**) and quiquesetinerviusin A (**1-134**).

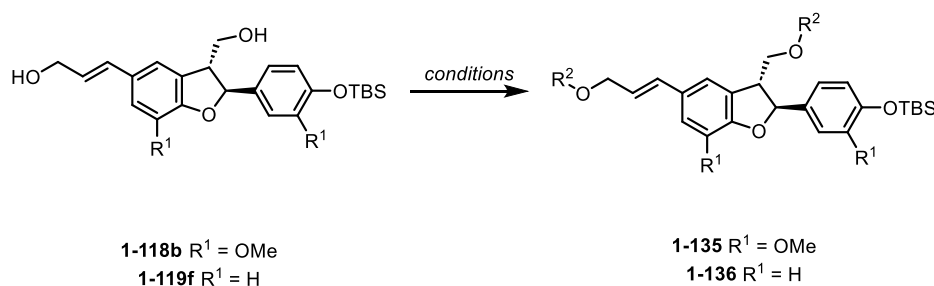
Although the first total synthesis of **quiquesetinerviusin A** was achieved already in 2017⁷⁴, no extensive biological evaluation of the targeted compounds was yet performed. To shed more light on the biological activity of the compound and with another objective that placed this compound as a possible 'marker' allowing the determination of the age of the marine

[†] Work in this subchapter was done in collaboration with Sylvie Lévayová, whom I co-supervised during her bachelor Thesis project. As a consequence, some results are based on the previous work of Sylvie Lévayová and were published in her Bachelor Thesis. After her Thesis was defended, the synthetic route was reconsidered, and several steps were re-optimized, changed or resynthesized.

grass layers in sediments, our intermediates previously prepared and used for the DCG-A (**1-108**) synthesis were reused in the quiquesetinerviusin A (**1-134**) synthesis.

The synthesis began from the previously prepared diols **1-118b** and **1-119f**, which were acetylated with the corresponding benzoyl chlorides (**Table 9**). Using standard reaction conditions, the benzoyl derivative **1-135a** (42%), the 4-methoxybenzoyl derivatives **1-135b** (62%) and **1-135c** (61 %) were prepared along with their *des*-Methoxy analogues **1-136a** (54 %) and **1-136b** (62 %) in good to very good yields.

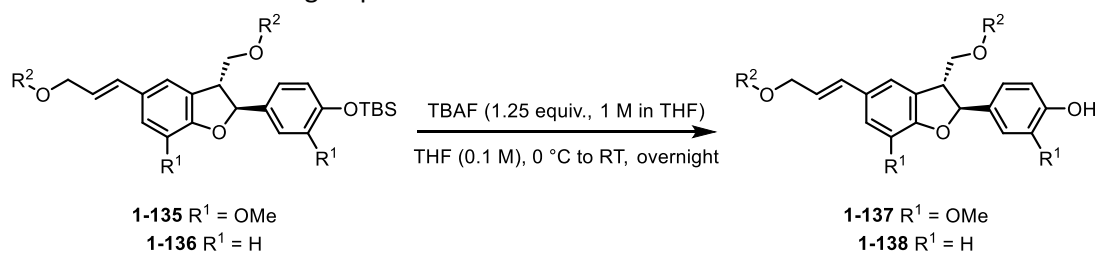
Table 9: Benzoylation of the free hydroxy groups. R² group introduction.



Entry	Conditions	R ¹	R ²	Product	Yields [%] ^a
1	BzCl (4.2 equiv.), TEA (6.0 equiv.) DCM (0.2 M), RT, 18 h	CH ₃		1-135a	42
2	4-methoxy BzCl (4.2 equiv.), TEA (6.0 equiv.) DCM (0.2 M), RT, 18 h	CH ₃		1-135b	62
3	4-(benzyloxy)benzoyl chloride (4.2 equiv.) TEA (6.0 equiv.), DCM (0.2 M), RT, 18 h	CH ₃		1-135c	61
4	BzCl (4.4 equiv.), TEA (6.0 equiv.) DCM (0.2 M), RT, 18 h	H		1-136a	54
5	4-methoxy BzCl (4.2 equiv.), TEA (6.0 equiv.) DCM (0.2 M), RT, 18 h	H		1-136b	62

a) Isolated yield after column chromatography on silica gel.

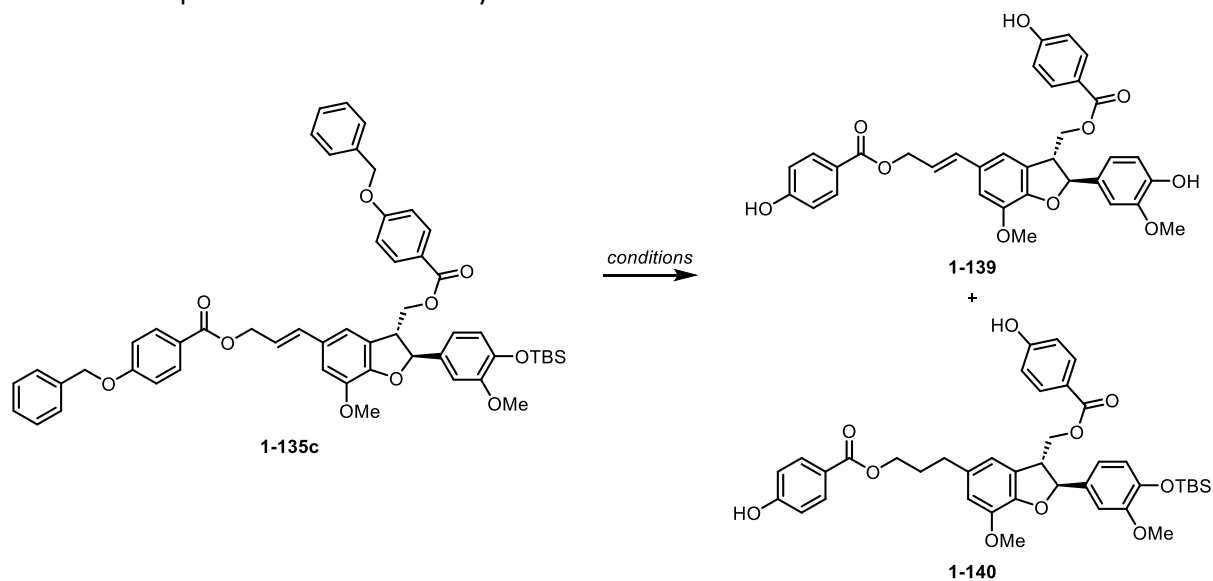
Similarly, the TBS group could be removed using TBAF in THF and the desired products **1-137a** (59 %), **1-137b** (61 %) and its *des*-Methoxy analogues **1-138a** (88%) and **1-138b** (71 %) were prepared in good yields. (**Table 10**).

Table 10: Removal of the TBS group in **1-135** and **1-136**.

Entry	R ¹	R ²	Product	Yields [%] ^a
1	CH ₃		1-137a	59
2	CH ₃		1-137b	61
3	H		1-138a	54
4	H		1-138b	62

a) Isolated yield after column chromatography on silica gel.

Ultimately, our goal was to prepare quiquesetinerviusin A **1-134**. Various Lewis acids were used to selectively remove the benzyl protecting group from **1-137**, but none of the attempted conditions resulted in the formation of the desired product (**entry 1 to 3**). Disappointed with the result, the Pd/C promoted hydrogenation was used (**entry 4**). As expected, the benzyl group was removed; however, the olefinic bond was reduced at the same time. The product of deprotection/reduction, compound **1-140**, a TBS protected dihydroquiquesetinerviusin A was isolated in a yield of 67% (**Table 11**).

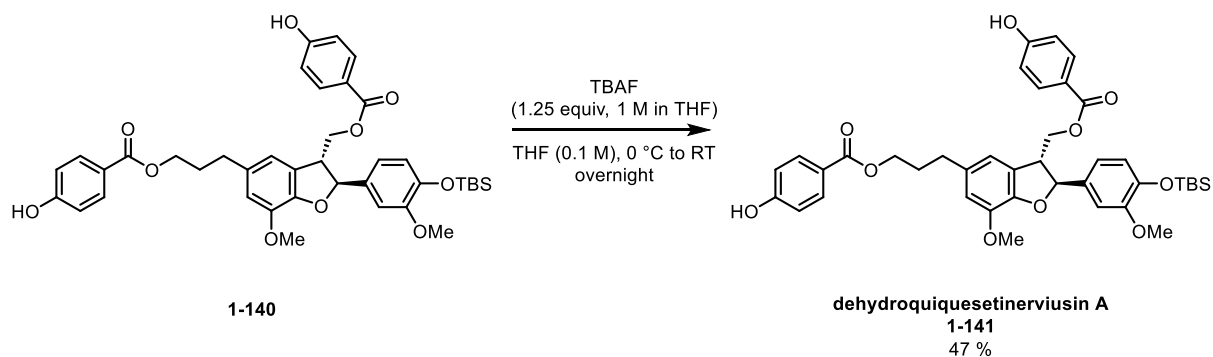
Table 11: Compound **1-139** and **1-140** synthesis.

Entry	Conditions	Product 1-139	Product 1-140	Comments
		[%] ^a	[%] ^a	
1	BCl ₃ (3.5 equiv.), DCM (0.2 M) -78 °C to RT, 2 h	-	-	decomposition ^b
2	BCl ₃ (3.5 equiv.), DCM (0.2 M) -78 °C to RT, 30 min	-	-	decomposition ^b
3	BBr ₃ (2.5 equiv.), DCM (0.2 M) -78 °C to RT, 1 h	-	-	decomposition ^b
4	Pd/C (20 mol%), H ₂ , MeOH (0.05 M), RT, 2h	-	67	

a) Isolated yield after column chromatography on silica gel.

b) Based on the ¹H NMR spectra of the crude reaction mixture analysis.

The last step of the synthesis, protection of the TBS group, resulted in the formation of a dehydroquiquetesinerviusin A-**1-141** with a yield of 47 %.

**Scheme 20:** TBS group removal that yielded compound **1-141**.

1.5. Biological activity evaluation results

1.5.1. Anthelmintic activity

C. elegans is a free-living soil nematode commonly used as a model to study various aspects of human diseases⁷⁵, thus it is routinely used in drug screenings.⁷⁶ The toxicity of our compounds was evaluated by the chitinase assay followed by microscopic evaluation. The constituted library of compounds containing compounds that were prepared during my theses was tested for anthelmintic activity at concentrations of 50 and 5 μ M concentrations. The standard anthelmintic drug ivermectin was used as a positive control in the experiment and DMSO was used as a negative control (**Figure 24**).



Figure 24: Typical microscope images obtained that are used to evaluate anthelmintic activity. A negative control (DMSO, left) and a positive control (ivermectin, right).

Based on the library evaluation, a compound **1-117c** was identified as a promising **HIT** compound, since it reduced the signal in the chitinase assay (quantifying egg hatching) at a concentration of 50 μ M and 5 μ M concentration. Activity values for representative examples of compounds from the evaluated chemical library are shown in **Figure 25**. All other compounds show none or insignificant activity in the test.

The hit compound **1-117c** was further evaluated for its **structure-activity relationship** (SAR, **Figure 26**). Our study proved that part A of **1-117c** is essential to maintain the activity of the molecule. Based on the results obtained, we hypothesized that the Michael acceptor generated *in situ* in **1-117c** could be responsible for the observed biological activity (**Figure 27**). However, none of the prepared compounds that would possess such a structural motive (including the open form of neolignan) showed similar biological activity as compound **1-117c**, suggesting that our hypothesis is wrong.

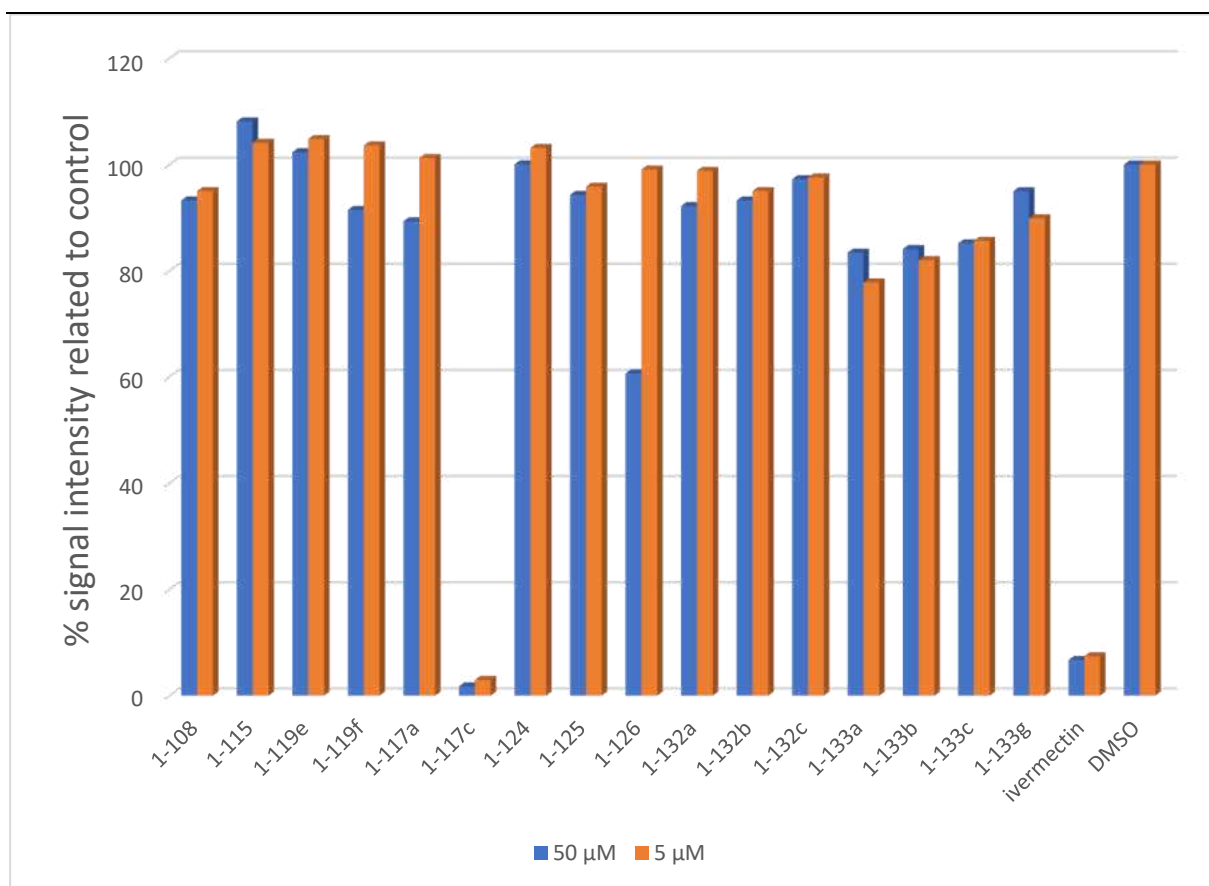


Figure 25: Anelmintic activity of the evaluated chemical library (selected examples). Compounds were evaluated for their activity against the *Caenorhabditis elegans* model nematode by means of a chitinase assay. The depicted values are the average values from 3 independent experiments \pm S.E.M. DMSO was used as negative control and ivermectine as positive control.

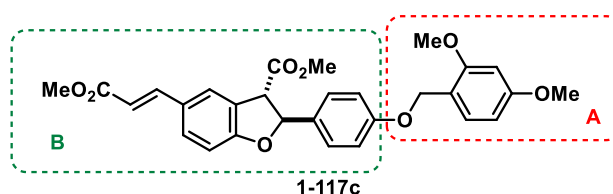


Figure 26: HIT compound **1-117c** and its evaluation within the SAR study (structural modifications). In turn, fragments A or B were modified.

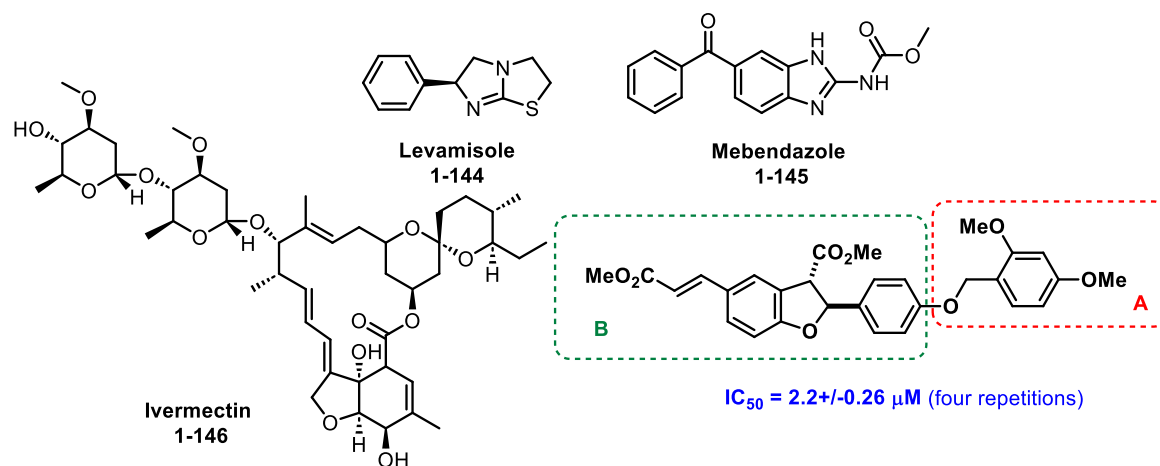


Figure 27: The action of **1-117c** against *C. elegans* proceeds via an unknown mode of action that is currently under investigation.

Meanwhile, and to check if we should further develop our HIT compound, we have decided to evaluate compound **1-117c** against Ivermectin, levamisol, and mebendazole (most commonly used drugs) resistant strains of *C. elegans* (Table 12). The compound **1-117c** has

been shown **to be highly active** against such strains, and therefore we are continuing in its development since (a) the mode of action of **1-117c** differs and (b) the mode of action is currently unknown.

Table 12: Commonly used antihelmintic drugs and IC_{50} values determined for **1-117c** in WT and *C. elegans* resistant lines.



strains of <i>C. elegans</i>	IC_{50}	SD	S.E.M.
N2 (WT)	2,20	0,52	0,26
CB221 (resistant to levomine)	1,85	0,17	0,10
ZZ15 (levamisole resistant)	3,09	1,75	1,01
CB3474 (metadazole resistant)	3,00	0,53	0,27
DA1316 (resistant to ivermectin)	2,96	0,23	0,13

1.5.2. Cytokinin activity

The second type of biological activity that we have evaluated during my thesis was the cytokinin activity. Cytokinins represent an important group of plant hormones that regulate plant growth and development. Naturally occurring cytokinins are adenine derivatives, such as *trans*-zeatine (**1-147**) or phenylurea derivatives, such as thidiazuron (**1-148**) (**Figure 28**).⁷⁷ These compounds are plant hormones, which promote cell division or cytokinesis in plant shoots and roots. Interestingly, more than three decades ago, **DCG-A**, a phenylpropanoid-derived plant metabolite, was identified as a compound with cytokinin-substituting and cell division-promoting activity.⁷⁸ Despite the data published in 1991, there were no follow-up studies of **DCG-A** mode of action, and its original activity has never been explored to the best of our knowledge by other researchers. At the same time as us, in 2023, Witvriuw et al. prepared **DCG-A** using its original synthetic protocol and carried

out various experiments and assays with the aim of proving the published activities. Unfortunately, no activity was observed. Based on those results, the group concluded that the original publication was wrong, and that **DCG-A** has no cytokinin-substituting activity.⁷⁹

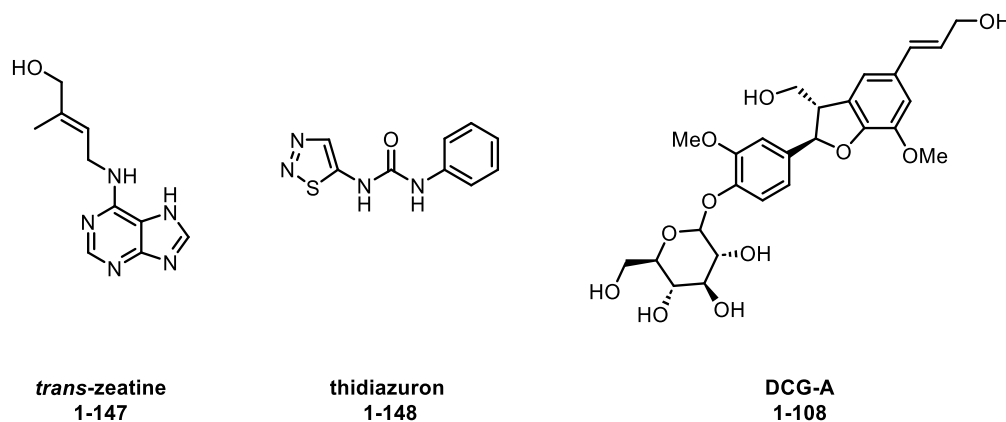


Figure 28: Structure of *trans*-zeatine 1-147, thidiazuron 1-148, and DCG-A.

This observation and conclusions were independently confirmed by our own research group by using different cytokinin bioassays approximately at the same time (*Amaranthus*, *tobacco callus*, wheat leaf senescence, and root elongation inhibition assay). In all these tests, **DCG-A** cytokinin activity was not observed (*trans*-zeatine was used as a positive standard) (**Figure 29** and **Figure 30**).

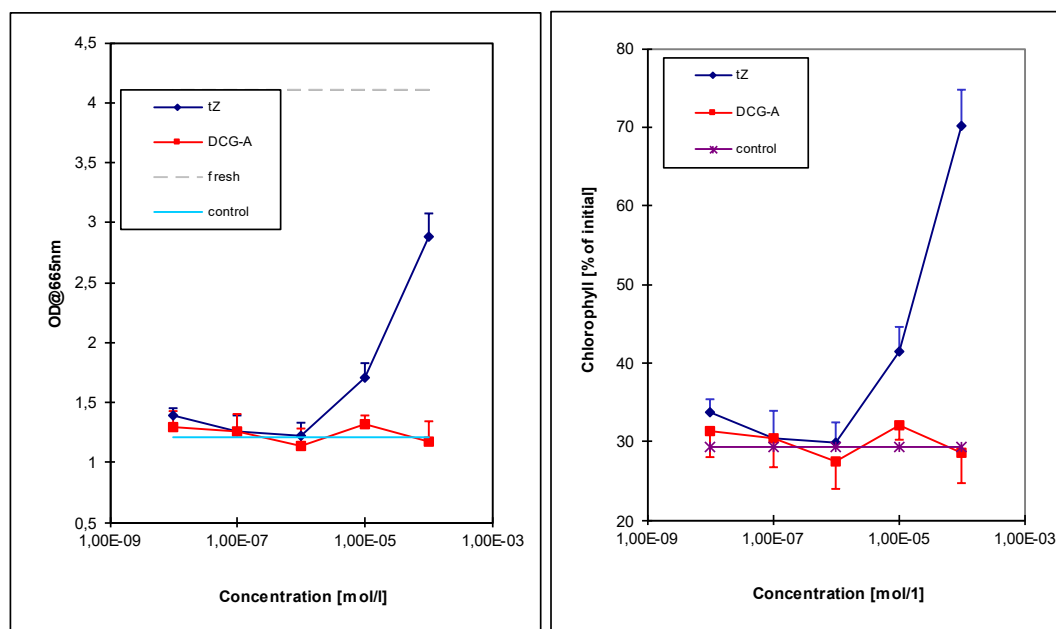


Figure 29: Dose response curves in *Amaranthus caudatus* var. *Artropurpurea* cotyledons treated with DCG-A and *trans*-zeatine. The dashed lines indicate values for the control treatment without any cytokinin. The error bars represent the standard deviation ($n = 5$).

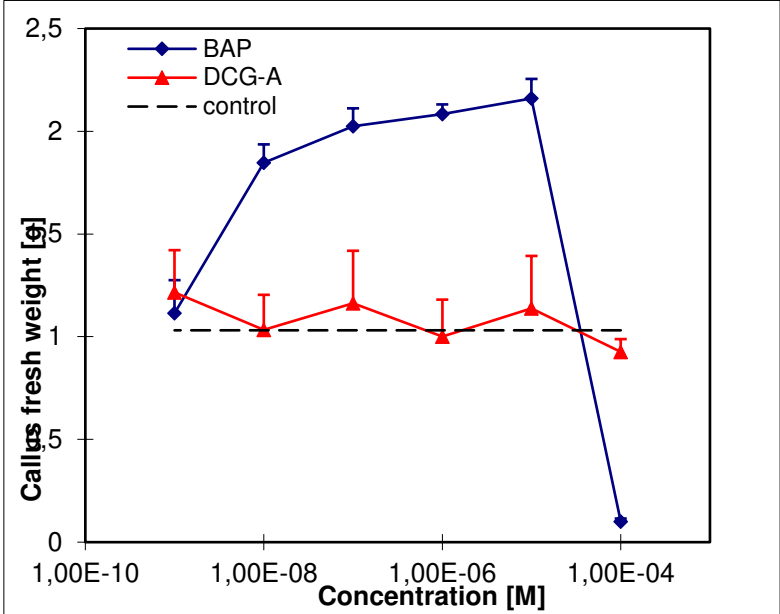


Figure 30: Tobacco callus bioassay, dose-response curves for cytokinin-dependent tobacco callus growth treated with a DCG-A and *trans*-zeatine. The dashed lines indicate values for the control treatment without any cytokinin. The error bars represent the standard deviation (n = 6).

1.6. Conclusions

We have successfully developed and optimized a reaction pathway for the synthesis of **DCG-A (1-108)** and its analogues in moderate to good overall yields. Additionally, we have explored the reactivity of 8,5' dimers and constituted a chemical library of 50 compounds of such a structural motive. Furthermore, with a bachelor student Silvie Levayová we have described a pathway towards **dehydroquiquesetinerviusin A (1-141)** and its analogues.

Our prepared compounds were tested for their anthelmintic activity (evaluated by Dr. A. Kadlecová) and cytokinin activity (evaluated by Dr. H. Vylíčilová).

In particular, compound **1-117c** was identified to be highly active in a chitinase assay (quantifying egg hatching) at a concentration of 50 μM and at a concentration of 5 μM . The IC_{50} values for this compound were stated to be $2.20 \mu\text{M} \pm 0.26$. In addition, this compound showed activity against *C. elegans* strains resistant to ivermectin, levamisole, and mebendazole (commonly used anthelmintic drugs), indicating a different mechanism of action, which is currently under investigation.

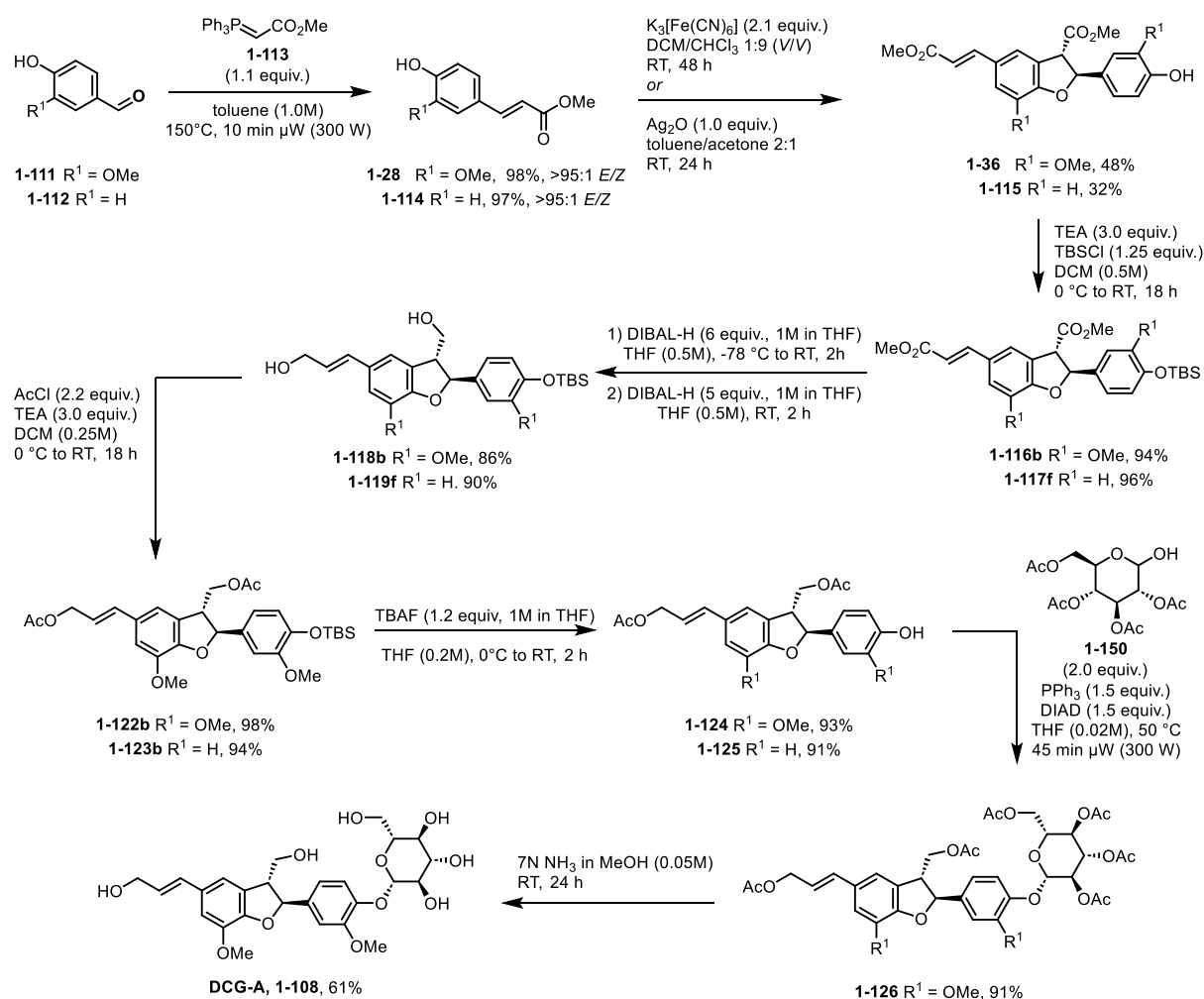
Next, cytokinin assays demonstrated that the **DCG-A** compound does not possess cytokinin activity, as it did not show significant cell division-promoting effects in standard callus and senescence assays.

In summary, our study not only established a robust synthetic pathway to **DCG-A** and its analogues but also provided valuable insights into their biological activities, highlighting the potential of these compounds in various biomedical applications. Future work will focus on further elucidating the mechanisms of action and expanding the biological evaluation of these compounds.

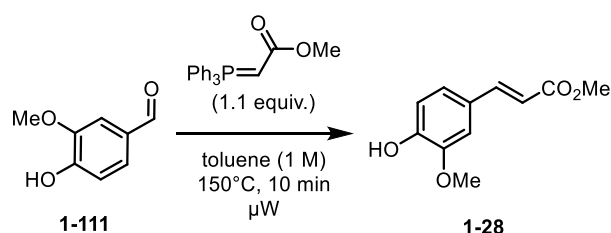
1.7. Experimental section

All starting materials were purchased from commercial suppliers and used without further purification, unless otherwise stated. All reactions were performed in round-bottom flasks fitted with rubber septa using standard laboratory techniques under positive pressure of argon (Air Liquide, >99.5% purity). In all reactions, unless stated otherwise, anhydrous solvents furnished by the Merck (Sigma-Aldrich) Company were used. The purification of reaction products was carried out by column chromatography using standard grade silica gel (60 Å, 230–400 mesh), or by preparative thin layer chromatography glass plates precoated with silica gel (silica gel G-200 F 254, particle size 0.040–0.063 mm). Analytical thin-layer chromatography was performed on a thin-layer chromatography (TLC) aluminum plates pre-coated with silica gel (silica gel 60 F 254). Visualization was accomplished with UV light, phosphomolybdic acid and potassium permanganate stains, followed by heating. The ^1H NMR and $^{13}\text{C}\{^1\text{H}\}$ NMR spectra were measured on JEOL ECA400II (400 and 101 MHz) or JEOL 500 ECA (500 and 126 MHz) in chloroform-*d*, acetone-*d*₆, DMSO-*d*₆ or methanol-*d*₄. Chemical shifts are reported in ppm, and their calibration was carried out (a) in the case of ^1H NMR experiments on the residual peak of non-deuterated solvent δ (CDCl_3) = 7.26 ppm or δ (CD_3OD) = 3.31 ppm, δ (DMSO-*d*₆) = 2.50 ppm, δ (acetone-*d*₆) = 2.05 ppm and in the case of ^{13}C NMR experiments on the middle peak of the ^{13}C signal in deuterated solvent δ (CDCl_3) = 77.16 ppm, δ (CD_3OD) = 49.00 ppm, (DMSO-*d*₆) = 39.52 ppm, (acetone-*d*₆) = 29.84 ppm. The proton coupling patterns are represented as a singlet (s), a doublet (d), a doublet of a doublet (dd), a triplet (t), a triplet of a triplet (tt), and a multiplet (m). High-resolution mass spectrometry (HRMS) was performed on LC chromatograph (Dionex UltiMate 3000, Thermo Fischer Scientific, MA, USA) and mass spectrometer Exactive Plus Orbitrap high-resolution (Thermo Fischer Scientific, MA, USA) with electrospray ionization (ESI) and a time-of-flight analyzer operating in a positive or negative full scan mode in the range of 100 – 1700 m/z. High-performance liquid chromatography (HPLC) was performed using an Agilent 1290 Infinity II system with UV-VIS detector and an Agilent InfinityLab LC/MSD mass detector. Purification using semiprep HPLC was carried out on Agilent 1290 Infinity II with UV-VIS and mass detector Agilent InfinityLab LC/MSD using the C18 reverse-phase column (Agilent 5Prep-C18 10x21.2 mm). The gradient was formed from water and methanol with a flow rate of 20 mL/min.

1.7.1. Synthesis of DCG-A and related compounds



Scheme 21: Synthesis of DCG-A and related compounds.

Methyl ferulate (**1-28**)

Was prepared according to⁵¹

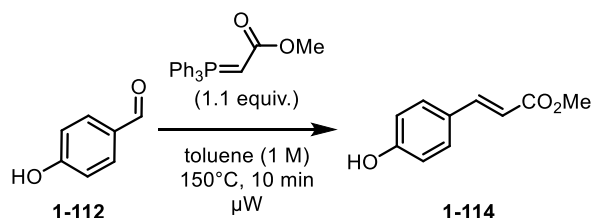
Vanillin **1-111** (6 g, 39.4 mmol, 1.0 equiv.) was dissolved in toluene (1 M, 39.4 mL), and phosphonium ylide (14.7 g, 43.4 mmol, 1.1 equiv.) was added. Mixture was placed to μW vial at RT. The vial was closed with Teflon tap and the whole mixture was heated to 150 °C for 10 min in the microwave reactor (300 W). After cooling to RT, organic solvents were removed under reduced pressure and the conversion of the ester was analyzed with help of the TLC. In case of incomplete conversion, the reaction was repeated. When the starting Vanillin was consumed, the crude product was purified by flash column chromatography (SiO_2 ; petroleum ether/EtOAc = 4:1 – 1:1) to afford **1-28** (8.1 g, 98 %).

^1H NMR (500 MHz, Chloroform-*d*) δ (ppm): δ 7.35 (dd, $J = 7.6, 1.5$ Hz, 1H), 7.21 (td, $J = 7.8, 1.7$ Hz, 1H), 6.96 (td, $J = 7.6, 1.2$ Hz, 1H), 6.79 (dd, $J = 7.9, 1.1$ Hz, 1H), 5.18 (s, 1H), 3.73 (s, 2H).

$^{13}\text{C}\{^1\text{H}\}$ NMR (126 MHz, Chloroform-*d*) δ (ppm): 152.8, 129.5, 129.3, 121.2, 117.7, 116.8, 115.1, 18.3.

MS (ESI) m/z (%): 209 $[\text{M}+\text{H}]^+$ (100).

HRMS (ESI) m/z : $[\text{M}+\text{H}]^+$ calculated for $\text{C}_{11}\text{H}_{13}\text{O}_4$: 209.0808; found: 209.0815.

Methyl *p*-coumarate (**1-114**)

Was prepared according to⁵¹

4-hydroxybenzaldehyde **1-112** (6 g, 39.4 mmol, 1.0 equiv.) was dissolved in toluene (1 M, 39.4 mL), and phosphonium ylide (14.7 g, 43.4 mmol, 1.1 equiv.) was added. Mixture was placed to μW vial at RT. The vial was closed with Teflon tap and the whole mixture was heated to

150 °C for 10 min in the microwave reactor (300 W). After cooling to RT, organic solvents were removed under reduced pressure and the conversion of the ester was analyzed with help of the TLC. In case of incomplete conversion, the reaction was repeated. When the starting Vanillin was consumed, the crude product was purified by flash column chromatography (SiO₂; petroleum ether/EtOAc = 4:1 – 1:1) to afford **1-114** (8 g, 97 %).

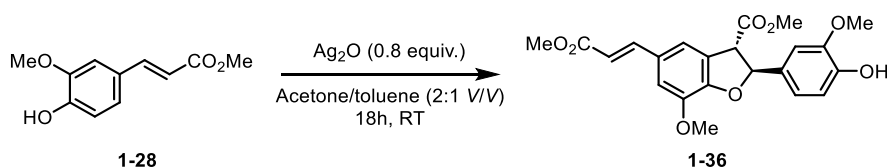
¹H NMR (500 MHz, Chloroform-d) δ (ppm): δ 7.64 (d, *J* = 15.9 Hz, 1H), 7.49 – 7.39 (m, 2H), 6.88 – 6.82 (m, 2H), 6.31 (d, *J* = 16.0 Hz, 1H), 5.18 (s, 1H), 3.80 (s, 3H).

¹³C {¹H} NMR (126 MHz, CDCl₃): 168.0, 157.6, 144.6, 130.1, 127.4, 115.9, 115.4, 51.8.

MS (ESI) *m/z* (%): 178 [M+H]⁺ (100).

HRMS (ESI) *m/z*: [M+H]⁺ calculated for C₁₀H₁₁O₃: 179.0703; found: 179.0702.

(±)-dehydrodiferrulate dimethyl ester (**1-36**)



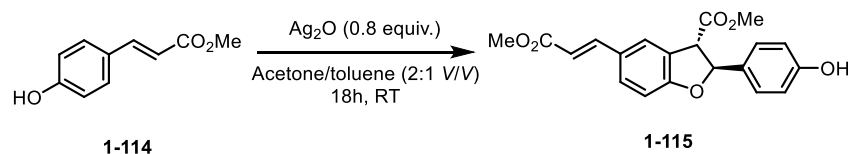
1-28 (16.4 g, 78.8 mmol, 1.0 equiv.) was dissolved in dry toluene/acetone (2:1 V/V, 600 mL), and flask was covered with aluminum foil. Next Ag₂O (14.6 g, 63 mmol, 0.8 equiv.) was added. After stirring for 18 h under aluminum foil, the mixture was filtered through a silica pad and evaporated under reduced pressure. The crude product was purified by gradient column chromatography (SiO₂; petroleum ether/EtOAc = 6:1 → 2:1) to afford **1-36** as a white solid (7.6 g, 48 %).

¹H NMR (500 MHz, Chloroform-d) δ (ppm): δ 7.65 (d, *J* = 15.9 Hz, 1H), 7.19 (t, *J* = 1.4 Hz, 1H), 7.02 (d, *J* = 2.0 Hz, 1H), 6.91 (dd, *J* = 3.6, 1.4 Hz, 3H), 6.32 (d, *J* = 15.9 Hz, 1H), 6.11 (d, *J* = 8.2 Hz, 1H), 5.64 (s, 1H), 4.35 (dt, *J* = 8.1, 0.8 Hz, 1H), 3.92 (s, 3H), 3.88 (s, 3H), 3.84 (s, 3H), 3.81 (s, 3H).

¹³C {¹H} NMR (126 MHz, Chloroform-d) δ (ppm): 170.9, 167.8, 150.1, 146.8, 146.2, 144.9, 144.9, 131.5, 128.7, 125.8, 119.6, 118.1, 115.7, 114.7, 112.2, 108.8, 87.6, 56.3, 56.2, 55.6, 53.0, 51.8.

MS (ESI) *m/z* (%): 415 [M+H]⁺ (100).

HRMS (ESI) *m/z*: [M+H]⁺ calculated for C₂₂H₂₃O₈: 415.1387 found: 415.1391.

(±) dehydrodicoumaric acid dimethyl ester (1-115)

1-114 (22 g, 123 mmol, 0.5 equiv.) was dissolved in solution of chloroform/dichloromethane (9:1 V/V, 610 mL), and the resulting mixture was stirred at RT for 5 min. Next potassium ferricyanide (97.6 g, 296 mmol, 1.2 equiv.) was dissolved in NaHCO_3 (0.45 M, 560 mL), and resulting brown solution was added dropwise into the mixture during 1h under argon atmosphere. Resulting mixture was stirred for 48 h at RT under argon atmosphere. Mixture was then evaporated and the water phase was extracted with EtOAc (4 x 400 mL), and combined organic layers were washed with brine (400 mL), dried over MgSO_4 , filtered, and the solvents were removed under reduced pressure. The crude product was purified by gradient column chromatography (SiO_2 ; petroleum ether/EtOAc = 8:1 \rightarrow 2:1) to afford **1-115** as a white solid (7 g, 32 %).

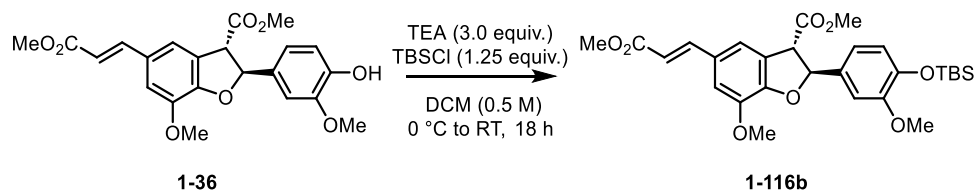
^1H NMR (500 MHz, Chloroform-d) δ (ppm): δ 7.66 (d, J = 15.9 Hz, 1H), 7.55 (t, J = 1.5 Hz, 1H), 7.42 (dd, J = 8.4, 1.9 Hz, 1H), 7.27 (d, J = 2.1 Hz, 1H), 7.26 (d, J = 2.2 Hz, 1H), 6.89 (d, J = 8.4 Hz, 1H), 6.85 – 6.82 (m, 2H), 6.32 (d, J = 16.0 Hz, 1H), 6.09 (d, J = 7.5 Hz, 1H), 5.59 – 5.16 (m, 1H), 4.27 (d, J = 7.5 Hz, 1H), 3.84 (s, 3H), 3.80 (s, 4H).

$^{13}\text{C}\{^1\text{H}\}$ NMR (126 MHz, Chloroform-d) δ (ppm): δ 171.0, 168.1, 161.3, 156.2, 144.8, 132.2, 131.0, 127.9, 127.7, 125.2, 125.1, 115.8, 115.3, 110.5, 86.5, 55.2, 53.1, 51.9.

MS (ESI) m/z (%): 355 $[\text{M}+\text{H}]^+$ (100).

HRMS (ESI) m/z : $[\text{M}+\text{H}]^+$ calculated for $\text{C}_{20}\text{H}_{19}\text{O}_6$: 355.1176; found: 355.1180.

Methyl 2-(4-((*tert*-butyldimethylsilyl)oxy)-3-methoxyphenyl)-7-methoxy-5-((*E*)-3-methoxy-3-oxoprop-1-en-1-yl)-2,3-dihydrobenzofuran-3-carboxylate (**1-116b**)



1-36 (1.1 g, 2.65 mmol, 1.0 equiv.) was dissolved in dry DCM (0.5 M, 6.21 mL), and the mixture was cooled to 0 °C. After 5 minutes at 0 °C TBSCl (0.5 g, 3.32 mmol, 1.25 equiv.) was added following addition of TEA (1.11 mL, 7.96 mmol, 3 equiv.). The resulting mixture was stirred at RT overnight. Next day 50 mL of NH₄Cl was added and the water phase was water phase was extracted with DCM (3 x 40 mL). Combined organic layers were washed with brine (40 mL), dried over MgSO₄, filtered, and the solvents were removed under reduced pressure. The crude product was purified by column chromatography (SiO₂; petroleum ether/EtOAc = 2:1) to afford **1-116b** as a white solid (1.33 g, 94 %).

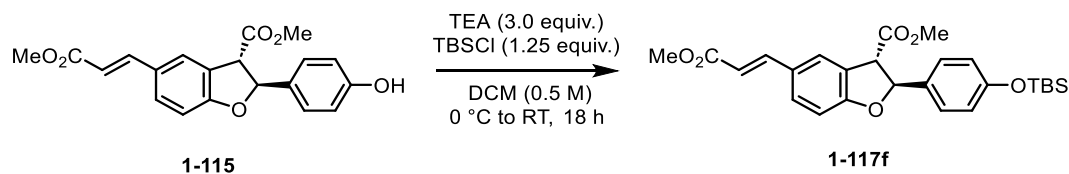
¹H NMR (500 MHz, Chloroform-d) δ (ppm): 7.65 (d, *J* = 15.9 Hz, 1H), 7.22 – 7.17 (m, 1H), 7.03 – 7.00 (m, 1H), 6.88 – 6.79 (m, 3H), 6.32 (dd, *J* = 15.9, 0.7 Hz, 1H), 6.12 (d, *J* = 8.0 Hz, 1H), 4.36 (dd, *J* = 8.1, 1.0 Hz, 1H), 3.92 (s, 3H), 3.83 (s, 3H), 3.80 (s, 3H), 3.78 (s, 3H), 0.98 (s, 10H), 0.13 (s, 6H).

¹³C{¹H} NMR (126 MHz, Chloroform-d) δ (ppm): 170.9, 167.8, 151.3, 150.1, 145.7, 144.9, 144.9, 133.0, 128.7, 125.9, 121.2, 118.9, 118.1, 115.7, 112.1, 110.3, 87.6, 56.3, 55.7, 55.6, 53.1, 51.8, 25.8, 18.6, -4.5.

MS (ESI) *m/z* (%): 529 [M+H]⁺ (100).

HRMS (ESI) *m/z*: [M+H]⁺ calculated for C₂₈H₃₇O₈Si: 529.2252; found:529.2253.

Methyl 2-(4-((*tert*-butyldimethylsilyl)oxy)phenyl)-5-((*E*)-3-methoxy-3-oxoprop-1-en-1-yl)-2,3-dihydrobenzofuran-3-carboxylate (**1-117f**)



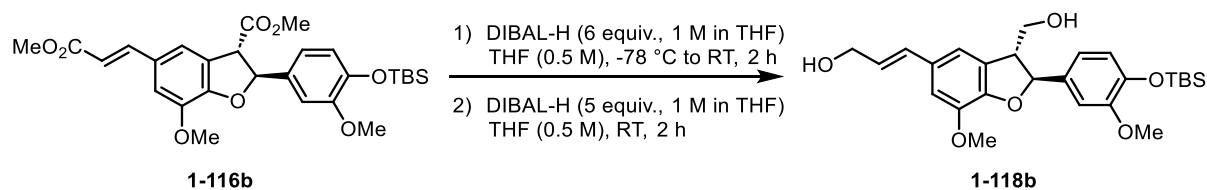
1-115 (1.1 g, 3.1 mmol, 1.0 equiv.) was dissolved in dry DCM (0.5 M, 6.21 mL), and the mixture was cooled to 0 °C. After 5 minutes at 0 °C TBSCl (0.59 g, 3.88 mmol, 1.25 equiv.) was added following addition of TEA (1.29 ml, 9.31 mmol, 3 equiv.). The resulting mixture was stirred at RT overnight. Next day 50 ml of NH₄Cl was added and the water phase was water phase was extracted with DCM (3 x 40 mL). Combined organic layers were washed with brine (40 mL), dried over MgSO₄, filtered, and the solvents were removed under reduced pressure. The crude product was purified by column chromatography (SiO₂; petroleum ether/EtOAc = 2:1) to afford **1-117f** as a white solid (1.42 g, 96 %).

¹H NMR (500 MHz, Chloroform-d) δ (ppm): 7.66 (d, *J* = 16.0 Hz, 1H), 7.57 – 7.55 (m, 1H), 7.43 (dd, *J* = 8.4, 1.9 Hz, 1H), 7.26 – 7.22 (m, 2H), 6.89 (d, *J* = 8.4 Hz, 1H), 6.87 – 6.78 (m, 2H), 6.32 (d, *J* = 16.0 Hz, 1H), 6.10 (d, *J* = 7.5 Hz, 1H), 4.28 (d, *J* = 7.5 Hz, 1H), 3.84 (s, 3H), 3.80 (s, 3H), 0.97 (s, 9H), 0.21 – 0.15 (m, 6H).

¹³C{¹H} NMR (126 MHz, Chloroform-d) δ (ppm): 171.0, 167.9, 161.3, 156.2, 144.7, 132.7, 130.9, 127.9, 127.3, 125.2, 125.1, 120.5, 115.4, 110.4, 86.6, 55.2, 53.0, 51.8, 29.8, 25.8, 18.3, -4.3.

MS (ESI) *m/z* (%): 469 [M+H]⁺ (100).

HRMS (ESI) *m/z*: [M+H]⁺ calculated for C₂₆H₃₃O₆Si: 469.2041; found: 469.2044.

(E)-3-(2-(4-((*tert*-butyldimethylsilyl)oxy)-3-methoxyphenyl)-3-(hydroxymethyl)-7-methoxy-2,3-dihydrobenzofuran-5-yl)prop-2-en-1-ol (1-118b)

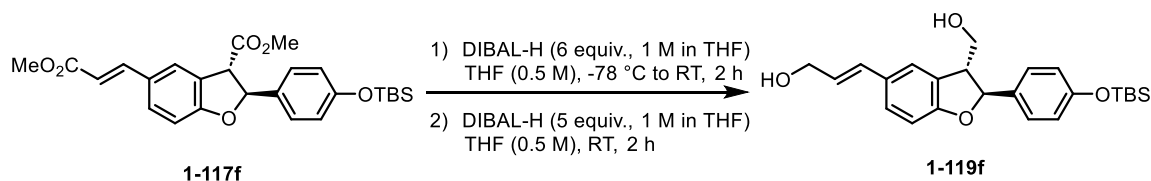
A solution of ester **1-116b** (3 g, 5.67 mmol, 1.0 equiv.) in THF (0.25 M, 22.7 mL) was cooled to -78 °C and DIBAL-H (1 M in THF, 34 mL, 34 mmol, 6 equiv.) was added dropwise over 10 minutes. The resulting mixture was stirred at -78 °C for 30 min before the cooling bath removal. To achieve full reduction, after 1h at RT, 5 more equivalents of DIBAL-H were added, and the reaction mixture was stirred for another 1 hour at RT. Then reaction was cooled to -78 °C and Aqueous saturated solution of Rochel salt (100 mL) was added carefully dropwise to quench the reaction. After addition of Rochel salt, solution was diluted with EtOAc 100 mL. The resulting mixture was stirred at RT till a milky suspension turned into the clear biphasic solution (usually takes around 16 h). Resulting phases were separated and the aqueous layer was extracted with DCM (3x 75mL). Combined organic layers were washed with brine (50 mL), dried over Na₂SO₄, filtered, and evaporated under reduced pressure. The crude product was purified by column chromatography (SiO₂; DCM/MeOH = 95:5) to afford **1-118b** as a colorless oil (2.3 g, 86 %).

¹H NMR (500 MHz, Chloroform-d) δ (ppm): 6.92 – 6.87 (m, 3H), 6.84 (dd, J = 8.1, 2.1 Hz, 1H), 6.80 (d, J = 8.1 Hz, 1H), 6.57 (dt, J = 15.8, 1.6 Hz, 1H), 6.25 (dt, J = 15.8, 5.9 Hz, 1H), 5.57 (d, J = 7.2 Hz, 1H), 4.31 (dd, J = 6.0, 1.5 Hz, 2H), 3.99 (dd, J = 11.0, 5.9 Hz, 1H), 3.93 – 3.91 (m, 1H), 3.91 (s, 3H), 3.77 (s, 3H), 3.64 (q, J = 5.8 Hz, 1H), 0.98 (s, 10H), 0.13 (s, 6H).

¹³C{¹H} NMR (126 MHz, Chloroform-d) δ (ppm): 151.2, 148.6, 145.3, 144.6, 134.4, 131.5, 130.9, 128.3, 126.5, 121.0, 118.9, 114.9, 110.5, 110.3, 88.4, 64.1, 64.0, 56.1, 55.7, 53.6, 25.8, 18.6, -4.5.

MS (ESI) *m/z* (%): 473 [M+H]⁺ (100).

HRMS (ESI) *m/z*: [M+H]⁺ calculated for C₂₆H₃₇O₆Si: 473.2354; found: 473.2355.

(E)-3-(2-(4-((*tert*-butyldimethylsilyl)oxy)phenyl)-3-(hydroxymethyl)-2,3-dihydrobenzofuran-5-yl)prop-2-en-1-ol (**1-119f**)

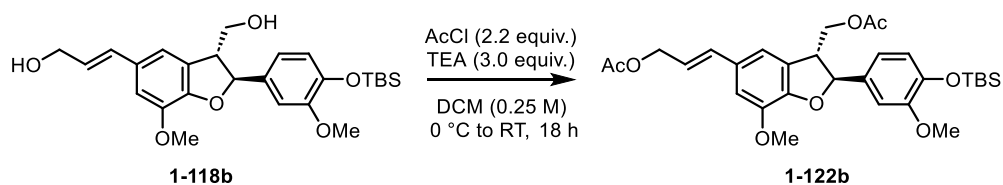
A solution of ester **1-117f** (1.4 g, 2.99 mmol, 1.0 equiv.) in THF (0.25 M, 5.97 mL) was cooled to -78 °C and DIBAL-H (1 M in THF, 17.9 mL, 17.9 mmol, 6 equiv.) was added dropwise over 10 minutes. The resulting mixture was stirred at -78 °C for 30 min before the cooling bath removal. To achieve full reduction, after 1 h at RT, 5 more equivalents of DIBAL-H were added, and the reaction mixture was stirred for another 1 hour at RT. Then reaction was cooled to -78 °C and Aqueous saturated solution of Rochel salt (100 mL) was added carefully dropwise to quench the reaction. After addition of Rochel salt, solution was diluted with EtOAc 100 mL. The resulting mixture was stirred at RT till a milky suspension turned into the clear biphasic solution (usually takes around 16 h). Resulting phases were separated and the aqueous layer was extracted with DCM (3x 75mL). Combined organic layers were washed with brine (50 mL), dried over Na₂SO₄, filtered, and evaporated under reduced pressure. The crude product was purified by column chromatography (SiO₂; DCM/MeOH = 95:5) to afford **1-119f** as a colorless oil (1.11 g, 90 %).

¹H NMR (500 MHz, Chloroform-d) δ (ppm): 7.29 (t, *J* = 1.4 Hz, 1H), 7.25 – 7.21 (m, 3H), 6.85 – 6.79 (m, 3H), 6.57 (d, *J* = 15.9, 1.6 Hz, 1H), 6.23 (dt, *J* = 15.8, 6.0 Hz, 1H), 5.56 (d, *J* = 6.4 Hz, 1H), 4.30 (dd, *J* = 6.0, 1.5 Hz, 2H), 3.97 (dd, *J* = 10.9, 6.2 Hz, 1H), 3.92 (dd, *J* = 10.9, 5.1 Hz, 1H), 3.56 (q, *J* = 5.9 Hz, 1H), 0.97 (s, 9H), 0.18 (s, 6H).

¹³C{¹H} NMR (126 MHz, Chloroform-d) δ (ppm): 160.0, 155.8, 134.2, 131.3, 129.9, 128.1, 127.6, 127.3, 126.0, 122.5, 120.4, 109.7, 87.3, 64.4, 64.0, 53.2, 25.8, 18.3, -4.3.

MS (ESI) *m/z* (%): 301 [M+H]⁺ (100).

HRMS (ESI) *m/z*: [M+H]⁺ calculated for C₂₄H₃₃O₄Si: 413.2143; found: 413.2165.

(E)-3-(3-(acetoxymethyl)-2-(4-((*tert*-butyldimethylsilyl)oxy)-3-methoxyphenyl)-7-methoxy-2,3-dihydrobenzofuran-5-yl)allyl acetate (1-122b**)**

Diol **1-118b** (1.72 g, 3.64 mmol, 1.0 equiv.) was dissolved in DCM (0.25 M, 14.55 mL), and solution was cooled to 0 °C. Then TEA (1.51 mL, 10.9 mmol, 3 equiv.) was added following by acetyl chloride (0.57 mL, 8.01 mmol, 2.2 equiv.). The reaction mixture was stirred at room temperature overnight. Reaction was quenched by addition of water (50 mL). The aqueous layer was extracted with EtOAc (3 × 30 mL). The combined organic layers were washed with brine, dried over anhydrous Na₂SO₄, filtered, and concentrated *in vacuo*. The crude product was purified by column chromatography (SiO₂; petroleum ether/EtOAc = 4:1) to afford **1-122b** as a colorless oil (2.0 g, 98 %).

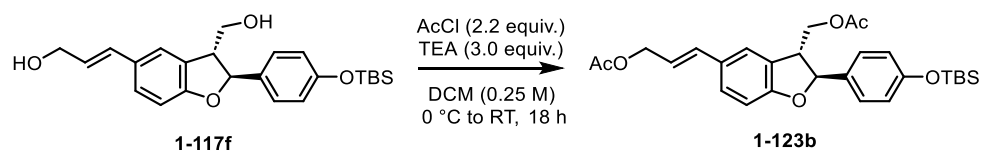
¹H NMR (500 MHz, Chloroform-d) δ (ppm): 6.89 – 6.86 (m, 3H), 6.84 – 6.79 (m, 2H), 6.60 (dd, *J* = 15.7, 1.3 Hz, 1H), 6.16 (dt, *J* = 15.8, 6.7 Hz, 1H), 5.47 (d, *J* = 7.5 Hz, 1H), 4.71 (dd, *J* = 6.7, 1.3 Hz, 2H), 4.45 (dd, *J* = 11.2, 5.4 Hz, 1H), 4.30 (dd, *J* = 11.1, 7.6 Hz, 1H), 3.91 (s, 3H), 3.82 – 3.78 (m, 1H), 3.77 (s, 3H), 2.10 (s, 3H), 2.01 (s, 3H), 0.98 (s, 9H), 0.13 (d, *J* = 0.9 Hz, 6H).

¹³C{¹H} NMR (126 MHz, Chloroform-d) δ (ppm): 171.1, 171.0, 151.3, 148.4, 145.4, 144.5, 134.6, 133.8, 130.5, 127.9, 121.2, 121.0, 119.1, 115.4, 110.5, 110.2, 89.1, 65.5, 65.4, 56.1, 55.7, 50.3, 25.8, 21.2, 21.0, 18.6, -4.5.

MS (ESI) *m/z* (%): 557 [M+H]⁺ (100).

HRMS (ESI) *m/z*: [M+H]⁺ calculated for C₃₀H₄₁O₈Si: 595.2124; found: 595.2123.

(*E*)-3-(3-(acetoxymethyl)-2-(4-((*tert*-butyldimethylsilyl)oxy)phenyl)-2,3-dihydrobenzofuran-5-yl)allyl acetate (**1-123b**)



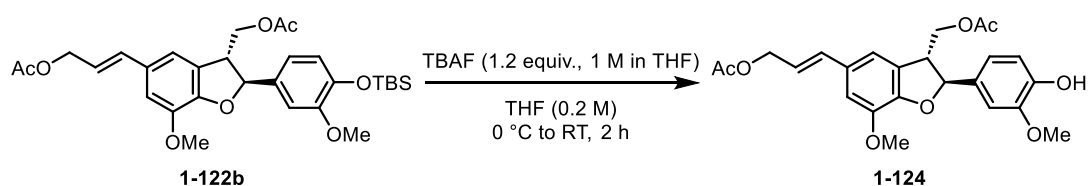
Diol **1-117f** (0.45 g, 1.09 mmol, 1.0 equiv.) was dissolved in DCM (0.25 M, 4.36 mL), and solution was cooled to 0 °C. Then TEA (0.46 mL, 3.27 mmol, 3 equiv.) was added following by acetyl chloride (0.17 mL, 2.4 mmol, 2.2 equiv.). The reaction mixture was stirred at room temperature overnight. Reaction was quenched by addition of water (30 mL). The aqueous layer was extracted with EtOAc (3 × 15 mL). The combined organic layers were washed with brine, dried over anhydrous Na₂SO₄, filtered, and concentrated *in vacuo*. The crude product was purified by column chromatography (SiO₂; petroleum ether/EtOAc = 4:1) to afford **1-123b** as a colorless oil (0.51 g, 94 %).

¹H NMR (500 MHz, Chloroform-*d*) δ (ppm): 7.28 – 7.26 (m, 1H), 7.26 – 7.20 (m, 3H), 6.84 – 6.80 (m, 3H), 6.61 (d, *J* = 15.9 Hz, 1H), 6.14 (dt, *J* = 15.7, 6.7 Hz, 1H), 5.46 (d, *J* = 6.7 Hz, 1H), 4.70 (dd, *J* = 6.6, 1.3 Hz, 2H), 4.44 (dd, *J* = 11.1, 5.5 Hz, 1H), 4.29 (dd, *J* = 11.1, 7.8 Hz, 1H), 3.74 – 3.69 (m, 1H), 2.09 (s, 3H), 2.04 (s, 3H), 0.97 (s, 9H), 0.18 (s, 6H).

¹³C{¹H} NMR (126 MHz, Chloroform-*d*) δ (ppm): 171.0, 170.9, 160.0, 155.9, 134.3, 133.5, 129.6, 128.5, 127.3, 127.0, 122.8, 120.8, 120.4, 109.8, 100.0, 88.0, 65.7, 65.4, 50.0, 25.8, 21.2, 20.9, 18.3, -4.3.

MS (ESI) *m/z* (%): 497 [M+H]⁺ (100).

HRMS (ESI) *m/z*: [M+H]⁺ calculated for C₂₈H₃₆KO₆Si: 535.1913; found: 535.1913.

(±)-dehydrodiconiferyl diacetate (1-124)

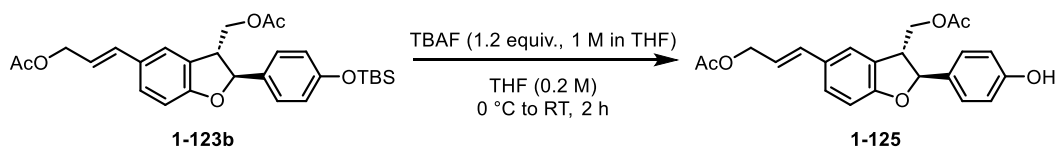
1-122b (1.9 g, 3.41 mmol, 1.0 equiv.) was dissolved in THF (0.2 M, 17.1 mL), and solution was cooled to 0 °C. After 5 minutes TBAF (4.1 mL, 1 M, 4.1 mmol, 1.2 equiv.) was added dropwise and the solution was stirred at RT for 2h. Reaction was quenched by addition of NH₄Cl (50 mL). The aqueous layer was extracted with DCM (3 × 30 mL). The combined organic layers were washed with brine, dried over anhydrous Na₂SO₄, filtered, and concentrated *in vacuo*. The crude product was purified by column chromatography (SiO₂; petroleum ether/EtOAc = 4:1) to afford **1-124** as a colorless oil (1.4 g, 93 %).

¹H NMR (500 MHz, Chloroform-d) δ (ppm): 6.91 – 6.86 (m, 5H), 6.60 (d, *J* = 15.8 Hz, 1H), 6.16 (dt, *J* = 15.8, 6.7 Hz, 1H), 5.63 (s, 1H), 5.47 (d, *J* = 7.3 Hz, 1H), 4.71 (dd, *J* = 6.6, 1.3 Hz, 2H), 4.44 (dd, *J* = 11.2, 5.4 Hz, 1H), 4.30 (dd, *J* = 11.1, 7.4 Hz, 1H), 3.91 (s, 3H), 3.87 (s, 3H), 3.80 – 3.75 (m, 1H), 2.10 (s, 3H), 2.03 (s, 3H).

¹³C{¹H} NMR (126 MHz, Chloroform-d) δ (ppm): 171.1, 171.0, 148.4, 146.8, 146.0, 144.6, 134.5, 132.4, 130.6, 127.8, 121.3, 119.7, 115.4, 114.4, 110.6, 108.7, 89.0, 65.4, 65.4, 56.1, 50.4, 21.2, 21.0.

MS (ESI) *m/z* (%): 443 [M+H]⁺ (100).

HRMS (ESI) *m/z*: [M+K]⁺ calculated for C₂₄H₂₆O₈K: 481.1259; found: 481.1262.

(±)-dehydrodi-*p*-coumaryl diacetate (1-125)

1-123b (1 g, 2.01 mmol, 1.0 equiv.) was dissolved in THF (0.2 M, 10.1 mL), and solution was cooled to 0 °C. After 5 minutes TBAF (2.42 mL, 1 M, 2.42 mmol, 1.2 equiv.) was added dropwise and the solution was stirred at RT for 2h. Reaction was quenched by addition of NH₄Cl (30 mL). The aqueous layer was extracted with DCM (3 × 20 mL). The combined organic layers were washed with brine, dried over anhydrous Na₂SO₄, filtered, and concentrated *in vacuo*. The

crude product was purified by column chromatography (SiO₂; petroleum ether/EtOAc = 4:1) to afford **1-125** as a colorless oil (0.7 g, 91 %).

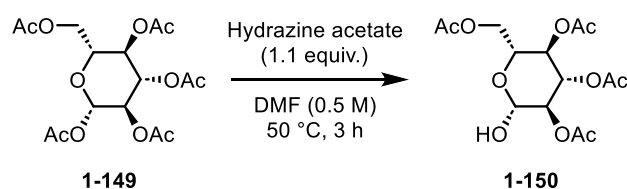
¹H NMR (500 MHz, Chloroform-d) δ (ppm): 7.25 – 7.17 (m, 3H), 6.81 (dd, *J* = 8.3, 2.9 Hz, 3H), 6.60 (d, *J* = 15.8 Hz, 1H), 6.49 (s, 1H), 6.13 (dt, *J* = 15.9, 6.6 Hz, 1H), 5.44 (d, *J* = 6.6 Hz, 1H), 4.74 – 4.68 (m, 2H), 4.43 (dd, *J* = 11.1, 5.5 Hz, 1H), 4.29 (dd, *J* = 11.1, 7.7 Hz, 1H), 3.70 (q, *J* = 6.6 Hz, 1H), 2.10 (s, 3H), 2.04 (s, 3H).

¹³C{¹H} NMR (126 MHz, Chloroform-d) δ (ppm): 171.6, 171.4, 159.8, 156.3, 134.4, 132.5, 129.6, 128.5, 127.5, 126.9, 122.8, 120.6, 115.7, 109.8, 87.8, 65.7, 65.6, 49.8, 21.2, 20.9.

MS (ESI) *m/z* (%): 383 [M+H]⁺ (100).

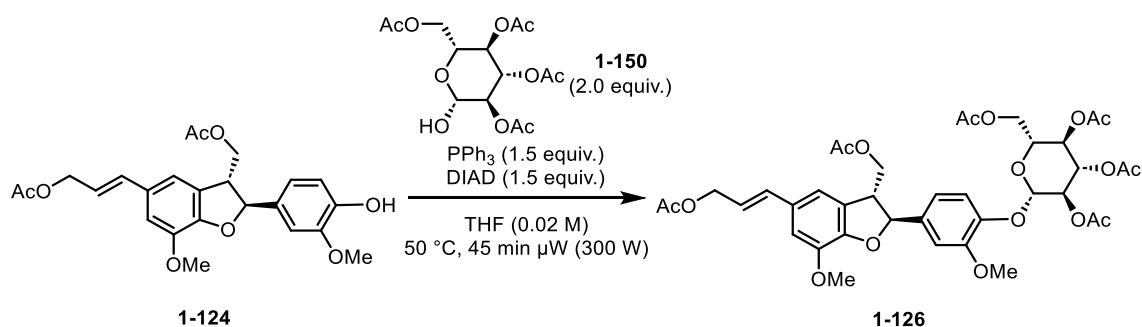
HRMS (ESI) *m/z*: [M+H]⁺ calculated for C₂₂H₂₂KO₆: 421.1048; found: 421.1048.

2,3,4,6-tetra-O-acetyl-β-D-glucopyranose (**1-150**)



Prepared according to a literature. Spectroscopic data match those in the literature.⁸⁰

Penta-O-acetyl-β-D-glucopyranose **1-149** (1 g, 2.51 mmol, 1.0 equiv.) was dissolved in DMF (0.5 M, 5.02 mL). Hydrazine acetate (0.26 g, 2.76 mmol, 1.1 equiv.) was added and the solution was warmed to 50 °C. Reaction was stirred for 3 h at 50 °C before it was cooled to RT and diluted by EtOAc (30 mL) and quenched by addition of water (30 mL). Mixture was transferred to a separatory funnel and was washed by NaCl (3x 30 mL). Organic phase was dried over anhydrous Na₂SO₄, filtered, and concentrated *in vacuo*. The crude product was purified by column chromatography (SiO₂; petroleum ether/EtOAc = 2:1) to afford **1-150** as a colorless oil (0.8 g, 91 %).

(±)-dehydrodiconiferyl alcohol-4-β-D-glucoside-hexaacetate (1-126)

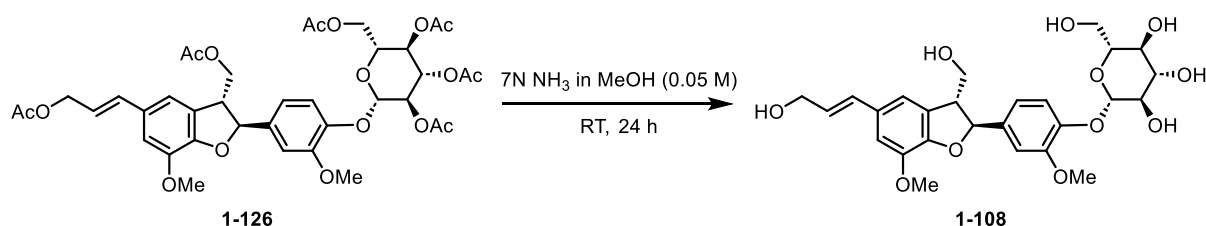
1-124 (0.1 g, 0.23 mmol, 1.0 equiv.) was dissolved in THF (0.02 M, 11.3 mL) in a microwave vial and **1-150** (0.16 g, 0.45 mmol, 2 equiv.) and PPh_3 (0.09 g, 0.34 mmol, 1.5 equiv.) was added followed by addition of DIAD (0.7 μL , 0.34 mmol, 1.5 equiv.). The vial was closed with Teflon tap and the whole mixture was heated to 50 $^\circ\text{C}$ for 45 min in the microwave reactor (100 W). After cooling to RT, organic solvents were removed under reduced pressure. The crude product was purified semipreparative chromatography using MeOH/water as an eluent to afford **1-126** as a colorless oil (0.7 g, 91 %).

$^1\text{H NMR}$ (500 MHz, Chloroform-*d*) δ (ppm): 7.08 (dt, $J = 8.3, 3.1$ Hz, 1H), 6.92 (dd, $J = 8.4, 2.1$ Hz, 1H), 6.90 – 6.85 (m, 3H), 6.60 (d, $J = 15.8$ Hz, 1H), 6.16 (dt, $J = 15.9, 6.6$ Hz, 1H), 5.50 (d, $J = 6.9$ Hz, 1H), 5.29 – 5.25 (m, 2H), 5.16 (dt, $J = 10.0, 4.2$ Hz, 1H), 4.95 – 4.89 (m, 1H), 4.71 (d, $J = 6.6$ Hz, 2H), 4.47 – 4.40 (m, 1H), 4.33 – 4.23 (m, 2H), 4.18 – 4.12 (m, 1H), 3.91 (s, 3H), 3.82 – 3.77 (m, 3H), 3.77 – 3.72 (m, 2H), 2.10 (s, 3H), 2.07 (s, 6H), 2.06 – 2.01 (m, 9H).

$^{13}\text{C}\{^1\text{H}\}$ NMR (126 MHz, Chloroform-*d*) δ (ppm): 171.0, 170.9, 170.8, 170.4, 169.6, 169.5, 151.1, 150.9, 148.3, 146.2, 144.5, 137.2, 134.4, 130.8, 127.5, 121.4, 120.4, 120.3, 118.8, 118.5, 115.4, 110.7, 110.3, 100.9, 88.3, 88.2, 72.7, 72.1, 71.3, 68.4, 65.4, 65.3, 62.0, 56.2, 56.2, 56.1, 50.5, 21.2, 21.0, 20.9, 20.8, 20.7.

MS (ESI) m/z (%): 773 $[\text{M}+\text{H}]^+$ (100).

HRMS (ESI) m/z : $[\text{M}+\text{K}]^+$ calculated for $\text{C}_{38}\text{H}_{44}\text{KO}_{17}$: 811.2216; found: 811.2201.

(±)-dehydrodiconiferyl alcohol 4-O-β-D-glucopyranoside (1-108)

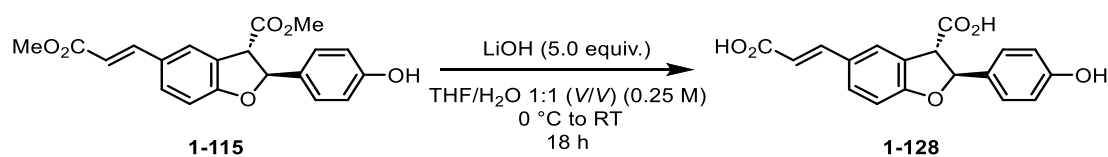
Glucoside **1-126** (0.24 g, 0.31 mmol, 1.0 equiv.) was dissolved in 7N ammonia methanol solution (0.025 M, 12.6 mL). The reaction was stirred overnight at RT. After there was no starting material on TLC, the reaction was stopped by addition of 10 mL of water and was extracted with EtOAc (3 × 20 mL). The combined organic layers were washed with brine, dried over anhydrous Na₂SO₄, filtered, and concentrated *in vacuo*. The crude product was purified semipreparative chromatography using MeOH/water as an eluent to afford **1-108** as a yellow solid (0.1 g, 61 %).

¹H NMR (500 MHz, Acetone-d₆) δ (ppm): 7.14 (d, *J* = 8.3 Hz, 1H), 7.08 (d, *J* = 2.0 Hz, 1H), 6.97 (d, *J* = 5.4 Hz, 2H), 6.93 (dd, *J* = 8.4, 2.0 Hz, 1H), 6.53 (dd, *J* = 15.9, 1.7 Hz, 1H), 6.24 (dt, *J* = 15.8, 5.5 Hz, 1H), 5.62 (d, *J* = 6.1 Hz, 1H), 4.91 (d, *J* = 7.2 Hz, 1H), 4.39 – 4.33 (m, 1H), 4.27 (s, 1H), 4.19 (d, *J* = 5.4 Hz, 2H), 3.94 – 3.89 (m, 1H), 3.88 (s, 3H), 3.86 – 3.82 (m, 2H), 3.81 (s, 3H), 3.71 – 3.65 (m, 2H), 3.60 – 3.51 (m, 3H), 3.49 – 3.41 (m, 4H).

¹³C{¹H} NMR (126 MHz, Acetone-d₆) δ (ppm): 150.8, 148.9, 147.6, 145.2, 137.7, 132.1, 130.4, 130.1, 128.5, 119.0, 117.9, 116.1, 111.7, 111.4, 111.4, 102.5, 88.2, 77.8, 74.6, 71.2, 64.6, 63.3, 62.5, 57.6, 56.5, 56.4, 54.9, 18.8.

MS (ESI) *m/z* (%): 521 [M+H]⁺ (100).

HRMS (ESI) *m/z*: [M+NH₄]⁺ calculated for C₂₆H₃₆NO₁₁: 538.2283; found: 538.2290.

(±)-dehydrodi-*p*-coumaric acid (1-128)

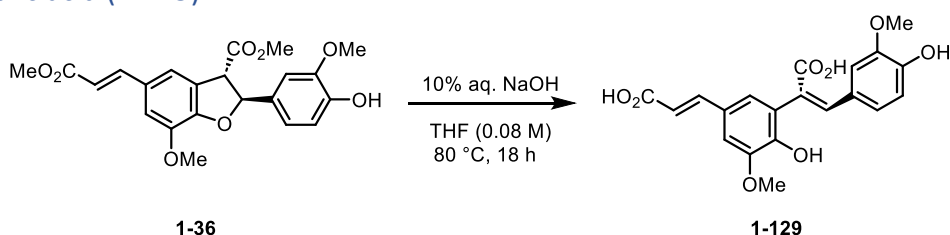
1-115 (0.30 g, 0.64 mmol, 1.0 equiv.) was dissolved in THF (0.5 M, 0.7 mL), and the solution was cooled to 0 °C. After 5 minutes at a solution of LiOH (0.14 g, 3.2 mmol, 5.0 equiv.) in water (0.5 M, 0.7 mL). The solution was slowly allowed to warm to room temperature while stirring overnight. The following day, the mixture was quenched by addition of 1 M HCl (15 mL) and extracted with EtOAc (3 × 25 mL). The combined organic layers were washed with brine, dried over anhydrous Na₂SO₄, filtered, and concentrated *in vacuo*. The crude product was purified by column chromatography (SiO₂; DCM:MeOH:AcOH = 20:1:0.1) to afford **1-128** as white solid (0.12 g, 57 %).

¹H NMR (500 MHz, Acetone-d₆) δ (ppm): 7.77 – 7.76 (m, 1H), 7.67 (d, *J* = 16.0 Hz, 1H), 7.62 – 7.59 (m, 1H), 7.32 – 7.28 (m, 2H), 6.92 (d, *J* = 8.3 Hz, 1H), 6.89 – 6.85 (m, 2H), 6.40 (d, *J* = 16.0 Hz, 1H), 6.04 (d, *J* = 7.3 Hz, 1H), 4.41 – 4.36 (m, 1H), 2.94 (bs, 2H).

¹³C{¹H} NMR (126 MHz, Acetone-d₆) δ (ppm): 172.0, 168.0, 162.1, 158.6, 145.3, 132.1, 131.6, 128.7, 128.5, 127.1, 126.0, 116.5, 116.3, 110.7, 87.8, 55.5.

MS (ESI) *m/z* (%): 327

HRMS (ESI) *m/z*: [M+H]⁺ calculated for C₁₈H₁₅O₆: 327.0863; found 327.0869.

8,5'-diferulic acid (**1-129**)

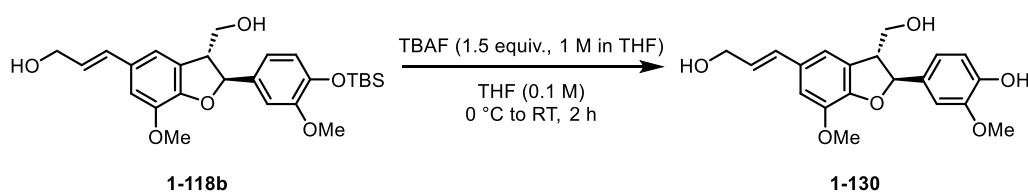
1-36 (0.3 g, 0.72 mmol, 1.0 equiv.) was dissolved in THF (0.08 M, 9 mL), and 10% aq. NaOH (9 mL) was added. The resulting mixture was stirred at RT. for 30 min before it was warmed to 80 °C overnight. Next day the resulting mixture was cool to RT and acidified with 2 M aq. HCl to pH 2. The water phase was water phase was extracted with EtOAc (3 x 20 mL). Combined organic layers were washed with brine (20 mL), dried over MgSO₄, filtered, and the solvents were removed under reduced pressure. The crude product was purified by column chromatography (SiO₂; CHCl₃:EtOAc:AcOH = 20:1:0.1-10:1:0.1) to afford **1-129** as a white solid (0.167 g, 60 %).

¹H NMR (500 MHz, Acetone-d₆) δ (ppm): 7.81 (s, 1H), 7.59 (d, *J* = 15.9 Hz, 1H), 7.39 (d, *J* = 2.0 Hz, 1H), 7.04 (d, *J* = 1.9 Hz, 1H), 6.86 (dd, *J* = 8.4, 2.0 Hz, 1H), 6.74 (d, *J* = 2.0 Hz, 1H), 6.72 (d, *J* = 8.2 Hz, 1H), 6.39 (d, *J* = 15.9 Hz, 1H), 3.97 (s, 3H), 3.46 (s, 3H).

¹³C{¹H} NMR (126 MHz, Acetone-d₆) δ (ppm): 168.6, 168.0, 149.1, 148.0, 147.9, 145.7, 141.7, 127.7, 127.4, 126.4, 125.7, 125.2, 116.3, 115.6, 113.3, 110.2, 56.6, 55.5.

MS (ESI) *m/z* (%): 387 [M+H]⁺ (100).

HRMS (ESI) *m/z*: [M+H]⁺ calculated for C₂₀H₁₉O₈: 387.1074; found: 387.1081.

(±)-dehydroconiferyl aldehyde (1-130)

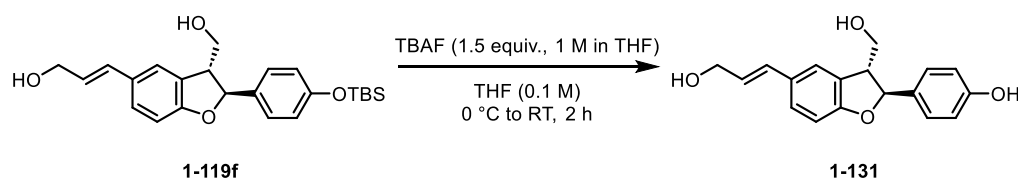
1-118b (0.25 g, 0.52 mmol, 1.0 equiv.) was dissolved in THF (0.1 M, 5.2 mL), and solution was cooled to 0 °C. After 5 minutes TBAF (0.21 g, 0.78 mmol, 1.5 equiv.) was added and the solution was stirred overnight at RT. Reaction was quenched by addition of NH₄Cl (50 mL). The aqueous layer was extracted with DCM (3 × 30 mL). The combined organic layers were washed with brine, dried over anhydrous Na₂SO₄, filtered, and concentrated *in vacuo*. The crude product was purified by column chromatography (SiO₂; petroleum DCM:MeOH = 10:1) to afford **1-130** as a white solid (0.15 g, 80 %).

¹H NMR (500 MHz, Acetone-d₆) δ (ppm): 7.03 (d, *J* = 2.0 Hz, 1H), 6.97 (t, *J* = 1.2 Hz, 1H), 6.94 (d, *J* = 1.6 Hz, 1H), 6.87 (dd, *J* = 8.1, 2.0 Hz, 1H), 6.80 (d, *J* = 8.1 Hz, 1H), 6.52 (dt, *J* = 15.9, 1.7 Hz, 1H), 6.24 (dt, *J* = 15.8, 5.6 Hz, 1H), 5.56 (d, *J* = 6.5 Hz, 1H), 4.19 (dd, *J* = 5.6, 1.6 Hz, 2H), 3.85 (s, 6H), 3.81 (s, 3H), 3.53 (q, *J* = 6.4 Hz, 1H).

¹³C{¹H} NMR (126 MHz, Acetone-d₆) δ (ppm): 148.8, 148.3, 147.1, 145.1, 134.3, 131.8, 130.5, 130.3, 128.2, 119.5, 116.0, 115.6, 111.5, 110.4, 88.4, 69.3, 69.2, 64.4, 63.2, 56.3, 56.2, 54.6.

MS (ESI) *m/z* (%): 357 [M-H]⁻ (100).

HRMS (ESI) *m/z*: [M+H]⁺ calculated for C₂₀H₂₃O₆: 357.1333 found: 357.1338.

(±)-dehydrodi-*p*-coumaryl alcohol (1-131)

1-119f (0.2 g, 0.48 mmol, 1.0 equiv.) was dissolved in THF (0.1 M, 4.85 mL), and solution was cooled to 0 °C. After 5 minutes TBAF (0.19 g, 0.73 mmol, 1.5 equiv.) was added and the solution was stirred overnight at RT. Reaction was quenched by addition of NH₄Cl (50 mL). The aqueous layer was extracted with DCM (3 × 30 mL). The combined organic layers were washed with brine, dried over anhydrous Na₂SO₄, filtered, and concentrated *in vacuo*. The crude product

was purified by column chromatography (SiO₂; petroleum DCM:MeOH = 10:1) to afford **1-131** as a white solid (0.12 g, 83 %).

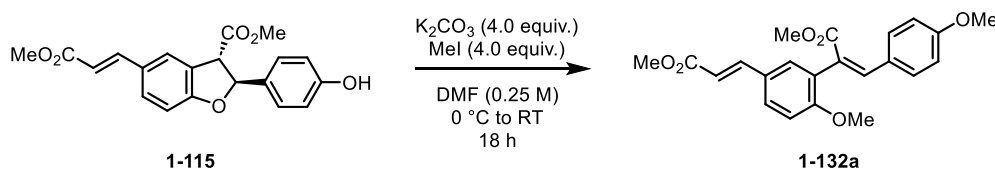
¹H NMR (500 MHz, Acetone-d₆) δ (ppm): δ 8.40 (bs, 1H), 7.43 – 7.36 (m, 1H), 7.28 – 7.17 (m, 3H), 6.84 – 6.81 (m, 2H), 6.74 (d, *J* = 8.2 Hz, 1H), 6.54 (dt, *J* = 15.7, 1.7 Hz, 1H), 6.23 (dt, *J* = 15.9, 5.5 Hz, 1H), 5.55 (d, *J* = 6.0 Hz, 1H), 4.19 (dd, *J* = 5.6, 1.5 Hz, 3H), 3.95 – 3.73 (m, 3H), 3.48 (q, *J* = 6.2 Hz, 1H).

¹³C{¹H} NMR (126 MHz, Acetone-d₆) δ (ppm): 160.5, 158.1, 134.1, 131.0, 130.3, 129.5, 128.2, 128.1, 128.1, 123.5, 116.1, 109.7, 88.0, 68.1, 64.8, 64.7, 63.4, 63.3, 54.4, 26.1.

MS (ESI) *m/z* (%): 297 [M-H]⁻ (100).

HRMS (ESI) *m/z*: [M-H]⁻ calculated for C₁₈H₁₇O₄: 297.1121; found: 297.1126.

methyl (*Z*)-2-(2-methoxy-5-((*E*)-3-methoxy-3-oxoprop-1-en-1-yl)phenyl)-3-(4-methoxyphenyl)acrylate (**1-132a**)



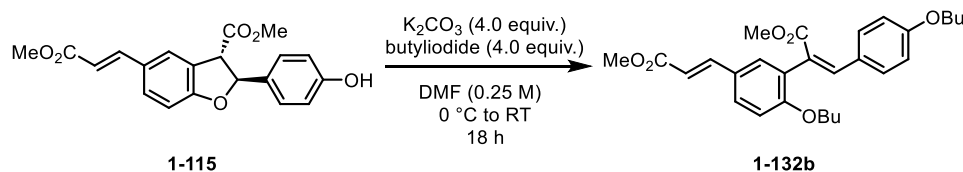
1-115 (0.1 g, 0.28 mmol, 1.0 equiv.) was dissolved in DMF (0.25 M, 1.1 mL), and the mixture was cooled to 0 °C. After 5 minutes at 0 °C K₂CO₃ (0.16 g, 0.113 mmol, 4.0 equiv.) was added following addition of methyl iodide (0.07 mL, 1.13 mmol, 4.0 equiv.). The resulting mixture was stirred at RT overnight. Next day 10 mL of NH₄Cl was added and the water phase was water phase was extracted with DCM (3 x 10 mL). Combined organic layers were washed with brine (20 mL), dried over MgSO₄, filtered, and the solvents were removed under reduced pressure. The crude product was purified by column chromatography (SiO₂; petroleum ether/EtOAc = 2:1) to afford **1-132a** as a white amorphous white solid (0,04 g, 79 %).

¹H NMR (500 MHz, Chloroform-d) δ (ppm): 7.82 (s, 1H), 7.59 (d, *J* = 16.0 Hz, 1H), 7.54 (dd, *J* = 8.6, 2.3 Hz, 1H), 7.28 (d, *J* = 2.3 Hz, 1H), 7.06 – 6.98 (m, 2H), 6.98 (d, *J* = 8.6 Hz, 1H), 6.72 – 6.65 (m, 2H), 6.24 (d, *J* = 16.0 Hz, 1H), 3.78 (s, 3H), 3.75 (s, 6H), 3.75 (s, 3H).

¹³C{¹H} NMR (126 MHz, Chloroform-d) δ (ppm): 168.4, 167.8, 160.5, 159.5, 144.4, 141.0, 132.1, 131.0, 130.0, 127.5, 127.2, 126.3, 126.0, 115.7, 113.9, 111.5, 56.0, 55.3, 52.4, 51.7.

MS (ESI) *m/z* (%): 383 [M+H]⁺ (100).

HRMS (ESI) *m/z*: [M+H]⁺ calculated for C₂₂H₂₅O₆: 383.1489; found: 383.1488.

methyl (Z)-2-(2-butoxy-5-((E)-3-methoxy-3-oxoprop-1-en-1-yl)phenyl)-3-(4-butoxyphenyl)acrylate (**1-132b**)

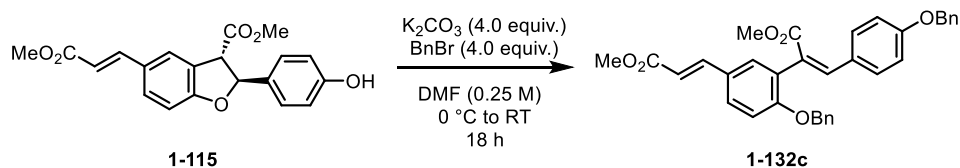
1-115 (0.1 g, 0.28 mmol, 1.0 equiv.) was dissolved in DMF (0.25 M, 1.1 mL), and the mixture was cooled to 0 °C. After 5 minutes at 0 °C K_2CO_3 (0.16 g, 0.13 mmol, 4.0 equiv.) was added following addition of 1-iodobutane (0.13 mL, 1.13 mmol, 4.0 equiv.). The resulting mixture was stirred at RT overnight. Next day 10 mL of NH_4Cl was added and the water phase was water phase was extracted with DCM (3 x 10 mL). Combined organic layers were washed with brine (20 mL), dried over MgSO_4 , filtered, and the solvents were removed under reduced pressure. The crude product was purified by column chromatography (SiO_2 ; petroleum ether/EtOAc = 4:1) to afford **1-132g** as a white solid (0.075 g, 58 %).

^1H NMR (500 MHz, Chloroform- d) δ (ppm): 8.03 (d, J = 2.4 Hz, 1H), 7.71 (dd, J = 8.7, 2.4 Hz, 1H), 7.65 (dd, J = 16.0, 4.6 Hz, 2H), 7.50 (dd, J = 8.4, 1.9 Hz, 1H), 7.41 (d, J = 1.9 Hz, 1H), 7.35 – 7.27 (m, 2H), 7.00 (dd, J = 10.7, 8.5 Hz, 2H), 6.88 (d, J = 6.5 Hz, 2H), 6.39 (d, J = 16.0 Hz, 1H), 6.32 (d, J = 16.0 Hz, 1H), 4.08 (t, J = 6.6 Hz, 2H), 3.95 (t, J = 6.5 Hz, 5H), 3.92 (s, 4H), 3.80 (s, 5H), 1.76 (p, J = 6.7 Hz, 4H), 1.53 – 1.42 (m, 4H), 0.98 (td, J = 7.4, 3.0 Hz, 6H).

$^{13}\text{C}\{^1\text{H}\}$ NMR (126 MHz, Chloroform- d) δ (ppm): 186.2, 172.4, 167.8, 167.4, 165.2, 162.6, 161.0, 159.6, 144.4, 143.0, 135.7, 131.9, 130.6, 128.9, 128.6, 127.7, 126.9, 126.8, 124.0, 123.2, 117.5, 116.0, 114.4, 113.1, 111.5, 94.1, 85.6, 69.3, 67.9, 53.2, 52.6, 51.9, 51.8, 31.4, 31.0, 29.8, 19.4, 19.1, 14.0, 13.9.

MS (ESI) m/z (%): 467 [M+H]⁺ (100).

HRMS (ESI) m/z : [M+H]⁺ calculated for $\text{C}_{28}\text{H}_{35}\text{O}_6$: 467.2428; found: 467.2427.

methyl (Z)-2-(2-(benzyloxy)-5-((E)-3-methoxy-3-oxoprop-1-en-1-yl)phenyl)-3-(4-(benzyloxy)phenyl)acrylate (**1-132c**)

1-115 (0.1 g, 0.28 mmol, 1.0 equiv.) was dissolved in DMF (0.25 M, 1.1 mL), and the mixture was cooled to 0 °C. After 5 minutes at 0 °C K_2CO_3 (0.16 g, 0.13 mmol, 4.0 equiv.) was added following addition of benzyl bromide (0.13 mL, 1.13 mmol, 4.0 equiv.). The resulting mixture was stirred at RT overnight. Next day 10 mL of NH_4Cl was added and the water phase was water phase was extracted with DCM (3 x 10 mL). Combined organic layers were washed with brine (20 mL), dried over $MgSO_4$, filtered, and the solvents were removed under reduced pressure. The crude product was purified by column chromatography (SiO_2 ; petroleum ether/EtOAc = 4:1) to afford **1-132c** as a white solid (0.12 g, 79 %).

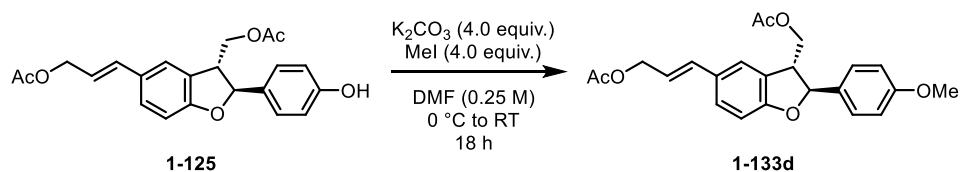
1H NMR (500 MHz, Chloroform-*d*) δ (ppm): 7.55 (d, J = 15.9 Hz, 1H), 7.42 – 7.37 (m, 4H), 7.37 – 7.35 (m, 1H), 7.35 – 7.30 (m, 1H), 7.25 – 7.19 (m, 3H), 7.14 – 7.10 (m, 2H), 6.89 – 6.84 (m, 5H), 6.70 (d, J = 1.8 Hz, 1H), 6.07 (d, J = 15.9 Hz, 1H), 5.63 (s, 1H), 5.03 (s, 2H), 3.81 (d, J = 13.1 Hz, 1H), 3.78 (s, 3H), 3.22 (s, 3H), 3.08 (d, J = 13.1 Hz, 1H).

$^{13}C\{^1H\}$ NMR (126 MHz, Chloroform-*d*) δ (ppm): 171.3, 168.0, 162.2, 159.1, 145.0, 136.8, 135.5, 130.8, 130.7, 129.7, 128.7, 128.3, 128.2, 128.1, 127.9, 127.7, 127.6, 127.5, 127.2, 115.1, 114.7, 110.0, 92.7, 70.0, 64.4, 52.1, 51.7, 45.3, 29.8.

MS (ESI) m/z (%): 535 $[M+H]^+$ (100).

HRMS (ESI) m/z : $[M+H]^+$ calculated for $C_{34}H_{31}O_6$: 535.2272; found:535.2118.

(E)-3-(3-(acetoxymethyl)-2-(4-methoxyphenyl)-2,3-dihydrobenzofuran-5-yl)allyl acetate
(1-133d)



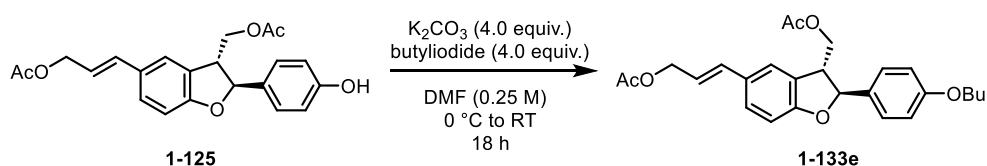
1-125 (0.05 g, 0.13 mmol, 1.0 equiv.) was dissolved in DMF (0.13 M, 1 mL), and the mixture was cooled to 0 °C. After 5 minutes at 0 °C K_2CO_3 (0.07 g, 0.52 mmol, 4.0 equiv.) was added following addition of methyl iodide (0.032 mL, 0.52 mmol, 4.0 equiv.). The resulting mixture was stirred at RT overnight. Next day 10 mL of NH_4Cl was added and the water phase was water phase was extracted with DCM (3 x 10 mL). Combined organic layers were washed with brine (20 mL), dried over $MgSO_4$, filtered, and the solvents were removed under reduced pressure. The crude product was purified by column chromatography (SiO_2 ; petroleum ether/EtOAc = 2:1) to afford **1-133d** as a white amorphous solid (0.04 g, 79 %).

1H NMR (500 MHz, Chloroform-*d*) δ (ppm): 7.28 – 7.22 (m, 4H), 6.90 – 6.86 (m, 2H), 6.81 (d, J = 8.2 Hz, 1H), 6.59 (d, J = 15.8 Hz, 1H), 6.13 (dt, J = 15.8, 6.6 Hz, 1H), 5.46 (d, J = 6.6 Hz, 1H), 4.69 (dd, J = 6.7, 1.3 Hz, 2H), 4.42 (dd, J = 11.1, 5.5 Hz, 1H), 4.28 (dd, J = 11.1, 7.8 Hz, 1H), 3.79 (s, 3H), 3.70 (q, J = 6.6 Hz, 1H), 2.08 (s, 3H), 2.03 (s, 3H).

$^{13}C\{^1H\}$ NMR (126 MHz, Chloroform-*d*) δ (ppm): 171.1, 171.0, 160.0, 159.8, 134.4, 133.0, 129.7, 128.5, 127.4, 127.0, 122.8, 120.9, 114.2, 109.9, 87.9, 65.7, 65.5, 55.5, 50.0, 21.2, 21.0.

MS (ESI) m/z (%): 397

HRMS (ESI) m/z : $[M+K]^+$ calculated for $C_{23}H_{25}O_6K$: 435.1204; found:435.1192.

(E)-3-(3-(acetoxymethyl)-2-(4-butoxyphenyl)-2,3-dihydrobenzofuran-5-yl)allyl acetate (1-133e)

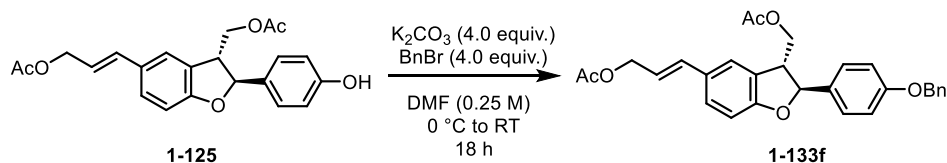
1-125 (0.05 g, 0.13 mmol, 1.0 equiv.) was dissolved in DMF (0.13 M, 1 mL), and the mixture was cooled to 0 °C. After 5 minutes at 0 °C K_2CO_3 (0.07 g, 0.52 mmol, 4.0 equiv.) was added following addition of 1-Iodobutane (0.06 mL, 0.52 mmol, 4.0 equiv.). The resulting mixture was stirred at RT overnight. Next day 10 mL of NH_4Cl was added and the water phase was water phase was extracted with DCM (3 x 10 mL). Combined organic layers were washed with brine (20 mL), dried over MgSO_4 , filtered, and the solvents were removed under reduced pressure. The crude was purified by column chromatography (SiO_2 ; petroleum ether/EtOAc = 2:1) to afford **1-133e** as a white solid (0.052 g, 91 %).

^1H NMR (500 MHz, Chloroform-d) δ (ppm): 7.28 – 7.24 (m, 4H), 6.90 – 6.86 (m, 2H), 6.83 (d, J = 8.3 Hz, 1H), 6.61 (d, J = 15.8 Hz, 1H), 6.15 (dt, J = 15.8, 6.6 Hz, 1H), 5.47 (d, J = 6.6 Hz, 1H), 4.71 (dd, J = 6.7, 1.3 Hz, 2H), 4.44 (dd, J = 11.2, 5.5 Hz, 1H), 4.30 (dd, J = 11.1, 7.8 Hz, 1H), 3.95 (t, J = 6.5 Hz, 2H), 3.72 (q, J = 6.5 Hz, 1H), 2.10 (s, 3H), 2.05 (s, 3H), 1.79 – 1.72 (m, 2H), 1.53 – 1.44 (m, 2H), 0.97 (t, J = 7.4 Hz, 3H).

$^{13}\text{C}\{^1\text{H}\}$ NMR (126 MHz, Chloroform-d) δ (ppm): 171.0, 171.0, 160.0, 159.4, 134.4, 132.7, 129.6, 128.5, 127.3, 127.0, 122.8, 120.8, 114.8, 109.8, 87.9, 67.8, 65.6, 65.4, 50.0, 31.4, 21.2, 20.9, 19.3, 14.0.

MS (ESI) m/z (%):

HRMS (ESI) m/z : $[\text{M}+\text{H}]^+$ calculated for $\text{C}_{26}\text{H}_{30}\text{O}_6\text{K}$: 477.1674; found: 477.1677.

(E)-3-(3-(acetoxymethyl)-2-(4-(benzyloxy)phenyl)-2,3-dihydrobenzofuran-5-yl)allyl acetate (1-133f)

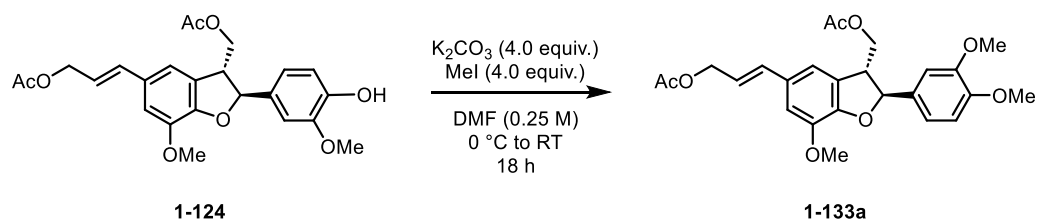
1-125 (0.05 g, 0.13 mmol, 1.0 equiv.) was dissolved in DMF (0.13 M, 1 mL), and the mixture was cooled to 0 °C. After 5 minutes at 0 °C K_2CO_3 (0.07 g, 0.52 mmol, 4.0 equiv.) was added following addition of benzyl bromide (0.062 mL, 0.52 mmol, 4.0 equiv.). The resulting mixture was stirred at RT overnight. Next day 10 mL of NH_4Cl was added and the water phase was water phase was extracted with DCM (3 x 10 mL). Combined organic layers were washed with brine (20 mL), dried over $MgSO_4$, filtered, and the solvents were removed under reduced pressure. The crude product was purified by column chromatography (SiO_2 ; petroleum ether/EtOAc = 2:1) to afford **1-133f** as a white solid (0.05 g, 81 %).

1H NMR (500 MHz, Chloroform- d) δ (ppm): 7.41 (dd, $J = 15.6, 7.4$ Hz, 4H), 7.35 – 7.30 (m, 2H), 7.29 – 7.23 (m, 3H), 6.99 – 6.94 (m, 2H), 6.83 (d, $J = 8.2$ Hz, 1H), 6.61 (d, $J = 15.8$ Hz, 1H), 6.14 (dt, $J = 15.7, 6.7$ Hz, 1H), 5.47 (d, $J = 6.5$ Hz, 1H), 5.07 (s, 2H), 4.74 – 4.66 (m, 2H), 4.44 (dd, $J = 11.1, 5.5$ Hz, 1H), 4.29 (dd, $J = 11.1, 7.8$ Hz, 1H), 3.71 (q, $J = 6.6$ Hz, 1H), 2.10 (s, 3H), 2.04 (s, 3H).

$^{13}C\{^1H\}$ NMR (126 MHz, Chloroform- d) δ (ppm): 171.4, 171.2, 159.9, 156.3, 134.4, 132.6, 129.6, 128.5, 127.6, 127.0, 122.8, 120.7, 115.7, 109.8, 87.9, 65.7, 65.6, 49.9, 21.2, 21.0.

MS (ESI) m/z (%): 473

HRMS (ESI) m/z : $[M+K]^+$ calculated for $C_{29}H_{28}O_6K$: 511.1517; found: 511.1519.

(E)-3-(3-(acetoxymethyl)-2-(3,4-dimethoxyphenyl)-7-methoxy-2,3-dihydrobenzofuran-5-yl)allyl acetate (**1-133a**)

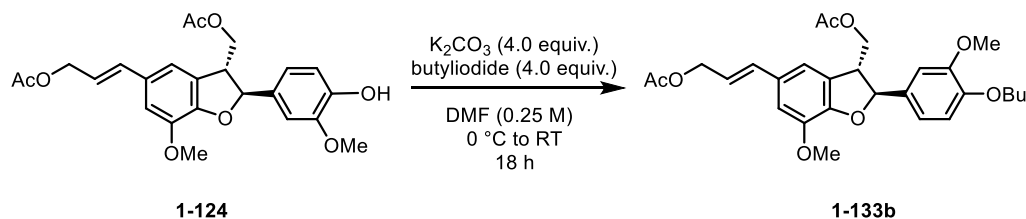
1-124 (0.05 g, 0.113 mmol, 1.0 equiv.) was dissolved in DMF (0.13 M, 1 mL), and the mixture was cooled to 0 °C. After 5 minutes at 0 °C K_2CO_3 (0.06 g, 0.45 mmol, 4 equiv.) was added following addition of methyl iodide (0.028 mL, 0.45 mmol, 4 equiv.). The resulting mixture was stirred at RT overnight. Next day 10 mL of NH_4Cl was added and the water phase was water phase was extracted with DCM (3 x 10 mL). Combined organic layers were washed with brine (20 mL), dried over MgSO_4 , filtered, and the solvents were removed under reduced pressure. The crude product was purified by column chromatography (SiO_2 ; petroleum ether/EtOAc = 2:1) to afford **1-133a** as a white solid (0.039 g, 76 %).

$^1\text{H NMR}$ (500 MHz, Chloroform-*d*) δ (ppm): 6.94 – 6.87 (m, 4H), 6.85 – 6.81 (m, 1H), 6.60 (d, J = 15.8 Hz, 1H), 6.16 (dt, J = 15.8, 6.6 Hz, 1H), 5.49 (d, J = 7.3 Hz, 1H), 4.71 (dd, J = 6.6, 1.2 Hz, 2H), 3.91 (s, 3H), 3.87 (s, 3H), 3.85 (s, 3H), 3.80 – 3.76 (m, 1H), 2.10 (s, 3H), 2.03 (s, 3H).

$^{13}\text{C}\{^1\text{H}\}$ NMR ($^{13}\text{C}\{^1\text{H}\}$ NMR (126 MHz, Chloroform-*d*) δ (ppm): 171.1, 171.0, 149.3, 148.4, 144.5, 134.5, 132.9, 130.6, 127.8, 121.3, 118.9, 115.4, 111.0, 110.6, 109.3, 88.8, 65.4, 65.4, 56.1, 56.1, 56.0, 50.4, 33.2, 21.2, 21.0, 20.2.

MS (ESI) m/z (%): 457

HRMS (ESI) m/z : $[\text{M}+\text{K}]^+$ calculated for $\text{C}_{25}\text{H}_{28}\text{O}_8\text{K}$: 495.1416; found: 495.1416.

(E)-3-(3-(acetoxymethyl)-2-(4-butoxy-3-methoxyphenyl)-7-methoxy-2,3-dihydrobenzofuran-5-yl) allyl acetate (1-133b)

1-124 (0.05 g, 0.113 mmol, 1.0 equiv.) was dissolved in DMF (0.13 M, 1 mL), and the mixture was cooled to 0 °C. After 5 minutes at 0 °C K_2CO_3 (0.06 g, 0.45 mmol, 4 equiv.) was added following addition of 1-Iodobutane (0.051 mL, 0.45 mmol, 4 equiv.). The resulting mixture was stirred at RT overnight. Next day 10 mL of NH_4Cl was added and the water phase was water phase was extracted with DCM (3 x 10 mL). Combined organic layers were washed with brine (20 mL), dried over MgSO_4 , filtered, and the solvents were removed under reduced pressure. The crude product was purified by column chromatography (SiO_2 ; petroleum ether/EtOAc = 2:1) to afford **1-133b** as a white amorphous solid (0.041 g, 73 %).

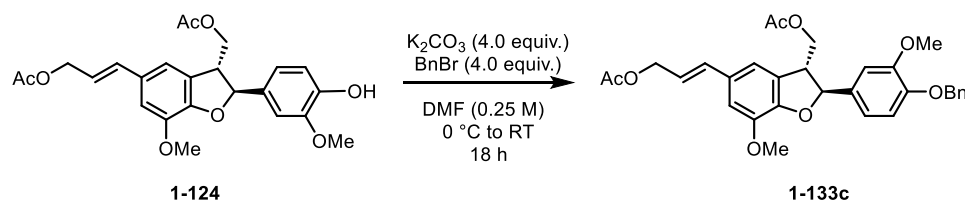
^1H NMR (500 MHz, Chloroform-*d*) δ (ppm): 6.92 – 6.87 (m, 4H), 6.83 (d, $J = 8.8$ Hz, 1H), 6.60 (d, $J = 15.8$ Hz, 1H), 6.15 (dt, $J = 15.8, 6.6$ Hz, 1H), 5.48 (d, $J = 7.3$ Hz, 1H), 4.71 (d, $J = 6.6$ Hz, 2H), 4.43 (dd, $J = 11.1, 5.4$ Hz, 1H), 4.30 (dd, $J = 11.2, 7.4$ Hz, 1H), 4.00 (t, $J = 6.8$ Hz, 2H), 3.90 (s, 3H), 3.83 (s, 3H), 3.81 – 3.76 (m, 1H), 2.10 (s, 3H), 2.03 (s, 3H), 1.81 (p, $J = 6.9$ Hz, 2H), 1.48 (h, $J = 7.4$ Hz, 2H), 0.96 (t, $J = 7.4$ Hz, 3H).

$^{13}\text{C}\{^1\text{H}\}$ NMR (126 MHz, Chloroform-*d*) δ (ppm): 171.1, 170.9, 149.7, 148.9, 148.4, 144.5, 134.5, 132.7, 130.5, 127.8, 121.2, 118.9, 115.4, 112.7, 110.6, 109.8, 88.8, 68.8, 65.4, 65.4, 56.2, 56.1, 50.3, 31.3, 21.2, 21.0, 19.3, 14.0.

MS (ESI) m/z (%): 499

HRMS (ESI) m/z : $[\text{M}+\text{K}]^+$ calculated for $\text{C}_{28}\text{H}_{34}\text{O}_8\text{K}$: 537.1885; found: 537.1885.

(*E*)-3-(3-(acetoxymethyl)-2-(4-(benzyloxy)-3-methoxyphenyl)-7-methoxy-2,3-dihydrobenzofuran-5-yl)allyl acetate (**1-133c**)



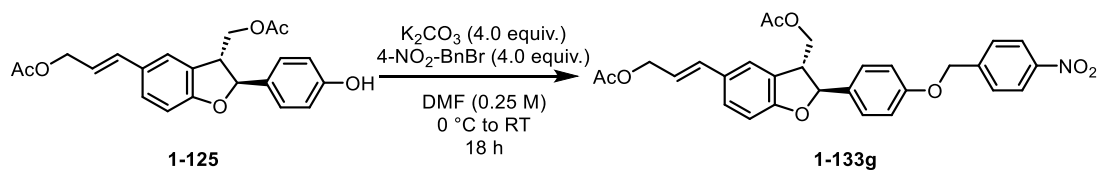
1-124 (0.05 g, 0.113 mmol, 1.0 equiv.) was dissolved in DMF (0.13 M, 1 mL), and the mixture was cooled to 0 °C. After 5 minutes at 0 °C K_2CO_3 (0.06 g, 0.45 mmol, 4 equiv.) was added following addition of benzyl bromide (0.054 mL, 0.45 mmol, 4 equiv.). The resulting mixture was stirred at RT overnight. Next day 10 mL of NH_4Cl was added and the water phase was water phase was extracted with DCM (3 x 10 mL). Combined organic layers were washed with brine (20 mL), dried over $MgSO_4$, filtered, and the solvents were removed under reduced pressure. The crude product was purified by column chromatography (SiO_2 ; petroleum ether/EtOAc = 2:1) to afford **1-133c** as a white solid (0.055 g, 92 %).

1H NMR (500 MHz, Chloroform-*d*) δ (ppm): 7.42 – 7.40 (m, 2H), 7.37 – 7.33 (m, 2H), 7.31 – 7.27 (m, 1H), 6.92 (d, J = 1.8 Hz, 1H), 6.88 (s, 2H), 6.85 – 6.82 (m, 2H), 6.60 (d, J = 15.9 Hz, 1H), 6.15 (dt, J = 15.7, 6.6 Hz, 1H), 5.47 (d, J = 7.3 Hz, 1H), 5.15 (s, 2H), 4.71 (dd, J = 6.7, 1.3 Hz, 2H), 4.43 (dd, J = 11.2, 5.4 Hz, 1H), 4.29 (dd, J = 11.2, 7.5 Hz, 1H), 3.90 (s, 3H), 3.86 (s, 3H), 3.80 – 3.75 (m, 1H), 2.10 (s, 3H), 2.01 (s, 3H).

$^{13}C\{^1H\}$ NMR (126 MHz, Chloroform-*d*) δ (ppm): 171.1, 170.9, 149.9, 148.3, 144.5, 137.1, 134.5, 133.4, 130.6, 128.7, 128.0, 127.7, 127.3, 121.2, 118.8, 115.4, 113.9, 110.6, 109.8, 88.7, 71.1, 65.4, 65.4, 56.2, 56.1, 50.3, 21.2, 20.9.

MS (ESI) m/z (%): 533

HRMS (ESI) m/z : $[M+H]^+$ calculated for $C_{31}H_{33}O_8$: 533.2170; found: 533.2193.

(E)-3-(3-(acetoxymethyl)-2-(4-((4-nitrobenzyl)oxy)phenyl)-2,3-dihydrobenzofuran-5-yl)allyl acetate (1-133g)

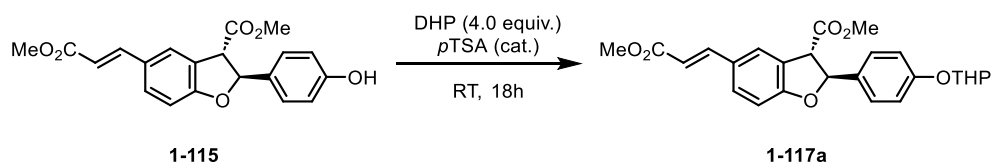
1-125 (0.05 g, 0.13 mmol, 1.0 equiv.) was dissolved in DMF (0.13 M, 1 mL), and the mixture was cooled to 0 °C. After 5 minutes at 0 °C K_2CO_3 (0.07 g, 0.52 mmol, 4.0 equiv.) was added following addition of 4-nitrobenzyl bromide (0.113 g, 0.52 mmol, 4.0 equiv.). The resulting mixture was stirred at RT overnight. Next day 10 mL of NH_4Cl was added and the water phase was water phase was extracted with DCM (3 x 10 mL). Combined organic layers were washed with brine (20 mL), dried over MgSO_4 , filtered, and the solvents were removed under reduced pressure. The crude product was purified by column chromatography (SiO_2 ; petroleum ether/EtOAc = 2:1) to afford **1-133g** as a white solid (0.046 g, 67 %).

^1H NMR (500 MHz, Chloroform-*d*) δ (ppm): 8.27 – 8.20 (m, 2H), 7.62 – 7.58 (m, 2H), 7.56 – 7.52 (m, 1H), 7.31 – 7.26 (m, 3H), 6.97 – 6.92 (m, 2H), 6.83 (d, J = 8.2 Hz, 1H), 6.61 (d, J = 15.8 Hz, 1H), 6.14 (dt, J = 15.7, 6.6 Hz, 1H), 5.48 (d, J = 6.5 Hz, 1H), 5.17 (s, 2H), 4.85 – 4.83 (m, 1H), 4.70 (d, J = 6.5 Hz, 2H), 4.44 (dd, J = 11.1, 5.5 Hz, 1H), 4.29 (dd, J = 11.1, 7.8 Hz, 1H), 3.70 (q, J = 6.6 Hz, 1H), 2.10 (s, 3H), 2.05 (s, 3H).

$^{13}\text{C}\{^1\text{H}\}$ NMR (126 MHz, Chloroform-*d*) δ (ppm): 171.1, 171.0, 159.9, 158.3, 147.7, 144.4, 134.3, 134.0, 129.8, 128.6, 127.7, 127.5, 127.1, 126.8, 124.0, 123.9, 122.9, 121.0, 115.1, 109.9, 68.8, 65.7, 65.4, 64.1, 50.1, 21.2, 21.0.

MS (ESI) m/z (%): 518

HRMS (ESI) m/z : $[\text{M}+\text{K}]^+$ calculated for $\text{C}_{29}\text{H}_{27}\text{NO}_8\text{K}$: 556.1368; found: 556.1368.

Methyl 5-((*E*)-3-methoxy-3-oxoprop-1-en-1-yl)-2-(4-((tetrahydro-2*H*-pyran-2-yl)oxy)phenyl)-2,3-dihydrobenzofuran-3-carboxylate (**1-117a**)

1-115 (0.60 g, 1.69 mmol, 1.0 equiv.) was dissolved in 3,4-dihydro-2*H*-pyran (0.62 mL, 6.77 mmol, 4.0 equiv.) and catalytic amount of *p*-toluene sulfonic acid was added. Mixture was stirred overnight at RT. The mixture was diluted with diethyl ether (20 mL), and 1 M NaOH (20 mL) was added. The aqueous layer was extracted with EtOAc (3 × 25 mL). The combined organic layers were washed with brine, dried over anhydrous Na₂SO₄, filtered, and concentrated *in vacuo*. The crude product was purified by column chromatography (SiO₂; petroleum ether/EtOAc = 4:1) to afford **1-117a** as a colorless oil (0.48 g, 65 %).

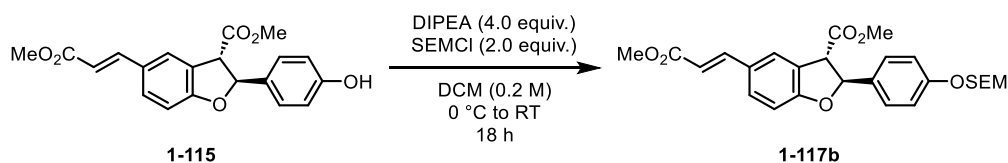
¹H NMR (500 MHz, Chloroform-*d*) δ (ppm): 7.66 (d, *J* = 15.9 Hz, 1H), 7.57 – 7.55 (m, 1H), 7.43 (dd, *J* = 8.3, 1.9 Hz, 1H), 7.32 – 7.28 (m, 2H), 7.07 – 7.03 (m, 1H), 6.89 (d, *J* = 8.4 Hz, 1H), 6.32 (d, *J* = 16.0 Hz, 1H), 6.14 – 6.08 (m, 1H), 5.44 – 5.41 (m, 1H), 4.30 – 4.26 (m, 1H), 3.90 – 3.86 (m, 1H), 3.84 (s, 3H), 3.80 (s, 3H), 3.61 – 3.56 (m, 1H), 2.04 – 1.94 (m, 1H), 1.90 – 1.80 (m, 2H), 1.74 – 1.51 (m, 4H).

¹³C{¹H} NMR (126 MHz, Chloroform-*d*) δ (ppm): 171.0, 167.9, 161.3, 157.4, 144.7, 132.9, 130.9, 127.9, 127.6, 127.3, 125.2, 125.0, 116.8, 115.8, 115.3, 110.4, 96.3, 86.5, 62.1, 55.1, 53.0, 51.8, 30.3, 25.2, 18.7.

MS (ESI) *m/z* (%): 439

HRMS (ESI) *m/z*: [M+H]⁺ calculated for C₂₅H₂₇O₇: 439.1751; found: 439.1759.

Methyl 5-((*E*)-3-methoxy-3-oxoprop-1-en-1-yl)-2-(4-((2-(trimethylsilyl)ethoxy)methoxy)phenyl)-2,3-dihydrobenzofuran-3-carboxylate (**1-117b**)



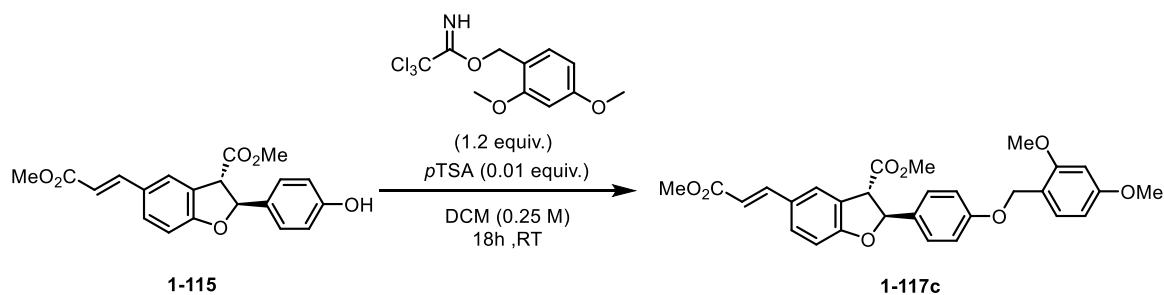
1-115 (0.20 g, 0.56 mmol, 1.0 equiv.) was dissolved in DCM (0.2 M, 2.8 mL), and the solution was cooled to 0 °C. After 5 minutes at 0 °C SEMCI (0.22 mL, 1.13 mmol, 2.0 equiv.) and DIPEA (0.40 mL, 2.26 mmol, 4.0 equiv.) was added. The solution was slowly allowed to warm to room temperature while stirring overnight. The following day, the mixture quenched by addition of NH_4Cl (15 mL), and the water phase was extracted with Et_2O (3 × 25 mL). The combined organic layers were washed with brine, dried over anhydrous Na_2SO_4 , filtered, and concentrated *in vacuo*. The crude product was purified by column chromatography (SiO_2 ; petroleum ether/ EtOAc = 4:1) to afford **1-117b** as a colorless oil (0.19 g, 70 %).

$^1\text{H NMR}$ (500 MHz, Chloroform-*d*) δ (ppm): 7.66 (d, J = 16.1 Hz, 1H), 7.56 (t, J = 1.5 Hz, 1H), 7.43 (dd, J = 8.3, 2.0 Hz, 1H), 7.33 – 7.29 (m, 2H), 7.06 – 7.02 (m, 2H), 6.89 (d, J = 8.3 Hz, 1H), 6.32 (d, J = 15.9 Hz, 1H), 6.11 (d, J = 7.7 Hz, 1H), 5.21 (s, 2H), 4.28 (d, J = 7.4 Hz, 1H), 3.84 (s, 3H), 3.79 (s, 3H), 3.76 – 3.71 (m, 2H), 0.97 – 0.92 (m, 2H), -0.01 (s, 9H).

$^{13}\text{C}\{^1\text{H}\}$ NMR (126 MHz, Chloroform-*d*) δ (ppm): 170.9, 167.9, 161.3, 157.9, 144.7, 133.1, 130.9, 128.0, 127.4, 125.2, 125.1, 116.6, 115.4, 110.5, 93.0, 86.5, 66.4, 55.2, 53.0, 51.8, 18.2, -1.3.

MS (ESI) m/z (%): 485

HRMS (ESI) m/z : $[\text{M}+\text{H}]^+$ calculated for $\text{C}_{26}\text{H}_{33}\text{O}_7\text{Si}$: 485.1990; found: 485.2002.

Methyl 2-(4-((2,4-dimethoxybenzyl)oxy)phenyl)-5-((*E*)-3-methoxy-3-oxoprop-1-en-1-yl)-2,3-dihydrobenzofuran-3-carboxylate (**1-117c**)

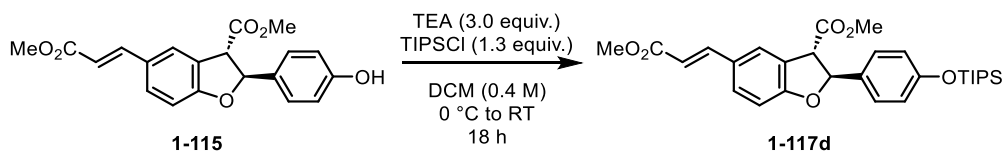
Formation of imidate: DBU (1.77 mL, 11.9 mmol, 0.1 equiv.) was added to a solution of 2,4-dimethoxybenzylalcohol (20 g, 119 mmol, 1.0 equiv.) in DCM (200 mL, 0.3 M) under argon atmosphere. The resulting mixture was stirred at RT for 15 min before it was cooled to 0 °C. After 5 min at 0 °C, trichloroacetonitril (14.3 mL, 143 mmol, 1.2 equiv.) was added and the resulting mixture was stirred at RT overnight. The resulting mixture was evaporated to dryness. The crude product was used in the next step without further purification. Spectroscopic data match those in the literature.⁸¹ Imidate (1.33 g, 3.75 mmol, 1.0 equiv.) was dissolved in DCM (0.25 M, 15 mL) at RT and imidate (1.41 g, 4.5 mmol, 1.2 equiv.) was added at one portion. After 5 minutes, *p*TSA (6.5 mg, 0.038 mmol, 1 mol%) was added. After stirring for 18 h, the mixture was evaporated. The crude product was purified by gradient column chromatography (SiO₂; petroleum ether/EtOAc = 4:1 → 2:1) to afford **1-117c** as a white solid (1.8 g, 95 %).

¹H NMR (500 MHz, Chloroform-*d*) δ (ppm): δ 7.66 (d, *J* = 16.0 Hz, 1H), 7.57 – 7.55 (m, 1H), 7.42 (dd, *J* = 8.4, 2.0 Hz, 1H), 7.33 – 7.28 (m, 3H), 7.00 – 6.96 (m, 2H), 6.89 (d, *J* = 8.3 Hz, 1H), 6.50 – 6.47 (m, 2H), 6.32 (d, *J* = 15.9 Hz, 1H), 6.10 (d, *J* = 7.6 Hz, 1H), 5.02 (s, 2H), 4.29 (d, *J* = 7.5 Hz, 1H), 3.84 (s, 3H), 3.82 (s, 3H), 3.81 (s, 3H), 3.80 (s, 3H).

¹³C{¹H} NMR (126 MHz, Chloroform-*d*) δ (ppm): δ 171.0, 167.9, 161.3, 161.1, 159.5, 158.4, 144.7, 132.0, 131.0, 130.3, 127.9, 127.4, 125.3, 125.1, 117.5, 115.3, 110.5, 104.3, 98.6, 86.6, 65.1, 55.6, 55.5, 55.2, 53.0, 51.8.

MS (ESI) *m/z* (%): 505 [M+H]⁺ (100).

HRMS (ESI) *m/z*: [M+H]⁺ calculated for C₂₉H₂₈O₈K: 543.1416; found: 543.1417.

Methyl 5-((*E*)-3-methoxy-3-oxoprop-1-en-1-yl)-2-(4-((triisopropylsilyl)oxy)phenyl)-2,3-dihydrobenzofuran-3-carboxylate (**1-117d**)

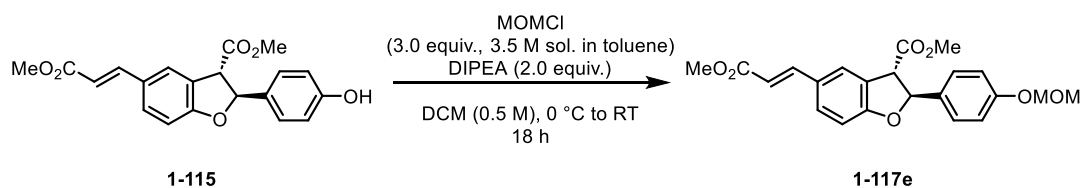
1-115 (0.10 g, 0.28 mmol, 1.0 equiv.) was dissolved in DCM (0.4 M, 0.7 mL), and the solution was cooled to 0 °C. After 5 minutes at 0 °C TEA (0.12 mL, 0.85 mmol, 3.0 equiv.) and TIPSCl (0.08 mL, 0.37 mmol, 1.3 equiv.) was added. The solution was slowly allowed to warm to room temperature while stirring overnight. The following day, the mixture was poured into cold water and extracted with Et₂O (3 × 25 mL). The combined organic layers were washed with brine, dried over anhydrous Na₂SO₄, filtered, and concentrated *in vacuo*. The crude product was purified by column chromatography (SiO₂; petroleum ether/EtOAc = 5:1) to afford **1-117d** as a colorless oil (0.11 g, 78 %).

¹H NMR (500 MHz, Chloroform-d) δ (ppm): 7.66 (d, *J* = 16.0 Hz, 1H), 7.56 (s, 1H), 7.42 (dd, *J* = 8.4, 2.0 Hz, 1H), 7.24 – 7.21 (m, 2H), 6.89 (d, *J* = 8.4 Hz, 1H), 6.88 – 6.85 (m, 2H), 6.32 (d, *J* = 16.0 Hz, 1H), 6.10 (d, *J* = 7.5 Hz, 1H), 4.28 (d, *J* = 7.3 Hz, 1H), 3.84 (s, 3H), 3.80 (s, 3H), 1.25 (ddt, *J* = 8.1, 6.1, 3.2 Hz, 3H), 1.09 (d, *J* = 7.4 Hz, 18H).

¹³C{¹H} NMR (126 MHz, Chloroform-d) δ (ppm): 171.0, 167.9, 156.6, 144.7, 132.4, 130.9, 127.9, 127.3, 125.3, 125.1, 120.3, 115.4, 110.5, 86.6, 55.2, 53.1, 51.8, 18.0, 12.8.

MS (ESI) *m/z* (%): 511

HRMS (ESI) *m/z*: [M+H]⁺ calculated for C₂₉H₃₉O₆Si: 511.2510; found: 511.2504.

Methyl 5-((E)-3-methoxy-3-oxoprop-1-en-1-yl)-2-(4-(methoxymethoxy)phenyl)-2,3-dihydrobenzofuran-3-carboxylate (**1-117e**)

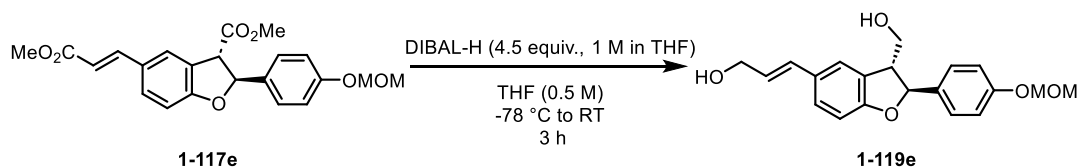
1-115 (1.33 g, 3.75 mmol, 1.0 equiv.) was dissolved in DCM (0.5 M, 7.5 mL), and the mixture was cooled to 0 °C. After 5 minutes at 0 °C DIPEA (1.3 mL, 7.51 mmol, 2.0 equiv.) was added following dropwise addition of methoxymethyl chloride solution in toluene (3.22 mL, 3.5 M, 11.3 mmol, 3.0 equiv.) during 1 h. The resulting mixture was stirred at RT overnight. Next day 50 mL of NH₄Cl was added and the water phase was water phase was extracted with EtOAc (3 x 100 mL). Combined organic layers were washed with brine (50 mL), dried over MgSO₄, filtered, and the solvents were removed under reduced pressure. The crude product was purified by column chromatography (SiO₂; petroleum ether/EtOAc = 2:1) to afford **1-117e** as a white solid (1.42 g, 95 %).

¹H NMR (500 MHz, Chloroform-d) δ (ppm) 7.69 – 7.60 (m, 2H), 7.56 (s, 1H), 7.49 – 7.37 (m, 2H), 7.33 – 7.29 (m, 2H), 7.05 – 7.02 (m, 2H), 7.01 – 6.97 (m, 1H), 6.89 (d, *J* = 8.4 Hz, 1H), 6.32 (d, *J* = 15.9 Hz, 1H), 6.11 (d, *J* = 7.5 Hz, 1H), 5.16 (s, 2H), 4.28 (d, *J* = 7.6 Hz, 1H), 3.83 (s, 3H), 3.79 (s, 3H), 3.46 (s, 3H).

¹³C{¹H} NMR (126 MHz, Chloroform-d) δ (ppm): 170.9, 167.8, 161.2, 157.6, 144.6, 133.3, 132.3, 130.9, 130.0, 128.0, 127.4, 125.2, 125.0, 116.6, 115.4, 110.4, 94.4, 86.4, 56.1, 55.2, 53.0, 51.7.

MS (ESI) *m/z* (%): 399 [M+H]⁺ (100).

HRMS (ESI) *m/z*: [M+H]⁺ calculated for C₂₂H₂₃O₇: 399.1438; found: 399.1438.

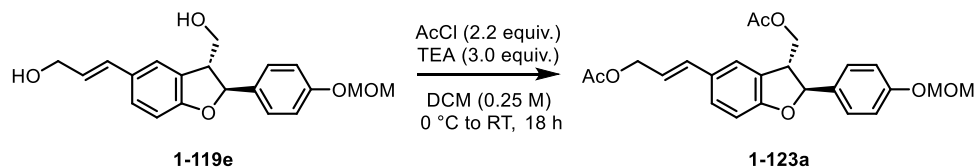
(E)-3-(3-(hydroxymethyl)-2-(4-(methoxymethoxy)phenyl)-2,3-dihydrobenzofuran-5-yl)prop-2-en-1-ol (1-119e)

A solution of ester **1-117e** (1.3 g, 3.26 mmol, 1.0 equiv.) in THF (0.5 M, 6.53 mL) was cooled to -78 °C and DIBAL-H (1 M in THF, 16.3 mL, 16.3 mmol, 4.5 equiv.) was added dropwise over 10 minutes. The resulting mixture was stirred at -78 °C for 30 min before the cooling bath removal. The reaction mixture was stirred for another 2 hours at RT. Then reaction was cooled to -78 °C and aqueous saturated solution of Rochel salt (100 mL) was added carefully dropwise to quench the reaction. After addition of Rochel salt, solution was diluted with EtOAc 100 mL. The resulting mixture was stirred at RT till a milky suspension turned into the clear biphasic solution (usually takes around 16 h). Resulting phases were separated and the aqueous layer was extracted with DCM (3x 75mL). Combined organic layers were washed with brine (50 mL), dried over Na₂SO₄, filtered, and evaporated under reduced pressure. The crude product was purified by column chromatography (SiO₂; DCM/MeOH = 95:5) to afford **1-119e** as a colorless oil (0.7 g, 63 %).

¹H NMR (500 MHz, Chloroform-d) δ (ppm): 7.32 – 7.29 (m, 2H), 7.28 – 7.27 (m, 1H), 7.25 – 7.22 (m, 1H), 7.04 – 7.00 (m, 2H), 6.83 (d, *J* = 8.2 Hz, 1H), 6.61 – 6.53 (m, 1H), 6.26 – 6.18 (m, 1H), 5.58 (d, *J* = 6.3 Hz, 1H), 5.17 (s, 2H), 4.31 – 4.27 (m, 2H), 4.00 – 3.90 (m, 2H), 3.56 (q, *J* = 5.7 Hz, 1H), 3.46 (s, 3H).

MS (ESI) *m/z* (%): 343

HRMS (ESI) *m/z*: [(M+H)⁺[-H₂O]]⁺ calculated for C₂₀H₂₁O₄: 325.1434; found: 325.1435.

(E)-3-(3-(acetoxymethyl)-2-(4-(methoxymethoxy)phenyl)-2,3-dihydrobenzofuran-5-yl)allyl acetate (1-123a)

Diol **1-119e** (0.6 g, 1.75 mmol, 1.0 equiv.) was dissolved in DCM (0.5 M, 3.5 mL), and solution was cooled to 0 °C. Then TEA (0.73 mL, 5.26 mmol, 3.0 equiv.) was added following by acetyl chloride (0.27 mL, 3.86 mmol, 2.2 equiv.). The reaction mixture was stirred at room temperature overnight. Reaction was quenched by addition of water (30 mL). The aqueous layer was extracted with EtOAc (3 × 25 mL). The combined organic layers were washed with brine, dried over anhydrous Na₂SO₄, filtered, and concentrated *in vacuo*. The crude product was purified by column chromatography (SiO₂; petroleum ether/EtOAc = 4:1) to afford **1-123a** as a yellowish oil (0.7 g, 93 %).

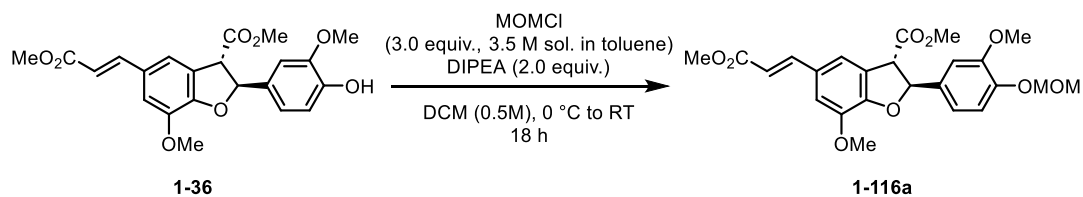
¹H NMR (500 MHz, Chloroform-d) δ (ppm): 7.31 – 7.26 (m, 3H), 7.26 – 7.23 (m, 1H), 7.05 – 6.98 (m, 2H), 6.83 (d, *J* = 8.3 Hz, 1H), 6.61 (d, *J* = 15.9 Hz, 1H), 6.14 (dt, *J* = 15.8, 6.7 Hz, 1H), 5.48 (d, *J* = 6.5 Hz, 1H), 5.17 (s, 2H), 4.70 (dd, *J* = 6.7, 1.3 Hz, 2H), 4.44 (dd, *J* = 11.1, 5.5 Hz, 1H), 4.29 (dd, *J* = 11.1, 7.8 Hz, 1H), 3.70 (q, *J* = 6.6 Hz, 1H), 3.47 (s, 3H), 2.10 (s, 3H), 2.06 (s, 3H).

¹³C{¹H} NMR (126 MHz, Chloroform-d) δ (ppm): 171.1, 171.0, 160.0, 157.4, 134.34, 134.26, 129.7, 128.5, 127.3, 126.9, 122.8, 120.9, 116.6, 109.9, 94.5, 87.7, 65.7, 65.5, 60.6, 56.1, 50.1, 21.2, 21.0, 14.3.

MS (ESI) *m/z* (%): 427

HRMS (ESI) *m/z*: [M+K]⁺ calculated for C₂₄H₂₆O₇K: 465.1310; found: 465.1310.

Methyl 7-methoxy-5-((*E*)-3-methoxy-3-oxoprop-1-en-1-yl)-2-(3-methoxy-4-(methoxymethoxy)phenyl)-2,3-dihydrobenzofuran-3-carboxylate (**1-116a**)



1-36 (2.0 g, 4.83 mmol, 1.0 equiv.) was dissolved in DCM (0.5 M, 9.65 mL), and the mixture was cooled to 0 °C. After 5 minutes at 0 °C DIPEA (1.67 mL, 9.65 mmol, 2.0 equiv.) was added following dropwise addition of methoxymethyl chloride solution in toluene (5.52 mL, 3.5 M, 19.3 mmol, 3.0 equiv.) during 1 h. The resulting mixture was stirred at RT overnight. Next day 50 mL of NH_4Cl was added and the water phase was water phase was extracted with EtOAc (3 x 100 mL). Combined organic layers were washed with brine (50 mL), dried over MgSO_4 , filtered, and the solvents were removed under reduced pressure. The crude product was purified by column chromatography (SiO_2 ; petroleum ether/EtOAc = 2:1) to afford **1-116a** as a white solid (2.05 g, 93 %).

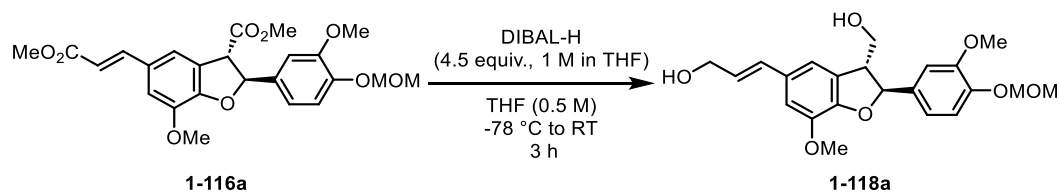
^1H NMR (500 MHz, Chloroform-*d*) δ (ppm): 7.65 (d, J = 15.9 Hz, 1H), 7.19 – 7.18 (m, 1H), 7.15 – 7.11 (m, 1H), 7.03 – 7.02 (m, 1H), 6.95 – 6.89 (m, 2H), 6.32 (d, J = 15.9 Hz, 1H), 6.14 (d, J = 8.2 Hz, 1H), 5.22 (s, 2H), 4.35 (d, J = 8.1 Hz, 1H), 3.92 (s, 3H), 3.86 (s, 3H), 3.84 (s, 3H), 3.80 (s, 3H), 3.49 (s, 3H).

$^{13}\text{C}\{^1\text{H}\}$ NMR (126 MHz, Chloroform-*d*) δ (ppm): 170.8, 167.8, 150.1, 146.9, 144.9, 133.8, 128.8, 125.7, 118.9, 118.1, 116.4, 115.7, 112.2, 109.8, 95.5, 87.4, 56.4, 56.3, 56.1, 55.6, 53.1, 51.8.

MS (ESI) m/z (%): 459

HRMS (ESI) m/z : $[\text{M}+\text{H}]^+$ calculated for $\text{C}_{24}\text{H}_{27}\text{O}_9$: 459.1650; found: 459.1651.

(*E*)-3-(3-(hydroxymethyl)-7-methoxy-2-(3-methoxy-4-(methoxymethoxy)phenyl)-2,3-dihydrobenzofuran-5-yl) prop-2-en-1-ol (**1-118a**)

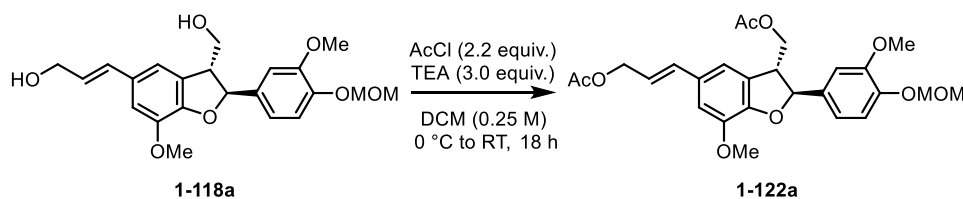


A solution of ester **1-116a** (2.0 g, 4.36 mmol, 1.0 equiv.) in THF (0.5 M, 6.53 mL) was cooled to -78 °C and DIBAL-H (1 M in THF, 21.8 mL, 21.8 mmol, 4.5 equiv.) was added dropwise over 10 minutes. The resulting mixture was stirred at -78 °C for 30 min before the cooling bath removal. The reaction mixture was stirred for another 2 hours at RT. Then reaction was cooled to -78 °C and aqueous saturated solution of Rochel salt (100 mL) was added carefully dropwise to quench the reaction. After addition of Rochel salt, solution was diluted with EtOAc 100 mL. The resulting mixture was stirred at RT till a milky suspension turned into the clear biphasic solution (usually takes around 16 h). Resulting phases were separated and the aqueous layer was extracted with DCM (3x 75mL). Combined organic layers were washed with brine (50 mL), dried over Na₂SO₄, filtered, and evaporated under reduced pressure. The crude product was purified by column chromatography (SiO₂; DCM/MeOH = 95:5) to afford **1-118a** as a colorless oil (1.16 g, 66 %).

¹H NMR (500 MHz, Chloroform-*d*) δ (ppm): 7.14 – 7.08 (m, 1H), 6.97 – 6.94 (m, 1H), 6.94 – 6.87 (m, 3H), 6.59 – 6.53 (m, 1H), 6.24 (dt, *J* = 15.8, 5.9 Hz, 1H), 5.61 (d, *J* = 7.0 Hz, 1H), 5.21 (s, 2H), 4.31 (dd, *J* = 6.0, 1.5 Hz, 2H), 3.98 (dd, *J* = 11.0, 6.0 Hz, 1H), 3.94 – 3.92 (m, 1H), 3.91 (s, 3H), 3.85 (s, 3H), 3.63 (q, *J* = 5.8 Hz, 1H), 3.50 (s, 3H).

MS (ESI) *m/z* (%): 403

HRMS (ESI) *m/z*: [M+K]⁺ calculated for C₂₂H₂₆O₇K: 441.1310; found: 441.1312.

(E)-3-(3-(acetoxymethyl)-7-methoxy-2-(3-methoxy-4-(methoxymethoxy)phenyl)-2,3-dihydrobenzofuran-5-yl)allyl acetate (1-122a)

Diol **1-118a** (0.41 g, 1.03 mmol, 1.0 equiv.) was dissolved in DCM (0.5 M, 4.1 mL), and solution was cooled to 0 °C. Then TEA (0.43 mL, 3.09 mmol, 3.0 equiv.) was added followed by acetyl chloride (0.16 mL, 2.27 mmol, 2.2 equiv.). The reaction mixture was stirred at room temperature overnight. Reaction was quenched by addition of water (30 mL). The aqueous layer was extracted with EtOAc (3 × 25 mL). The combined organic layers were washed with brine, dried over anhydrous Na₂SO₄, filtered, and concentrated *in vacuo*. The crude product was purified by column chromatography (SiO₂; petroleum ether/EtOAc = 4:1) to afford **1-122a** as a colorless oil (0.44 g, 88 %).

¹H NMR (500 MHz, Chloroform-d) δ (ppm): 7.10 (d, *J* = 8.3 Hz, 1H), 6.95 – 6.88 (m, 2H), 6.87 (s, 2H), 6.58 (d, *J* = 15.8 Hz, 1H), 6.14 (dt, *J* = 15.8, 6.6 Hz, 1H), 5.49 (d, *J* = 7.0 Hz, 1H), 4.69 (d, *J* = 6.6 Hz, 2H), 4.44 – 4.40 (m, 1H), 4.31 – 4.26 (m, 1H), 3.89 (s, 3H), 3.84 (s, 3H), 3.76 (q, *J* = 7.2 Hz, 1H), 3.48 (s, 3H), 2.08 (s, 3H), 2.03 (s, 3H).

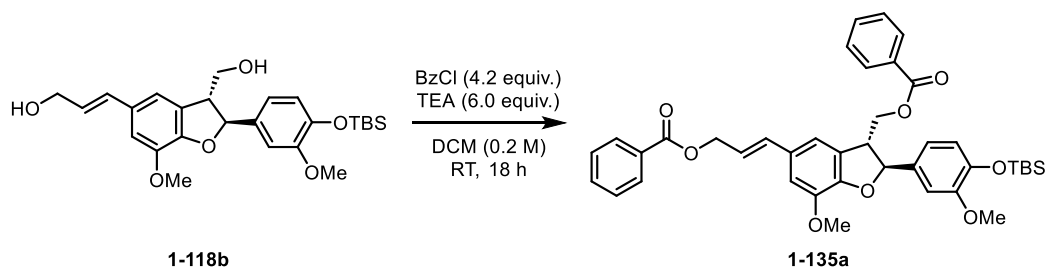
¹³C{¹H} NMR (126 MHz, Chloroform-d) δ (ppm): 170.9, 170.8, 150.0, 148.3, 146.6, 144.5, 134.6, 134.4, 130.6, 127.6, 121.2, 118.7, 116.2, 115.4, 115.4, 110.6, 109.6, 95.5, 88.5, 65.4, 65.3, 65.2, 56.2, 56.1, 56.0, 56.0, 55.9, 50.4, 21.1, 20.9.

MS (ESI) *m/z* (%): 487

HRMS (ESI) *m/z*: [M+K]⁺ calculated for C₂₆H₃₀O₉K: 525.1521; found: 525.1523.

1.7.2. Synthesis of dehydroquivesetinerviusin A and related compounds

(*E*)-3-(3-((benzoyloxy)methyl)-2-(4-((*tert*-butyldimethylsilyl)oxy)-3-methoxyphenyl)-7-methoxy-2,3-dihydrobenzofuran-5-yl)allyl benzoate (**1-135a**)

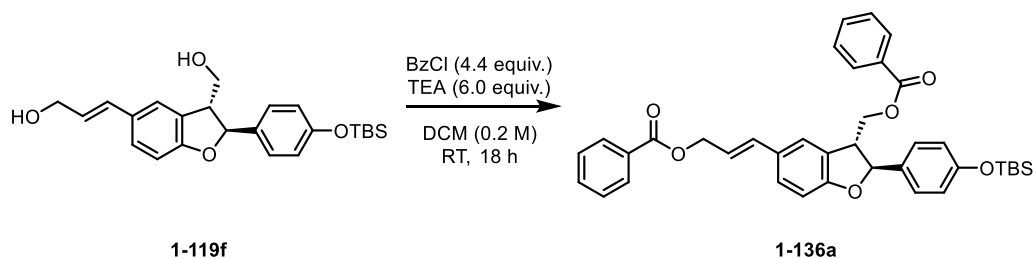


1-118b (0.3 g, 0.63 mmol, 1.0 equiv.) was dissolved in DCM (0.2 M, 3.1 mL), and solution was cooled to 0 °C. After 5 minutes TEA (0.53 mL, 3.77 mmol, 6.0 equiv.) and benzoyl chloride (0.32 mL, 2.76 mmol, 4.4 equiv.) was added to the solution. The solution was stirred at RT overnight. Reaction was quenched by addition of NH₄Cl (15 mL). The aqueous layer was extracted with DCM (3 × 20 mL). The combined organic layers were washed with brine, dried over anhydrous Na₂SO₄, filtered, and concentrated *in vacuo*. The crude product was purified by column chromatography (SiO₂; petroleum ether/EtOAc = 2:1) to afford **1-135a** as a white solid (0.18 g, 42 %).

¹H NMR (500 MHz, Chloroform-*d*) δ (ppm): 8.10 – 8.07 (m, 2H), 7.96 – 7.93 (m, 2H), 7.59 – 7.54 (m, 2H), 7.46 – 7.39 (m, 4H), 6.99 – 6.97 (m, 1H), 6.92 (d, *J* = 1.5 Hz, 1H), 6.87 – 6.84 (m, 2H), 6.80 – 6.77 (m, 1H), 6.71 – 6.66 (m, 1H), 6.27 (dt, *J* = 15.7, 6.5 Hz, 1H), 5.59 (d, *J* = 7.3 Hz, 1H), 4.97 (dd, *J* = 6.6, 1.2 Hz, 2H), 4.71 (dd, *J* = 11.2, 5.4 Hz, 1H), 4.54 (dd, *J* = 11.1, 7.9 Hz, 1H), 3.99 – 3.95 (m, 1H), 3.92 (s, 3H), 3.70 (s, 3H), 0.98 (s, 9H), 0.12 (s, 6H).

MS (ESI) *m/z* (%): 680 [M+H]⁺ (100).

(*E*)-3-(3-((benzyloxy)methyl)-2-(4-((*tert*-butyldimethylsilyl)oxy)phenyl)-2,3-dihydrobenzofuran-5-yl)allyl benzoate (**1-136a**)



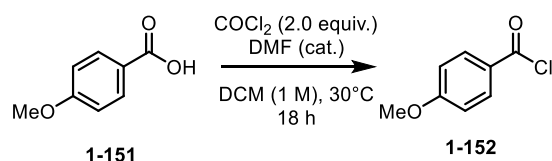
1-119f (0.25 g, 0.61 mmol, 1.0 equiv.) was dissolved in DCM (0.2 M, 3.1 mL), and solution was cooled to 0 °C. After 5 minutes TEA (0.51 mL, 3.64 mmol, 6.0 equiv.) and benzoyl chloride (0.31 mL, 2.76 mmol, 4.4 equiv.) was added to the solution. The solution was stirred at RT overnight. Reaction was quenched by addition of NH₄Cl (15 mL). The aqueous layer was extracted with DCM (3 × 20 mL). The combined organic layers were washed with brine, dried over anhydrous Na₂SO₄, filtered, and concentrated *in vacuo*. The crude product was purified by column chromatography (SiO₂; petroleum ether/EtOAc = 2:1) to afford **1-136a** as a white solid (0.21 g, 54 %).

¹H NMR (500 MHz, Chloroform-*d*) δ (ppm): 8.10 – 8.07 (m, 2H), 7.99 – 7.93 (m, 2H), 7.59 – 7.53 (m, 2H), 7.47 – 7.40 (m, 4H), 7.38 (t, *J* = 1.4 Hz, 1H), 7.29 (dd, *J* = 8.2, 1.9 Hz, 1H), 7.26 – 7.23 (m, 2H), 6.86 (d, *J* = 8.3 Hz, 1H), 6.83 – 6.77 (m, 2H), 6.70 (d, *J* = 15.8 Hz, 1H), 6.25 (dt, *J* = 15.8, 6.6 Hz, 1H), 5.56 (d, *J* = 6.6 Hz, 1H), 4.98 – 4.94 (m, 2H), 4.69 (dd, *J* = 11.1, 5.5 Hz, 1H), 4.55 (dd, *J* = 11.1, 7.8 Hz, 1H), 3.89 (q, *J* = 6.6 Hz, 1H), 0.97 (s, 9H), 0.18 (s, 6H).

¹³C{¹H} NMR (126 MHz, Chloroform-*d*) δ (ppm): 166.6, 166.5, 160.1, 156.0, 134.4, 133.5, 133.4, 133.1, 130.4, 129.80, 129.77, 129.67, 128.7, 128.6, 128.5, 127.4, 127.1, 122.9, 121.0, 120.5, 109.9, 88.2, 66.4, 65.9, 50.1, 25.8, 18.3, -4.3.

MS (ESI) *m/z* (%): 620 [M+H]⁺ (100).

HRMS (ESI) *m/z*: [M+NH₄]⁺ calculated for C₃₈H₄₄NO₆Si: 638.2932; found: 638.2947.

4-methoxybenzoyl chloride (**1-152**)

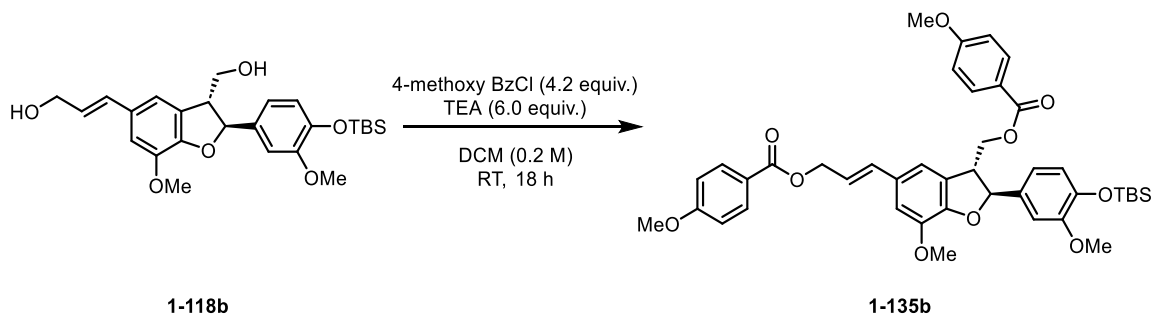
To the solution of 4-methoxybenzoic acid **1-151** (1 g, 7.24 mmol, 1.0 equiv.) in DCM (1 M, 7.24 mL) was added oxalyl chloride (1.26 mL, 14.5 mmol, 2.0 equiv.) and few drops of DMF. The solution was warmed to 30 °C and left stirring overnight. Next day reaction evaporated to dryness. The crude product **1-152** was used in the next step without further purification.

¹H NMR (500 MHz, Chloroform-d) δ (ppm): 8.08 (dd, *J* = 8.9, 1.9 Hz, 2H), 6.99 – 6.93 (m, 2H), 3.90 (s, 3H).

¹³C{¹H} NMR (126 MHz, Chloroform-d) δ (ppm): 167.3, 165.5, 134.2, 125.6, 114.4, 55.9.

MS (ESI) *m/z* (%): 170 [M+H]⁺ (100).

(E)-3-(2-(4-((*tert*-butyldimethylsilyl)oxy)-3-methoxyphenyl)-7-methoxy-3-(((4-methoxybenzoyl)oxy)methyl)-2,3-dihydrobenzofuran-5-yl)allyl 4-methoxybenzoate (**1-135b**)



1-118b (0.2 g, 0.42 mmol, 1.0 equiv.) was dissolved in DCM (0.2 M, 4.2 mL), and solution was cooled to 0 °C. After 5 minutes TEA (0.35 mL, 2.51 mmol, 6.0 equiv.) and **1-152** (0.3 g, 1.76 mmol, 4.2 equiv.) was added to the solution. The solution was stirred at RT overnight. Reaction was quenched by addition of NH₄Cl (15 mL). The aqueous layer was extracted with DCM (3 × 20 mL). The combined organic layers were washed with brine, dried over anhydrous Na₂SO₄, filtered, and concentrated *in vacuo*. The crude product was purified by column chromatography (SiO₂; petroleum ether/EtOAc = 2:1) to afford **1-135b** as a white solid (0.19 g, 62 %).

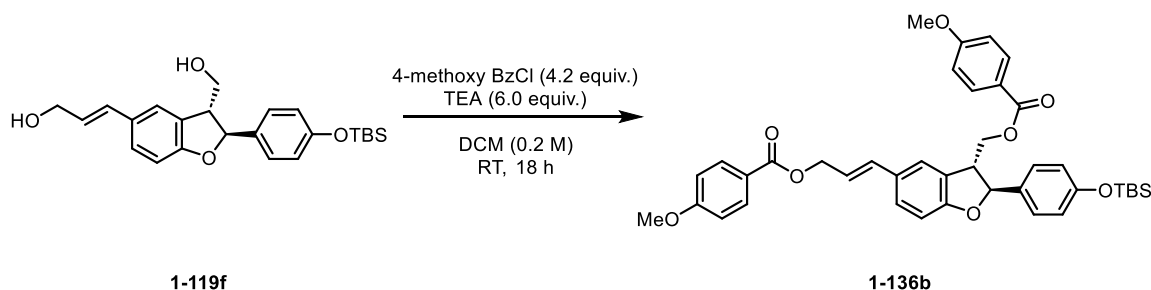
¹H NMR (500 MHz, Chloroform-d) δ (ppm): 8.05 – 8.02 (m, 2H), 7.91 – 7.87 (m, 2H), 7.00 – 6.95 (m, 2H), 6.95 – 6.91 (m, 3H), 6.90 – 6.87 (m, 2H), 6.87 – 6.84 (m, 2H), 6.79 (d, *J* = 7.9 Hz,

1H), 6.69 – 6.64 (m, 1H), 6.26 (dt, $J = 15.8, 6.5$ Hz, 1H), 5.57 (d, $J = 7.3$ Hz, 1H), 4.93 (dd, $J = 6.6, 1.3$ Hz, 2H), 4.68 (dd, $J = 11.1, 5.3$ Hz, 1H), 4.50 (dd, $J = 11.1, 8.0$ Hz, 1H), 3.92 (s, 3H), 3.87 (s, 3H), 3.85 (s, 3H), 3.70 (s, 3H), 0.98 (s, 9H), 0.12 (s, 6H).

$^{13}\text{C}\{^1\text{H}\}$ NMR (126 MHz, Chloroform- d) δ (ppm): 166.4, 166.2, 163.7, 163.5, 151.2, 148.5, 145.4, 144.6, 134.3, 133.9, 133.0, 132.5, 131.8, 130.7, 127.9, 122.8, 122.2, 121.6, 121.0, 119.1, 115.5, 114.3, 113.84, 113.76, 110.6, 110.3, 89.5, 66.0, 65.6, 56.1, 55.6, 55.5, 50.6, 25.8, 18.6, -4.5.

MS (ESI) m/z (%): 740 $[\text{M}+\text{H}]^+$ (100).

(E)-3-(2-(4-((*tert*-butyldimethylsilyl)oxy)phenyl)-3-(((4-methoxybenzoyl)oxy)methyl)-2,3-dihydrobenzofuran-5-yl)allyl 4-methoxybenzoate (**1-136b**)



1-119f (0.21 g, 0.52 mmol, 1.0 equiv.) was dissolved in DCM (0.2 M, 5.2 mL), and solution was cooled to 0 °C. After 5 minutes TEA (0.44 mL, 3.14 mmol, 6.0 equiv.) and **1-152** (0.38 g, 2.2 mmol, 4.2 equiv.) was added to the solution. The solution was stirred at RT overnight. Reaction was quenched by addition of NH_4Cl (15 mL). The aqueous layer was extracted with DCM (3 × 20 mL). The combined organic layers were washed with brine, dried over anhydrous Na_2SO_4 , filtered, and concentrated *in vacuo*. The crude product was purified by column chromatography (SiO_2 ; petroleum ether/EtOAc = 2:1) to afford **1-136b** as a white solid (0.19 g, 62 %).

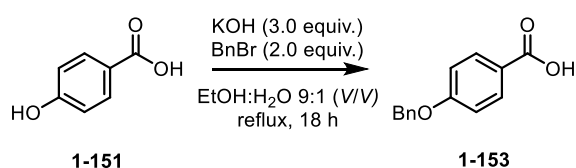
^1H NMR (500 MHz, Chloroform- d) δ (ppm): 8.04 – 8.02 (m, 2H), 7.92 – 7.87 (m, 2H), 7.38 – 7.35 (m, 1H), 7.28 (dd, $J = 8.3, 1.9$ Hz, 1H), 7.25 – 7.22 (m, 2H), 6.93 – 6.89 (m, 4H), 6.85 (d, $J = 8.3$ Hz, 1H), 6.82 – 6.78 (m, 2H), 6.68 (dd, $J = 15.9, 1.4$ Hz, 1H), 6.25 (dt, $J = 15.9, 6.6$ Hz, 1H), 5.55 (d, $J = 6.6$ Hz, 1H), 4.92 (dd, $J = 6.6, 1.3$ Hz, 2H), 4.66 (dd, $J = 11.0, 5.5$ Hz, 1H), 4.51 (dd, $J = 11.1, 7.8$ Hz, 1H), 3.86 (s, 3H), 3.85 (s, 3H), 0.97 (s, 9H), 0.18 (s, 6H).

$^{13}\text{C}\{^1\text{H}\}$ NMR (126 MHz, Chloroform- d) δ (ppm): 166.4, 166.2, 163.7, 163.5, 160.0, 156.0, 134.1, 133.0, 132.5, 131.8, 129.8, 128.6, 127.4, 127.2, 122.9, 122.8, 122.2, 121.2, 120.4, 117.2, 114.3, 113.9, 113.7, 109.9, 66.1, 65.7, 55.6, 25.8, 18.3, -4.3.

MS (ESI) m/z (%): 680 $[\text{M}+\text{H}]^+$ (100).

HRMS (ESI) m/z : $[\text{M}+\text{H}]^+$ calculated for $\text{C}_{40}\text{H}_{45}\text{O}_8\text{Si}$: 681.2878; found: 681.2880.

4-(benzyloxy)benzoic acid (**1-153**)



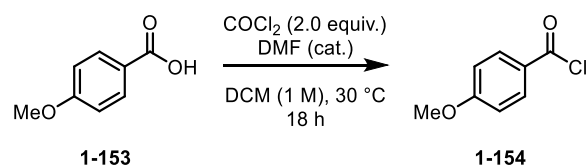
KOH (2.38 g, 86.7 mmol, 3.0 equiv.) and benzyl bromide (6.91 mL, 57.8 mmol, 2.0 equiv.) were added to a solution of 4-hydroxybenzoic acid **1-151** (4 g, 28.9 mmol, 1.0 equiv.) in EtOH:H₂O 9:1 (90:10 mL). The mixture was heated under reflux for 20 h. Next a 20% KOH solution (20 mL) was added, and the mixture was maintained under reflux for another 4 h. The mixture was then diluted with H₂O (60 mL) and acidified with 20% HCl solution. The precipitate formed was filtered and washed with water and *n*-hexane to give the pure **1-153** as a white solid (6.6g, 99 %).

^1H NMR (500 MHz, DMSO- d_6) δ (ppm): 7.47 – 7.40 (m, 2H), 7.04 – 6.99 (m, 2H), 6.99 – 6.92 (m, 2H), 6.91 – 6.87 (m, 1H), 6.68 – 6.62 (m, 2H), 4.73 (s, 2H).

$^{13}\text{C}\{^1\text{H}\}$ NMR (126 MHz, DMSO- d_6) δ (ppm): 167.0, 162.0, 136.6, 131.4, 128.5, 128.1, 127.9, 123.2, 114.6, 69.5.

MS (ESI) m/z (%): 228 $[\text{M}+\text{H}]^+$ (100).

HRMS (ESI) m/z : $[\text{M}+\text{NH}_4]^+$ calculated for $\text{C}_{14}\text{H}_{13}\text{O}_3$: 229.0859; found: 229.0861.

4-(benzyloxy)benzoyl chloride (**1-154**)

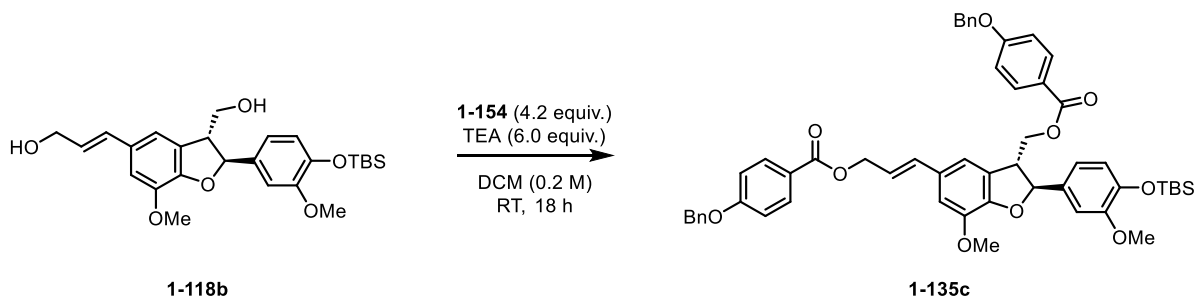
To the solution of **1-153** (0.5 g, 2.17 mmol, 1.0 equiv.) in DCM (1 M, 4.34 mL) was added oxalyl chloride (0.38 mL, 4.34 mmol, 2 equiv.) and few drops of DMF. The solution was warmed to 30 °C and left stirring overnight. Next day reaction evaporated to dryness. The crude **1-154** product was used in the next step without further purification.

¹H NMR (500 MHz, Chloroform-d) δ (ppm): 8.12 – 8.06 (m, 2H), 7.47 – 7.40 (m, 4H), 7.06 – 7.01 (m, 2H), 5.16 (s, 2H).

¹³C{¹H} NMR (126 MHz, Chloroform-d) δ (ppm): 167.3, 164.6, 135.7, 134.2, 128.9, 128.6, 127.7, 125.8, 115.2, 70.6.

MS (ESI) m/z (%): 246 [M+H]⁺ (100).

(E)-3-(3-(((4-(benzyloxy)benzoyl)oxy)methyl)-2-(4-((*tert*-butyldimethylsilyl)oxy)-3-methoxyphenyl)-7-methoxy-2,3-dihydrobenzofuran-5-yl)allyl 4-(benzyloxy)benzoate (**1-135c**)



1-118b (0.5 g, 1.05 mmol, 1.0 equiv.) was dissolved in DCM (0.2 M, 21 mL), and solution was cooled to 0 °C. After 5 minutes TEA (0.88 mL, 6.28 mmol, 6.0 equiv.) and **1-154** (1.15 g, 4.61 mmol, 4.2 equiv.) was added to the solution. The solution was stirred at RT overnight. Reaction was quenched by addition of NH₄Cl (15 mL). The aqueous layer was extracted with DCM (3 × 20 mL). The combined organic layers were washed with brine, dried over anhydrous Na₂SO₄, filtered, and concentrated *in vacuo*. The crude product was purified by gradient column chromatography (SiO₂; petroleum ether/EtOAc = 10:1 → 2:1) to afford **1-135c** as a white solid (0.55 g, 61 %).

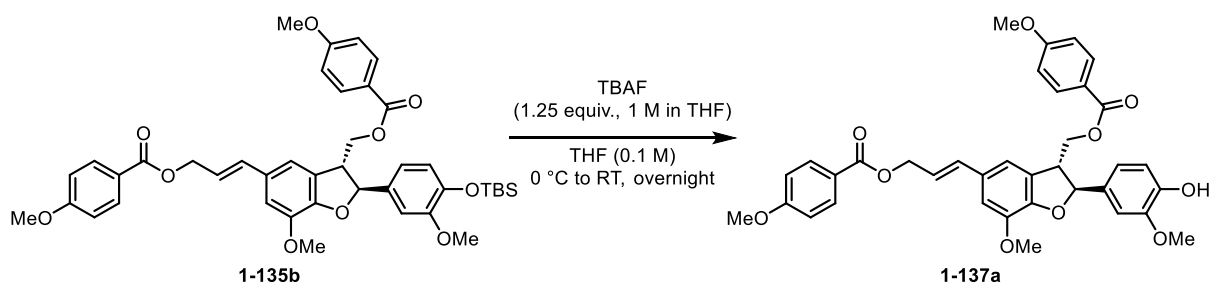
¹H NMR (500 MHz, Chloroform-d) δ (ppm): 8.06 – 8.02 (m, 2H), 7.92 – 7.88 (m, 2H), 7.44 – 7.38 (m, 8H), 7.36 – 7.33 (m, 2H), 7.01 – 6.95 (m, 5H), 6.92 (s, 1H), 6.89 – 6.83 (m, 2H), 6.82 –

6.77 (m, 1H), 6.67 (d, $J = 15.6$ Hz, 1H), 6.26 (dt, $J = 16.0, 6.5$ Hz, 1H), 5.58 (d, $J = 7.3$ Hz, 1H), 5.11 (d, $J = 2.8$ Hz, 4H), 4.93 (d, $J = 6.5$ Hz, 2H), 4.68 (dd, $J = 11.1, 5.3$ Hz, 1H), 4.50 (dd, $J = 11.1, 7.9$ Hz, 1H), 3.98 – 3.93 (m, 1H), 3.92 (s, 3H), 3.69 (s, 3H), 0.98 (s, 9H), 0.13 (s, 6H).

$^{13}\text{C}\{^1\text{H}\}$ NMR (126 MHz, Chloroform- d) δ (ppm): 166.3, 166.1, 162.8, 162.7, 151.2, 148.5, 145.4, 144.6, 136.35, 136.28, 134.3, 133.9, 132.0, 131.9, 130.7, 128.8, 128.39, 128.36, 127.8, 127.64, 127.62, 123.0, 122.4, 121.6, 121.0, 119.0, 115.5, 114.7, 114.6, 114.5, 110.7, 110.2, 89.4, 70.2, 66.0, 65.6, 56.1, 55.5, 50.6, 29.8, 25.8, 25.8, 18.6, -4.5.

MS (ESI) m/z (%): 893 $[\text{M}+\text{H}]^+$ (100).

(*E*)-3-(2-(4-hydroxy-3-methoxyphenyl)-7-methoxy-3-(((4-methoxybenzoyl)oxy)methyl)-2,3-dihydrobenzofuran-5-yl)allyl 4-methoxybenzoate (**1-137a**)

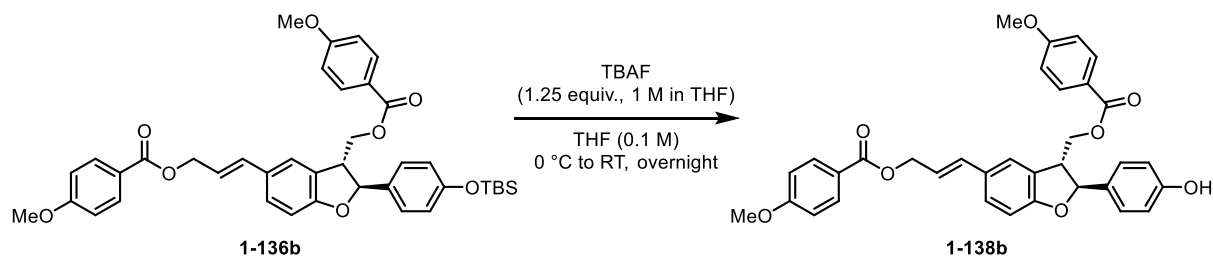


1-135b (0.185 g, 0.247 mmol, 1.0 equiv.) was dissolved in THF (0.1 M, 2.5 mL), and solution was cooled to 0 °C. After 5 minutes TBAF (0.309 mL, 0.309 mmol, 1 M, 1.25 equiv.) was added and the solution was stirred at RT overnight. Reaction was quenched by addition of NH_4Cl (15 mL). The aqueous layer was extracted with DCM (3×15 mL). The combined organic layers were washed with brine, dried over anhydrous Na_2SO_4 , filtered, and concentrated *in vacuo*. The crude product was purified by gradient column chromatography (SiO_2 ; petroleum ether/EtOAc = 4:1 \rightarrow 1:1) to afford **1-137a** (0.092 g, 59 %).

^1H NMR (500 MHz, Chloroform- d) δ (ppm): 8.05 – 8.02 (m, 2H), 7.90 – 7.86 (m, 2H), 6.97 (d, $J = 1.4$ Hz, 1H), 6.95 – 6.85 (m, 9H), 6.67 (d, $J = 15.8$ Hz, 1H), 6.30 – 6.24 (m, 1H), 5.61 (s, 1H), 5.57 (d, $J = 7.4$ Hz, 1H), 4.93 (dd, $J = 6.6, 1.3$ Hz, 2H), 4.68 (dd, $J = 11.2, 5.4$ Hz, 1H), 4.50 (dd, $J = 11.1, 7.9$ Hz, 1H), 3.92 (s, 3H), 3.87 (s, 3H), 3.85 (s, 3H), 3.79 (s, 3H).

$^{13}\text{C}\{^1\text{H}\}$ NMR (126 MHz, Chloroform- d) δ (ppm): 166.4, 166.2, 163.7, 163.5, 148.4, 146.8, 145.9, 144.6, 134.3, 132.43, 132.40, 131.8, 130.7, 127.8, 122.8, 122.1, 121.7, 119.8, 115.5, 114.4, 113.93, 113.91, 113.83, 113.75, 110.6, 108.8, 89.4, 65.9, 65.6, 56.1, 56.0, 55.61, 55.58, 50.7.

MS (ESI) m/z (%): 627 $[\text{M}+\text{H}]^+$ (100); HRMS (ESI) m/z : $[\text{M}+\text{NH}_4]^+$ calculated for $\text{C}_{36}\text{H}_{38}\text{O}_{10}\text{N}$: 644.2490; found: 644.2504.

(E)-3-(2-(4-hydroxyphenyl)-3-(((4-methoxybenzoyl)oxy)methyl)-2,3-dihydrobenzofuran-5-yl)allyl 4-methoxybenzoate (1-138b)

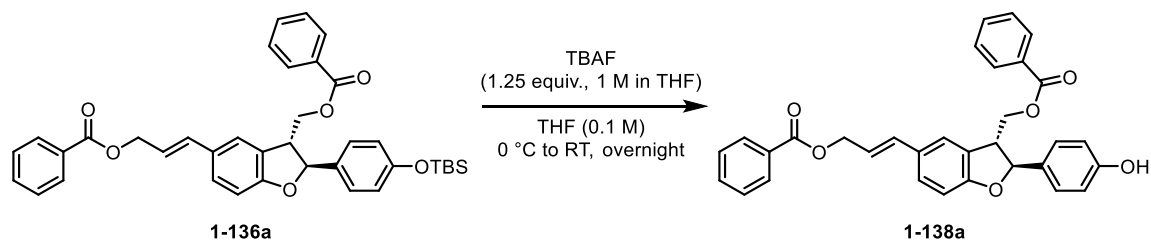
1-136b (0.1 g, 0.15 mmol, 1.0 equiv.) was dissolved in THF (0.2 M, 0.7 mL), and solution was cooled to 0 °C. After 5 minutes TBAF-3H₂O (0.05g, 0.18 mmol, 1.25 equiv.) was added and the solution was stirred at RT overnight. Reaction was quenched by addition of NH₄Cl (15 mL). The aqueous layer was extracted with DCM (3 × 15 mL). The combined organic layers were washed with brine, dried over anhydrous Na₂SO₄, filtered, and concentrated *in vacuo*. The crude product was purified by gradient column chromatography (SiO₂; petroleum ether/EtOAc = 3:1 → 2:1) to afford **1-138b** (0.059 g, 71 %).

¹H NMR (500 MHz, Chloroform-d) δ (ppm): 8.03 (d, *J* = 9.0 Hz, 2H), 7.90 (d, *J* = 8.8 Hz, 2H), 7.36 (d, *J* = 1.8 Hz, 1H), 7.27 (t, *J* = 8.8 Hz, 3H), 6.92 (d, *J* = 8.1 Hz, 2H), 6.90 (d, *J* = 8.1 Hz, 2H), 6.85 (d, *J* = 8.3 Hz, 1H), 6.81 (d, *J* = 8.5 Hz, 2H), 6.68 (d, *J* = 15.8 Hz, 1H), 6.25 (dt, *J* = 15.8, 6.5 Hz, 1H), 5.55 (d, *J* = 6.5 Hz, 1H), 4.92 (dd, *J* = 6.6, 1.2 Hz, 2H), 4.76 (s, 1H), 4.66 (dd, *J* = 11.0, 5.5 Hz, 1H), 4.51 (dd, *J* = 11.0, 7.8 Hz, 1H), 3.86 (s, 3H), 3.86 (s, 3H).

¹³C{¹H} NMR (126 MHz, Chloroform-d) δ (ppm): 166.4, 166.3, 163.7, 163.5, 160.0, 155.9, 134.1, 133.1, 131.8, 129.8, 128.6, 127.7, 127.1, 122.9, 122.8, 122.1, 121.2, 115.7, 113.9, 113.7, 109.9, 88.1, 66.1, 65.7, 55.60, 55.57, 50.2.

MS (ESI) *m/z* (%): 565 [M-H]⁻ (100).

HRMS (ESI) *m/z*: [M-H]⁻ calculated for C₃₄H₂₉O₈: 565.1868; found: 565.1868.

(E)-3-(3-((benzyloxy)methyl)-2-(4-hydroxyphenyl)-2,3-dihydrobenzofuran-5-yl)allylbenzoate (**1-138a**)

1-136a (0.5 g, 0.727 mmol, 1.0 equiv.) was dissolved in THF (0.1 M, 7.27 mL), and solution was cooled to 0 °C. After 5 minutes TBAF (0.909 mL, 1 M, 0.18 mmol, 1.25 equiv.) was added and the solution was stirred at RT overnight. Reaction was quenched by the addition of NH₄Cl (25 mL). The aqueous layer was extracted with DCM (3 × 30 mL). The combined organic layers were washed with brine, dried over anhydrous Na₂SO₄, filtered, and concentrated *in vacuo*. The crude product was purified by column chromatography (SiO₂; petroleum ether/EtOAc = 2:1) to afford **1-138a** (0.363 g, 88 %).

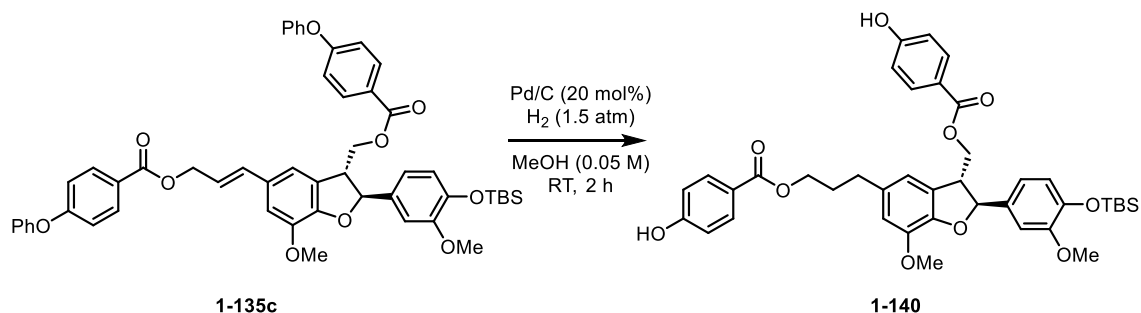
¹H NMR (500 MHz, Chloroform-d) δ (ppm): 8.09 – 8.05 (m, 2H), 7.96 – 7.92 (m, 2H), 7.58 – 7.53 (m, 2H), 7.47 – 7.41 (m, 4H), 7.37 (s, 1H), 7.31 – 7.29 (m, 1H), 7.28 – 7.24 (m, 2H), 6.86 (d, *J* = 8.3 Hz, 1H), 6.83 – 6.79 (m, 2H), 6.70 (d, *J* = 15.8 Hz, 1H), 6.25 (dt, *J* = 15.9, 6.6 Hz, 1H), 5.55 (d, *J* = 6.5 Hz, 1H), 5.12 (s, 1H), 4.96 (d, *J* = 6.6 Hz, 2H), 4.69 (dd, *J* = 11.1, 5.5 Hz, 1H), 4.54 (dd, *J* = 11.1, 7.8 Hz, 1H), 3.88 (q, *J* = 6.5 Hz, 1H).

¹³C{¹H} NMR (126 MHz, Chloroform-d) δ (ppm): 166.7, 166.5, 160.0, 156.0, 134.4, 133.4, 133.2, 133.0, 130.3, 129.81, 129.77, 129.7, 128.7, 128.6, 128.5, 127.7, 127.0, 122.9, 121.0, 115.7, 109.9, 88.1, 66.4, 66.0, 50.1.

MS (ESI) *m/z* (%): 507 [M+H]⁺ (100).

HRMS (ESI) *m/z*: [M+NH₄]⁺ calculated for C₃₂H₃₀O₆N: 524.2068; found: 524.2072.

3-(2-(4-((*tert*-butyldimethylsilyl)oxy)-3-methoxyphenyl)-3-(((4-hydroxybenzoyl)oxy)methyl)-7-methoxy-2,3-dihydrobenzofuran-5-yl)propyl 4-hydroxybenzoate (**1-140**)



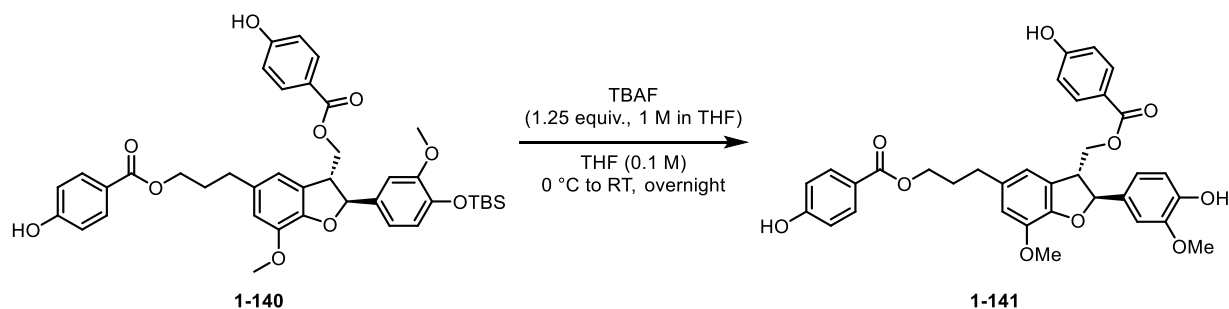
1-135c (0.113 g, 0.127 mmol, 1.0 equiv.) was dissolved in MeOH (0.05 M, 2.53 mL), and 20mol% Pd/C (0.027 g, 0.0025 mmol, 0.2 equiv.) was added under Argon atmosphere. Then the Argon atmosphere was changed for Hydrogen atmosphere (1 atm) and the solution was stirred at RT overnight. Reaction mixture was filtered through[®], filter cake was washed by EtOAc (2x 10 mL), and solvent was concentrated *in vacuo*. The crude product was purified by column chromatography (SiO₂; petroleum ether/EtOAc = 2:1) to afford **1-140** (0.067 g, 47 %).

¹H NMR (500 MHz, Chloroform-d) δ (ppm): 7.94 – 7.91 (m, 2H), 7.85 – 7.81 (m, 2H), 6.90 – 6.77 (m, 5H), 6.69 (d, *J* = 19.0 Hz, 2H), 5.97 (bs, 2H), 5.52 (d, *J* = 7.6 Hz, 1H), 4.66 – 4.61 (m, 1H), 4.53 – 4.46 (m, 1H), 4.34 – 4.29 (m, 2H), 3.92 (q, *J* = 7.2 Hz, 1H), 3.87 (s, 3H), 3.71 (d, *J* = 1.4 Hz, 3H), 2.09 – 2.03 (m, 2H), 0.98 – 0.97 (m, 9H), 0.13 – 0.12 (m, 6H).

¹³C{¹H} NMR (126 MHz, Chloroform-d) δ (ppm): 166.8, 166.4, 160.4, 160.2, 151.2, 146.4, 145.2, 144.3, 135.1, 134.2, 132.1, 132.0, 127.5, 122.8, 122.2, 121.0, 119.2, 116.4, 115.5, 115.4, 112.6, 110.4, 89.0, 66.2, 64.3, 56.1, 55.6, 50.8, 32.4, 30.8, 25.8, 18.6, -4.5.

MS (ESI) *m/z* (%): 515 [M+H]⁺ (100).

HRMS (ESI) *m/z*: [M-H]⁻ calculated for C₄₀H₄₅O₁₀Si: 713.2788; found: 713.2794.

3-(2-(4-hydroxy-3-methoxyphenyl)-3-(((4-hydroxybenzoyl)oxy)methyl)-7-methoxy-2,3-dihydrobenzofuran-5-yl)propyl 4-hydroxybenzoate (**1-141**)

1-140 (0.056 g, 0.078 mmol, 1.0 equiv.) was dissolved in THF (0.1 M, 0.78 mL), and solution was cooled to 0 °C. After 5 minutes TBAF-3H₂O (0.031 g, 0.098 mmol, 1.25 equiv.) was added and the solution was stirred at RT overnight. Reaction was quenched by addition of NH₄Cl (5 mL). The aqueous layer was extracted with EtOAc (3 × 15 mL). The combined organic layers were washed with brine, dried over anhydrous Na₂SO₄, filtered, and concentrated *in vacuo*. The crude product was purified by gradient column chromatography (SiO₂; petroleum ether/EtOAc = 2:1 → 1:2, 1% AcOH) to afford **1-141** (0.022 g, 47 %).

¹H NMR (500 MHz, Chloroform-d) δ (ppm): 7.93 (d, *J* = 8.4 Hz, 2H), 7.80 (d, *J* = 8.4 Hz, 2H), 6.93 – 6.90 (m, 2H), 6.88 – 6.84 (m, 3H), 6.82 – 6.78 (m, 2H), 6.71 (s, 1H), 6.68 (s, 1H), 5.50 (d, *J* = 7.6 Hz, 1H), 4.64 (dd, *J* = 11.0, 5.5 Hz, 1H), 4.49 (dd, *J* = 11.0, 7.7 Hz, 1H), 4.31 (t, *J* = 6.4 Hz, 2H), 3.95 – 3.88 (m, 1H), 3.87 (s, 3H), 3.79 (s, 3H), 2.73 (t, *J* = 7.6 Hz, 2H), 2.09 – 2.02 (m, 2H).

¹³C{¹H} NMR (126 MHz, Chloroform-d) δ (ppm): 166.6, 166.3, 160.3, 160.1, 146.8, 146.4, 145.8, 144.3, 135.1, 132.6, 132.1, 132.0, 127.6, 122.9, 122.2, 119.8, 116.4, 115.43, 115.40, 114.4, 112.6, 108.9, 89.1, 66.0, 64.2, 56.1, 56.0, 50.8, 32.4, 30.8.

MS (ESI) *m/z* (%): 599 [M-H]⁻ (100).

HRMS (ESI) *m/z*: [M-H]⁻ calculated for C₃₄H₃₁O₁₀: 599.1912; found: 599.1927.

CHAPTER II

2. Nitro fatty acids

2.1. Nitro Fatty Acids: An Introduction

Nitro fatty acids (**NO₂FAs**) and the corresponding nitrated lipids belong to a class of compounds formed endogenously by reaction of unsaturated fatty acids (UFAs) with reactive nitrogen species (for example, monoxide radical (NO·) or nitrite anions (NO₂⁻)). These highly reactive nitrated organic species have been found in tissues and biological fluids of mammals; however, the most interesting is the fact that **NO₂FA** were found mainly in the brain. They have also been reported to form in healthy human plasma and urine.^{82,83} Examples of nitrated FAs are shown in **Figure 31**.

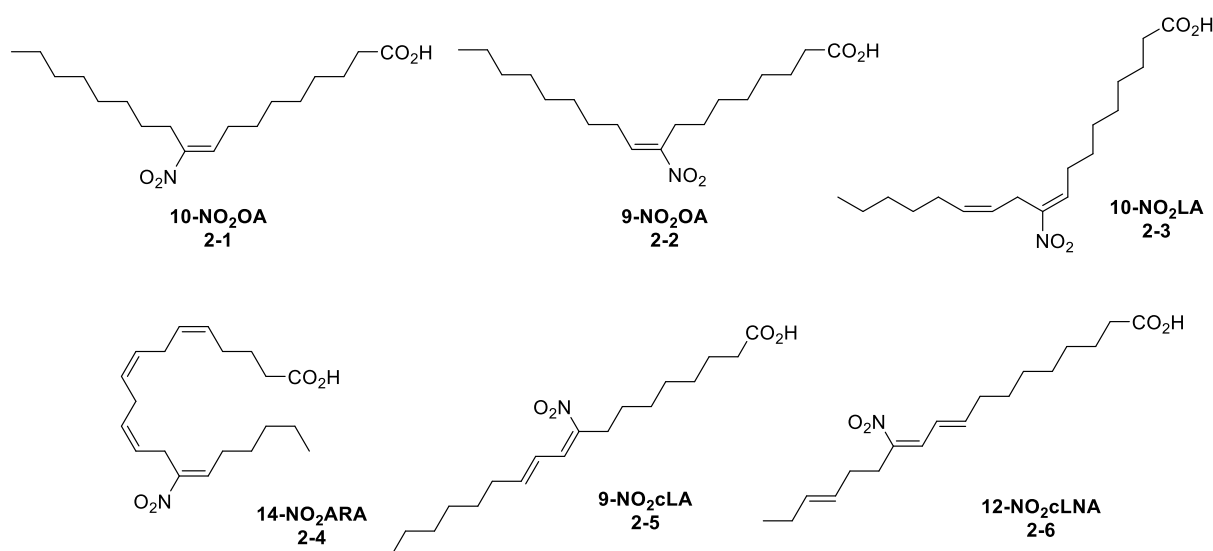
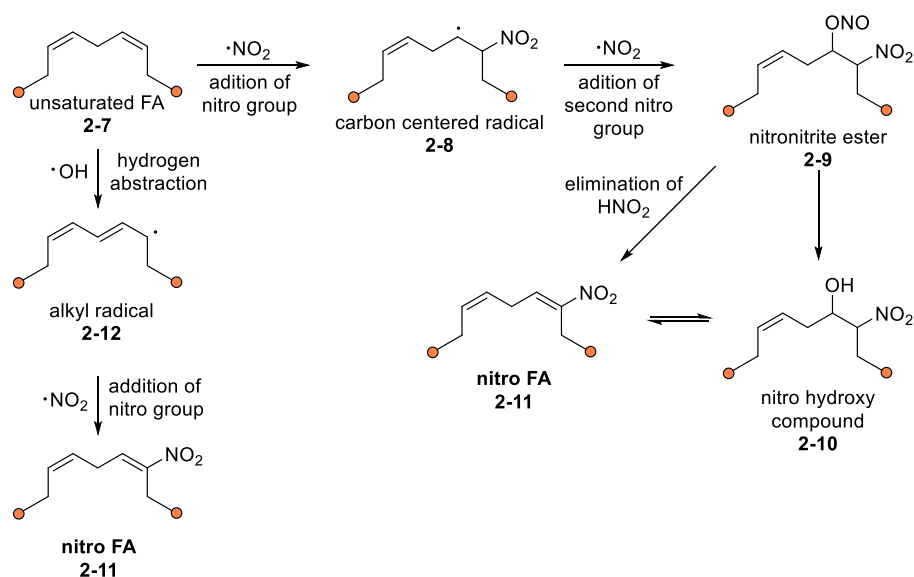


Figure 31: Examples of different NO₂FAs detected in mammals. Structure of 9- and 10-NO₂ oleic acid **2-1** and **2-2**, 10-NO₂ linoleic acid **2-3**, 14-NO₂ arachidonic acid **2-4**, 9-NO₂ conjugated linoleic acid **2-5** (nitro rumenic acid) and 12-NO₂ octadeca-9,11,15-trienoic acid **2-6** (nitro rumenelic acid).

From advanced studies, it is known that **NO₂FAs** are generated from fatty acids (**FAs**) by nitration in hydrophobic compartments such as the lipid bilayer of cellular membranes or the lipophilic core of lipoproteins,⁸⁴ and during digestion^{85,86}. Reactive nitrogen species can modify unsaturated **FA** and produce various derivatives of **FA** that contain functional groups of hydroxyl, hydroperoxy, nitro, and nitrohydroxy functional groups.⁸⁴ Although, the exact formation of **NO₂FAs** *in vivo* remains unknown, two different mechanisms were proposed. One mechanism suggests that the first generation of carbon-centered radical **2-8** is formed which is further transformed to nitronitrite **2-9** and nitrohydroxy **2-10** compounds. The further elimination of nitrous acid (HNO₂) or water yields the final product, **NO₂FA**

derivative **2-11 (Scheme 22)**. The second mechanism involves the formation of the alkyl radical **2-12** that further undergoes to the addition of nitro group addition.^{87,88}



Scheme 22: Endogenous nitration of UFAs.⁸⁷

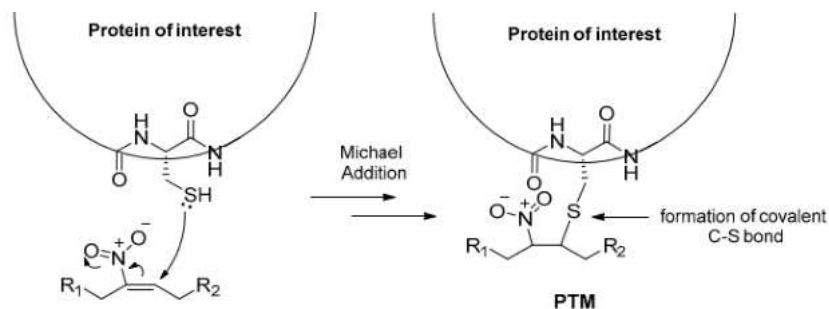
In general, the structure of **NO₂FAs** contains at least one nitro olefinic bond, giving them a property of Michael acceptors. Therefore, these compounds are highly reactive to nucleophiles and can react endogenously with Michael donors forming a covalent Michael addition product. Such donors (nucleophiles) are, for example, the amino acids cysteine and lysine.^{89–91}

2.1.1. Biological activity

The presence of Michael acceptor motive within the **NO₂FAs** structure predetermines that **NO₂FAs** should be expected to be a highly reactive species. And, as a consequence, various biological activities observed in the presence of **NO₂FAs** are attributed to these structures. For example, they form adducts with cysteine residues due to the high nucleophilic reactivity of the $-\text{SH}$ group. This formation of adducts between cysteine and **NO₂FAs** plays a crucial role in many biochemical pathways that result in the activation of Nrf2. This activation induces the expression of genes responsible for antioxidant and cell protection function and induces anti-inflammatory cell signaling.^{87,92–94} Addition of cysteine residues from a protein of interest causes structural change in protein and its function. This change

Chapter II: Biological activity

is called post-translation modification (**Scheme 23**).⁸⁷ Therefore, **NO₂FAs** are expected to be a Nrf2 activator.



Scheme 23: Post-translational modification of protein of interest (adapted from⁸⁷).

NO₂FAs are also reported to interact with p65 and p50 cysteine residues of nuclear factor κ B preventing the formation of various pro-inflammatory mediators responsible for diseases such as vascular inflammation and pro-fibrotic responses.⁹⁵ They also interact with regulatory proteins, such as keep-1 and peroxisome proliferator-activated receptor γ (PPAR γ), heat shock proteins, 5-lipoxygenase, and others, in order to regulate many diseases.^{95–98} To understand the way **NO₂FAs** interact with proteins is the foremost priority for the SAR to maximize the therapeutic effect of **NO₂FAs** and minimize harmful side effects.

One of the most studied **NO₂FAs** is 10-NO₂ oleic acid **2-1** (clinical name CXA-10, or generally 10-NO₂OA) was already in **PHASE II** clinical studies against pulmonary arterial hypertension, focal segmental glomerulosclerosis, and asthma. 10-NO₂OA **2-1** was also reported to significantly increase the antiproliferative effects of some known antineoplastic DNA damaging agents such as olaparib **2-13**, cisplatin **2-14**, and doxorubicin **2-15** against triple negative breast cancer (**Figure 32**).⁹⁹ 10-NO₂OA significantly reduces the growth of triple negative breast cancer epithelial cells by inhibiting the nuclear factor kappa-light chain enhancer of the activated B cells (NF- κ B) signaling pathway. This inhibition occurs through the ability of 10-NO₂OA to modify specific cysteine residues in the NF- κ B subunit kinase IKK β and NF- κ B RelA protein. This modification prevents DNA binding and subsequent degradation of proteins induced by the RelA protein. Additionally, 10-NO₂OA inhibits NF- κ B activity induced by TNF α , leading to suppression of target genes responsible for the expression of metastasis-related proteins such as ICAM-1 and the urokinase-type plasminogen activator.^{99,100}

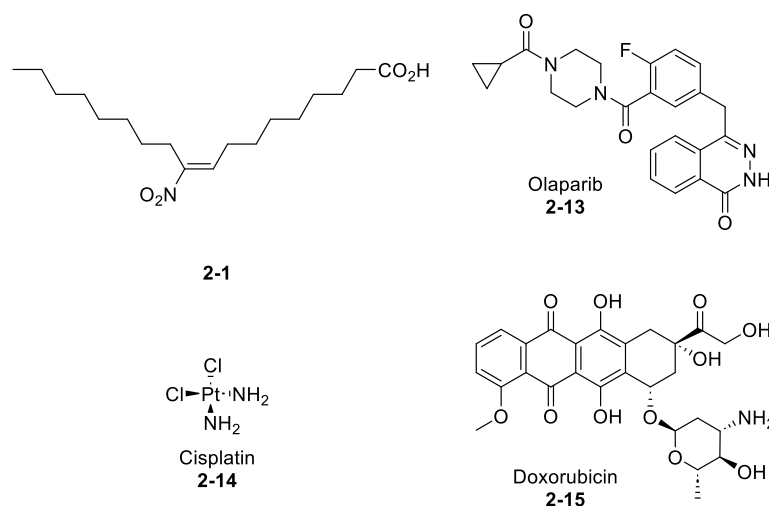


Figure 32: Structure of 10-NO₂OA **2-1** in comparison to other antineoplastic DNA-damaging agents.

In contrast, another variant of the well-known 10-NO₂OA, namely 9-nitro oleic acid **2-2** (**9-NO₂OA**), has demonstrated its potential as a cytotoxic agent against the colorectal cancer cell lines HCT-116 and HT-29. The presence of 9-NO₂OA significantly inhibited the cell viability of these cancer cells by inducing caspase-dependent apoptosis through the intrinsic apoptotic pathway. This anticancer effect can be attributed to the antioxidant properties of **NO₂FAs**, with 9-NO₂OA specifically targeting mitochondria and causing disruption of their membrane and respiratory functions. Ultimately, this disruption leads to apoptosis of cancer cells.¹⁰¹ Recent research has shown that NO₂OA (a mixture of regio isomers was used in this study) plays a key role in the regulation of pluripotency and differentiation of mouse embryonic stem cells through STAT3 signaling. 9/10-NO₂OA was shown to influence mESC pluripotency by regulating STAT3 phosphorylation. It also affected cardiac differentiation and directed mESCs to a neural fate.¹⁰²

Nitro linoleic acid **2-3** (NO₂LA) and nitro arachidonic acid **2-4** (NO₂ARA) belonging to polyunsaturated **FAs** (**Figure 33**).

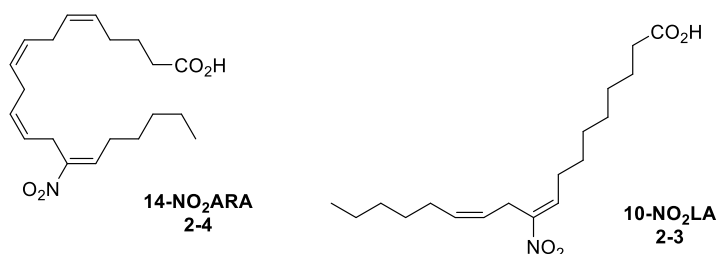


Figure 33: Examples of polyunsaturated FAs. Structure of 14-NO₂ARA **2-4** and 10-NO₂LA **2-3**.

These FAs are targets for peroxidation by nonenzymatic autocatalytic oxidation reactions due to their unsaturated double bonds.^{103–105} Arguably, more important of these two,

Chapter II: Biological activity

arachidonic acid (**ARA**), a 20-carbon polyunsaturated FA with four double bonds is a precursor to prostaglandins and thromboxanes and a powerful signaling molecules. ARA nitration by inflammatory stimuli alters the 'normal metabolic pathway' of ARA leading to new responses.¹⁰⁶ Since NO_2ARA is the most abundant polyunsaturated FA in biological membranes, NO_2ARA could therefore function as a new signaling molecule and a specific biological marker of inflammation. Until today, NO_2ARA was prepared only by acidic nitration (NaNO_2) and was characterized as a mixture of 9-, 12-, 14-, and 15- NO_2 isomers. Biological evaluation of this NO_2ARA mixture showed that the compound exhibited anti-inflammatory activity by inhibiting POX activity, being a new poorly reversible POX inhibitor of PGHS-2103, the ability to release NO, induces vasorelaxation due to its capacity to release NO, and modulates macrophage activation and NOS2 expression.^{107,108} Additionally, NO_2ARA exhibits antioxidant¹⁰⁹ and neuroprotective activity¹¹⁰ due to the Nrf2 activation.

Conjugated FAs (**Figure 34**) are commonly found in a diet composed mainly of ruminic acid (conjugated linoleic acid, cLA) and rumelenic acid (conjugated α -linolenic acid, cLNA). To date, there is no clear consensus on the role of cLA in inflammatory diseases. Under normal conditions, these compounds are nitrated in the gastric compartment, mainly forming 9- NO_2cLA **2-5**, 12- NO_2cLA **2-6**, and 9- NO_2cLNA .¹¹¹

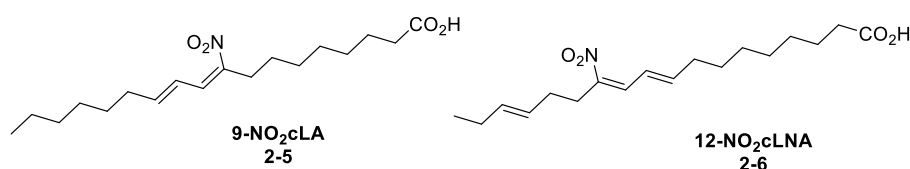
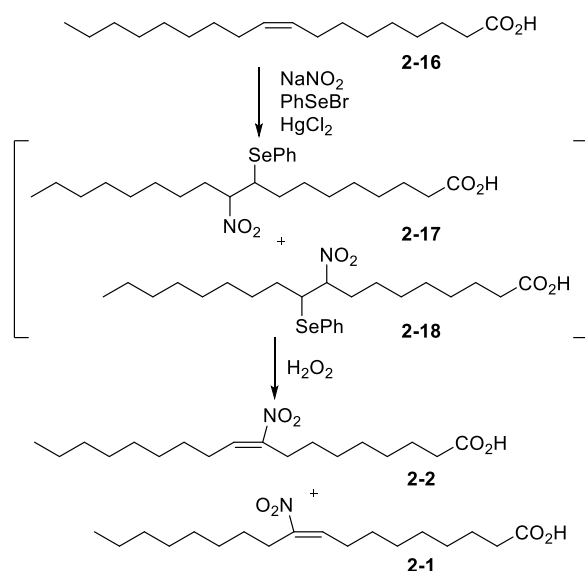


Figure 34: Examples of conjugated FAs. Structures of 9- NO_2cLA **2-5**, 12- NO_2cLA **2-6**.

In conclusion, the activity of **NO_2FAs** in various biological systems is evident. Furthermore, **NO_2FAs** are endogenous compounds produced by our body. Thus, their potential as a possible drug candidate is huge. However, the specific mode of action underlying their effects remains largely unknown. Previous studies have often focused on mixtures of stereo and regio isomers, which limits our understanding of the individual contributions of each regio isomer. Therefore, it is crucial to synthesize and isolate pure regio isomers of **NO_2FAs** to further investigate their biological activities. From our point of view, the biological testing of **NO_2FAs** should be carried out again but this time only pure regio and stereoisomers should be used to provide exact insights into the mechanisms of action of those molecules and improve our understanding of the various biological effects exhibited by **NO_2FAs** .

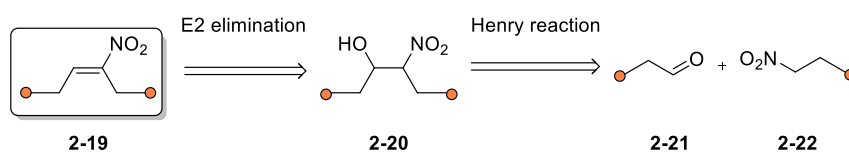
2.1.2. Synthesis of NO₂FAs

As mentioned previously, **NO₂FAs** are endogenously biosynthesized during inflammation by reactive nitrogen species.^{87,88} Their importance and potential for additional applications however, led chemists to develop additional synthetic routes to their preparation. Currently, two different pathways are synthetically used. The first is biomimetic and explores the direct nitration of a double bond of unsaturated FAs which, for example, in the case of oleic acid **2-16**, delivers a mixture of 9- and 10-NO₂OAs **2-1** and **2-2** as final products (**Scheme 24**).^{112,113} The situation is complicated when more double bonds are present. As mentioned in the previous chapter, the position of the nitro group is very important, therefore having a mixture of regio isomers is not optimal for biological evaluation and expensive separation of these isomers must (should) be performed.



Scheme 24: Direct nitration radical protocol (nitro-selenation/oxidation).¹¹³

The second approach is based on step-by-step synthesis which usually involves Henry reaction between nitro alkane/alkene **2-22** and aldehyde **2-21** followed by E2 elimination of the hydroxy group from nitro/hydroxy compound **2-20**. In such a case, the regio-defined isomer **2-19** with various degrees of *E/Z*-stereoselectivity is formed (**Scheme 25**).^{114,115}

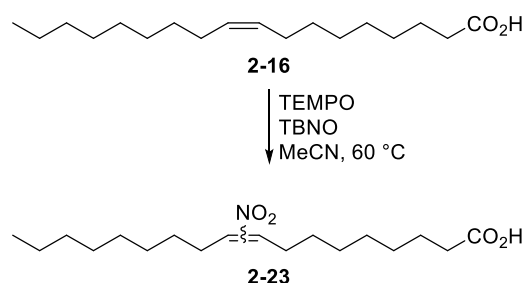


Scheme 25: Two possible retrosynthetic approaches towards NO₂FAs **2-19**.

2.2. Results and discussion^o

2.2.1. Introduction

Over the last 3 years our group is interested in the **NO₂FAs** and their physical and biological properties. In 2022, our group has started a new collaboration with a group of Prof. Jan Vacek from Palacký University. The goal of this collaboration was to prepare **NO₂FAs** with stereo and regio control since most biological assays^{116–118}, redox properties evaluation¹¹⁹, stability testing and measurement of electrophilic characteristics^{120–122} were performed on mixtures of positional isomers (especially on mixture of 9-/10-NO₂ oleic acid **2-23**) prepared by relatively new optimized direct nitration radical protocol of oleic acid **2-16**¹¹⁸, which eliminated nitro-selenation/oxidation¹¹³ to avoid mercury contamination (**Scheme 26**).

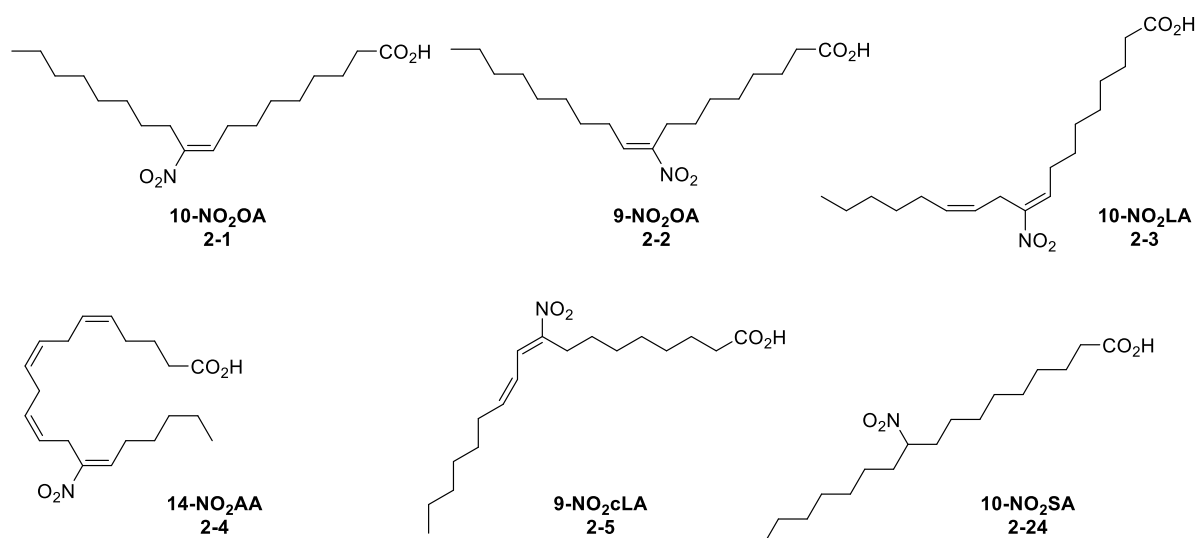


Scheme 26: Novel protocol for direct nitration.¹¹⁸

Our initial phase included the synthesis of specific regio and stereo isomers including 9- and 10-NO₂ oleic acid **2-1** and **2-2**, 10-NO₂ linoleic acid **2-3**, 14-NO₂ arachidonic acid **2-4**, 9-NO₂ conjugated linoleic acid **2-5** (nitro rumenic acid) and as a control for mechanistic and biological studies a fully saturated 10-NO₂ stearic acid **2-24** (**Scheme 27**).

^oThis work was supported by Grant Agency of the Czech Republic (no.23-06051S) and by the Palacký University Internal Grant Agency (IGA_PrF_2022_016, IGA_PrF_2022_022, IGA_PrF_2023_031 and IGA_PrF_2023_020). Part of the results presented in this chapter were published in a full paper that covers the development of novel modification of Julia-Kocienski olefination (stereoselective synthesis of *E* and *Z* olefins; I am shared 1st author: *Adv. Synth. Catal.* **2024**, 366, 480-487, doi: 10.1002/adsc.202301054) and the olefination reaction was further put in context of all olefination reactions of such type in recent review (I am 1st author, *Molecules* **2024**, 29(12), 2719; doi: 10.3390/molecules29122719). As a primary researcher in the project, I was responsible for designing and conducting experimental procedures and measurements, analyzing the data, and interpreting the results. Additionally, I am now writing a synthesis related part of the manuscripts that are in preparation and will be published with our colleagues. Additional research that is based on compounds I prepared is summarized in chapter 2.3.

Chapter II: Results and discussion

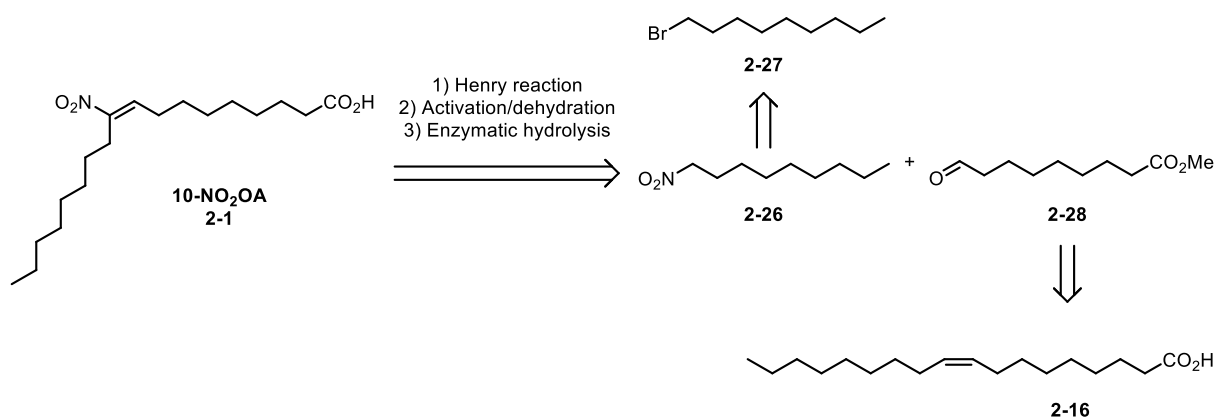


Scheme 27: Structures of targeted nitrated FAs.

In following chapters, the synthesis of each NO₂FA will be discussed separately.

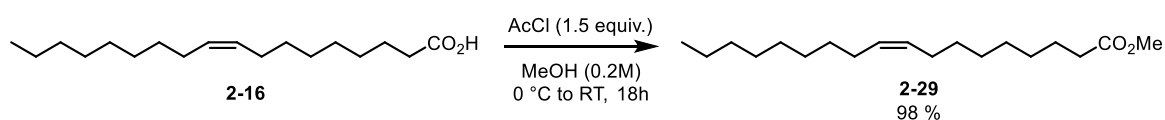
2.2.2. 10-NO₂ oleic acid

First, we tackled the synthesis of the 10-NO₂OA **2-1**. Our retrosynthetic plan was based on the Henry reaction¹²³ that required a reunion of the nitrononane **2-26** prepared from 1-bromononane **2-27** and of the methyl 9-oxononanoate **2-28** readily available from oleic acid **2-16** (Scheme 28).



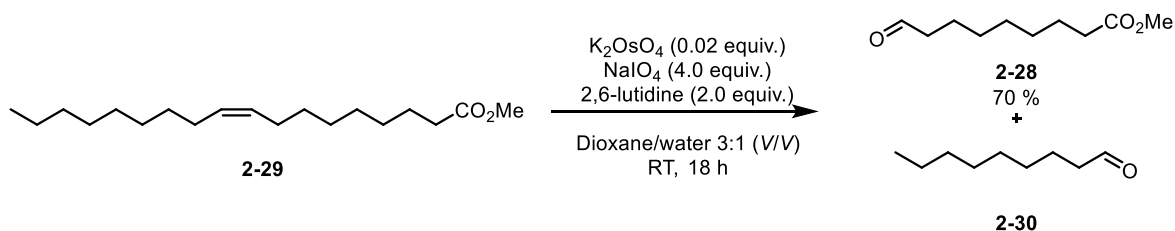
Scheme 28: Retrosynthetic plan towards 10-NO₂OA **2-1**.

The synthesis of 9-oxononanoate **2-28** began with the transformation of oleic acid to its methyl ester **2-29**. The methyl ester **2-29** was prepared from oleic acid **2-16** using AcCl/MeOH protocol in a yield of 98 % yield (Scheme 29).



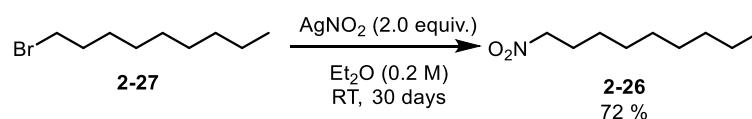
Scheme 29: Acylation of oleic acid **2-16**.

Oxidative cleavage of the olefinic bond in **2-29** carried out with the help of potassium osmate(VI) dihydrate in the presence of NaIO₄ (oxidant) and 2,6-lutidine yielded aldehyde **2-28** in 70 % yield (Scheme 30).



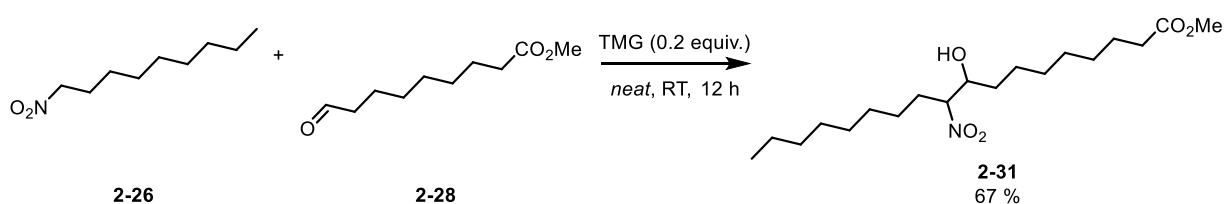
Scheme 30: Oxidative cleavage of methyl ester of oleic acid **2-29**.

Aldehyde **2-28** was then reacted with the nitro reagent **2-26** that was prepared by nitro/bromide exchange in the presence of silver nitrite. After 30 days of stirring in the dark, the reaction produced the desired product in a yield of 72 % yield (**Scheme 31**).¹²⁴



Scheme 31: Nitro/bromine exchange. Synthesis of the nitrogen compound **2-26**.

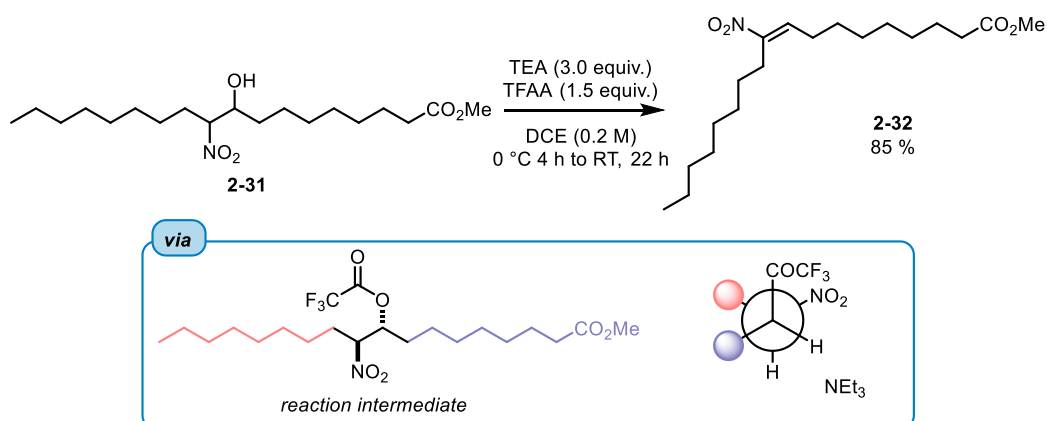
The reaction of nitro alkane **2-26** and with aldehyde **2-28** produced nitro aldol (Henry reaction) **2-31** with a yield of 67 %. The addition step of the sequence is crucial, since (a) it fixes the regiochemistry of the nitro group by combination of known precursors (nitro group is at the C10 position), and (b) it determines the *E/Z* stereochemical outcome of the subsequent *antiperiplanar* E2 elimination (**Scheme 32**). Under thermodynamic reaction conditions (use of TMG as a base) produces the predominantly *anti*-**2-31** adduct is produced. The desired adduct **2-31** must be immediately submitted to the elimination reaction to avoid any unwanted degradation. The elimination step that is mediated by the TFAA anhydride generates an activated intermediate *in situ* that in the presence of base undergoes an *anti*-elimination to yield *E*-olefin (*E*)-**2-32** in 85 % yield. The reaction proceeds under very mild conditions, yields the desired product as virtually a single stereoisomer (no traces of *Z* isomer as judged by the ¹H NMR spectra of the crude reaction mixture analysis), and only a small amount of unwanted side reaction products (in most cases) (**Scheme 33**).



Scheme 32: Formation of hydroxy nitro intermediate **2-31**.

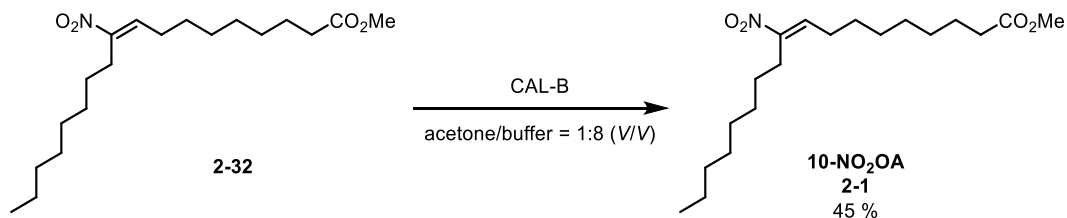
Next step, activation/dehydration generated the nitroalkene moiety **2-32** in an 85 % yield. Notably, this reaction proceeds under mild conditions, and yields clean stereoisomers, with very few side products observed (in most cases) (**Scheme 33**).

Chapter II: Results and discussion: 10-NO₂ oleic acid



Scheme 33: Elimination of **2-31** that gives (*E*)-10-NO₂ methyl oleate **2-32**.

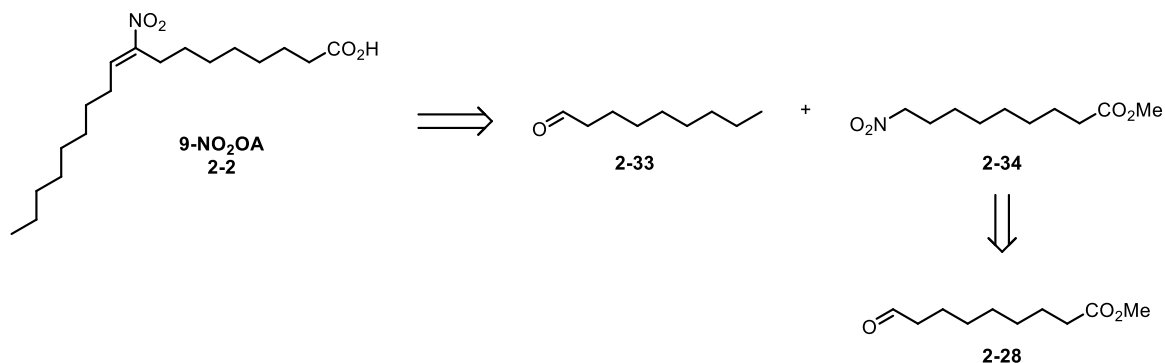
The final step of the synthesis involves the hydrolysis of the ester group in 10-NO₂ methyl oleate **2-32**. After several unsuccessful attempts and a very careful literature search of the reaction conditions, we opted for ester hydrolysis under mild enzyme-promoted conditions using lipase B from *Candida antarctica* (CAL-B). Conditions that should avoid side product formations and the final product, acid **2-1** degradation. This resulted in the formation of 10-NO₂OA **2-1** with a yield of 45 % and a 95:5 *E/Z* ratio (**Scheme 34**).



Scheme 34: Formation of 10-NO₂OA (**2-1**).

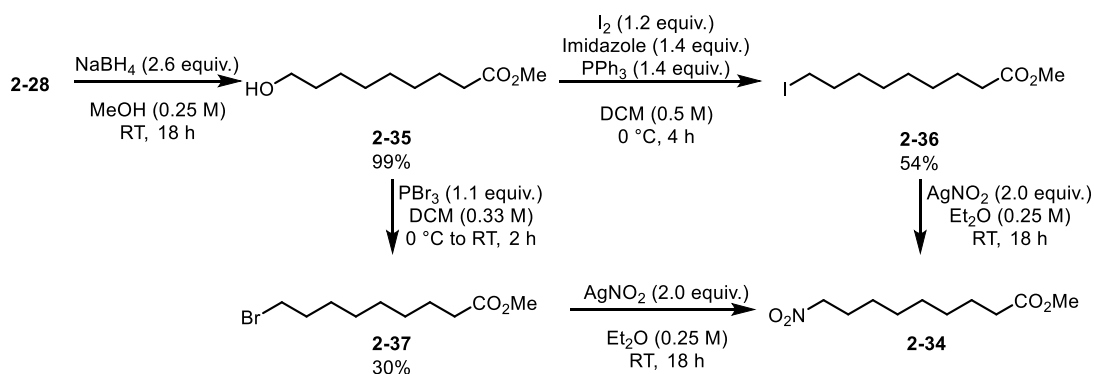
2.2.3. 9-NO₂ oleic acid

The retrosynthetic strategy for the synthesis of 9-NO₂OA **2-2** involves the same methodology, but the use of two different coupling partners for the Henry reaction. In this case, aldehyde **2-33** and methyl 9-nitrononanoate **2-34** must be used. While the first partner, aldehyde **2-33**, is commercial, the nitro derivative **2-28** must be prepared from aldehyde **2-28** (Scheme 35).



Scheme 35: Retrosynthetic plan towards 9-NO₂OA, **2-2**.

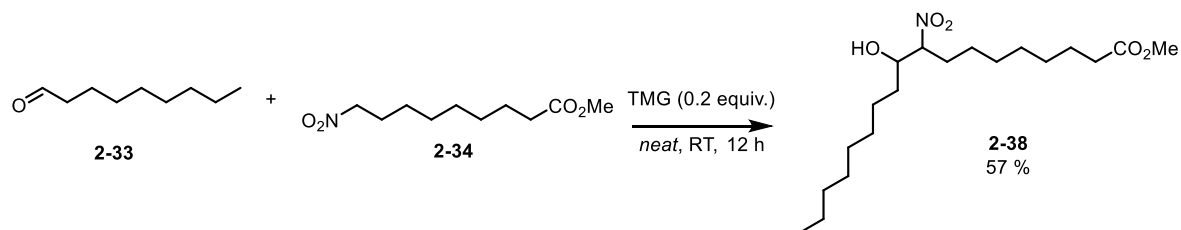
Thus, the nitro compound **2-34** is prepared from aldehyde **2-28** by reducing the aldehyde to alcohol **2-35** and the resulting alcohol is transformed into bromide **2-37** using PBr₃ in 30 % yield (Scheme 36). The bromide **2-37** was then transformed to methyl 9-nitrononanoate **2-34** in the presence of AgNO₂. However, the substitution reaction proceeds very slowly, and the desired product was isolated only in 23 % yield. The product of O-substitution (-ONO derivative) was isolated in 45 % isolated yield. To increase the isolated yield of a nitroalkane **2-34**, iodide **2-36** was prepared and reacted instead of the corresponding bromine derivative. This slight change resulted in an increased reaction yield and the final methyl 9-nitrononanoate **2-34** was isolated in 88 % yield. The whole protocol in addition eliminated all undesired side products.



Scheme 36: Formation of methyl 9-nitrononanoate (**2-34**).

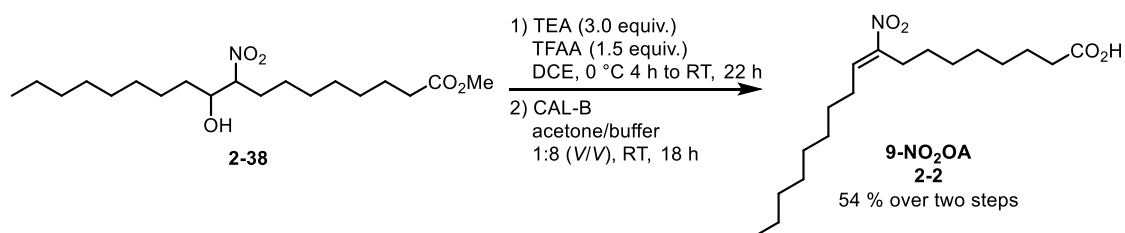
Chapter II: Results and discussion: 9-NO₂ oleic acid

When the synthesis of methyl 9-nitrononanoate **2-34** was accomplished, a Henry reaction could be performed (**Scheme 37**). The desired Henry adduct **2-38** was isolated in a satisfactory 57 % yield.



Scheme 37: Formation of the Henry adduct **2-38**.

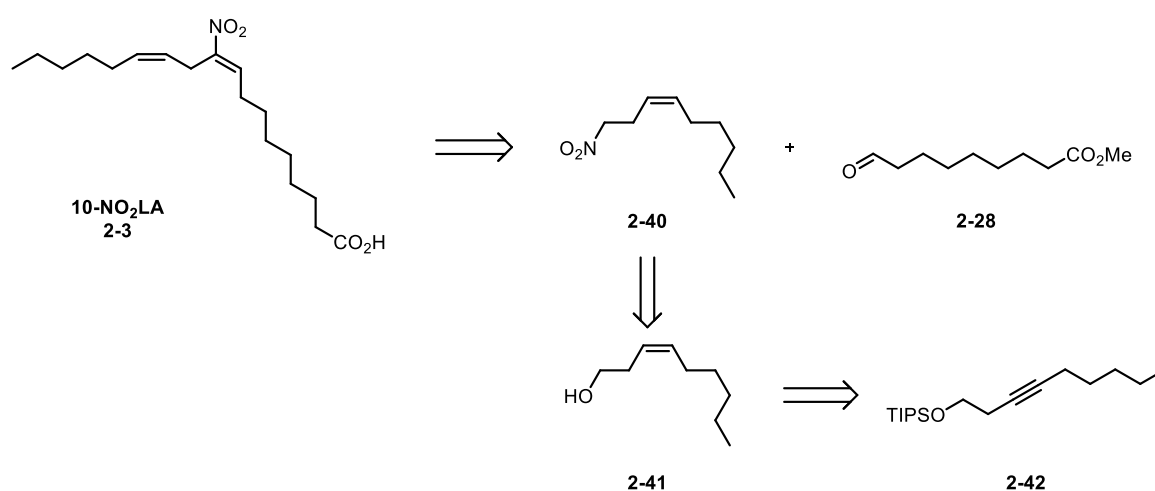
Intermediate **2-38** then reacted in the presence of TFAA and TEA and produced selectively 9-NO₂ methyl oleate **2-39** with an isolated yield of 81 % and >95:5 *E/Z* selectivity. The final step again involved enzymatic hydrolysis of ester promoted by CAL-B that furnished the desired 9-NO₂ oleic acid **2-2** in 66 % yield (54 % over two steps) and >95:5 *E/Z* selectivity (**Scheme 38**).



Scheme 38: Formation of 9-NO₂OA (**2-2**).

2.2.4. 10-NO₂ linoleic acid

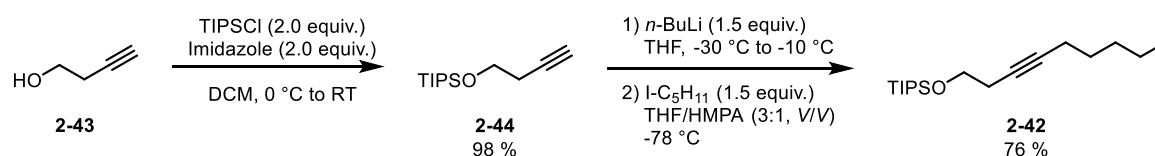
Synthesis of 10-NO₂LA proved to be more challenging compared to previous synthesis of nitro oleic acid, as it involved the construction of the first partner, nitro alkene **2-40**, before the subsequent Henry reaction with aldehyde **2-28** could be attempted. Nitro alkene **2-40** was designed to be synthesized from alcohol **2-41**, which could be prepared from TIPS-protected alkyne **2-42** (Scheme 39). Alternatively, our recently developed protocol, which employs the modified Julia-Kocienski reaction could be also used (for details, see chapter 2.5.8).¹²⁵



Scheme 39: Retrosynthetic plan towards polyunsaturated **10-NO₂LA**, **2-3**.

- “Classical approach”

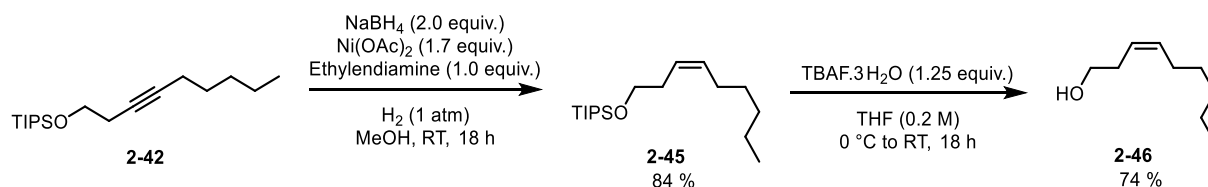
First, we have employed the standard organic chemistry-based approach, where the synthesis began with TIPSCl protection of 3-butynol **2-43** (98 % yield) that was followed by alkylation of the terminal alkyne with 1-iodopentane (**Scheme 40**). The substitution reaction was performed with the help of a lithium acetylene-type reagent, which is known to have low reactivity in substitution reactions. To increase its reactivity, we added HMPA, a well-known lithium scavenger solvent, to the reaction mixture to generate a more reactive 'naked' alkyne anion. Under such reaction conditions, the substitution reaction proceeded smoothly and produced the desired **2-42** product with a yield of 76 %.



Scheme 40: TIPS protected internal alkyne **2-42** synthesis.

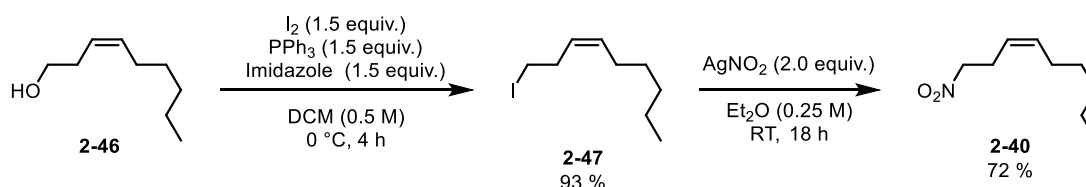
Chapter II: Results and discussion: 10-NO₂ linoleic acid

Subsequently, a (*Z*) selective reduction of the triple bond was carried out using NaBH₄/Ni(OAc)₂/ethylenediamine protocol, yielding TIPS-protected (*Z*) alkene **2-45** in 84 % yield and >95:5 *E/Z* selectivity. The deprotection of the TIPS group mediated by TBAF then resulted in the formation of alcohol **2-46** with a yield of 74 % (**Scheme 41**).



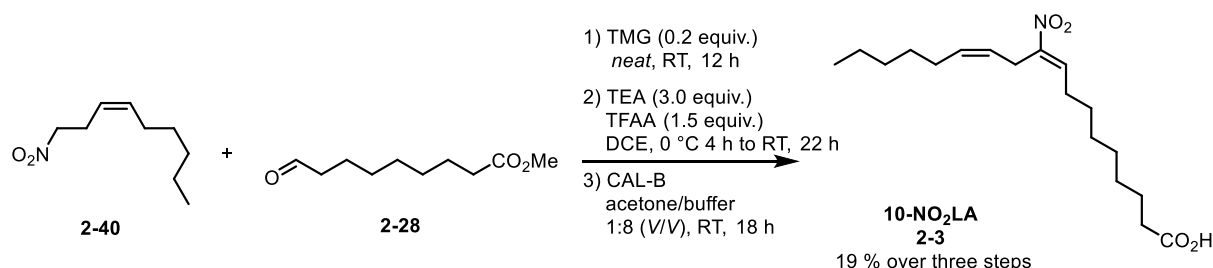
Scheme 41: Preparation of (*Z*)-alkene **2-46**.

Generated alcohol was transformed into the corresponding iodide **2-47** with help of I₂/PPh₃/imidazole protocol (93 % yield), and the reaction of **2-47** with AgNO₂ finally produced the nitro coupling partner **2-40** in 72 % (**Scheme 42**).



Scheme 42: Preparation of nitro alkene **2-40**.

The nitrogen coupling partner was then reacted with aldehyde **2-28** under the standard Henry coupling reaction protocol. The generated adduct was eliminated in the presence of TFAA/TEA, and the prepared ester was hydrolyzed to produce the desired **10-NO₂LA (2-3)**. The overall yield of the transformation (3 steps) was 19 % and the acid was formed in >95:5; 5:>95 *E/Z,E/Z* ratio (**Scheme 43**).



Scheme 43: End game in the synthesis of **10-NO₂LA (2-3)**.

- **Modified Julia-Kocienski approach**

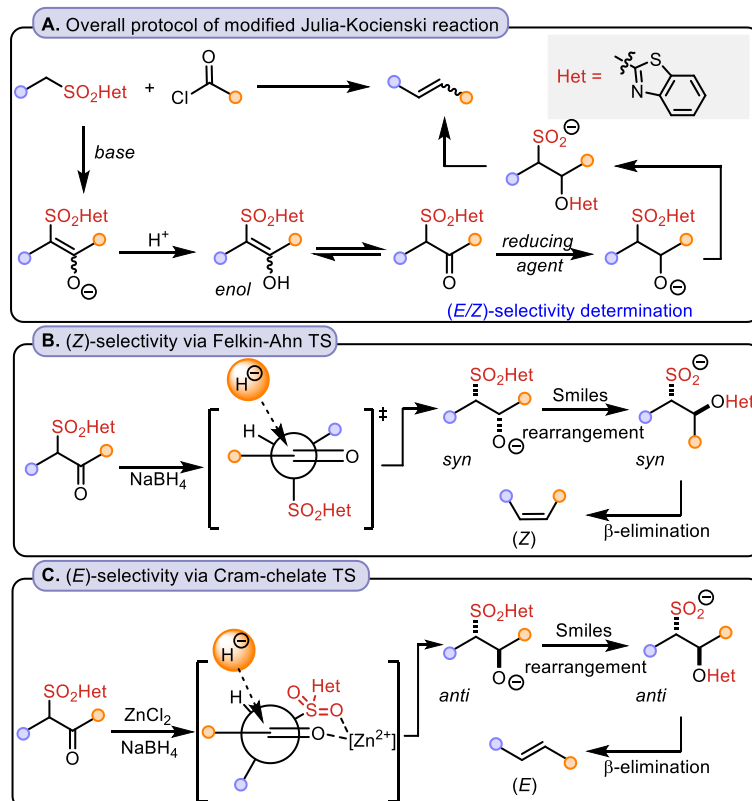
Alternatively, the *Z* olefin which is used in the preparation of **10-NO₂LA (2-3)** could also be prepared using our recently developed protocol, which transforms the well-known Julia-Kocienski reaction into a new type of the olefination reaction that allows for the stereoselective formation of *E* as well as *Z* olefins (

Scheme 44A).^{125,126} The reaction sequence is based on the reaction of alkyl BT-sulfone with acyl chloride in the presence of an excess of a non-nucleophilic base. The reunion of the two reagents generates the desired *b*-keto sulfone that is present in the reaction mixture in the form of the corresponding enolate. The addition of MeOH results in *in situ* protonation of the enolate to the corresponding enol that, when present in its keto-form, can be reduced to the corresponding *b*-hydroxy sulfone by an external reducing agent. The reduction is the key for the stereochemical outcome of the reaction, since if the reduction proceeds under the Felkin-Ahn transition state conditions (NaBH₄), the *Z* olefin is formed (

Scheme 44B). On the other hand, when the reduction proceeds under the Cram-chelate conditions (NaBH₄/ZnCl₂) then produce the desired olefin as the *E* isomer (

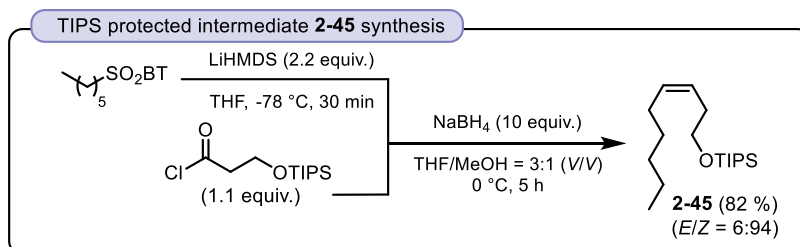
Scheme 44C). The reason is that stereoselective reduction produces *syn* or *anti*-hydroxy BT sulfone that is further transformed *via* the stereospecific *anti*-elimination process and yields *E* or *Z* olefin.

Chapter II: Results and discussion: 10-NO₂ linoleic acid



Scheme 44: Modified Julia-Kocienski Like olefination method.¹²⁵

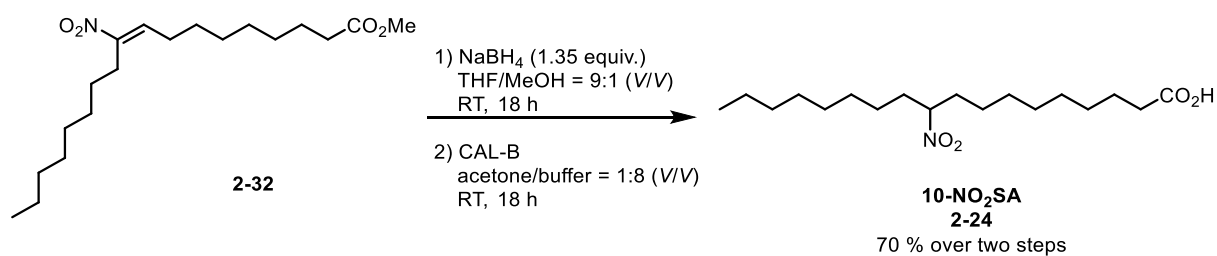
In the context of our project, the reaction intermediate, TIPS-ether **2-45**, was prepared using this protocol in an 82% yield and 6:94 *E/Z* ratio (**Scheme 45**).



Scheme 45: Application of modified Julia-Kocienski Like olefination method in the preparation of TIPS-ether **2-45**.

2.2.5. 10- NO₂ stearic acids

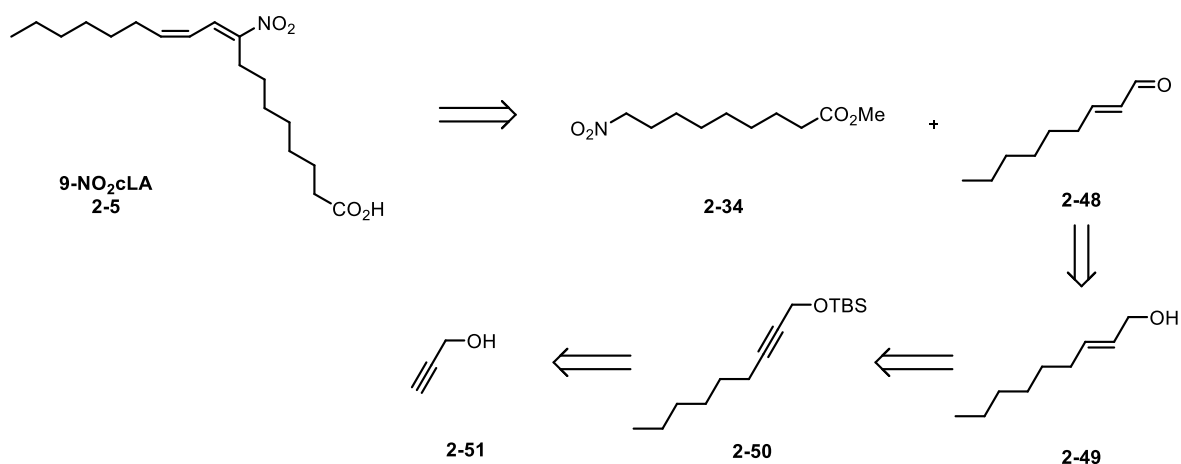
The synthesis of the 10-nitro derivative of stearic acid (**SA**) **2-24** involved a straightforward reduction of NaBH₄ **2-32** followed by enzyme-promoted ester hydrolysis. This two-step reaction sequence resulted in the formation of compound **2-24** and yielded the desired product with a yield of 70 % (**Scheme 46**).



Scheme 46: Preparation of **10-NO₂SA, 2-24**.

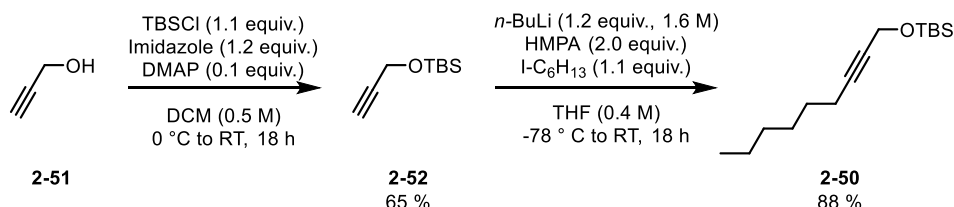
2.2.6. 9-NO₂ conjugated linoleic acid

The next challenge was the synthesis of 9-NO₂ conjugated linoleic acid (**9-NO₂cLA**, **2-5**) synthesis. The compound itself is known for its lability to both a basic and an acidic environment, and therefore its synthesis was quite a challenge. Our retrosynthesis was based on the Henry reaction between methyl 9-nitrononanoate **2-34** and aldehyde **2-48**. Aldehyde **2-48** was expected to be prepared from (*E*)-alcohol **2-49**, which, in turn, can be prepared from propargyl alcohol **2-51** (**Scheme 47**).



Scheme 47: Retrosynthetic plan of **9-NO₂cLA** (**2-5**).

The synthesis of the first coupling partner, methyl 9-nitrononanoate **2-34**, was already described in the context of the synthesis of 9-NO₂OA and therefore will not be discussed. However, aldehyde **2-48** synthesis was not yet described (**Scheme 48**). As mentioned above, the synthesis started with propargyl alcohol **2-51** that was transformed to its TBS-ether **2-52** (65 % yield). Alkyn **2-52** was transformed into the corresponding organolithiated species that was further alkylated in the presence of HMPA with 1-iodohexane. Alkylated alkyne **2-50** was isolated in 88 % yield.

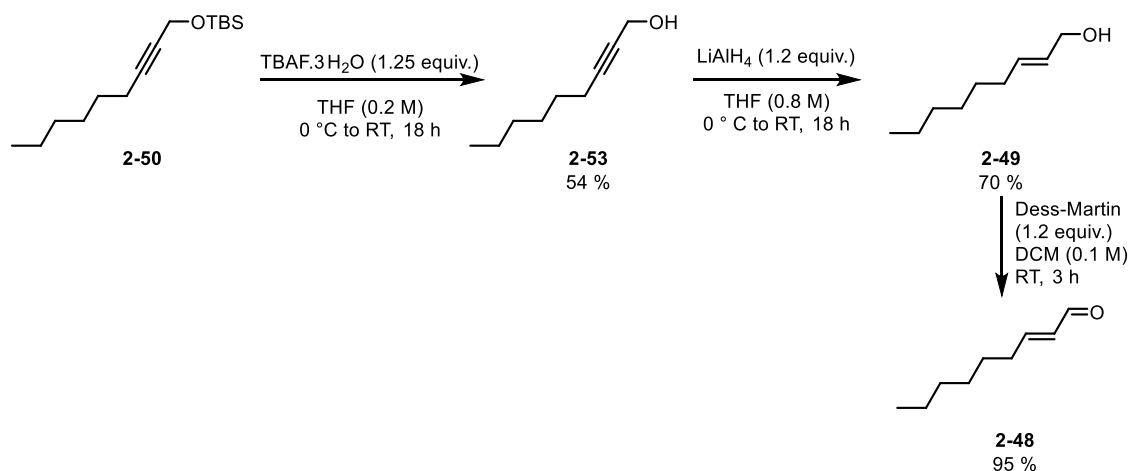


Scheme 48: Preparation of protected alkyne **2-50**.

The removal of the TBAF-mediated TBS group produced alcohol **2-53** with a yield of 54 % and its (*E*) selective reduction of LiAlH₄ resulted in the formation of *E*-allylic alcohol **2-49**

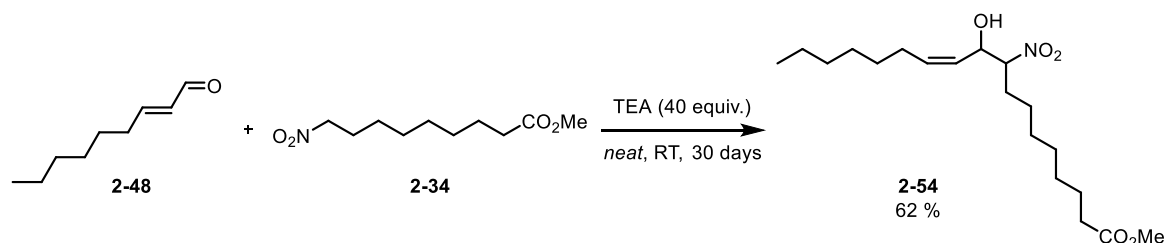
Chapter II: Results and discussion: 9-NO₂ conjugated linoleic acid

with a yield of 70 % and >95:5 *E/Z* ratio. Dess-Martin periodinate promoted oxidation of allylic alcohol to aldehyde, yielding unsaturated aldehyde **2-48** in a yield of 95 % (**Scheme 49**).



Scheme 49: Preparation of aldehyde **2-48**.

Having both reaction partners for the Henry reaction, the coupling step was attempted. First, a published protocol by Woodcock et al.¹¹¹ was evaluated. However, our substrates and those used in the work of Woodcock et al. differ, since in the referenced paper, *tert*-butyl 9-nitrononanoate is used as the starting material. We used a 9-nitrononanoate methyl ester **2-34**. The difference proved to be crucial since in our case, no product of the reaction was observed even after 3-5 days (reaction time of the original protocol). The desired product formation **2-54** was detected only after 10 days from the beginning of the reaction. Given the sluggish reaction progress, the reaction was monitored for an extended period of 30 days, after which the workup that consisted of TEA removal by stream of N₂ was used. In 30 days, the conversion of the methyl ester was only 70 % and the isolated yield of **2-54** was 62 %. Nitro-hydroxyl adduct **2-54** obtained was immediately used in the next step due to the reported low stability of the adduct (**Scheme 50**).

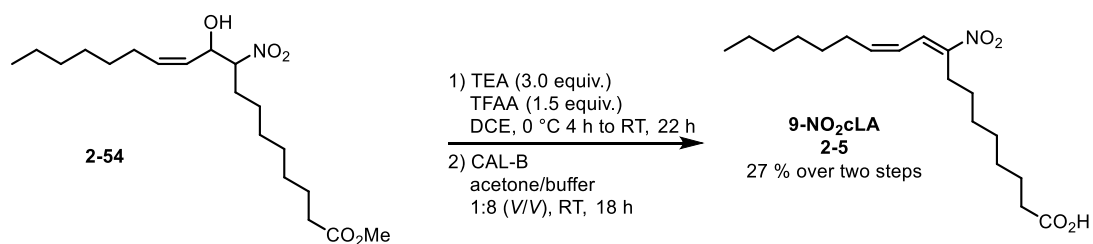


Scheme 50: Henry reaction. Adduct **2-54** synthesis.

The elimination step and the additional hydrolysis step of methyl ester required for the transformation of **2-54** to 9-NO₂cLA **2-5** proceeded without any further problems

Chapter II: Results and discussion: 9-NO₂ conjugated linoleic acid

and the desired product 9-NO₂cLA **2-5** was isolated in two mentioned steps in a modest isolated yield of 27 % and >95:5; >95:5 *E/Z,E/Z* selectivity (**Scheme 51**).



Scheme 51: Final steps of **9-NO₂cLA (2-5)** synthesis.

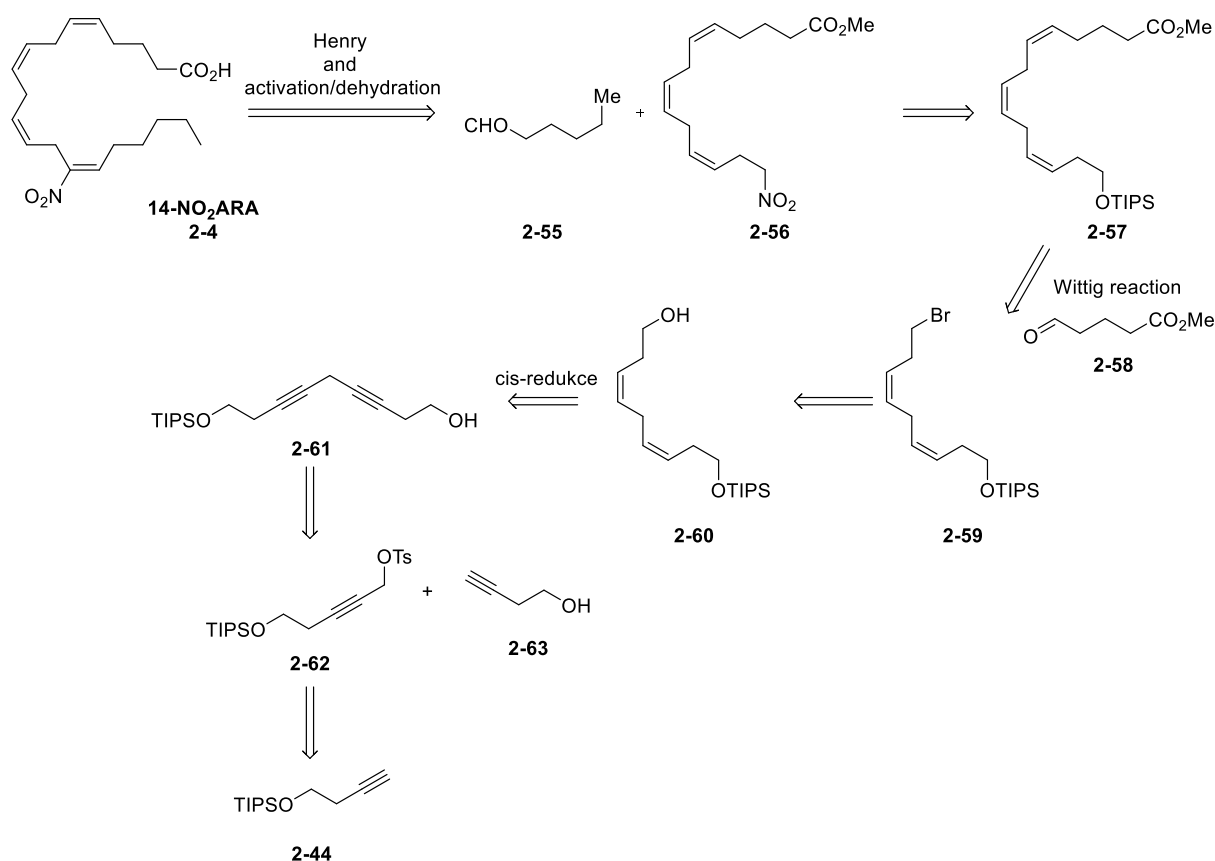
2.2.7. 14-NO₂ arachidonic acid

The next target of the synthesis was the synthesis of 14-NO₂ arachidonic acid (14-NO₂ARA, **2-4**). Our interest in this molecule is dated back to the year 2022 when our collaborators from the faculty of medicine and dentistry UPOL showed great interest in the evaluation of the molecule and we have found that there is no reported total synthesis of the molecule. Our journey to complete the synthesis of this molecule are described in the next few pages of this thesis.

2.2.7.1. First approach

First approach towards 14-NO₂ARA **2-4** was based on the similar retrosynthetic pathway described previously for the preparation of simpler NO₂FAs (**Scheme 52**). Compound **2-4** that contains three skipped (*Z*) 1,2-disubstituted olefins and one (*E*) (nitro containing) olefin was retrosynthetically divided along the nitro olefinic bond that could be established *via* Henry reaction/elimination protocol. This retrosynthetic step left us with aldehyde **2-55** and nitro-containing triene **2-56**. Triene **2-56** could be traced back to TIPS-ether **2-44**. However, to reach all *Z* triene **2-56** from the alcohol derivative **2-44** would require several steps where we identified two key ones: installation of the ester group *via* the *Z*-selective Wittig reaction (step inspired by the work of Suto et al.¹²⁷) and dialkyne **2-61** synthesis and further all *Z* reduction.

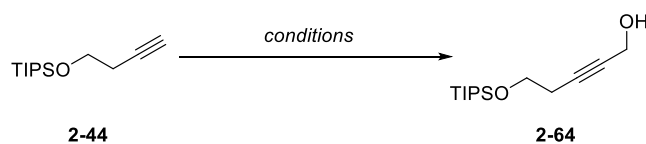
Chapter II: Biological evaluation



Scheme 52: Our first retrosynthetic approach to **14-NO₂ARA (2-4)**.

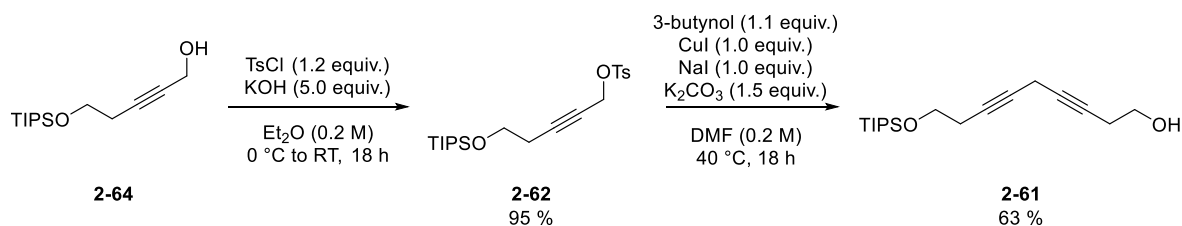
The synthesis of the targeted molecule started with the TIPS protected 3-butynol **2-44** preparation. TIPS-ether **2-44** was then formylated using the published procedure¹²⁸, where the first step involved the formation of an aldehyde by the reaction of the generated alkyne anion with DMF, followed by the reduction of the aldehyde to alcohol (**Table 13, entry 1**). However, in our hands, this protocol proved to be low-yielding (product **2-64** was isolated only 40% in two steps) and we faced reproducibility issues due to the rapid decomposition of the aldehyde-containing intermediate. The issue becomes significant when the reaction was carried out in a larger scale. Therefore, an alternative one-step protocol based on the use of paraformaldehyde was used (**Table 13, entry 2**).¹²⁹ In this case the desired product was formed in 80 % isolated yield.

Tosylation of the alcohol **2-64** followed by copper(I)-promoted substitution reaction of the resulting activated propargylic alcohol in **2-62** with 3-butynol group produces the desired skipped dialkyne **2-61** in 95 % yield (**Scheme 53**).

Table 13: Alcohol **2-64** synthesis.

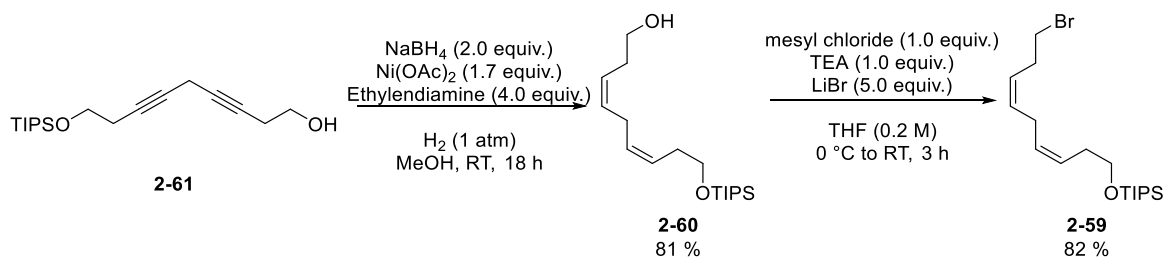
Entry	Conditions	Yields [%] ^a
1	1) <i>n</i> -BuLi (2.5 equiv., 1.6 M), DMF (2.0 equiv.), THF (0.4 M), -40 °C to RT, 2 h.	40
	2) 2) NaBH ₄ (2.0 equiv.), MeOH (0.2 M), 0 °C, 15 min.	
2	<i>n</i> -BuLi (1.1 equiv., 1.6 M), paraformaldehyde (2.5 equiv.), THF (0.4 M), -78 °C to RT, 12 h	80

a) Isolated yield after column chromatography on silica gel.



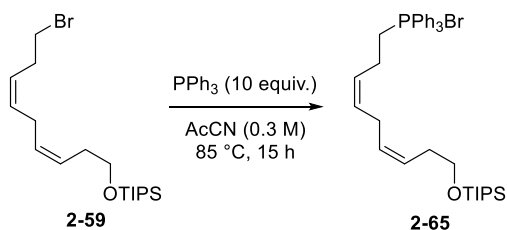
Scheme 53: Alkyne **2-61** preparation that features the copper(I) promoted substitution of activated propargylic alcohol.

After diene **2-61** formation, a *cis* reduction of the two triple bonds to the corresponding *Z* olefins was carried out under the hydrogen atmosphere with the help of the NiH₂ reducing agent (generated *in situ* from the NaBH₄/Ni(OAc)₂/ethylenediamine mixture) (**Scheme 54**). Skipped *Z,Z* dialkene **2-60** was isolated in 81 % and 5:>95; 5:>95 *E/Z,E/Z* ratio. Subsequently, bromide **2-59** was prepared from the alcohol **2-60** with a yield of 82 % over two steps. The reaction proceeded *via in situ* generated mesylate intermediate.

**Scheme 54:** Formation of bromide **2-59**.

The reaction of the bromide **2-59** with PPh₃ then yielded the desired phosphonium salt **2-65** (**Scheme 55**). At this stage, we failed to purify the Wittig salt and even though it appeared not as important, our inability to purify the **2-65** salt to >95% purity proved to be crucial in the next Wittig olefination step.

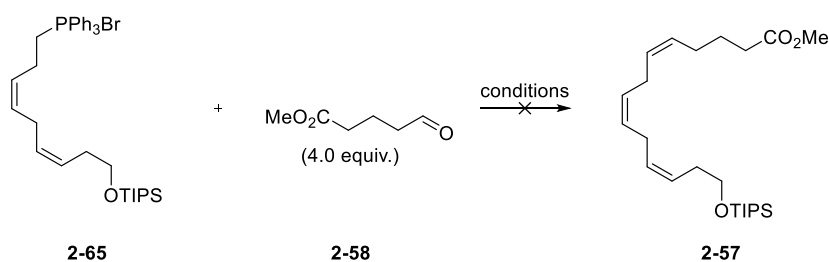
Chapter II: Biological evaluation



Scheme 55: Formation of triphenylphosphine bromide **2-65**.

All our attempts to react crude phosphonium salt **2-65** with aldehyde **2-58** under various Wittig olefination conditions were unsuccessful and the desired product **2-57** was never observed (**Table 14**). Instead, various unidentified products were isolated; however, their structure was not clearly identified due to the spectra complexity and our inability to obtain them in pure form as an individual entity.

Table 14: Optimization of Wittig reaction between salt **2-65** and aldehyde **2-58**.



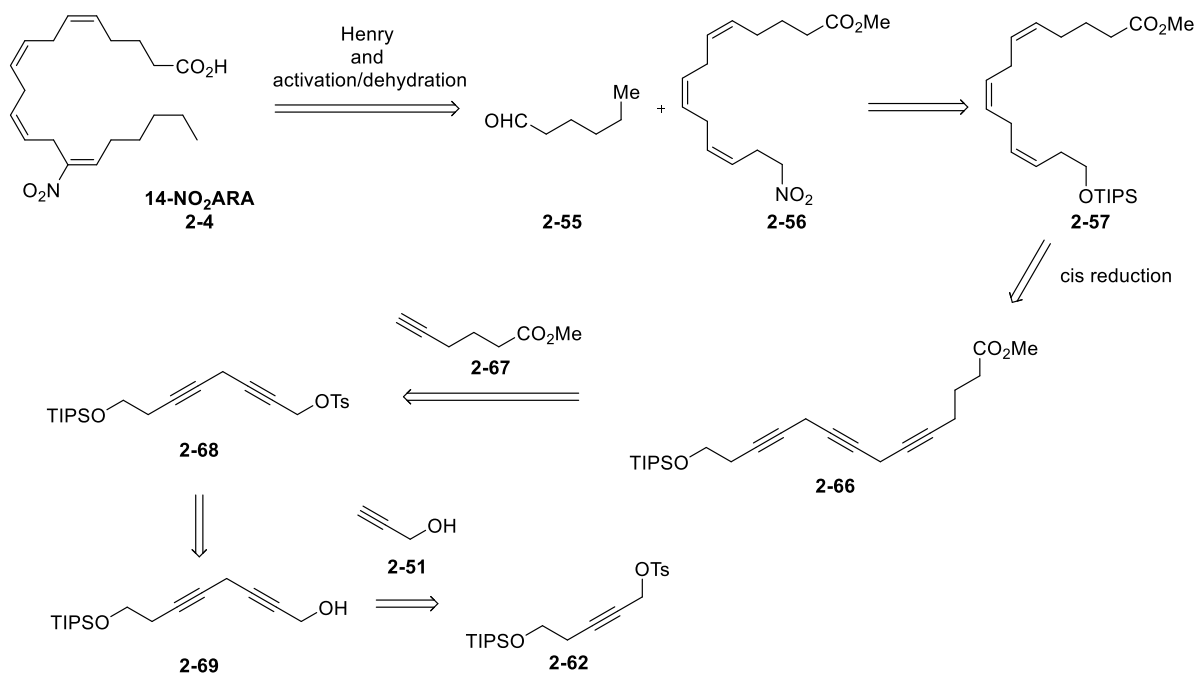
Entry	Conditions	Comments ^a
1	NaHMDS (2.1 equiv.), THF (0.1 M), 2 h	No desired product observed
2	NaHMDS (2.1 equiv.), THF (0.1 M), 4 h	No desired product observed
3	LiHMDS (2.1 equiv.), THF (0.1 M), 4 h	No desired product observed
4	LiHMDS (3.1 equiv.), THF (0.1 M), 18 h	decomposition

a) Based on the ¹H NMR spectra of the crude reaction mixture analysis.

Considering the problems related to the Wittig reaction (no traces of product) and our inability to purify the phosphonium salt **2-65**, our further efforts in this direction were abandoned and our synthetic strategy was revised.

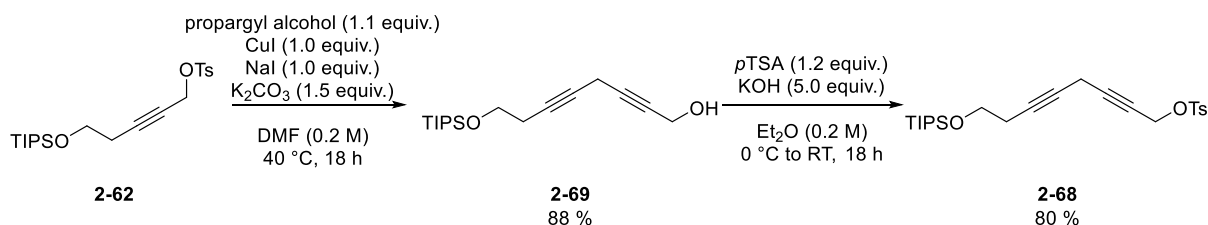
2.2.7.2. Second approach

In our second approach to Henry coupling partner **2-56**, we have replaced the trouble-making Wittig reaction with a step-by-step buildup strategy.¹³⁰ The final steps of the synthesis thus were unchanged, but TIPS-ether **2-57** should be prepared *via* all *cis* reduction of skipped trialkyne **2-66** intermediate. The skipped alkyne motive supposed to be built up *via* a sequence of copper(I)-promoted substitution reactions of activated propargylic hydroxyls with appropriate alkynes (**Scheme 56**).



Scheme 56: Second retrosynthetic analysis of **14-NO₂ARA (2-4)**.

Building on the progress made in our initial approach, we utilized intermediate **2-62** and successfully synthesized product **2-69** in a yield of 88 % by utilization of copper(I)-promoted substitution reaction (**Scheme 57**). The tosylation of the resulting alcohol then furnished the desired activated propargylic alcohol **2-68** in 80 %.



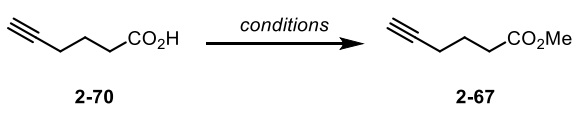
Scheme 57: Formation of tosylate **2-68**.

The second substitution reaction should then be carried out. However, first we had to prepare the required nucleophile, ester **2-67** (**Table 15**). Its synthesis started from the commercially

Chapter II: Biological evaluation

available 5-hexynoic acid **2-70** that was first esterified under acidic conditions (**entry 1** and **2**) using the MeOH/*p*TSA system or the SOCl₂/MeOH system. However, both methods yielded suboptimal results, since the desired ester **2-67** was isolated in reaction yields of 68 % (**entry 1**) and 49 % (**entry 2**), respectively. Consequently, we employed freshly generated diazomethane (**entry 3**) as a methylating agent. Under such conditions, the desired ester was formed in a quantitative manner.

Table 15: Methyl ester **2-67** synthesis. Optimization of the protocol.

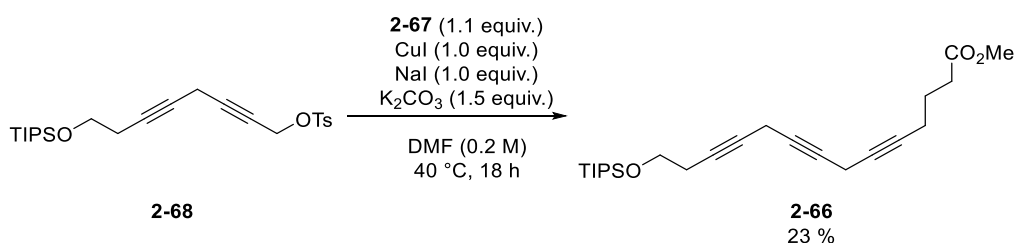


2-70 $\xrightarrow{\text{conditions}}$ **2-67**

Entry	Conditions	Yields [%] ^a
1	MeOH (5 M), <i>p</i> TSA (0.01 equiv.), DCM (2.5 M), reflux, 24 h	68
2	Thionyl chloride (3.0 equiv.), MeOH (0.2 M), 0 °C to RT, 18 h	49
3	CH ₂ N ₂ (2.2 equiv.), Et ₂ O (0.2 M), 0 °C, 30 min.	99

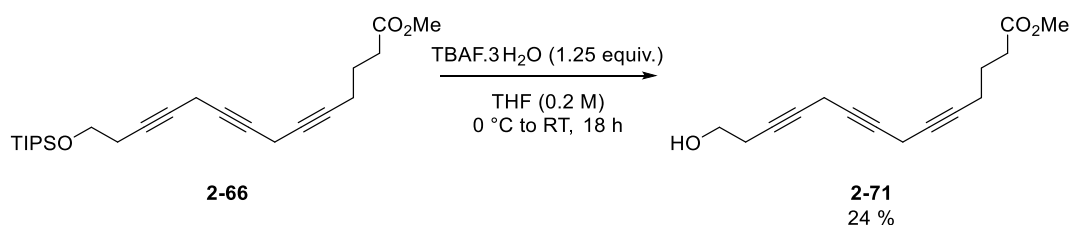
a) Isolated yield after column chromatography on silica gel.

Subsequent reaction with methyl ester of 5-hexynoic acid **2-67** led to the formation of a product **2-66** which embody 3 triple bonds, unfortunately in an unimpressive yield of 23 % and low purity (**Scheme 58**).



Scheme 58: Formation of alkyne **2-66**.

Although, the deprotection of **2-66** resulted in the formation of an alcohol **2-71**, with another discouraging yield of only 24 % and again in low purity (**Scheme 59**).



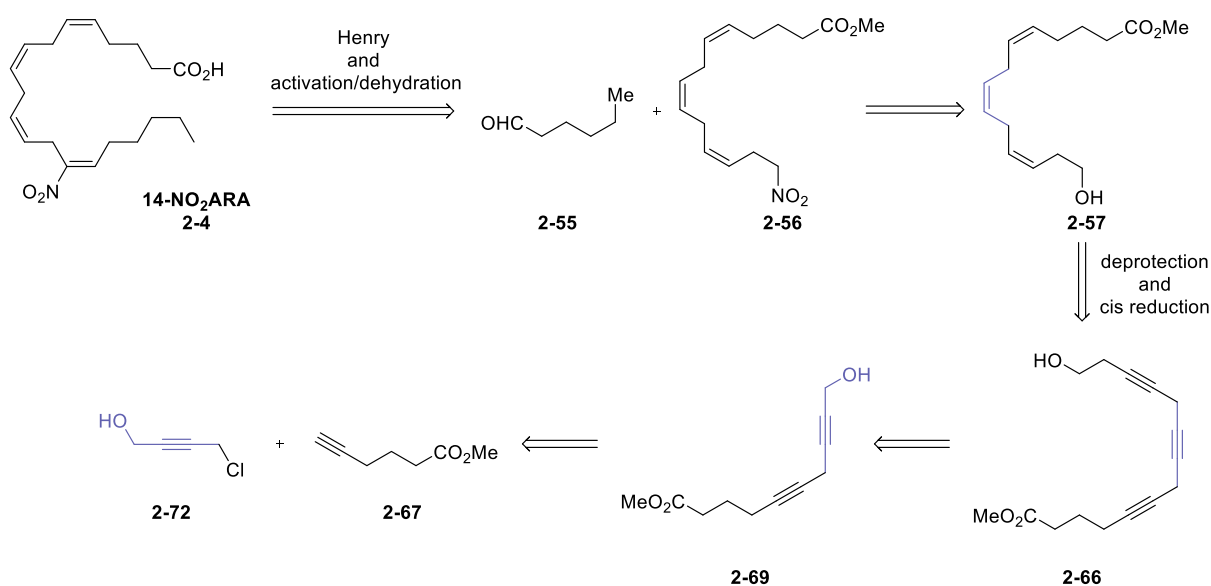
Scheme 59: Deprotection of **2-66**.

Chapter II: Biological evaluation

At this point, because of the low reaction yields, particularly in the last two steps, we have decided to abandon this pathway and explore a third alternative approach.

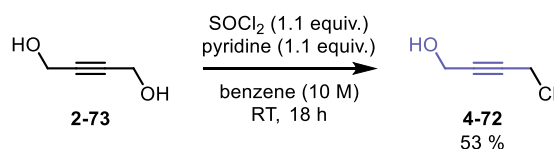
2.2.7.2.1. Third approach

The third and final approach is again based on the literature precedented transformations^{130,131} and similarly to the second approach the key intermediate was trialkyn **2-66** (Scheme 60). However, while^{125,126} the final steps remain the same, the opening transformations are way different. In this approach, we have decided to build up the whole carbon chain starting from the methyl ester of 5-hexynoic acid **2-67** and 4-chlorobut-2-yn-1-ol **2-72**



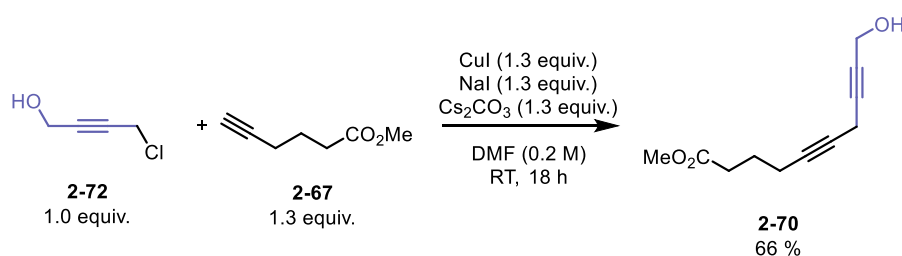
Scheme 60: Third approach to **14-NO₂ARA (2-4)**. Retrosynthetic consideration.

The first step of the sequence is the monochlorination of the diol **2-73** that was carried out with the help of SOCl₂ (Scheme 61). The reaction proceeded in benzene and in the presence of pyridine and yielded the desired hydroxy chloride **4-72** in 53 % yield.



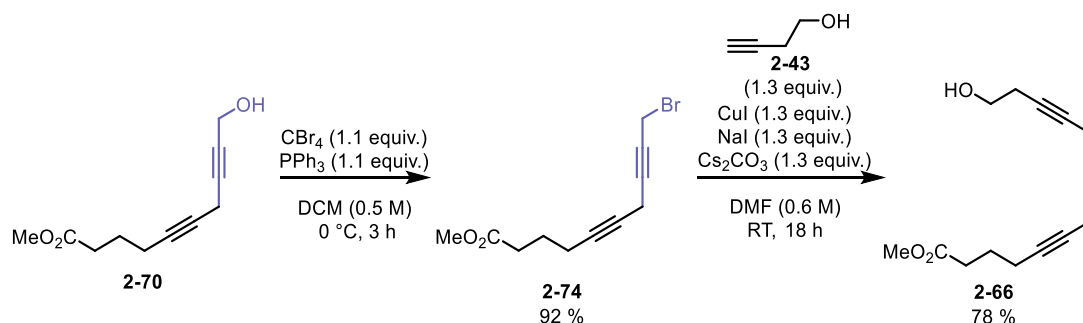
Scheme 61: Chlorination of **2-73**.

Next, the copper(I) promoted substitution reaction of alkyne **2-67** with the previously generated chloride **4-72** yielded alcohol **2-70** in a yield of 66 % (Scheme 62).¹³⁰



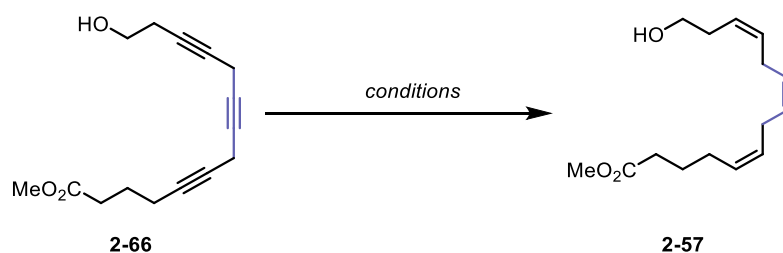
Scheme 62: Coupling of chloride **2-72** and methyl 5-hexynoate **2-67**.

The alcohol **2-70** was then converted to the corresponding bromide **2-74** using the Appel reaction conditions (92 %), and the bromide **2-74** was reacted again in the presence of copper(I) salts with 3-butynol **2-43** and yielded alkyne **2-66** with three skipped triple bonds in a 78 % yield (**Scheme 63**).



Scheme 63: Formation of alkyne **2-66**.

At this stage a challenging all *cis* reduction of alkynes to olefins in **2-66** was evaluated (**Table 16**). First, hydrogenation promoted with the Lindlar catalyst was attempted, but only partial reduction of alkyne or partial/complete overreduction of alkynes to alkanes was observed (**entry 1-5**). Therefore, we switched the reducing system and used NiH₂ as a reducing agent (generated *in situ* from NaBH₄/Ni(OAc)₂/ethylenediamine in the presence of H₂). Under these conditions, the desired product was isolated in the yield of 42 % and 46 %, respectively (**entry 6 and 7**). Change in the solvent from methanol to ethanol resulted in complete decomposition (**entry 8**), but when the chelating diamine ligand equivalents were decreased from 4.0 to 2.0, the desired product **2-57** was formed in an increased 57 % yield (**entry 9**).

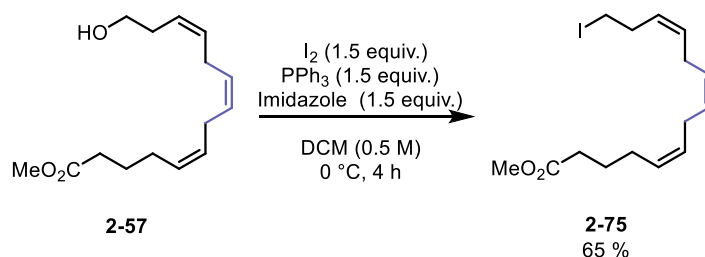
Table 16: Optimization of reduction of alkyne **2-66** to triple skipped alkene **2-57**.

Entry	Conditions	Yields [%] ^a	comments
1	Lindlar catalyst (20 mg/1 mmol), MeOH (0.5 M), 4 h	-	partial overreduction
2	Lindlar catalyst (20 mg/1 mmol), quinoline (0.02 equiv.), H ₂ (1 atm), Et ₂ O (0.5 M), RT, 3.5 h	-	no conversion
3	Lindlar catalyst (20 mg/1 mmol), quinoline (0.3 equiv.) H ₂ (1 atm), THF/Et ₂ O (0.115 M, 1:1 (V/V)), RT, overnight	-	complete overreduction
4	Lindlar catalyst (60 mg/1 mmol), quinoline (0.3 equiv.) H ₂ (1 atm), Et ₂ O (0.5 M), RT, 3 h	-	Partial overreduction
5	Lindlar catalyst (60 mg/1 mmol), quinoline (0.3 equiv.) H ₂ (1 atm), Et ₂ O (0.25 M), RT, overnight	-	complete overreduction
6	NaBH ₄ (1.3 equiv.), Ni(OAc) ₂ (1.2 equiv.), ethylenediamine, (4.0 equiv.), H ₂ (1 atm), MeOH (0.5 M), RT, 3 h	42	-
7	NaBH ₄ (1.3 equiv.), Ni(OAc) ₂ (1.2 equiv.), ethylenediamine, (4.0 equiv.), H ₂ (1 atm), MeOH (0.75 M), RT, 4 h	46	-
8	NaBH ₄ (1.3 equiv.), Ni(OAc) ₂ (1.2 equiv.), ethylenediamine, (2.0 equiv.), H ₂ (1 atm), EtOH (0.75 M), RT, 18 h	-	decomposition
9	NaBH ₄ (1.3 equiv.), Ni(OAc) ₂ (1.2 equiv.), ethylenediamine, (2.0 equiv.), H ₂ (1 atm), MeOH (0.75 M), RT, 4 h	57	-

a) Isolated yield after column chromatography on silica gel.

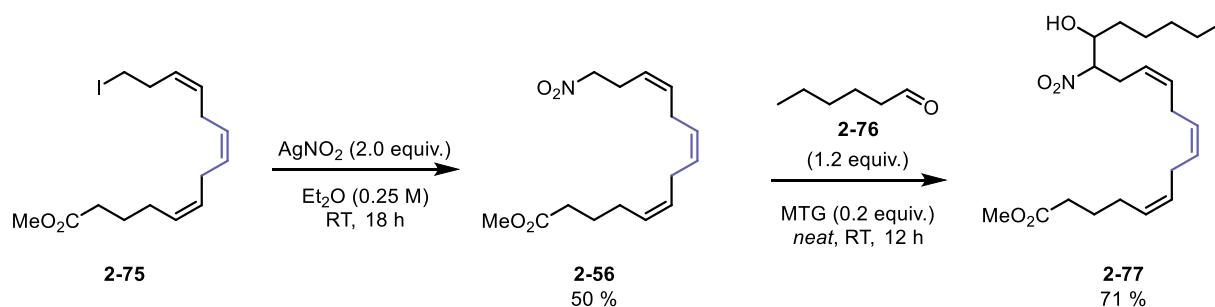
b) Based on the ¹H NMR spectra of the crude reaction mixture analysis.

The prepared alcohol **2-57** was then transformed into iodide **2-75** using I₂/PPh₃/imidazole system (65 % yield) (**Scheme 64**) and the iodo derivative **2-75** was transformed with the help of AgNO₂ into the corresponding nitro precursor for the Henry reaction (**Scheme 65**). Nitro derivative **2-56** was prepared in 50 % yield.

**Scheme 64:** Formation of Iodide **2-75**.

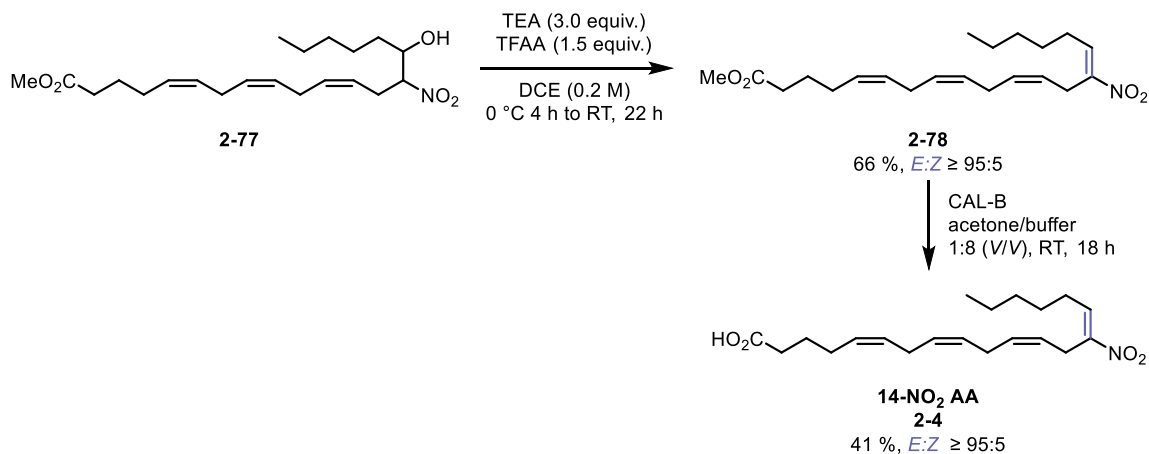
Chapter II: Biological evaluation

Finally, the Henry reaction of the nitro compound **2-56** with aldehyde **2-76** could be attempted (**Scheme 65**). Gratifyingly, the desired adduct **2-77** was formed under standard reaction conditions in just 12 h and a yield of 71 % (**Scheme 65**).



Scheme 65: Formation of nitro-alkene **2-56** and subsequent Henry reaction.

At this stage there were only two steps left in the sequence. First, adduct **2-77** underwent elimination reaction promoted with TFAA/TEA system and formed methyl ester of 14-nitro arachidonic acid **2-78** with a yield of 66 % and >95:5; 5:>95; 5:>95; 5:>95 *E/Z, E/Z, E/Z, E/Z* ratio. Subsequent enzymatic hydrolysis of **2-78** promoted with the CAL-B enzyme produced the final acid **2-4** in a yield of 41 % and an *E/Z, E/Z, E/Z, E/Z* ratio of >95:5; 5:>95; 5:>95; 5:>95 (**Scheme 66**).



Scheme 66: Elimination and ester hydrolysis. First synthesis of **14-NO₂ARA (2-4)**.

2.2.8. 14-NO₂ anandamide

Anandamide (**2-79**) - the arachidonic acid ethanolamide, together with 2-arachidonoylglycerol (2-AG, **2-80**) was found in the brain and intestine, and both belong to lipids classified as endocannabinoids (**Figure 35**).

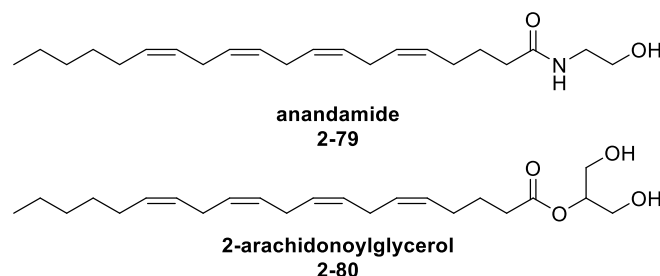


Figure 35: Structure of anandamide **2-79** and 2-arachidonoylglycerol **2-80**.

Cannabis sativa is a common plant that is known to contain various psychotropic compounds. Therefore, it is not surprising that the plant found its utility in many applications in medicine and is also known as a “readily available” intoxicant and/or as a drug. Recently, it has been reported that the plant has therapeutic effects, most probably due to cannabinoids.¹³² Cannabinoids are products typically derived from cannabis plant flowers such as Δ^9 -tetrahydrocannabinol (THC, **2-82**) and the cannabidiol (CBD, **2-81**) (**Figure 36**). The identification of THC structure in 1960s^{133,134} and mechanistic bioactivity studies of THC led to the identification of cannabinoid receptors in the 1990s^{135,136}, as well as the identification of endogenous ligands of these receptors, endocannabinoids¹³⁷.

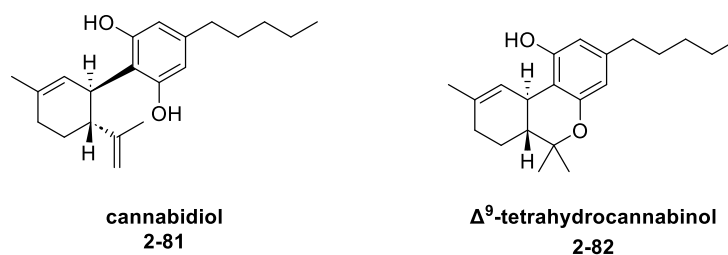


Figure 36: Structure of CBD **2-81** and THC **2-82**.

Cannabinoid receptors and endocannabinoids were found to be pleiotropic and involved in restoring homeostasis following pathological insults, suggesting their therapeutic opportunities.¹³⁸ The use of radiolabeled THC analogues led to the identification of binding sites in the brain, cannabinoid receptor 1 (CB1) and cannabinoid receptor 2 (CB2) which led to the identification of CB1 and CB2 ligands.^{136,137} **Anandamide** and

2-arachidonoylglycerol were found in the brain and intestine. They were also shown to activate CB1 and CB2 with high affinity and efficacy.^{139–141}

Endocannabinoids play a crucial role in the regulation of various physiological processes, mainly including those related to the nervous system. Studies in animal models suggest that in neurological disorders, endocannabinoids can become dysregulated and contribute to disease in different ways.¹⁴² For example, in Parkinson's disease^{143,144}, and Alzheimer's disease^{145–147}, Huntington disease^{148,149}, Multiple sclerosis^{150,151} and Epilepsy^{152,153}, altered levels or functions of endocannabinoids and their receptors have been observed, suggesting their potential as therapeutic targets. The action of endocannabinoids and their receptors in these neurological disorders is complex and diverse, often mitigating immune cell infiltration into the CNS and promoting anti-inflammatory responses through receptors such as CB2, TRPV1, or PPAR γ .^{154,155} Major efforts have been made to develop endocannabinoid-targeted drugs. The first promising drugs against Parkinson's disease, Alzheimer's disease, and multiple sclerosis are nabixomols (a mixture of THC and CBD), CBD, and palmitoylethanolamide (**Figure 36**, **Figure 37**). The efficacy of such drugs is attributed to their multitarget nature.

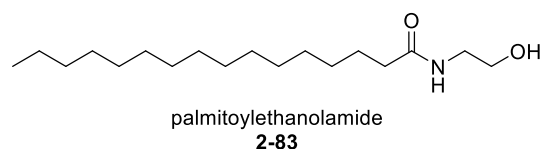


Figure 37: Structure of palmitoylethanolamide **2-83**.

2.2.8.1. Preparation of 14-NO₂ anandamide

We have decided to prepare the nitrated version of anandamide at C14 position **2-84** and test its biological properties. Since we have successfully prepared 14-NO₂ arachidonic acid (**2-4**), we have expected that the synthesis of the nitro derivative of anandamide will not be a problem, especially since various total syntheses of anandamide have been reported in the literature.^{156–160} Initially, we have decided to allow 14-NO₂ arachidonic acid (**2-4**) to react with O-protected aminoethanol by means of amide coupling (**Table 17**). First conditions we tried focused on the use of CDI and DCC coupling reagents, but in all cases no product was observed. We believe that the main reason for this observation is the reactivity of the free amine group that presumably attacked the Michael acceptor (nitroolefin) within the **2-4** structure and caused the decomposition of the starting material.

2.3. Biological evaluation

All newly prepared **NO₂FAs** were subjected to a biological activity evaluation, especially focusing on their activation of Nrf2 factor. Nrf2 is a well-known short-lived protein that works as a transcription factor, associated with the expression of numerous cytoprotective genes involved in xenobiotic metabolism and antioxidant responses.¹⁶¹ Over the past decade, studies have highlighted its crucial role in combating oxidative stress and potential implications in neurodegenerative diseases such as Alzheimer's and Parkinson's disease. Collaborative research has been conducted with Prof. Jan Vacek of Palacký University Olomouc, Faculty of Medicine, to explore the application of these compounds. Furthermore, the stability, redox properties, and electrophilic characteristics of methyl esters and acids were evaluated in collaboration with Prof. Ludvík Jiří and Dr. Liška Alan from the Jan Heyrovsky Institute of Physical Chemistry, Czech Academy of Sciences. Furthermore, the compounds were evaluated for their radioprotective properties in collaboration with Dr. Tomáš Perečko and Dr. Jana Perečková from the Institute of Biophysics, Czech Academy of Sciences. This activity, known to be related to Nrf2 activation in a wide variety of cells, is mediated by increasing DNA repair responses, neutralizing reactive oxygen species (ROS), reducing apoptosis, and regulating the cell cycle.¹⁶²

2.4. Conclusion

In conclusion, this chapter presents our efforts to optimize the synthesis of NO₂FAs. We successfully developed efficient reaction conditions, leading to the synthesis of five NO₂FAs, including 9- and 10-NO₂ oleic acid (**2-1** and **2-2**), 10-NO₂ linoleic acid (**2-3**), 9-NO₂ conjugated linoleic acid (**2-5**, nitro rumenic acid) and we have disclosed the first total synthesis of 14-NO₂ arachidonic acid (**2-4**). Additionally, a saturated NO₂ acid, 10-NO₂ stearic acid (**2-24**) was prepared (**Figure 38**). The preparation of 14-NO₂ anandamide has so far not been successful and a different approach will have to be developed.

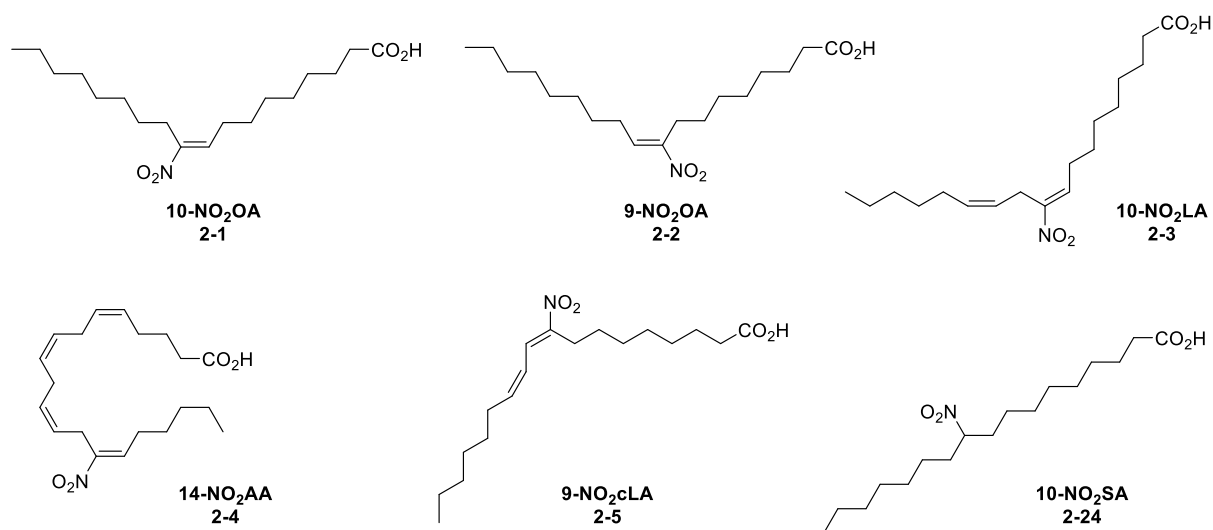


Figure 38: Structures of prepared FAs.

Biological evaluation, radioprotective properties, stability of NO₂FAs in water, their redox properties, and electrophilic characteristics of prepared compounds are currently being evaluated. The ongoing studies focus on detailed mechanistic investigations and further biological evaluations to fully elucidate the therapeutic potential of these NO₂FAs. We aim to explore their efficacy in various disease models and understand their mechanism of action at the molecular level. This work sets the foundation for the future development of NO₂FAs as potential therapeutic agents, because, for the first time, it allows the systematic study of **JUST ONE** stereoisomer of NO₂FAs that is in addition undoubtedly described and characterized.

The results from these collaborative efforts will be compiled and published in four independent articles, expected to be released in late 2024 and early 2025.

2.5. Experimental section

All starting materials were purchased from commercial suppliers and used without further purification, unless otherwise stated. All reactions were performed in round-bottom flasks fitted with rubber septa using standard laboratory techniques under positive pressure of argon (Air Liquide, >99.5% purity). In all reactions, unless stated otherwise, anhydrous solvents furnished by the Merck (Sigma-Aldrich) Company were used. Alternatively, tetrahydrofuran, acetonitrile and dichloromethane were dried using a solvent purification system equipped with alumina drying columns under argon. **Caution! HMPA and DCE are toxic. CARE SHOULD BE TAKEN!** Purification of reaction products was carried out by column chromatography using standard grade silica gel (60 Å, 230–400 mesh), or by preparative thin layer chromatography glass plates precoated with silica gel (silica gel G-200 F 254, particle size 0.040–0.063 mm). Analytical thin-layer chromatography was performed on a thin-layer chromatography (TLC) aluminum plates pre-coated with silica gel (silica gel 60 F 254). Visualization was accomplished with UV light, phosphomolybdic acid and potassium permanganate stains, followed by heating. The ^1H NMR and $^{13}\text{C}\{^1\text{H}\}$ NMR spectra were measured on JEOL ECA400II (400 and 101 MHz) or JEOL 500 ECA (500 and 126 MHz) in Chloroform- d . Chemical shifts are reported in ppm, and their calibration was carried out (a) in the case of ^1H NMR experiments on the residual peak of non-deuterated solvent δ (CDCl_3) = 7.26 ppm or δ (CD_3OD) = 3.31 ppm, δ ($\text{DMSO}-d_6$) = 2.50 ppm, δ ($\text{acetone}-d_6$) = 2.05 ppm and in the case of ^{13}C NMR experiments on the middle peak of the ^{13}C signal in deuterated solvent δ (CDCl_3) = 77.16 ppm, δ (CD_3OD) = 49.00 ppm, ($\text{DMSO}-d_6$) = 39.52 ppm, ($\text{acetone}-d_6$) = 29.84 ppm. The proton coupling patterns are represented as a singlet (s), a doublet (d), a doublet of a doublet (dd), a triplet (t), a triplet of a triplet (tt), and a multiplet (m). High-resolution mass spectrometry (HRMS) was performed on LC chromatograph (Dionex UltiMate 3000, Thermo Fischer Scientific, MA, USA) and mass spectrometer Exactive Plus Orbitrap high-resolution (Thermo Fischer Scientific, MA, USA) with electrospray ionization (ESI) and a time-of-flight analyzer operating in a positive or negative full scan mode in the range of 100 – 1700 m/z. High-performance liquid chromatography (HPLC) was performed using an Agilent 1290 Infinity II system with UV-VIS detector and an Agilent InfinityLab LC/MSD mass detector. Purification using semiprep HPLC was carried out on Agilent 1290 Infinity II with UV-VIS and mass detector Agilent InfinityLab LC/MSD using

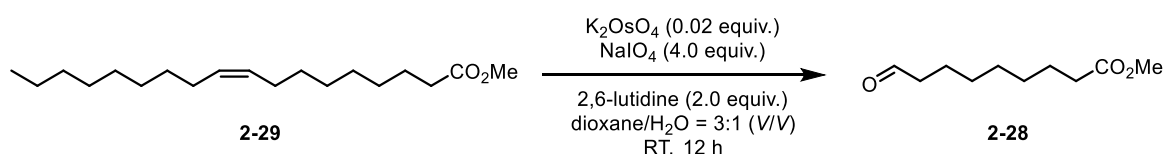
Chapter II: Experimental section

the C18 reverse-phase column (Agilent 5Prep-C18 10x21.2 mm). The gradient was formed from water and methanol with a flow rate of 20 mL/min. CAL-B - Lipase B *Candida antarctica* immobilized on Immobead 150 (≥ 2000 units/g IUBMB 3.1.1.3, EC number 232-619-9) was purchased from Merck.

Chapter II: Experimental section

2.5.1. 10-NO₂OA

methyl 9-oxononanoate (2-28)



2,6-lutidine (7.83 mL, 66.8 mmol, 2.0 equiv.), K₂OsO₄ (250 mg, 0.67 mmol, 0.02 equiv.) and NaIO₄ (28.8 g, 134 mmol, 4.0 equiv.) were sequentially added at room temperature to a stirred solution of **2-29** (10 g, 33.4 mmol, 1.0 equiv.) in dioxane/water = 3:1 (V/V, 300 mL). The reaction mixture was stirred at room temperature overnight before being filtered over a pad of Celite[®]. The filter cake was successfully washed with CHCl₃ (3x 200 mL). The combined filtrates were further washed with water (2x150 mL), brine (150 mL), dried over MgSO₄ and the solvents were removed under reduced pressure. The crude product was purified by flash column chromatography (SiO₂; petroleum ether:EtOAc = 1000:1) and gave a product **2-28** (4.36 g, 70 %) as a colorless oil.

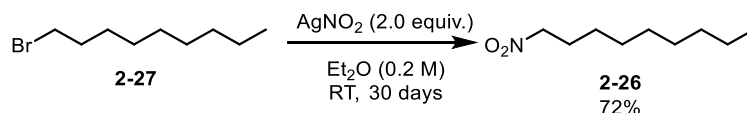
¹H NMR (500 MHz, Chloroform-*d*) δ (ppm): 9.76 (s, 1H), 3.66 (s, 3H), 2.42 (td, *J* = 7.3, 1.7 Hz, 2H), 2.30 (t, *J* = 7.5 Hz, 2H), 1.66 – 1.59 (m, 4H), 1.35 – 1.30 (m, 6H).

¹³C {¹H} NMR (126 MHz, Chloroform-*d*) δ (ppm): 203.0, 174.4, 67.2, 60.6, 51.6, 44.0, 34.2, 29.1, 29.1, 29.0, 25.0, 22.1, 14.3.

R_f = 0.7 (PMA; petroleum ether:EtOAc = 10:1)

Data matched to those previously reported.¹⁶³

1-nitrononane (2-26)



To a solution of bromide **2-27** (4 g, 19.3 mmol, 1.0 equiv.) in Et₂O (0.2 M, 96 mL) was added AgNO₂ (6 g, 38.6 mmol, 2.0 equiv.). The flask was stoppered and covered with aluminum foil to protect from light. The suspension was stirred for 30 days at RT. The mixture was diluted with EtOAc and filtered through a short plug of Celite[®]. The filter pad was rinsed with additional amounts of EtOAc (2x 100 mL), and the combined filtrates were concentrated under reduced

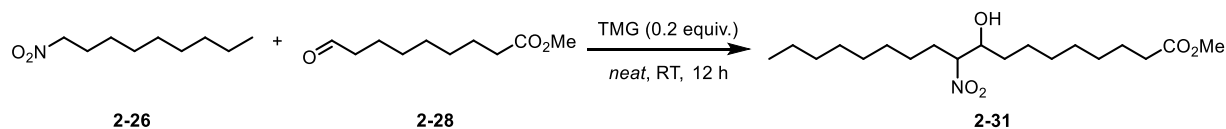
Chapter II: Experimental section

pressure. The crude product was purified by flash column chromatography (SiO₂; petroleum ether:EtOAc = 1000:1) and gave a product **2-26** (2.43 g, 72 % yield,) as a colorless oil.

¹H NMR (500 MHz, Chloroform-*d*) δ (ppm): 4.37 (t, *J* = 7.1 Hz, 2H), 2.03 – 1.96 (m, 2H), 1.41 – 1.19 (m, 12 h), 0.87 (t, *J* = 6.9 Hz, 3H).

¹³C {¹H} NMR (126 MHz, Chloroform-*d*) δ (ppm): 75.9, 31.9, 29.4, 29.3, 29.0, 27.6, 26.4, 22.8, 14.2.

methyl 9-hydroxy-10-nitrooctadecanoate (**2-31**)



Neat mixture of 1-nitrononane **2-26** (0.5 g, 2.28 mmol, 1.0 equiv.) and aldehyde **2-28** (0.4 g, 2.73 mmol, 1.2 equiv.) was cooled to 0 °C and 1,1,3,3-tetramethylguanidine (0.053 g, 0.2 mmol, 0.2 equiv.) was added. The resulting mixture was stirred for 18 h at room temperature before being cooled to 0 °C and the reaction was terminated with the addition of H₂O (10 mL). The resulting mixture was extracted with EtOAc (3×25 mL), and the combined organic phases were dried over Na₂SO₄. The solvent was removed *in vacuo* and the crude product was purified by flash column chromatography (SiO₂; petroleum ether:EtOAc = 50:1) to yield the adduct **2-31** (0.55 g, 67 %; *d.r.* = 1.48:1) as a pale-yellow oil. Product **2-31** was obtained as a mixture of two diastereoisomers in a 1.48:1 *d.r.* ratio (based on the ¹H NMR spectra analysis).

¹H NMR (500 MHz, Chloroform-*d*) δ (ppm): 4.43 (ttd, *J* = 9.3, 4.0, 1.7 Hz, 1H), 4.00 (ddq, *J* = 8.7, 4.7, 2.0 Hz, 0.5H), 3.85 (pd, *J* = 7.3, 6.4, 2.8 Hz, 0.5H), 3.66 (s, 3H), 2.34 (dd, *J* = 4.9, 3.0 Hz, 0.5H), 2.30 (t, *J* = 7.5 Hz, 2H), 2.18 (dd, *J* = 8.0, 3.4 Hz, 0.5H), 2.14 – 1.95 (m, 1H), 1.83 – 1.72 (m, 1H), 1.63 – 1.59 (m, 2H), 1.53 – 1.40 (m, 3H), 1.33 – 1.23 (m, 18 h), 0.87 (t, *J* = 7.0 Hz, 3H).

¹³C {¹H} NMR (126 MHz, Chloroform-*d*) δ (ppm): 174.5, 93.1, 92.5, 72.4, 72.1, 51.6, 34.1, 33.6, 33.2, 31.9, 30.5, 29.3, 29.2, 29.2, 29.1, 29.0, 28.1, 26.1, 25.8, 25.6, 25.2, 24.9, 22.7, 14.2.

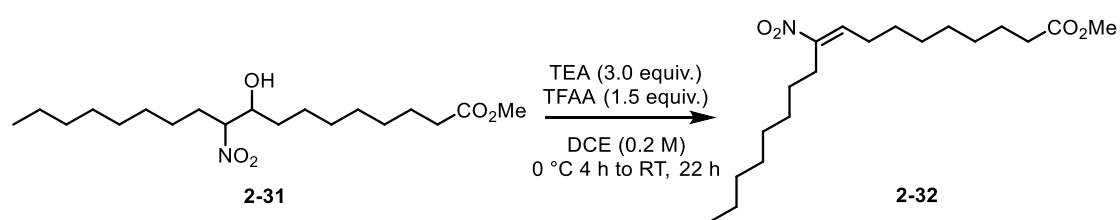
MS (ESI) *m/z* (%): 361 [M+H]⁺.

HRMS (ESI) *m/z*: [M+H]⁺ calculated for C₁₉H₃₈NO₅: 360.2744; found: 360.2748.

R_f = 0.19 (PMA, *n*-hexane:EtOAc = 10:1)

Chapter II: Experimental section

methyl (*E*)-10-nitrooctadec-9-enoate (**2-32**)



Adduct **2-31** (0.24 g, 0.66 mmol, 1.0 equiv.) was dissolved in DCE (3.3 mL, 0.2 M) and cooled to 0 °C. TEA (0.28 mL, 1.98 mmol, 3.0 equiv.) and TFAA (0.14 mL, 0.99 mmol, 1.5 equiv.) were sequentially added and the resulting mixture was stirred at 0 °C for 4 h and then at room temperature for next 22 h. The whole mixture was cooled to 0 °C and water (10 mL) was added in order to terminate the reaction. The resulting mixture was extracted with EtOAc (3×15 mL), and organic phases were combined, dried over MgSO₄, and the volatiles were removed *in vacuo*. The crude product was purified using semipreparative chromatography (C18 reverse-phase column; MeOH:H₂O) to yield the desired nitro olefin **2-32** (0.19g, 85 %; *E/Z* ≥ 95:5 (based on the ¹H NMR spectra analysis) in a form of a colorless oil.

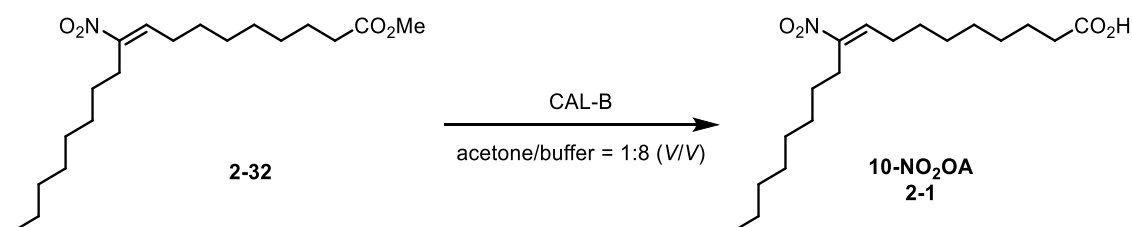
¹H NMR (500 MHz, Chloroform-*d*) δ (ppm): 7.07 (t, *J* = 7.9 Hz, 1H), 3.67 (d, *J* = 1.0 Hz, 3H), 2.60 – 2.53 (m, 2H), 2.31 (t, *J* = 7.5 Hz, 2H), 2.21 (q, *J* = 7.6 Hz, 2H), 1.62 (p, *J* = 7.2 Hz, 2H), 1.48 (h, *J* = 8.8, 8.2 Hz, 4H), 1.38 – 1.23 (m, 16H), 0.88 (t, *J* = 7.0 Hz, 3H).

¹³C {¹H} NMR (126 MHz, Chloroform-*d*) δ (ppm): 174.4, 152.1, 136.4, 51.6, 34.1, 32.0, 29.4, 29.32, 29.29, 29.14, 29.11, 28.6, 28.12, 28.05, 26.5, 25.0, 22.8, 14.2.

MS (ESI) *m/z* (%): 343 [M+H]⁺.

HRMS (ESI) *m/z*: [M+H]⁺ calculated for C₁₉H₃₆NO₄: 342.2639; found: 342.2642.

(*E*)-10-nitrooctadec-9-enoic acid (**10-NO₂OA**, **2-1**)



CAL-B (400 mg) was added to a solution of methyl ester **2-32** (0.3 g, 0.88 mmol, 1.0 equiv.) in acetone (11 mL, 0.08 M) and aqueous phosphate buffer (88 mL, 0.01 M, pH 7.4). The solution was vigorously stirred (magnetic stirrer, 1000 rpm) at room temperature for 18 h. 1 M HCl solution was added to adjust the pH of the solution to pH = 3. The whole mixture was

Chapter II: Experimental section

then extracted with EtOAc (5x20 mL), and the combined organic layers were dried over MgSO₄, filtered, and the volatiles were removed *in vacuo*. The crude product was purified using semipreparative chromatography (C18 reverse-phase column; MeOH:H₂O) to yield the desired acid **10-NO₂OA, 2-1** (0.13 g, 45 %, *E/Z* ≥ 95:5; based on the ¹H NMR spectra analysis).

¹H NMR (500 MHz, Chloroform-*d*) δ (ppm): 10.50 (bs, 1H), 7.07 (t, *J* = 7.9 Hz, 1H), 2.59 – 2.54 (m, 2H), 2.36 (t, *J* = 7.5 Hz, 2H), 2.21 (q, *J* = 7.6 Hz, 2H), 1.67 – 1.60 (m, 2H), 1.53 – 1.44 (m, 4H), 1.39 – 1.32 (m, 6H), 1.32 – 1.24 (m, 10H), 0.88 (t, *J* = 6.8 Hz, 3H).

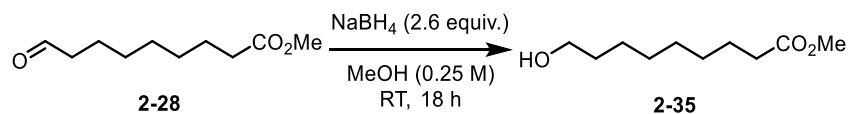
¹³C {¹H} NMR (126 MHz, Chloroform-*d*) δ (ppm): 152.1, 136.4, 33.8, 32.0, 29.4, 29.38, 29.32, 29.1, 29.0, 28.6, 28.12, 28.05, 26.5, 24.7, 22.8, 14.2.

MS (ESI) *m/z* (%): 327 [M-H]⁻.

HRMS (ESI) *m/z*: [M-H]⁻ calculated for C₁₈H₃₂NO₄: 326.2337; found: 326.2340.

2.5.2. 9-NO₂OA

methyl 9-hydroxynonanoate (2-35)

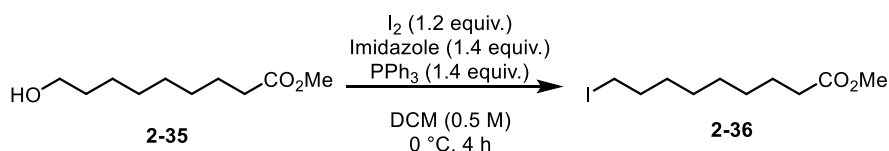


NaBH₄ (1.7 g, 44.2 mmol, 2.6 equiv.) was added to a cold (0 °C) solution of methyl oxoester **2-28** (3.2 g, 17 mmol, 1.0 equiv.) in MeOH (68 mL, 0.25 mL) and the resulting mixture was stirred at RT overnight. Water (50 mL), and EtOAc (100 mL) were added at room temperature and the resulting phases were separated. Aqueous layer was extracted with EtOAc (3x50 mL), and the combined organic layers were dried over MgSO₄, filtered, and the volatiles were removed *in vacuo*. The crude product was purified by flash column chromatography (SiO₂; petroleum ether:EtOAc = 10:1) to yield the desired nitro alkane **2-35** (3.17 g, 99 %) as a colorless oil.

¹H NMR (500 MHz, Chloroform-*d*) δ (ppm): 3.66 (d, *J* = 2.0 Hz, 3H), 3.63 (t, *J* = 6.6 Hz, 2H), 2.30 (td, *J* = 7.4, 2.0 Hz, 2H), 1.64 – 1.59 (m, 2H), 1.59 – 1.52 (m, 2H), 1.37 – 1.26 (m, 8H).

¹³C {¹H} NMR (126 MHz, Chloroform-*d*) δ (ppm): 174.5, 63.2, 51.6, 34.2, 32.9, 29.3, 29.3, 29.2, 25.8, 25.0.

methyl 9-iodononanoate (2-36)



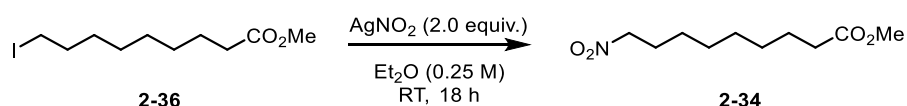
To an ice-cold solution of alcohol **2-35** (3.1 g, 2.14 mmol) in DCM (0.5 M, 33 mL) were added imidazole (1.57 g, 22.8 mmol, 1.4 equiv.), PPh₃ (6.05 g, 22.8 mmol, 1.4 equiv.), and I₂ (5 g, 19.6 mmol, 1.2 equiv.). After 3.5 h at 0 °C, the solution was diluted with EtOAc (100 mL), and a solution was filtered through a pad of silica gel to afford crude product. The crude product was purified by flash column chromatography (SiO₂; petroleum ether:EtOAc = 10:1) to yield the desired iodide **2-36** (4 g, 83 %) as a pale orange

¹H NMR (500 MHz, Chloroform-*d*) δ (ppm): 3.67 (s, 3H), 3.18 (t, *J* = 7.0 Hz, 2H), 2.30 (t, *J* = 7.5 Hz, 2H), 1.81 (p, *J* = 7.1 Hz, 2H), 1.64 – 1.59 (m, 2H), 1.41 – 1.35 (m, 2H), 1.34 – 1.23 (m, 6H).

¹³C {¹H} NMR (126 MHz, Chloroform-*d*) δ (ppm): 174.4, 51.6, 34.2, 33.6, 30.5, 29.2, 29.2, 28.5, 25.0, 7.4.

Chapter II: Experimental section

methyl 9-nitrononanoate (**2-34**)

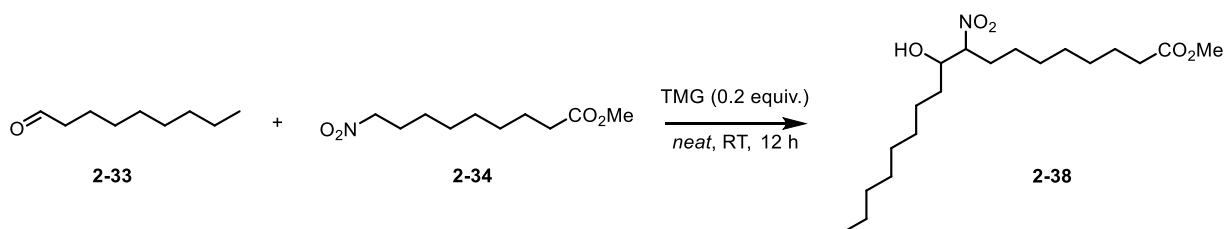


To a solution of iodide **2-36** (4 g, 13.3 mmol, 1.0 equiv.) in Et₂O (0.2 M, 66 mL) was added AgNO₂ (4.1 g, 26.6 mmol, 2.0 equiv.). The flask was stoppered and covered with aluminum foil to protect from light. The suspension was stirred overnight at RT. The mixture was diluted with EtOAc (100 mL) and filtered through a short plug of Celite[®]. The filter pad was rinsed with additional amounts of EtOAc (2x 100 mL), and the combined filtrates were concentrated under reduced pressure. Purification of the crude residue by flash column chromatography (SiO₂; petroleum ether:EtOAc = 4:1) afforded the desired nitro alkane **2-34** (4 g, 88 %) as a colorless oil.

¹H NMR (500 MHz, Chloroform-*d*) δ (ppm): 4.37 (t, *J* = 7.0 Hz, 2H), 3.66 (s, 3H), 2.30 (t, *J* = 7.5 Hz, 2H), 2.00 (p, *J* = 7.1 Hz, 2H), 1.62 (q, *J* = 7.4 Hz, 2H), 1.41 – 1.26 (m, 8H).

¹³C {¹H} NMR (126 MHz, Chloroform-*d*) δ (ppm): 174.4, 75.8, 51.6, 51.6, 34.1, 29.0, 29.0, 28.8, 27.5, 26.3, 24.9.

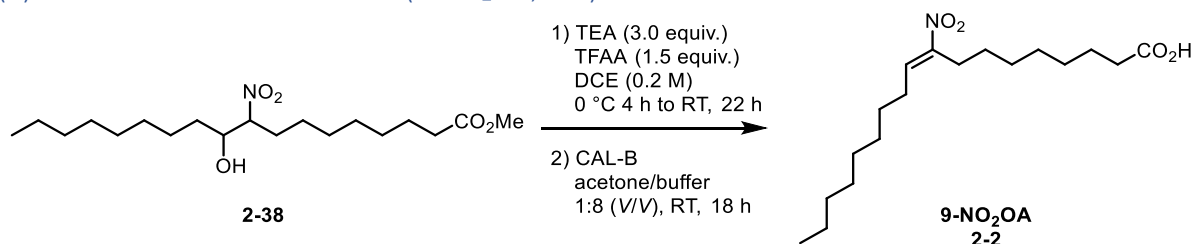
methyl 10-hydroxy-9-nitrooctadecanoate (**2-38**)



Neat mixture of nitroalkane **2-34** (1.2 g, 5.47 mmol, 1.0 equiv.) and nonanal **2-33** (0.96 g, 6.56 mmol, 1.2 equiv.) was cooled to 0 °C and 1,1,3,3-tetramethylguanidine (0.14 g, 1.1 mmol, 0.2 equiv.) was added. The resulting mixture was stirred for 12 h at room temperature before being cooled to 0 °C and the reaction was terminated with the addition of H₂O (25 mL). The resulting mixture was extracted with EtOAc (3x30 mL), and the combined organic phases were dried over MgSO₄. The solvent was removed *in vacuo* and the crude product **2-38** was used directly without further purification in the next step.

Chapter II: Experimental section

(*E*)-9-nitrooctadec-9-enoic acid (**9-NO₂OA**, **2-2**)



Adduct **2-38** (0.24 g, 0.66 mmol, 1.0 equiv.) was dissolved in DCE (3.3 mL, 0.2 M) and cooled to 0 °C. TEA (0.28 mL, 1.98 mmol, 3.0 equiv.) and TFAA (0.14 mL, 0.99 mmol, 1.5 equiv.) were sequentially added and the resulting mixture was stirred at 0 °C for 4 h and then at room temperature for next 22 h. The whole mixture was cooled to 0 °C and water (10 mL) was added in order to terminate the reaction. The resulting mixture was extracted with EtOAc (3×15 mL), and organic phases were combined, dried over MgSO₄, and the volatiles were removed *in vacuo*. The crude product was purified using semipreparative chromatography (C18 reverse-phase column; MeOH:H₂O) to yield the desired methyl 9-nitro oleate **2-39** (0.13 g, 57 %).

¹H NMR (500 MHz, Chloroform-*d*) δ (ppm): 7.08 (t, *J* = 7.9 Hz, 1H), 3.66 (s, 3H), 2.60 – 2.53 (m, 2H), 2.30 (t, *J* = 7.5 Hz, 2H), 2.21 (q, *J* = 7.6 Hz, 2H), 1.61 (p, *J* = 7.2 Hz, 2H), 1.48 (h, *J* = 7.5 Hz, 4H), 1.37 – 1.22 (m, 16H), 0.90 – 0.83 (m, 3H).

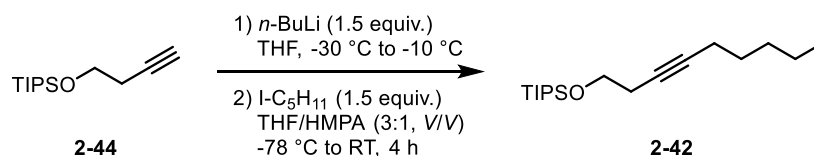
¹³C {¹H} NMR (126 MHz, Chloroform-*d*) δ (ppm): 174.4, 151.9, 136.7, 51.6, 34.2, 31.9, 29.5, 29.4, 29.3, 29.2, 29.1, 29.1, 28.7, 28.2, 28.0, 26.5, 25.0, 22.8, 14.2.

CAL-B (400 mg) was added to a solution of methyl ester **2-39** (0.13 g, 0.38 mmol, 1.0 equiv.) in acetone (4.7 mL, 0.08 M) and aqueous phosphate buffer (38 mL, 0.01 M, pH 7.4). The solution was vigorously stirred (magnetic stirrer, 1000 rpm) at room temperature for 18 h. 1 M HCl solution was added to adjust the pH of the solution to pH = 3. The whole mixture was then extracted with EtOAc (5×20 mL), and the combined organic layers were dried over MgSO₄, filtered, and the volatiles were removed *in vacuo*. The crude product was purified using semipreparative chromatography (C18 reverse-phase column; MeOH:H₂O) to yield the desired acid **9-NO₂OA**, **2-2** (0.1 g, 81 %, *E/Z* ≥ 95:5; based on the ¹H NMR spectra analysis).

¹H NMR (500 MHz, Chloroform-*d*) δ (ppm): 11.53 (s, 1H), 7.07 (t, *J* = 7.9 Hz, 1H), 2.60 – 2.51 (m, 2H), 2.34 (t, *J* = 7.5 Hz, 2H), 2.20 (q, *J* = 7.6 Hz, 2H), 1.62 (p, *J* = 7.4 Hz, 2H), 1.48 (h, *J* = 7.2 Hz, 4H), 1.37 – 1.29 (m, 6H), 1.32 – 1.21 (m, 10H), 0.92 – 0.83 (m, 3H).

¹³C {¹H} NMR (126 MHz, Chloroform-*d*) δ (ppm): 152.1, 136.4, 33.9, 32.0, 29.4, 29.3, 29.3, 29.1, 29.0, 28.6, 28.1, 28.1, 26.5, 24.7, 22.8, 14.2.

HRMS (ESI) *m/z*: [M-H]⁻ calculated for C₁₈H₃₂NO₄: 326.2337; found: 326.2326.

2.5.3. 10-NO₂LATriisopropyl(oct-3-yn-1-yloxy)silane (**2-42**)

A solution of TIPS protected acetylene **2-44** (10 g, 43.7 mmol, 1.0 equiv.) in THF (109 mL, 0.4 M) was cooled to -30 °C (dry ice/acetone) and *n*-BuLi (41 mL, 64 mmol, 1.5 equiv.; 1.6 M sol. in hexane) was added dropwise. The resulting mixture was brought to -10 °C and stirred for 1 hour. The whole mixture was cooled to -78 °C (dry ice/acetone) and a mixture of 1-iodopentane (8.7 mL, 43.7 mmol, 1.5 equiv.) in THF:HMPA = 3:1 (V/V; 88 mL) was added dropwise. The whole mixture was stirred at -78 °C for 1 h and then was allowed to warm up to room temperature over a period of 4 h. Water (50 mL) was added and the whole mixture was extracted with Et₂O (3x100 mL). The combined organic layers were washed with brine (50 mL), washed over Na₂SO₄, filtered and the volatiles were removed under reduced pressure. The crude product was purified by flash column chromatography (SiO₂; petroleum ether:EtOAc = 100:1) and yielded acetylene **2-42** (9.86 g, 76 %) in the form of a colorless oil.

¹H NMR (500 MHz, Chloroform-*d*) δ (ppm): 3.77 (t, *J* = 7.4 Hz, 2H), 2.42 – 2.36 (m, 2H), 2.13 (tt, *J* = 7.2, 2.4 Hz, 2H), 1.48 (p, *J* = 7.0 Hz, 2H), 1.39 – 1.27 (m, 3H), 1.14 – 1.01 (m, 20H), 0.90 (t, *J* = 7.1 Hz, 3H).

¹³C {¹H} NMR (126 MHz, Chloroform-*d*) δ (ppm): 62.8, 31.2, 28.9, 23.4, 22.4, 18.9, 18.7, 18.1, 14.1, 12.12, 12.09.

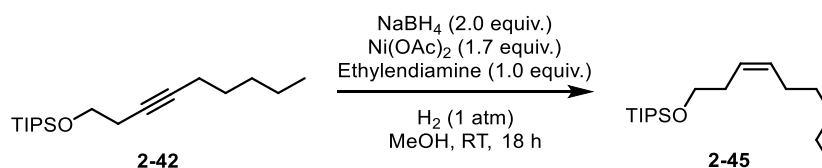
MS (ESI) *m/z* (%): 298 [M+H]⁺.

HRMS (ESI) *m/z*: [M+H]⁺ calculated for C₁₈H₃₉OSi: 297.2608; found: 297.2605.

R_f = 0.45 (vanillin, orange spot; petroleum ether:EtOAc = 10:1)

Chapter II: Experimental section

(*Z*)-triisopropyl(non-3-en-1-yloxy)silane (**2-45**)



NaBH₄ (9.86 g, 65.8 mmol, 2.0 equiv.) was added to a stirred solution of Ni(OAc)₂ (14.2 g, 56 mmol, 1.7 equiv.) in dry MeOH (330 mL, 0.1 M) at room temperature under positive pressure of argon. Argon atmosphere (balloon) was replaced with hydrogen (double layer balloon) and ethylenediamine (3.29 mL, 32.9 mmol, 10 M, 1.0 equiv.) was added. After 5 min, alkyne **2-42** (9.86 g, 32.9 mmol, 1.0 equiv.) in MeOH (20 mL) was added and the resulting mixture was stirred for 4 h. The whole mixture was filtered through a pad of Celite[®] and the filter cake was washed with Et₂O (200 mL). Filtrate was diluted with brine (150 mL), and EtOAc (150 mL), and the resulting layers were separated. The aqueous phase was extracted with EtOAc (3x150 mL), and the combined organic layers were washed with brine (50 mL), dried over MgSO₄, filtered, and the volatiles were removed under reduced pressure. The crude product was purified by flash column chromatography (SiO₂; petroleum ether:EtOAc = 100:1) and yielded a product **2-45** (8.25 g, 84 %) in the form of a colorless oil.

¹H NMR (500 MHz, Chloroform-*d*) δ (ppm): 5.48 – 5.35 (m, 2H), 3.68 – 3.65 (m, 2H), 2.30 (q, *J* = 7.2 Hz, 2H), 2.04 (q, *J* = 7.3 Hz, 2H), 1.35 – 1.27 (m, 6H), 1.06 (dd, *J* = 5.5, 2.3 Hz, 21H), 0.90 – 0.86 (m, 3H).

¹³C{¹H} NMR (126 MHz, Chloroform-*d*) δ (ppm): 132.0, 125.7, 63.4, 31.7, 31.4, 29.6, 27.5, 22.7, 18.2, 14.2, 12.2.

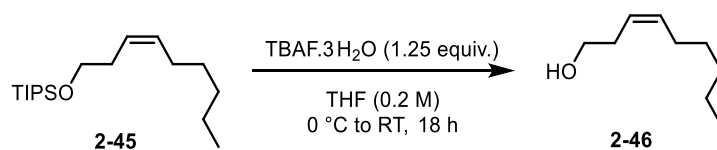
MS (ESI) *m/z* (%): 300 [M+H]⁺.

HRMS (ESI) *m/z*: [M+H]⁺ calculated for C₁₈H₃₉OSi: 299.2765; found: 299.2768.

R_f = 0.55 (PMA, petroleum ether:EtOAc = 10:1)

Chapter II: Experimental section

(Z)-non-3-en-1-ol (**2-46**)



Alkene **2-45** (6 g, 19.9 mmol, 1.0 equiv.) was dissolved in THF (99.5 mL, 0.2 M) and the resulting mixture was cooled to 0 °C (ice/water). TBAF·3H₂O (8 g, 24.9 mmol, 1.25 equiv.) was added dropwise and the resulting mixture was stirred at 0 °C for 3 h. Sat. aq. NH₄Cl (50 mL) was added, and the resulting mixture was extracted with EtOAc (3x100 mL). The combined organic layers were washed with brine (100 mL), dried over MgSO₄, filtered and the solvents were removed under reduced pressure. The crude product was purified by column flash column chromatography (SiO₂; petroleum ether:EtOAc = 10:1) and gave a product **2-46** (2.11 g, 74 %) as a colorless oil.

¹H NMR (500 MHz, Chloroform-*d*) δ (ppm): 5.62 – 5.51 (m, 1H), 5.42 – 5.29 (m, 1H), 3.67 – 3.57 (m, 2H), 2.33 (qd, *J* = 6.6, 1.5 Hz, 2H), 2.06 (qd, *J* = 7.3, 1.6 Hz, 2H), 1.39 – 1.23 (m, 7H), 0.88 (t, *J* = 6.9 Hz, 3H).

¹³C {¹H} NMR (126 MHz, Chloroform-*d*) δ (ppm): 133.8, 125.1, 62.5, 31.6, 30.9, 29.5, 27.5, 22.7, 18.7, 14.2.

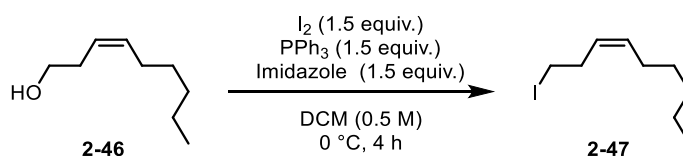
MS (ESI) *m/z* (%): 143 [M+H]⁺.

HRMS (ESI) *m/z*: [M+H]⁺ calculated for C₉H₁₉O: 143.1430; found: 143.1429.

R_f = 0.3 (vanillin, blue-green spot; petroleum ether:EtOAc = 4:1)

Chapter II: Experimental section

(Z)-1-iodonon-3-ene (2-47)



A solution of **2-46** (2.11 g, 14.7 mmol, 1.0 equiv.) in DCM (147 mL, 0.1 M) was cooled to 0 °C and PPh_3 (5.84 g, 22 mmol, 1.5 equiv.), imidazole (1.51 g, 22 mmol, 1.5 equiv.), and iodine (5.65 g, 22 mmol, 1.5 equiv.) was sequentially added. The resulting mixture was allowed to warm up to room temperature, and the reaction progress was monitored by TLC. Water (50 mL) was added to terminate the reaction and the resulting phases were separated. The aqueous phase was extracted with EtOAc (3x50 mL), and the combined organic phases were washed with brine (50 mL), dried over $MgSO_4$ and the volatiles were removed under reduced pressure. The crude product was purified by flash column chromatography (SiO_2 ; petroleum ether:EtOAc = 10:1) and yielded **2-47** (3.45, 93 %) as colorless oil.

1H NMR (500 MHz, Chloroform-*d*) δ (ppm): 5.57 – 5.50 (m, 1H), 5.34 – 5.28 (m, 1H), 3.13 (t, J = 7.3 Hz, 2H), 2.63 (q, J = 7.3 Hz, 2H), 2.02 (q, J = 7.4 Hz, 2H), 1.38 – 1.25 (m, 6H), 0.89 (t, J = 6.8 Hz, 3H).

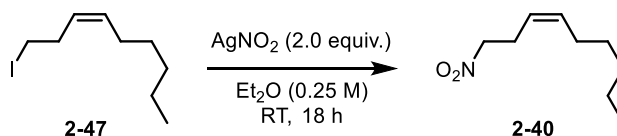
$^{13}C\{^1H\}$ NMR (126 MHz, Chloroform-*d*) δ (ppm): 132.9, 127.8, 31.7, 31.6, 29.3, 27.6, 22.7, 14.2, 5.7.

MS (ESI) m/z (%): 253 [$M+H$] $^+$.

HRMS (ESI) m/z : [$M+H$] $^+$ calculated for $C_9H_{18}I$: 253.0448; found: 253.0450.

R_f = 0.8 (vanillin; petroleum ether:EtOAc = 10:1)

(Z)-1-nitronon-3-ene (2-40)



At room temperature, a silver nitrite (4.2 g, 27.1 mmol, 2.0 equiv.) was added in one portion to an aluminum foil-covered flask containing a stirred solution of **2-47** (3.45 g, 13.5 mmol, 1.0 equiv.) in Et_2O (54 mL, 0.25 M). The resulting mixture was stirred at room temperature for 18 h before being filtered through a short pad of Celite[®]. The filter cake was washed with EtOAc (3x50 mL), and the resulting layers were separated. The aqueous layer was extracted with EtOAc (3x50 mL), and the organic layers were combined, washed with brine, dried over

Chapter II: Experimental section

MgSO₄ and the solvents were removed under reduced pressure. The crude product was purified by flash column chromatography (SiO₂; petroleum ether:EtOAc =10:1) and yielded a product **2-40** (1.67 g, 72 %) as a colorless oil.

¹H NMR (500 MHz, Chloroform-*d*) δ (ppm): 5.58 (dtt, *J* = 16.4, 7.5, 1.5 Hz, 1H), 5.29 (dtt, *J* = 16.5, 7.5, 1.7 Hz, 1H), 4.37 (t, *J* = 7.2 Hz, 2H), 2.83 – 2.68 (m, 2H), 2.08 – 2.01 (m, 2H), 1.36 – 1.25 (m, 6H), 0.89 (t, *J* = 6.9 Hz, 3H).

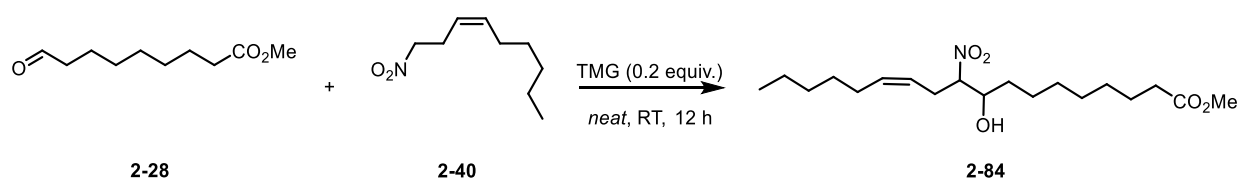
¹³C {¹H} NMR (126 MHz, Chloroform-*d*) δ (ppm): 135.1, 122.2, 75.3, 31.6, 29.2, 27.4, 25.6, 22.7, 14.2.

MS (ESI) *m/z* (%): 172 [M+H]⁺.

HRMS (ESI) *m/z*: [M+H]⁺ calculated for C₉H₁₈NO₂: 172.1332; found: 172.1335.

R_f = 0.4 (petroleum ether:EtOAc = 10:1)

methyl (*Z*)-9-hydroxy-10-nitrooctadec-12-enoate (**2-84**)



Neat mixture of nitroalkane **2-40** (0.3 g, 1.73 mmol, 1.0 equiv.) and aldehyde **2-28** (0.49 g, 2.6 mmol, 1.2 equiv.) was cooled to 0 °C and 1,1,3,3-tetramethylguanidine (0.04 g, 0.35 mmol, 0.2 equiv.) was added. The resulting mixture was stirred for 12 h at room temperature before being cooled to 0 °C and the reaction was terminated with the addition of H₂O (5 mL). The resulting mixture was extracted with EtOAc (3×15 mL), and the combined organic phases were dried over MgSO₄. The solvent was removed *in vacuo* and the crude product was purified by flash column chromatography (SiO₂; petroleum ether:EtOAc = 50:1) to yield the adduct **2-84** (0.5 g, 81 %; *d.r.* = 1.17:1) in the form of a colorless oil. Product **2-84** was obtained as a mixture of two diastereoisomers in a 1.17:1 *d.r.* ratio (based on the ¹H NMR spectra analysis).

¹H NMR (500 MHz, Chloroform-*d*) δ (ppm): 5.62 – 5.53 (m, 1H), 5.33 – 5.24 (m, 1H), 4.48 – 4.39 (m, 1H), 4.05 (dq, *J* = 8.5, 4.2 Hz, 0.5H, *major diastereoisomer*), 3.91 – 3.85 (m, 0.5H, *minor diastereoisomer*), 3.66 (s, 3H), 2.94 – 2.76 (m, 1H), 2.62 – 2.52 (m, 1H), 2.36 (d, *J* = 4.8 Hz, 0.5H), 2.30 (t, *J* = 7.5 Hz, 2H), 2.21 (d, *J* = 8.2 Hz, 0.5H), 2.02 (q, *J* = 7.4 Hz, 2H), 1.62 (p, *J* = 7.3 Hz, 2H), 1.58 – 1.39 (m, 4H), 1.34 – 1.26 (m, 12H), 0.88 (t, *J* = 6.9 Hz, 3H).

Chapter II: Experimental section

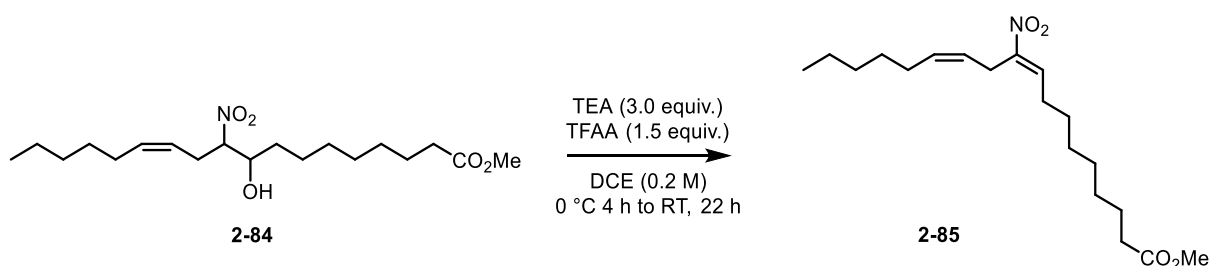
^{13}C { ^1H } NMR (126 MHz, Chloroform-*d*) δ (ppm): 174.4, 135.5, 135.2, 122.3, 121.6, 92.3, 92.0, 72.2, 71.7, 51.6, 34.2, 33.7, 33.3, 31.6, 29.25, 29.22, 29.17, 29.07, 28.7, 27.4, 26.3, 25.6, 25.4, 25.0, 22.7, 14.2.

MS (ESI) m/z (%): 359 [M+H]⁺.

HRMS (ESI) m/z : [M+H]⁺ calculated for C₁₉H₃₆NO₅: 358.2588; found: 358.2590.

R_f = 0.2 (PMA; petroleum ether:EtOAc = 10:1)

methyl (9*E*,12*Z*)-10-nitrooctadeca-9,12-dienoate (**2-85**)



Adduct **2-84** (0.5 g, 1.4 mmol, 1.0 equiv.) was dissolved in DCE (7 mL, 0.2 M) and cooled to 0 °C. TEA (0.59 mL, 4.2 mmol, 3.0 equiv.) and TFAA (0.3 mL, 2.1 mmol, 1.5 equiv.) were sequentially added and the resulting mixture was stirred at 0 °C for 4 h and then at room temperature for next 22 h. The whole mixture was cooled to 0 °C and water (10 mL) was added to terminate the reaction. The resulting mixture was extracted with EtOAc (3×25 mL), and organic phases were combined, dried over MgSO₄, and the volatiles were removed *in vacuo*. The crude product was purified by flash column chromatography (SiO₂; petroleum ether:EtOAc = 20:1) to yield the desired nitro olefin **2-85** (0.26 g, 55 %; *E/Z* ≥ 95:5 (based on the ¹H NMR spectra analysis) in a form of a colorless oil.

^1H NMR (500 MHz, Chloroform-*d*) δ (ppm): 7.08 (t, *J* = 7.9 Hz, 1H), 5.49 (dtt, *J* = 10.8, 7.3, 1.8 Hz, 1H), 5.25 (dtt, *J* = 10.5, 7.0, 1.7 Hz, 1H), 3.66 (s, 3H), 3.33 (dd, *J* = 7.0, 1.8 Hz, 2H), 2.30 (t, *J* = 7.5 Hz, 2H), 2.24 (q, *J* = 7.7 Hz, 2H), 2.12 (qd, *J* = 7.3, 1.6 Hz, 2H), 1.62 (dd, *J* = 9.9, 4.6 Hz, 2H), 1.49 (dt, *J* = 11.5, 7.2 Hz, 2H), 1.41 – 1.23 (m, 12H), 0.91 – 0.87 (m, 3H).

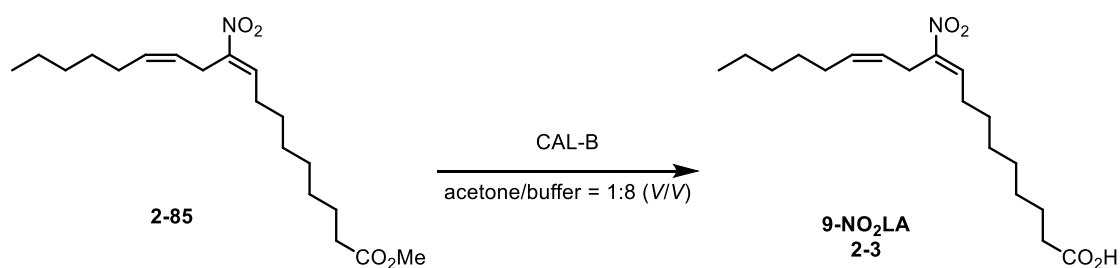
^{13}C { ^1H } NMR (126 MHz, Chloroform-*d*) δ (ppm): 174.3, 150.8, 136.6, 133.2, 123.4, 51.6, 34.1, 31.7, 29.29, 29.23, 29.12, 29.10, 28.5, 28.1, 27.5, 25.0, 22.7, 14.2.

MS (ESI) m/z (%): 340 [M+H]⁺ (100).

HRMS (ESI) m/z : [M+H]⁺ calculated for C₁₉H₃₄NO₄: 340.2482; found: 340.2486.

Chapter II: Experimental section

(9E,12Z)-10-nitrooctadeca-9,12-dienoic acid (9-NO₂LA, 2-3)



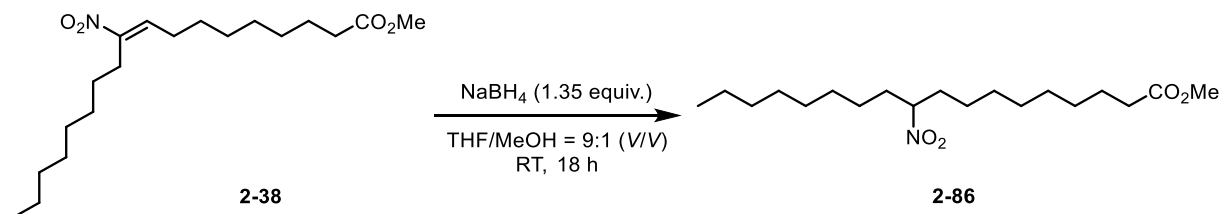
CAL-B (400 mg) was added to a solution of methyl ester **2-85** (0.3 g, 0.24 mmol, 1.0 equiv.) in acetone (11 mL, 0.08 M) and aqueous phosphate buffer (88 mL, 0.01 M, pH 7.4). The solution was vigorously stirred (magnetic stirrer, 1000 rpm) at room temperature for 18 h. 1 M aq. HCl solution was added to adjust the pH of the solution to pH = 3. The whole mixture was then extracted with EtOAc (5x20 mL), and the combined organic layers were dried over MgSO₄, filtered, and the volatiles were removed *in vacuo*. The crude product was purified using semipreparative chromatography (C18 reverse-phase column; MeOH:H₂O) to yield the desired acid **10-NO₂LA, 2-3** (0.12 g, 42 %, *E/Z* ≥ 95:5; based on the ¹H NMR spectra analysis).

¹H NMR (500 MHz, Chloroform-*d*) δ (ppm): δ 11.14 (bs, 1H), 7.08 (t, *J* = 7.9 Hz, 1H), 5.49 (dtt, *J* = 10.9, 7.3, 1.8 Hz, 1H), 5.25 (dtt, *J* = 10.7, 6.9, 1.7 Hz, 1H), 3.34 (dd, *J* = 7.0, 1.8 Hz, 2H), 2.35 (t, *J* = 7.4 Hz, 2H), 2.24 (q, *J* = 7.6 Hz, 2H), 2.12 (q, *J* = 7.3 Hz, 2H), 1.65 – 1.61 (m, 2H), 1.53 – 1.47 (m, 2H), 1.38 – 1.29 (m, 12 h), 0.90 (t, *J* = 6.8 Hz, 3H).

¹³C {¹H} NMR (126 MHz, Chloroform-*d*) δ (ppm): 179.6, 150.8, 136.6, 133.2, 123.4, 34.0, 31.7, 29.3, 29.2, 29.1, 29.0, 28.5, 28.1, 27.6, 25.0, 24.7, 22.7, 14.2.

MS (ESI) *m/z* (%): 324 [M-H]⁻ (100).

HRMS (ESI) *m/z*: [M-H]⁻ calculated for C₁₈H₃₀NO₄: 324.2169; found: 324.2179.

2.5.4. 10-NO₂SAmethyl 10-nitrooctadecanoate (**2-86**)

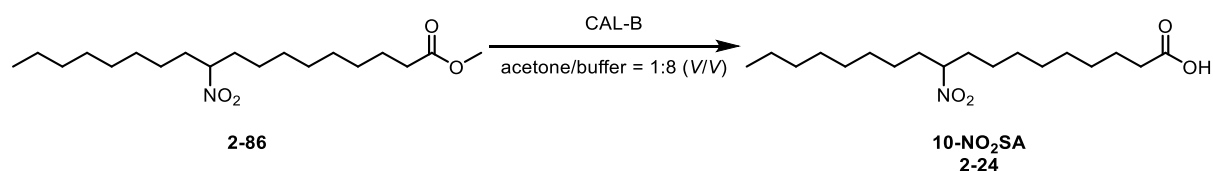
NaBH₄ (0.058 g, 1.5 mmol, 1.35 equiv.) was added to a cold (0 °C) solution of methyl (*E*)-9-nitrooctadec-9-enoate **2-38** (0.400 g, 1.1 mmol, 1.0 equiv.) in THF/MeOH (5.5 mL, 9:1 (V/V)) and the resulting mixture was stirred at RT for 14 h. Water (5 mL), and EtOAc (5 mL) were added at room temperature and the resulting phases were separated. Aqueous layer was extracted with EtOAc (5x20 mL), and the combined organic layers were dried over MgSO₄, filtered, and the volatiles were removed *in vacuo*. The crude product was purified by flash column chromatography (SiO₂; petroleum ether:EtOAc = 10:1) to yield the desired nitro alkane **2-86** (0.27 g, 73 %) as a colorless oil.

¹H NMR (500 MHz, Chloroform-*d*) δ (ppm): 4.45 (tt, *J* = 9.3, 4.5 Hz, 1H), 3.66 (s, 3H), 2.30 (t, *J* = 7.5 Hz, 2H), 1.94 (dtd, *J* = 14.0, 8.9, 4.3 Hz, 2H), 1.67 (dp, *J* = 15.2, 5.4, 5.0 Hz, 2H), 1.59 (dt, *J* = 12.4, 6.1 Hz, 2H), 1.34 – 1.20 (m, 22H), 0.87 (t, *J* = 6.9 Hz, 3H).

¹³C {¹H} NMR (126 MHz, Chloroform-*d*) δ (ppm): 174.5, 89.2, 51.6, 34.2, 34.1, 34.0, 31.9, 29.4, 29.3, 29.20, 29.17, 29.1, 29.0, 25.93, 25.91, 25.0, 22.8, 14.2.

MS (ESI) *m/z* (%): 345 [M+H]⁺.

HRMS (ESI) *m/z*: [M+H]⁺ calculated for C₁₉H₃₈NO₄: 344.2795; found: 344.2796.

10-nitrooctadecanoic acid (10-NO₂SA, **2-24**)

CAL-B (0.4 g) was added to a solution of methyl ester **2-86** (0.18 g, 0.52 mmol, 1.0 equiv.) in acetone (6.50 mL, 0.08 M) and aqueous phosphate buffer (52.4 mL, 0.01 M, pH 7.4). The solution was vigorously stirred (magnetic stirrer, 1000 rpm) at room temperature for 18 h. 1 M aq. HCl solution was added to adjust the pH of the mixture to pH = 3. The whole mixture was then extracted with EtOAc (5x20 mL), and the combined organic layers were dried over

Chapter II: Experimental section

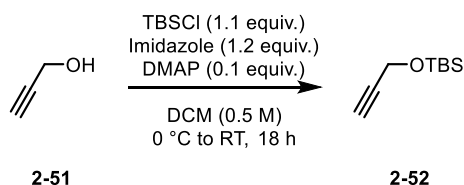
MgSO₄, filtered, and the volatiles were removed *in vacuo*. The crude product was purified by flash column chromatography (SiO₂; petroleum ether:EtOAc = 10:1) to yield the adduct **10-NO₂SA, 2-24** (0.17 g, 96 %) as a colorless oil.

¹H NMR (500 MHz, Chloroform-*d*) δ (ppm): 11.15 (bs, 1H), 4.45 (tt, *J* = 9.3, 4.5 Hz, 1H), 2.34 (t, *J* = 7.5 Hz, 2H), 1.99 – 1.89 (m, 2H), 1.72 – 1.58 (m, 4H), 1.36 – 1.22 (m, 22H), 0.87 (t, *J* = 7.0 Hz, 3H).

¹³C {¹H} NMR (126 MHz, Chloroform-*d*) δ (ppm): 179.7, 89.2, 34.1, 34.0, 31.9, 29.4, 29.3, 29.19, 29.17, 29.11, 29.06, 29.02, 25.93, 25.90, 24.7, 22.8, 14.2.

MS (ESI) *m/z* (%): 329 [M-H]⁻.

HRMS (ESI) *m/z*: [M-H]⁻ calculated for C₁₈H₃₄NO₄: 328.2493; found: 328.2496.

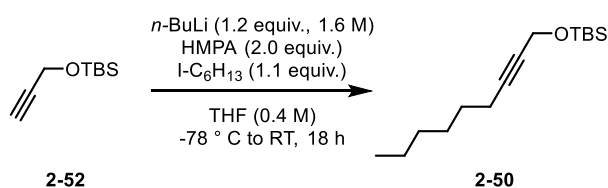
2.5.5. 9-NO₂cLA*tert*-butyldimethyl(prop-2-yn-1-yloxy)silane (2-52)

A solution of imidazole (22.0 g, 323 mmol, 1.2 equiv.) in DCM (539 mL, 0.5 M) was cooled to 0 °C and propargyl alcohol **2-51** (15.1 g, 269 mmol, 1.0 equiv.) was added. DMAP (3.36 g, 26.9 mmol, 0.1 equiv.) and TBSCl (51.3 mL, 296 mmol, 1.1 equiv.) were added and the whole mixture was stirred at room temperature overnight. Sat. aq. NH₄Cl (150 mL) was added, and the resulting layers were separated. The aqueous layer was extracted with DCM (3x150 mL). The combined organic layers were washed with brine (100 mL), dried over Na₂SO₄, filtered, and concentrated under reduced pressure. The crude product was purified by flash column chromatography (SiO₂; petroleum ether:EtOAc = 100:1) and yielded product **2-52** (30.0 g, 65 %) in the form of a colorless oil.

¹H NMR (500 MHz, Chloroform-*d*) δ (ppm): 4.31 (m, 2H), 2.39 (td, *J* = 2.4, 0.8 Hz, 1H), 0.91 (m, 9H), 0.13 – 0.12 (m, 6H).

¹³C {¹H} NMR (126 MHz, Chloroform-*d*) δ (ppm): 82.5, 73.0, 51.7, 26.1, 25.9, 18.4, -5.1.

R_f = 0.55 (hexane:EtOAc, 10:1)

tert-butyldimethyl(oct-2-yn-1-yloxy)silane (2-50)

To a solution of TBS protected alcohol **2-52** (6.85 g, 40 mmol, 1.0 equiv.) in THF (100 mL, 0.4 M) at -78 °C was added *n*-BuLi (29.9 mL, 47.8 mmol, 1.6 M in hexane) dropwise and stirring was continued at -78 °C for 1 h. Then, 1-iodohexane (6.46 mL, 43.8 mmol, 1.1 equiv.) was added to the reaction mixture followed by HMPA (13.9 mL, 79.6 mmol, 2.0 equiv.). The reaction mixture was allowed to warm to RT and left stirring overnight. Sat. aq. NH₄Cl (100 mL) was added. The organic layer was separated, and the aqueous phase was extracted by EtOAc (3x 100mL). Combined organic layers were dried with MgSO₄, filtered and concentrated

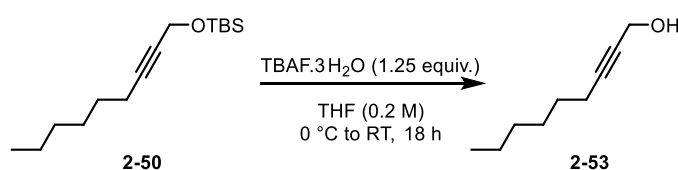
Chapter II: Experimental section

under vacuum. The crude product was purified by flash column chromatography (SiO₂; petroleum ether:EtOAc = 100:1) and yielded product **2-50** (8.45 g, 88 %) in the form of a colorless oil.

¹H NMR (500 MHz, Chloroform-*d*) δ (ppm): 4.30 (t, *J* = 2.2 Hz, 2H), 2.19 (tt, *J* = 7.1, 2.2 Hz, 2H), 1.53 – 1.45 (m, 2H), 1.42 – 1.34 (m, 2H), 1.33 – 1.24 (m, 4H), 0.91 (d, *J* = 0.5 Hz, 9H), 0.88 (t, *J* = 7.0 Hz, 3H), 0.12 (d, *J* = 0.5 Hz, 6H).

¹³C {¹H} NMR (126 MHz, Chloroform-*d*) δ (ppm): 85.7, 78.7, 52.2, 31.5, 28.7, 26.0, 25.9, 22.7, 18.9, 18.5, 14.2, -5.0.

non-2-yn-1-ol (2-53)



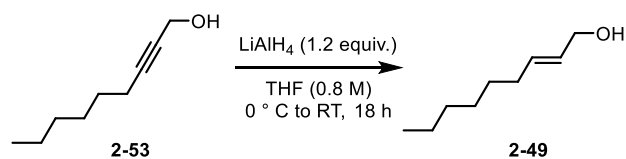
Alkene **2-50** (8.45 g, 32.9 mmol, 1.0 equiv.) was dissolved in THF (164 mL, 0.2 M) and the resulting mixture was cooled to 0 °C (ice/water). TBAF·3H₂O (13.2 g, 41.1 mmol, 1.25 equiv.) was added and the resulting mixture was stirred at 0 °C for 3 h. Sat. aq. NH₄Cl (100 mL) was added, and the resulting mixture was extracted with EtOAc (5x50mL). The combined organic layers were washed with brine (25 mL), dried over MgSO₄, filtered and the solvents were removed under reduced pressure. The crude product was purified by column flash column chromatography (SiO₂; petroleum ether:EtOAc = 40:1) and gave a product **2-53** (0.1 g, 24 %) as a yellowish oil.

¹H NMR (500 MHz, Chloroform-*d*) δ (ppm): 4.25 (dtd, *J* = 5.9, 2.2, 1.3 Hz, 2H), 2.21 (dddd, *J* = 7.2, 5.1, 2.2, 1.1 Hz, 2H), 1.59 – 1.55 (m, 2H), 1.54 – 1.45 (m, 3H), 1.40 – 1.34 (m, 2H), 1.33 – 1.24 (m, 4H), 0.91 (d, *J* = 1.2 Hz, 3H), 0.90 – 0.86 (m, 3H).

¹³C {¹H} NMR (126 MHz, Chloroform-*d*) δ (ppm): 86.9, 78.4, 51.6, 31.5, 28.7, 25.8, 22.7, 18.9, 14.2.

Chapter II: Experimental section

(*E*)-non-2-en-1-ol (**2-49**)



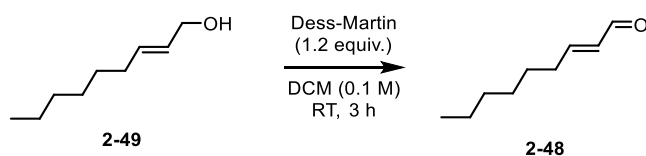
To a suspension of LiAlH_4 (0.89 g, 23.3 mmol, 1.2 equiv.) at 0 °C in dry THF (24.3 mL, 0.8 M) was added compound alcohol **2-53** (2.75 g, 19.4 mmol) dissolved in dry THF (19.4 mL, 1 M). The reaction was stirred at 0 °C for 10 min before it was allowed to warm to room temperature and allowed to stir overnight. Upon completion, the reaction was carefully quenched at 0 °C by the addition of water (2 mL) and 3 M NaOH followed by water (3x 15 mL). The mixture was filtered, and the filter cake was washed repeatedly with diethyl ether (5x 20 mL) and DCM (3x 5 mL). Concentration in vacuo followed by purification by column flash column chromatography (SiO_2 ; petroleum ether:EtOAc = 4:1) and gave a product **2-49** (1.75 g, 70 %) as a yellowish oil.

$R_f = 0.69$ (hexane:EtOAc, 4:1).

$^1\text{H NMR}$ (500 MHz, Chloroform-*d*) δ (ppm): 5.66 (qt, $J = 15.4, 6.0$ Hz, 2H), 4.08 (d, $J = 5.5$ Hz, 2H), 2.04 (q, $J = 7.0$ Hz, 2H), 1.40 – 1.33 (m, 2H), 1.32 – 1.22 (m, 6H), 0.88 (t, $J = 6.7$ Hz, 3H).

^{13}C { ^1H } NMR (126 MHz, Chloroform-*d*) δ (ppm): 133.8, 128.9, 64.0, 32.4, 31.9, 29.2, 29.0, 22.8, 14.2.

(*E*)-non-2-enal (**2-48**)



To a stirred solution of the alcohol **2-48** (1.5 g, 11.7 mmol, 1 equiv.) in DCM (117 mL, 0.1 M) was added Dess-Martin periodinane (6.37 g, 14.3 mmol, 1.22 equiv.). The resulting milky suspension was stirred for 3 h followed by the addition of sat. aq. NaHCO_3 solution (50 mL). Within 20 min the solution became clear and biphasic. The mixture was extracted with DCM (3x 50 mL), dried over MgSO_4 , filtered and the solvents were removed under reduced pressure. The crude product was purified by column flash column chromatography (SiO_2 ; petroleum ether:EtOAc = 4:1) and gave a product **2-53** (1.5 g, 95 %) as a yellowish oil.

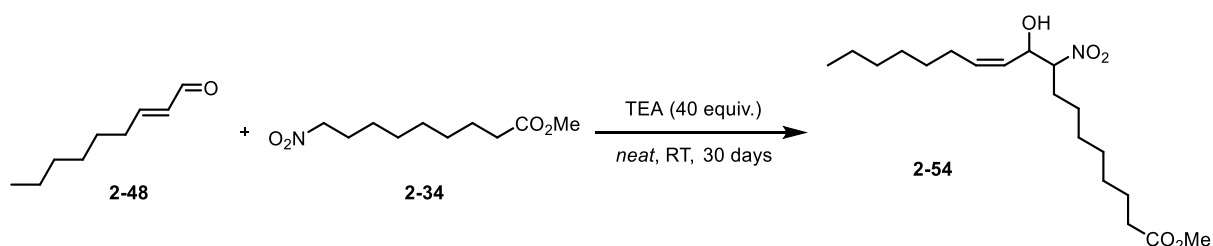
Chapter II: Experimental section

¹H NMR (500 MHz, Chloroform-*d*) δ (ppm): 9.51 (d, J = 7.9 Hz, 1H), 6.85 (dt, J = 15.6, 6.8 Hz, 1H), 6.12 (ddt, J = 15.6, 7.9, 1.6 Hz, 1H), 2.38 – 2.29 (m, 2H), 1.51 (p, J = 7.3 Hz, 2H), 1.37 – 1.24 (m, 6H), 0.90 – 0.87 (m, 3H).

¹³C {¹H} NMR (126 MHz, Chloroform-*d*) δ (ppm): 194.4, 159.3, 133.1, 32.9, 31.7, 28.9, 27.9, 22.7, 14.2.

HRMS (ESI) m/z : [M+H]⁺ calculated for C₉H₁₆O: 141.1274; found: 141.1277.

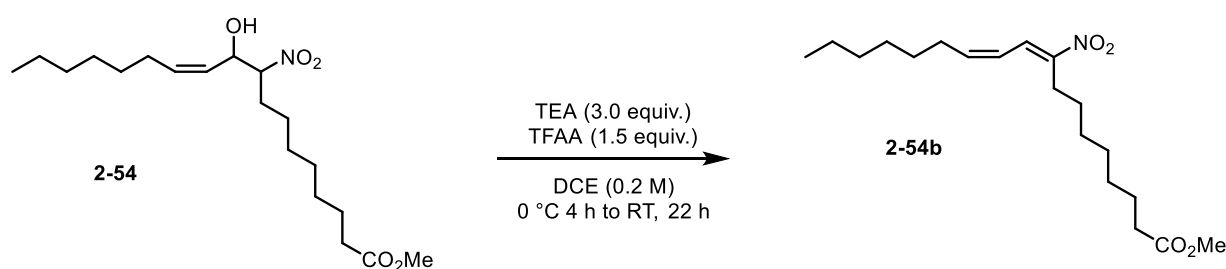
methyl (*Z*)-10-hydroxy-9-nitrooctadec-11-enoate (**2-54**)



Aldehyde **2-48** (0.95 g, 6.7 mmol, 1.7 equiv.) and nitro ester **2-34** (0.86 g, 3.94 mmol, 1 equiv.) were mixed and TEA (22 mL, 158 mmol, 40 equiv.) was added. The reaction was monitored until starting materials were consumed. After 30 days, the reaction was evaporated with a stream of nitrogen to remove triethylamine solvent then the crude oil redissolved in 20 mL Et₂O. The ether solution was transferred to a separatory funnel and washed with 30 mL \times 2 aqueous 0.1 M HCl, 30 mL \times 2 water, and 30 mL brine. The resulting solution was dried over anhydrous sodium sulfate, filtered through a plug of silica gel and Celite[®], then concentrated by rotary evaporation. The crude product was purified by gradient column flash column chromatography (SiO₂; petroleum ether:EtOAc = 30:1 \rightarrow 1:1) to separate starting materials from the product. The product was isolated and gave a product **2-54** (1.15 g, 60 %, *d.r.* 31:69) as a yellowish oil together with isolated aldehyde (0.2 g) and nitro ester (0.18 g). The product **2-54** was then immediately used in the next step

Chapter II: Experimental section

methyl (9*E*,11*Z*)-9-nitrooctadeca-9,11-dienoate (**2-54b**)



Adduct **2-54** (1.15 g, 3.2 mmol, 1.0 equiv.) was dissolved in DCE (16 mL, 0.2 M) and cooled to 0 °C. TEA (0.98 mL, 9.6 mmol, 3.0 equiv.) and TFAA (1.01 mL, 4.8 mmol, 1.5 equiv.) were sequentially added and the resulting mixture was stirred at 0 °C for 4 h and then at room temperature for next 22 h. The whole mixture was cooled to 0 °C and water (20 mL) was added to terminate the reaction. The resulting mixture was extracted with EtOAc (3×25 mL), and organic phases were combined, dried over MgSO₄, and the volatiles were removed *in vacuo*. The crude product was purified by flash column chromatography (SiO₂; petroleum ether:EtOAc = 20:1) to yield the desired nitro olefin **2-54b** (0.5 g, 47 %; *E/Z* ≥ 95:5 (based on the ¹H NMR spectra analysis) in a form of a colorless oil.

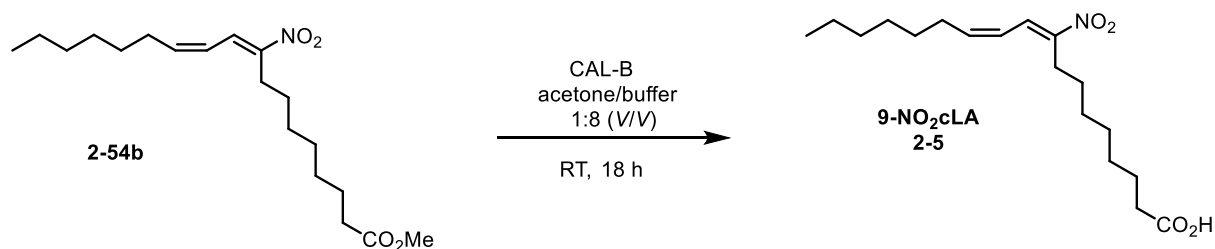
¹H NMR (500 MHz, Chloroform-*d*) δ (ppm): 7.54 (d, *J* = 11.3 Hz, 1H), 6.34 (dt, *J* = 14.5, 7.0 Hz, 1H), 6.19 (ddt, *J* = 14.8, 11.4, 1.4 Hz, 1H), 3.66 (s, 3H), 2.71 – 2.60 (m, 2H), 2.30 (t, *J* = 7.5 Hz, 2H), 2.25 (q, *J* = 7.8, 7.2 Hz, 2H), 1.62 (dd, *J* = 10.1, 4.5 Hz, 2H), 1.50 (q, *J* = 6.3, 5.4 Hz, 2H), 1.50 – 1.37 (m, 2H), 1.39 – 1.22 (m, 12H), 0.89 (t, *J* = 6.8 Hz, 3H).

¹³C {¹H} NMR (126 MHz, Chloroform-*d*) δ (ppm): 174.4, 149.5, 149.2, 134.1, 123.7, 51.6, 34.2, 33.8, 31.7, 29.1, 29.1, 29.1, 29.0, 28.7, 28.2, 26.7, 25.0, 22.7, 14.2.

HRMS (ESI) *m/z*: [M+H]⁺ calculated for C₁₉H₃₃NO₄: 340.2482; found: 340.2480.

Chapter II: Experimental section

(9E,11Z)-9-nitrooctadeca-9,11-dienoic acid, 9-NO₂cLA (**2-5**)



CAL-B (600 mg) was added to a solution of methyl ester **2-54b** (1.115 g, 3.2 mmol, 1.0 equiv.) in acetone (11 mL, 0.08 M) and aqueous phosphate buffer (88 mL, 0.01 M, pH 7.4). The solution was vigorously stirred (magnetic stirrer, 1000 rpm) at room temperature for 18 h. 1 M aq. HCl solution was added to adjust the pH of the solution to pH = 3. The whole mixture was then extracted with EtOAc (5x20 mL), and the combined organic layers were dried over MgSO₄, filtered, and the volatiles were removed *in vacuo*. The crude product was purified using semipreparative chromatography (C18 reverse-phase column; MeOH:H₂O) to yield the desired acid **9-NO₂cLA**, **2-3** (0.12 g, 42 %, *E/Z* ≥ 95:5; based on the ¹H NMR spectra analysis).

¹H NMR (500 MHz, Chloroform-*d*) δ (ppm): 7.56 – 7.52 (m, 1H), 6.35 (dt, *J* = 14.5, 7.0 Hz, 1H), 6.19 (ddt, *J* = 15.0, 11.4, 1.4 Hz, 1H), 2.69 – 2.62 (m, 2H), 2.35 (t, *J* = 7.5 Hz, 2H), 2.27 – 2.22 (m, 2H), 1.63 (p, *J* = 7.9, 7.1 Hz, 2H), 1.52 (d, *J* = 7.3 Hz, 2H), 1.48 – 1.42 (m, 2H), 1.37 – 1.25 (m, 12H), 0.94 – 0.85 (m, 3H).

¹³C {¹H} NMR (126 MHz, Chloroform-*d*) δ (ppm): 178.3, 149.5, 149.2, 134.1, 123.7, 33.8, 33.8, 31.7, 29.1, 29.1, 29.0, 29.0, 28.7, 28.2, 26.7, 24.7, 22.7, 14.2.

HRMS (ESI) *m/z*: [M-H]⁻ calculated for C₁₈H₃₀NO₄: 324.2180; found: 324.2178.

R_f = 0.33 (hexane/EtOAc; 3:1)

Chapter II: Experimental section

chromatography (SiO₂; petroleum ether/EtOAc = 20:1 → 10:1) to afford **2-64** (5.4 g, 80 %) as a colorless oil.

¹H NMR (500 MHz, Chloroform-*d*) δ (ppm): 4.25 – 4.22 (m, 1H), 3.80 (td, *J* = 7.3, 1.2 Hz, 1H), 2.49 – 2.44 (m, 1H), 1.08 – 1.03 (m, 21H).

¹³C {¹H} NMR (126 MHz, Chloroform-*d*) δ (ppm): 83.6, 79.6, 62.2, 51.5, 23.3, 18.1, 12.1.

5-((triisopropylsilyl)oxy)pent-2-yn-1-yl 4-methylbenzenesulfonate (**2-62**)

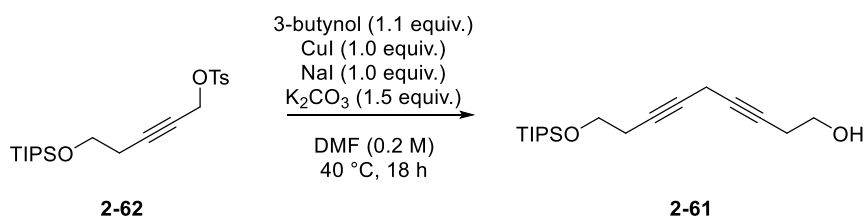


KOH (7.64 g, 116 mmol, 5.0 equiv.) was added to a solution of alcohol **2-62** (6 g, 18.5 mmol, 1.0 equiv.), *p*-toluenesulfonyl chloride (5.41 g, 27.8 mmol, 1.2 equiv.) and Et₂O (116 mL, 0.2 M) at 0 °C. The mixture was stirred for 2 h at 0 °C, after which the reaction was warmed to RT. Next day, the reaction was quenched with saturated aqueous NH₄Cl (50 mL) and extracted with EtOAc (3x 50 mL). The combined organic extracts were washed with brine (50 mL), dried over Na₂SO₄, and concentrated. The residue was purified by silica gel column chromatography (SiO₂; petroleum ether/EtOAc = 20:1) to afford tosylate **2-62** (9 g, 95 %) as a colorless oil.

¹H NMR (500 MHz, Chloroform-*d*) δ (ppm): 7.84 – 7.78 (m, 2H), 7.36 – 7.32 (m, 2H), 4.68 (t, *J* = 2.2 Hz, 2H), 3.68 (t, *J* = 7.2 Hz, 2H), 2.45 (s, 3H), 2.33 (tt, *J* = 7.2, 2.2 Hz, 2H), 1.07 – 1.00 (m, 21H).

¹³C {¹H} NMR (126 MHz, Chloroform-*d*) δ (ppm): 145.0, 133.4, 129.8, 128.2, 87.6, 73.0, 61.6, 58.7, 23.2, 21.8, 18.0, 17.8, 12.4, 12.0.

9-((triisopropylsilyl)oxy)nona-3,6-diyn-1-ol (**2-61**)



K₂CO₃ (7.68 g, 55.6 mmol, 3.0 equiv.) was added to a mixture of tosylate **2-62** (7.5 g, 18.1 mmol, 1.0 equiv.), 3-butyn-1-ol (1.45 mL, 19 mmol, 1.0 equiv.), CuI (3.51 g, 18.1 mmol, 1.0 equiv.), NaI (2.74 g, 18.1 mmol, 1.0 equiv.), and DMF (90 mL, 0.2 M) at RT. The mixture was heated to 40 °C, stirred for 18 h at this temperature, and quenched with saturated aqueous NH₄Cl (50

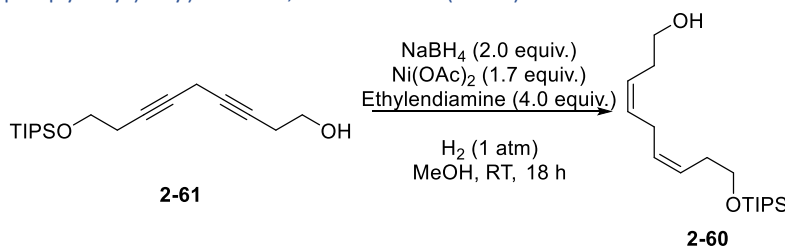
Chapter II: Experimental section

mL). The resulting mixture was filtrated through a pad of Celite®. After the organic layer was separated, the resulting aqueous layer was extracted with Et₂O (3x 50 mL). The combined organic extracts were washed with brine (50 mL), dried over Na₂SO₄, and concentrated. The crude product was purified by gradient column chromatography (SiO₂; petroleum ether/EtOAc = 20:1 → 10:1) to afford 1,4-diyne **2-61** (3.5 g, 63 %) as a colorless oil.

¹H NMR (500 MHz, Chloroform-*d*) δ (ppm): 3.78 (t, J = 7.3 Hz, 2H), 3.70 (q, J = 6.0 Hz, 2H), 3.13 (m, 2H), 2.44 (ddt, J = 8.2, 6.7, 2.2 Hz, 2H), 2.41 (dq, J = 7.3, 2.5 Hz, 2H), 1.11 – 1.01 (m, 21H).

¹³C {¹H} NMR (126 MHz, Chloroform-*d*) δ (ppm): 77.8, 77.0, 76.8, 75.3, 62.3, 61.2, 23.3, 23.3, 18.1, 12.1, 12.1, 9.9.

(3*Z*,6*Z*)-9-((triisopropylsilyl)oxy)nona-3,6-dien-1-ol (**2-60**)



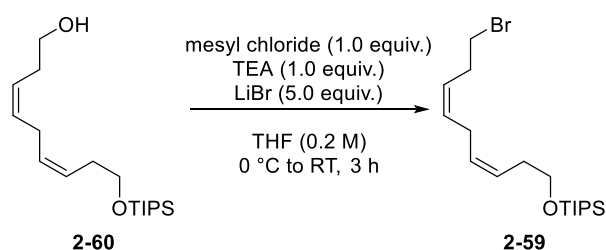
NaBH₄ (0.89 g, 23.1 mmol, 2.0 equiv.) was added to a stirred solution of Ni(OAc)₂ (5 g, 19.6 mmol, 1.7 equiv.) in dry MeOH (116 mL, 0.1 M) at RT under positive pressure of argon. Argon atmosphere (balloon) was replaced with hydrogen (double layer balloon) and ethylenediamine (4.6 mL, 46.2 mmol, 4.0 equiv., 10 M) was added. After 5 min, alkyne **2-61** (3.6 g, 11.6 mmol, 1.0 equiv.) in MeOH (20 mL) was added and the resulting mixture was stirred overnight. The whole mixture was filtered through a pad of Celite® and the filter cake was washed with Et₂O (2x100 mL). Filtrate was diluted with brine (150 mL), and EtOAc (150 mL), and the resulting layers were separated. The aqueous phase was extracted with EtOAc (3x150 mL), and the combined organic layers were washed with brine (50 mL), dried over MgSO₄, filtered, and the volatiles were removed under reduced pressure. The crude product was purified by flash column chromatography (SiO₂; petroleum ether:EtOAc = 20:1) and yielded a product **2-60** (2.93 g, 81 %) in the form of a colorless oil.

¹H NMR (500 MHz, Chloroform-*d*) δ (ppm): 5.54 (q, J = 8.1 Hz, 1H), 5.50 – 5.36 (m, 3H), 3.67 (dt, J = 18.4, 6.7 Hz, 4H), 2.85 (t, J = 6.7 Hz, 2H), 2.35 (dq, J = 13.4, 6.7 Hz, 4H), 1.06 (m, 21H).

¹³C {¹H} NMR (126 MHz, Chloroform-*d*) δ (ppm): 131.5, 129.4, 126.7, 125.6, 63.2, 62.4, 31.4, 31.0, 26.0, 18.2, 18.1, 12.13, 12.08.

Chapter II: Experimental section

(((3Z,6Z)-9-bromonona-3,6-dien-1-yl)oxy)triisopropylsilane (**2-59**)



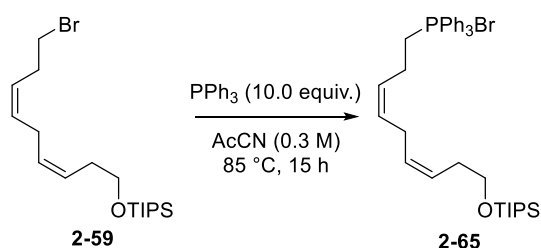
Mesyl chloride (1.37 mL, 17.4 mmol, 2.0 equiv.) was added to a solution of 1,4-diene **2-60** (2.74 g, 8.68 mmol, 1.0 equiv.), TEA (2.4 mL, 2.7 mmol, 2.0 equiv.), and THF (87 mL, 0.1 M) at 0 °C. After the solution was maintained for 1 h at 0 °C, lithium bromide (7.6 g, 86.8 mmol, 10.0 equiv.) was added to the solution. The resulting mixture was then heated to 50 °C, maintained for 3 h at this temperature after which it was cooled to RT and left overnight. Next day, the reaction was quenched with saturated aqueous NaHCO₃ (50 mL) and extracted with EtOAc (3x 50 mL). The combined organic extracts were washed with brine (50 mL), dried over Na₂SO₄, and concentrated. The crude product was purified by flash column chromatography (SiO₂; petroleum ether:EtOAc = 20:1) and yielded a product **2-59** (2.65 g, 82 %) in the form of a colorless oil.

¹H NMR (500 MHz, Chloroform-*d*) δ (ppm): 5.58 – 5.47 (m, 1H), 5.49 – 5.35 (m, 3H), 3.69 (t, J = 7.0 Hz, 2H), 3.38 (t, J = 7.1 Hz, 2H), 2.82 (t, J = 7.0 Hz, 2H), 2.65 (q, J = 7.2 Hz, 2H), 2.33 (q, J = 7.0 Hz, 2H), 1.16 – 1.01 (m, 21H).

¹³C {¹H} NMR (126 MHz, Chloroform-*d*) δ (ppm): 131.2, 129.1, 126.8, 126.4, 63.2, 32.5, 31.4, 30.9, 26.1, 18.2, 12.1.

Chapter II: Experimental section

bromotriphenyl((3Z,6Z)-9-((triisopropylsilyl)oxy)nona-3,6-dien-1-yl)-15-phosphane (2-65)



PPh_3 (18.5 g, 69.9 mmol, 10.0 equiv.) was dissolved in AcCN (23.3 mL, 0.3 M) and bromide **2-59** (2.65 g, 6.99 mmol, 1.0 equiv.) was added at RT. The solution was heated to 85 °C, maintained for 15 h at this temperature, after which it was cooled and evaporated. The crude product was purified by flash column chromatography (SiO_2 ; petroleum ether:EtOAc = 10:1) and yielded a product **2-65** in the form of a colorless oil.

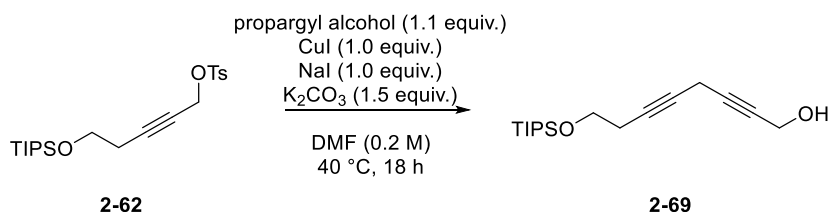
^1H NMR (500 MHz, Chloroform-*d*) δ (ppm): 7.91 – 7.85 (m, 6H), 7.79 (m, 4H), 7.70 (m, 5H), 5.64 (m, 1H), 5.42 – 5.32 (m, 2H), 5.28 – 5.20 (m, 1H), 4.00 (m, 2H), 3.61 (t, $J = 6.9$ Hz, 2H), 2.54 (t, $J = 7.3$ Hz, 2H), 2.46 (q, $J = 8.6, 7.3$ Hz, 2H), 2.17 (m, 2H, overlapping signal with impurity), 1.14 – 0.97 (m, 21H).

^{13}C { ^1H } NMR (126 MHz, Chloroform-*d*) δ (ppm): 135.1, 134.0, 133.9, 130.7, 130.6, 130.4, 128.8, 126.8, 118.9, 118.2, 63.1, 31.4, 25.8, 23.3, 20.6, 18.2, 12.1.

Chapter II: Experimental section

2.5.6.2. Second approach

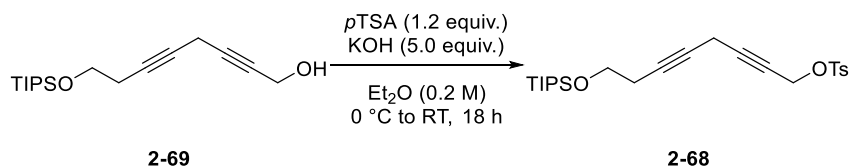
8-((triisopropylsilyl)oxy)octa-2,5-diyne-1-ol (**2-69**)



K₂CO₃ (4 g, 28.9 mmol, 1.5 equiv.) was added to a mixture of tosylate **2-62** (8 g, 19.3 mmol, 1.0 equiv.), propargyl alcohol (1.2 mL, 20.3 mmol, 1.0 equiv.), CuI (3.75 g, 19.3 mmol, 1.0 equiv.), NaI (2.92 g, 19.3 mmol, 1.0 equiv.), and DMF (96 mL, 0.2 M) at RT. The mixture was heated to 40 °C, stirred for 18 h at this temperature, and quenched with saturated aqueous NH₄Cl (50 mL). The resulting mixture was filtrated through a pad of Celite®. After the organic layer was separated, the resulting aqueous layer was extracted with Et₂O (3x 50 mL). The combined organic extracts were washed with brine (50 mL), dried over Na₂SO₄, and concentrated. The crude product was purified by gradient column chromatography (SiO₂; petroleum ether/EtOAc = 20:1 → 10:1) to afford 1,4-diyne **2-69** (4.97 g, 88 %) as a colorless oil.

¹H NMR (500 MHz, Chloroform-*d*) δ (ppm): 4.26 (dt, *J* = 6.2, 2.2 Hz, 2H), 3.78 (t, *J* = 7.3 Hz, 2H), 3.18 (p, *J* = 2.3 Hz, 2H), 2.41 (tt, *J* = 7.3, 2.4 Hz, 2H), 1.52 (t, *J* = 6.2 Hz, 1H), 1.09 – 1.03 (m, 21H).
¹³C {¹H} NMR (126 MHz, Chloroform-*d*) δ (ppm): 80.7, 78.6, 78.2, 74.6, 62.3, 62.3, 62.2, 51.5, 51.4, 23.3, 23.2, 18.1, 12.1, 10.0.

8-((triisopropylsilyl)oxy)octa-2,5-diyne-1-yl 4-methylbenzenesulfonate (**2-68**)



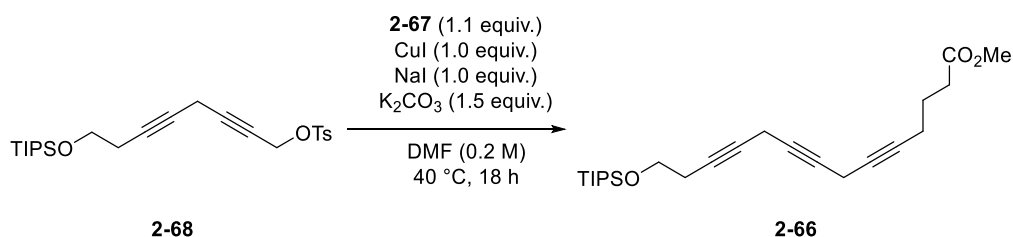
KOH (5.51 g, 83.5 mmol, 5.0 equiv.) was added to a solution of alcohol **2-69** (4.97 g, 16.7 mmol, 1.0 equiv.), *p*-toluenesulfonyl chloride (3.9 g, 20 mmol, 1.2 equiv.) and Et₂O (83 mL, 0.2 M) at 0 °C. The mixture was stirred for 2 h at 0 °C, after it was warmed to RT and left overnight. Next day, the reaction was quenched with saturated aqueous NH₄Cl (50 mL) and extracted with EtOAc (3x 50 mL). The combined organic extracts were washed with brine (50 mL), dried over Na₂SO₄, and concentrated. The residue was purified by silica gel column chromatography (SiO₂; petroleum ether/EtOAc = 20:1) to afford tosylate **2-68** (6 g, 80 %) as a colorless oil.

Chapter II: Experimental section

^1H NMR (500 MHz, Chloroform-*d*) δ (ppm): 7.84 – 7.80 (m, 2H), 7.35 (d, J = 8.0 Hz, 2H), 4.69 (t, J = 2.2 Hz, 2H), 3.76 (t, J = 7.3 Hz, 2H), 3.04 (p, J = 2.3 Hz, 2H), 2.45 (s, 3H), 2.39 (tt, J = 7.3, 2.4 Hz, 2H), 1.08 – 1.02 (m, 21H).

^{13}C { ^1H } NMR (126 MHz, Chloroform-*d*) δ (ppm): 145.2, 133.3, 129.9, 128.3, 84.5, 78.6, 73.6, 72.2, 62.2, 58.3, 23.2, 21.8, 18.1, 17.8, 12.4, 12.1, 10.0.

methyl 14-((triisopropylsilyl)oxy)tetradeca-5,8,11-triynoate (**2-66**)

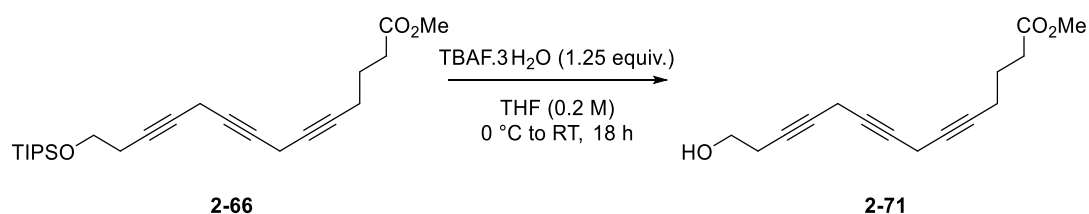


To a mixture of tosylate **2-68** (3.91 g, 8.63 mmol, 1.0 equiv.) in DMF (43 mL, 0.2 M), NaI (1.31 g, 8.63 mmol, 1.0 equiv.), CuI (1.68 g, 8.63 mmol, 1.0 equiv.), and K₂CO₃ (1.81 g, 12.9 mmol, 1.5 equiv.) were sequentially added at RT. After 2 min, methyl 5-hexynoate **2-67** (1.21 g, 9.49 mmol, 1.1equiv.) was added and the resulting mixture was stirred at RT for 12 h. The whole mixture was then diluted with EtOAc (50 mL), and the resulting mixture was filtered through a pad of Celite®. Resulting filtrate was washed with saturated aq. NH₄Cl (20 mL), and the aqueous layer was back extracted with EtOAc (3x 50 mL). The combined organic phases were washed with brine (50 mL), dried over MgSO₄, filtered, and the solvents were removed under reduced pressure. The crude product was purified by column chromatography (SiO₂; petroleum ether/EtOAc = 2:1) to afford **2-66** (0.87 g, 23 %).

^1H NMR (500 MHz, Chloroform-*d*) δ (ppm): 3.77 (t, J = 7.3 Hz, 1H), 3.68 (d, J = 2.9 Hz, 2H), 3.13 (q, J = 2.0, 1.5 Hz, 2H), 2.50 – 2.37 (m, 2H), 2.25 (dddd, J = 16.2, 9.3, 7.0, 2.5 Hz, 1H), 1.82 (tt, J = 14.4, 7.2 Hz, 1H), 1.05 (d, J = 5.5 Hz, 21H).

Chapter II: Experimental section

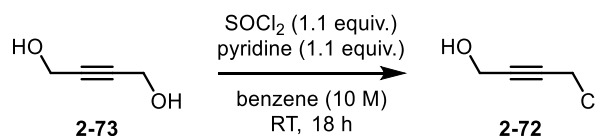
methyl 14-hydroxytetradeca-5,8,11-triynoate (**2-71**)



Alkene **2-66** (0.74 g, 1.81 mmol, 1.0 equiv.) was dissolved in THF (9.1 mL, 0.2 M) and the resulting mixture was cooled to 0 °C (ice/water). TBAF·3H₂O (0.73 g, 2.27 mmol, 1.25 equiv.) was added and the resulting mixture was stirred at 0 °C for 3 h. Sat. aq. NH₄Cl (50 mL) was added, and the resulting mixture was extracted with EtOAc (5x25 mL). The combined organic layers were washed with brine (25 mL), dried over MgSO₄, filtered and the solvents were removed under reduced pressure. The crude product was purified by column flash chromatography (SiO₂; petroleum ether:EtOAc = 10:1) and gave a product **2-71** (0.1 g, 24 %) as a yellowish oil.

¹H NMR (500 MHz, Chloroform-*d*) δ (ppm): 3.71 (t, *J* = 6.3 Hz, 2H), 3.68 (s, 3H), 3.15 (dp, *J* = 14.2, 2.4 Hz, 3H), 2.48 – 2.41 (m, 4H), 2.24 (tt, *J* = 6.9, 2.3 Hz, 2H), 1.82 (p, *J* = 7.2 Hz, 2H).

¹³C {¹H} NMR (126 MHz, Chloroform-*d*) δ (ppm): 173.9, 79.6, 76.1, 75.0, 74.8, 74.6, 61.1, 51.7, 32.9, 23.9, 23.1, 18.2, 18.0, 11.9, 9.9, 9.8.

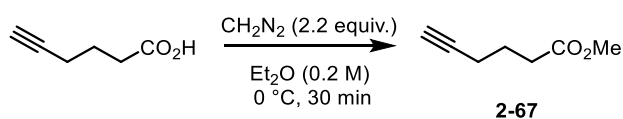
2.5.6.3. Third approach4-chlorobut-2-yne-1-ol (**2-72**)

To a solution of but-2-yne-1,4-diol **2-73** (10.0 g, 116 mmol, 1 equiv.) in benzene (11.6 mL, 10 M), dry pyridine (10.3 mL, 128 mmol, 1.1 equiv.) was added. The mixture was cooled to 0 °C and stirred for 5 min before SOCl₂ (9.3 mL, 128 mmol, 1.1 equiv.) was added dropwise. The mixture was then allowed to stir overnight at RT. After consumption of the starting material (TLC), the mixture was poured into ice-water mixture (10 g/10 mL). The resulting layers were separated, and the aqueous layer was extracted with EtOAc (3x 50 mL). Combined organic layers were then washed with saturated aqueous NaHCO₃ (50 mL), and brine (50 mL), dried over MgSO₄, filtered, and solvents were removed under reduced pressure. The crude product was purified by gradient column chromatography (SiO₂; petroleum ether/EtOAc = 10:1 → 2:1) to afford **2-72** (6.39 g, 53 %).

$R_f = 0.23$ (petroleum ether/EtOAc 4:1)

¹H NMR (500 MHz, Chloroform-d) δ (ppm): 4.33 (t, $J = 3.0$ Hz, 1H), 4.18 (dt, $J = 2.5, 2.0$ Hz, 2H), 1.74 (d, $J = 2.6$ Hz, 2H).

¹³C{¹H} NMR (126 MHz, Chloroform-d) δ (ppm): 84.8, 80.7, 51.2, 30.4.

methyl hex-5-ynoate (**2-67**)

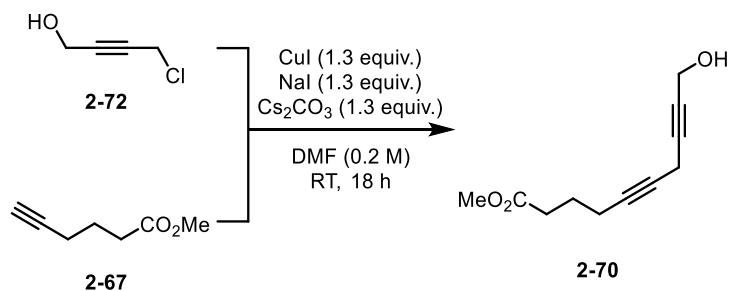
Freshly prepared ether solution of diazomethane [KOH (12 mL, 12 M) was slowly added to *N*-nitroso-*N*-methyl urea (8.4 g, 81.4 mmol, 2.2 equiv.) mixture in Et₂O (164 mL, 0.225 M), and stirred at 0 °C until all *N*-nitroso-*N*-methyl urea dissolves] was added dropwise to 5-hexynoic acid (4.15 g, 37 mmol, 1 equiv.) solution in Et₂O (16.4 mL, 2.25 M) at 0 °C. The resulting mixture was stirred at 0 °C for 1h and the N₂ was bubbled through the solution to remove an excess of the diazomethane (change of color from yellowish to clear). The whole mixture was then concentrated under reduced pressure, and the crude product was purified by column chromatography (SiO₂; petroleum ether/EtOAc = 2:1) to afford **2-67** (4.7g, 99 %).

Chapter II: Experimental section

¹H NMR (500 MHz, Chloroform-d) δ (ppm): 3.68 (s, 3H), 2.46 (t, *J* = 7.4 Hz, 2H), 2.27 (td, *J* = 7.0, 2.7 Hz, 2H), 1.97 (t, *J* = 2.7 Hz, 1H), 1.85 (p, *J* = 7.2 Hz, 2H).

¹³C{¹H} NMR (126 MHz, CDCl₃): 173.7, 83.4, 69.3, 51.7, 51.7, 32.8, 23.7, 18.0.

methyl 10-hydroxydeca-5,8-diynoate (**2-70**)



To a mixture of propargyl chloride **2-72** (2.7 g, 25.8 mmol, 1.0 equiv.) in DMF (52 mL, 0.5 M), NaI (5.08 g, 33.6 mmol, 1.3 equiv.), CuI (6.53 g, 33.6 mmol, 1.3 equiv.), and Cs₂CO₃ (4.69 g, 33.6 mmol, 1.3 equiv.) were sequentially added at RT. After 2 min, methyl hex-5-ynote **2-67** (4.32 g, 33.6 mmol, 1.3 equiv.) was added and the resulting mixture was stirred at RT for 12 h. The whole mixture was then diluted with EtOAc (50 mL), and the resulting mixture was filtered through a pad of Celite®. Resulting filtrate was washed with saturated aq. NH₄Cl (20 mL), and the aqueous layer was back extracted with EtOAc (3x 50 mL). The combined organic phases were washed with brine (50 mL), dried over MgSO₄, filtered, and the solvents were removed under reduced pressure. The crude product was purified by column chromatography (SiO₂; petroleum ether/EtOAc = 2:1) to afford **2-70** (3.38 g, 66 %).

R_f = 0.3 (petroleum ether/EtOAc 7:3)

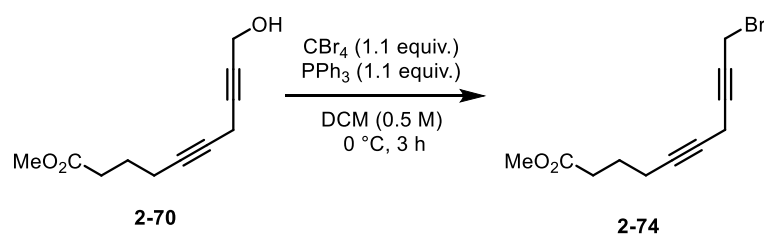
¹H NMR (500 MHz, Chloroform-d) δ (ppm): 4.26 (t, *J* = 2.4 Hz, 2H), 3.68 (s, 2H), 3.18 (td, *J* = 2.3, 1.2 Hz, 2H), 2.44 (t, *J* = 7.5 Hz, 2H), 2.24 (dddd, *J* = 6.9, 5.7, 3.0, 1.8 Hz, 2H), 1.88 – 1.76 (m, 2H).

¹³C {¹H} NMR (126 MHz, CDCl₃): 173.8, 80.7, 79.9, 78.7, 74.6, 51.8, 51.4, 33.0, 23.9, 18.3, 10.0.

HRMS (ESI) *m/z*: [M+H]⁺ calculated for C₁₁H₁₄O₃ [M+Na]⁺: 217.0835; found: 217.0834.

Chapter II: Experimental section

methyl 10-bromodeca-5,8-diynoate (**2-74**)



Diene **2-70** (5.07 g, 25.8 mmol, 1.0 equiv.) was dissolved in DCM (25.8 mL, 1 M) and PPh_3 (7.53 g, 28.4 mmol, 1.1 equiv.) and CBr_4 (9.52 g, 28.4 mmol, 1.1 equiv.) were added. After being stirred at $0\text{ }^\circ\text{C}$ for 3 h, the mixture was diluted with hexane/EtOAc (1:1, V/V; 100 mL), and the whole mixture was filtered through a plug of silica. The filtrate was concentrated under reduced pressure and the residue was purified by column chromatography (petroleum ether/EtOAc = 10:1) to afford **2-74** (6.1 g, 92 %).

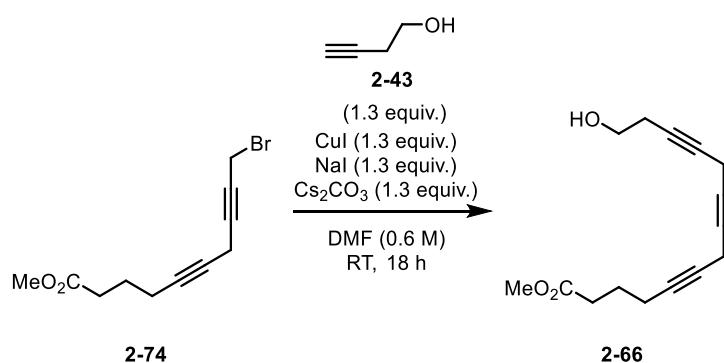
R_f = 0.6 (petroleum ether/EtOAc 7:1)

$^1\text{H NMR}$ (500 MHz, Chloroform- d) δ (ppm): 3.92 – 3.90 (m, 2H), 3.68 (s, 3H), 3.22 – 3.18 (m, 2H), 2.43 (t, J = 7.4 Hz, 2H), 2.26 – 2.22 (m, 2H), 1.82 (p, J = 7.0 Hz, 2H).

$^{13}\text{C}\{^1\text{H}\}$ NMR (126 MHz, Chloroform- d) δ (ppm): 173.8, 82.0, 80.2, 75.5, 74.0, 51.7, 33.0, 23.9, 18.3, 14.9, 10.2.

HRMS (ESI) m/z : $[\text{M}+\text{H}]^+$ calculated for $\text{C}_{11}\text{H}_{14}\text{O}_2\text{Br}$: 257.0172; found: 257.0171.

Methyl 14-hydroxytetradeca-5,8,11-triynoate (**2-66**)



To a mixture of 3-butyn-1-ol (2.6 mL, 3.33 mmol, 1.3 equiv.), NaI (5.09 g, 3.33 mmol, 1.3 equiv.), CuI (6.47 g, 3.33 mmol, 1.3 equiv.), and Cs_2CO_3 (10.95 g, 33.3 mmol, 1.3 equiv.) in DMF (43 mL, 0.6 M) at RT was added bromide **2-66** (6.7 g, 25.8 mmol, 1.0 equiv.) in DMF (5 mL) at RT. After being stirred overnight at RT, the mixture was diluted with EtOAc (100 mL), and the whole mixture was filtered through a pad of Celite[®]. Filter cake was rinsed with EtOAc (2x100 mL),

Chapter II: Experimental section

and combined filtrates were washed with saturated aq. NH_4Cl (50 mL). The aqueous layer was back extracted with EtOAc (3x 50 mL), and combined organic layers were washed with brine (100 mL), dried over MgSO_4 , filtered, and the solvents were removed under reduced pressure. The crude product was purified by column chromatography (SiO_2 ; petroleum ether/EtOAc = 2:1) to afford **2-66** (5 g, 78 %).

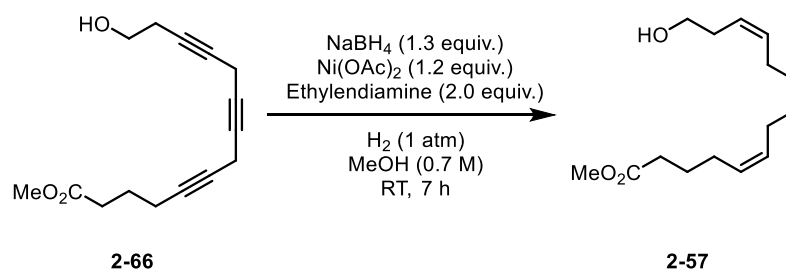
R_f = 0.5 (petroleum ether/EtOAc 1:1)

^1H NMR (500 MHz, Chloroform- d) δ (ppm): 3.74 – 3.69 (m, 2H), 3.68 (s, 3H), 3.21 – 3.07 (m, 4H), 2.44 (J = 8.4, 4.8 Hz, 4H), 2.27 – 2.21 (m, 2H), 1.82 (p, J = 7.2 Hz, 2H).

$^{13}\text{C}\{^1\text{H}\}$ NMR (126 MHz, Chloroform- d) δ (ppm): 173.9, 79.7, 76.3, 75.1, 74.9, 74.6, 61.2, 51.7, 33.0, 24.0, 23.2, 18.3, 10.0, 9.9.

HRMS (ESI) m/z : $[\text{M}+\text{H}]^+$ calculated for $\text{C}_{15}\text{H}_{19}\text{O}_3$: 247.1329; found: 247.1329.

Methyl (5Z,8Z,11Z)-14-hydroxytetradeca-5,8,11-trienoate (**2-57**)



To a solution of $\text{Ni}(\text{OAc})_2 \cdot 4\text{H}_2\text{O}$ (2.47 g, 9.73 mmol, 1.21 equiv.) in MeOH (11.5 mL, 0.75 M) at 0 °C, NaBH_4 (403 mg, 10.5 mmol, 1.3 equiv.) was added. The flask was purged with hydrogen, and ethylenediamine (1.61 mL, 10 M, 2 equiv.) was added to the mixture. After 10 min, triene **2-71** (2.0 g, 8.05 mmol, 1.0 equiv.) in MeOH (2.0 mL) was added. The mixture was stirred at RT for 5 h. Then the mixture was diluted with hexane/EtOAc (1:1, 50 mL), and the whole mixture was filtered through a pad of silica. Filter cake was washed with EtOAc (2x20 mL), and combined filtrates were washed with saturated aq. NH_4Cl (50 mL). The aqueous layer was back extracted with EtOAc (3x 50 mL), and combined organic layers were washed with brine (50 mL), dried over MgSO_4 , filtered, and the solvents were removed under reduced pressure. The crude product was purified by column chromatography (SiO_2 ; petroleum ether/EtOAc = 6:1 \rightarrow 2:1) to afford triene **2-57** (1.17 g, 58 %).

^1H NMR (500 MHz, Chloroform- d) δ (ppm): 5.57 – 5.50 (m, 1H), 5.44 – 5.33 (m, 5H), 3.66 (s, 3H), 2.87 – 2.75 (m, 4H), 2.39 – 2.29 (m, 4H), 2.15 – 2.07 (m, 2H), 1.74 – 1.66 (m, 2H).

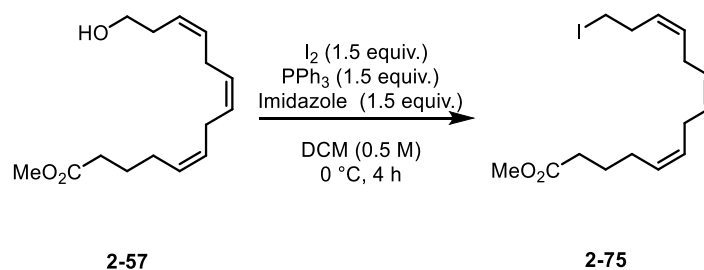
Chapter II: Experimental section

$^{13}\text{C}\{^1\text{H}\}$ NMR (126 MHz, Chloroform-d) δ (ppm): 174.3, 131.2, 129.1, 128.9, 128.5, 128.1, 125.8, 62.3, 51.7, 33.6, 31.0, 26.7, 25.9, 25.7, 24.9.

HRMS (ESI) m/z : $[\text{M}+\text{H}]^+$ calculated for $\text{C}_{15}\text{H}_{25}\text{O}_3$: 253.1798; found: 253.1799.

R_f = 0.5 (petroleum ether/EtOAc 2:1)

methyl (5Z,8Z,11Z)-14-iodotetradeca-5,8,11-trienoate (**2-75**)



To an ice-cold solution of triene **2-57** (2.42 g, 9.5 mmol, 1 equiv.) in DCM (19 mL, 0.5 M), imidazole (0.91 g, 13.3 mmol, 1.4 equiv.), PPh_3 (3.53 g, 13.3 mmol, 1.4 equiv.), and I_2 (2.93 g, 11.4 mmol, 1.2 equiv.) were sequentially added. After 3 h at 0 °C, the solution was diluted with petroleum ether/ether mixture (4:1, 50 mL), and the whole mixture was filtered through a pad of silica to afford unstable iodide **2-75** (2.25 g, 65 %) that was used immediately in the next step of the synthesis.

^1H NMR (500 MHz, Chloroform-d) δ (ppm): 5.56 – 5.46 (m, 1H), 5.40 – 5.30 (m, 5H), 3.65 (s, 3H), 3.13 (t, J = 7.2 Hz, 2H), 2.83 – 2.73 (m, 4H), 2.65 (q, J = 7.2 Hz, 2H), 2.31 (t, J = 7.5 Hz, 2H), 2.13 – 2.04 (m, 2H), 1.73 – 1.64 (m, 2H).

$^{13}\text{C}\{^1\text{H}\}$ NMR (126 MHz, Chloroform-d) δ (ppm): 174.1, 130.5, 129.1, 128.8, 128.6, 128.4, 127.7, 51.6, 33.5, 31.6, 26.7, 26.6, 25.9, 25.7, 24.8, 5.3.

R_f = 0.65 (hexane/EtOAc 5:1)

Chapter II: Experimental section

methyl (5Z,8Z,11Z)-14-nitrotetradeca-5,8,11-trienoate (**2-56**)



To a solution of **2-75** (3.3 g, 9.02 mmol, 1.0 equiv.) in Et₂O (36.1 mL, 0.25 M) placed in aluminum foil wrapped flask was at RT added in one portion silver nitrite (2.8 g, 18 mmol, 2.0 equiv.). The resulting mixture was stirred for 12 h before it was filtered through a short pad of Celite[®]. Filter cake was washed with EtOAc (3x100 mL), and the solvents were removed under reduced pressure. The crude product was purified by column chromatography (SiO₂; petroleum ether/EtOAc = 10:1) to afford triene **2-56** (1.26 g, 50 %).

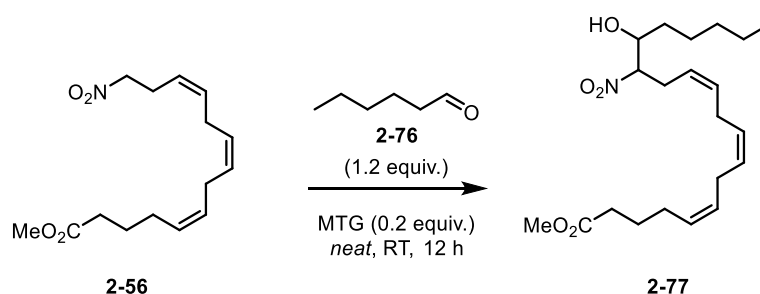
¹H NMR (500 MHz, Chloroform-d) δ (ppm): 5.59 – 5.52 (m, 1H), 5.41 – 5.28 (m, 5H), 4.38 (t, *J* = 7.1 Hz, 2H), 3.65 (s, 3H), 2.85 – 2.80 (m, 2H), 2.80 – 2.74 (m, 4H), 2.31 (t, *J* = 7.5 Hz, 2H), 2.12 – 2.05 (m, 2H), 1.74 – 1.64 (m, 2H).

¹³C{¹H} NMR (126 MHz, Chloroform-d) δ (ppm): 174.1, 132.7, 129.2, 128.9, 128.7, 127.3, 122.9, 75.0, 51.6, 33.5, 26.6, 25.7, 25.5, 24.8.

HRMS (ESI) *m/z*: [M+H]⁺ calculated for C₁₅H₂₄NO₄: 282.1700; found: 282.1695.

R_f = 0.3 (hexane/EtOAc 10:1)

methyl (5Z,8Z,11Z)-15-hydroxy-14-nitroicosa-5,8,11-trienoate (**2-77**)



A mixture of nitroalkane **2-56** (1.25 g, 4.4 mmol, 1.0 equiv.) and hexanal **2-76** (0.66 mL, 5.3 mmol, 1.2 equiv.) (neat) was cooled to 0 °C and 1,1,3,3-tetramethylguanidine (113 μL, 0.88 mmol, 0.2 equiv.) was added. Resulting mixture was stirred at RT for 12 h before it was again cooled to 0 °C. H₂O (30 mL) was added and the whole mixture was extracted with EtOAc (3× 50 mL). The combined organic phases were dried over Na₂SO₄, filtered and the solvents were

Chapter II: Experimental section

removed under reduced pressure. The crude product was purified by column chromatography (SiO₂; petroleum ether/EtOAc = 40:1 → 20:1) to afford triene **2-77** (1.2 g, 71 %).

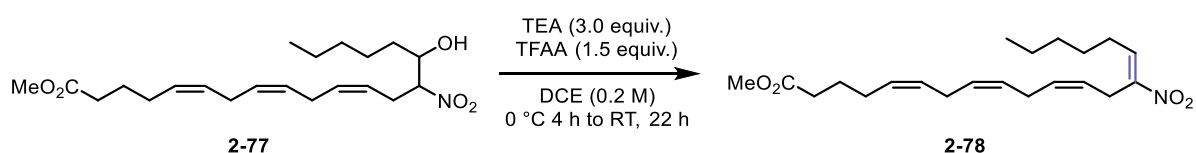
¹H NMR (500 MHz, Chloroform-d) δ (ppm): 5.61 – 5.51 (m, 1H), 5.43 – 5.27 (m, 5H), 4.49 – 4.42 (m, 1H), 4.06 (dq, *J* = 8.7, 4.4 Hz, 1H), 3.92 – 3.84 (m, 1H), 3.67 (s, 3H), 2.91 – 2.77 (m, 4H), 2.64 – 2.59 (m, 1H), 2.35 – 2.29 (m, 3H), 2.14 – 2.09 (m, 2H), 1.71 (p, *J* = 7.5 Hz, 2H), 1.56 – 1.43 (m, 3H), 1.35 – 1.28 (m, 5H), 0.91 – 0.87 (m, 3H).

¹³C{¹H} NMR (126 MHz, Chloroform-d) δ (ppm): 174.3, 133.2, 129.2, 129.0, 128.8, 127.4, 122.4, 92.0, 71.7, 51.7, 33.8, 33.6, 31.6, 28.7, 26.7, 25.8, 25.7, 25.2, 24.9, 22.6, 14.1.

HRMS (ESI) *m/z*: [M+H]⁺ calculated for C₂₁H₃₆NO₅: 382.2588; found:382.2587.

R_f = 0.25 (hexane/EtOAc 7:1)

methyl (5*Z*,8*Z*,11*Z*,14*E*)-14-nitricosa-5,8,11,14-tetraenoate (**2-78**)



Adduct **2-77** (1.5 g, 3.9 mmol, 1.0 equiv.) was dissolved in DCE (19.5 mL, 0.2 M) and the resulting mixture was cooled to 0 °C. TEA (0.14 mL, 11.7 mmol, 3.0 equiv.) and TFAA (0.82 mL, 5.84 mmol, 1.5 equiv.) were sequentially added and the resulting reaction mixture was stirred at 0 °C for 4 h and then at RT for 22 h. The whole mixture was cooled to 0 °C, and water (100 mL) was added to terminate the reaction. The resulting mixture was extracted with EtOAc (3×100 mL), and the combined organic layers were dried over MgSO₄, filtered, and the solvents were removed under reduced pressure. The crude product was purified by column flash column chromatography (SiO₂; petroleum ether/EtOAc = 30:1) to afford tetraene **2-78** (0.93 g, 66 %; *E/Z* (newly generated olefinic bond) ≥ 95:5) as a colorless oil.

R_f = 0.4 (hexane/EtOAc 5:1)

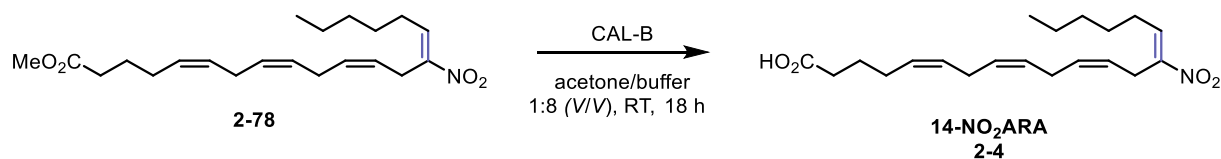
¹H NMR (500 MHz, Chloroform-d) δ (ppm): 7.12 (t, *J* = 7.9 Hz, 1H), 5.51 – 5.24 (m, 6H), 3.67 (s, 3H), 3.38 (d, *J* = 6.6 Hz, 2H), 2.93 (t, *J* = 6.5 Hz, 2H), 2.82 (t, *J* = 6.0 Hz, 2H), 2.15 – 2.08 (m, 2H), 1.71 (p, *J* = 7.5 Hz, 2H), 1.54 – 1.48 (m, 2H), 1.36 – 1.30 (m, 4H), 0.92 – 0.89 (m, 3H).

¹³C{¹H} NMR (126 MHz, Chloroform-d) δ (ppm): 174.2, 137.0, 130.9, 129.2, 128.9, 128.8, 127.6, 124.1, 51.6, 33.6, 31.6, 29.8, 28.3, 28.1, 26.7, 25.9, 25.8, 25.0, 24.9, 22.5, 14.1.

HRMS (ESI) *m/z*: [M+H]⁺ calculated for C₂₁H₃₄NO₄: 364.2482; found: 364.2479.

Chapter II: Experimental section

(5Z,8Z,11Z,14E)-14-nitroicosa-5,8,11,14-tetraenoic acid; 14-nitro arachidonic acid (**14-NO₂ARA**, **2-4**)



CAL-B (1400 mg) was added to a solution of methyl ester **2-78** (880 mg, 0.24 mmol, 1.0 equiv.) in acetone (30 mL, 0.08 M) and aqueous phosphate buffer (240 mL, 0.01 M, pH 7.4). The solution was vigorously stirred (magnetic stirrer, 1000 rpm) at room temperature for 18 h. 1 M HCl was added to terminate the reaction and to adjust the pH of the solution to pH = 3. The whole mixture was then transferred to separatory funnel and layers were separated. Aqueous layer was extracted with EtOAc (5x80 mL), and the combined organic layers were dried over MgSO₄, filtered, and the volatiles were removed *in vacuo*. The crude product was purified using semipreparative chromatography (C18 reverse- phase column; MeOH:H₂O) to yield the desired acid **14-NO₂ARA** **2-4** (350 mg, 41 %, *E/Z* ≥ 95:5; based on the ¹H NMR spectra analysis).

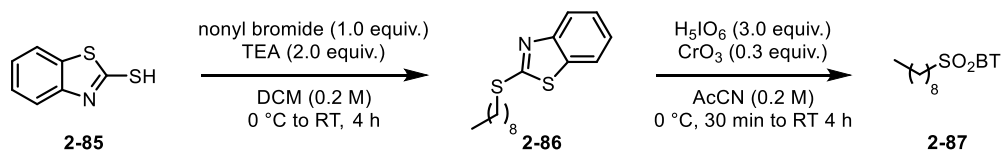
¹H NMR (500 MHz, Chloroform-d) δ (ppm): 7.12 (t, *J* = 7.9 Hz, 1H), 5.50 – 5.24 (m, 6H), 3.37 (d, *J* = 6.7 Hz, 2H), 2.93 (t, *J* = 6.6 Hz, 2H), 2.83 (t, *J* = 6.1 Hz, 2H), 2.37 (t, *J* = 7.4 Hz, 2H), 2.25 (q, *J* = 7.6 Hz, 2H), 2.17 – 2.10 (m, 2H), 1.72 (p, *J* = 7.5 Hz, 2H), 1.54 – 1.46 (m, 2H), 1.35 – 1.30 (m, 4H), 0.91 – 0.87 (m, 3H).

¹³C{¹H} NMR (126 MHz, Chloroform-d) δ (ppm): 177.9, 150.4, 137.1, 130.9, 129.1, 129.0, 128.9, 127.6, 124.1, 33.1, 31.6, 28.3, 28.1, 26.6, 25.9, 25.8, 25.0, 24.6, 22.5, 14.1.

HRMS (ESI) *m/z*: [M+H]⁺ calculated for C₂₀H₃₂NO₄: 350.2326; found: 350.2331.

R_f = 0.45 (hexane/EtOAc 2:1)

2.5.7. oleic acid synthesis using modified Julia-Kocienski method

2-(nonylsulfonyl)benzo[d]thiazole (**2-87**)

A benzothiazole-2-thiol **2-85** (10.0 g, 60 mmol, 1.0 equiv.) and nonyl bromide (12.4 g, 60 mmol, 1.0 equiv.) were dissolved in DCM (0.2 M, 300 mL) and the mixture was cooled to 0 °C (ice/water, external). TEA (12.1 mL, 120 mmol, 2.0 equiv.) was added dropwise, and the resulting mixture was allowed to warm to RT and stirred for additional 4 hours. 2 M aq. HCl (150 mL) was added to the reaction mixture at RT, and the resulting layers were separated. The aqueous layer was extracted with DCM (3x100mL) and organic layers were combined, washed with water (50 mL), brine (50 mL), dried over MgSO₄, and the solvents were evaporated under reduced pressure. The crude product **2-86** was used in the next step without further purification.

The crude sulfide **2-86** (10 g, 20 mmol, 1.0 equiv.) and periodic acid (13.7 g, 60 mmol, 3.0 equiv.) were dissolved in acetonitrile (0.2 M, 100 mL) and the resulting mixture was cooled to 0 °C. CrO₃ (0.6 g, 6 mmol, 0.3 equiv.) was added portion-wise, and the resulting mixture was stirred for an additional 30 minutes at 0 °C, before being allowed to warm to RT. The resulting mixture was stirred for an additional 4 hours before it was cooled to 0 °C and the reaction was terminated by adding sat. aq. Na₂SO₃ (150 mL). The whole mixture was filtered through a short pad of Celite®. Filter cake was washed with EtOAc (3x50 mL). Resulting layers were separated, and the organic phase was washed with sat. aq. Na₂SO₃ (2x50 mL), water (2x50mL), brine (2x20mL) and dried over MgSO₄. Solvents were removed under the reduced pressure and purified with help of column chromatography (SiO₂; petroleum ether:EtOAc = 10:1->4:1->2:1) to yield sulfone **2-87** (11.5 g, 59 % over two steps).

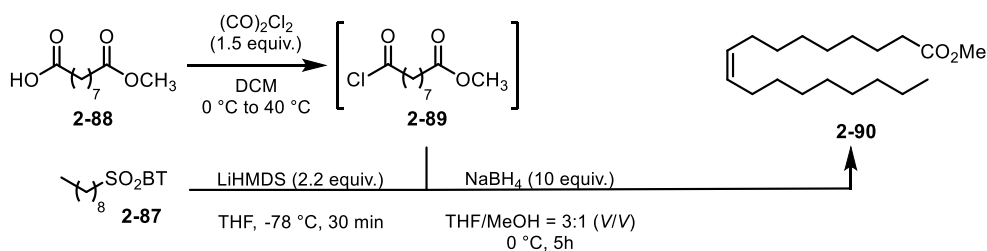
¹H NMR (500 MHz, Chloroform-d) δ (ppm): 8.24 (dd, J = 7.8, 1.5 Hz, 1H), 8.03 (dd, J = 7.7, 1.5 Hz, 1H), 7.66–7.57 (m, 2H), 3.54– 3.49 (m, 2H), 1.90–1.82 (m, 2H), 1.52–1.43 (m, 2H), 1.39–1.29 (m, 10H), 0.93 (t, J = 7.3 Hz, 3H).

¹³C{¹H} NMR (126 MHz, Chloroform-d) δ (ppm): 166.0, 152.9, 136.9, 128.1, 127.8, 125.6, 122.5, 54.6, 30.9, 27.7, 22.2, 22.1, 22.0, 21.9, 13.6.

MS (ESI) m/z (%): 326 [M+H]⁺.

Chapter II: Experimental section

methyl oleate (**2-90**)



Oxalyl chloride (804 μL , 10.3 mmol, 1.65 equiv.) was added at RT to an azelaic acid monomethyl ester **2-88** (1.37 g, 6.75 mmol, 1.1 equiv.) and the resulting mixture was gently stirred till the evolution of the gas ceased (25 min). The resulting mixture was then stirred at reflux for additional 2h before it was cooled to RT. The whole mixture was then concentrated under vacuum (excess of $(\text{CO})_2\text{Cl}_2$ removal) and the resulting acyl chloride **2-89** was dissolved in dry THF (5 mL) and cooled to -78 °C.

In a separated flask, sulfone **2-87** (2 g, 6.14 mmol; 1.0 equiv.) was dissolved in dry THF (31 mL, 0.2 M) and cooled to -78 °C (acetone/dry ice; external). After 5 minutes, LiHMDS (13.5 mL, 13.5 mmol; 2.2 equiv; 1.0 M solution in THF) was added dropwise over a period of 5 minutes. The reaction mixture turned light orange upon its addition. Previously prepared acyl chloride **2-89** was then added in one shot *via* HPLC Teflon cannula (\varnothing 1.5 mm) at -78 °C.

The resulting reaction mixture was allowed to stir at -78 °C for 30 minutes before the cooling bath was removed. The reaction mixture was then allowed to stir at RT for additional 30 min before MeOH (11 mL; THF/MeOH = 3:1 (V/V)) was added. After additional 5 min at RT, the reaction mixture was cooled to 0 °C and stirred for an additional 5 minutes. NaBH₄ (2.32 g, 61.4 mmol, 10 equiv.) was added portion wise at 0 °C and the resulting reaction mixture was stirred at 0 °C for an additional 6 h, before being quenched with 0.5M aq. HCl (40 mL). The resulting mixture was stirred at RT for 10 h. The whole reaction mixture was extracted with EtOAc (4x50 mL), and the organic layers were combined, washed with water (25 mL), brine (50 mL), dried over Na₂SO₄, filtered and solvents were removed under reduce pressure. The crude reaction mixture was purified by flash column chromatography (SiO₂; petroleum ether:Et₂O = 20:1) and gave the desired product **2-90** (1.02 g, 63%) as a pure (*Z*)-isomer (¹H NMR, *E/Z* = 1:>99) in form of colorless oil.

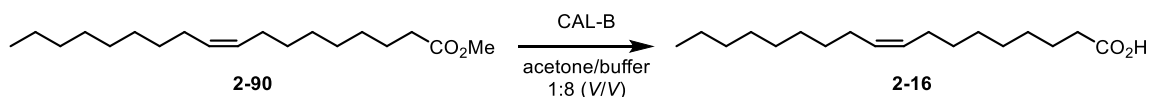
¹H NMR (500 MHz, Chloroform-d) δ (ppm): 5.44 – 5.26 (m, 2H), 3.66 (s, 2H), 2.30 (t, *J* = 7.5 Hz, 2H), 2.06 – 1.94 (m, 4H), 1.62 (p, *J* = 7.1 Hz, 2H), 1.28 (q, *J* = 9.9, 7.5 Hz, 21H), 0.88 (t, *J* = 6.7 Hz, 3H).

Chapter II: Experimental section

$^{13}\text{C}\{^1\text{H}\}$ NMR (126 MHz, Chloroform-d) δ (ppm):174.5, 130.1, 129.9, 51.6, 34.2, 32.0, 29.9, 29.8, 29.7, 29.5, 29.3, 29.3, 29.2, 27.4, 27.3, 25.1, 22.8, 14.3.

MS (ESI) m/z (%): 297 $[\text{M}+\text{H}]^+$, 319 $[\text{M}+\text{Na}]^+$.

oleic acid (**2-16**)



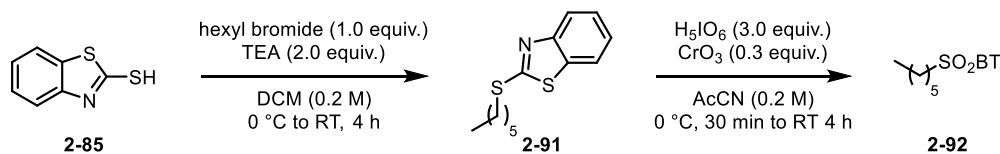
CAL-B (70 mg/mmol) was added to a solution of methyl ester **2-90** (0.3 g, 0.88 mmol, 1.0 equiv.) in acetone (11 mL, 0.08 M) and aqueous phosphate buffer (88 mL, 0.01 M, pH 7.4). The solution was vigorously stirred (magnetic stirrer, 1000 rpm) at room temperature for 18 h. 1 M HCl solution was added to adjust the pH of the solution to pH = 3. The whole mixture was then extracted with EtOAc (5x20 mL), and the combined organic layers were dried over MgSO_4 , filtered, and the volatiles were removed *in vacuo*. The crude product was purified using semipreparative chromatography (C18 reverse-phase column; MeOH:H₂O) to yield the desired acid **oleic acid, 2-16** (0.255g 82%, E/Z = 1:>99; based on the ^1H NMR spectra analysis).

^1H NMR (500 MHz, methanol- d_4) δ (ppm):5.40 – 5.30 (m, 2H), 4.90 (bs, 1H), 2.28 (t, J = 7.5 Hz, 2H), 2.10 – 2.00 (m, 4H), 1.60 (p, J = 7.3 Hz, 2H), 1.43 – 1.25 (m, 20H), 0.90 (t, J = 6.8 Hz, 3H).

$^{13}\text{C}\{^1\text{H}\}$ NMR (101 MHz, methanol- d_4) δ (ppm): 177.7, 130.9, 130.8, 35.0, 33.1, 30.9, 30.8, 30.6, 30.5, 30.4, 30.3, 30.3, 30.2, 28.1, 26.1, 23.8, 14.5.

MS (ESI) m/z (%): 283 $[\text{M}+\text{H}]^+$, 305 $[\text{M}+\text{Na}]^+$.

2.5.8. linoleic acid synthesis using modified Julia-Kocienski method

2-(hexylsulfonyl)benzo[d]thiazole (**2-92**)

A benzothiazole-2-thiol **2-85** (10.0 g, 60 mmol, 1.0 equiv.) and hexyl bromide (9.87 g, 60 mmol, 1.0 equiv.) were dissolved in DCM (0.2 M, 300 mL) and the mixture was cooled to 0 °C (ice/water, external). TEA (12.1 mL, 120 mmol, 2.0 equiv.) was added dropwise, and the resulting mixture was allowed to warm to RT and stirred for additional 4 hours. 2 M aq. HCl (150 mL) was added to the reaction mixture at RT, and the resulting layers were separated. The aqueous layer was extracted with DCM (3x100mL) and organic layers were combined, washed with water (50 mL), brine (50 mL), dried over MgSO₄, and the solvents were evaporated under reduced pressure. The crude product **2-91** was used in the next step without further purification.

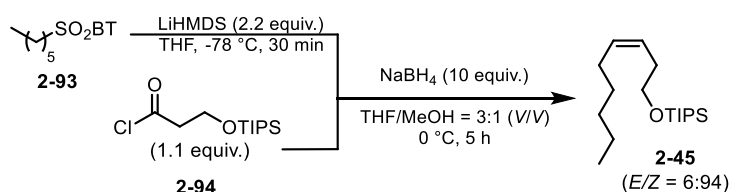
The crude sulfide **2-91** (10 g, 20 mmol, 1.0 equiv.) and periodic acid (13.7 g, 60 mmol, 3.0 equiv.) were dissolved in acetonitrile (0.2 M, 100 mL) and the resulting mixture was cooled to 0 °C. CrO₃ (0.6 g, 6 mmol, 0.3 equiv.) was added portion-wise, and the resulting mixture was stirred for an additional 30 minutes at 0 °C, before being allowed to warm to RT. The resulting mixture was stirred for an additional 4 hours before it was cooled to 0 °C and the reaction was terminated by adding sat. aq. Na₂SO₃ (150 mL). The whole mixture was filtered through a short pad of Celite®. Filter cake was washed with EtOAc (3x50 mL). Resulting layers were separated, and the organic phase was washed with sat. aq. Na₂SO₃ (2x50 mL), water (2x50mL), brine (2x20mL) and dried over MgSO₄. Solvents were removed under the reduced pressure and purified with help of column chromatography (SiO₂; petroleum ether:EtOAc = 10:1->4:1->2:1) to yield sulfone **2-92** (10 g, 58 % over two steps).

¹H NMR (500 MHz, Chloroform-d) δ (ppm): 8.21 (ddd, J = 7.9, 1.4, 0.8 Hz, 1H), 8.01 (ddd, J = 7.7, 1.4, 0.8 Hz, 1H), 7.63 (ddd, J = 8.5, 7.2, 1.4 Hz, 1H), 7.58 (ddd, J = 8.5, 7.3, 1.6 Hz, 1H), 3.50 (t, J = 8.0 Hz, 2H), 1.87 (q, J = 7.7 Hz, 2H), 1.43 (q, J = 7.5 Hz, 2H), 1.27 (dq, J = 7.1, 3.6 Hz, 4H), 0.85 (t, J = 7.1 Hz, 3H). ¹³C{¹H} NMR (101 MHz, Chloroform-d) δ (ppm): 166.0, 152.8, 136.9, 128.1, 127.8, 125.6, 122.5, 54.8, 31.2, 28.0, 22.31, 22.28, 14.0.

MS (ESI) *m/z* (%): 284 [M+H]⁺.

Chapter II: Experimental section

(Z)-triisopropyl(non-3-en-1-yloxy)silane (**2-45**)



Sulfone **2-93** (1.5 g, 5.29 mmol; 1.0 equiv.) was dissolved in dry THF (50 mL, 0.1M) and cooled to $-78\text{ }^\circ\text{C}$ (acetone/dry ice; external). After 5 minutes, LiHMDS (11.65 mL, 11.64 mmol; 2.2 equiv; 1.0 M solution in THF) was added over 2 min period. The reaction mixture turned light orange upon its addition. TiPSO-propionyl chloride **2-94** (1.54 g, 5.82 mmol, 1.1 equiv.) in dry THF (5 mL) was cooled to $-78\text{ }^\circ\text{C}$ (dry ice/acetone ; extern.) and then added in one shot *via* HPLC Teflon cannula (\varnothing 1.5 mm) at $-78\text{ }^\circ\text{C}$ to the solution of sulfone 1e. The resulting reaction mixture was allowed to stir at $-78\text{ }^\circ\text{C}$ for 30 minutes before the cooling bath was removed. The reaction mixture was allowed to stir at RT for 20 min before MeOH (14 mL; THF/MeOH = 3:1 (V/V)) was added. The mixture was cooled to $0\text{ }^\circ\text{C}$ and stirred for an additional 5 minutes, before NaBH_4 (2.0 g, 53 mmol; 10 equiv.) was added at $0\text{ }^\circ\text{C}$. The resulting reaction mixture was stirred at $0\text{ }^\circ\text{C}$ for an additional 4h, before being quenched with 0.5M aq. HCl (50 mL). The resulting mixture was stirred at RT for 4 h. Resulting phases were separated, and the aqueous phase was extracted with EtOAc (3 x 75 mL). Organic layers were combined and washed with water (50 mL), brine (50 mL), dried over Na_2SO_4 , filtered and solvents were removed under reduced pressure. The residue was purified by column chromatography (SiO_2 ; petroleum ether:EtOAc = 200:1- \rightarrow 100:1) and yielded the desired product **2-45** (1.3 g, 82%, E/Z = 6:94) in form of colorless oil.

$^1\text{H NMR}$ (500 MHz, Chloroform-*d*) δ (ppm): 5.48 – 5.35 (m, 2H), 3.68 – 3.65 (m, 2H), 2.30 (q, J = 7.2 Hz, 2H), 2.04 (q, J = 7.3 Hz, 2H), 1.35 – 1.27 (m, 6H), 1.06 (dd, J = 5.5, 2.3 Hz, 21H), 0.90 – 0.86 (m, 3H).

$^{13}\text{C}\{^1\text{H}\}$ NMR (126 MHz, Chloroform-*d*) δ (ppm): 132.0, 125.7, 63.4, 31.7, 31.4, 29.6, 27.5, 22.7, 18.2, 14.2, 12.2.

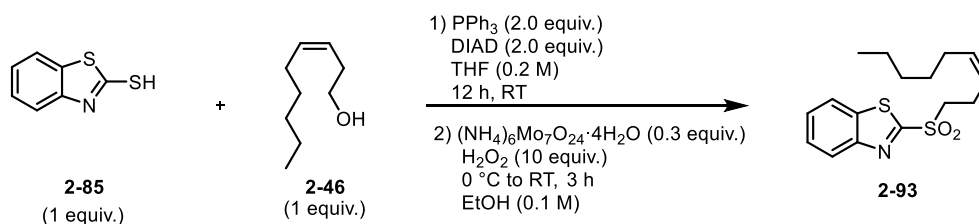
MS (ESI) m/z (%): 300 $[\text{M}+\text{H}]^+$.

HRMS (ESI) m/z : $[\text{M}+\text{H}]^+$ calculated for $\text{C}_{18}\text{H}_{39}\text{OSi}$: 299.2765; found: 299.2768.

R_f = 0.55 (PMA, petroleum ether:EtOAc = 10:1)

Chapter II: Experimental section

(Z)-2-(non-3-en-1-ylsulfonyl)benzo[d]thiazole (**2-93**)



Alcohol **2-46** (0.128 g, 0.891 mmol, 1.0 equiv.), benzothiazole **2-85** (0.149 g, 0.891 mmol, 1.0 equiv.), and triphenylphosphine (0.467 g, 1.78 mmol, 2.0 equiv.) were dissolved in THF (9.0 mL, 0.1 M) at RT and DIAD (0.354 mL, 1.78 mmol, 2.0 equiv.) was added dropwise. The resulting mixture was allowed to stir at RT for 12 h and solvents were removed under reduced pressure. The residue was dissolved in EtOH (8.9 mL, 0.1 M) and the whole mixture was cooled to 0 °C (ice/water; extern). In separate flask was placed ammonium molybdate (0.334 g, 0.267 mmol, 0.3 equiv.) and H₂O₂ (0.505 mL, 8.91 mmol, 10 equiv.; 50% in H₂O) was added to it. The resulting yellow clear solution was cooled to 0 °C and added with help of Pipette Pasteur to the solution of sulfide in EtOH. The resulting mixture was stirred at 0 °C for 3 h (TLC monitoring) before it was diluted with H₂O (20 mL). The resulting mixture was extracted with DCM (3x75 mL) and combined organic layers were washed with brine (15 mL), dried over MgSO₄, filtered and solvents were removed under reduced pressure. The residue was purified by column chromatography (SiO₂; petroleum ether:EtOAc = 5:1) and gave the desired sulfone **2-93** (0.265 g, 92%, E/Z = 1:>99) as a slightly yellow oil.

¹H NMR (500 MHz, Chloroform-d) δ (ppm): 8.23 (d, J = 8.3 Hz, 1H), 8.04 (d, J = 7.7 Hz, 1H), 7.69 – 7.58 (m, 2H), 5.48 (ddt, J = 10.6, 7.3, 1.0 Hz, 1H), 5.30 (qt, J = 10.5, 7.5, 7.1, 1.8, 0.8 Hz, 1H), 3.61 – 3.52 (m, 2H), 2.64 (q, J = 7.7 Hz, 2H), 1.99 (q, J = 7.2 Hz, 2H), 1.37 – 1.15 (m, 4H), 0.86 (t, J = 7.0 Hz, 3H).

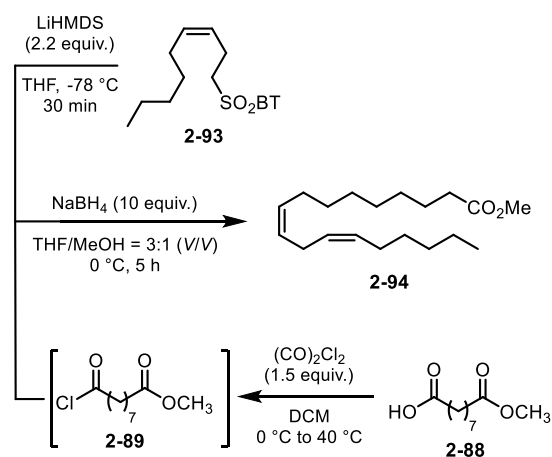
¹³C{¹H} NMR (101 MHz, Chloroform-d) δ (ppm): 166.25, 153.19, 137.24, 134.36, 128.51, 128.15, 125.93, 124.03, 122.82, 54.86, 31.86, 29.48, 27.64, 22.94, 21.02, 14.49.

MS (ESI) m/z (%): 324 [M+H]⁺.

HRMS (ESI) m/z: [M+H]⁺ calculated for C₁₆H₂₁NO₂S₂Na [M+Na]⁺: 346.0906; found: 346.0912.

Chapter II: Experimental section

methyl linoleate (2-94)

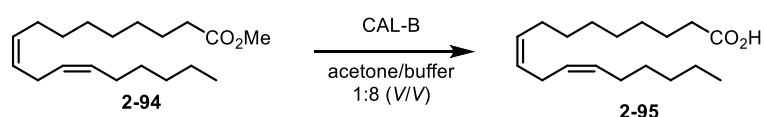


Oxalyl chloride (0.583 mL, 6.80 mmol, 1.65 equiv.) was added at RT to an azelaic acid monomethyl ester **2-88** (1.0 g, 4.94 mmol, 1.2 equiv.) and the resulting mixture was gently stirred till the evolution of the gas ceased (25 min). The resulting mixture was then stirred at reflux for additional 2h before it was cooled to RT. The whole mixture was then concentrated under

vacuum (excess of (CO)₂Cl₂ removal) and the resulting acyl chloride **2-89** was dissolved in dry THF (5 mL) and cooled to -78 °C. In a separated flask, sulfone **2-93** (1.33 g, 4.12 mmol, 1.0 equiv.) was dissolved in dry THF (20 mL, 0.2 M) and cooled to -78 °C (acetone/dry ice; external). After 5 minutes, LiHMDS (9.1 mL, 9.06 mmol; 2.2 equiv.; 1.0 M solution in THF) was added dropwise over a period of 5 minutes. The reaction mixture turned light orange upon its addition. Previously prepared acyl chloride **2-89** was then added in one shot to the resulting yellow-orange solution *via* HPLC Teflon cannula (ø 1.5 mm) at -78 °C. The resulting reaction mixture was allowed to stir at -78 °C for 30 minutes before the cooling bath was removed. The reaction mixture was then allowed to stir at RT for additional 30 min before MeOH (10 mL; THF/MeOH = 3:1 (V/V)) was added. After additional 5 min at RT, the reaction mixture was cooled to 0 °C and stirred for an additional 5 minutes. NaBH₄ (1.56 g, 41.2 mmol, 10 equiv.) was added portion wise at 0 °C and the resulting reaction mixture was stirred at 0 °C for an additional 6h, before being quenched with 0.5M aq. HCl (40 mL). The resulting mixture was stirred at RT for 10 h. The whole reaction mixture was extracted with EtOAc (4x75 mL), and the organic layers were combined, washed with water (50 mL), brine (50 mL), dried over Na₂SO₄, filtered and solvents were removed under reduced pressure. The crude reaction mixture was purified by column chromatography (SiO₂; petroleum ether:EtOAc = 10:1) and gave the desired product **2-94** (0.630 g, 52%, *Z/E:Z/Z* = 1:>99) in form of yellowish oil. ¹H NMR (500 MHz, Chloroform-d) δ (ppm): 5.41 – 5.28 (m, 4H), 3.66 (s, 3H), 2.81 – 2.68 (m, 1H), 2.38 – 2.25 (m, 2H), 2.05 (qd, J = 6.8, 1.3 Hz, 4H), 1.66 – 1.58 (m, 2H), 1.41 – 1.22 (m, 19H), 0.89 (t, J = 7.0 Hz, 3H). ¹³C{¹H} NMR (101 MHz, Chloroform-d) δ (ppm): 174.49, 130.37, 130.20, 128.18, 128.04, 51.61, 34.25, 31.67, 29.73, 29.49, 29.30, 29.26, 29.24, 27.34, 27.33, 25.76, 25.08, 22.72, 14.23. MS (ESI) *m/z* (%): 317 [M+Na]⁺.

Chapter II: Experimental section

linoleic acid (2-95)



CAL-B (70 mg/mmol) was added to a solution of methyl ester **2-94** (0.3 g, 1 mmol, 1.0 equiv.) in acetone (12.7 mL, 0.08 M) and aqueous phosphate buffer (102 mL, 0.01 M, pH 7.4). The solution was vigorously stirred (magnetic stirrer, 1000 rpm) at room temperature for 18 h. 1 M HCl solution was added to adjust the pH of the solution to pH = 3. The whole mixture was then extracted with EtOAc (5x25 mL), and the combined organic layers were dried over MgSO₄, filtered, and the volatiles were removed *in vacuo*. The crude product was purified using semipreparative chromatography (C18 reverse-phase column; MeOH:H₂O) to yield the desired acid **linoleic acid, 2-95** (0.22 g 75%, *E/Z* = 1:>99; based on the ¹H NMR spectra analysis).

¹³C{¹H} NMR (101 MHz, methanol-d₄) δ (ppm): 5.52 – 5.26 (m, 4H), 4.90 (bs, 1H) 2.78 (dd, J = 6.7, 5.5 Hz, 2H), 2.28 (t, J = 7.4 Hz, 2H), 2.13 – 2.03 (m, 4H), 1.68 – 1.54 (m, 2H), 1.43 – 1.25 (m, 14H), 0.94 – 0.85 (m, 3H).

¹³C{¹H} NMR (101 MHz, methanol-d₄) δ (ppm): 177.72, 130.93, 130.87, 129.11, 129.06, 34.96, 32.69, 30.71, 30.50, 30.33, 30.24, 28.18, 28.15, 26.54, 26.10, 23.65, 14.44.

MS (ESI) *m/z* (%): 303 [M+Na]⁺.

CHAPTER III

3. Sulfonamides

3.1. Introduction to Sulfonamides

Sulfonamides, also known under the name 'sulfa drugs', are a class of compounds that contain the $R^1SO_2-NH_2$ moiety that can vary in nitrogen atom substitution. For this reason, sulfonamides are further divided into three subcategories – non-substituted, primary and secondary sulfonamides (**Figure 39**).

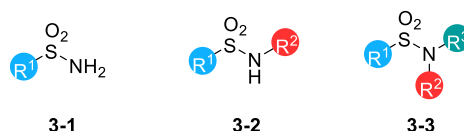


Figure 39: General structure of primary (left), secondary (middle) and tertiary (right) sulfonamides.

3.1.1. Biological activity of sulfonamides

Compounds that include a sulfonamide motive within their structure possess huge biological activities, such as antibacterial¹⁶⁴, oral hypoglycemic¹⁶⁵, antitumor¹⁶⁶, antiviral^{164,167}, antiepileptic¹⁶⁸, antihypertensive¹⁶⁹, antiprotozoal¹⁷⁰, antifungal¹⁷¹, anticancer^{164,167}, anti-inflammatory¹⁷², diuretic¹⁷³, activity against Alzheimer's¹⁷⁴ and Parkinson's disease¹⁷⁵, anti-inflammatory Activity¹⁷⁶ etc.

'Sulfa drugs' as antibacterial agents were first mentioned in the 1930s and in 1939 the Nobel prize was awarded to Gerhard Domagk for the discovery of the antibacterial effect of Prontosil, which bears a structure without substituted sulfonamide. Since then, these substances have gained popularity in the field of medicinal chemistry. However, eventually bacteria started to develop resistance to sulfonamides and penicillin replaced the use Prontosil as a first-line treatment.¹⁷⁷ While antibiotic resistance is an issue, sulfonamides are still commonly used to treat a variety of bacterial infections. The most widely used sulfonamides are, for example, celecoxib, zonisamide, and sulfasarazine which belong to primary sulfonamides. Celecoxib as a member of primary sulfonamides acts as a COX-2 inhibitor, which is a group of compounds that acts as a non-steroidal anti-inflammatory drug (NSAID).¹⁷⁸ NSAIDs are usually used to treat pain and inflammation.¹⁷⁸ Celecoxib is the 98th most prescribed medication in the United States. In 2020, zonisamide was the 278th most prescribed medication for the treatment of epilepsy and Parkinson's disease.¹⁷⁹ Sulfasarazine belongs to the family of secondary sulfonamides and is used against Crohn's disease and rheumatoid

Chapter III: Introduction

arthritis.¹⁸⁰ Glyburide antidiabetic properties and therefore is used to treat type 2 diabetes¹⁸¹

One of the few examples of tertiary sulfonamides is darunavir, which has been approved for the treatment of HIV infection as part of highly active antiretroviral therapy, in combination with other anti-HIV agents (**Figure 40**).¹⁸²

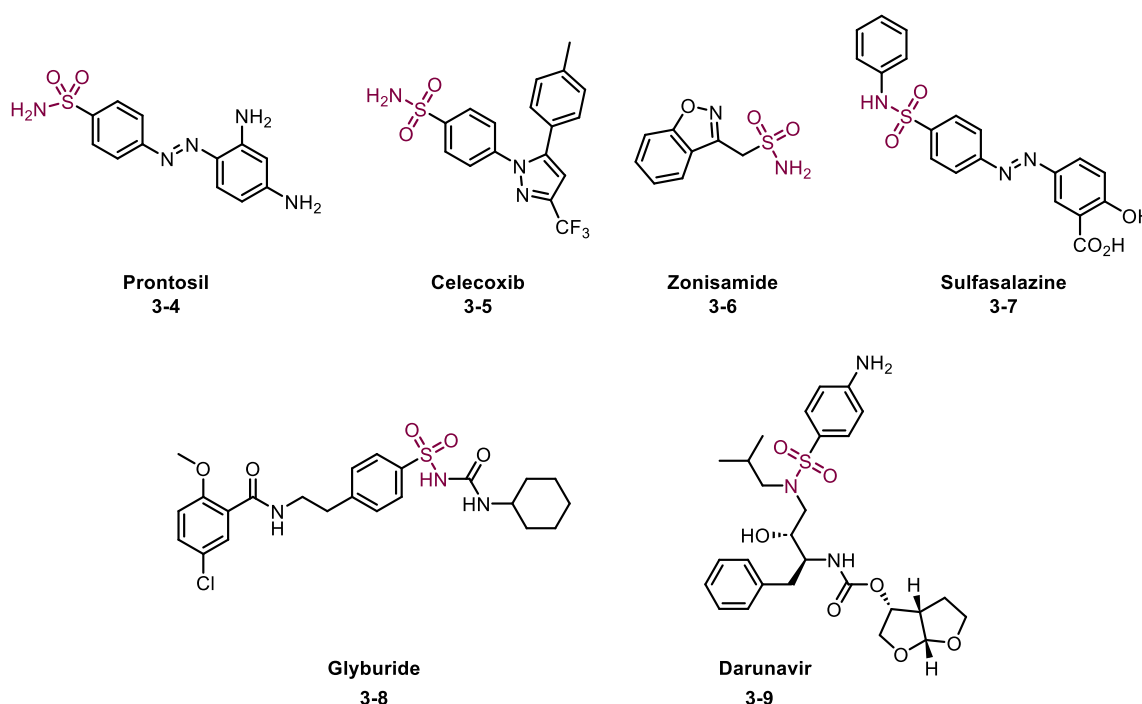


Figure 40: Structure of sulfonamides used as drugs.

Thanks to their extensive biological effects, sulfonamides are being revived and have recently become a point of interest for medicinal chemists, as new ways of using them in the fight against various types of infection have been discovered. Overall, sulfonamides remain an important group of drugs in the fight against infectious diseases and their research and development will continue in the future.

3.2. General approaches towards sulfonamides

The most used synthetic routes to sulfonamides have traditionally been divided into three approaches. The first approach involved the use of sulfonyl chlorides, which can be obtained by chlorosulfonylation of arenes,¹⁸³ sulfochlorination of alkyl chains,¹⁸⁴ or oxidation¹⁸⁵/chlorination¹⁸⁶ of thiols (**Figure 41A**). However, these methods have certain limitations, including the low thermal stability of (heteroaryl)sulfonyl chlorides and relatively limited functional group tolerance.¹⁸⁷ These limitations led to the second approach, which used sulfinic acid salts (ester hydrolysis),¹⁸⁸ or by sulfonylation using DABSO (**Figure 41B**).¹⁸⁹ The third most common alternative is a well-known SuFEx approach. (**Figure 41C**). The last approach, which is newly added and rarely used, relies on the conversion of thiols into sulfenamides, which are subsequently oxidized to form sulfonamides. The drawback of this oxidation of sulfenamides to sulfonamides are low yields (**Figure 41D**).^{190,191}

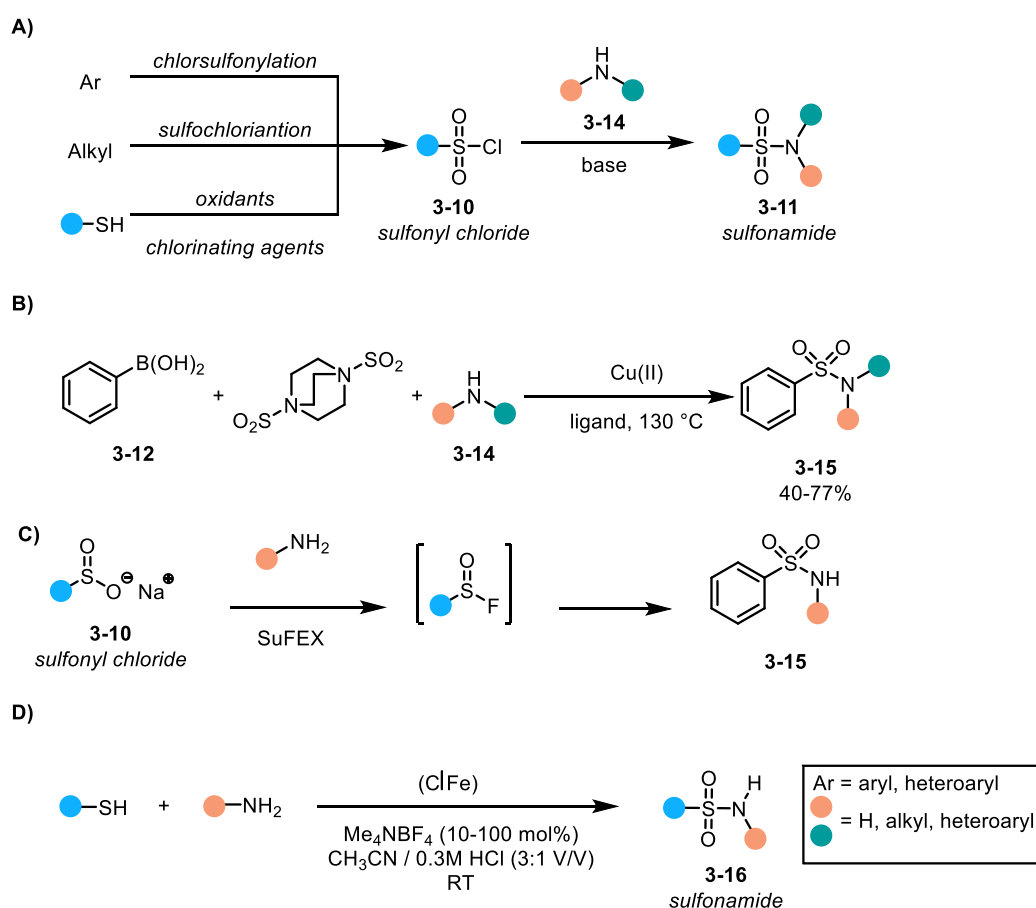
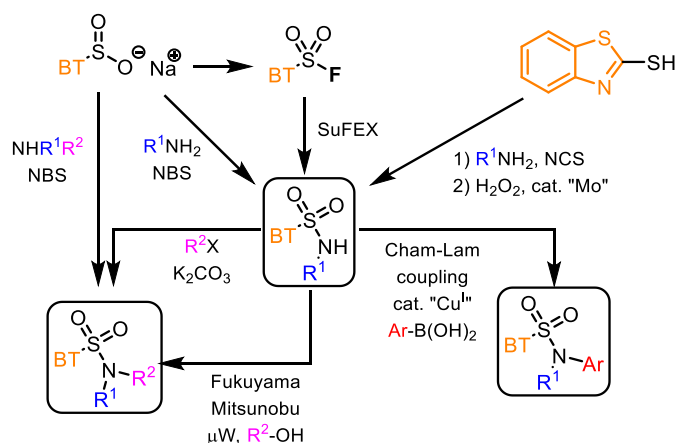


Figure 41: Approaches towards sulfonamides. **A)** Classical approach to sulfonamides. **B)** DABSO-based approach. **C)** SuFEX approach. **D)** Electrochemical oxidative coupling.

Chapter III: Synthetic approaches to sulfonamides

During recent years, our research group focused on the chemistry of **heteroaryl sulfonamides**.^{187,192} While the above-mentioned methods are generally effective for the synthesis of alkyl and aryl sulfonamides, they present challenges when applied to heteroaryl sulfonamides.¹⁸⁷ These challenges include the instability of reaction intermediates, the need for harsh reaction conditions, and low reaction yields.^{193–195} Therefore, our group focused on developing a method that would eliminate these challenges related to the synthesis of *N*-monoalkyl, *N,N*-dialkyl, and *N,N*-alkyl aryl benzothiazole sulfonamides. After a huge amount of time and efforts, a unified approach to *N*-substituted and *N,N*-disubstituted benzothiazole (BT) sulfonamides was developed by Zálešák et al.¹⁸⁷ It was demonstrated that various substrates and sulfonamides or their precursors need to be prepared using various synthetic strategies. The only criterion was that the developed methods are based on readily available building blocks that should be further interconnected through various strategies, including **1**) S-oxidation/S-N coupling with primary and secondary amines, **2**) S-N coupling /S-oxidation sequence, and **3**) S-oxidation/S-F bond formation/SuFEX approach. These three mentioned methods allowed the synthesis of a basic common intermediate that could be further functionalized to *N,N*-disubstituted BT-sulfonamides by base-promoted alkylation with alkyl halides and/or stereospecific Fukuyama Mitsunobu alkylation by reaction with alkyl alcohol. The aryl substituents were installed using the Cham-Lam coupling reaction. (**Scheme 67**).



Scheme 67: Overview of the general routes to BT sulfonamides (adapted from¹⁸⁷).

3.3. Amino acids

The second class of compounds that I will discuss in my theses are amino acids **3-19** (AA) (**Figure 42**). Along with its non-disputable function in living organisms, where they serve as building blocks of proteins and play crucial roles in various biological processes, AAs are also common, structurally very useful, and chiral chemical pools for organic synthesis.

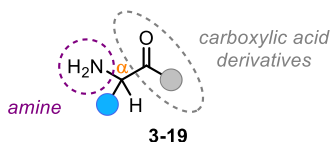


Figure 42: General structure of α -amino acids.

As mentioned above, AAs are essential for the structure and function of enzymes, receptors, and signaling molecules, as well as fundamental building blocks in biology (more than 500 AAs have been identified in nature).^{196,197} The name comes from the fact that all AAs contain at least one amine and one carboxylic acid moiety, which makes them attractive building blocks. The presence of these functional groups results in relatively high hydrophilicity, a property that is currently exploited for the enhancement of drug delivery. The incorporation of AAs in drugs proved to improve the biopharmaceutical properties of targeted molecules such as permeability, stability, and solubility.¹⁹⁸

From a biosynthetic point of view, the biosynthesis of AAs is a complex process that involves numerous enzymatic steps. All 20 naturally occurring AAs that can be easily found in proteins are α -amino acids that differ with the side chains. And this difference strongly influences the inherent properties of AAs as well as of proteins and/or other compounds that are generated starting from them.^{196,199}

The unique properties of AAs are explored in a wide range of applications across several scientific fields, from organic synthesis and biochemistry to material science. One of the reasons why they are so commonly used is that there is a desire to “escape from flatland”.²⁰⁰ A concept that answers the search of the pharmaceutical industry for better drug and candidate selectivity, the concept of searching for compounds that selectively interact only with the chosen receptor, the target place of biological action. The situation is favored using drug candidates with several chiral centers, which allows for better selectivity of the drug candidate.

Chapter III: α,α -disubstituted- α -amino-acids

For this and other reasons, numerous approaches for amino acid synthesis were developed and are now available as a chemical tool for organic chemists. Such tools vary in many ways, and they range from enzymatic applications,²⁰¹ *via* transition-metal catalysis,²⁰² organocatalysis,²⁰³ to radical chemistry-based²⁰⁴ methods. And still there are many novel and modern synthetic ways that are waiting to be disclosed and added to the tool of modern organic synthetic chemist. Such methods aim to synthesize specific structural motives that include AAs or to develop a synthesis of previously unknown AAs with the goal of adding new synthetic possibilities and previously unknown building blocks to the hands of medicinal chemists.

3.4. α,α -disubstituted- α -amino-acids

The most interesting and for the moment developed motive in AA chemistry is the synthesis of enantioenriched α,α -disubstituted α -AAs **3-20**. All these compounds are non-proteinogenic AAs, since the α -carbon atom next to the carboxylic function does not have a hydrogen atom and instead another alkyl substituent is placed (**Figure 43**). The 'double' substitution of the α position gives special properties to the AAs. For example, double substitution blocks/changes the way proteins fold, blocks active centers of proteins, and is resistant to oxidation, etc. In the case of plants, the cyclic form of the disubstituted AAs (which contain a cyclopropane scaffold in the building block) serves as a source of ethylene, a plant signaling molecule.

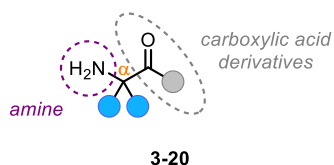


Figure 43: General structure of α,α -disubstituted α -AAs.

Interestingly, such a type of skeleton (α,α -disubstituted AA) is present in many natural products, as well as in synthetic drugs since recently. It is not surprising that the pharmaceutical industry is paying much more attention to the development of new synthetic routes for novel disubstituted AAs. The new type of structure, when incorporated into advanced molecular scaffolds, could further increase, for example, biostability, rigidity, increase biopharmaceutical properties, or allow for better selectivity of new or already existing drugs.^{205–207} However, preparation of a carbon atom with four distinct non-hydrogen

substituents remains a synthetic challenge, where the steric hindrance generated between the substituents is one of them. In general, the synthesis of the quaternary homochiral stereogenic center requires a multistep approach with several functional group interconversions.

3.4.1. Biological activity of α,α -disubstituted α -AAs.

A few examples of biologically active synthetic molecules are mentioned in **Figure 44**. Eglumegad **3-21**, also known as LY-354740, is a compound developed by Eli Lilly and Company, which acts as a group-selective agonist for group II metabotropic glutamate receptors and is being investigated in the treatment of anxiety and drug addiction.²⁰⁸ Another example can be fidarestat **3-22**, also known as SNK-860. Compound **3-22** belongs to the group of hydantoin heterocycles that are also known to be an aldose reductase inhibitor. This compound was in advanced Phase III clinical studies for the treatment of diabetic peripheral neuropathy; however, the study was discontinued in 2006.²⁰⁹

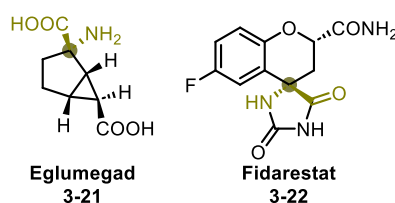


Figure 44: Examples of synthetic biologically active α,α -disubstituted α AA.^{208,209}

Naturally occurring biologically active α,α -disubstituted α -AAs are more common than we think (**Figure 45**). One of the examples is **spHINGOFUNGIN E 3-26** that was isolated from a fermentation of *Paecilomyces variotii*. This inosine-like compound inhibits serine palmitoyl transferase, an enzyme essential in the biosynthesis of sphingolipids, with an IC_{50} of 7.2 nM.²¹⁰ **Lactacystin 3-23** and its cell-permeable β -lactone form, **omuralide 3-24**, are both compounds naturally synthesized by bacteria of the genus *Streptomyces lactacystenaeus*, first identified in 1991. Both have selective and potent irreversible inhibitory effects on the 20S proteasome, a large polymolecular protein that is responsible for the degradation of ubiquitin-labeled proteins.^{206,211} **Coronatine 3-25** is a phytotoxin produced by *Pseudomonas syringae*, which is involved in chlorosis in leaves and that forces the stomata to reopen after closing in response to pathogen-associated molecular patterns.²¹²

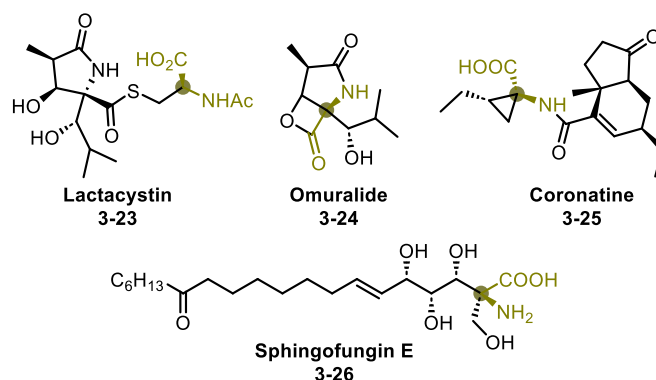
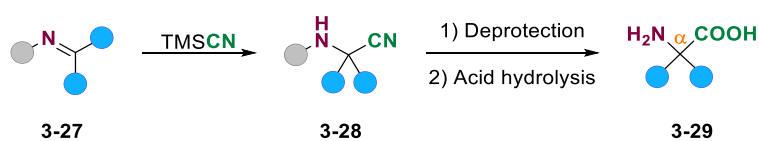


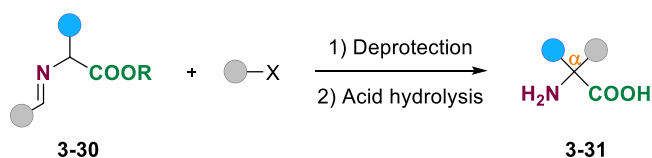
Figure 45: Examples of naturally occurring biologically active α,α -disubstituted α AA. ^{206,210–212}

3.4.2. Known methodologies of α,α -disubstituted α AA and their derivatives synthesis

Over the past few decades, numerous methods for the selective and enantioselective synthesis of α,α -disubstituted α AAs and their derivatives have been developed. The methods were developed with the aim to prepare natural products and other biologically active compounds. In general, developed methods require several steps (5-7 steps), to achieve the α,α -disubstituted AAs, and therefore the overall yields of the synthetic sequence are usually low.²¹³ Oldest, but still employed synthetic strategy that allows for α,α -disubstituted AA synthesis was described already in 1850. The method is called the Strecker synthesis and its asymmetric versions are still commonly used (**Scheme 68**).²¹³ Similarly, a bit younger coupling of Schiff-base enolates with various electrophiles derives α -amino esters (**Scheme 69**).^{214,215}



Scheme 68. Strecker synthesis of α,α -disubstituted α AA. ²¹³



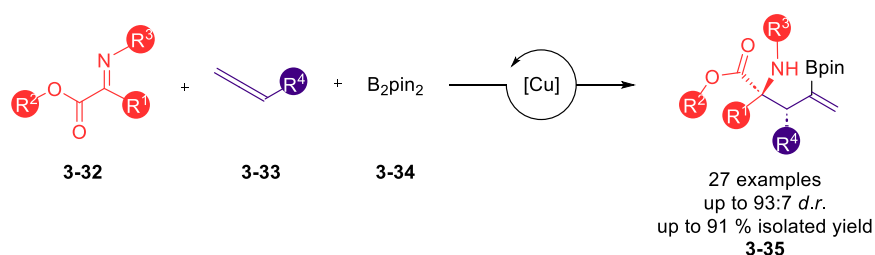
Scheme 69: Schiff-base synthesis of α,α -disubstituted α AA. ^{214,215}

The aim of this chapter is to briefly summarize the most important and recent methods employed in the synthesis of α,α -disubstituted α -AAs and its derivatives with a primary focus on methods developed in the past decade. These strategies include the formation of C-C

Chapter III: α,α -disubstituted- α -amino-acids

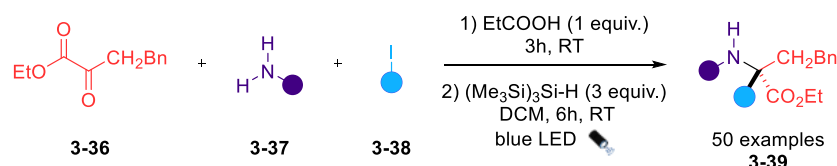
bonds using synergistic catalysis through common Cu/Pd, Ni/Cu and other cooperative systems to achieve the enantioselectivity^{216–219}, α -functionalization of general α -AAs (especially arylation and alkenylation)^{220–222}, direct α -C-H bond functionalization of α -amino acid²²³ or hydrocarboxylation of amines or imines.²²⁴

In 2019, the Proctet group developed a copper-catalyzed borylative allylation conditions that allowed the modification of ketiminoesters **3-32** with allenes **3-33** and bis(pinacolato)diborane **3-34** and produced quaternary α -amino esters **3-35** (Scheme 70).²²⁵



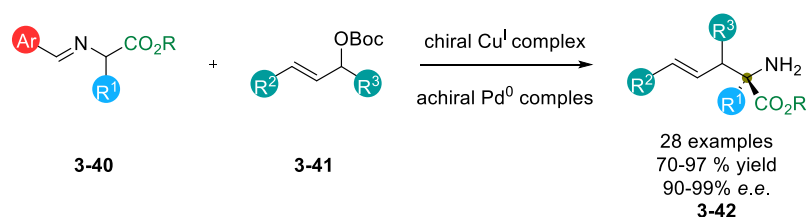
Scheme 70: Copper-catalyzed borylative allylation of ketiminoesters.²²⁵

In 2022, Gaunt group developed a protocol for the synthesis of α -tertiary amino esters **3-39** starting from primary alkylamine **3-37**, alkyl α -ketoesters **3-36**, and 1°, 2° or 3° alkyl iodides **3-38**. In this one-pot protocol, a broad scope of adducts could be prepared (Scheme 71).²²⁶



Scheme 71: Synthesis of α -tertiary amino ester *via* photoredox process.²²⁶

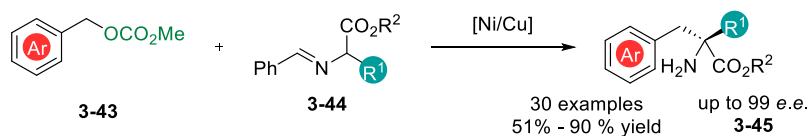
In 2017, Wang et al. described the enantioselective α -allylic alkylation of readily available aldimine esters **3-40** catalyzed by a synergistic Cu^I/Pd⁰ catalyst system to produce nonproteinogenic α,α -disubstituted α AAs **3-42** in high yields and with excellent enantioselectivity (Scheme 72).²¹⁶



Scheme 72: Cu^I/Pd⁰ cooperative catalysis for enantioselective alkylation of aldimine esters.²¹⁶

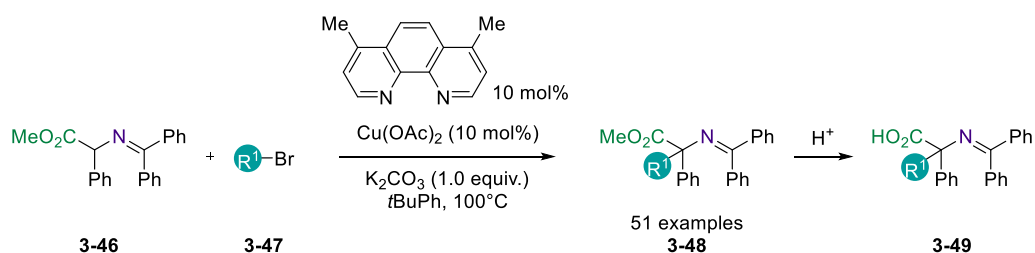
Chapter III: α,α -disubstituted- α -amino-acids

More recently, in 2022, Zhang's group reported the first synergistic asymmetric Ni/Cu-catalyzed benzylic alkylation of aldimine esters **3-44** in high yields and enantioselectivities (**Scheme 73**).²¹⁷



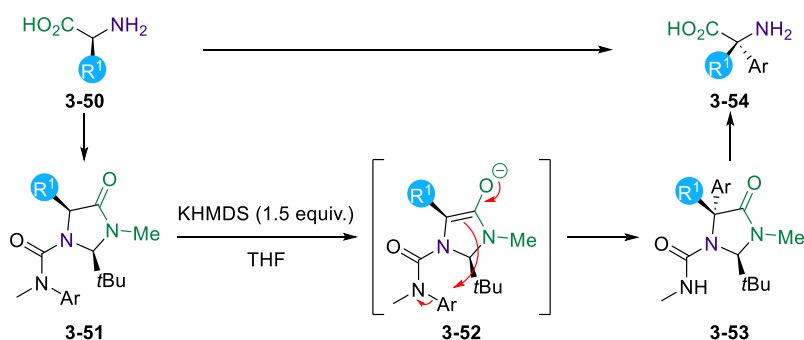
Scheme 73: Ni/Cu-catalysed benzylic alkylation of prochiral aldimine esters.²¹⁷

In 2020, the Ohshima group developed a method that was different from traditional systems that used Schiff bases. In previous examples, Schiff bases generally reacted with primary and very limited secondary alkyl halides **3-47**. In this work, α,α -disubstituted α -amino acid derivatives are prepared in moderate to high yields by radical-radical coupling of two radical species that are obtained through a one-electron process. α,α -disubstituted α -AAs **3-49** are then obtained by acid hydrolysis (**Scheme 74**).²²⁷



Scheme 74: Amino acid Schiff bases merging with copper catalysis.²²⁷

The Clayden Group reported in 2018 a construction of α,α -disubstituted α -AAs **3-54** via the α -arylation process where generated *N*-aryl ureas from AAs are converted to imidazolidinones **3-51**. Upon treatment with a base, the enolate **3-52** is formed in which the aromatic substituent of urea migrates stereoselectively, and the migration is directed by the bulky *tert*-butyl group. Hydrolysis of the product provides the quaternary α -aryl amino acids **3-54** (**Scheme 75**).²²⁸



Scheme 75: Metal-free stereoselective arylation of amino acids.²²⁸

3.5. α -heteroaryl α -substituted α -AAs

In our group, during our quest for heteroarylsulfonamides, we became interested in α -heteroaryl α -substituted α -amino acids (HAA), compounds that have proved to be virtually non-existing in chemical space of our universe. Indeed, only a very detailed literature search can reveal a few existing examples of molecules that would embody such a molecular scaffold. We are talking about HAAs with a heterocycle with at least two heteroatoms. From our point of view, such a molecular scaffold was very promising, since it combined the structure and functional potential of α,α -disubstituted α -AAs (used in the construction of non-natural peptides and proteins) and the power of the polyheteroatom containing heteroaryl structural motives (crucial for many drugs and drug-like molecules). As mentioned in previous chapters, a prominent subgroup of α -AAs are α,α -disubstituted α -AAs, AAs with unique pharmacological and biological capabilities. The heteroaryl group present in the α position, should even improve the unique chemical and biological properties already known for “simple” α,α -disubstituted α -AAs (**Figure 46**).

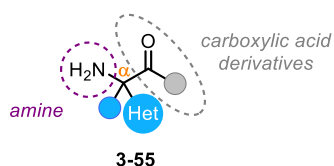


Figure 46: General structure of α -heteroaryl α -substituted α -AAs (HAA).

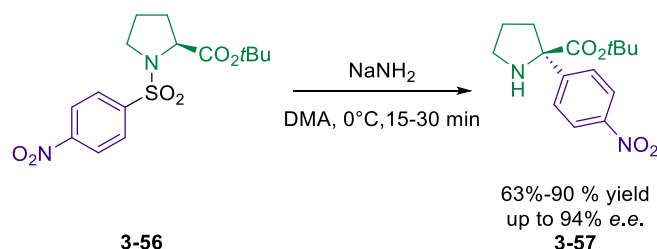
As mentioned above and to our knowledge, there are only few examples of $\alpha\alpha$ HAAs in the literature^{229–232}, and in most cases, the heteroaryl moiety of HAA is restricted to the pyridine ring and/or HAA is formed as an unwanted side product or is present in racemic form. Since such compounds are mostly unknown, we reasoned that the development of a robust and general route to homochiral HAAs is of interest to synthetic chemists (development of a novel synthetic method potentially broadly applicable), medicinal, and material (new building blocks with potentially interesting properties).

3.5.1. Synthesis of α -heteroaryl α -substituted α -amino acid derivatives

As we could see in Chapter 3.4.2, various synthetic approaches to α,α -disubstituted α -AAs were developed, but only few were reported for $\alpha\alpha$ HAAs. One of them is the reaction of proline-modified 4-NO₂phenyl sulfonamide **3-56**, which upon treatment with NaNH₂

Chapter III: α -heteroaryl α -substituted α -amino-acids

undergoes Smiles rearrangement and yields α -arylated proline derivative **3-57** in good yield and enantioselectivity (**Scheme 76**). Unfortunately, it was shown that the reaction conditions are limited to proline AA and the phenyl ring must contain an electron withdrawing group (EWG) in the *para* position of the phenyl ring and thus are limited to mono and dinitrophenyl sulfonamides).²³³

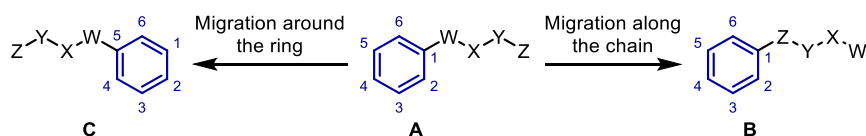


Scheme 76: Enantioselective rearrangement of proline sulfonamides.²³³

The reaction was first reported and further developed by Foschi et al.²³³ and it is one of the examples where the stereoselectivity of the reaction is dictated by the concept of a **Memory of Chirality**. In detail, the chirality of the modified stereogenic center is maintained only due to the fast intramolecular **Smiles rearrangement** step. The presence of the EWG group(s) on the phenyl ring is important for the stabilization of the polar Meisenheimer complex intermediate. In the next two subchapters a concept of **Smiles rearrangement** and concept of **Memory of chirality**, which are relevant for the results and discussion of chapter 3.8, and therefore will be described in detail on the following pages.

3.6. Truce Smiles rearrangement

Arguably, one of the most efficient and elegant ways to functionalize aromatic rings involves selective migration of the aryl moiety (rearrangement reactions). A rearrangement changes the attachment point between the arene ring and the atom it was originally connected to, and it is thus an inherently high atom economy. Starting with a relatively simple substrate, rearrangement reactions facilitate the creation of more complex molecules. Additionally, these reactions often achieve selectivity that their intermolecular counterparts cannot, thanks to increased reactivity resulting from a lower entropy of activation.²³⁴ These reactions involving arenes can be classified into two families: migration along the ring (**A** to **C**, e.g., Claisen rearrangement²³⁵) and migration along the chain (**A** to **B**, e.g., Smiles rearrangement²³⁶, **Scheme 77**)

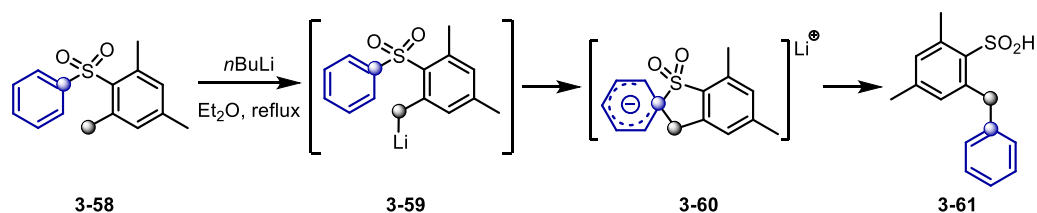


Scheme 77: Aryl migration strategies.

The Smiles rearrangement belongs to the migration along the chain family of rearrangements. This process has been widely studied and applied in a variety of fields, including drug discovery, materials science, and natural product synthesis.^{234,237–240} One important aspect of Smiles rearrangement is the role of reaction conditions in controlling the outcome of the reaction. The reaction can proceed under acidic or basic conditions, and the choice of conditions can have a significant impact on the selectivity and efficiency of the reaction. For example, in some cases, the use of Lewis acids can improve the yield of the reaction and enhance the stereoselectivity, while in other cases Lewis acids can lead to undesired side reactions and reduced selectivity.²⁴⁰ The choice of solvent can also affect the outcome of the reaction, with some solvents promoting faster reaction rates and others promoting greater selectivity. The mechanism of Smiles rearrangement has been the subject of much study and debate. Although the basic principles of the reaction are well established, the details of the reaction mechanism can vary depending on the specific reaction conditions and the structure of the starting material. Seminal base-catalyzed example of the Polar Truce-Smiles rearrangement mechanism is described in **Scheme 78**. In this example, a carbon-based nucleophile **3-59** is formed by lithiation of mesitylphenylsulfone **3-58**. Intermediate **3-59**

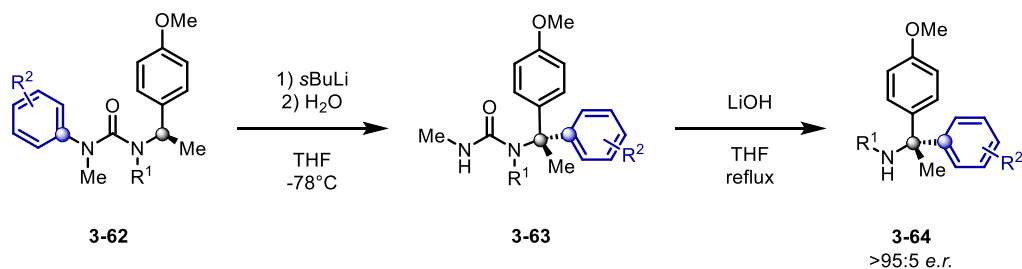
Chapter III: Smiles rearrangement

rearranges through the formation of a polar Meisenheimer spirocyclic intermediate **3-60**, delivering the corresponding lithium sulfonate. After protonation, the corresponding sulfonic acid **3-61** is obtained.²³⁴



Scheme 78: Typical tandem Polar Truce–Smiles rearrangement.²⁴⁰

One of the pioneering works in asymmetric Truce-smiles rearrangement was reported by Clayden et al.²³³ where they prepared substituted diarylmethylamines **3-64** through the stereospecific intramolecular electrophilic aryl migration of chiral ureas **3-62** (**Scheme 79**).



Scheme 79: Clayden asymmetric Smiles rearrangement.²⁴¹

Overall, Smiles rearrangement is a powerful tool in organic synthesis with a wide range of applications in drug discovery, materials science, and natural product synthesis. The reaction can be used to create complex molecules from simpler building blocks, and the ability to control the stereochemistry of the reaction makes it a valuable tool in the synthesis of chiral compounds and natural products.

3.7. Memory of chirality

Memory of chirality²⁴² is a concept introduced by Kawabata nearly 40 years ago that describes the 'conservation' of chirality in the case of reactions that proceed directly on the stereogenic center of the substrate (**Figure 47**). In short, the stereogenic center, for example on the sp^3 carbon atom, is destroyed (e.g., transformed to enolate), however, the original chirality of the starting material is 'conserved' ('memorized' / retained in the form of dynamic sp^2 chirality) and 'recuperated' by the reaction with the external reagent, most commonly electrophile. Memorization in this context means converting *the point chirality* (typically around the carbon stereocenter) to *the dynamic chirality* (typically through the "frozen" conformation to the 'special' chirality, chirality of the environment) and then recuperating back from the *dynamic chirality* to the *point chirality* (typically back to the carbon-based stereogenic center) chirality. During the process, either retention or inversion of chirality might occur.²⁴³

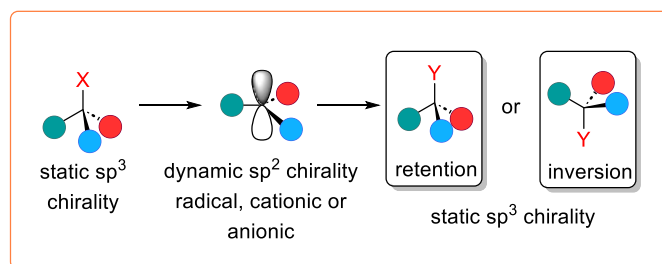
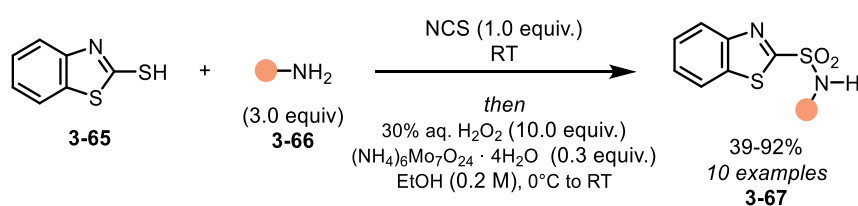


Figure 47: Concept of "Memory of chirality". Chirality is transferred from enantioenriched starting material to enantioenriched product.²⁴³

3.8. Results and discussion[#]

3.8.1. Introduction to sulfonamides synthesis

Over the past decade, we have been interested in exploring new ways to sulfonamides. As mentioned in Chapter 3.2 our group has developed a unified approach towards *N*-substituted and *N,N*-disubstituted BT sulfonamides (**Scheme 67**). From the newly developed routes to BT-sulfonamides, especially those based on the sulfenamide precursor gained much interest within our group due to its operational simplicity and high yield (**Scheme 80**). The problem with the method was that its scope and limitations were not fully disclosed.



Scheme 80: Approaches towards *N*-substituted benzo[*d*]thiazole-2-yl sulfonamides from benzo[*d*]thiazole-2-thiol and alkyl amines.

Thus, my first objective was to expand the application of this method to additional heterocyclic thiols, mainly nitrogen-containing heterocycles pyridine, pyrimidine, imidazole, benzo[*d*]imidazole and purine-2,6-dione, oxygen-containing heterocycles such as benzo[*d*]oxazole and oxazoles, and to sulfur-containing benzeno[*d*]thiazole and thiazole.

[#]This work was supported by the European Regional Development Fund-Project 'Centre for Experimental Plant Biology' (no. CZ.02.1.01/0.0/0.0/16_019/0000738) and by the Palacký University Internal Grant Agency (IGA_PrF_2022_016, IGA_PrF_2022_022, IGA_PrF_2023_031 and IGA_PrF_2023_020). Part of the research was published in *Org. Biomol. Chem.* **2022**, *20*, 3154-3159; DOI: 10.1039/D2OB00345G. The research presented in chapter **Chyba! Nenalezen zdroj odkazů.** were in part carried out by MSc. Jozef Kristek, with whom I did collaborate on the method development. The results obtained by him are presented only in the Results and discussion part to enrich the discussion. No experimental data are present in such case in the experimental part, since those will be integral part of his Thesis. The manuscript, where we both will be shared 1st authors is currently under preparation. The work was done in collaboration with prof. Freija De Vleeschouwer (DFT calculations) and Dr. Tomáš Pospíšil (advanced NMR experiments). As a co-primary researcher (shared with MSc J. Kristek) in the project, I was responsible for designing and conducting experimental procedures and measurements, analyzing the data, and interpreting the results. Additionally, I am co-writing a first draft of the manuscript.

3.8.1.1. Evaluation of sulfonamides *in silico*

Our work on the extension of the methodology started with the *in silico* evaluation of the selected heterocycle stability and reactivity. The reason for such 'project opening' was our previous experience with the preparation of derivatives from BT where the stability of intermediates and compounds was sometimes disputable and slight changes in reaction or further storage conditions had a huge impact on the reaction yields or stability. And we expected that the instability is caused by the C_α on a sulfone/sulfonamide of the heterocycle that is undergoing nucleophilic attack. Therefore, selected structures were evaluated *via* DFT calculation methods by Prof. Freija De Vleeschouwer and her Ph.D. student Eline Desmedt from Vrije Universiteit Brussel. In particular, we were interested in the local electrophilicity $\omega_{C\alpha}^+$ at C_α carbon of selected heteroarylsulfenamides (

Figure 48).¹⁹² The calculations found that the evaluated structures can be present in solution in two very different conformers, linear (expected) and sandwich (unexpected), and that local electrophilicity of such conformers might be significantly different (for example difference in case of **D1** and **D2**).

Chapter III: Results and discussion

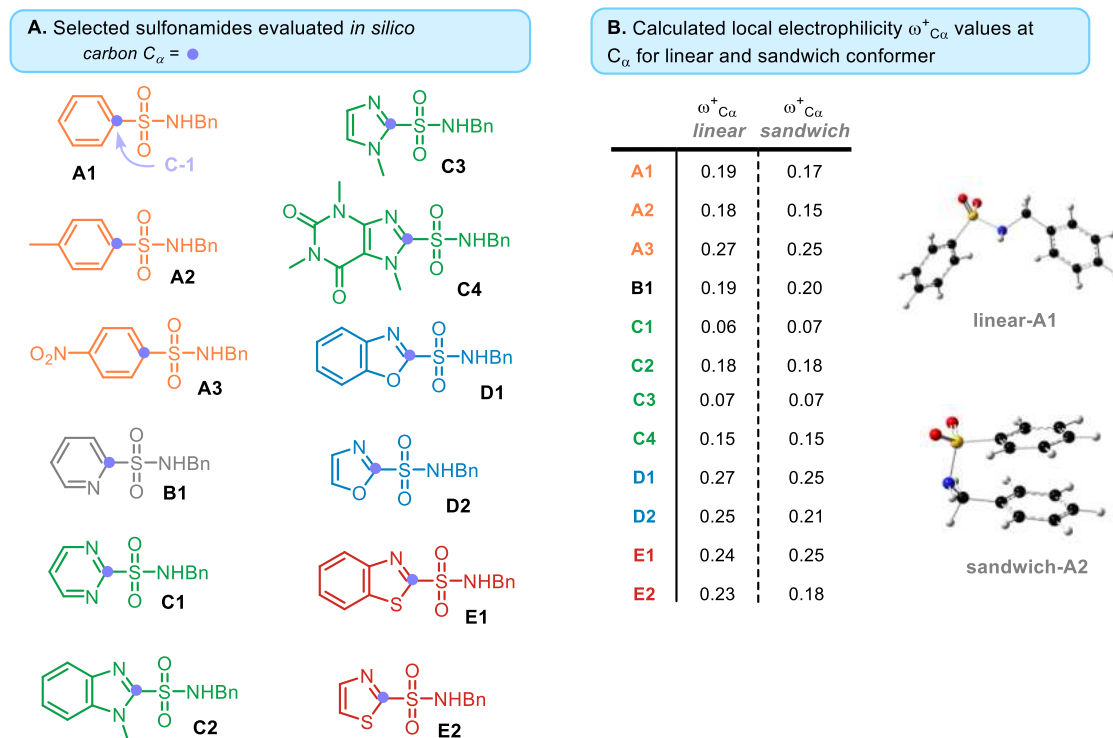


Figure 48: Local electrophilicity $\omega_{C_{\alpha}}^+$ at C_{α} carbon of selected heteroarylsulfenamides.

As a consequence, two different conclusions emerged from the calculations: (1) oxygen-containing heterocycles should be due to the highest electrophilicity index our ideal substrate for reaction optimization (should be the most prone to react with external electrophiles), and (2) the sandwich conformation brought us to the expectation that heteroarylsulfenamides might be a suitable substrate for the development of the 'Memory of Chirality' concept.

3.8.1.2. Optimization

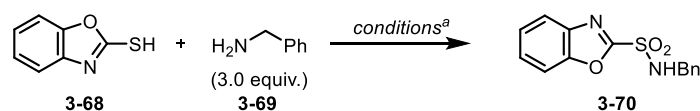
As mentioned above, our optimization of the heteroaryl sulfenamide reaction conditions began with benzo[*d*]oxazole **3-68** since it was the most sensitive substrate to nucleophilic attack (based on *in silico* results). Initial conditions for the synthesis of benzo[*d*]oxazole sulfenamide **3-70** were taken from the previously developed reaction protocol, although only traces of the desired product were observed (

Table 19). Detailed investigation of the formation and degradation of sulfenamide (equivalents of H_2O_2 and other reagents, including reaction workup and product purification) followed by oxidation to sulfonamide together with purification (crystallization turned out to be the only method for purification method) then allowed us to isolate the desired product in

Chapter III: Results and discussion

35 % yield (**entry 4**). This experience led us to conclude two things: (1) if one-pot protocol fails, the intermediate sulfenamide needs to be purified, and (2) oxidation step needs to be checked for the stability of generated sulfonamide (if product unstable, crystallization conditions need to be searched).

Table 19: Optimization of benzo[*d*]oxazole sulfonamide synthesis



Entry	Conditions	NMR Yields [%] ^b	Isolated Yield [%] ^c
1	NCS (1.0 equiv.), DCM, RT, 30 min, then (NH ₄) ₆ MoO ₄ ·4H ₂ O (0.3 equiv.), H ₂ O ₂ (20 equiv.), EtOH, 0 °C to RT, 5h	34	0
2	NCS (1.0 equiv.), DCE, RT, 1h, then (NH ₄) ₆ MoO ₄ ·4H ₂ O (0.3 equiv.), H ₂ O ₂ (20 equiv.), EtOH, 0 °C to RT, 5h	59	8
3	NCS (1.0 equiv.), DCE, RT, 1h, then (NH ₄) ₆ MoO ₄ ·4H ₂ O (0.3 equiv.), H ₂ O ₂ (10 equiv.), EtOH, 0 °C (30 min) to RT, 12 h	69	16
4 ^d	NCS (1.0 equiv.), DCE, RT, 1h, then (NH ₄) ₆ MoO ₄ ·4H ₂ O (0.3 equiv.), H ₂ O ₂ (10 equiv.), EtOH, 0 °C (30 min) to RT, 12 h	68	35

^a) The reactions were performed on benzo[*d*]oxazole-2-thiol (1 mmol) and benzylamine (3 mmol) scale.

^b) NMR yield determined using dimethylsulfone as an internal standard.

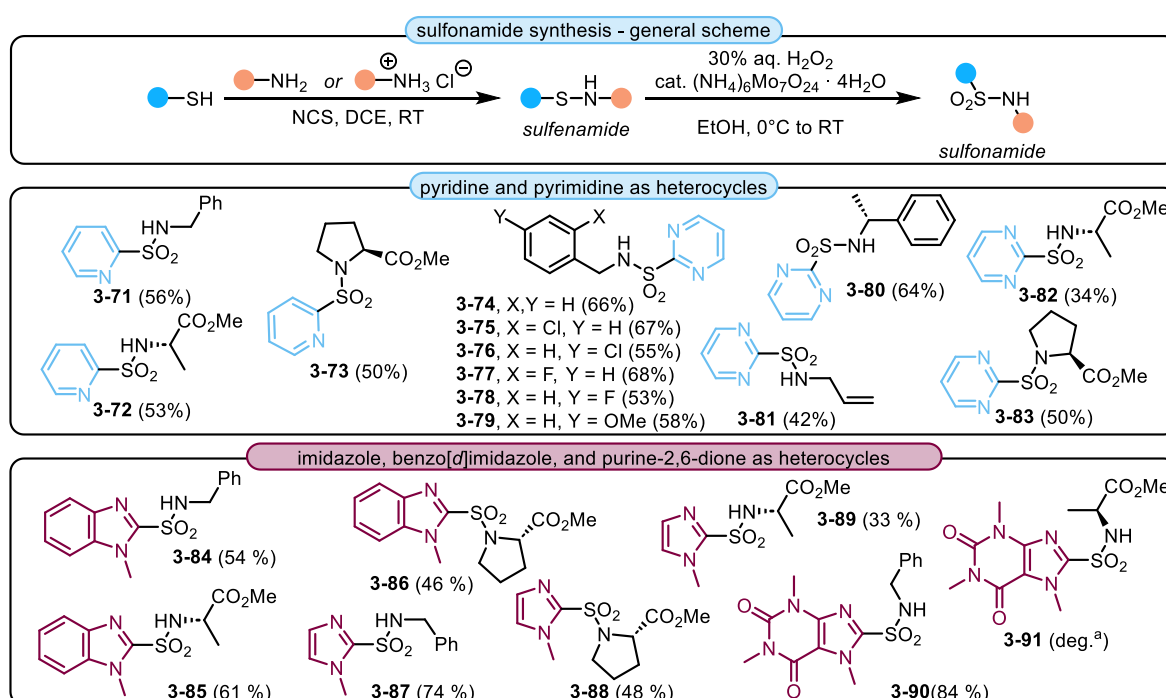
^c) Obtained *via* crystallization.

^d) Reaction performed on benzo[*d*]oxazole-2-thiol (5 mmol) and benzyl amine (15 mmol) scale.

3.8.1.3. Scope and limitations of heteroaryl sulfonamides synthesis

Although a comprehensive description of the developed synthetic approach towards the final conjugates can be found in a published paper ¹⁹², it is important to provide to the reader a summary of scope and limitations of the method. All compounds that were prepared by me during this project are then summarized in the experimental part of this chapter and their full characterization is provided.

The optimal conditions (entry 4, **Table 19**) for a preparation of *N*-substituted sulfonamides were used as the standard reaction conditions, however, in some cases several deviations from the standard protocol were applied especially with the regard of the product isolation and purification. The scope of the reaction started with the evaluation of pyridines, pyrimidines, imidazoles, benzo[*d*]imidazoles and purine-2,6-diones (**Scheme 81**). All these substrates proved to be suitable for the reaction and the desired compounds were isolated in good to very good yields.

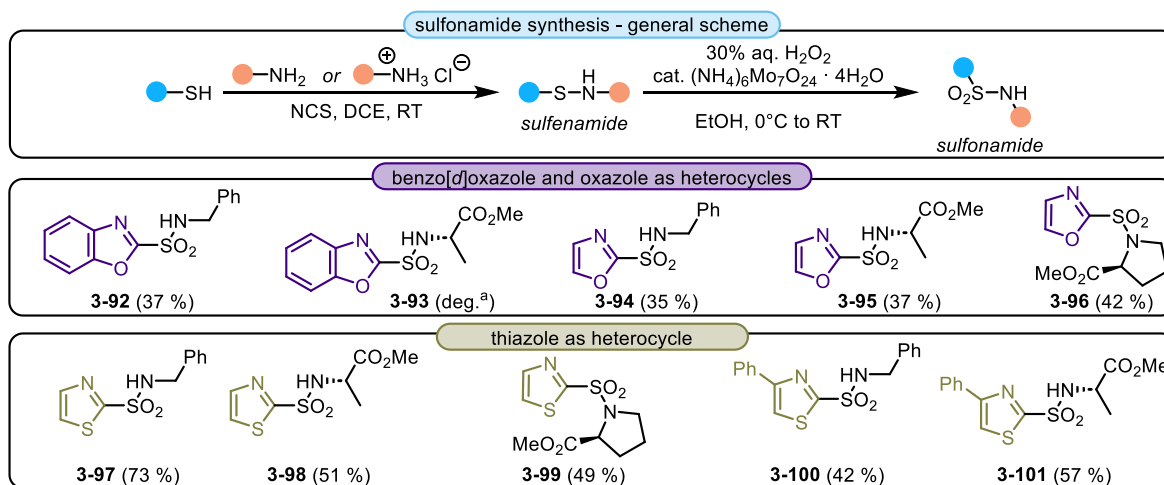


Scheme 81: Scope of the oxidative coupling between heteroaryl thiols (for pyridines, pyrimidines, imidazoles, benzo[*d*]imidazoles, purine-2,6-diones, benzo[*d*]oxazoles and oxazoles and thiazoles) and different amines. Yields refer to pure isolated compounds after two steps. All reactions were typically performed on a 5 mmol scale of the corresponding heteroaryl thiol. ^aSulfonamides detected by ¹H NMR; however, all attempts to isolate it failed.

Next, benzo[*d*]oxazoles and oxazoles and thiazoles were evaluated (**Scheme 82**). In this case it was observed that the stability of generated products is in many cases low and desired

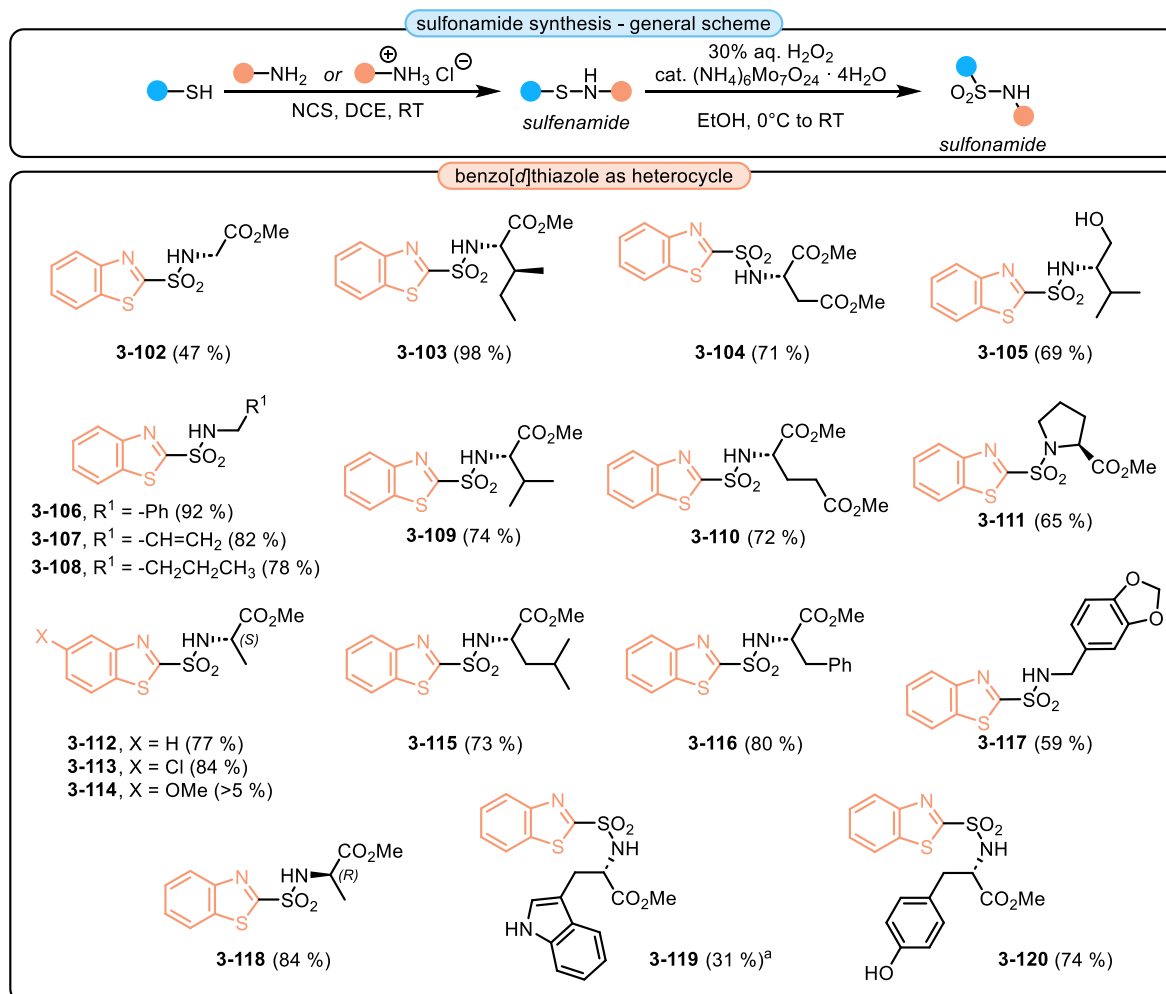
Chapter III: Results and discussion

products degraded either during the reaction workup or during the purification. Interestingly, once the final compounds were pure, they proved to be bench stable for several months.



Scheme 82: Scope of the oxidative coupling between heteroaryl thiols (benzo[*d*]oxazoles and oxazoles and thiazoles) and different amines. Yields refer to pure isolated compounds after two steps. All reactions were typically performed on a 5 mmol scale of the corresponding heteroaryl thiol.

We have also quite substantially broadened the scope for benzo[*d*]thiazoles sulfonamides (**Scheme 83**) and included other amino acids (many of obtained sulfonamides derived from AA are not part of the original publication¹⁹²), such as glycine **3-102**, both enantiomers of alanine **3-112** and **3-118**, isoleucine **3-103**, leucine **3-115**, proline **3-111**, valine **3-109**, phenylalanine **3-116**, tryptophan **3-119**, tyrosine **3-120**, and aspartic **3-104** and glutamic acid **3-110** besides other amines. Benzo[*d*]thiazoles sulfonamides proved to be the most stable group of sulfonamides generated *via* our protocol and their yields vary from good to excellent.



Scheme 83: Scope of the oxidative coupling between benzo[d]thiazole-2-thiols and different amines. Yields refer to pure isolated compounds after two steps. All reactions were typically performed on a 5 mmol scale of the corresponding heteroaryl thiol. ^aProduct **3-119** is sensitive to oxygen and upon concentration decomposes.

On the other hand, several substrates prove to be inappropriate substrates for the reaction (**Figure 49Chyba! Nenalezen zdroj odkazů.**). The partially saturated heteroaryl sulfonamides **3-122** and **3-123**, purine **3-124**, and triazole **3-125** react in the first step and produce sulfenamides smoothly. However, the subsequent oxidation step to sulfonamide was unsuccessful, most probably due to the oxidative decomposition of the sulfenamide. In the case of **3-121** and aromatic amines, the first step of the sequence, formation of sulfenamide, failed. We believe that the presence of a free N-H bond on the heterocycle is responsible for this behaving. In the case of tetrazole **3-126** both steps, sulfenamide formation and further oxidation, occurred and the desired product was clearly identifiable from the ¹H NMR spectra of the crude reaction mixture analysis, however, the purification of the product failed regardless of the isolation technique used.

Chapter III: Results and discussion

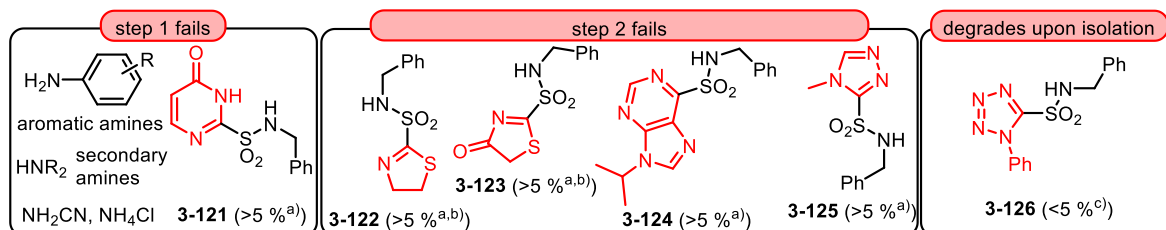
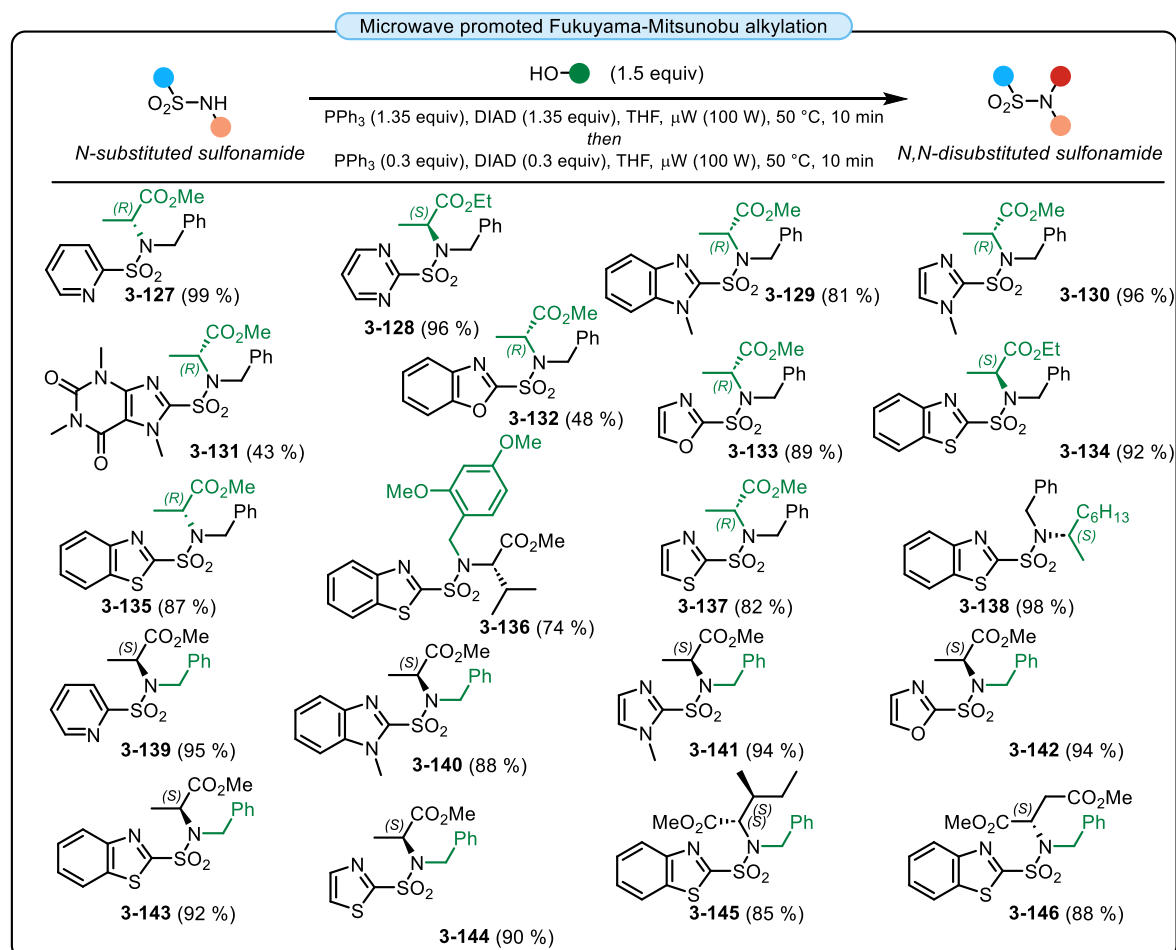


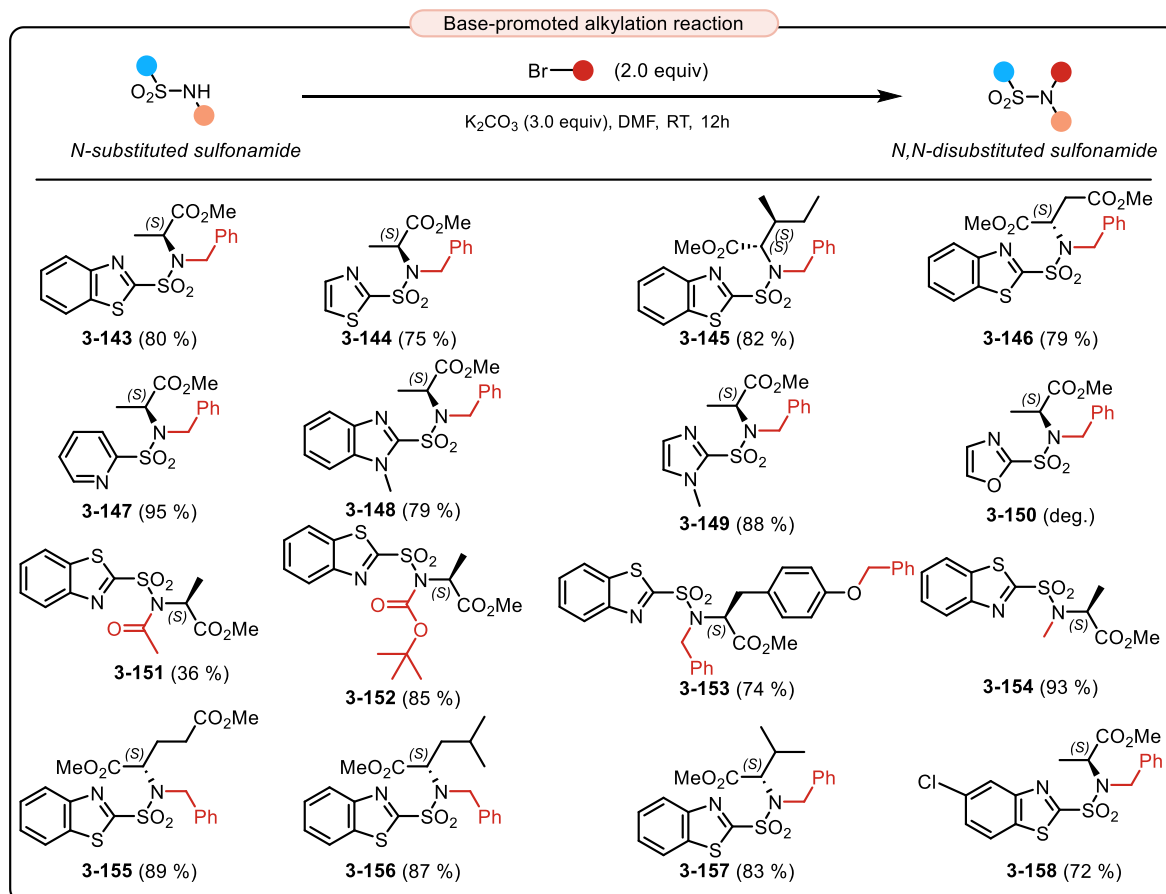
Figure 49: Limitations of the oxidative coupling between heteroaryl thiols and different amines. ^aNo product formation was observed. Only intermediate sulfenamide was detected. ^bThe oxidative opening of the heterocycle occurred during the oxidation step. Only side products were formed ^cDesired product **3-126** isolated only as a mixture of **3-126** with phenyl tetrazole (1 : 5). All attempts to purify compound **3-126** failed due to compound **3-126** decomposition.

Next, prepared *N*-monosubstituted heteroaryl sulfonamides were transformed to a *N,N*-disubstituted one. To achieve selective alkylation, two different methods were used. The first method explores the use of alcohols as alkylating agents and is based on the microwave-promoted Fukuyama–Mitsunobu alkylation reaction (**Scheme 84**).



Scheme 84: *N,N*-disubstituted sulfonamide synthesis. Scope of the microwave-promoted Fukuyama–Mitsunobu alkylation reaction. Yields refer to pure isolated compounds.

The second method uses alkyl bromides as alkylating agents and proceeds under basic conditions (**Scheme 85**).



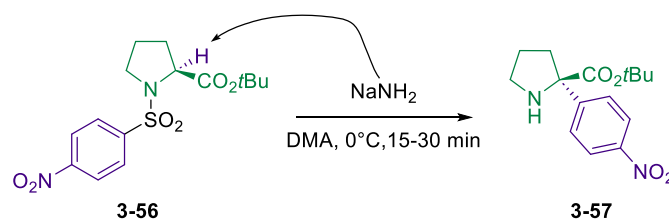
Scheme 85: *N,N*-disubstituted sulfonamide synthesis. Scope of the base-mediated alkylation reaction. Yields refer to pure isolated compounds.

In both cases, the expected products formed in good to excellent yields, and in the case of Fukuyama-Mitsunobu reaction, the reaction proceeded with complete inversion of the stereochemistry with regards to the original stereogenic center present in the starting alcohol. Again, *N*-substituted and *N,N*-disubstituted heteroaryl sulfonamides prepared by me during the scope and limitations determination are listed in the Experimental part with their full characterization data.

3.8.2. Introduction to α -heteroaryl α -substituted α -AAs synthesis

In Chapters 3.4.2 and 3.5, we have discussed extensive methodologies for the synthesis of α,α -disubstituted α AA and their derivatives. The methods depicted are quite broad and applicable on many substrates; however, when it comes to α -heteroaryl α -substituted α -AAs the power of such methods is vanishing.

As mentioned earlier, *in silico* evaluation of simple heteroaryl sulfonamides demonstrated that such compounds can be readily found in sandwich-like conformation (**Figure 48**), and such information in combination with the knowledge of Kawabata's principle of Memory of chirality, led us to the conclusion that such AA-derived heteroaryl sulfonamides could be explorative substrates to a new previously unknown class of α -heteroaryl α -substituted α -AAs and their derivatives. In this context, the literature precedent²³³ that describes the transformation of the proline-type sulfonamide **3-56** *via* Smiles rearrangement to α,α -disubstituted α AA ester **3-57**, was a great encouragement.



Scheme 86: Enantioselective rearrangement of proline sulfonamides.²³³

The primary motivation for the α -heteroaryl α -substituted α -AAs (**HAAs**) synthesis was, however, its application potential. We believe that this unique class of compounds can have a huge impact in at least two areas of research (**Figure 50**): (1) a design of a novel class of tunable organocatalysts, such as Hayashi-Jorgensen-like organocatalyst **3-161**, and (2) in a preparation of previously unexplored variety of Xeno nucleic acids, such as C8-Ala-Ado **3-163**. The with stability of such Xeno nucleic acids is obviously unknown, but we believe that it might be sufficient to be explorative in context of DNA or RNA.

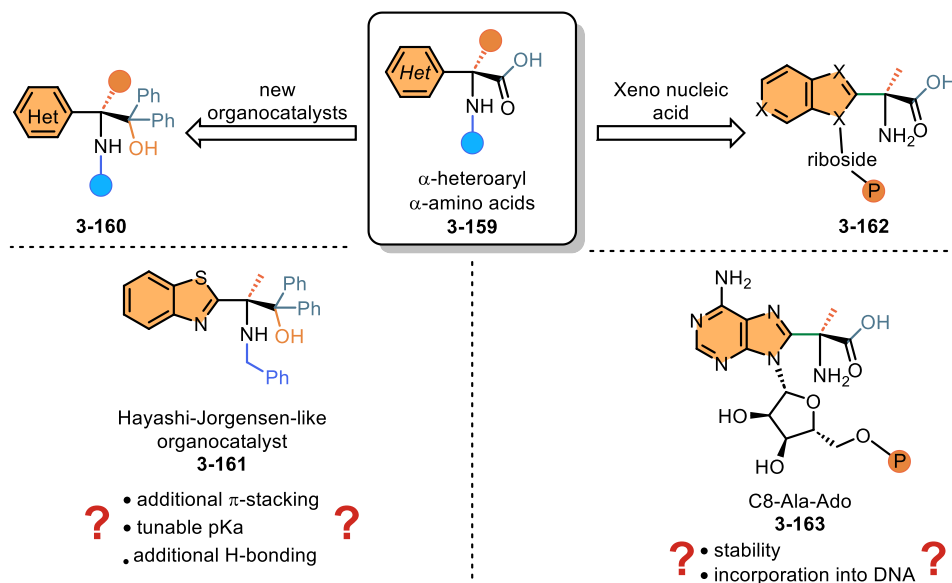


Figure 50: Two research domains where α -heteroaryl α -substituted α -AAs (**HAAs**) might play a key role in the future.

3.8.2.1. Evaluation of sulfonamides *in silico*

As previously, our first steps led to our colleagues from the theoretical department, and we led them to evaluate our idea of 'fixed' required for the Memory of Chirality concept the *in silico*. This approach that was used even later during our study allowed us to rationalize our ideas and definitely pushed us to test our Smiles rearrangement-based hypothesis towards the experimental evaluation. In particular we were interested in two outcomes: (1) the electrophilicity of the C_{α} electrophilic center in the heterocycle, and (2) the position of the acidic hydrogen atom placed in the a position to ester group (**Figure 51**). Theoretical approach suggested that both preliminary conditions are achieved, ((1) the C_{α} electrophilic center in the heterocycle is highly electrophilic, and (2) the acidic proton a to the ester is well suited to be deprotonated with a strong base) in the evaluated molecules at the same time. We thus conclude that the Smiles rearrangement is possible and can successfully occur.

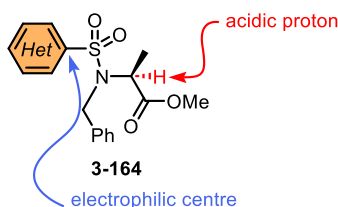
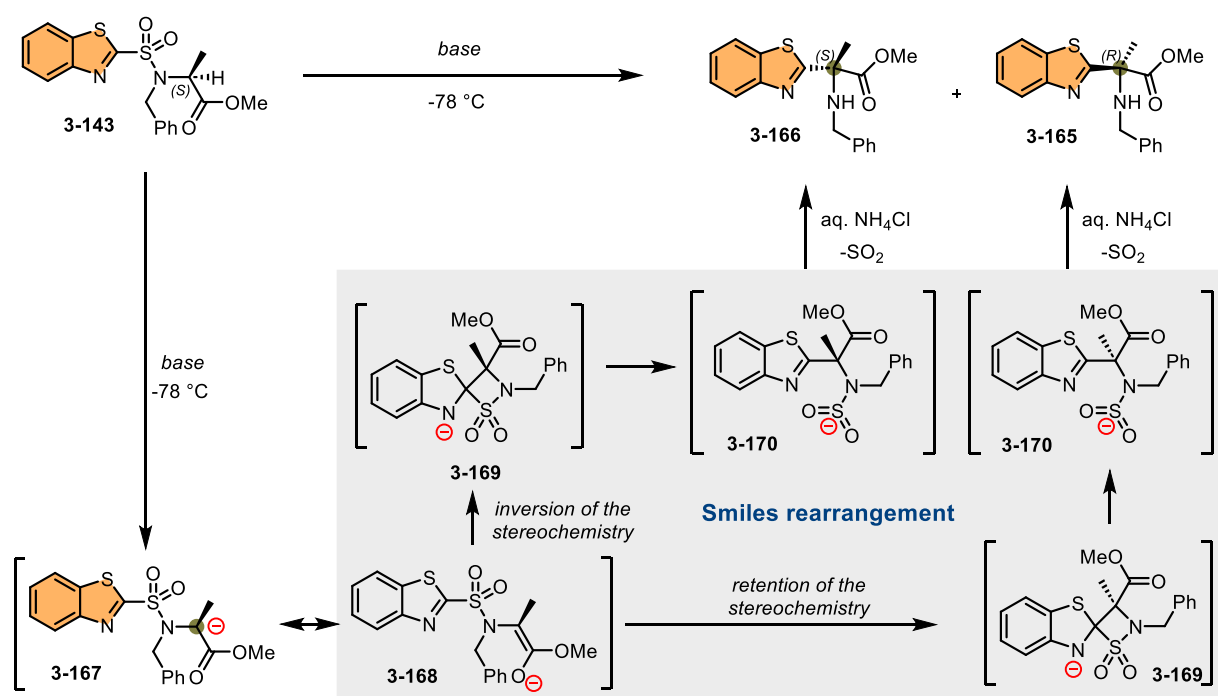


Figure 51: Necessity of the two reactive centers, (1) electrophilic center in the heterocycle, and (2) well-placed hydrogen atom in a position to ester group.

With this information in hand, we have taken advantage of our developed synthetic pathway to optically pure electron-deficient *N,N*-disubstituted heteroaryl sulfonamides

Chapter III: Results and discussion

and used compound **3-143** as the model substrate for the base-promoted Smiles rearrangement (**Scheme 87**). We expected that the reaction will proceed according to the following scenario: sulfonamide **3-143** will be deprotonated with a nonnucleophilic base and the generated anion will be either (**A**) conformationally stable or, more likely, (**B**) the generated enolate will preserve the conformation the molecule kept before the deprotection. In addition, we expected that the Smiles rearrangement will be a rapid process that will proceed faster than the inevitable conformational change would occur. The corresponding α -amino ester with retention **3-165** or inversion **3-166** of configuration. First, the deprotonation to form **3-167** occurs, followed by tautomerization to its enol form **3-168**. Next, the formation of Meisenheimer complex **3-169** followed by Smiles rearrangement proceeds to form **3-170**, which upon aquatic workup protonates and releases SO_2 .



Scheme 87: Expected reaction mechanism of heteroaryl sulfonamide **3-143** transformation to HAA **3-165** or **3-166** that should proceed *via* Smiles rearrangement.

3.8.2.2. Optimization

To validate our hypothesis, the reaction conditions that would yield the desired rearrangement product were searched (**Table 20**). In the first attempt, 6.0 equiv. of LDA was added to sulfonamide **3-143** at $-78\text{ }^\circ\text{C}$ and the reaction was allowed to stir at that temperature for 30 min (**Entry 1**). The degradation of the starting material

Chapter III: Results and discussion

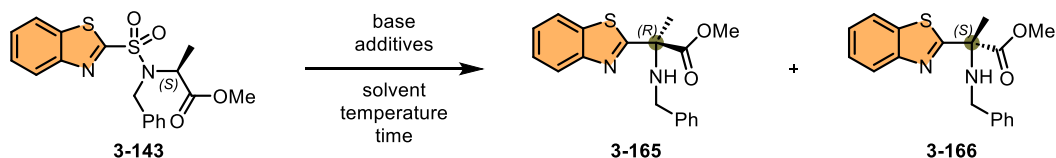
was observed, however, a comprehensive analysis of the ^1H NMR spectra of the crude reaction mixture revealed some traces of a new compound that was later identified as our product **3-166**. Next, KHMDS (1.5 equiv.) in Et_2O was used (**entry 2**). The reaction proceeded smoothly, and the spectra of the crude reaction mixture were quite clean. Additionally, based on the TLC analysis, the overall transformation proceeded within 10 min (conversion of the starting material). The desired product **3-166** was formed and after the HPLC separation method was established that the enantiomeric ratio of **3-166** to its enantiomer **3-165** is 81:19. The reaction yield was 92 %. Next, a screening of the optimal reaction conditions started. First, the influence of the solvents was established (**entries 2-5**) identifying THF as the best reaction solvent. Next, based on our longstanding tradition reaction of KHMDS at $-78\text{ }^\circ\text{C}$ in the presence of 18-crown-6 was carried out (**entry 6**).²⁴⁴ The addition of 18-crown-6 should allow the Smiles rearrangement to proceed faster since the potassium cation should be scavenged and to further increase already nice enantiomeric ratio of the reaction. Much to our surprise, after the reaction workup and determination of the enantiomeric purity, the opposite enantiomer, compound **3-165**, was formed as a major product of the reaction (**3-165:3-166** = 93:7). When 1.5 equiv. of KHMDS with 3.0 equiv. of 18-crown-6 was used at $-95\text{ }^\circ\text{C}$, the enantiomeric ration increased slightly (**entry 7**, 95:5). The results were encouraging, but confusing. Thus, other bases such as LiHMDS and NaHMDS and additives were screened, and very interesting results were obtained. LiHMDS without any additional additives gave at $-78\text{ }^\circ\text{C}$ (**entry 8**, *e.r.* = 87:13) the same result as KHMDS/18-crown-6 mixture. The addition of HMPA led to a decrease in reaction selectivity (**entry 9**, 75:25). Decreasing the temperature from $-78\text{ }^\circ\text{C}$ to $-90\text{ }^\circ\text{C}$ also helped the selectivity, and *e.r.* increased to 96:4 (**entry 10**). NaHMDS without any additives provided only poor selectivity of 67:33 (**entry 11**), but when 3.0 equiv. of 18-crown-6 was added, the selectivity increased to excellent **97:3** (**entry 12**).

The conditions obtained were excellent; however, they did not answer the question how reversed selectivity could be repetitively achieved (**entry 5**, *e.r.* = 17:83). Our hypothesis was that the size of the cation and/or additive might play a role in the selectivity switch. The task of finding out if the hypothesis is correct was taken over by my colleague, MSc. Jozef Kristek, who devoted his time to searching for the right reaction conditions that would allow us to prepare enantiomer **3-166** as the main product of the reaction starting from the same

Chapter III: Results and discussion

starting material as me, who is able to prepare enantiomer **3-165**. The results obtained during his optimization are for clarity of the discussion summarized in **Table 21** and **Table 22**.

Table 20: Optimization of the reaction conditions of the Smiles rearrangement.



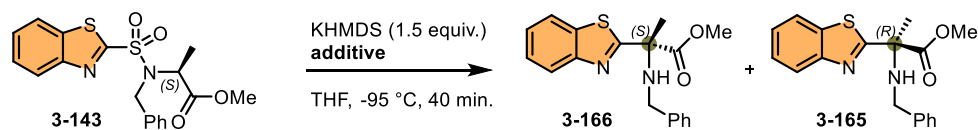
Entry	Base (equiv.)	Additive (equiv.)	Solvent ^a	Temp. [°C]	Time [min]	Conv. [%] ^b	Yield [%] ^c	<i>e.r.</i> ^d
1	LDA (6.0)	-	THF	-78	30	≥98	n.d.	-
2	KHMDS (1.5)	-	Et ₂ O	-78	30	≥98	n.d.	19:81
3	KHMDS (1.5)	-	Et ₂ O	-95	30	≥98	n.d.	15:85
4	KHMDS (1.5)	-	DMF	-50	30	≥98	n.d.	17:83
5	KHMDS (1.5)	-	THF	-95	30	≥95	63	17:83
6	KHMDS (1.5)	18-crown-6 (3.0)	THF	-78	30	≥98	69	93:7
7	KHMDS (1.5)	18-crown-6 (3.0)	THF	-95	30	≥99	73	90:10
8	LiHMDS (1.5)	-	THF	-78	30	≥98	n.d.	87:13
9	LiHMDS (1.5)	HMPA (3.0)	THF	-78	30	≥98	n.d.	75:25
10	LiHMDS (1.5)	-	THF	-95	30	≥98	75	97:3
11	NaHMDS (1.5)	-	THF	-78	30	≥99	n.d.	67:33
12	NaHMDS (1.5)	18-crown-6 (3.0)	THF	-78	30	≥99	90	97:3

a) All reactions were performed in 0.1 M concentration; b) Based on ¹H NMR spectra of the crude reaction mixture or by HPLC; c) Refers to pure isolated product; d) Determined by chiral HPLC analysis.

First, screening of different additives that were added to the reaction mixture prior the base, KHMDS, was performed (**Table 21**). It was observed that product **3-166** in high enantiomeric ratios might be obtained. The best *e.r.* was obtained in the case CuOTf (**entry 14**).

Chapter III: Results and discussion

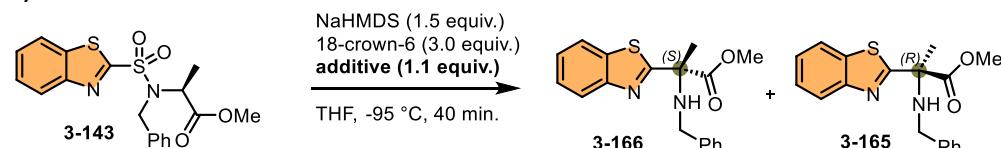
Table 21: Evaluation of the role of the additional metal salts given to the reaction mixture *prior* cooling down to -95 °C.



Entry ^a	Additive	Additive equiv.	Conv. [%] ^b	e.r. ^c
1	LiCl	1.1	>98	46:53
2	NaCl	1.1	>98	13:87
3	KCl	1.1	>98	13:87
4	KCl	3.0	>98	13:87
5	KCl	5.0	>98	20:80
6	CsF	1.1	>98	13:87
7	MgCl ₂	1.1	70	32:68
8	CaCl ₂	1.1	>98	13:87
9	Yb(OTf) ₃	1.1	>98	13:87
10	Sc(OTf) ₃	1.1	70	25:75
11	Zn(OTf) ₂	1.1	>98	12:88
12	Zn(OTf) ₂	3.0	70	20:80
13	Zn(OTf) ₂	5.0	30	35:65
14	CuOTf	1.1	>98	10:90
15	CuOTf	3.0	30	35:65
16	CuOTf	5.0	15	30:70
17	CuCl	1.1	>98	30:70
18	ZnCl ₂	1.1	>98	82:18
19	AgOTf	1.1	>98	85:15
20	AgNO ₃	1.1	>98	85:15

^aReactions were performed with sulfonamide **3-143** (20.0 mg, 0.05 mmol, 1.0 equiv) in THF (0.1 M) at -95 °C with KHMDS (0.08 mmol, 1.5 equiv) and different inorganic salts. ^bAll conversions were determined by crude HPLC analysis or by NMR. ^cThe enantiomeric ratio (e.r.) was determined by chiral HPLC analysis.

The same optimization was performed for the NaHMDS/18-crown-6 system (**Table 22**). Interestingly, in this case the reaction yielded the enantiomer **3-165** as the main product of the reaction suggesting that the addition of the 18-crown-6 additive hampers any influence that additional salt addition has on the reaction selectivity.

Table 22: Influence of added cations to the NaHMDS/18-crown-6 system on the reaction selectivity.


Entry ^a	Additive	Additive equiv.	Conv. [%] ^b	e.r. ^c
1	LiCl	1.1	>98	99:1
2	NaCl	1.1	>98	82:18
3	KCl	1.1	>98	82:18
4	CsF	1.1	>98	81:19
5	MgCl ₂	1.1	>98	86:14
6	CaCl ₂	1.1	>98	94:6
7	Yb(OTf) ₃	1.1	50	85:15
8	Sc(OTf) ₃	1.1	40	81:19
9	Zn(OTf) ₂	1.1	43	93:7
10	CuOTf	1.1	61	95:5

^aReactions were performed with sulfonamide **3-143** (20.0 mg, 0.05 mmol, 1.0 equiv) and 18-crown-6 (0.15 mmol, 3.0 equiv) in THF (0.1 M) at -95 °C with NaHMDS (0.08 mmol, 1.5 equiv) and different inorganic salts (0.06 mmol, 1.1 equiv). ^bAll conversions were determined by crude HPLC analysis or by NMR. ^cThe enantiomeric ratio (e.r.) was determined by chiral HPLC analysis.

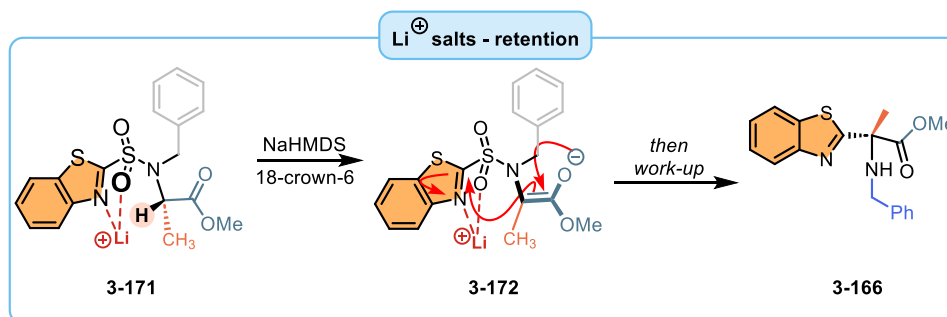
To conclude, extensive optimization of the reaction conditions identified two sets of the reaction conditions that can selectively furnish compound **3-165** or **3-166** starting from the same homochiral starting material. When 1.5 equiv. of NaHMDS with 3.0 equiv. of 18-crown-6 and 1.1 equiv. of LiCl were used, stereoselective formation of the **3-165** enantiomer increased to 99:1 (**entry 1, Table 22**), and when 1.5 equiv. of KHMDS with 1.1 equiv. of CuOTf was used, the opposite enantiomer **3-166** was isolated in 95:5 e.r. (**entry 13, Table 20**).

3.8.2.3. Mechanistic studies of Li⁺ and Cu²⁺ salts

Given the intriguing results from the initial screening and our success in synthesizing both enantiomers from a same starting material, we reached out to our collaborators Dr. Freija De Vleeschouwer from Vrije Universiteit Brussel for assistance with density functional theory (DFT) calculations and Dr. Tomáš Pospíšil for NMR experiments. With their expertise, we computed the transitional states and proposed a coordination mechanism involving two distinct cations, shedding light on the reaction mechanism.

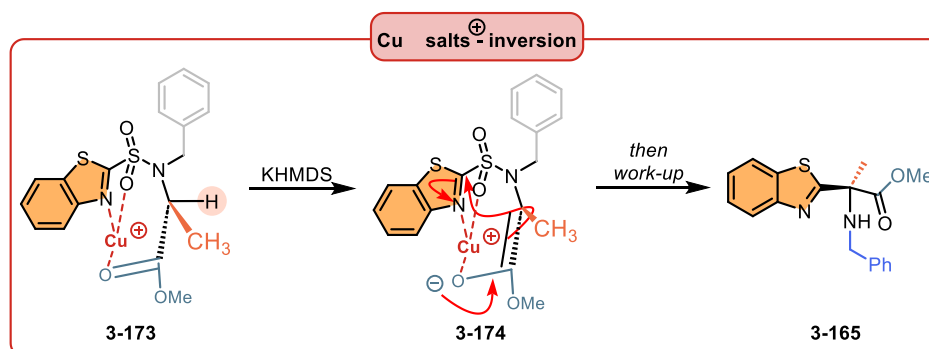
Chapter III: Results and discussion

First, we propose that lithium(I) cation from LiCl coordinates to oxygen of the sulfonamide group and nitrogen of the BT-heteroaryl and forms intermediate **3-171**. Since the Li(I) is a small cation, it does not sterically interfere with the ester part of the molecule. Consequently, after deprotonation by NaHMDS, the nucleophilic attack of the enolate **3-172** happens from the front side of the molecule and the rearrangement proceeds with the retention of the stereochemistry. Aqueous work up then yields to product **3-166** and the reaction proceeds overall with retention of configuration (**Scheme 88**).



Scheme 88: Proposed formation of **3-166** using LiCl additive.

When copper triflate is added, the overall picture changes. Copper(I) coordinates presumably with the oxygen of the sulfonamide, the nitrogen of the BT group, and the oxygen of the ester group. The change in the cation size is a reason for the observed change in the mode of coordination. The generated conformer **3-173** than placing the acidic hydrogen atom outside of the complex and its subsequent deprotonation then forces the Smile rearrangement to proceed *via* the inversion of the configuration. The aqueous work then yields the final product with the opposite configuration, when compared to the original configuration of the starting material (**Scheme 89**).



Scheme 89: Proposed formation of **3-165** using CuOTf additive.

3.8.2.4. Determination of absolute configuration

Of course, the reaction mechanism could not be suggested before the determination of the absolute configuration of compounds **3-165** and **3-166** was achieved. We have tried many ways of doing it. First, the transformation of generated products to Mosher amides was carried out, but no product formation was observed. Co-crystallization of generated compounds with various chiral acids failed again presumably due to a low basicity of sulfonamide. Therefore, the only possibility left was to prepare a single crystal for X-ray analysis. Thus, the crystallization of **3-166** by dissolving it in DCM and allowing it to crystallize in the hexane atmosphere allowed us to obtain a monocrystal, which was suitable for X-Ray analysis. Single X-Ray analysis of the product was performed by Dr. Ivan Němec (Palacký University Olomouc) (**Figure 52**).

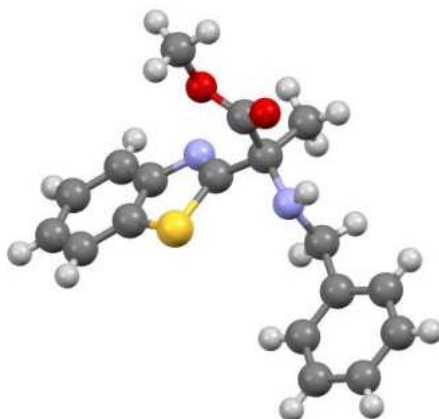
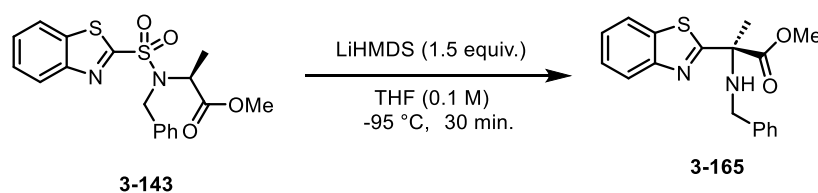


Figure 52: Crystalline structure of **3-166**.

3.8.2.5. Competitive reactivity in the presence of other functional groups

We also wanted to find out which functional groups are tolerated during the Smiles rearrangement. Therefore, we have performed a competitive reaction of our model substrate **3-143** with LiHMDS in the presence of 4-methoxyacetophenone ($pK_a \approx 21$, keton group), *p*-anisaldehyd ($pK_a \approx 16$, aldehyde group), ethylacetate ($pK_a \approx 25$, ester group), silylated BT sulfonamide ($pK_a \approx 6$) and monitored conversion (**Table 23**). Competitive experiments suggested that the reaction cannot be carried out in the presence of substrates with readily available (accessible) acidic hydrogen atoms that have lower pK_a compared to the acidic proton in heteroaryl sulfone **3-143** ($pK_a \sim 25-28$). However, if a sterically hindered acidic proton is present, the Smiles rearrangement might proceed smoothly.

Table 23: Functional group tolerance experiments.

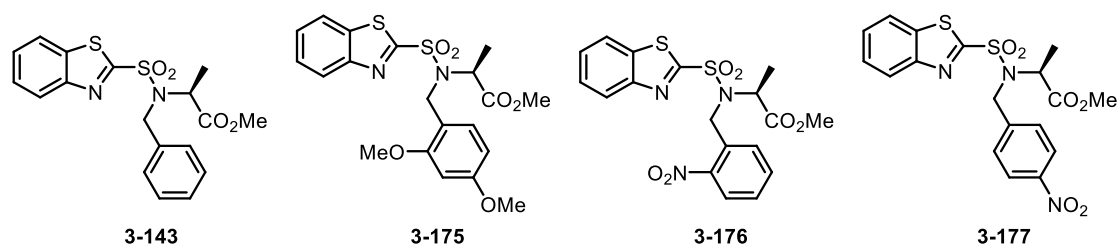
Entry	Additive (1.0 equiv.)	pKa	Product formation [%] ^a
1	4-methoxyacetophenone	≈ 25	29
2	<i>p</i> -anisaldehyd	≈ 16	≤1
3	ethylacetate	≈ 25	≤1
4	silylated BT sulfonamide	≈ 6	≥99

a) Based on ¹H NMR spectra of the crude reaction mixture

3.8.2.6. Effects of nitro group

We have also prepared three other BT sulfonamides (**3-175** – **3-177**), together with the **3-143** model substrate according to our developed protocol¹⁹² with different substitution on the benzyl group. These substrates should allow us to evaluate the influence of the substitution on the aromatic ring on the Smiles rearrangement (**Table 24**). In addition, the role of substitution might prove to be crucial when the pre-rearrangement conformation of the substrates is adapted.

From **Table 24** it is clear that the electron-donating dimethoxybenzyl **3-175** gives the best selectivity during the reaction for both inversion and retention products (**entry 5** and **6**) whereas electron-withdrawing 2-nitrobenzyl **3-176** gives the worst selectivity (**entries 10** and **11**). The change in the nitro group position to *para* makes the reaction proceed and if LiHMDS is used as a base, the desired product **3-177** (**entry 8**) can be isolated albeit with modes stereoselectivity. Those results had an important impact on our scope and limitations determination campaign. Since dimethoxybenzyl group increases the reaction stereoselectivity of the rearrangement process (presumably due to a better conformation stability) it was used in the cases where worse reaction yields, or selectivity were observed during the scope and the limitation evaluation.

Table 24: Impact of the benzylic group substitution on the reaction yields and selectivity.

Entry	compound	base	salt/additive	Time [min]	Temp [°C]	Conv. [%] ^a	<i>e.r.</i>
1	3-143	LiHMDS	-	30	-95	~99%	96 : 4
2	3-143	KHMDS	18-crown-6	30	-95	~99%	72 : 28
3	3-143	NaHMDS	LiCl, 18-crown-6	60	-95	~90%	98 : 2
4	3-143	KHMDS	CuOTf	30	-78	99%	10:90
5	3-175	KHMDS	CuOTf	60	-78	~75%	7 : 93
6	3-175	NaHMDS	LiCl, 18-crown-6	60	-78	~99%	99:1
7	3-177	KHMDS	CuOTf	60	-78	~30%	35:65
8	3-177	NaHMDS	LiCl, 18-crown-6	60	-78	~30%	95:5
9	3-177	LiHMDS	-	60	-78	~54%	-
10	3-176	KHMDS	CuOTf	60	-78	~<5%	-
11	3-176	NaHMDS	LiCl, 18-crown-6	60	-95	~<5%	-
12	3-176	KHMDS	18-crown-6	60	-78	~60%	-
13	3-176	LiHMDS	-	60	-78	~95%	76:24

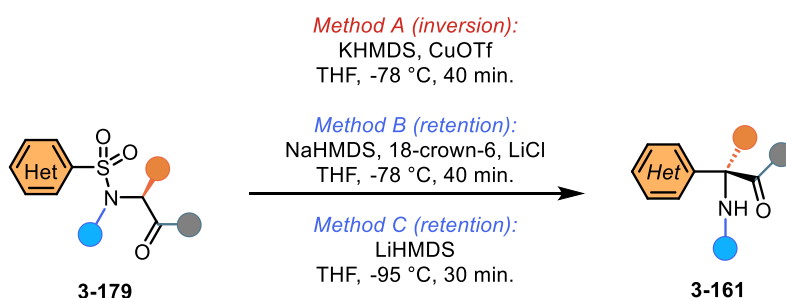
a) Based on ¹H NMR spectra of the crude reaction mixture

b) Determined by chiral HPLC analysis.

3.8.2.7. Scope and limitations of α -heteroaryl α -substituted α -AA derivatives

With the proof-of-concept established and optimized reaction conditions in hand, the scope and limitations of the method could be established. Three protocols were evaluated: one for inversion of the stereochemistry - **Method A** (KHMDS (1.5 equiv.), CuOTf (1.1 equiv.), THF (0.1 M)) and two for retention of the stereochemistry - **Method B** and **Method C** (LiHMDS (1.5 equiv.), THF (0.1 M) or NaHMDS (1.5 equiv.), 18-crown-6 (3.0 equiv.), LiCl (1.1 equiv.), THF (0.1 M)). Two different methods for the retention of stereochemistry were selected since they proved to be complementary in their reaction outcomes (**Scheme 90**). At this point, it should be noted that all starting substrates for the rearrangement reaction, heteroaryl sulfonamides, were prepared according to a protocol developed in our group¹⁹² and their synthesis, if not presented earlier, is summarized in the Experimental part. My part in this project focused on the evaluation of the role of *N*-alkyl substitution, amino acid

substitution (substitution excluding the ester part) part, and partially in the heterocycles scope. The influence and scope of the ester and heterocycle parts (majority) were the responsibility of my colleague Jozef Kristek.



Scheme 90: Optimal conditions for Smiles rearrangement.

First, the influence of the alkyl group on the nitrogen atom of sulfonamide was evaluated (**Figure 53**). Various groups were evaluated with respect to their structural diversity and steric hindrance. The screening of the influence of the alkyl chains (such as: -benzyl **3-167**, methyl **3-181**, butyl **3-182**, isopropyl **3-183**, allyl **3-185**, and **3-186**) revealed that in all cases the rearrangement proceeded in good yields and selectivity if retention of the configuration is considered. In case of inversion of the configuration, moderate to good selectivity was reached. Carbonyl groups (-COCH₃ **3-180** and *t*-butoxycarbonyl **3-187**) were also successfully incorporated, as well as various substituted benzylic groups.

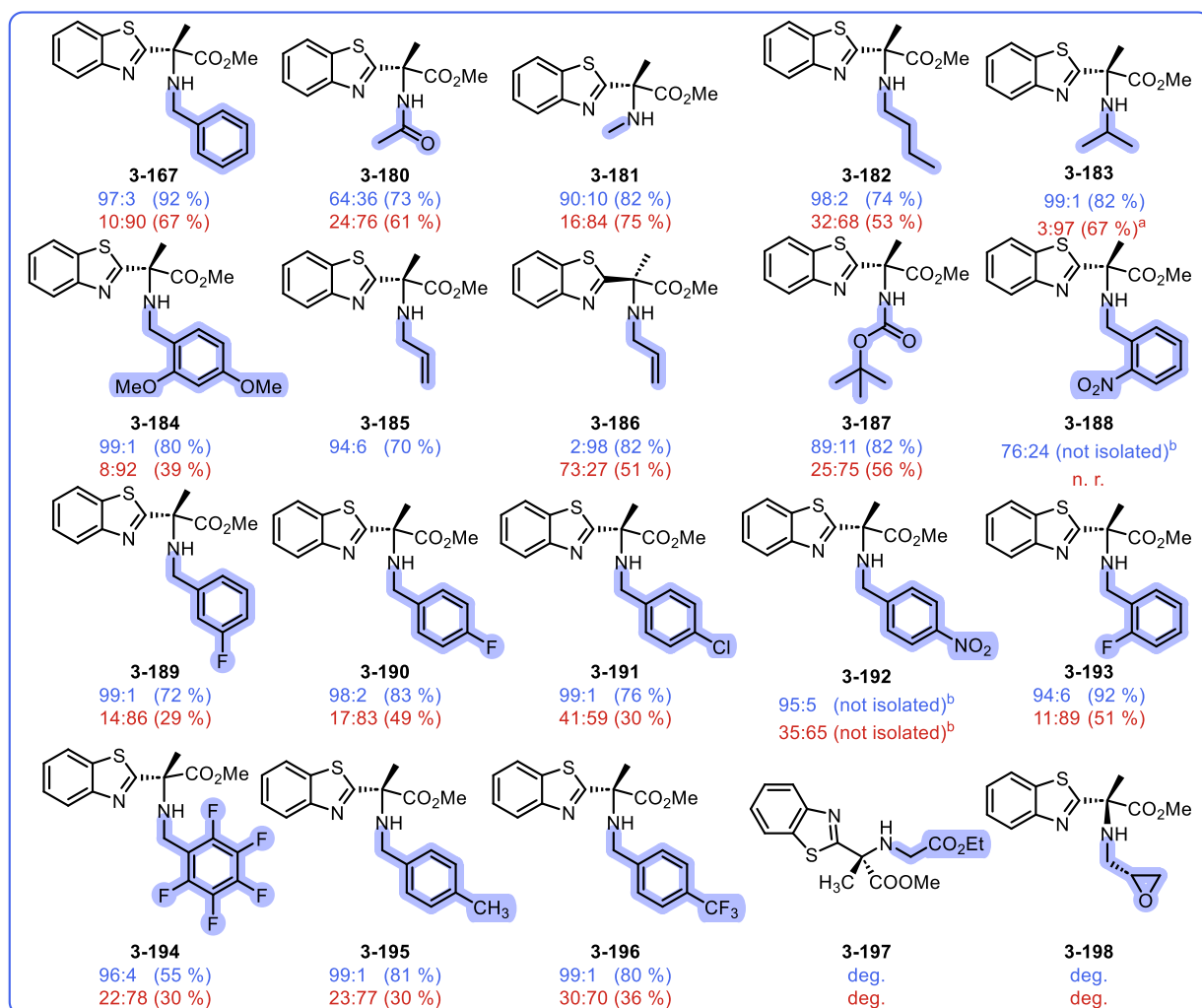


Figure 53: The scope and limitations of nitrogen substitution. Yields refer to pure isolated compounds. ^aPartial conversion, yield calculated on the recuperated starting material; n.r. = no reaction; deg. = degradation of starting material ^bnot purified, NMR conversion and HPLC were measured on crude reaction mixture.

Next, the diversity of the heterocycles was investigated. We have successfully incorporated pyrimidine **3-199** and **3-207**, oxazole **3-200**, thiazol **3-201**, pyridine **3-203**, benzimidazol **3-204**, imidazole **3-205**, as well as chlorinated BT sulfonamide **3-208** into the rearranged HAAs (**Figure 54**). Substituted BT heterocycles in different positions were not prepared due to the intermediate instability and therefore could not be tested under the reaction conditions. One of our goals was also the incorporation of the purine heterocycle, which we have successfully formed as a C6 rearranged product with alanine **3-206**, but due to the problematic separation of the peaks in the chiral HPLC, we were unable to determine the optical purity of the product.

Chapter III: Results and discussion

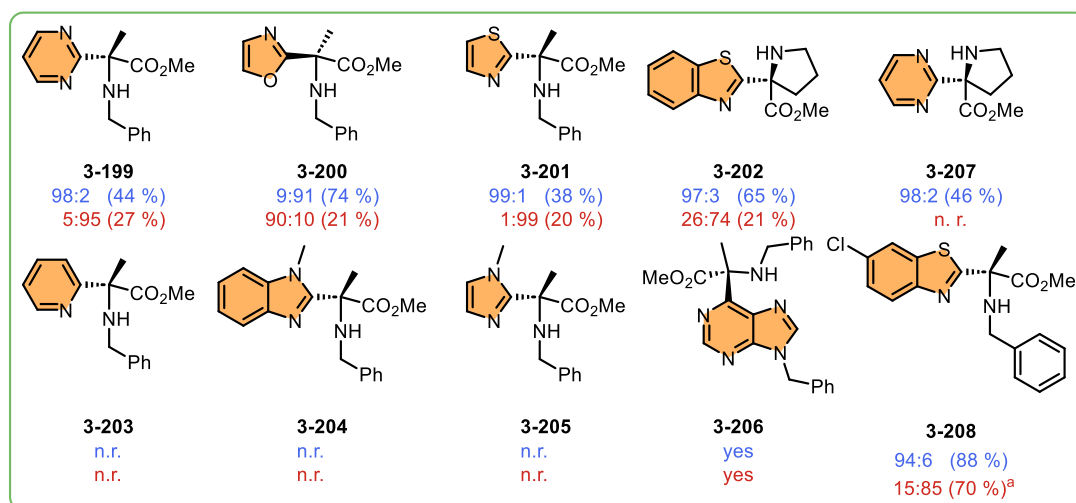


Figure 54: Heterocyclic scope and limitations. ^aPartial conversion, yield calculated on the recuperated starting material; n.r. = no reaction; deg. = degradation of starting material; ^bnot purified, NMR conversion and HPLC were measured on crude reaction mixture.

We have also screened various ester groups as well as amides. In all cases, the products were obtained with good to excellent yields and enantioselectivity (**Figure 55**).

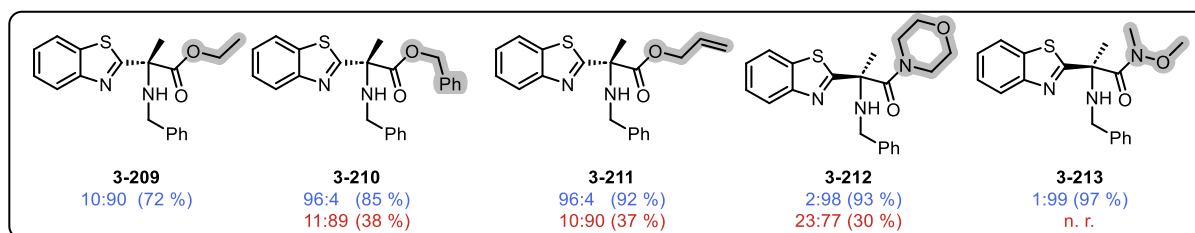


Figure 55: Scope and limitations of the ester and amide parts. Yields refer to pure isolated compounds.

A high degree of flexibility was found in the incorporation of different amino acids (**Figure 56**). This included methyl esters of alanine as our model substrate **3-167** and **3-184**, as well as valine **3-218** and **3-215**, leucine **3-214** and **3-217**, proline **3-224**, **3-202** and **3-207**, glutamic acid **3-178** and **3-219**, tryptophan **3-221**, phenylalanine **3-216** and benzyl-protected tyrosine **3-222**. Glycine **3-220** produced the product as racemate in both cases. The isoleucine substrate **3-209** was obtained only under modified conditions using LiHMDS with the addition of 6.0 equiv. of HMPA, resulting in the formation of the racemic product. Incorporation of methoxy groups **3-208** into the substrate did not help in this case.

It was observed that in case of more complex AA-based sulfonamide substrates, only the conditions for **retention** of the configuration (**Method B/C**) allowed the preparation of the desired HAA in good yield and stereoselectivity. In such cases, **Method A**, which is supposed to yield the product with inversion of the configuration, produced only an unchanged starting material (no racemization was observed) suggesting that the reaction conditions do not allow for the acidic proton removal.

Chapter III: Results and discussion

However, in most cases, the products were obtained with good yields and excellent enantioselectivities. In some cases, partial and/or low conversion was observed. Other amino acid-containing starting materials, such as methionine, cysteine, lysine, and arginine, were problematic to prepare and therefore were not tested.

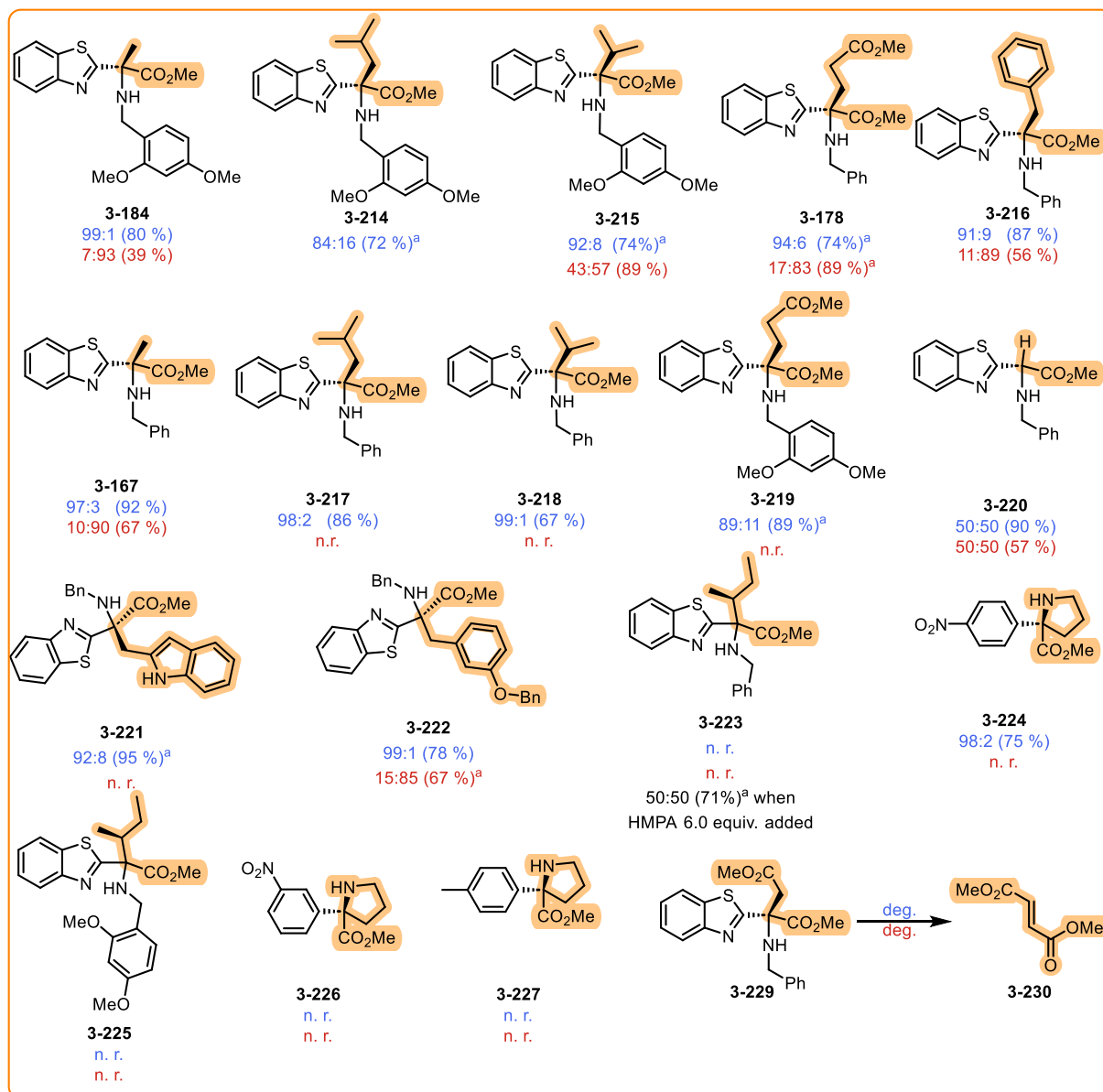


Figure 56: Amino ester part – scope and limitations. ^aPartial conversion, yield calculated on the recuperated starting material; n.r. = no reaction; deg. = degradation of starting material; Yields refer to pure isolated compounds.

Asparagic acid containing substrate **3-212** was degraded to dimethylformate **3-213** most probably due to competitive deprotonation of protons in β position

3.9. Conclusion

In this chapter, we successfully found conditions for our previously developed method for the heteroaryl sulfonamide synthesis, that broadened the scope of the method to additional heterocycles. This expansion included nitrogen-containing heterocycles such as pyridines, pyrimidines, imidazoles, benzo[*d*]imidazoles, and purine-2,6-diones, as well as oxygen-containing benzo[*d*]oxazoles and oxazoles, and sulfur-containing benzo[*d*]thiazoles and thiazoles. Our results showed that such heteroaryl sulfonamides are prone to nucleophilic attack at the α -carbon, making them suitable candidates for Smiles rearrangement.

The advantage of observed reactivity was used to develop a novel methodology for the asymmetric synthesis of quaternary α -heteroaryl α -substituted α -amino acids. Our mechanistic investigations, supported by detailed computational studies (DFT calculations), indicated that the selectivity of the rearrangement products is influenced by the concept of Memory of chirality. This allowed us to achieve selective synthesis of products with either inversion or retention of stereochemistry from a single starting material.

In conclusion, we have developed a robust and selective protocol for the synthesis of α -heteroaryl α -substituted α -AAs, which can be used further in the design of novel organocatalysts and/or the preparation of Xeno nucleic acids. This methodology provides significant advances in the field of asymmetric synthesis, offering new opportunities for the development of complex structures.

3.10. Experimental section

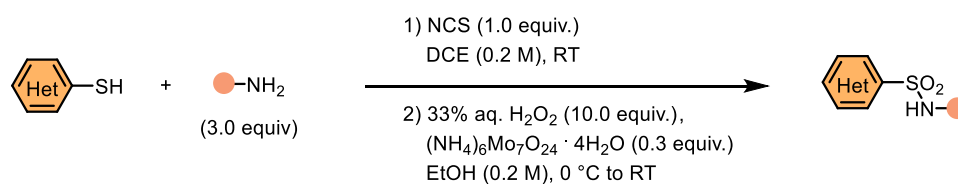
All starting materials were purchased from commercial suppliers and used without further purification, unless otherwise stated. All reactions were performed in round-bottom flasks fitted with rubber septa using standard laboratory techniques under positive pressure of argon (Air Liquide, >99.5% purity). Anhydrous Tetrahydrofuran (THF), dichloromethane (DCM) and 1,2-dichloroethane (DCE) were purchased from Sigma-Aldrich. **Caution! HMPA and DCE are toxic. CARE SHOULD BE TAKEN!** Purification of reaction products was carried out by column chromatography using standard grade silica gel (60 Å, 230–400 mesh), or by preparative thin layer chromatography glass plates precoated with silica gel (silica gel G-200 F₂₅₄, particle size 0.040–0.063 mm). Analytical thin-layer chromatography was performed on a thin-layer chromatography (TLC) aluminum plates pre-coated with silica gel (silica gel 60 F₂₅₄). Visualization was accomplished with UV light, phosphomolybdic acid, and potassium permanganate stains, followed by heating. Reactions run at temperatures of -78 °C (N₂/acetone) or -95 °C (N₂/methanol) were carried out using a cooling bath, and indicated temperatures refers to the cooling bath temperature. The determination of melting points was done on a Büchi melting point apparatus. The ¹H NMR and ¹³C{¹H} NMR spectra were measured on JEOL ECA400II (400 and 101 MHz) or JEOL 500 ECA (500 and 126 MHz) in Chloroform-d or CD₃OD. Chemical shifts are reported in ppm, and their calibration was carried out (a) in the case of ¹H NMR experiments on the residual peak of non-deuterated solvent δ (CDCl₃) = 7.26 ppm or δ (CD₃OD) = 3.31 ppm, δ (DMSO-*d*₆) = 2.50 ppm, δ (acetone-*d*₆) = 2.05 ppm and in the case of ¹³C NMR experiments on the middle peak of the ¹³C signal in deuterated solvent δ (CDCl₃) = 77.16 ppm, δ (CD₃OD) = 49.00 ppm, (DMSO-*d*₆) = 39.52 ppm, (acetone-*d*₆) = 29.84 ppm. The proton coupling patterns are represented as a singlet (s), a doublet (d), a doublet of a doublet (dd), a triplet (t), a triplet of a triplet (tt), and a multiplet (m). High-resolution mass spectrometry (HRMS) on Agilent 6230 high-resolution mass spectrometer with electrospray ionization (ESI) and a time-of-flight analyzer operating in a positive or negative full scan mode in the range of 100 – 1700 m/z. High-performance liquid chromatography (HPLC) was performed using an Agilent 1290 Infinity II system with UV-VIS detector and an Agilent InfinityLab LC/MSD mass detector. Purification using semiprep HPLC was carried out on Agilent 1290 Infinity II with UV-VIS and mass detector Agilent InfinityLab LC/MSD using the C18 reverse-phase column (Agilent 5Prep-C18 10x21.2 mm). The gradient

Chapter III: Experimental section

was formed from 15 mM aqueous ammonium acetate (buffer) and methanol with a flow rate of 20 mL/min. Chiral analysis was performed on Waters Alliance 2695 with autosampler and UV-VIS detector Waters 2996 PDA using chiral columns (CHIRAL ART Amylose-SA 250x4,6 mm, 5 μ m; CHIRALCEL Cellulose OD-H, 250x4,6 mm, 5 μ m; CHIRALCEL Cellulose OZ-H, 250x4,6 mm, 5 μ m). All solvents used were HPLC-grade solvents purchased from Merck. The column employed and the respective solvent mixture are indicated for each experiment. Specific rotations ($[\alpha]_D^T$) were measured with Perkin Elmer Polarimeter 241 Automatic (Massachusetts, USA) at the indicated temperature. Measurements were performed in a 1 mL cell (50 mm length) with concentrations (g/(100 mL)) reported in corresponding solvent. All microwave irradiation experiments were carried out in a dedicated CEM-*discover* mono-mode microwave apparatus. The reactor was used in the standard configuration as delivered, including proprietary software. The reactions were carried out in 10- or 35-mL glass vials that were sealed with silicone/PTFE caps, which can be exposed to a maximum of 250 °C and 20 bar internal pressure. The temperature was measured with an IR sensor on the outer surface of the process vial. After the irradiation period, the reaction vessels were cooled to ambient temperature by gas jet cooling.

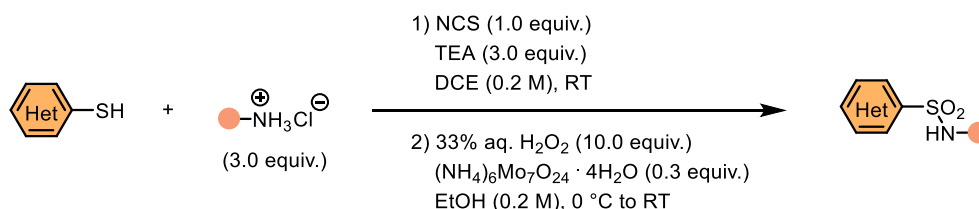
Chapter III: Experimental section

Method A



Heterocyclic thiol (1 mmol, 1.0 equiv.) and amine (3 mmol, 3.0 equiv.) were suspended in DCE (0.2 M) at RT and the resulting mixture was stirred at RT for 10 min. NCS (1 mmol, 1.0 equiv.) was added portion wise over a period of 5 min, and the whole mixture was stirred for additional 2 h at RT. The whole slurry was filtered, filter cake was washed with DCM, and the combined filtrates were evaporated *in vacuo*. Residue was dissolved in EtOH (0.2 M), cooled to 0 °C and a premixed cold (0 °C) bright yellow solution of 33% aq. H₂O₂ (10 mmol, 10.0 equiv.) and (NH₄)₆Mo₇O₂₄·4H₂O (0.3 mmol, 0.3 equiv.) was added with help of pipette Pasteur (*CAUTION: the use of metallic needle must be avoided!*). The resulting mixture was stirred at 0 °C for 0.5 h before it was allowed to warm to RT (cooling bath removed) and stirred for additional 8 h at RT. The whole mixture was cooled to 0 °C (ice/water) and sat. aq. Na₂SO₃ was added. The whole mixture was stirred at 0 °C for 10 min (*presence of peroxide was checked by iodide paper and if necessary additional of Na₂SO₃ was added*) before it was filtered. Filter cake was washed with EtOH, and the combined filtrates were concentrated under reduced pressure. The residue was diluted by water and the whole mixture was extracted with DCM. Combined organic layers were washed with H₂O, brine, dried over Na₂SO₄, and the volatiles were removed under reduced pressure. The crude product was washed with hexane and purified by recrystallization or by column chromatography.

Method B

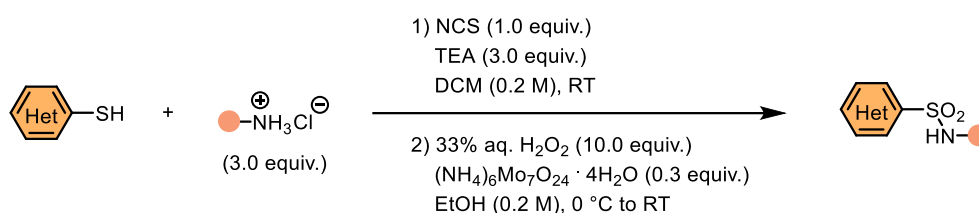


Heterocyclic thiol (1 mmol, 1.0 equiv.), TEA (3.0 mmol, 3.0 equiv.) and amine hydrochloride (3 mmol, 3.0 equiv.) were suspended in DCE (0.2 M) at RT and the resulting mixture was stirred at RT for 10 min. NCS (1 mmol, 1.0 equiv.) was added portion wise over a period of 5 min, and the whole mixture was stirred for additional 2 h at RT. The whole slurry was filtered, filter cake was washed with DCM, and the combined filtrates were evaporated *in vacuo*. Residue was dissolved in EtOH (0.2 M), cooled to 0 °C and a premixed cold (0 °C) bright yellow solution of

Chapter III: Experimental section

33% aq. H_2O_2 (10 mmol, 10 equiv.) and $(\text{NH}_4)_6\text{Mo}_7\text{O}_{24}\cdot 4\text{H}_2\text{O}$ (0.3 mmol, 0.3 equiv.) was added with help of pipette Pasteur (*CAUTION: the use of metallic needle must be avoided!*). The resulting mixture was stirred at 0 °C for 0.5 h before it was allowed to warm to RT (cooling bath removed) and stirred for additional 8 h at RT. The whole mixture was cooled to 0 °C (ice/water) and sat. aq. Na_2SO_3 was added. The whole mixture was stirred at 0 °C for 10 min (*presence of peroxide was checked by iodide paper and if necessary additional of Na_2SO_3 was added*) before it was filtered. Filter cake was washed with EtOH, and the combined filtrates were concentrated under reduced pressure. The residue was diluted by water and the whole mixture was extracted with DCM. Combined organic layers were washed with H_2O , brine, dried over Na_2SO_4 , and the volatiles were removed under reduced pressure. The crude product was washed with hexane and purified by recrystallization or by column chromatography.

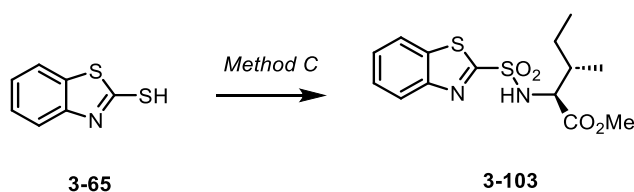
Method C



Heterocyclic thiol (1 mmol, 1.0 equiv.), TEA (3.0 mmol, 3.0 equiv.) and amine hydrochloride (3 mmol, 3.0 equiv.) were suspended in DCM (0.2 M) at RT and the resulting mixture was stirred at RT for 10 min. NCS (1 mmol, 1.0 equiv.) was added portion wise over a period of 5 min, and the whole mixture was stirred until TLC indicated consumption of starting material. The whole slurry was filtered, filter cake was washed with DCM, and the combined filtrates were evaporated *in vacuo*. Residue was dissolved in EtOH (0.2 M), cooled to 0 °C and a premixed cold (0 °C) bright yellow solution of 33% aq. H_2O_2 (10 mmol, 10 equiv.) and $(\text{NH}_4)_6\text{Mo}_7\text{O}_{24}\cdot 4\text{H}_2\text{O}$ (0.3 mmol, 0.3 equiv.) was added with help of pipette Pasteur (*CAUTION: the use of metallic needle must be avoided!*). The resulting mixture was stirred at 0 °C for 0.5 h before it was allowed to warm to RT (cooling bath removed) and stirred until TLC indicated consumption of starting material. Mixture was diluted with H_2O and DCM following extraction. Combined organic layers were washed brine, dried over Na_2SO_4 , and the volatiles were removed under reduced pressure. The crude product was washed with hexane and purified by recrystallization or by column chromatography.

Chapter III: Experimental section

methyl (benzo[*d*]thiazol-2-ylsulfonyl)-L-isoleucinate (**3-103**)



Method C: Starting from 2-mercaptobenzothiazol **3-65** (1 g, 5.9 mmol, 1.0 equiv.) and L-isoleucine methylester hydrochloride (3.23 g, 17.8 mmol, 3.0 equiv.). The crude sulfenamide had to be purified prior the oxidation step, otherwise the decomposition occurred (column chromatography SiO₂; petroleum ether/EtOAc = 10:1 – 5:1). The crude sulfonamide **3-103** was purified by column chromatography (SiO₂; petroleum ether/EtOAc = 4:1) to afford pure **3-103** (1.88 g, 98 %, *d.r.* ≥ 99:1).

¹H NMR (500 MHz, Chloroform-*d*) δ (ppm): 8.12 (dd, *J* = 8.2, 1.7 Hz, 1H), 7.97 (dd, *J* = 7.7, 1.9 Hz, 1H), 7.60 (ddd, *J* = 8.3, 7.2, 1.4 Hz, 1H), 7.55 (ddd, *J* = 8.4, 7.2, 1.3 Hz, 1H), 5.68 (d, *J* = 9.7 Hz, 1H), 4.32 (dd, *J* = 9.7, 4.9 Hz, 1H), 3.49 (s, 3H), 1.92 (dq, *J* = 9.2, 6.8, 4.7 Hz, 1H), 1.42 (dtd, *J* = 14.8, 7.4, 4.4 Hz, 1H), 1.19 (ddq, *J* = 14.4, 9.2, 7.4 Hz, 1H), 0.99 (d, *J* = 6.9 Hz, 3H), 0.91 (t, *J* = 7.4 Hz, 3H).

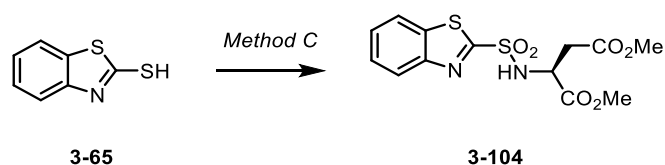
¹³C {¹H} NMR (126 MHz, Chloroform-*d*) δ (ppm): 171.6, 165.7, 152.4, 136.4, 127.8, 127.6, 125.1, 122.4, 61.5, 52.6, 38.6, 24.7, 15.6, 11.5.

MS (ESI) *m/z* (%): 343 [M+H]⁺ (100).

HRMS (ESI) *m/z*: [M+H]⁺ calculated for C₁₄H₁₉N₂O₄S₂: 343.0786; found: 343.0782.

R_f = 0.60 (hexane/ EtOAc = 3:1)

[α]_D²⁵ = +36.5° (*c* 1.0, CHCl₃)

dimethyl (benzo[*d*]thiazol-2-ylsulfonyl)-L-aspartate (**3-104**)

Method C: Starting from 2-mercaptobenzothiazol **3-65** (1.0 g, 6.0 mmol, 1.0 equiv.) and L-aspartic acid dimethylester hydrochloride (3.58 g, 17.9 mmol, 3.0 equiv.). The crude product was purified by crystallization from 40% ethanol to afford **3-104** as white crystal (1.52 g, 71 % yield, *e.r.* = \geq 99:1).

^1H NMR (500 MHz, Chloroform-*d*) δ (ppm): 8.15 (dd, $J = 8.0, 1.4$ Hz, 1H), 7.98 (dd, $J = 8.0, 1.5$ Hz, 1H), 7.59 (dtd, $J = 21.7, 7.3, 1.4$ Hz, 2H), 6.19 (d, $J = 8.4$ Hz, 1H), 4.67 (dt, $J = 8.5, 4.3$ Hz, 1H), 3.67 (s, 3H), 3.55 (s, 3H), 3.15 – 3.01 (m, 2H).

^{13}C { ^1H } NMR (126 MHz, Chloroform-*d*) δ (ppm): 171.0, 170.0, 165.7, 152.4, 136.5, 127.9, 127.6, 125.2, 122.4, 53.3, 53.0, 52.4, 37.6.

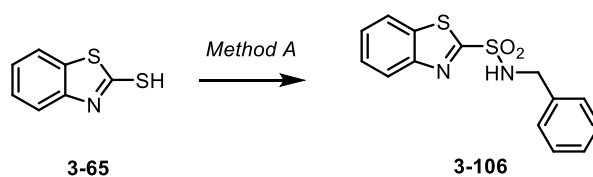
MS (ESI) m/z (%): 358 [M+H]⁺ (100).

HRMS (ESI) m/z : [M+H]⁺ calculated for C₁₃H₁₅N₂O₆S₂: 359.0366; found: 359.0359.

R_f = 0.30 (hexane/ EtOAc = 2:1)

$[\alpha]_D^{23}$ = +38.0° (*c* 1.0, CHCl₃)

m. p. = 100-102 °C

N-benzylbenzo[*d*]thiazole-2-sulfonamide (**3-106**)

Method A: Starting from 2-mercaptobenzothiazol **3-65** (1.45 g, 8.7 mmol, 1.0 equiv.) and benzylamine (2.85 g, 26.1 mmol, 3.0 equiv.). The crude product was purified by column chromatography (SiO₂; petroleum ether/EtOAc = 8:1) to afford **3-106** as yellow solid (2.48 g, 92 % yield).

^1H NMR (400 MHz, Chloroform-*d*) δ (ppm): 8.17 – 8.14 (m, 1H), 7.99 – 7.95 (m, 1H), 7.66 – 7.57 (m, 1H), 7.59 – 7.54 (m, 1H), 7.31 – 7.26 (m, 4H), 7.26 – 7.22 (m, 1H), 5.46 (t, $J = 5.4$ Hz, 1H), 4.44 (d, $J = 6.1$ Hz, 2H).

Chapter III: Experimental section

^{13}C { ^1H } NMR (126 MHz, Chloroform-*d*) δ (ppm): 166.0, 152.4, 136.5, 135.7, 128.9, 128.3, 128.2, 127.8, 127.6, 125.2, 122.3, 48.2.

MS (ESI) m/z (%): 305 [M+H]⁺ (100).

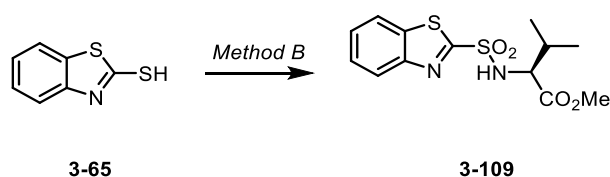
HRMS (ESI) m/z : [M+H]⁺ calculated for C₁₄H₁₃N₂O₂S₂: 305.0413; found: 305.0412.

R_f = 0.50 (hexane/ EtOAc = 3:1)

$[\alpha]_{\text{D}}^{23}$ = +38.1° (c 1.0, CHCl₃)

m. p. = 108-112 °C

methyl (benzo[*d*]thiazol-2-ylsulfonyl)-L-valinate (**3-109**)



Method B: Starting from 2-mercaptobenzothiazole **3-65** (1.0 g, 6.0 mmol, 1.0 equiv.) and L-valine methylester hydrochloride (3.0 g, 17.9 mmol, 3.0 equiv.). The crude product was purified by crystallization from 40% ethanol to afford **3-109** as white crystal (1.45 g, 74 % yield, *e.r.* = ≥ 99:1).

^1H NMR (500 MHz, Chloroform-*d*) δ (ppm): 8.11 (dd, *J* = 8.1, 1.6 Hz, 1H), 7.97 (dd, *J* = 7.4, 1.2 Hz, 1H), 7.63 – 7.52 (m, 2H), 5.89 – 5.60 (m, 1H), 4.28 (dd, *J* = 9.9, 4.6 Hz, 1H), 3.50 (s, 3H), 2.17 (pd, *J* = 6.8, 4.7 Hz, 1H), 1.04 (d, *J* = 6.8 Hz, 3H), 0.90 (d, *J* = 6.9 Hz, 3H).

^{13}C { ^1H } NMR (126 MHz, Chloroform-*d*) δ (ppm): 171.6, 165.7, 152.4, 136.4, 127.8, 127.6, 125.1, 122.4, 62.1, 52.7, 31.7, 19.1, 17.3.

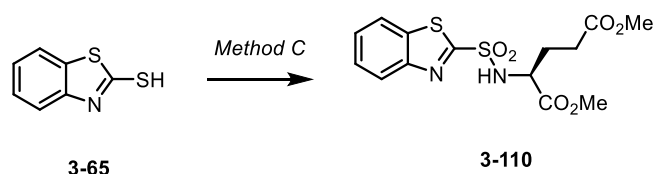
MS (ESI) m/z (%): 329 [M+H]⁺ (100).

HRMS (ESI) m/z : [M+H]⁺ calculated for C₁₃H₁₇N₂O₄S₂: 329.0624; found: 329.0629.

R_f = 0.50 (hexane/ EtOAc = 3:1)

$[\alpha]_{\text{D}}^{24}$ = +52.8° (c 1.0, CHCl₃)

m. p. = 106-107 °C

dimethyl (benzo[*d*]thiazol-2-ylsulfonyl)-L-glutamate (**3-110**)

Method C: Starting from 2-mercaptobenzothiazol **3-65** (1.0 g, 6.0 mmol, 1.0 equiv.) and L-glutamic acid dimethylester hydrochloride (3.84 g, 17.9 mmol, 3.0 equiv.). The crude product was purified by crystallization from 40% ethanol to afford **3-110** as white crystal (1.61 g, 72 % yield, *e.r.* = \geq 99:1).

^1H NMR (500 MHz, Chloroform-*d*) δ (ppm): 8.11 (ddd, J = 8.2, 1.4, 0.7 Hz, 1H), 7.97 (ddd, J = 7.9, 1.4, 0.7 Hz, 1H), 7.62 – 7.54 (m, 2H), 5.83 (d, J = 8.8 Hz, 1H), 4.50 (td, J = 8.7, 4.6 Hz, 1H), 3.66 (s, 3H), 3.59 (s, 3H), 2.61 – 2.48 (m, 2H), 2.31 – 2.22 (m, 1H), 2.01 (dddd, J = 14.2, 8.8, 7.7, 6.4 Hz, 1H).

^{13}C { ^1H } NMR (126 MHz, Chloroform-*d*) δ (ppm): 173.1, 171.5, 165.6, 152.3, 136.4, 127.9, 127.6, 125.1, 122.4, 56.2, 53.1, 52.0, 29.7, 28.3.

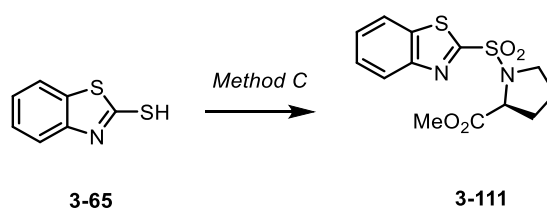
MS (ESI) m/z (%): 373 [$\text{M}+\text{H}$] $^+$ (100).

HRMS (ESI) m/z : [$\text{M}+\text{H}$] $^+$ calculated for $\text{C}_{14}\text{H}_{17}\text{N}_2\text{O}_6\text{S}_2$: 373.0523; found: 373.0531.

R_f = 0.50 (hexane/ EtOAc = 1:1)

$[\alpha]_D^{23}$ = +38.1 $^\circ$ (*c* 1.0, CHCl_3)

m. p. = 106-108 $^\circ\text{C}$

methyl (benzo[*d*]thiazol-2-ylsulfonyl)-L-prolinate (**3-111**)

Method C: Starting from 2-mercaptobenzothiazol **3-65** (1.0 g, 5.8 mmol, 1.0 equiv.), 3.5 equiv. of TEA and L-proline methylester hydrochloride (2.2 g, 17.4 mmol, 3.0 equiv.). The crude product was purified by column chromatography (SiO_2 ; petroleum ether/EtOAc = 3:2) to afford **3-111** as a slightly yellowish crystals (1.27 g, 65 % yield, *e.r.* = \geq 99:1).

^1H NMR (500 MHz, Chloroform-*d*) δ (ppm): 8.18 (d, J = 8.2 Hz, 1H), 7.99 (d, J = 7.9 Hz, 1H), 7.65 – 7.59 (m, 1H), 7.57 (td, J = 7.7, 7.3, 1.2 Hz, 1H), 4.71 (dd, J = 8.6, 3.5 Hz, 1H), 3.85 – 3.77

Chapter III: Experimental section

(m, 1H), 3.74 (s, 3H), 3.64 (dt, $J = 9.8, 7.4$ Hz, 1H), 2.26 – 2.14 (m, 1H), 2.14 – 1.99 (m, 2H), 1.97 – 1.85 (m, 1H).

^{13}C { ^1H } NMR (126 MHz, Chloroform-*d*) δ (ppm): 172.0, 164.5, 152.6, 136.3, 127.7, 127.5, 125.3, 122.2, 61.4, 52.7, 49.5, 31.1, 24.8.

MS (ESI) m/z (%): 327 [M+H]⁺ (100).

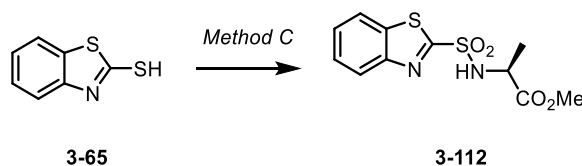
HRMS (ESI) m/z : [M+H]⁺ calculated for C₁₃H₁₅N₂O₄S₂: 327.0468; found 327.0467.

R_f = 0.30 (hexane/ EtOAc = 2:1)

$[\alpha]_{\text{D}}^{24} = -214.8^\circ$ (c 1.01, CHCl₃)

m. p. = 74-75 °C

methyl (benzo[*d*]thiazol-2-ylsulfonyl)-L-alaninate (**3-112**)



Method C: Starting from 2-mercaptobenzothiazol **3-65** (1.45 g, 8.7 mmol, 1.0 equiv.) and L-alanine methylester hydrochloride (3.65 g, 26.1 mmol, 3.0 equiv.). The crude product was purified by column chromatography (SiO₂; petroleum ether/EtOAc = 3:1) to afford **3-112** as orange solid (2.01g, 77 % yield, *e.r.* = $\geq 99:1$).

^1H NMR (500 MHz, Chloroform-*d*) δ (ppm): 8.14 (dt, $J = 7.5, 1.6$ Hz, 1H), 7.97 (dt, $J = 8.7, 1.3$ Hz, 1H), 7.63 – 7.58 (m, 1H), 7.58 – 7.54 (m, 1H), 5.87 (d, $J = 7.8$ Hz, 1H), 4.52 – 4.43 (m, 1H), 3.60 (s, 3H), 1.51 (d, $J = 7.1$ Hz, 3H).

^{13}C { ^1H } NMR (126 MHz, Chloroform-*d*) δ (ppm): 172.4, 165.9, 152.4, 136.4, 127.9, 127.7, 127.6, 125.2, 122.4, 53.0, 52.6, 20.1.

MS (ESI) m/z (%): 301 [M+H]⁺ (100).

HRMS (ESI) m/z : [M+K]⁺ calculated for C₁₁H₁₂KN₂O₄S₂: 338.9876; found: 338.9873.

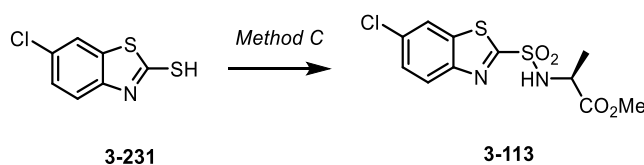
R_f = 0.40 (hexane/EtOAc = 3:1)

$[\alpha]_{\text{D}}^{21} = +15.9^\circ$ (c 0.45, CHCl₃)

m. p. = 116-118 °C

Chapter III: Experimental section

methyl ((6-chlorobenzo[*d*]thiazol-2-yl)sulfonyl)-L-alaninate (**3-113**)



Method C: Starting from 5-chloro-2-mercaptobenzothiazol **3-231** (0.33 g, 2.4 mmol, 1.0 equiv.) and L-alanine methylester hydrochloride (1.01 g, 7.3 mmol, 3.0 equiv.). The crude sulfenamide had to be purified prior the oxidation step, otherwise the decomposition occurred (column chromatography SiO₂; petroleum ether/EtOAc = 10:1 – 5:1). The crude sulfonamide **3-113** was purified by column chromatography (SiO₂; petroleum ether/EtOAc = 4:1) to afford pure **3-113** (0.44 g, 84 %, *e.r.* = ≥ 99:1).

¹H NMR (500 MHz, Chloroform-*d*) δ (ppm): 8.12 (d, *J* = 2.0 Hz, 1H), 7.90 (d, *J* = 8.7 Hz, 1H), 7.54 (dd, *J* = 8.6, 2.0 Hz, 1H), 5.86 (d, *J* = 8.1 Hz, 1H), 4.51 – 4.45 (m, 1H), 3.64 (s, 3H), 1.52 (d, *J* = 7.4 Hz, 3H).

¹³C {¹H} NMR (126 MHz, Chloroform-*d*) δ (ppm): 172.4, 167.8, 153.1, 134.6, 133.9, 128.6, 124.8, 123.2, 53.1, 52.6, 20.1.

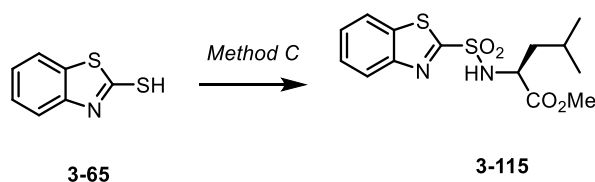
MS (ESI) *m/z* (%): 334 [M+H]⁺ (100).

HRMS (ESI) *m/z*: [M+H]⁺ calculated for C₁₁H₁₂ClN₂O₄S₂: 334.9922; found: 334.9929.

R_f = 0.50 (hexane/ EtOAc = 3:1)

[α]_D²⁵ = -36.8° (*c* 1.0, CHCl₃)

methyl (benzo[*d*]thiazol-2-ylsulfonyl)-L-leucinate (**3-115**)



Method C: Starting from 2-mercaptobenzothiazol **3-65** (1.0 g, 6.0 mmol, 1.0 equiv.) and L-Leucine methylester hydrochloride (3.2 g, 17.9 mmol, 3.0 equiv.). The crude product was purified by crystallization from 40% ethanol to afford **3-105** as white crystal (1.49 g, 73 % yield, *e.r.* = ≥ 99:1).

¹H NMR (500 MHz, Chloroform-*d*) δ (ppm): 8.17 – 8.09 (m, 1H), 8.01 – 7.93 (m, 1H), 7.62 – 7.54 (m, 2H), 5.50 (d, *J* = 10.6 Hz, 1H), 4.44 (td, *J* = 9.4, 5.5 Hz, 1H), 3.50 (s, 3H), 1.88 (dh, *J* = 8.3, 6.5 Hz, 1H), 1.63 – 1.55 (m, 2H), 0.97 (d, *J* = 6.6 Hz, 3H), 0.94 (d, *J* = 6.7 Hz, 3H).

Chapter III: Experimental section

^{13}C { ^1H } NMR (126 MHz, Chloroform-*d*) δ (ppm): 172.6, 165.7, 152.4, 136.5, 127.8, 127.6, 125.1, 122.4, 55.6, 52.8, 42.5, 24.5, 22.9, 21.5.

MS (ESI) m/z (%): 343 [M+H]⁺ (100).

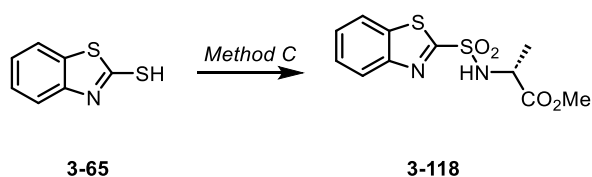
HRMS (ESI) m/z : [M+H]⁺ calculated for C₁₄H₁₉N₂O₄S₂: 343.0781; found: 343.0773.

R_f = 0.40 (hexane/ EtOAc = 3:1)

$[\alpha]_{\text{D}}^{22}$ = +27.8° (c 1.0, CHCl₃)

m. p. = 110-112 °C

methyl (benzo[*d*]thiazol-2-ylsulfonyl)-D-alaninate (**3-118**)



Method C: Starting from 2-mercaptobenzothiazol **3-65** (1.36 g, 7.9 mmol, 1.0 equiv.) and D-alanine methylester hydrochloride (3.33 g, 23.6 mmol, 3.0 equiv.). The crude product was purified by gradient column chromatography (SiO₂; petroleum ether/EtOAc = 6:1 → 4:1) to afford **3-118** as orange solid (2.01 g, 84 % yield, *e.r.* = ≥ 1:99).

^1H NMR (500 MHz, Chloroform-*d*) δ (ppm): 8.16 – 8.12 (m, 1H), 8.02 – 7.93 (m, 1H), 7.63 – 7.58 (m, 1H), 7.58 – 7.54 (m, 1H), 5.78 (d, *J* = 7.7 Hz, 1H), 4.48 (p, *J* = 7.3 Hz, 1H), 3.61 (s, 3H), 1.52 (d, *J* = 7.1 Hz, 3H).

^{13}C { ^1H } NMR (126 MHz, Chloroform-*d*) δ (ppm): 172.4, 165.9, 152.4, 136.5, 127.9, 127.6, 125.2, 122.4, 53.0, 52.6, 20.1.

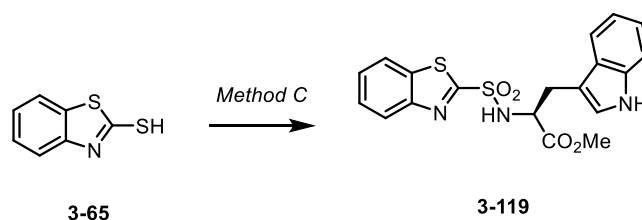
MS (ESI) m/z (%): 301 [M+H]⁺ (100).

HRMS (ESI) m/z : [M+H]⁺ calculated for C₁₁H₁₃N₂O₄S₂: 301.0317; found: 301.0319.

R_f = 0.40 (hexane/EtOAc = 3:1)

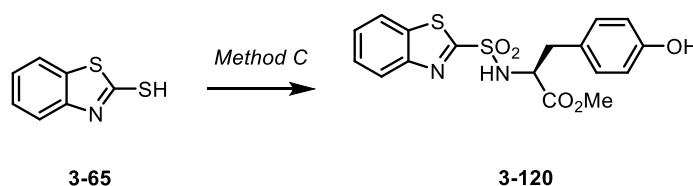
$[\alpha]_{\text{D}}^{20}$ = -17.0° (c 1.0, CHCl₃)

m. p. = 115-117 °C

methyl (benzo[*d*]thiazol-2-ylsulfonyl)-L-tryptophanate (**3-119**)

Method C: Starting from 2-mercaptobenzothiazol **3-65** (1.36 g, 8.1 mmol, 1.0 equiv.) and L-tryptophan methylester hydrochloride (6.3 g, 24.2 mmol, 3.0 equiv.). The crude sulfenamide had to be purified prior the oxidation step, otherwise the decomposition occurred (column chromatography SiO₂; petroleum ether/EtOAc = 10:1 – 5:1). **The solution was concentrated to ~ 0.1 M solution of sulfonamide 3-119 in DCM due to decomposition.** The product was used in the next step without further purification.

CAUTION! If concentrated to dryness the product decomposes!

methyl (benzo[*d*]thiazol-2-ylsulfonyl)-L-tyrosinate (**3-120**)

Method C: Starting from 2-mercaptobenzothiazol **3-65** (1.0 g, 5.8 mmol, 1.0 equiv.) and L-tyrosine methylester hydrochloride (4.03 g, 17.4 mmol, 3.0 equiv.). The crude sulfenamide had to be purified prior the oxidation step, otherwise the decomposition occurred (SiO₂; petroleum ether/EtOAc = 4:1). The crude sulfonamide **3-120** was purified by column chromatography (SiO₂; petroleum ether/EtOAc = 4:1) to afford pure **3-120** (0.95 g, 74 %).

¹H NMR (500 MHz, Chloroform-*d*) δ (ppm): 8.15 – 8.10 (m, 1H), 7.96 (d, *J* = 8.0 Hz, 1H), 7.60 (t, *J* = 7.6 Hz, 1H), 7.56 (t, *J* = 7.6 Hz, 1H), 6.99 – 6.93 (m, 2H), 6.68 – 6.61 (m, 2H), 5.53 (d, *J* = 8.5 Hz, 1H), 4.79 (s, 1H), 4.68 (dt, *J* = 8.4, 5.7 Hz, 1H), 3.55 (s, 3H), 3.09 (qd, *J* = 14.0, 5.6 Hz, 2H). ¹³C {¹H} NMR (126 MHz, Chloroform-*d*) δ (ppm): 171.0, 165.6, 155.0, 152.4, 136.5, 130.8, 127.8, 127.6, 126.7, 125.2, 122.4, 115.7, 57.7, 52.8, 38.7.

MS (ESI) *m/z* (%): 373 [M+H]⁺ (100).

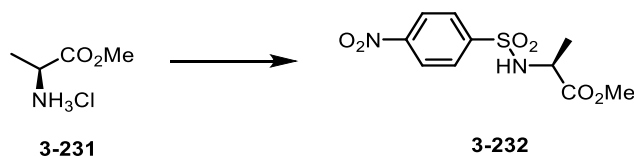
HRMS (ESI) *m/z*: [M+H]⁺ calculated for C₁₇H₁₆N₂O₅S₂: 393.0573; found: 393.0575.

R_f = 0.50 (hexane/ EtOAc = 4:1)

[α]_D²³ = +38.1° (*c* 1.0, CHCl₃) **m. p.** = 106-108 °C

Chapter III: Experimental section

methyl ((4-nitrophenyl)sulfonyl)-L-alaninate (**3-232**)

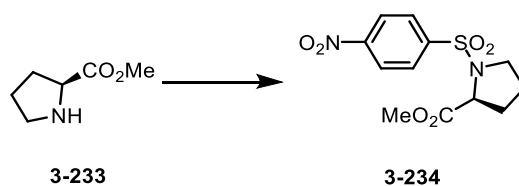


Prepared according to a literature. Spectroscopic data match those in the literature.²⁴⁵

To a solution L-alanine methyl ester hydrochloride **3-231** (1 g, 7.16 mmol, 1.0 equiv.) in DCM (10 mL, 0.5 M) was added TEA (3.0 mL, 21.5 mmol, 3.0 equiv.) followed by 4-nitrobenzenesulfonyl chloride (1.76 g, 7.9 mmol, 1.1 equiv.) at 0 °C and the mixture was stirred at room temperature for 16 hours. The mixture was diluted with DCM, washed with brine, dried over anhydrous Na₂SO₄, filtered, and concentrated to dryness. The crude product **3-232** was used in the next step without further purification (1.95g, 99 % yield, *e.r.* = ≥ 99:1).

¹H NMR (500 MHz, Chloroform-*d*) δ (ppm): 8.37 – 8.33 (m, 2H), 8.07 – 8.03 (m, 2H), 4.07 (q, *J* = 7.2 Hz, 1H), 3.59 (s, 3H), 2.96 (q, *J* = 7.2 Hz, 1H), 1.43 (d, *J* = 7.2 Hz, 3H).

methyl ((4-nitrophenyl)sulfonyl)-L-prolinate (**3-234**)



Prepared according to a literature. Spectroscopic data match those in the literature.²⁴⁶

To a solution of L-Proline methyl ester **3-233** (0.34 g, 2.0 mmol, 1.0 equiv.) in DCM (8 mL, 0.25 M) was added TEA (0.84 mL, 6.0 mmol, 3.0 equiv.) followed by 4-nitrobenzenesulfonyl chloride (0.49 g, 2.2 mmol, 1.1 equiv.) at 0 °C and the mixture was stirred at room temperature for 16 hours. Then, the mixture was quenched with water and the layers were separated. The aqueous layer was extracted using DCM (3 x 50 mL). Combined organic layers were washed with brine (100 mL), dried over MgSO₄, filtered and the solvents were concentrated under reduced pressure. The crude product was purified by column chromatography (SiO₂; petroleum ether/EtOAc = 4:1) to afford **3-234** as a colorless oil (0.45 g, 72 % yield, *e.r.* = ≥ 99:1).

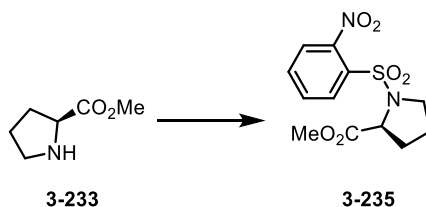
¹H NMR (500 MHz, Chloroform-*d*) δ (ppm): 8.39 – 8.36 (m, 2H), 8.10 – 8.07 (m, 2H), 4.47 (dd, *J* = 8.6, 3.8 Hz, 1H), 3.71 (s, 3H), 3.48 – 3.43 (m, 2H), 2.22 – 2.15 (m, 1H), 2.08 – 1.99 (m, 2H), 1.95 – 1.87 (m, 1H).

Chapter III: Experimental section

^{13}C { ^1H } NMR (126 MHz, Chloroform-*d*) δ (ppm): 172.3, 150.2, 144.8, 128.8, 124.3, 60.7, 52.7, 48.4, 31.1, 24.9.

$[\alpha]_{\text{D}}^{22}$ = -69.5° (*c* 1.0, CHCl_3)

methyl ((2-nitrophenyl)sulfonyl)-L-prolinate (**3-235**)



Prepared according to a literature. Spectroscopic data match those in the literature.²⁴⁶

To a solution of *L*-Proline methyl ester **3-233** (0.40 g, 2.42 mmol, 1.0 equiv.) in DCM (9.7 mL, 0.25 M) was added TEA (1.02 mL, 7.26 mmol, 3.0 equiv.) followed by 2-nitrobenzenesulfonyl chloride (0.66 g, 2.91 mmol, 1.2 equiv.) at 0 °C and the mixture was stirred at room temperature for 16 hours. Then, the mixture was quenched with water and the layers were separated. The aqueous layer was extracted using DCM (3 x 50 mL). Combined organic layers were washed with brine (100 mL), dried over MgSO_4 , filtered and the solvents were concentrated under reduced pressure. The crude product was purified by column chromatography (SiO_2 ; petroleum ether/EtOAc = 4:1) to afford **3-235** as a colorless oil (0.58 g, 77 % yield, *e.r.* = \geq 99:1).

^1H NMR (500 MHz, Chloroform-*d*) δ (ppm): 8.74 (q, J = 1.9 Hz, 1H), 8.44 (ddt, J = 8.3, 2.3, 1.1 Hz, 1H), 8.23 (ddt, J = 4.1, 2.8, 1.9, 1.1 Hz, 1H), 7.75 (t, J = 8.0 Hz, 1H), 4.51 (ddd, J = 8.9, 3.8, 2.0 Hz, 1H), 3.72 (s, 3H), 3.51 – 3.41 (m, 2H), 2.25 – 2.15 (m, 1H), 2.10 – 2.03 (m, 1H), 2.03 – 1.89 (m, 2H).

^{13}C { ^1H } NMR (126 MHz, Chloroform-*d*) δ (ppm): 172.3, 148.4, 141.4, 133.1, 130.4, 127.3, 122.8, 60.7, 52.7, 48.4, 31.1, 24.9.

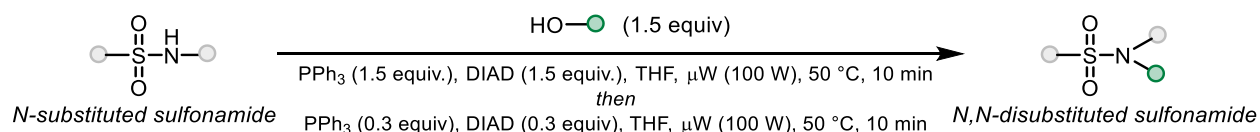
MS (ESI) m/z (%): 353 [$\text{M}+\text{H}$]⁺ (100).

HRMS (ESI) m/z : [$\text{M}+\text{K}$]⁺ calculated for $\text{C}_{12}\text{H}_{14}\text{N}_2\text{O}_6\text{SK}$: 353.0204; found: 353.0217.

R_f = 0.40 (PE/ EtOAc = 2:1)

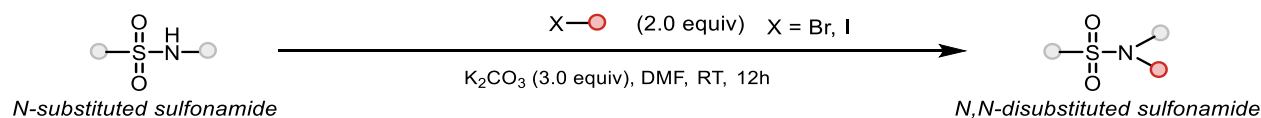
Chapter III: Experimental section

Method D: Fukuyama-Mitsunobu reaction protocol (FMR protocol)

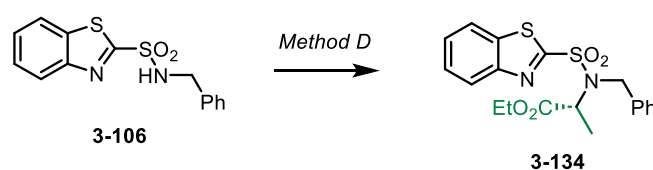


Sulfonamide (1.0 equiv.) and PPh_3 (1.5 equiv.) in dry THF (0.05 M) were placed to μW vial at RT, and alcohol (1.5 equiv.) followed by DIAD (1.5 equiv.) were added. The vial was closed with Teflon tap and the whole mixture was heated to 50 °C for 10 min in the microwave reactor (100 W). After cooling to RT, organic solvents were removed under reduced pressure and the conversion of the sulfonamide was analyzed with help of the ^1H NMR experiments. In case of incomplete conversion, the whole mixture was redissolved in dry THF (0.05 M), additional PPh_3 (0.3 equiv.) and DIAD (0.3 equiv.) were added and the whole procedure was repeated. In case of missing signals of the starting alcohol, an additional 0.3 equiv. of the corresponding alcohol was also added. When the starting sulfonamide was consumed, the crude product was purified by flash column chromatography on silica gel.

Method E: Alkylation protocol



Sulfonamide (1.0 equiv.) was dissolved in DMF (0.1 M) and K_2CO_3 (3.0 equiv.) was added. The resulting mixture was stirred at RT for 5 min, and alkyl bromide or alkyl iodide (2.0 equiv.) was added dropwise over a period of 5 min. The whole mixture was stirred at RT for 16 h, before it was diluted with H_2O . The whole mixture was extracted with EtOAc, and combined organic layers were washed with, dried over MgSO_4 , filtered, and the solvents were removed under reduced pressure.

ethyl *N*-(benzo[*d*]thiazol-2-ylsulfonyl)-*N*-benzyl-L-alaninate **3-134**

Prepared according to a literature. Spectroscopic data match those in the literature.¹⁸⁷

Method D: Starting from sulfonamide **3-106** (0.1 g, 0.33 mmol, 1.0 equiv.) and alcohol L(-)lactate (0.04 mL, 0.33 mmol, 1.0 equiv.). The crude product was purified by column chromatography (SiO₂; petroleum ether/EtOAc = 4:1) to afford **3-134** as a slightly yellow oil (0.13 g, 98 % yield, *e.r.* = ≥ 99:1).

¹H NMR (400 MHz, Chloroform-*d*) δ (ppm): 8.21 – 8.15 (m, 1H), 8.00 – 7.95 (m, 1H), 7.61 (ddd, *J* = 8.3, 7.2, 1.4 Hz, 1H), 7.56 (ddd, *J* = 8.5, 7.2, 1.4 Hz, 1H), 7.44 – 7.41 (m, 2H), 7.34 – 7.25 (m, 3H), 4.93 (d, *J* = 16.4 Hz, 1H), 4.86 (q, *J* = 7.3 Hz, 1H), 4.54 (d, *J* = 16.4 Hz, 1H), 3.86 – 3.72 (m, 2H), 1.34 (d, *J* = 7.4 Hz, 3H), 0.96 (t, *J* = 7.1 Hz, 3H).

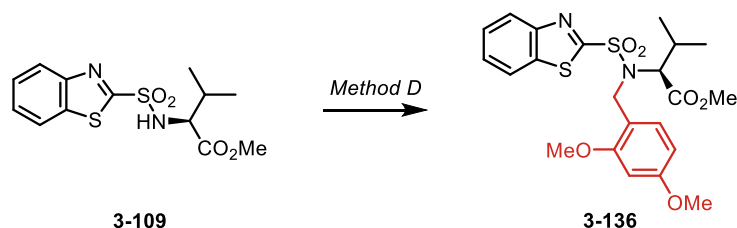
¹³C {¹H} NMR (101 MHz, Chloroform-*d*) δ (ppm): 170.7, 165.6, 152.7, 137.0, 136.5, 128.6, 128.2, 127.9, 127.7, 127.5, 125.2, 122.2, 61.6, 56.4, 50.3, 16.9, 13.8.

MS (ESI) *m/z* (%): 405 [M+H]⁺ (100).

HRMS (ESI) *m/z*: [M+H]⁺ calculated for C₁₉H₂₁N₂O₄S₂: 405.0937; found: 405.0938.

R_f = 0.53 (hexane/ EtOAc = 3:1)

[α]_D²² = +26.3° (c 1.0, CHCl₃)

methyl *N*-(benzo[*d*]thiazol-2-ylsulfonyl)-*N*-(2,4-dimethoxybenzyl)-L-valinate (**3-136**)

Method D: Starting from sulfonamide **3-109** (0.2 g, 0.61 mmol, 1.0 equiv.) and 2,4-dimethoxybenzylalcohol (0.21 g, 1.22 mmol, 2.0 equiv.). The crude product was purified by column chromatography (petroleum ether/EtOAc = 10:1) to afford **3-136** as a yellow oil (0.18 g, 61 % yield, *e.r.* = ≥ 99:1).

¹H NMR (500 MHz, Chloroform-*d*) δ (ppm): 8.17 (d, *J* = 8.2 Hz, 1H), 7.96 (d, *J* = 7.7 Hz, 1H), 7.62 – 7.57 (m, 1H), 7.57 – 7.51 (m, 2H), 6.45 (dd, *J* = 8.5, 2.5 Hz, 1H), 6.37 – 6.34 (m, 1H), 4.85

Chapter III: Experimental section

(d, $J = 16.2$ Hz, 1H), 4.76 (d, $J = 16.1$ Hz, 1H), 4.28 (d, $J = 10.3$ Hz, 1H), 3.78 (s, 3H), 3.75 (s, 3H), 3.26 (s, 3H), 2.16 – 2.06 (m, 1H), 0.86 (d, $J = 6.6$ Hz, 3H), 0.81 (d, $J = 6.6$ Hz, 3H).

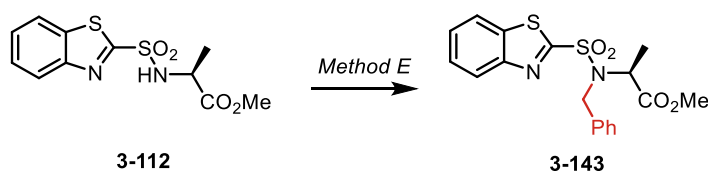
^{13}C $\{^1\text{H}\}$ NMR (126 MHz, Chloroform-*d*) δ (ppm): 170.1, 165.9, 160.6, 158.2, 152.6, 136.6, 131.8, 130.4, 127.5, 127.4, 125.2, 122.2, 117.1, 104.2, 98.1, 66.9, 55.5, 55.4, 51.7, 44.5, 28.4, 20.0, 19.8.

MS (ESI) m/z (%): 479 [M+H]⁺ (100).

HRMS (ESI) m/z : [M+H]⁺ calculated for C₁₄H₁₇N₂O₅S₂: 479.1311; found: 479.1305.

R_f = 0.38 (hexane/ EtOAc = 5:1)

methyl *N*-(benzo[*d*]thiazol-2-ylsulfonyl)-*N*-benzyl-L-alaninate (**3-143**)



Method E: Starting from sulfonamide **3-112** (0.3 g, 1.0 mmol, 1.0 equiv.) and benzyl bromide (0.24 mL, 2.0 mmol, 2.0 equiv.). The crude product was purified by gradient column chromatography (SiO₂; petroleum ether/EtOAc = 10:1 → 4:1) to afford **3-143** as slightly yellow oil (0.33 g, 84 % yield, *e.r.* = ≥ 99:1).

^1H NMR (400 MHz, Chloroform-*d*) δ (ppm): 8.19 (ddd, $J = 8.1, 1.4, 0.6$ Hz, 1H), 8.03 – 7.93 (m, 1H), 7.62 (ddd, $J = 8.3, 7.2, 1.4$ Hz, 1H), 7.56 (ddd, $J = 8.0, 7.2, 1.4$ Hz, 1H), 7.45 – 7.40 (m, 2H), 7.36 – 7.26 (m, 3H), 4.92 – 4.83 (m, 2H), 4.60 (d, $J = 16.3$ Hz, 1H), 3.34 (s, 3H), 1.36 (d, $J = 7.3$ Hz, 3H).

^{13}C $\{^1\text{H}\}$ NMR (101 MHz, Chloroform-*d*) δ (ppm): 171.1, 165.6, 152.7, 136.8, 136.5, 128.6, 128.3, 127.9, 127.7, 127.5, 125.3, 122.3, 56.2, 52.3, 50.3, 16.6.

MS (ESI) m/z (%): 391 [M+H]⁺ (100).

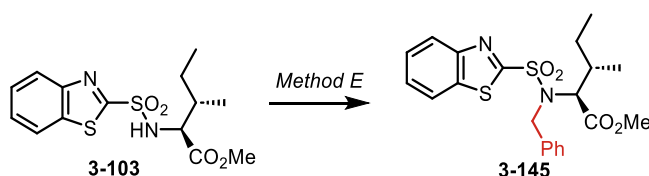
HRMS (ESI) m/z : [M+H]⁺ calculated for C₁₈H₁₉N₂O₄S₂: 391.0786; found: 391.0784.

R_f = 0.40 (hexane/ EtOAc = 3:1)

$[\alpha]_{\text{D}}^{23} = -29.1^\circ$ (*c* 1.0, CHCl₃)

Chapter III: Experimental section

methyl *N*-(benzo[*d*]thiazol-2-ylsulfonyl)-*N*-benzyl-L-isoleucinate (**3-145**)



Method E: Starting from sulfonamide **3-103** (0.365 g, 1.06 mmol, 1.0 equiv.) and benzyl bromide (0.25 mL, 2.11 mmol, 2.0 equiv.). The crude product was purified by column chromatography (SiO₂; petroleum ether/EtOAc = 4:1) to afford **3-145** as colorless oil (0.24 g, 52 % yield, *e.r.* = ≥ 99:1).

¹H NMR (500 MHz, Chloroform-*d*) δ (ppm): 8.17 (ddd, *J* = 8.2, 1.3, 0.7 Hz, 1H), 7.98 (ddd, *J* = 8.0, 1.4, 0.7 Hz, 1H), 7.63 – 7.52 (m, 4H), 7.35 – 7.31 (m, 2H), 7.30 – 7.26 (m, 1H), 5.09 (d, *J* = 16.1 Hz, 1H), 4.73 (d, *J* = 16.1 Hz, 1H), 4.35 (d, *J* = 10.7 Hz, 1H), 3.26 (s, 3H), 1.70 – 1.61 (m, 1H), 1.47 (dtd, *J* = 15.1, 7.5, 2.4 Hz, 1H), 0.90 – 0.82 (m, 1H), 0.74 (d, *J* = 6.6 Hz, 3H), 0.38 (t, *J* = 7.4 Hz, 3H).

¹³C {¹H} NMR (126 MHz, Chloroform-*d*) δ (ppm): 170.4, 165.6, 152.5, 137.1, 136.5, 129.1, 128.5, 127.9, 127.7, 127.5, 125.1, 122.2, 65.8, 51.7, 50.2, 34.7, 25.5, 15.7, 10.4.

MS (ESI) *m/z* (%): 433 [M+H]⁺ (100).

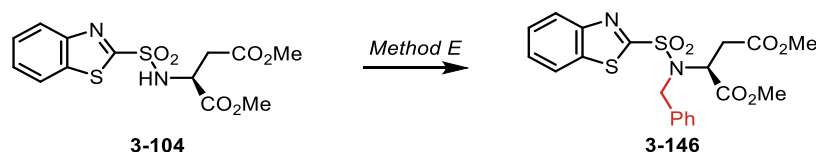
HRMS (ESI) *m/z*: [M+K]⁺ calculated for C₂₁H₂₄KN₂O₄S₂: 471.0809; found: 471.0811.

R_f = 0.50 (PE/ EtOAc = 2:1)

[α]_D²³ = -32.7° (*c* 1.2, CHCl₃)

Chapter III: Experimental section

dimethyl *N*-(benzo[*d*]thiazol-2-ylsulfonyl)-*N*-benzyl-L-aspartate (**3-146**)



Method E: Starting from sulfonamide **3-104** (1.0 g, 2.79 mmol, 1.0 equiv.) and benzyl bromide (0.67 mL, 5.58 mmol, 2.0 equiv.). The crude product was purified by gradient column chromatography (SiO₂; petroleum ether/EtOAc = 20:1 → 5:1) to afford **3-146** as a colorless solid (1.05 g, 84 % yield, *e.r.* = ≥ 99:1).

¹H NMR (500 MHz, Chloroform-*d*) δ (ppm): 8.20 – 8.17 (m, 1H), 8.01 – 7.98 (m, 1H), 7.63 (ddt, *J* = 8.1, 7.0, 1.1 Hz, 1H), 7.58 (ddt, *J* = 8.2, 7.1, 1.2 Hz, 1H), 7.43 (dd, *J* = 7.9, 1.6 Hz, 2H), 7.35 – 7.29 (m, 3H), 5.02 (dd, *J* = 8.4, 5.8 Hz, 1H), 4.89 (d, *J* = 15.7 Hz, 1H), 4.51 (d, *J* = 15.7 Hz, 1H), 3.53 (s, 3H), 3.34 (s, 3H), 2.99 (dd, *J* = 17.0, 8.4 Hz, 1H), 2.76 (dd, *J* = 17.0, 5.7 Hz, 1H).

¹³C {¹H} NMR (126 MHz, Chloroform-*d*) δ (ppm): 170.6, 169.5, 165.7, 152.5, 136.5, 135.5, 128.9, 128.7, 128.4, 127.8, 127.6, 125.3, 122.3, 56.9, 52.7, 52.1, 52.0, 35.4.

MS (ESI) *m/z* (%): 449 [M+H]⁺ (100).

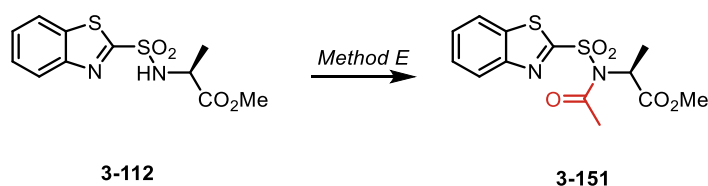
HRMS (ESI) *m/z*: [M+H]⁺ calculated for C₂₀H₂₁N₂O₆S₂: 449.0836; found: 449.0829.

R_f = 0.44 (PE/ EtOAc = 5:1)

[α]_D²² = -50.6° (*c* 1.0, CHCl₃)

m. p. = 110-112 °C

methyl *N*-acetyl-*N*-(benzo[*d*]thiazol-2-ylsulfonyl)-L-alaninate (**3-151**)



Sulfonamide **3-112** (0.5 g, 1.65 mmol, 1.0 equiv.) was dissolved in THF (8.2 mL, 0.2 M) followed by addition of NaH (60% suspension in mineral oil; 0.1 g, 5.5 mmol, 1.5 equiv.). The mixture was cooled to 0 °C and acetyl chloride (0.24 mL, 3.3 mmol, 2.0 equiv.) was added and the reaction mixture was stirred at RT for 16 h. After that H₂O mixture evaporated and the crude product was purified by gradient column chromatography (SiO₂; petroleum ether/EtOAc = 10:1 → 4:1) to afford **3-151** as a slightly yellow oil (0.2g, 36 % yield, *e.r.* = ≥ 99:1).

Chapter III: Experimental section

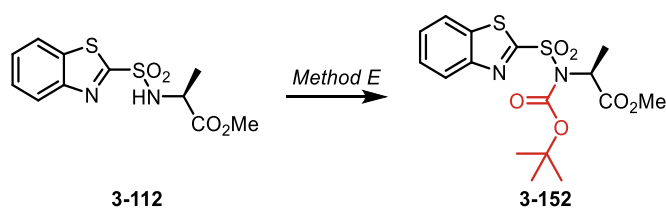
¹H NMR (500 MHz, Chloroform-*d*) δ (ppm): 8.21 (dd, *J* = 8.1, 1.8 Hz, 1H), 8.01 (dd, *J* = 7.9, 1.5 Hz, 1H), 7.64 (ddd, *J* = 15.4, 7.2, 1.4 Hz, 2H), 5.06 (q, *J* = 6.9 Hz, 1H), 3.50 (s, 3H), 2.70 (s, 3H), 1.63 (d, *J* = 6.9 Hz, 3H).

¹³C {¹H} NMR (126 MHz, Chloroform-*d*) δ (ppm): 170.2, 169.9, 163.8, 152.2, 136.7, 128.6, 128.1, 125.8, 122.4, 56.6, 52.7, 25.9, 16.0.

MS (ESI) *m/z* (%): 343 [M+H]⁺ (100).

HRMS (ESI) *m/z*: [M+H]⁺ calculated for C₁₃H₁₅N₂O₅S₂: 343.0417; found: 343.0426.

methyl *N*-(benzo[*d*]thiazol-2-ylsulfonyl)-*N*-(*tert*-butoxycarbonyl)-L-alaninate (**3-152**)



Method E: Sulfonamide **3-112** (0.2 g, 0.66 mmol, 1.0 equiv.) was dissolved in DCE (1.3 mL, 0.5 M) followed by addition of TEA (0.112 mL, 0.8 mmol, 1.2 equiv.). Subsequently, (Boc)₂O (0.43 g, 2.0 mmol, 3.0 equiv.) was added and the reaction mixture was stirred at 60 °C for 16 h. Then, the mixture evaporated, and the crude product was purified by gradient column chromatography (SiO₂; petroleum ether/EtOAc = 10:1 → 4:1) to afford **3-152** as a slightly yellow oil (0.225 g, 85 % yield, *e.r.* = ≥ 99:1).

¹H NMR (500 MHz, Chloroform-*d*) δ (ppm): 8.20 (dd, *J* = 8.5, 1.2 Hz, 1H), 8.00 (dd, *J* = 7.7, 1.7 Hz, 1H), 7.67 – 7.53 (m, 2H), 5.24 (q, *J* = 7.0 Hz, 1H), 3.75 (s, 3H), 1.77 (d, *J* = 7.0 Hz, 3H), 1.36 (s, 10H).

¹³C {¹H} NMR (126 MHz, Chloroform-*d*) δ (ppm): 173.0, 170.4, 164.6, 151.8, 149.6, 137.1, 128.1, 127.7, 125.6, 122.3, 86.5, 86.4, 56.1, 52.8, 28.7, 27.9, 27.9, 16.6.

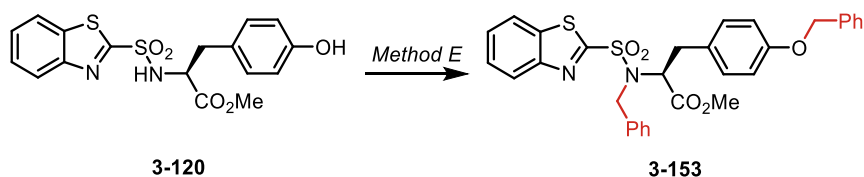
MS (ESI) *m/z* (%): 401 [M+H]⁺ (100).

HRMS (ESI) *m/z*: [M+H]⁺ calculated for C₁₆H₂₁N₂O₆S₂: 401.0836; found: 401.0831.

R_f = 0.52 (hexane/ EtOAc = 4:1)

Chapter III: Experimental section

methyl (S)-2-(N-benzylbenzo[d]thiazole-2-sulfonamido)-3-(4-(benzyloxy)phenyl)propanoate (3-153)



Method E: Starting from sulfonamide **3-120** (0.3 g, 0.76 mmol, 1.0 equiv.) and benzyl bromide (0.27 mL, 2.3 mmol, 3.0 equiv.). The crude product was purified by column chromatography (SiO₂; petroleum ether/EtOAc = 10:1) to afford **3-153** as a slightly yellow oil (0.95 g, 74 % yield, *e.r.* = ≥ 99:1).

¹H NMR (500 MHz, Chloroform-*d*) δ (ppm): 8.17 (d, *J* = 8.2 Hz, 1H), 7.97 (d, *J* = 8.0 Hz, 1H), 7.61 (td, *J* = 7.4, 1.2 Hz, 1H), 7.56 (td, *J* = 7.5, 1.3 Hz, 1H), 7.43 – 7.36 (m, 7H), 7.34 – 7.27 (m, 4H), 6.92 (d, *J* = 8.3 Hz, 2H), 6.73 (d, *J* = 8.4 Hz, 2H), 4.95 (s, 2H), 4.87 – 4.82 (m, 2H), 4.72 (d, *J* = 15.7 Hz, 1H), 3.22 (s, 3H), 3.13 (dd, *J* = 14.1, 8.5 Hz, 1H), 2.85 (dd, *J* = 14.1, 6.6 Hz, 1H).

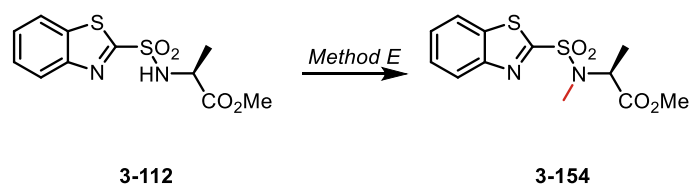
¹³C {¹H} NMR (126 MHz, Chloroform-*d*) δ (ppm): 170.0, 165.8, 157.7, 152.6, 137.1, 136.5, 136.1, 130.3, 128.8, 128.7, 128.6, 128.6, 128.1, 128.1, 127.7, 127.6, 127.6, 125.2, 122.2, 114.8, 70.0, 61.9, 52.2, 50.8, 35.8, 29.8.

MS (ESI) *m/z* (%): 573 [M+H]⁺ (100).

HRMS (ESI) *m/z*: [M+H]⁺ calculated for C₁₈H₁₈N₃O₆S₂: 573.1512; found: 573.1511.

[α]_D²³ = -7.2° (c 1, CHCl₃)

methyl N-(benzo[d]thiazol-2-ylsulfonyl)-N-methyl-L-alaninate (3-154)



Method E: Starting from sulfonamide **3-112** (0.2 g, 0.67 mmol, 1.0 equiv.) and iodomethane (0.08 mL, 1.33 mmol, 2.0 equiv.). The crude product was purified by column chromatography (SiO₂; petroleum ether/EtOAc = 8:1) to afford **3-154** as a colorless oil (0.193 g, 93 % yield, *e.r.* = ≥ 99:1).

¹H NMR (500 MHz, Chloroform-*d*) δ (ppm): 8.17 (ddd, *J* = 8.3, 1.2, 0.7 Hz, 1H), 7.97 (ddd, *J* = 8.1, 1.6, 0.7 Hz, 1H), 7.60 (ddd, *J* = 8.3, 7.2, 1.4 Hz, 1H), 7.55 (ddd, *J* = 8.4, 7.3, 1.3 Hz, 1H), 4.93 (q, *J* = 7.3 Hz, 1H), 3.48 (s, 3H), 3.07 (s, 3H), 1.46 (d, *J* = 7.3 Hz, 3H).

Chapter III: Experimental section

^{13}C $\{^1\text{H}\}$ NMR (126 MHz, Chloroform-*d*) δ (ppm): 171.1, 164.9, 152.7, 136.4, 127.7, 127.5, 125.2, 122.2, 55.6, 52.5, 31.0, 15.6.

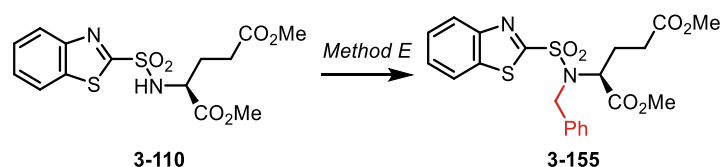
MS (ESI) m/z (%): 315 $[\text{M}+\text{H}]^+$ (100).

HRMS (ESI) m/z : $[\text{M}+\text{H}]^+$ calculated for $\text{C}_{12}\text{H}_{15}\text{N}_2\text{O}_4\text{S}_2$: 315.0468; found: 315.0478.

R_f = 0.35 (PE/ EtOAc = 2:1)

$[\alpha]_{\text{D}}^{23} = -30.3^\circ$ (*c* 1.0, CHCl_3)

dimethyl *N*-(benzo[*d*]thiazol-2-ylsulfonyl)-*N*-benzyl-L-glutamate (**3-155**)



Method E: Starting from sulfonamide **3-110** (1.0 g, 2.69 mmol, 1.0 equiv.) and benzyl bromide (0.65 mL, 5.48 mmol, 2.0 equiv.). The crude product was purified by gradient column chromatography (SiO_2 ; petroleum ether/EtOAc = 20:1 \rightarrow 5:1) to afford **3-155** as a colorless solid (1.1 g, 89 % yield, *e.r.* = \geq 99:1).

^1H NMR (500 MHz, Chloroform-*d*) δ (ppm): 8.18 (ddd, J = 8.2, 1.4, 0.7 Hz, 1H), 7.99 (ddd, J = 8.1, 1.4, 0.7 Hz, 1H), 7.62 (ddd, J = 8.3, 7.2, 1.3 Hz, 1H), 7.59 – 7.55 (m, 1H), 7.48 – 7.45 (m, 2H), 7.34 – 7.27 (m, 3H), 5.00 (d, J = 15.9 Hz, 1H), 4.74 (dd, J = 9.9, 4.9 Hz, 1H), 4.45 (d, J = 15.9 Hz, 1H), 3.57 (s, 3H), 3.30 (s, 3H), 2.36 – 2.23 (m, 1H), 2.25 – 2.09 (m, 2H), 1.88 – 1.77 (m, 1H).

^{13}C $\{^1\text{H}\}$ NMR (126 MHz, Chloroform-*d*) δ (ppm): 172.8, 170.1, 165.3, 152.6, 136.5, 136.2, 128.9, 128.7, 128.2, 127.7, 127.6, 125.2, 122.3, 60.1, 52.4, 51.8, 51.0, 29.9, 25.1.

MS (ESI) m/z (%): 463 $[\text{M}+\text{H}]^+$ (100).

HRMS (ESI) m/z : $[\text{M}+\text{H}]^+$ calculated for $\text{C}_{21}\text{H}_{23}\text{N}_2\text{O}_6\text{S}_2$: 463.0992; found: 463.1001.

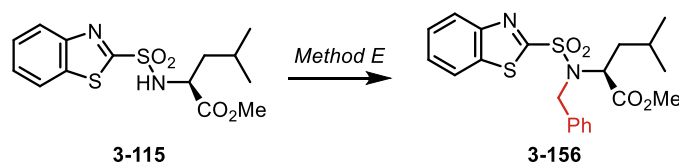
R_f = 0.42 (PE/ EtOAc = 5:1)

$[\alpha]_{\text{D}}^{23} = -26.3^\circ$ (*c* 0.4, CHCl_3)

m. p. = 58-60 $^\circ\text{C}$

Chapter III: Experimental section

methyl *N*-(benzo[*d*]thiazol-2-ylsulfonyl)-*N*-benzyl-L-leucinate (**3-156**)



Method E: Starting from sulfonamide **3-115** (1.0 g, 2.92 mmol, 1.0 equiv.) and benzyl bromide (0.71 mL, 5.84 mmol, 2.0 equiv.). The crude product was purified by gradient column chromatography (SiO₂; petroleum ether/EtOAc = 15:1 → 5:1) to afford **3-156** as a colorless solid (1.94 g, 87 % yield, *e.r.* = ≥ 99:1).

¹H NMR (500 MHz, Chloroform-*d*) δ (ppm): 8.19 – 8.16 (m, 1H), 7.99 (dt, *J* = 8.0, 1.0 Hz, 1H), 7.62 (ddd, *J* = 8.3, 7.2, 1.4 Hz, 1H), 7.57 (ddt, *J* = 8.0, 7.1, 1.6 Hz, 1H), 7.50 – 7.46 (m, 2H), 7.33 (td, *J* = 6.9, 1.2 Hz, 2H), 7.30 – 7.27 (m, 1H), 5.02 (d, *J* = 16.3 Hz, 1H), 4.80 (dd, *J* = 8.3, 6.4 Hz, 1H), 4.51 (d, *J* = 16.4 Hz, 1H), 3.29 (s, 3H), 1.54 – 1.49 (m, 2H), 1.44 (dt, *J* = 13.1, 6.5 Hz, 1H), 0.86 (d, *J* = 6.3 Hz, 3H), 0.49 (d, *J* = 6.5 Hz, 3H).

¹³C {¹H} NMR (126 MHz, Chloroform-*d*) δ (ppm): 171.2, 165.4, 152.7, 137.1, 136.5, 128.6, 128.6, 127.9, 127.7, 127.5, 125.2, 122.3, 59.3, 52.3, 50.6, 39.1, 24.4, 22.4, 21.4.

MS (ESI) *m/z* (%): 433 [M+H]⁺ (100).

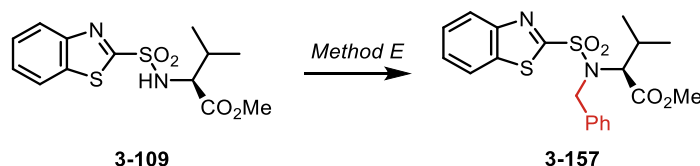
HRMS (ESI) *m/z*: [M+H]⁺ calculated for C₂₁H₂₅N₂O₄S₂: 433.1250; found: 433.1263.

R_f = 0.35 (PE/ EtOAc = 5:1)

[α]_D²³ = -66.8° (*c* 1.2, CHCl₃)

m. p. = 100-102 °C

methyl *N*-(benzo[*d*]thiazol-2-ylsulfonyl)-*N*-benzyl-L-valinate (**3-157**)



Method E: Starting from sulfonamide **3-109** (1.0 g, 3.04 mmol, 1.0 equiv.) and benzyl bromide (0.74 mL, 6.08 mmol, 2.0 equiv.). The crude product was purified by gradient column chromatography (SiO₂; petroleum ether/EtOAc = 15:1 → 5:1) to afford **3-157** as a colorless solid (1.19 g, 93 % yield, *e.r.* = ≥ 99:1).

¹H NMR (500 MHz, Chloroform-*d*) δ (ppm): 8.17 (ddd, *J* = 8.4, 1.2, 0.7 Hz, 1H), 7.98 (ddd, *J* = 8.1, 1.3, 0.7 Hz, 1H), 7.61 (ddd, *J* = 8.3, 7.2, 1.3 Hz, 1H), 7.56 (ddd, *J* = 8.3, 7.1, 1.3 Hz, 1H), 7.54

Chapter III: Experimental section

– 7.50 (m, 2H), 7.34 – 7.26 (m, 3H), 5.02 (d, $J = 15.9$ Hz, 1H), 4.69 (d, $J = 15.9$ Hz, 1H), 4.27 (d, $J = 10.7$ Hz, 1H), 3.24 (s, 3H), 2.04 – 1.94 (m, 1H), 0.81 (d, $J = 6.6$ Hz, 3H), 0.73 (d, $J = 6.6$ Hz, 3H).

^{13}C $\{^1\text{H}\}$ NMR (126 MHz, Chloroform-*d*) δ (ppm): 170.2, 165.8, 152.5, 136.8, 136.5, 129.3, 128.5, 128.0, 127.7, 127.5, 125.1, 122.2, 67.1, 51.8, 50.4, 28.7, 19.7, 19.4.

MS (ESI) m/z (%): 419 $[\text{M}+\text{H}]^+$ (100).

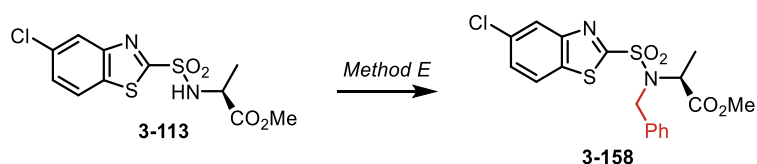
HRMS (ESI) m/z : $[\text{M}+\text{H}]^+$ calculated for $\text{C}_{20}\text{H}_{23}\text{N}_2\text{O}_4\text{S}_2$: 419.1094; found: 419.1110.

$R_f = 0.49$ (PE/ EtOAc = 5:1)

$[\alpha]_{\text{D}}^{23} = -40.7^\circ$ (c 1.0, CHCl_3)

m. p. = 110-112 $^\circ\text{C}$

methyl *N*-benzyl-*N*-((6-chlorobenzo[*d*]thiazol-2-yl)sulfonyl)-*L*-alaninate (**3-158**)



Method E: Starting from sulfonamide **3-113** (0.39 g, 1.16 mmol, 1.0 equiv.) and benzyl bromide (0.28 mL, 2.32 mmol, 2.0 equiv.). The crude product was purified by gradient column chromatography (SiO_2 ; petroleum ether/EtOAc = 10:1 \rightarrow 5:1) to afford **3-158** as a slightly yellowish oil (0.36 g, 72 % yield, *e.r.* = $\geq 99:1$).

^1H NMR (500 MHz, Chloroform-*d*) δ (ppm): 8.17 (dd, $J = 2.1, 0.5$ Hz, 1H), 7.90 (dd, $J = 8.6, 0.5$ Hz, 1H), 7.54 (dd, $J = 8.6, 2.0$ Hz, 1H), 7.42 – 7.39 (m, 2H), 7.34 – 7.30 (m, 2H), 7.29 – 7.25 (m, 1H), 4.91 – 4.82 (m, 2H), 4.56 (d, $J = 16.3$ Hz, 1H), 3.38 (s, 3H), 1.36 (d, $J = 7.3$ Hz, 3H).

^{13}C $\{^1\text{H}\}$ NMR (126 MHz, Chloroform-*d*) δ (ppm): 171.1, 167.5, 153.4, 136.6, 134.7, 133.7, 128.6, 128.4, 128.4, 128.2, 128.0, 124.8, 123.1, 56.3, 52.5, 50.3, 16.7.

MS (ESI) m/z (%): 425 $[\text{M}+\text{H}]^+$ (100).

HRMS (ESI) m/z : $[\text{M}+\text{H}]^+$ calculated for $\text{C}_{18}\text{H}_{18}\text{ClN}_2\text{O}_4\text{S}_2$: 425.0391; found: 425.0394.

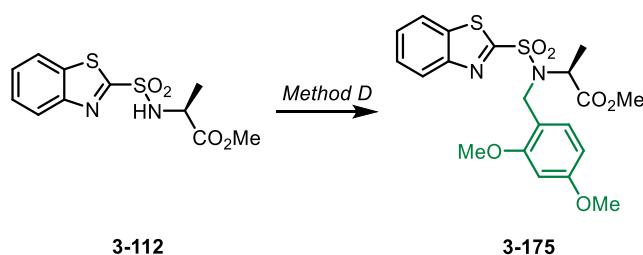
$R_f = 0.45$ (hexane/ EtOAc = 3:1)

$[\alpha]_{\text{D}}^{23} = -24.9^\circ$ (c 1.0, CHCl_3)

m. p. = 110-112 $^\circ\text{C}$

Chapter III: Experimental section

methyl *N*-(benzo[*d*]thiazol-2-ylsulfonyl)-*N*-(2,4-dimethoxybenzyl)-*L*-alaninate (**3-175**)



Method D: Starting from sulfonamide **3-112** (0.7 g, 2.33 mmol, 1.0 equiv.), 2,4-dimethoxybenzylalcohol (0.6 g, 3.50 mmol, 1.5 equiv.), PPh₃ (1.2 g, 4.66 mmol, 2.0 equiv.) and DIAD (0.9 mL, 4.66 mmol, 2.0 equiv.). The crude product was purified by gradient column chromatography (SiO₂; hexane/EtOAc = 10:1 → 3:1) to afford **3-175** as a slightly blue solid (0.78 g, 74 % yield, *e.r.* = ≥ 99:1).

¹H NMR (500 MHz, Chloroform-*d*) δ (ppm): δ 8.21 – 8.15 (m, 1H), 7.99 – 7.94 (m, 1H), 7.63 – 7.57 (m, 1H), 7.57 – 7.52 (m, 1H), 7.46 (d, *J* = 8.4 Hz, 1H), 6.47 (dd, *J* = 8.5, 2.4 Hz, 1H), 6.34 (d, *J* = 2.3 Hz, 1H), 4.85 (q, *J* = 7.3 Hz, 1H), 4.72 (d, *J* = 16.2 Hz, 1H), 4.57 (d, *J* = 16.3 Hz, 1H), 3.78 (s, 3H), 3.71 (s, 3H), 3.36 (s, 3H), 1.39 (d, *J* = 7.3 Hz, 3H).

¹³C {¹H} NMR (126 MHz, Chloroform-*d*) δ (ppm): 171.3, 165.7, 160.6, 157.9, 152.6, 136.5, 131.0, 127.6, 127.4, 125.2, 122.2, 117.0, 104.3, 98.0, 56.2, 55.5, 55.3, 52.3, 44.3, 16.0.

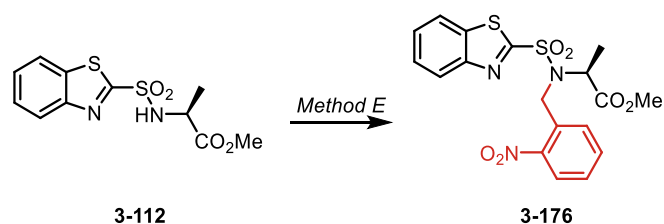
MS (ESI) *m/z* (%): 451 [M+H]⁺ (100).

HRMS (ESI) *m/z*: [M+K]⁺ calculated for C₂₀H₂₂N₂O₆S₂: 489.0551; found: 489.0555.

R_f = 0.28 (hexane/EtOAc = 3:1)

[α]_D³¹ = -12.7° (*c* 1.0, CHCl₃)

m. p. = 88-90 °C

methyl *N*-(benzo[*d*]thiazol-2-ylsulfonyl)-*N*-(2-nitrobenzyl)-L-alaninate (**3-176**)

Method E: Starting from sulfonamide **3-112** (0.2 g, 0.66 mmol, 1.0 equiv.) and 2-nitrobenzyl bromide (0.29 mL, 1.33 mmol, 2.0 equiv.). The crude product was purified by gradient column chromatography (SiO₂; petroleum ether/EtOAc = 10:1 → 4:1) to afford **3-176** as a slightly yellow oil (0.26 g, 90 % yield, *e.r.* = ≥ 99:1).

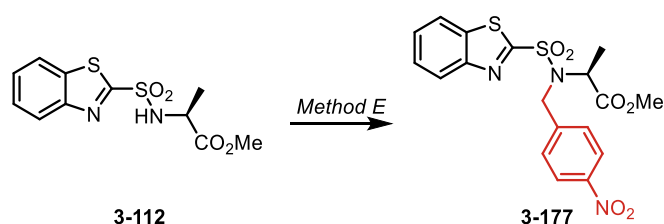
¹H NMR (500 MHz, Chloroform-*d*) δ (ppm): 8.20 (dt, *J* = 8.4, 0.9 Hz, 1H), 8.06 (dt, *J* = 8.3, 1.1 Hz, 1H), 8.04 – 7.97 (m, 2H), 7.74 – 7.67 (m, 1H), 7.63 (ddt, *J* = 15.5, 7.2, 1.1 Hz, 1H), 7.58 (ddt, *J* = 15.4, 7.2, 1.1 Hz, 1H), 7.46 (t, *J* = 7.7 Hz, 1H), 5.31 (d, *J* = 18.8 Hz, 1H), 5.00 (q, *J* = 7.4 Hz, 1H), 4.95 (d, *J* = 18.8 Hz, 1H), 3.34 (s, 3H), 1.35 (d, *J* = 7.3 Hz, 3H).

¹³C {¹H} NMR (126 MHz, Chloroform-*d*) δ (ppm): 170.7, 164.2, 152.6, 147.6, 136.5, 133.9, 133.8, 130.0, 128.4, 128.0, 127.7, 125.3, 125.1, 122.3, 56.8, 52.6, 47.4, 16.6.

MS (ESI) *m/z* (%): 436 [M+H]⁺ (100).

HRMS (ESI) *m/z*: [M+H]⁺ calculated for C₁₈H₁₈N₃O₆S₂: 436.0632; found: 436.0627.

R_f = 0.35 (hexane/ EtOAc = 4:1)

methyl *N*-(benzo[*d*]thiazol-2-ylsulfonyl)-*N*-(4-nitrobenzyl)-L-alaninate (**3-177**)

Method E: Starting from sulfonamide **3-112** (0.2 g, 0.66 mmol, 1.0 equiv.) and 4-nitrobenzyl bromide (0.29 mL, 1.33 mmol, 2.0 equiv.). The crude product was purified by gradient column chromatography (SiO₂; petroleum ether/EtOAc = 10:1 → 4:1) to afford **3-177** as a slightly yellow oil (0.27 g, 93 % yield, *e.r.* = ≥ 99:1).

¹H NMR (500 MHz, Chloroform-*d*) δ (ppm): 8.20 (ddt, *J* = 9.3, 8.2, 1.2 Hz, 3H), 8.00 (dq, *J* = 8.0, 1.0 Hz, 1H), 7.66 – 7.62 (m, 3H), 7.59 (ddd, *J* = 8.3, 7.2, 1.3 Hz, 1H), 5.06 (d, *J* = 17.4 Hz, 1H), 4.96 (q, *J* = 7.4 Hz, 1H), 4.65 (d, *J* = 17.4 Hz, 1H), 3.38 (s, 3H), 1.35 (d, *J* = 7.4 Hz, 3H).

Chapter III: Experimental section

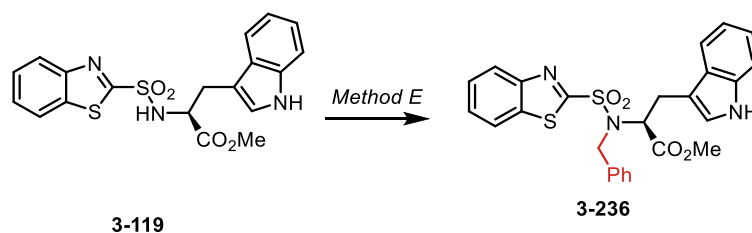
^{13}C { ^1H } NMR (126 MHz, Chloroform-*d*) δ (ppm): 171.0, 164.7, 152.6, 147.6, 145.1, 136.4, 128.5, 128.0, 127.8, 125.3, 123.9, 122.3, 56.4, 52.6, 49.4, 17.0.

MS (ESI) m/z (%): 436 [M+H]⁺ (100).

HRMS (ESI) m/z : [M+H]⁺ calculated for C₁₈H₁₈N₃O₆S₂: 436.0632; found: 436.0628.

R_f = 0.40 (hexane/ EtOAc = 4:1)

methyl *N*-(benzo[*d*]thiazol-2-ylsulfonyl)-*N*-benzyl-L-tryptophanate (**3-236**)



Modified Method E: To the solution of sulfonamide **3-119** in DMF (0.1 M, 20.5 mL) was added followed by addition of K₂CO₃ (0.85 g, 6.14 mmol, 3 equiv.). Subsequently, benzyl bromide (0.49 mL, 4.09 mmol, 2 equiv.) was added dropwise and the reaction mixture was stirred at room temperature for 16 h. Then, the mixture was quenched with water and the layers were separated. The aqueous layer was extracted using EtOAc (3 x 20 mL). Combined organic layers were washed with brine (50 mL), dried over MgSO₄, filtered and the solvents were concentrated under reduced pressure. The crude product was purified by column chromatography (SiO₂; petroleum ether/EtOAc = 6:1 to 2:1) to afford **3-236** in 30 % yield over 2 steps (0.3g, *e.r.* = \geq 98:2) as a slightly orange oil.

^1H NMR (500 MHz, Chloroform-*d*) δ (ppm): 8.16 (dd, *J* = 8.3, 1.8 Hz, 1H), 7.94 (dd, *J* = 8.1, 1.5 Hz, 1H), 7.79 (s, 1H), 7.61 (ddd, *J* = 8.2, 7.1, 1.3 Hz, 1H), 7.56 (ddd, *J* = 8.2, 7.2, 1.3 Hz, 1H), 7.45 – 7.41 (m, 3H), 7.30 – 7.25 (m, 2H), 7.23 (dd, *J* = 9.6, 2.5 Hz, 1H), 7.14 (ddd, *J* = 8.1, 7.0, 1.2 Hz, 1H), 7.06 (ddd, *J* = 8.1, 7.0, 1.2 Hz, 1H), 6.89 – 6.86 (m, 1H), 4.98 (ddd, *J* = 8.3, 6.6, 1.6 Hz, 1H), 4.88 (d, *J* = 15.9 Hz, 1H), 4.76 (d, *J* = 16.0 Hz, 1H), 3.38 (dd, *J* = 14.7, 8.5 Hz, 1H), 3.20 (s, 3H), 3.12 (dd, *J* = 14.7, 6.5 Hz, 1H).

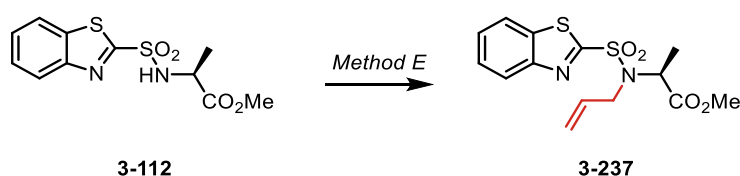
^{13}C { ^1H } NMR (126 MHz, Chloroform-*d*) δ (ppm): 170.2, 165.9, 152.6, 136.5, 136.2, 136.0, 128.8, 128.5, 128.0, 127.6, 127.5, 127.1, 125.1, 123.5, 122.3, 122.2, 119.7, 118.7, 111.2, 110.4, 60.6, 52.2, 50.8, 26.6.

MS (ESI) m/z (%): 506 [M+H]⁺ (100). **HRMS (ESI) m/z :** [M+K]⁺ calculated for C₂₆H₂₃KN₃O₄S₂: 544.0762; found: 544.0772.

R_f = 0.30 (hexane/ EtOAc = 3:1); [α]_D²² = -16.3° (c 0.9, CHCl₃)

Chapter III: Experimental section

methyl *N*-allyl-*N*-(benzo[*d*]thiazol-2-ylsulfonyl)-*L*-alaninate (**3-237**)



Method E: Starting from sulfonamide **3-112** (0.21 g, 0.70 mmol, 1.0 equiv.) and allyl bromide (0.12 mL, 1.40 mmol, 2.0 equiv.). The crude product was purified by column chromatography (SiO₂; petroleum ether/EtOAc = 8:1) to afford **3-237** as a colorless oil (0.17 g, 72 % yield, *e.r.* = ≥ 99:1).

¹H NMR (500 MHz, Chloroform-*d*) δ (ppm): 8.17 (d, *J* = 7.5 Hz, 1H), 7.97 (d, *J* = 7.8 Hz, 1H), 7.60 (ddd, *J* = 8.3, 7.3, 1.2 Hz, 1H), 7.55 (ddd, *J* = 8.3, 7.3, 1.2 Hz, 1H), 5.93 (ddt, *J* = 16.4, 10.3, 6.2 Hz, 1H), 5.26 (dd, *J* = 17.2, 1.3 Hz, 1H), 5.16 (dd, *J* = 10.2, 1.2 Hz, 1H), 4.87 (q, *J* = 7.3 Hz, 1H), 4.24 (dd, *J* = 16.6, 6.1 Hz, 1H), 4.00 (dd, *J* = 16.6, 6.1 Hz, 1H), 3.47 (s, 3H), 1.50 (d, *J* = 7.3 Hz, 3H).

¹³C {¹H} NMR (126 MHz, Chloroform-*d*) δ (ppm): 171.4, 165.7, 152.6, 136.4, 134.6, 127.7, 127.5, 125.2, 122.3, 118.4, 56.1, 52.5, 49.2, 16.6.

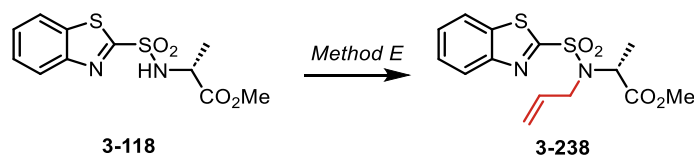
MS (ESI) *m/z* (%): 340 [M+H]⁺ (100).

HRMS (ESI) *m/z*: [M+H]⁺ calculated for C₁₄H₁₇N₂O₄S₂: 341.0624; found: 341.0626.

R_f = 0.45 (PE/ EtOAc = 4:1)

[α]_D²⁴ = +29.8° (c 1.0, CHCl₃)

methyl *N*-allyl-*N*-(benzo[*d*]thiazol-2-ylsulfonyl)-*D*-alaninate (**3-238**)



Method E: Starting from sulfonamide **3-118** (0.6 g, 2.0 mmol, 1.0 equiv.) and allyl bromide (0.35 mL, 4.0 mmol, 2.0 equiv.). The crude product was purified by column chromatography (SiO₂; petroleum ether/EtOAc = 8:1) to afford **3-238** as a colorless oil (0.5 g, 74 % yield, *e.r.* = ≥ 1:99).

¹H NMR (500 MHz, Chloroform-*d*) δ (ppm): 8.17 (dt, *J* = 8.4, 0.9 Hz, 1H), 7.97 (dt, *J* = 8.0, 1.0 Hz, 1H), 7.60 (ddd, *J* = 8.2, 7.2, 1.3 Hz, 1H), 7.55 (ddd, *J* = 8.4, 7.1, 1.3 Hz, 1H), 5.93 (ddt, *J* = 17.2, 10.2, 6.1 Hz, 1H), 5.26 (dq, *J* = 17.2, 1.5 Hz, 1H), 5.16 (dq, *J* = 10.2, 1.3 Hz, 1H), 4.87 (q, *J*

Chapter III: Experimental section

= 7.3 Hz, 1H), 4.24 (ddt, $J = 16.7, 6.2, 1.6$ Hz, 1H), 4.00 (ddt, $J = 16.6, 6.2, 1.4$ Hz, 1H), 3.46 (s, 3H), 1.50 (d, $J = 7.4$ Hz, 3H).

^{13}C { ^1H } NMR (126 MHz, Chloroform-*d*) δ (ppm): 171.4, 165.7, 152.6, 136.4, 134.6, 127.7, 127.5, 125.2, 122.3, 118.4, 56.1, 52.5, 49.2, 16.6.

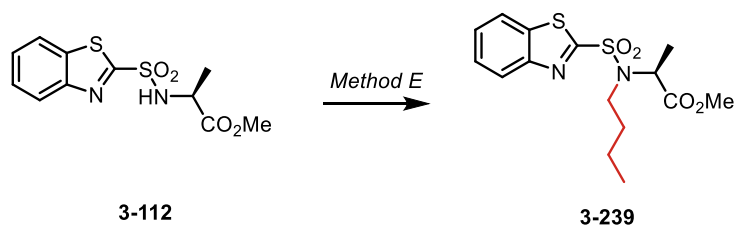
MS (ESI) m/z (%): 340 [M+H]⁺ (100).

HRMS (ESI) m/z : [M+H]⁺ calculated for C₁₄H₁₇N₂O₄S₂: 341.0624; found: 341.0628.

$R_f = 0.45$ (PE/ EtOAc = 4:1)

$[\alpha]_D^{24} = -25.0^\circ$ (c 0.8, CHCl₃)

methyl *N*-(benzo[*d*]thiazol-2-ylsulfonyl)-*N*-butyl-L-alaninate (**3-239**)



Method E: Starting from sulfonamide **3-112** (0.6 g, 2.0 mmol, 1.0 equiv.) and 1-iodobutane (0.46 mL, 4.0 mmol, 2.0 equiv.). The crude product was purified by gradient column chromatography (SiO₂; petroleum ether/EtOAc = 10:1 → 5:1) to afford **3-239** as a colorless solid (0.55 g, 77 % yield, *e.r.* = ≥ 1:99).

^1H NMR (500 MHz, Chloroform-*d*) δ (ppm): 8.16 (dt, $J = 8.7, 0.8$ Hz, 1H), 7.97 (dt, $J = 8.0, 0.9$ Hz, 1H), 7.60 (ddd, $J = 8.3, 7.2, 1.4$ Hz, 1H), 7.55 (ddd, $J = 8.3, 7.2, 1.3$ Hz, 1H), 4.85 (q, $J = 7.3$ Hz, 1H), 3.57 (ddd, $J = 15.6, 10.9, 5.1$ Hz, 1H), 3.45 (s, 3H), 3.21 (ddd, $J = 15.0, 11.0, 5.5$ Hz, 1H), 1.83 – 1.74 (m, 1H), 1.67 – 1.60 (m, 1H), 1.51 (d, $J = 7.3$ Hz, 3H), 1.37 – 1.30 (m, 2H), 0.93 (t, $J = 7.3$ Hz, 3H).

^{13}C { ^1H } NMR (126 MHz, Chloroform-*d*) δ (ppm): 171.6, 165.6, 152.6, 136.4, 127.6, 127.5, 125.2, 122.2, 56.2, 52.5, 46.9, 33.3, 20.2, 16.7, 13.9.

MS (ESI) m/z (%): 357 [M+H]⁺ (100).

HRMS (ESI) m/z : [M+H]⁺ calculated for C₁₅H₂₁N₂O₄S₂: 357.0937; found: 357.0945.

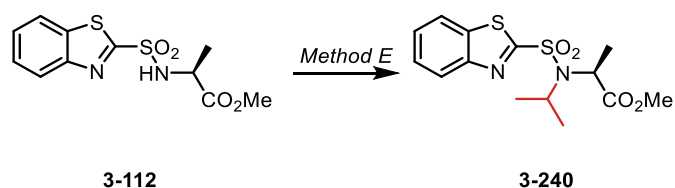
$R_f = 0.55$ (PE/ EtOAc = 2:1)

$[\alpha]_D^{23} = -50.1^\circ$ (c 1.2, CHCl₃)

m. p. = 53-55 °C

Chapter III: Experimental section

methyl *N*-(benzo[*d*]thiazol-2-ylsulfonyl)-*N*-isopropyl-L-alaninate (**3-240**)



Method D: Starting from sulfonamide **3-112** (0.11 g, 0.37 mmol, 1.0 equiv.) and isopropanol (0.06 mL, 0.73 mmol, 2.0 equiv.). The crude product was purified by column chromatography (SiO₂; petroleum ether/EtOAc = 4:1) to afford **3-240** as a colorless oil (0.1 g, 80 % yield, *e.r.* = ≥ 99:1).

¹H NMR (500 MHz, Chloroform-*d*) δ (ppm): 8.13 (dt, *J* = 8.5, 0.9 Hz, 1H), 7.95 (dt, *J* = 7.6, 0.8 Hz, 1H), 7.58 (ddd, *J* = 8.3, 7.1, 1.4 Hz, 1H), 7.53 (ddd, *J* = 8.3, 7.1, 1.3 Hz, 1H), 4.33 (q, *J* = 7.2 Hz, 1H), 4.27 (p, *J* = 6.8 Hz, 1H), 3.69 (s, 3H), 1.63 (d, *J* = 7.2 Hz, 3H), 1.38 (d, *J* = 6.8 Hz, 3H), 1.27 (d, *J* = 6.8 Hz, 3H).

¹³C {¹H} NMR (126 MHz, Chloroform-*d*) δ (ppm): 171.9, 167.7, 152.4, 136.4, 127.5, 127.3, 125.1, 122.2, 53.8, 52.7, 52.1, 21.9, 21.6, 17.6.

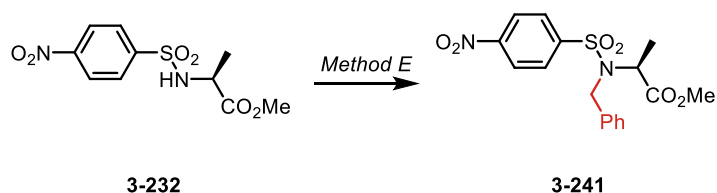
MS (ESI) *m/z* (%): 343 [M+H]⁺ (100).

HRMS (ESI) *m/z*: [M+H]⁺ calculated for C₁₄H₁₉N₂O₄S₂: 343.0781; found: 343.0783.

R_f = 0.40 (PE/ EtOAc = 2:1)

[α]_D²³ = +17.8° (c 1.1, CHCl₃)

methyl *N*-benzyl-*N*-((4-nitrophenyl)sulfonyl)-L-alaninate (**3-241**)



Prepared according to a literature. Spectroscopic data match those in the literature.²⁴⁵

To the mixture of nosyl-protected alanine methyl ester **3-232** (1.95 g, 6.76 mmol, 1.0 equiv.) and K₂CO₃ (0.6g, 7.4 mmol, 1.5 equiv.) in DMF (14 mL, 0.5 M) was added benzyl bromide (0.89 mL, 7.4 mmol, 1.05 equiv.) at 0 °C. The mixture was stirred overnight at room temperature for 16 h. Upon completion, the solid was removed by filtration through cotton wool. The filtrate was washed with HCl (1 M), saturated NaHCO₃ (15 mL) solution and brine (15 mL), dried with

Chapter III: Experimental section

anhydrous Na₂SO₄. The crude product **3-241** was used in the next step without further purification (2.3 g, 86 % yield, *e.r.* = ≥ 99:1).

¹H NMR (500 MHz, Chloroform-*d*) δ (ppm): 8.32 – 8.27 (m, 2H), 7.97 – 7.91 (m, 2H), 7.30 – 7.27 (m, 4H), 4.73 (q, *J* = 7.3 Hz, 1H), 4.64 (d, *J* = 15.9 Hz, 1H), 4.38 (d, *J* = 15.9 Hz, 1H), 3.53 (s, 3H), 1.36 (d, *J* = 7.3 Hz, 3H).

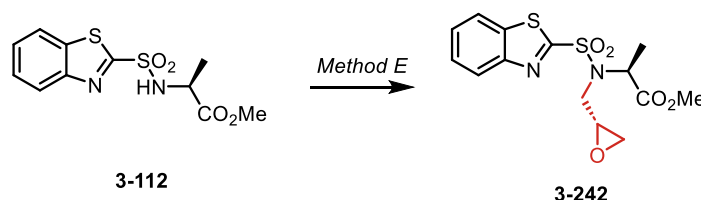
¹³C {¹H} NMR (126 MHz, Chloroform-*d*) δ (ppm): 171.3, 150.0, 146.0, 136.4, 128.7, 128.7, 128.3, 128.0, 124.1, 56.01, 52.5, 49.8, 17.1.

MS (ESI) *m/z* (%): 379 [M+H]⁺ (100).

HRMS (ESI) *m/z*: [M+H]⁺ calculated for C₁₇H₁₉N₂O₆S₂: 379.0964; found: 379.1031.

[α]_D²³ = -34.9° (*c* 1.0, CHCl₃)

methyl *N*-(benzo[*d*]thiazol-2-ylsulfonyl)-*N*-(((*R*)-oxiran-2-yl)methyl)-*L*-alaninate (**3-242**)



Method D: Starting from sulfonamide **3-112** (0.09 g, 0.3 mmol, 1.0 equiv.) and (*R*)-Glycidol (0.04 mL, 0.6 mmol, 2.0 equiv.). The crude product was purified by semipreparative HPLC using gradient (MeOH:AcCN = 90:10 → 30:70 → 90:10) to afford **2-242** as a slightly yellow oil (0.066 g, 92 % yield, *e.r.* = ≥ 99:1).

¹H NMR (500 MHz, Chloroform-*d*) δ (ppm): 8.16 (dt, *J* = 8.3, 1.0 Hz, 1H), 8.00 – 7.96 (m, 1H), 7.61 (ddd, *J* = 8.4, 7.2, 1.3 Hz, 1H), 7.56 (ddd, *J* = 8.4, 7.2, 1.3 Hz, 1H), 4.89 (q, *J* = 7.3 Hz, 1H), 3.87 – 3.82 (m, 1H), 3.54 (s, 3H), 3.45 (dd, *J* = 16.0, 5.9 Hz, 1H), 3.36 – 3.31 (m, 1H), 2.84 (t, *J* = 4.3 Hz, 1H), 2.63 (dd, *J* = 4.7, 2.6 Hz, 1H), 1.49 (d, *J* = 7.3 Hz, 3H).

¹³C {¹H} NMR (126 MHz, Chloroform-*d*) δ (ppm): 171.3, 165.4, 152.6, 136.4, 127.8, 127.6, 125.2, 122.3, 56.2, 52.7, 51.1, 48.3, 46.2, 15.9.

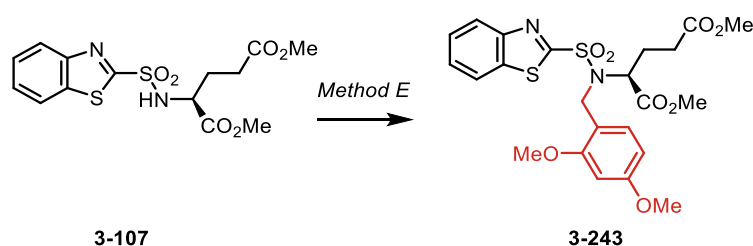
MS (ESI) *m/z* (%): 357 [M+H]⁺ (100).

HRMS (ESI) *m/z*: [M+H]⁺ calculated for C₁₄H₁₇N₂O₅S₂: 357.0573; found: 357.0582.

[α]_D²³ = -440° (*c* 0.25, DCM)

Chapter III: Experimental section

dimethyl *N*-(benzo[*d*]thiazol-2-ylsulfonyl)-*N*-(2,4-dimethoxybenzyl)-L-glutamate (**3-243**)



Method D: Starting from sulfonamide **3-107** (0.2 g, 0.54 mmol, 1.0 equiv.) and 2,4-dimethoxybenzylalcohol (0.184 g, 1.07 mmol, 2.0 equiv.). The crude product was purified by column chromatography (petroleum ether/EtOAc = 10:1) to afford **3-243** as a yellow oil (0.2 g, 72 % yield, *e.r.* = \geq 99:1).

¹H NMR (500 MHz, Chloroform-*d*) δ (ppm): 8.18 (dd, *J* = 8.5, 1.9 Hz, 1H), 7.97 (dd, *J* = 8.0, 1.6 Hz, 1H), 7.60 (ddd, *J* = 8.4, 7.2, 1.3 Hz, 1H), 7.55 (ddd, *J* = 8.3, 7.2, 1.2 Hz, 1H), 7.48 (d, *J* = 8.5 Hz, 1H), 6.47 (dd, *J* = 8.5, 2.4 Hz, 1H), 6.32 (d, *J* = 2.4 Hz, 1H), 4.73 (d, *J* = 15.5 Hz, 1H), 4.73 – 4.64 (m, 2H), 4.62 (d, *J* = 15.4 Hz, 1H), 3.78 (s, 3H), 3.67 (s, 3H), 3.58 (s, 3H), 3.35 (s, 3H), 2.36 – 2.19 (m, 3H), 1.95 (qd, *J* = 12.0, 10.1, 3.4 Hz, 1H).

¹³C {¹H} NMR (126 MHz, Chloroform-*d*) δ (ppm): 173.1, 170.4, 165.7, 161.1, 158.3, 152.7, 136.6, 132.3, 127.6, 127.5, 125.2, 122.2, 116.3, 104.6, 98.2, 60.0, 55.5, 55.3, 52.4, 51.7, 44.8, 30.2, 24.6.

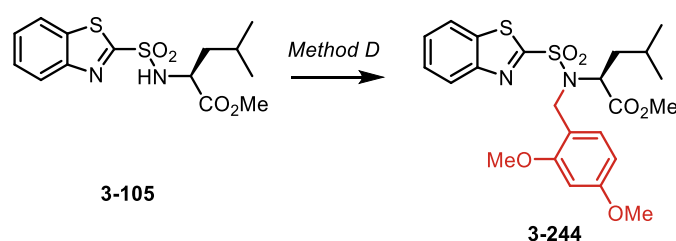
MS (ESI) *m/z* (%): 523 [M+H]⁺ (100).

HRMS (ESI) *m/z*: [M+K]⁺ calculated for C₂₃H₂₆N₂O₈S₂: 561.0768; found: 531.0755.

R_f = 0.35 (hexane/ EtOAc = 5:1)

Chapter III: Experimental section

methyl *N*-(benzo[*d*]thiazol-2-ylsulfonyl)-*N*-(2,4-dimethoxybenzyl)-*L*-leucinate (**3-244**)



Method D: Starting from sulfonamide **3-105** (0.2 g, 0.61 mmol, 1.0 equiv.) and 2,4-dimethoxybenzylalcohol (0.21 g, 1.22 mmol, 2.0 equiv.). The crude product was purified by column chromatography (petroleum ether/EtOAc = 10:1) to afford **3-244** as a colorless oil (0.2 g, 70 % yield, *e.r.* = \geq 99:1).

^1H NMR (500 MHz, Chloroform-*d*) δ (ppm): 8.18 (dt, J = 8.3, 0.9 Hz, 1H), 8.01 – 7.95 (m, 1H), 7.60 (ddd, J = 8.4, 7.3, 1.4 Hz, 1H), 7.58 – 7.53 (m, 2H), 6.50 (dd, J = 8.5, 2.4 Hz, 1H), 6.37 (d, J = 2.4 Hz, 1H), 4.77 – 4.71 (m, 2H), 4.67 (d, J = 16.4 Hz, 1H), 3.80 (s, 3H), 3.72 (s, 3H), 3.31 (s, 3H), 1.58 (t, J = 7.0 Hz, 2H), 1.50 (dt, J = 13.2, 6.6 Hz, 1H), 0.86 (d, J = 6.3 Hz, 3H), 0.61 (d, J = 6.6 Hz, 3H).

^{13}C { ^1H } NMR (126 MHz, Chloroform-*d*) δ (ppm): 171.3, 165.6, 160.7, 157.8, 152.7, 136.6, 131.5, 130.4, 127.6, 127.4, 125.2, 122.2, 117.3, 104.5, 98.1, 59.2, 55.5, 55.3, 52.2, 44.1, 38.6, 24.6, 22.7, 21.6.

MS (ESI) m/z (%): 493 [M+H]⁺ (100).

HRMS (ESI) m/z : [M+H]⁺ calculated for C₂₃H₂₉N₂O₆S₂: 493.1462; found: 493.1459.

R_f = 0.40 (hexane/ EtOAc = 5:1)

Chapter III: Experimental section

Method A: Smiles rearrangement

Method A: A tertiary sulfonamide (1 equiv.) was dissolved in THF (0.1 M), and the solution was cooled to -95 °C (N₂/methanol). After 10 minutes 18-crown-6 (3 equiv.) and the solution of KHMDS (1 M in THF, 1.5 equiv.) were added. The reaction was kept at -95 °C and the progress was monitored by TLC. Resulting mixture was quenched after 30 minutes (unless stated otherwise) by NH₄Cl (15 mL) and EtOAc (15 mL) was added. Resulting layers were separated and the aqueous layer was extracted with EtOAc (3 x 15 mL). Combined organic layers were washed with brine (15 mL), dried over MgSO₄, filtered, and the solvents were removed under reduced pressure to yield the crude product.

Method B: Smiles rearrangement

Method B: A tertiary sulfonamide (1 equiv.) was dissolved in THF (0.1 M), and the solution was cooled to -95 °C (N₂/methanol). After 10 minutes the solution of LiHMDS (1 M in THF, 1.5 equiv.) were added. The reaction was kept at -95 °C and the progress was monitored by TLC. Resulting mixture was quenched after 30 minutes (unless stated otherwise) by NH₄Cl (15 mL) and EtOAc (15 mL) was added. Resulting layers were separated and the aqueous layer was extracted with EtOAc (3 x 15 mL). Combined organic layers were washed with brine (15 mL), dried over MgSO₄, filtered, and the solvents were removed under reduced pressure to yield the crude product.

Method C: Smiles rearrangement

Method C: To a solution of HMDS (1.5 equiv.) in tetrahydrofuran (0.1 M) cooled in an ice-water bath was added *n*-BuLi (1.5 equiv.) *via* syringe. The mixture was stirred at room temperature for 15-30 min prior to use. After that, solution was cooled to -95 °C (N₂/methanol) and sulfonamide (1 equiv.) was added. After 30 minutes (unless stated otherwise) the reaction was quenched with sat. NH₄Cl and EtOAc (15 mL) was added. Resulting layers were separated and the aqueous layer was extracted with EtOAc (3 x 15 mL). Combined organic layers were washed with brine (15 mL), dried over MgSO₄, filtered, and the solvents were removed under reduced pressure to yield the crude product.

Method D: Smiles rearrangement

Method D: A tertiary sulfonamide (1 equiv.) was dissolved in THF (0.1 M), and the solution was cooled to -78 °C (N₂/acetone or dry ice/acetone). Then 18-crown-6 (3 equiv.) and LiCl (1.1 equiv.) were added following addition of NaHMDS (1 M in THF, 1.5 equiv.). The reaction was

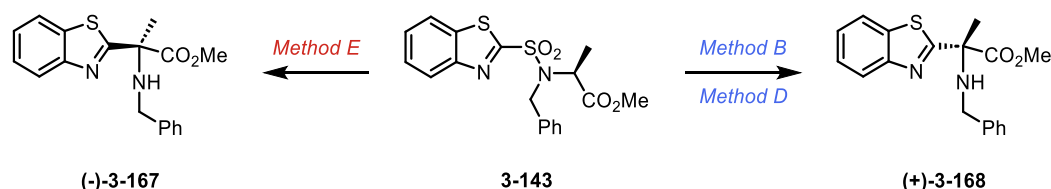
Chapter III: Experimental section

kept at -78 °C and the progress was monitored by TLC. Resulting mixture was quenched after 30 minutes (unless stated otherwise) by NH₄Cl (15 mL) and EtOAc (15 mL) was added. Resulting layers were separated and the aqueous layer was extracted with EtOAc (3 x 15 mL). Combined organic layers were washed with brine (15 mL), dried over MgSO₄, filtered, and the solvents were removed under reduced pressure to yield the crude product.

Method E: Smiles rearrangement inversion

Method E: A tertiary sulfonamide (1 equiv.) was dissolved in THF (0.1 M), and the solution was cooled to -78 °C (N₂/acetone or dry ice/acetone). Then CuOTf (1.1 equiv.) was added following addition of KHMDS (1 M in THF, 1.5 equiv.). The reaction was kept at -78 °C and the progress was monitored by TLC. Resulting mixture was quenched after 30 minutes (unless stated otherwise) by NH₄Cl (15 mL) and EtOAc (15 mL) was added. Resulting layers were separated and the aqueous layer was extracted with EtOAc (3 x 15 mL). Combined organic layers were washed with brine (15 mL), dried over MgSO₄, filtered, and the solvents were removed under reduced pressure to yield the crude product.

methyl 2-(benzo[d]thiazol-2-yl)-2-(benzylamino)propanoate



The crude product was purified by column chromatography (SiO₂; petroleum ether/EtOAc = 4:1) and obtained as colorless oil. **Method B:** Starting from 0.100 g (0.26 mmol, 1 equiv.) of **3-143**, yielded 0.061 g (73 %) of **(+)-3-167**, *e.r.* = ≥ 97:3 [α]_D²⁰ = + 17.3° (*c* 1.2, CHCl₃); **Method D:** 0.2 g (0.51 mmol, 1 equiv.) of **(+)-3-143**, yielded 0.15 g (92 %) of **3-167**, *e.r.* = ≥ 96:4, [α]_D²⁴ = - 11.7° (*c* 1, CHCl₃). **Method E:** Starting from 0.1 g (0.26 mmol, 1 equiv.) of **3-143**, yielded 0.055 g (67 %) of **(-)-3-167**, *e.r.* = ≥ 10:90, [α]_D²⁴ = - 15.8° (*c* 1, CHCl₃).

¹H NMR (400 MHz, Chloroform-*d*) δ (ppm): 8.04 (dt, *J* = 8.1, 1.0 Hz, 1H), 7.89 (dt, *J* = 8.0, 0.9 Hz, 1H), 7.50 – 7.33 (m, 6H), 7.31 – 7.26 (m, 1H), 3.84 – 3.79 (m, 1H), 3.79 (s, 3H), 2.83 (bs, 1H), 1.96 (s, 3H).

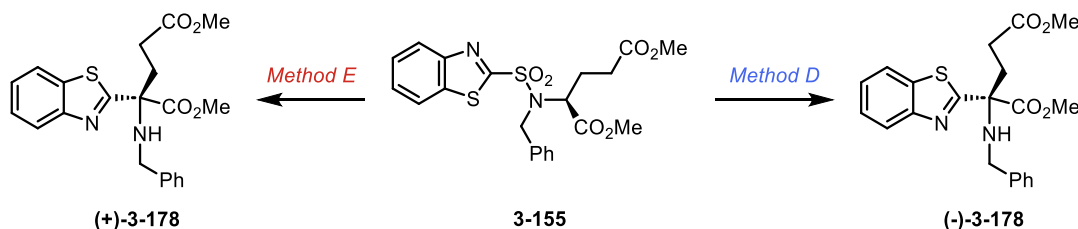
¹³C NMR (101 MHz, Chloroform-*d*) δ (ppm): 175.2, 172.9, 153.5, 139.7, 135.6, 128.6, 128.4, 127.4, 126.1, 125.3, 123.5, 121.8, 66.5, 53.2, 48.2, 23.7.

MS (ESI) *m/z* (%) 327: [M+H]⁺ (100).

HRMS (ESI) m/z : $[M+H]^+$ calc. for $C_{18}H_{19}N_2O_2S$, 327.1167; found: 327.1156.

HPLC (AD-H, Hexane : iPrOH = 90:10, 0.5 mL/min, 298 K, 220 nm): t_{R1} = 11.95 min, t_{R2} = 14.95 min.

dimethyl 2-(benzo[*d*]thiazol-2-yl)-2-(benzylamino)pentanedioate



Reaction time was increased to 1h and 3 equiv. of $LiNTMS_2$ were used. The crude product was purified using preparative TLC (SiO_2 ; petroleum ether/EtOAc = 2:1) and obtained as white solid. **Method D:** 0.185 g (0.4 mmol, 1 equiv.) of **3-155**, yielded 0.089 g (55 %, 74 % after recuperating starting material) of **(-)-3-178**, *e.r.* = $\geq 94:6$; $[\alpha]_D^{20}$ = -12.1° (*c* 1.2, $CHCl_3$).

Method E: 0.05 g (0.1 mmol, 1 equiv.) of **3-155**, yielded 0.022 g (89 %) of **(+)-3-178** after recuperating starting material (conversion = 50 %), *e.r.* = $\geq 17:83$, $[\alpha]_D^{22}$ = $+15.2$ (*c* 0.5, $CHCl_3$).

1H NMR (500 MHz, Chloroform-*d*) δ (ppm): 8.05 (dt, J = 8.2, 0.8 Hz, 1H), 7.89 (dt, J = 7.9, 0.9 Hz, 1H), 7.49 (ddd, J = 8.3, 7.2, 1.3 Hz, 1H), 7.45 – 7.37 (m, 3H), 7.40 – 7.30 (m, 3H), 7.33 – 7.24 (m, 2H), 3.78 (s, 3H), 3.78 – 3.66 (m, 5H), 3.63 (s, 3H), 2.90 – 2.80 (m, 1H), 2.80 – 2.68 (m, 1H), 2.46 (t, J = 8.1 Hz, 2).;

^{13}C $\{^1H\}$ NMR (126 MHz, Chloroform-*d*) δ (ppm): 173.3, 173.0, 171.8, 153.3, 139.3, 135.4, 128.6, 128.6, 128.3, 128.2, 127.5, 126.2, 125.4, 123.6, 121.8, 68.7, 53.2, 51.9, 47.5, 30.1, 28.8.

MS (ESI) m/z (%) 361: $[M+H]^+$ (100).

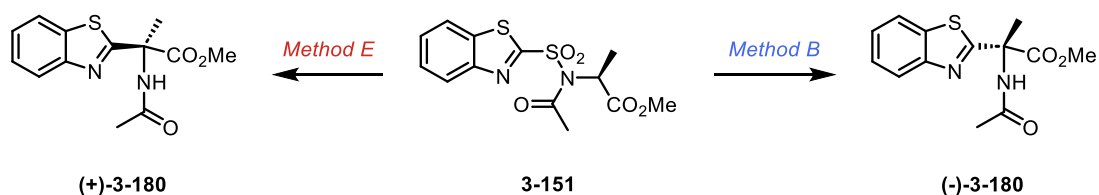
HRMS (ESI) m/z : $[M+H]^+$ calc. for $C_{21}H_{23}N_2O_4S$, 399.1373; found: 399.1380.

HPLC (AD-H, Hexane : iPrOH = 80:20, 0.5 mL/min, 298 K, 220 nm): t_{R1} = 15.20 min, t_{R2} = 18.38 min.

m. p. = 80 – 82 $^\circ C$

Chapter III: Experimental section

methyl 2-acetamido-2-(benzo[d]thiazol-2-yl)propanoate (**3-180**)



The crude product was purified by column chromatography (SiO₂; petroleum ether/EtOAc = 4:1) and obtained as colorless oil. **Method D:** Starting from 0.1 g (0.29 mmol, 1 equiv.) of **3-151**, yielded 0.061 g (73 %) of **(-)-3-180**, *e.r.* = ≥ 64:36 [α]_D²² = -3.2° (*c* 0.6, CHCl₃).; **Method E:** 0.1 g (0.29 mmol, 1 equiv.) of **3-151** yielded 0.05 g (61 %) of **(+)-3-180**, *e.r.* = ≥ 24:76, [α]_D²¹ = +5.3° (*c* 1.1, CHCl₃).

¹H NMR (500 MHz, Chloroform-*d*) δ (ppm): 8.03 (dt, *J* = 8.3, 0.9 Hz, 1H), 7.87 (dt, *J* = 8.0, 0.9 Hz, 1H), 7.58 (s, 1H), 7.50 (ddd, *J* = 8.3, 7.2, 1.2 Hz, 1H), 7.41 (ddd, *J* = 8.3, 7.2, 1.1 Hz, 1H), 3.75 (s, 3H), 2.14 (s, 3H), 2.13 (s, 3H).

¹³C {¹H} NMR (126 MHz, Chloroform-*d*) δ (ppm): 171.0, 170.1, 169.6, 152.0, 135.7, 126.5, 125.9, 123.5, 121.9, 62.9, 53.8, 24.8, 23.6.

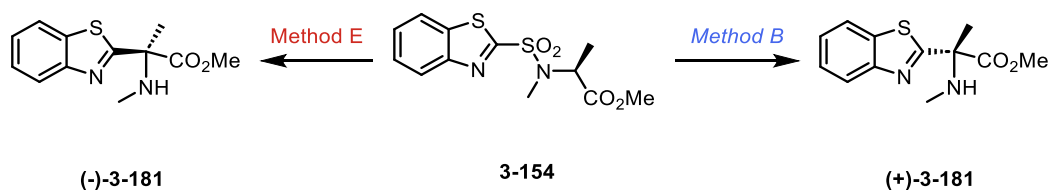
MS (ESI) *m/z* (%) 279: [M+H]⁺ (100).

HRMS (ESI) *m/z*: [M+H]⁺ calculated for C₁₃H₁₄N₂O₃S: 279.0798 found: 279.0800.

R_f = (hexane/ EtOAc = 5:1)

HPLC (AD-H, Hexane : iPrOH = 90:10, 0.5 mL/min, 298 K, 220 nm): *t*_{R1} = 12.00 min, *t*_{R2} = 12.53 min.

methyl 2-(benzo[d]thiazol-2-yl)-2-(methylamino)propanoate (**3-181**)



The crude product was purified by column chromatography (SiO₂; petroleum ether/EtOAc = 10:1) and obtained as colorless oil. **Method B:** 0.150 g (0.48 mmol, 1 equiv.) of **3-154**, yielded 0.098 g (82 %) of **(+)-3-181**, *e.r.* = ≥ 90:10 [α]_D²⁰ = + 7 (*c* 1.2, CHCl₃). **Method E:** 0.042 g (0.134 mmol, 1 equiv.) of **3-154**, yielded 0.025 g (75 %) of **(-)-3-181**, *e.r.* = ≥ 16:84, [α]_D²⁵ = - 6.5 ° (*c* 1, CHCl₃).

Chapter III: Experimental section

¹H NMR (500 MHz, Chloroform-*d*) δ (ppm): 8.02 (dt, *J* = 8.1, 1.0, 0.6 Hz, 2H), 7.88 (dt, *J* = 8.0, 1.3, 0.6 Hz, 1H), 7.47 (ddd, *J* = 8.3, 7.2, 1.3 Hz, 1H), 7.38 (ddd, *J* = 8.2, 7.2, 1.2 Hz, 1H), 3.79 (s, 3H), 2.43 (s, 3H), 1.85 (s, 3H).

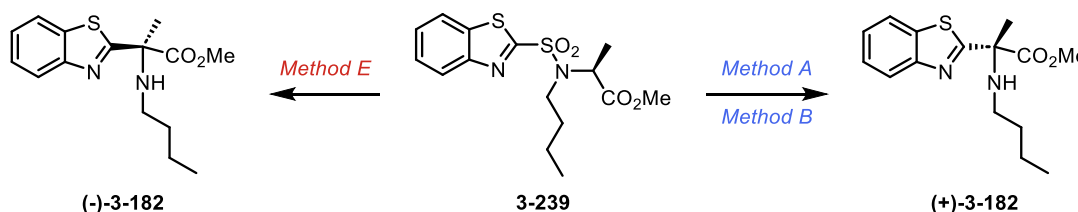
¹³C {¹H} NMR (126 MHz, Chloroform-*d*) δ (ppm): 175.0, 173.0, 153.4, 135.5, 126.1, 125.3, 123.5, 121.8, 66.8, 53.2, 30.5, 22.8.

MS (ESI) *m/z* (%): 251: [M+H]⁺ (100).

HRMS (ESI) *m/z*: [M+H]⁺ calc. for C₁₂H₁₅N₂O₂S, 251.0849; found: 251.0849.

HPLC (AD-H, Hexane : iPrOH = 90:10, 0.5 mL/min, 298 K, 220 nm): t_{R1} = 10.55 min, t_{R2} = 12.98 min.

methyl 2-(benzo[*d*]thiazol-2-yl)-2-(butylamino)propanoate (**3-182**)



The crude product was purified using preparative TLC (SiO₂; petroleum ether/EtOAc = 4:1) and obtained as colorless oil. **Method A:** Starting from 0.150 g (0.42 mmol, 1 equiv.) of **3-239**, yielded 0.090 g (73 %) of **(+)-3-182**, *e.r.* = ≥ 77:23, [α]_D²⁰ = + 2.2° (c 1, CHCl₃); **Method B:** 0.07 g (0.21 mmol, 1 equiv.) of **3-239**, yielded 0.091 g (74 %) of **3-182**, *e.r.* = ≥ 98:2, [α]_D²¹ = + 16.9° (c 1, CHCl₃). **Method E:** 0.05 g (0.14 mmol, 1 equiv.) of **3-239**, yielded 0.022 g (53 %) of **(-)-3-182** after recuperated starting material (conversion = 50 %), *e.r.* = ≥ 32:68, [α]_D²⁰ = - 2.1° (c 1, CHCl₃).

¹H NMR (500 MHz, Chloroform-*d*) δ (ppm): 8.01 (dt, *J* = 8.2, 0.9 Hz, 1H), 7.87 (dt, *J* = 8.0, 1.0 Hz, 1H), 7.45 (ddd, *J* = 8.3, 7.2, 1.3 Hz, 1H), 7.36 (ddd, *J* = 8.2, 7.1, 1.2 Hz, 1H), 3.77 (s, 3H), 2.66 – 2.51 (m, 2H), 2.49 (bs, 1H), 1.86 (s, 3H), 1.58 – 1.48 (m, 2H), 1.39 (h, *J* = 7.3 Hz, 2H), 0.91 (t, *J* = 7.3 Hz, 3H).

¹³C {¹H} NMR (126 MHz, Chloroform-*d*) δ (ppm): 175.6, 173.1, 153.4, 135.5, 126.0, 125.9, 125.2, 125.1, 123.4, 121.8, 66.3, 53.1, 43.5, 32.7, 23.4, 20.5, 14.1.

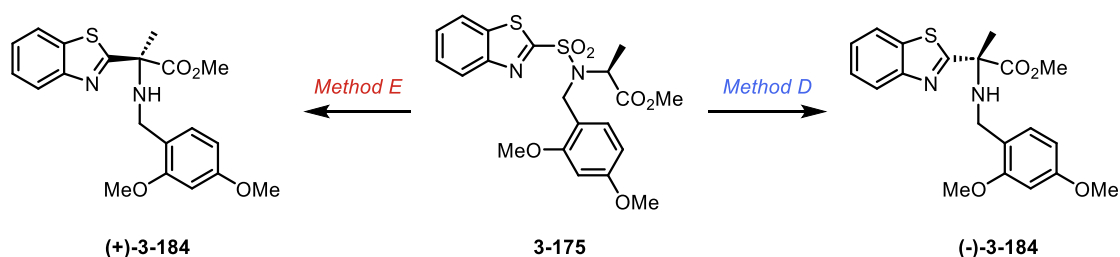
MS (ESI) *m/z* (%): 293 [M+H]⁺ (100).

HRMS (ESI) *m/z*: [M+H]⁺ calc. for C₁₅H₂₁N₂O₂S, 293.1324; found: 293.1326.

HPLC (AD-H, Hexane : iPrOH = 90:10, 0.5 mL/min, 298 K, 220 nm): t_{R1} = 9.07 min, t_{R2} = 10.67 min.

Chapter III: Experimental section

methyl 2-(benzo[d]thiazol-2-yl)-2-((2,4-dimethoxybenzyl)amino)propanoate (**3-184**)



The crude product was purified by gradient column chromatography (SiO₂; hexane/EtOAc = 15:1 → 5:1) and obtained as colorless oil. **Method D**: Starting from sulfonamide **3-175** (0.075 g, 0.17 mmol, 1.0 equiv.), yielded 0.031 g (80 %) of (-)-**3-184**, *e.r.* = 99:1, [α]_D³¹ = -6.8° (c 1, CHCl₃). **Method E**: Starting from sulfonamide **3-175** (0.075 g, 0.17 mmol, 1.0 equiv.), yielded 0.023 g (39 %) of (+)-**3-184**, *e.r.* = 8:92, [α]_D³¹ = +5.9° (c 1, CHCl₃).

¹H NMR (500 MHz, Chloroform-*d*) δ (ppm): 8.02 (dt, *J* = 8.3, 0.8 Hz, 1H), 7.91 – 7.83 (m, 1H), 7.46 (ddd, *J* = 8.4, 7.3, 1.2 Hz, 1H), 7.37 (ddd, *J* = 8.3, 7.1, 1.1 Hz, 1H), 7.26 (d, *J* = 0.8 Hz, 1H), 6.51 – 6.40 (m, 2H), 3.80 (d, *J* = 1.4 Hz, 7H), 3.69 (s, 3H), 1.94 (s, 3H).

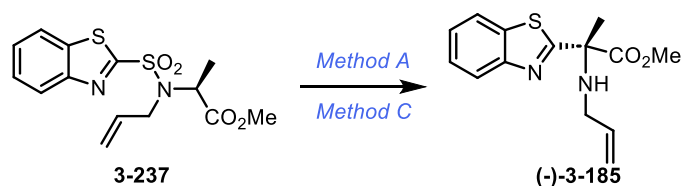
¹³C {¹H} NMR (126 MHz, Chloroform-*d*) δ (ppm): δ 176.1, 172.9, 160.3, 158.6, 153.5, 135.6, 130.4, 126.0, 125.1, 123.4, 121.8, 120.2, 104.0, 98.6, 66.2, 55.5, 55.4, 53.1, 42.9, 23.4.

MS (ESI) *m/z* (%): 387 [M+H]⁺ (100).

HRMS (ESI) *m/z*: [M+H]⁺ calculated for C₂₀H₂₂N₂O₄S: 387.1373; found: 387.1382.

R_f = 0.58 (hexane/EtOAc = 3:1)

HPLC (AD-H, Hexane : iPrOH = 90:10, 0.5 mL/min, 298 K, 220 nm): t_{R1} = 15.35 min, t_{R2} = 18.32 min.

methyl 2-(allylamino)-2-(benzo[*d*]thiazol-2-yl)propanoate (**3-185**)

The crude product was purified by column chromatography (SiO₂; petroleum ether/EtOAc = 10:1) and obtained as colorless oil. **Method A:** Starting from 0.075 g (0.22 mmol, 1 equiv.) of **3-237**, yielded 0.043 g (71 %) **(-)-3-185**, *e.r.* = ≥ 81:19, $[\alpha]_{\text{D}}^{24} = -3.6^{\circ}$ (*c* 1, CHCl₃); **Method C:** 0.045 g (0.13 mmol, 1 equiv.) of **3-237**, yielded 0.027 g (70 %) **(-)-3-185**, *e.r.* = ≥ 94:6, $[\alpha]_{\text{D}}^{24} = -6.8^{\circ}$ (*c* 1, CHCl₃).

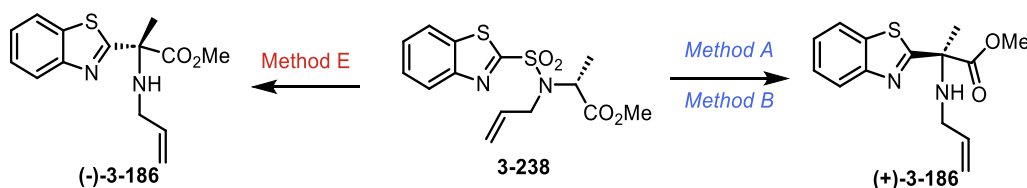
¹H NMR (500 MHz, Chloroform-*d*) δ (ppm): 8.02 (dd, *J* = 8.2, 1.0 Hz, 1H), 7.87 (dd, *J* = 7.9, 1.1 Hz, 1H), 7.46 (ddt, *J* = 8.1, 7.1, 1.1 Hz, 1H), 7.37 (ddt, *J* = 7.9, 7.0, 0.9 Hz, 1H), 6.00 – 5.91 (m, 1H), 5.33 – 5.22 (m, 1H), 5.18 – 5.09 (m, 1H), 3.78 (s, 3H), 3.34 – 3.20 (m, 2H), 1.90 (s, 3H).

¹³C {¹H} NMR (126 MHz, Chloroform-*d*) δ (ppm): 175.0, 172.8, 153.4, 136.0, 135.6, 126.1, 125.3, 123.5, 121.8, 116.7, 66.2, 53.2, 46.6, 23.4.

MS (ESI) *m/z* (%) 277: [M+H]⁺ (100).

HRMS (ESI) *m/z*: [M+H]⁺ calc. for C₁₄H₁₇N₂O₂S, 277.1005; found: 277.1008.

HPLC (AD-H, Hexane: iPrOH = 90:10, 0.5 mL/min, 298 K, 220 nm): *t*_{R1} = 9.70 min, *t*_{R2} = 11.12 min.

methyl 2-(allylamino)-2-(benzo[*d*]thiazol-2-yl)propanoate (**3-186**)

The crude product was purified by column chromatography (SiO₂; petroleum ether/EtOAc = 10:1) and obtained as colorless oil. **Method A:** Starting from 0.15 g (0.44 mmol, 1 equiv.) of **3-238**, yielded 0.098 g (80 %) of **(+)-3-186**, *e.r.* = ≥ 24:76, $[\alpha]_{\text{D}}^{24} = +1.3^{\circ}$ (*c* 0.7, CHCl₃); **Method B:** 0.150 g (0.44 mmol, 1 equiv.) of **3-238**, yielded 0.1 g (82 %) of **(+)-3-186**, *e.r.* = ≥ 2:98, $[\alpha]_{\text{D}}^{24} = +5.5^{\circ}$ (*c* 0.7, CHCl₃). **Method E:** 0.05 g (0.15 mmol, 1 equiv.) of **3-238**, yielded 0.025 g (51 %) of **(-)-3-186** after recuperated starting material (conversion = 30 %), *e.r.* = ≥ 73:27, $[\alpha]_{\text{D}}^{25} = -1.5^{\circ}$ (*c* 1, CHCl₃).

Chapter III: Experimental section

¹H NMR (500 MHz, Chloroform-*d*) δ (ppm): 8.02 (dt, *J* = 8.1, 1.0 Hz, 1H), 7.88 (dt, *J* = 7.8, 0.9 Hz, 1H), 7.47 (ddd, *J* = 8.3, 7.2, 1.3 Hz, 1H), 7.38 (ddd, *J* = 8.2, 7.2, 1.2 Hz, 1H), 5.96 (ddt, *J* = 17.0, 10.1, 5.8 Hz, 1H), 5.28 (dq, *J* = 17.1, 1.7 Hz, 1H), 5.14 (dq, *J* = 10.4, 1.4 Hz, 1H), 3.78 (s, 3H), 3.31 – 3.21 (m, 2H), 1.89 (s, 3H).

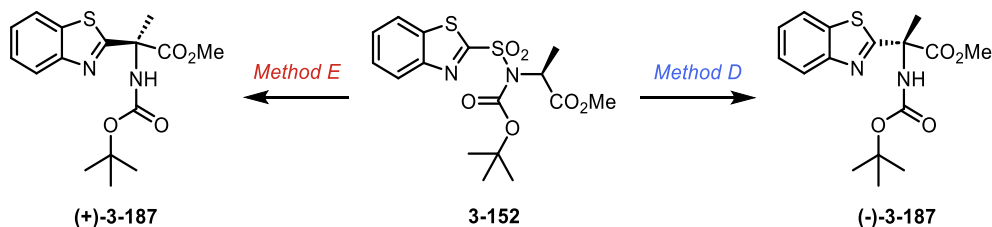
¹³C {¹H} NMR (126 MHz, Chloroform-*d*) δ (ppm): 175.2, 173.0, 153.5, 136.1, 135.6, 126.1, 125.3, 123.5, 121.8, 116.5, 66.2, 53.2, 46.6, 23.5.

MS (ESI) *m/z* (%) 277: [M+H]⁺ (100).

HRMS (ESI) *m/z*: [M+H]⁺ calc. for C₁₄H₁₇N₂O₂S, 277.1005; found: 277.1009.

HPLC (AD-H, Hexane: iPrOH = 90:10, 0.5 mL/min, 298 K, 220 nm): *t*_{R1} = 9.68 min, *t*_{R2} = 11.13 min.

methyl 2-(benzo[*d*]thiazol-2-yl)-2-((*tert*-butoxycarbonyl)amino)propanoate (**3-187**)



The crude product was purified by column chromatography (SiO₂; petroleum ether/EtOAc = 4:1) and obtained as colorless oil. **Method D:** starting from 0.1 g (0.25 mmol, 1 equiv.) of **3-230**, yielded 0.069 g (82 %) of **(-)-3-187**, *e.r.* = ≥ 89:11 [α]_D²² = -14.8° (*c* 1.2, CHCl₃).; **Method E:** 0.02 g (0.05 mmol, 1 equiv.) of **3-230** yielded 0.01 g (56 %) of **(+)-3-187** (conversion = 60%), *e.r.* = ≥ 25:75, [α]_D²¹ = +5.2° (*c* 1.2, CHCl₃).

¹H NMR (500 MHz, Chloroform-*d*) δ (ppm): 8.03 (dd, *J* = 8.0, 0.8 Hz, 1H), 7.86 (dd, *J* = 8.0, 1.4 Hz, 1H), 7.48 (ddd, *J* = 15.4, 8.6, 1.3 Hz, 1H), 7.40 (ddd, *J* = 15.1, 8.7, 1.3 Hz, 1H), 6.56 (bs, 1H), 3.75 (s, 3H), 2.13 (s, 3H), 1.48 – 1.38 (m, 9H).

¹³C {¹H} NMR (126 MHz, Chloroform-*d*) δ (ppm): 171.3, 170.7, 152.4, 135.9, 126.4, 125.7, 123.6, 121.8, 62.9, 53.7, 28.4.

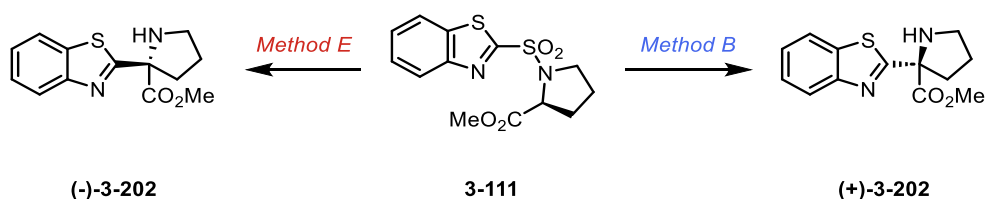
MS (ESI) *m/z* (%) 337: [M+H]⁺ (100).

HRMS (ESI) *m/z*: [M+H]⁺ calc. for C₁₆H₂₀N₂O₄S, 337.1217; found: 337.1215.

HPLC (OZ-H, Hexane : iPrOH = 95:5, 0.5 mL/min, 298 K, 220 nm): *t*_{R1} = 12.85 min, *t*_{R2} = 14.00 min.

Chapter III: Experimental section

methyl 2-(benzo[*d*]thiazol-2-yl)pyrrolidine-2-carboxylate (**3-202**)



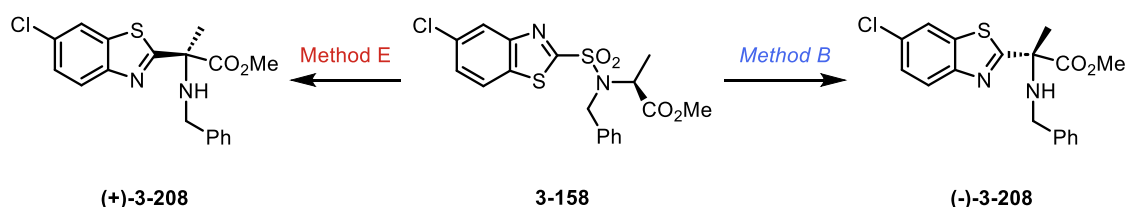
The crude product was purified by column chromatography (SiO₂; petroleum ether/EtOAc = 10:1) and obtained as colorless oil. **Method B**: 0.1 g (0.3 mmol, 1 equiv.) of **3-110**, yielded 0.061 g (76 %) of **3-216**, *e.r.* = ≥ 98:2; [α]_D²⁰ = + 22° (1.2 c; CHCl₃). **Method E**: Starting from sulfonamide **3-110** (0.050 g, 0.15 mmol, 1.0 equiv.), yielded 0.008 g (21 %) of **3-216** (conversion = 50 %), *e.r.* = 6:94; [α]_D²² = - 18° (1.0 c; CHCl₃).

¹H NMR (400 MHz, Chloroform-*d*) δ (ppm): 8.01 (ddd, *J* = 8.1, 1.2, 0.7 Hz, 1H), 7.86 (ddd, *J* = 8.0, 1.3, 0.6 Hz, 1H), 7.44 (ddd, *J* = 8.3, 7.2, 1.3 Hz, 1H), 7.35 (ddd, *J* = 8.3, 7.3, 1.2 Hz, 1H), 3.80 (s, 3H), 3.36 (bs, 1H), 3.22 – 3.10 (m, 2H), 2.69 – 2.54 (m, 2H), 1.95 – 1.85 (m, 2H).

¹³C NMR (101 MHz, Chloroform-*d*) δ (ppm): 177.3, 173.1, 154.3, 135.9, 125.9, 125.0, 123.3, 121.8, 72.4, 53.6, 47.1, 38.0, 26.1.

HPLC (AD-H, Hexane : iPrOH = 90:10, 0.5 mL/min, 298 K, 220 nm): *t*_{R1} = 14.25 min, *t*_{R2} = 15.30 min.

methyl 2-(benzylamino)-2-(6-chlorobenzo[*d*]thiazol-2-yl)propanoate (**3-208**)



The crude product was purified by column chromatography (SiO₂; petroleum ether/EtOAc = 10:1) and obtained as colorless oil. **Method B**: 0.040 g (0.094 mmol, 1 equiv.) of **3-158**, yielded 0.030 g (88 %) of **(-)-3-208**, *e.r.* = ≥ 94:6; [α]_D²⁰ = - 12.1° (c 1.2, CHCl₃). **Method E**: 0.032 g (0.075 mmol, 1 equiv.) of **3-158**, yielded 0.012 g (70 % after recuperating starting material) of **(+)-3-208** (conversion = 50 %), *e.r.* = ≥ 15:85, [α]_D²³ = + 11 ° (c 1, CHCl₃).

¹H NMR (500 MHz, Chloroform-*d*) δ (ppm): 8.02 (dd, *J* = 2.0, 0.5 Hz, 1H), 7.79 (dd, *J* = 8.5, 0.5 Hz, 1H), 7.44 – 7.41 (m, 2H), 7.37 – 7.34 (m, 3H), 7.30 – 7.27 (m, 1H), 3.82 – 3.75 (m, 5H; two signals overlap s 3H and q 2H), 2.86 (bs, 1H), 1.94 (s, 3H).

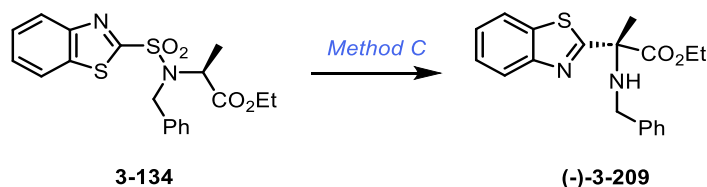
^{13}C { ^1H } NMR (126 MHz, Chloroform-*d*) δ (ppm): 177.5, 172.7, 154.4, 139.5, 133.9, 132.1, 128.7, 128.4, 127.5, 125.8, 123.3, 122.6, 66.5, 53.3, 48.1, 23.7.

MS (ESI) m/z (%): 361: $[\text{M}+\text{H}]^+$ (100).

HRMS (ESI) m/z : $[\text{M}+\text{H}]^+$ calc. for $\text{C}_{18}\text{H}_{18}\text{ClN}_2\text{O}_2\text{S}$, 361.0772; found: 361.0775.

HPLC (AD-H, Hexane : iPrOH = 90:10, 0.5 mL/min, 298 K, 220 nm): $t_{\text{R}1}$ = 12.07 min, $t_{\text{R}2}$ = 14.90 min.

ethyl 2-(benzo[*d*]thiazol-2-yl)-2-(benzylamino)propanoate (**3-209**)



The crude product was purified using preparative TLC (SiO_2 ; petroleum ether/EtOAc = 3:1) and obtained as colorless oil. **Method C**: 0.1 g (0.25 mmol, 1 equiv., *e.r.* = \geq 90:10) of **3-130**, yielded 0.061 g (72 %) of **(-)-3-209**, *e.r.* = \geq 90:10, $[\alpha]_{\text{D}}^{21} = -3.4^\circ$ (*c* 0.5, CHCl_3). **Method A**: 0.1 g (0.25 mmol, 1 equiv., *e.r.* = \geq 90:10) of **3-134**, yielded 0.057 g (65 %) of **3-209**, *e.r.* = \geq 50:50.

^1H NMR (500 MHz, Chloroform-*d*) δ (ppm): 8.05 (dt, $J = 8.2, 0.8$ Hz, 1H), 7.89 (dt, $J = 7.9, 0.8$ Hz, 1H), 7.48 (ddd, $J = 8.3, 7.1, 1.3$ Hz, 1H), 7.46 – 7.43 (m, 2H), 7.41 – 7.34 (m, 3H), 7.31 – 7.26 (m, 1H), 4.27 (q, $J = 7.1$ Hz, 2H), 3.84 – 3.77 (m, 2H), 2.85 (bs, 1H), 1.96 (s, 3H), 1.26 (t, $J = 7.1$ Hz, 3H).

^{13}C { ^1H } NMR (126 MHz, Chloroform-*d*) δ (ppm): 175.2, 172.3, 153.4, 139.7, 135.6, 128.6, 128.4, 127.4, 126.0, 125.2, 123.5, 121.8, 66.4, 62.2, 48.1, 23.6, 14.2.

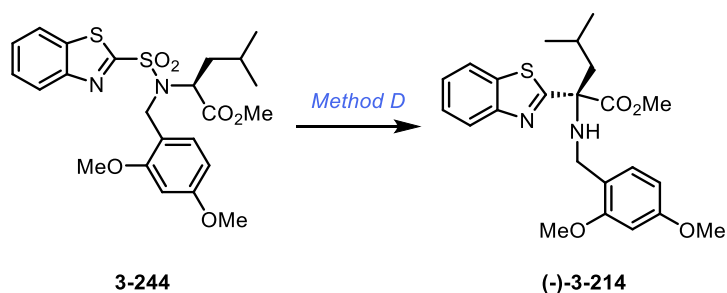
MS (ESI) m/z (%): 341 $[\text{M}+\text{H}]^+$ (100).

HRMS (ESI) m/z : $[\text{M}+\text{H}]^+$ calculated for $\text{C}_{19}\text{H}_{21}\text{N}_2\text{O}_2\text{S}$: 341.1318; found: 341.1319.

HPLC (AD-H, Hexane : iPrOH = 90:10, 0.5 mL/min, 298 K, 220 nm): $t_{\text{R}1}$ = 11.05 min, $t_{\text{R}2}$ = 13.65 min.

Chapter III: Experimental section

methyl 2-(benzo[*d*]thiazol-2-yl)-2-((2,4-dimethoxybenzyl)amino)-4-methylpentanoate (**3-214**)



The crude product was purified by column chromatography (SiO₂; petroleum ether/EtOAc = 4:1) and obtained as colorless oil. **Method D**: 0.045 g (0.09 mmol, 1 equiv.) of **3-244** yielded 0.054 g (72 %) **(-)-3-214** after recuperating starting material (conversion = 60 %), *e.r.* = ≥ 84:16, [α]_D²¹ = -18.6° (*c* 0.7, CHCl₃).

¹H NMR (500 MHz, Chloroform-*d*) δ (ppm): 8.05 (d, *J* = 8.2 Hz, 1H), 7.87 (d, *J* = 8.0 Hz, 1H), 7.46 (td, *J* = 8.3, 7.8, 1.5 Hz, 1H), 7.44 – 7.32 (m, 1H), 7.24 (d, *J* = 8.2 Hz, 1H), 6.49 – 6.40 (m, 2H), 3.79 (d, *J* = 6.8 Hz, 6H), 3.72 (d, *J* = 12.5 Hz, 1H), 3.68 (d, *J* = 1.1 Hz, 3H), 3.48 (d, *J* = 12.4 Hz, 1H), 3.09 (bs, 1H), 2.52 (dd, *J* = 14.7, 7.1 Hz, 1H), 2.37 (dd, *J* = 14.6, 4.7 Hz, 1H), 1.87 (ddt, *J* = 13.3, 11.2, 6.6 Hz, 1H), 0.93 (dd, *J* = 11.8, 6.7 Hz, 6H).

¹³C {¹H} NMR (126 MHz, Chloroform-*d*) δ (ppm): 175.6, 172.7, 160.3, 158.6, 153.6, 135.9, 130.3, 125.9, 125.1, 123.5, 121.8, 120.4, 104.0, 98.6, 68.9, 55.5, 55.4, 52.9, 43.2, 42.2, 29.9, 24.4, 23.8, 23.4.

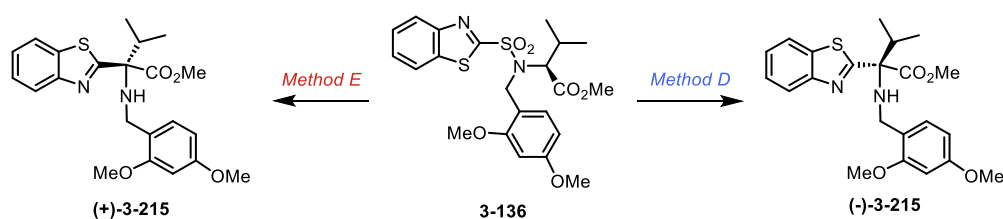
MS (ESI) *m/z* (%) 429: [M+H]⁺ (100).

HRMS (ESI) *m/z*: [M+H]⁺ calc. for C₂₃H₂₈N₂O₄S, 429.1843; found: 429.1845.

HPLC (AD-H, Hexane : iPrOH = 90:10, 0.5 mL/min, 298 K, 220 nm): *t*_{R1} = 11.47 min, *t*_{R2} = 12.27 min.

Chapter III: Experimental section

methyl 2-(benzo[*d*]thiazol-2-yl)-2-((2,4-dimethoxybenzyl)amino)-3-methylbutanoate (**3-215**)



The crude product was purified using preparative TLC (SiO₂; petroleum ether/EtOAc = 3:1) and obtained as colorless oil. **Method D**: 0.050 g (0.1 mmol, 1 equiv.) of **3-136** yielded 0.018 mg (42 %) of **(-)-3-215** (conversion = 50%) *e.r.* = ≥ 84:16, [α]_D²¹ = -16.3° (c 1, CHCl₃).

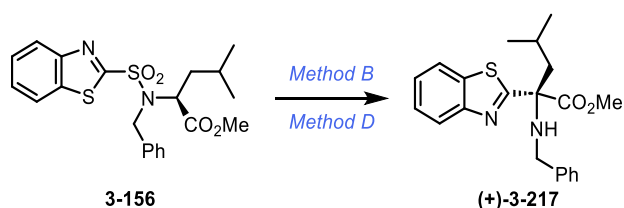
Method E: 0.050 g (0.1 mmol, 1 equiv.) of **3-136** yielded 0.016 mg (37, 75 %) of **(+)-3-215** after recuperating starting material (conversion = 52%) *e.r.* = ≥ 43:57 [α]_D²² = +8.2° (c 1, CHCl₃).

¹H NMR (500 MHz, Chloroform-*d*) δ (ppm): 8.07 (dt, *J* = 8.3, 1.4 Hz, 1H), 7.88 (dd, *J* = 8.0, 1.4 Hz, 1H), 7.49 – 7.43 (m, 1H), 7.39 – 7.34 (m, 1H), 7.30 – 7.22 (m, 2H), 6.46 (dt, *J* = 8.3, 2.0 Hz, 1H), 6.45 – 6.43 (m, 1H), 3.80 (s, 3H), 3.79 (s, 2H), 3.78 (s, 3H), 3.74 – 3.61 (m, 2H), 2.70 (hept, *J* = 13.8, 7.6, 3.4 Hz, 1H), 1.12 (dd, *J* = 6.7, 1.7 Hz, 3H), 0.99 (dd, *J* = 6.9, 1.7 Hz, 3H).

¹³C {¹H} NMR (126 MHz, Chloroform-*d*) δ (ppm): 172.4, 172.2, 160.3, 158.6, 153.5, 135.4, 130.2, 125.7, 124.9, 123.5, 121.5, 120.5, 104.0, 98.6, 73.0, 55.5, 55.4, 52.4, 43.8, 35.9, 18.4, 17.6.

HPLC (OZ-H, Hexane : iPrOH = 95:5, 0.5 mL/min, 298 K, 220 nm): *t*_{R1} = 16.25 min, *t*_{R2} = 29.68 min.

methyl 2-(benzo[*d*]thiazol-2-yl)-2-(benzylamino)-4-methylpentanoate (**3-217**)



The crude product was purified using preparative TLC (SiO₂; petroleum ether/EtOAc = 3:1) and obtained as colorless oil. **Method B**: Starting from 0.1 g (0.23 mmol, 1 equiv.) of **3-156**, yielded 0.134 g (73 %) of **(+)-3-217**, *e.r.* = ≥ 98:2; [α]_D²³ = +9.2 (1 c, CHCl₃). **Method D**: Starting from 0.22 g (0.5 mmol, 1 equiv.) of **3-156**, yielded 0.134 g (86 %) of **(+)-3-217**, *e.r.* = ≥ 95:5; [α]_D²⁴ = + 9.0 (1 c, CHCl₃).

¹H NMR (500 MHz, Chloroform-*d*) δ (ppm): 8.06 (dd, *J* = 8.2, 1.0 Hz, 1H), 7.89 (dd, *J* = 8.0, 1.1 Hz, 1H), 7.48 (ddd, *J* = 8.2, 7.3, 1.3 Hz, 1H), 7.45 – 7.41 (m, 2H), 7.41 – 7.38 (m, 1H), 7.37 – 7.33

Chapter III: Experimental section

(m, 2H), 7.30 – 7.27 (m, 1H), 3.74 (s, 3H), 3.72 – 3.63 (m, 2H), 2.96 (bs, 1H), 2.53 (dd, $J = 14.6$, 7.3 Hz, 1H), 2.43 – 2.34 (m, 1H), 1.87 (hd, $J = 6.8$, 4.8 Hz, 1H), 0.97 (d, $J = 6.7$ Hz, 3H), 0.93 (d, $J = 6.6$ Hz, 3H).

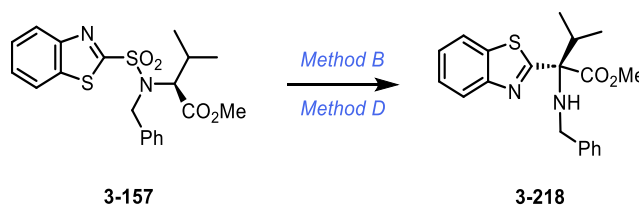
^{13}C { ^1H } NMR (126 MHz, Chloroform-*d*) δ (ppm): 172.5, 153.4, 135.8, 128.6, 128.4, 127.4, 126.1, 125.3, 123.5, 121.9, 69.1, 53.1, 47.5, 43.3, 24.4, 24.1, 23.2.

MS (ESI) m/z (%) 369: $[\text{M}+\text{H}]^+$ (100).

HRMS (ESI) m/z : $[\text{M}+\text{H}]^+$ calc. for $\text{C}_{21}\text{H}_{25}\text{N}_2\text{O}_2\text{S}$, 369.1631; found: 369.1625.

HPLC (AD-H, Hexane : iPrOH = 80:10, 0.5 mL/min, 298 K, 220 nm): $t_{\text{R}1} = 10.72$ min, $t_{\text{R}2} = 11.58$ min.

methyl 2-(benzo[*d*]thiazol-2-yl)-2-(benzylamino)-3-methylbutanoate (**3-218**)



The crude product was purified by semipreparative HPLC and obtained as colorless oil.

Method B: Starting from 0.2 g (0.473 mmol, 1 equiv.) of **3-157** yielded 0.102 mg (75 %) of **(+)-3-218**, (conversion = 60 %); *e.r.* = $\geq 85:15$; $[\alpha]_{\text{D}}^{22} = +31.7$ (*c* 0.6, CHCl_3).

Method D: Starting from 0.1 g (0.23 mmol, 1 equiv.) of **3-157** yielded 0.55 g (67 %) of **(+)-3-218**, *e.r.* = $\geq 99:1$; $[\alpha]_{\text{D}}^{23} = +50.5$ (1 *c*, CHCl_3).

^1H NMR (500 MHz, Chloroform-*d*) δ (ppm): 8.09 (dt, $J = 8.1$, 0.8 Hz, 1H), 7.90 (ddd, $J = 7.9$, 1.3, 0.6 Hz, 1H), 7.50 – 7.42 (m, 3H), 7.40 – 7.33 (m, 3H), 7.31 – 7.26 (m, 1H), 3.85 (s, 3H), 3.78 (d, $J = 12.5$ Hz, 1H), 3.69 (d, $J = 12.5$ Hz, 1H), 2.69 (h, $J = 6.8$ Hz, 1H), 2.47 (bs, 1H), 1.12 (d, $J = 6.7$ Hz, 3H), 1.00 (d, $J = 6.9$ Hz, 3H).

^{13}C { ^1H } NMR (126 MHz, Chloroform-*d*) δ (ppm): 172.1, 171.7, 153.3, 139.8, 135.4, 128.6, 128.3, 127.4, 125.8, 125.1, 123.5, 121.5, 73.4, 52.6, 49.1, 36.9, 18.4, 17.7.

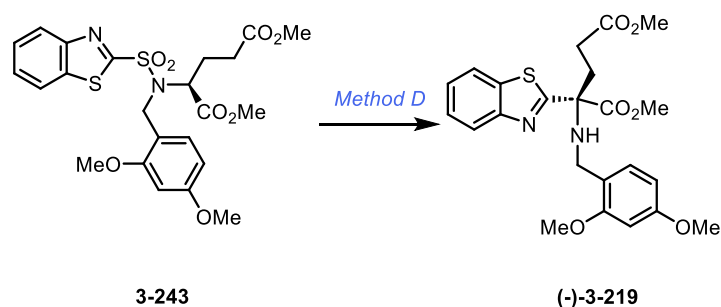
MS (ESI) m/z (%) 355: $[\text{M}+\text{H}]^+$ (100).

HRMS (ESI) m/z : $[\text{M}+\text{H}]^+$ calc. for $\text{C}_{20}\text{H}_{23}\text{N}_2\text{O}_2\text{S}$, 355.1475; found: 355.1471.

HPLC (AD-H, Hexane : iPrOH = 90:10, 0.5 mL/min, 298 K, 220 nm): $t_{\text{R}1} = 10.12$ min, $t_{\text{R}2} = 14.18$ min.

Chapter III: Experimental section

dimethyl 2-(benzo[*d*]thiazol-2-yl)-2-((2,4-dimethoxybenzyl)amino)pentanedioate (**3-219**)



The crude product was purified by column chromatography (SiO₂; petroleum ether/EtOAc = 4:1) and obtained as colorless oil. **Method D**: Starting from 0.05 g (0.096 mmol, 1 equiv.) of **3-243**, yielded 0.022 g (58 %; 89 % after recuperating starting material) of **(-)-3-219** (conversion = 70 %), *e.r.* = ≥ 89:11 [α]_D²² = -18.6° (c 1.1, CHCl₃).

¹H NMR (500 MHz, Chloroform-*d*) δ (ppm): 8.18 (dd, *J* = 8.5, 1.9 Hz, 1H), 7.97 (dd, *J* = 8.0, 1.6 Hz, 1H), 7.60 (ddd, *J* = 8.4, 7.2, 1.3 Hz, 1H), 7.55 (ddd, *J* = 8.3, 7.2, 1.2 Hz, 1H), 7.48 (d, *J* = 8.5 Hz, 1H), 6.47 (dd, *J* = 8.5, 2.4 Hz, 1H), 6.32 (d, *J* = 2.4 Hz, 1H), 4.73 (d, *J* = 15.5 Hz, 1H), 4.73 – 4.64 (m, 2H), 4.62 (d, *J* = 15.4 Hz, 1H), 3.78 (s, 3H), 3.67 (s, 3H), 3.58 (s, 3H), 3.35 (s, 3H), 2.36 – 2.19 (m, 3H), 1.95 (qd, *J* = 12.0, 10.1, 3.4 Hz, 1H).

¹³C {¹H} NMR (126 MHz, Chloroform-*d*) δ (ppm): 173.9, 173.6, 172.0, 160.4, 158.7, 153.5, 135.5, 130.5, 126.1, 125.3, 123.6, 121.8, 119.9, 104.0, 98.6, 68.4, 55.5, 55.4, 53.1, 51.8, 42.4, 29.8, 28.7.

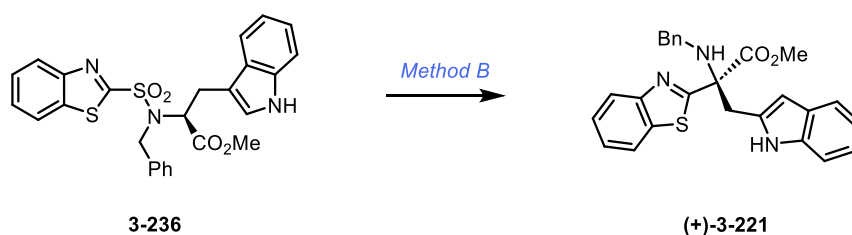
MS (ESI) *m/z* (%) 459: [M+H]⁺ (100).

HRMS (ESI) *m/z*: [M+H]⁺ calc. for C₁₇H₁₉N₂O₄, 459.1584; found: 459.1580.

HPLC (AD-H, Hexane : iPrOH = 90:10, 0.5 mL/min, 298 K, 220 nm): *t*_{R1} = 16.00 min, *t*_{R2} = 21.37 min.

Chapter III: Experimental section

methyl 2-(benzo[*d*]thiazol-2-yl)-2-(benzylamino)-3-(1*H*-indol-2-yl)propanoate (**3-221**)



The crude product was purified by preparative TLC (SiO₂; petroleum ether/EtOAc = 7:2) and obtained as colorless oil. **Method B**: Starting from 0.04 g (0.078 mmol, 1 equiv.) of **3-236**, yielded 0.025 g (73 %, 95 % rsm) **(+)-3-221**, *e.r.* = ≥ 92:8; [α]_D²² = +18.2 (*c* 1.2, CHCl₃).

¹H NMR (500 MHz, Chloroform-*d*) δ (ppm): 8.13 – 8.06 (m, 2H), 7.87 (dt, *J* = 8.0, 1.0 Hz, 1H), 7.60 (dt, *J* = 8.1, 0.9 Hz, 1H), 7.50 (ddd, *J* = 8.2, 7.2, 1.2 Hz, 1H), 7.41 – 7.38 (m, 3H), 7.33 – 7.30 (m, 3H), 7.26 – 7.23 (m, 1H), 7.15 (ddd, *J* = 8.0, 6.9, 1.1 Hz, 1H), 7.09 – 7.07 (m, 1H), 7.05 (ddd, *J* = 8.0, 7.0, 1.0 Hz, 1H), 4.18 (dd, *J* = 15.1, 0.8 Hz, 1H), 3.92 – 3.81 (m, 3H), 3.61 (s, 3H).

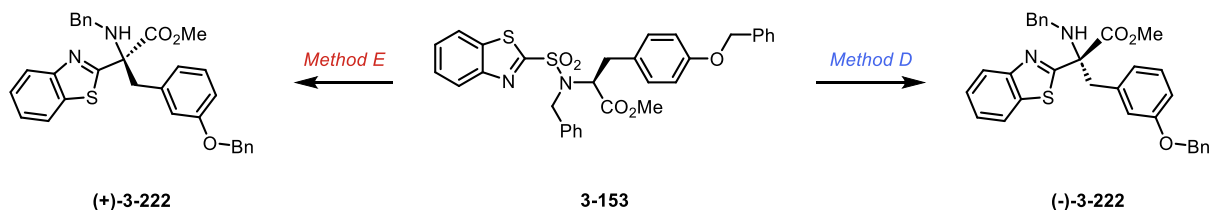
¹³C {¹H} NMR (126 MHz, Chloroform-*d*) δ (ppm): 173.9, 171.9, 153.3, 139.7, 136.1, 135.8, 128.5, 128.3, 128.1, 127.3, 126.0, 125.3, 123.6, 123.4, 122.2, 121.8, 119.6, 118.9, 111.2, 109.2, 70.2, 53.1, 47.7, 31.5.

MS (ESI) *m/z* (%) 442: [M+H]⁺ (100).

HRMS (ESI) *m/z*: [M+H]⁺ calc. for C₂₆H₂₄N₃O₂S, 442.1584; found: 442.1578.

HPLC (AD-H, Hexane : iPrOH = 90:10, 0.5 mL/min, 298 K, 220 nm): *t*_{R1} = 16.63 min, *t*_{R2} = 19.25 min.

dimethyl 2-(benzo[*d*]thiazol-2-yl)-2-((2,4-dimethoxybenzyl)amino)pentanedioate (**3-222**)



The crude product was purified by column chromatography (SiO₂; petroleum ether/EtOAc = 4:1) and obtained as colorless oil. **Method D**: Starting from 0.223 g (0.4 mmol, 1 equiv.) of **3-153**, yielded 0.158 g (78 %) of **(-)-3-222**, *e.r.* = ≥ 99:1 [α]_D²¹ = -25.6° (*c* 1.2, CHCl₃).; **Method E**: 0.03 g (0.05 mmol, 1 equiv.) of **3-153** yielded 0.018 g (67 %) of **(+)-3-222** (conversion was 50 %), *e.r.* = ≥ 15:85, [α]_D²¹ = +18.6° (*c* 1.2, CHCl₃).

¹H NMR (500 MHz, Chloroform-*d*) δ (ppm): 8.09 (d, *J* = 8.2 Hz, 1H), 7.88 (d, *J* = 8.0 Hz, 1H), 7.50 (t, *J* = 7.7 Hz, 1H), 7.44 – 7.36 (m, 7H), 7.34 (t, *J* = 7.9 Hz, 3H), 7.32 – 7.22 (m, 2H), 7.06 (d,

Chapter III: Experimental section

$J = 8.1$ Hz, 2H), 6.88 – 6.81 (m, 2H), 5.01 (s, 2H), 3.91 (dd, $J = 17.3, 13.4$ Hz, 2H), 3.80 (d, $J = 12.7$ Hz, 1H), 3.71 (d, $J = 1.4$ Hz, 3H), 3.65 (d, $J = 14.3$ Hz, 1H).

^{13}C $\{^1\text{H}\}$ NMR (126 MHz, Chloroform-*d*) δ (ppm): 173.6, 171.5, 158.1, 153.2, 139.5, 137.1, 136.0, 131.2, 128.7, 128.6, 128.3, 128.1, 127.7, 127.6, 127.4, 126.0, 125.4, 123.6, 121.9, 114.9, 70.8, 70.1, 53.0, 47.7, 40.4.

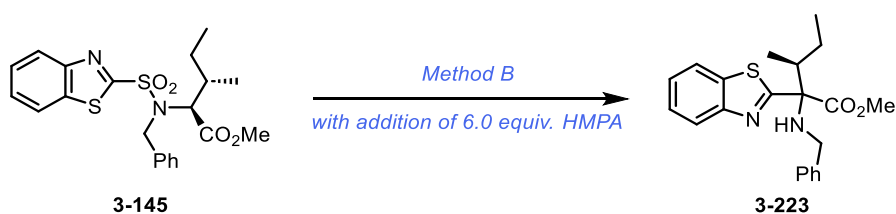
MS (ESI) m/z (%) 459: $[\text{M}+\text{H}]^+$ (100).

HRMS (ESI) m/z : $[\text{M}+\text{H}]^+$ calc. for $\text{C}_{17}\text{H}_{19}\text{N}_2\text{O}_4$, 459.1584; found: 459.1580.

$R_f = 0.65$ (hexane/ EtOAc = 4:1)

HPLC (AD-H, Hexane : iPrOH = 80:20, 0.5 mL/min, 298 K, 220 nm): $t_{R1} = 19.32$ min, $t_{R2} = 27.33$ min.

mixture of (3*S*) methyl 2-(benzo[*d*]thiazol-2-yl)-2-(benzylamino)-3-methylpentanoate (**3-223**)



The crude product was purified using preparative TLC (SiO_2 ; petroleum ether/EtOAc = 3:1) and obtained as colorless oil. **Modified method B:** Reaction time was increased to 1h, 3 equiv. of LiHMDS were used and HMPA (6.0 equiv.) was added. Starting from 0.050 g (0.114 mmol, 1 equiv., *e.r.* = 99:1) of **3-145**, yielded (54 %; 78 % on recuperating starting material) of **3-223** 0.023 g, *e.r.* = $\geq 52:48$, (conversion = 55 %).

^1H NMR (500 MHz, Chloroform-*d*) δ (ppm): 8.08 (dd, $J = 8.2, 3.7$ Hz, 2H), 7.89 (d, $J = 7.9$ Hz, 2H), 7.49 – 7.43 (m, 6H), 7.40 – 7.33 (m, 6H), 7.30 – 7.26 (m, 2H), 3.85 (d, $J = 3.9$ Hz, 6H), 3.80 – 3.74 (m, 2H), 3.69 (dd, $J = 12.4, 6.6$ Hz, 2H), 2.40 – 2.33 (m, 2H), 1.95 – 1.83 (m, 2H), 1.13 (d, $J = 6.7$ Hz, 3H), 1.00 (d, $J = 6.9$ Hz, 3H), 0.94 (t, $J = 7.4$ Hz, 3H), 0.91 – 0.87 (m, 3H).

^{13}C $\{^1\text{H}\}$ NMR (126 MHz, Chloroform-*d*) δ (ppm): 172.3, 172.1, 172.1, 172.1, 153.4, 153.3, 139.9, 139.8, 135.4, 135.4, 128.6, 128.3, 128.3, 127.4, 127.4, 125.8, 125.1, 123.5, 123.5, 121.5, 73.7, 73.7, 52.6, 52.6, 49.1, 49.1, 44.0, 43.8, 25.4, 24.3, 14.6, 13.9, 12.7, 12.6.

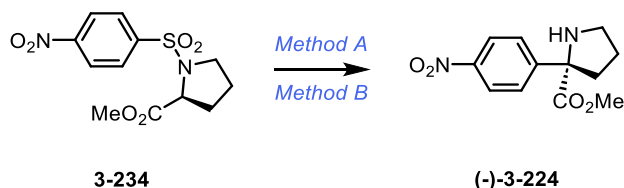
MS (ESI) m/z (%) 369: $[\text{M}+\text{H}]^+$ (100).

HRMS (ESI) m/z : $[\text{M}+\text{H}]^+$ calc. for $\text{C}_{18}\text{H}_{18}\text{ClN}_2\text{O}_2\text{S}$, 369.1631; found: 369.1633.

HPLC (AD-H, Hexane: iPrOH = 90:10, 0.5 mL/min, 298 K, 220 nm): $t_{R1} = 9.92$ min, $t_{R2} = 12.63$ min.

Chapter III: Experimental section

methyl 2-(4-nitrophenyl)pyrrolidine-2-carboxylate (**3-224**)



The crude product was purified using preparative TLC (SiO₂; petroleum ether/EtOAc = 4:1) and obtained as colorless oil. **Method A:** Starting from 0.07 g (0.21 mmol, 1 equiv.) of **3-224**, yielded 0.041 g (74 %) of **(-)-3-224**, *e.r.* = ≥ 91:9, [α]_D²⁰ = - 8° (c 1, CHCl₃); **Method B:** Starting from 0.07 g (0.21 mmol, 1 equiv.) of **3-234**, yielded 0.042 g (75 %) **(-)-3-224**, *e.r.* = ≥ 98:2, [α]_D²¹ = - 9.1° (c 1, CHCl₃).

¹H NMR (500 MHz, Chloroform-*d*) δ (ppm): 8.20 – 8.14 (m, 2H), 7.77 – 7.73 (m, 2H), 3.71 (s, 3H), 3.10 (dddd, *J* = 32.3, 10.0, 7.6, 6.3 Hz, 2H), 2.76 (ddd, *J* = 12.9, 7.7, 5.5 Hz, 1H), 2.05 (dt, *J* = 12.8, 8.2 Hz, 1H), 1.88 – 1.80 (m, 2H).

¹³C {¹H} NMR (126 MHz, Chloroform-*d*) δ (ppm): 175.1, 150.5, 147.3, 127.5, 123.5, 72.3, 53.3, 46.2, 37.8, 25.2.

MS (ESI) *m/z* (%): 251 [M+H]⁺ (100).

HRMS (ESI) *m/z*: [M+H]⁺ calculated for C₁₂H₁₅N₂O₄: 251.1026; found: 251.1029.

HPLC (AD-H, Hexane : iPrOH = 90:10, 0.5 mL/min, 298 K, 220 nm): t_{R1} = 17.10 min, t_{R2} = 19.85 min.

Overall conclusion

4. Global conclusion

This thesis summarizes the successful development and optimization of several synthetic pathways and the exploration of their respective biological activities. We have established a robust method for the synthesis of DCG-A molecule **1-108** and its analogues, producing a library of 50 compounds with notable activities against various biological targets. Specifically, compound **1-117c** demonstrated significant anthelmintic activity, including efficacy against resistant strains of *C. elegans*, indicating a novel mechanism of action. Furthermore, the candidate worked on the development of a versatile 'non-symmetrical' route toward dihydrobenzofurans using squareamide or thiourea organocatalysts (since this project is not finished, it was not included in this Thesis).

In the second project, we have successfully optimized the synthetic pathway towards various NO₂FAs including (10- and 9-NO₂OA, 10-NO₂LA, 9-NO₂cLA, 14-NO₂ARA, and 10-NO₂SA). These compounds are currently being evaluated extensively in biological tests to determine their therapeutic potential, with promising preliminary results suggesting radioprotective properties. This work lay the foundation for the future development of NO₂FAs as potential therapeutic agents. Furthermore, the candidate partially worked on the development of a Julia-Kocienski olefination method and its application in the synthesis of various FA and NO₂FA.

1. Bon, D.J.-Y.D.; Chrenko, D.; Kováč, O.; Ferugová, V.; Lasák, P.; Fuksová, M.; Zálešák, F. & Pospíšil, J. *Adv. Synth.Catal.* **366**, 480–4 (2024).
2. **Chrenko, D.**; Pospíšil, J. *Molecules* , **29** (12), 2719 (2024).

In the third part, we have successfully expanded the scope of heteroaryl sulfonamide synthesis to include various heterocycles and leveraged these compounds in a novel developed methodology for the asymmetric synthesis of α -heteroaryl α -substituted α -amino acid derivatives which proceeds under the polar Truce-Smiles rearrangement. We have also successfully proposed a mechanism of rearrangement based on detailed experimental and computational studies.

3. Iakovenko, R. O.; **Chrenko, D.**; Kristek, J.; Desmedt, E.; Zálešák, F.; De Vleeschouwer, F. & Pospíšil, J. *Org. Biomol. Chem.* **20**, 3154–3159 (2022).

Overall conclusion

During a research stay at JKU Linz in 2022, in a group of prof. Mario Waser, the candidate worked on developing and applying new phase-transfer catalysts. The results obtained during the research stay were published in 2023.

4. Zebrowski, P., Röser, K., **Chrenko, D.**, Pospíšil, J. & Waser, M. *Synthesis* **55**, 1706–1713 (2023). (Included in Special Issue dedicated to Prof. Dr. Cristina Nevado, Recipient of the 2021 Dr. Margaret Faul Women in Chemistry Award)

Additionally, during the research stay at UZH Zurich in 2023, in the group of prof. Cristina Nevado, the candidate worked on the synthesis of new ligands for asymmetric dual Ni/photoredox catalysis and photoredox-dual catalyzed silylarylation of unactivated alkenes.

In summary, this thesis presents not only significant synthetic advancements, but also biological insight. Future research will continue to build on these foundations.

5. Literature

1. Teponno, R. B. et al. *Nat. Prod. Rep.* **33**, 1044–1092 (2016).
2. Cushnie, T. P. T. et al. *Int. J. Antimicrob. Agents* **44**, 377–386 (2014).
3. Ludwiczuk, A. et al. *Pharmacognosy* 233–266 (2017).
4. Lin, D. et al. *Molecules* **21**, 1374 (2016).
5. Zálešák, F. et al. *Pharmacol. Res.* **146**, 104284 (2019).
6. Jones, A. W. *Perspectives in Drug Discovery A Collection of Essays on the History and Development of Pharmaceutical Substances.* (2010).
7. Dong, K. et al. *Org. Lett.* **23**, 2816–2820 (2021).
8. Vogt, T. *Mol. Plant* **3**, 2–20 (2010).
9. Biała, W. et al. *Front. Plant Sci.* **9**, 1–8 (2018).
10. Satake, H. et al. *J. Agric. Food Chem.* **61**, 11721–11729 (2013).
11. Constantin, M.-A. et al. *Green Chem.* **14**, 2375 (2012).
12. Tatsumi, K et al. *Environ. Sci. Technol.* **28**, 210–215 (1994).
13. Higuchi, T. *Plant Carbohydrates II* 194–224 (Springer, Berlin, Heidelberg, 1981).
14. Paniagua, C. et al. *J. Exp. Bot.* **68**, 3287–3301 (2017).
15. Zoia, L. et al. *Molecules* **13**, 129–148 (2008).
16. Orlandi, M. et al. *Tetrahedron* **57**, 371–378 (2001).
17. Daquino, C. et al. *Eur. J. Org. Chem.* **2009**, 6289–6300 (2009).
18. Dias, H. et al. *J. Braz. Chem. Soc.* **32**, (2020).
19. Kuo, Y. H. et al. *Experientia* **39**, 991–993 (1983).
20. Wasserman, H. H. et al. *J. Am. Chem. Soc.* **107**, 519–521 (1985).
21. Chioccaro, F. et al. *Acta Chem. Scand.* **47**, 610–616 (1993).
22. Miao, Y. et al. *RSC Adv.* **9**, 27510–27540 (2019).
23. Park, J. Y. et al. *Bioorg. Med. Chem. Lett.* **27**, 3060–3064 (2017).
24. Wang, Y. et al. *Chem. Nat. Compd.* **52**, 396–398 (2016).
25. Cabral, M. M. O. et al. *Exp Parasitol* **124**, 319–324 (2010).
26. Li, J. et al. *J. Agric. Food Chem.* **70**, 1122–1133 (2022).
27. Su, T. et al. *Nat. Prod. Res.* **37**, 3798–3805 (2023).
28. Sun, Z.-L. et al. *RSC Adv.* **6**, 43518–43525 (2016).

Literature

29. Cunha, M. R. et al. *Molecules* **26**, 1521 (2021).
30. Tshitenge, D. T. et al. *J. Nat. Prod.* **80**, 1604–1614 (2017).
31. Suh, W. S. et al. *Bioorg. Med. Chem. Lett.* **26**, 1877–1880 (2016).
32. Ye, F. et al. *Phytochem. Lett.* **17**, 263–269 (2016).
33. Morikawa, T. et al. *J. Nat. Med.* **72**, 464–473 (2018).
34. Lee, W. et al. *Biochem. Biophys. Res. Commun.* **495**, 2242–2248 (2018).
35. Lee, W. et al. *J. Nat. Prod.* **81**, 1343–1356 (2018).
36. Varadaraju, T. G. et al. *Org. Biomol. Chem.* **10**, 5456 (2012).
37. Jiang, R.-W. et al. *Curr. Med. Chem.* **12**, 237–246 (2005).
38. Forsythe, W. G. et al. *Green Chem.* **15**, 3031 (2013).
39. Pieters, L. et al. *J. Med. Chem.* **42**, 5475–5481 (1999).
40. Nascimento, I. R. et al. *Tetrahedron* **56**, 9181–9193 (2000).
41. Bernal, F. A. et al. *Eur. J. Med. Chem.* **205**, 112493 (2020).
42. Shiba, T. et al. *J. Mol. Catal. B Enzym.* **10**, 605–615 (2000).
43. Zhao, Q. et al. *Chem. Sci.* **11**, 3909–3913 (2020).
44. Jha, B. K. et al. *RSC Adv.* **10**, 38588–38591 (2020).
45. Lu, Z. et al. *J. Org. Chem.* **86**, 7625–7635 (2021).
46. Zhu, D.-X. et al. *J. Am. Chem. Soc.* **143**, 8583–8589 (2021).
47. Guan, C.-Y. et al. *Green Synth. Catal.* **4**, 258–262 (2023).
48. Chen, M.-W. et al. *Chem. Comm.* **49**, 1660 (2013).
49. Tan, J.-P. et al. *Org. Lett.* **21**, 7298–7302 (2019).
50. Barbušáková, Z. et al. *Monatsh. Chem.* **149**, 737–748 (2018).
51. Konrádová, D. et al. *Eur. J. Org. Chem.* **2017**, 5204–5213 (2017).
52. Konrádová, D. et al. *J. Org. Chem.* **83**, 12229–12238 (2018).
53. Yuen, M. S. M. et al. *Tetrahedron* **54**, 12429–12444 (1998).
54. Sugamoto, K. et al. *Tetrahedron* **67**, 5346–5359 (2011).
55. Han, J. H. et al. *Tetrahedron* **66**, 1673–1677 (2010).
56. Juhász, L. et al. *Tetrahedron Lett.* **41**, 2491–2494 (2000).
57. Cooksey, J. et al. *Synthesis* **44**, 2779–2785 (2012).
58. Zanatta, S. D. et al. *Aust. J. Chem.* **63**, 946 (2010).
59. Shih-Yuan Lee, A. et al. *Tetrahedron* **57**, 2121–2126 (2001).
60. Peng, Y. et al. *Synth. Commun.* **34**, 4325–4330 (2004).

Literature

61. Ahmed, N. et al. *Tetrahedron Lett.* **55**, 3683–3687 (2014).
62. Huang, Q. et al. *J. Am. Chem. Soc.* **126**, 7460–7461 (2004).
63. Cuevas, C. et al. *Org. Lett.* **2**, 2545–2548 (2000).
64. Li, L. et al. *J. Med. Chem.* **57**, 71–77 (2014).
65. Kumar, V. et al. *Eur. J. Org. Chem.* **2010**, 3377–3381 (2010).
66. Mitchell, S. A. et al. *J. Org. Chem.* **66**, 2327–2342 (2001).
67. Srikanth, V. et al. *Eur. J. Med. Chem.* **109**, 134–145 (2016).
68. Nagano, T. et al. *Chem. - Eur. J.* **15**, 9697–9706 (2009).
69. Rye, C. S. et al. *J. Am. Chem. Soc.* **124**, 9756–9767 (2002).
70. Kishida, M. et al. *Tetrahedron Lett.* **46**, 4123–4125 (2005).
71. Kværnø, L. et al. *Angew. Chem. Int. Ed.* **43**, 4653–4656 (2004).
72. Chang, C.-L. et al. *J. Nat. Prod.* **73**, 1482–1488 (2010).
73. Bitam, F. et al. *Phytochem. Lett.* **5**, 696–699 (2012).
74. Xia, Y. et al. *J. Chem. Res.* **41**, 296–300 (2017).
75. Corsi, A. K. et al. *Genetics* **200**, 387–407 (2015).
76. Iškauskienė, M. et al. *Arch. Pharm.* **354**, 2100001 (2021).
77. Aina, O. et al. *Crop Sci.* **52**, 1076–1083 (2012).
78. Teutonico, R. A. et al. *Plant Physiol.* **97**, 288–297 (1991).
79. Witvrouw, K. et al. *Proc. Natl. Acad. Sci. U.S.A.* **120**, (2023).
80. Cheng, H. et al. *J. Med. Chem.* **48**, 645–652 (2005).
81. Mahajani, N. S. et al. *J. Org. Chem.* **84**, 7871–7882 (2019).
82. Rubbo, H. et al. *Biochim. Biophys. Acta* **1780**, 1318–1324 (2008).
83. Trostchansky, A. et al. *Biochemistry* **46**, 4645–4653 (2007).
84. Rubbo, H. et al. *Arch. Biochem. Biophys.* **324**, 15–25 (1995).
85. Bonacci, G. et al. *J. Biol. Chem.* **287**, 44071–44082 (2012).
86. Greenwood, D. M. et al. *Free Radic. Biol. Med.* **89**, 333–341 (2015).
87. Freeman, B. A. et al. *J. Biol. Chem.* **283**, 15515–15519 (2008).
88. Aranda-Caño, L. et al. *Plants*, **8**, 82 (2019).
89. Baker, L. M. S. et al. *J. Biol. Chem.* **282**, 31085–31093 (2007).
90. Turell, L. et al. *J. Biol. Chem.* **292**, 1145–1159 (2017).
91. Batthyany, C. et al. *J. Biol. Chem.* **281**, 20450–20463 (2006).
92. Kansanen, E. et al. *J. Biol. Chem.* **284**, 33233–33241 (2009).

Literature

93. Cole, M. P. et al. *Circ. Res.* **105**, 965–972 (2009).
94. Tsujita, T. et al. *Genes Cells* **16**, 46–57 (2011).
95. Ambrozova, G. et al. *Free Radic. Biol. Med.* **90**, 252–260 (2016).
96. Netto, L. E. S. et al. *Comp. Biochem. Physiol. C* **146**, 180–193 (2007).
97. Villacorta, L. et al. *Cardiovasc. Res.* **98**, 116–124 (2013).
98. Cui, T. et al. *J. Biol. Chem.* **281**, 35686–35698 (2006).
99. Asan, A. et al. *J. Biol. Chem.* **294**, 397–404 (2019).
100. Woodcock, C.-S. C. et al. *J. Biol. Chem.* **293**, 1120–1137 (2018).
101. Kühn, B. et al. *Biochem. Pharmacol.* **155**, 48–60 (2018).
102. Pereckova, J. et al. *Int. J. Mol. Sci.* **22**, 9981 (2021).
103. Marwah, S. S. et al. *Am. J. Hematol.* **69**, 144–146 (2002).
104. Higdon, A. et al. *Biochem. J.* **442**, 453–464 (2012).
105. Schopfer, F. J. et al. *Chem. Rev.* **111**, 5997–6021 (2011).
106. Rubbo, H. et al. *Biochemistry of Oxidative Stress* 79–93 (2016).
107. Trostchansky, A. et al. *Biochemistry* **46**, 4645–4653 (2007).
108. Trostchansky, A. et al. *J. Biol. Chem.* **15**, 12891–12900, 286 (2011)
109. Sánchez-Calvo, B. et al. *PLOS One* **11**, e0154651 (2016).
110. Diaz-Amarilla, P. et al. *Free Radic. Biol. Med.* **95**, 112–120 (2016).
111. Woodcock, S. R. et al. *Tetrahedron Lett.* **81**, 153371 (2021).
112. Maity, S. et al. *J. Am. Chem. Soc.* **135**, 3355–3358 (2013).
113. Woodcock, S. R. et al. *Free Radic. Biol. Med.* **59**, 14–26, (2013).
114. Gorczynski, M. et al. *Org. Lett.* **8**, 2305–2308 (2006).
115. Woodcock, S. R. et al. *Tetrahedron Lett.* **81**, 153371 (2021).
116. Zatloukalová, M. et al. *Redox Biol.* **46**, 102097 (2021).
117. Novák, D. et al. *Free Radic. Biol. Med.* **164**, 381–389 (2021).
118. Hernychova, L. et al. *Int. J. Biol. Macromol.* **203**, 116–129 (2022).
119. Zatloukalova, M. et al. *Redox Biol.* **24**, 101213, (2019).
120. Grippo, V. et al. *Redox Biol.* **38**, 101756 (2021).
121. Novak, D. et al. *J. Mol. Liq.* **383**, 122020 (2023).
122. Sobczak, K. et al. *J. Mol. Liq.* **365**, 120110 (2022).
123. Henry, L. *Comptes rendus.* **120**, 1265–1268 (1895).
124. Woodcock, S. R. et al. *Org. Lett.* **8**, 3931–3934 (2006).

Literature

125. Bon, D. J. Y. D. et al. *Adv. Synth. Catal.* **366**, 480–487 (2024).
126. Chrenko, D. et al. *Molecules* **29**, 2719, (2024).
127. Suto, T. et al. *J. Am. Chem. Soc.* **139**, 2952–2955 (2017).
128. Langille, N. F. et al. *Org. Lett.* **8**, 3761–3764 (2006).
129. Gobé, V. et al. *Chem. - Eur. J.* **21**, 8511–8520 (2015).
130. Nanba, Y. et al. *Org. Biomol. Chem.* **15**, 8614–8626 (2017).
131. Krishnamurthy, V. R. et al. *J. Org. Chem.* **76**, 5433–5437 (2011).
132. Alexander, S. P. H. *Prog. Neuro-Psychopharmacol. Biol. Psychiatry* **64**, 157–166 (2016).
133. Mechoulam, R. et al. *J. Am. Chem. Soc.* **87**, 3273–3275 (1965).
134. Mechoulam, R. et al. *Tetrahedron* **19**, 2073–2078 (1963).
135. Matsuda, L. A. et al. *Nature* **346**, 561–564 (1990).
136. Munro, S. et al. *Nature* **365**, 61–65 (1993).
137. Devane, W. A. et al. *Science* **258**, 1946–1949 (1992).
138. Mazzola, C. et al. *Eur. J. Pharmacol.* **477**, 219–225 (2003).
139. Devane, W. A. et al. *Science* **258**, 1946–1949 (1992).
140. Mechoulam, R. et al. *Biochem. Pharmacol.* **50**, 83–90 (1995).
141. Sugiura, T. et al. *Biochem. Biophys. Res. Commun.* **215**, 89–97 (1995).
142. Di Marzo, V. *Nat. Rev. Drug Discov.* **17**, 623–639 (2018).
143. Pisani, A. et al. *Ann. Neurol.* **57**, 777–779 (2005).
144. Stelt, M. et al. *FASEB J.* **19**, 1140–1142 (2005).
145. Van Der Stelt, M. et al. *Cell. Mol. Life Sci.* **63**, 1410–1424 (2006).
146. Mulder, J. et al. *Brain* **134**, 1041–1060 (2011).
147. Vázquez, C. et al. *Neurobiol. Aging* **36**, 3008–3019 (2015).
148. Cristino, L. et al. *Nat. Rev. Neurol.* **2019 16:1** **16**, 9–29 (2019).
149. Dowie, M. J. et al. *Neuroscience* **163**, 456–465 (2009).
150. Cabranes, A. et al. *Neurobiol. Dis.* **20**, 207–217 (2005).
151. Baker, D. et al. *FASEB J.* **15**, 300–302 (2001).
152. Marsicano, G. et al. *Science* **302**, 84–88 (2003).
153. Lerner, R. et al. *Biochim. Biophys. Acta Mol. Cell Biol. Lipids* **1862**, 255–267 (2017).
154. Chiurchiù, V. et al. *Pharmacol. Res.* **113**, 313–319 (2016).
155. Franco, R. et al. *Prog. Neurobiol.* **131**, 65–86 (2015).
156. Quintana, P. G. et al. *Eur. J. Org. Chem.* **2016**, 518–528 (2016).

Literature

157. Boger, D. L. et al. *Bioorg. Med. Chem. Lett.* **9**, 1151–1154 (1999).
158. Ferreri, C. et al. *Bioorg. Med. Chem.* **16**, 8359–8365 (2008).
159. Abadji, V. et al. *J. Med. Chem.* **37**, 1889–1893 (1994).
160. Qi, L. et al. *Org. Lett.* **6**, 1673–1675 (2004).
161. Suzen, S. et al. *Pharmaceuticals* **15**, 692 (2022).
162. Mercurio, V. et al. *Antioxidants*, **9**, 641 (2020).
163. Takashina, K. et al. *Org. Lett.* **24**, 2253–2257 (2022).
164. Scozzafava, A. et al. *Curr. Med. Chem.* **10**, 925–953 (2005).
165. Abd El-Karim, S. S. et al. *Bioorg. Chem.* **81**, 481–493 (2018).
166. Said, M. A. et al. *Eur. J. Med. Chem.* **189**, (2020).
167. Moskalik, M. Y. *Molecules* **28**, (2023).
168. Van Berkel, M. A. et al. *Am. J. Health-Syst. Pharm.* **75**, 524–531 (2018).
169. Masaret, G. S. et al. *ChemistrySelect* **5**, 13995–14003 (2020).
170. Dolensky, J. et al. *Molecules* **27**, 1–14 (2022).
171. Khan, F. A. et al. *Curr. Org. Chem.* **22**, 818–830 (2018).
172. Abdel-Aziz, A. A.-M. et al. *Bioorg. Chem.* **84**, 260–268 (2019).
173. Ferraroni, M. et al. *J. Mol. Struct.* **1268**, 133672 (2022).
174. Košák, U. et al. *J. Med. Chem.* **61**, 119–139 (2018).
175. Shetnev, A. et al. *Bioorg. Med. Chem. Lett.* **29**, 126677 (2019).
176. Sarnpitak, P. et al. *Eur. J. Med. Chem.* **84**, 160–172 (2014).
177. Domagk, G. *DMW - Deutsche Medizinische Wochenschrift* **61**, 250–253 (1935).
178. Antman, E. M. et al. *Circulation* **115**, 1634–1642 (2007).
179. Grover, N. et al. *Indian J. Pharmacol.* **45**, 547 (2013).
180. Nunokawa, T. et al. *J. Infect. Chemother* **29**, 193–197 (2023).
181. Surendiran, A. et al. *Eur. J. Clin. Pharmacol.* **67**, 797–801 (2011).
182. Lascar, R. et al. *HIV/AIDS* **1**, 31-39, (2009).
183. Nie, Z. et al. *J. Med. Chem.* **48**, 1596–1609 (2005).
184. Mallireddigari, M. R. et al. *Synthesis* **2005**, 3639–3643 (2005).
185. Kellogg, R. M. et al. *Synthesis* **2003**, 1626–1638 (2003).
186. Aquino, A. M. et al. *J. Am. Chem. Soc.* **112**, 5819–5824 (1990).
187. Zálešák, F. et al. *J. Org. Chem.* **86**, 11291–11309 (2021).
188. Day, J. J. et al. *Org. Lett.* **19**, 3819–3822 (2017).

Literature

189. Woolven, H. et al. *Org. Lett.* **13**, 4876–4878 (2011).
190. Tang, S. et al. *Org. Biomol. Chem.* **17**, 1370–1374 (2019).
191. Brownbridge, P. et al. *Phosphorus, Sulfur Relat. Elem.* **35**, 311–318 (1988).
192. Iakovenko, R. O. et al. *Org. Biomol. Chem.* **20**, 3154–3159 (2022).
193. Bornholdt, J. et al. *Chem. - Eur. J.* **16**, 12474–12480 (2010).
194. Bahrami, K. et al. *Synlett* **2009**, 2773–2776 (2009).
195. Bornholdt, J. et al. *Tetrahedron* **65**, 9280–9284 (2009).
196. Nelson, D. L. et al. *Lehninger Principles of Biochemistry*. (Elsevier, 2005).
197. Walsh, C. T. et al. *Angew. Chem. Int. Ed.* **52**, 7098–7124 (2013).
198. Tilborg, A. et al. *Eur. J. Med. Chem.* **74**, 411–426 (2014).
199. Buchanani, B. B. et al. *Biochemistry and Molecular Biology of Plants*. (Willey, 2015).
200. Lovering, F. et al. *J. Med. Chem.* **52**, 6752–6756 (2009).
201. Pollegioni, L. et al. *Int. J. Mol. Sci.* **21**, 3206 (2020).
202. Trowbridge, A. et al. *Chem. Rev.* **120**, 2613–2692 (2020).
203. Cabrera, S. et al. *J. Am. Chem. Soc.* **130**, 12031–12037 (2008).
204. Aguilar Troyano, F. J. et al. *Angew. Chem. Int. Ed.* **60**, 1098–1115 (2021).
205. Vogt, H. et al. *Org. Biomol. Chem.* **5**, 406–430 (2007).
206. COREY, E. J. et al. *Chem. Pharm. Bull.* **47**, 1–10 (1999).
207. Shiozaki, M. et al. *J. Med. Chem.* **54**, 2839–2863 (2011).
208. SCHOEPP, D. D. et al. *Neuropharmacology* **36**, 1–11 (1997).
209. Mei, H. et al. *Eur. J. Med. Chem.* **186**, 111826 (2020).
210. HORN, W. S. et al. **45**, 1692–1696 (1992).
211. Ōmura, S. et al. *J. Antibiot.* **72**, 189–201 (2019).
212. Koda, Y. et al. *Phytochemistry* **41**, 93–96 (1996).
213. Ohfuné, Y. et al. *Eur. J. Org. Chem.* **2005**, 5127–5143 (2005).
214. Schöllkopf, U. *Tetrahedron* **39**, 2085–2091 (1983).
215. Nájera, C. et al. *Chem. Rev.* **107**, 4584–4671 (2007).
216. Wei, L. et al. *Angew. Chem. Int. Ed.* **56**, 12312–12316 (2017).
217. Peng, Y. et al. *Angew. Chem. Int. Ed.* **61**, e202203448 (2022).
218. Huo, X. et al. *J. Am. Chem. Soc.* **140**, 2080–2084 (2018).
219. Wei, L. et al. *J. Am. Chem. Soc.* **140**, 1508–1513 (2018).
220. Panahi, F. et al. *Chem. Sci.* **12**, 7388–7392 (2021).

Literature

221. Abas, H. et al. *Angew. Chem. Int. Ed.* **58**, 2418–2422 (2019).
222. Leonard, D. J. et al. *Chem. Sci.* **12**, 9386–9390 (2021).
223. Li, K. et al. *Nat. Commun.* **6**, 8404 (2015).
224. Ju, T. et al. *Angew. Chem. Int. Ed.* **57**, 13897–13901 (2018).
225. Yeung, K. et al. *ACS Catal.* **9**, 1655–1661 (2019).
226. Blackwell, J. H. et al. *J. Am. Chem. Soc.* **143**, 1598–1609 (2021).
227. Matsumoto, Y. et al. *J. Am. Chem. Soc.* **142**, 8498–8505 (2020).
228. Leonard, D. J. et al. *Nature* **562**, 105–109 (2018).
229. Bouet, A. et al. *Tetrahedron* **66**, 498–503 (2010).
230. Cochrane, E. J. et al. *Chem. Commun.* **50**, 9910–9913 (2014).
231. Agafonova, A. V. et al. *Org. Lett.* **23**, 8045–8049 (2021).
232. Xu, G. et al. *Chem. - Eur. J.* **16**, 10667–10670 (2010).
234. Henderson, A. R. P. et al. *Can. J. Chem.* **95**, 483–504 (2017).
235. Martín Castro, A. M. *Chem. Rev.* **104**, 2939–3002 (2004).
236. Truce, W. E. et al. *J. Am. Chem. Soc.* **80**, 3625–3629 (1958).
237. Holden, C. M. et al. *Chem. - Eur. J.* **23**, 8992–9008 (2017).
238. Allart-Simon, I. et al. *Molecules* **21**, (2016).
239. Allen, A. R. et al. *Chem. Rev.* **122**, 2695–2751 (2022).
240. Whalley, D. M. et al. *Synthesis* **54**, 1908–1918 (2022).
241. Clayden, J. et al. *J. Am. Chem. Soc.* **129**, 7488–7489 (2007).
242. Kawabata, T. et al. *Angew. Chem. Int. Ed.* **39**, (2000).
243. Alezra, V. et al. *Synthesis* **48**, 2997–3016 (2016).
244. Pospíšil, J. *Tetrahedron Lett.* **52**, 2348–2352 (2011).
245. Zhu, R. et al. *J. Am. Chem. Soc.* **139**, 5724–5727 (2017).
246. Foschi, F. et al. *Chem. - Eur. J.* **16**, 10667–10670 (2010).

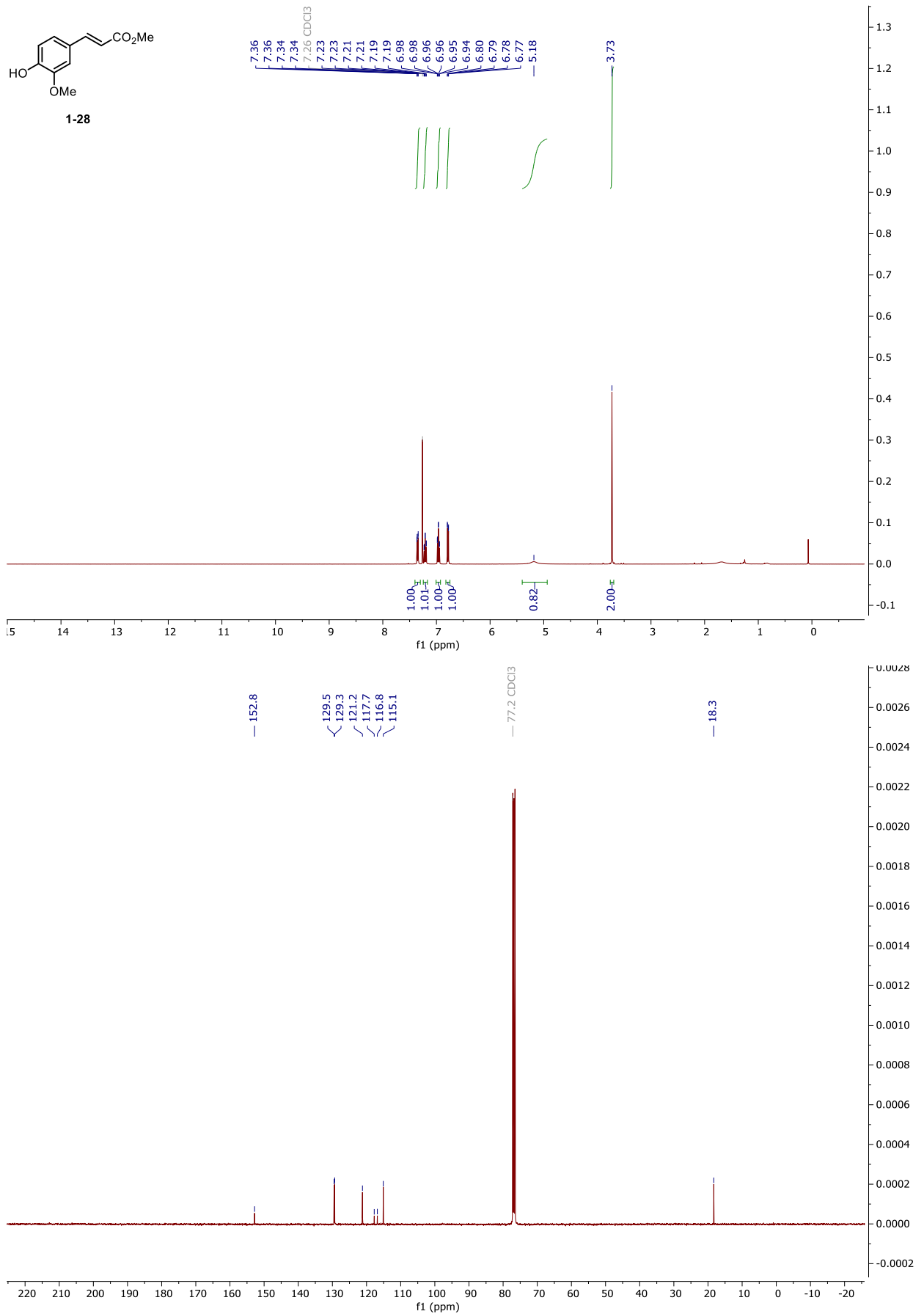
6. NMR and HPLC

The ^1H NMR and $^{13}\text{C}\{^1\text{H}\}$ NMR spectra were measured on Jeol ECA400II (400 and 101 MHz) or Jeol 500 ECA (500 and 126 MHz) in Chloroform- d or CD_3OD . Chemical shifts are reported in ppm, and their calibration was carried out (a) in the case of ^1H NMR experiments on the residual peak of non-deuterated solvent δ (CDCl_3) = 7.26 ppm or δ (CD_3OD) = 3.31 ppm, δ ($\text{DMSO}-d_6$) = 2.50 ppm, δ (acetone- d_6) = 2.05 ppm and in the case of ^{13}C NMR experiments on the middle peak of the ^{13}C signal in deuterated solvent δ (CDCl_3) = 77.16 ppm, δ (CD_3OD) = 49.00 ppm, ($\text{DMSO}-d_6$) = 39.52 ppm, (acetone- d_6) = 29.84 ppm. The proton coupling patterns are represented as a singlet (s), a doublet (d), a doublet of a doublet (dd), a triplet (t), a triplet of a triplet (tt), and a multiplet (m). ***NMR spectra were recorded from a pure compounds, purified by column chromatography, preparative TLC or in some cases semipreparative HPLC.***

Chiral analysis was performed on Waters Alliance 2695 with autosampler and UV-VIS detector Waters 2996 PDA using chiral columns (CHIRAL ART Amylose-SA 250x4,6 mm, 5 μm ; CHIRALCEL Cellulose OD-H, 250x4,6 mm, 5 μm ; CHIRALCEL Cellulose OZ-H, 250x4,6 mm, 5 μm). All solvents used were HPLC-grade solvents purchased from Merck. The column employed and the respective solvent mixture are indicated for each experiment. ***HPLC chromatograms were recorded mostly from pure compounds but in some cases crude reaction mixture was measured instead.***

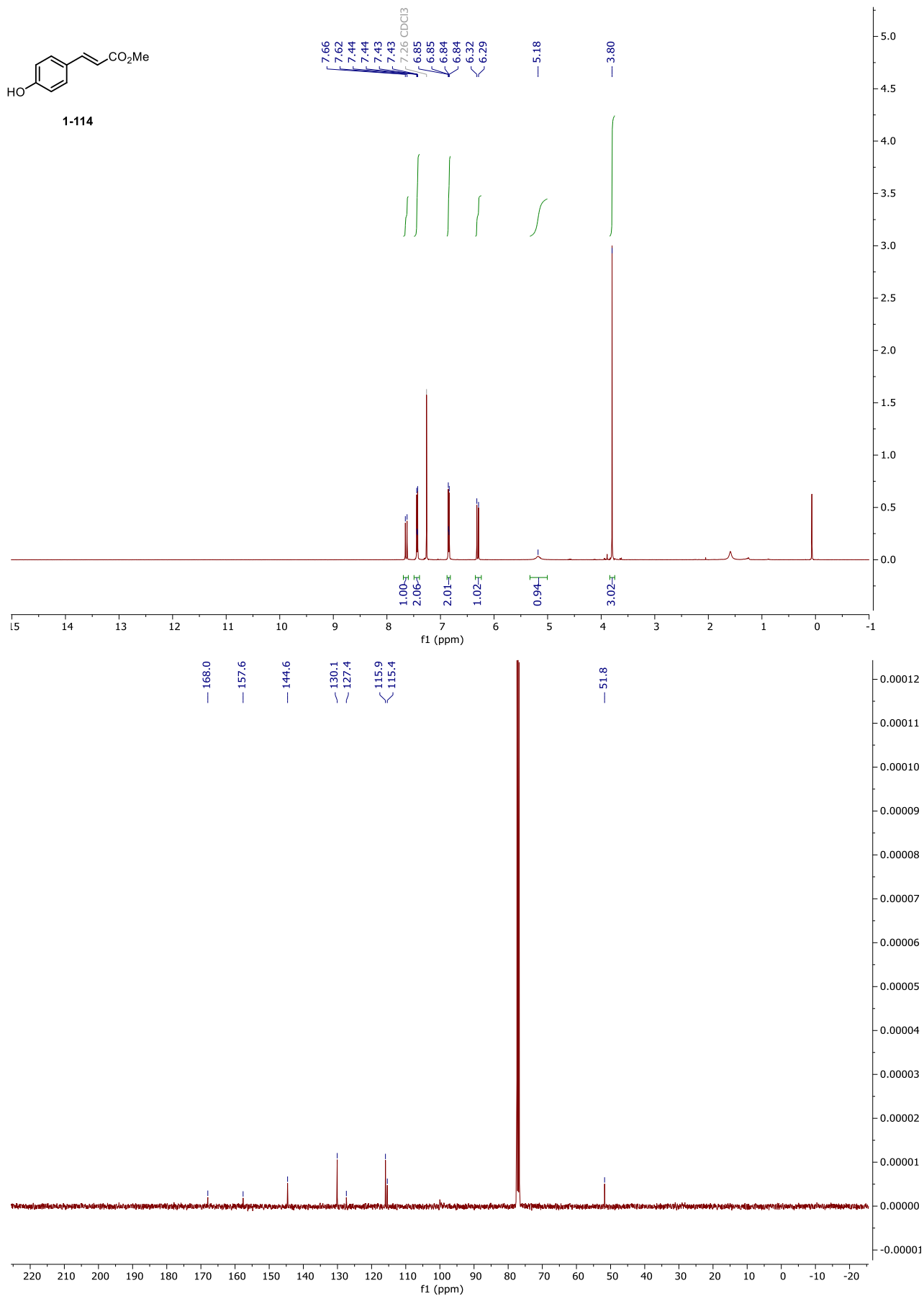
NMR and HPLC

Copy of ^1H and $^{13}\text{C}\{^1\text{H}\}$ spectra of 1-28



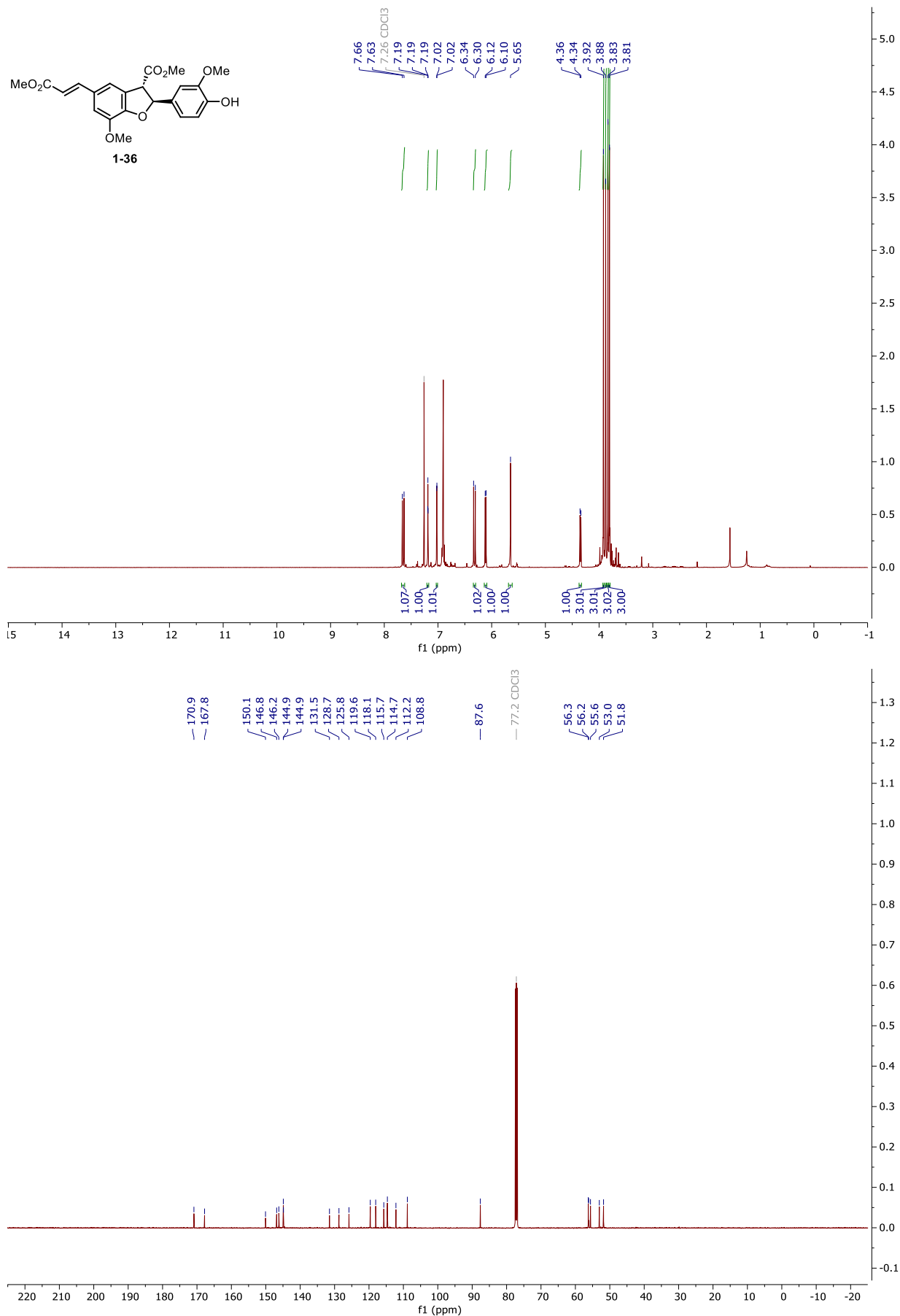
NMR and HPLC

Copy of ^1H and $^{13}\text{C}\{^1\text{H}\}$ spectra of 1-114



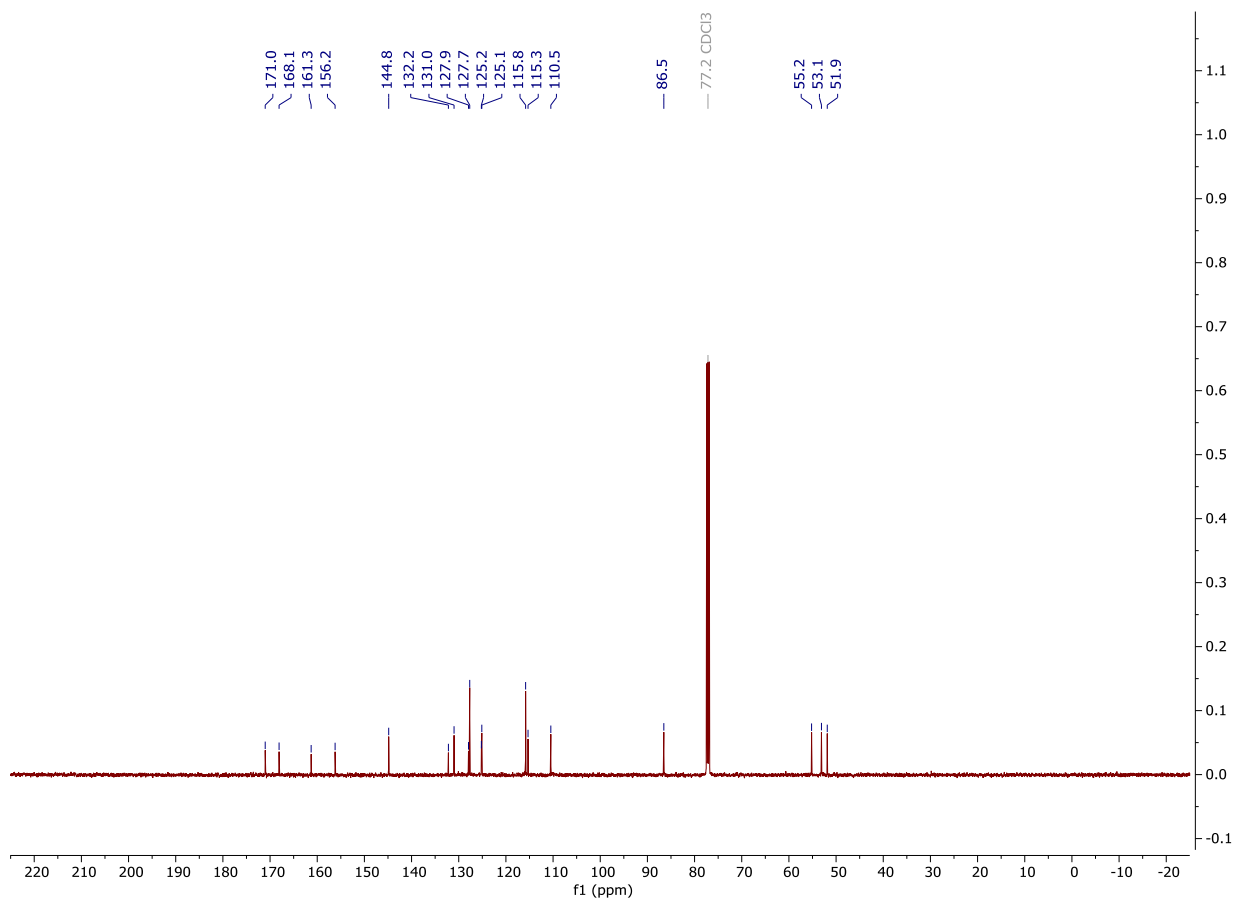
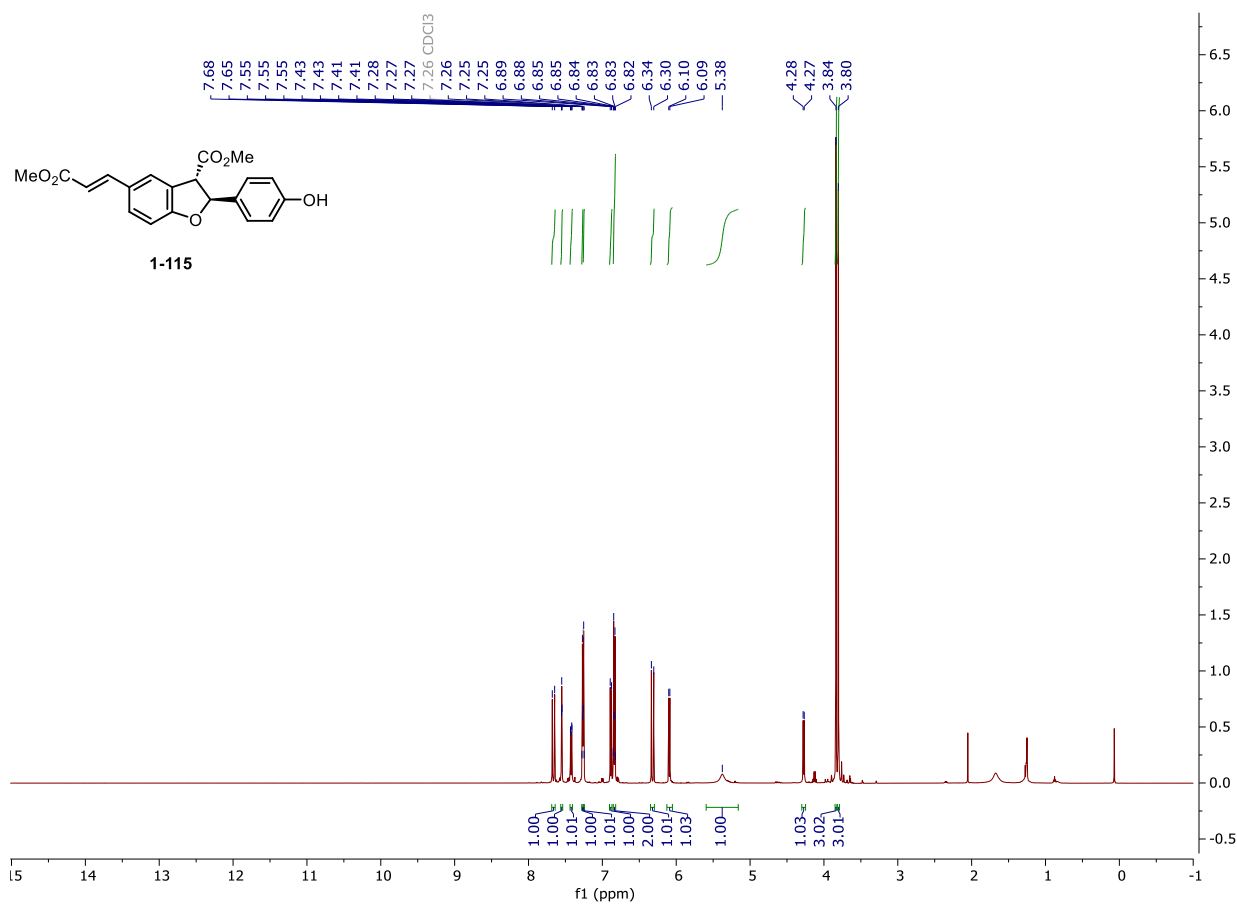
NMR and HPLC

Copy of ^1H and $^{13}\text{C}\{^1\text{H}\}$ spectra of 1-36



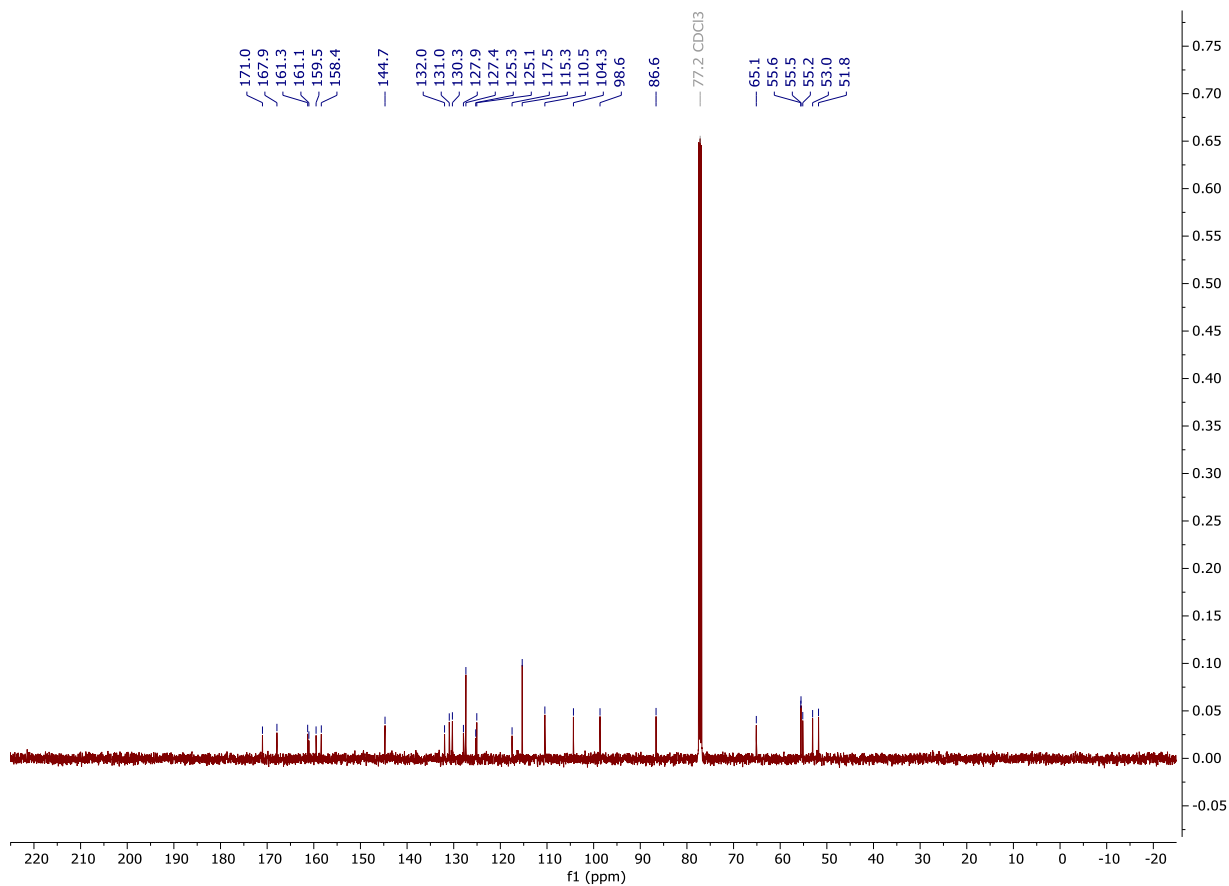
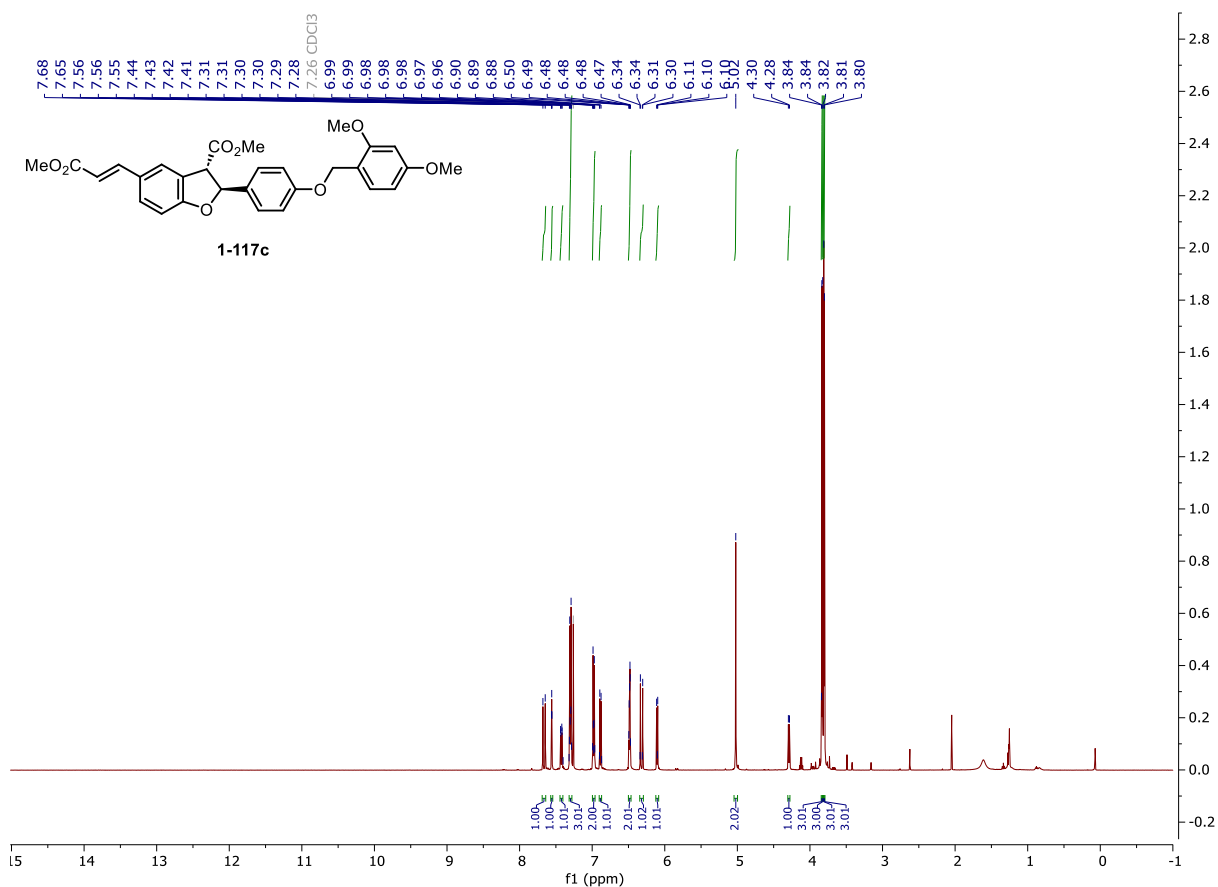
NMR and HPLC

Copy of ^1H and $^{13}\text{C}\{^1\text{H}\}$ spectra of 1-115



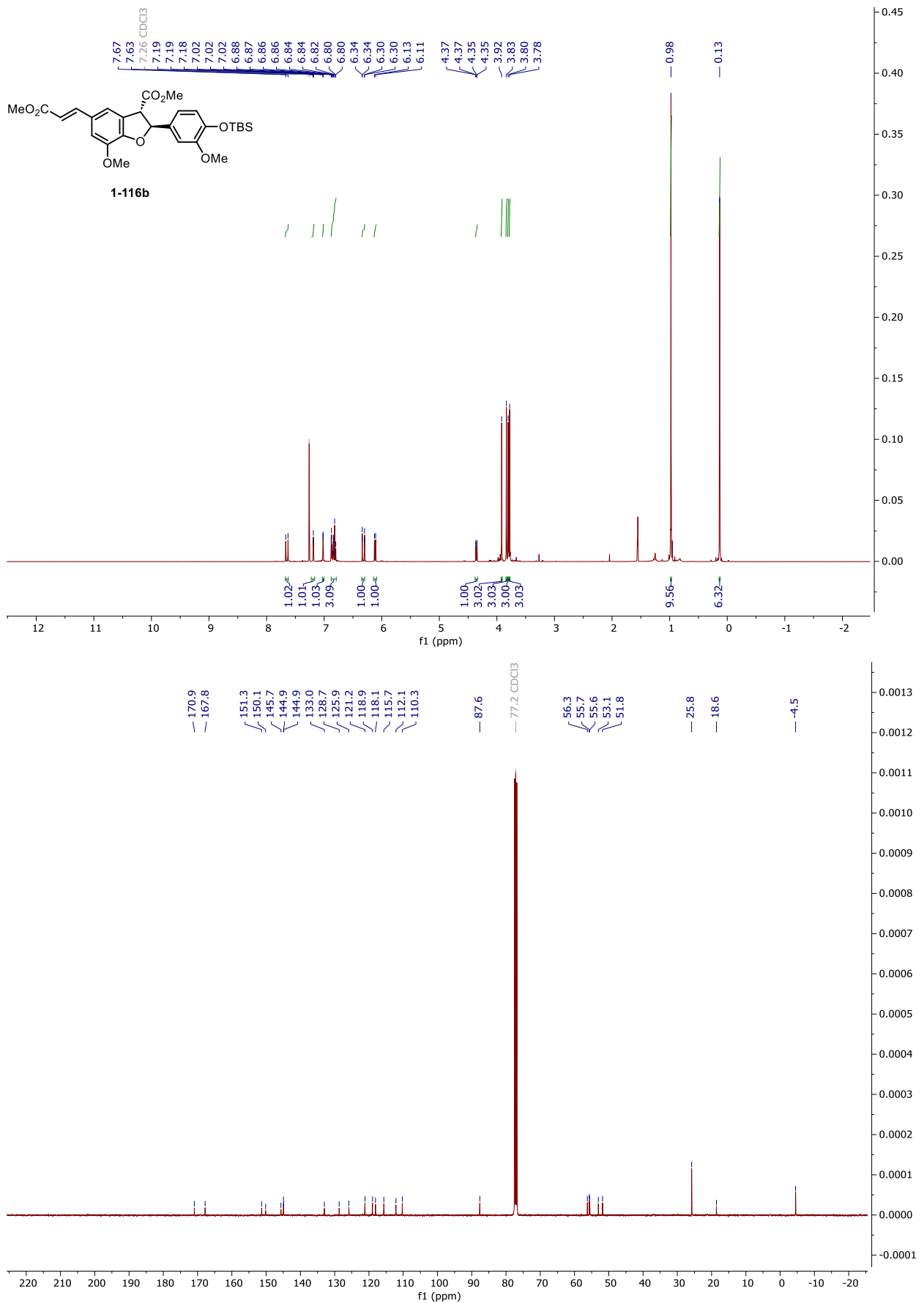
NMR and HPLC

Copy of ^1H and $^{13}\text{C}\{^1\text{H}\}$ spectra of 1-117c



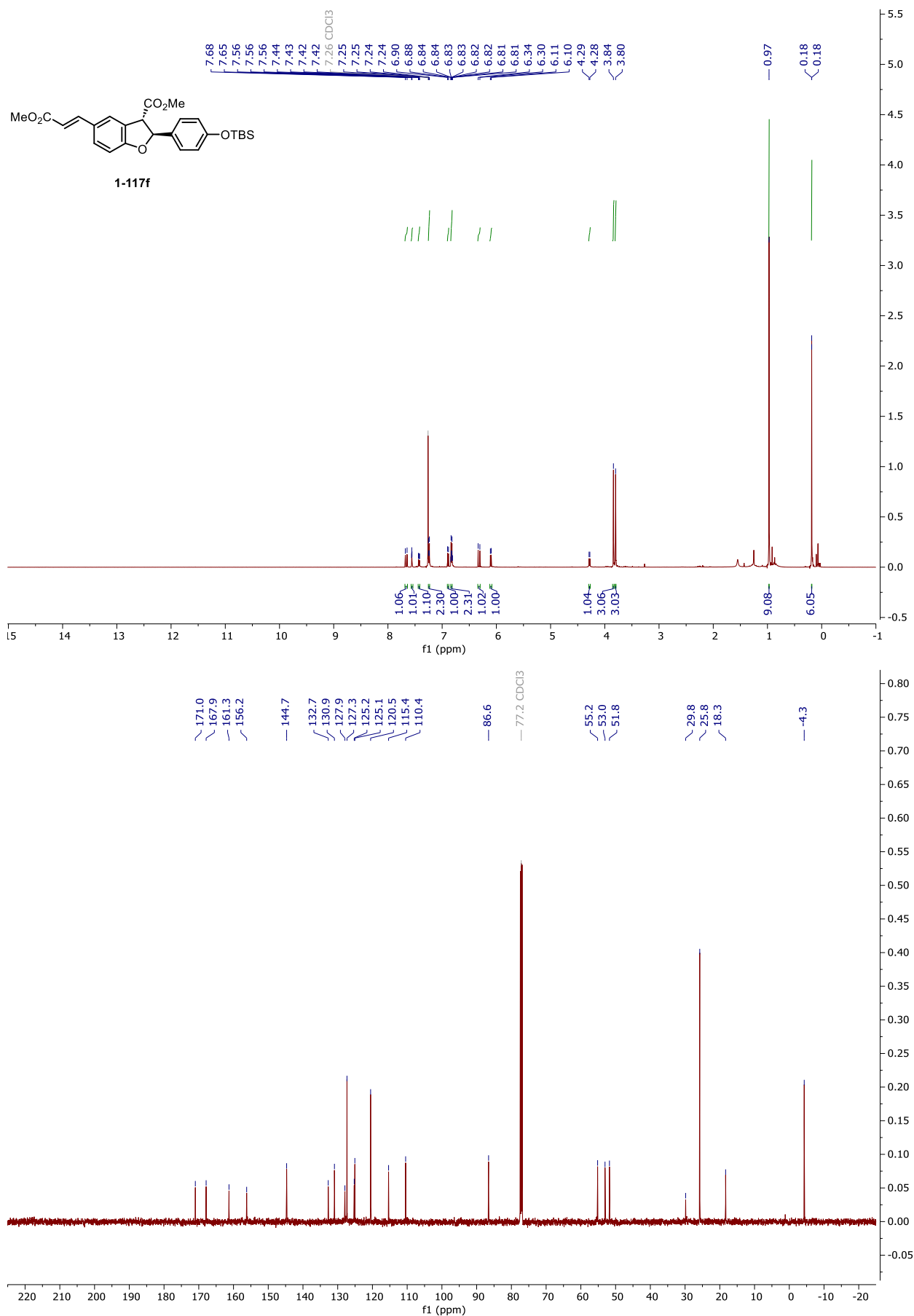
NMR and HPLC

Copy of ^1H and $^{13}\text{C}\{^1\text{H}\}$ spectra of 1-116b



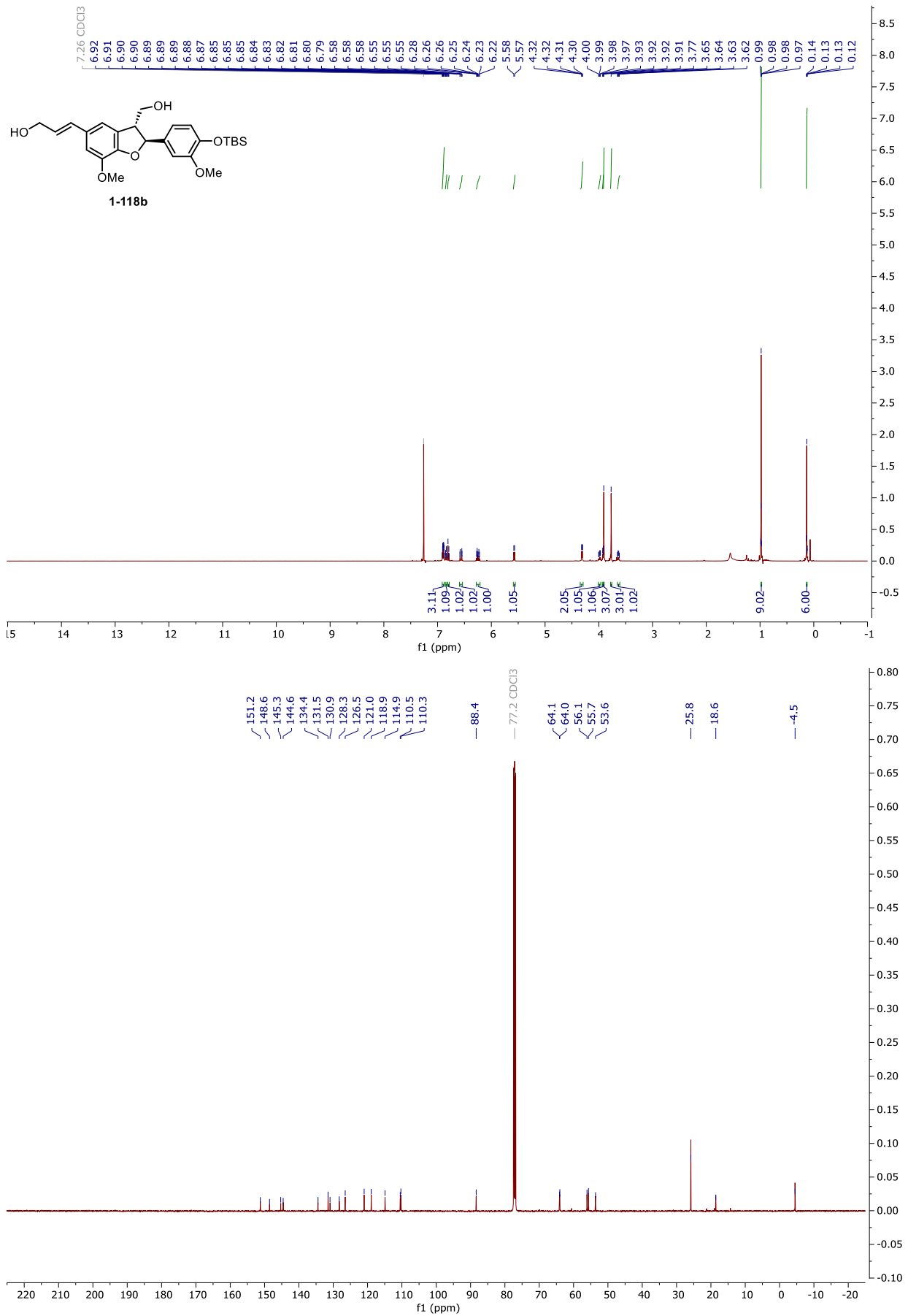
NMR and HPLC

Copy of ^1H and $^{13}\text{C}\{^1\text{H}\}$ spectra of 1-117f



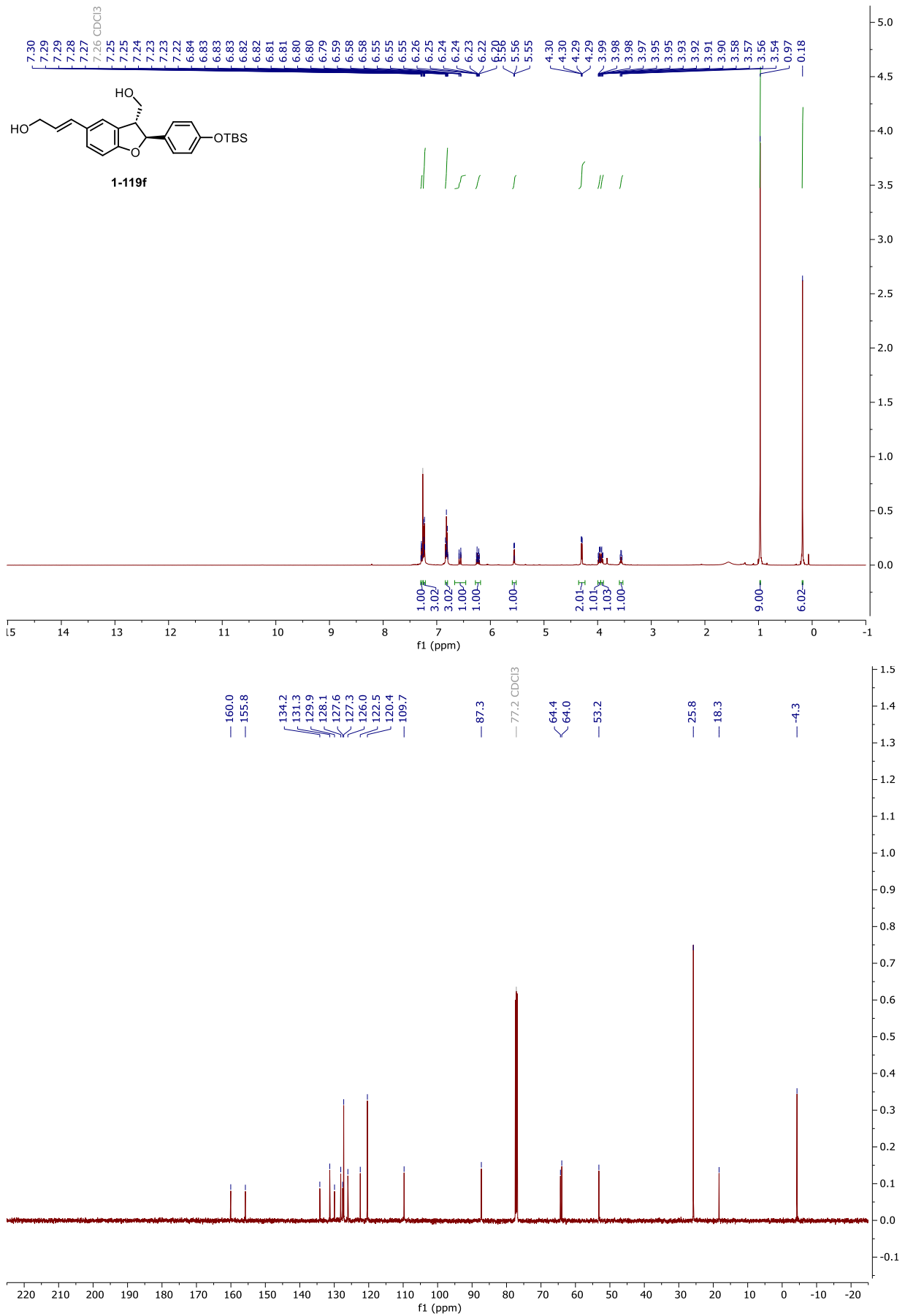
NMR and HPLC

Copy of ^1H and $^{13}\text{C}\{^1\text{H}\}$ spectra of 1-118b



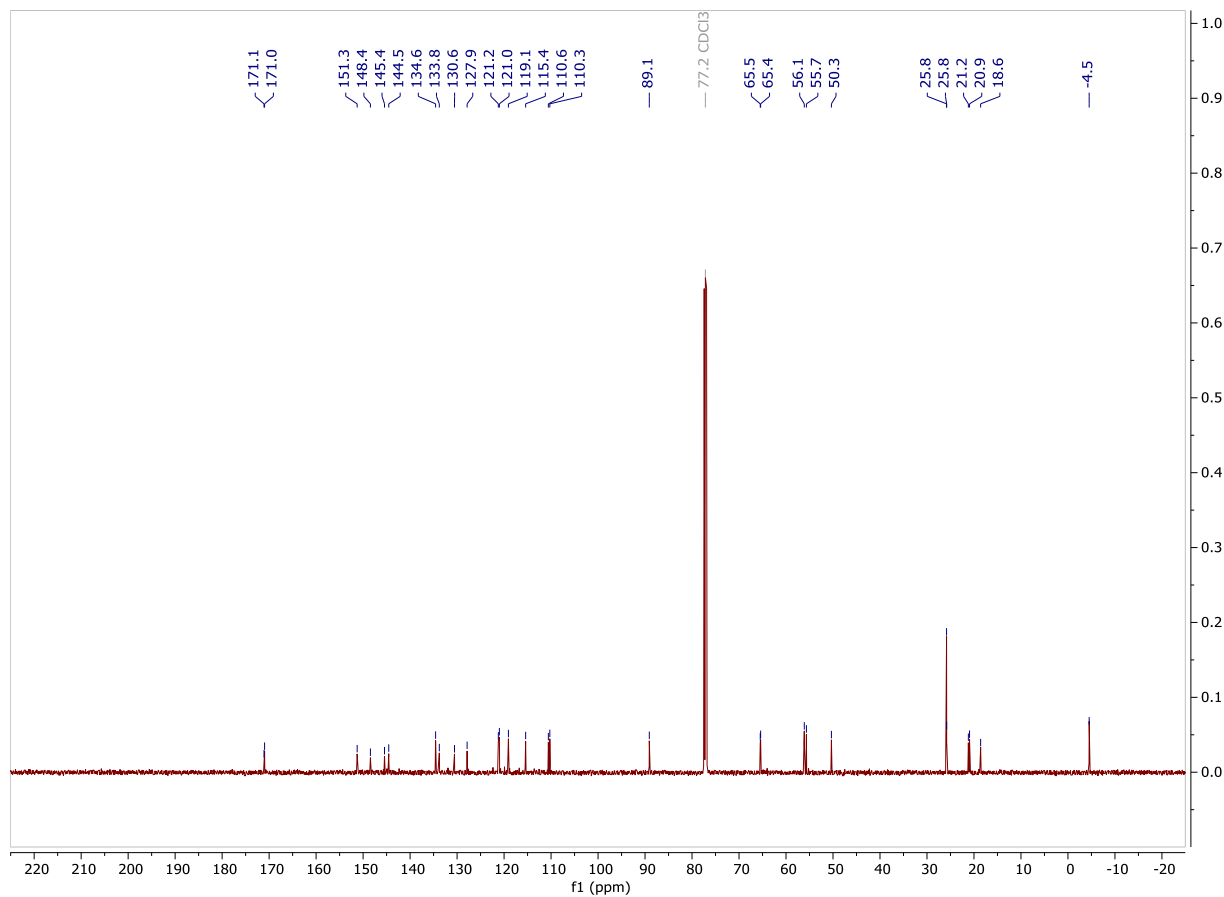
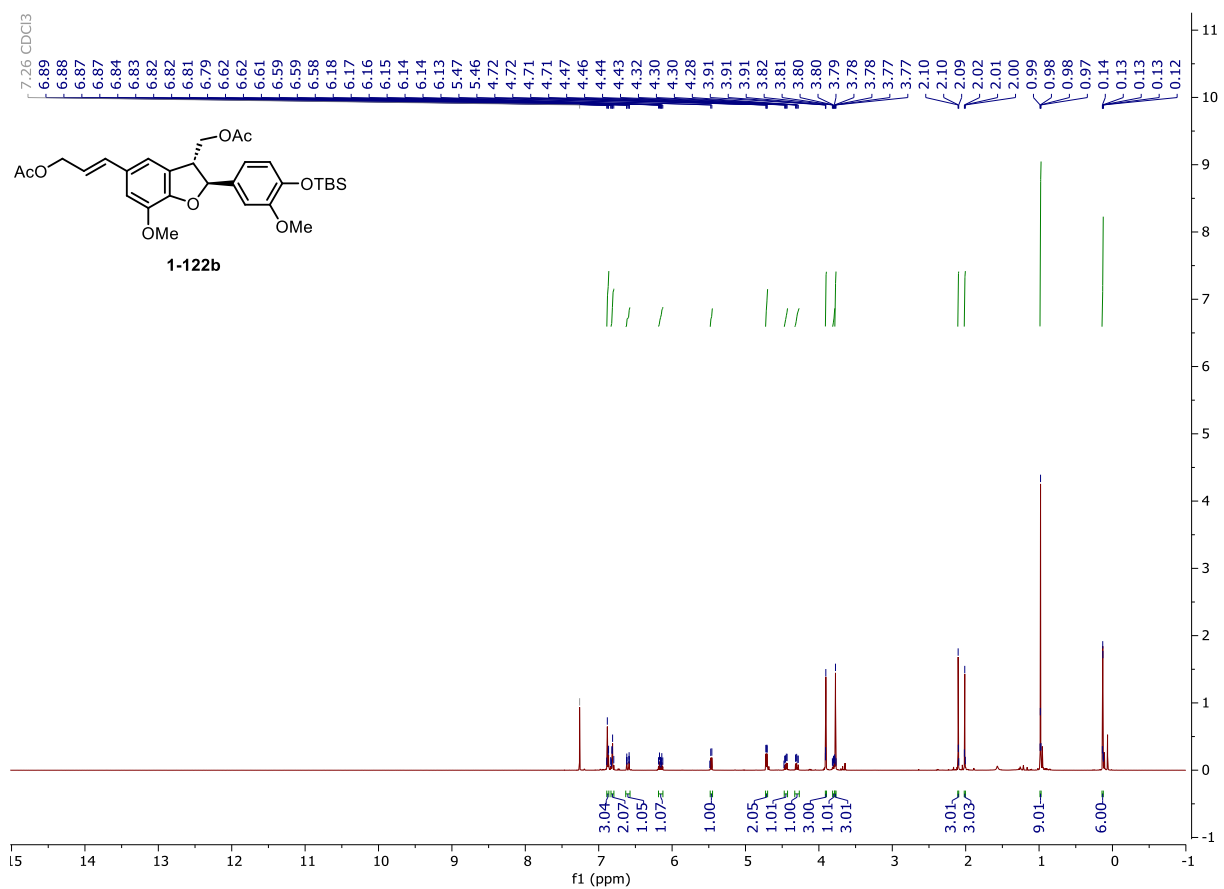
NMR and HPLC

Copy of ^1H and $^{13}\text{C}\{^1\text{H}\}$ spectra of 1-119f



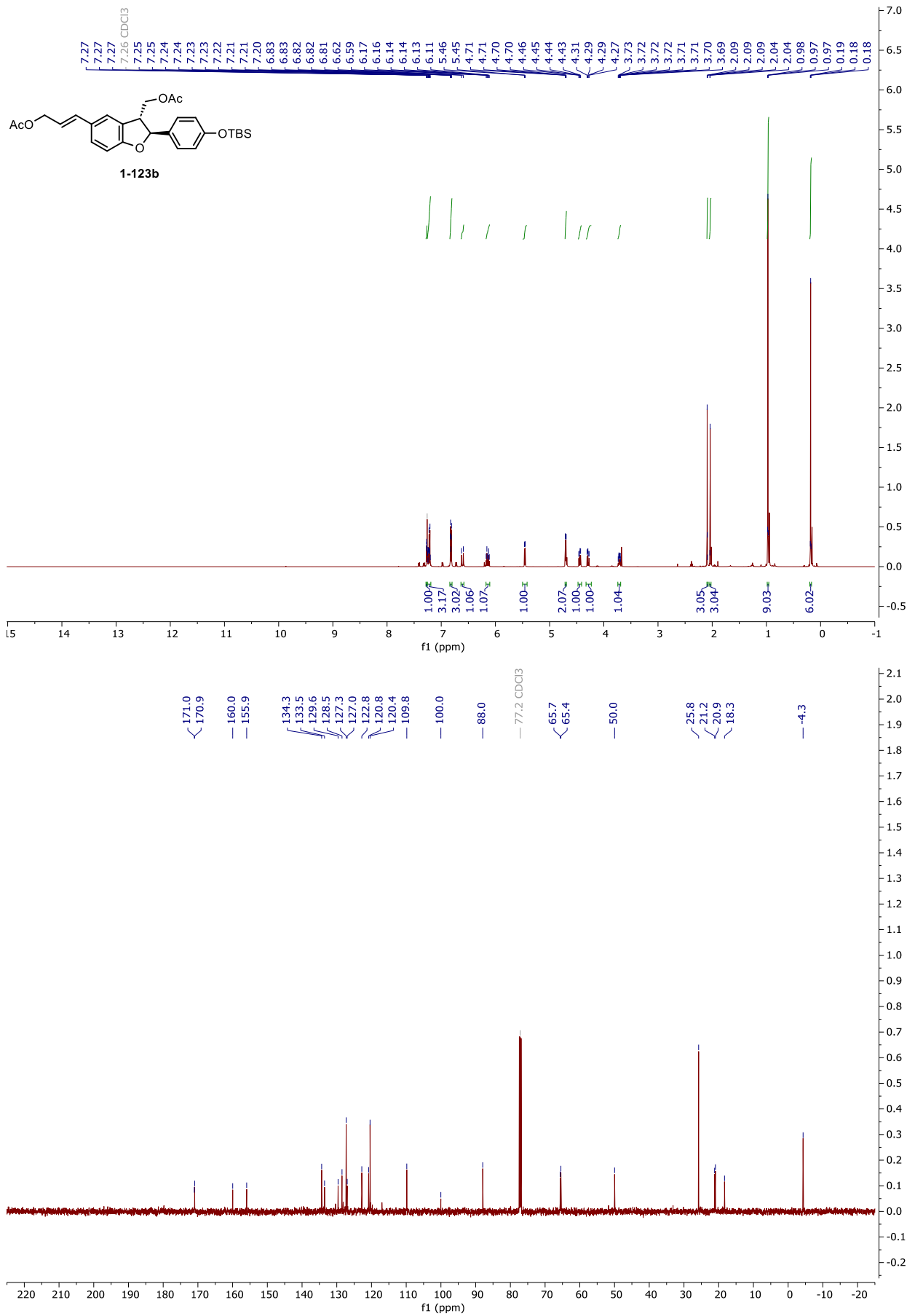
NMR and HPLC

Copy of ^1H and $^{13}\text{C}\{^1\text{H}\}$ spectra of 1-122b



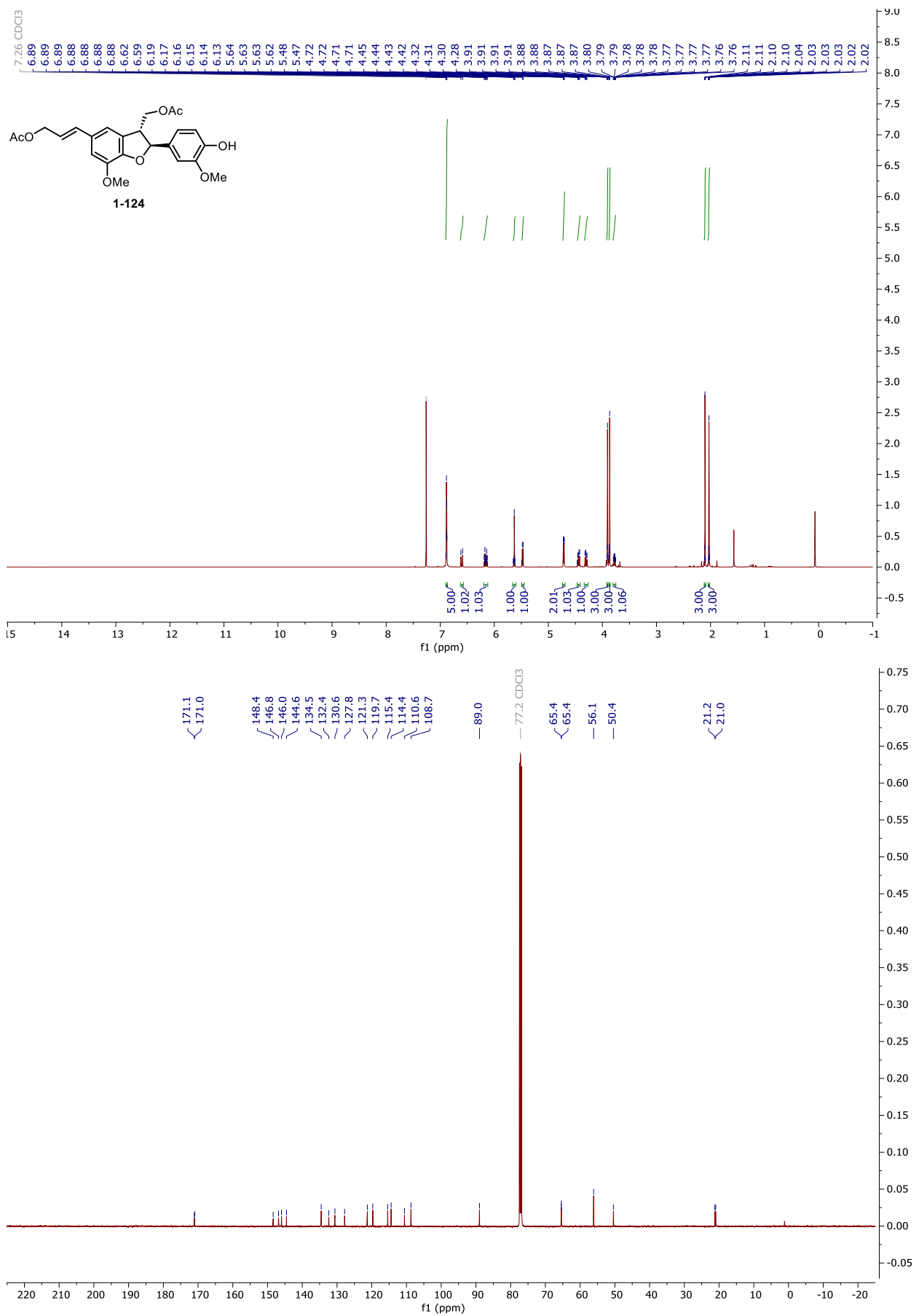
NMR and HPLC

Copy of ^1H and $^{13}\text{C}\{^1\text{H}\}$ spectra of 1-123b



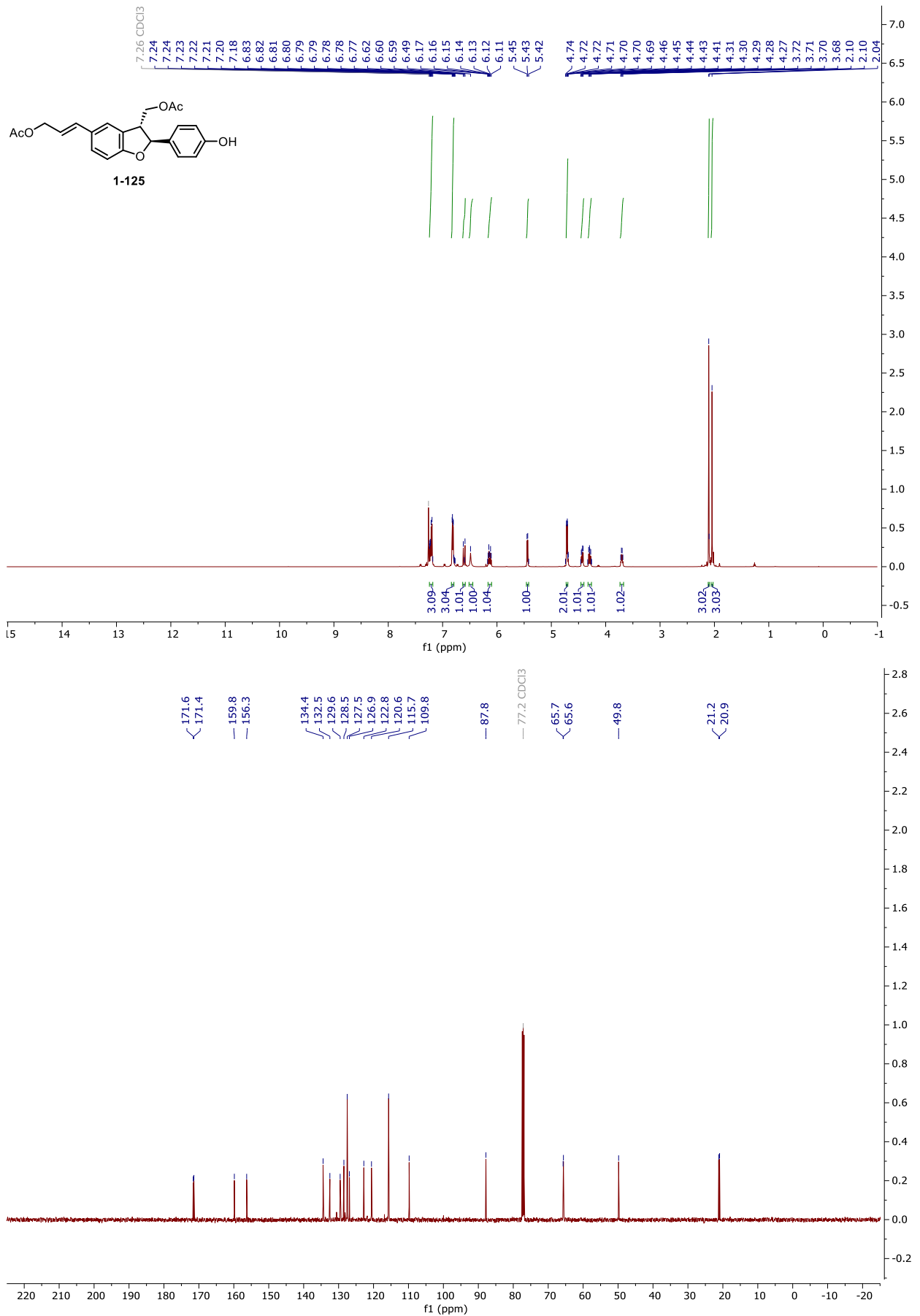
NMR and HPLC

Copy of ^1H and $^{13}\text{C}\{^1\text{H}\}$ spectra of 1-124



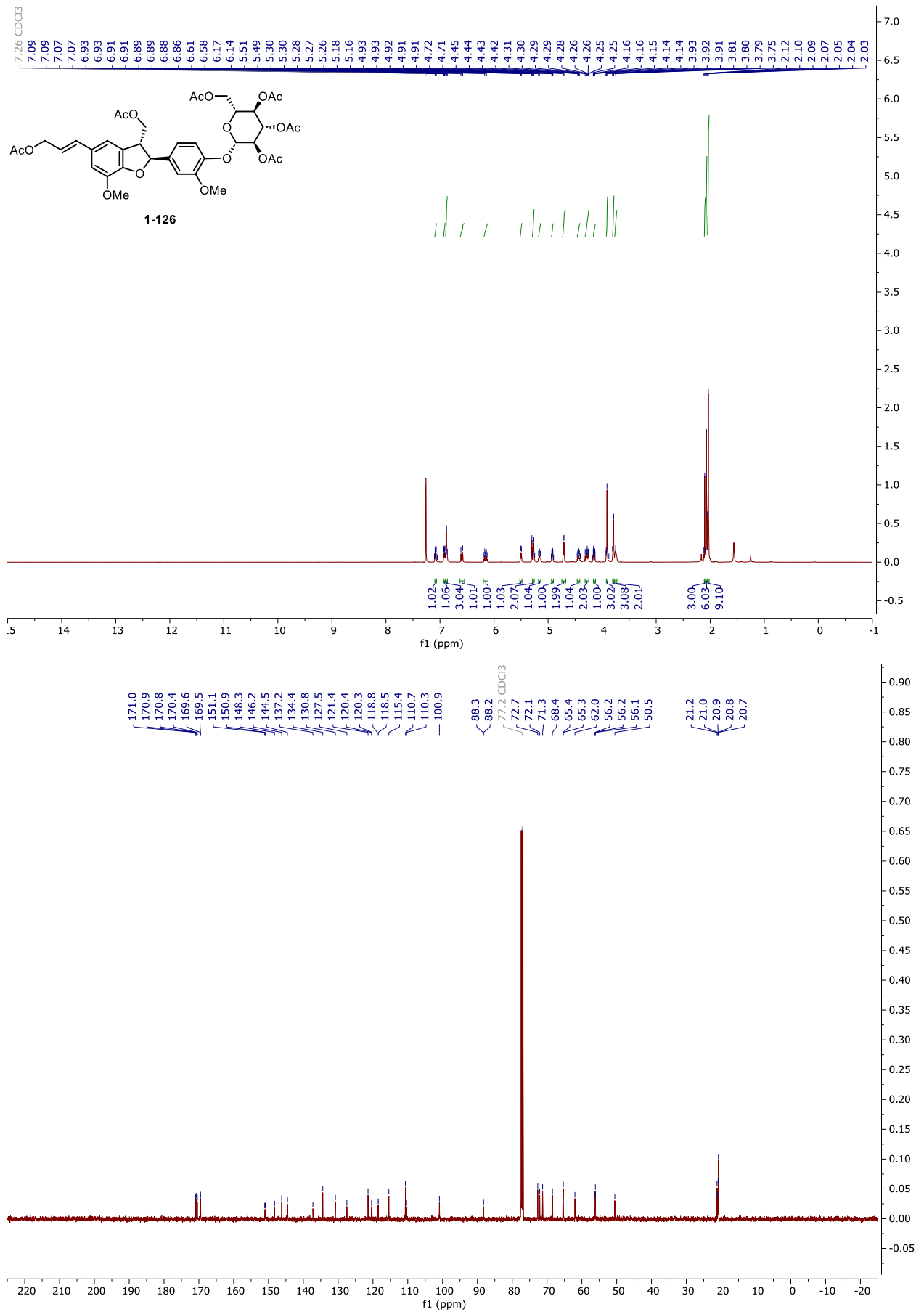
NMR and HPLC

Copy of ^1H and $^{13}\text{C}\{^1\text{H}\}$ spectra of 1-125



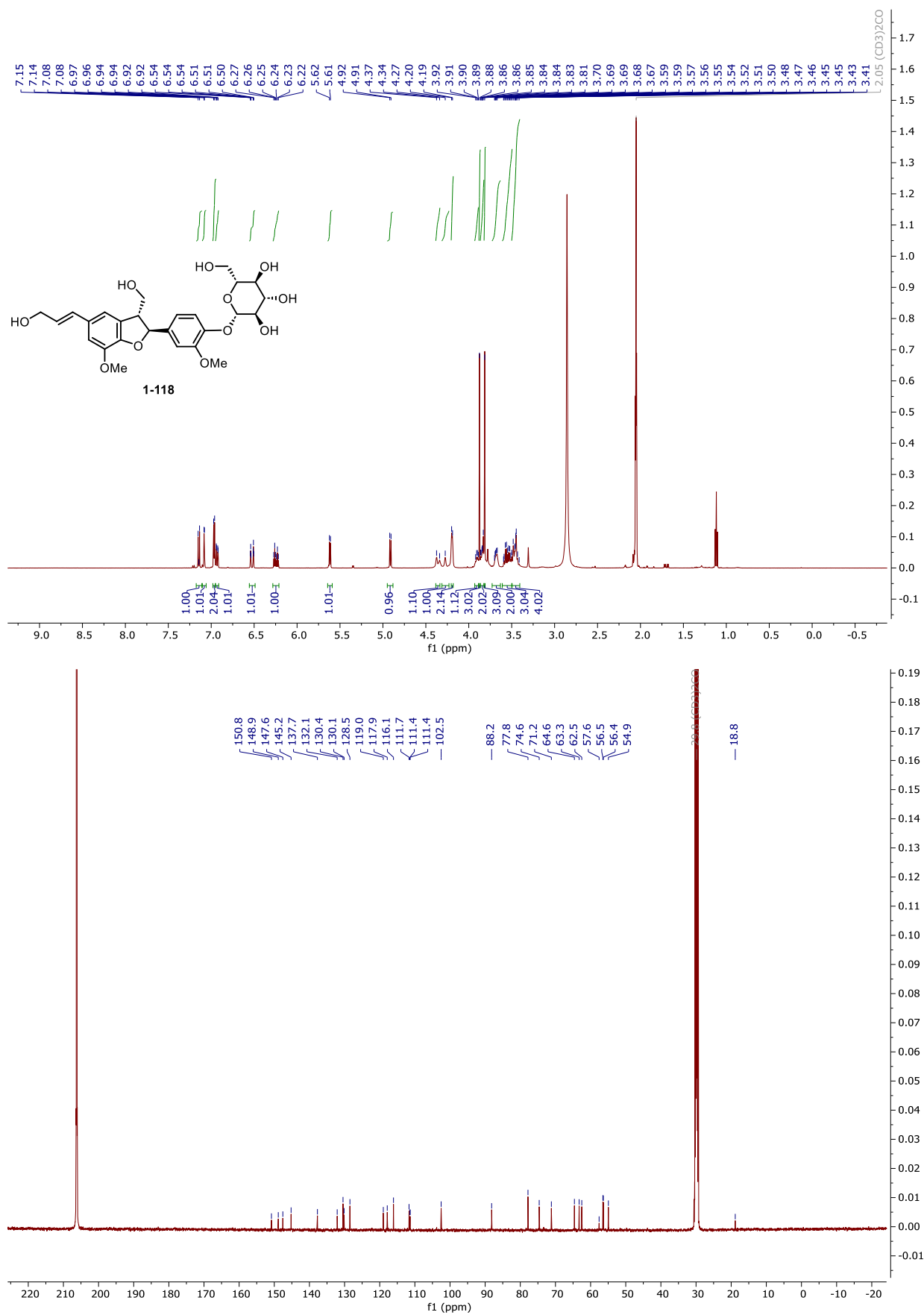
NMR and HPLC

Copy of ^1H and $^{13}\text{C}\{^1\text{H}\}$ spectra of 1-126



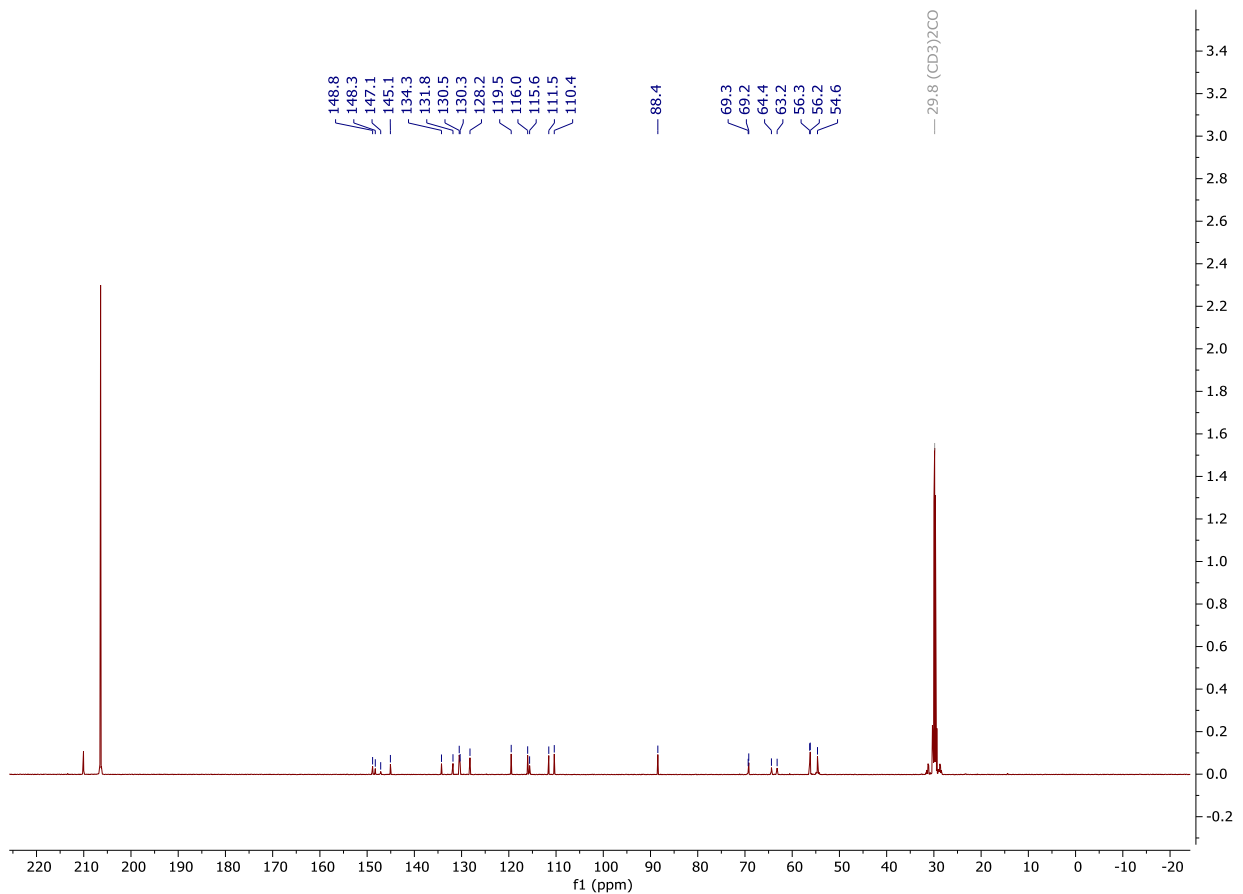
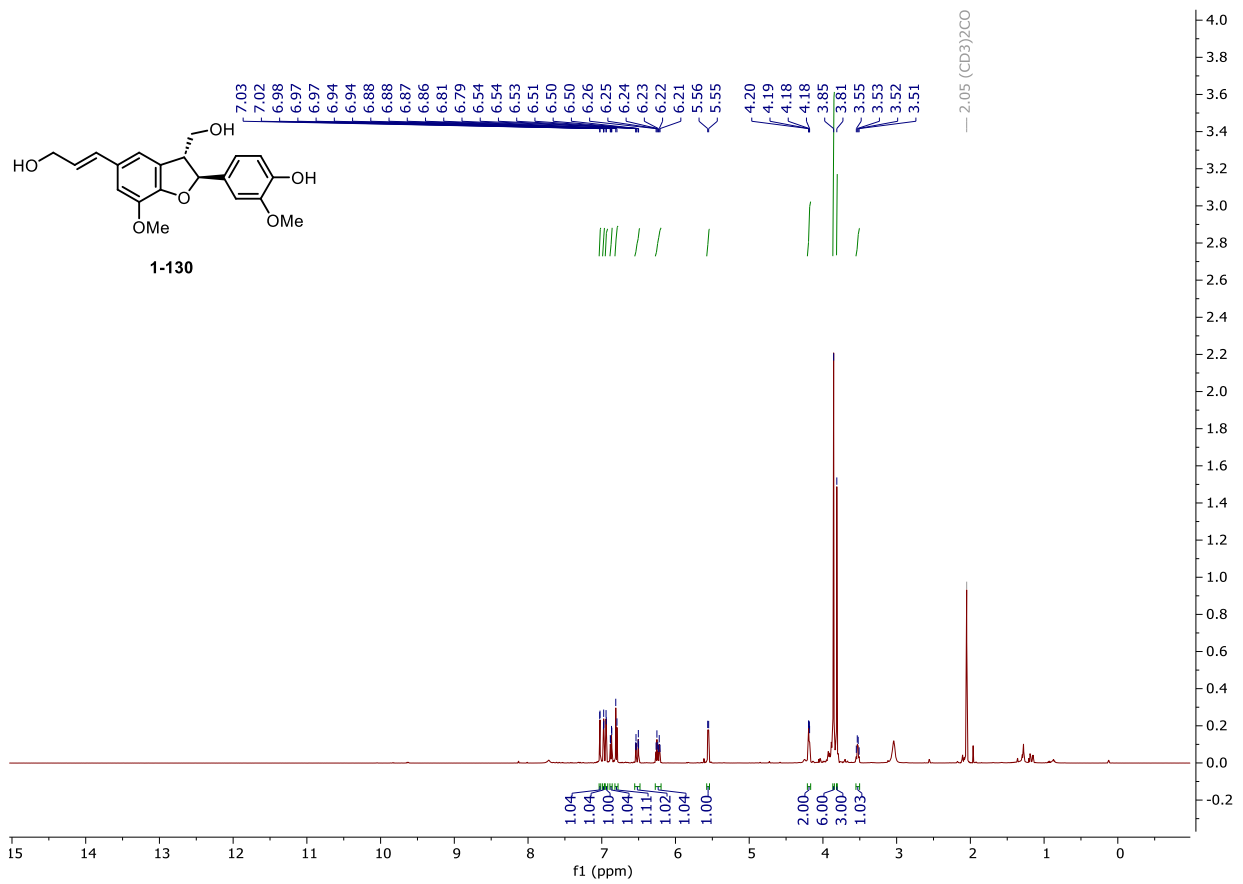
NMR and HPLC

Copy of ^1H and $^{13}\text{C}\{^1\text{H}\}$ spectra of DCG-A, 1-108



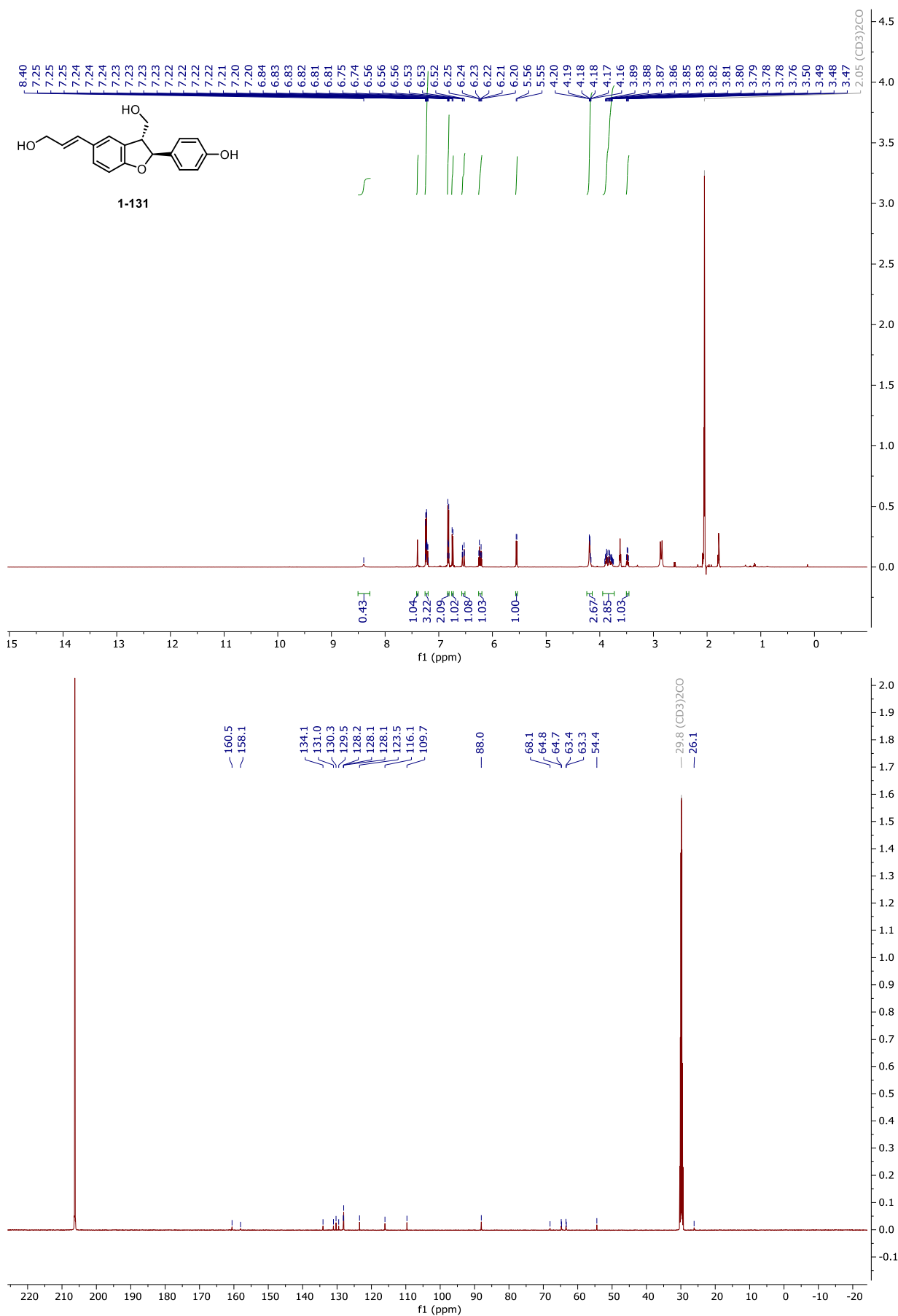
NMR and HPLC

Copy of ^1H and $^{13}\text{C}\{^1\text{H}\}$ spectra of 1-130



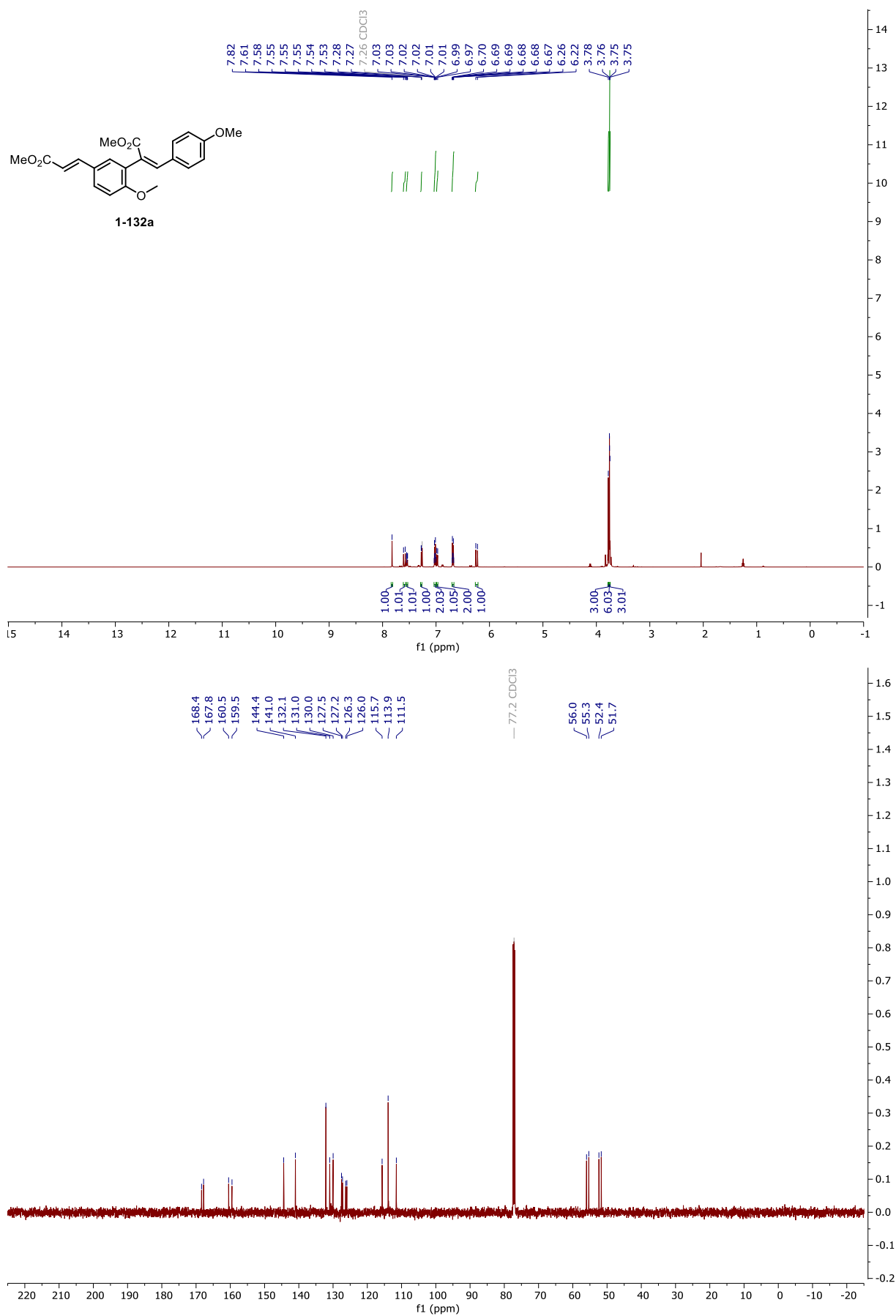
NMR and HPLC

Copy of ^1H and $^{13}\text{C}\{^1\text{H}\}$ spectra of 1-131



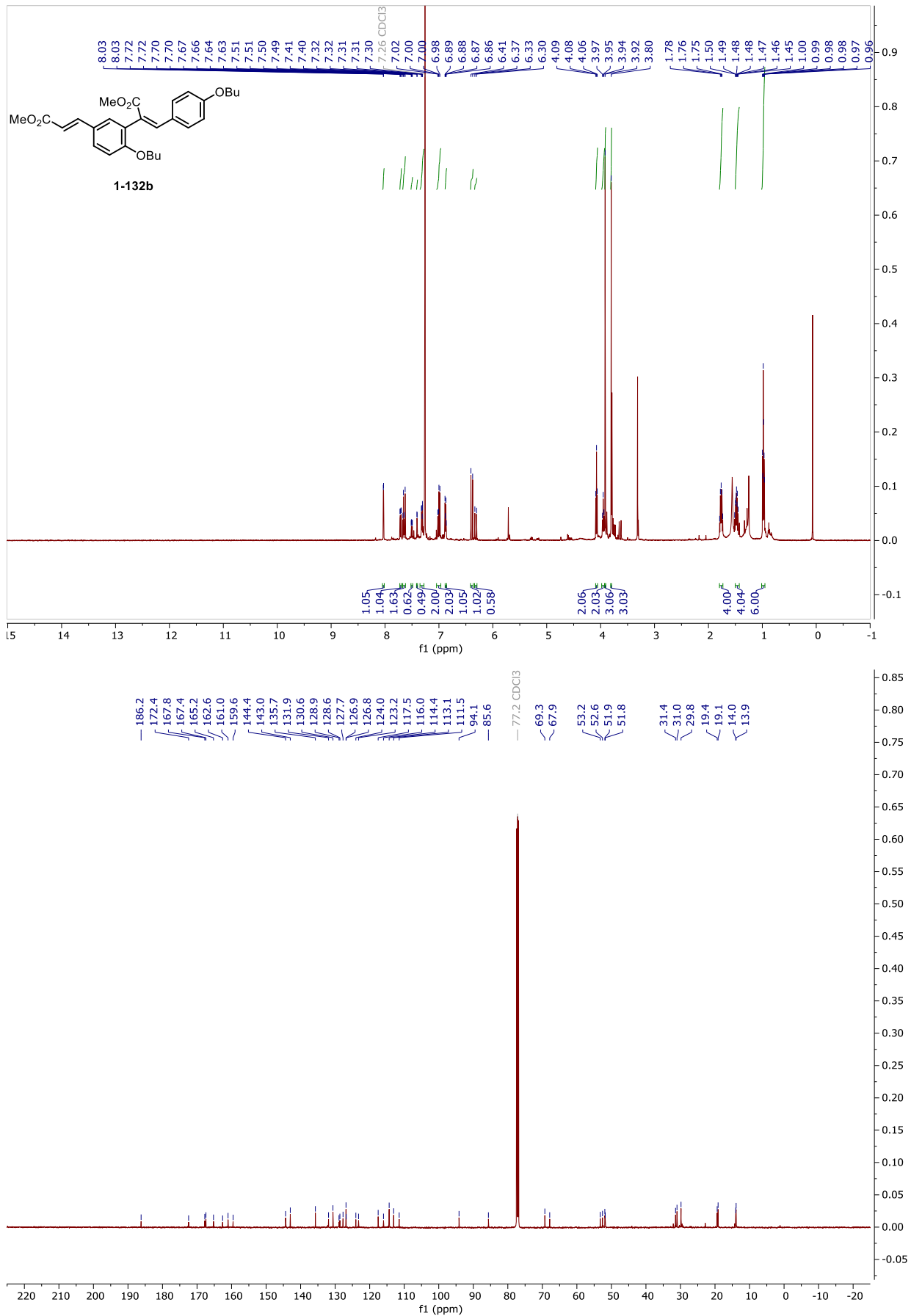
NMR and HPLC

Copy of ^1H and $^{13}\text{C}\{^1\text{H}\}$ spectra of 1-132a



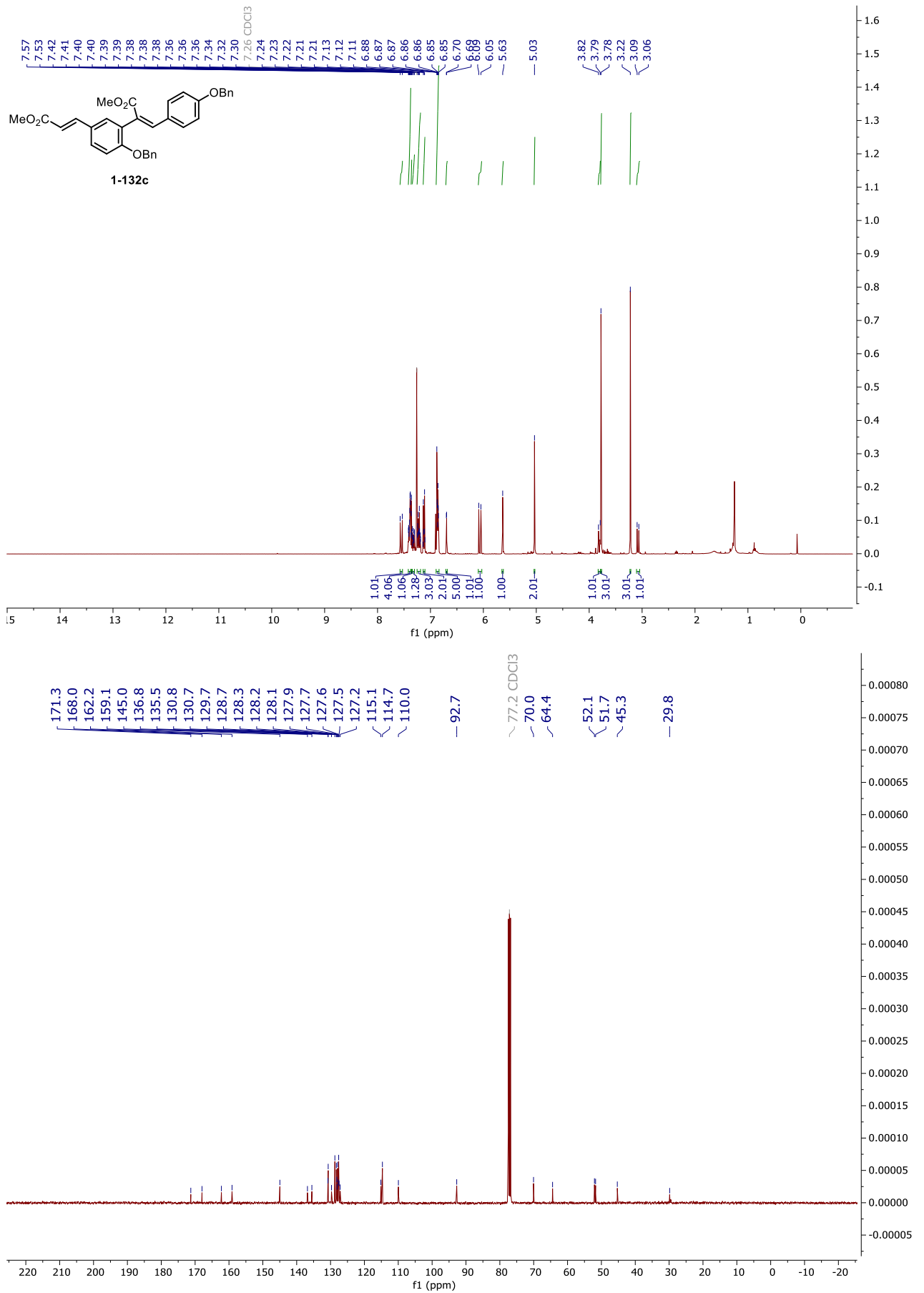
NMR and HPLC

Copy of ^1H and $^{13}\text{C}\{^1\text{H}\}$ spectra of 1-132b



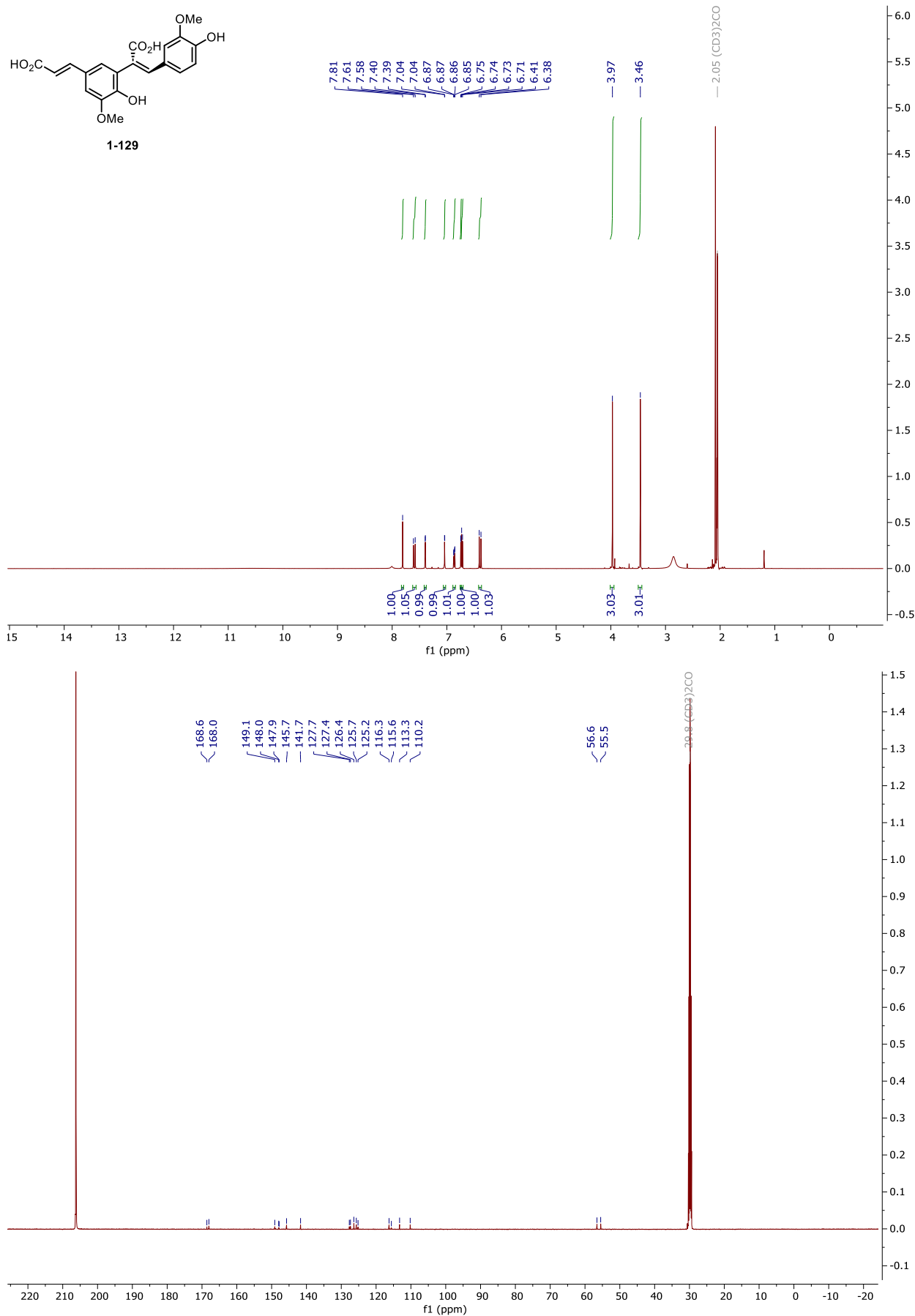
NMR and HPLC

Copy of ^1H and $^{13}\text{C}\{^1\text{H}\}$ spectra of 1-132c



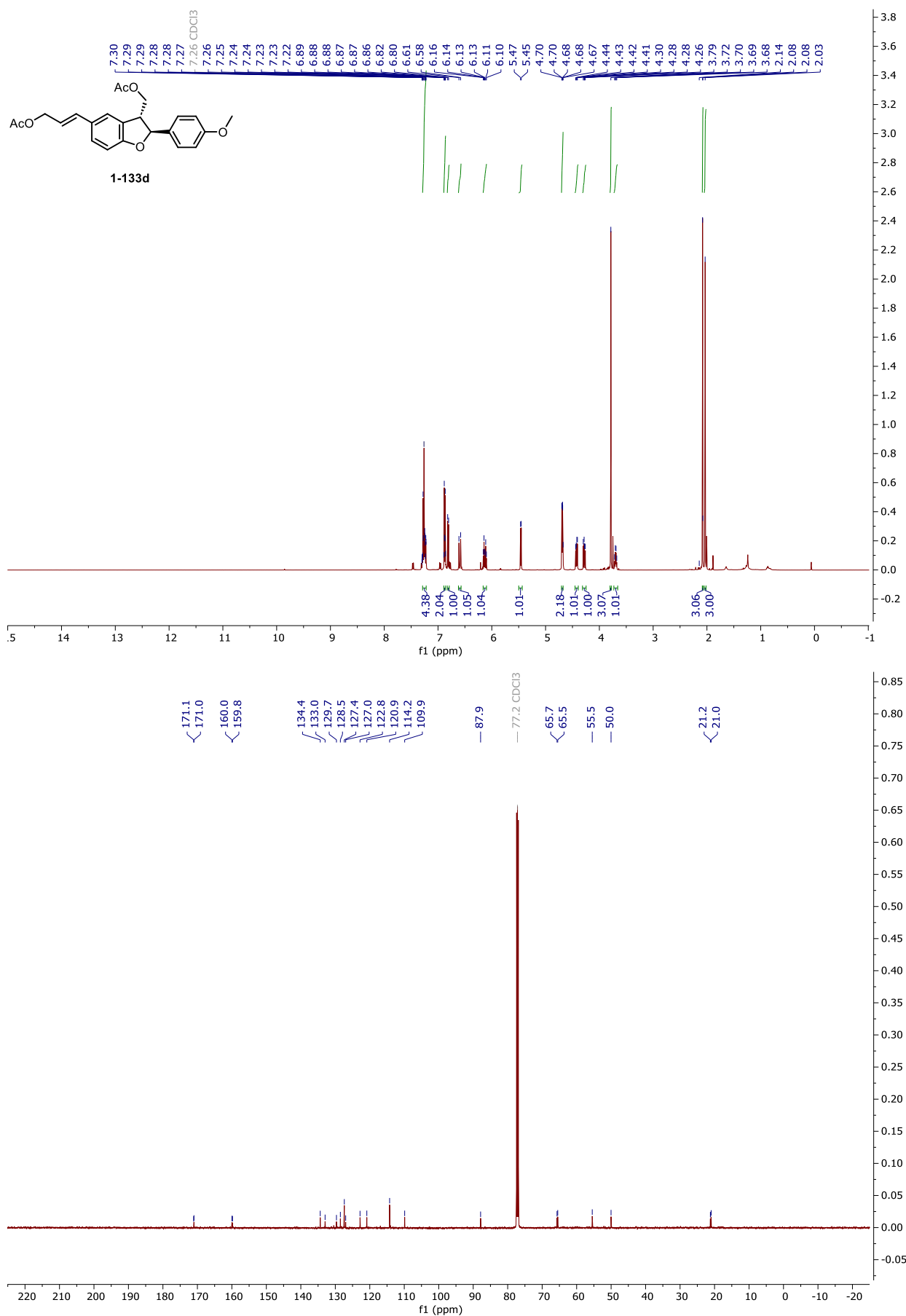
NMR and HPLC

Copy of ^1H and $^{13}\text{C}\{^1\text{H}\}$ spectra of 1-129



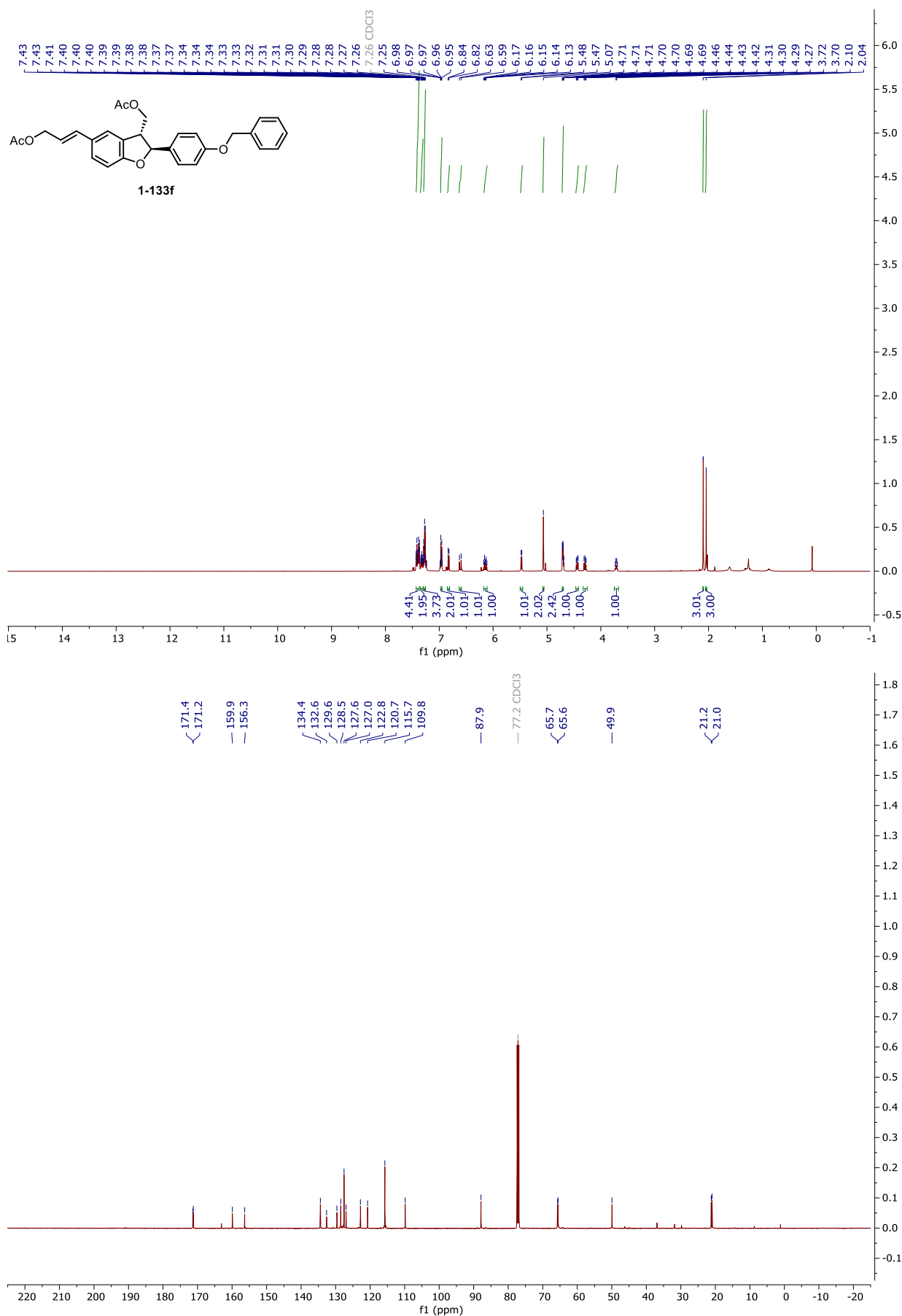
NMR and HPLC

Copy of ^1H and $^{13}\text{C}\{^1\text{H}\}$ spectra of 1-133d



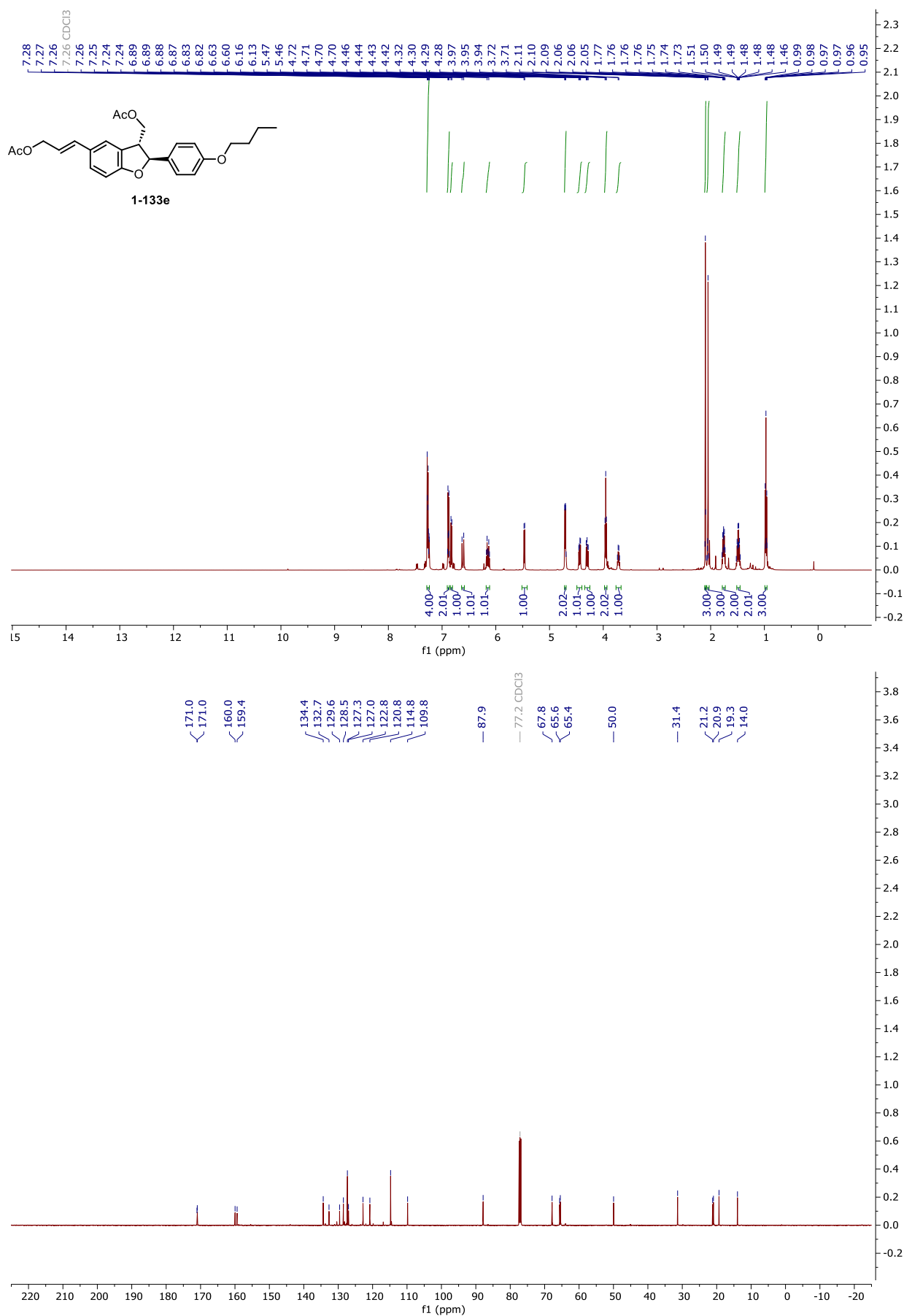
NMR and HPLC

Copy of ^1H and $^{13}\text{C}\{^1\text{H}\}$ spectra of 1-133f



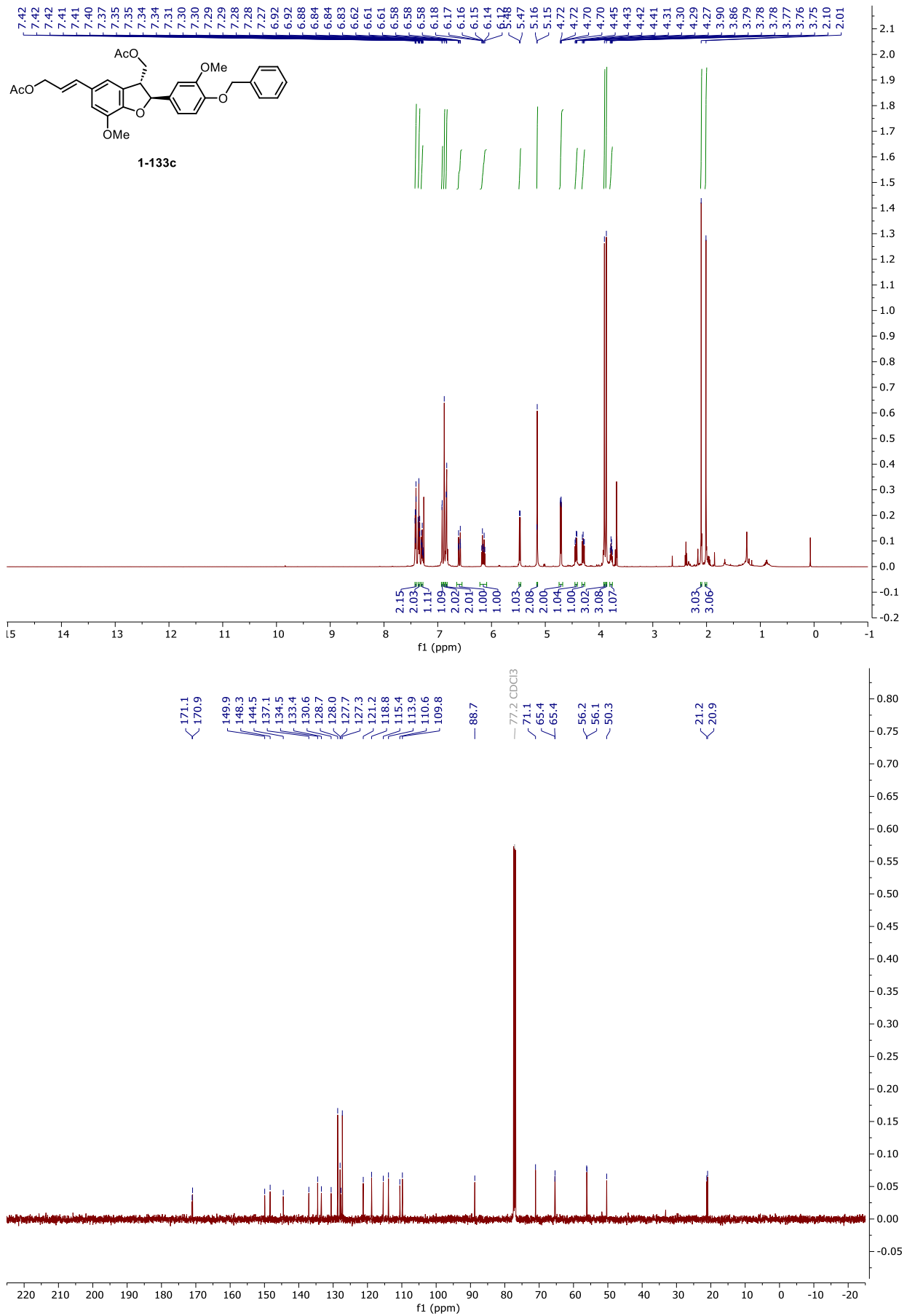
NMR and HPLC

Copy of ^1H and $^{13}\text{C}\{^1\text{H}\}$ spectra of 1-133e



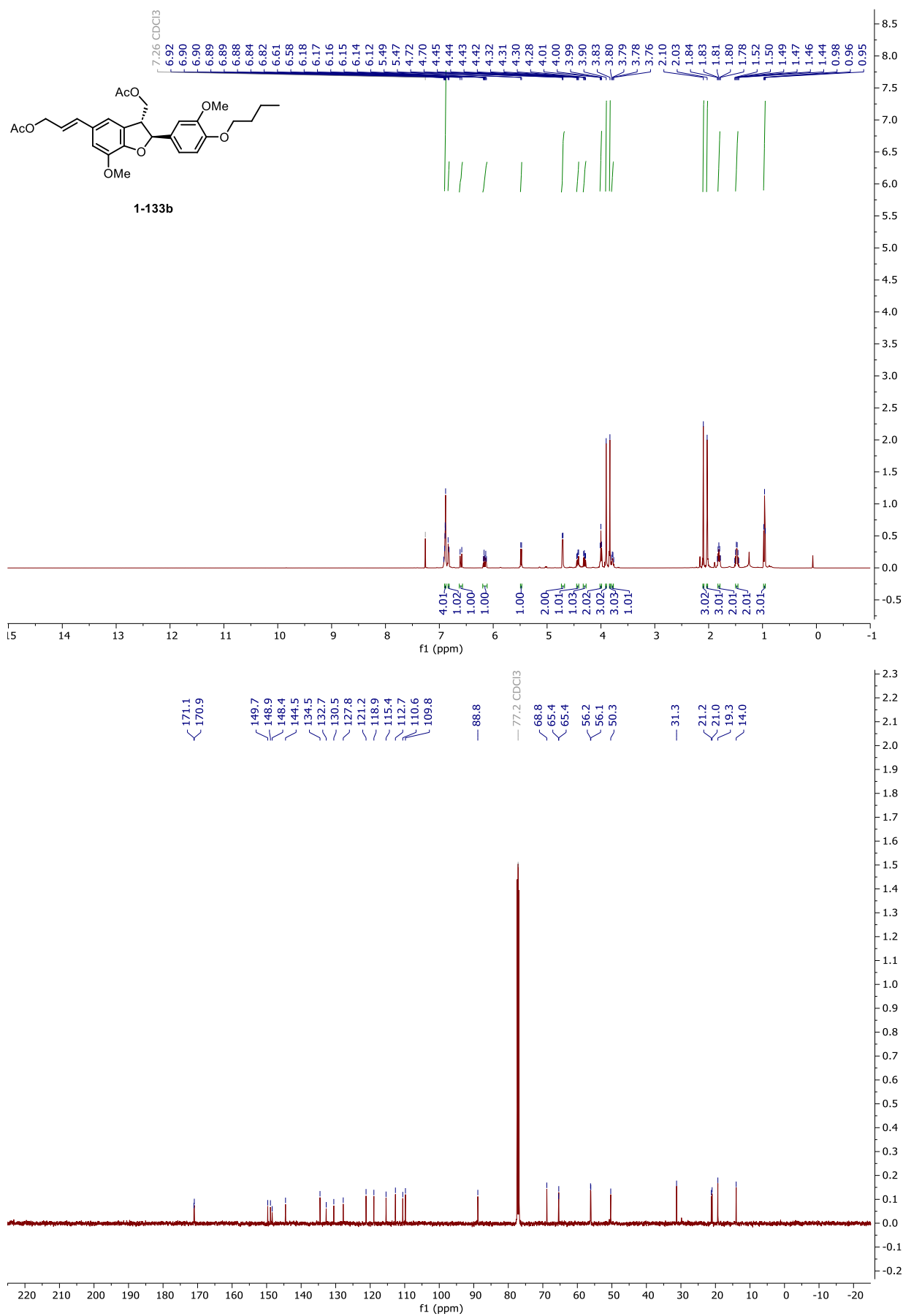
NMR and HPLC

Copy of ^1H and $^{13}\text{C}\{^1\text{H}\}$ spectra of 1-133c



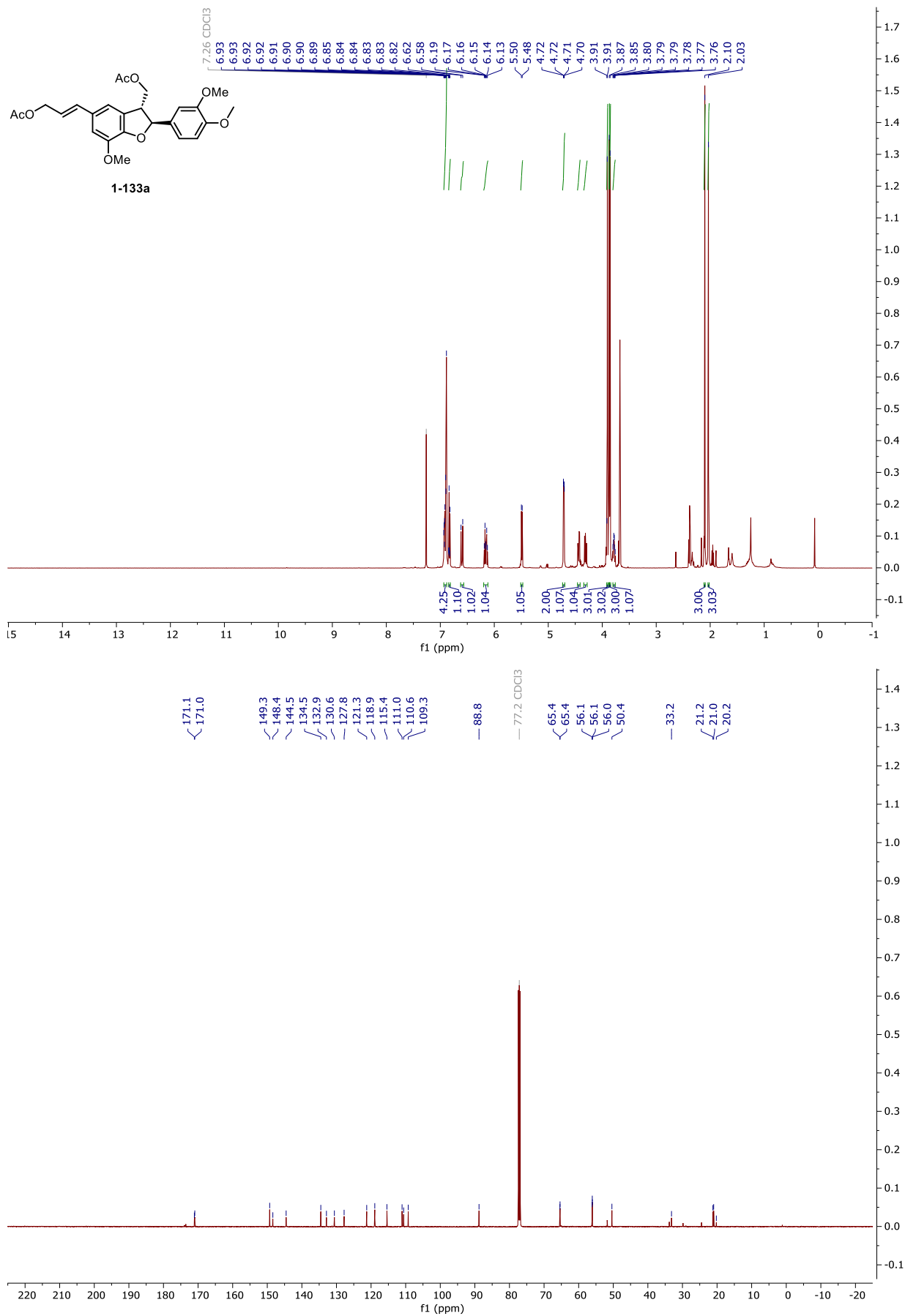
NMR and HPLC

Copy of ^1H and $^{13}\text{C}\{^1\text{H}\}$ spectra of 1-133b



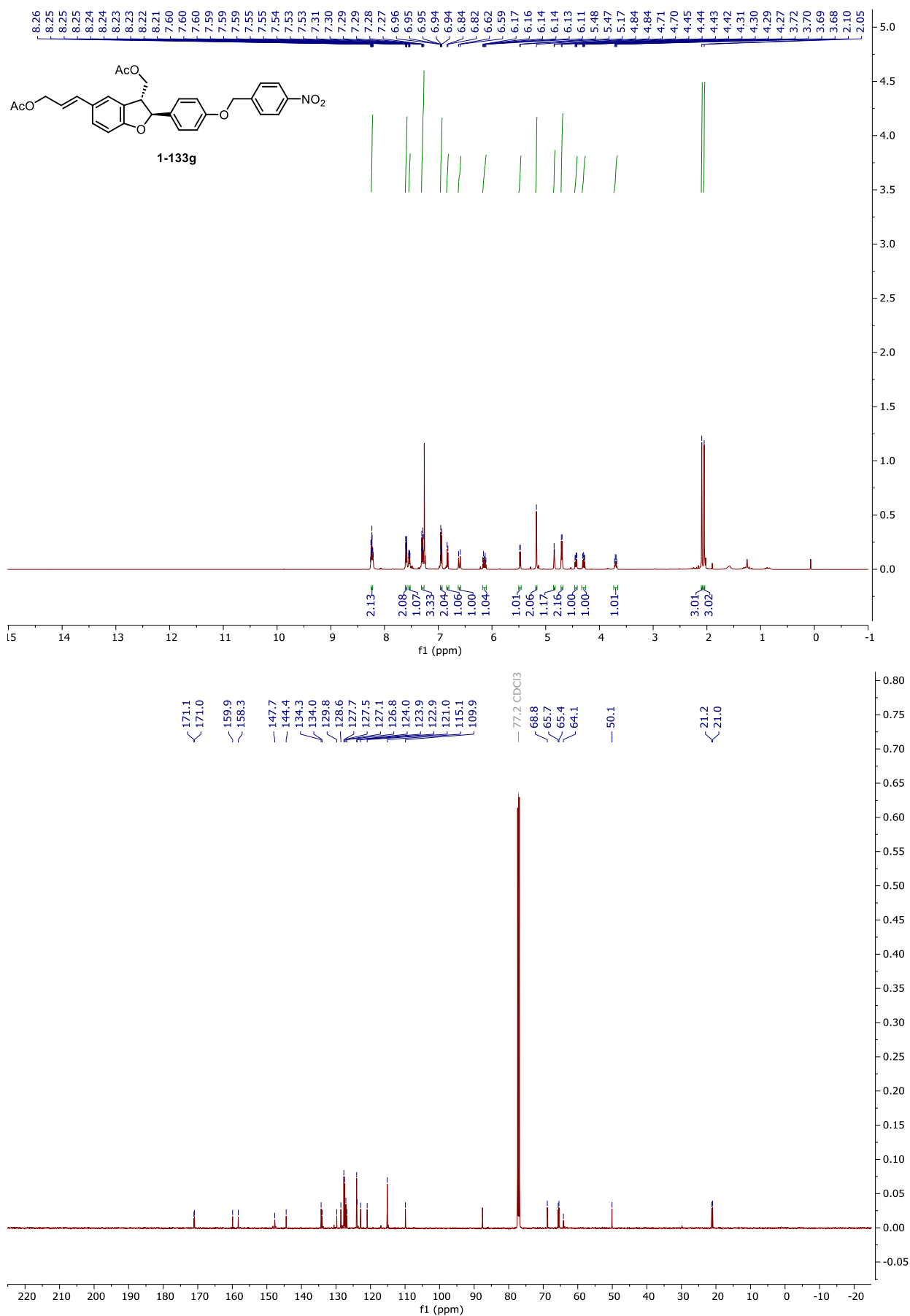
NMR and HPLC

Copy of ¹H and ¹³C{¹H} spectra of 1-133a



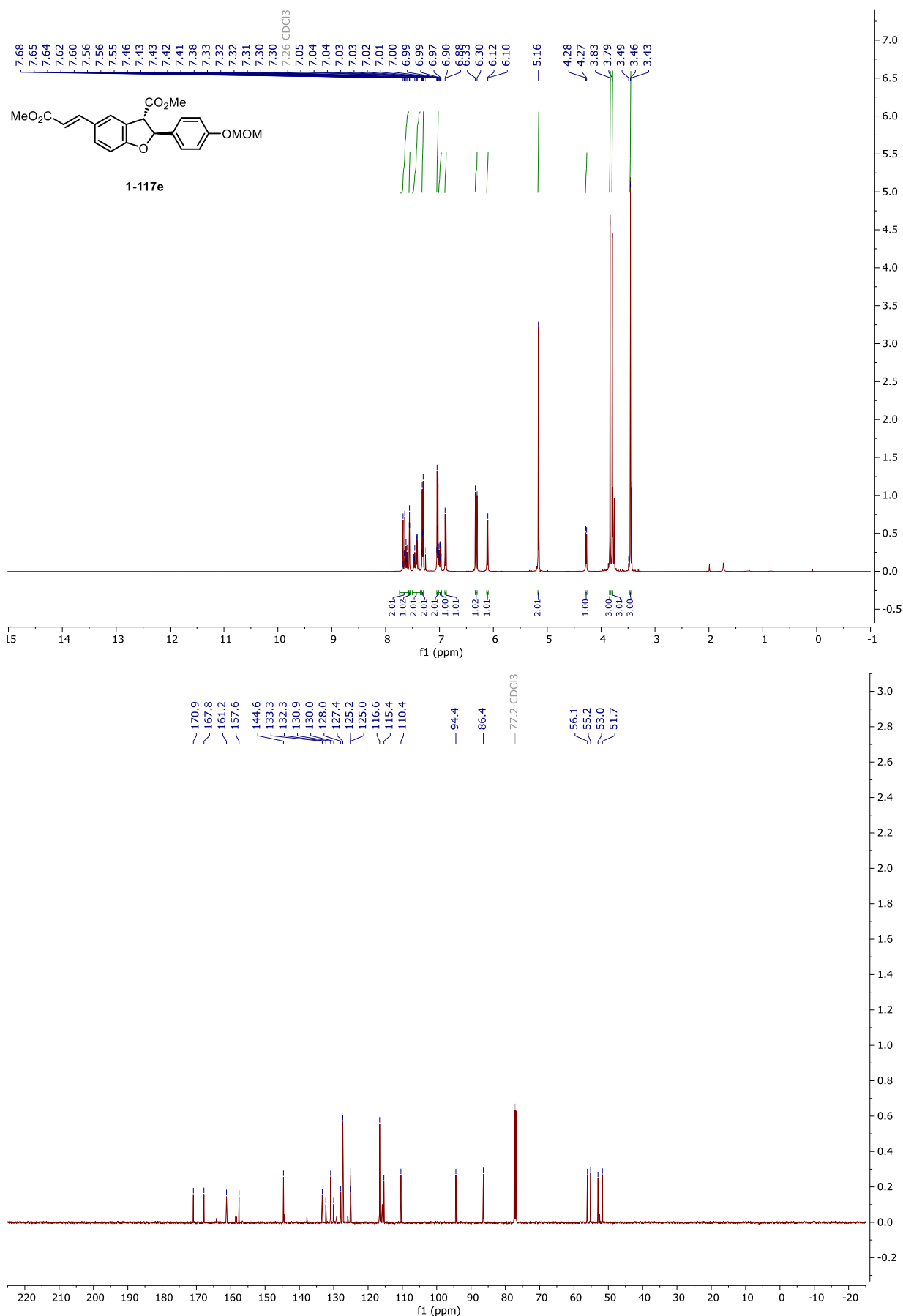
NMR and HPLC

Copy of ^1H and $^{13}\text{C}\{^1\text{H}\}$ spectra of 1-133g



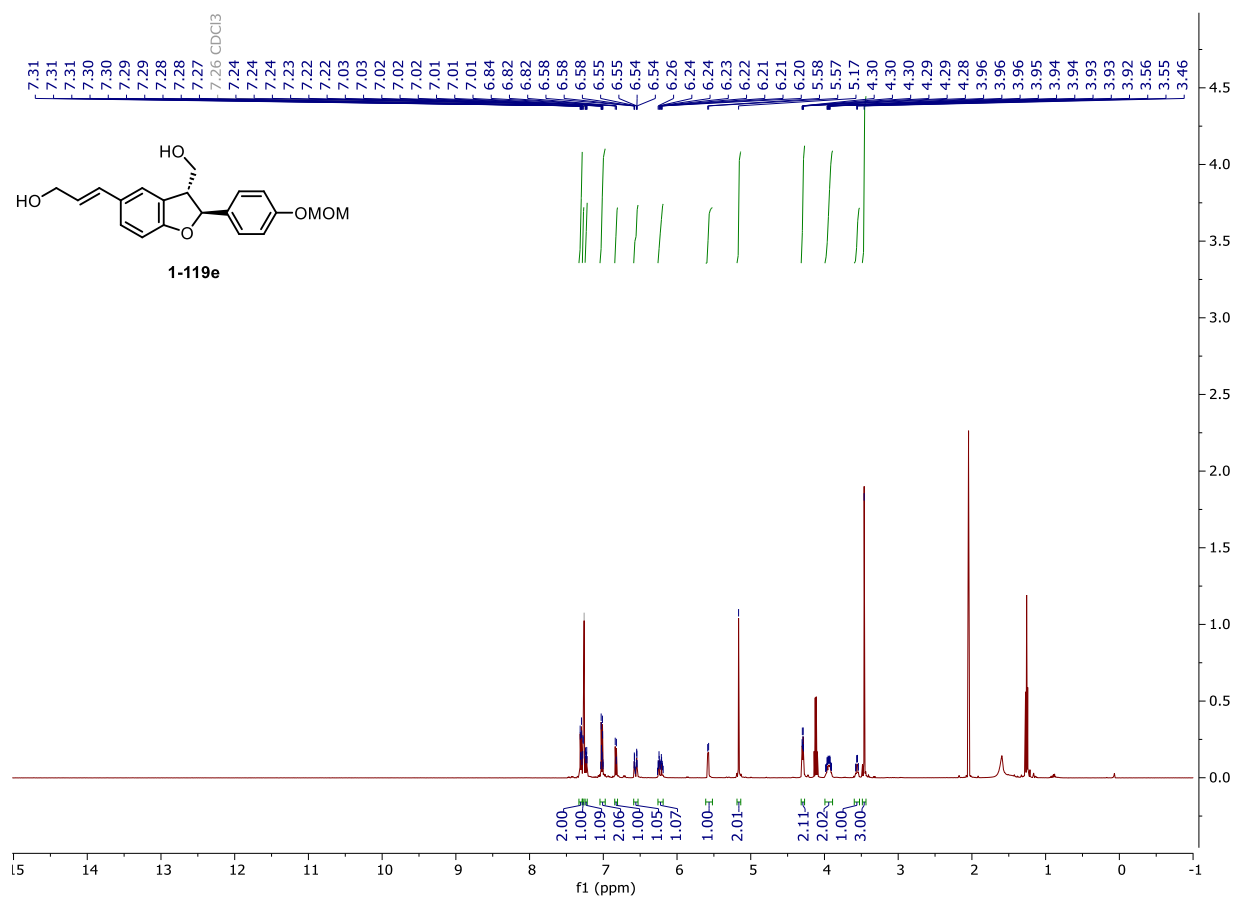
NMR and HPLC

Copy of ^1H and $^{13}\text{C}\{^1\text{H}\}$ spectra of 1-117e



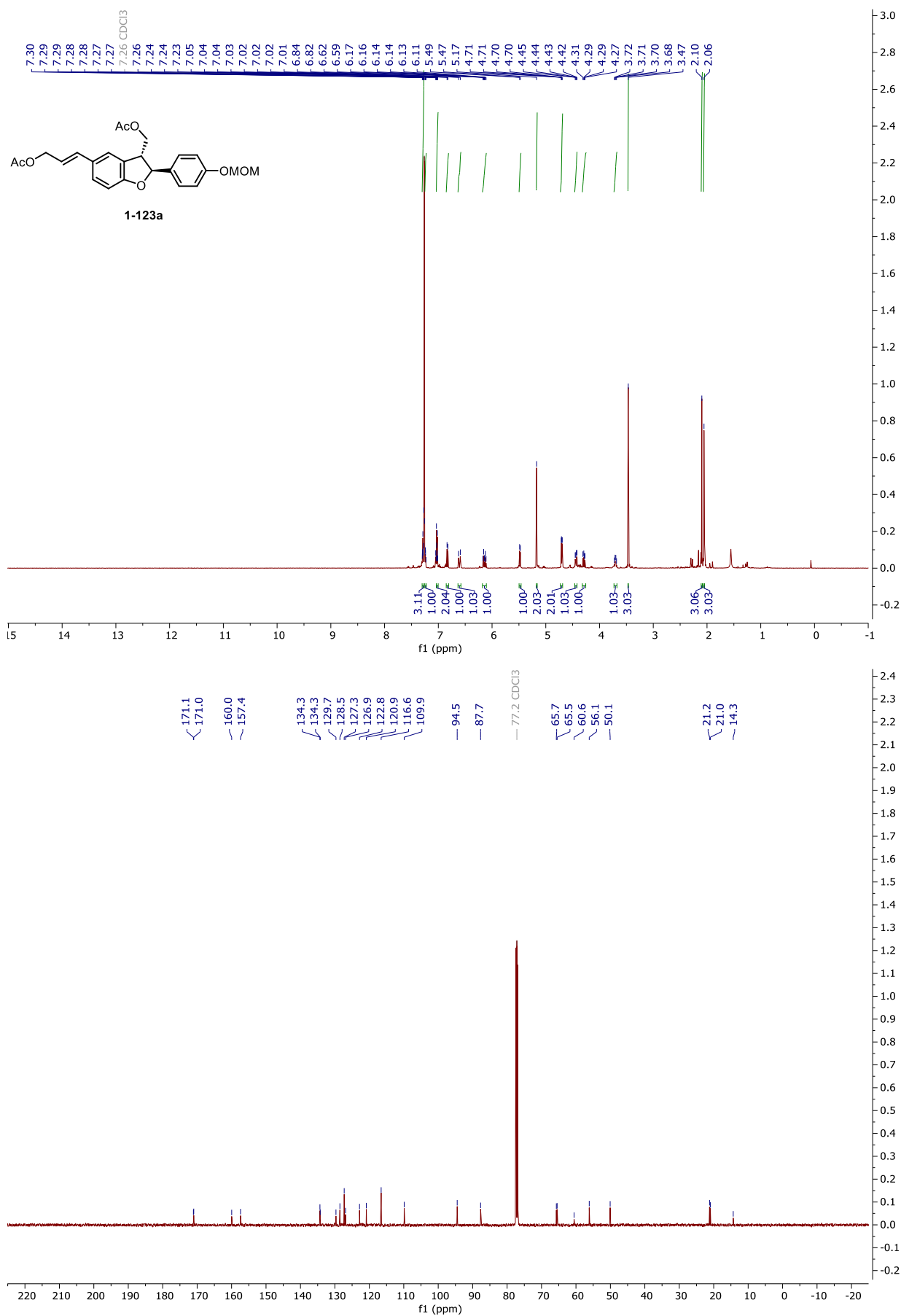
NMR and HPLC

Copy of ^1H and $^{13}\text{C}\{^1\text{H}\}$ spectra of 1-119e



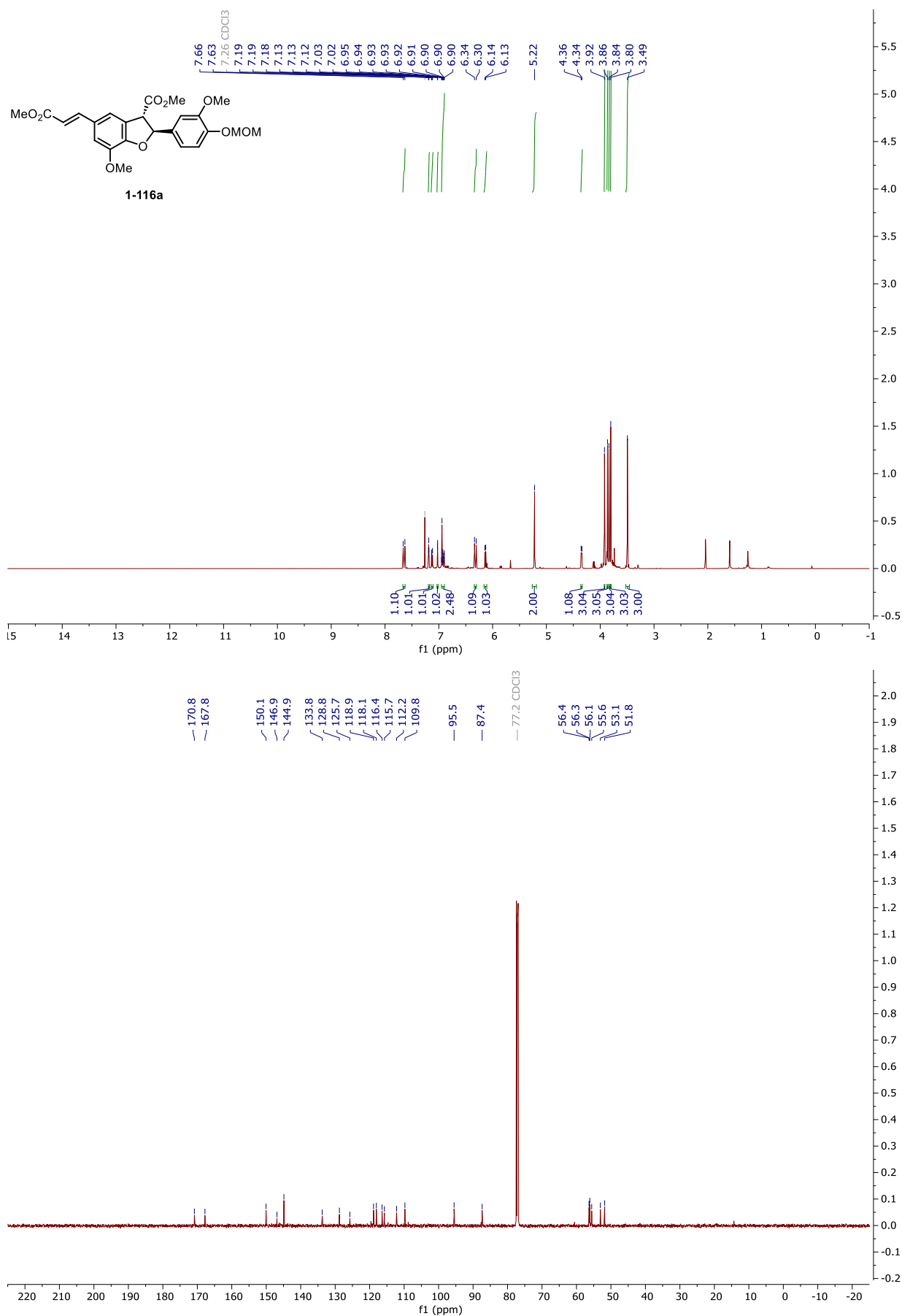
NMR and HPLC

Copy of ^1H and $^{13}\text{C}\{^1\text{H}\}$ spectra of 1-123a



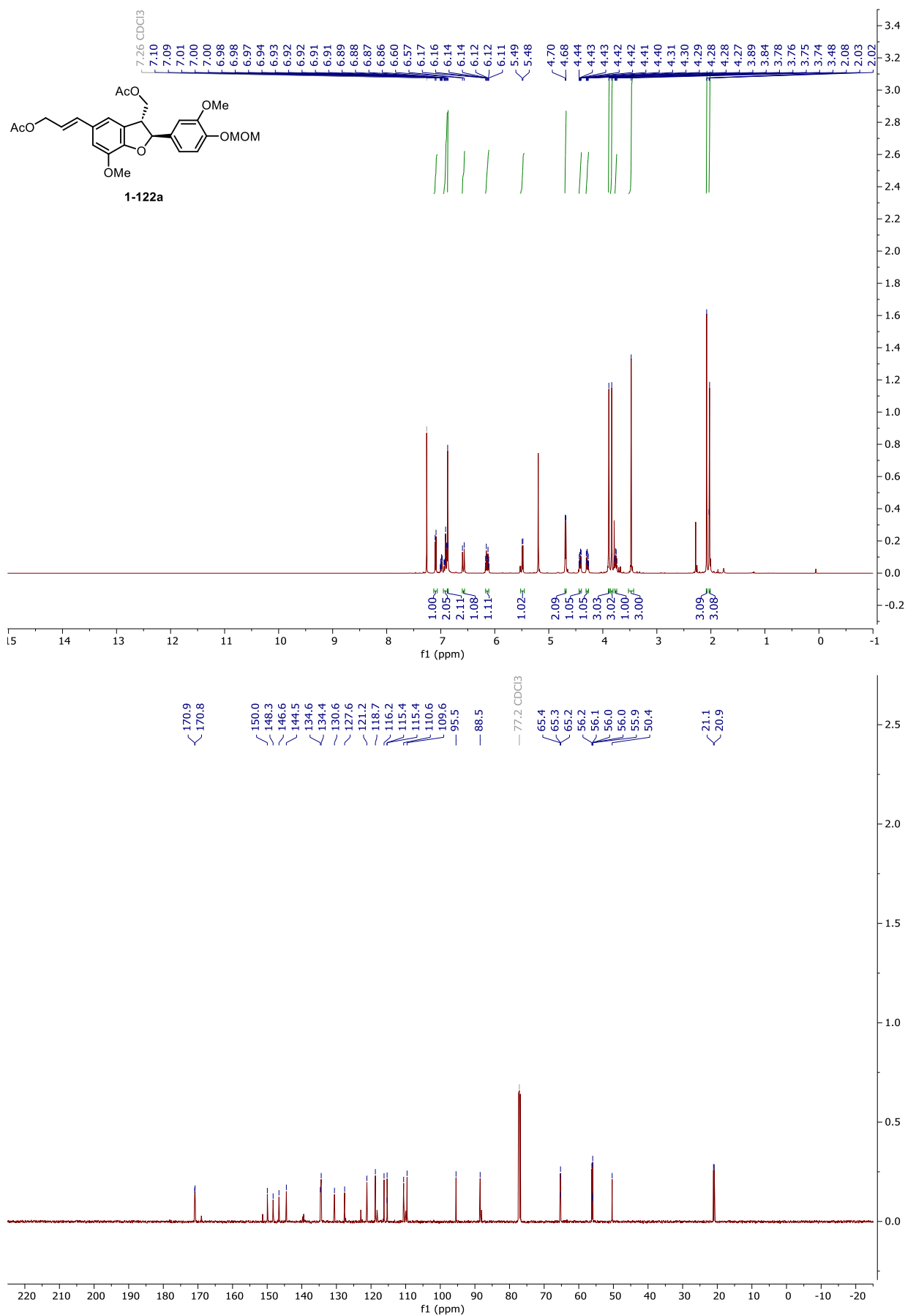
NMR and HPLC

Copy of ^1H and $^{13}\text{C}\{^1\text{H}\}$ spectra of 1-116a



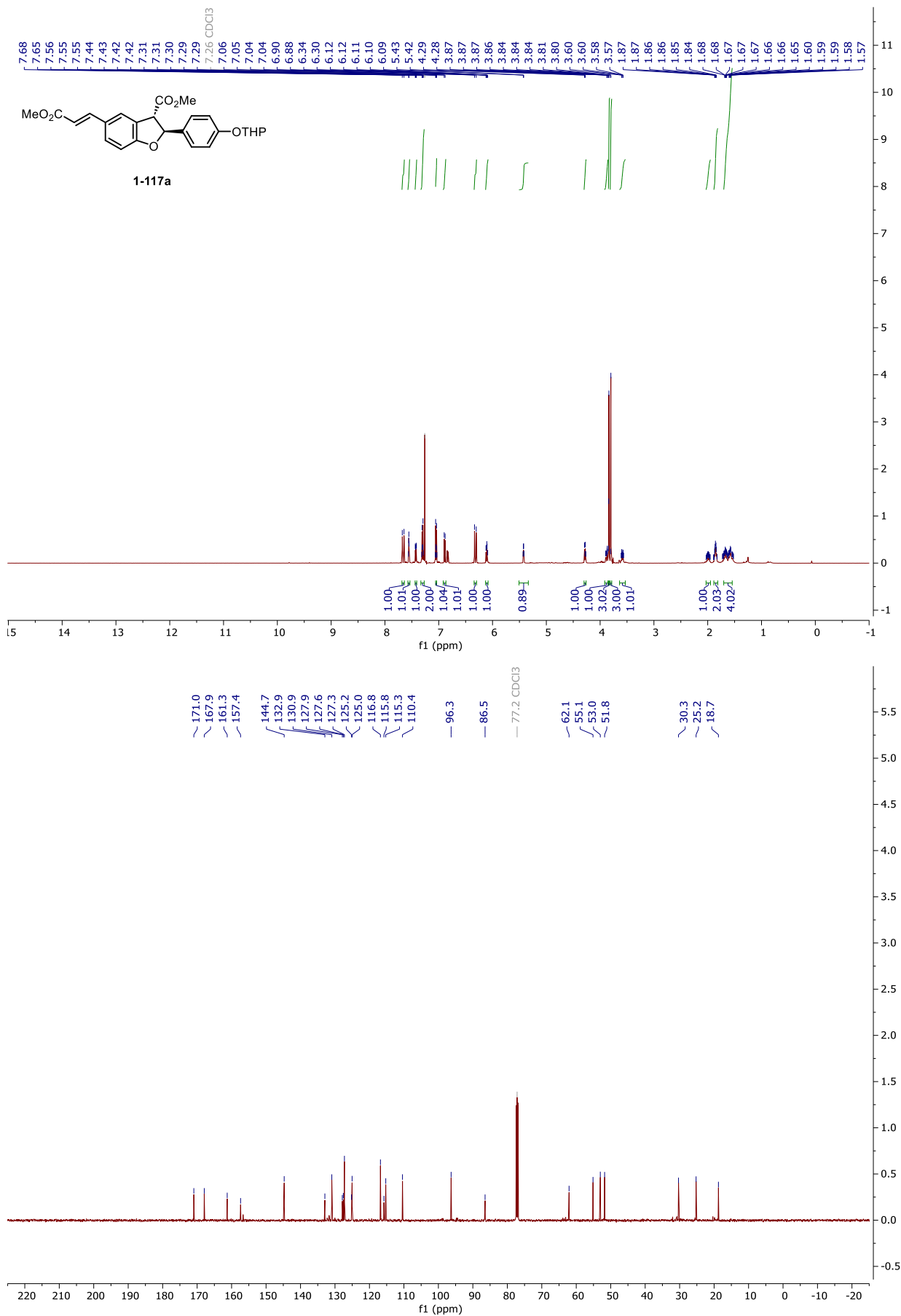
NMR and HPLC

Copy of ^1H and $^{13}\text{C}\{^1\text{H}\}$ spectra of 1-122a



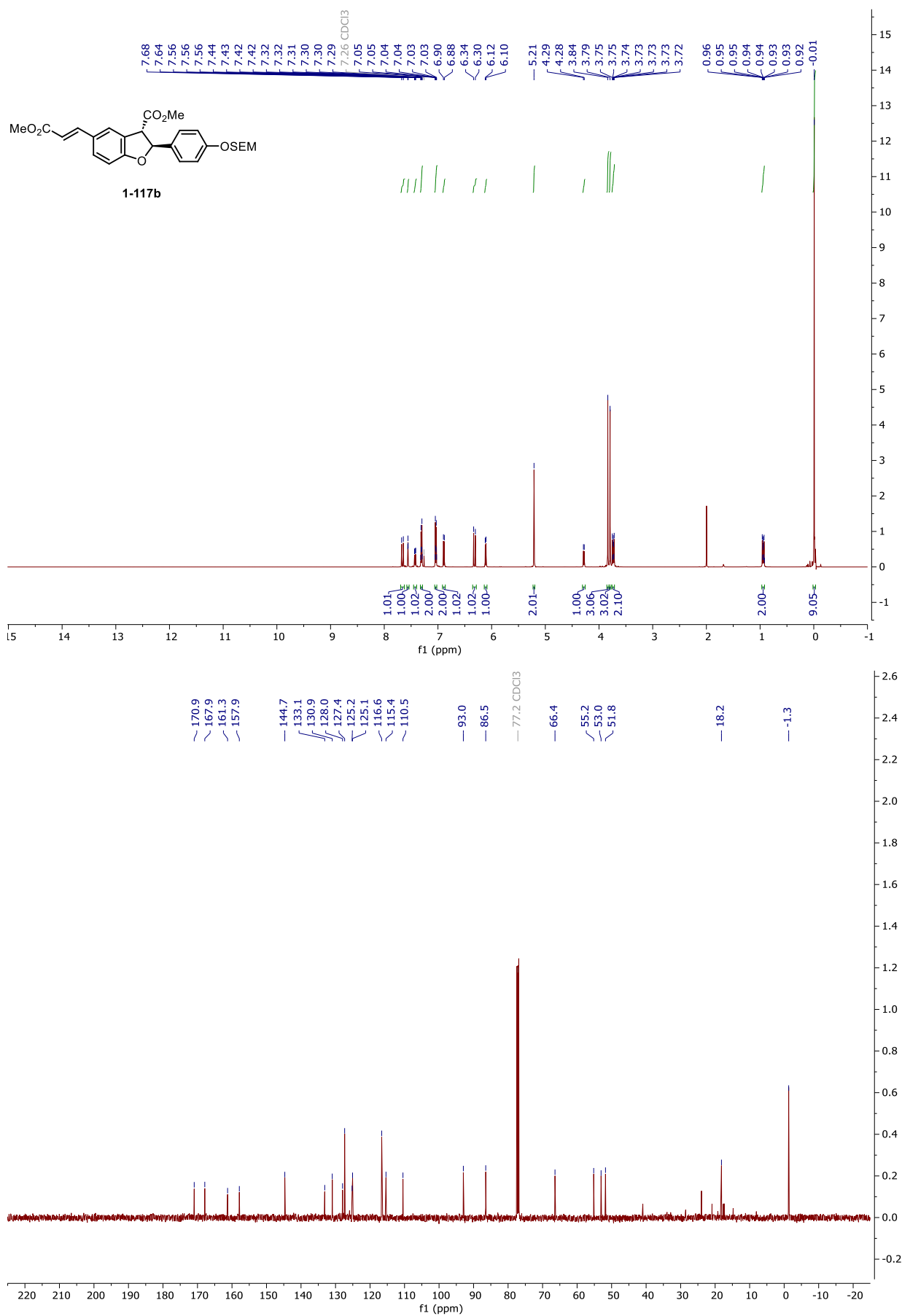
NMR and HPLC

Copy of ^1H and $^{13}\text{C}\{^1\text{H}\}$ spectra of 1-117a



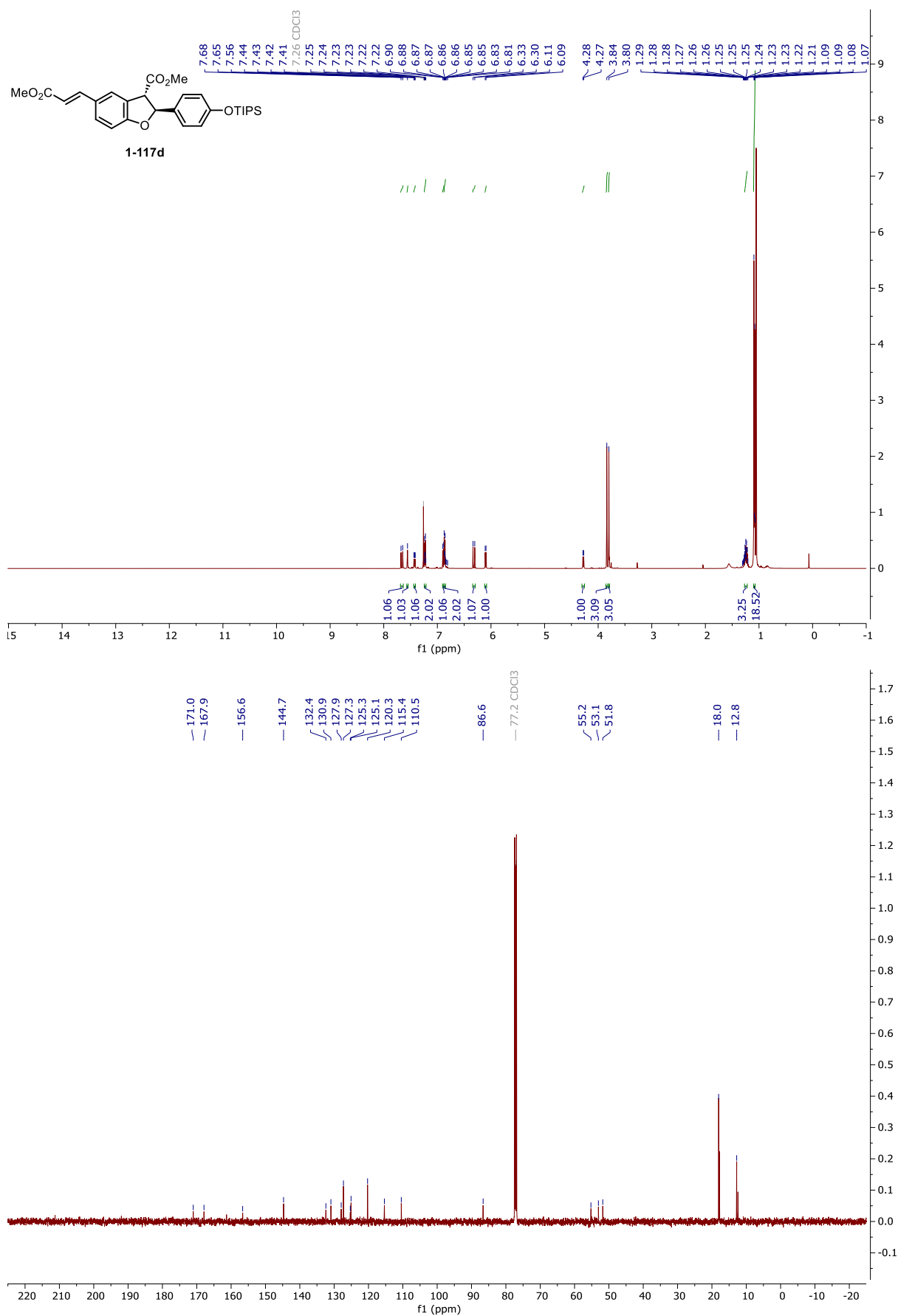
NMR and HPLC

Copy of ^1H and $^{13}\text{C}\{^1\text{H}\}$ spectra of 1-117b



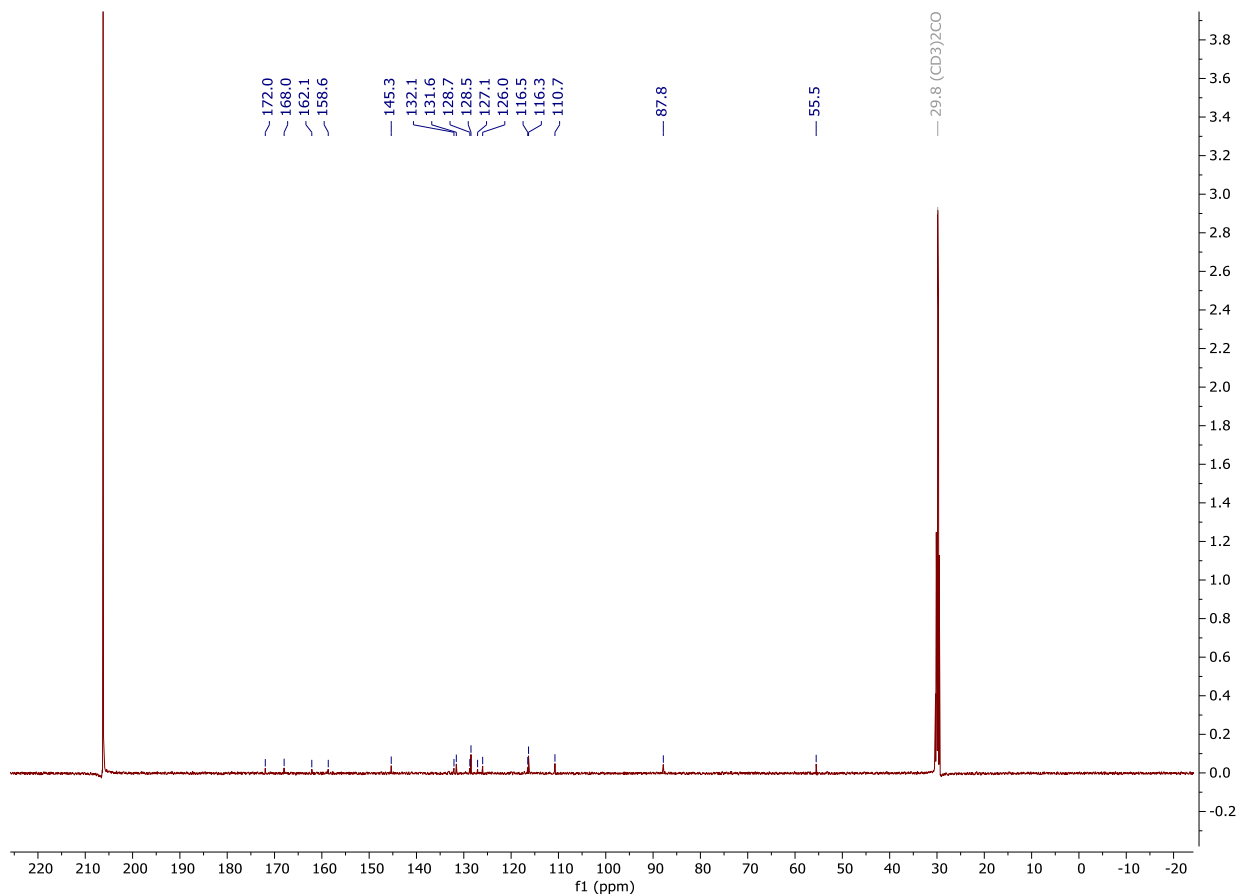
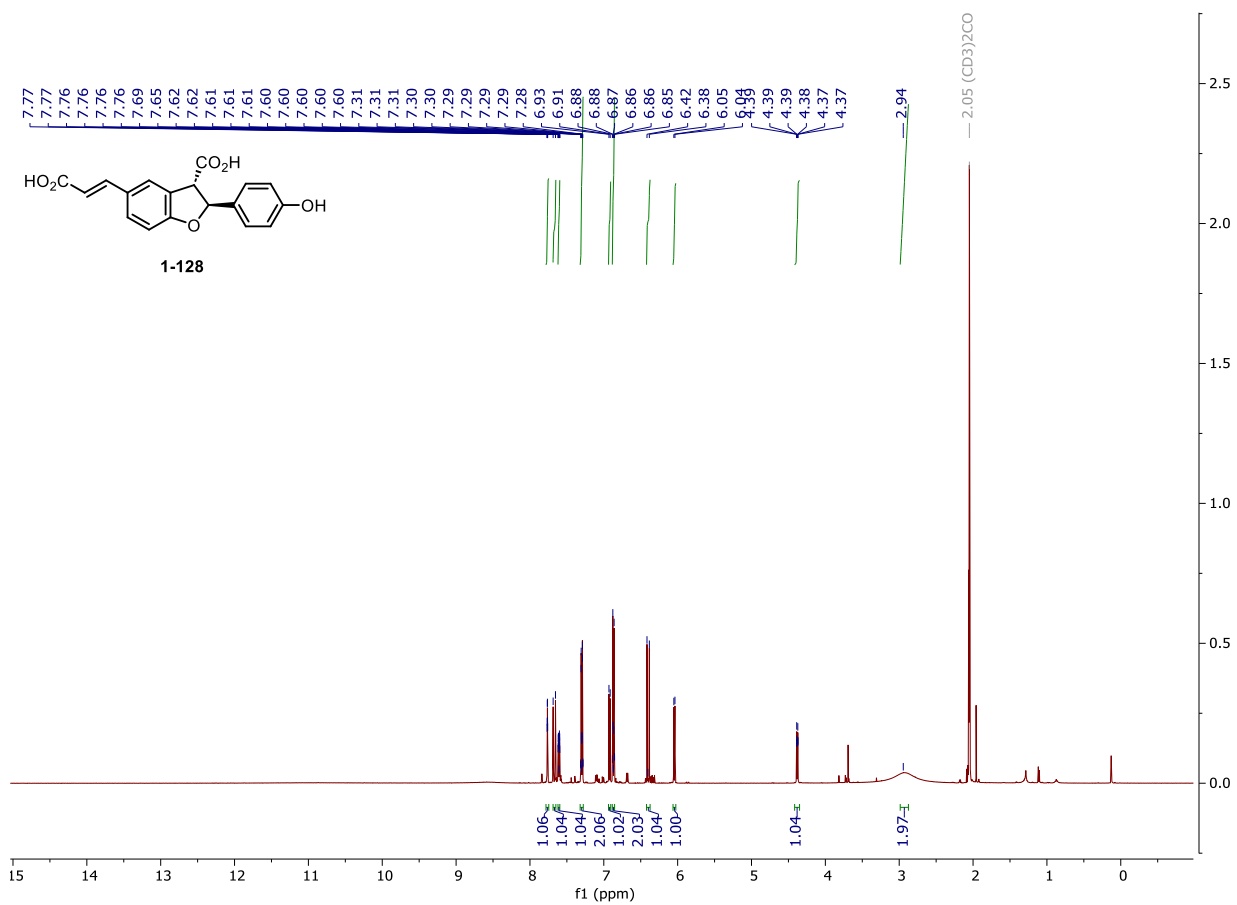
NMR and HPLC

Copy of ^1H and $^{13}\text{C}\{^1\text{H}\}$ spectra of 1-117d



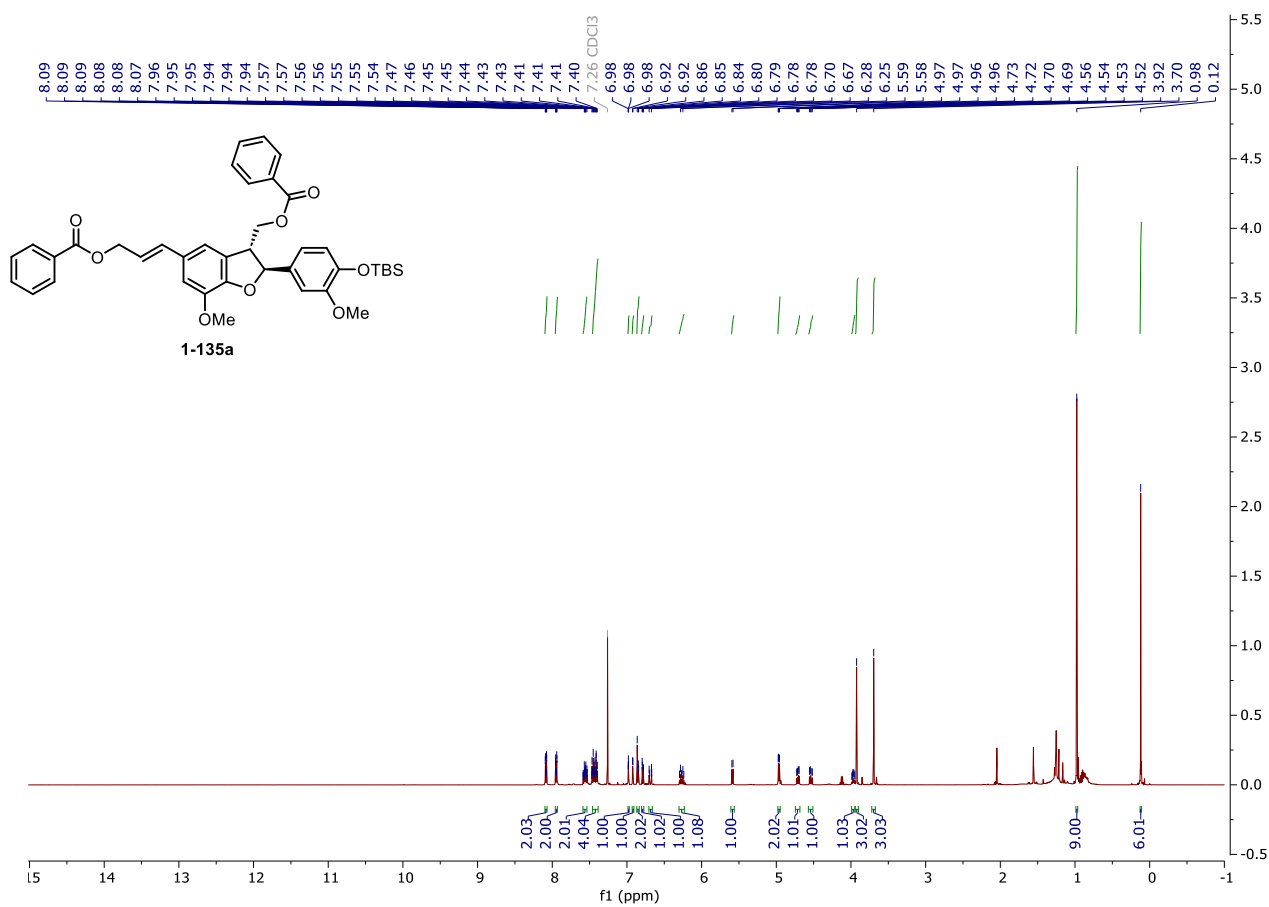
NMR and HPLC

Copy of ^1H and $^{13}\text{C}\{^1\text{H}\}$ spectra of 1-128



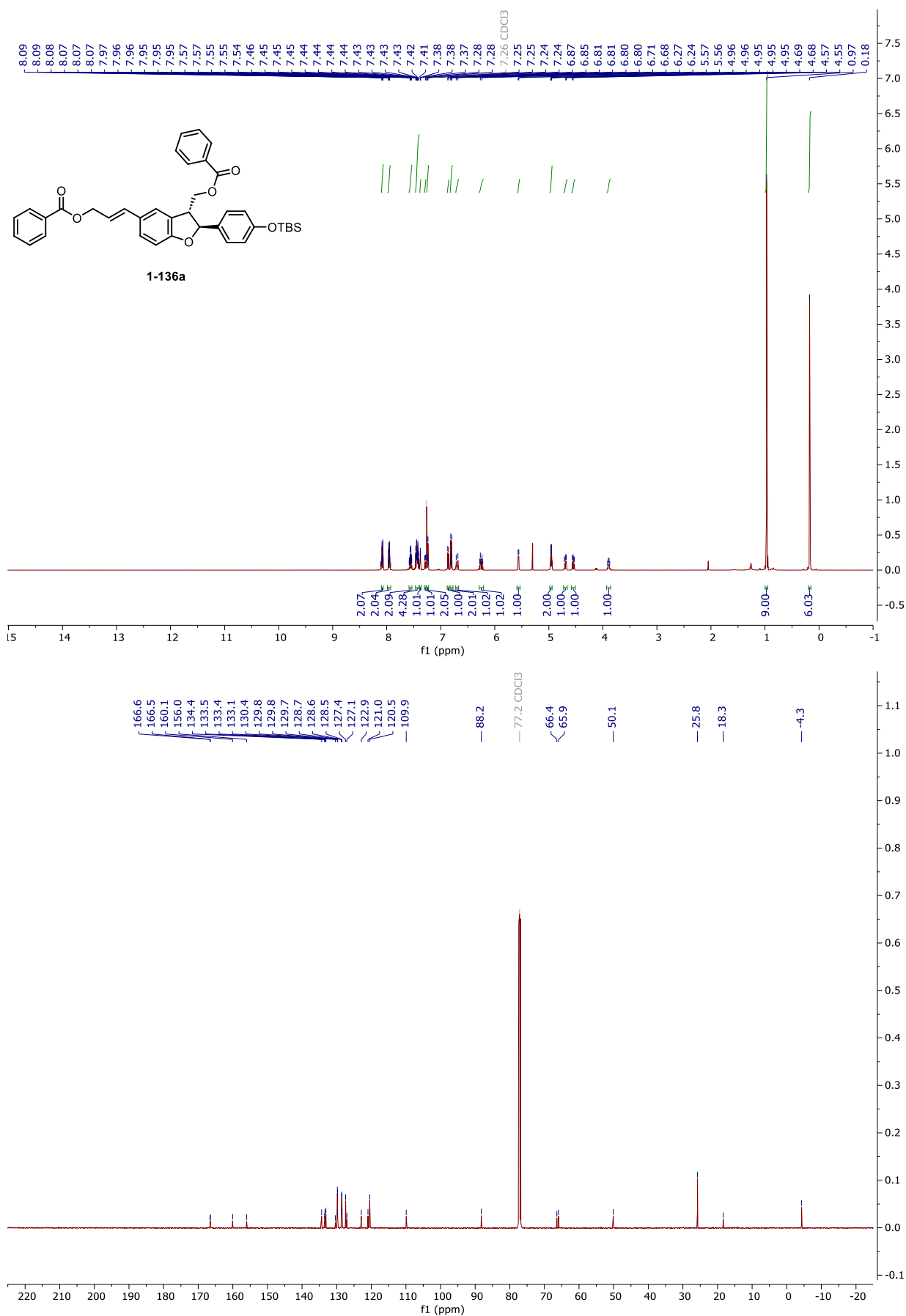
NMR and HPLC

Copy of ^1H and $^{13}\text{C}\{^1\text{H}\}$ spectra of 1-135a



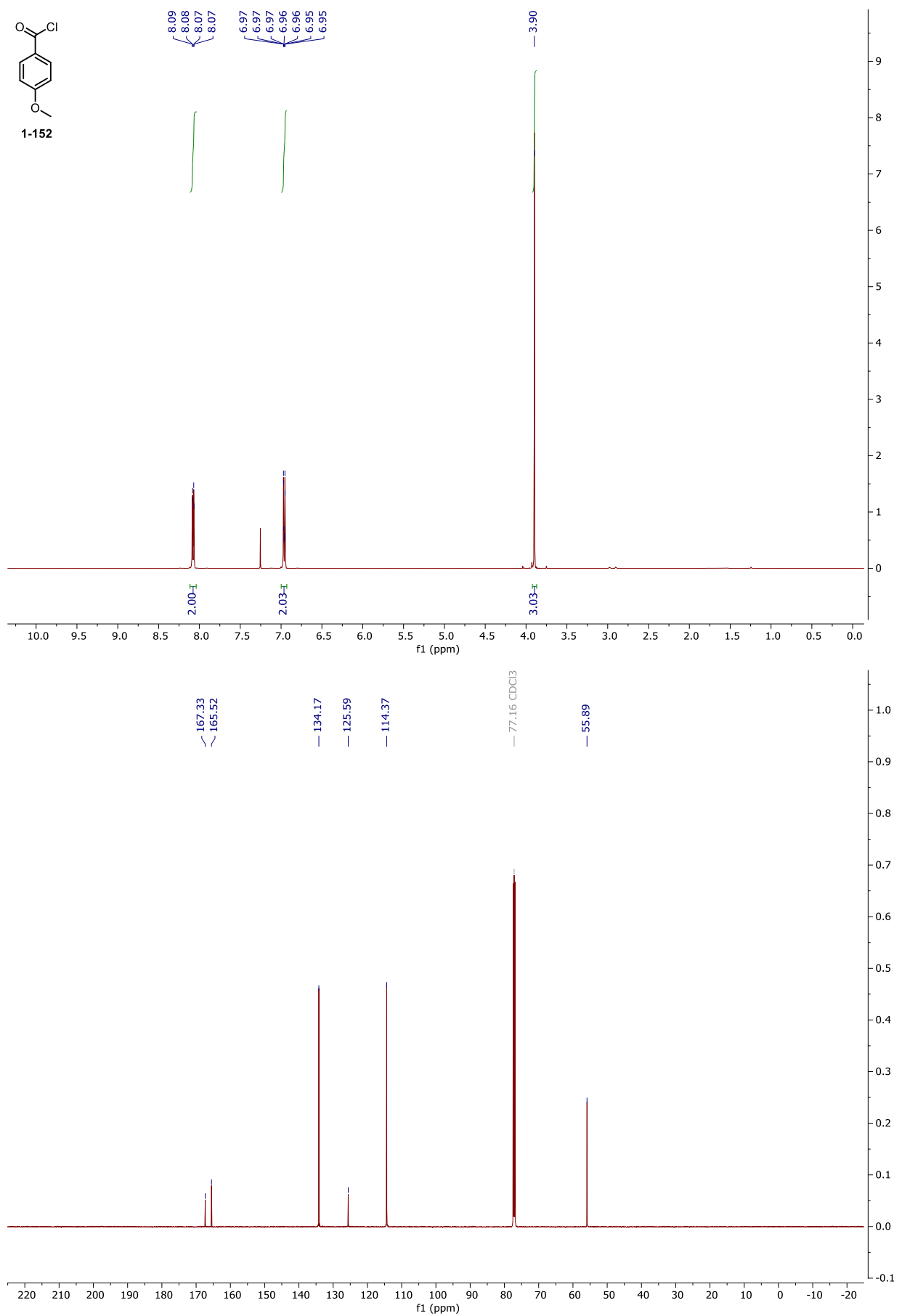
NMR and HPLC

Copy of ^1H and $^{13}\text{C}\{^1\text{H}\}$ spectra of 1-136a



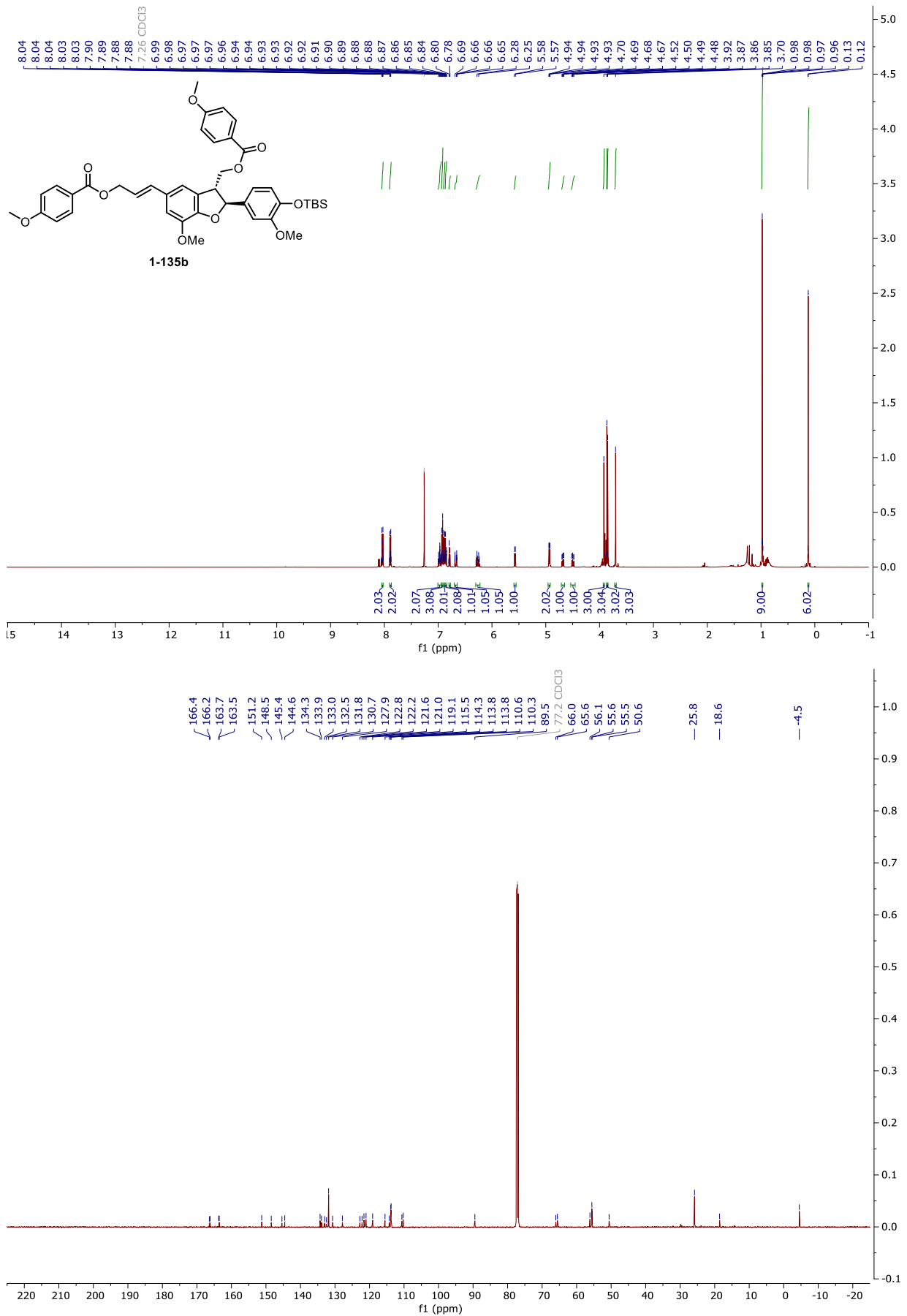
NMR and HPLC

Copy of ^1H and $^{13}\text{C}\{^1\text{H}\}$ spectra of 1-152



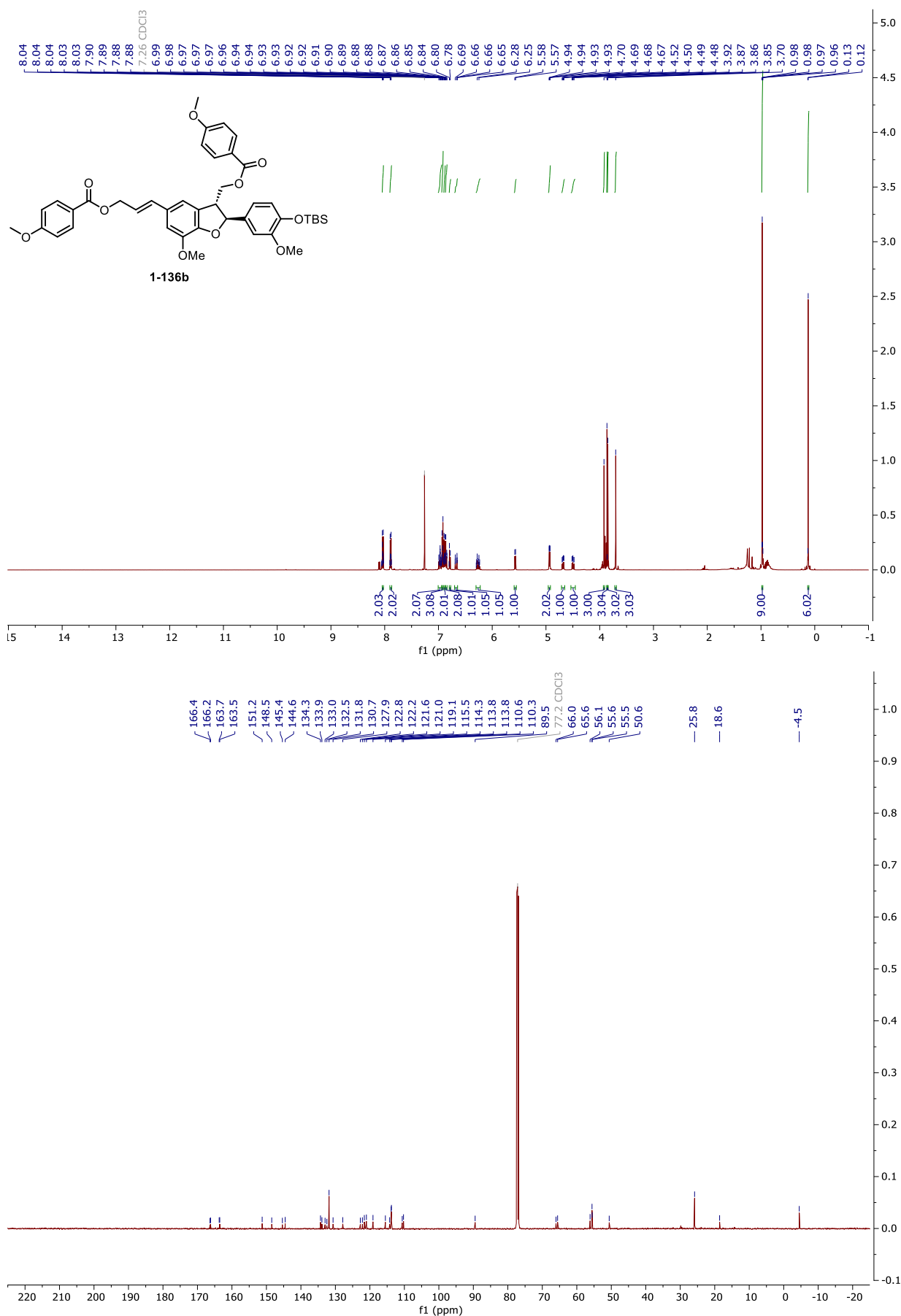
NMR and HPLC

Copy of ^1H and $^{13}\text{C}\{^1\text{H}\}$ spectra of 1-135b



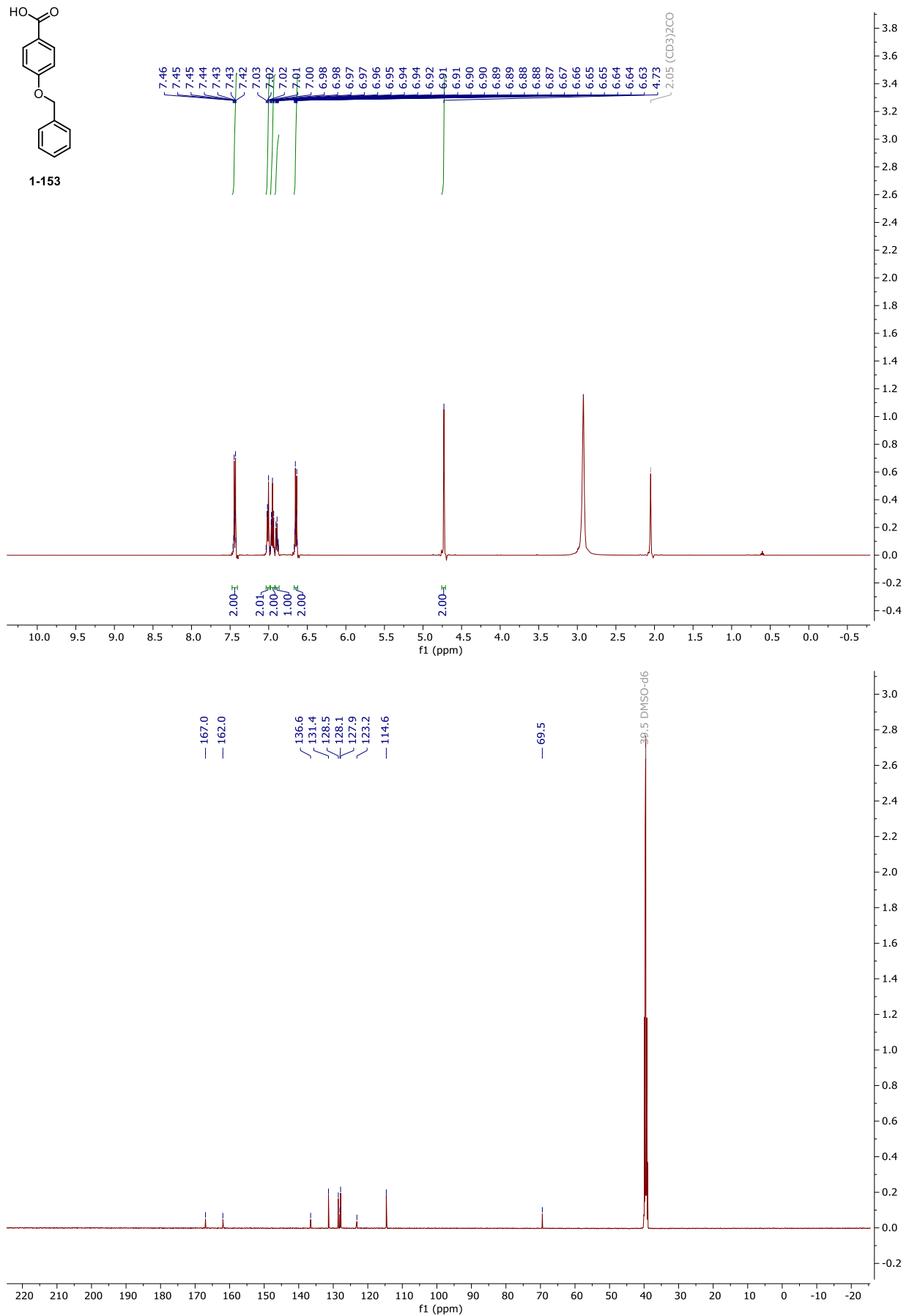
NMR and HPLC

Copy of ¹H and ¹³C{¹H} spectra of 1-136b



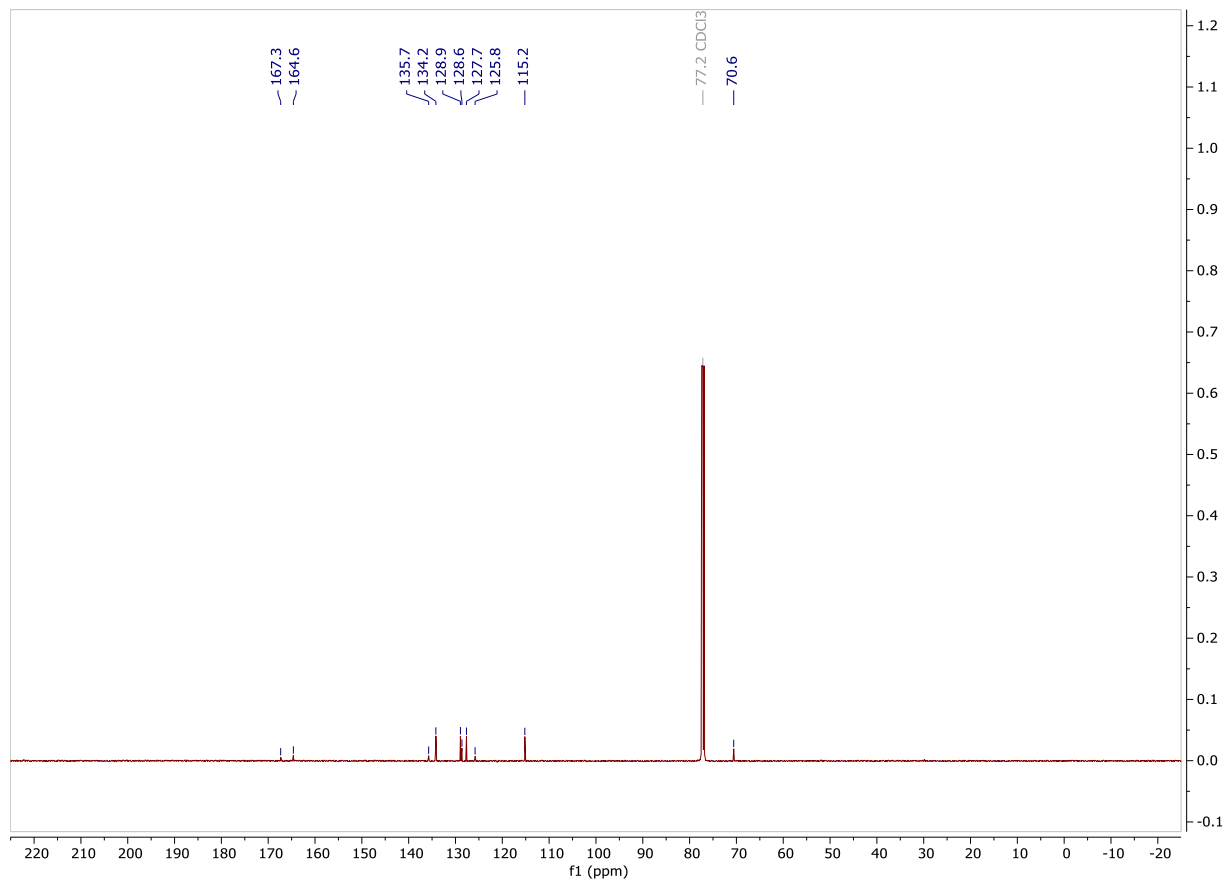
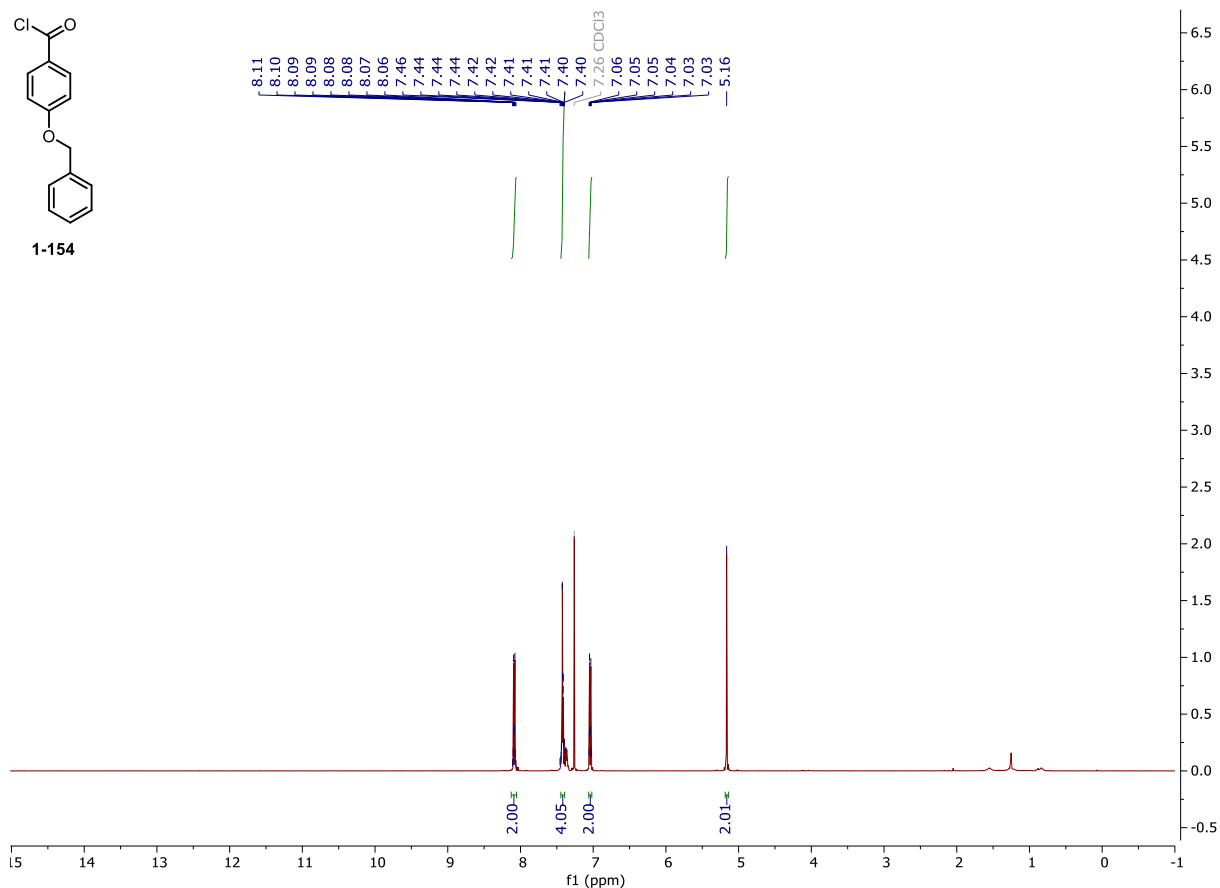
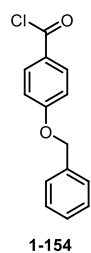
NMR and HPLC

Copy of ^1H and $^{13}\text{C}\{^1\text{H}\}$ spectra of 1-153



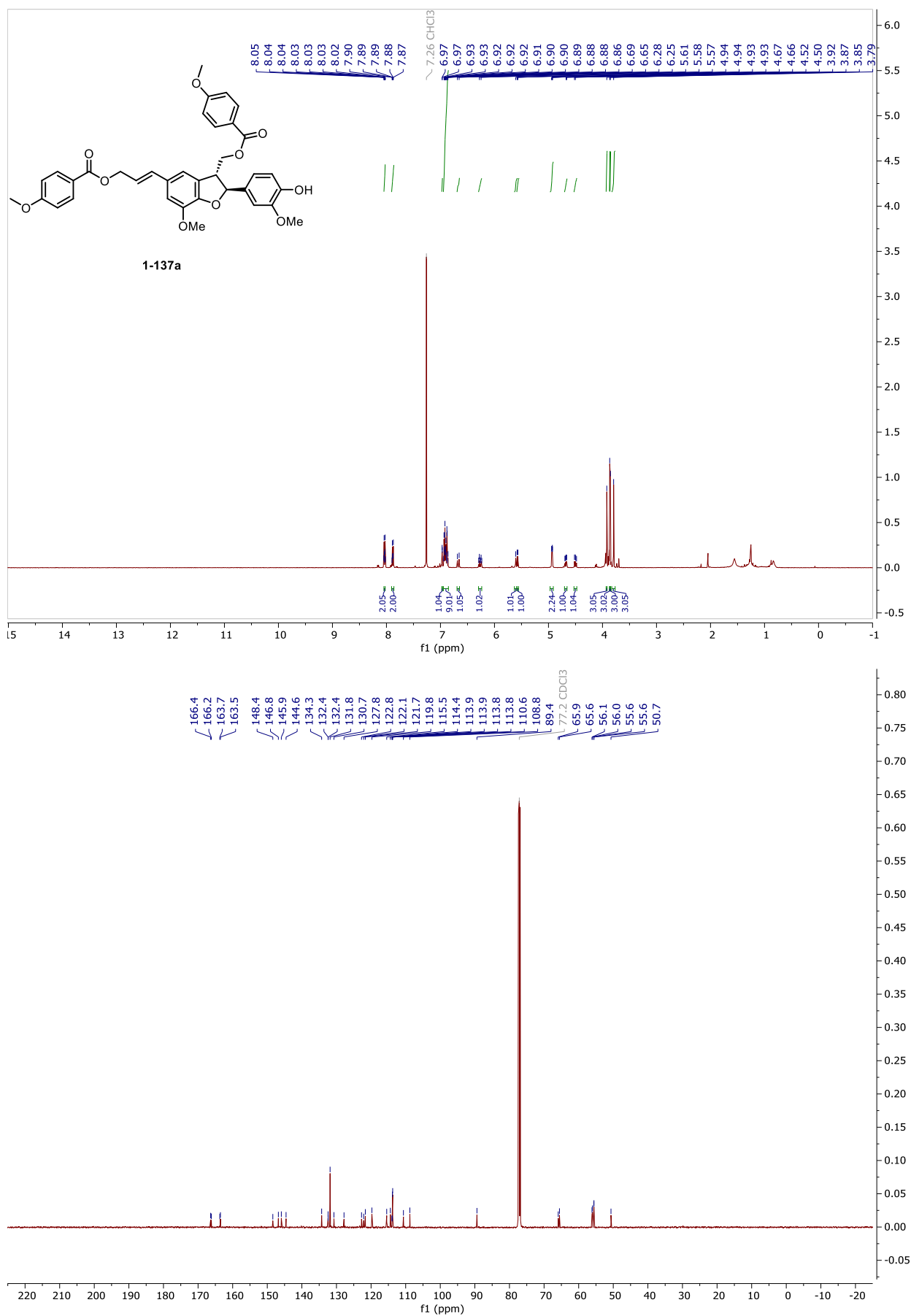
NMR and HPLC

Copy of ^1H and $^{13}\text{C}\{^1\text{H}\}$ spectra of 1-154



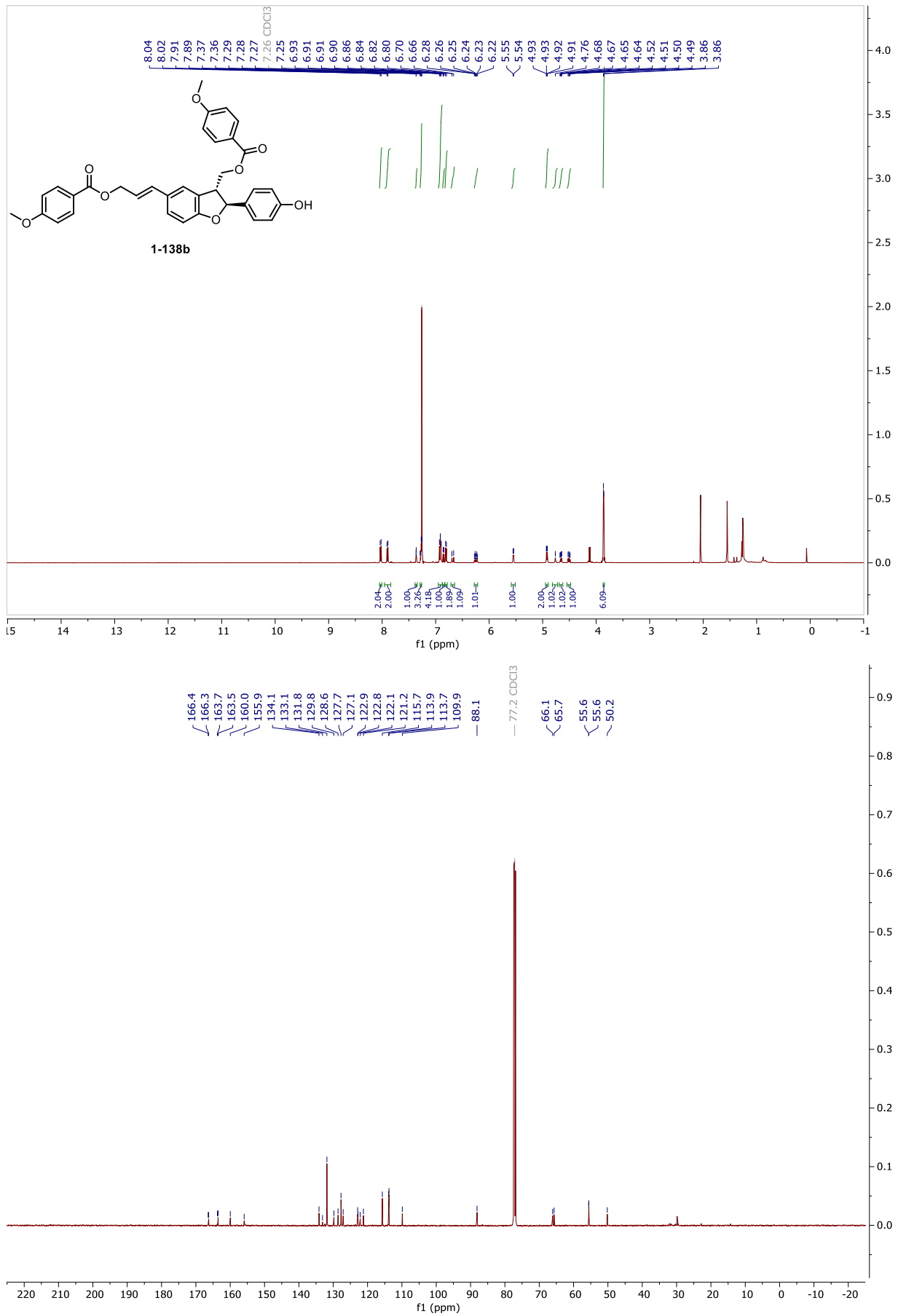
NMR and HPLC

Copy of ^1H and $^{13}\text{C}\{^1\text{H}\}$ spectra of 1-137a



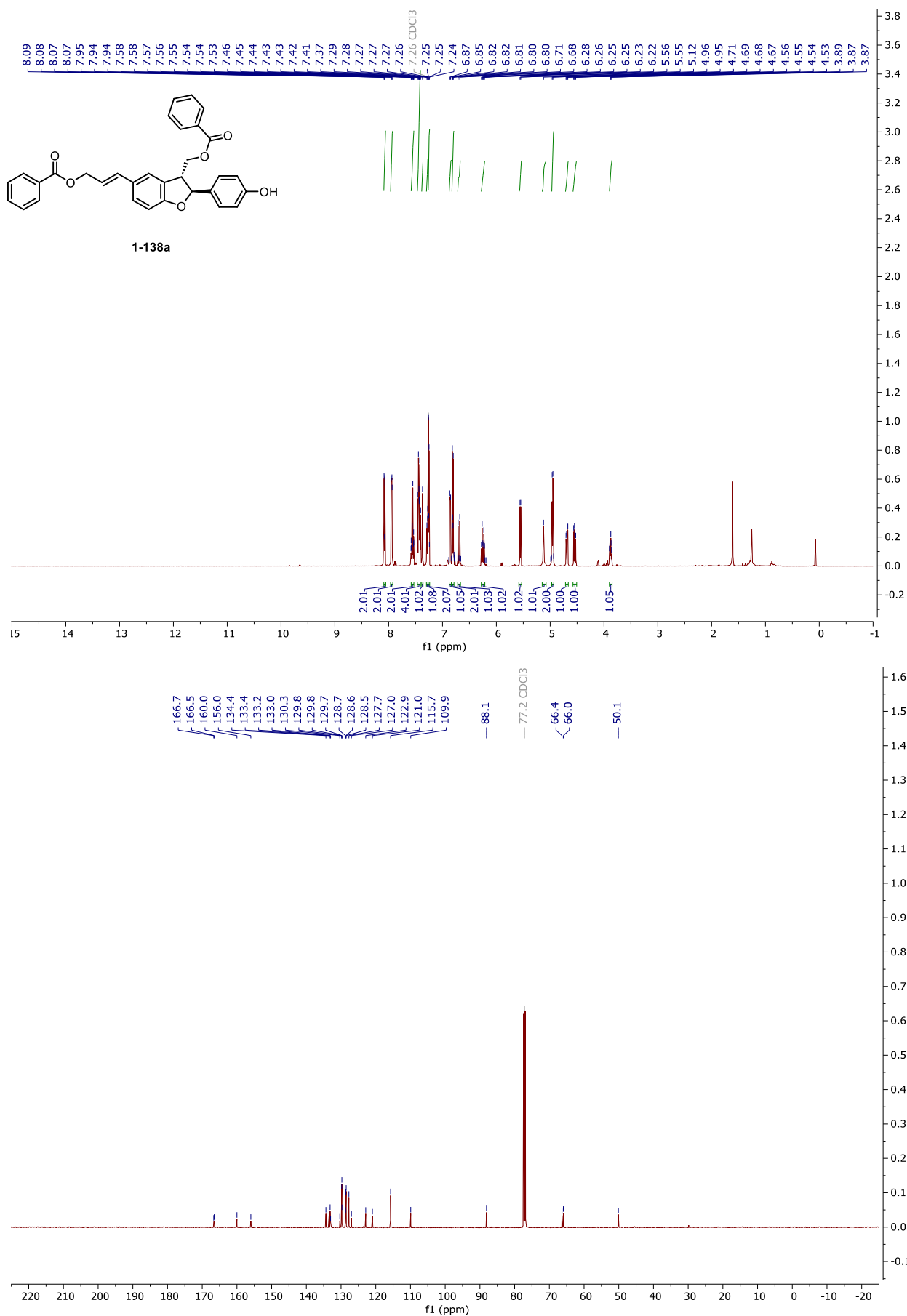
NMR and HPLC

Copy of ^1H and $^{13}\text{C}\{^1\text{H}\}$ spectra of 1-138b



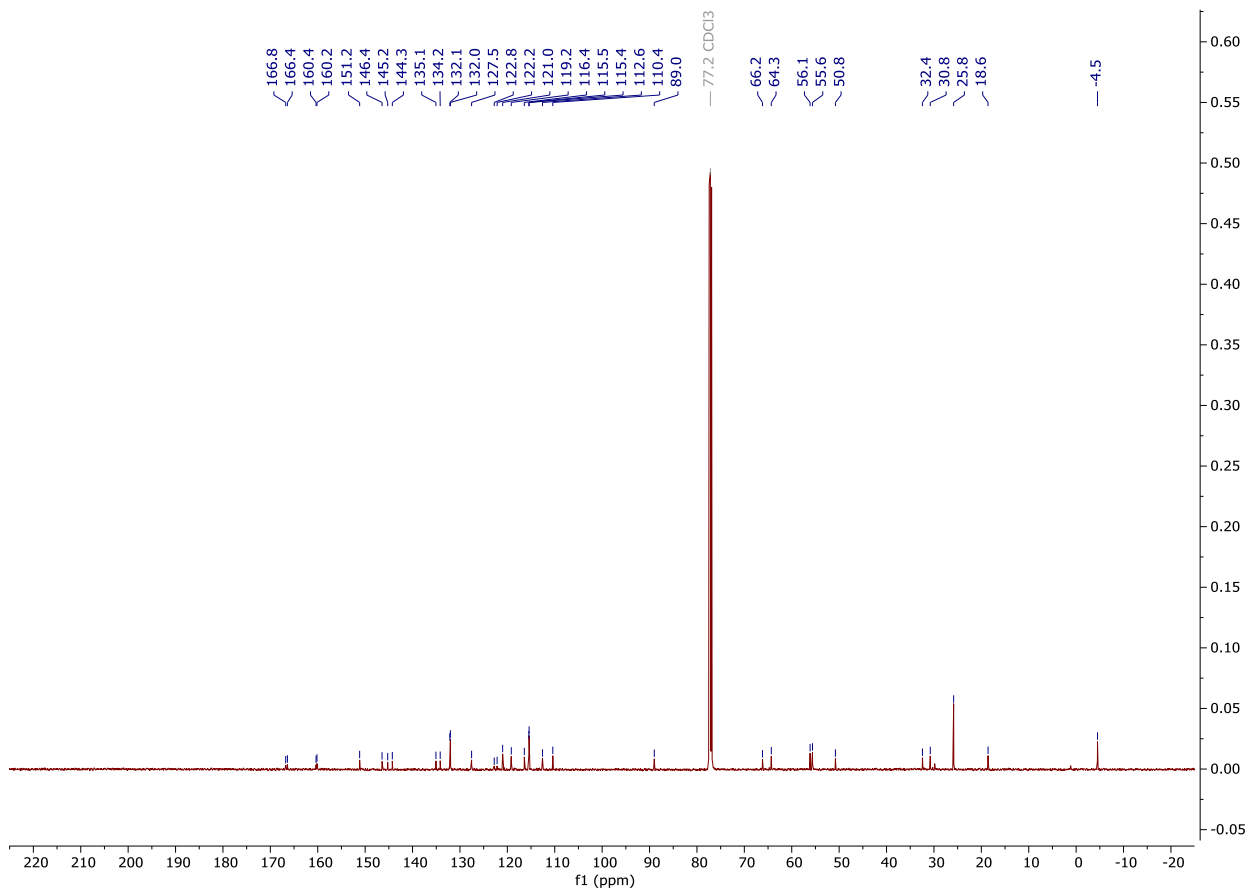
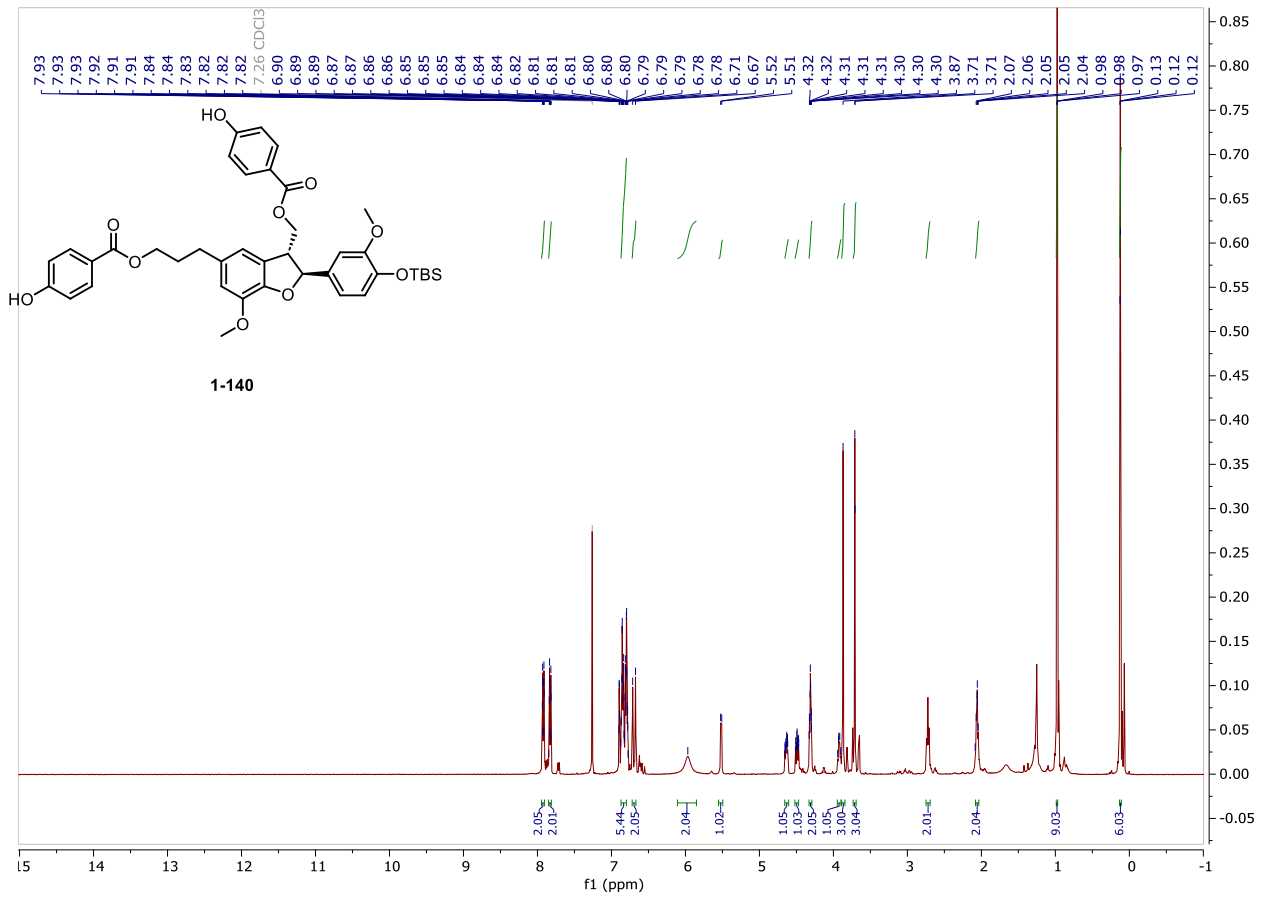
NMR and HPLC

Copy of ^1H and $^{13}\text{C}\{^1\text{H}\}$ spectra of 1-138a



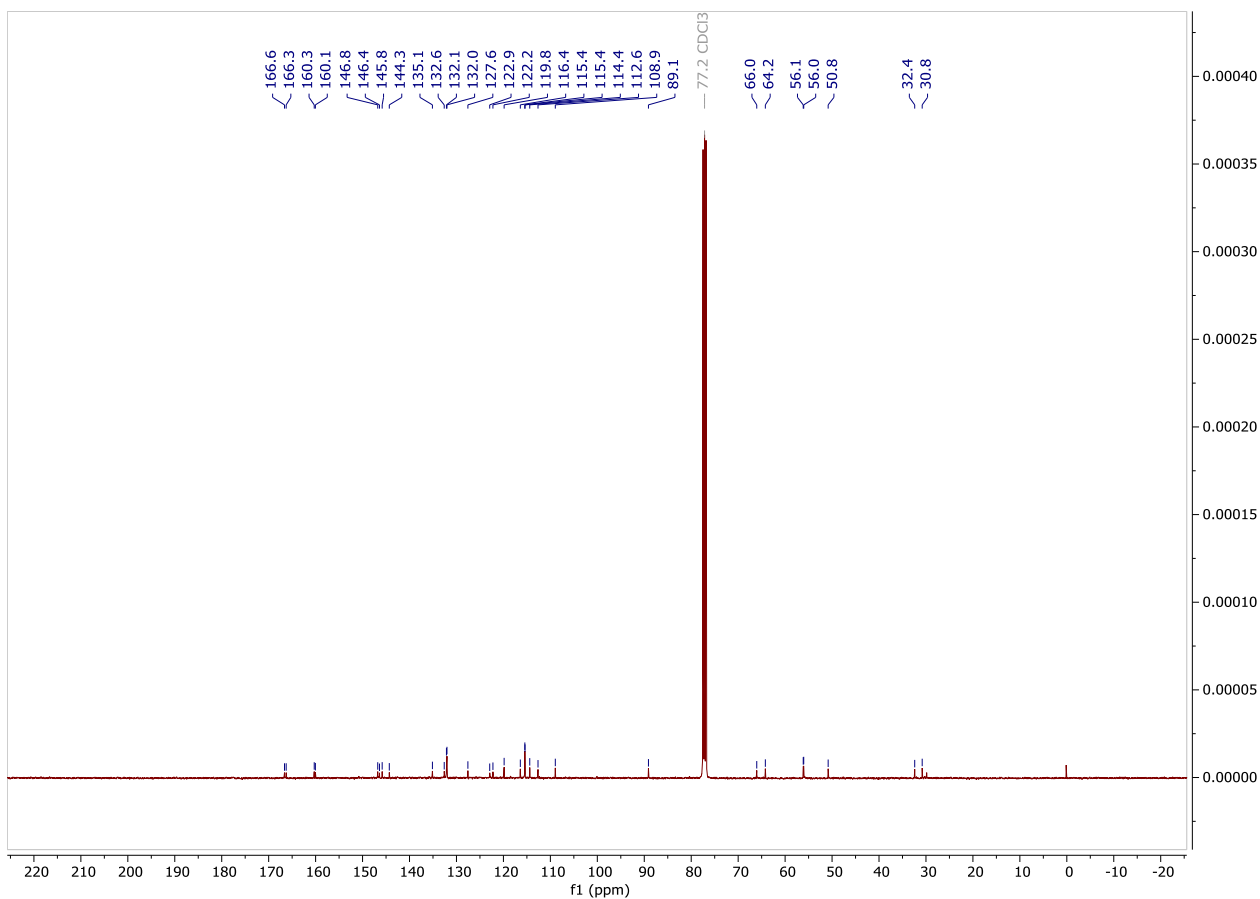
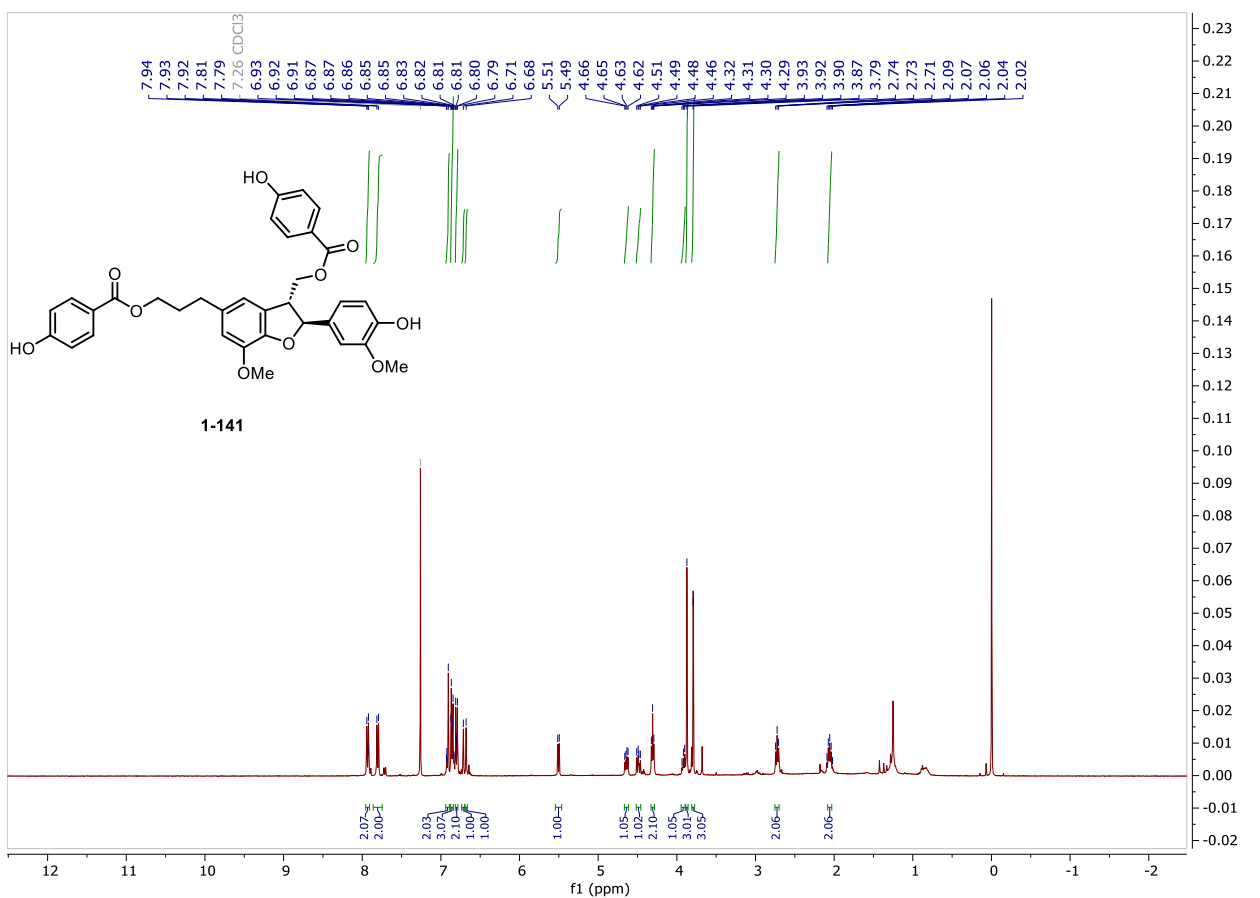
NMR and HPLC

Copy of ^1H and $^{13}\text{C}\{^1\text{H}\}$ spectra of 1-140



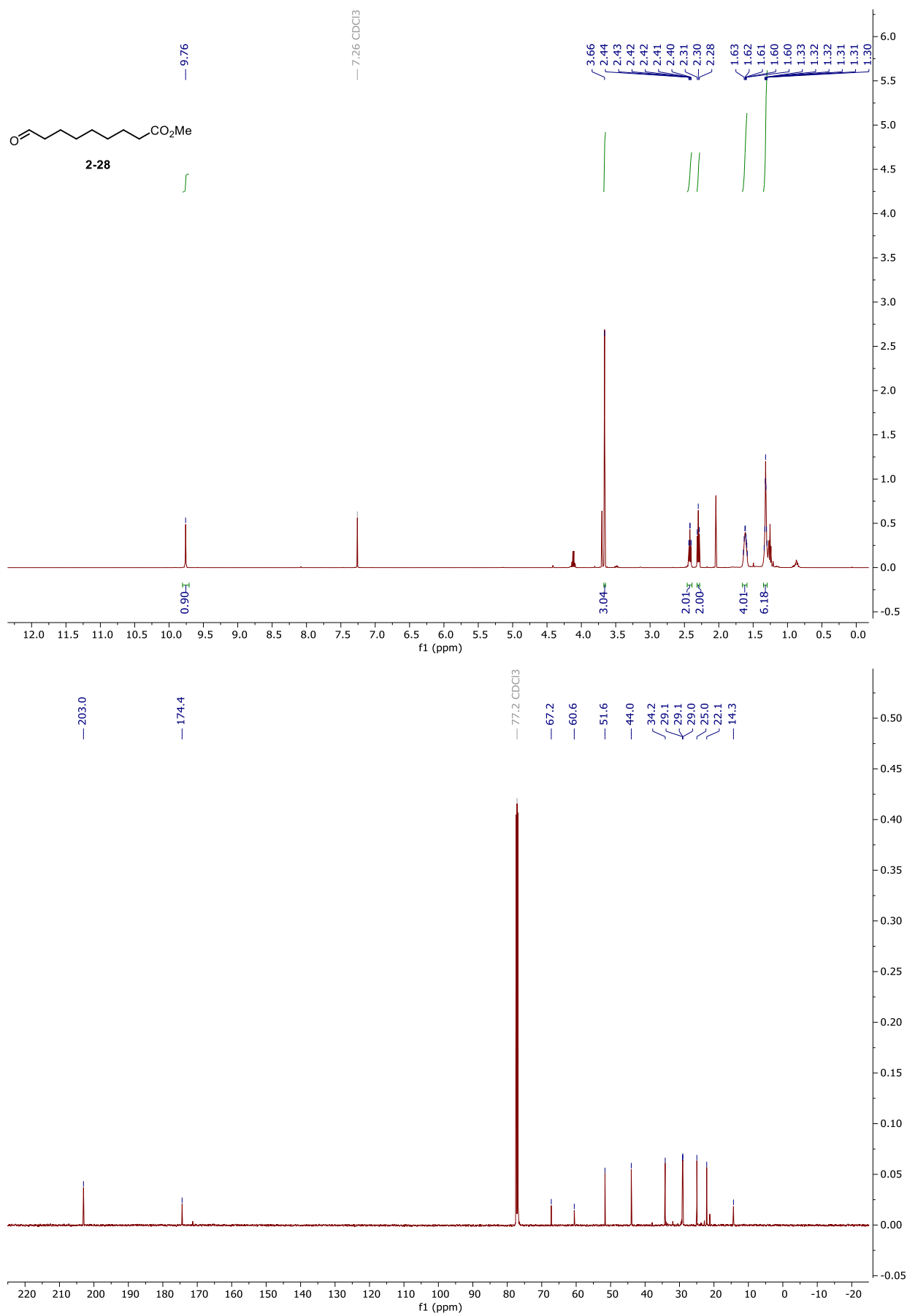
NMR and HPLC

Copy of ^1H and $^{13}\text{C}\{^1\text{H}\}$ spectra of 1-141



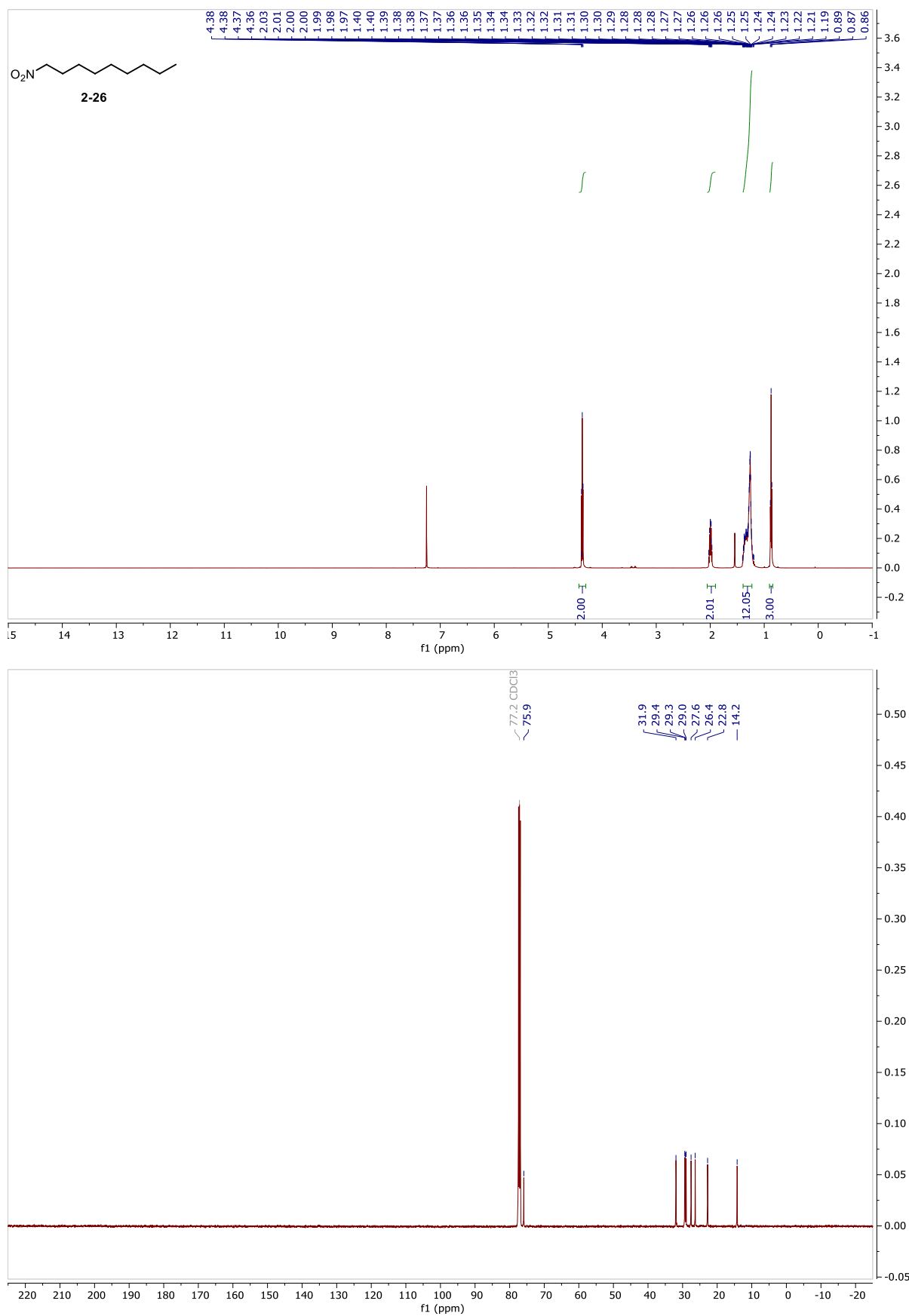
NMR and HPLC

Copy of ^1H and $^{13}\text{C}\{^1\text{H}\}$ spectra of 2-28



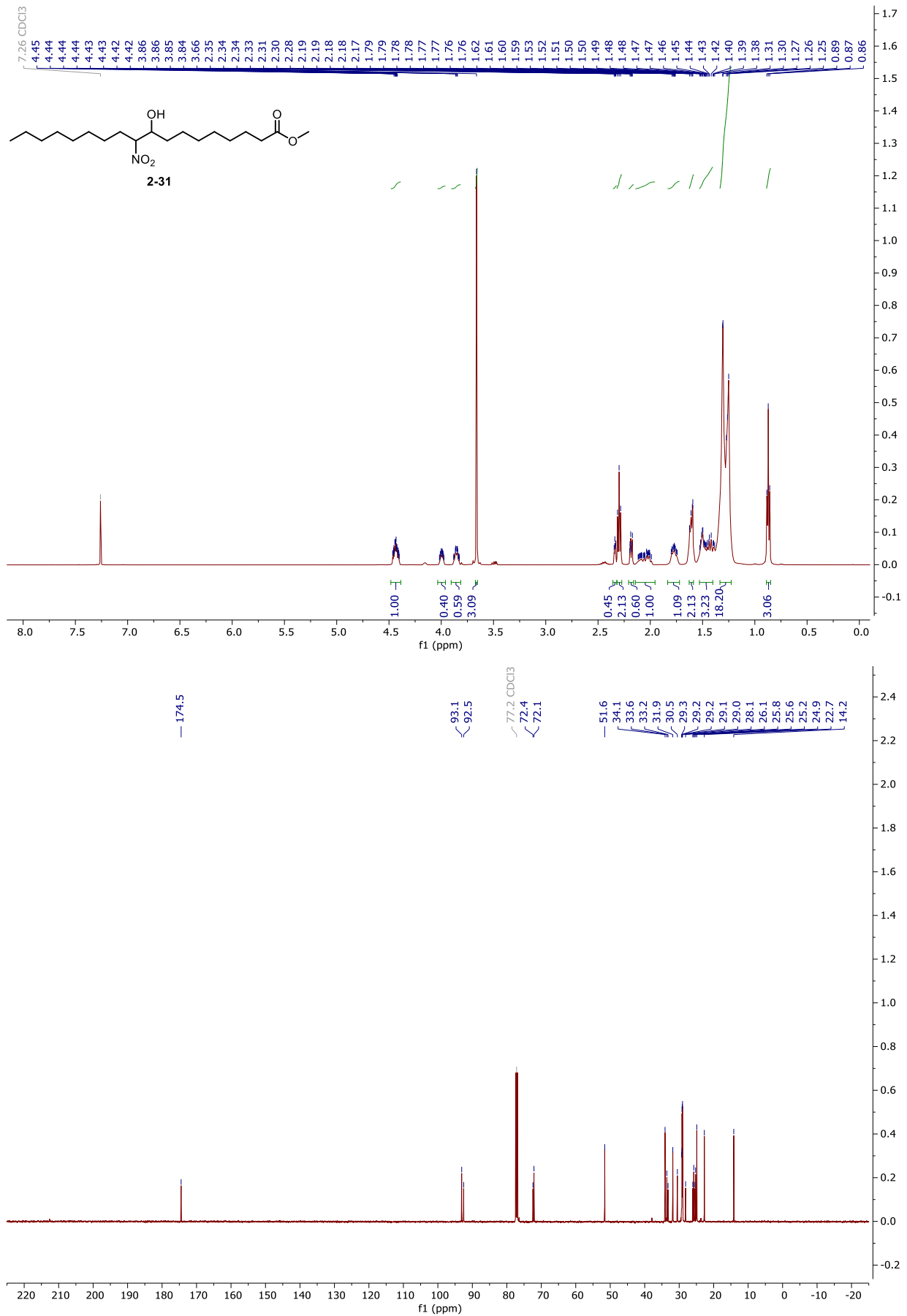
NMR and HPLC

Copy of ^1H and $^{13}\text{C}\{^1\text{H}\}$ spectra of 2-26



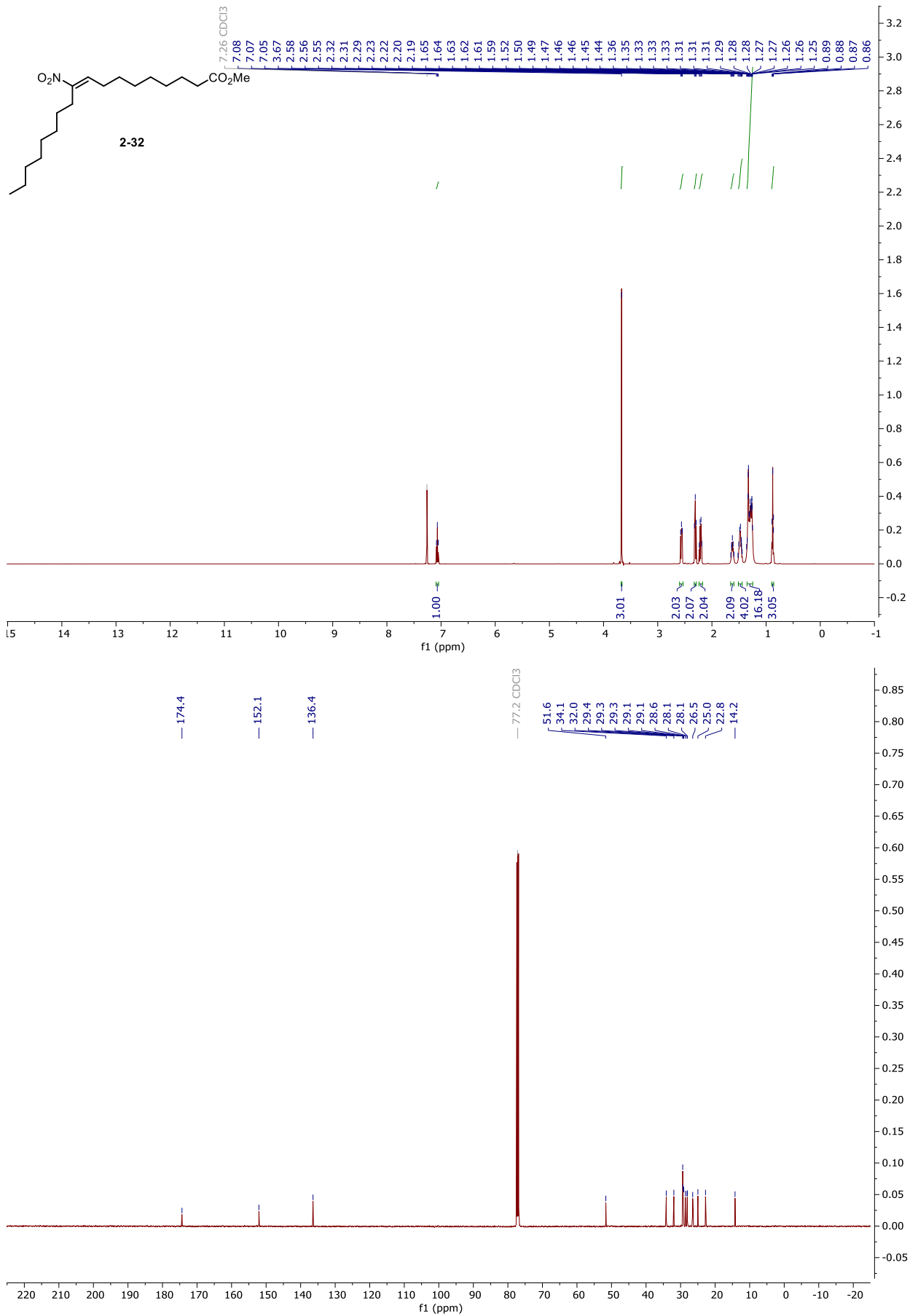
NMR and HPLC

Copy of ^1H and $^{13}\text{C}\{^1\text{H}\}$ spectra of 2-31



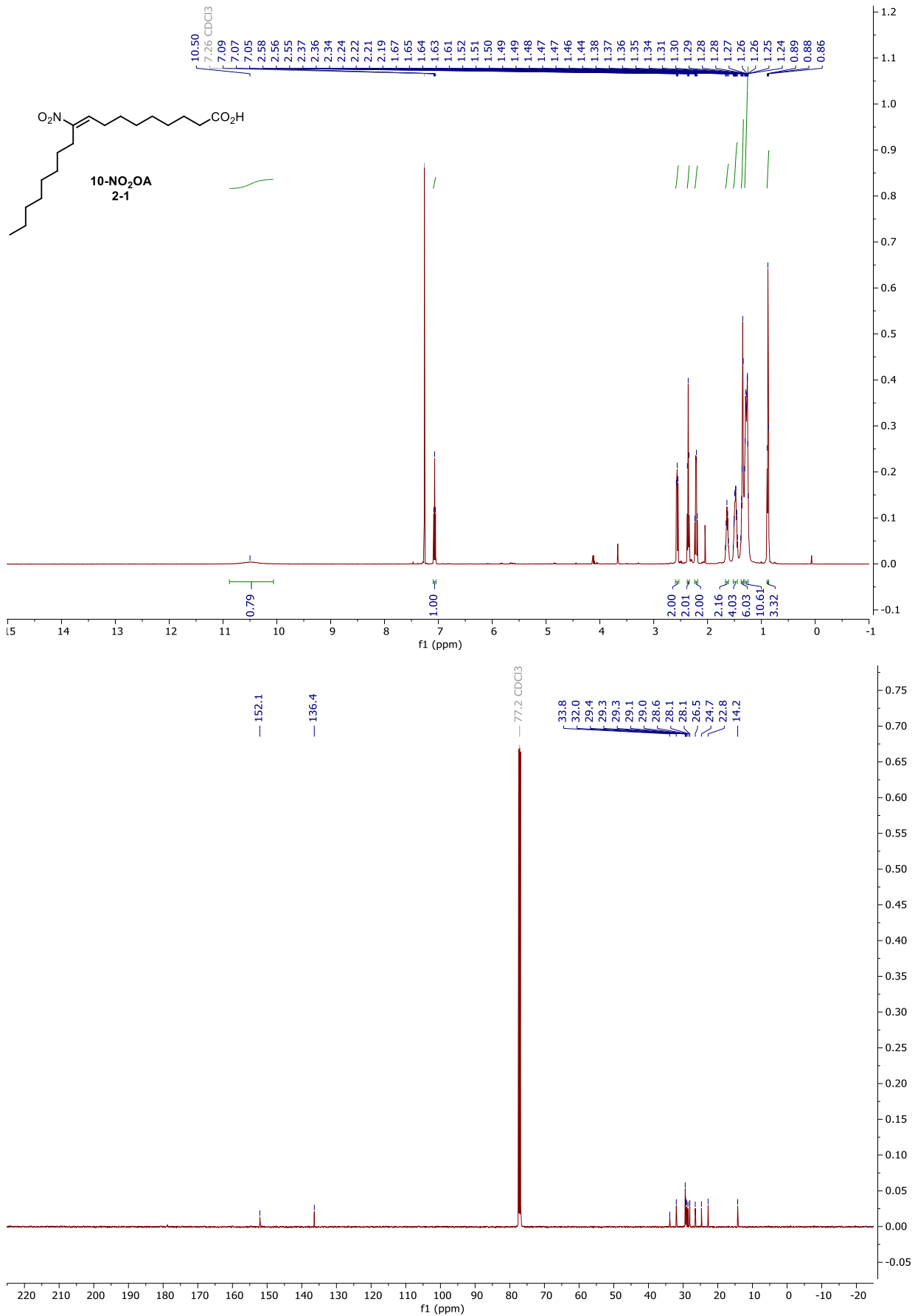
NMR and HPLC

Copy of ^1H and $^{13}\text{C}\{^1\text{H}\}$ spectra of 2-32



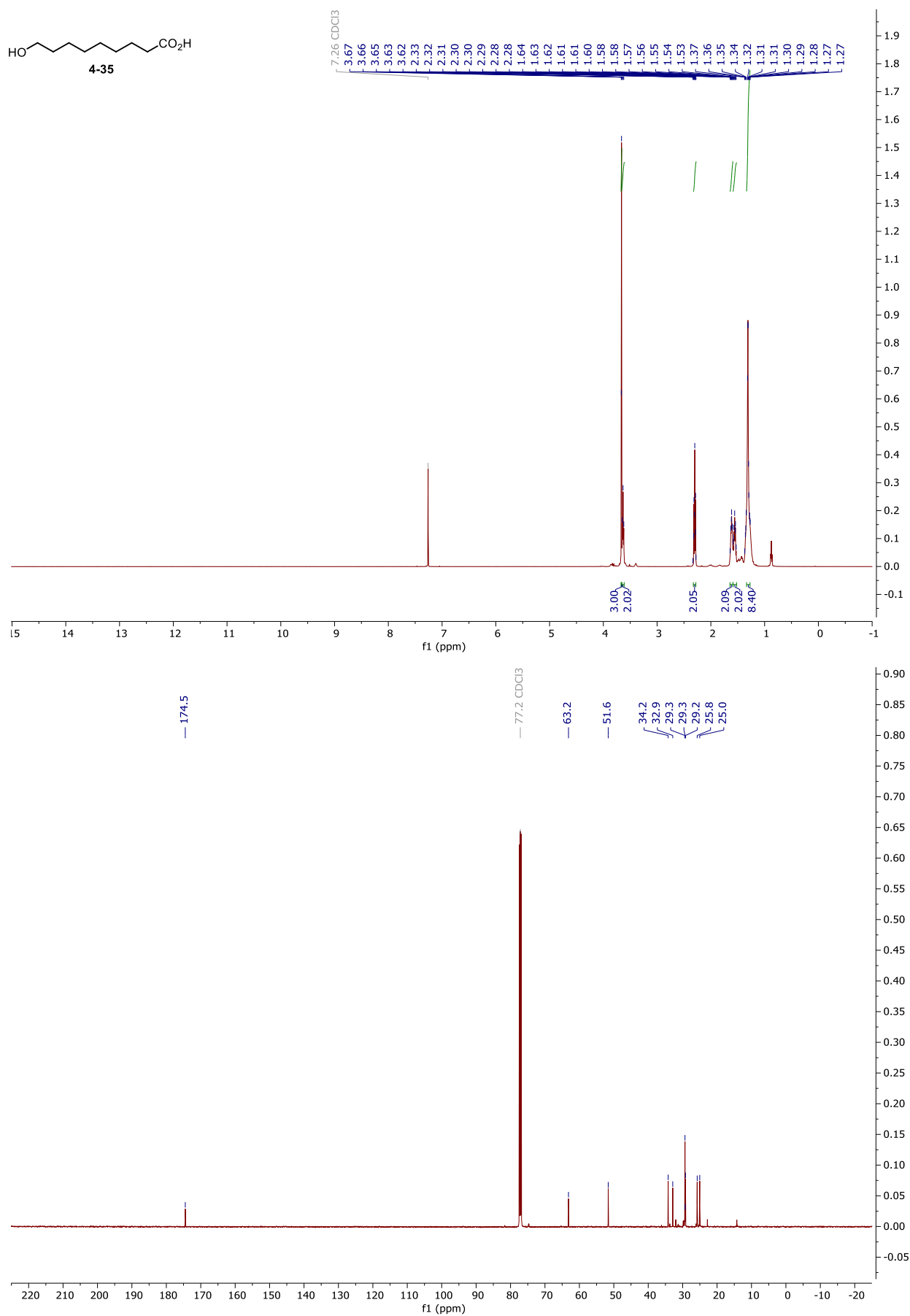
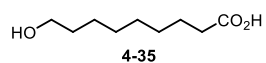
NMR and HPLC

Copy of ^1H and $^{13}\text{C}\{^1\text{H}\}$ spectra of 10-NO₂OA, 2-1



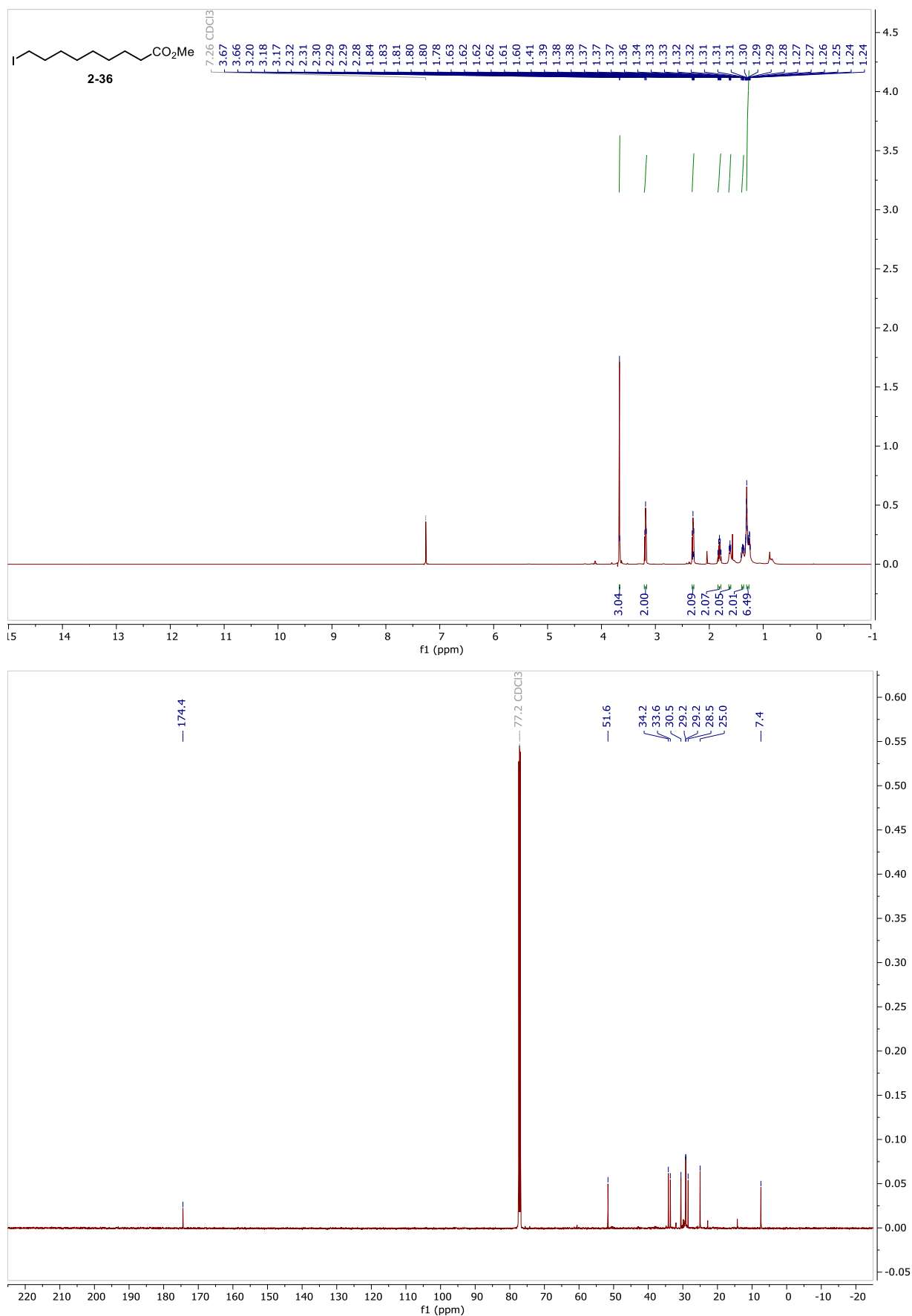
NMR and HPLC

Copy of ^1H and $^{13}\text{C}\{^1\text{H}\}$ spectra of 2-35



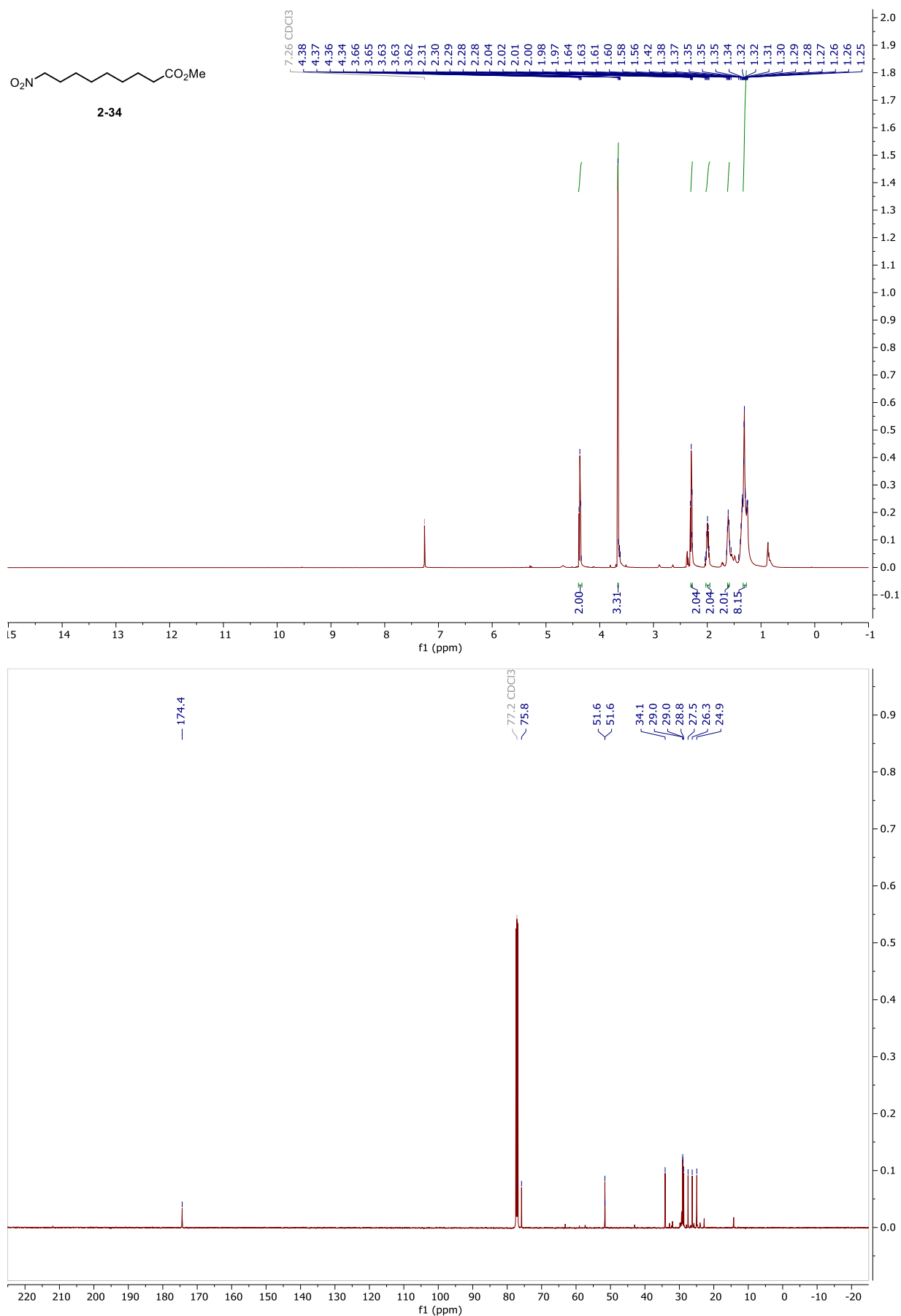
NMR and HPLC

Copy of ^1H and $^{13}\text{C}\{^1\text{H}\}$ spectra of 2-36



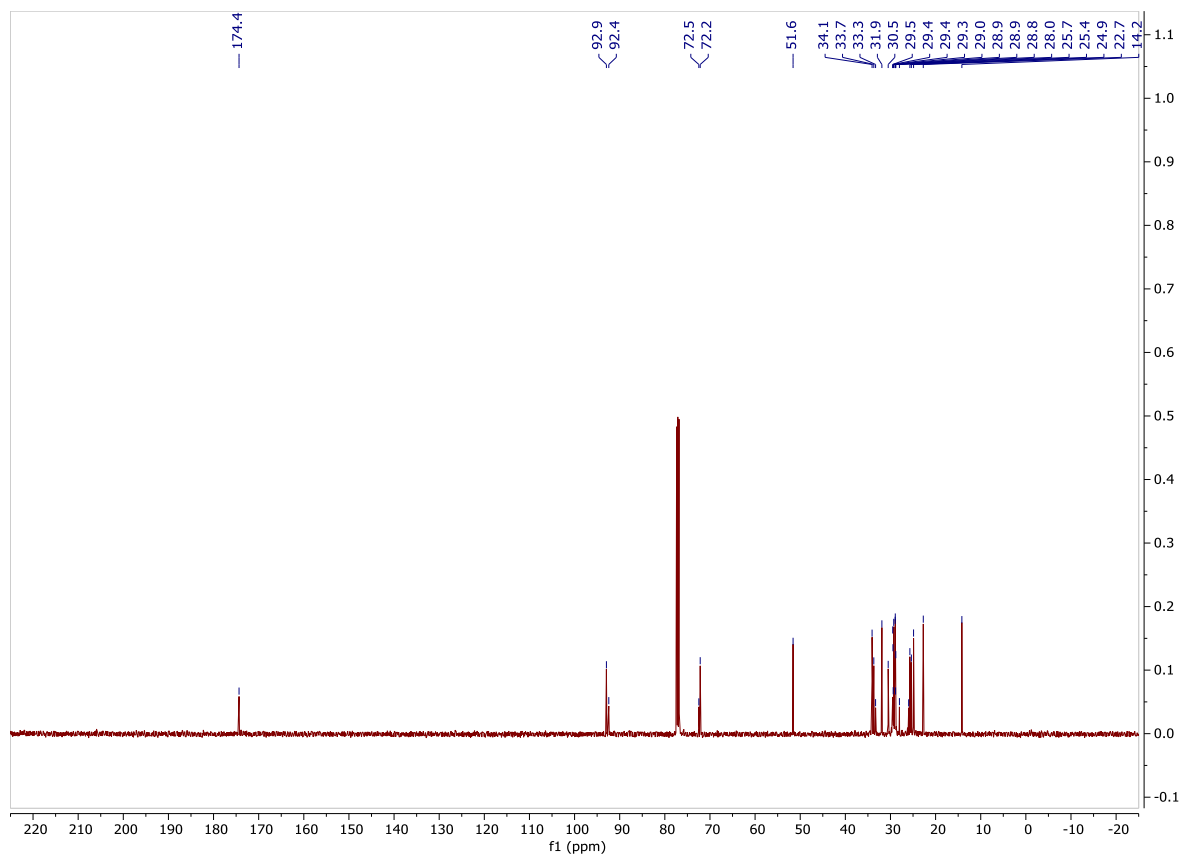
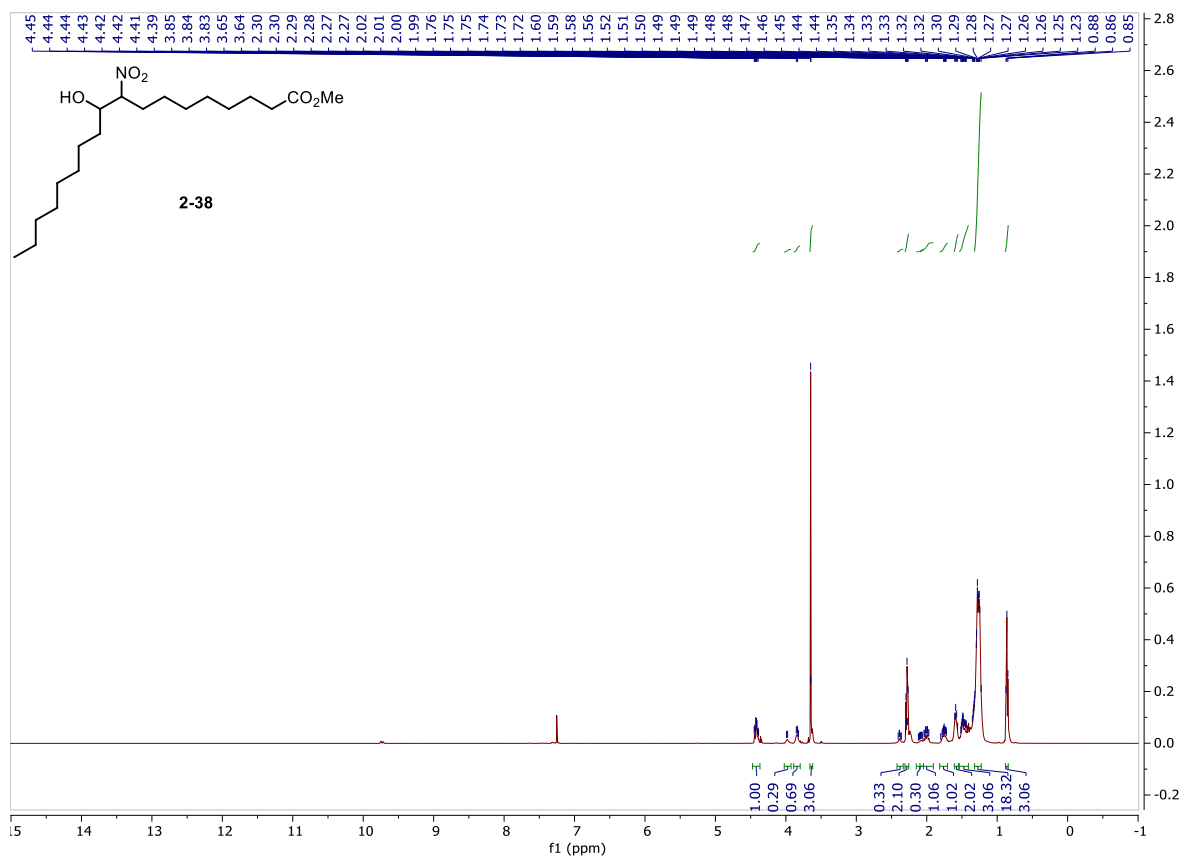
NMR and HPLC

Copy of ^1H and $^{13}\text{C}\{^1\text{H}\}$ spectra of 2-34



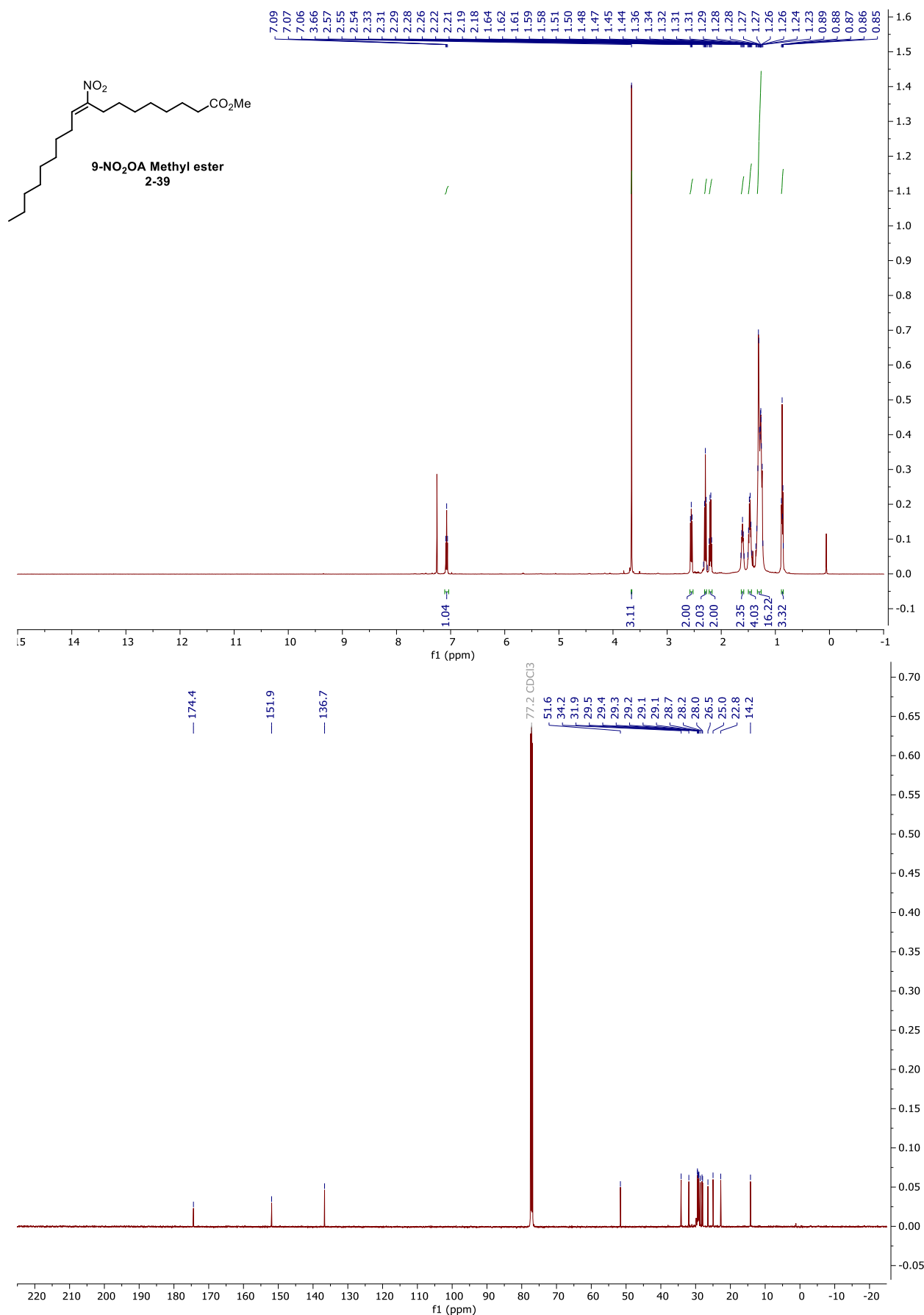
NMR and HPLC

Copy of ^1H and $^{13}\text{C}\{^1\text{H}\}$ spectra of 2-38



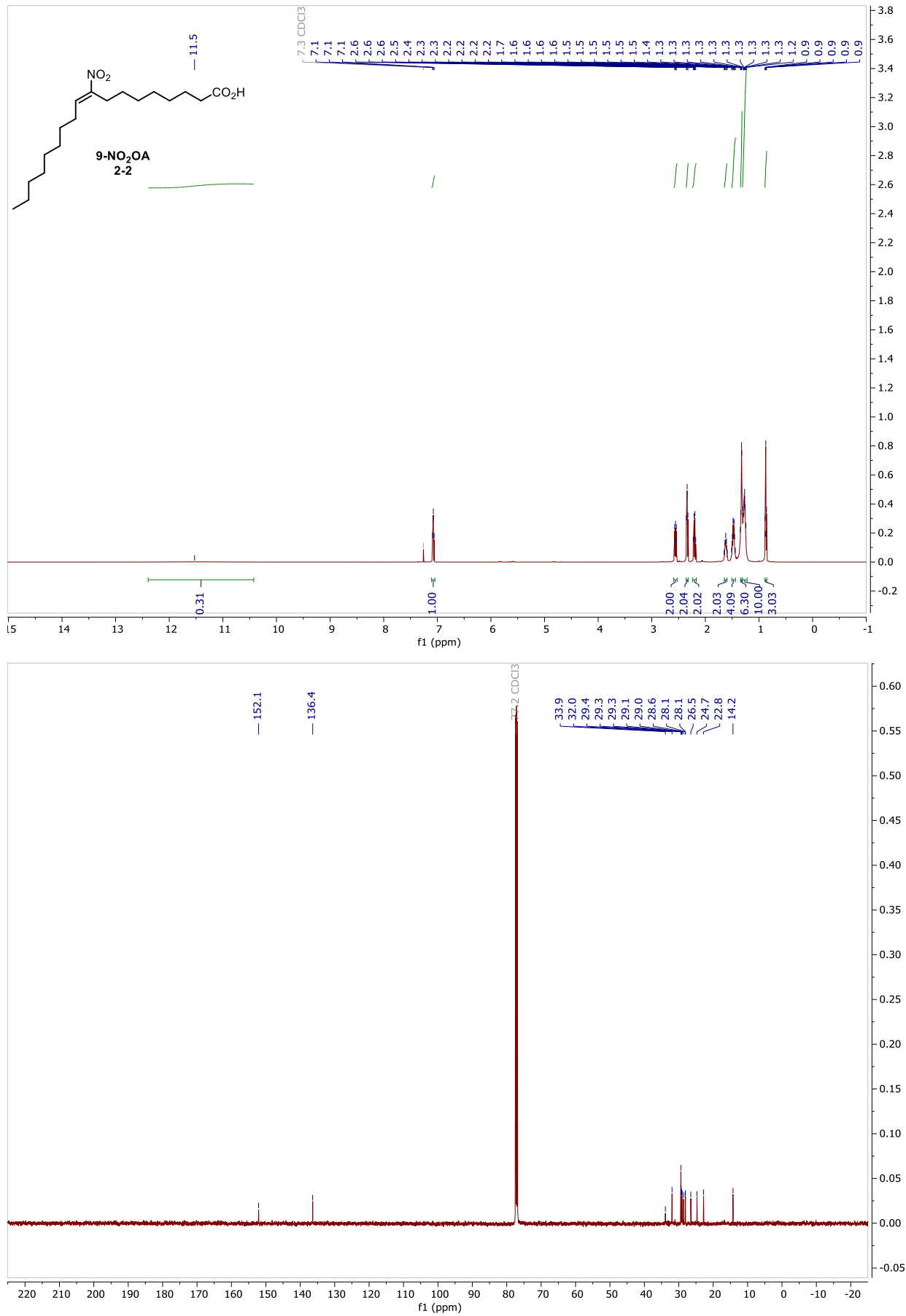
NMR and HPLC

Copy of ^1H and $^{13}\text{C}\{^1\text{H}\}$ spectra of 2-39



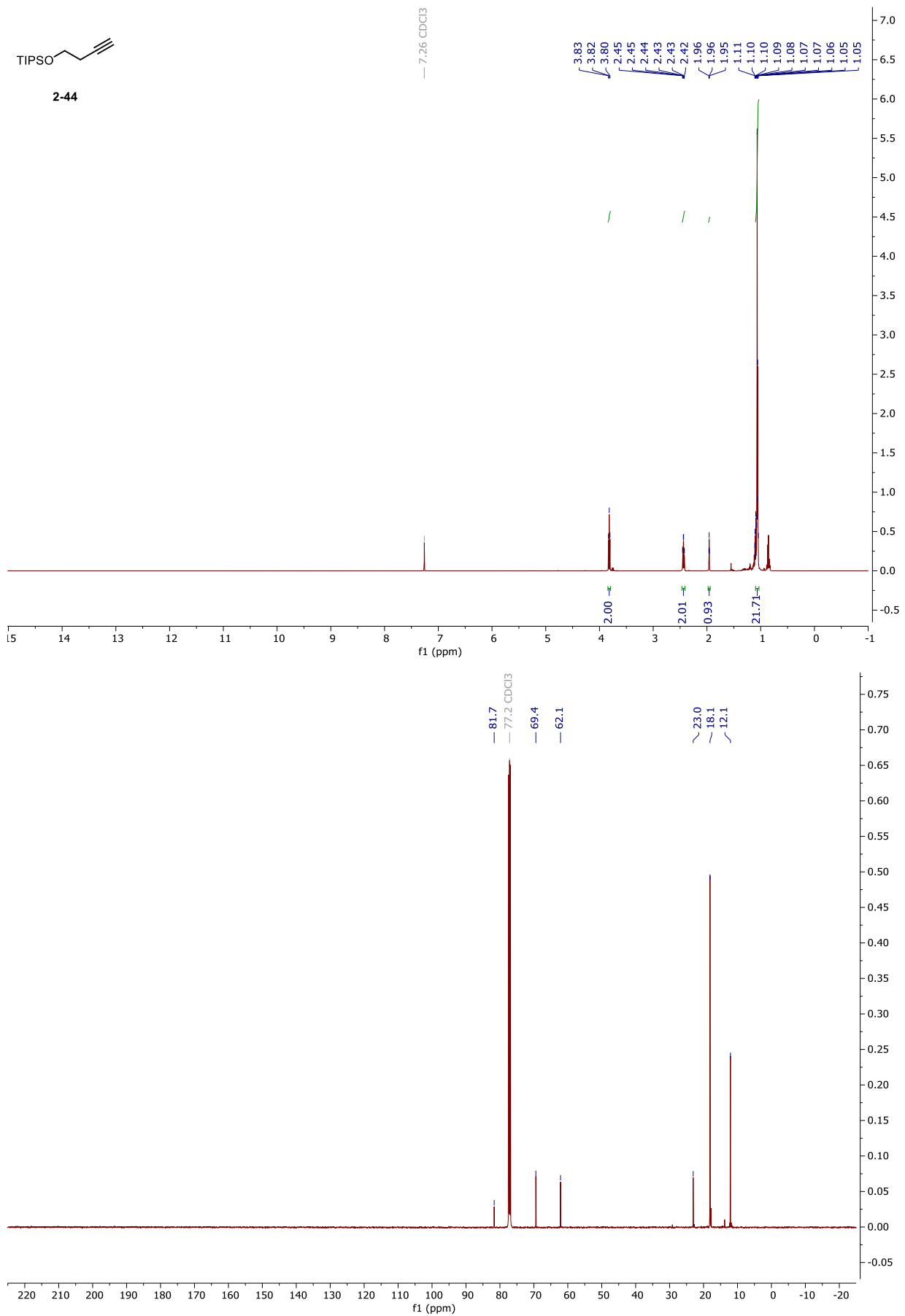
NMR and HPLC

Copy of ^1H and $^{13}\text{C}\{^1\text{H}\}$ spectra of 9-NO₂OA, 2-2



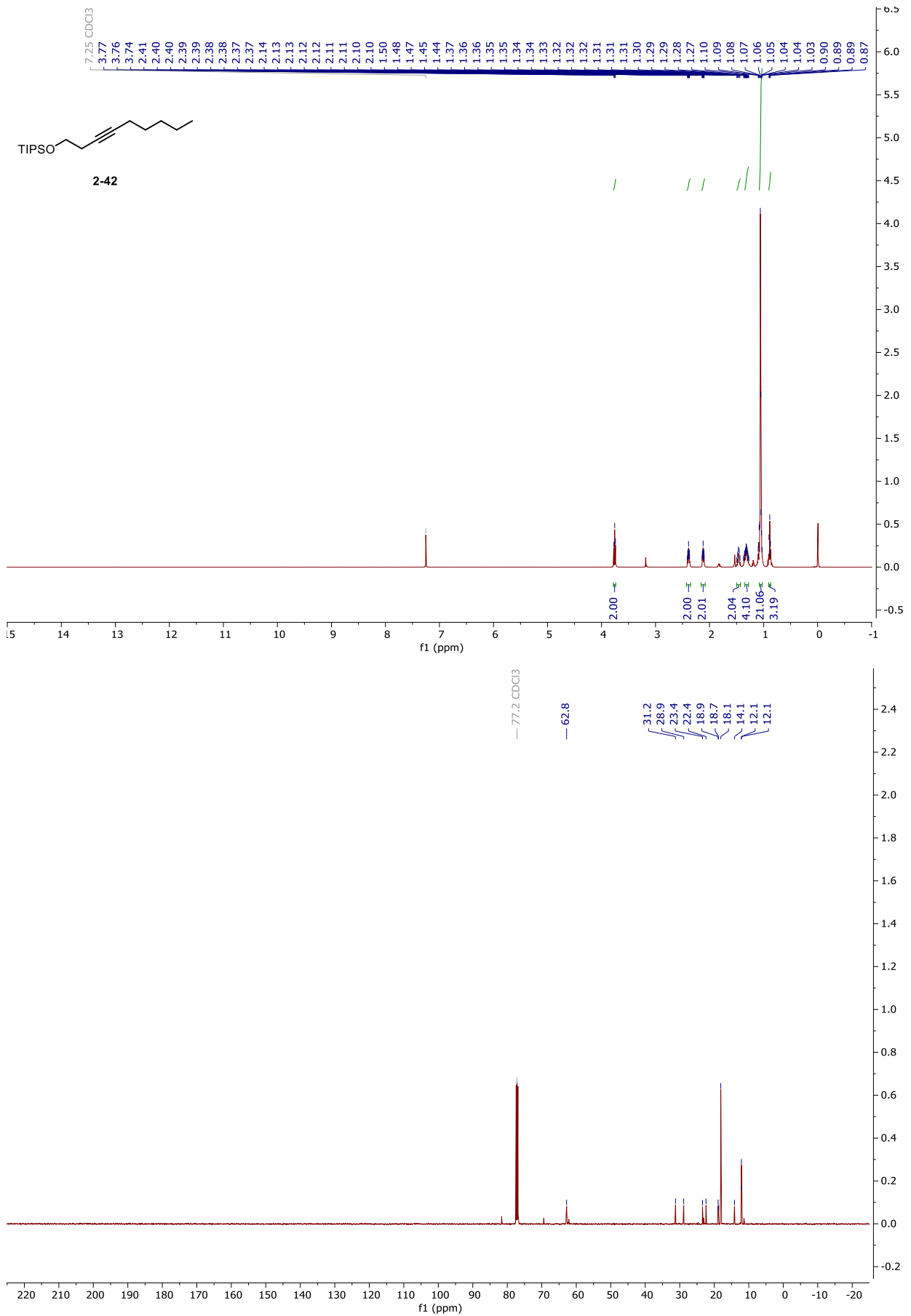
NMR and HPLC

Copy of ^1H and $^{13}\text{C}\{^1\text{H}\}$ spectra of 2-44



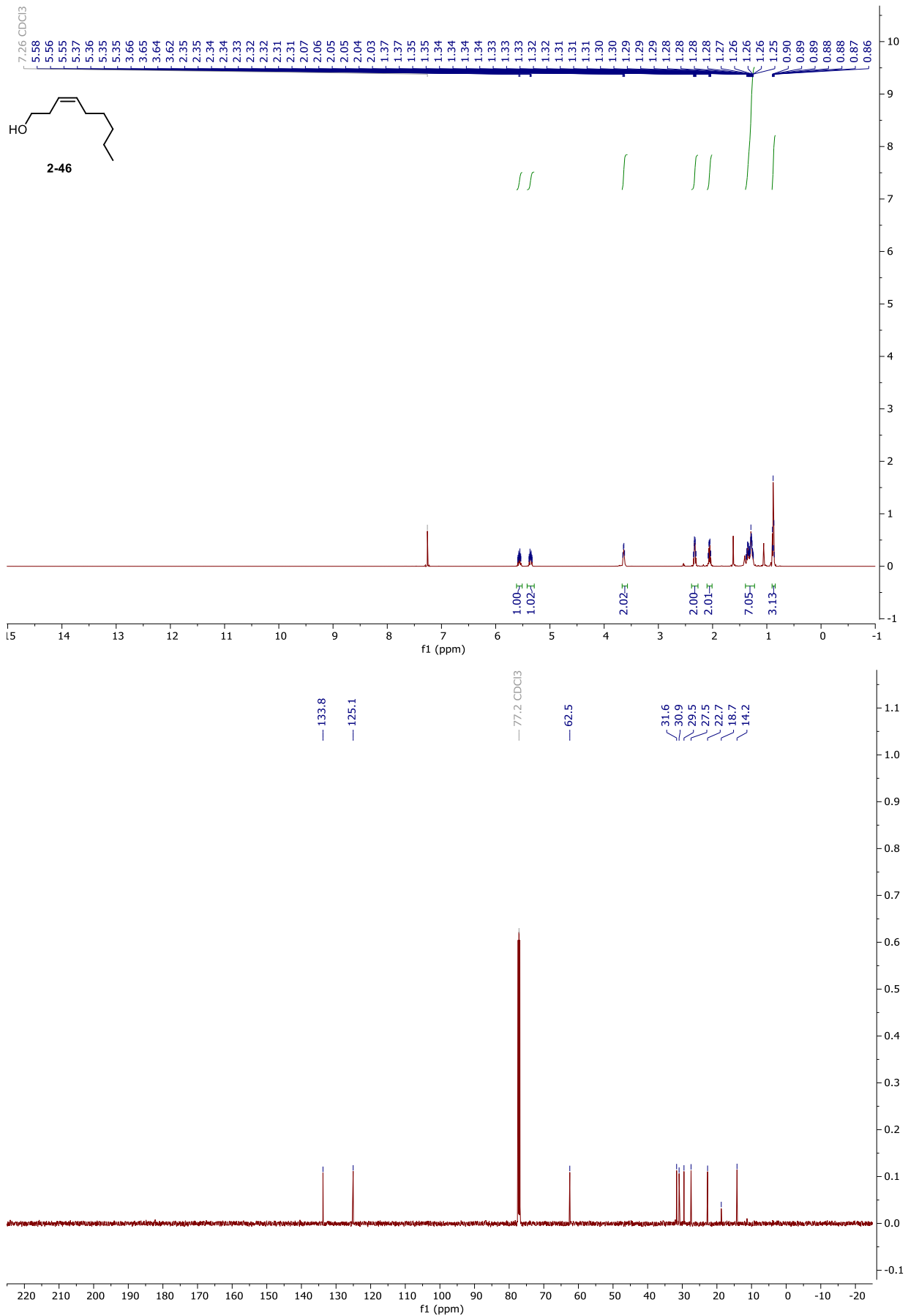
NMR and HPLC

Copy of ^1H and $^{13}\text{C}\{^1\text{H}\}$ spectra of 2-42



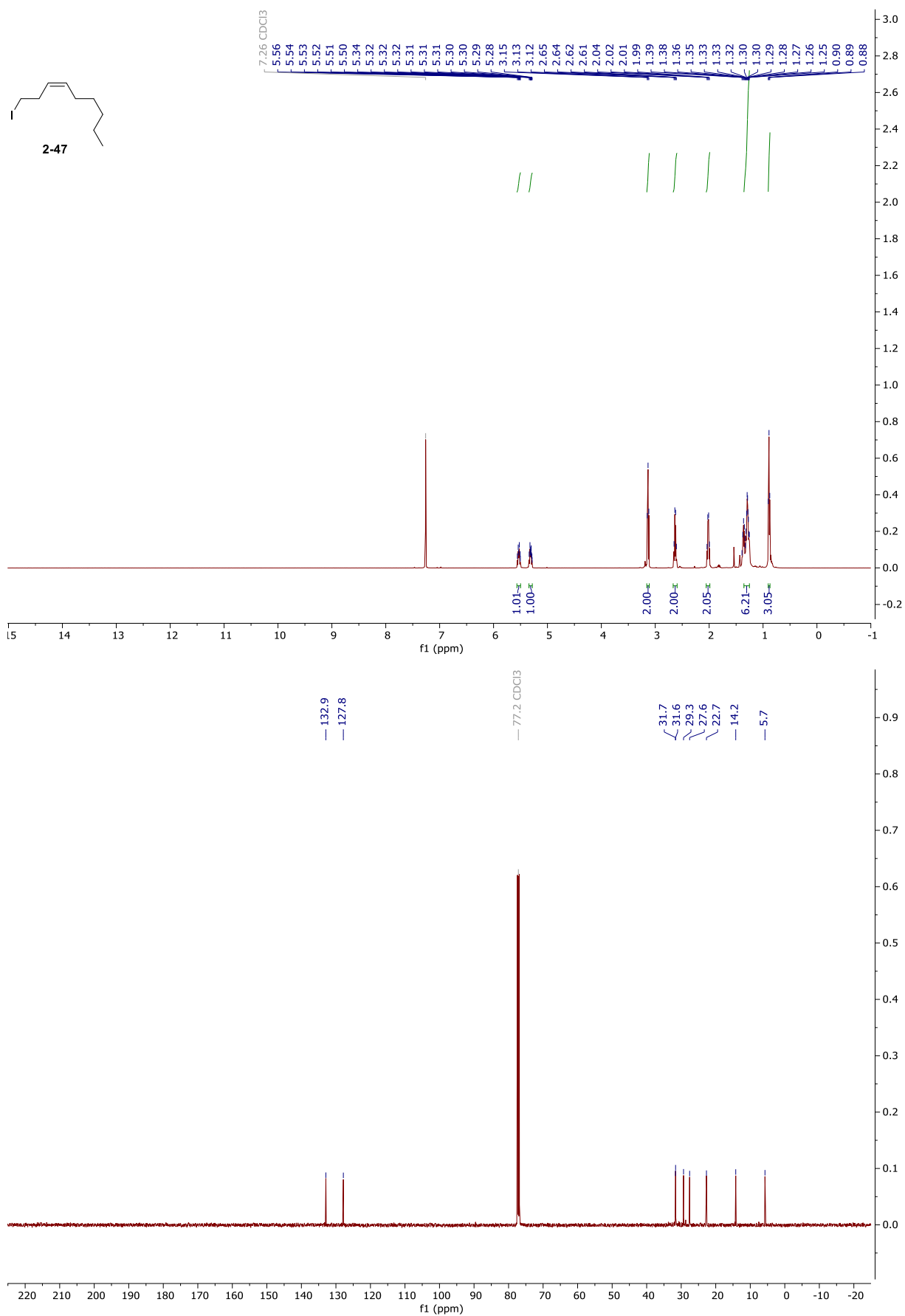
NMR and HPLC

Copy of ^1H and $^{13}\text{C}\{^1\text{H}\}$ spectra of 2-46



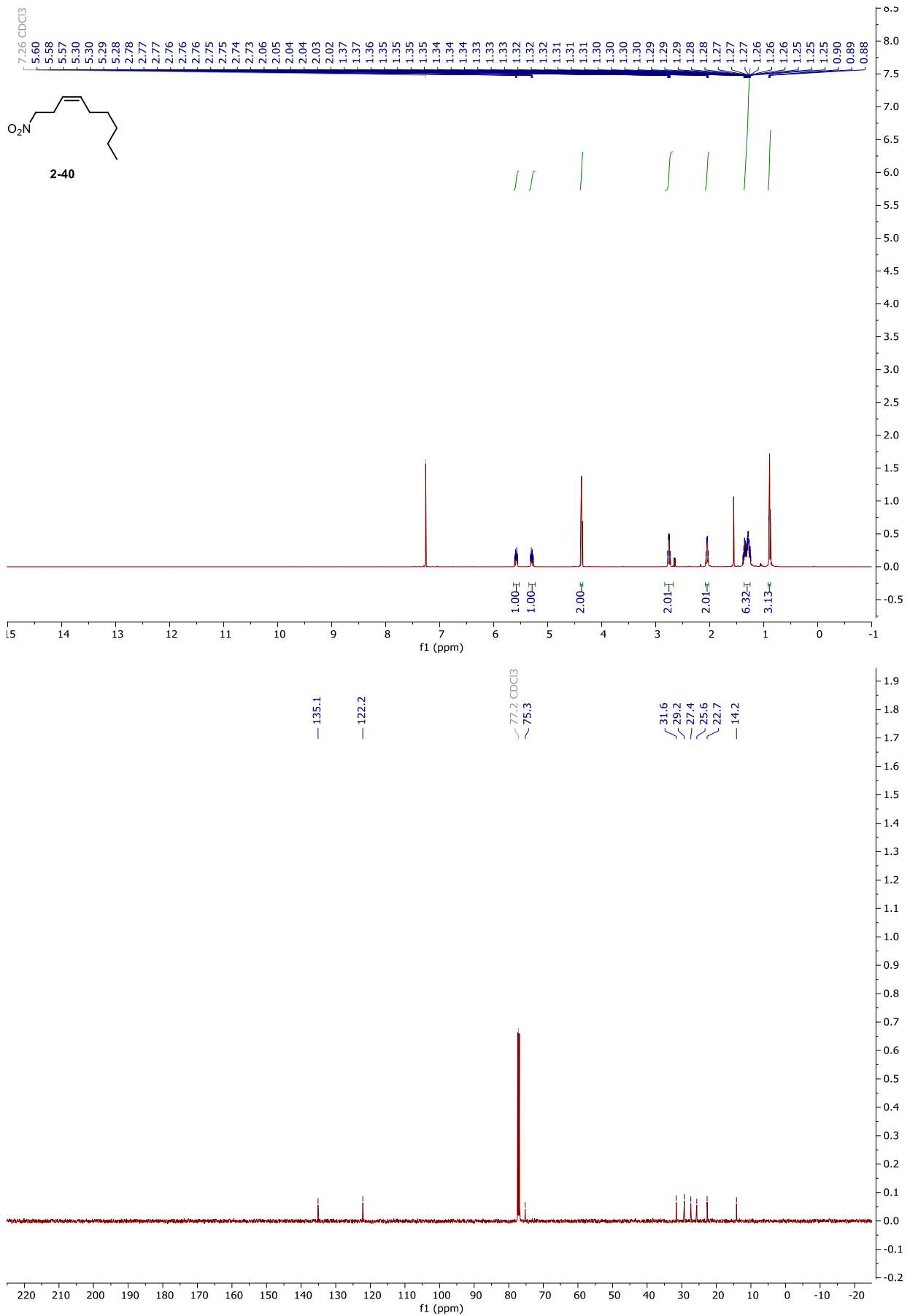
NMR and HPLC

Copy of ^1H and $^{13}\text{C}\{^1\text{H}\}$ spectra of 2-47



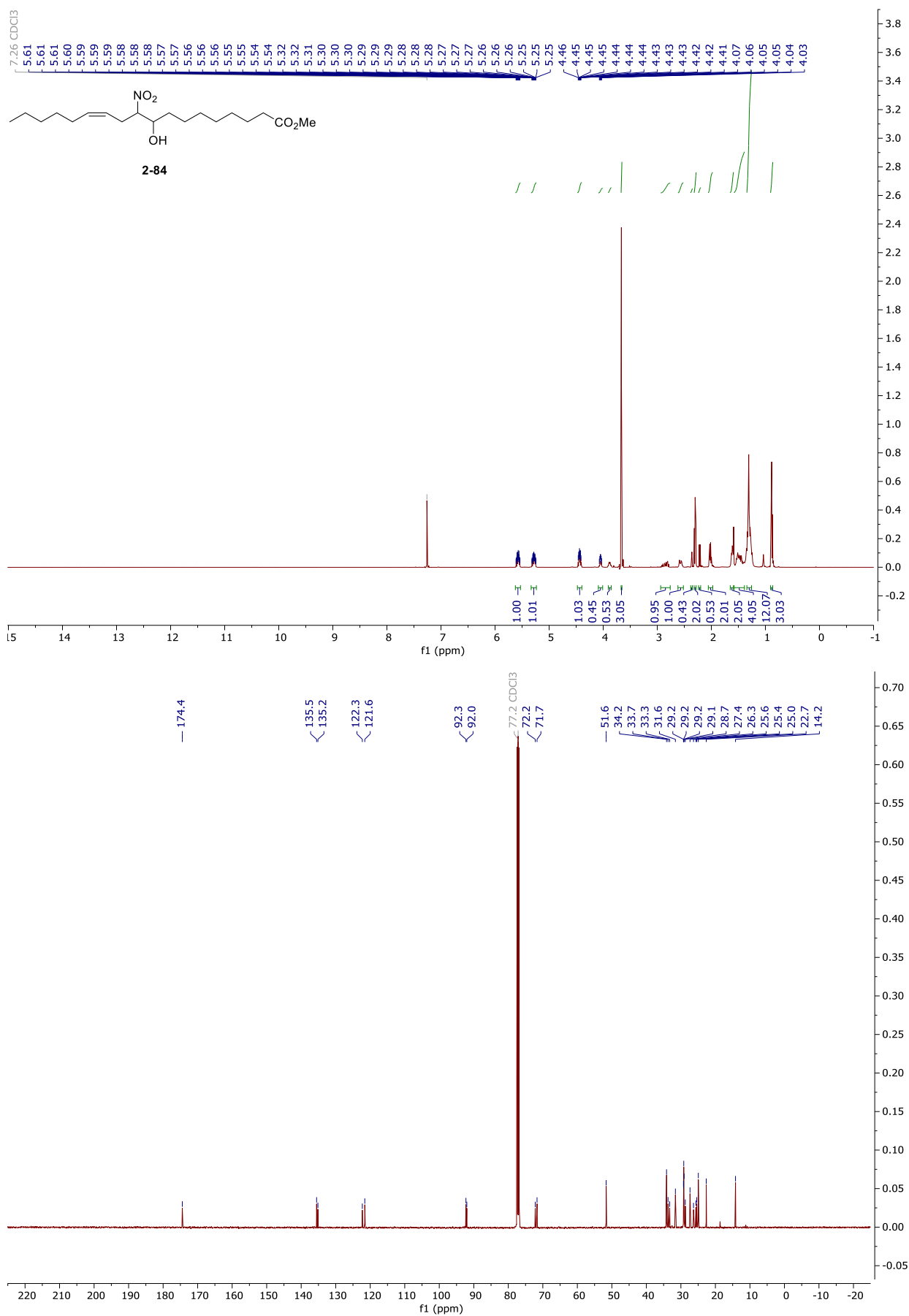
NMR and HPLC

Copy of ^1H and $^{13}\text{C}\{^1\text{H}\}$ spectra of 2-40



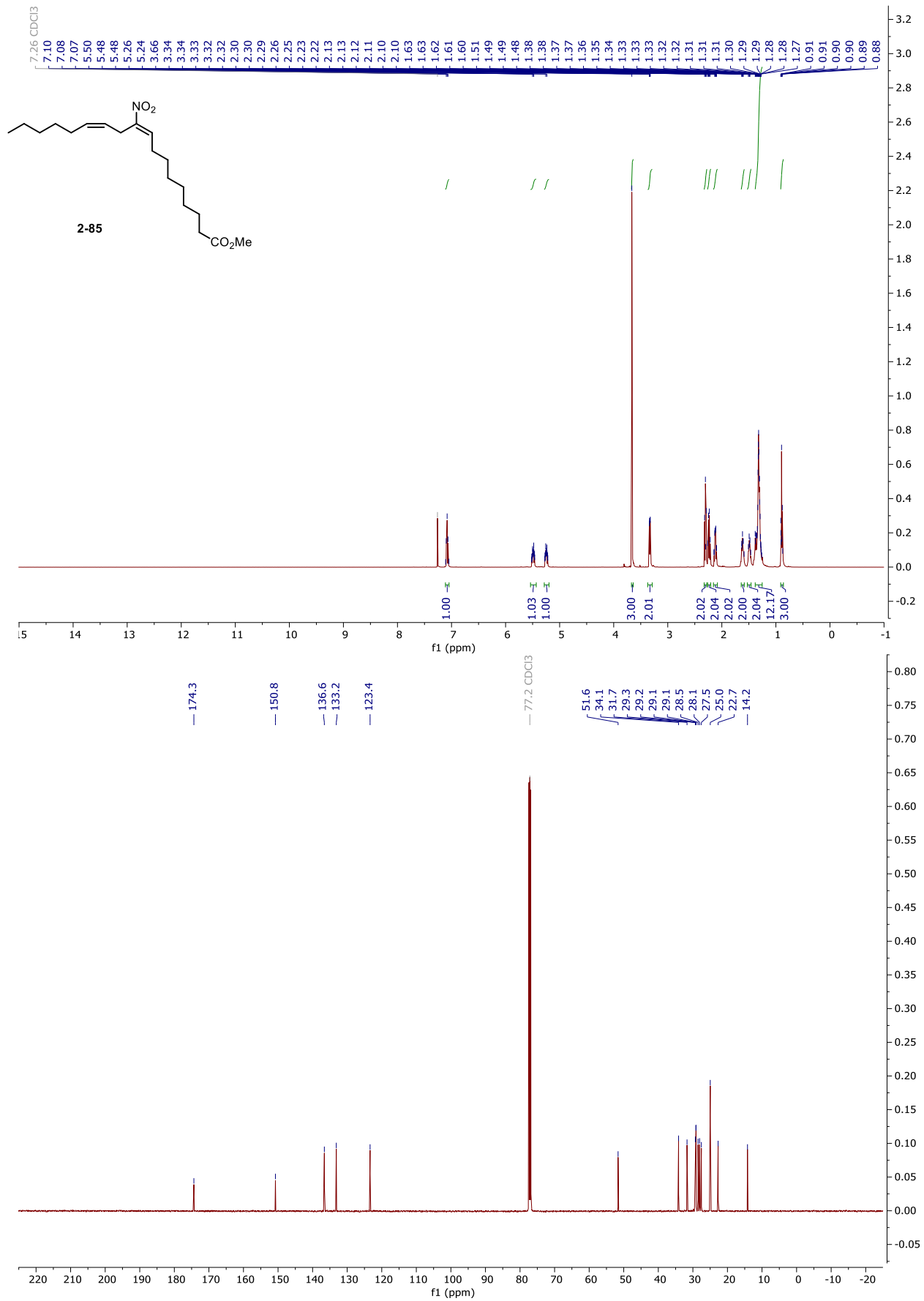
NMR and HPLC

Copy of ^1H and $^{13}\text{C}\{^1\text{H}\}$ spectra of 2-84



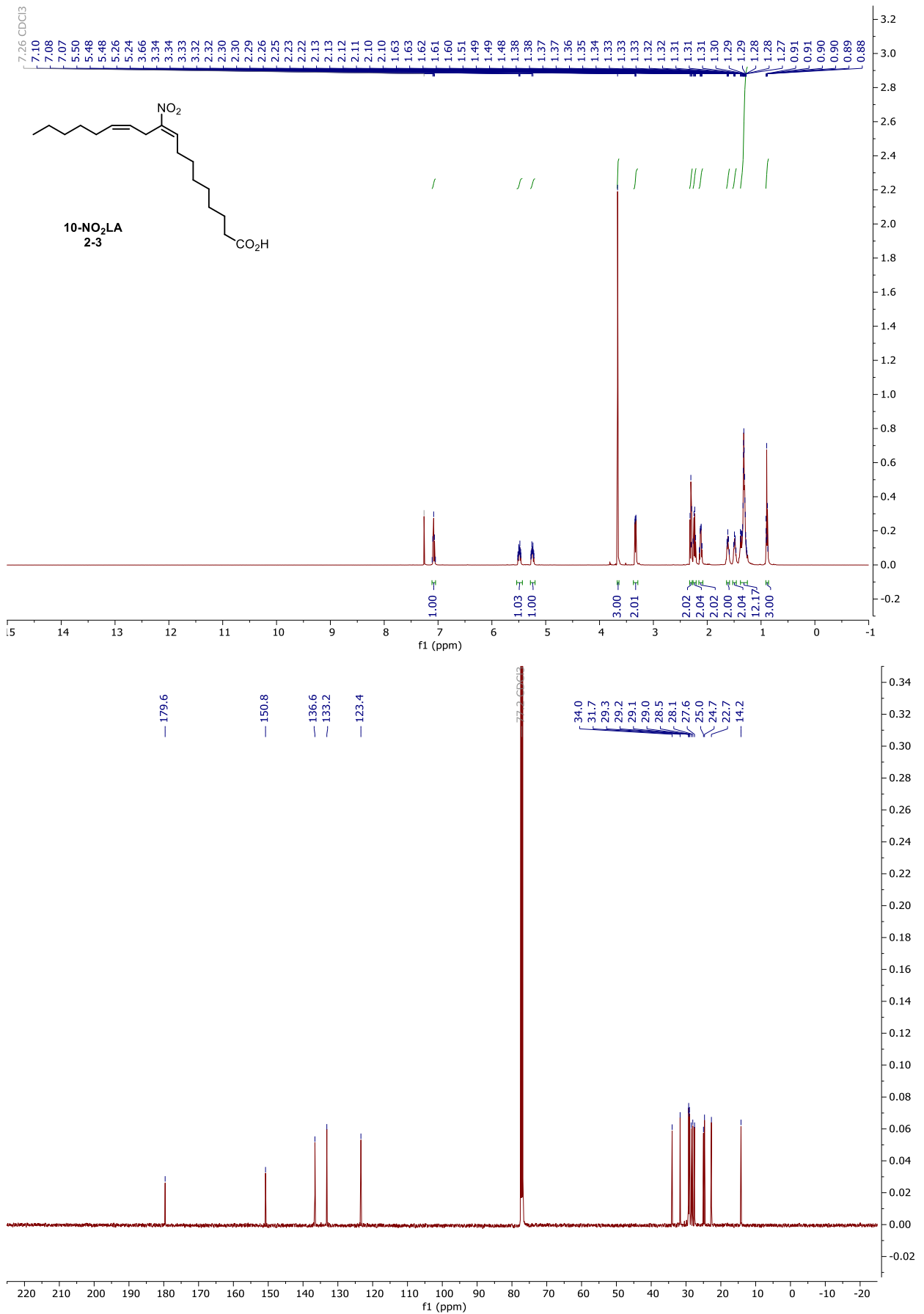
NMR and HPLC

Copy of ^1H and $^{13}\text{C}\{^1\text{H}\}$ spectra of 2-85



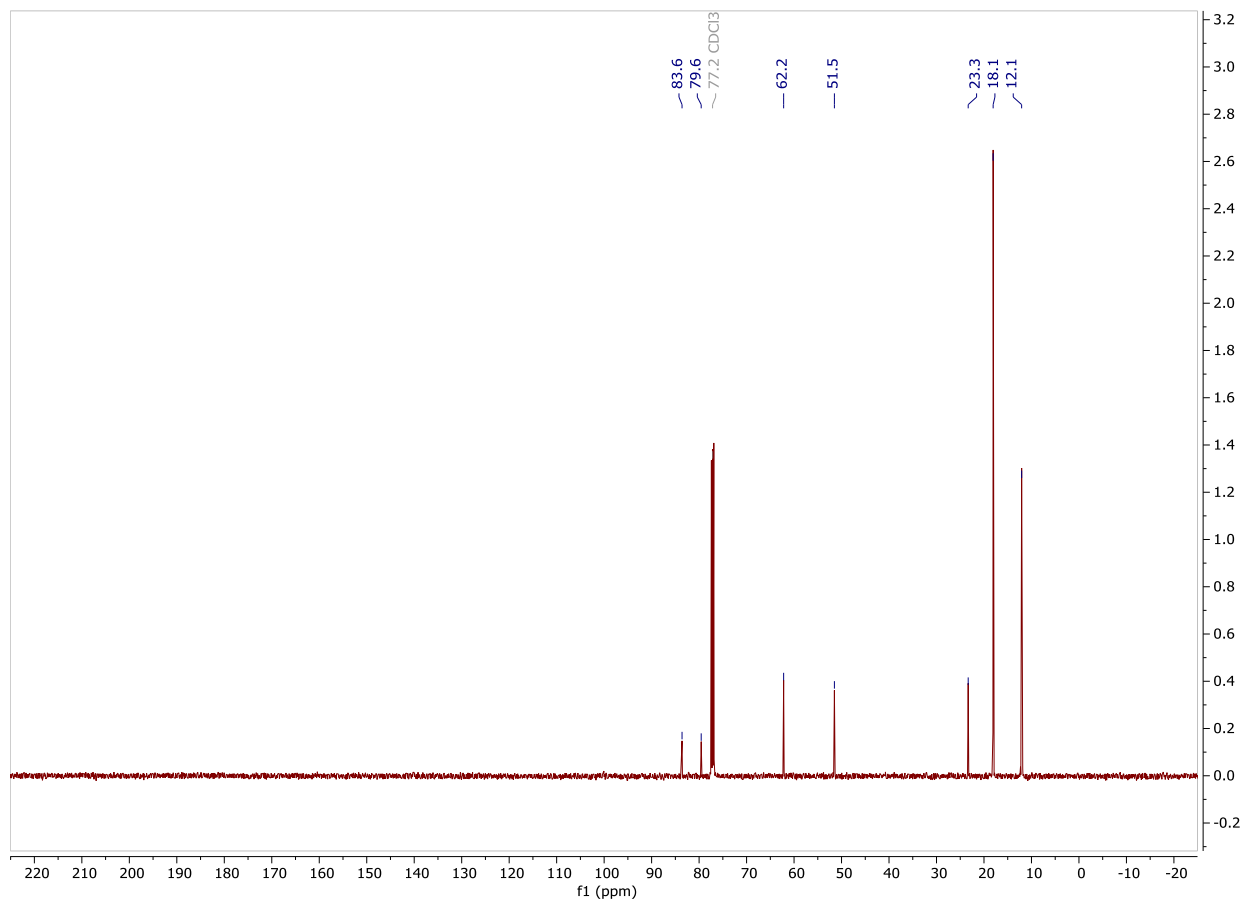
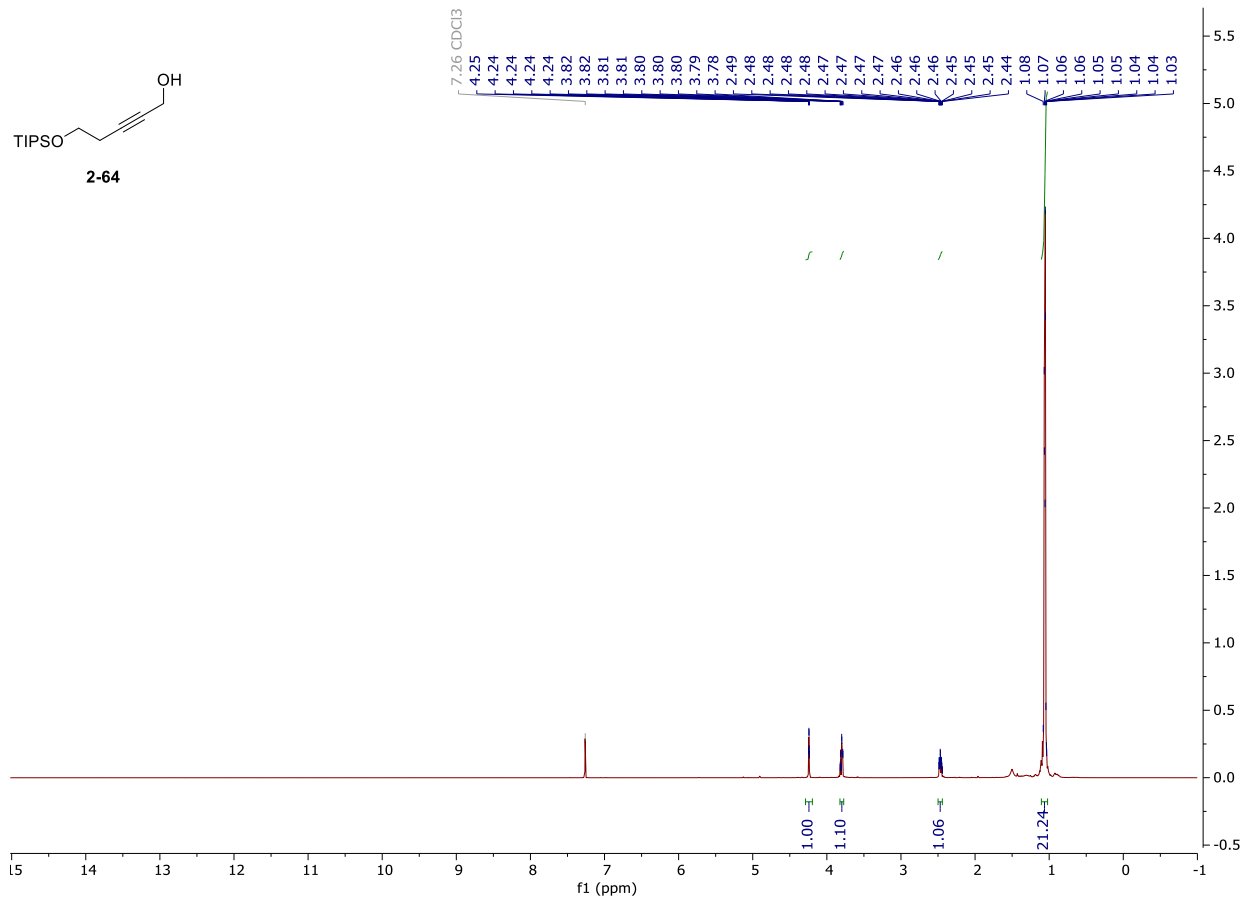
NMR and HPLC

Copy of ^1H and $^{13}\text{C}\{^1\text{H}\}$ spectra of 10- NO_2LA , 2-3



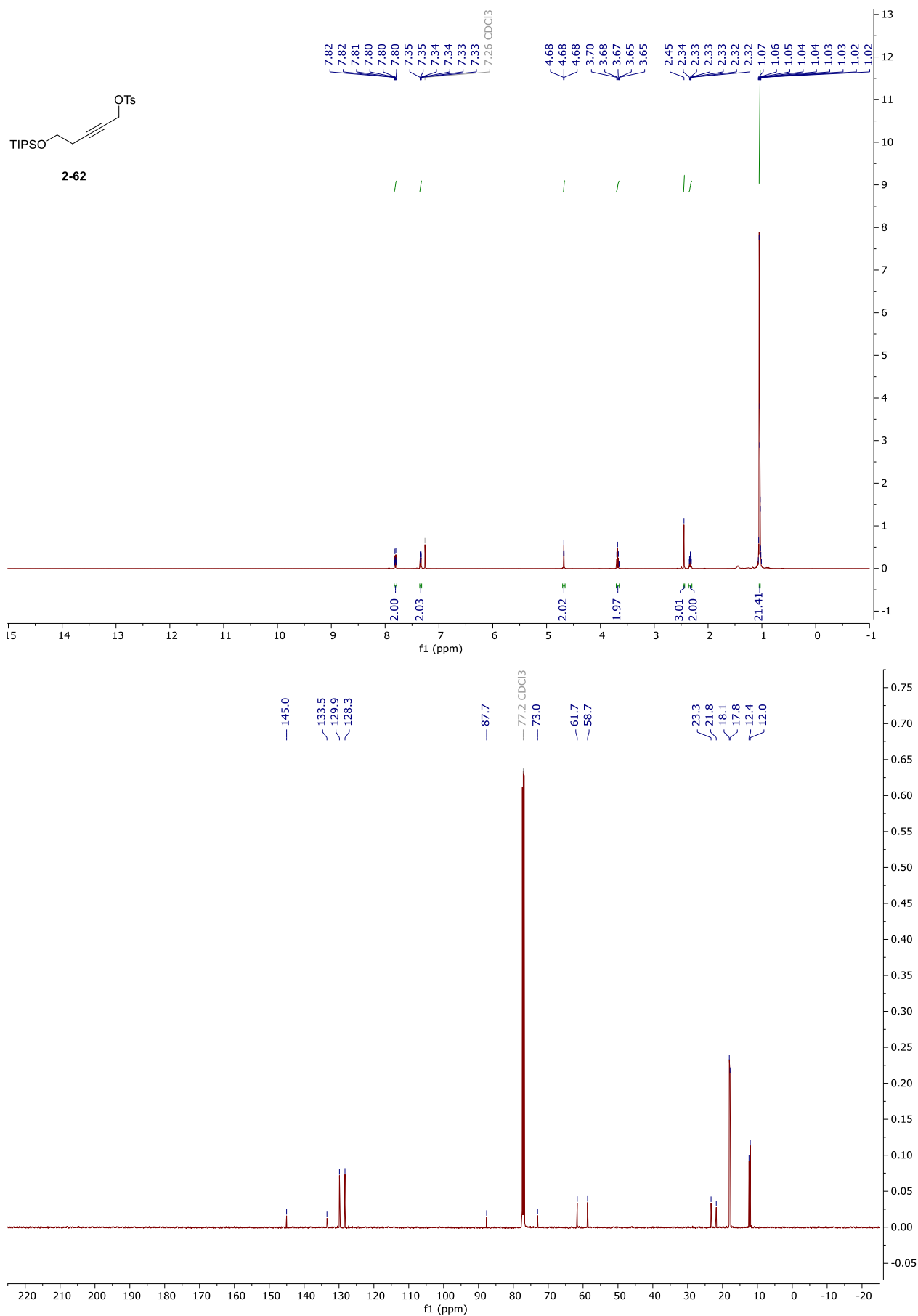
NMR and HPLC

Copy of ^1H and $^{13}\text{C}\{^1\text{H}\}$ spectra of 2-64



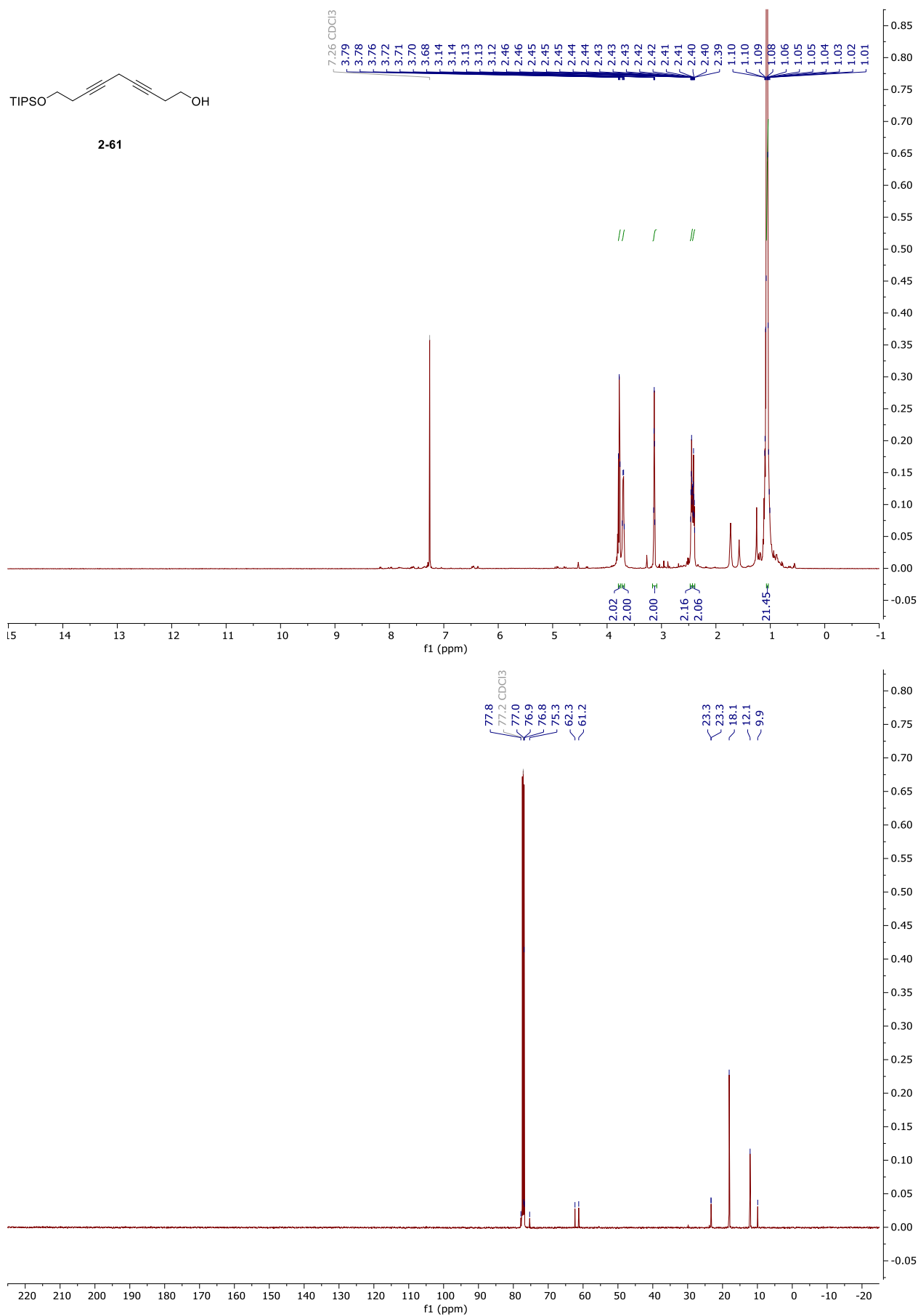
NMR and HPLC

Copy of ^1H and $^{13}\text{C}\{^1\text{H}\}$ spectra of 2-62



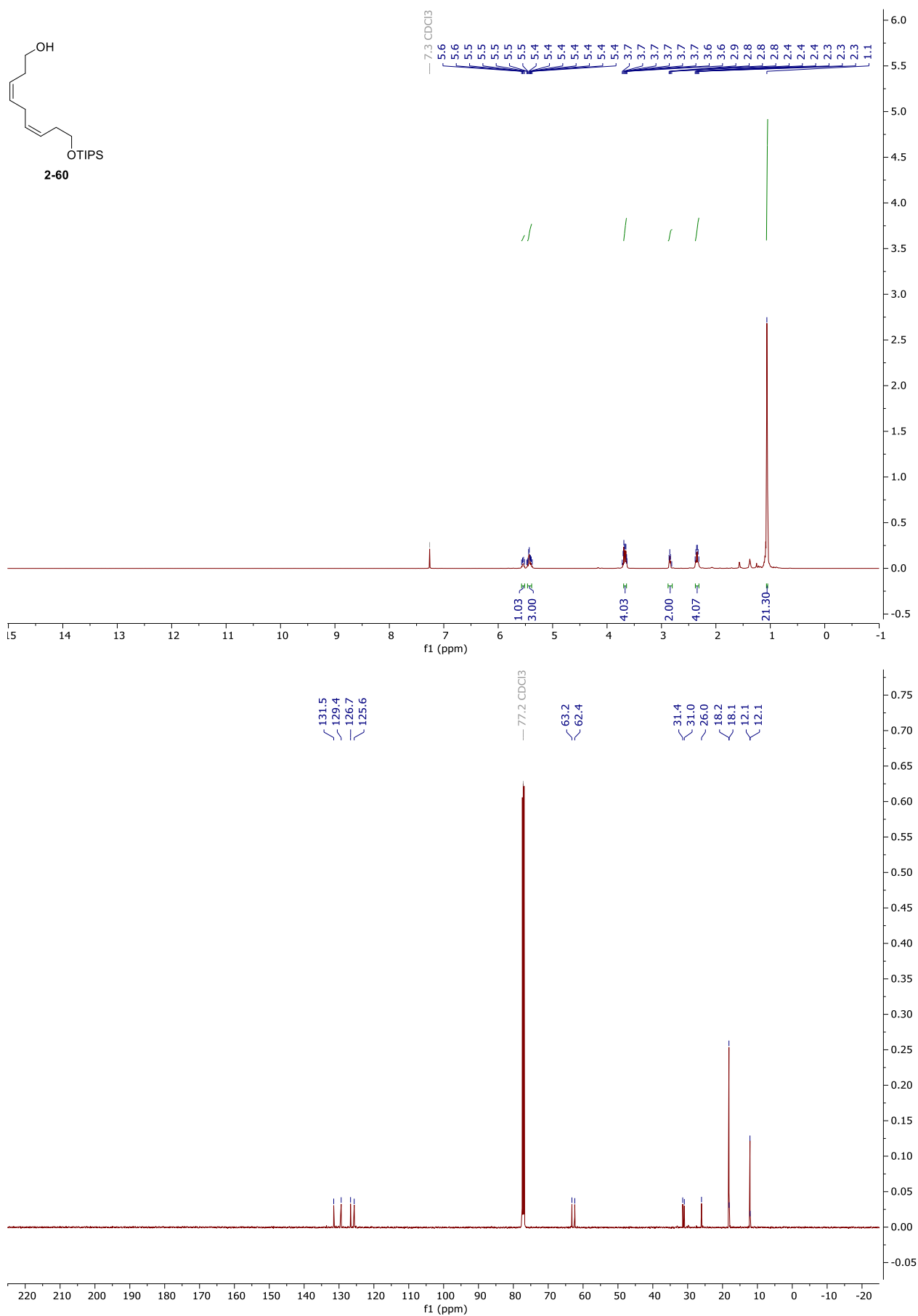
NMR and HPLC

Copy of ^1H and $^{13}\text{C}\{^1\text{H}\}$ spectra of 2-61



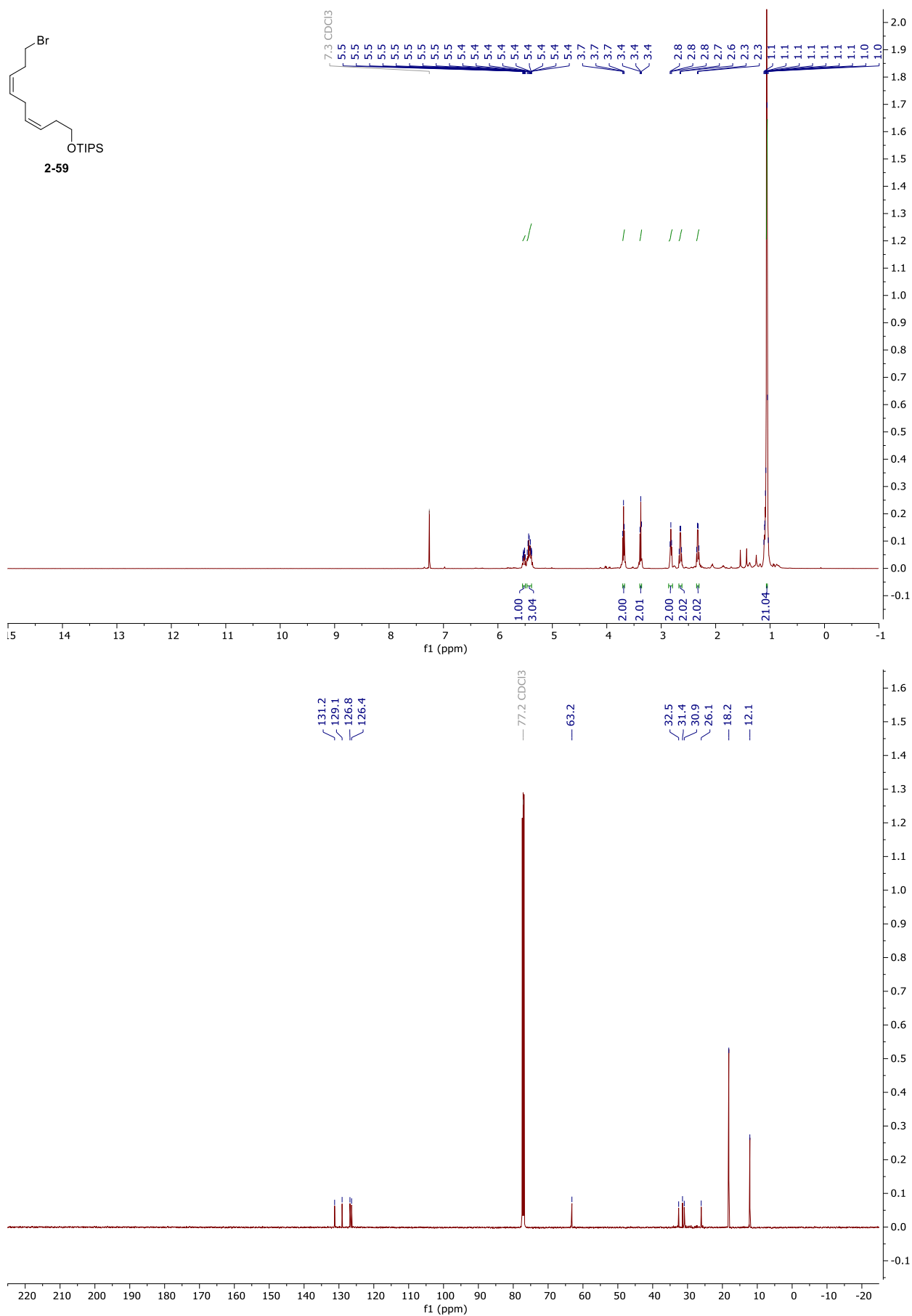
NMR and HPLC

Copy of ^1H and $^{13}\text{C}\{^1\text{H}\}$ spectra of 2-60



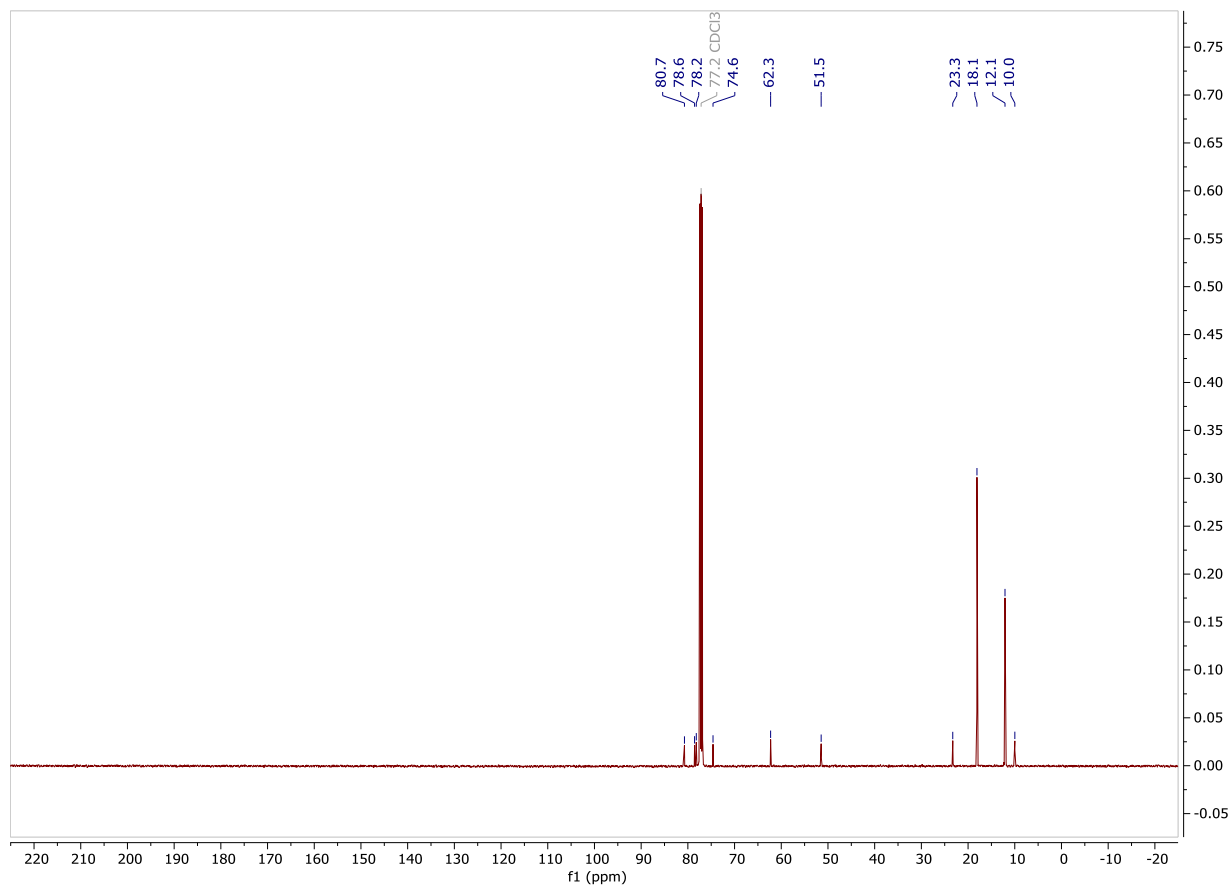
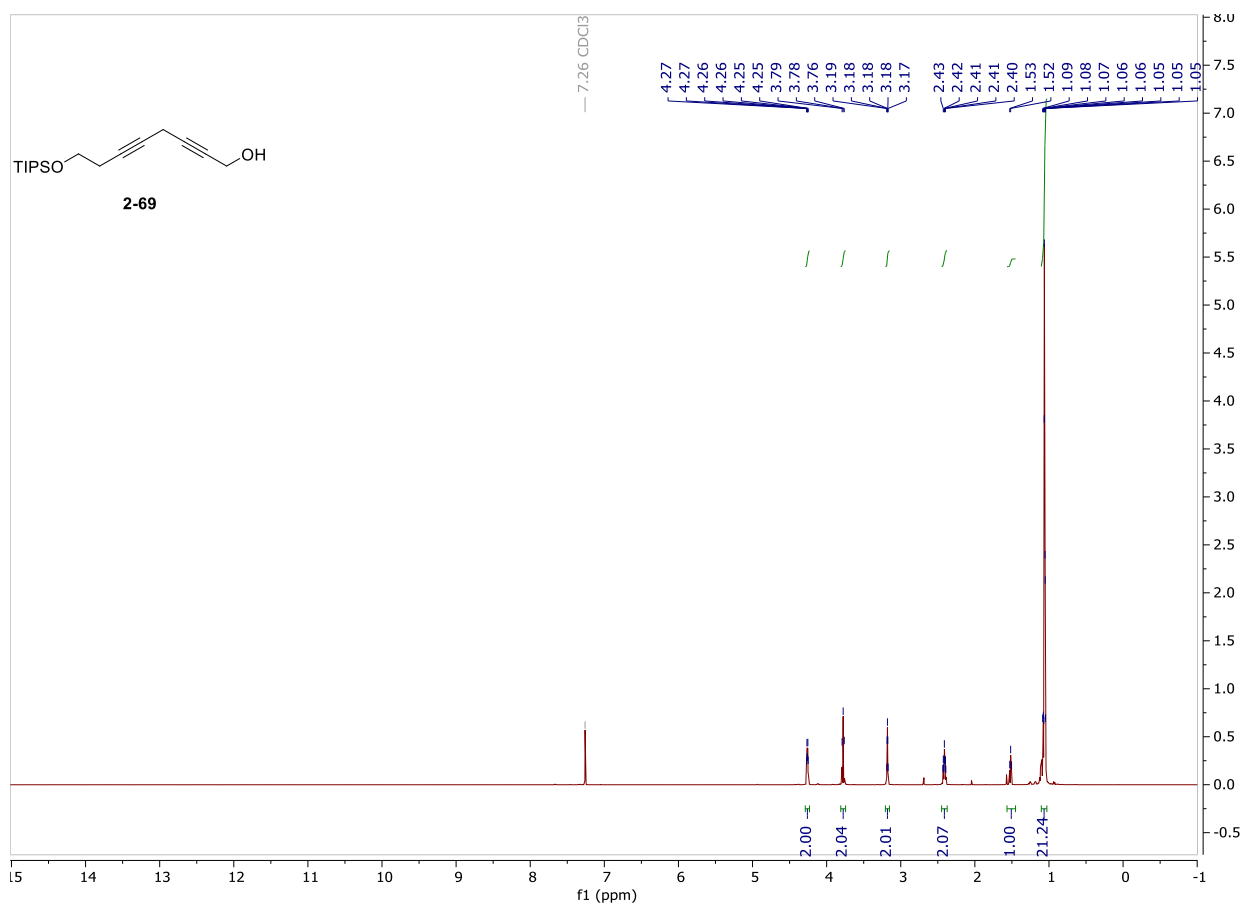
NMR and HPLC

Copy of ^1H and $^{13}\text{C}\{^1\text{H}\}$ spectra of 2-59



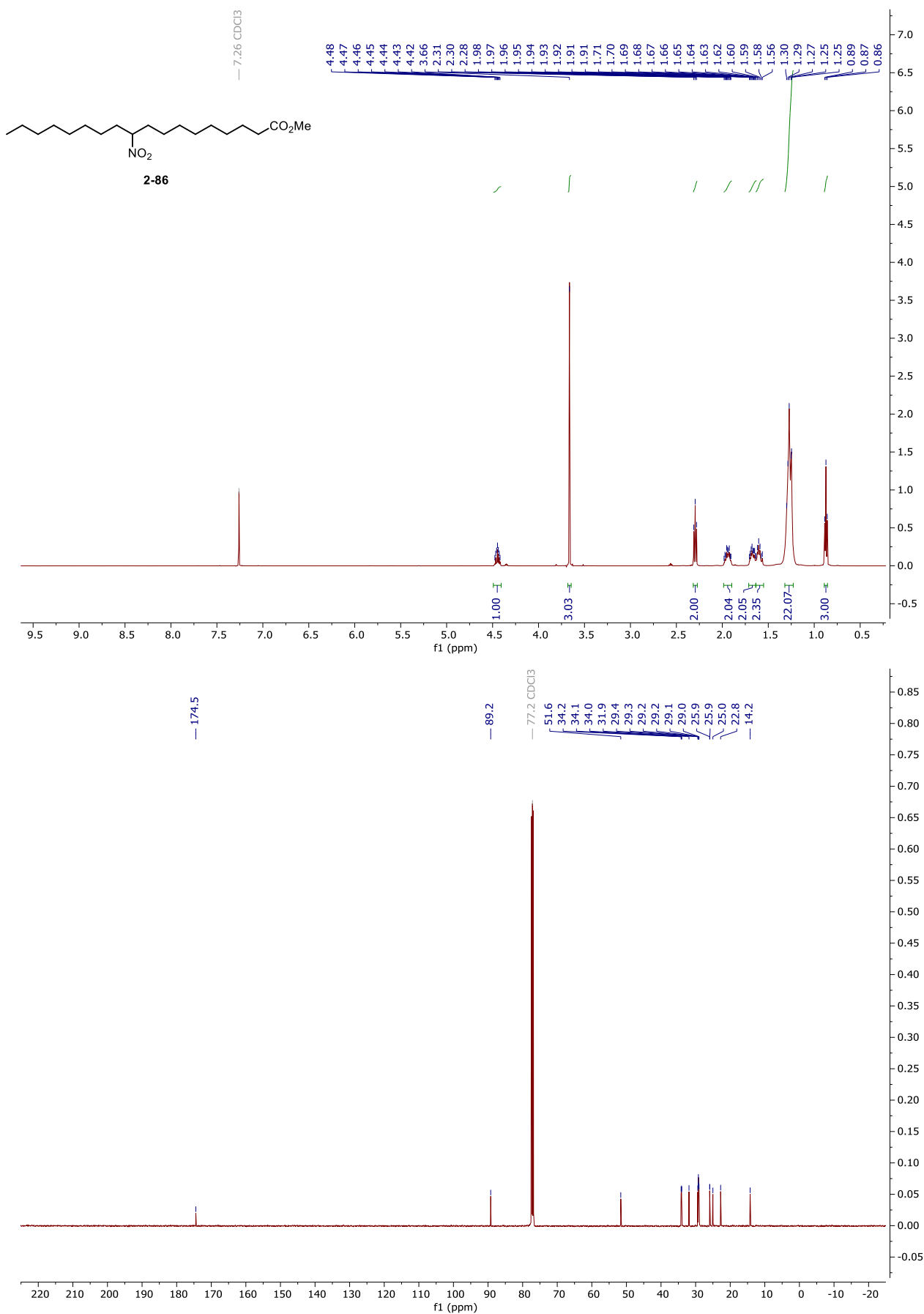
NMR and HPLC

Copy of ^1H and $^{13}\text{C}\{^1\text{H}\}$ spectra of 2-69



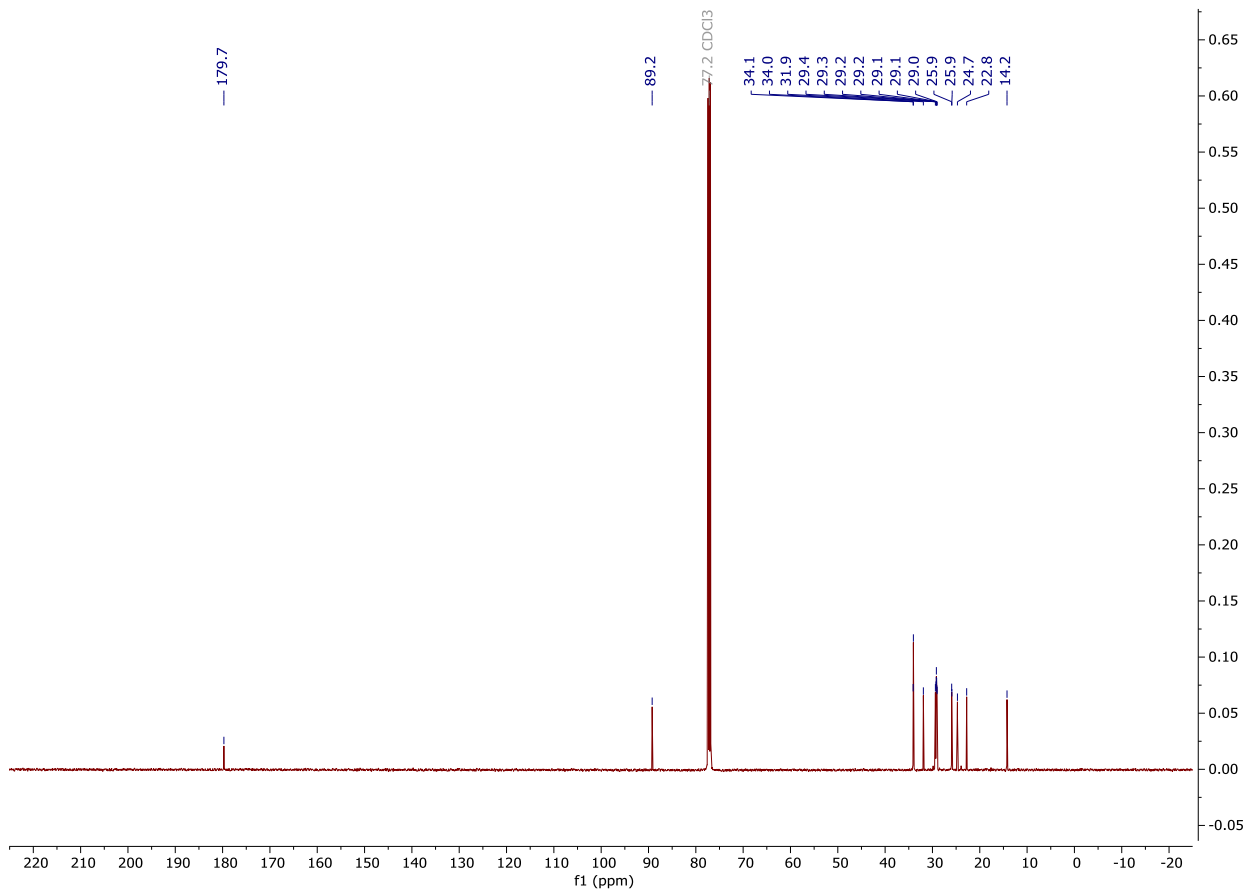
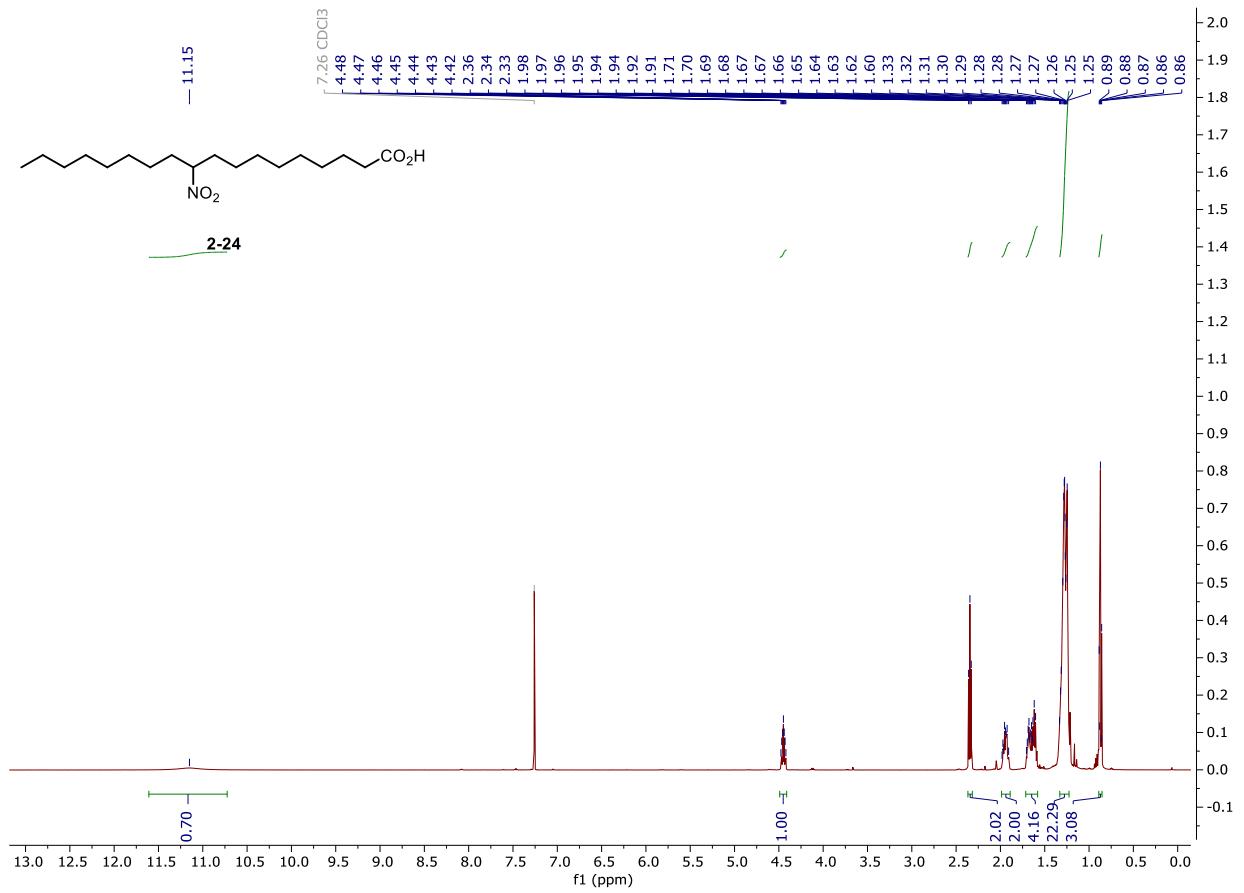
NMR and HPLC

Copy of ^1H and $^{13}\text{C}\{^1\text{H}\}$ spectra of 2-86



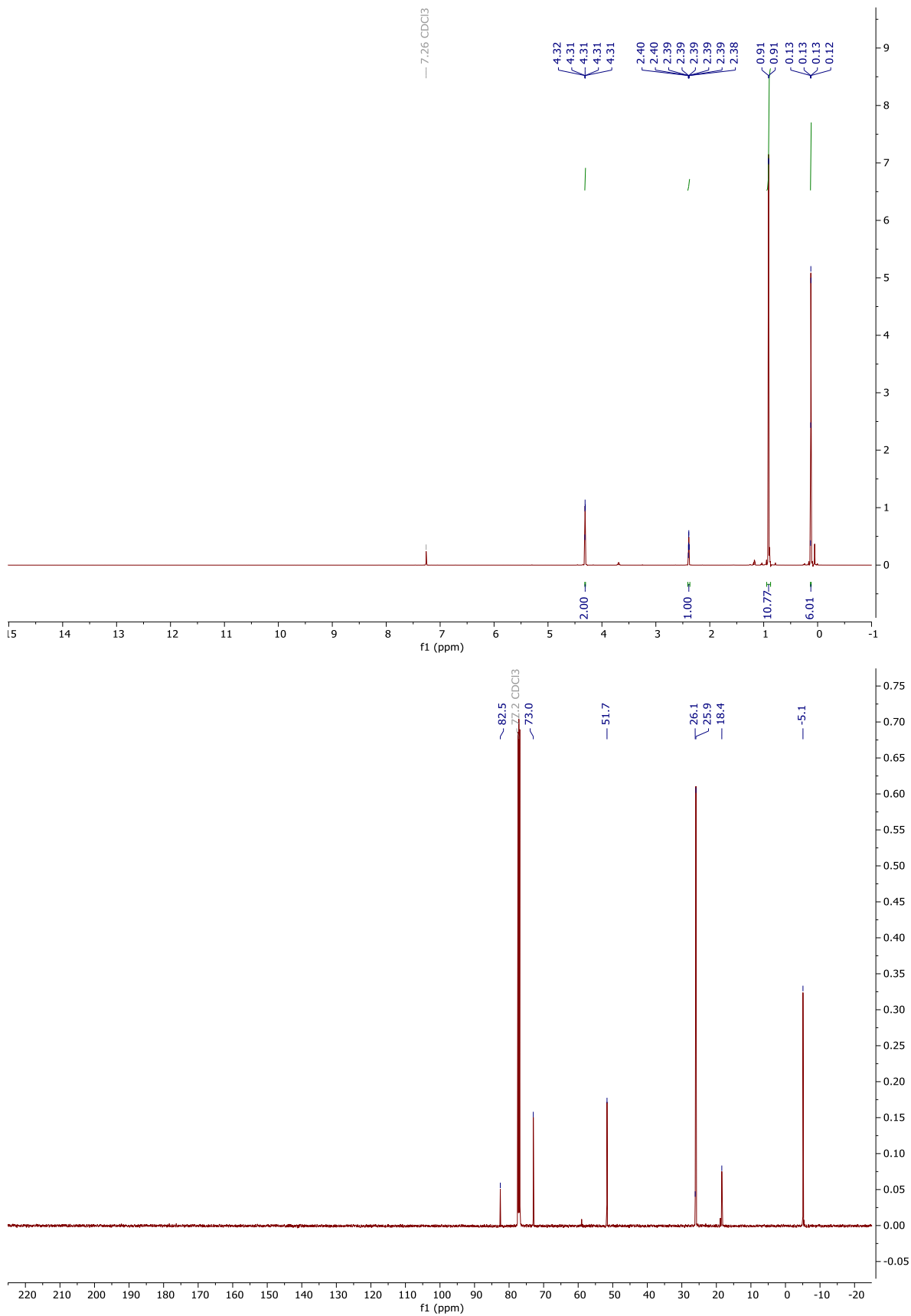
NMR and HPLC

Copy of ^1H and $^{13}\text{C}\{^1\text{H}\}$ spectra of 10- NO_2SA , 2-24



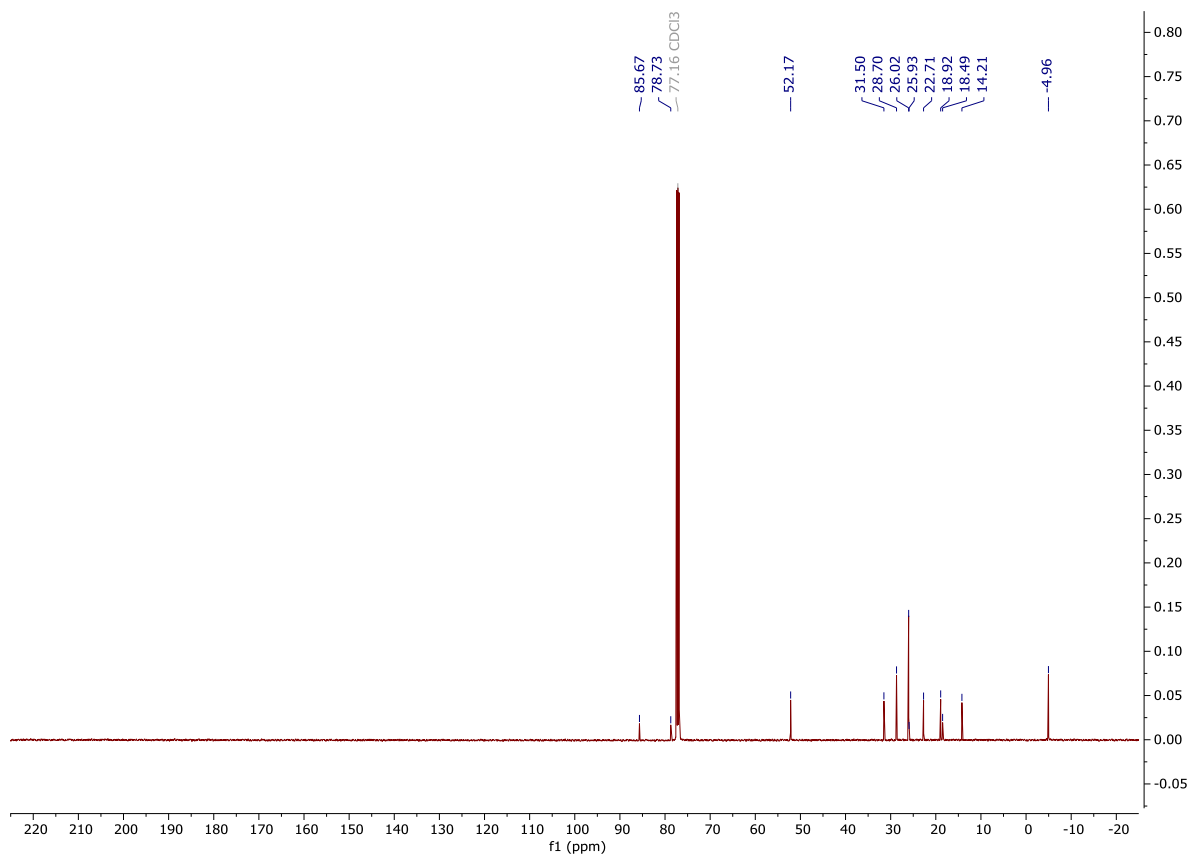
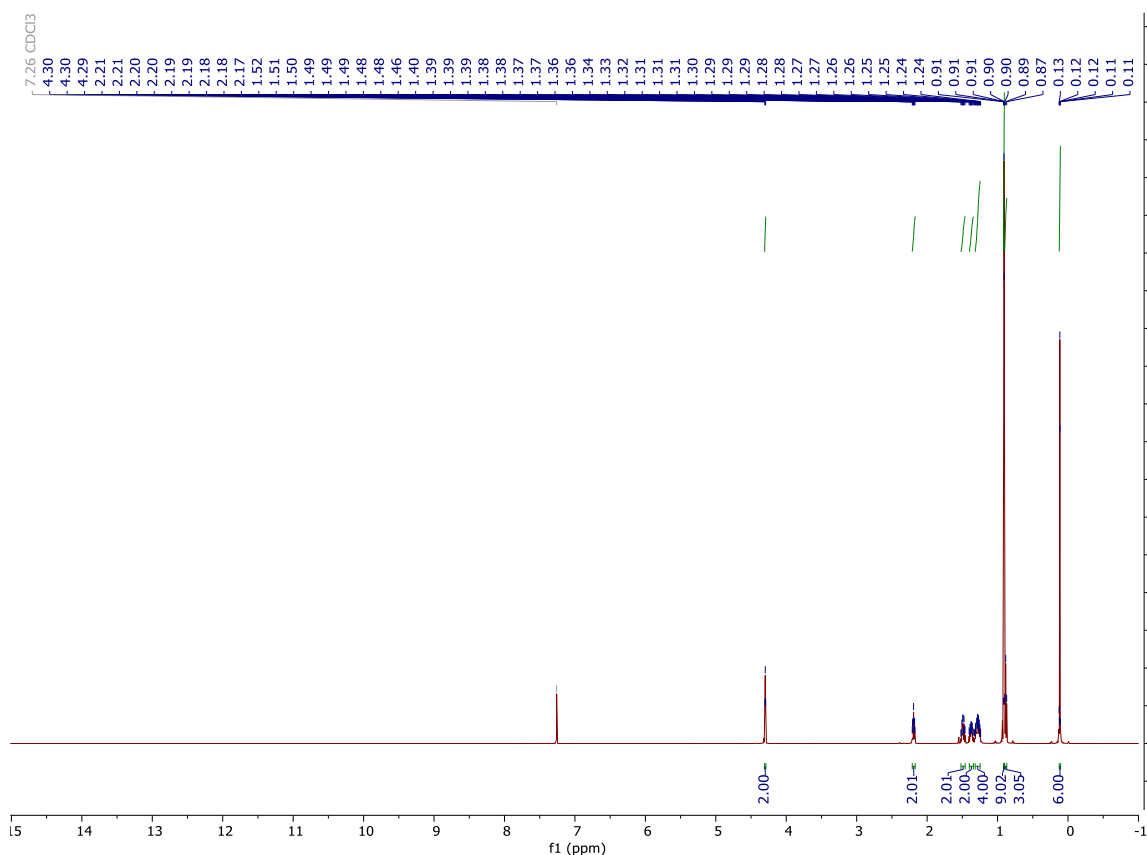
NMR and HPLC

Copy of ^1H and $^{13}\text{C}\{^1\text{H}\}$ spectra of 2-52



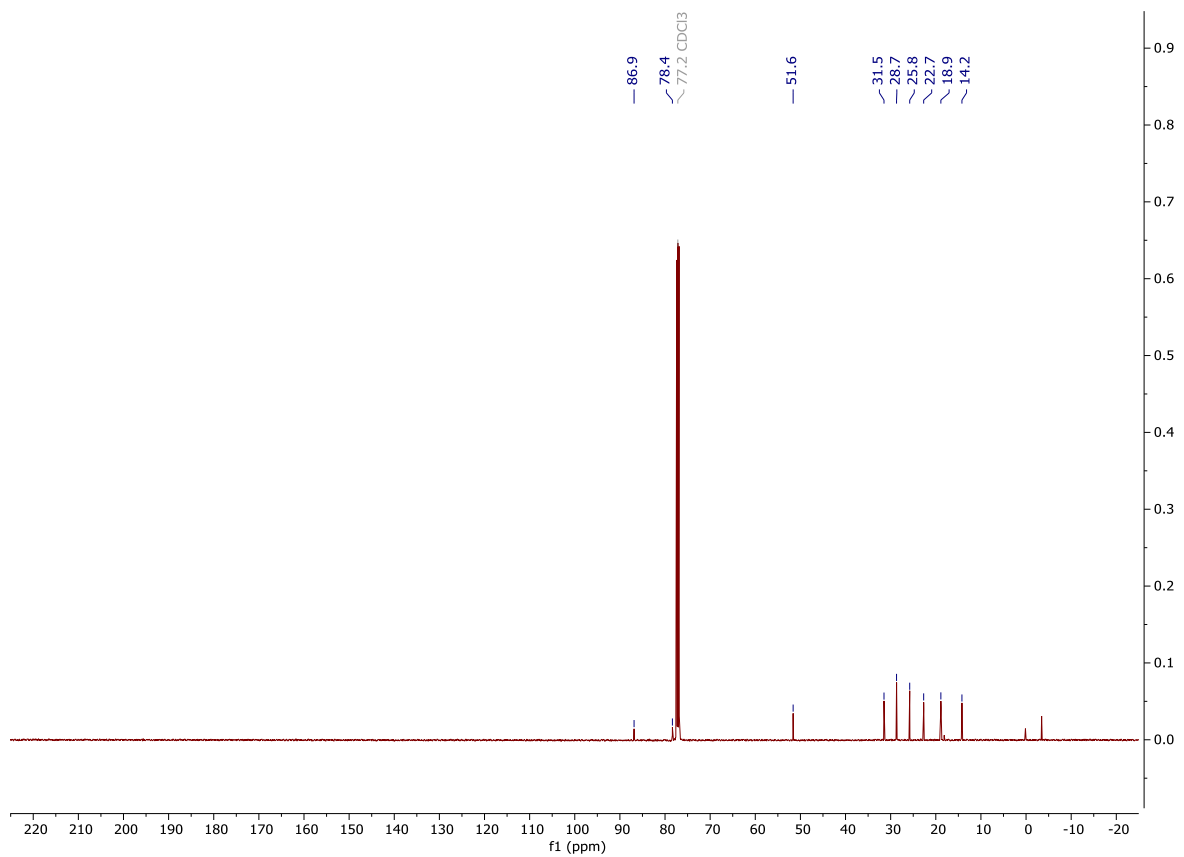
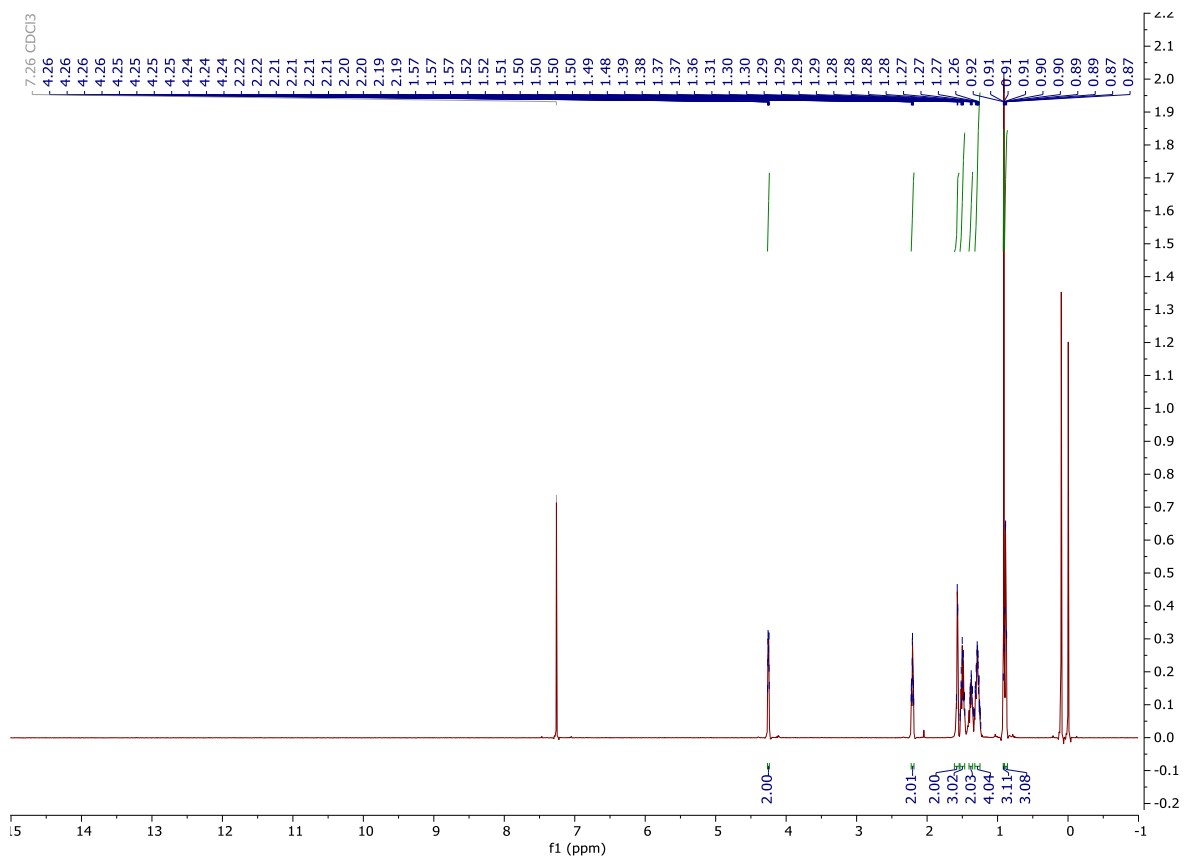
NMR and HPLC

Copy of ^1H and $^{13}\text{C}\{^1\text{H}\}$ spectra of 2-50



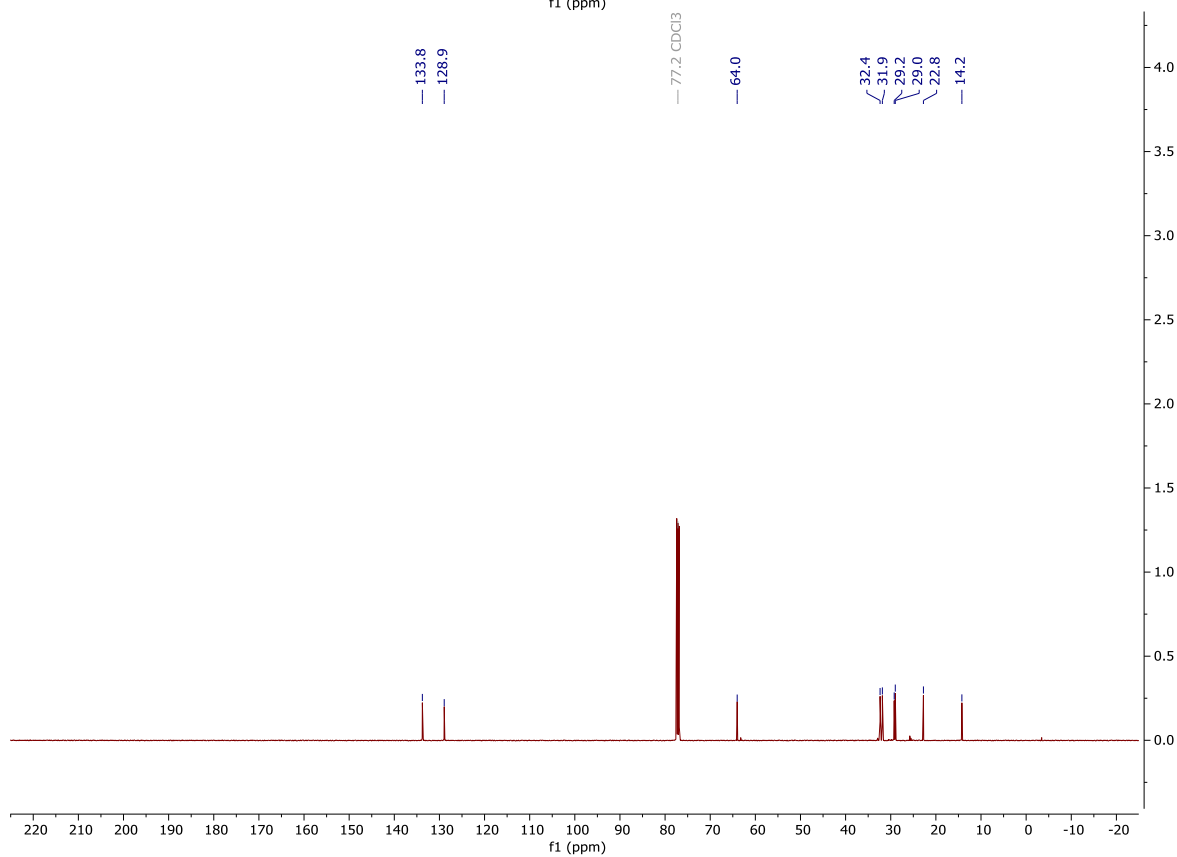
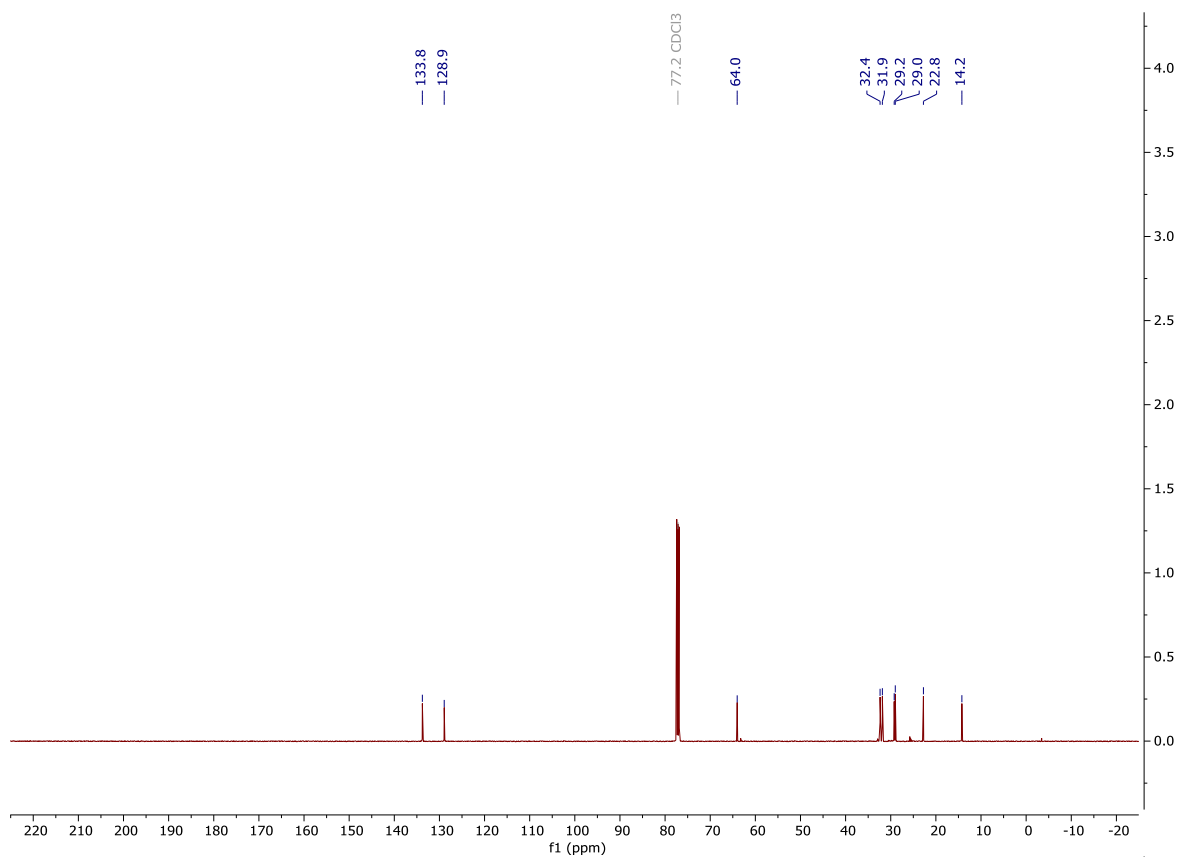
NMR and HPLC

Copy of ^1H and $^{13}\text{C}\{^1\text{H}\}$ spectra of 2-53



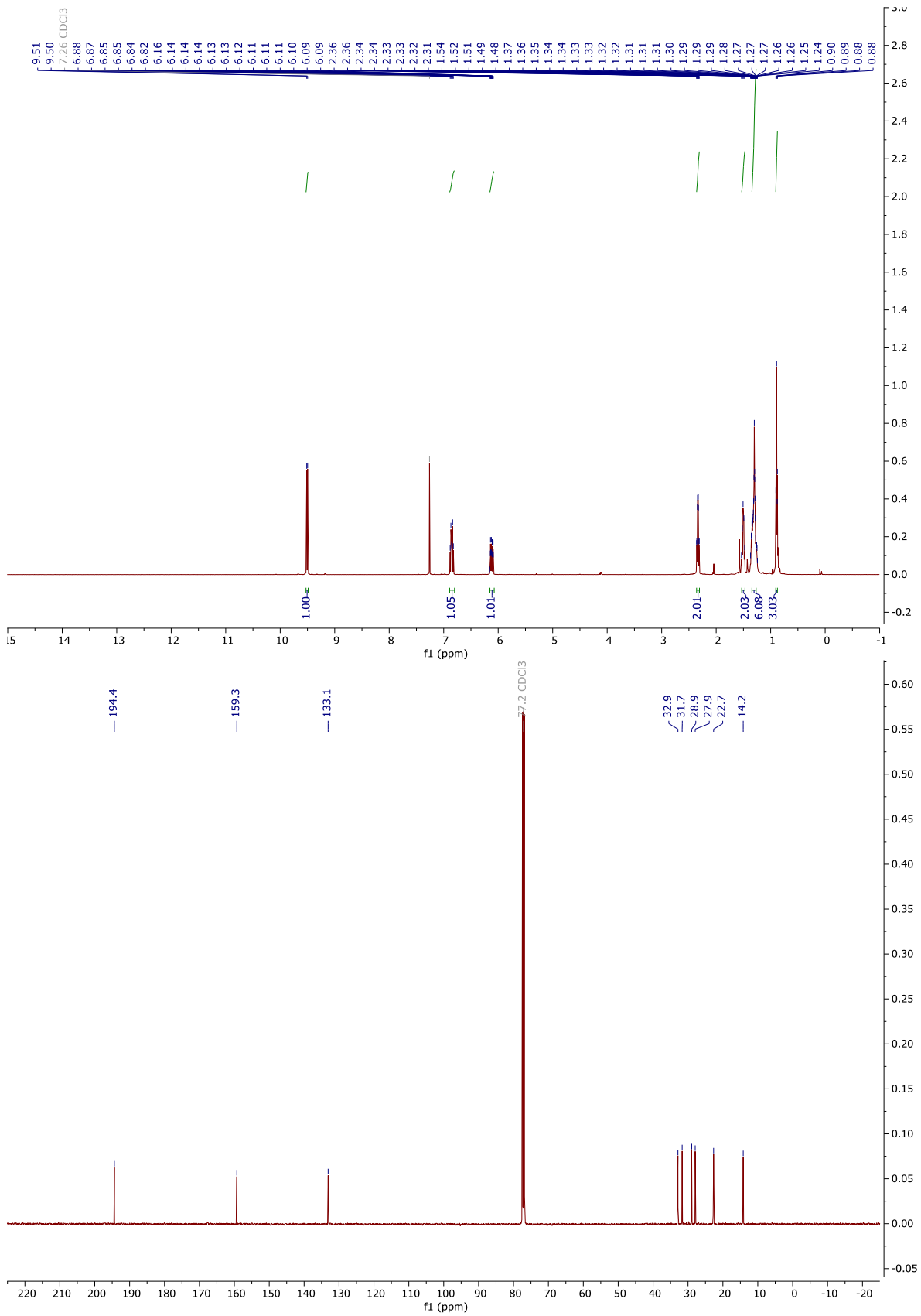
NMR and HPLC

Copy of ^1H and $^{13}\text{C}\{^1\text{H}\}$ spectra of 2-49



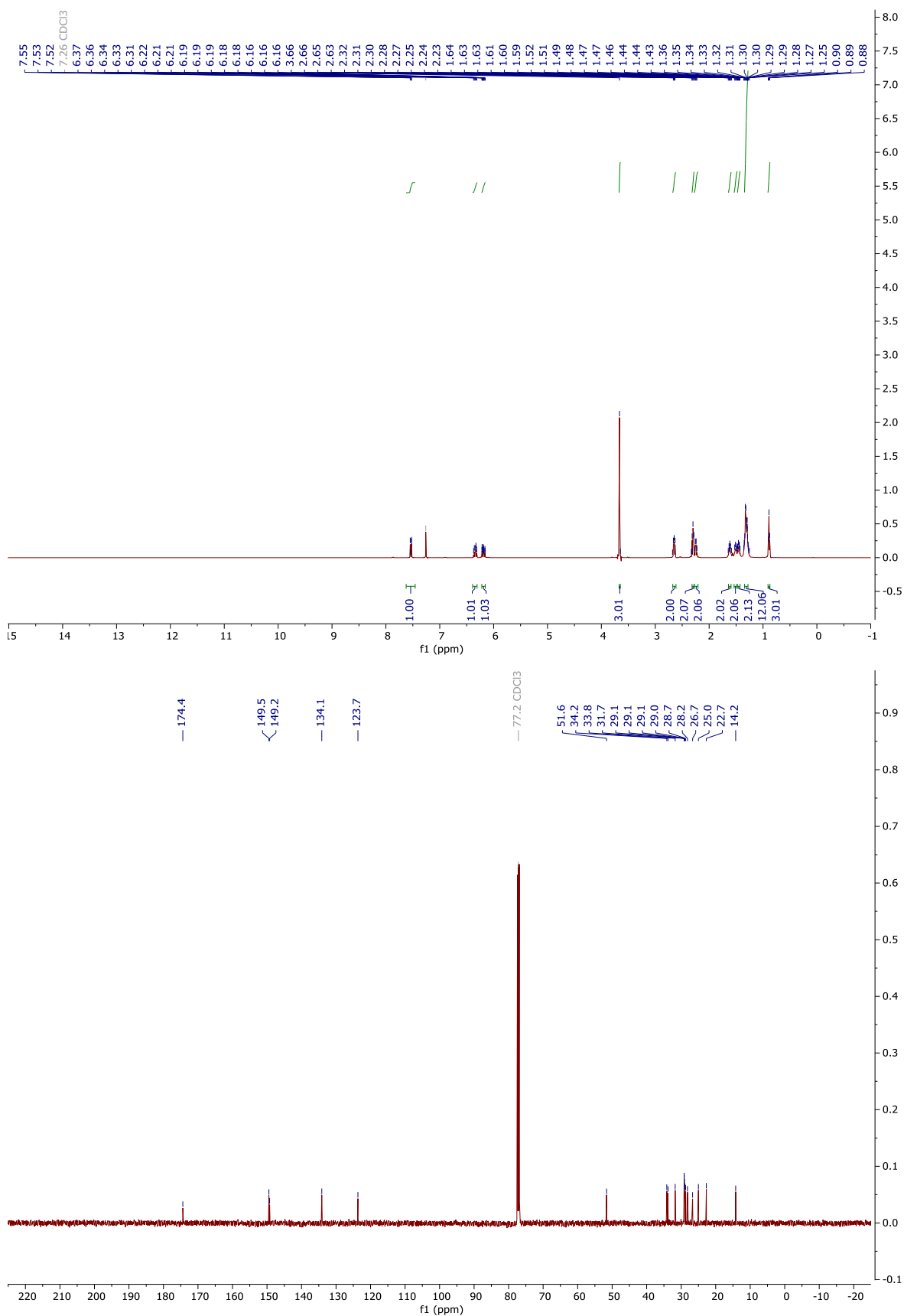
NMR and HPLC

Copy of ^1H and $^{13}\text{C}\{^1\text{H}\}$ spectra of 2-48



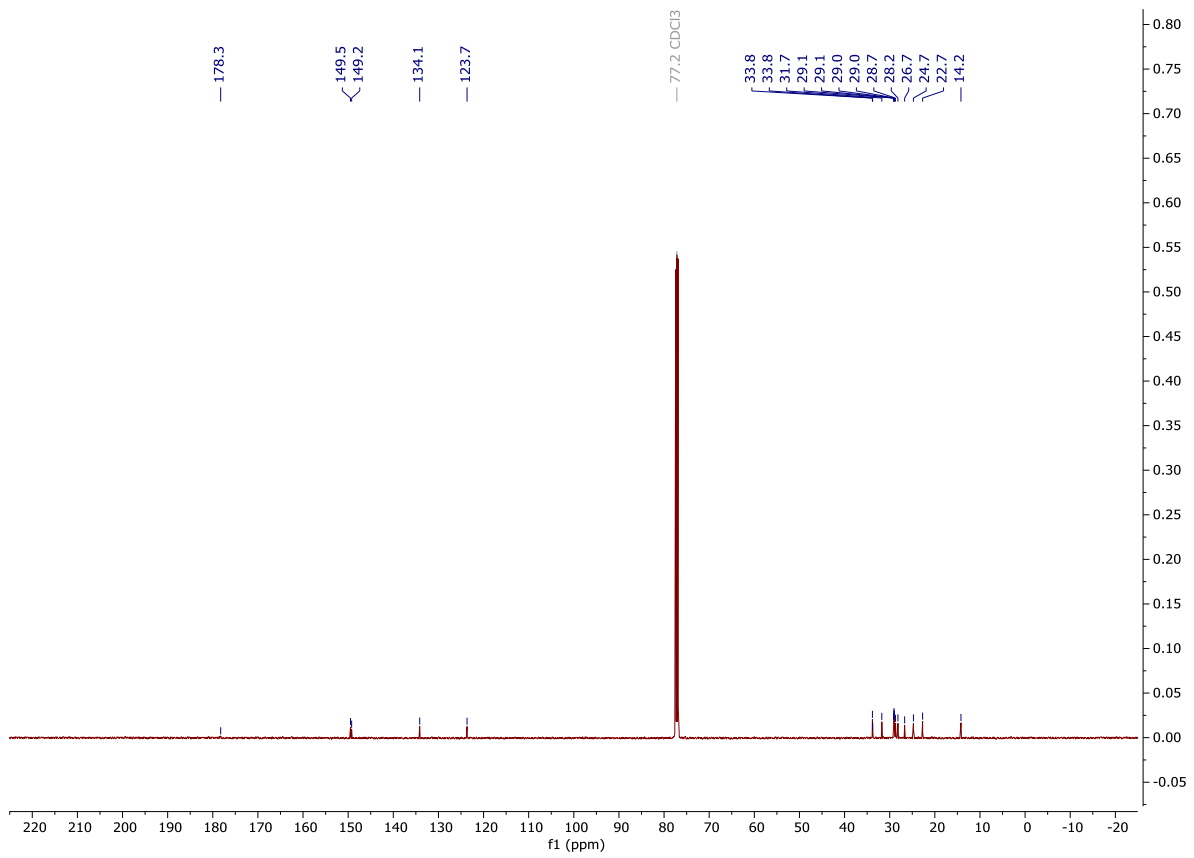
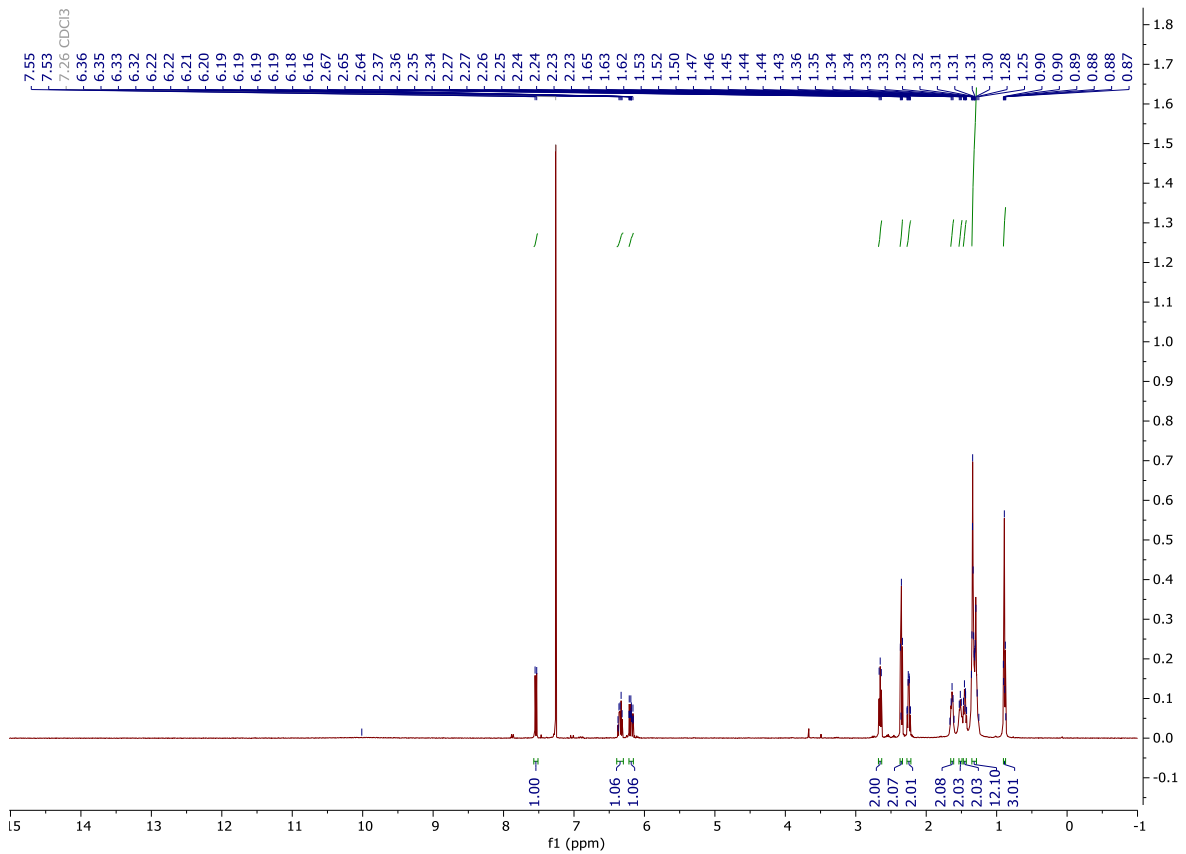
NMR and HPLC

Copy of ^1H and $^{13}\text{C}\{^1\text{H}\}$ spectra of 2-54b



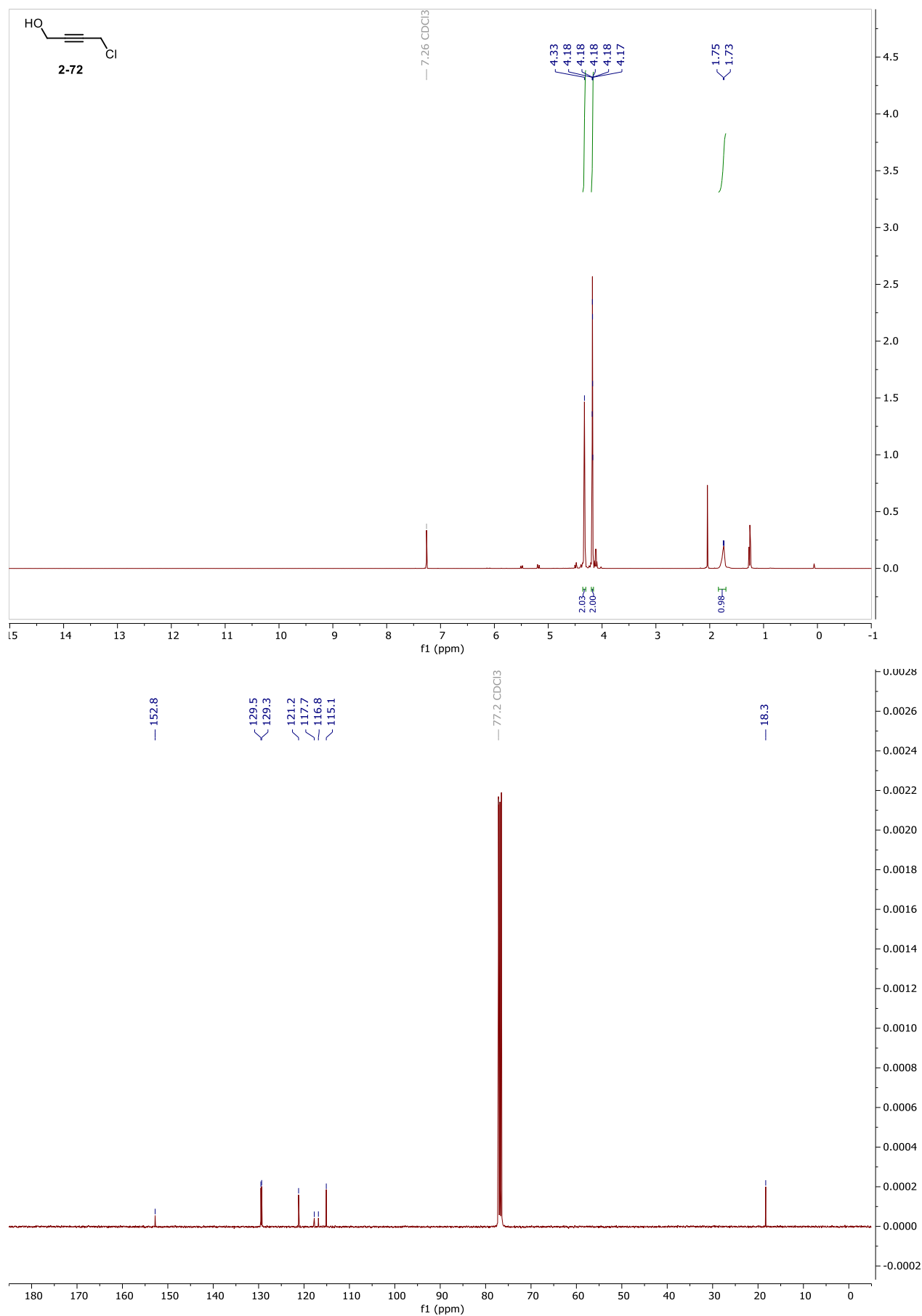
NMR and HPLC

Copy of ^1H and $^{13}\text{C}\{^1\text{H}\}$ spectra of 9- NO_2cLA , 2-5



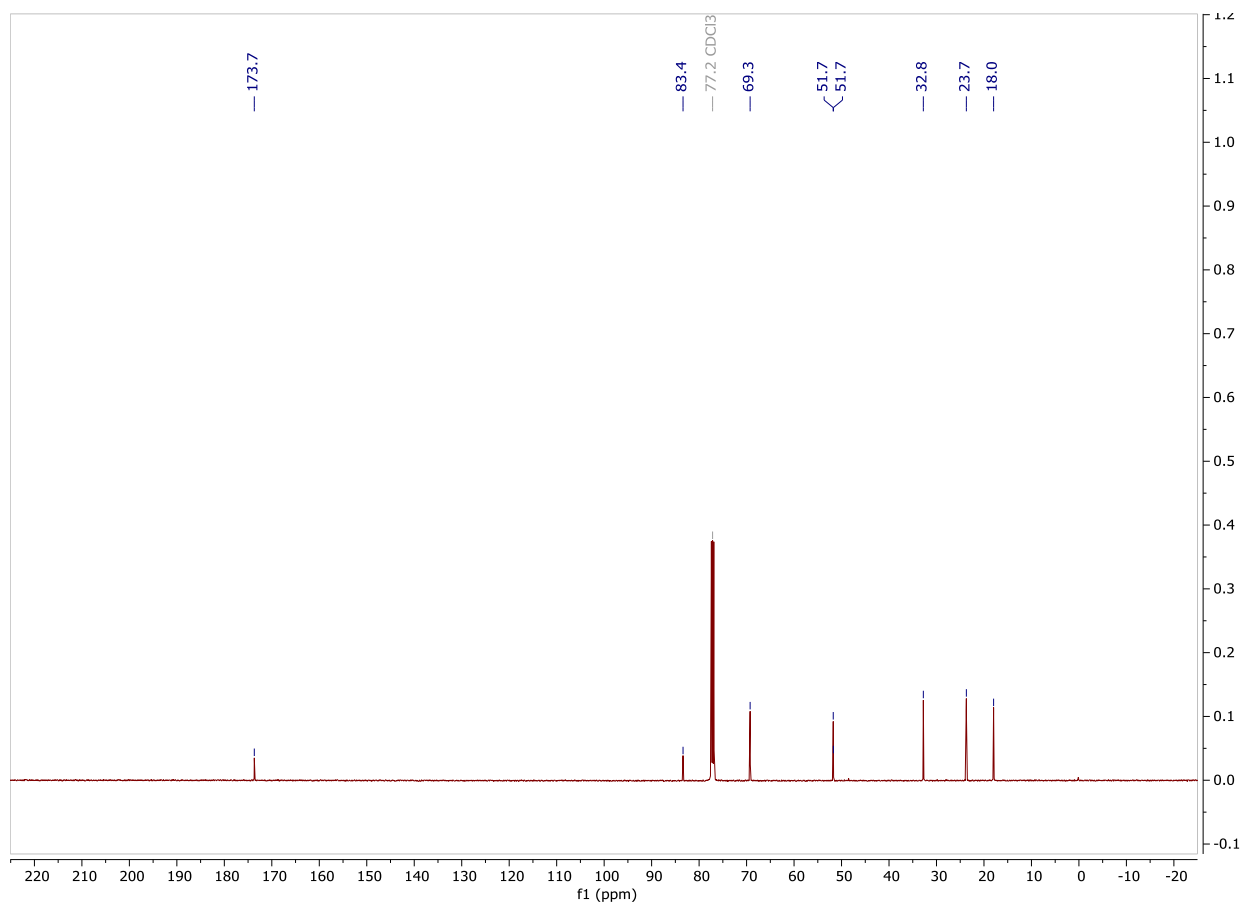
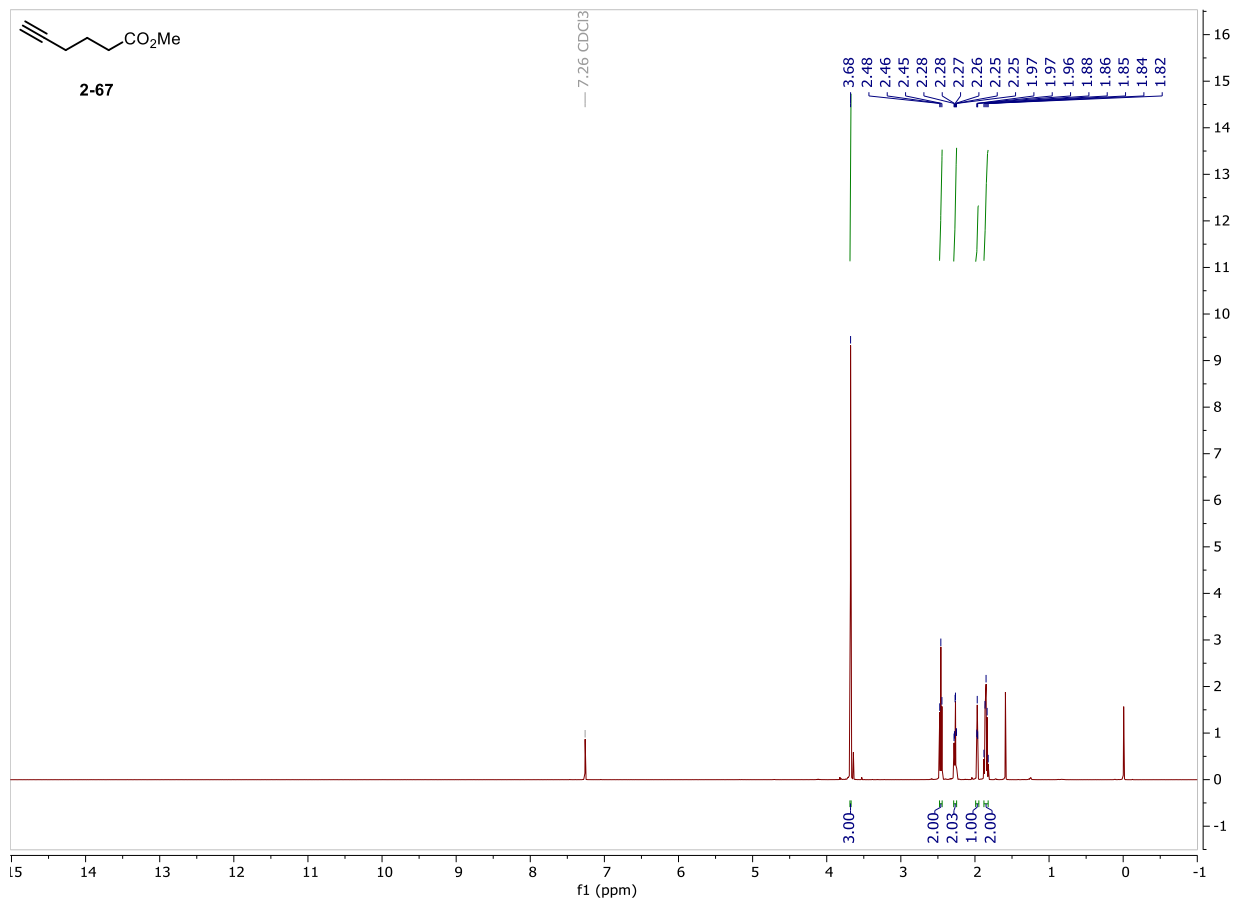
NMR and HPLC

Copy of ^1H and $^{13}\text{C}\{^1\text{H}\}$ spectra of 2-72



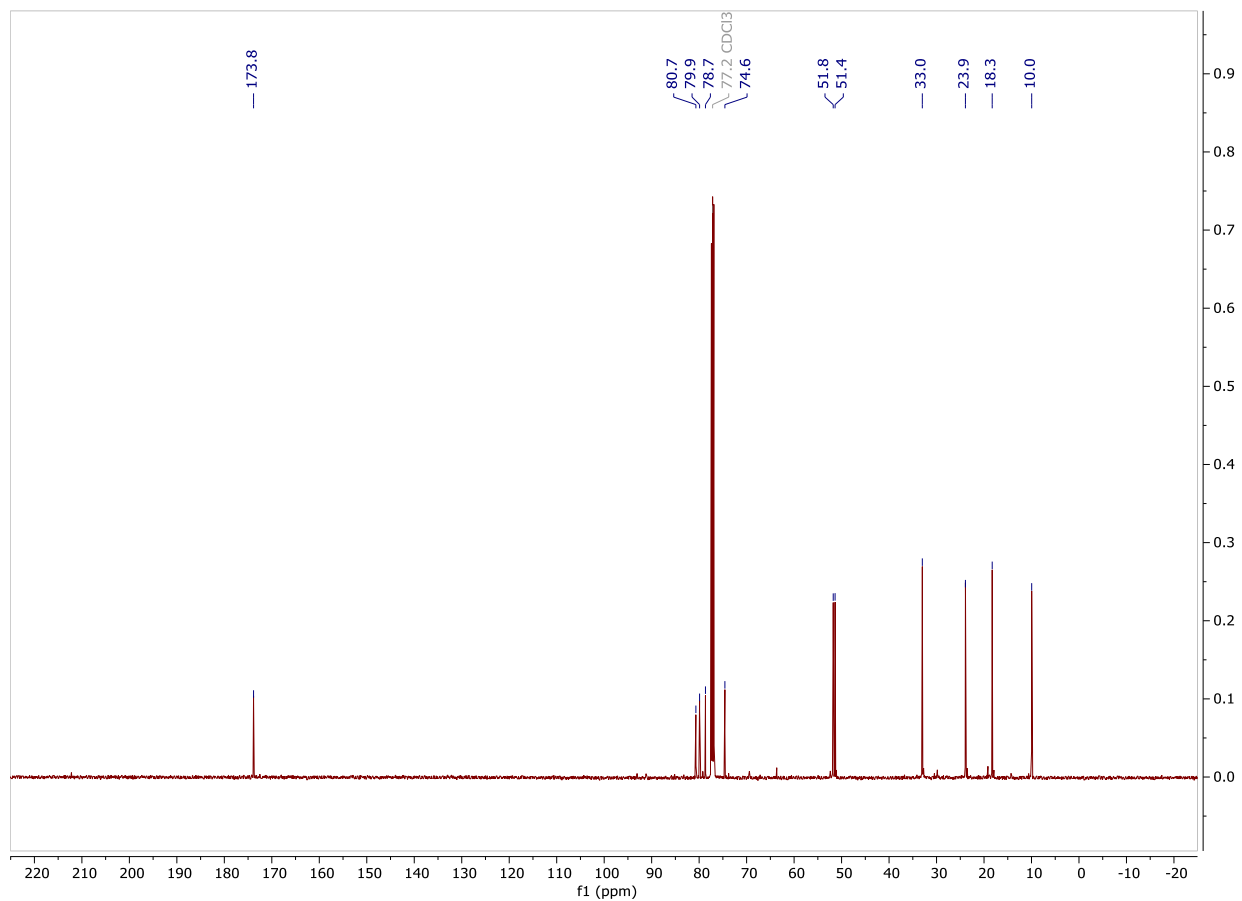
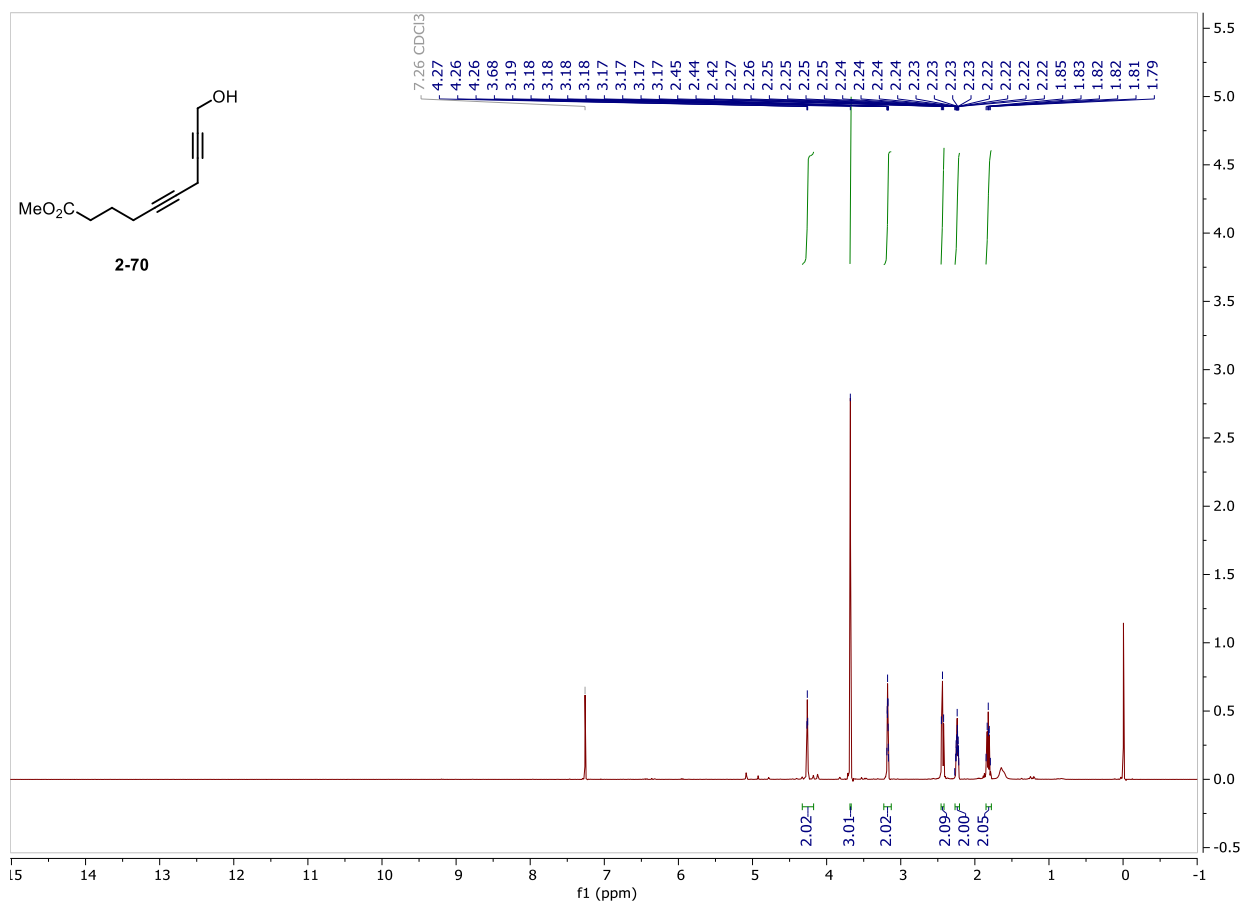
NMR and HPLC

Copy of ^1H and $^{13}\text{C}\{^1\text{H}\}$ spectra of 2-67



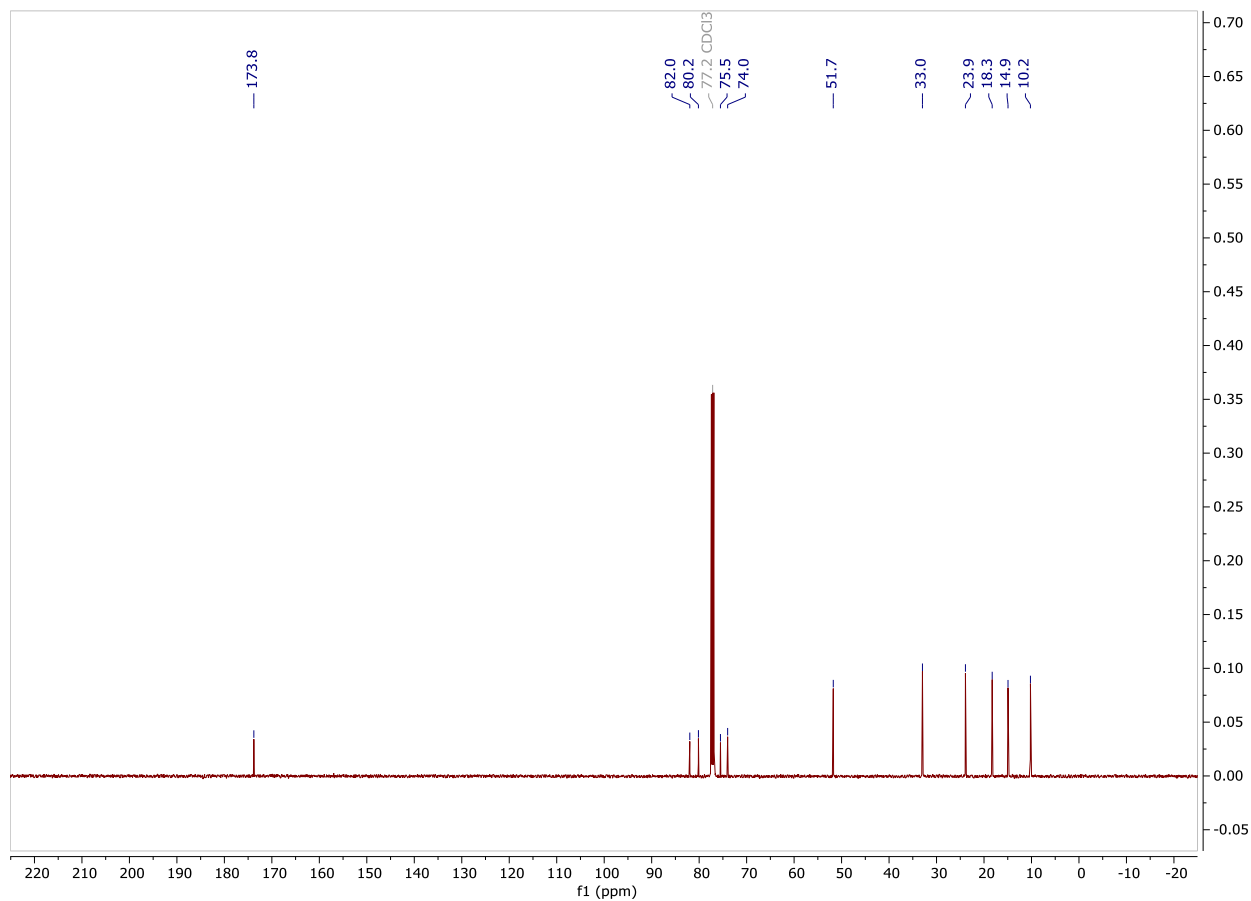
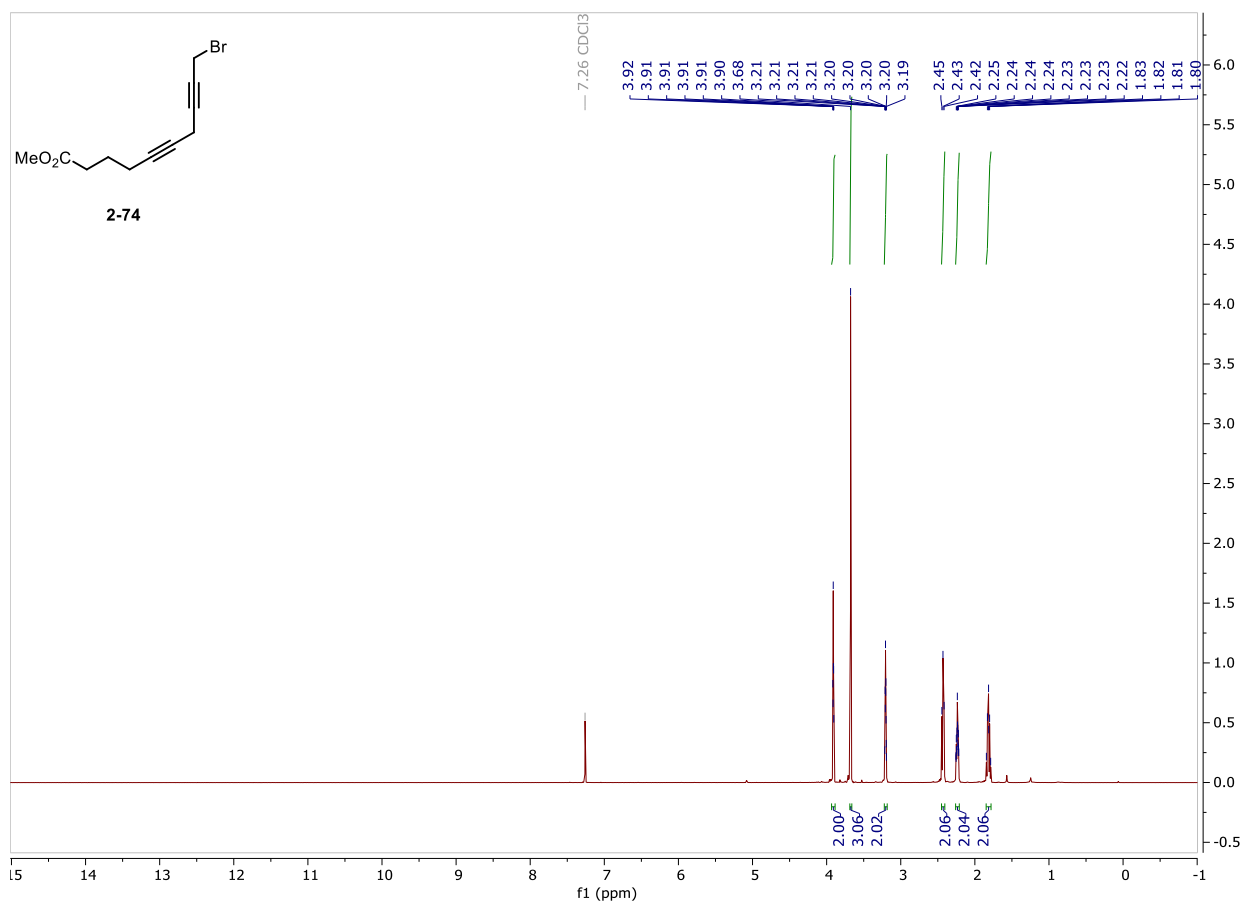
NMR and HPLC

Copy of ^1H and $^{13}\text{C}\{^1\text{H}\}$ spectra of 2-70



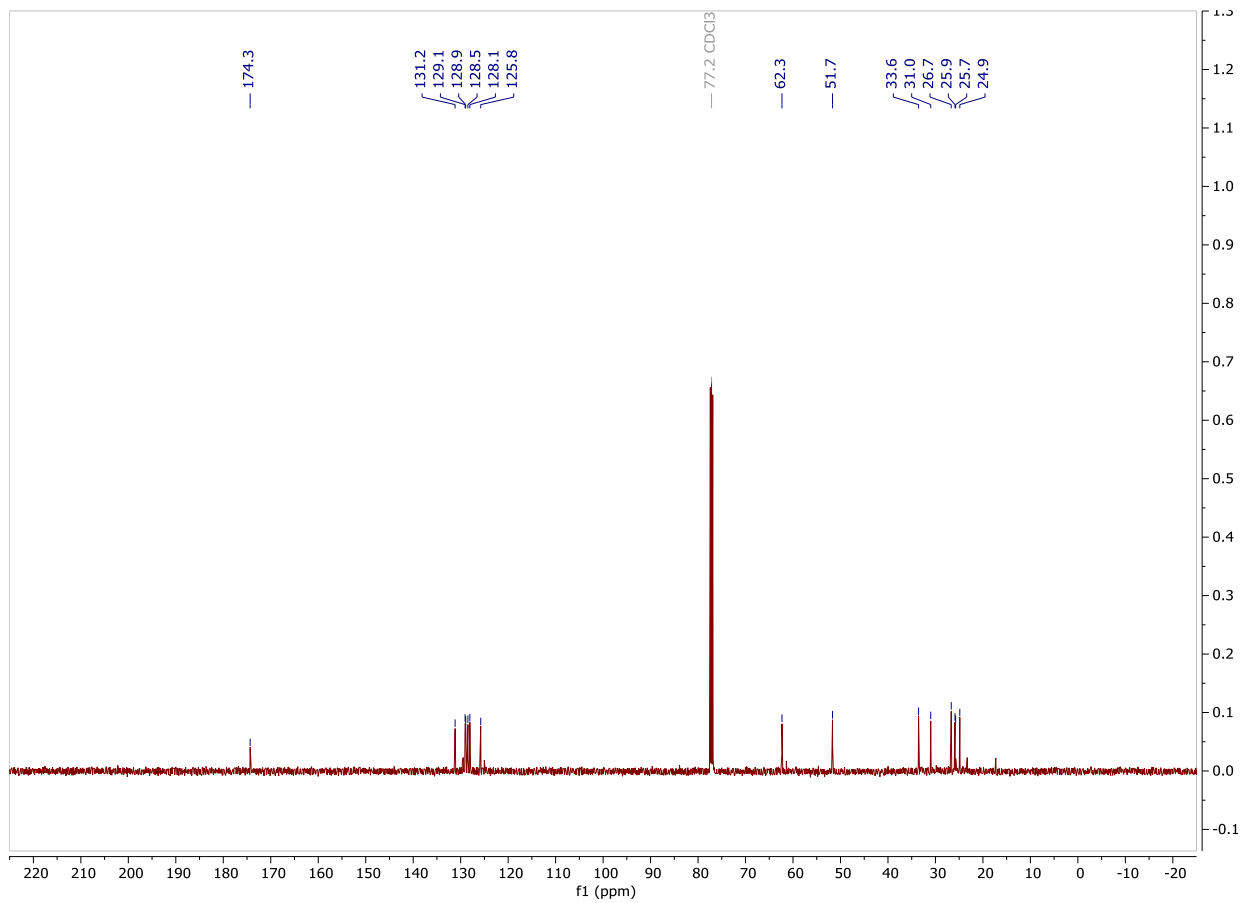
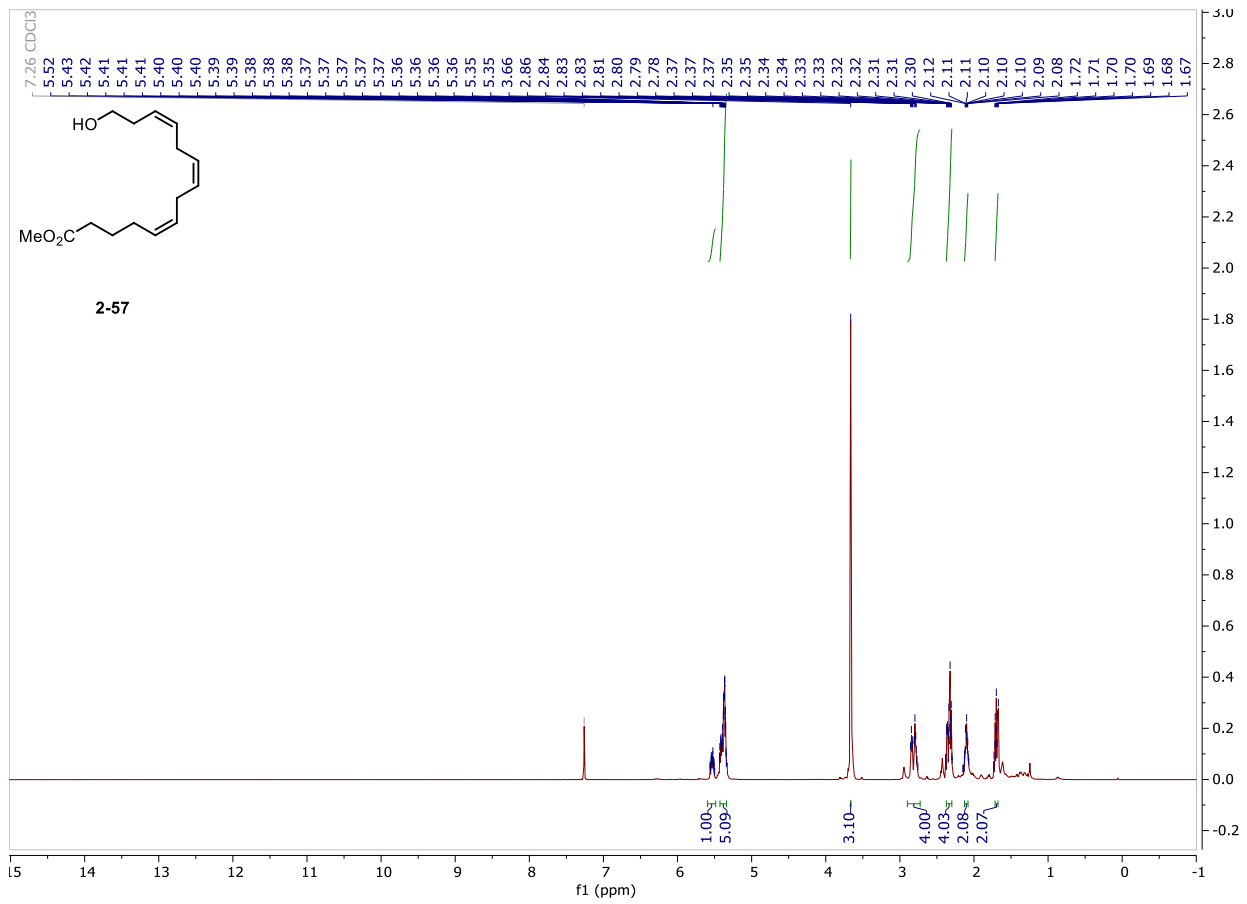
NMR and HPLC

Copy of ^1H and $^{13}\text{C}\{^1\text{H}\}$ spectra of 2-74



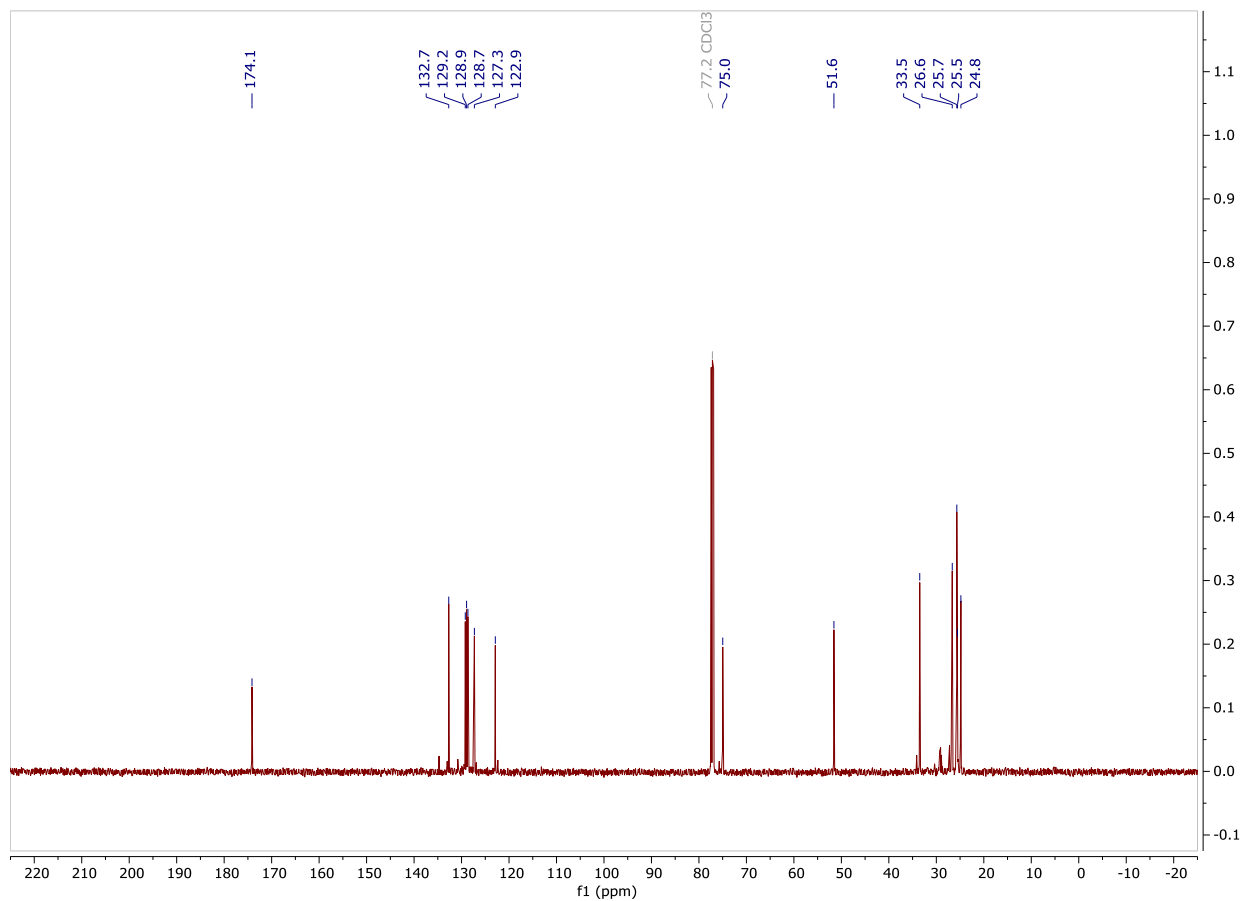
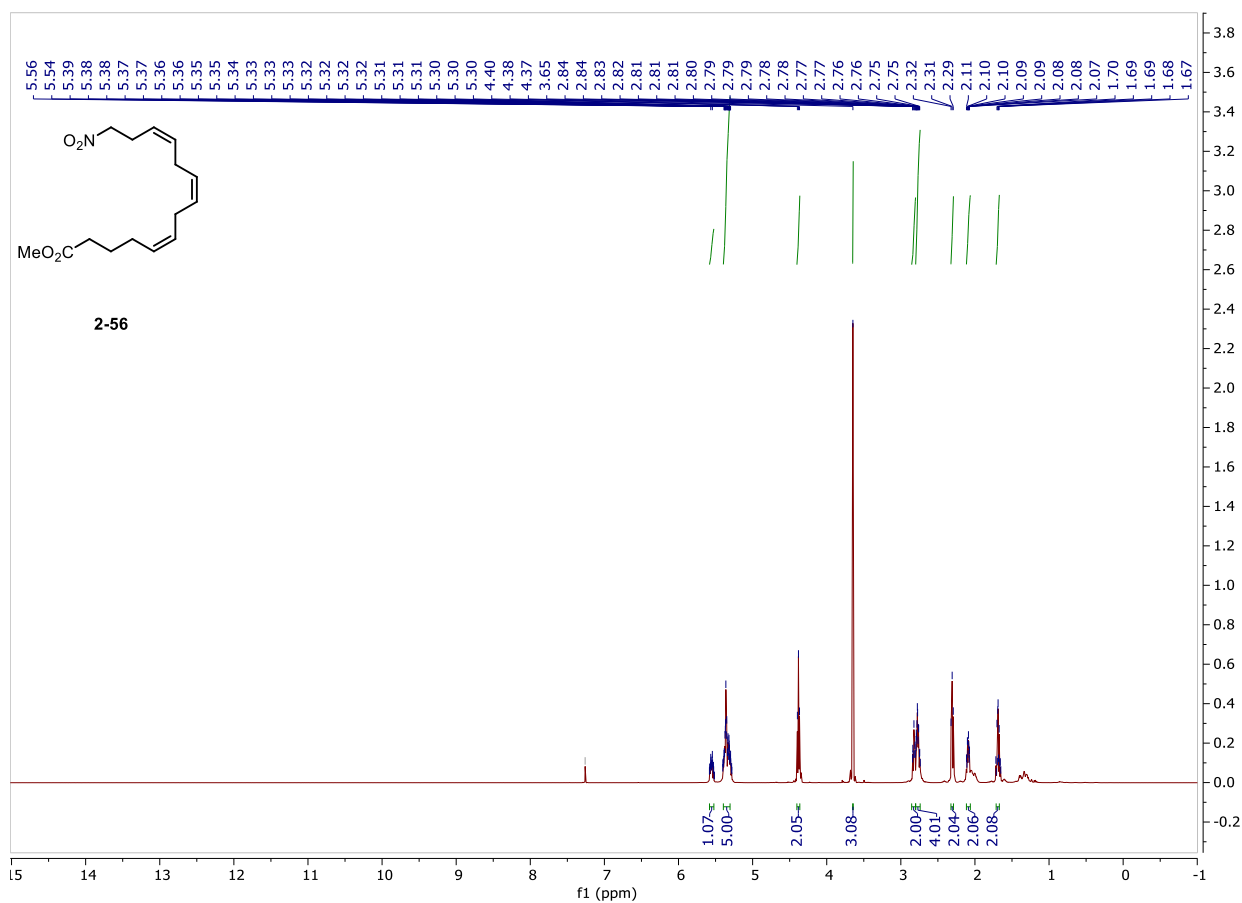
NMR and HPLC

Copy of ^1H and $^{13}\text{C}\{^1\text{H}\}$ spectra of 2-57



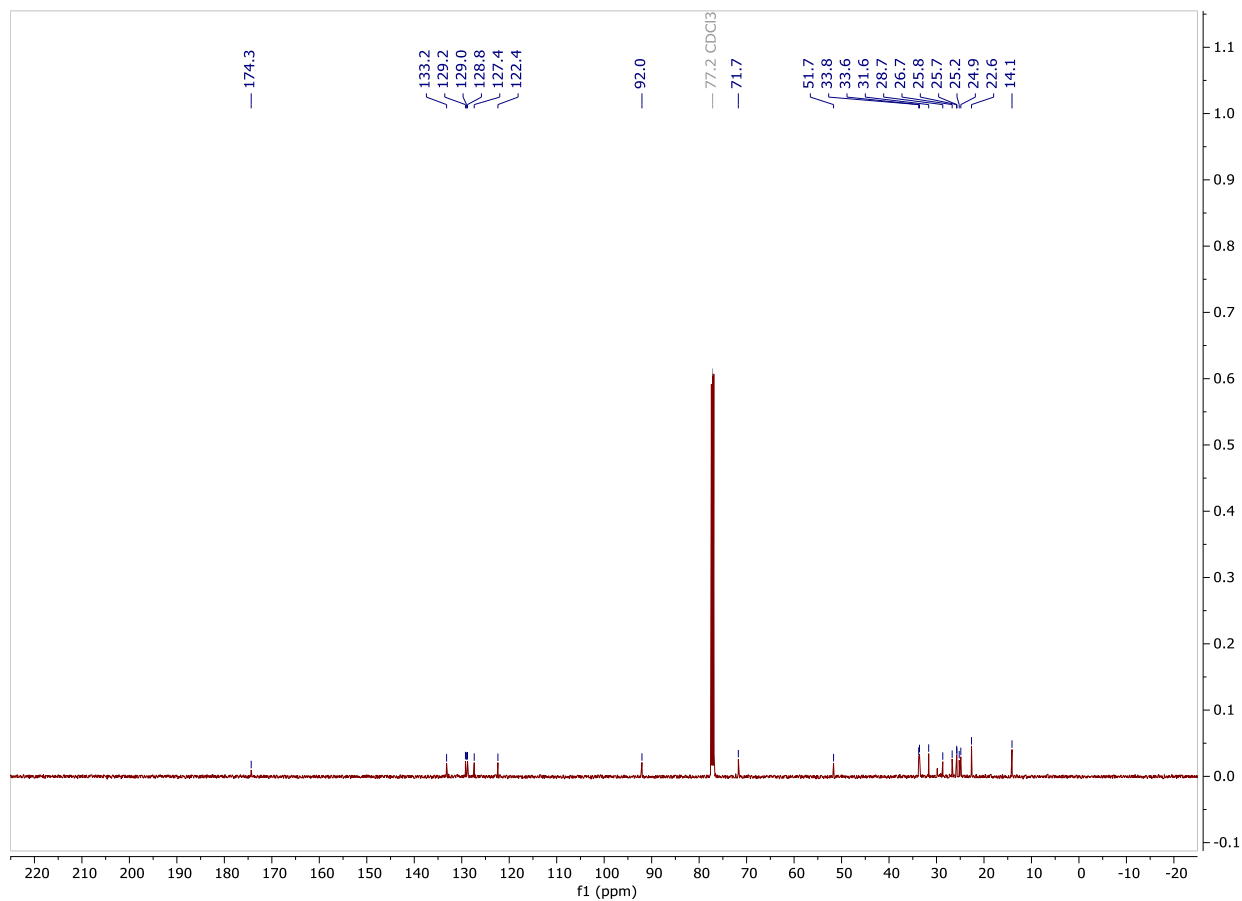
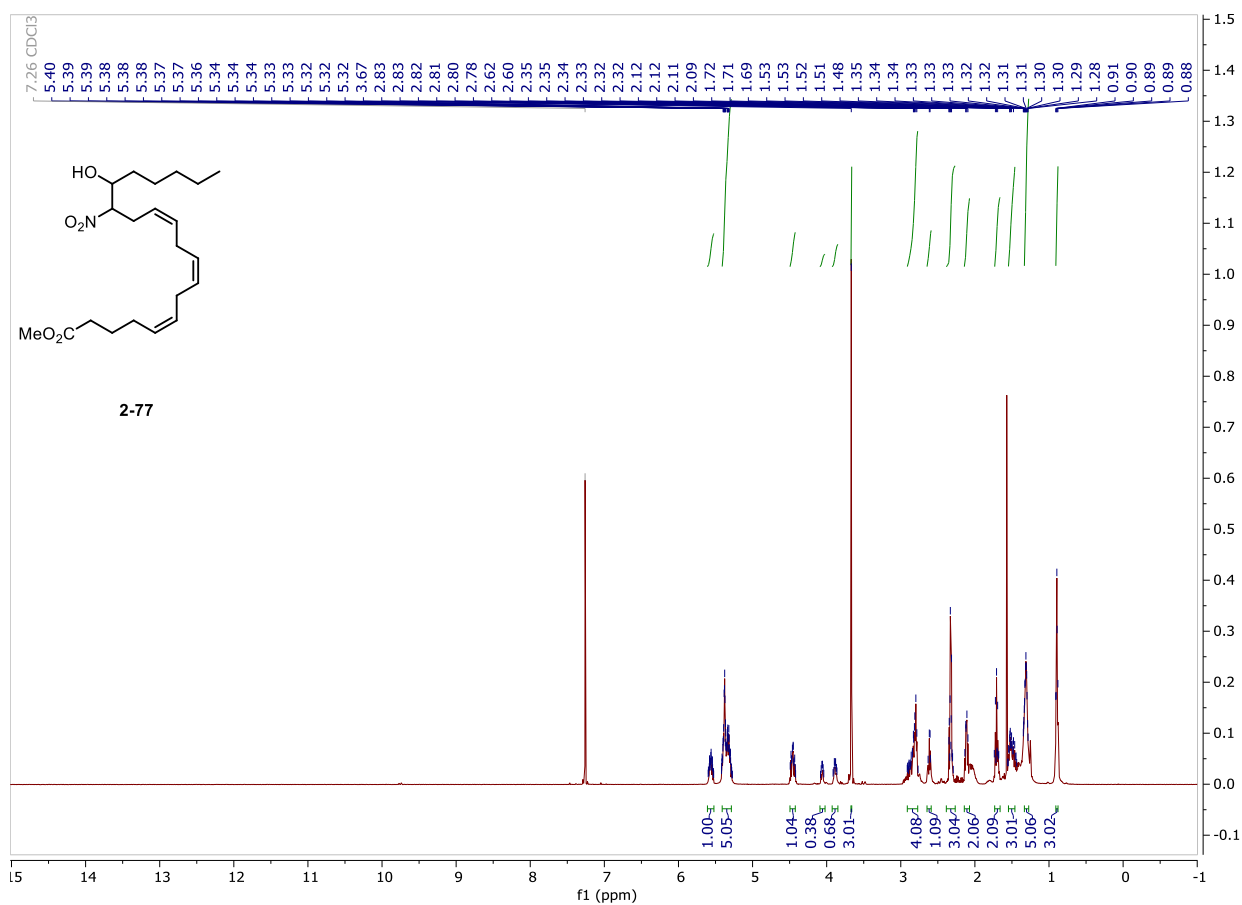
NMR and HPLC

Copy of ^1H and $^{13}\text{C}\{^1\text{H}\}$ spectra of 2-56



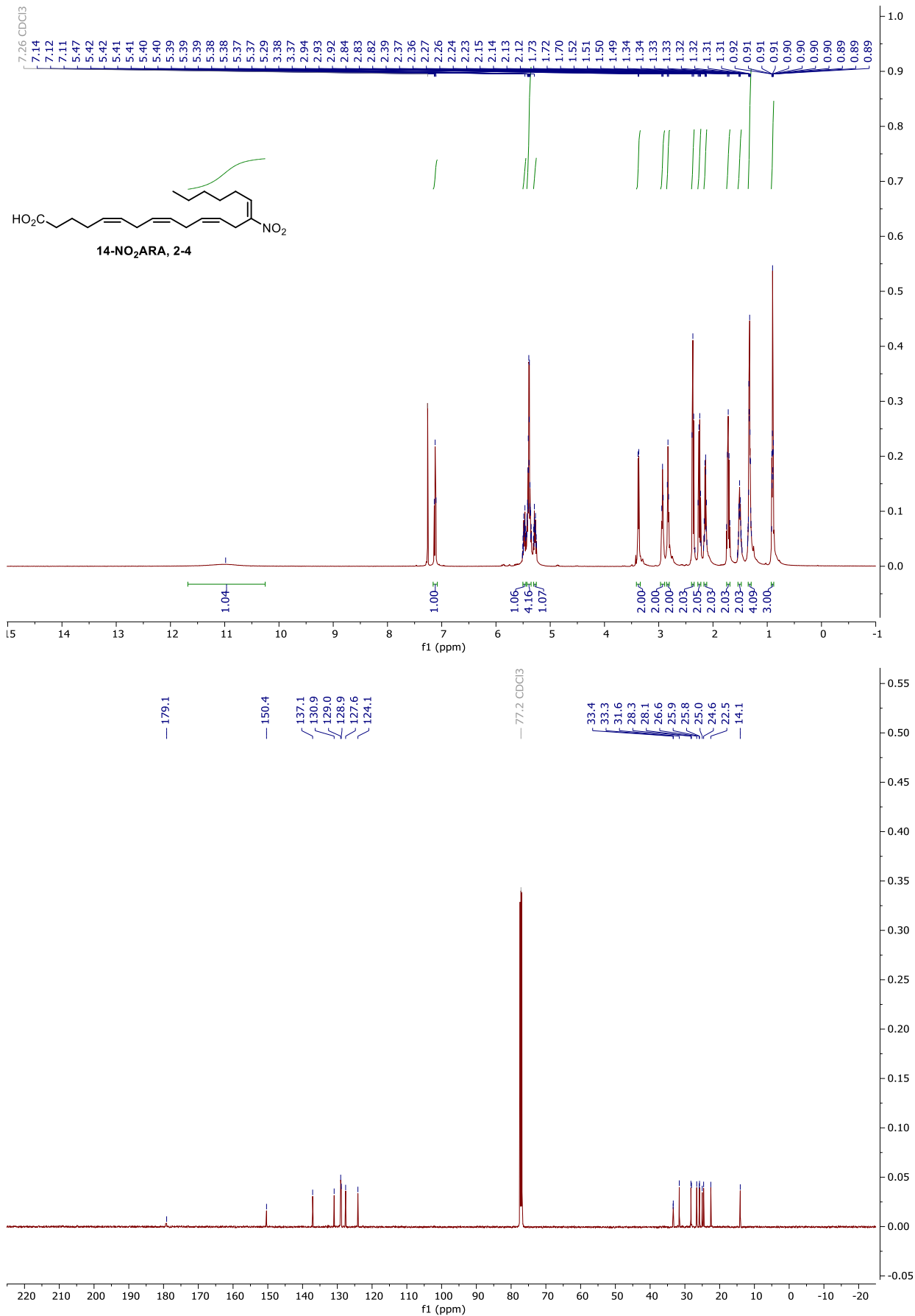
NMR and HPLC

Copy of ^1H and $^{13}\text{C}\{^1\text{H}\}$ spectra of 2-77



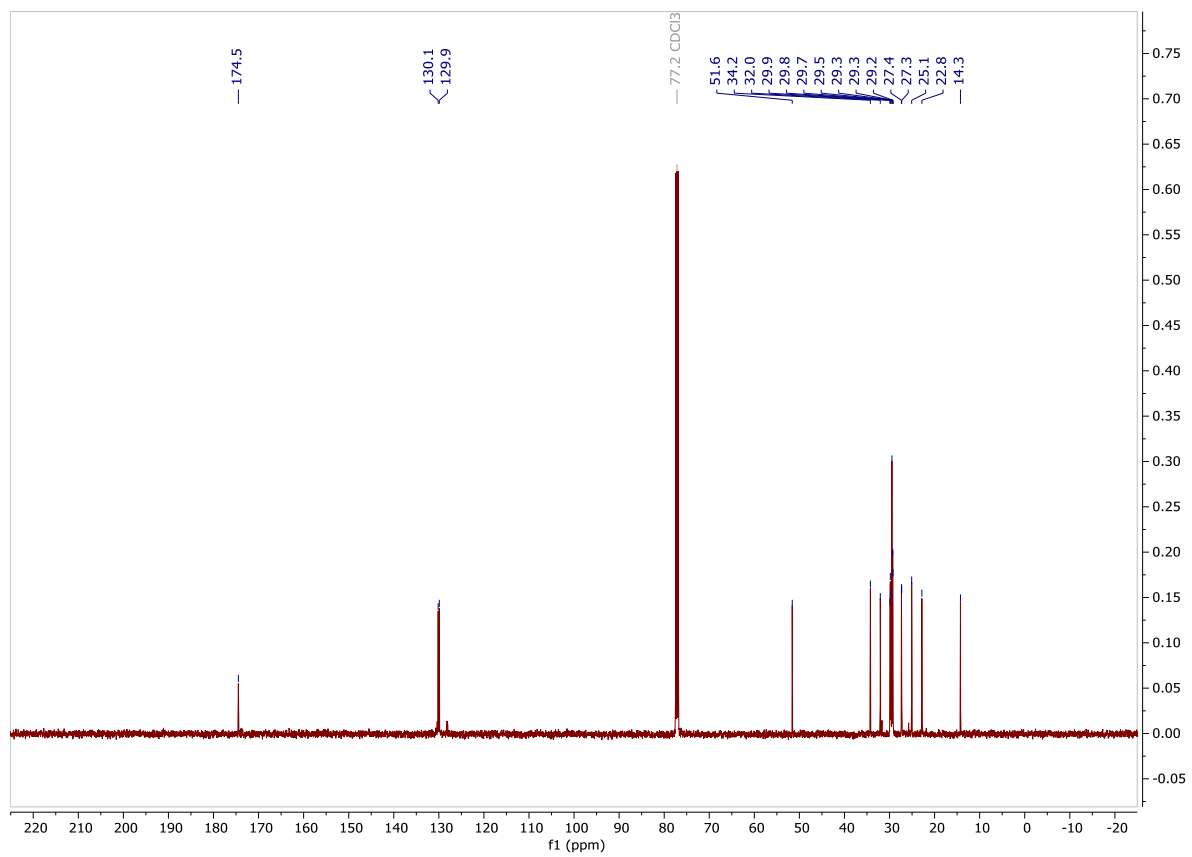
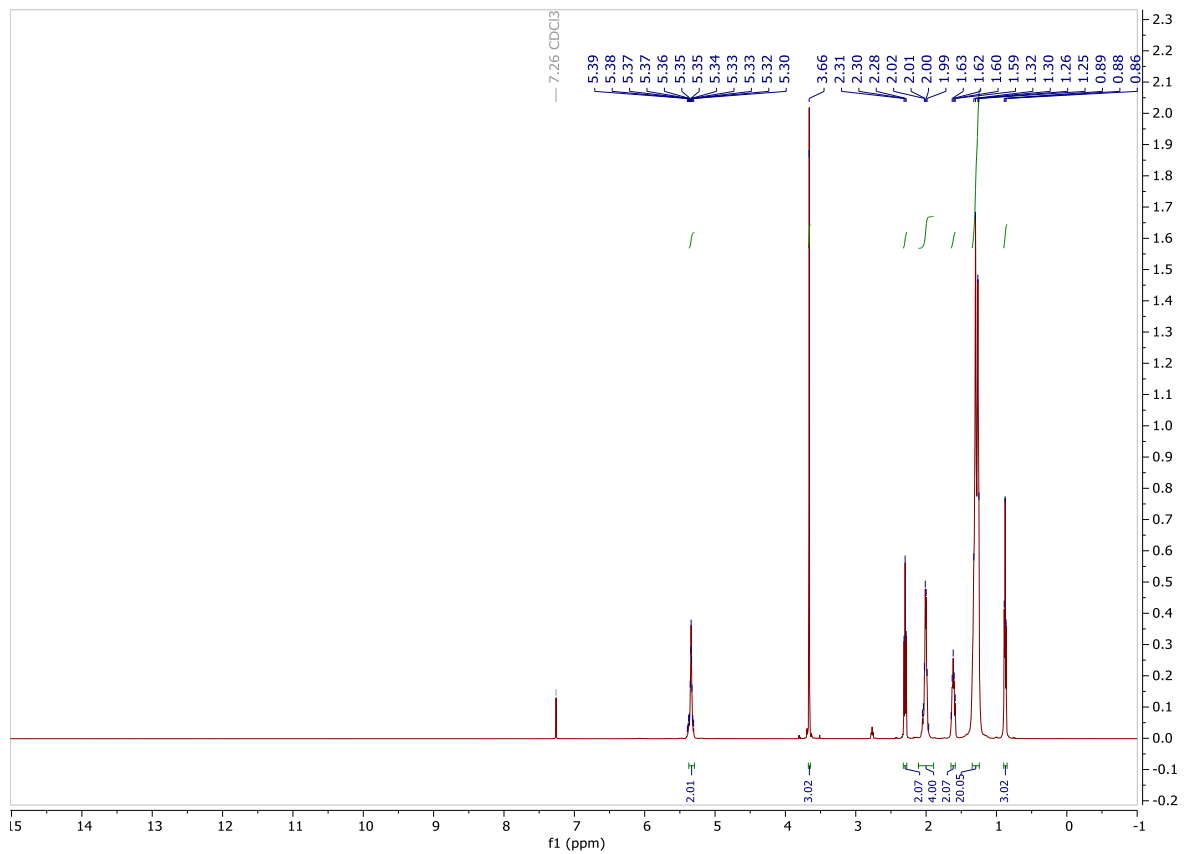
NMR and HPLC

Copy of ^1H and $^{13}\text{C}\{^1\text{H}\}$ spectra of 14- NO_2ARA , 2-4



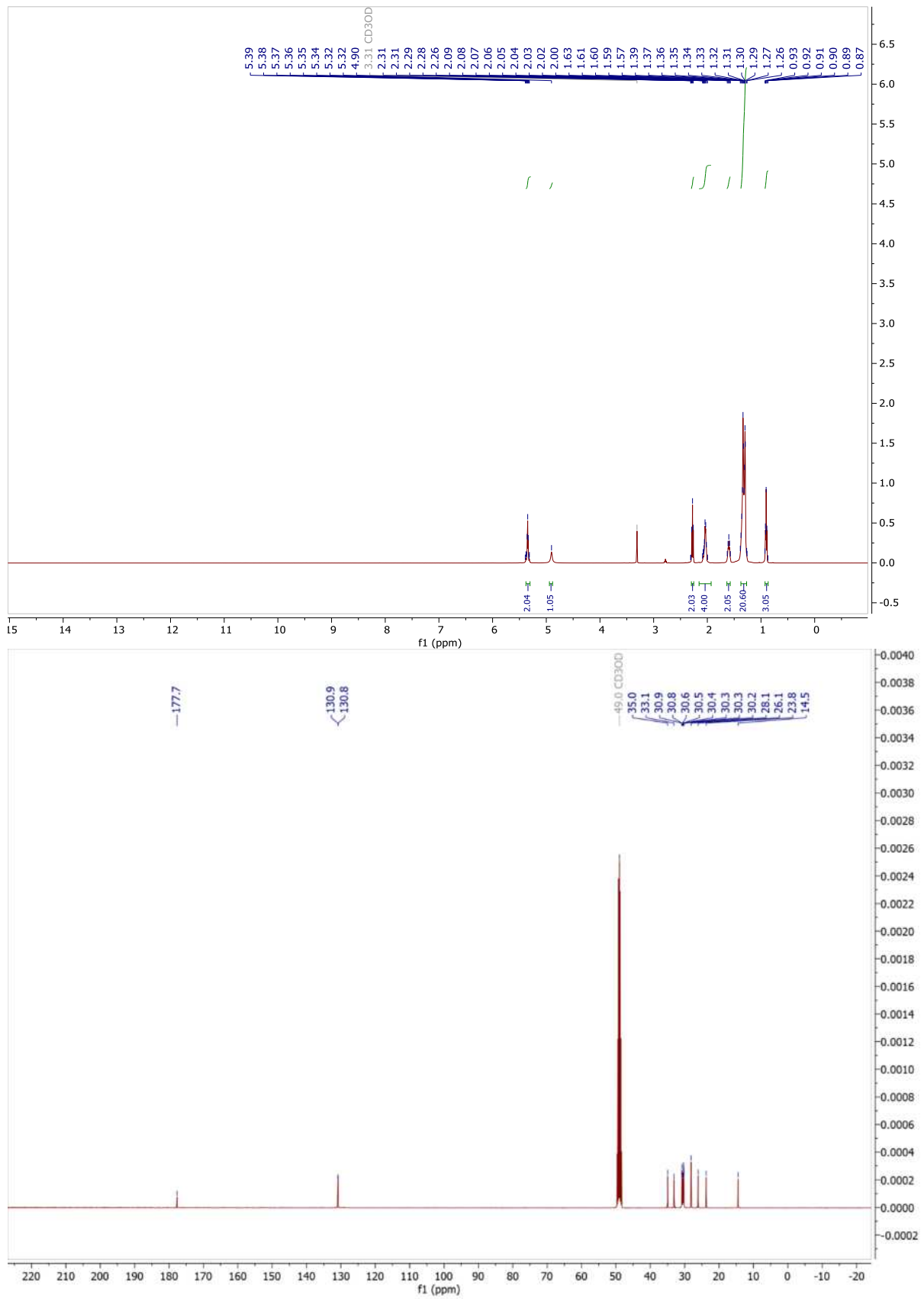
NMR and HPLC

Copy of ^1H and $^{13}\text{C}\{^1\text{H}\}$ spectra of 2-90



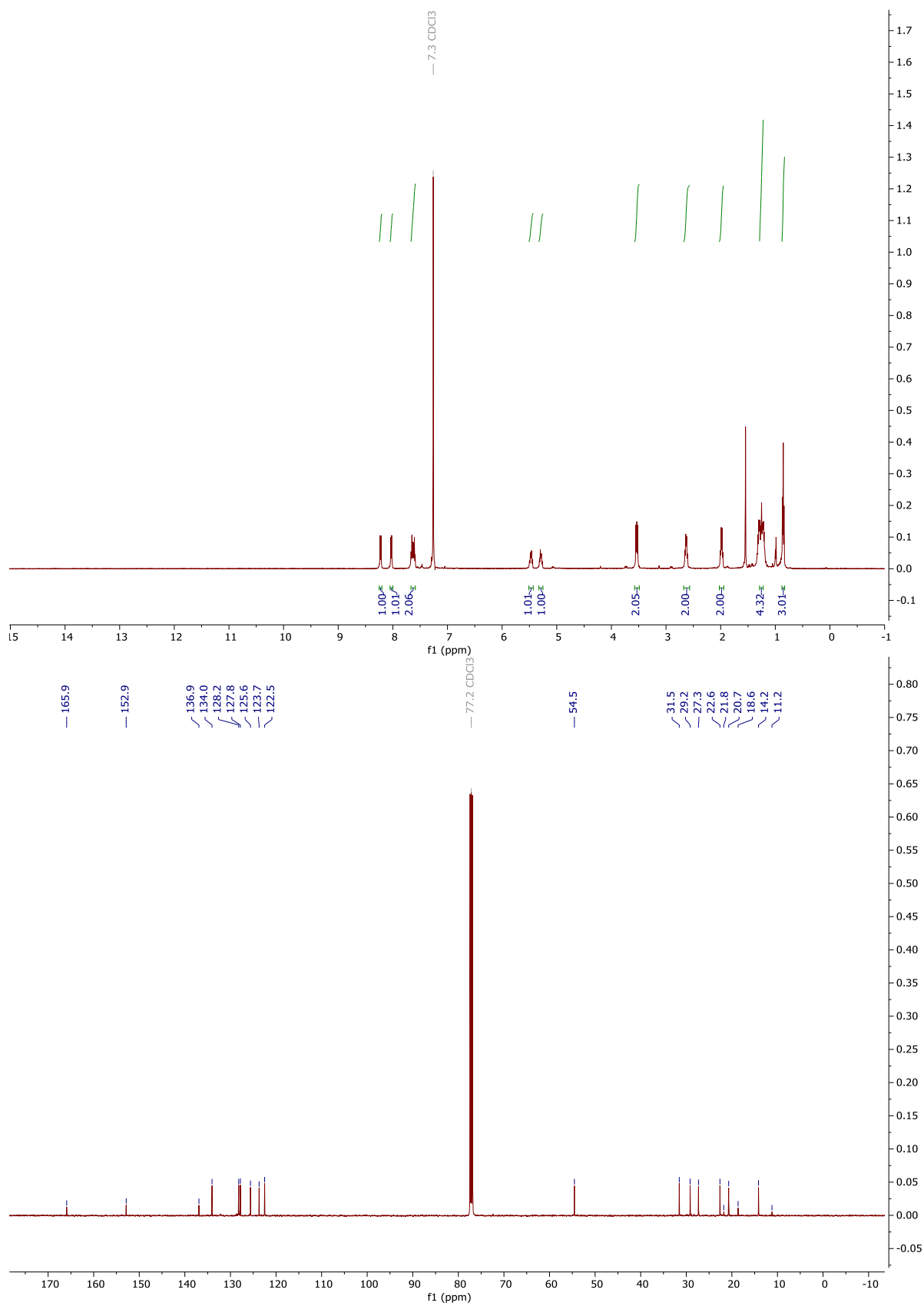
NMR and HPLC

Copy of ^1H and $^{13}\text{C}\{^1\text{H}\}$ spectra of 2-16



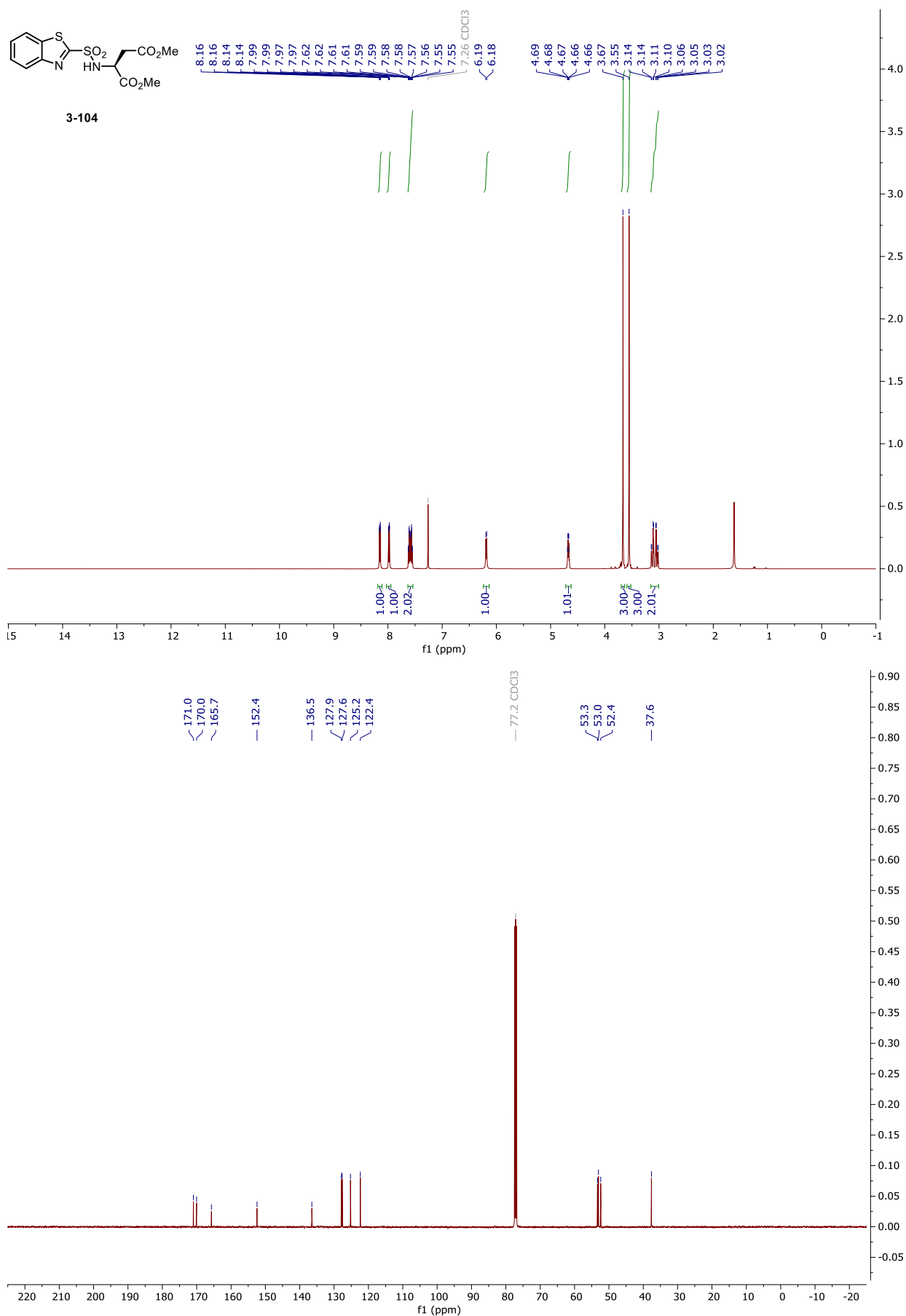
NMR and HPLC

Copy of ^1H and $^{13}\text{C}\{^1\text{H}\}$ spectra of 2-93



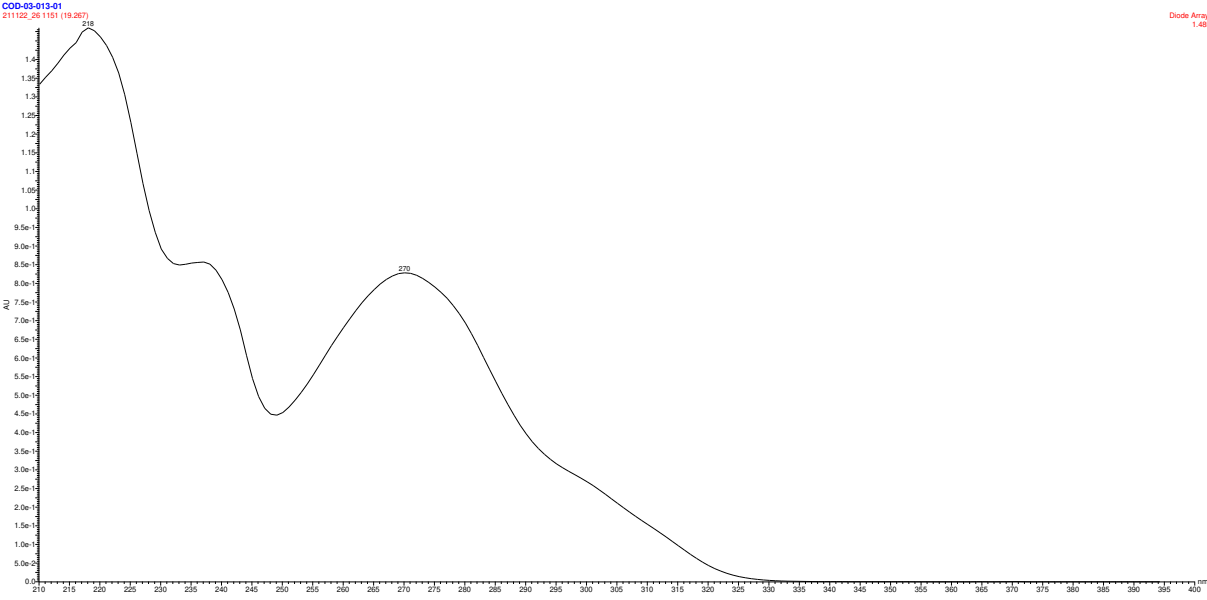
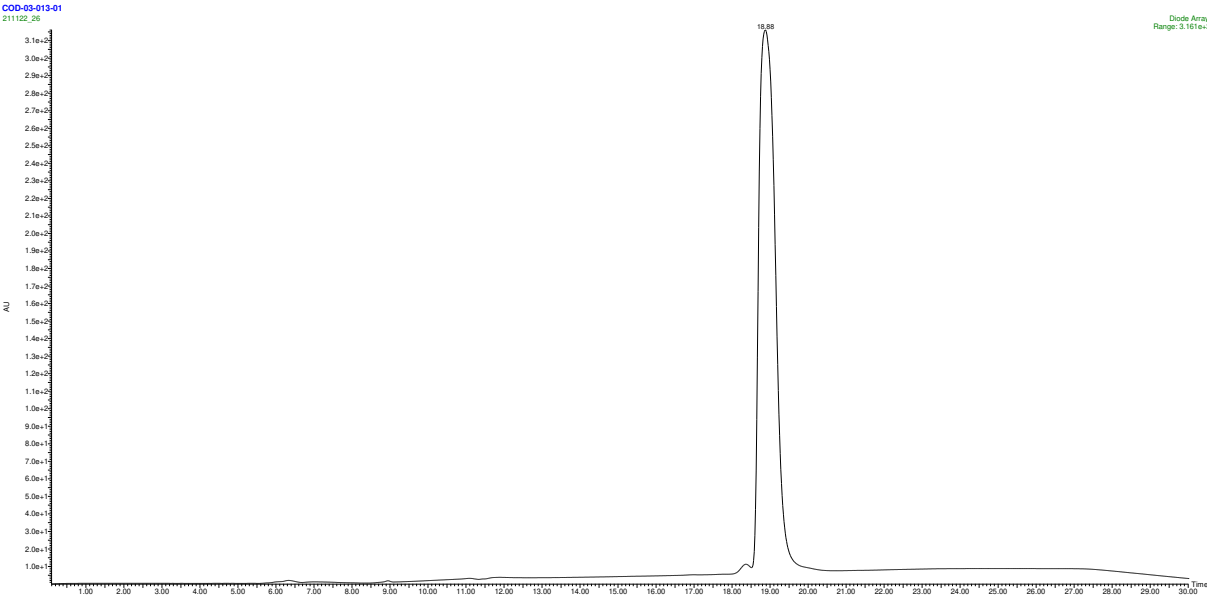
NMR and HPLC

Copy of ^1H , $^{13}\text{C}\{^1\text{H}\}$ spectra of 3-104



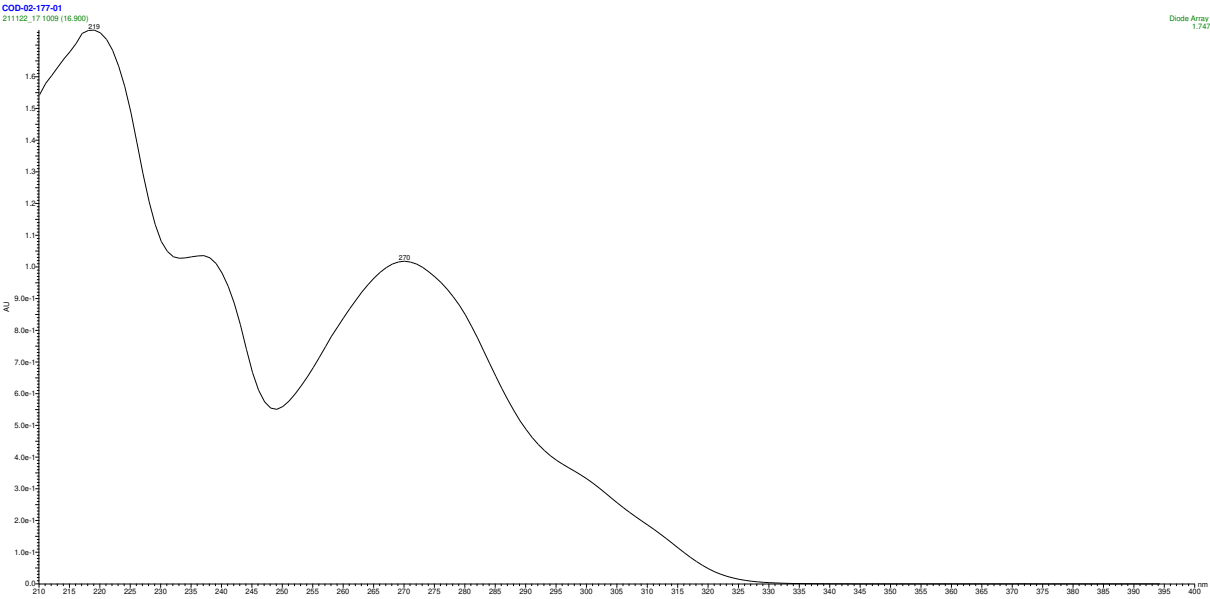
NMR and HPLC

HPLC chromatograms of 3-104



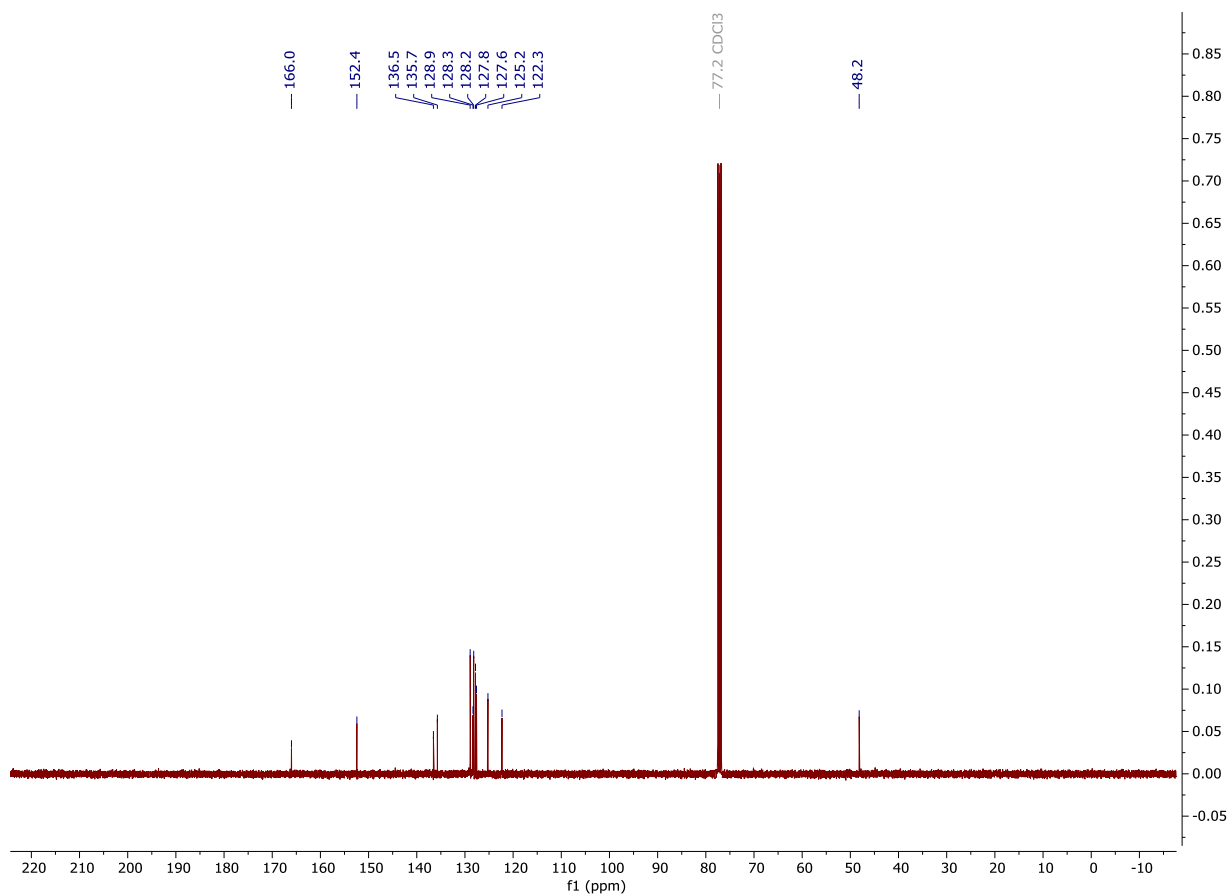
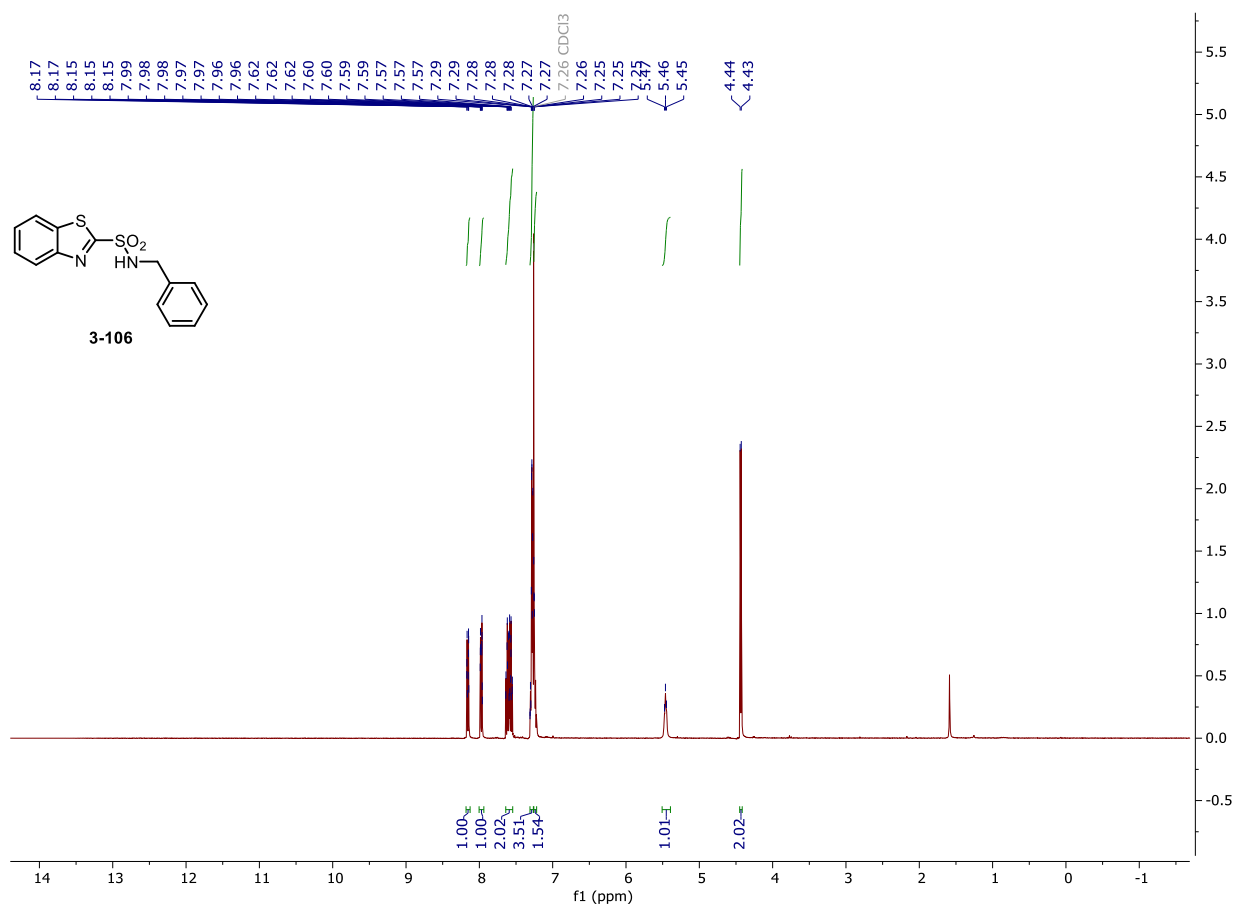
NMR and HPLC

HPLC chromatograms of 3-103



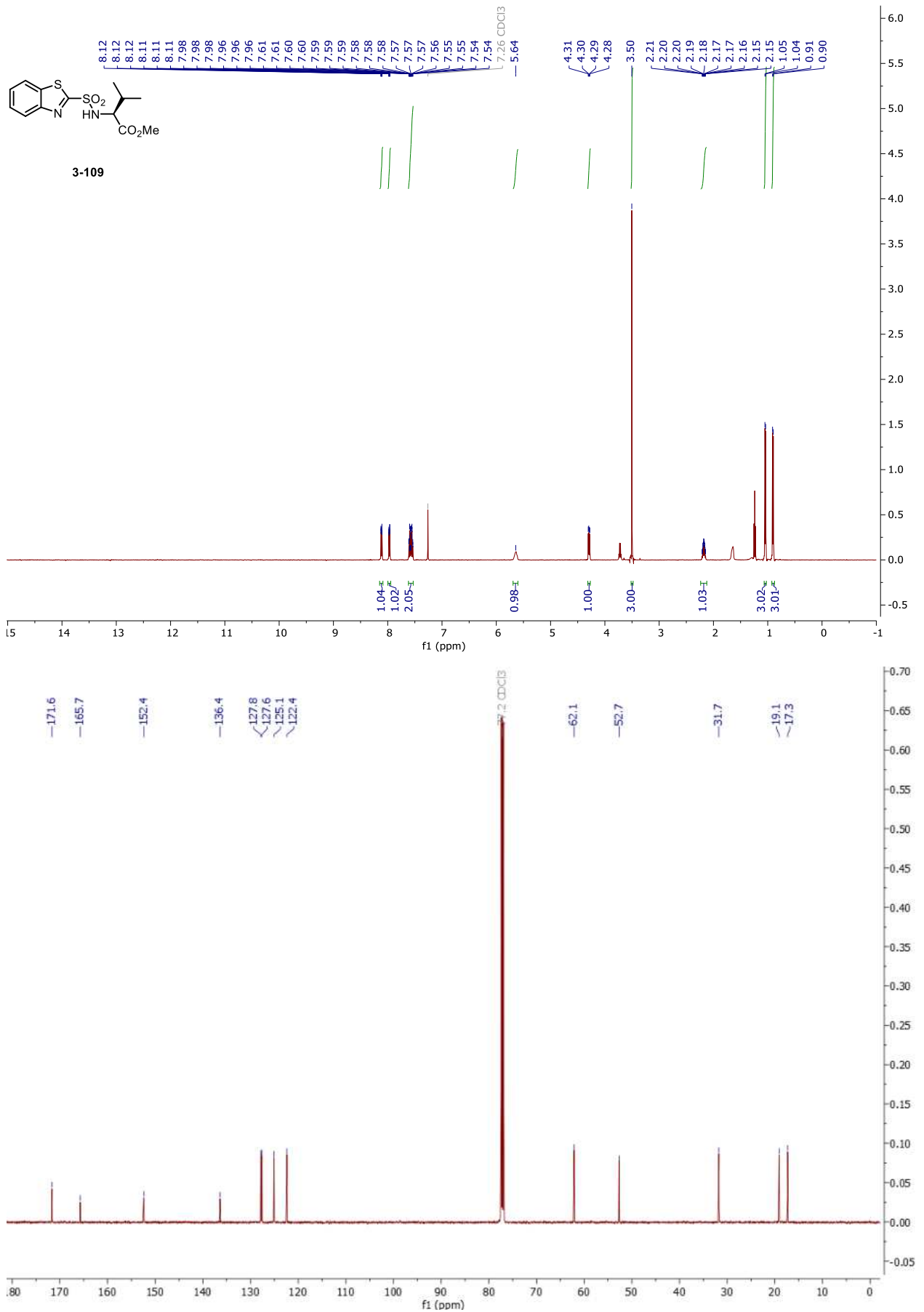
NMR and HPLC

Copy of ^1H , $^{13}\text{C}\{^1\text{H}\}$ spectra of 3-106



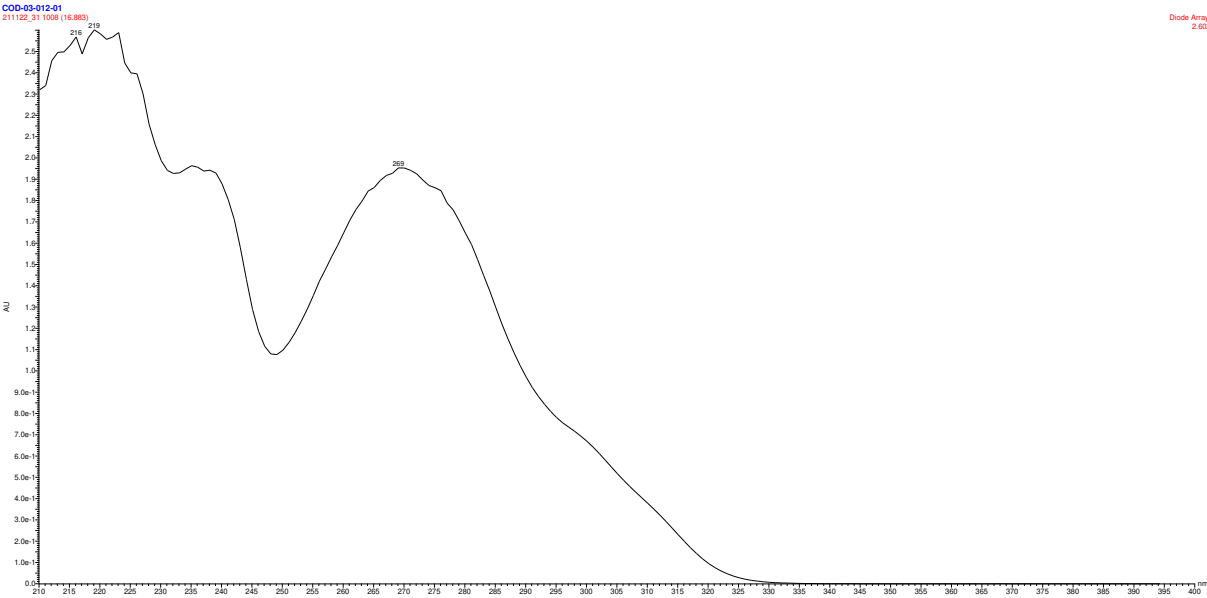
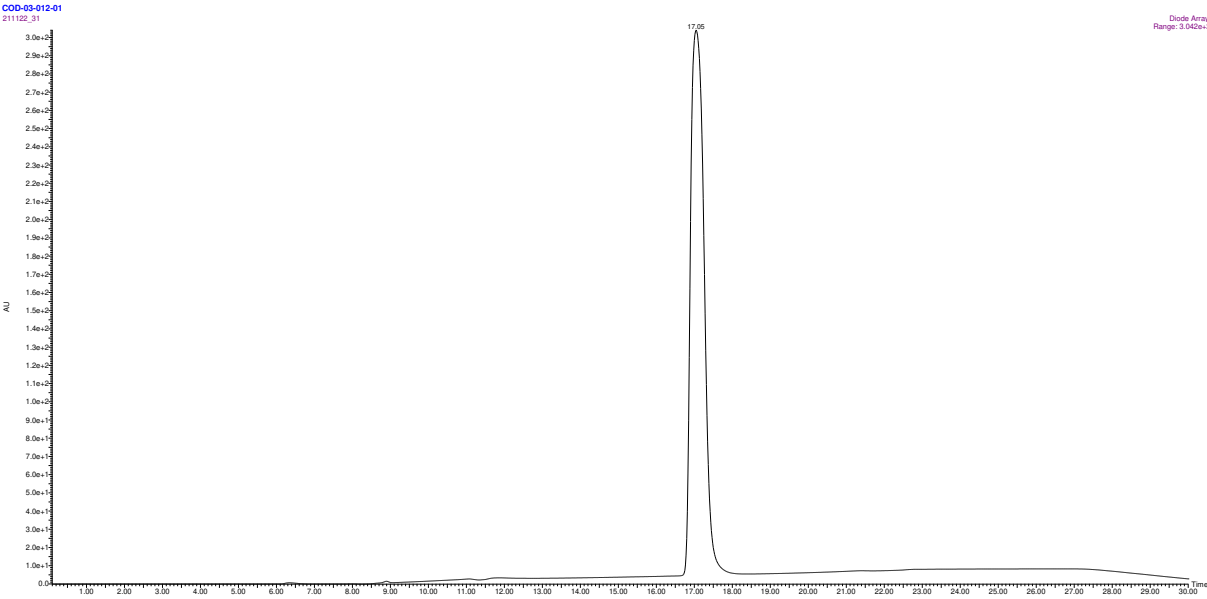
NMR and HPLC

Copy of ^1H , $^{13}\text{C}\{^1\text{H}\}$ spectra of **3-109**



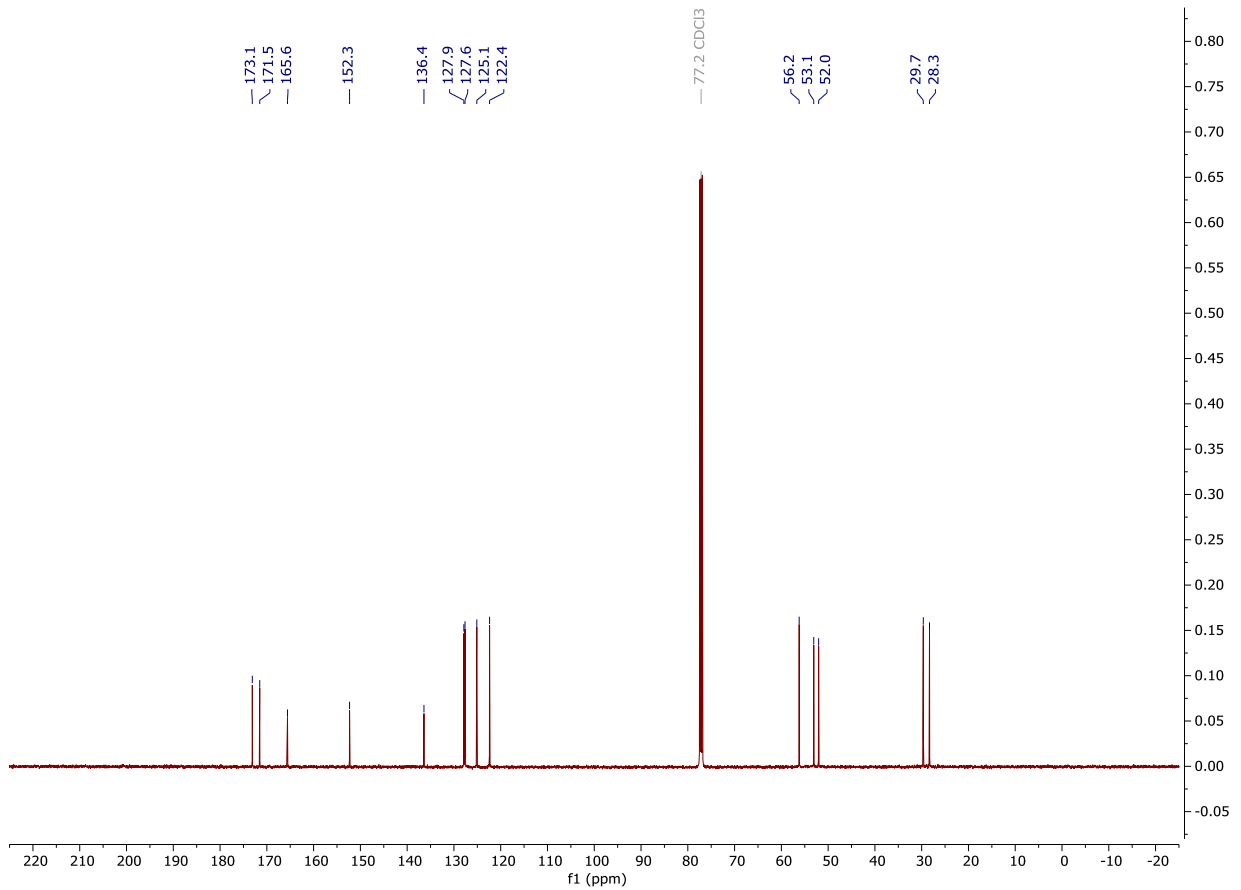
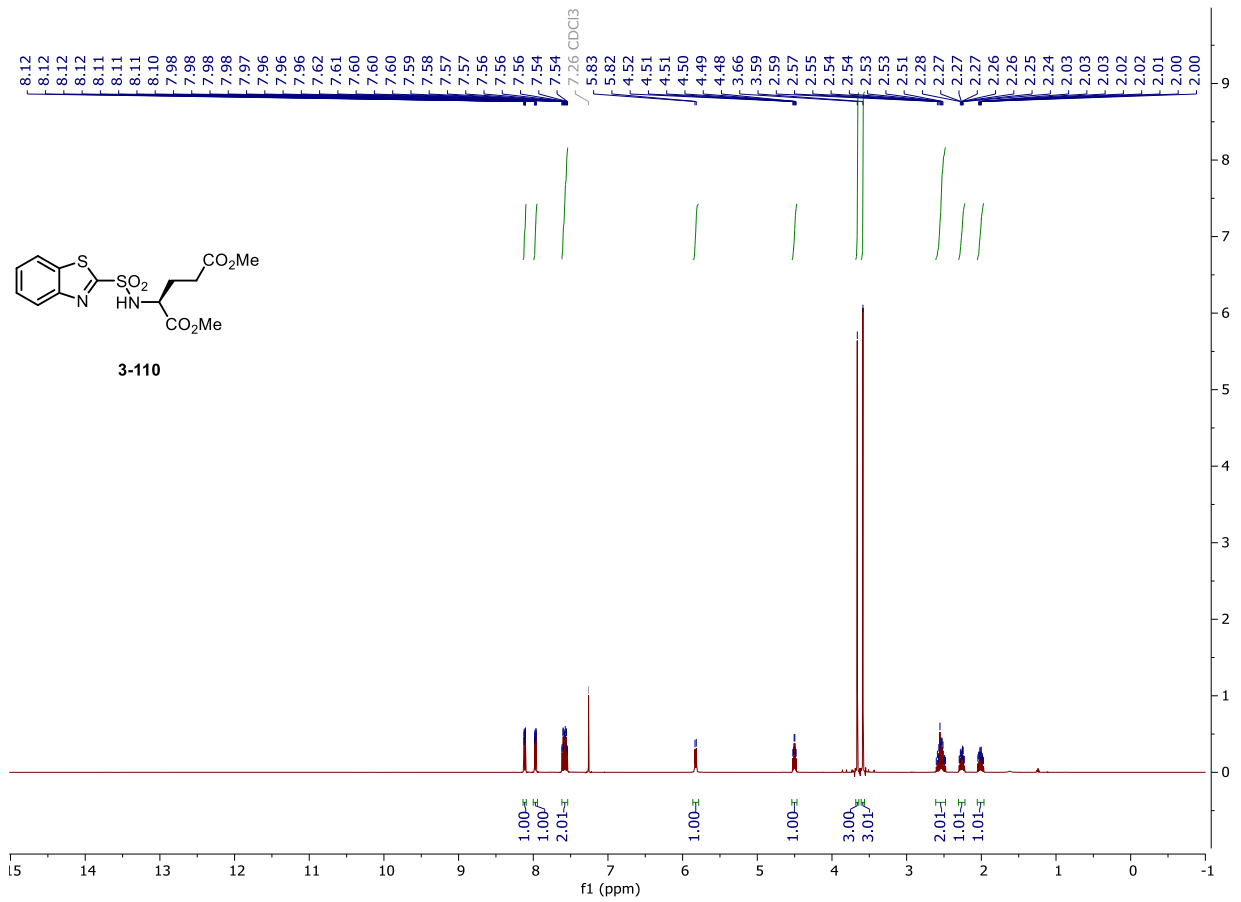
NMR and HPLC

HPLC chromatograms of 3-109



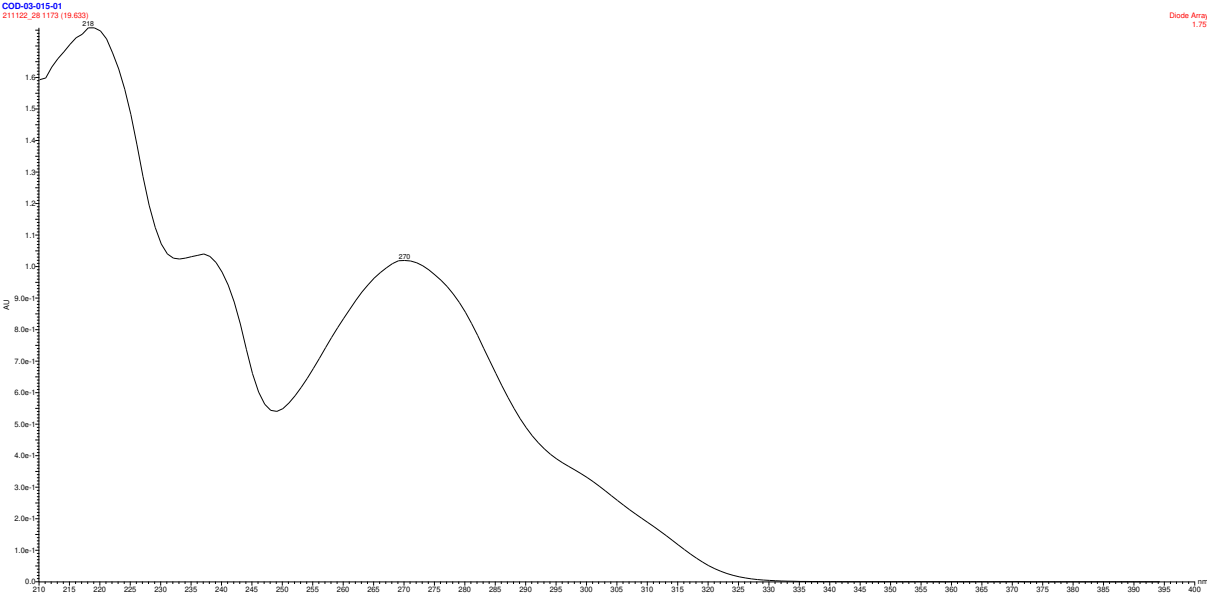
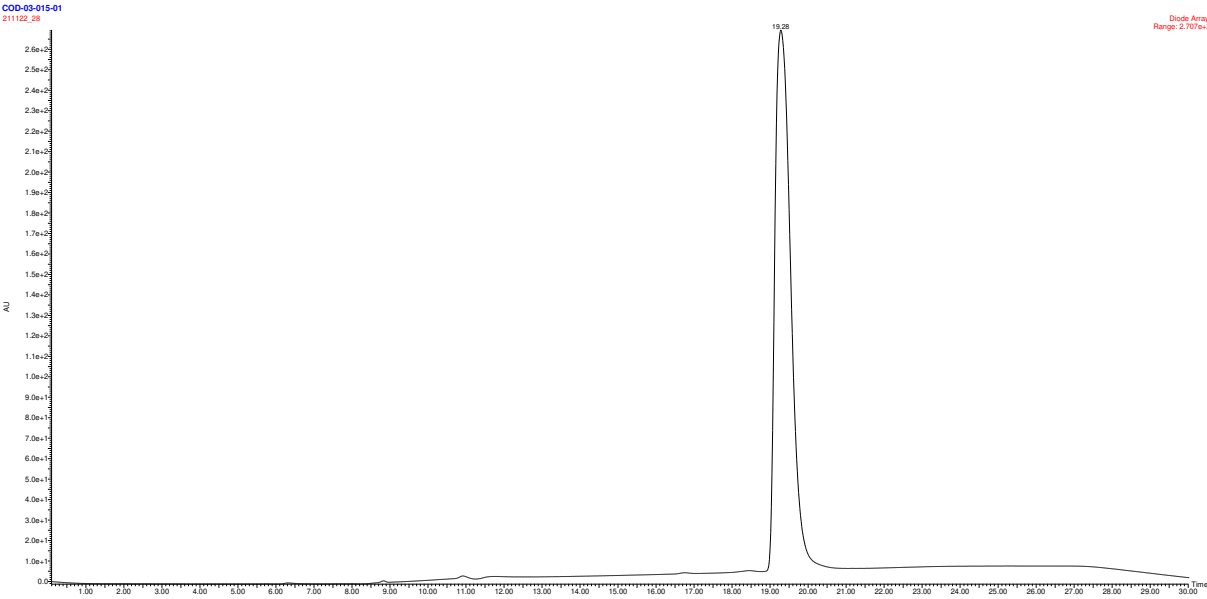
NMR and HPLC

Copy of ^1H , $^{13}\text{C}\{^1\text{H}\}$ spectra of 3-110



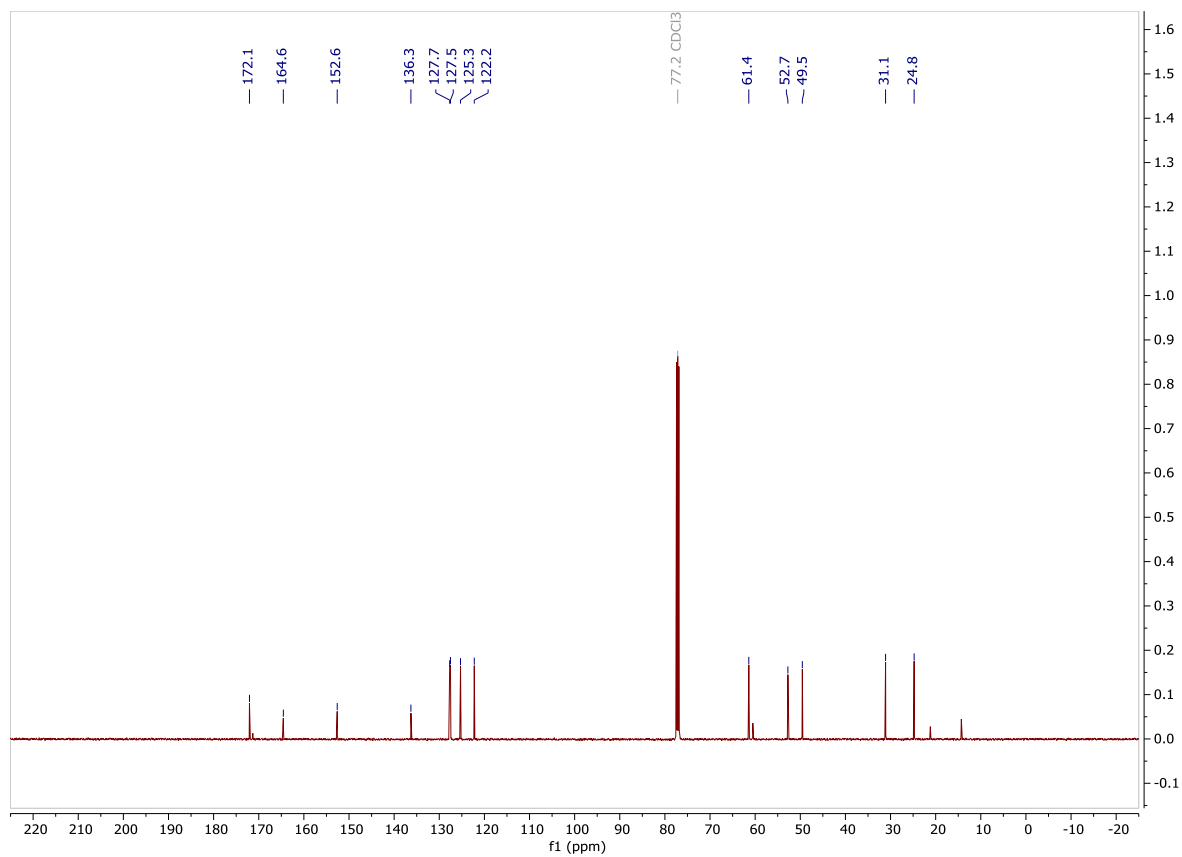
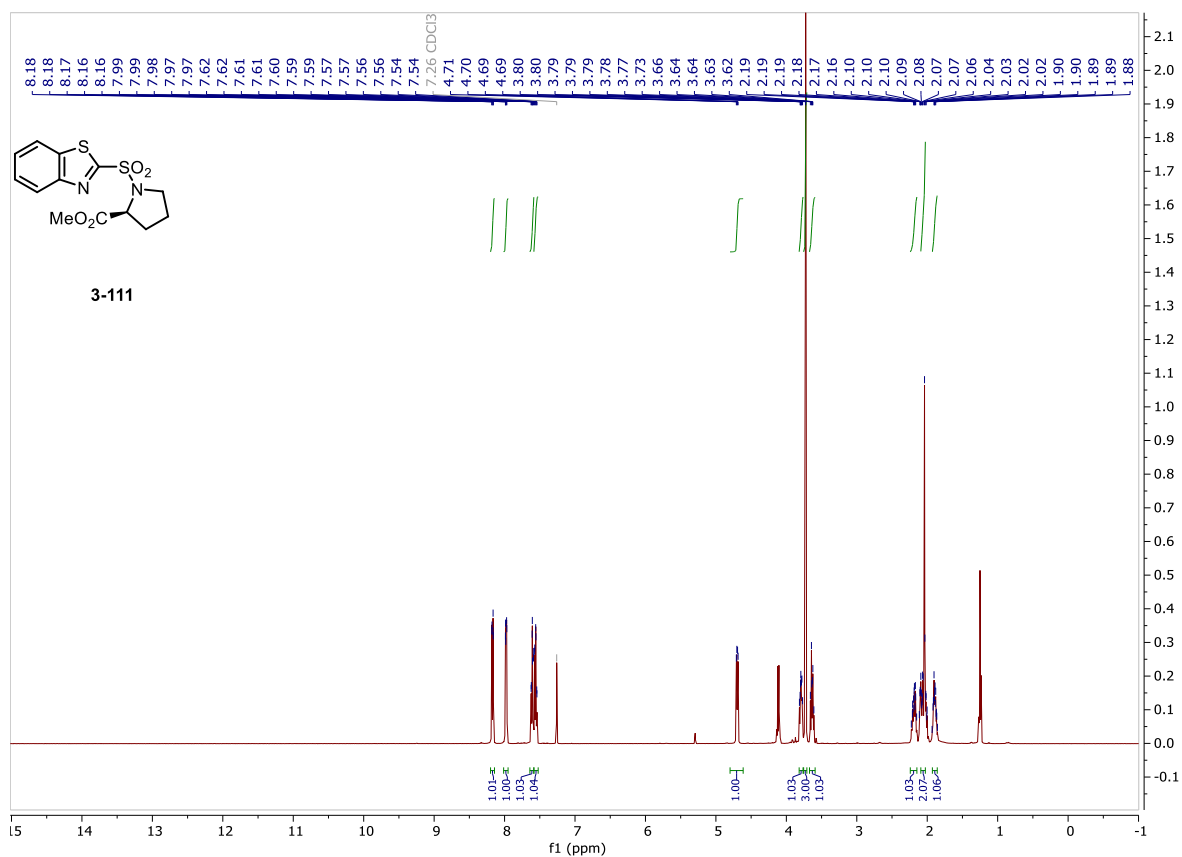
NMR and HPLC

HPLC chromatograms of 3-110



NMR and HPLC

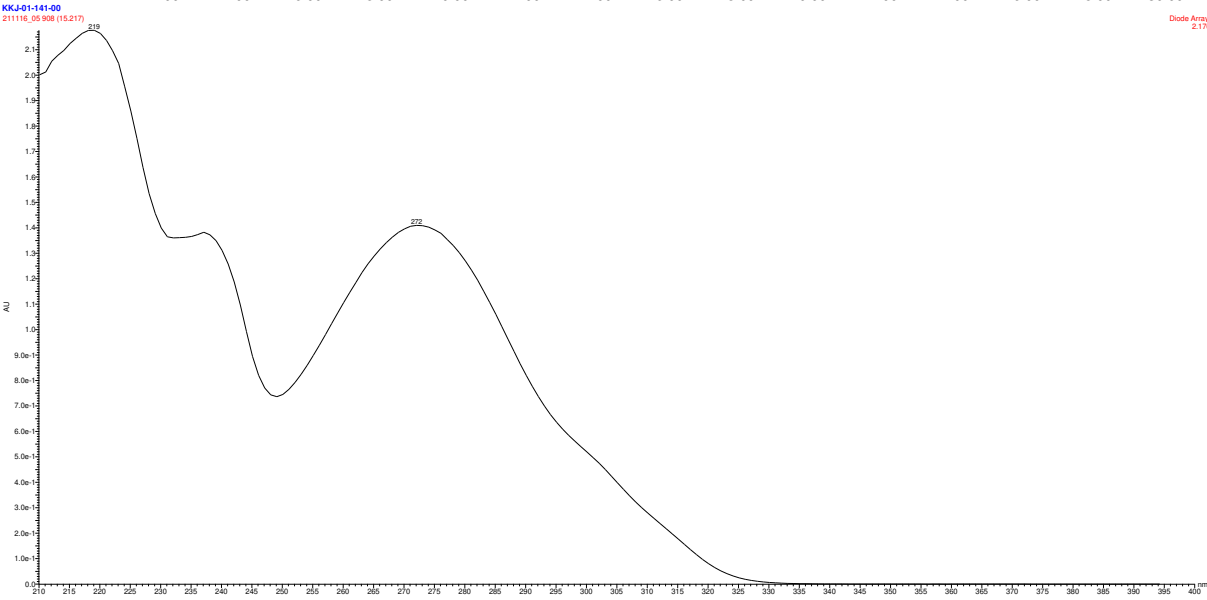
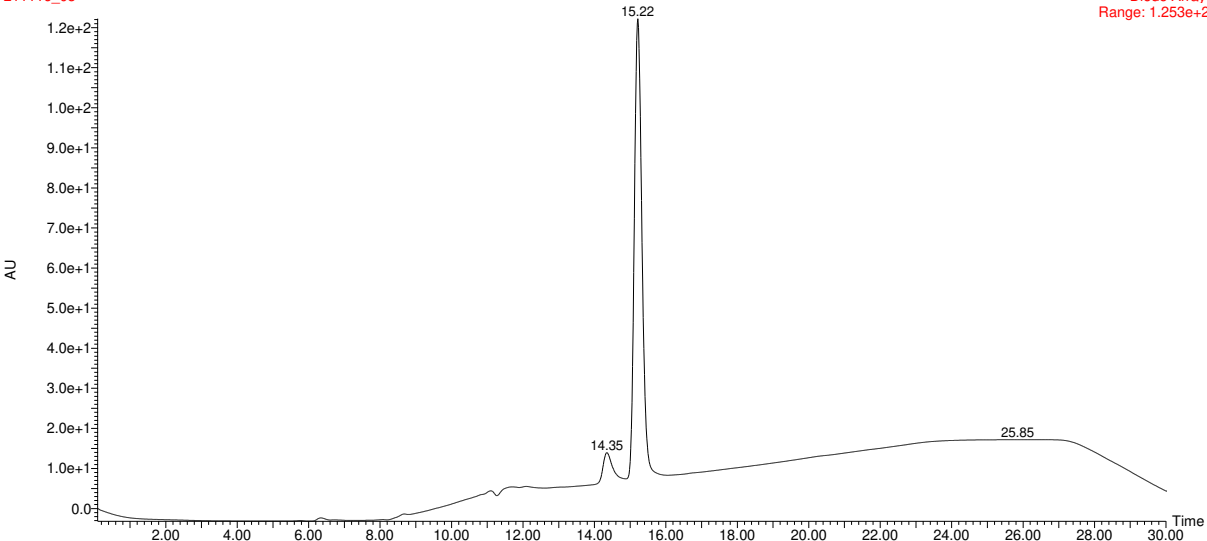
Copy of ^1H , $^{13}\text{C}\{^1\text{H}\}$ spectra of 3-111



NMR and HPLC

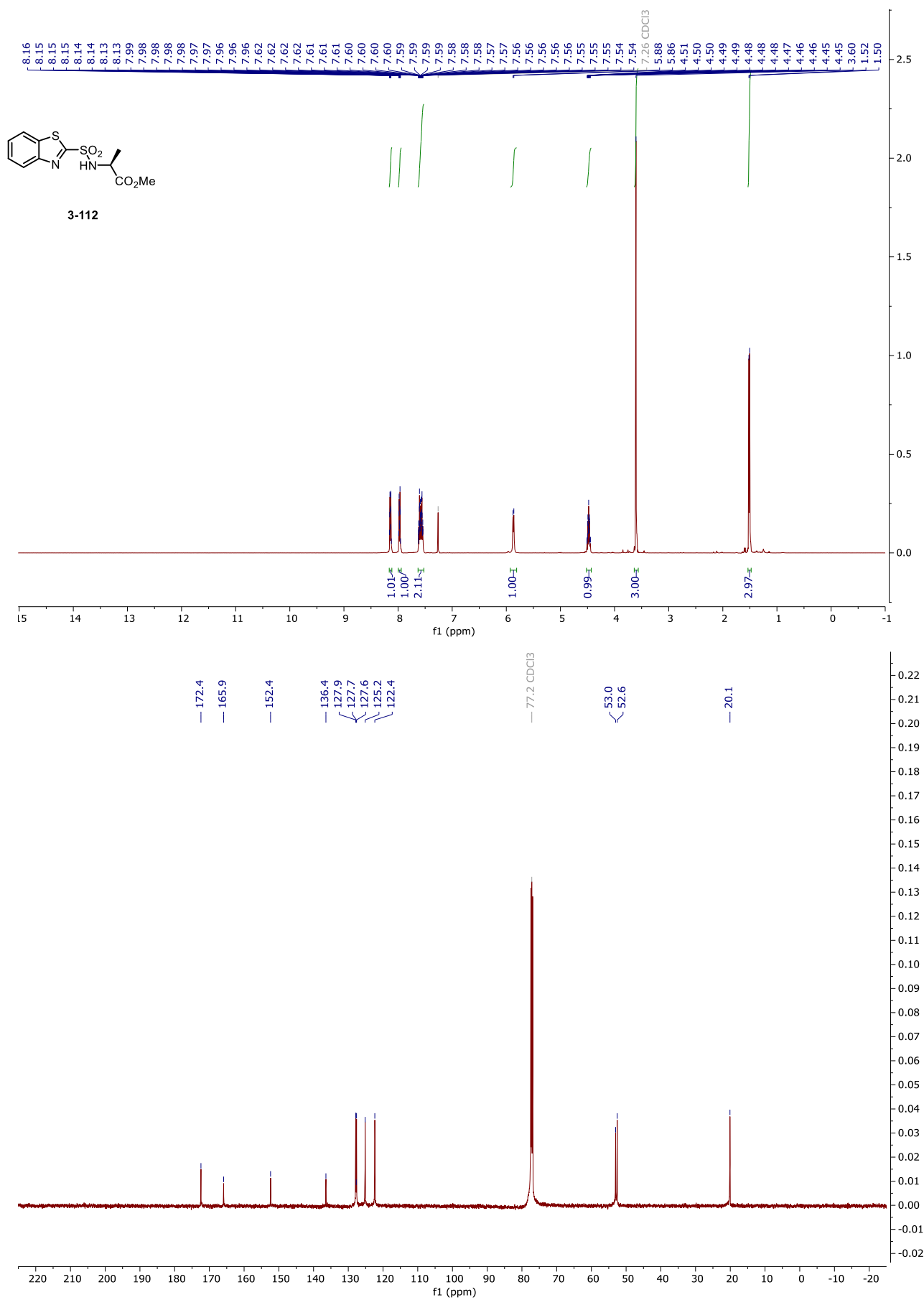
HPLC chromatograms of 3-111

KKJ-01-141-00
211116_05



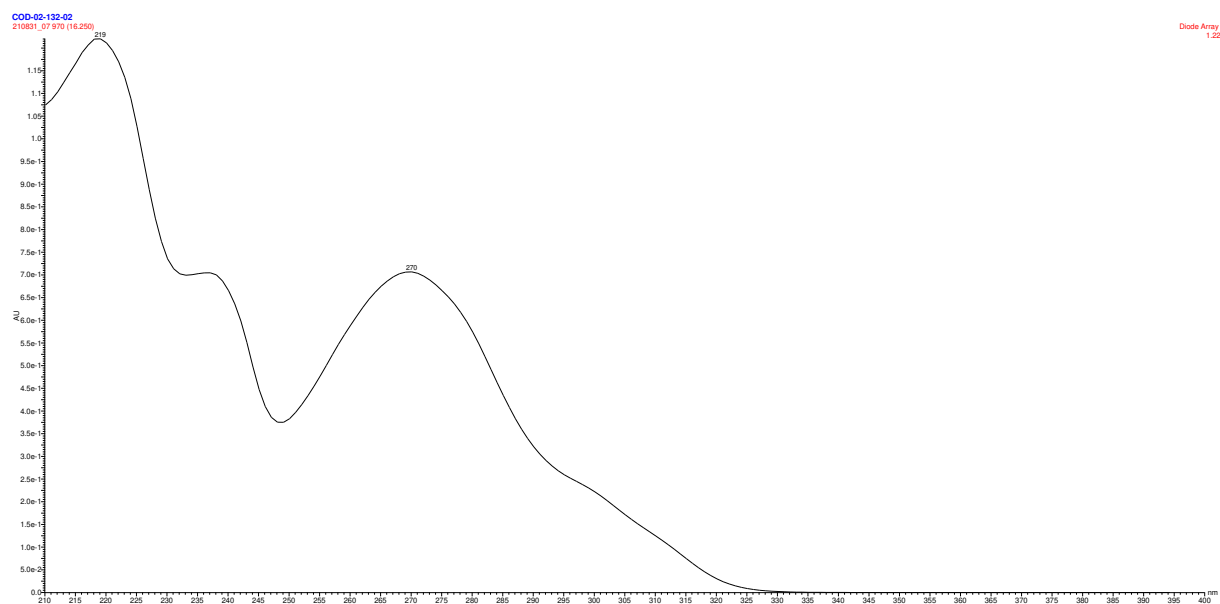
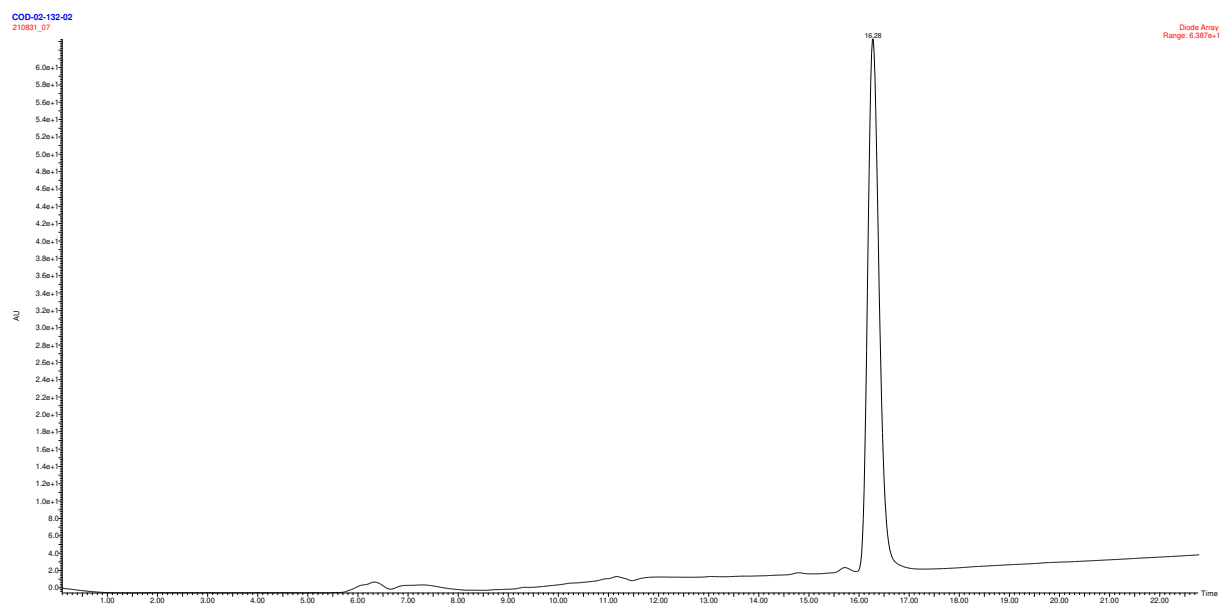
NMR and HPLC

Copy of ^1H , $^{13}\text{C}\{^1\text{H}\}$ spectra of 3-112



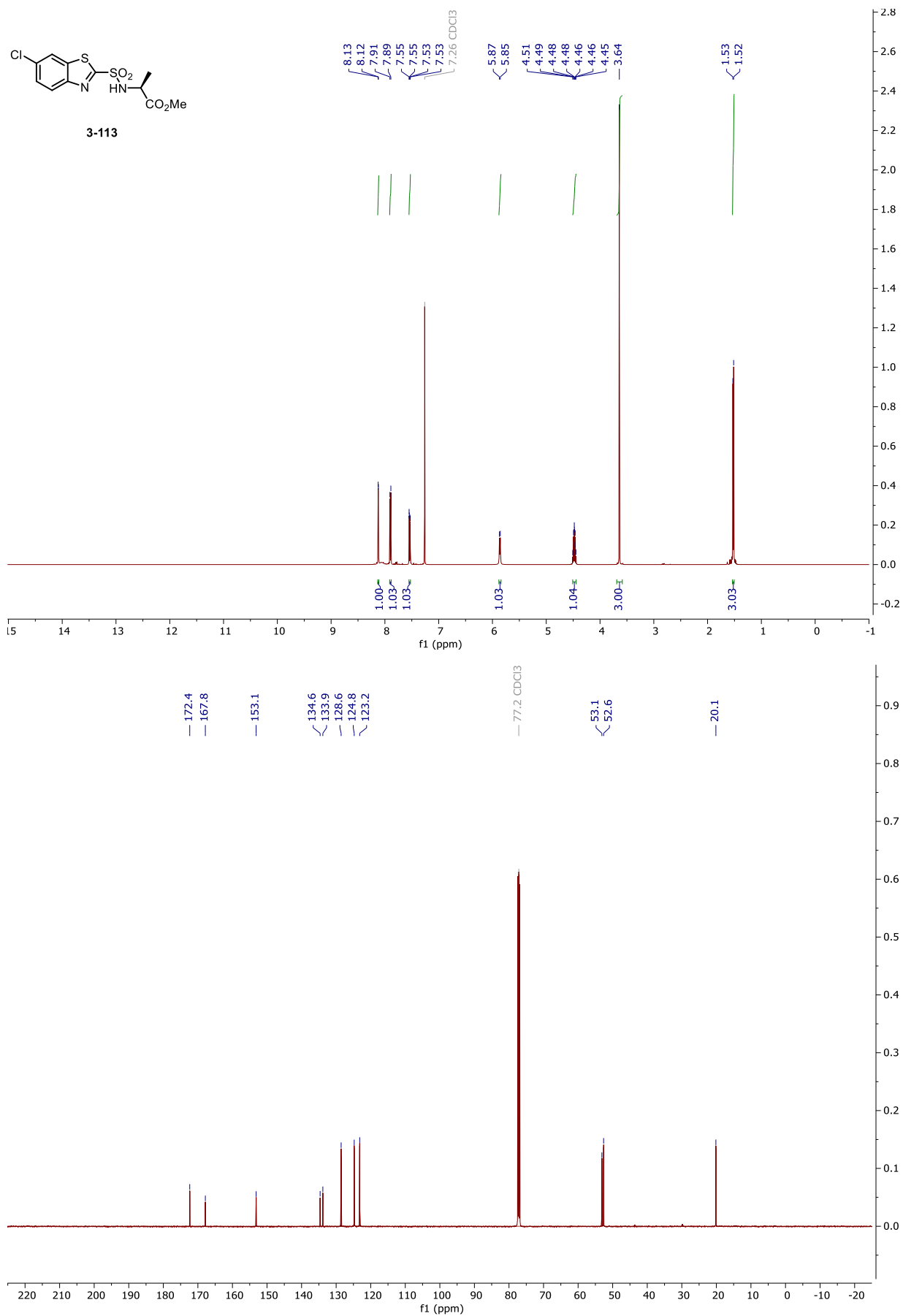
NMR and HPLC

HPLC chromatograms of 3-112



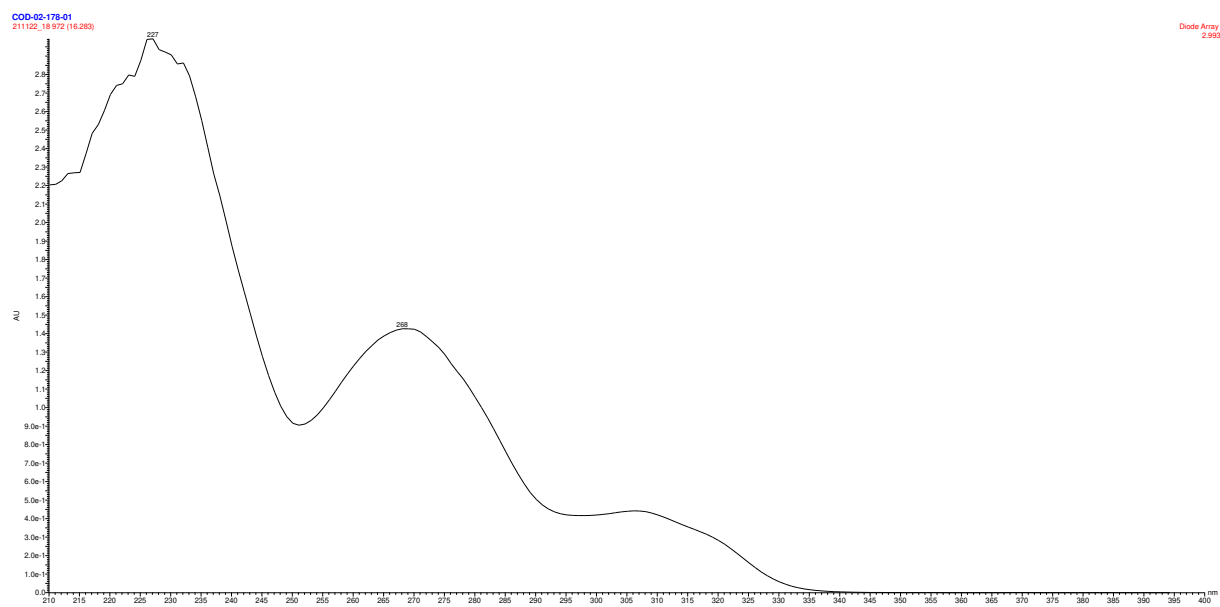
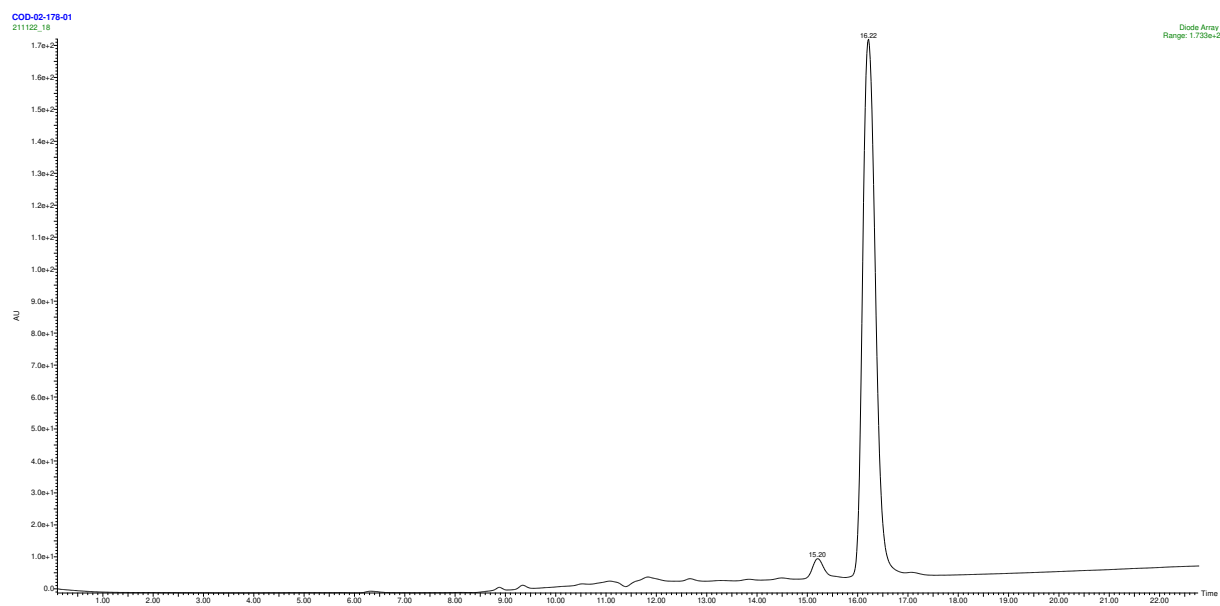
NMR and HPLC

Copy of ^1H , $^{13}\text{C}\{^1\text{H}\}$ spectra of 3-113



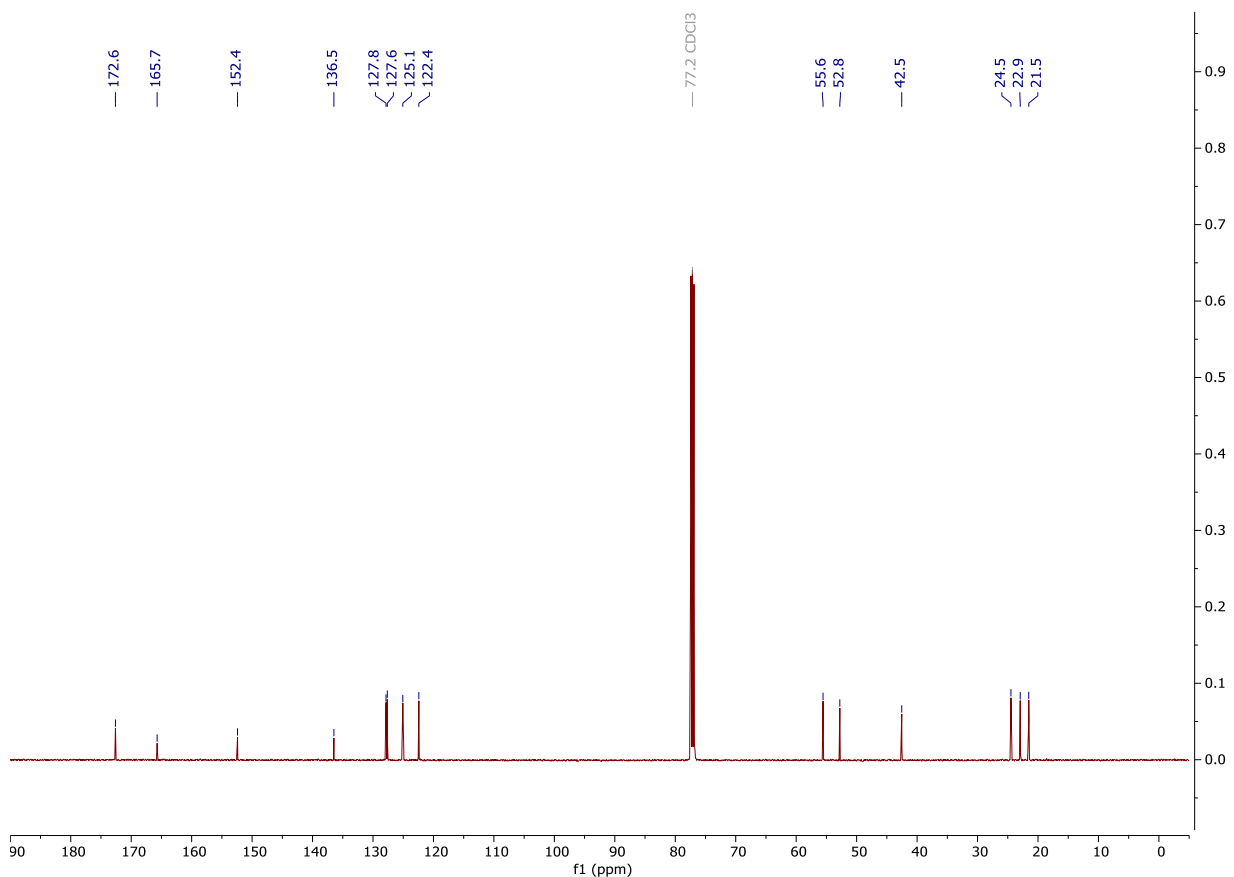
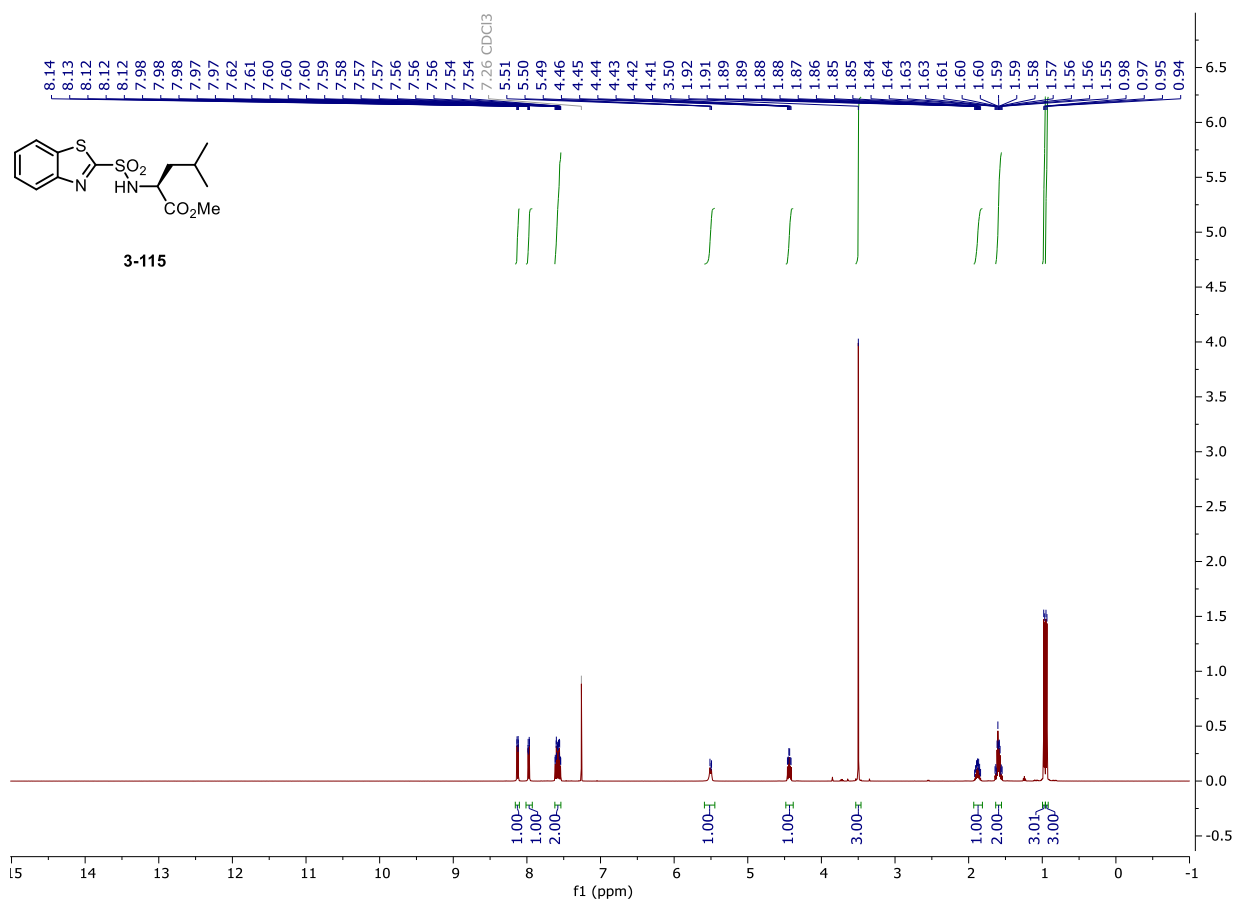
NMR and HPLC

HPLC chromatograms of 3-113



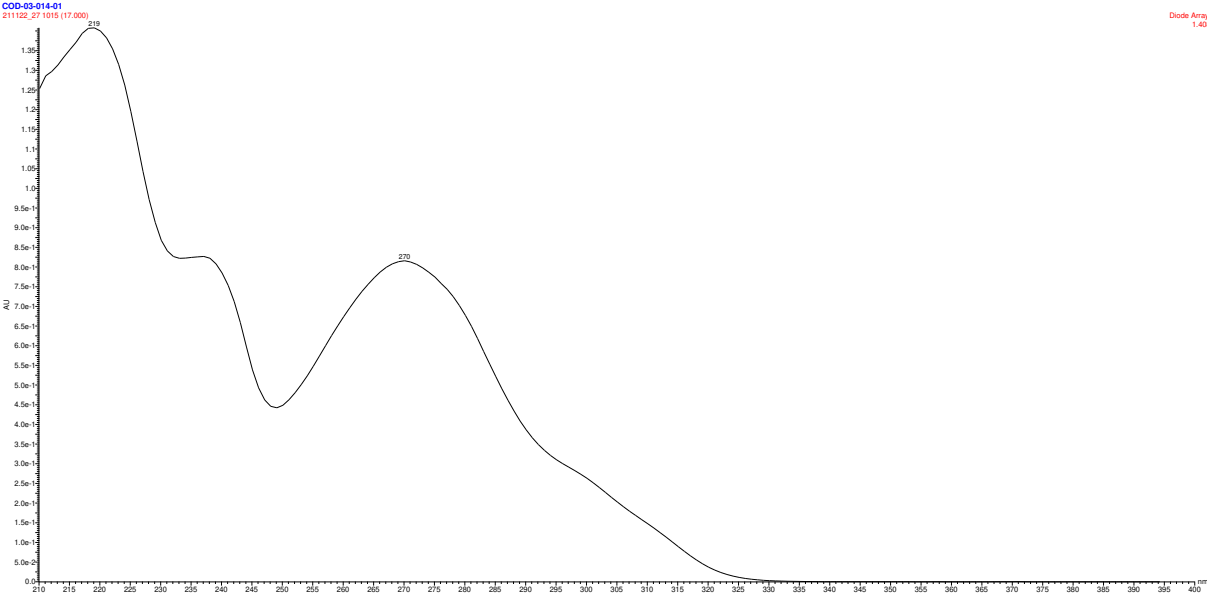
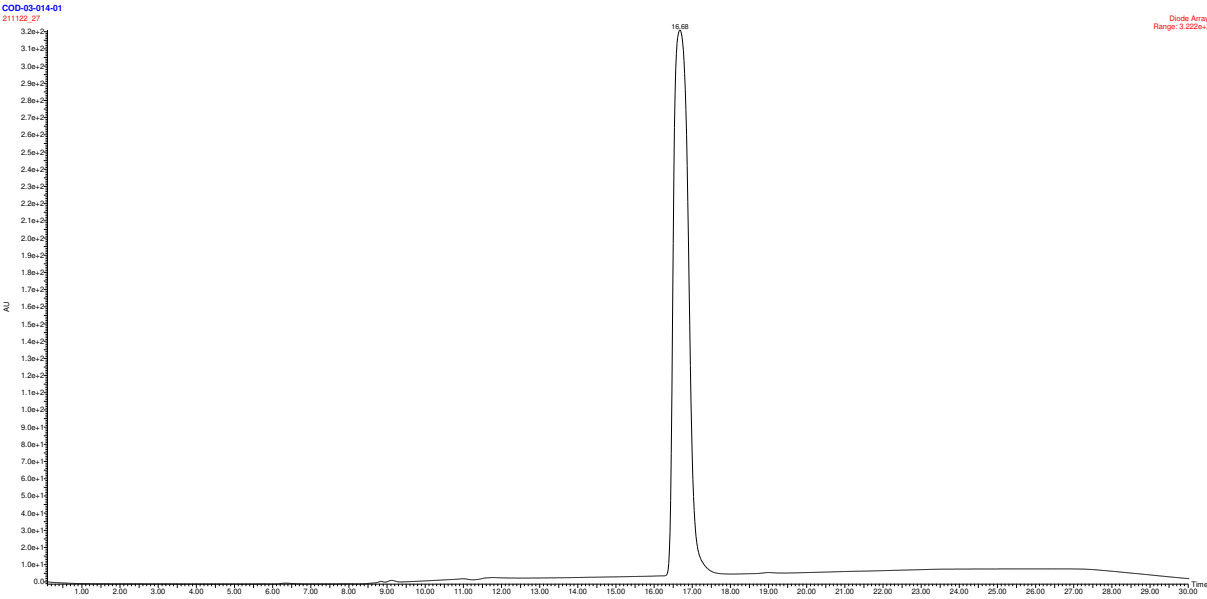
NMR and HPLC

Copy of ^1H , $^{13}\text{C}\{^1\text{H}\}$ spectra of 3-115



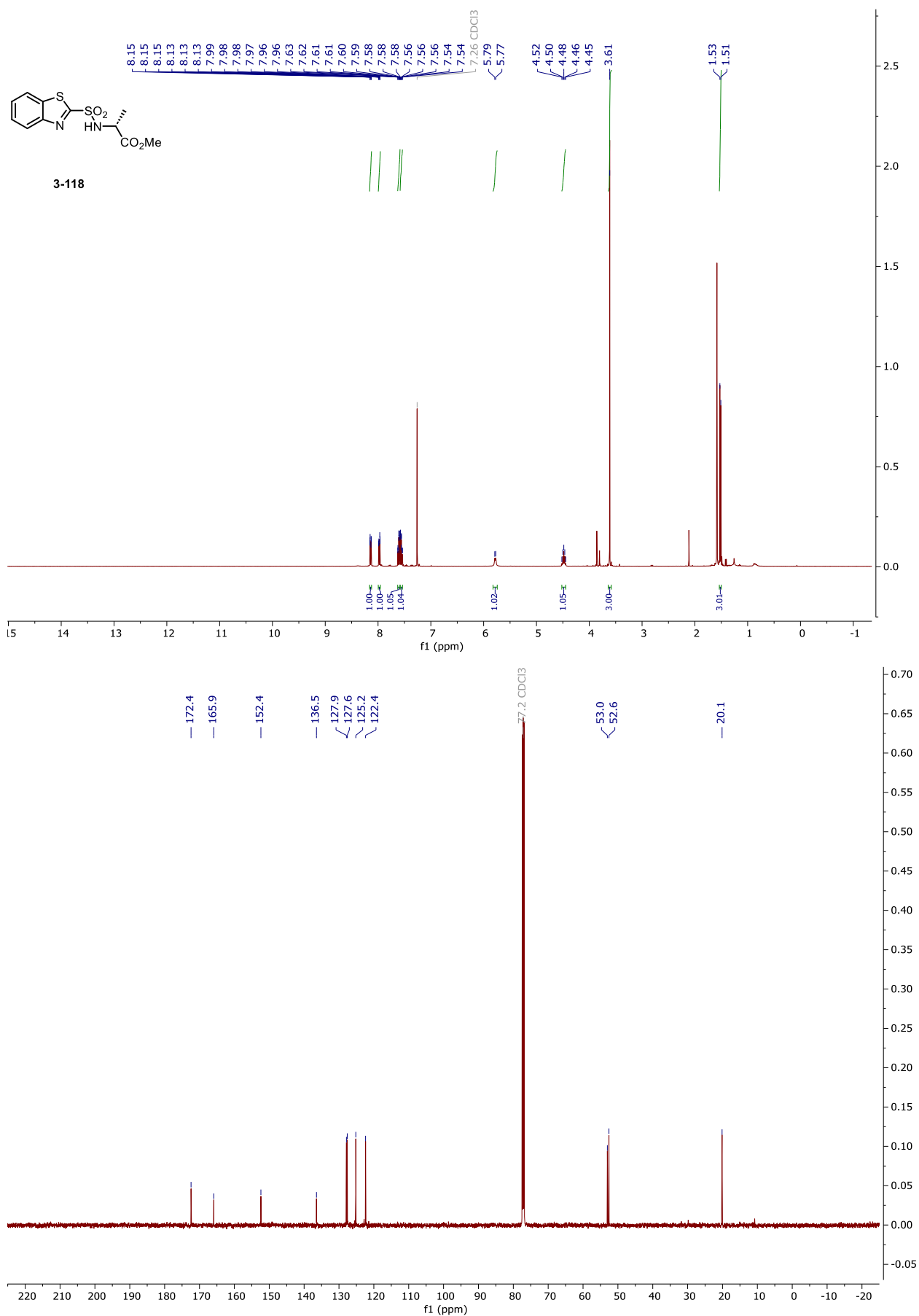
NMR and HPLC

HPLC chromatograms of 3-115



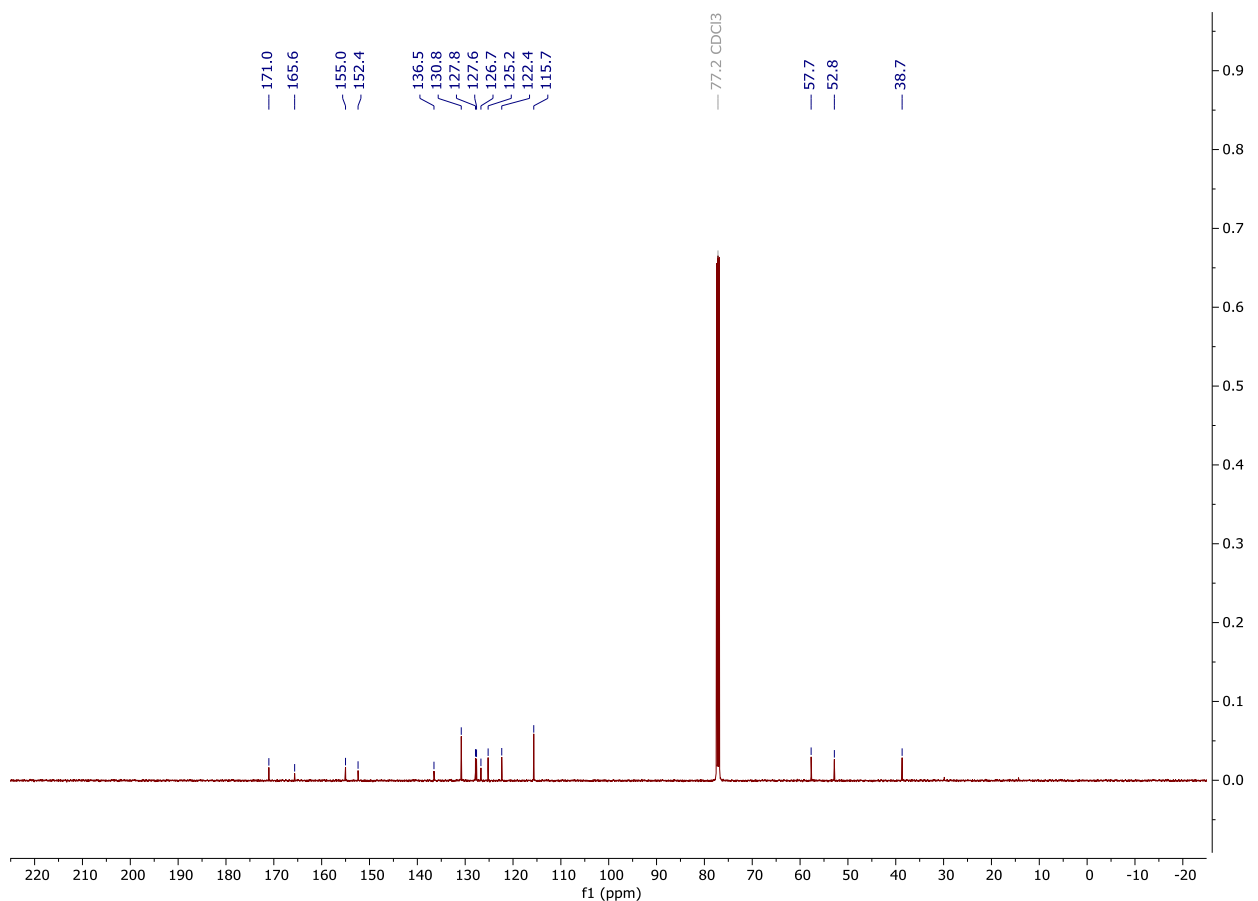
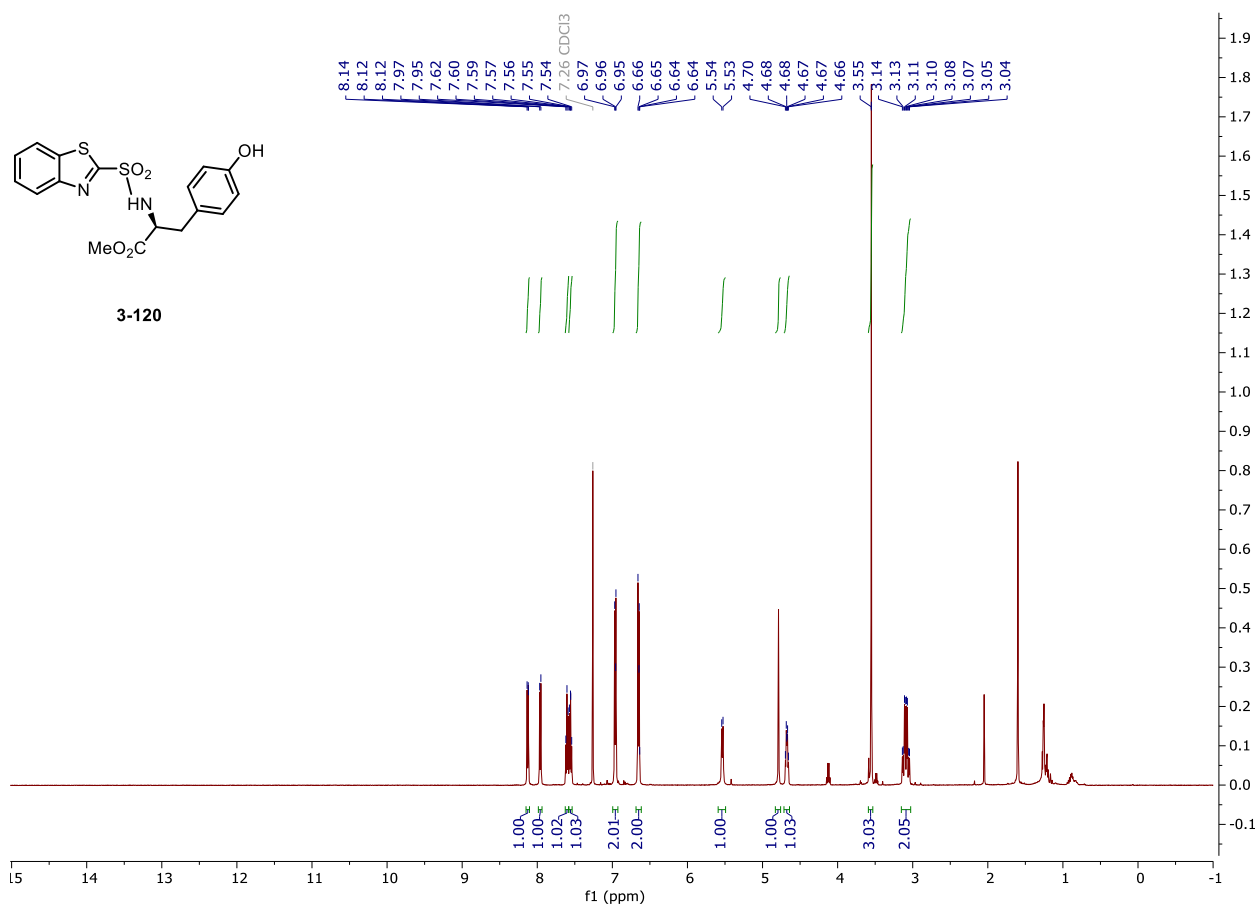
NMR and HPLC

Copy of ^1H , $^{13}\text{C}\{^1\text{H}\}$ spectra of 3-118

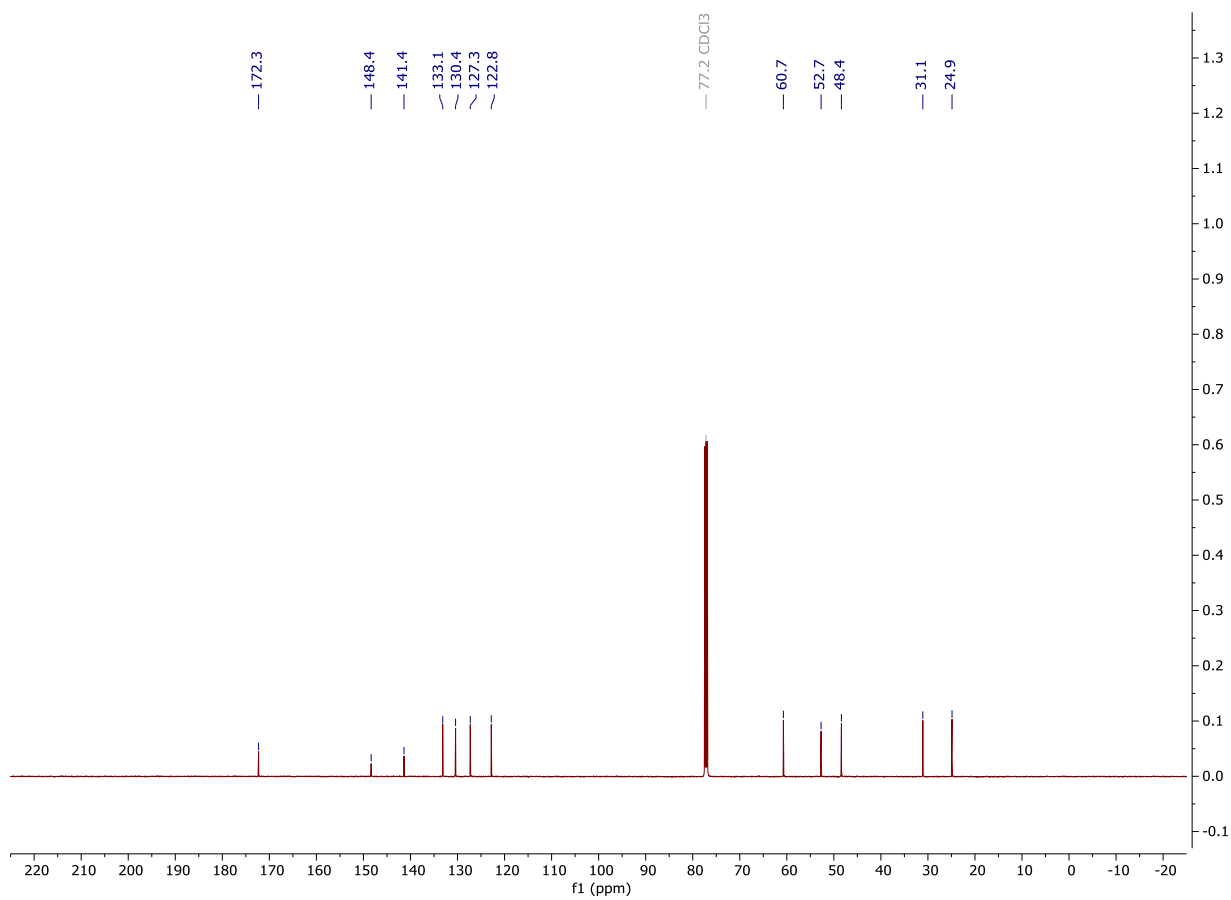
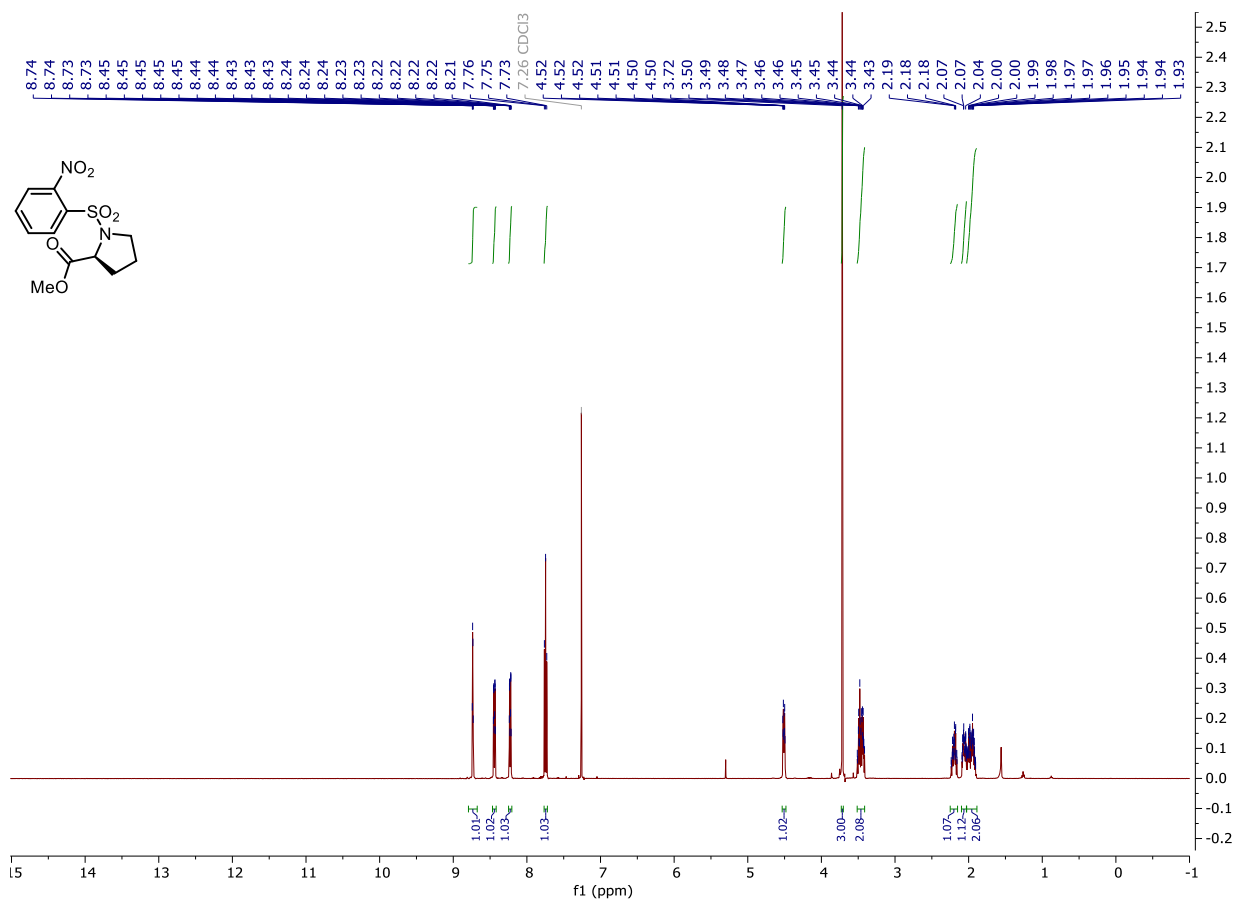


NMR and HPLC

Copy of ^1H , $^{13}\text{C}\{^1\text{H}\}$ spectra of 3-120

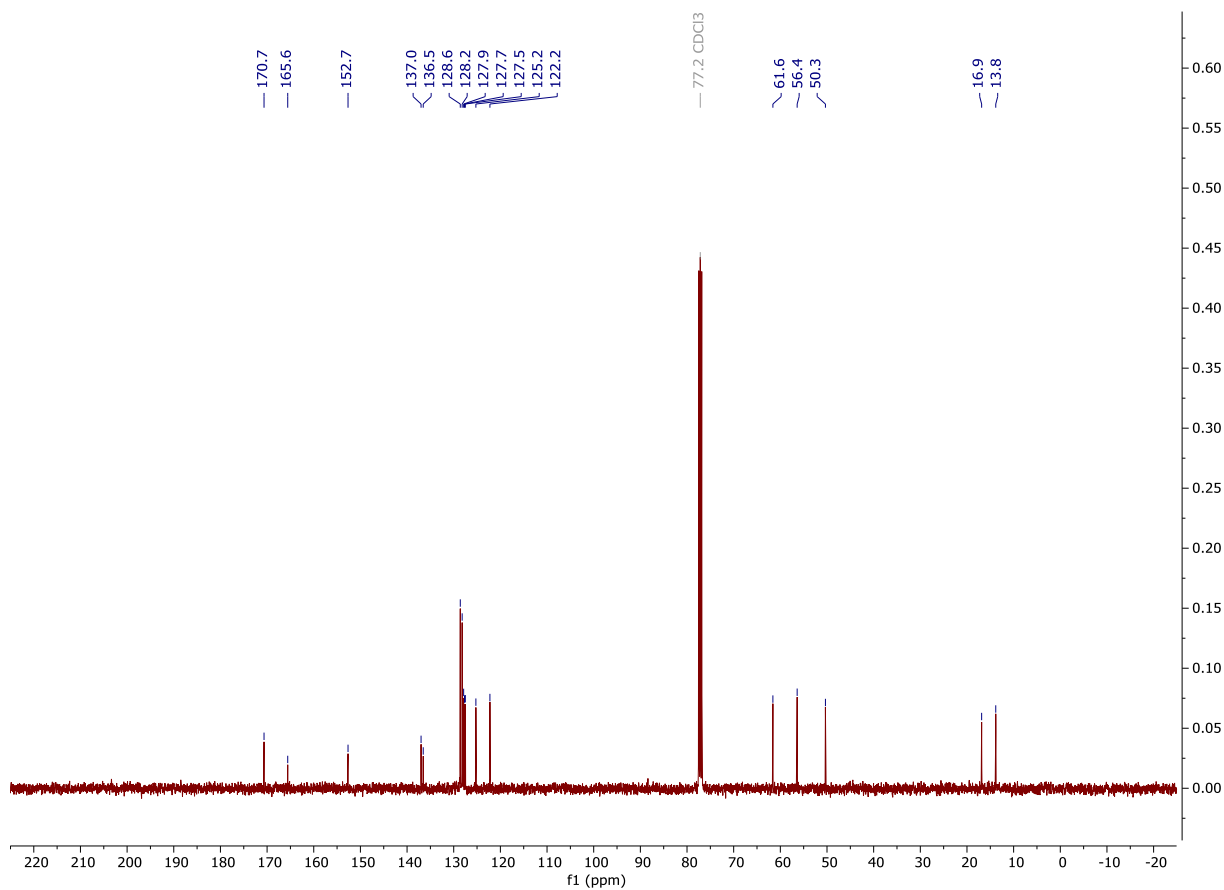
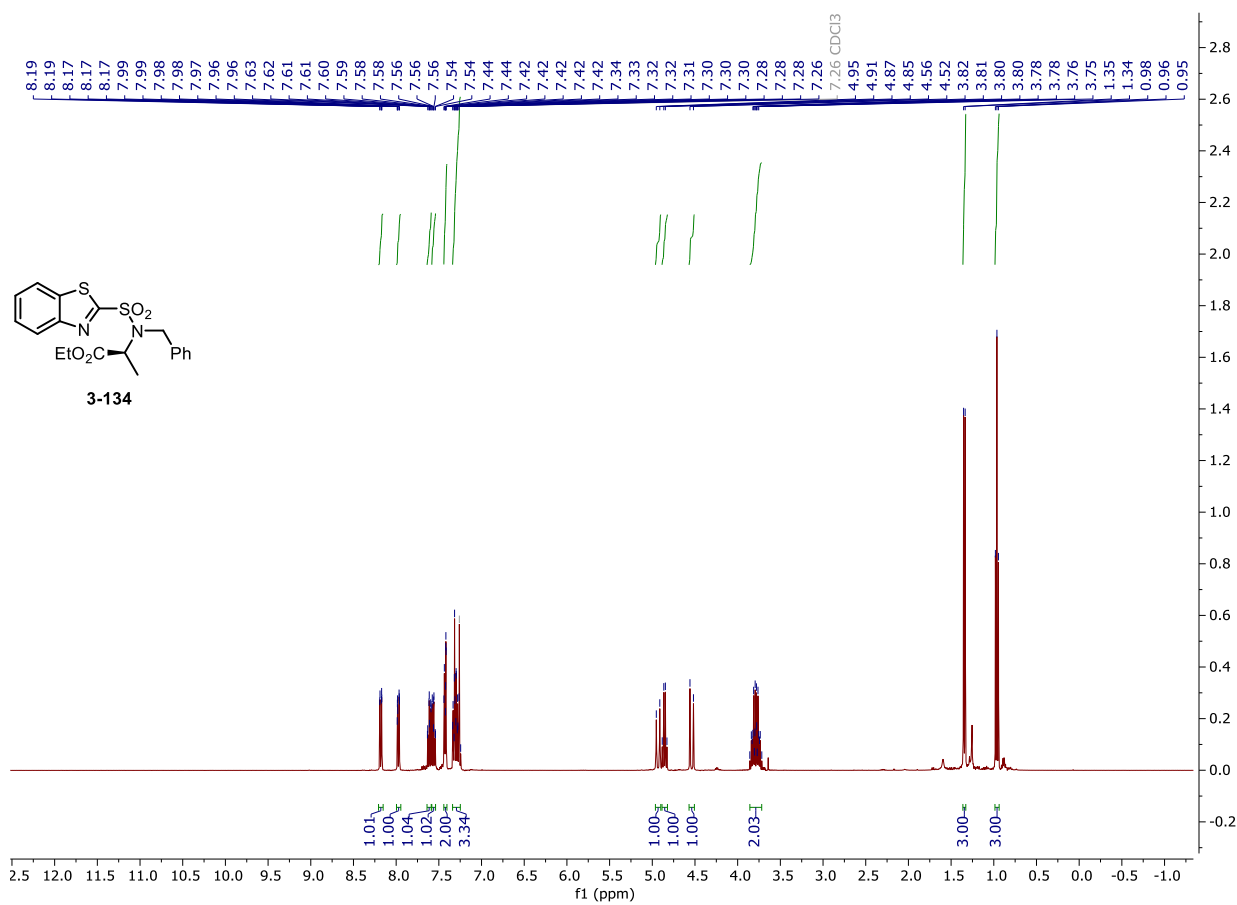


NMR and HPLC



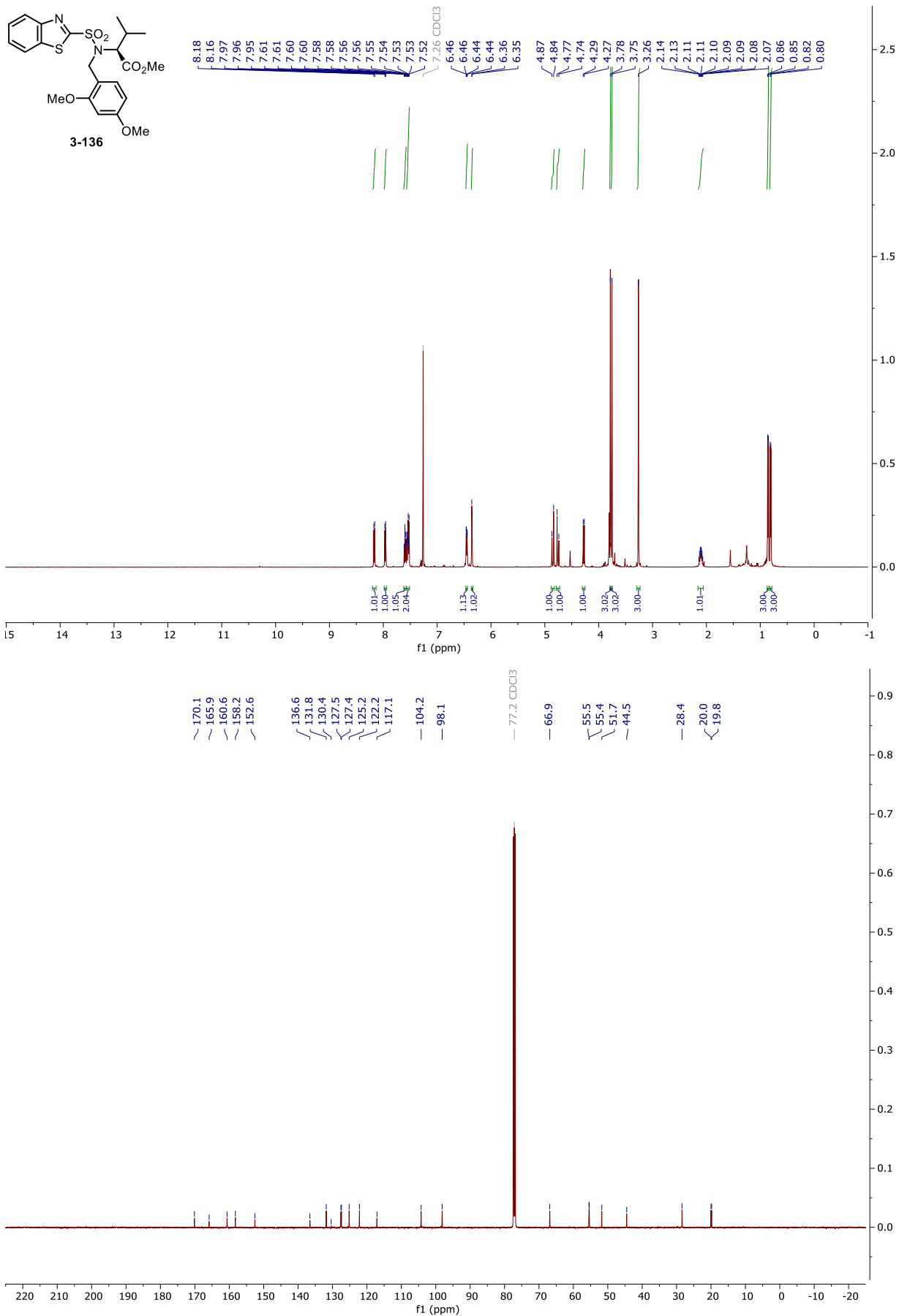
NMR and HPLC

Copy of ¹H, ¹³C{¹H} spectra of 3-134



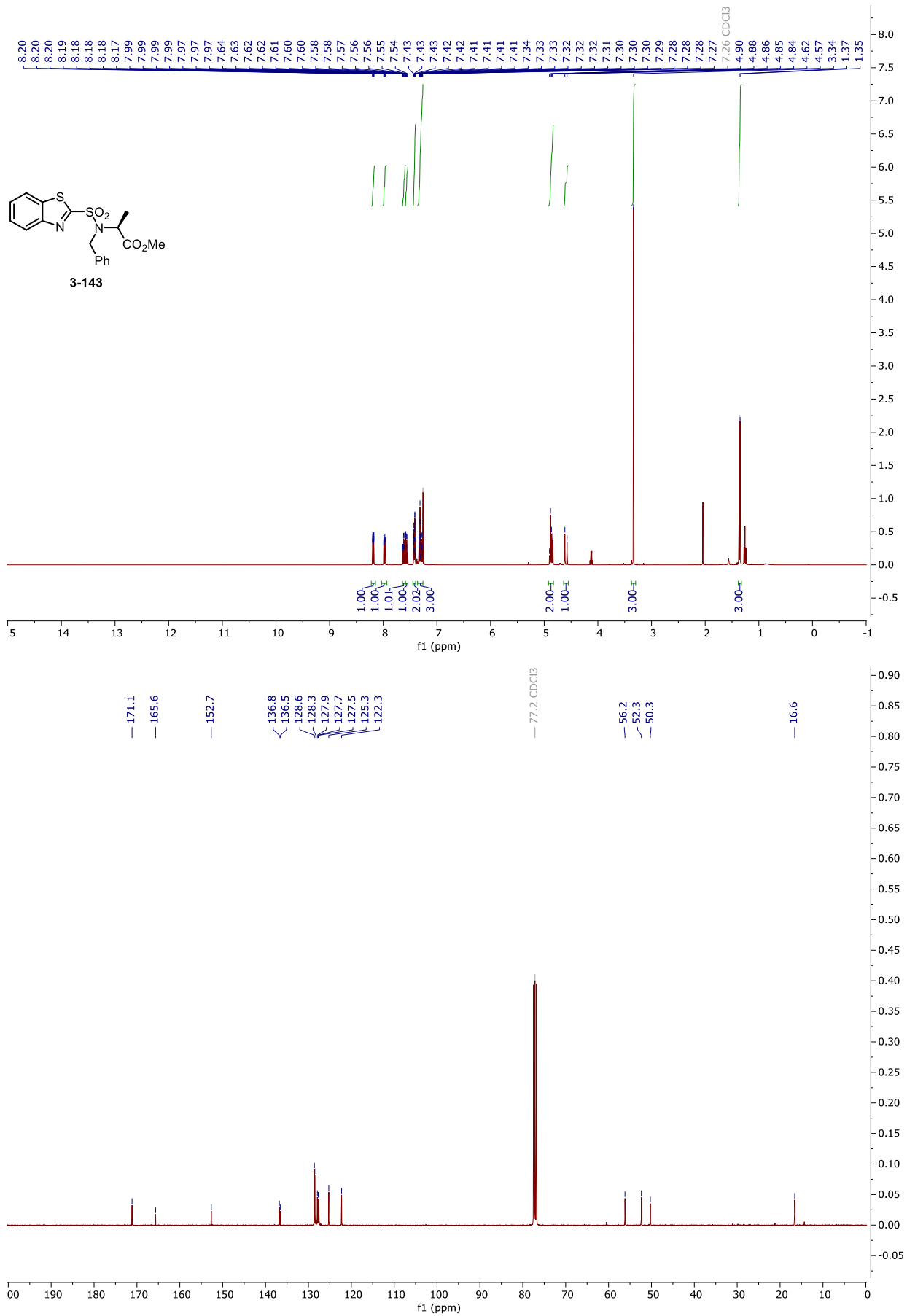
NMR and HPLC

Copy of ^1H , $^{13}\text{C}\{^1\text{H}\}$ spectra of **3-136**



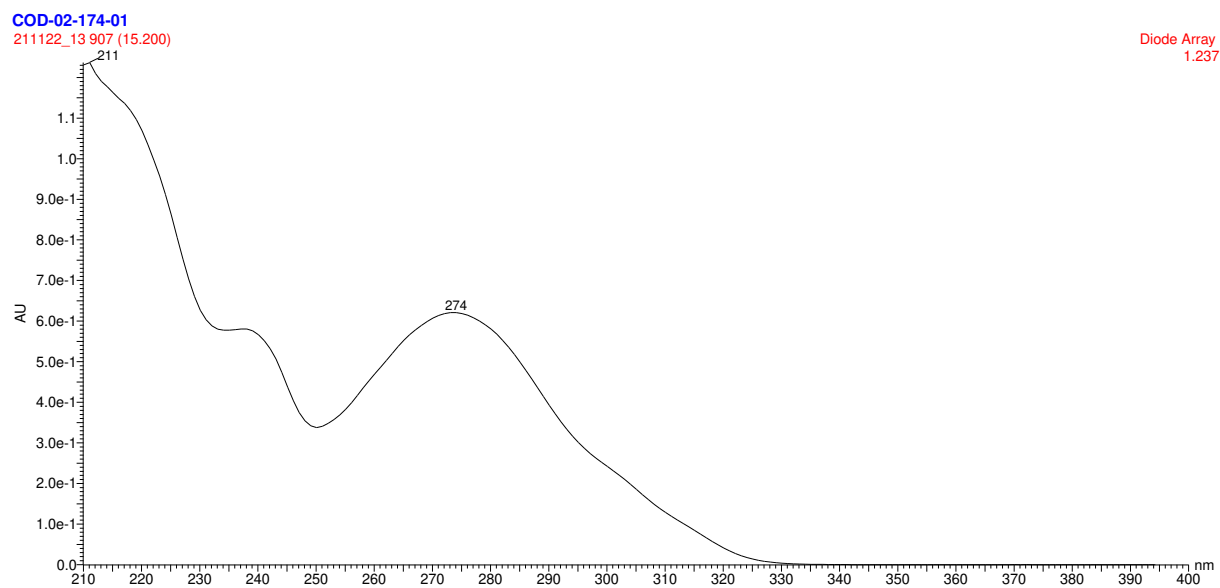
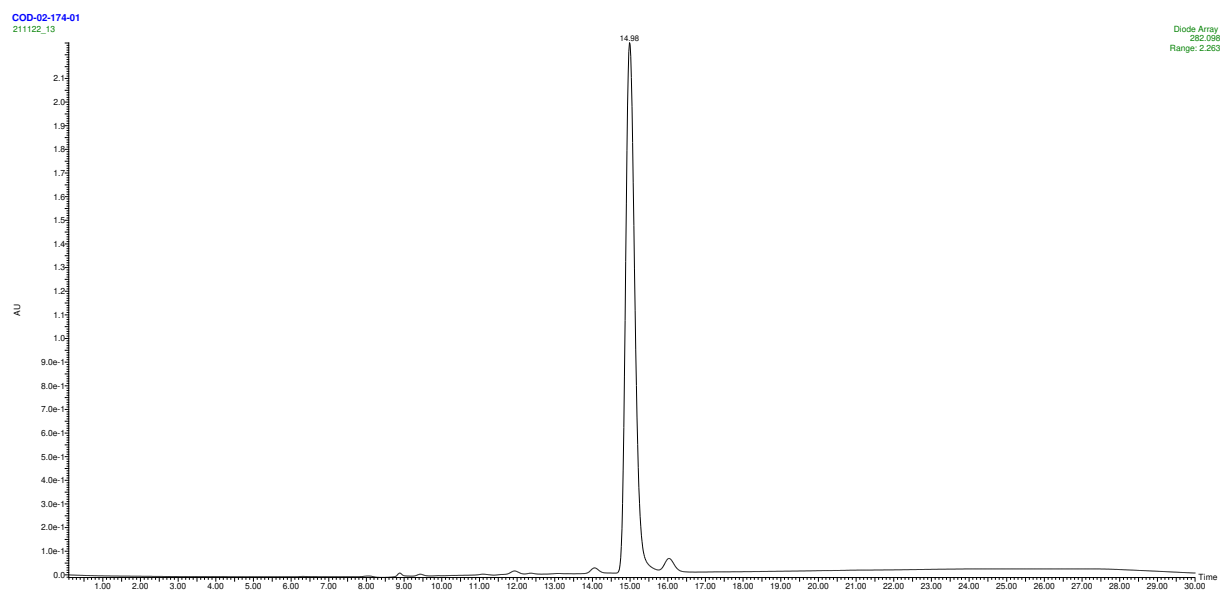
NMR and HPLC

Copy of ^1H , $^{13}\text{C}\{^1\text{H}\}$ spectra of 3-143



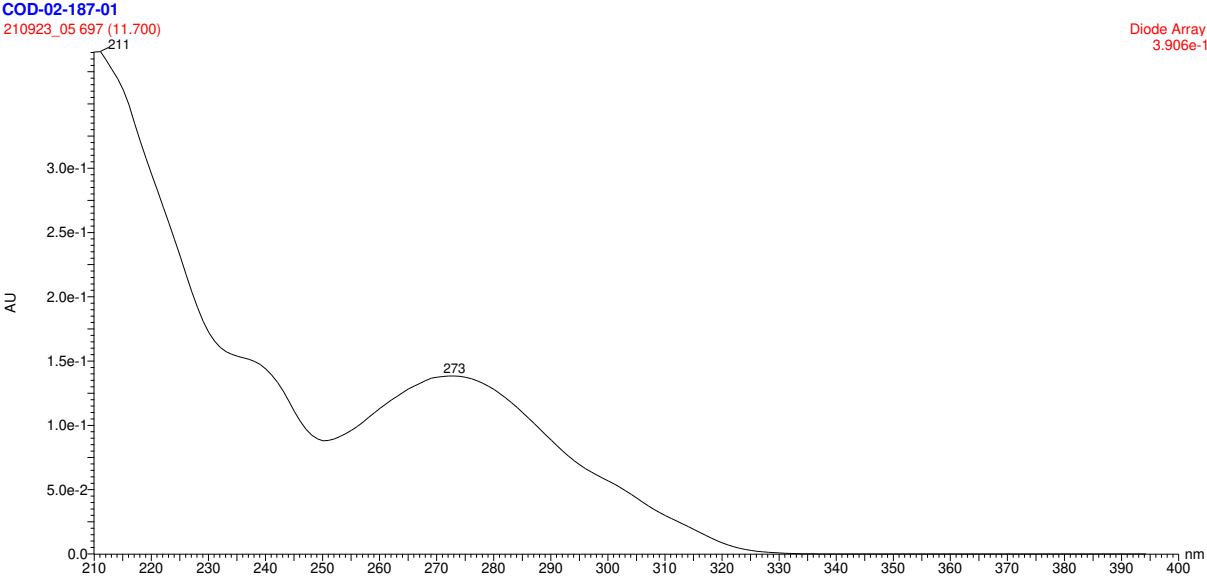
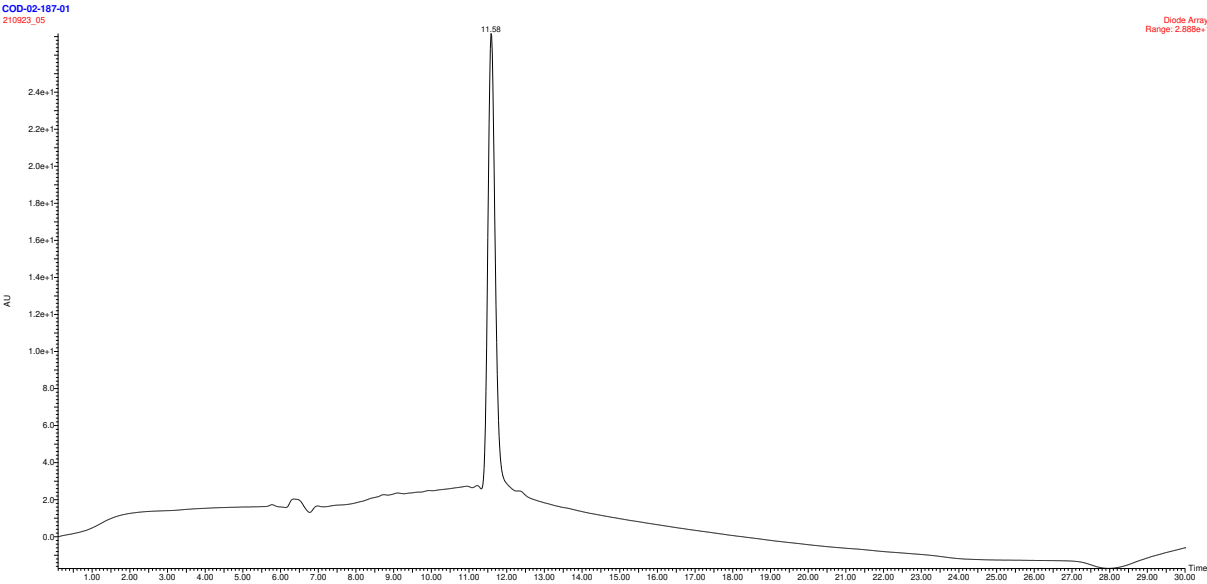
NMR and HPLC

HPLC chromatograms of 3-143



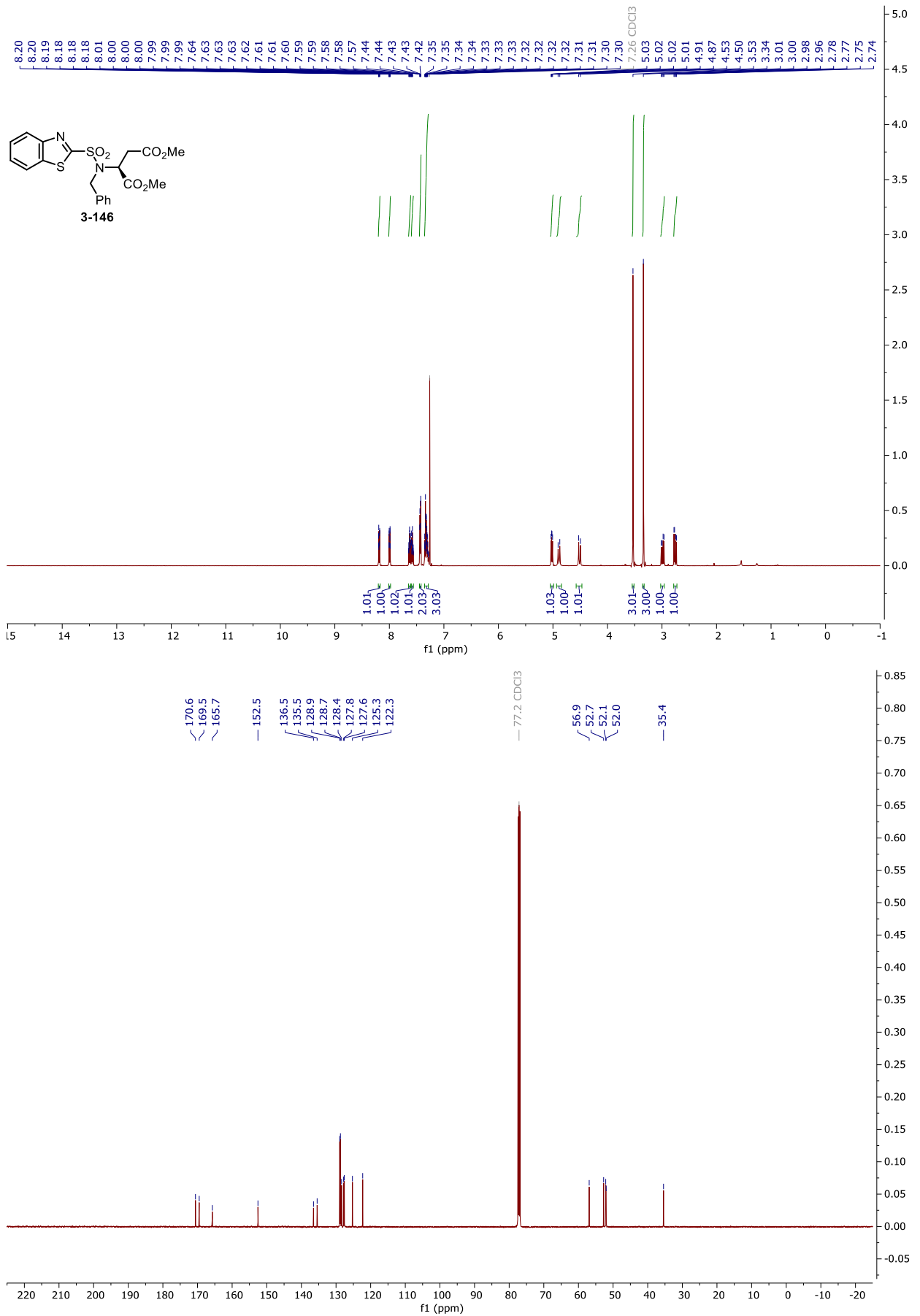
NMR and HPLC

HPLC chromatograms of 3-145



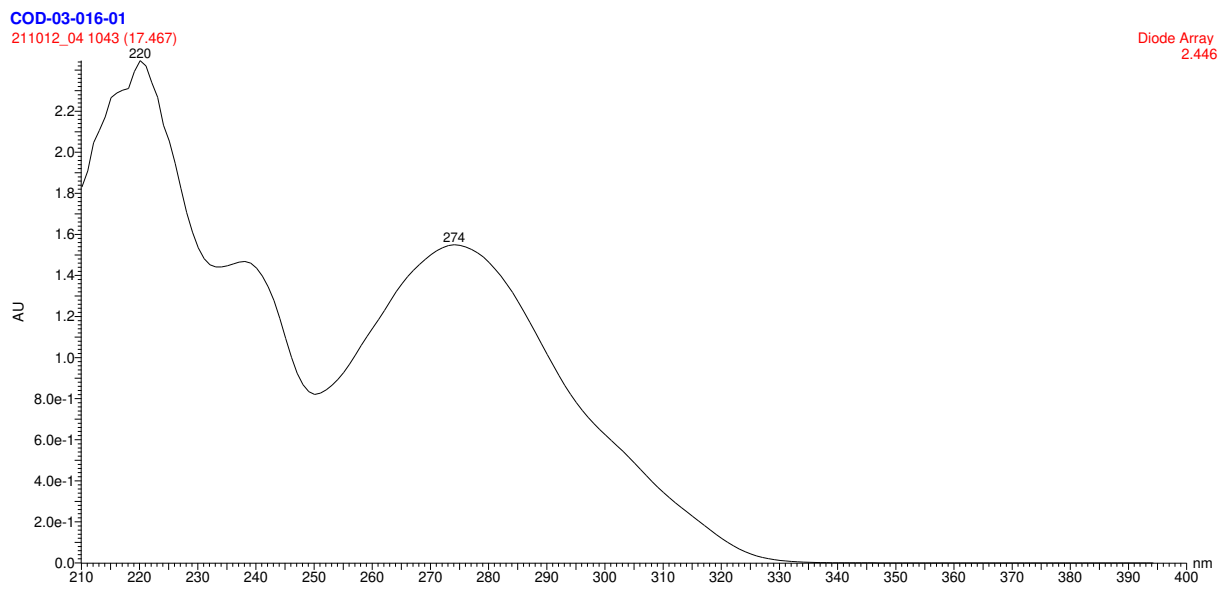
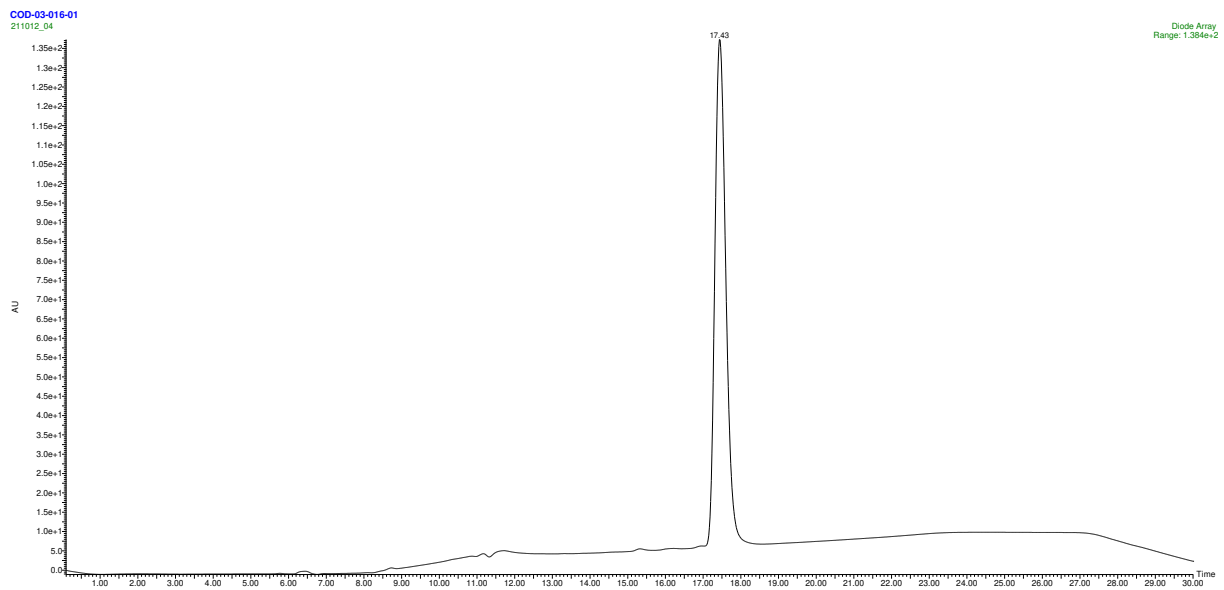
NMR and HPLC

Copy of ^1H , $^{13}\text{C}\{^1\text{H}\}$ spectra of **3-146**



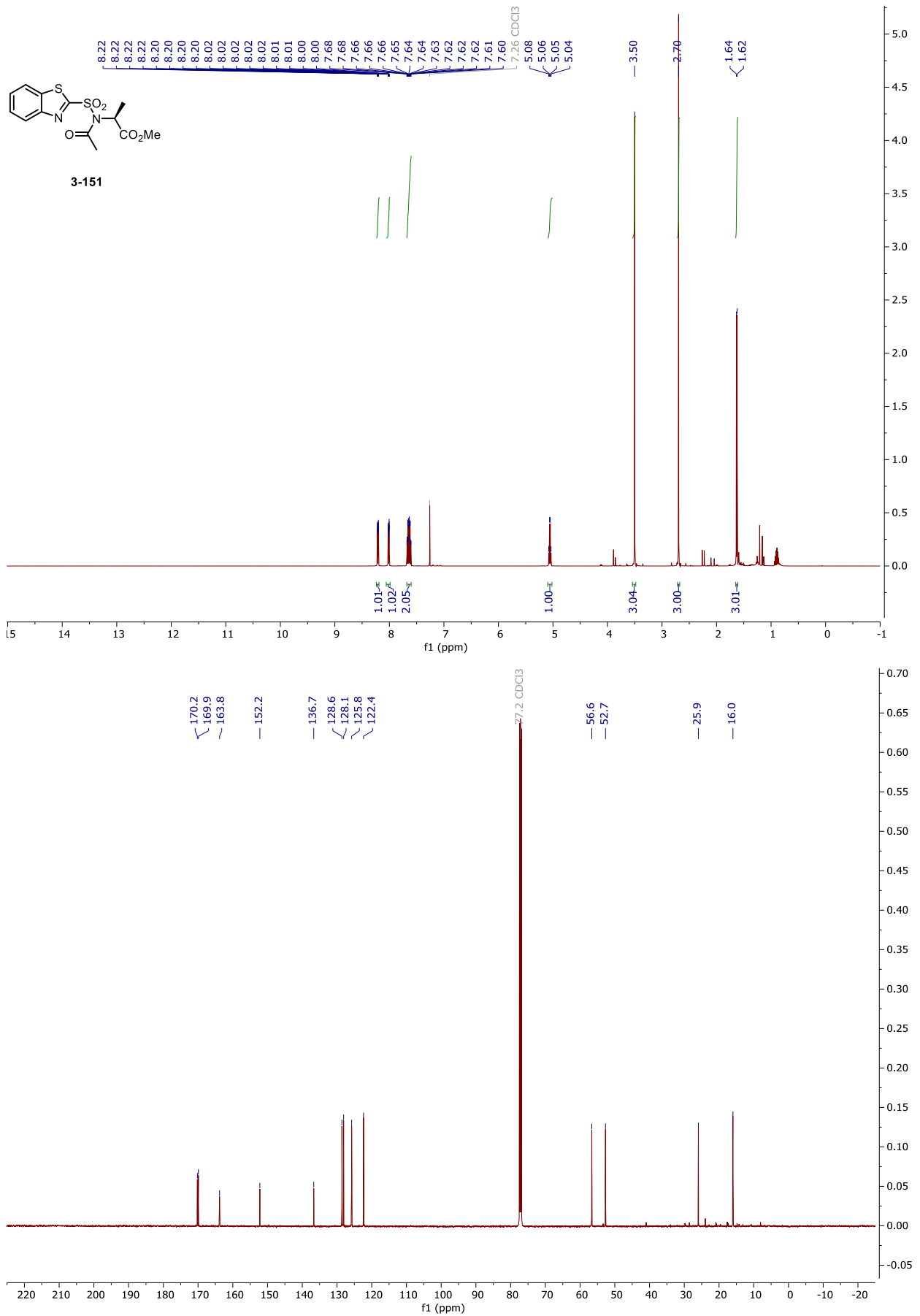
NMR and HPLC

HPLC chromatograms of 3-146

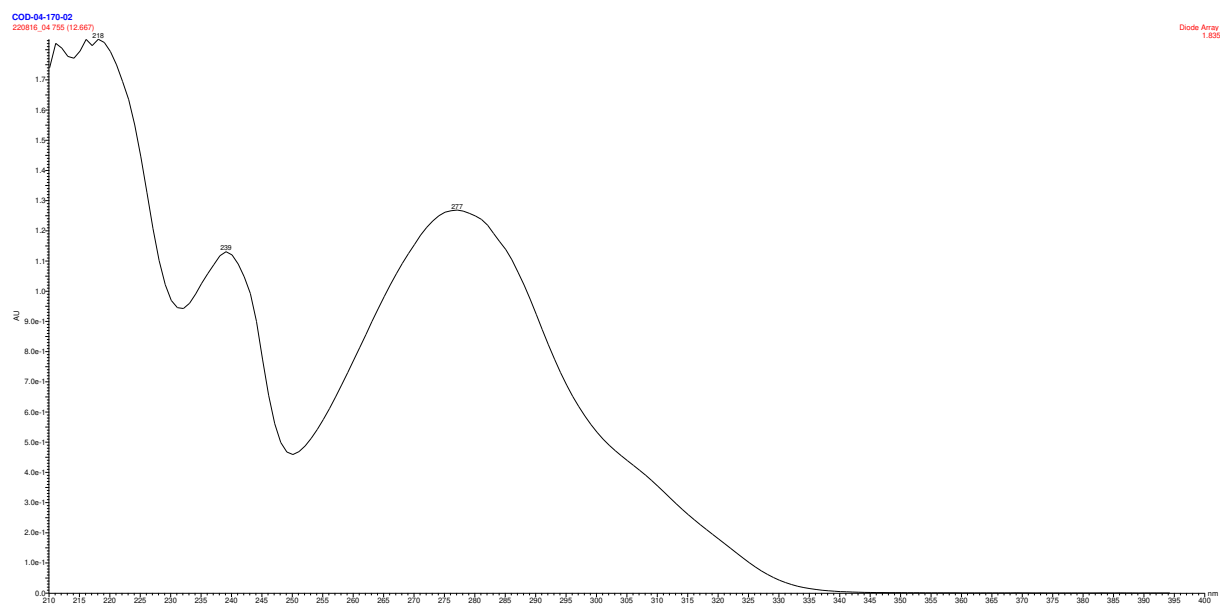
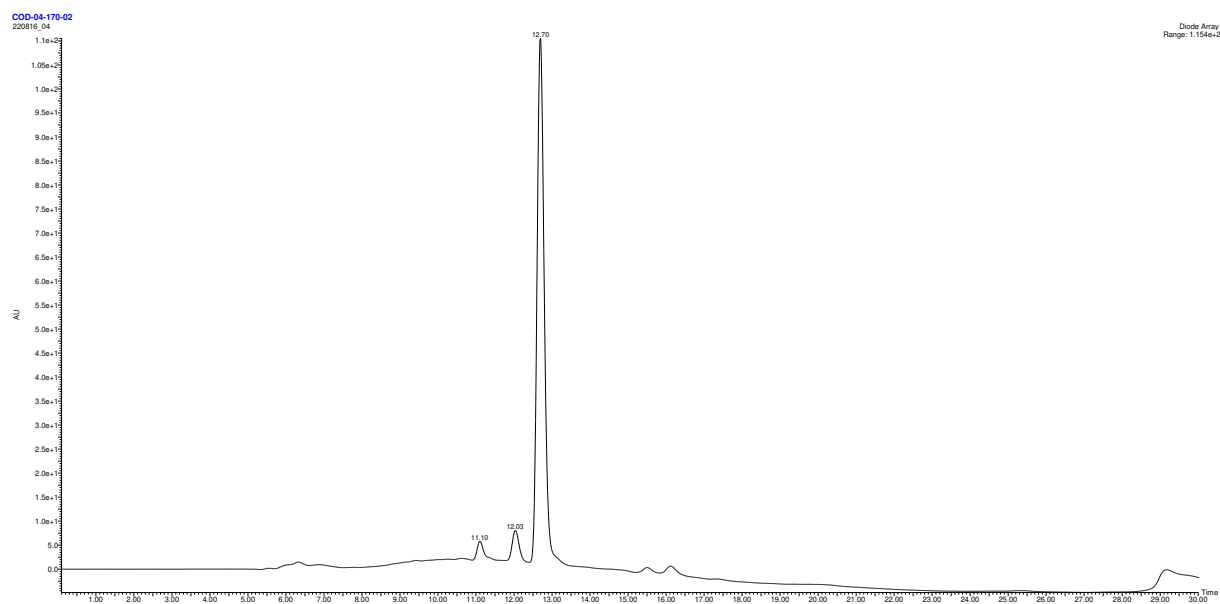


NMR and HPLC

Copy of ^1H , $^{13}\text{C}\{^1\text{H}\}$ spectra of **3-151**

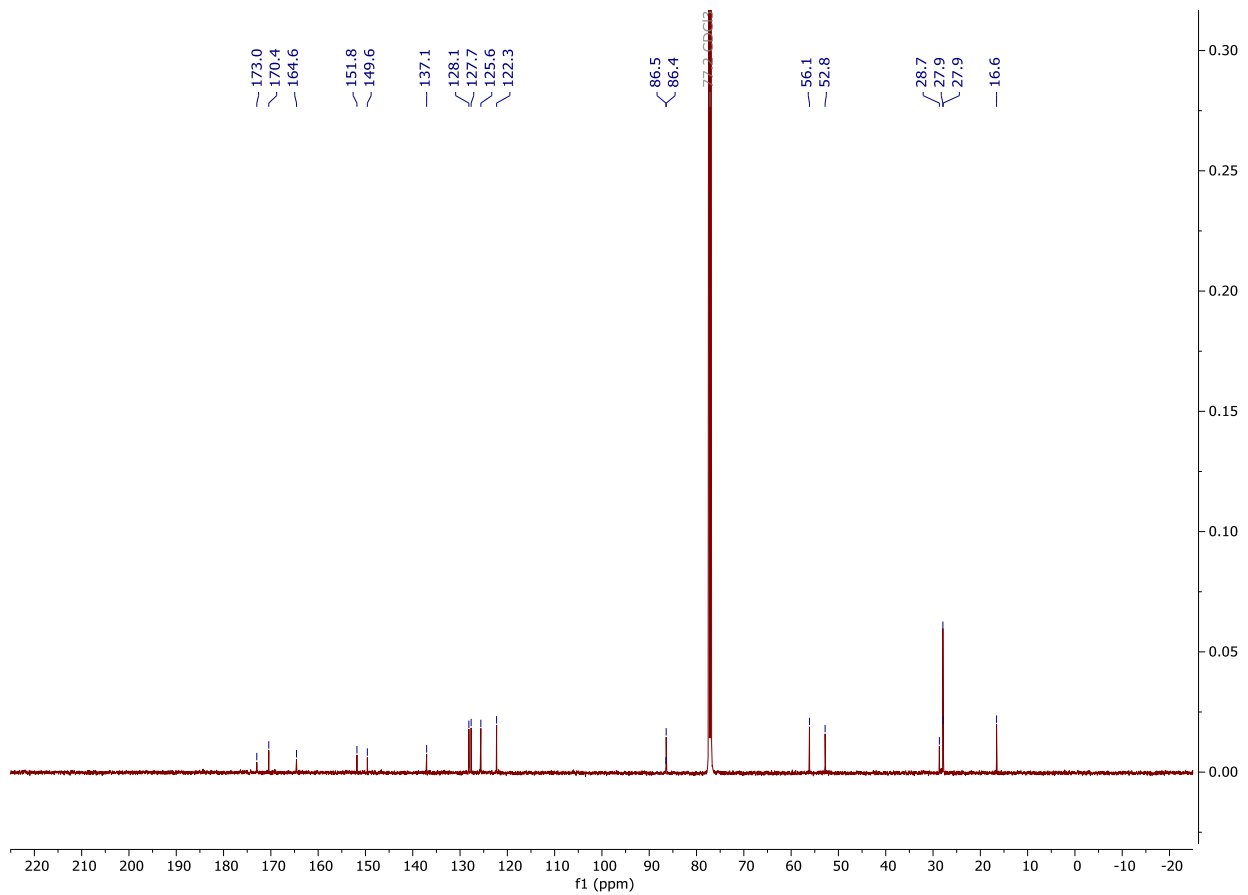
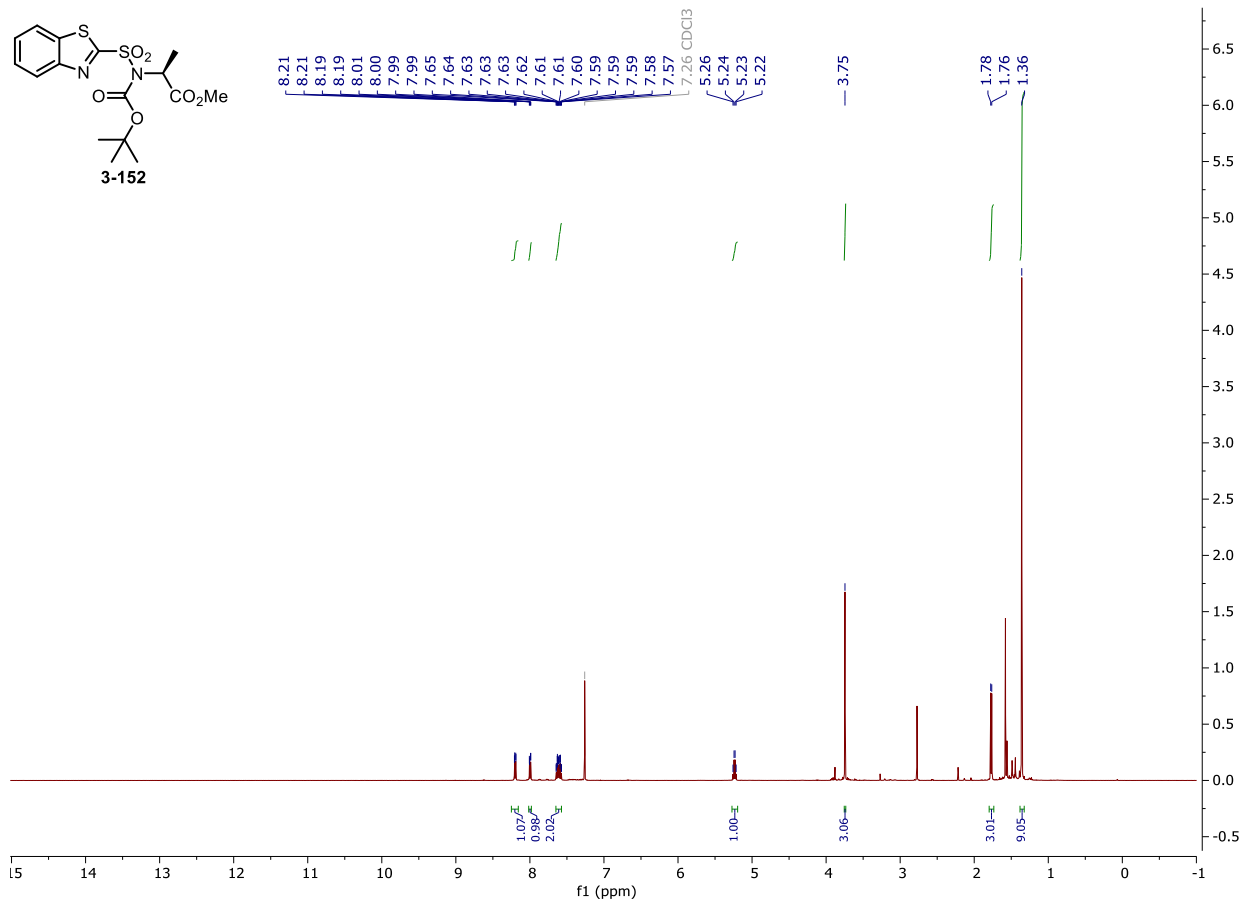
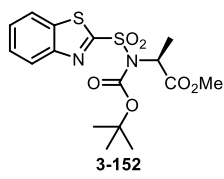


NMR and HPLC



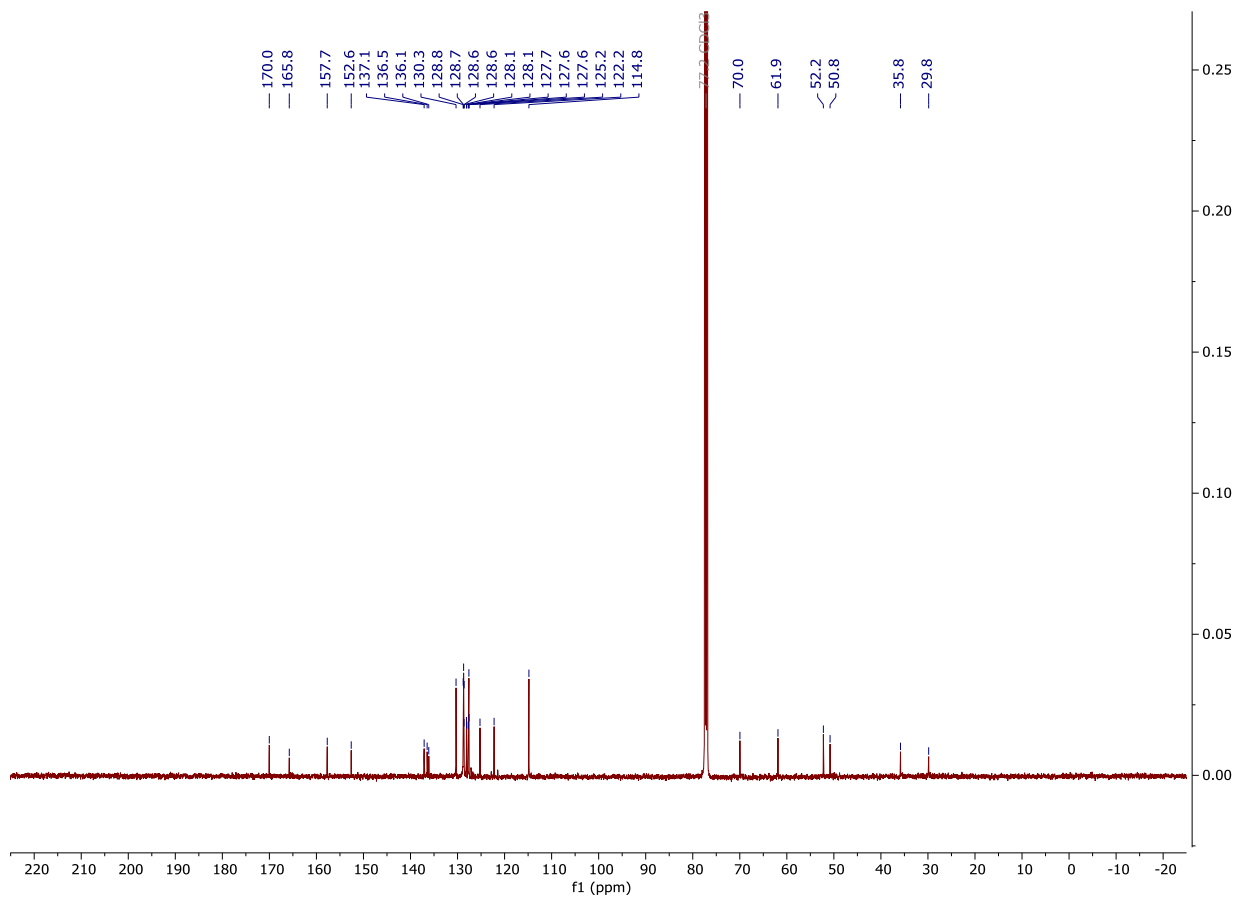
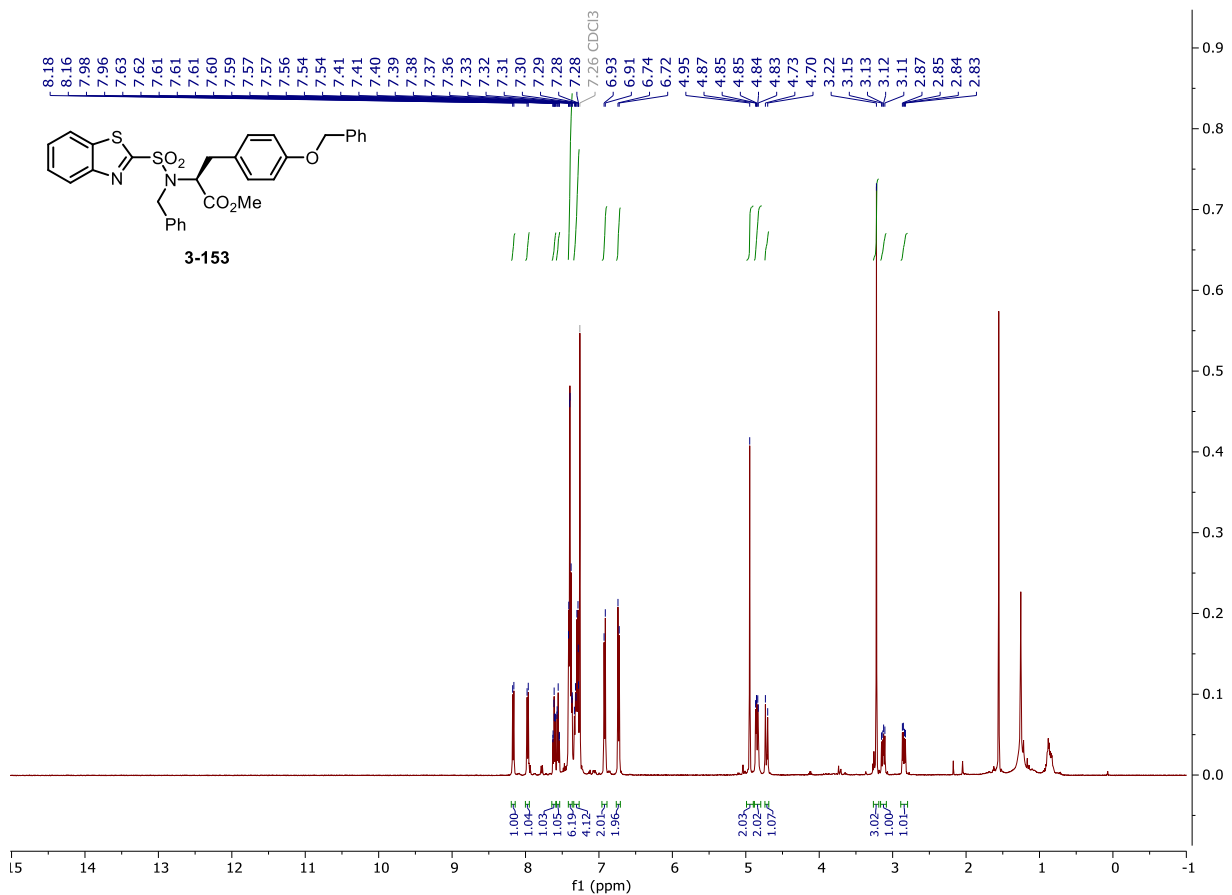
NMR and HPLC

Copy of ^1H , $^{13}\text{C}\{^1\text{H}\}$ spectra of 3-152



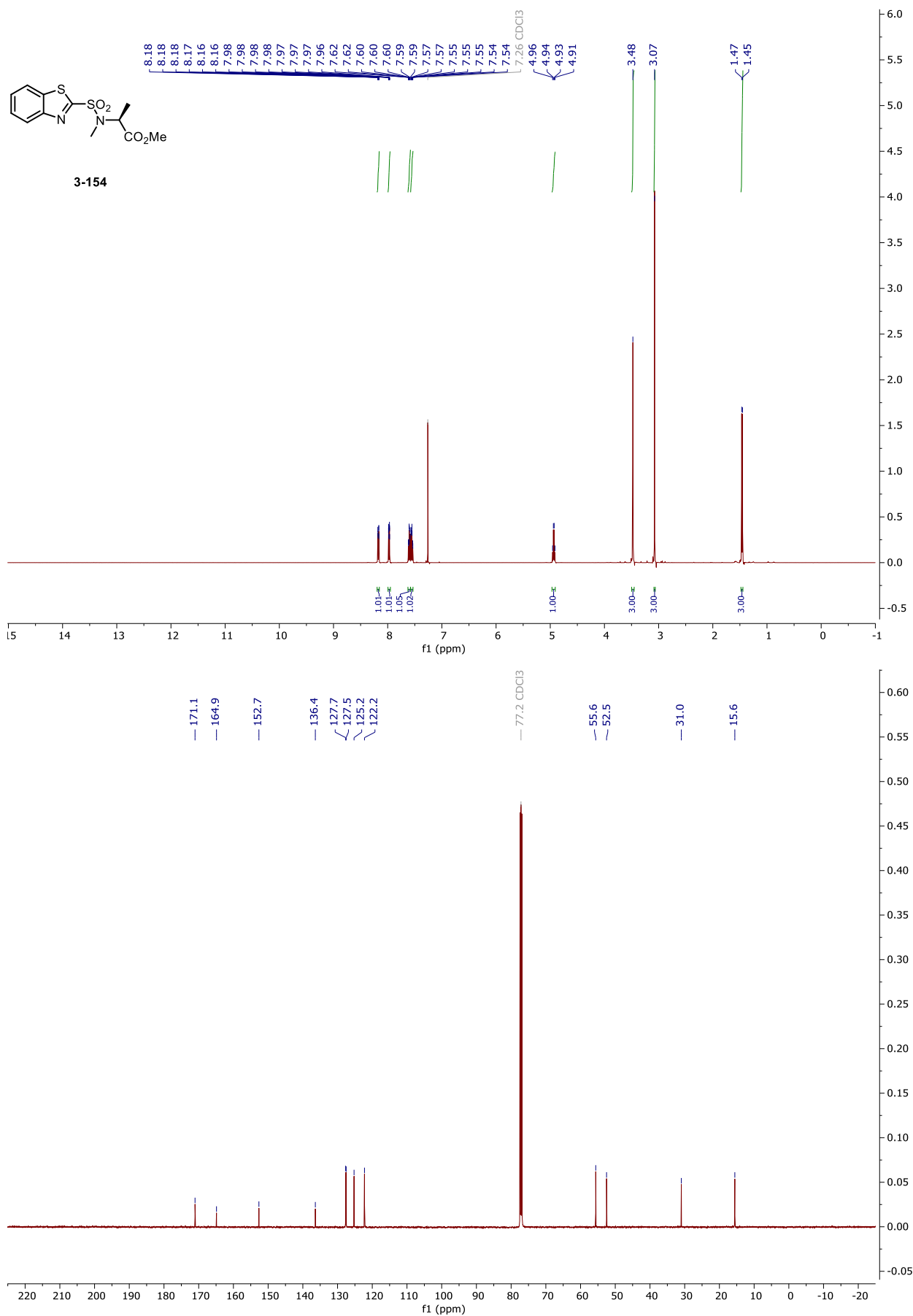
NMR and HPLC

Copy of ^1H , $^{13}\text{C}\{^1\text{H}\}$ spectra of **3-153**



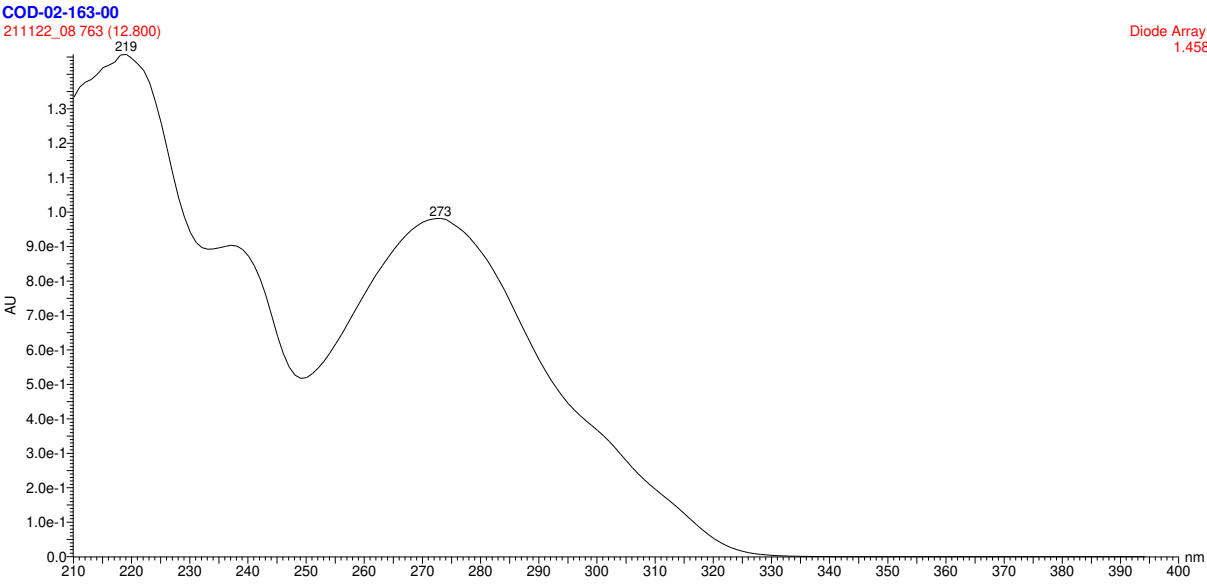
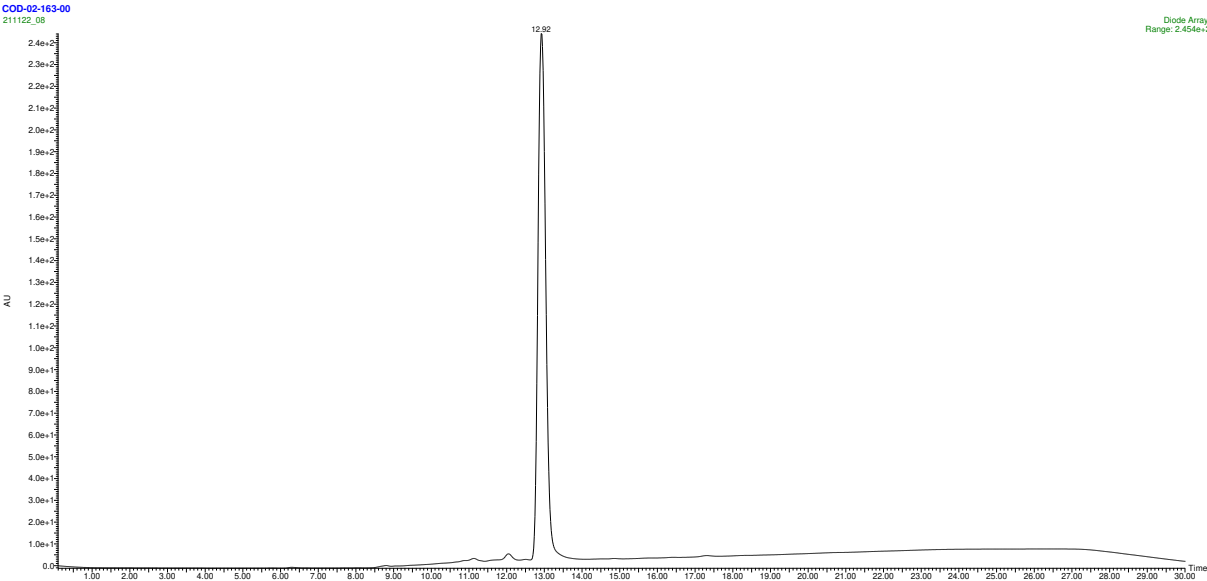
NMR and HPLC

Copy of ^1H , $^{13}\text{C}\{^1\text{H}\}$ spectra of 3-154



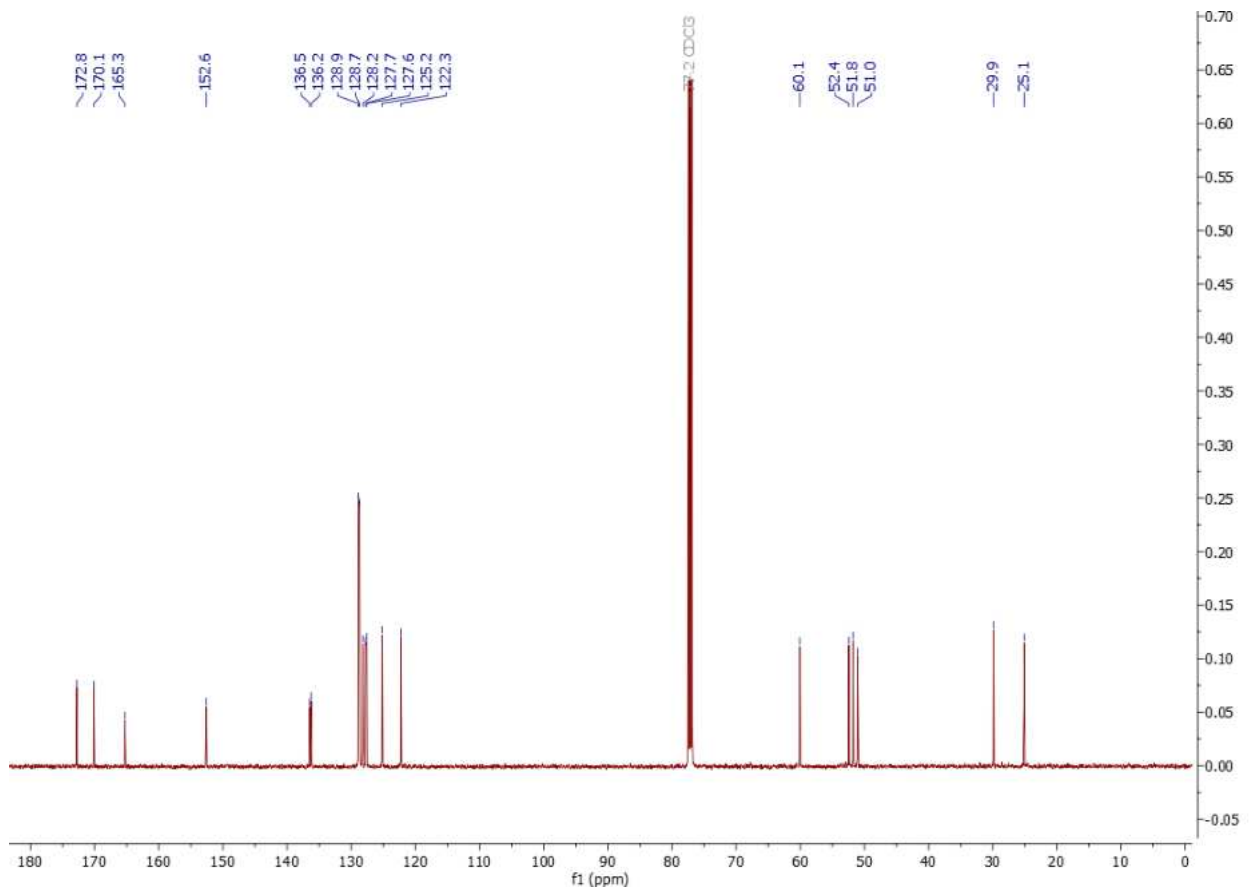
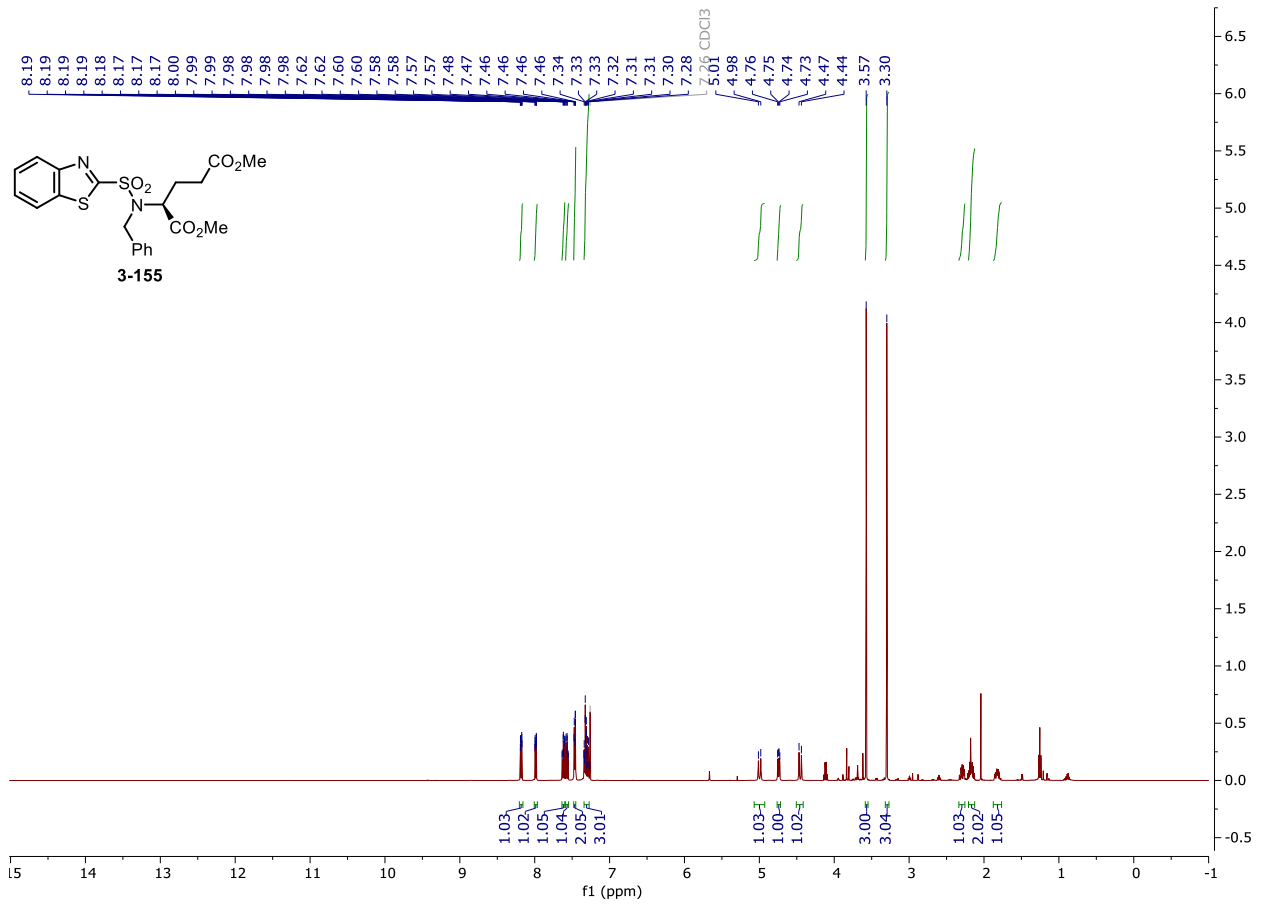
NMR and HPLC

HPLC chromatograms of 3-154



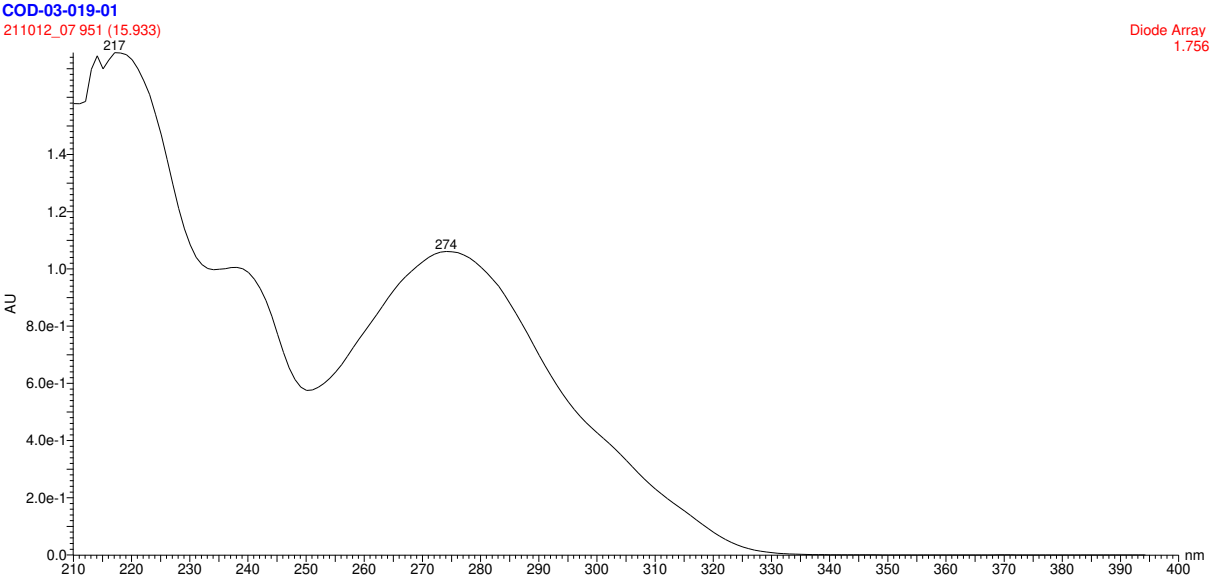
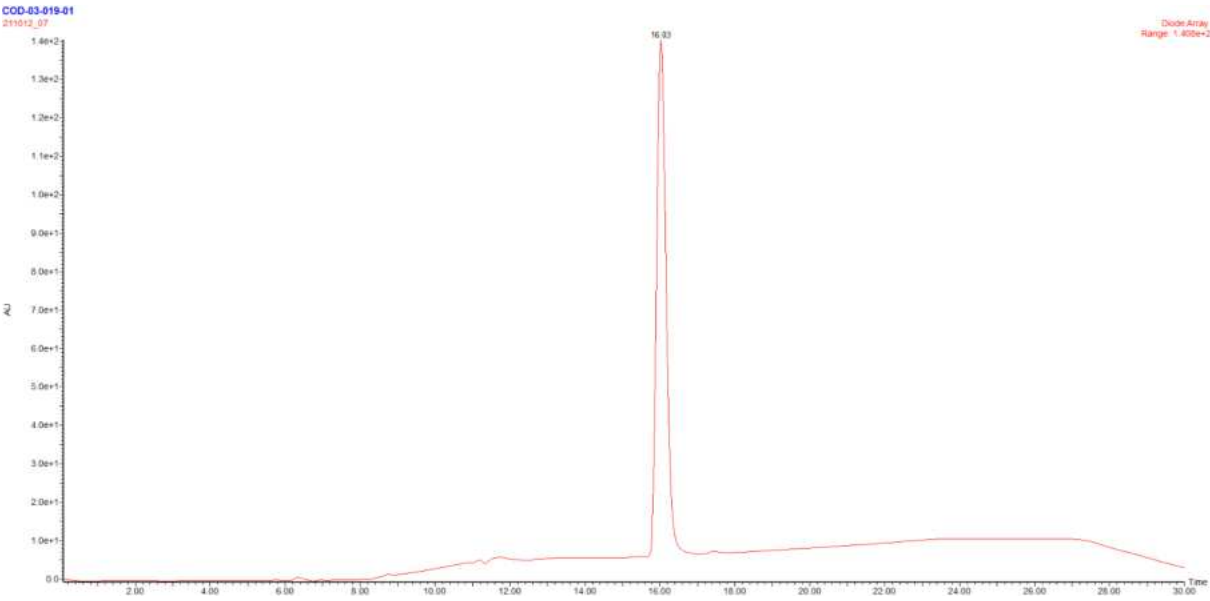
NMR and HPLC

Copy of ^1H , $^{13}\text{C}\{^1\text{H}\}$ spectra of 3-155



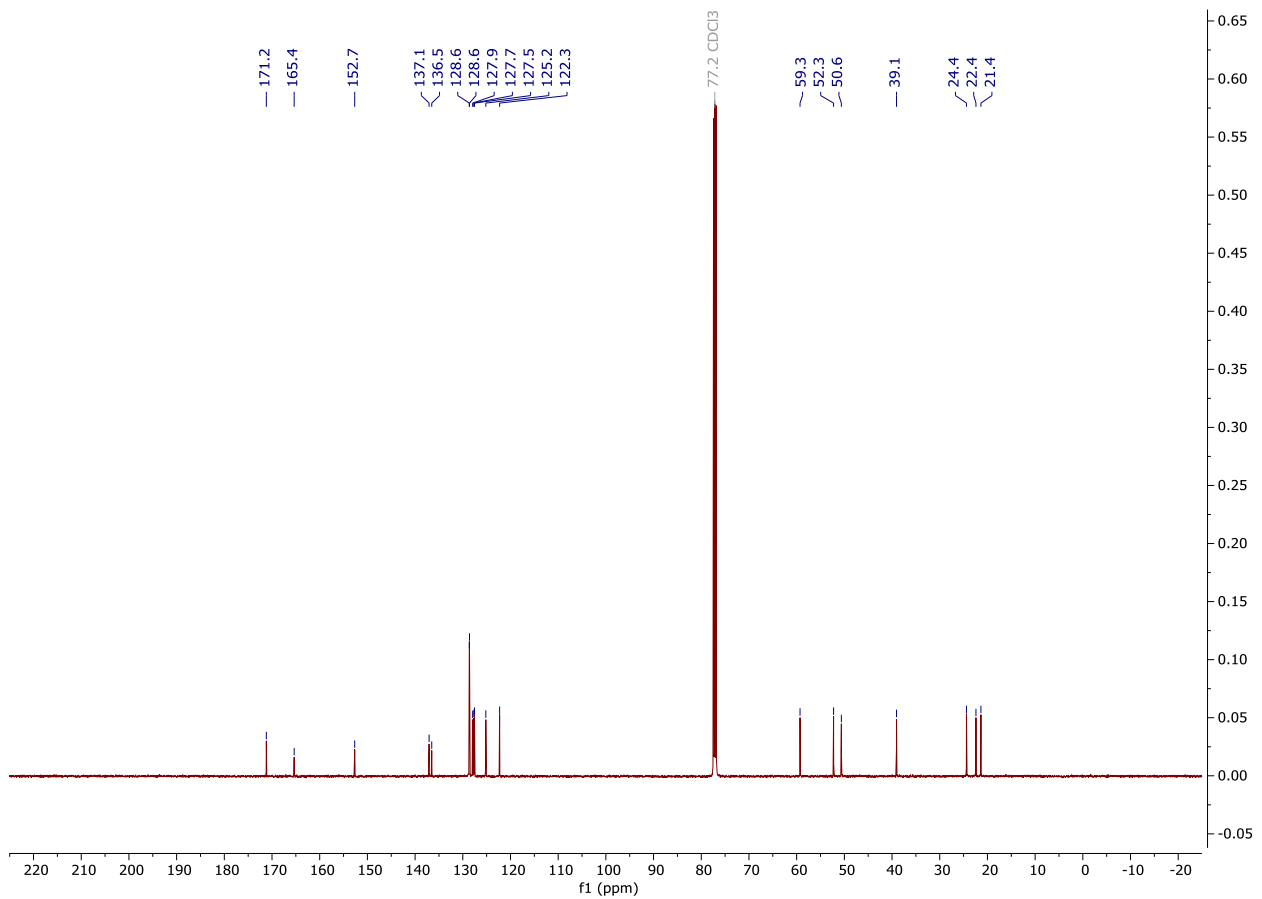
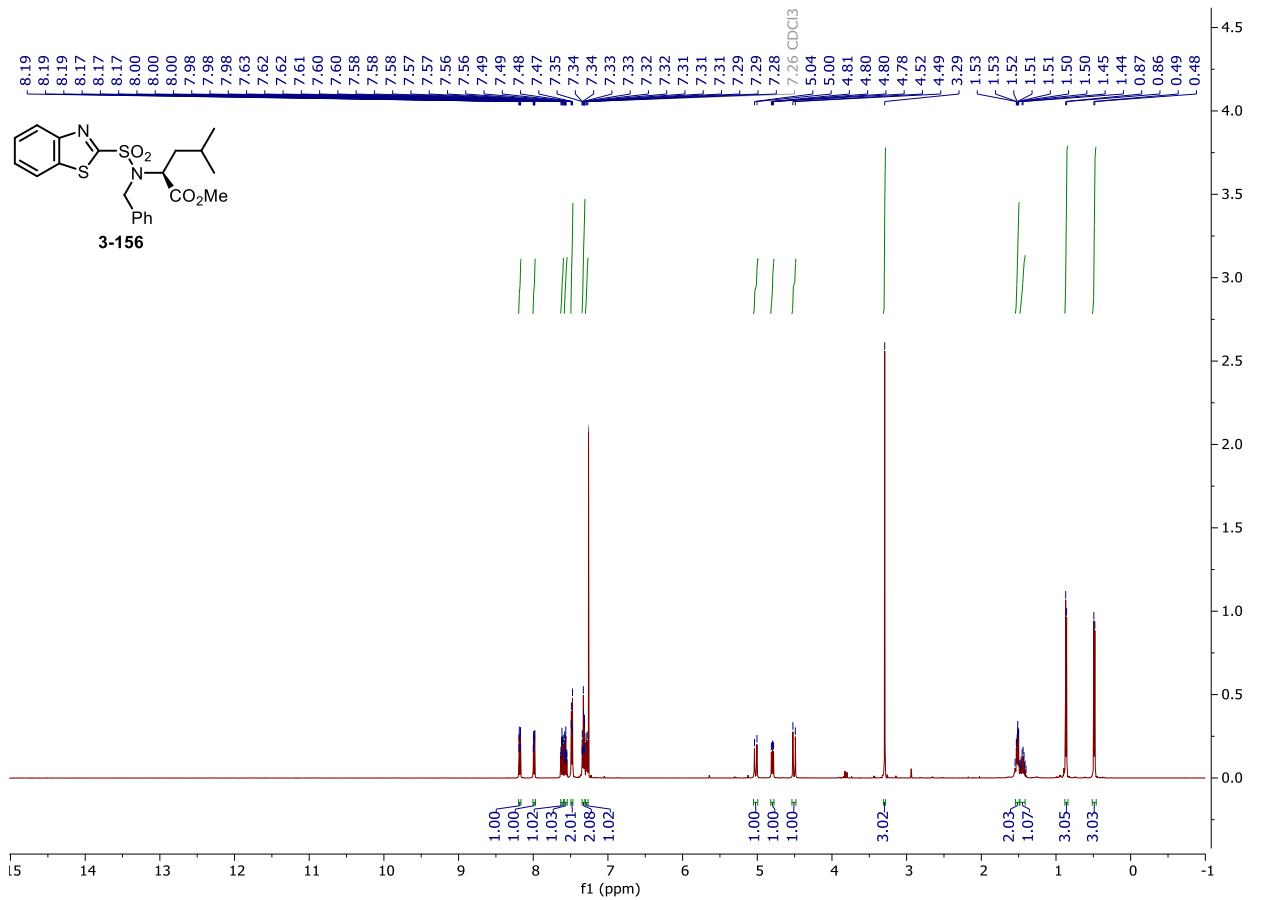
NMR and HPLC

HPLC chromatograms of 3-155



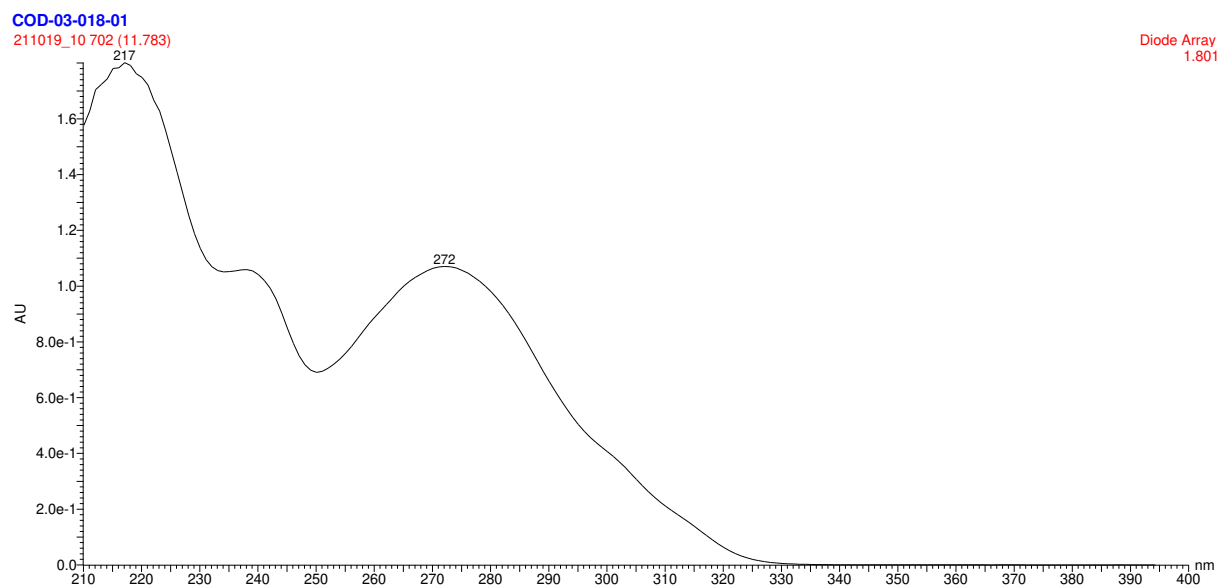
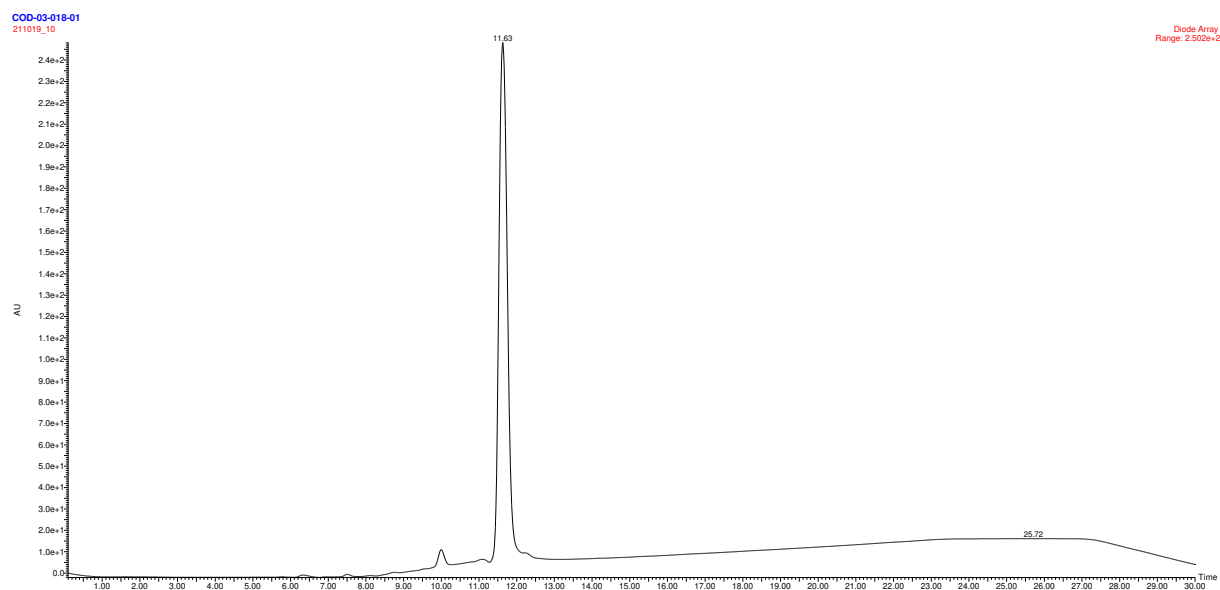
NMR and HPLC

Copy of ^1H , $^{13}\text{C}\{^1\text{H}\}$ spectra of **3-156**



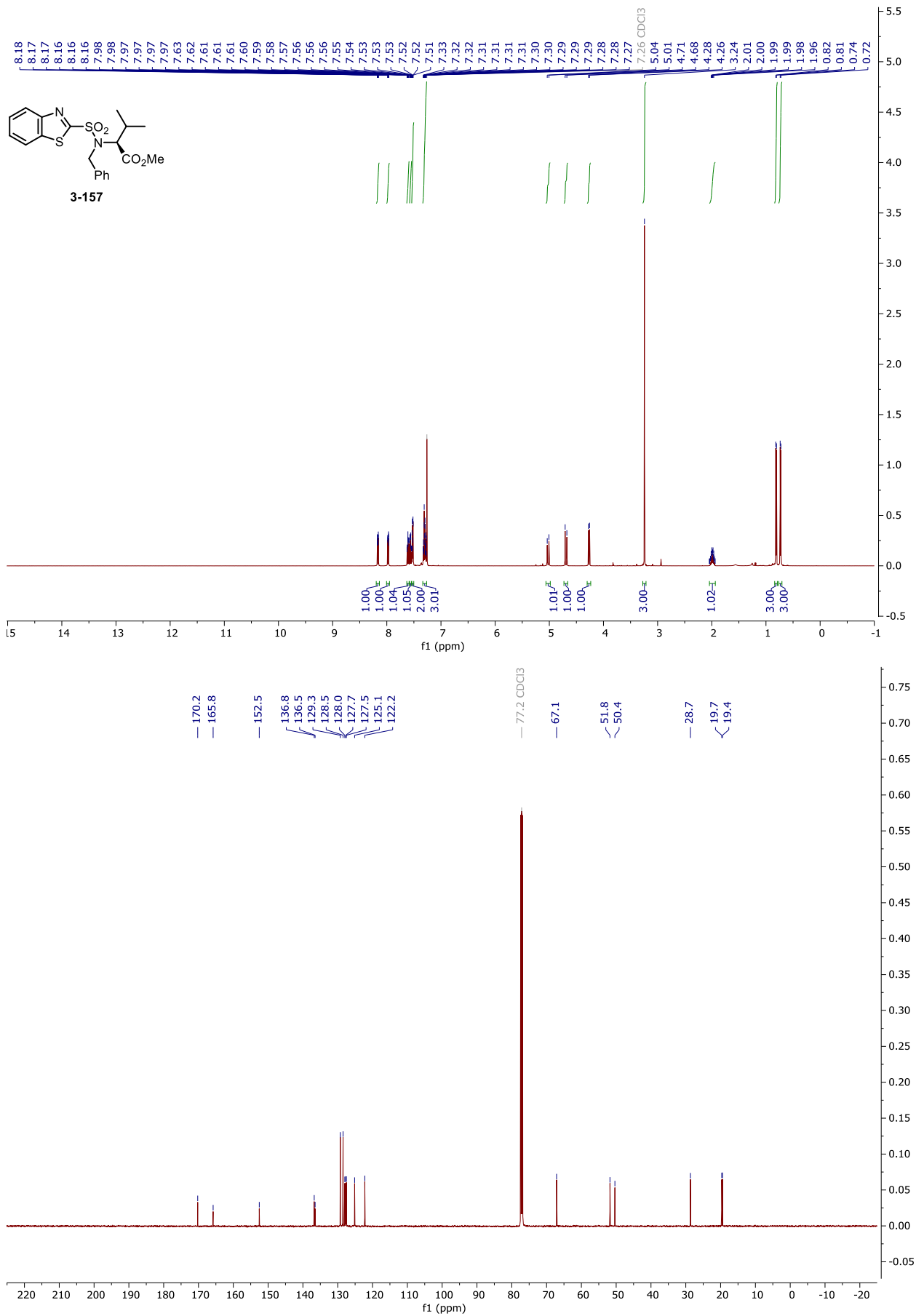
NMR and HPLC

HPLC chromatograms of 3-156



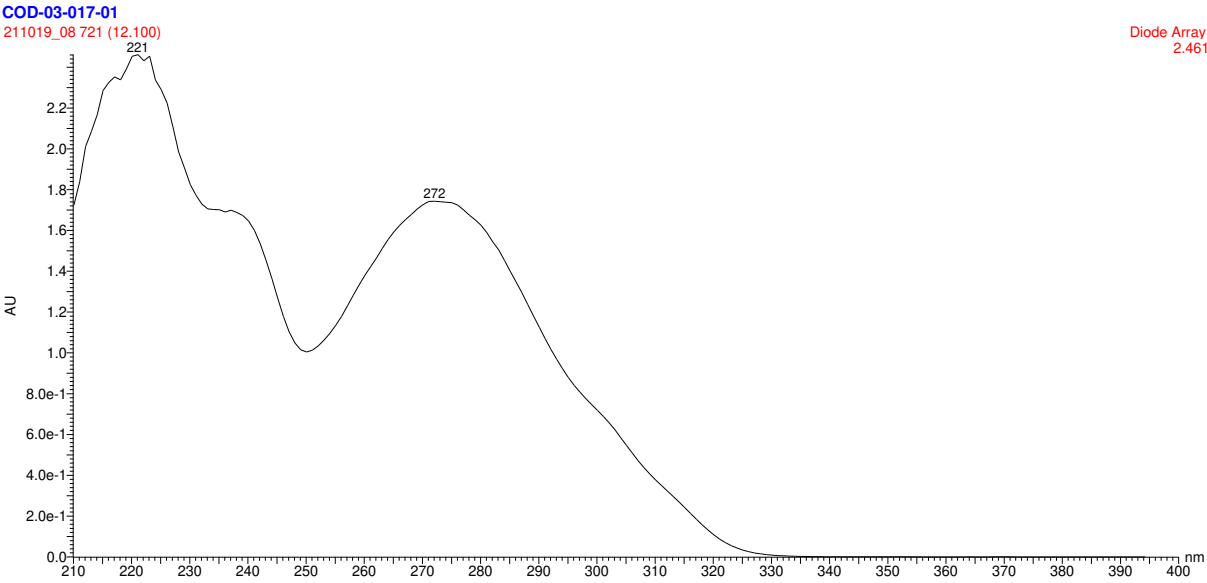
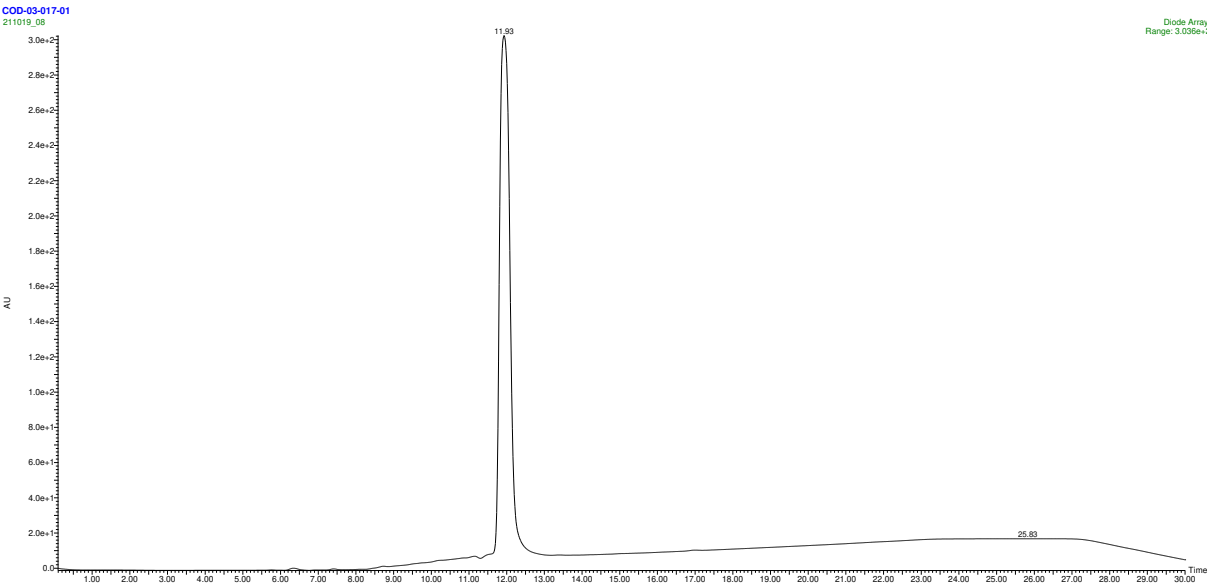
NMR and HPLC

Copy of ^1H , $^{13}\text{C}\{^1\text{H}\}$ spectra of **3-157**



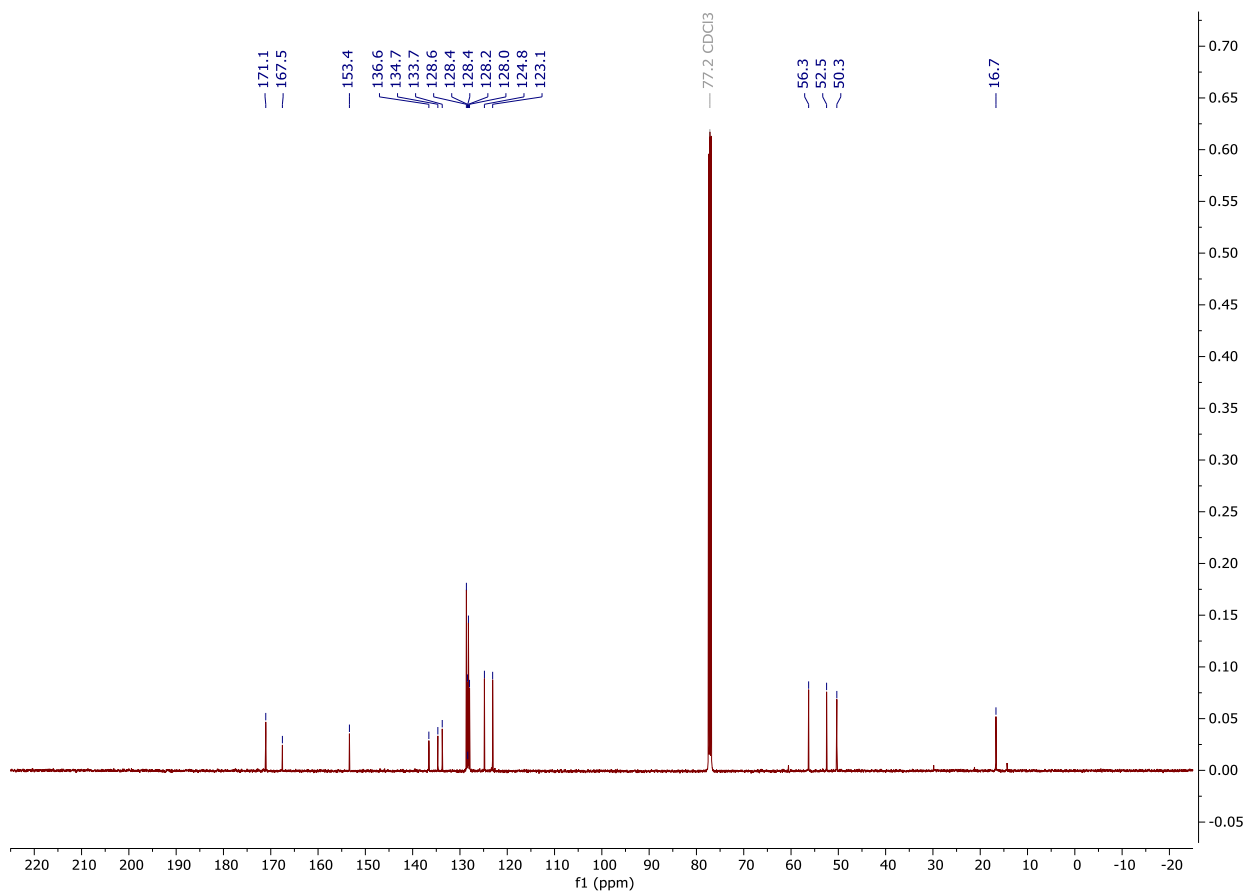
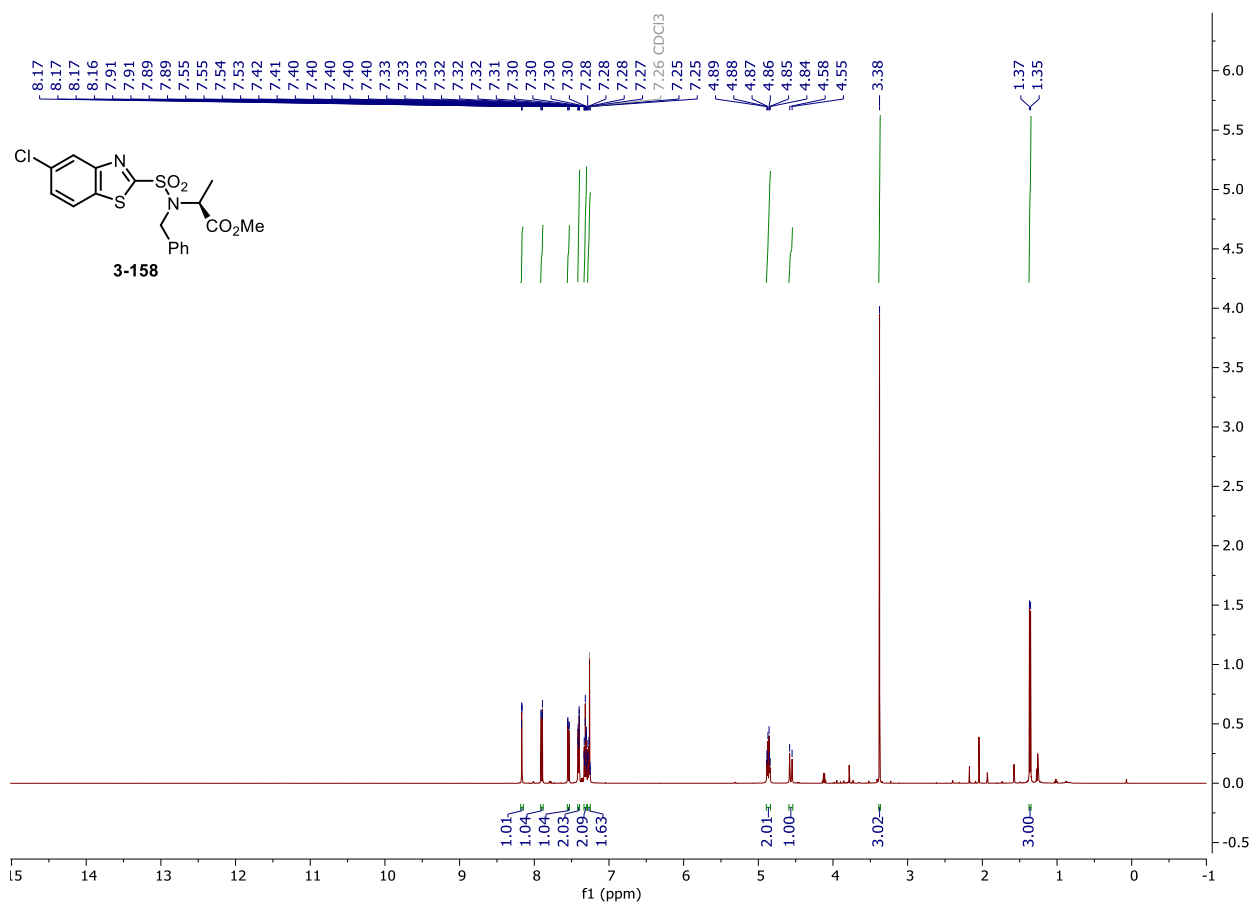
NMR and HPLC

HPLC chromatograms of 3-157



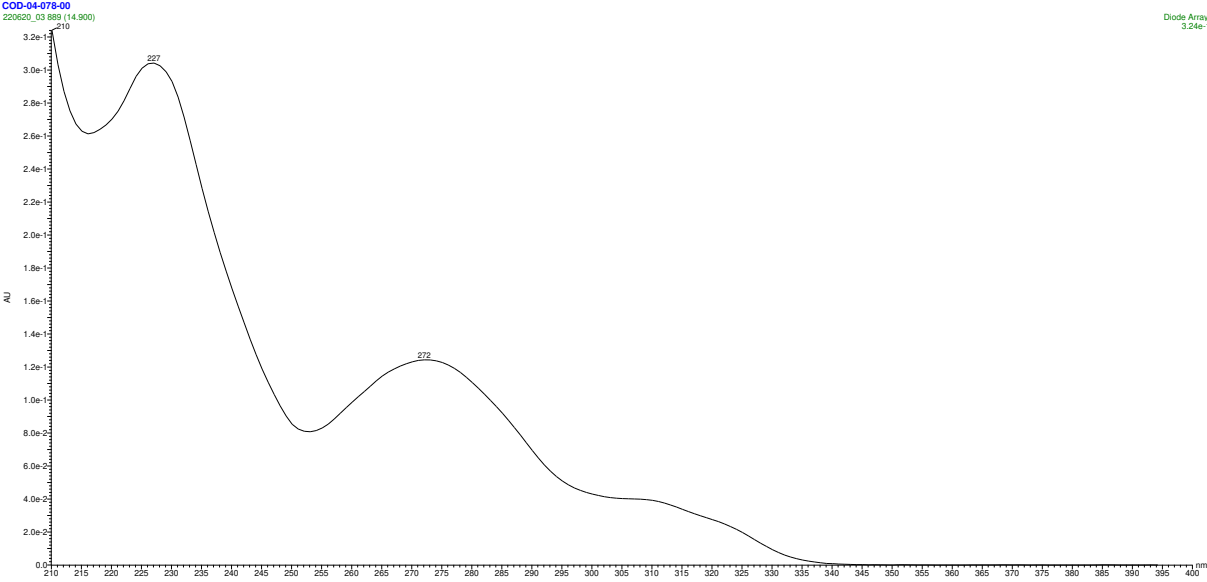
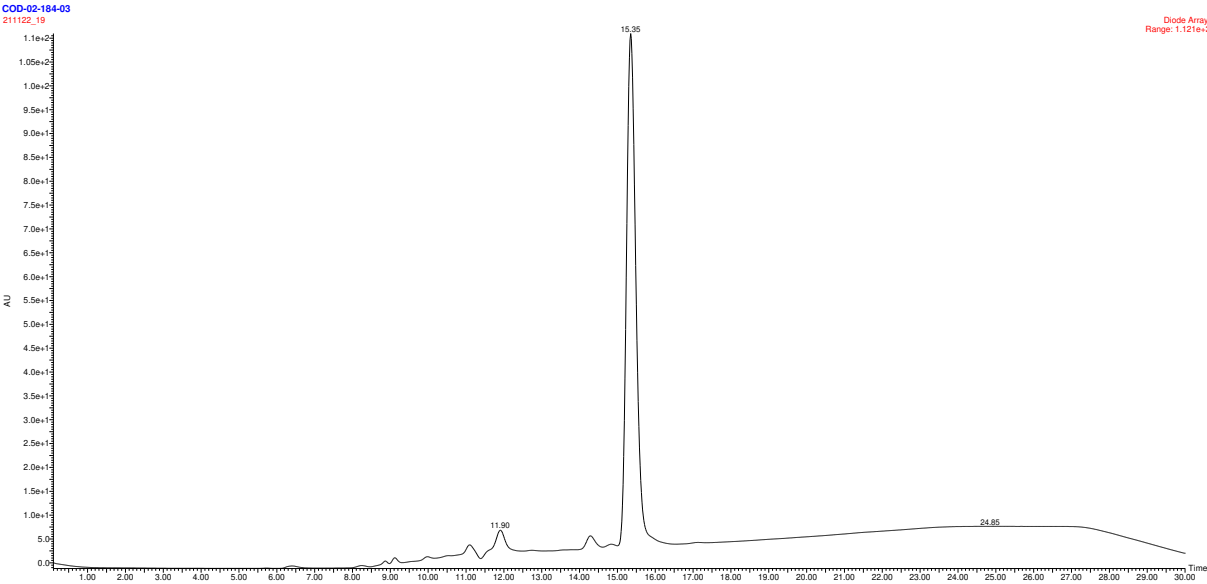
NMR and HPLC

Copy of ^1H , $^{13}\text{C}\{^1\text{H}\}$ spectra of 3-158



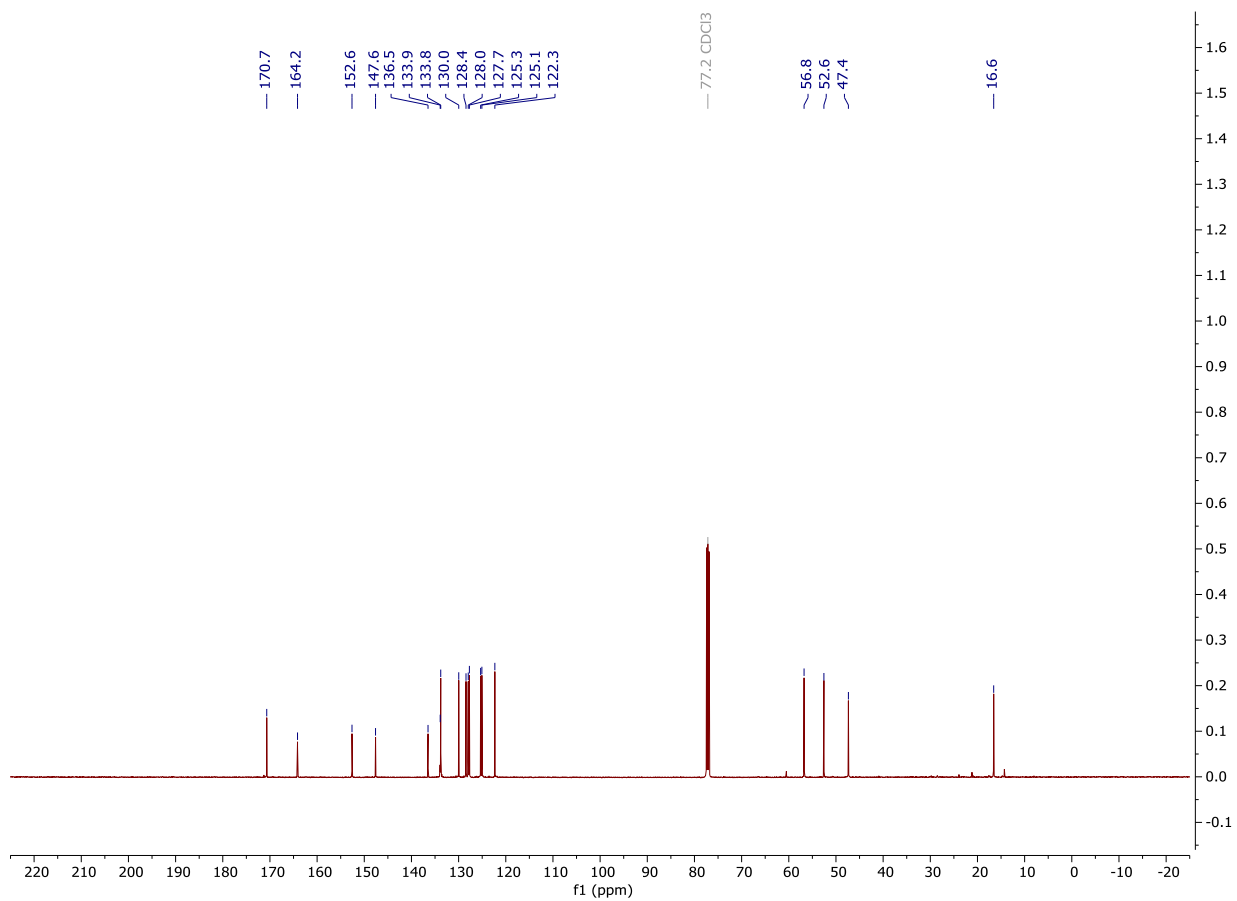
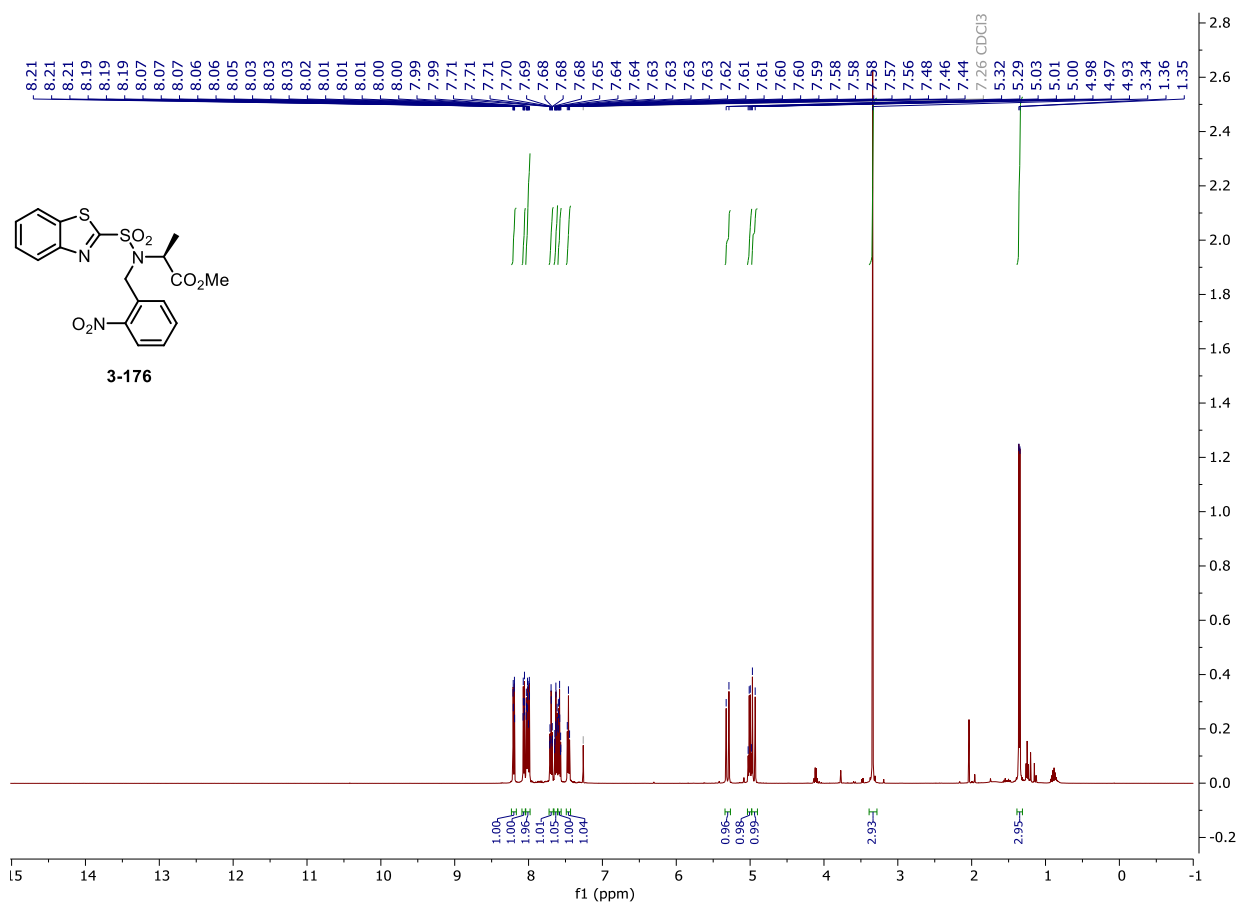
NMR and HPLC

HPLC chromatograms of 3-158



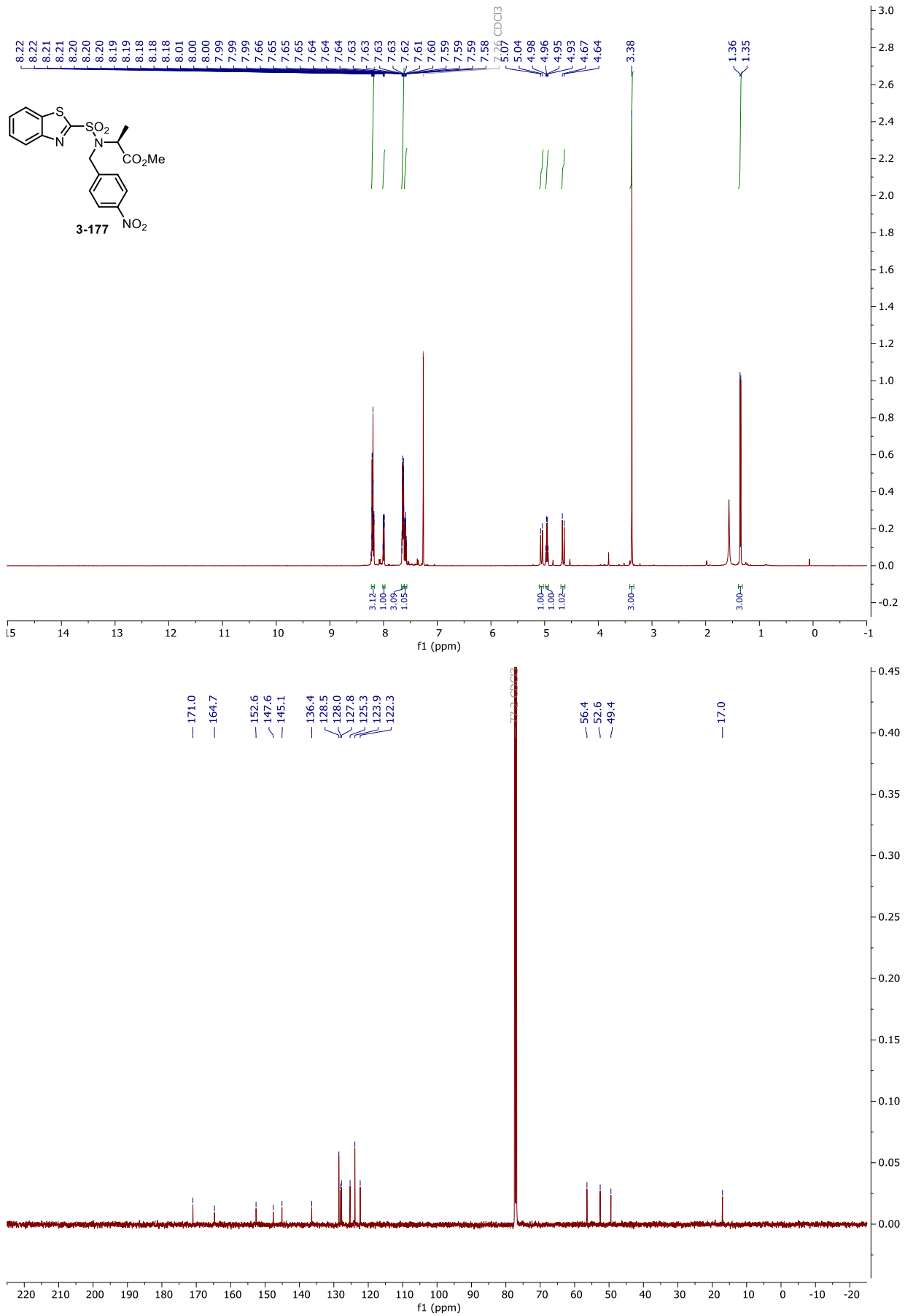
NMR and HPLC

Copy of ^1H , $^{13}\text{C}\{^1\text{H}\}$ spectra of 3-176



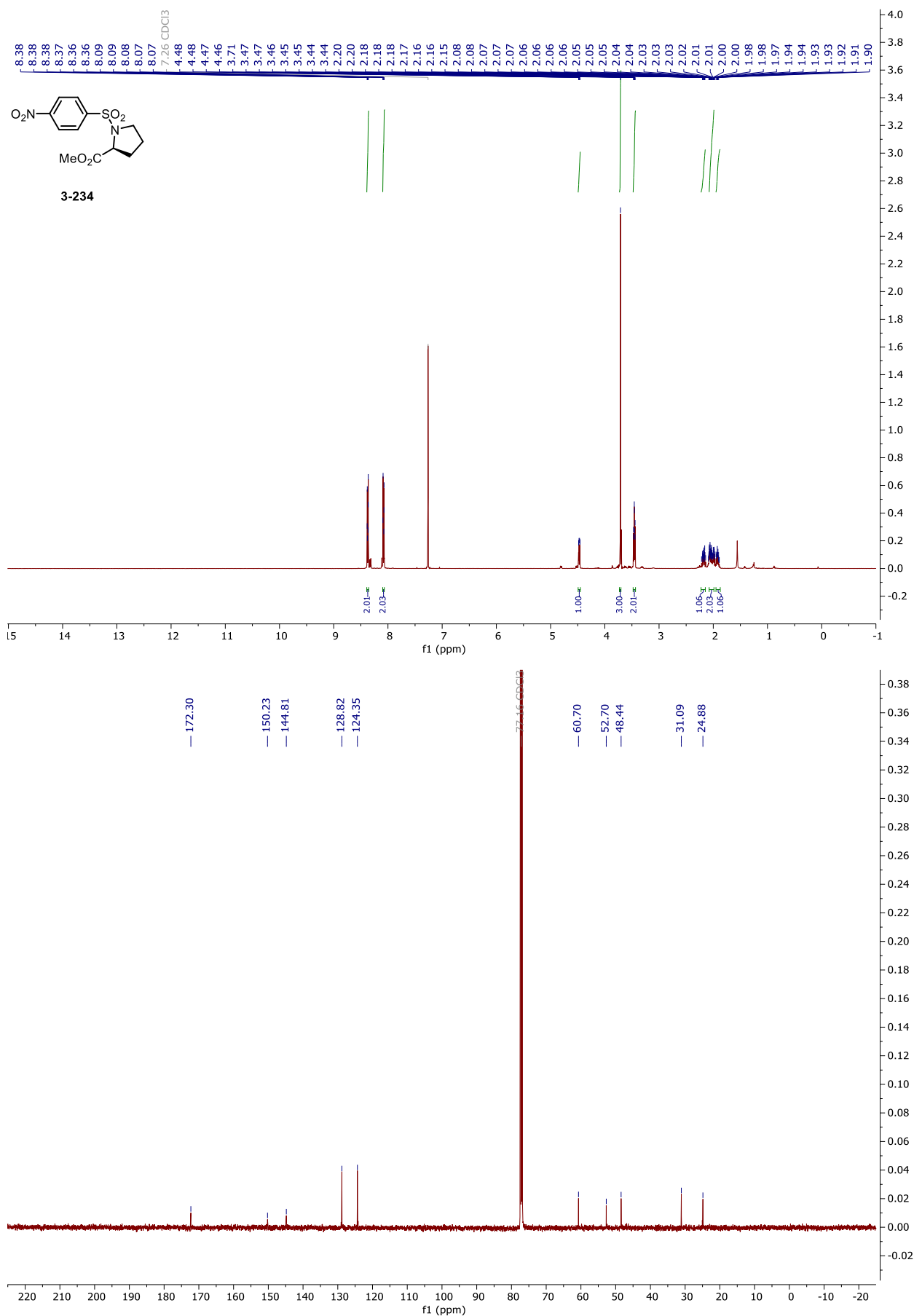
NMR and HPLC

Copy of ^1H , $^{13}\text{C}\{^1\text{H}\}$ spectra of 3-177



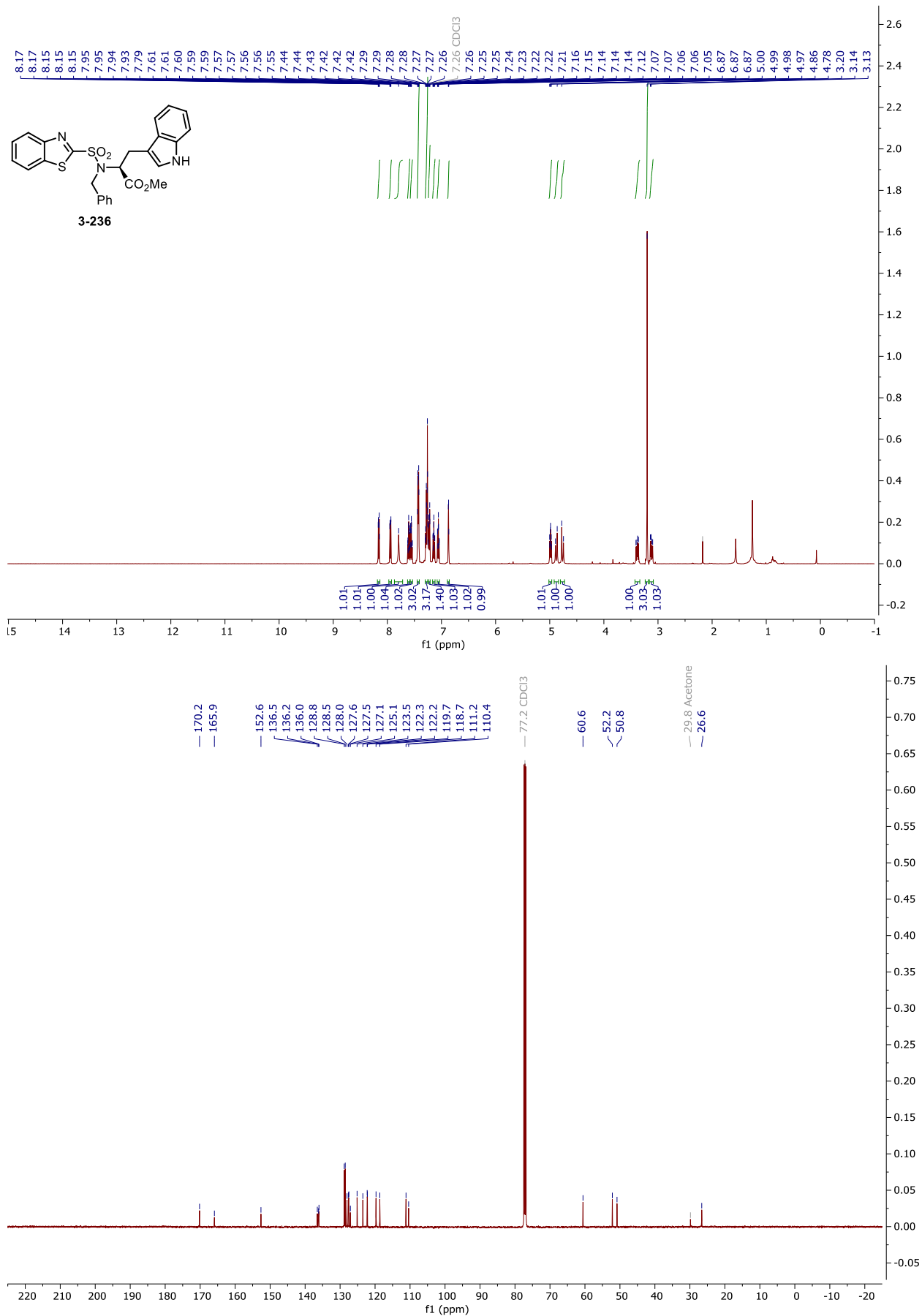
NMR and HPLC

Copy of ^1H , $^{13}\text{C}\{^1\text{H}\}$ spectra of 3-234



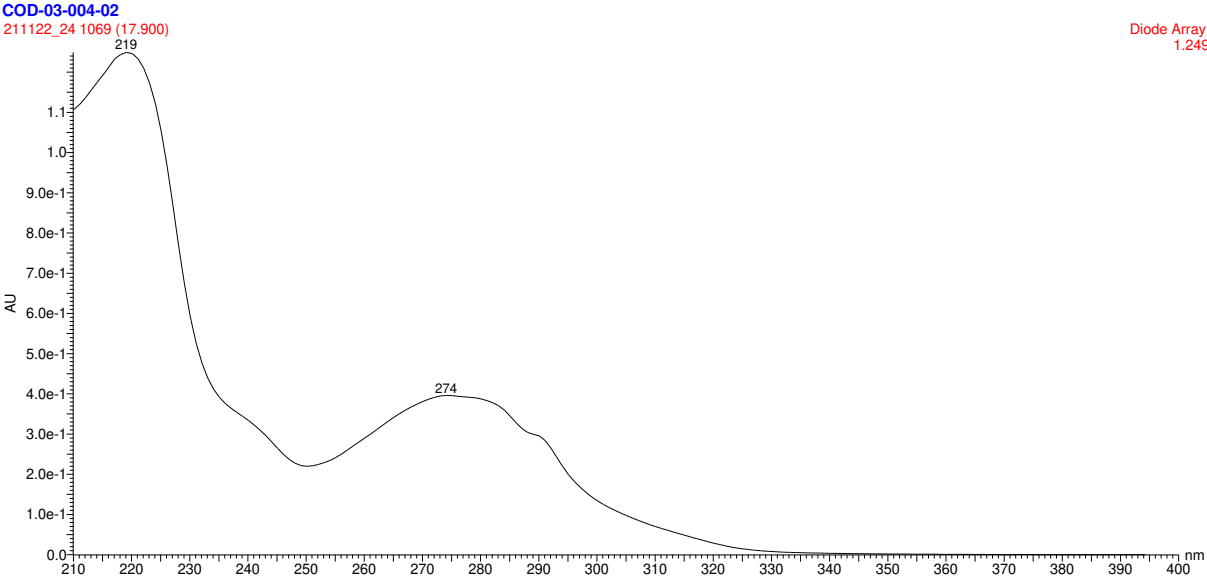
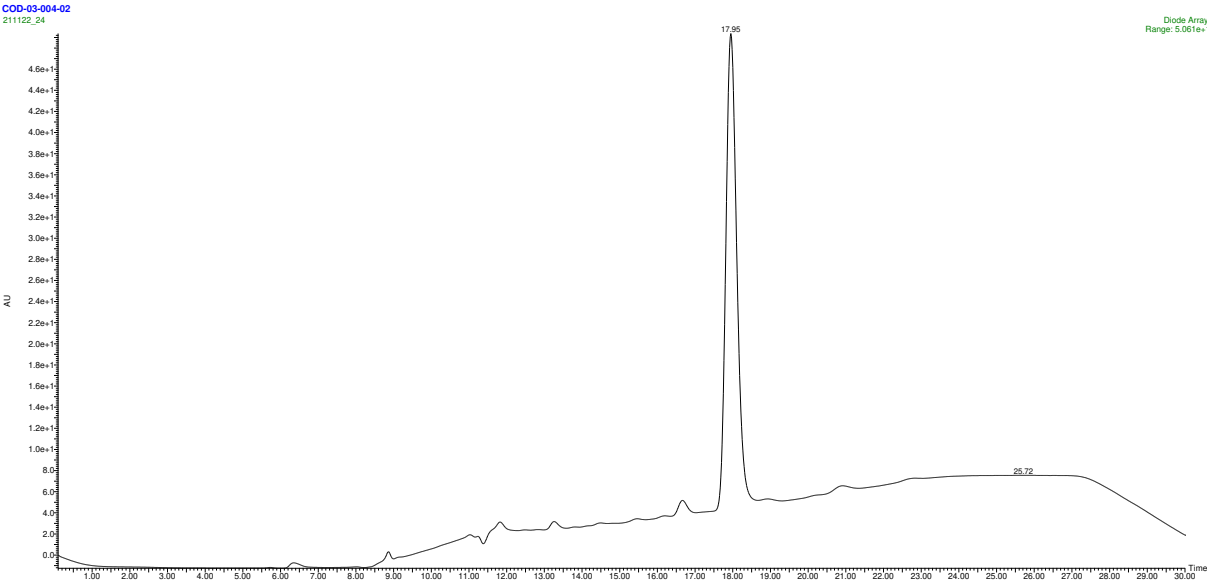
NMR and HPLC

Copy of ^1H , $^{13}\text{C}\{^1\text{H}\}$ spectra of 3-236



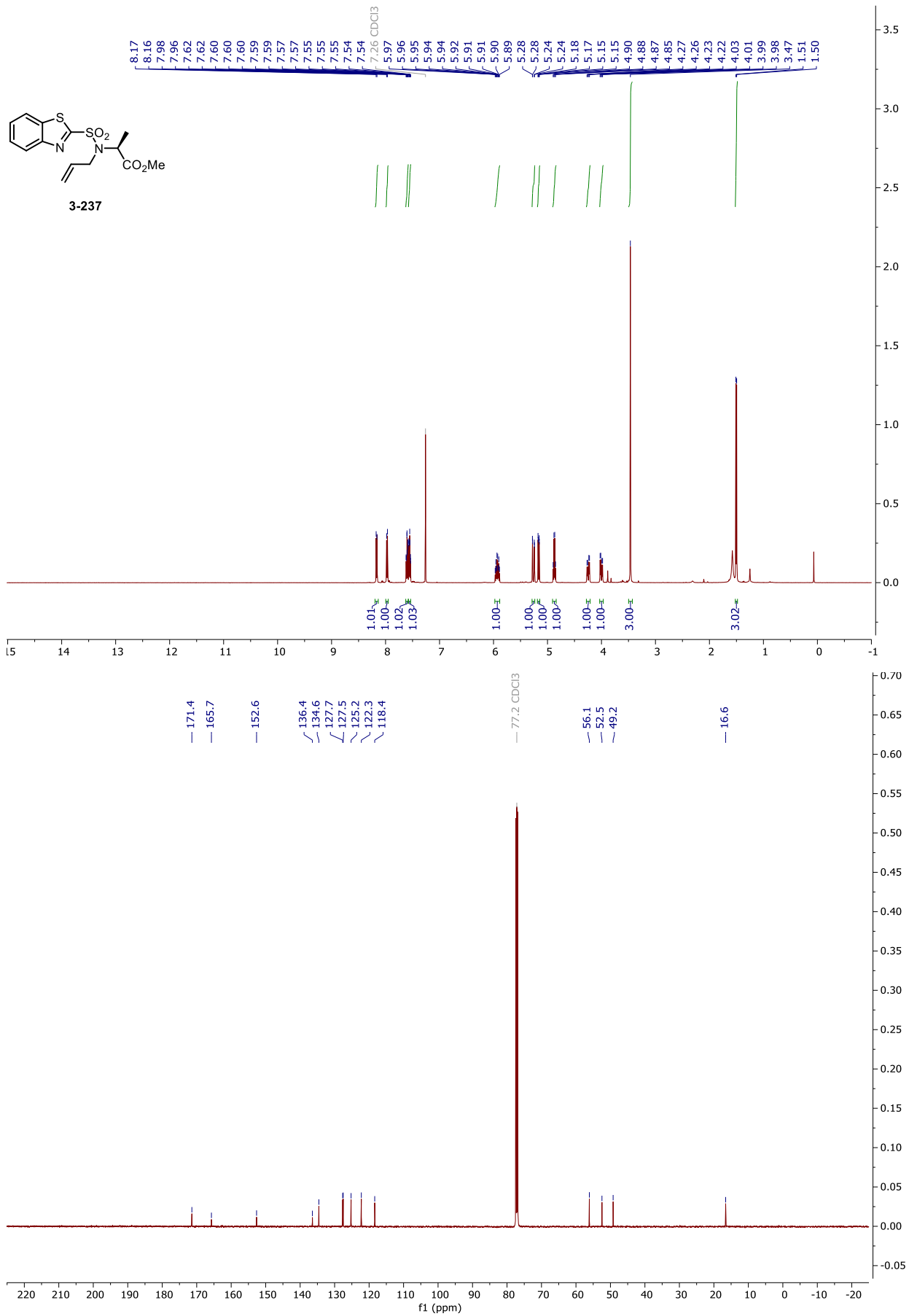
NMR and HPLC

HPLC chromatograms of 3-236



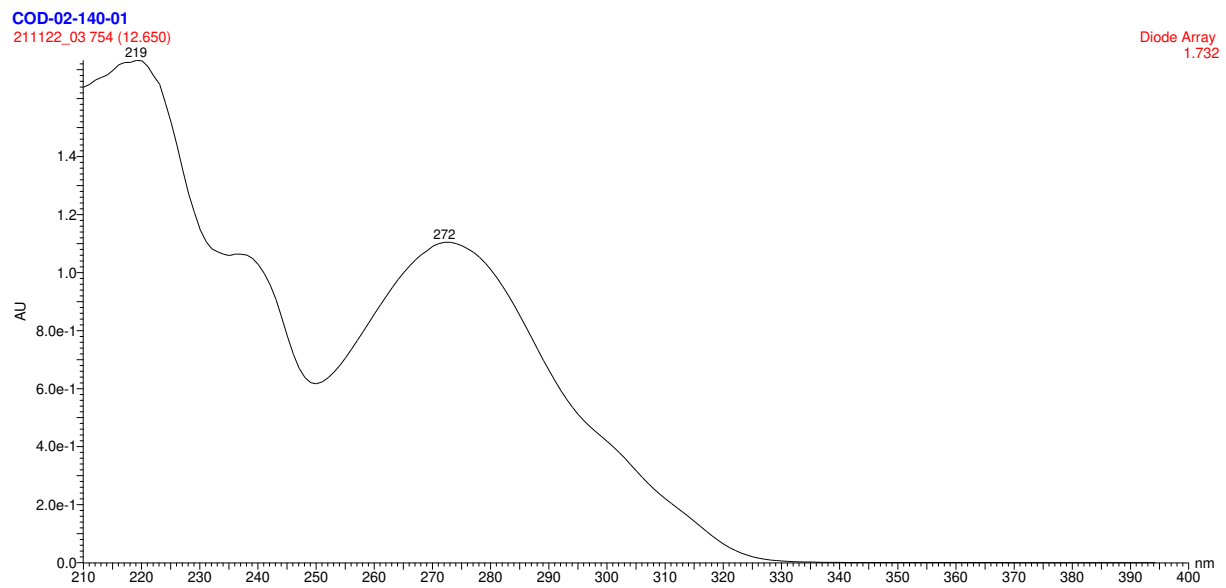
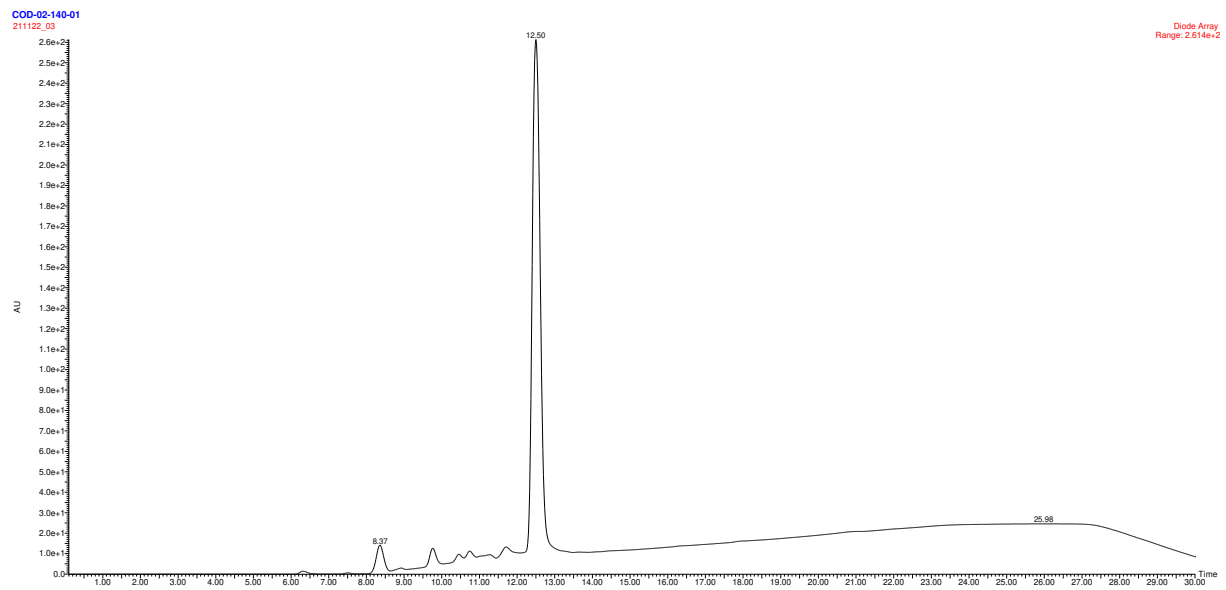
NMR and HPLC

Copy of ^1H , $^{13}\text{C}\{^1\text{H}\}$ spectra of 3-237



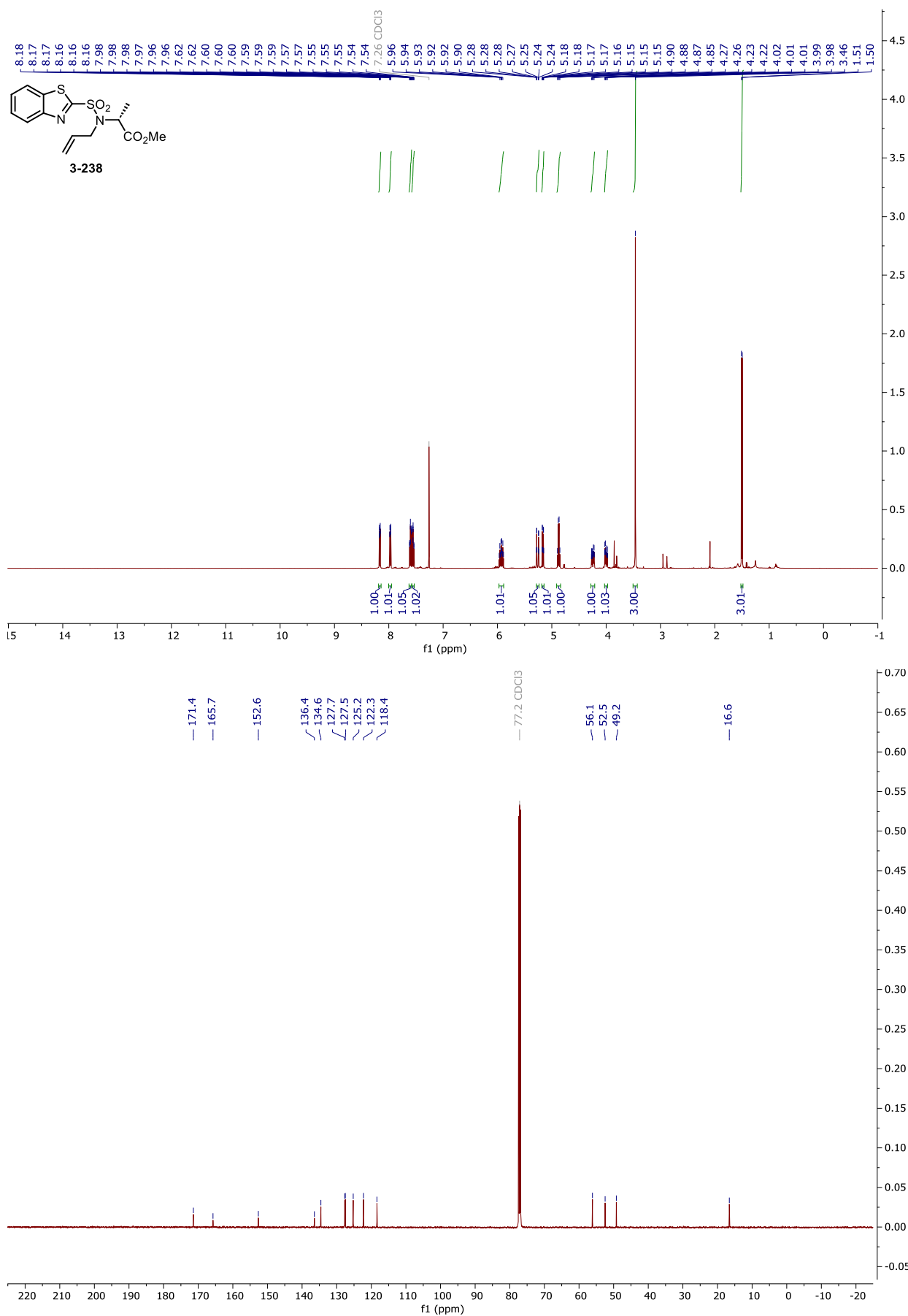
NMR and HPLC

HPLC chromatograms of 3-237



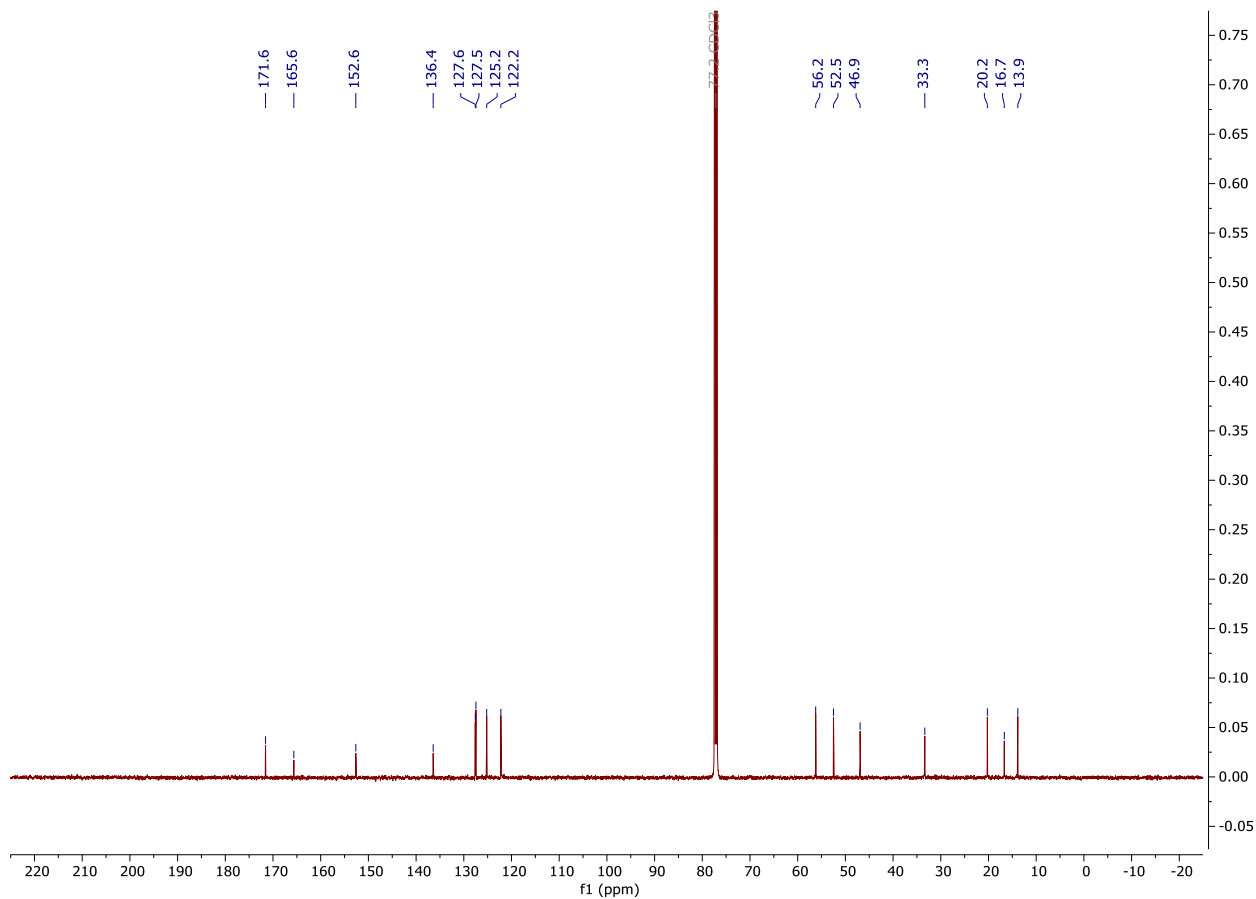
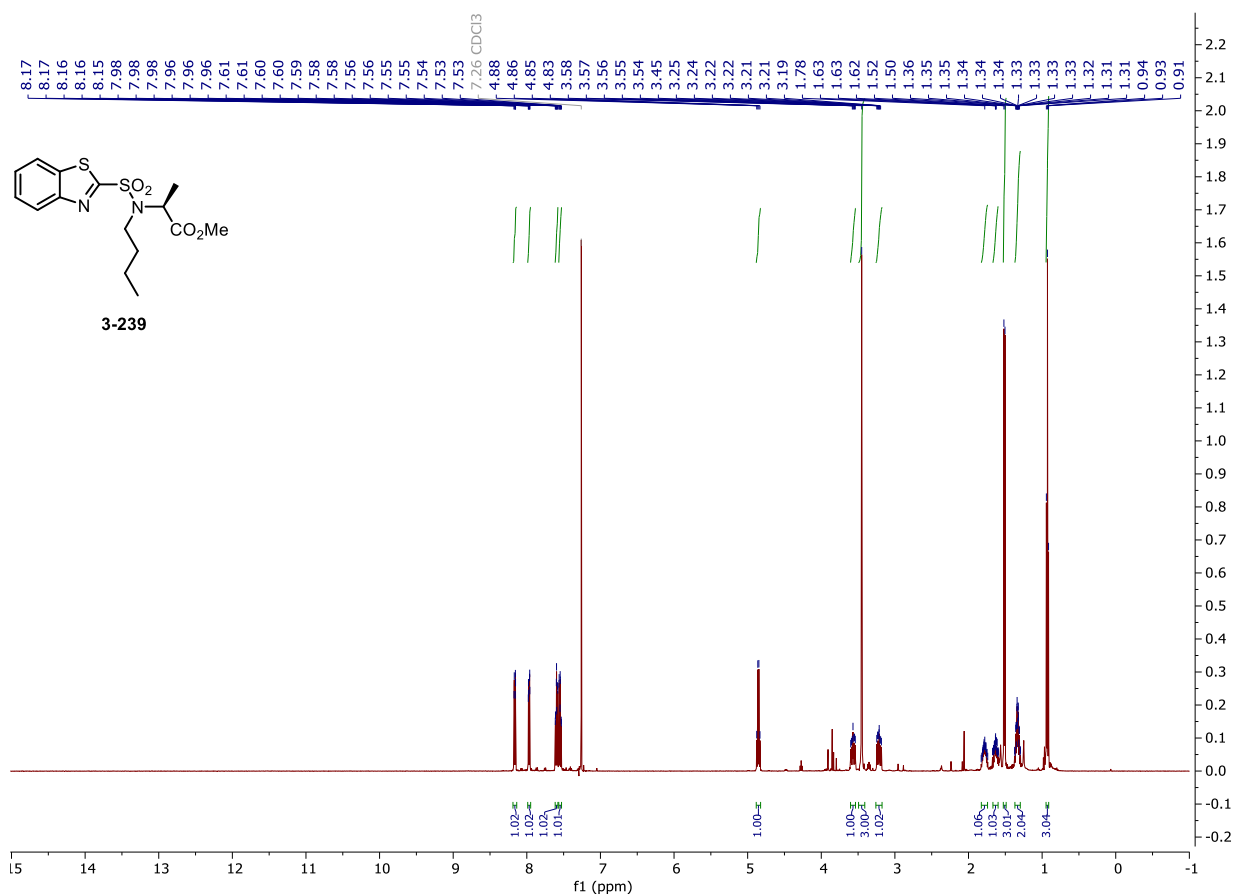
NMR and HPLC

Copy of ^1H , $^{13}\text{C}\{^1\text{H}\}$ spectra of 3-238



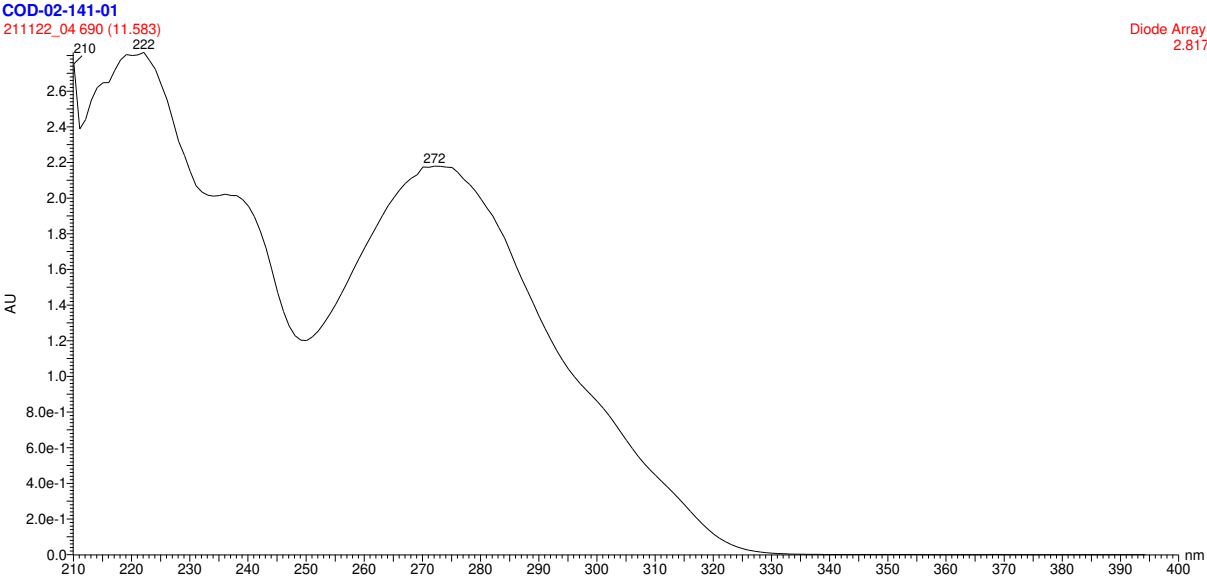
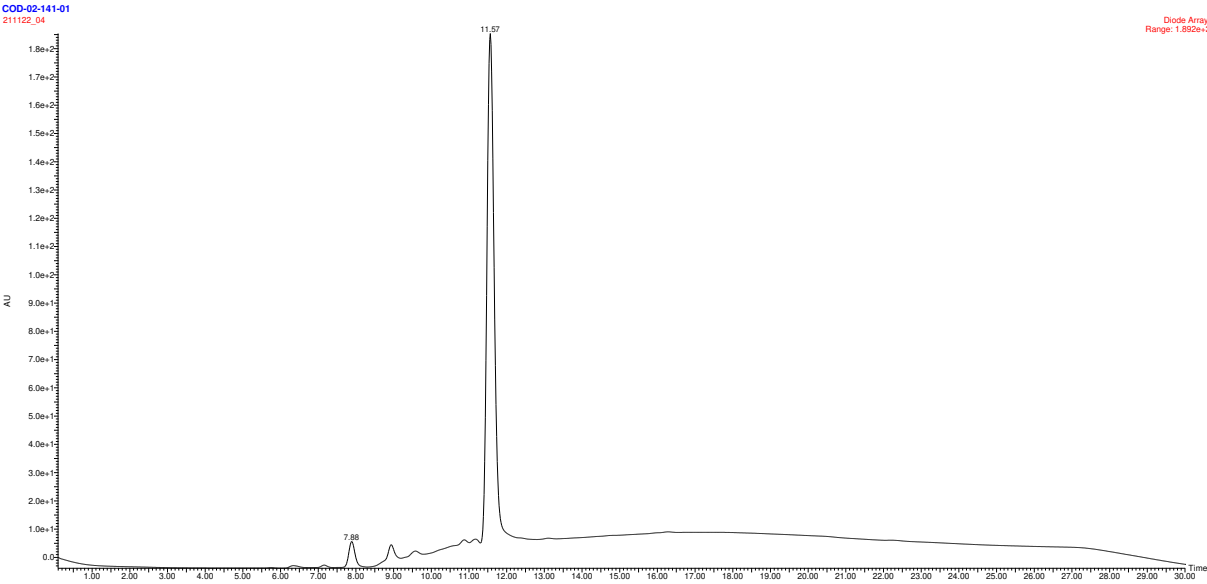
NMR and HPLC

Copy of ^1H , $^{13}\text{C}\{^1\text{H}\}$ spectra of 3-239



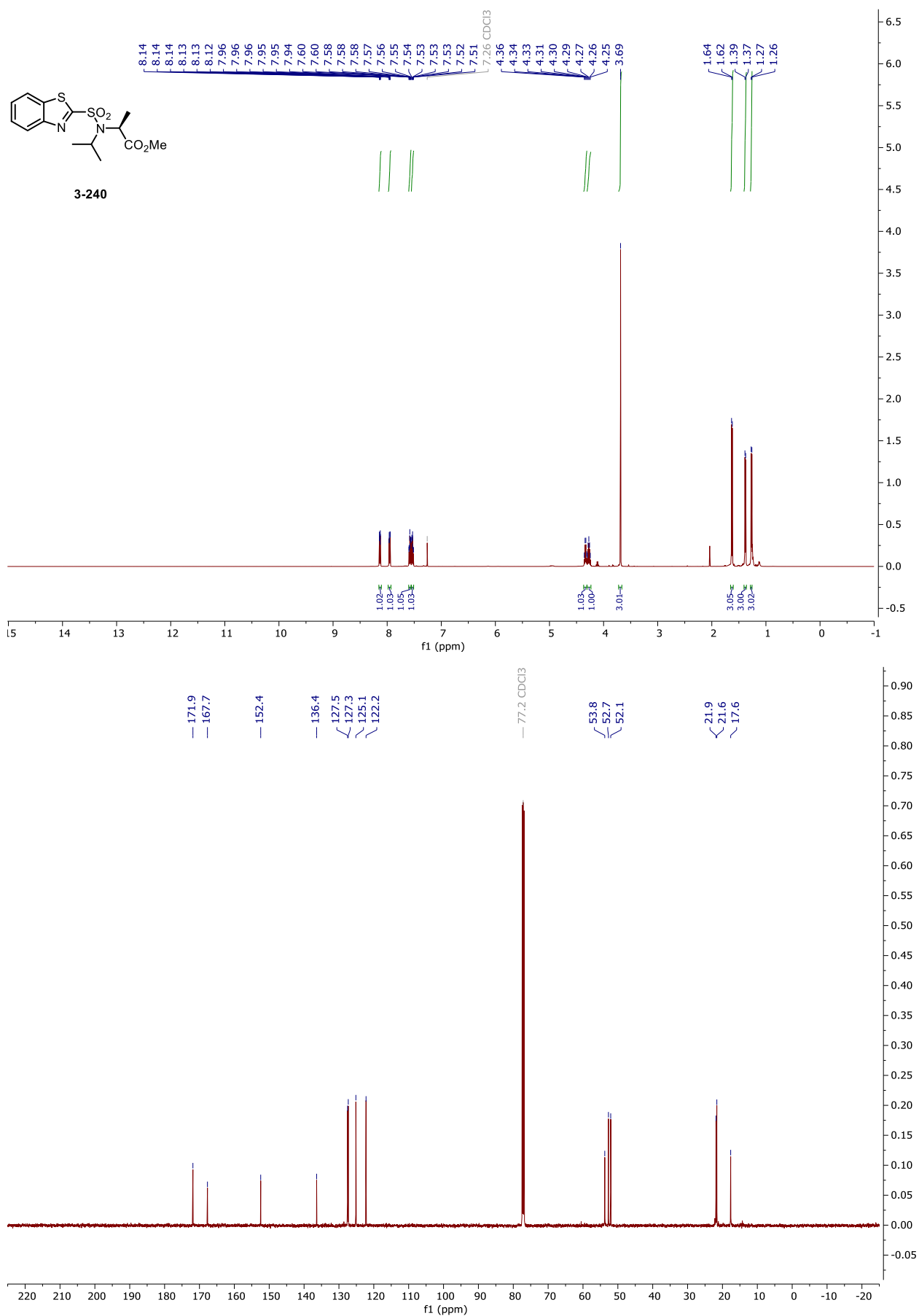
NMR and HPLC

HPLC chromatograms of 3-239



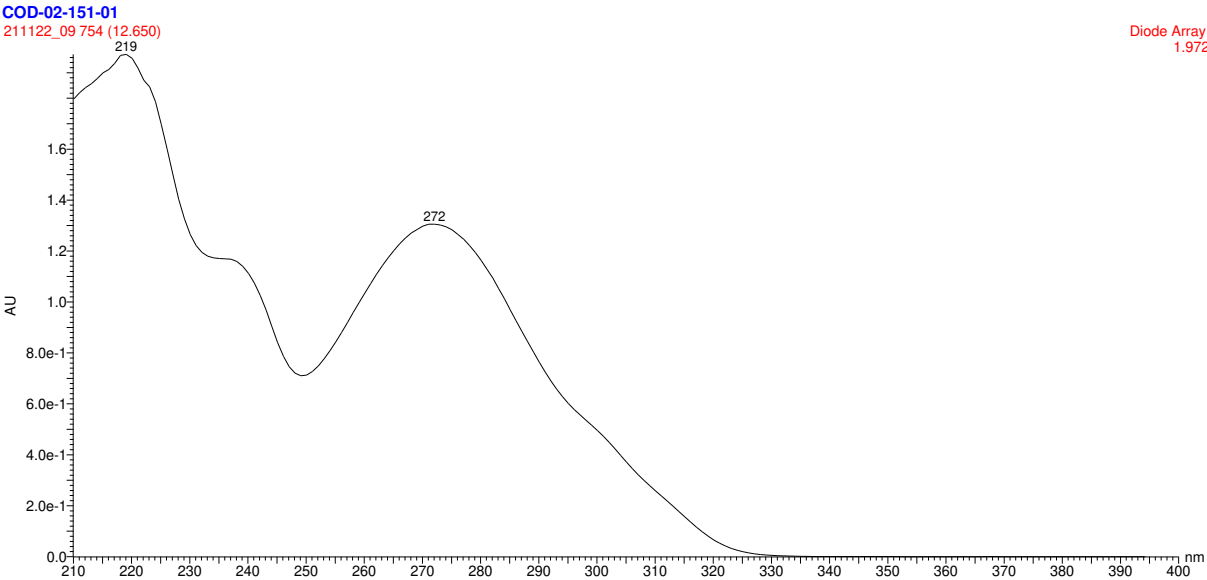
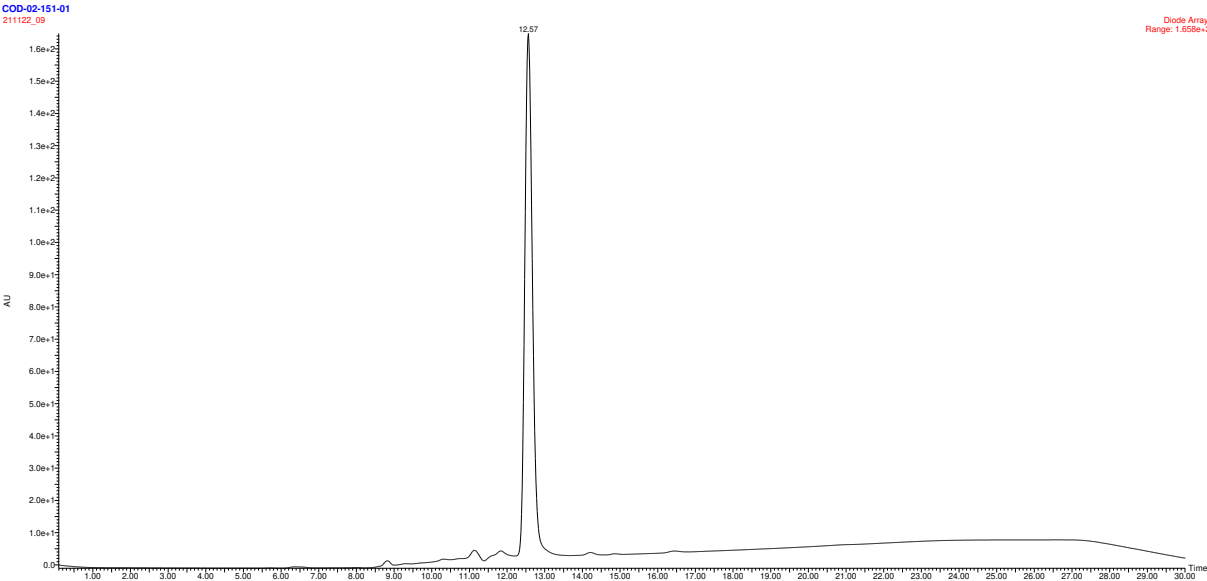
NMR and HPLC

Copy of ^1H , $^{13}\text{C}\{^1\text{H}\}$ spectra of 3-240



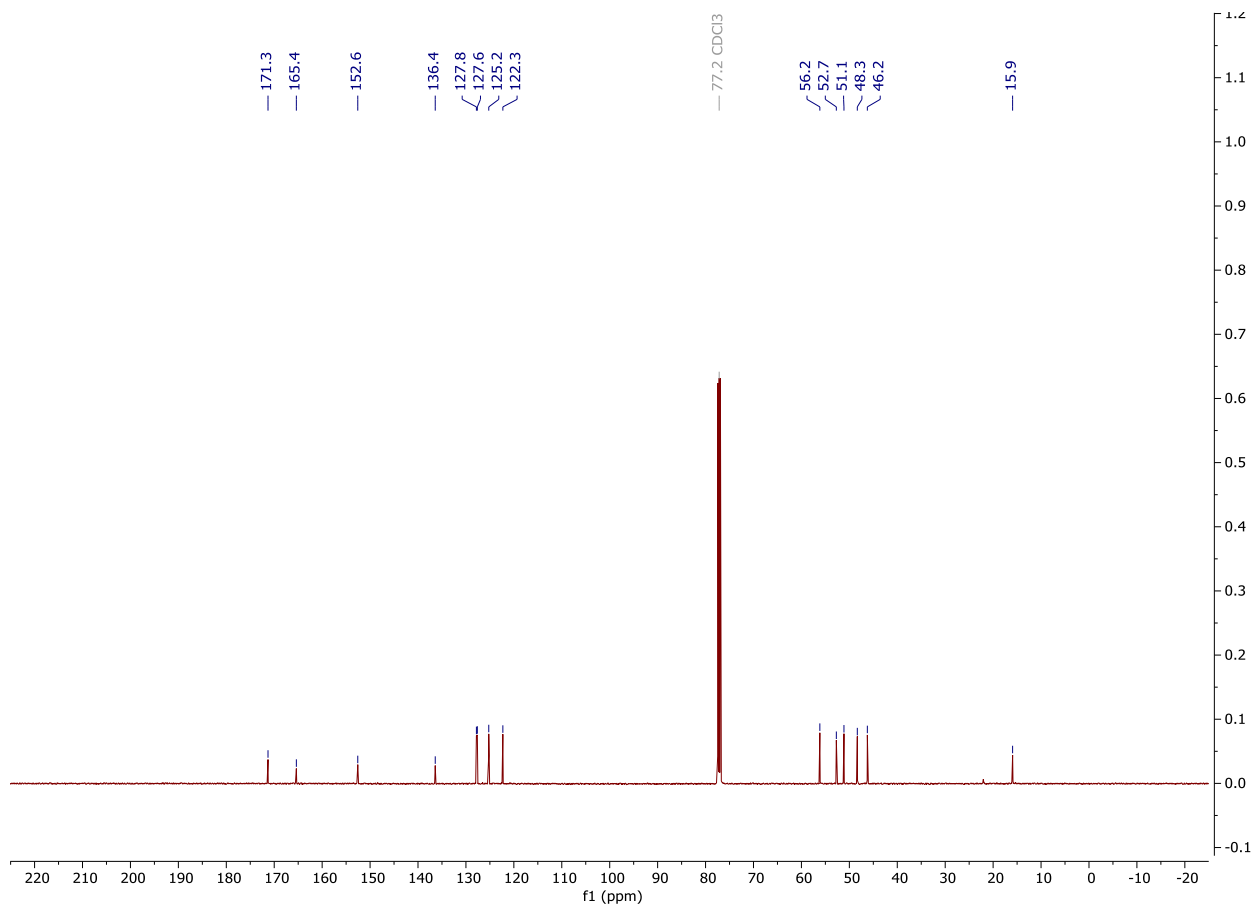
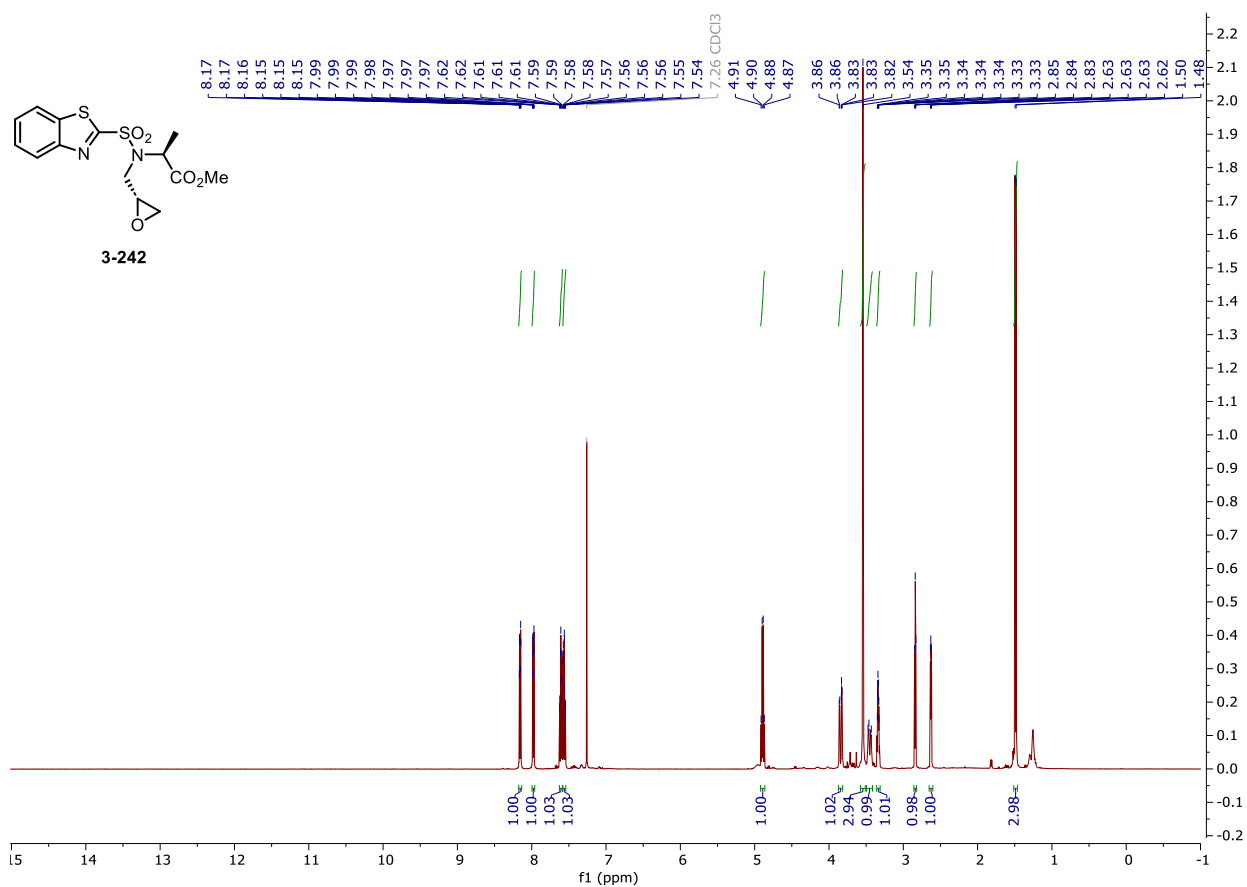
NMR and HPLC

HPLC chromatograms of 3-240



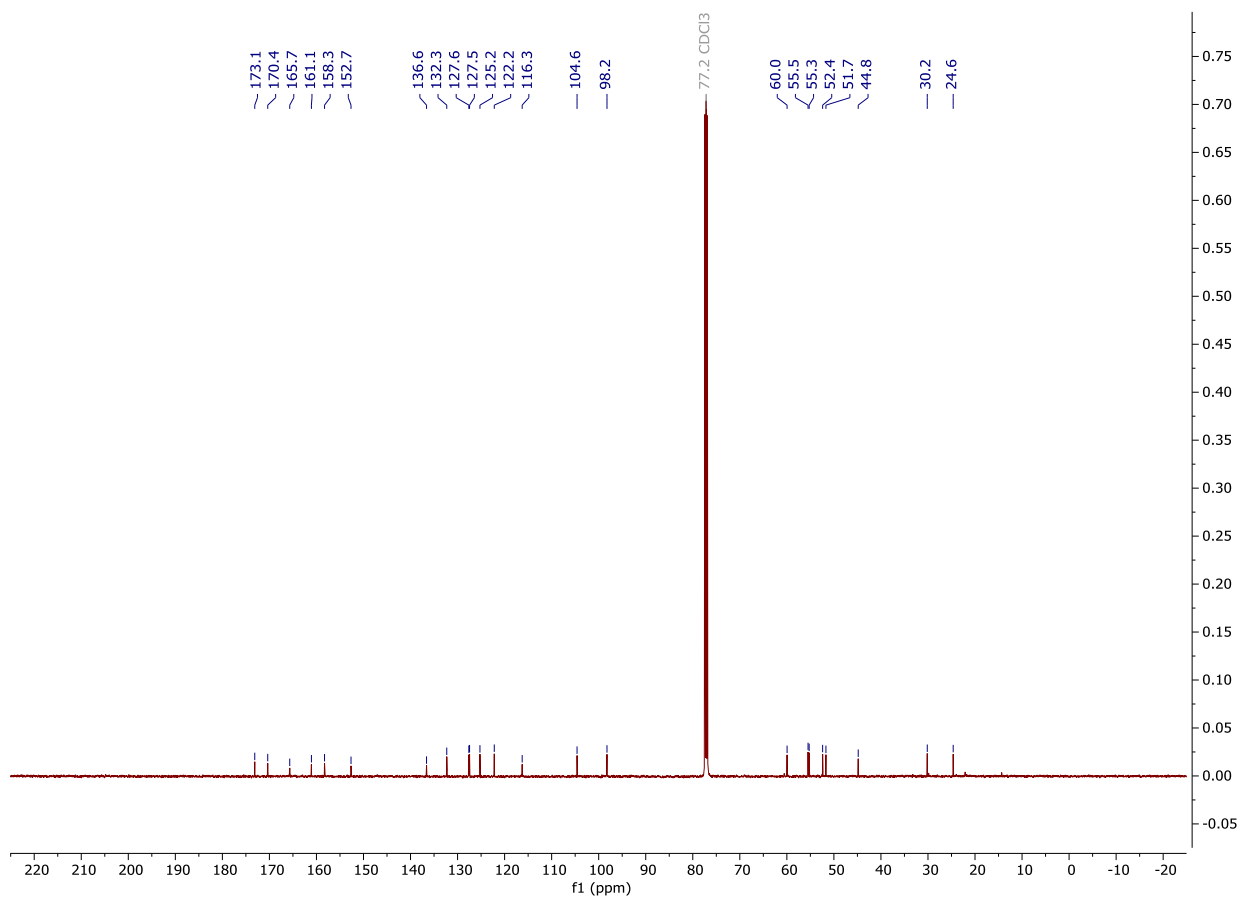
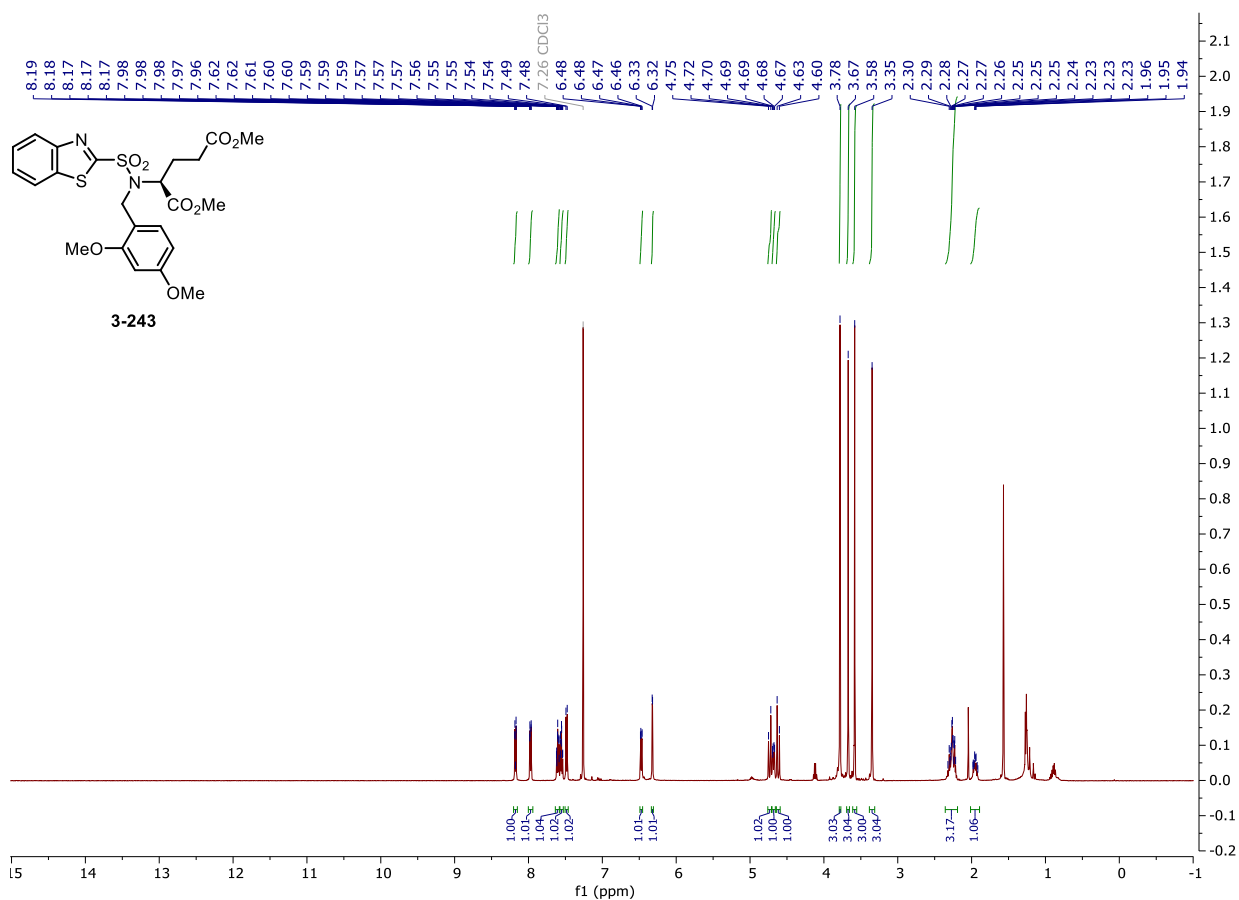
NMR and HPLC

Copy of ^1H , $^{13}\text{C}\{^1\text{H}\}$ spectra of 3-242



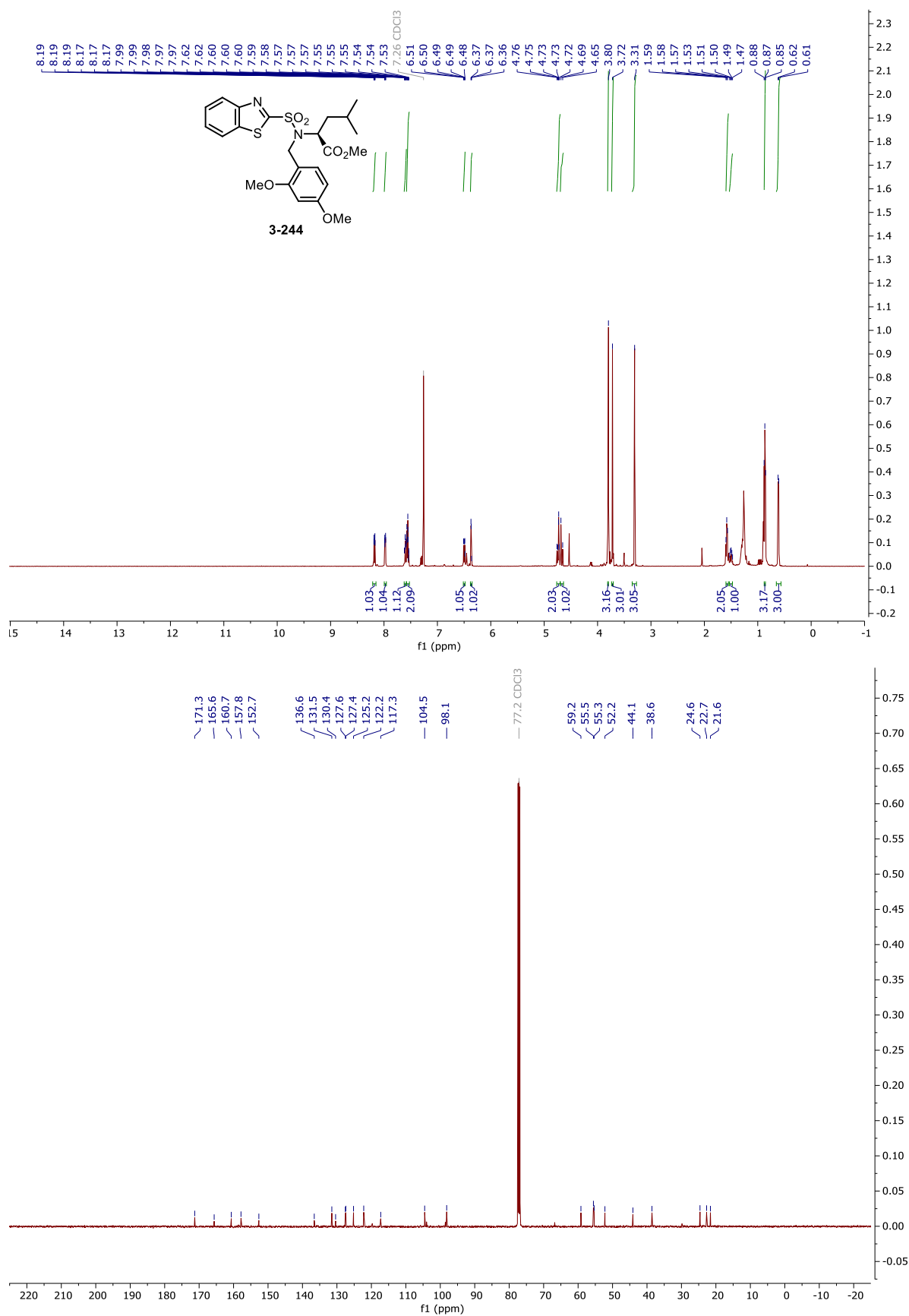
NMR and HPLC

Copy of ^1H , $^{13}\text{C}\{^1\text{H}\}$ spectra of 3-243



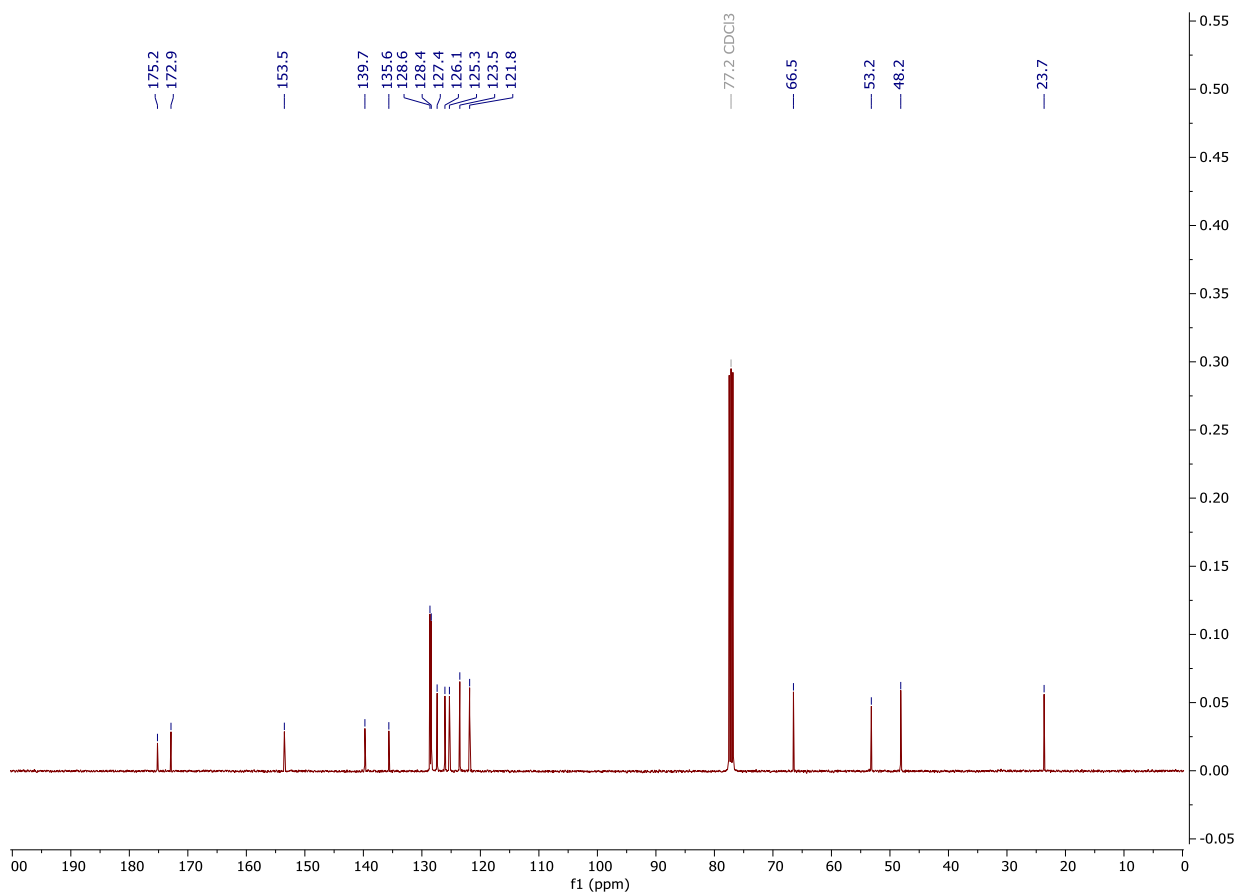
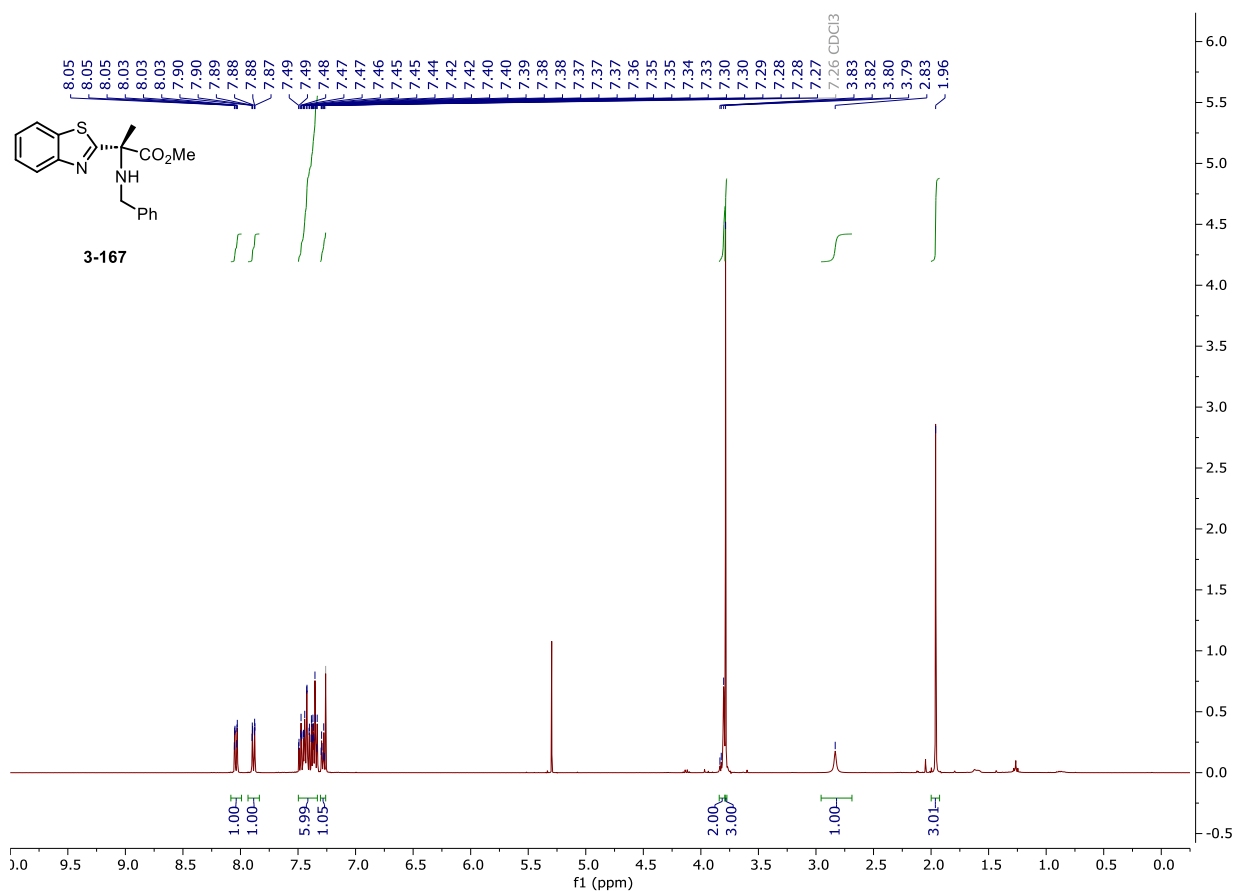
NMR and HPLC

Copy of ^1H , $^{13}\text{C}\{^1\text{H}\}$ spectra of 3-244



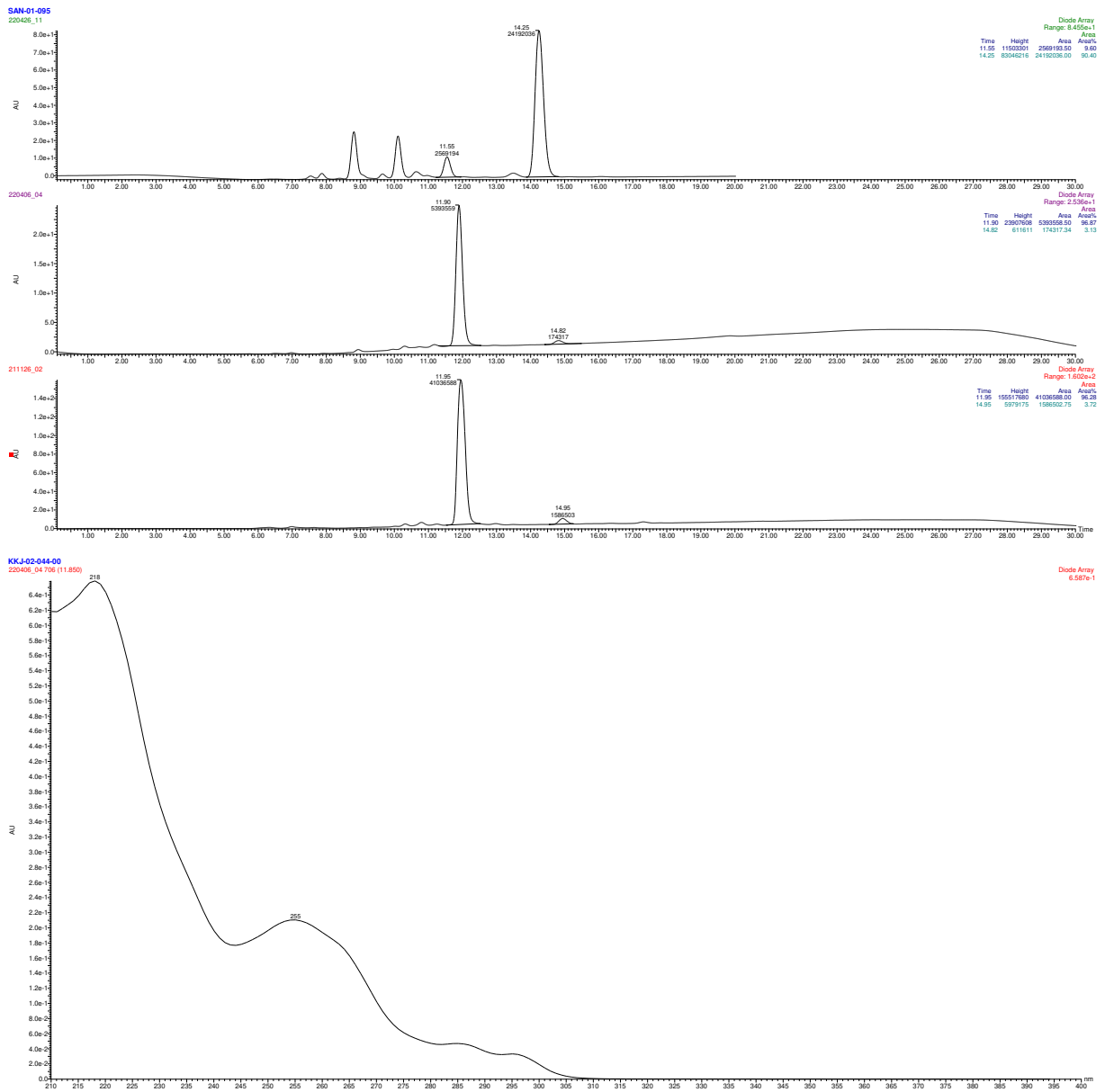
NMR and HPLC

Copy of ^1H , $^{13}\text{C}\{^1\text{H}\}$ spectra of **3-167**



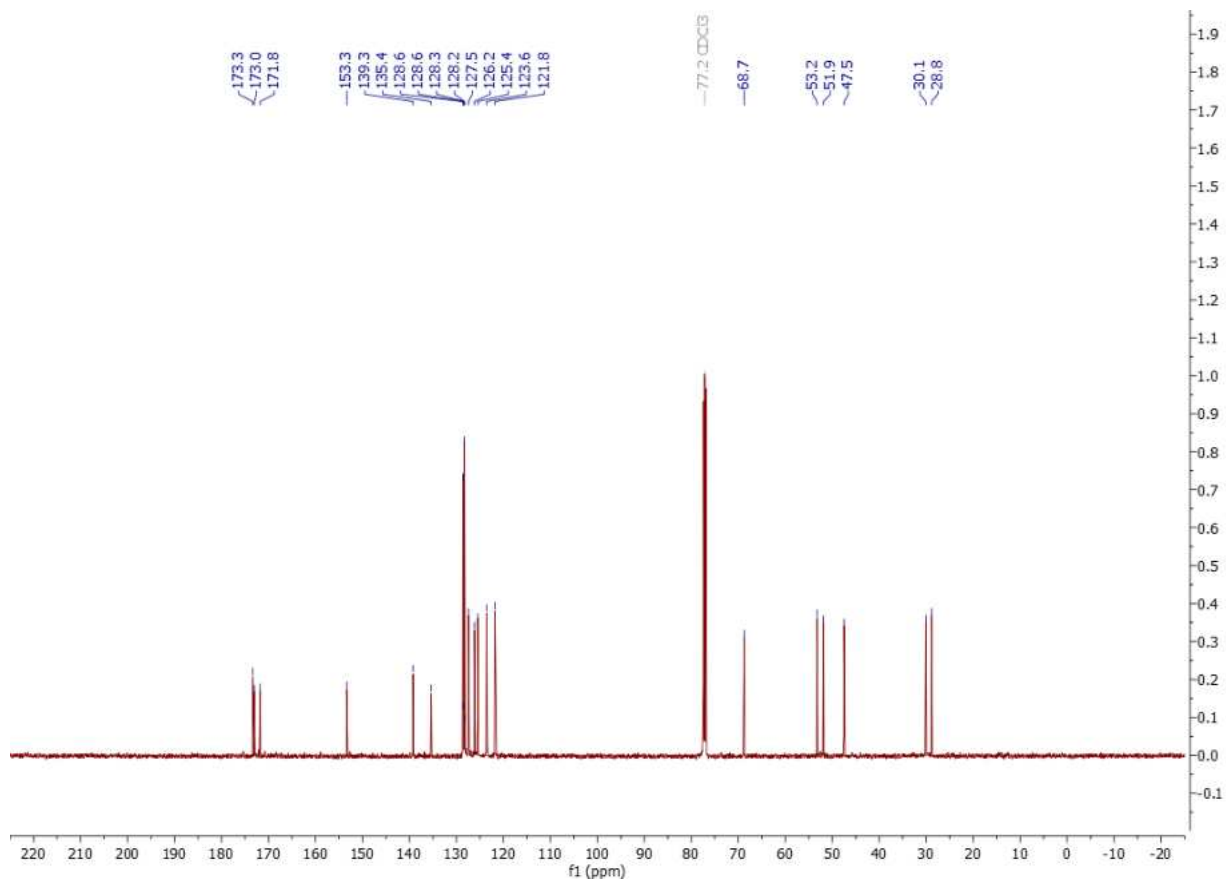
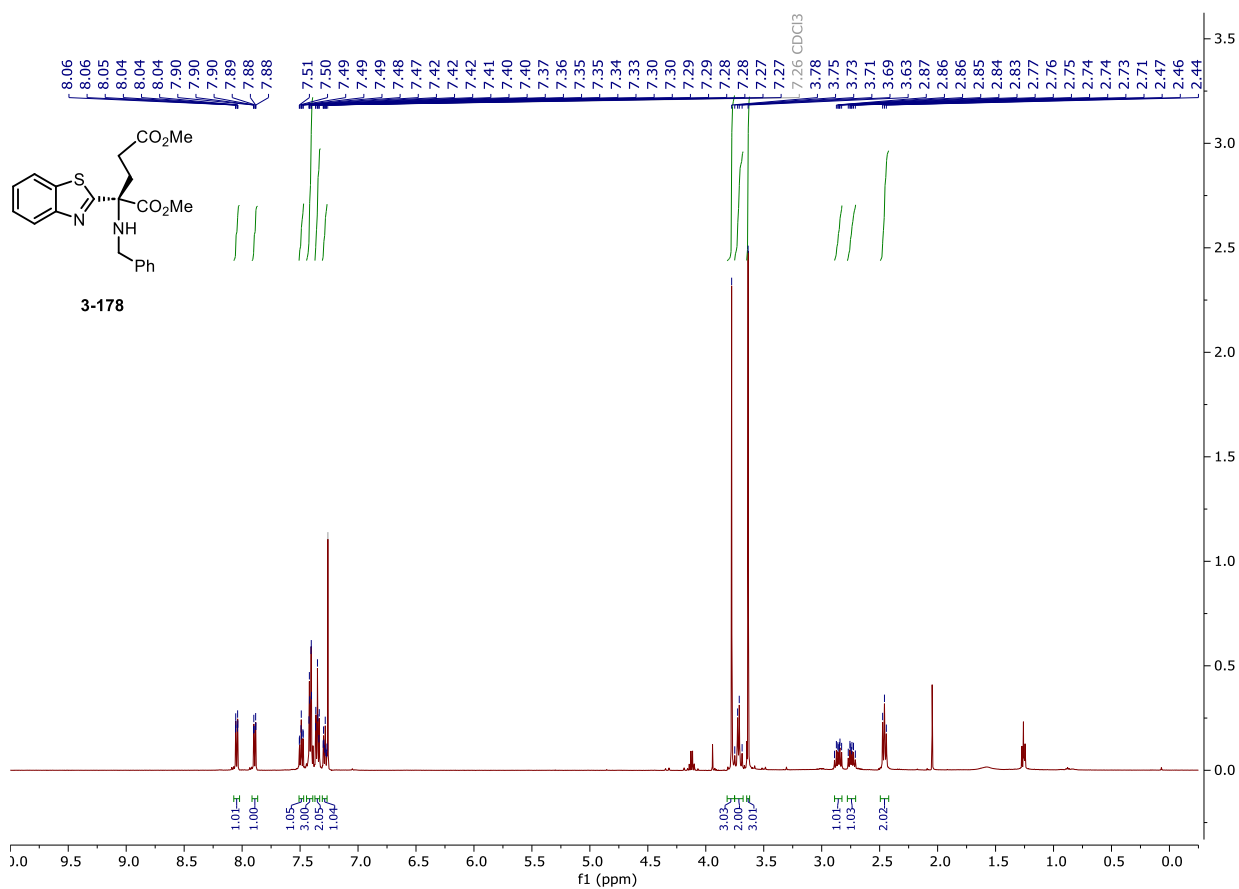
NMR and HPLC

HPLC chromatograms of 3-167



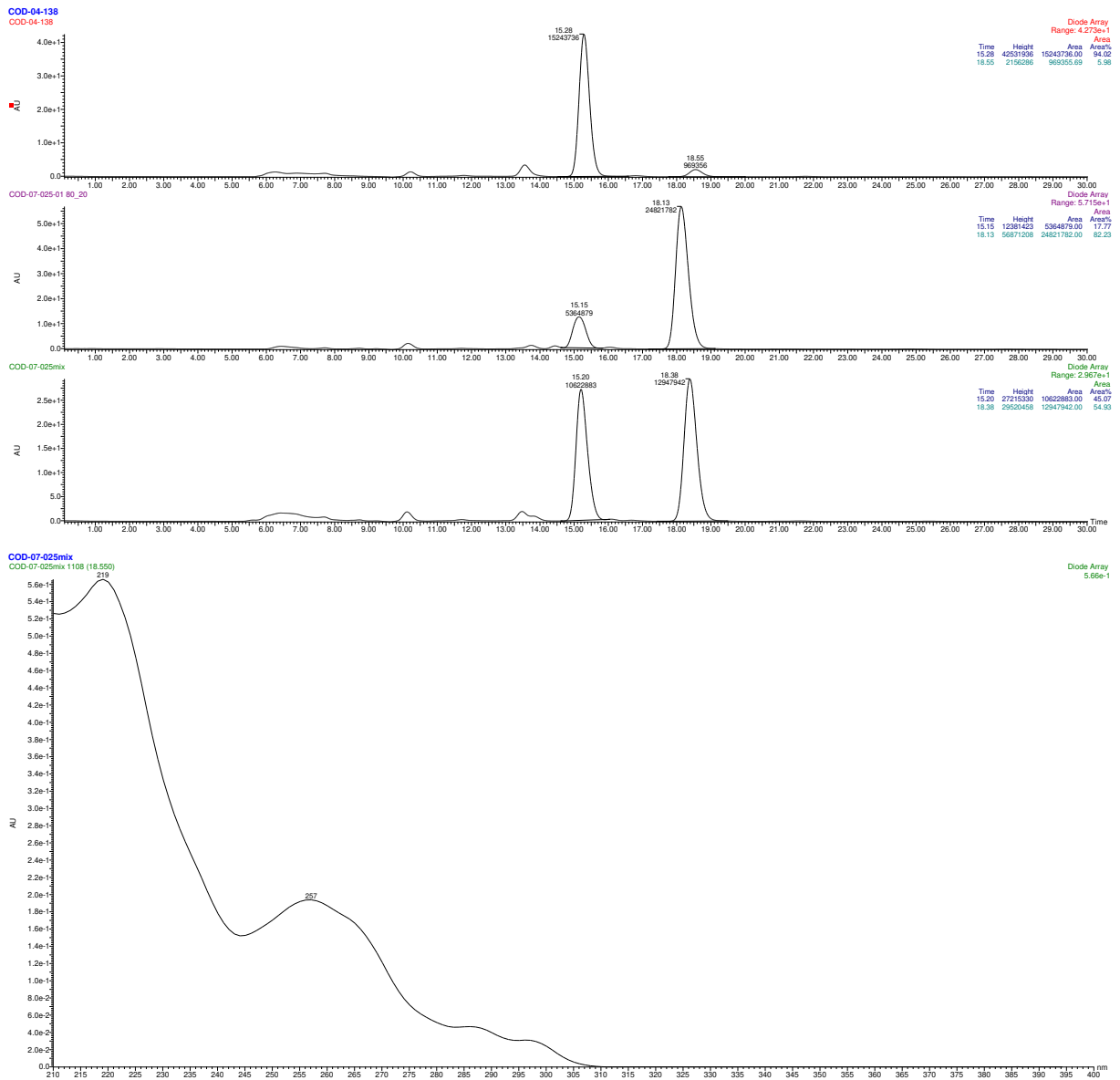
NMR and HPLC

Copy of ^1H , $^{13}\text{C}\{^1\text{H}\}$ spectra of 3-178



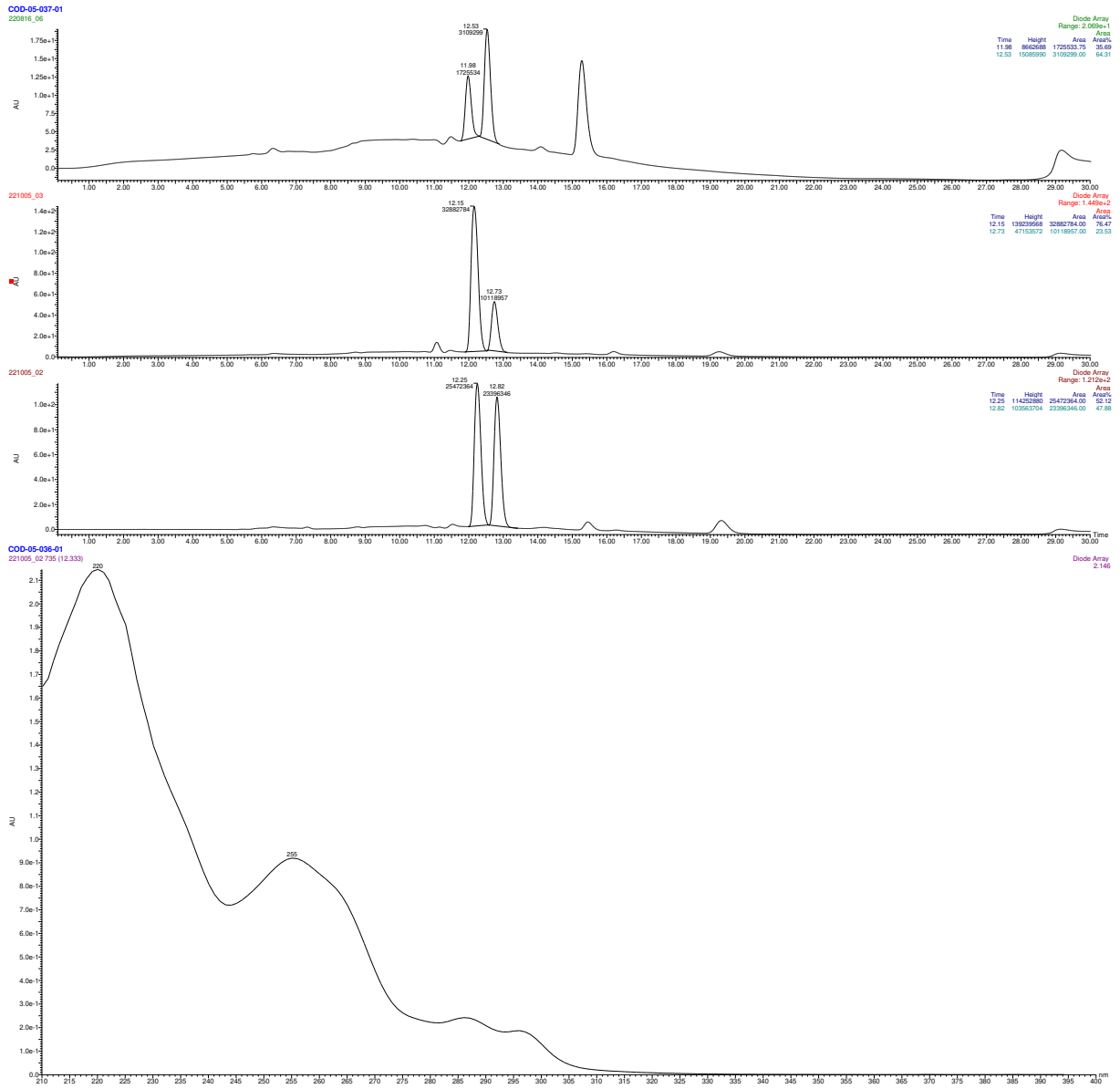
NMR and HPLC

HPLC chromatograms of 3-178



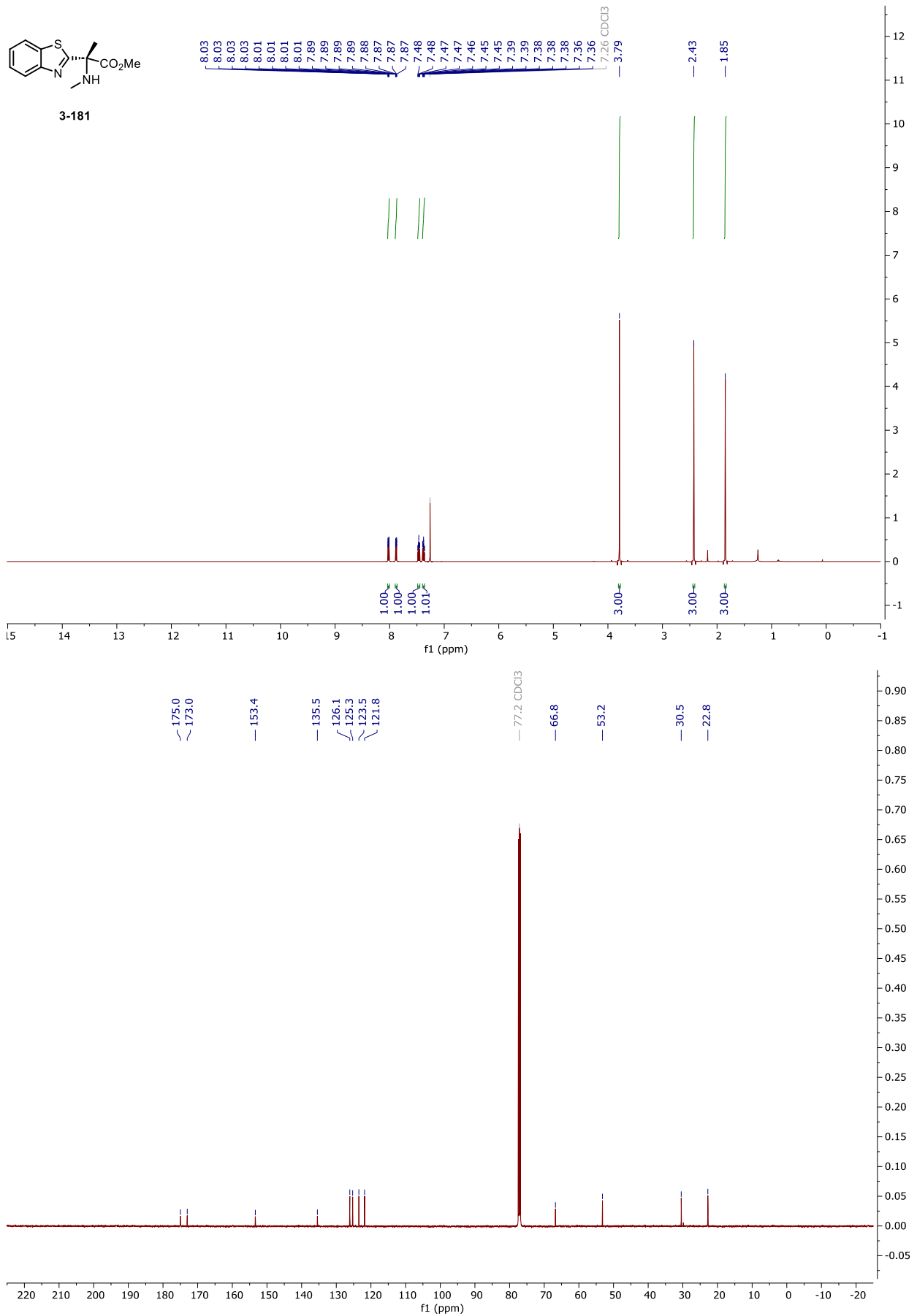
NMR and HPLC

HPLC chromatograms of 3-180



NMR and HPLC

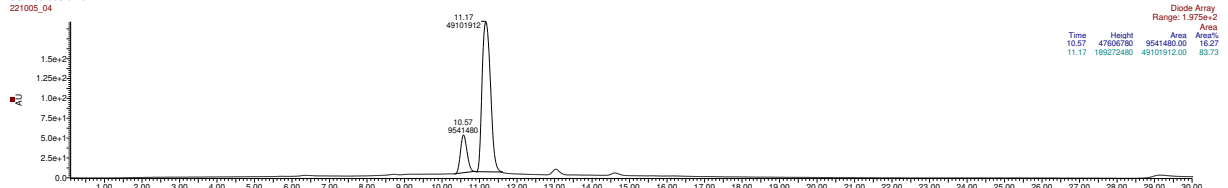
Copy of ^1H , $^{13}\text{C}\{^1\text{H}\}$ spectra of **3-181**



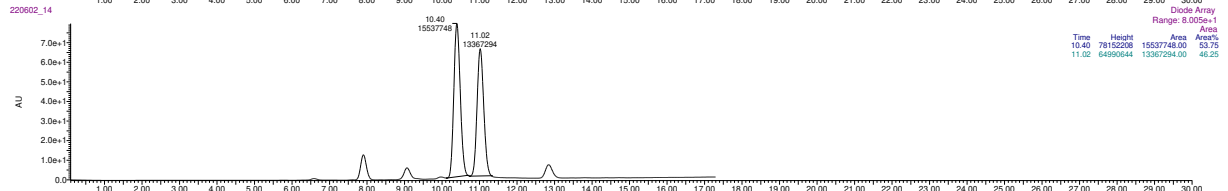
NMR and HPLC

HPLC chromatograms of 3-181

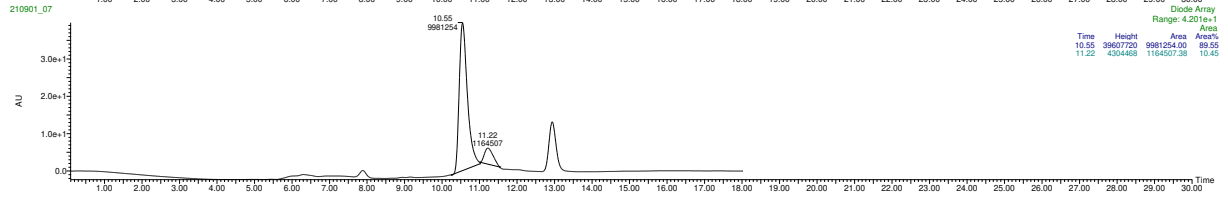
COD-05-039-02-01
221005_04



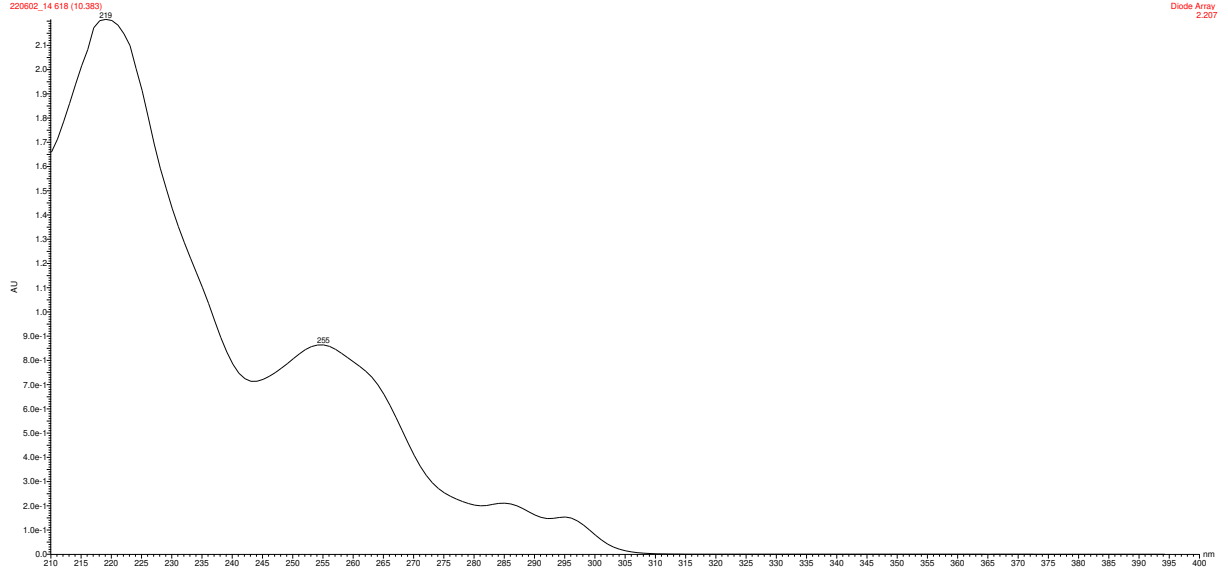
220602_14



210801_07

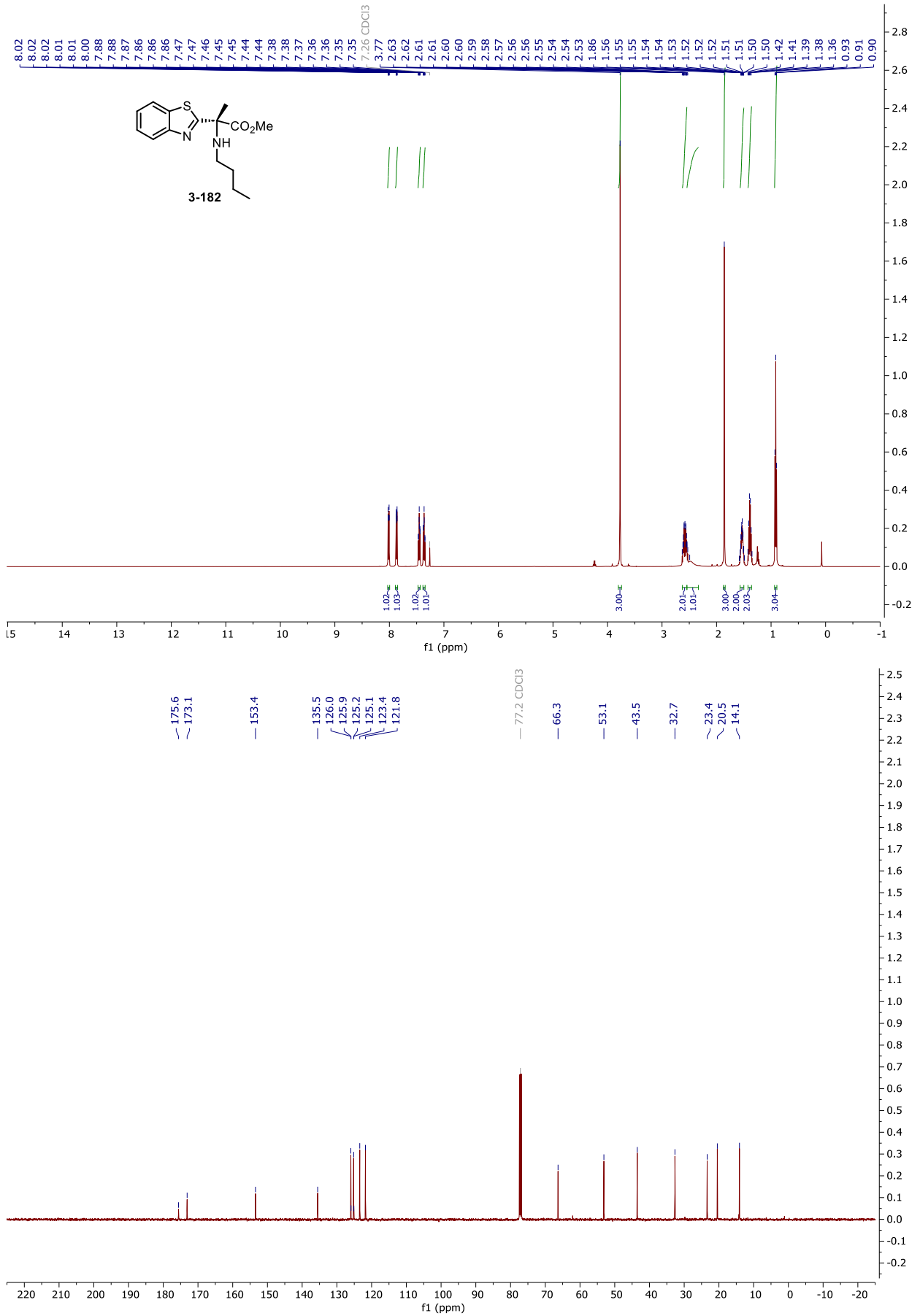


COD-04-057-00



NMR and HPLC

Copy of ^1H , $^{13}\text{C}\{^1\text{H}\}$ spectra of 3-182

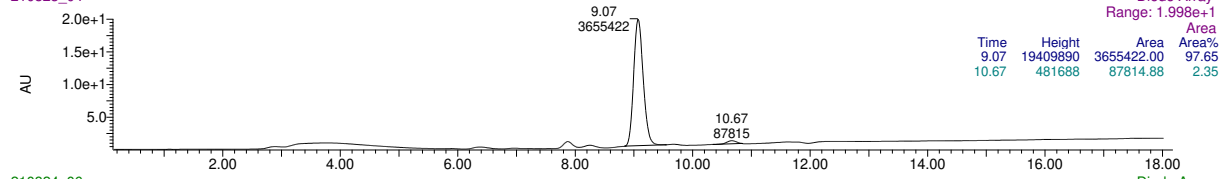


NMR and HPLC

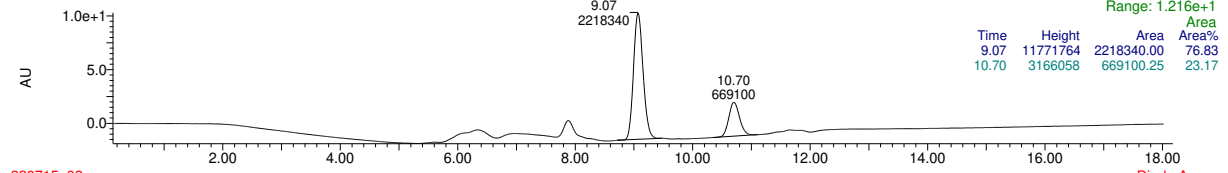
HPLC chromatograms of 3-182

COD-04-125-00

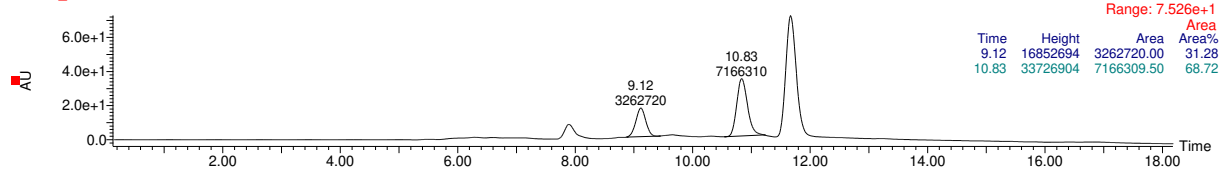
210823_04



210824_06

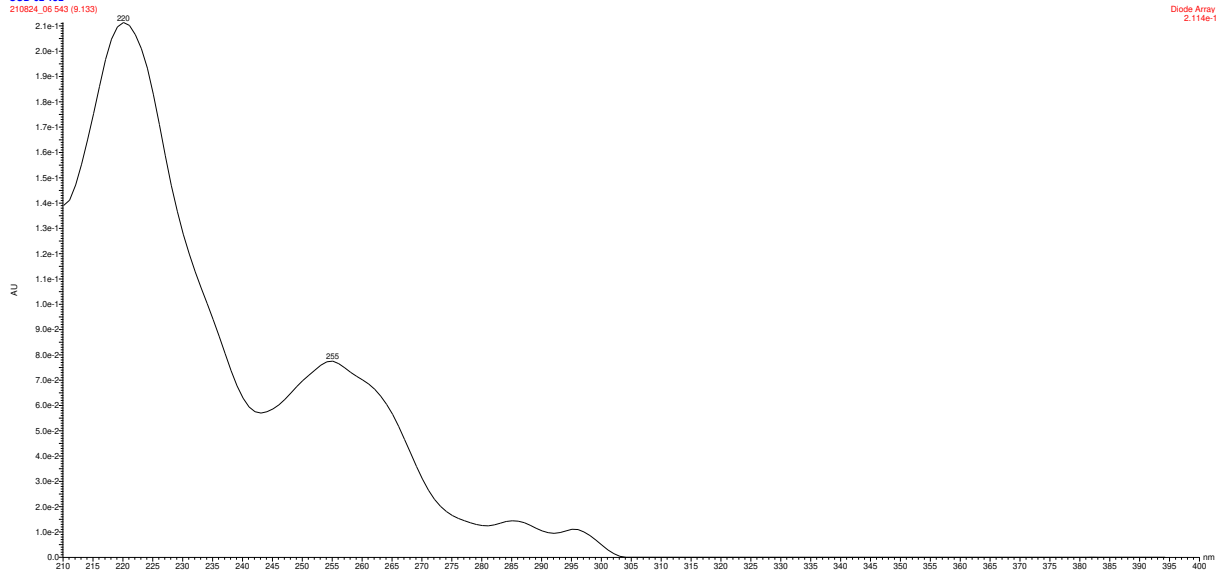


220715_02



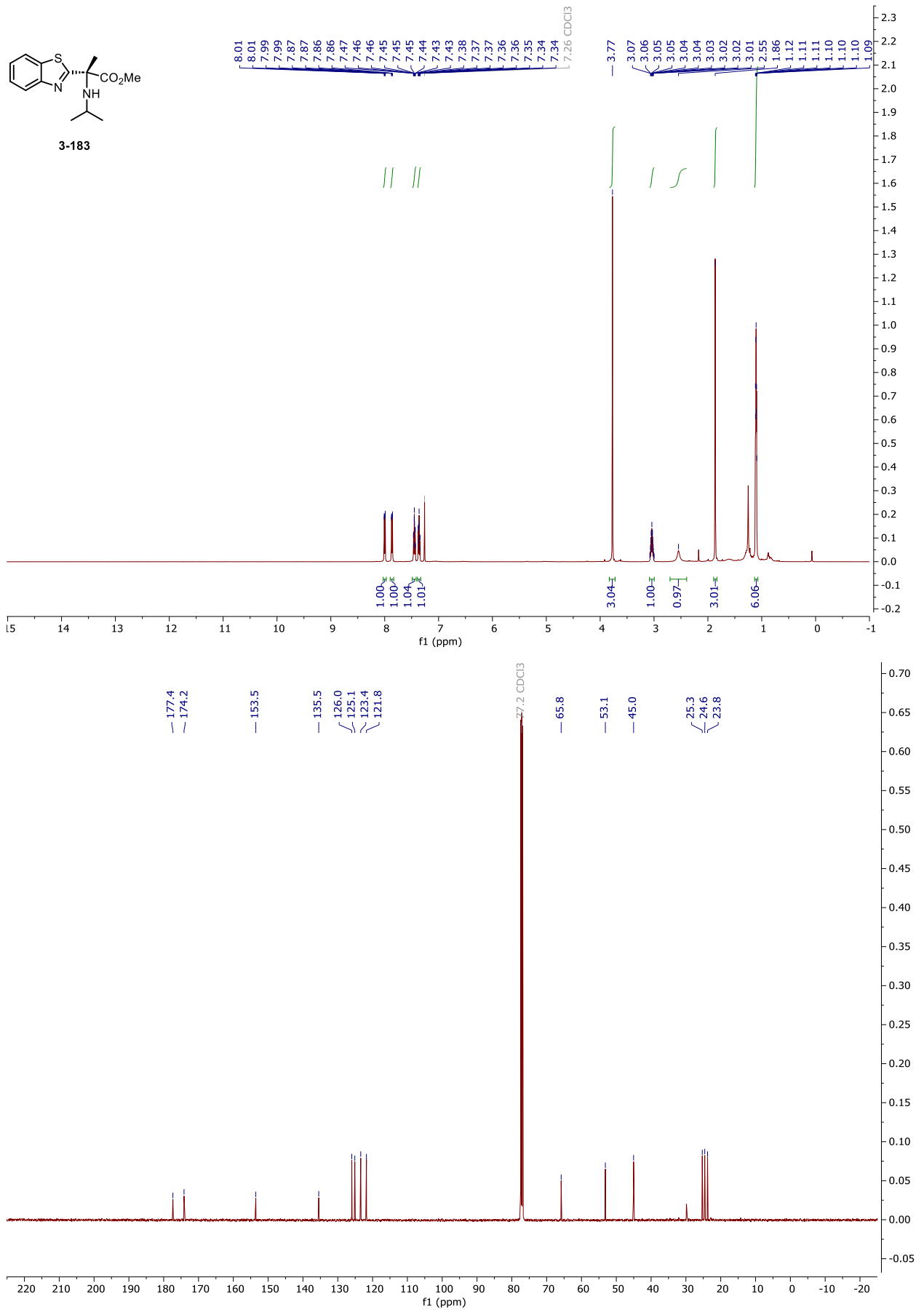
COD-02-152

210824_06 942 (9.133)



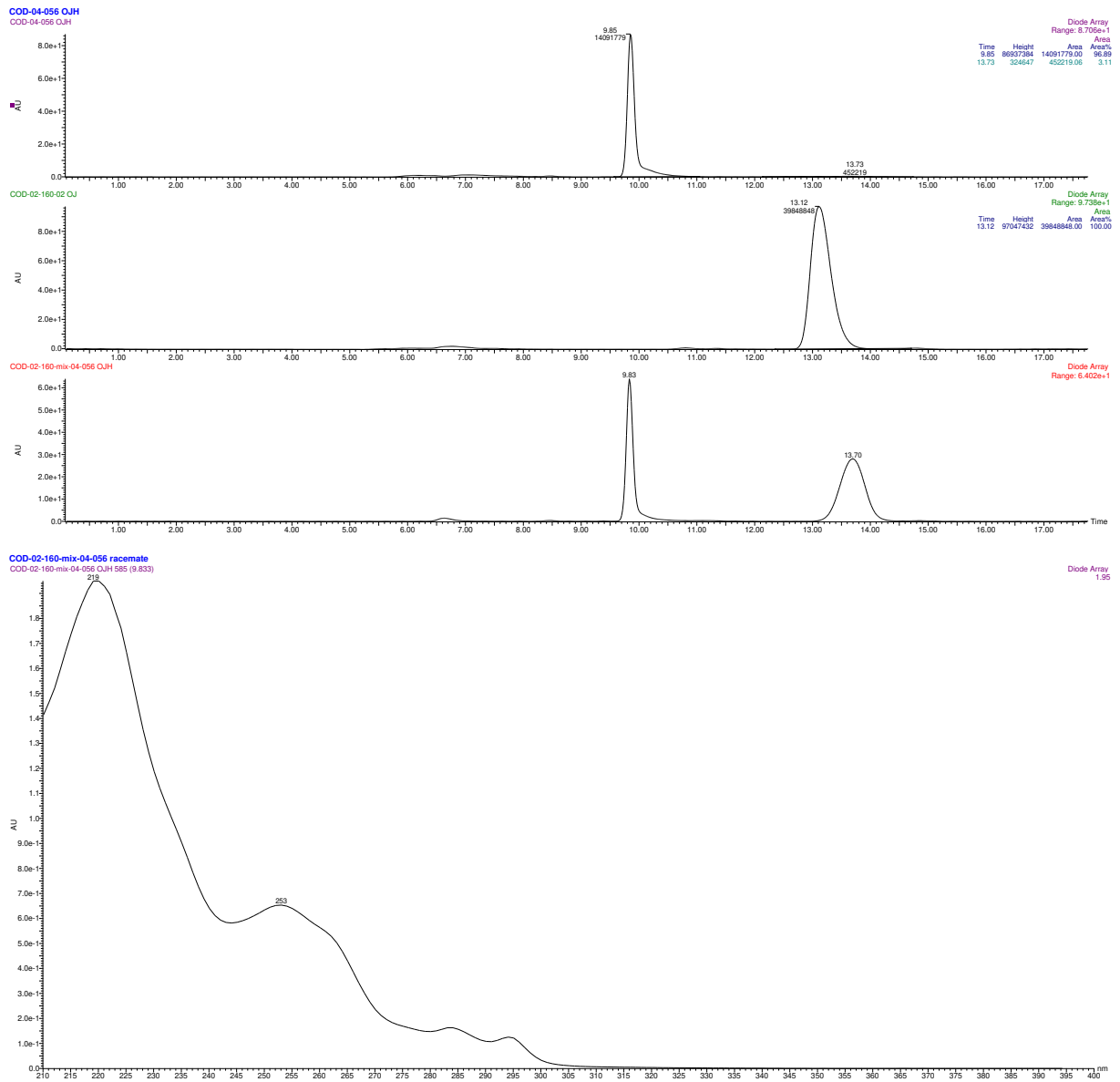
NMR and HPLC

Copy of ^1H , $^{13}\text{C}\{^1\text{H}\}$ spectra of **3-183**



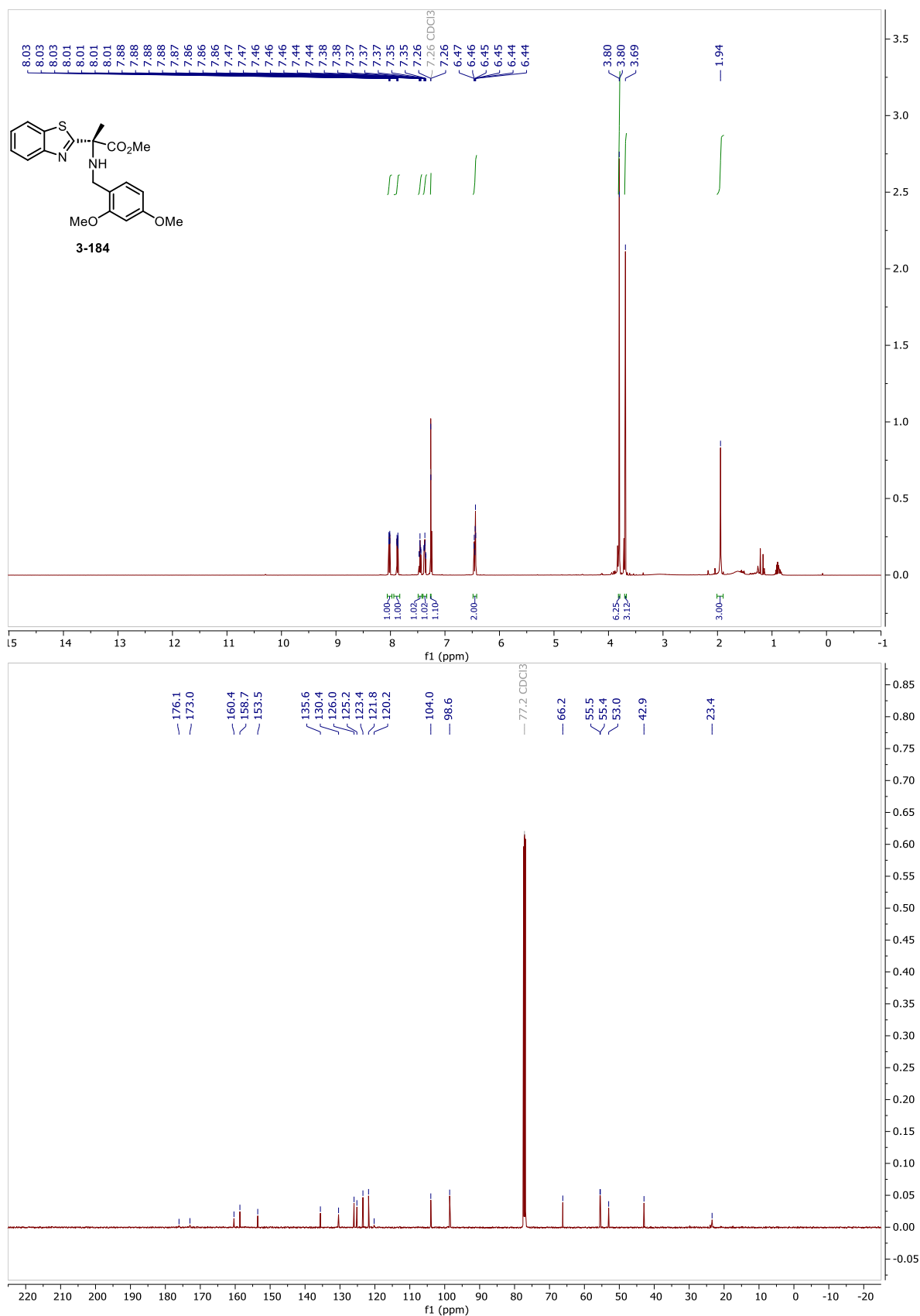
NMR and HPLC

HPLC chromatograms of 3-183



NMR and HPLC

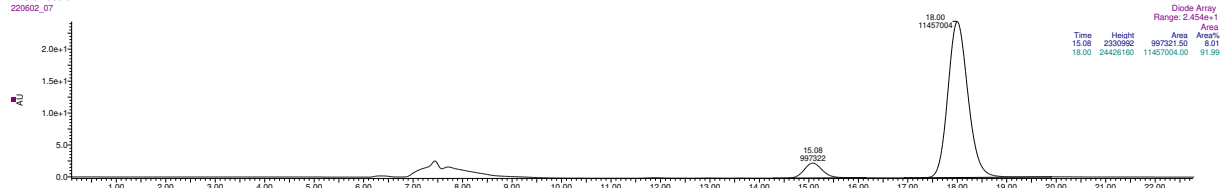
Copy of ^1H , $^{13}\text{C}\{^1\text{H}\}$ spectra of **3-184**



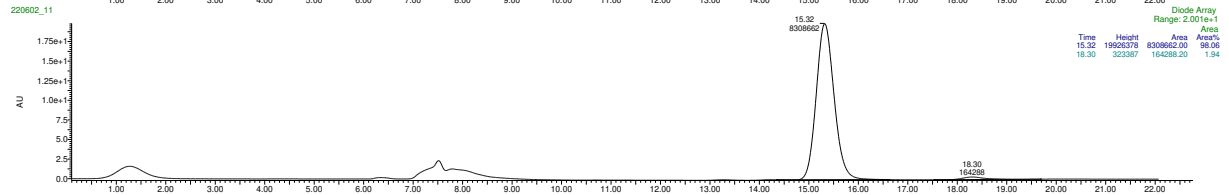
NMR and HPLC

HPLC chromatograms of 3-184

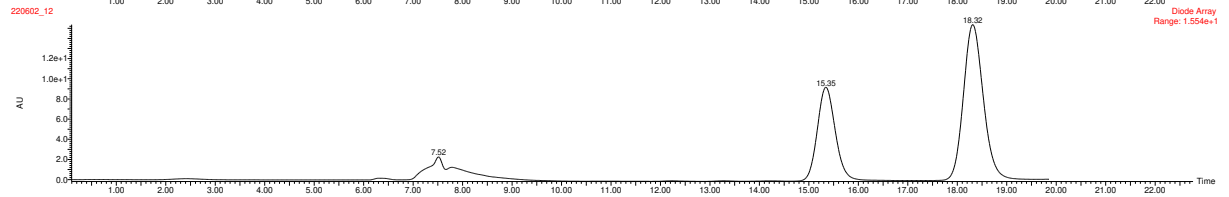
KK-02-066-01
220602_07



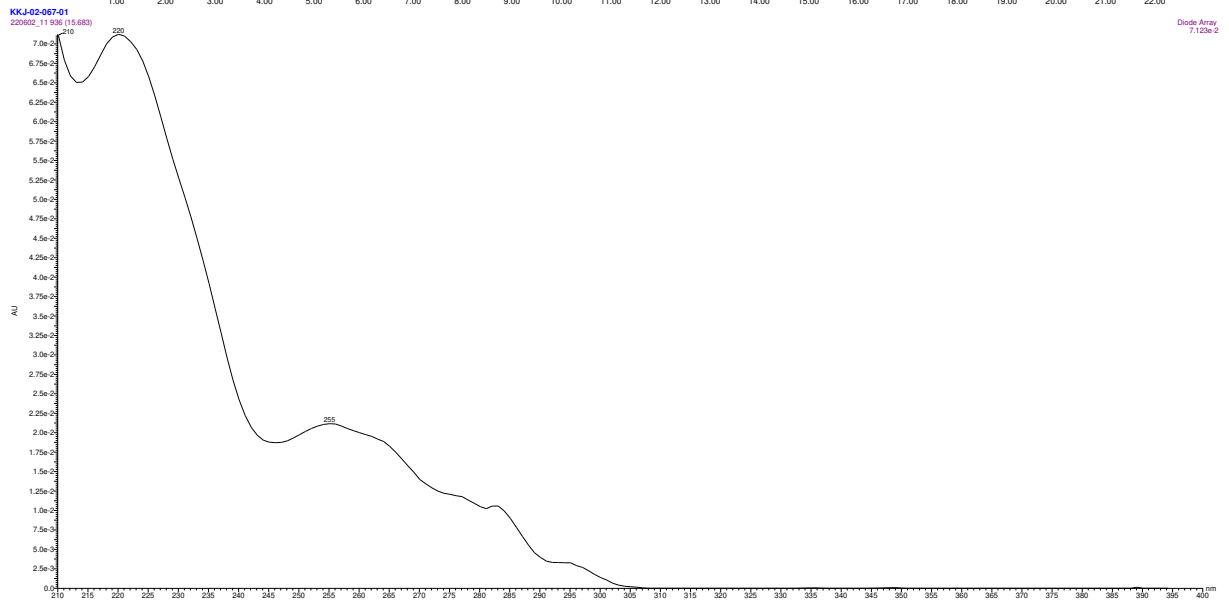
220602_11



220602_12

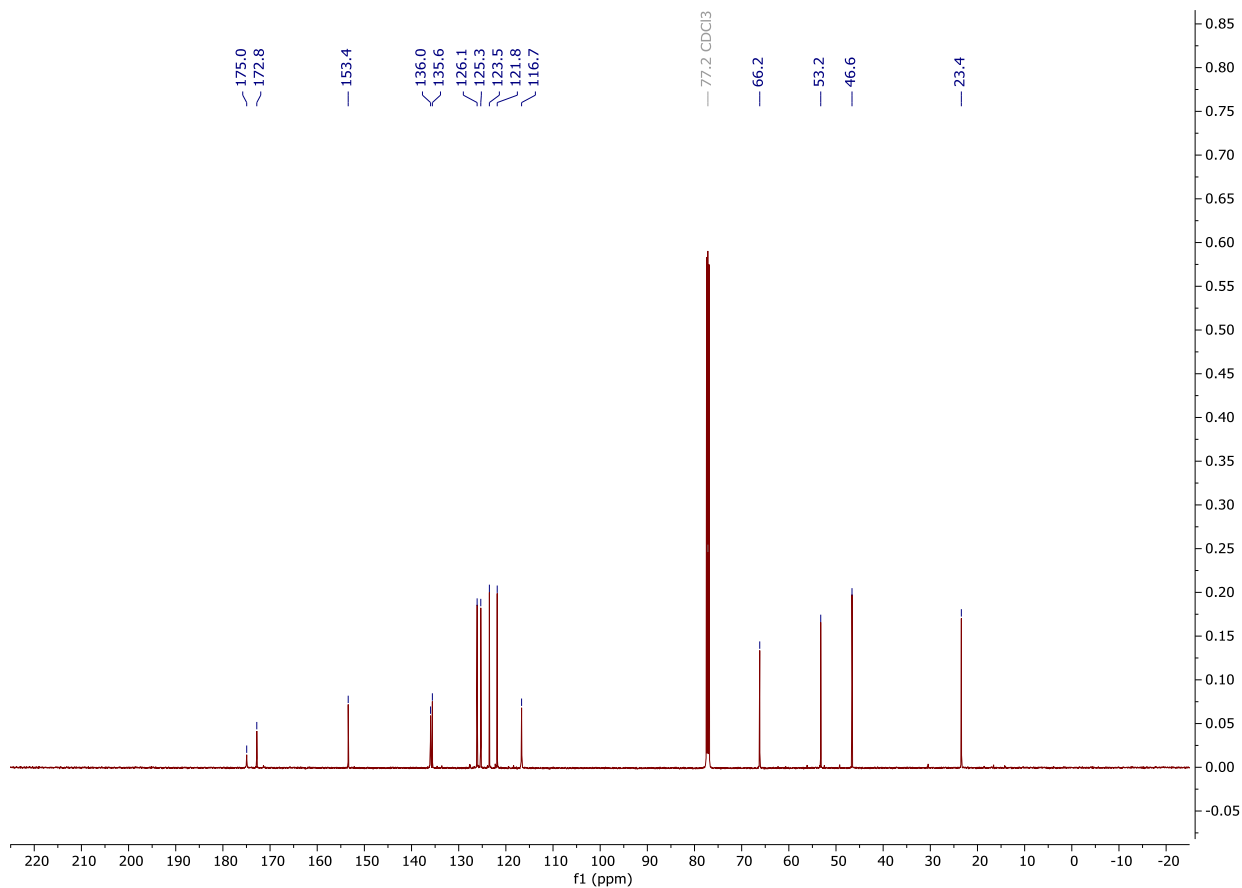
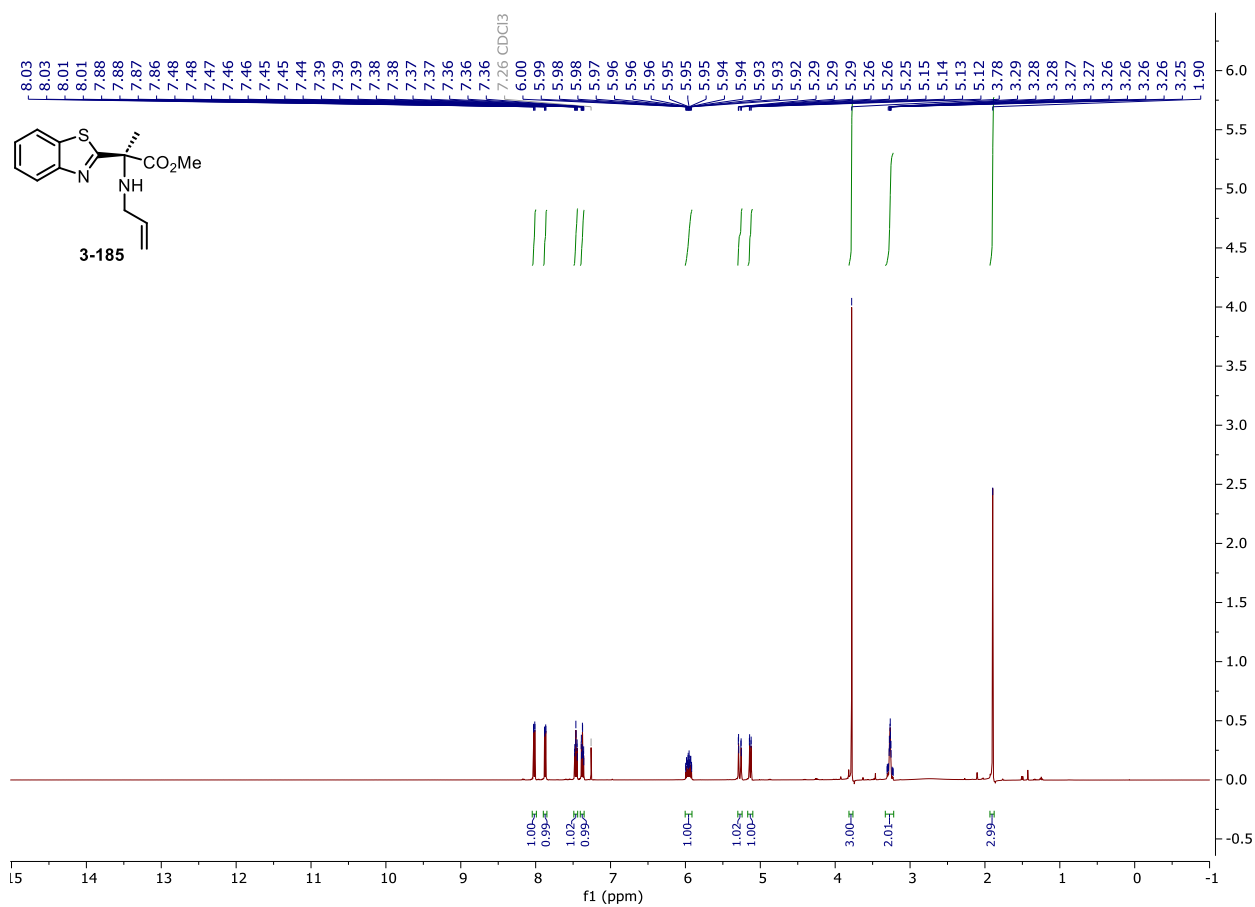


KK-02-067-01



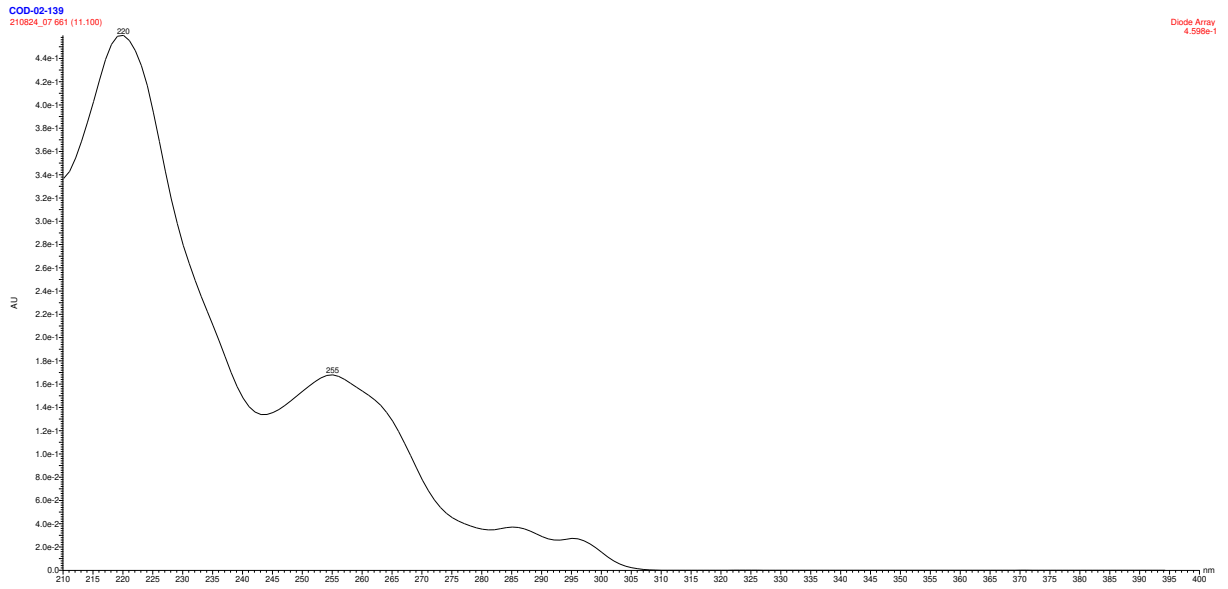
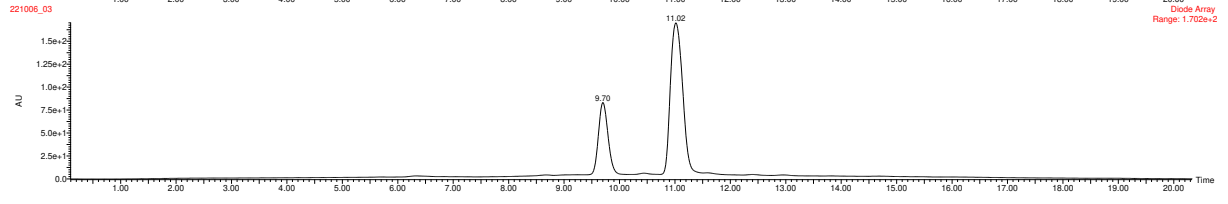
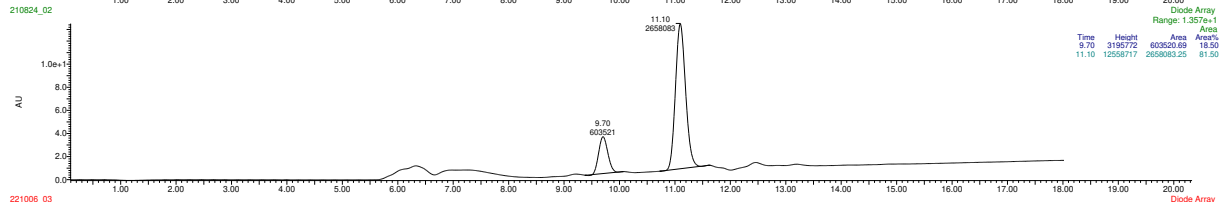
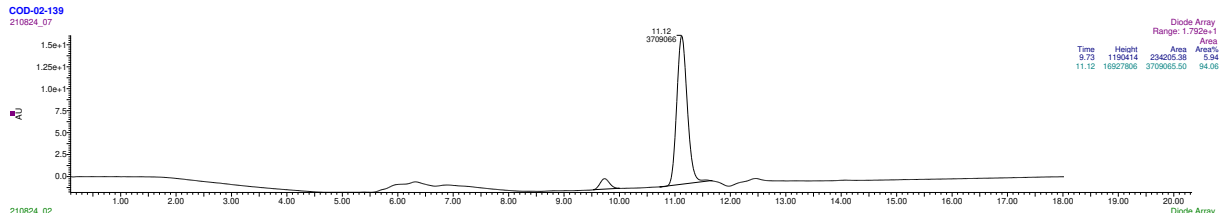
NMR and HPLC

Copy of ^1H , $^{13}\text{C}\{^1\text{H}\}$ spectra of 3-185



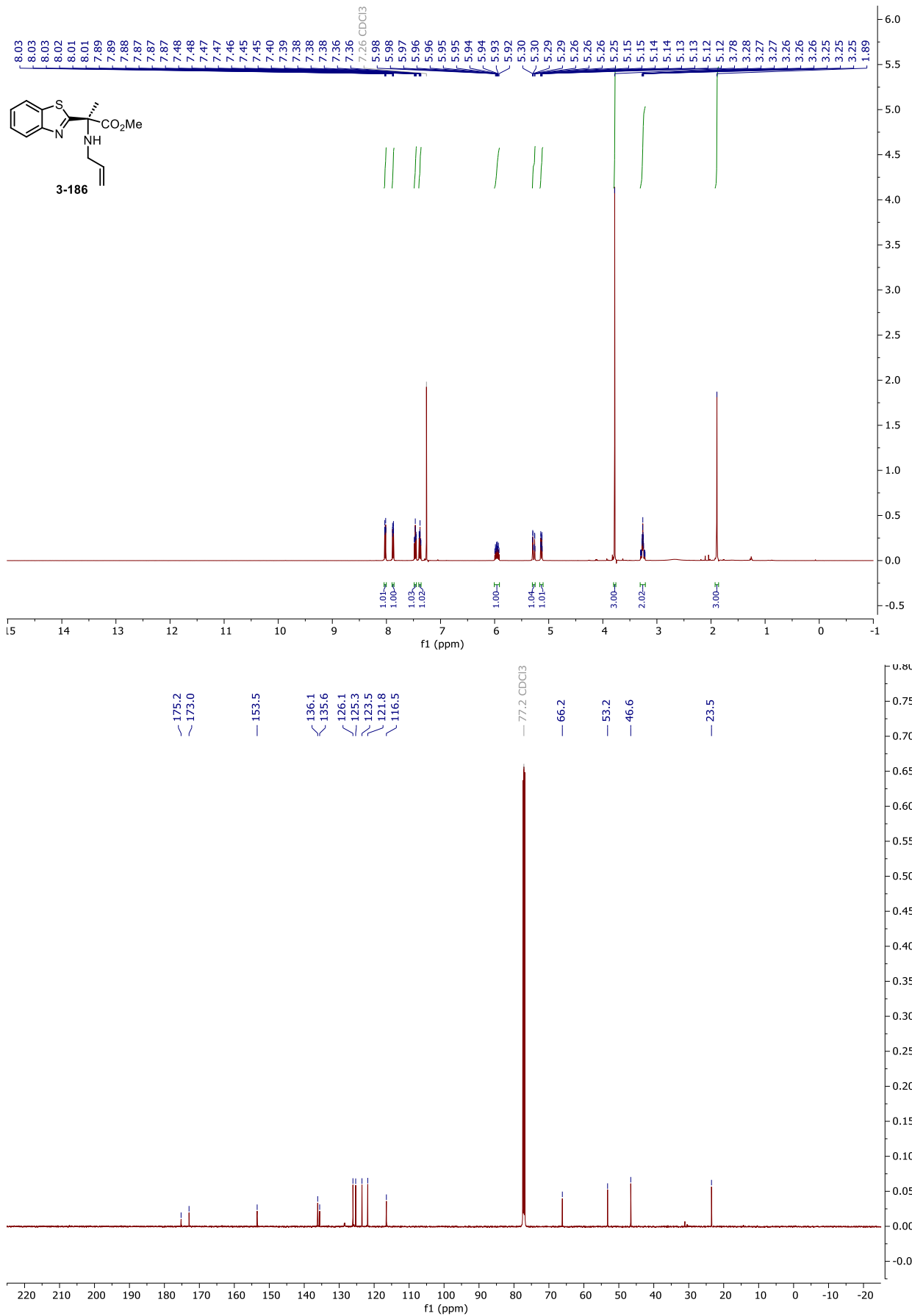
NMR and HPLC

HPLC chromatograms of 3-185



NMR and HPLC

Copy of ^1H , $^{13}\text{C}\{^1\text{H}\}$ spectra of **3-186**

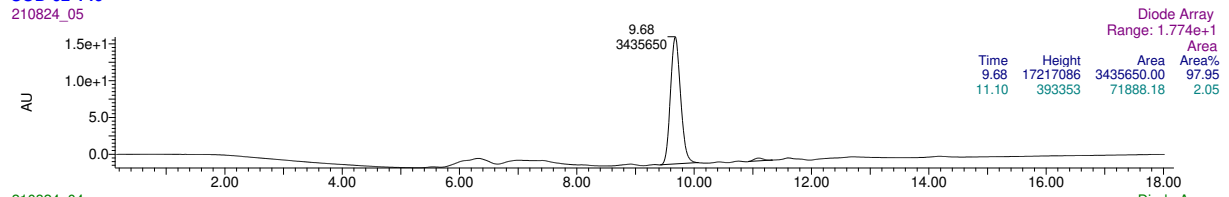


NMR and HPLC

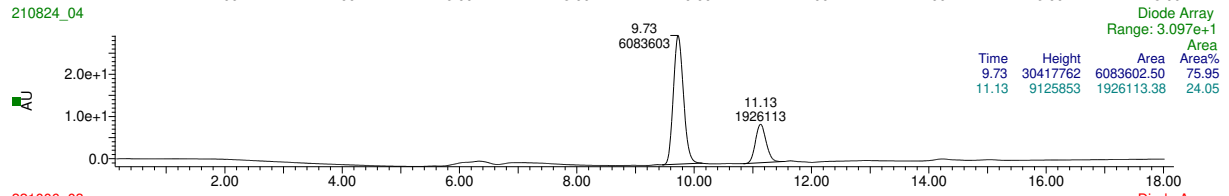
HPLC chromatograms of 3-186

COD-02-146

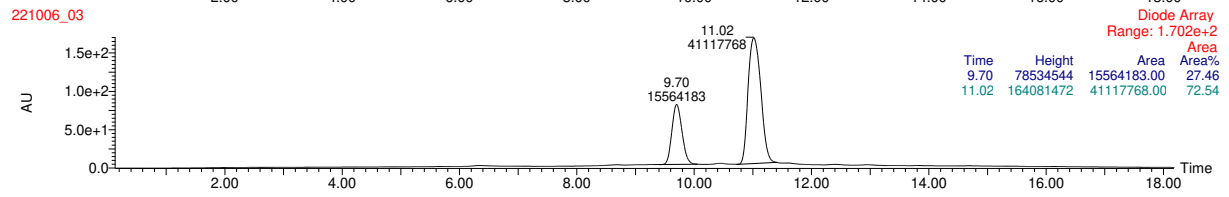
210824_05



210824_04

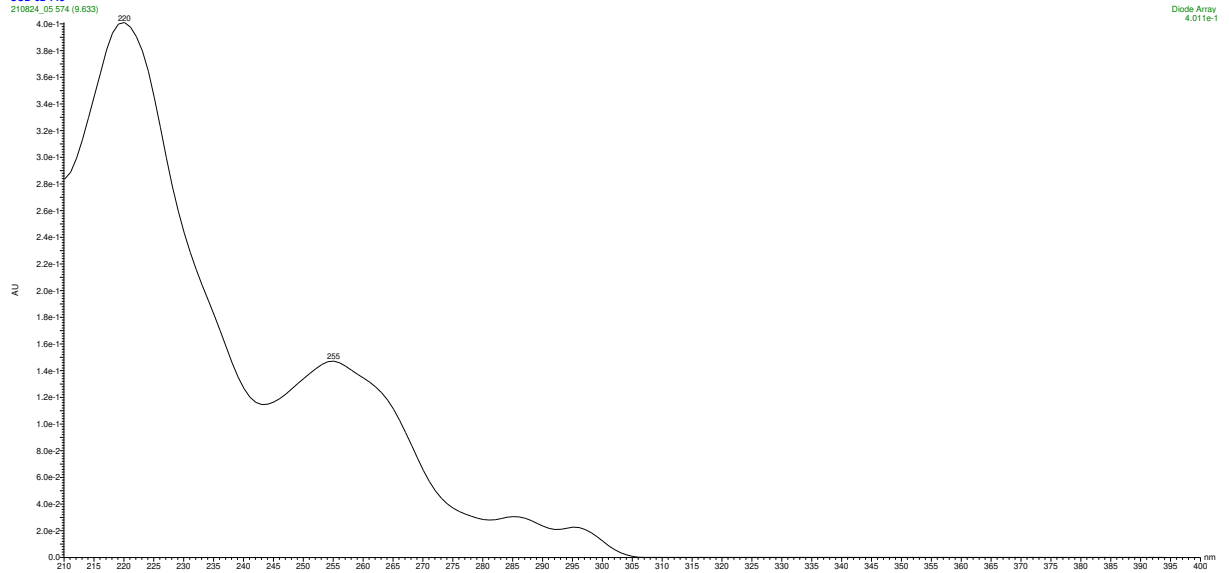


221006_03



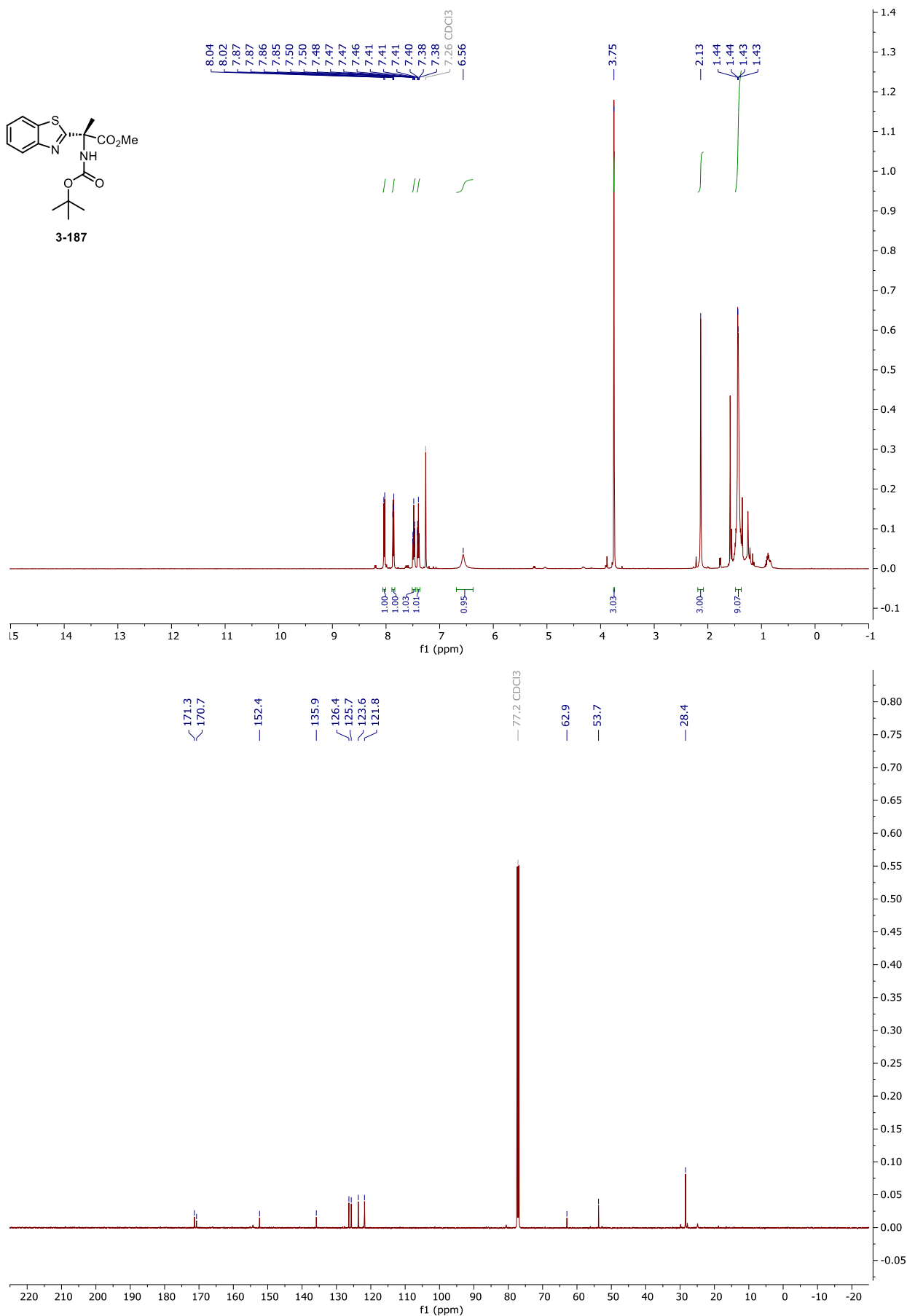
COD-02-148

210824_05 574 (9.533)



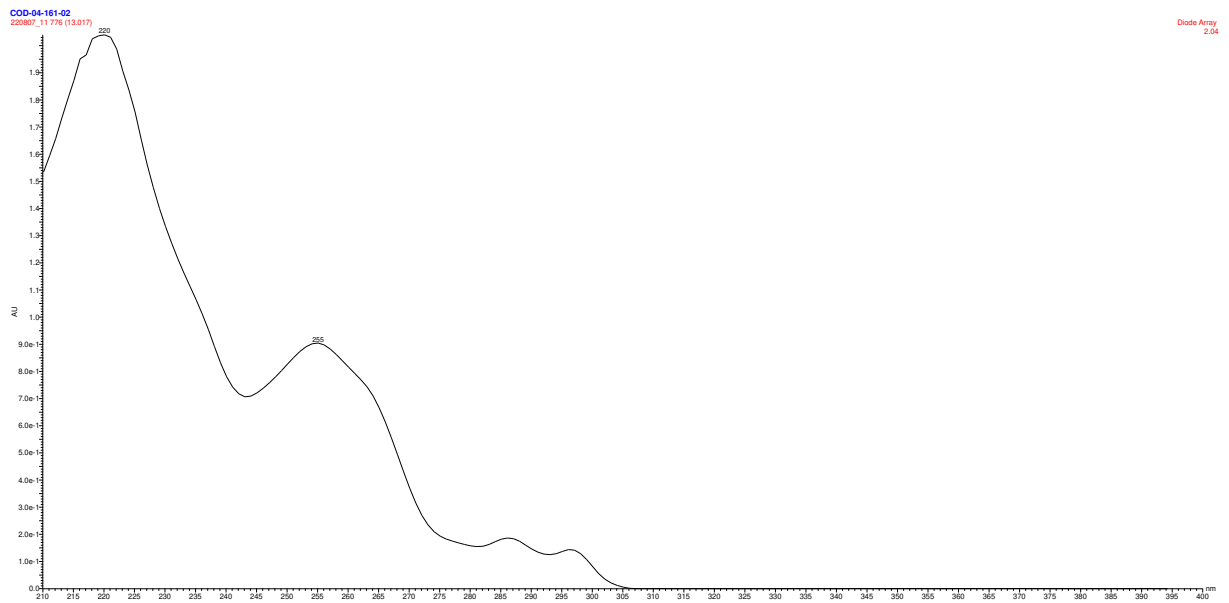
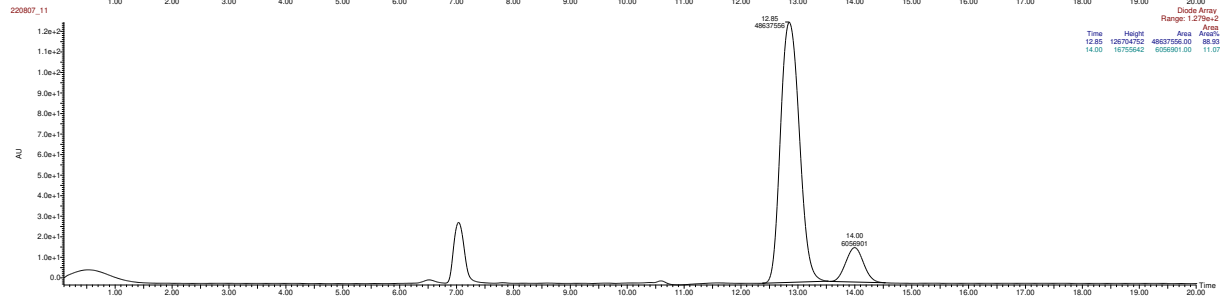
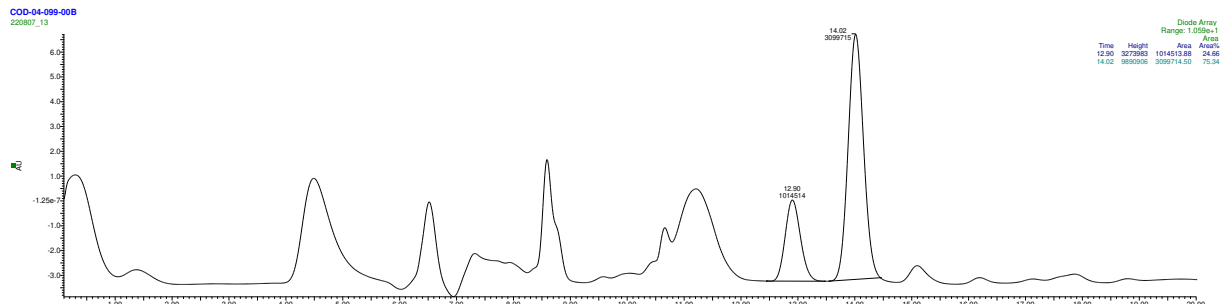
NMR and HPLC

Copy of ^1H , $^{13}\text{C}\{^1\text{H}\}$ spectra of 3-187



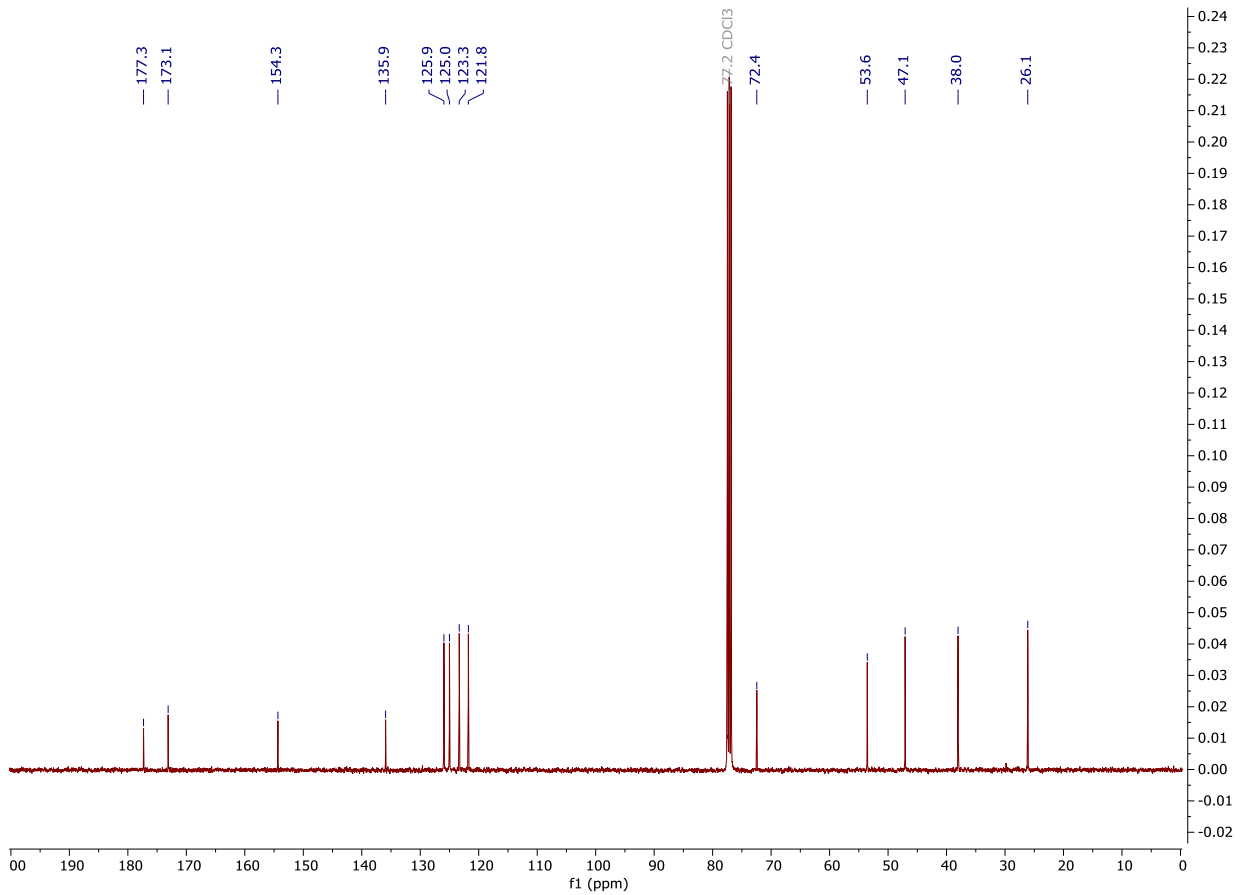
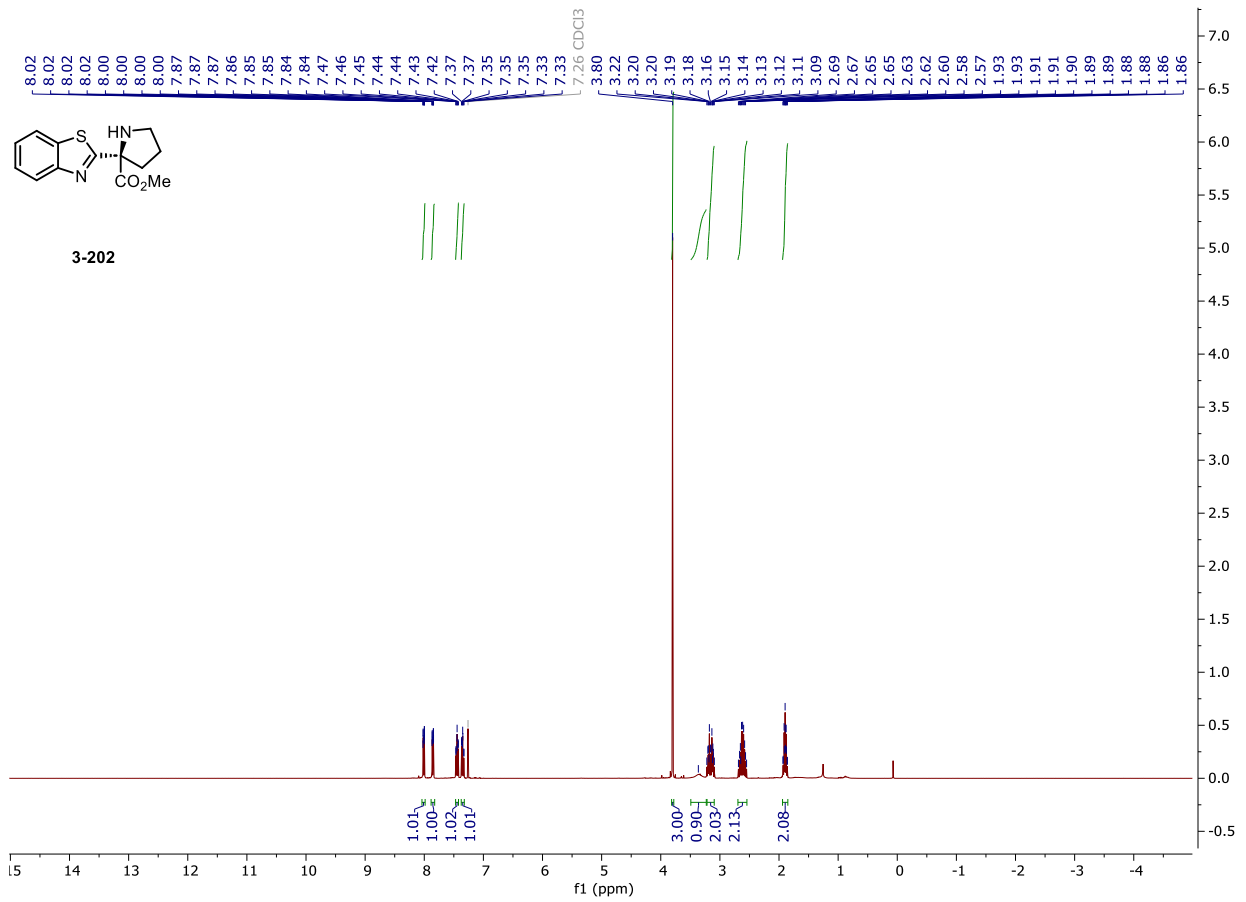
NMR and HPLC

HPLC chromatograms of 3-187



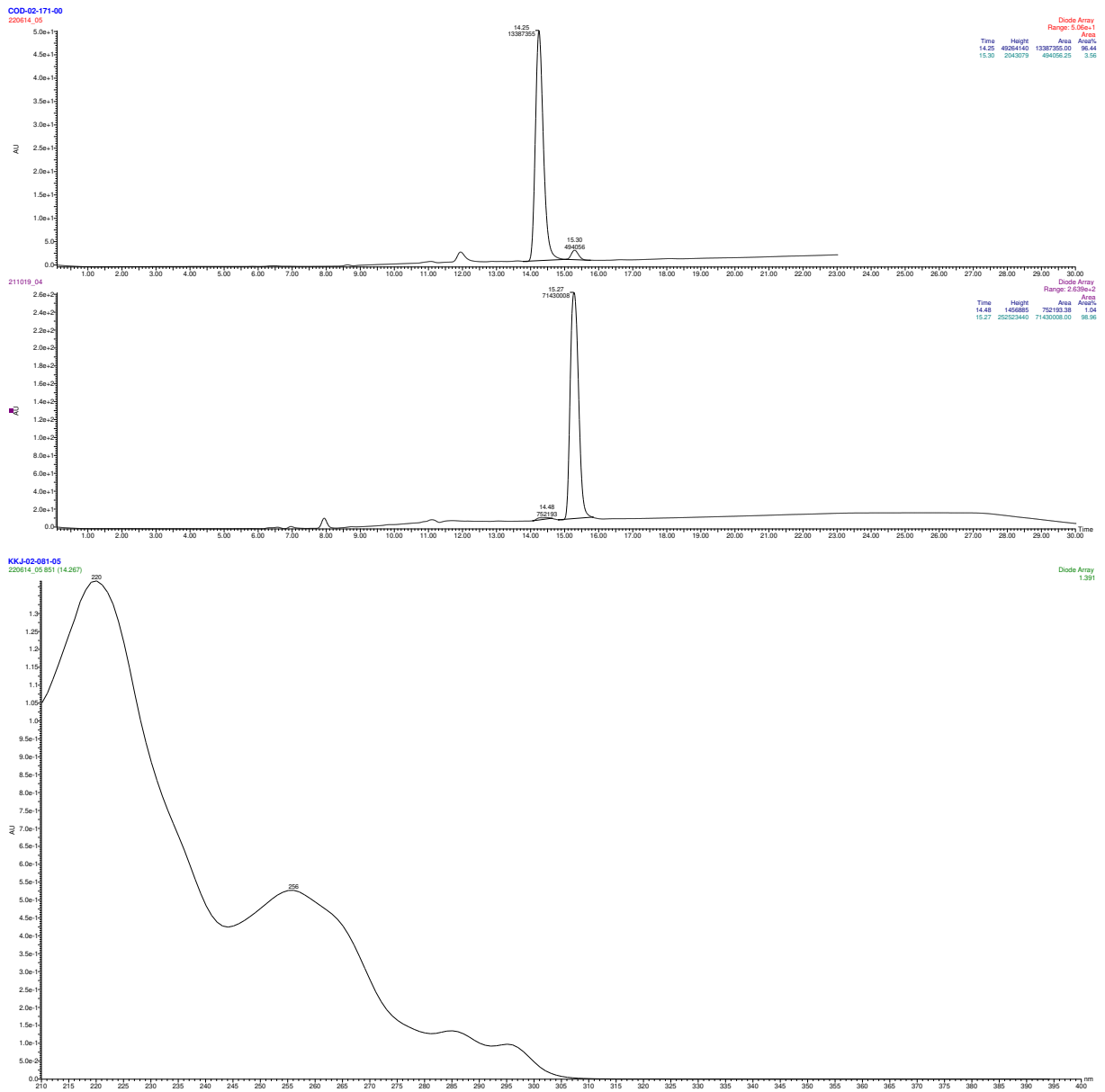
NMR and HPLC

Copy of ^1H , $^{13}\text{C}\{^1\text{H}\}$ spectra of 3-202



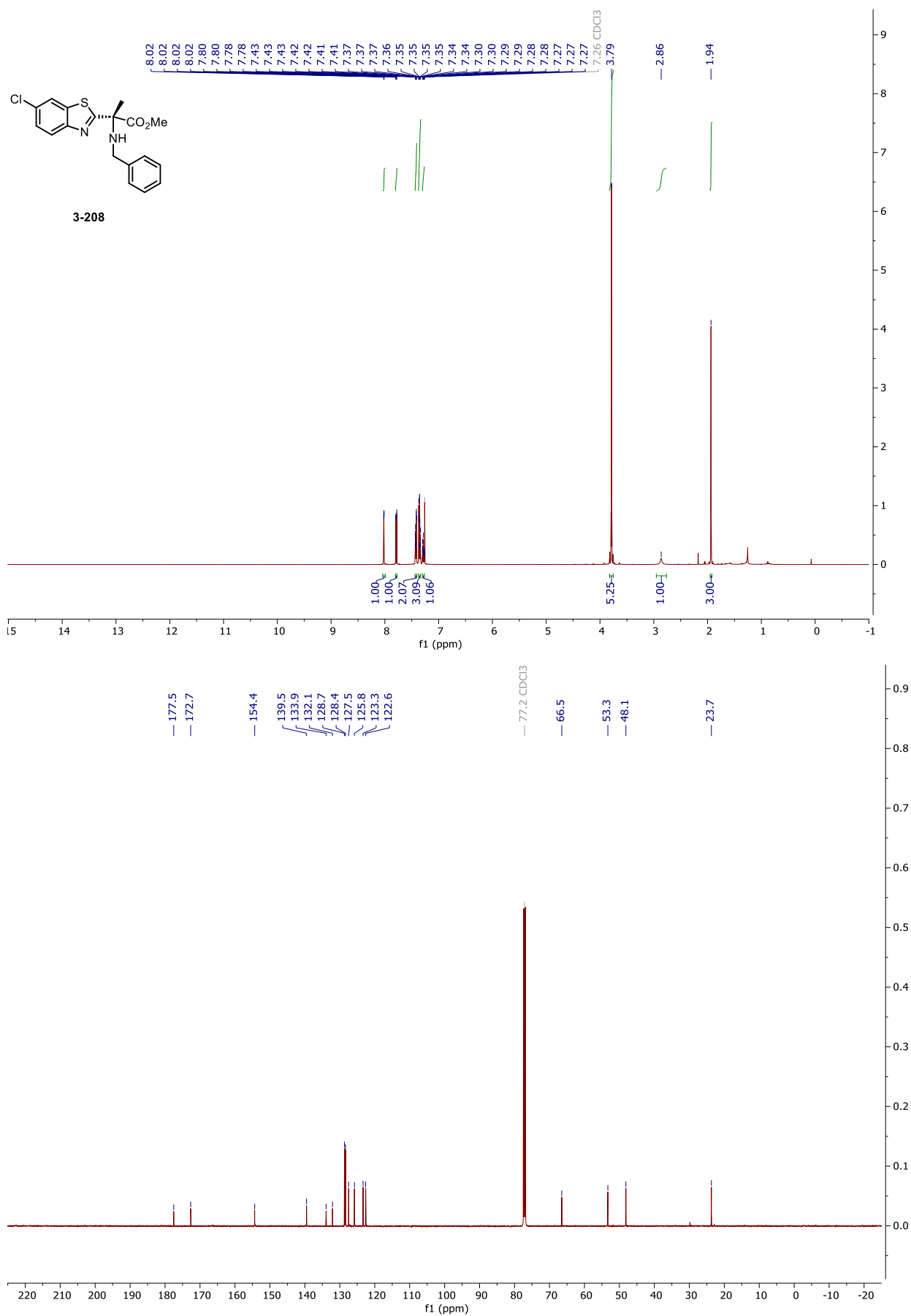
NMR and HPLC

HPLC chromatograms of 3-202



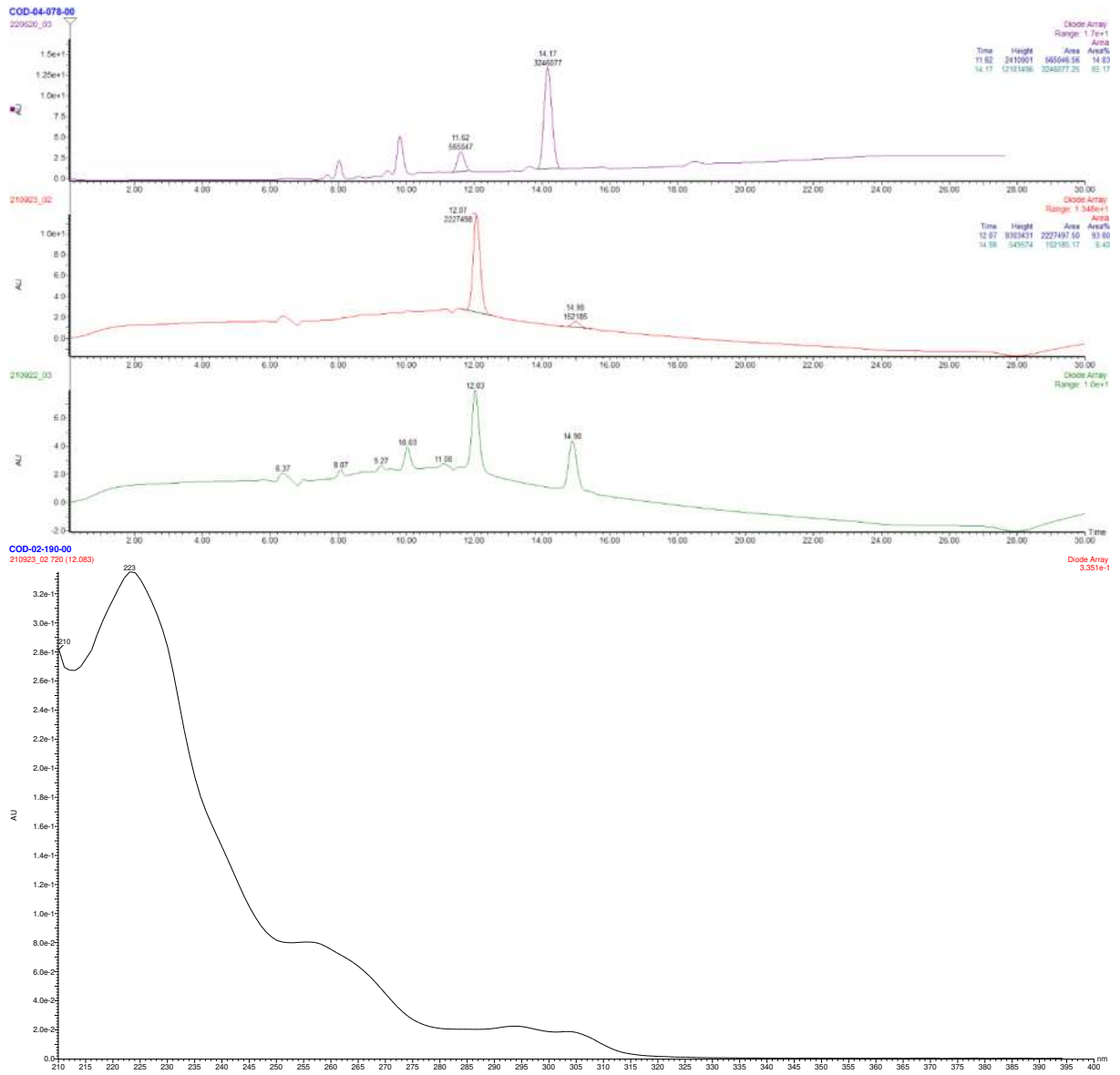
NMR and HPLC

Copy of ^1H , $^{13}\text{C}\{^1\text{H}\}$ spectra of 3-208



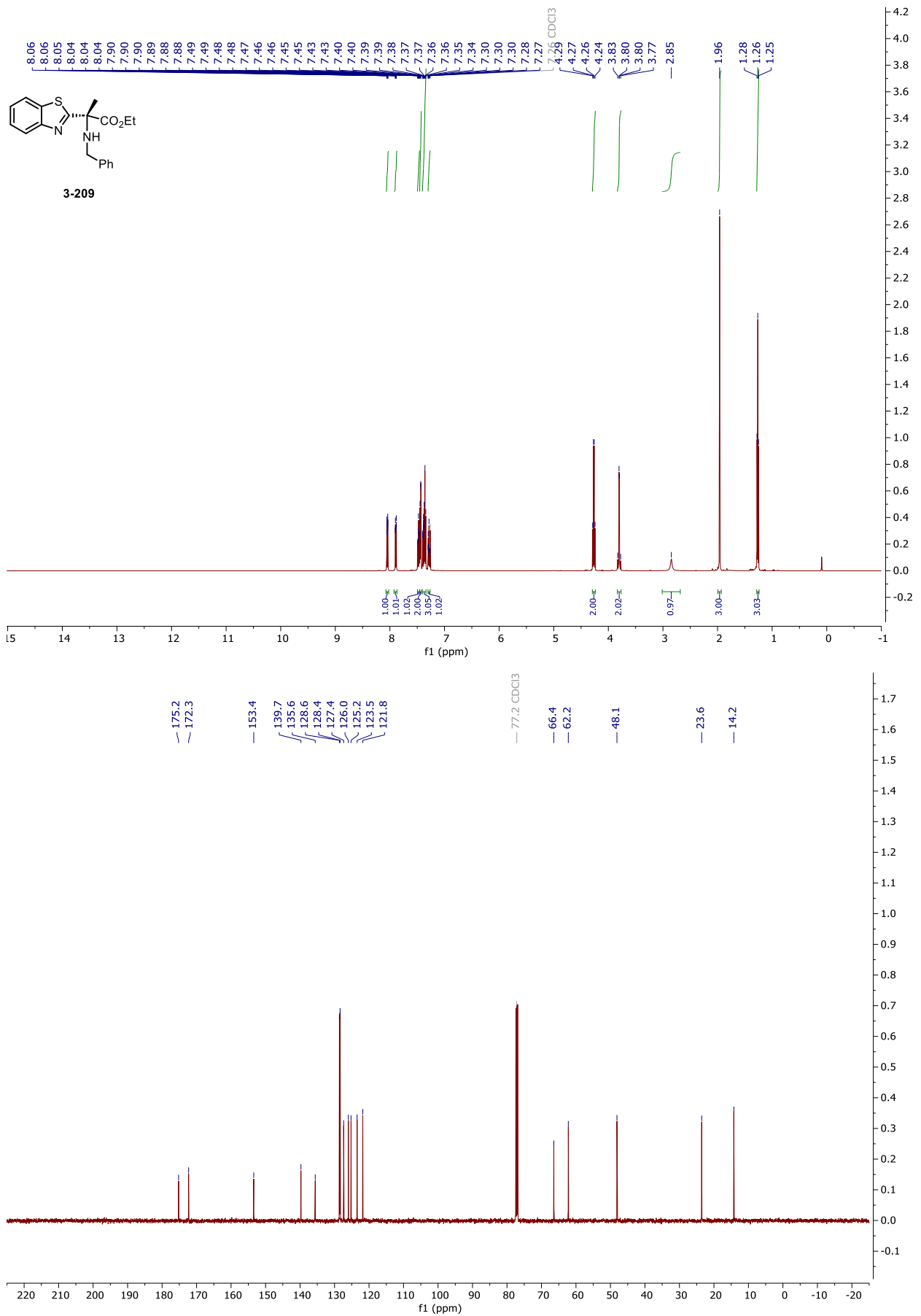
NMR and HPLC

HPLC chromatograms of 3-208



NMR and HPLC

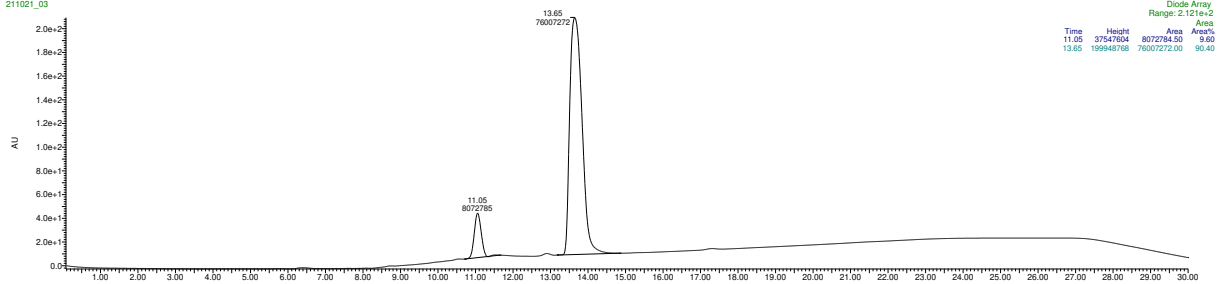
Copy of ^1H , $^{13}\text{C}\{^1\text{H}\}$ spectra of 3-209



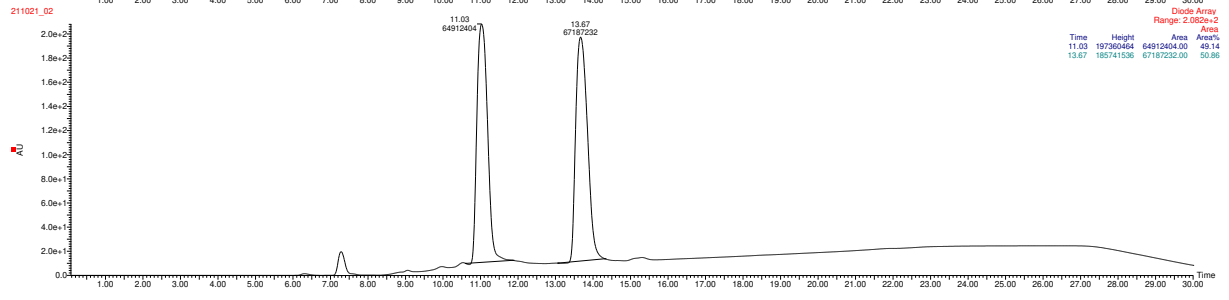
NMR and HPLC

HPLC chromatograms of 3-209

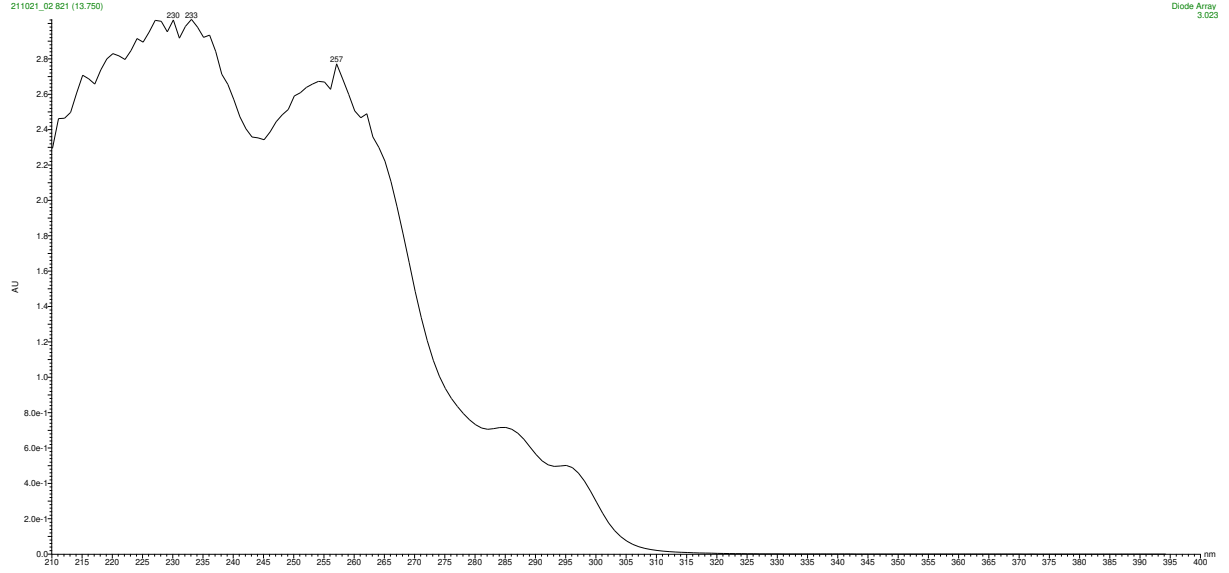
COD-02-134-01
211021_03



211021_02

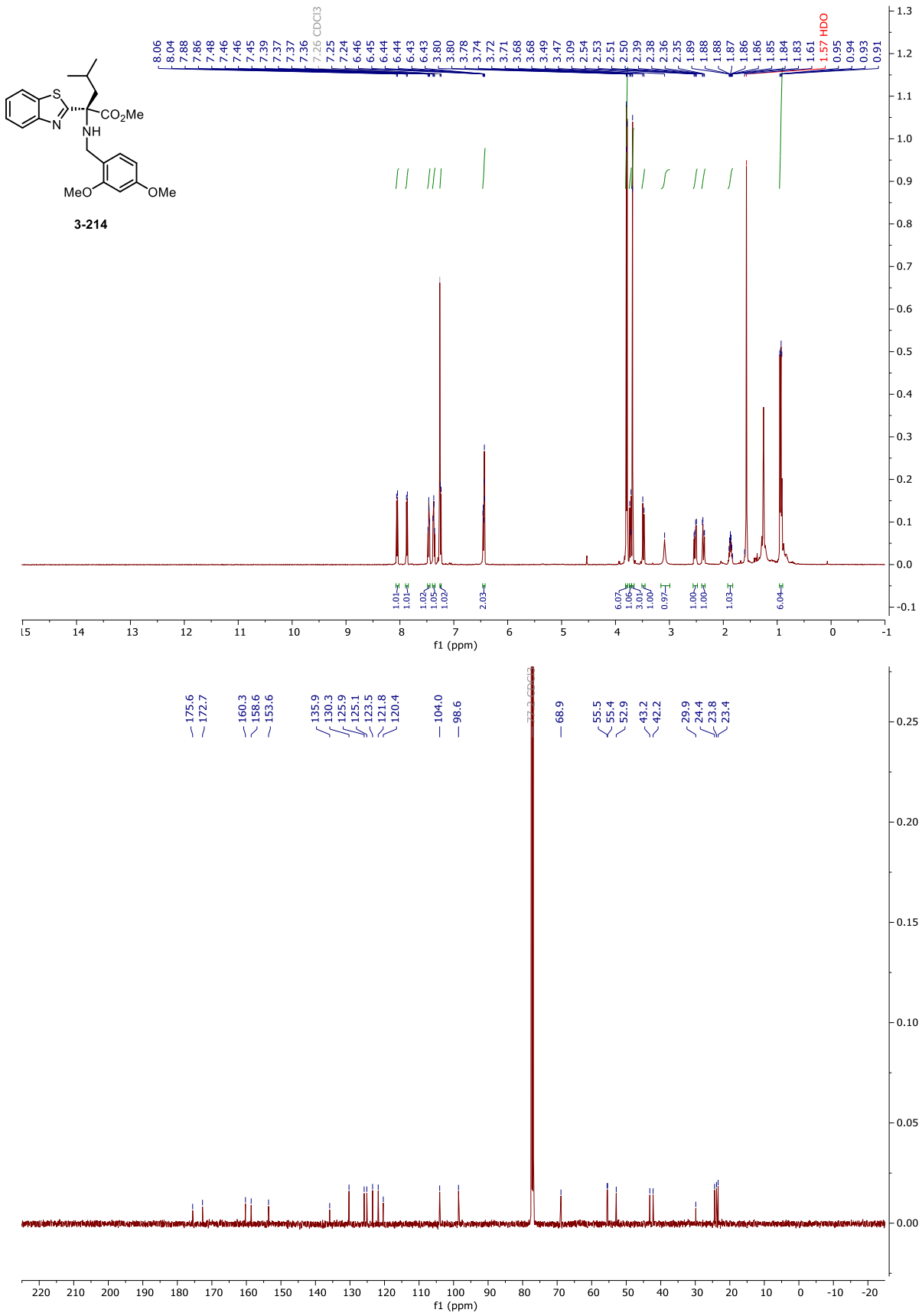


COD-02-134-01
211021_02 821 (13.750)



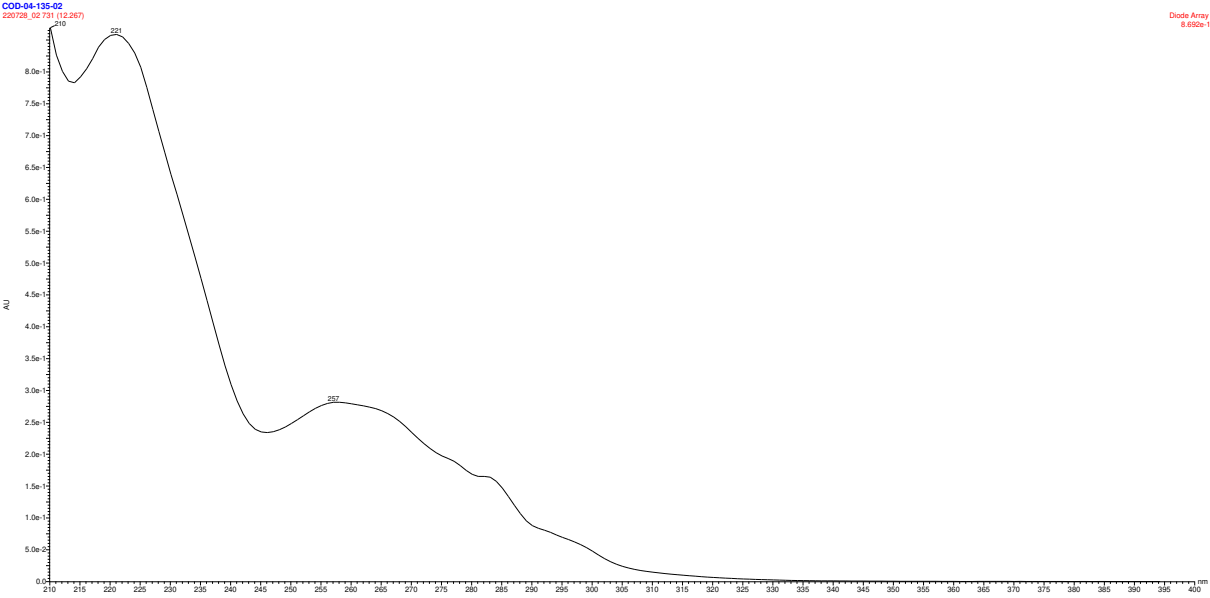
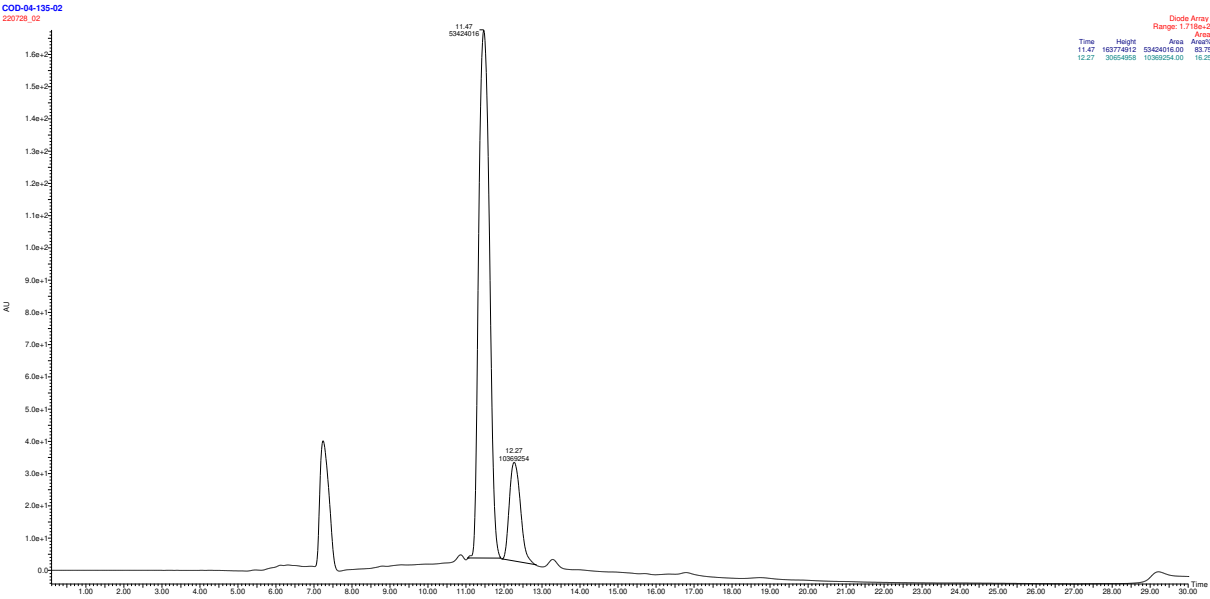
NMR and HPLC

Copy of ^1H , $^{13}\text{C}\{^1\text{H}\}$ spectra of 3-214



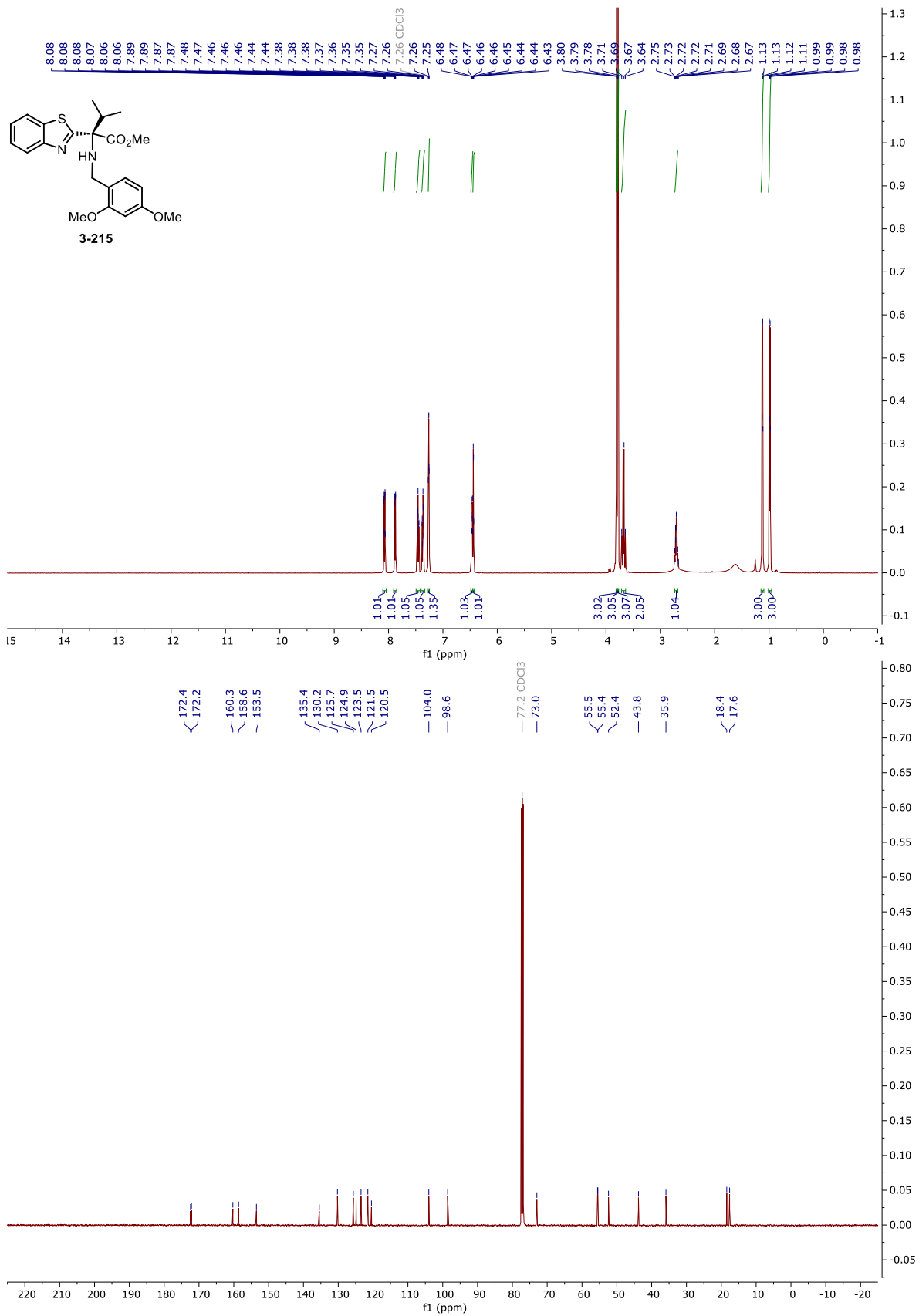
NMR and HPLC

HPLC chromatograms of 3-214



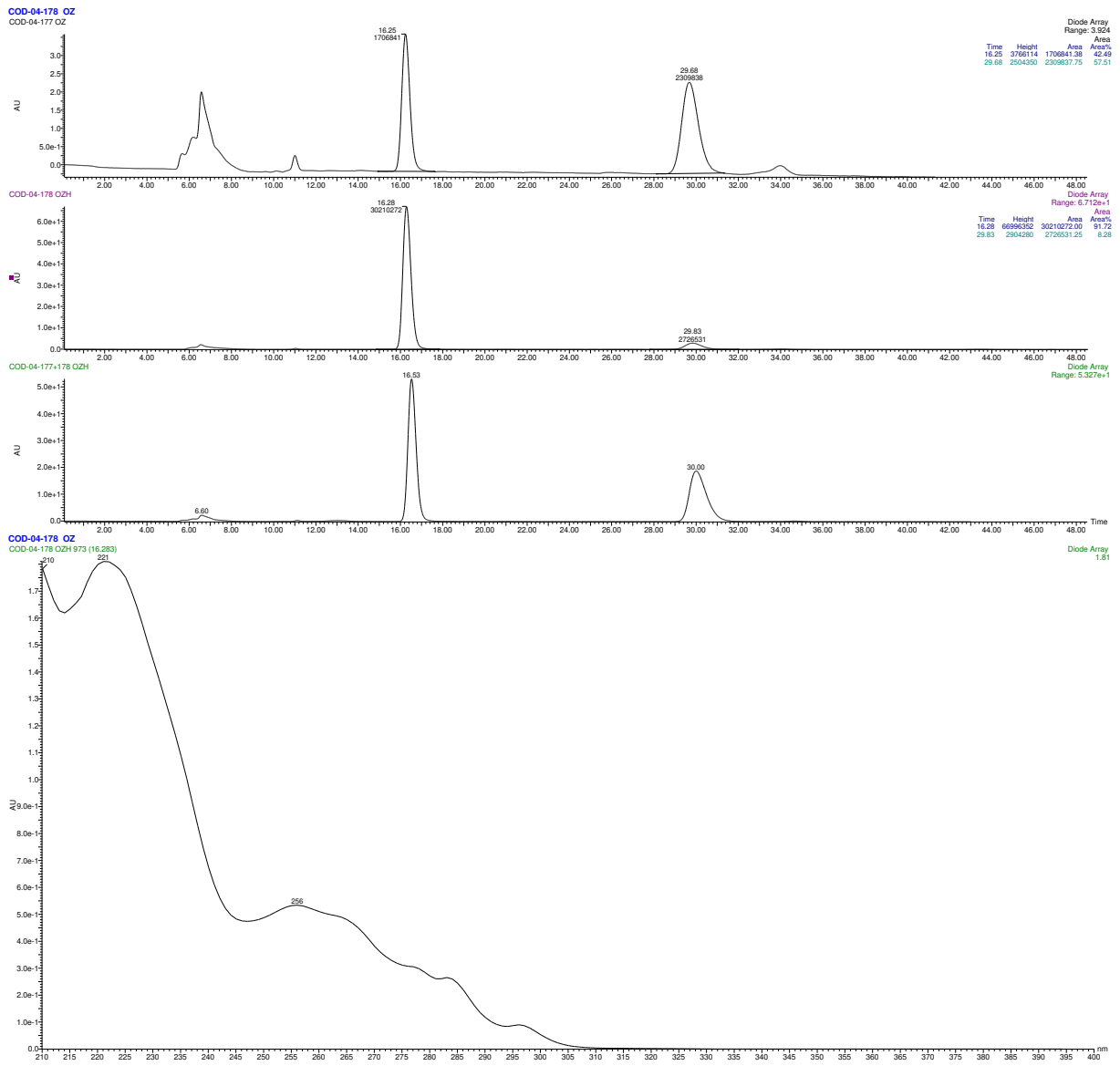
NMR and HPLC

Copy of ^1H , $^{13}\text{C}\{^1\text{H}\}$ spectra of 3-215



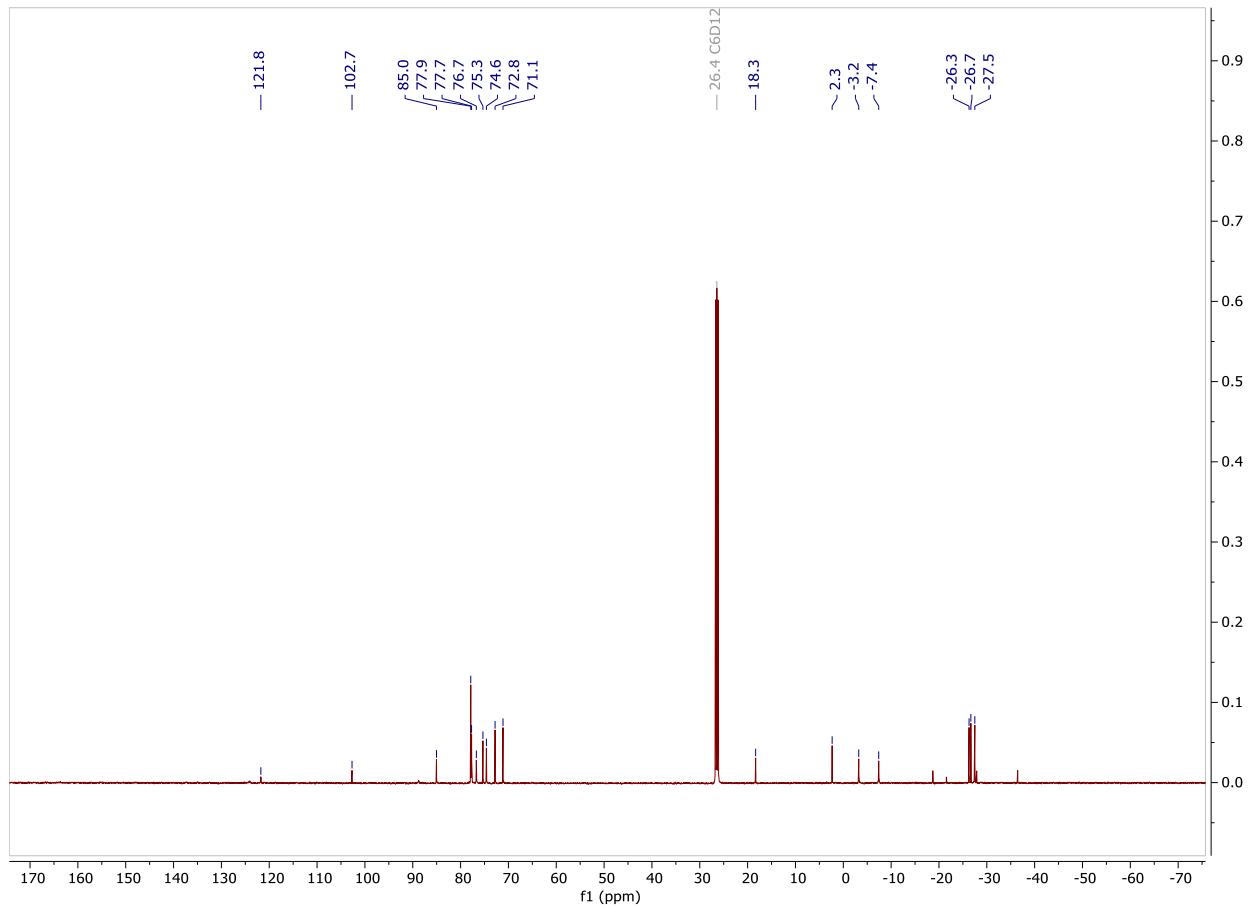
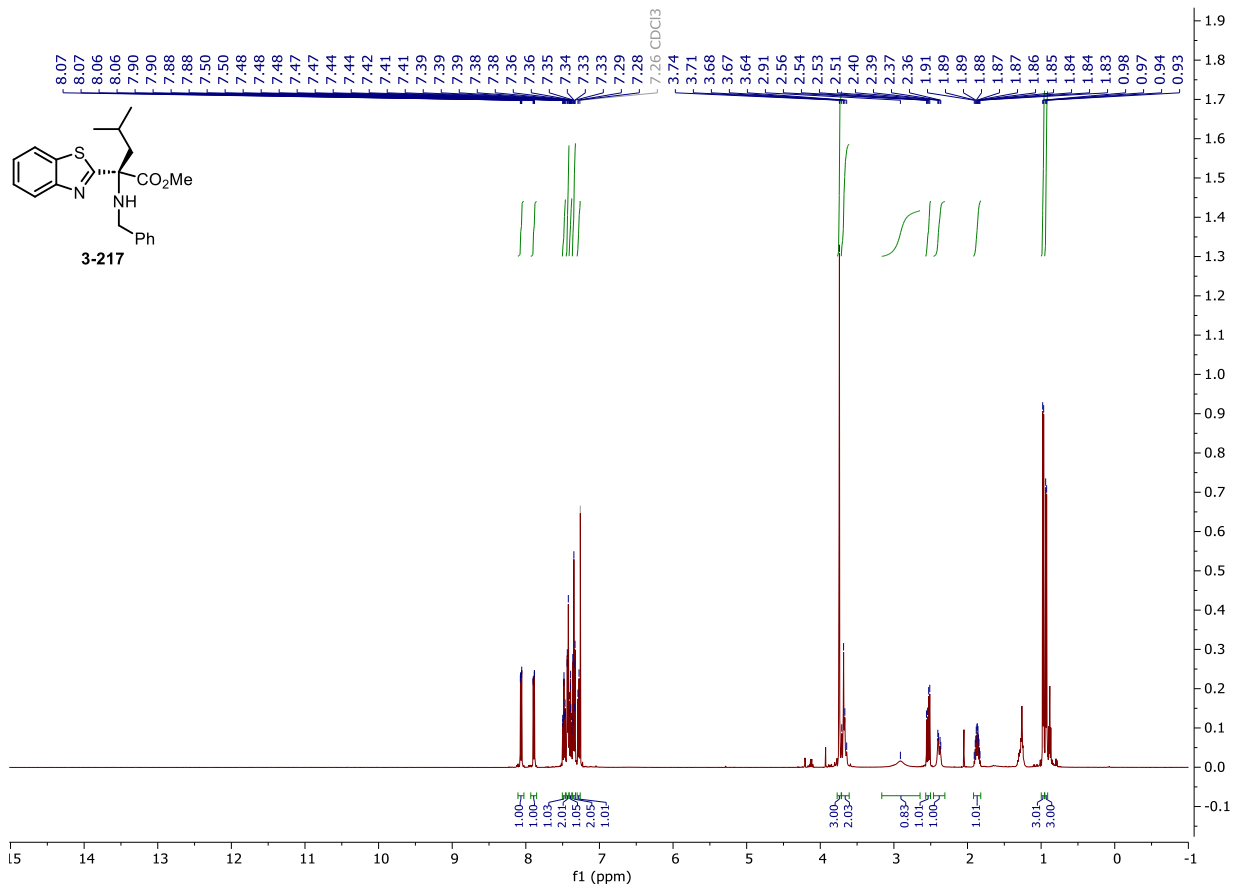
NMR and HPLC

HPLC chromatograms of 3-215



NMR and HPLC

Copy of ^1H , $^{13}\text{C}\{^1\text{H}\}$ spectra of 3-217

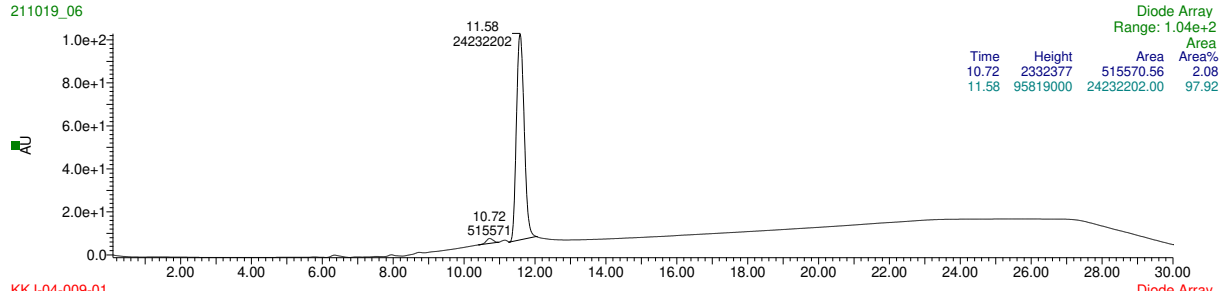


NMR and HPLC

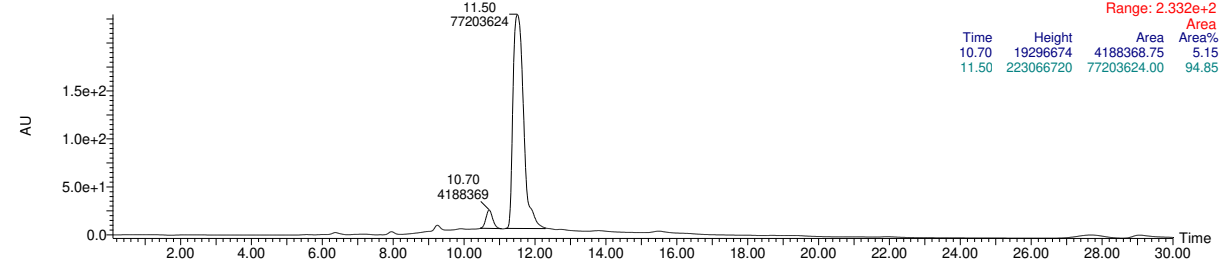
HPLC chromatograms of 3-217

COD-03-033-01

211019_06

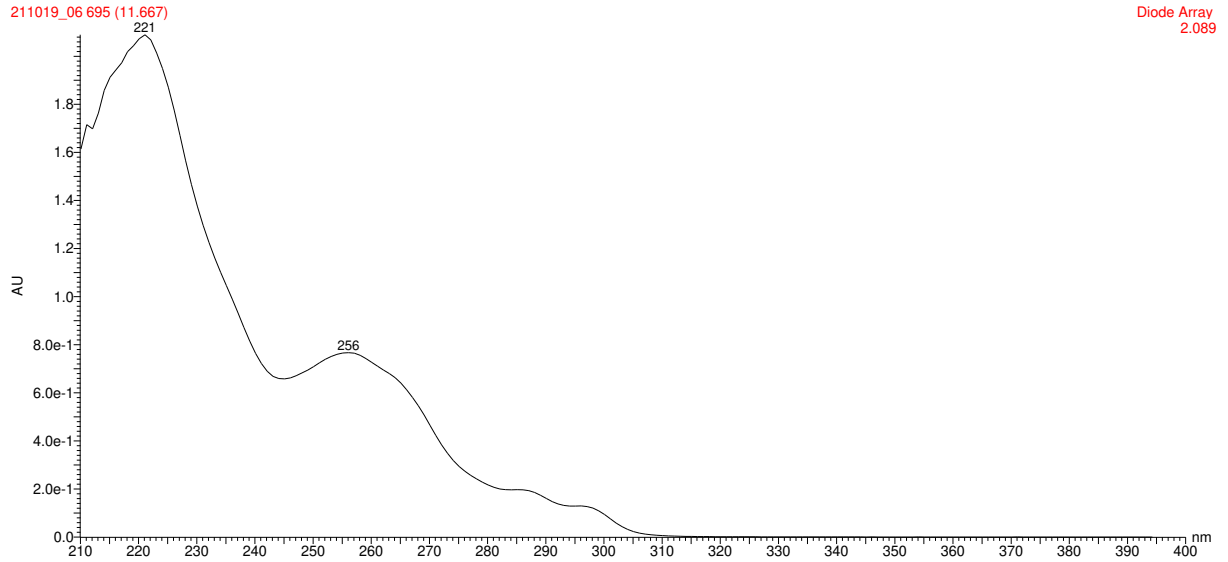


KKJ-04-009-01



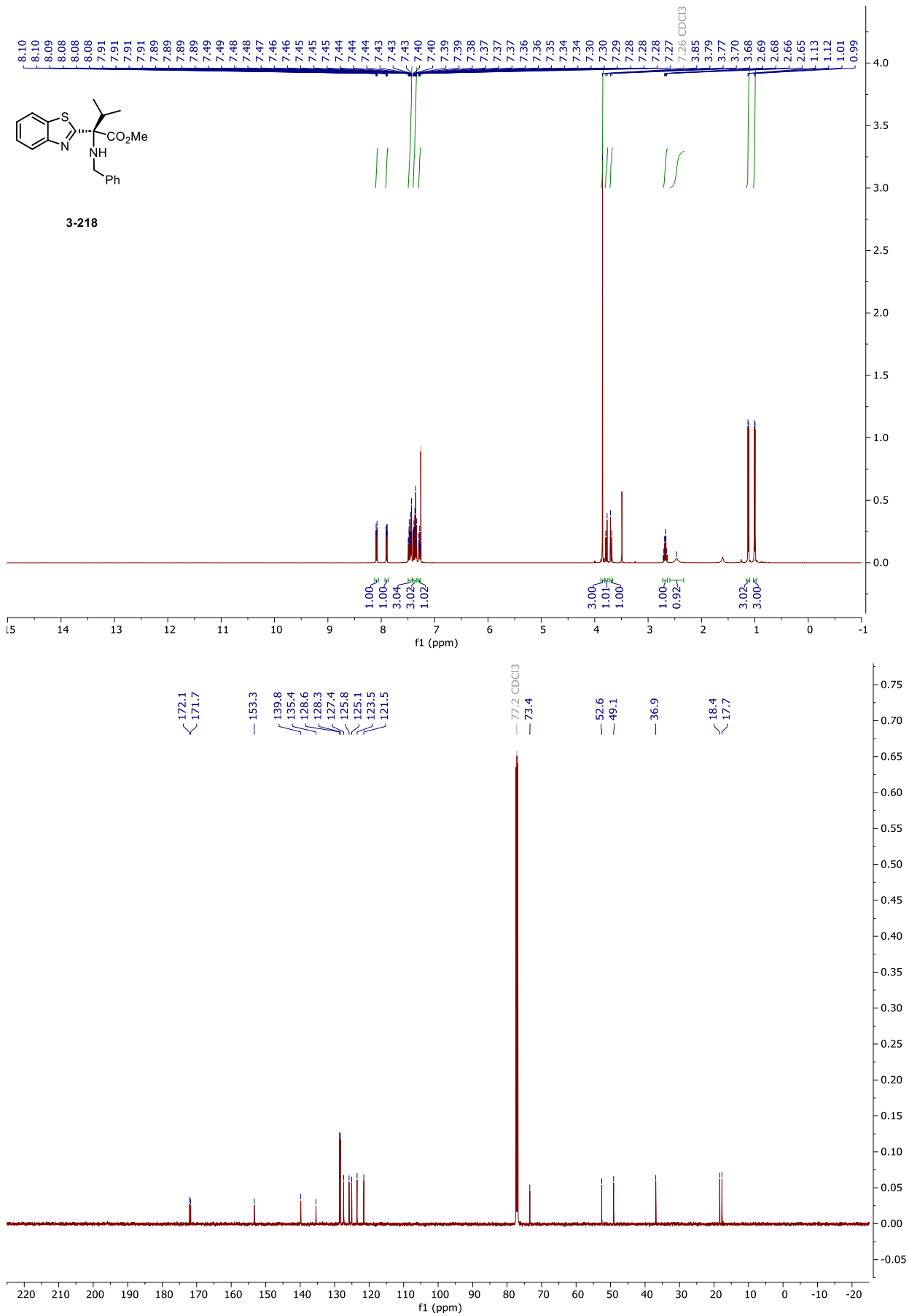
COD-03-033-01

211019_06 695 (11.667)



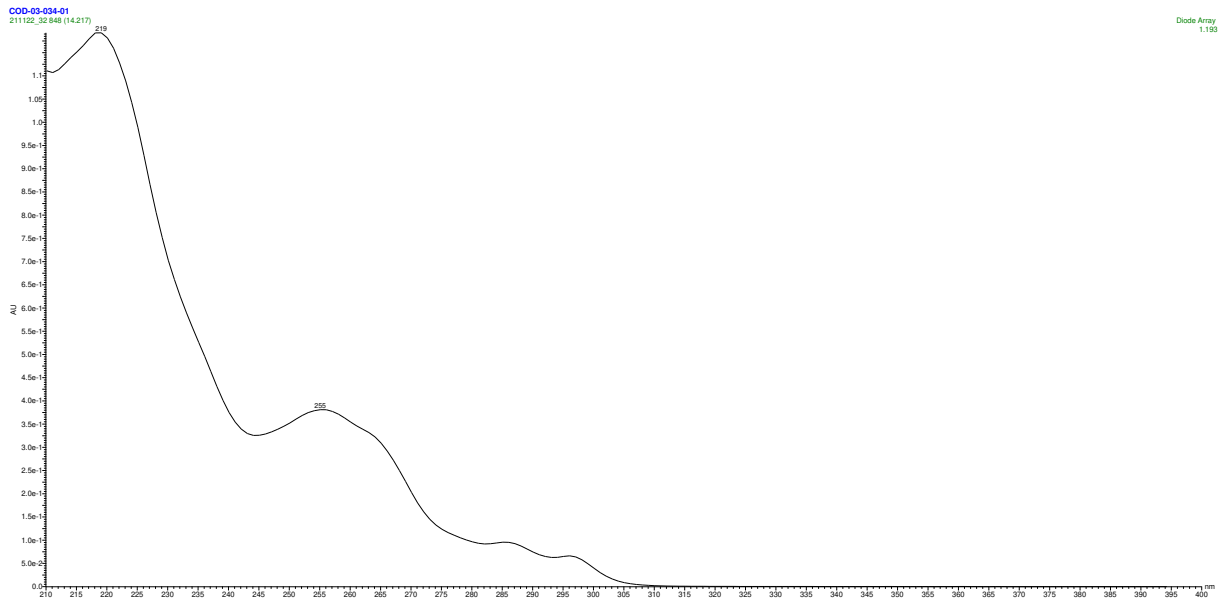
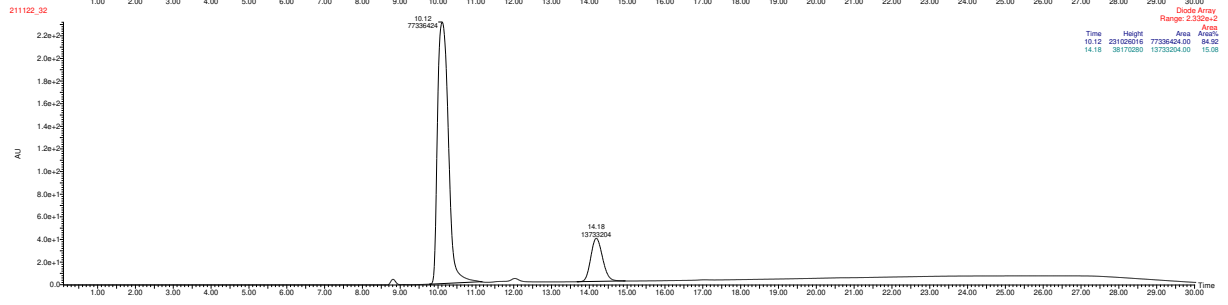
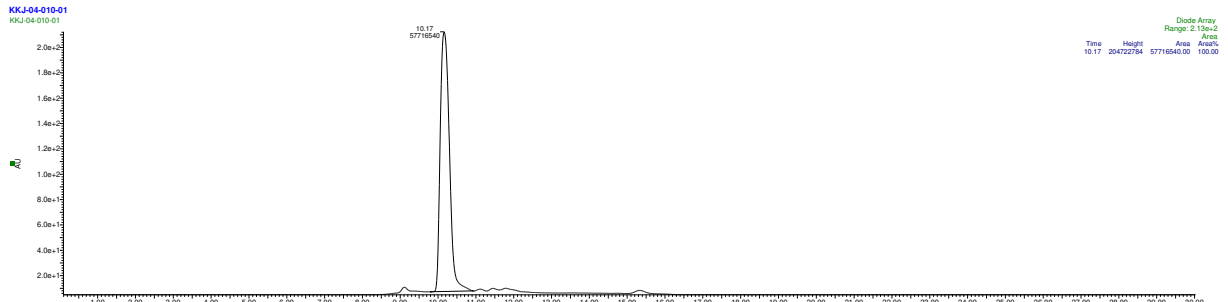
NMR and HPLC

Copy of ^1H , $^{13}\text{C}\{^1\text{H}\}$ spectra of 3-218



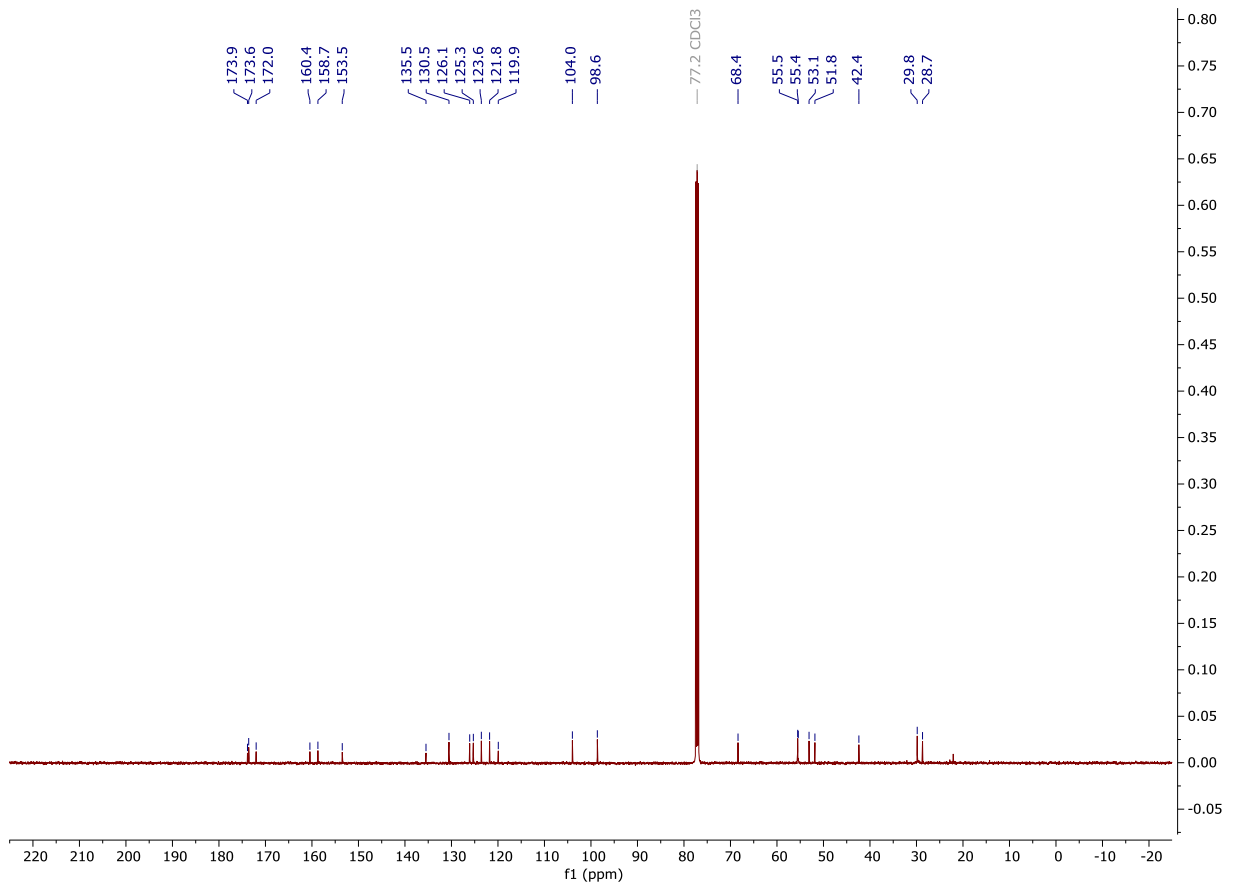
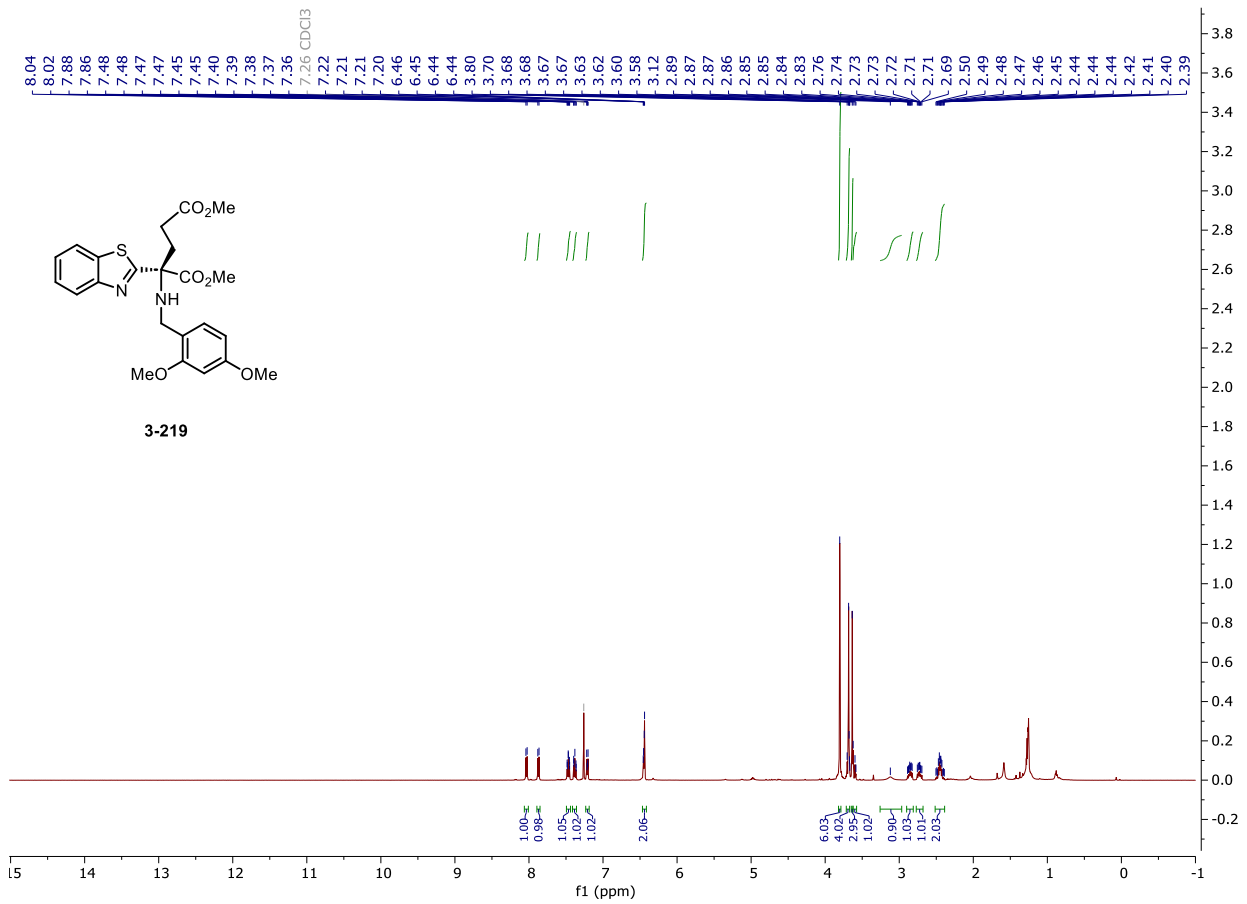
NMR and HPLC

HPLC chromatograms of 3-218



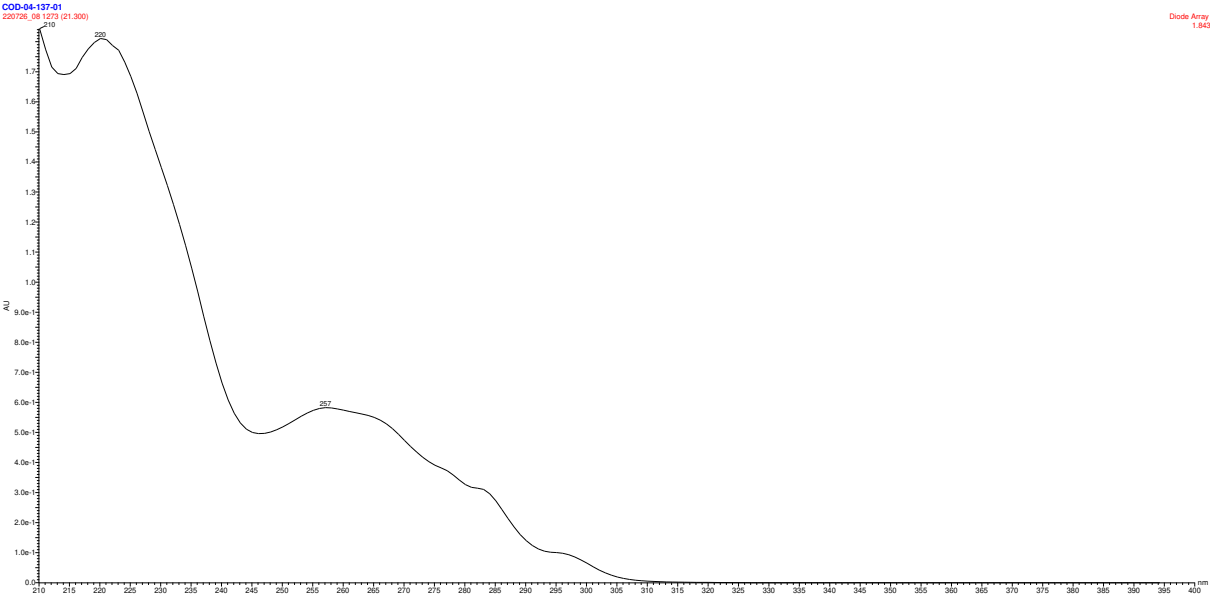
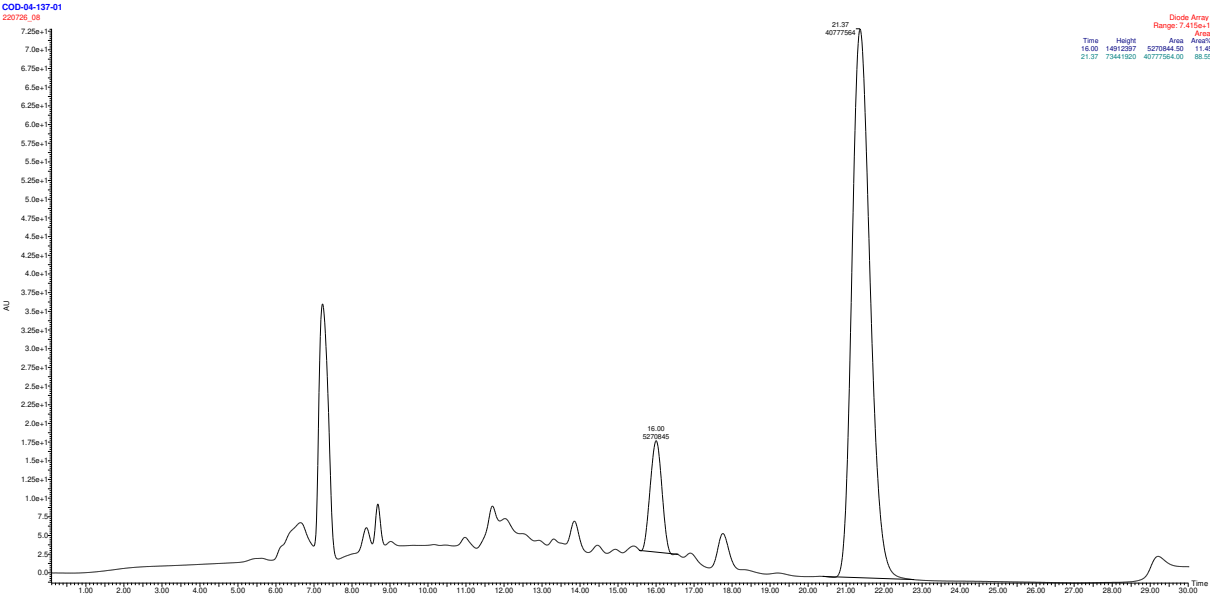
NMR and HPLC

Copy of ^1H , $^{13}\text{C}\{^1\text{H}\}$ spectra of 3-219



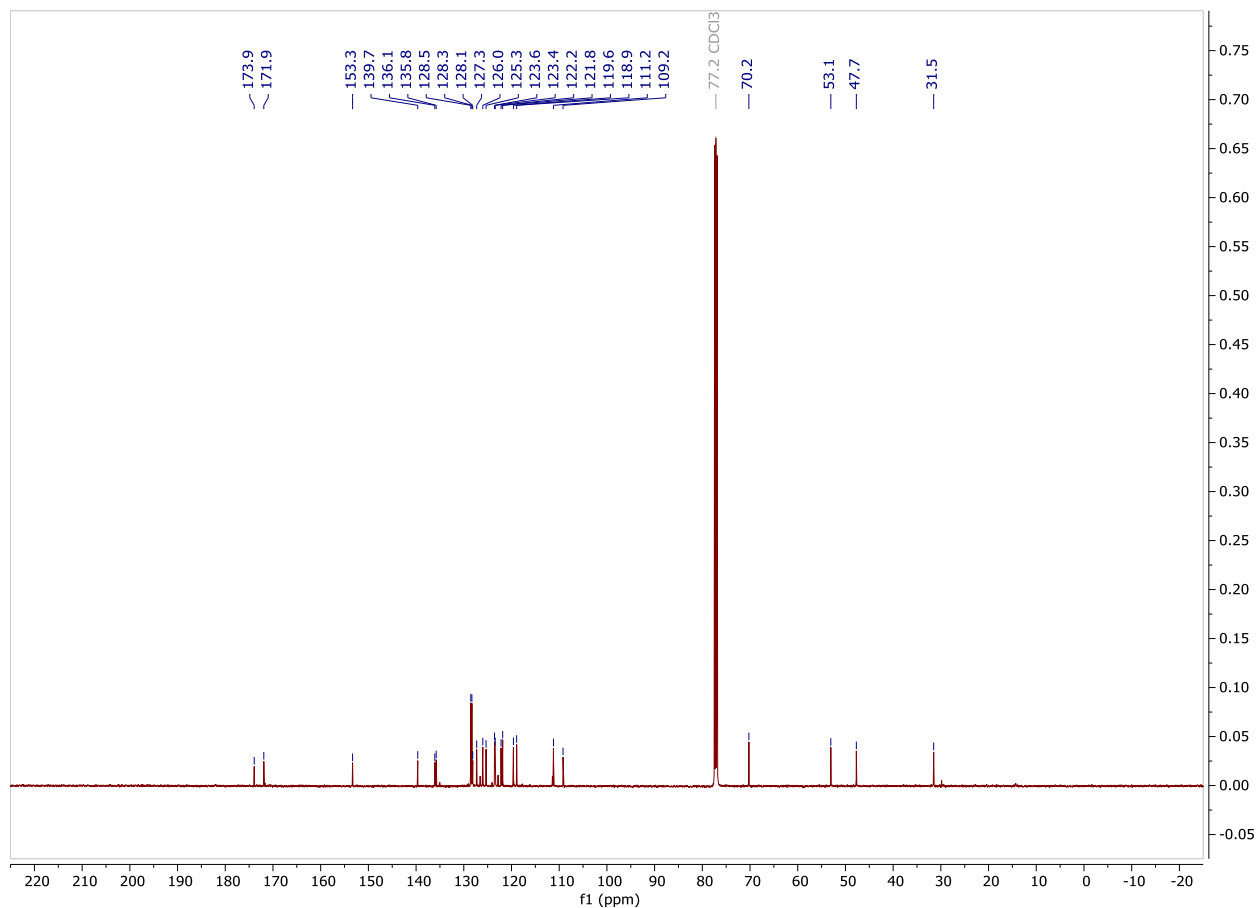
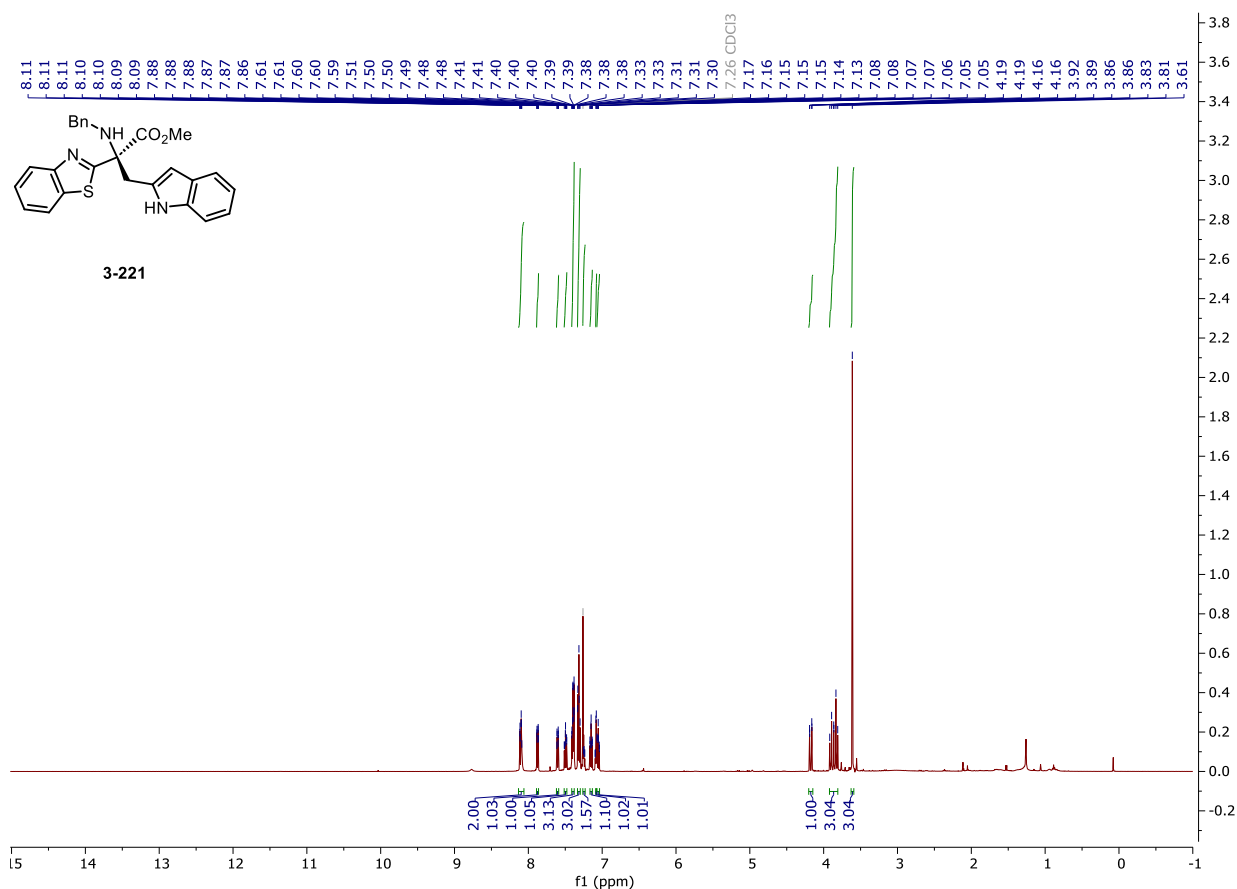
NMR and HPLC

HPLC chromatograms of 3-219



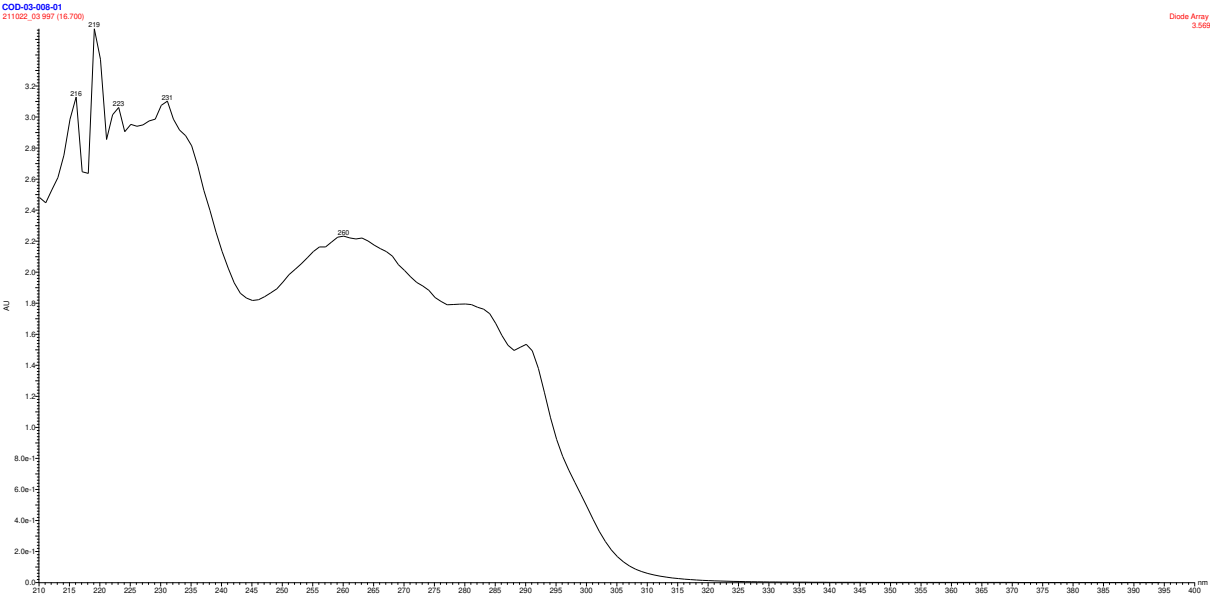
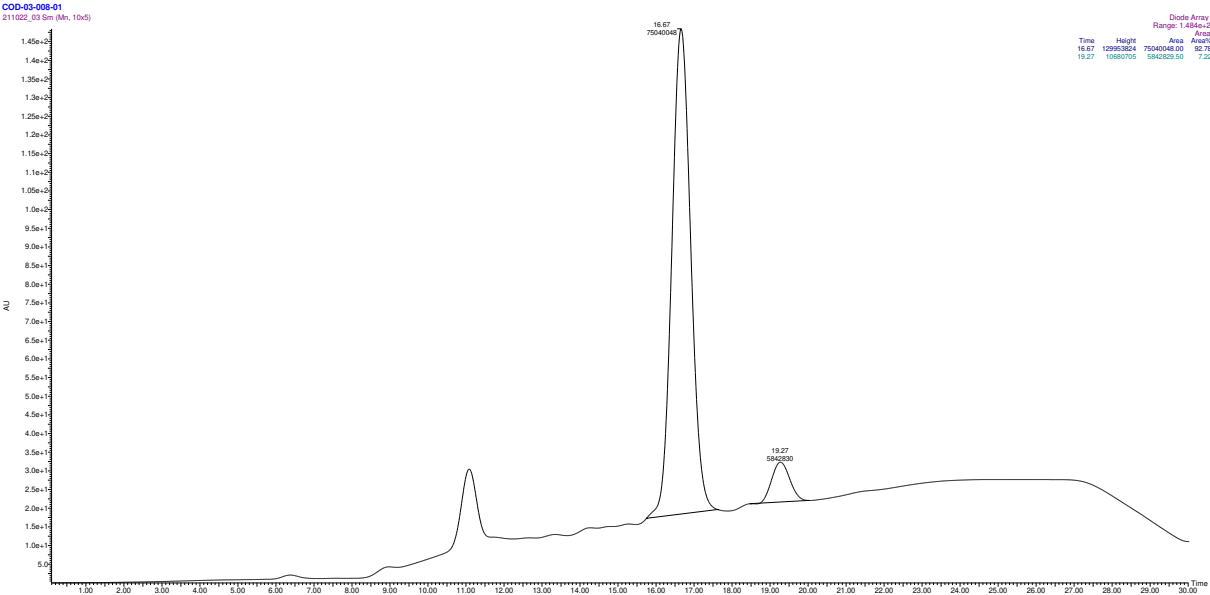
NMR and HPLC

Copy of ^1H , $^{13}\text{C}\{^1\text{H}\}$ spectra of 3-221



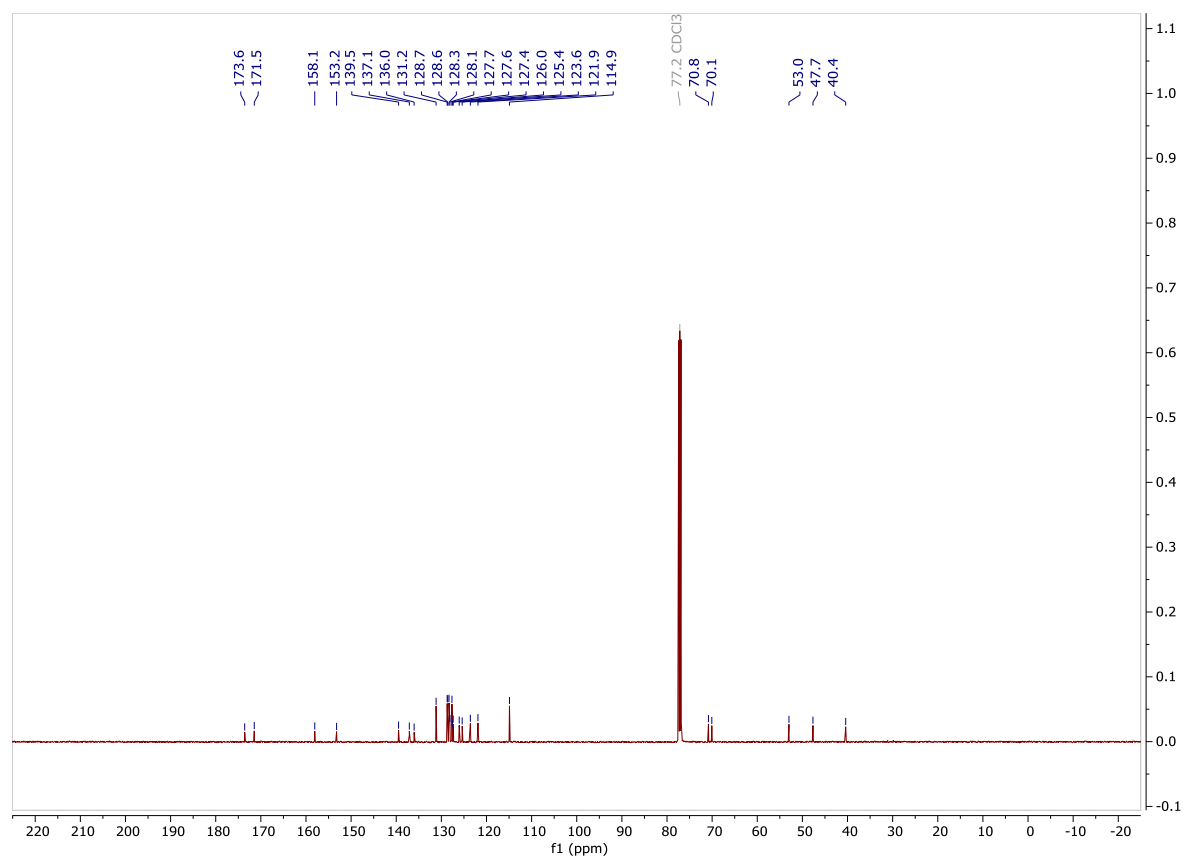
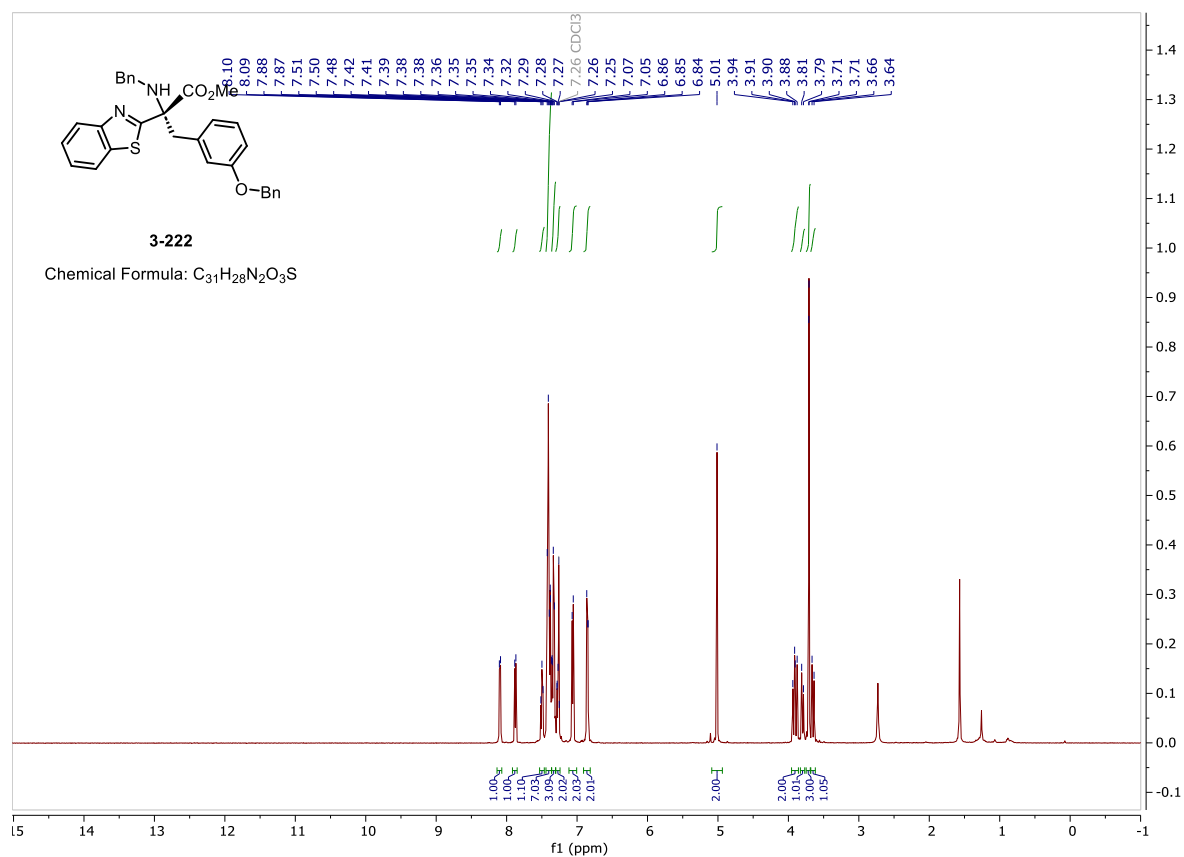
NMR and HPLC

HPLC chromatograms of 3-221



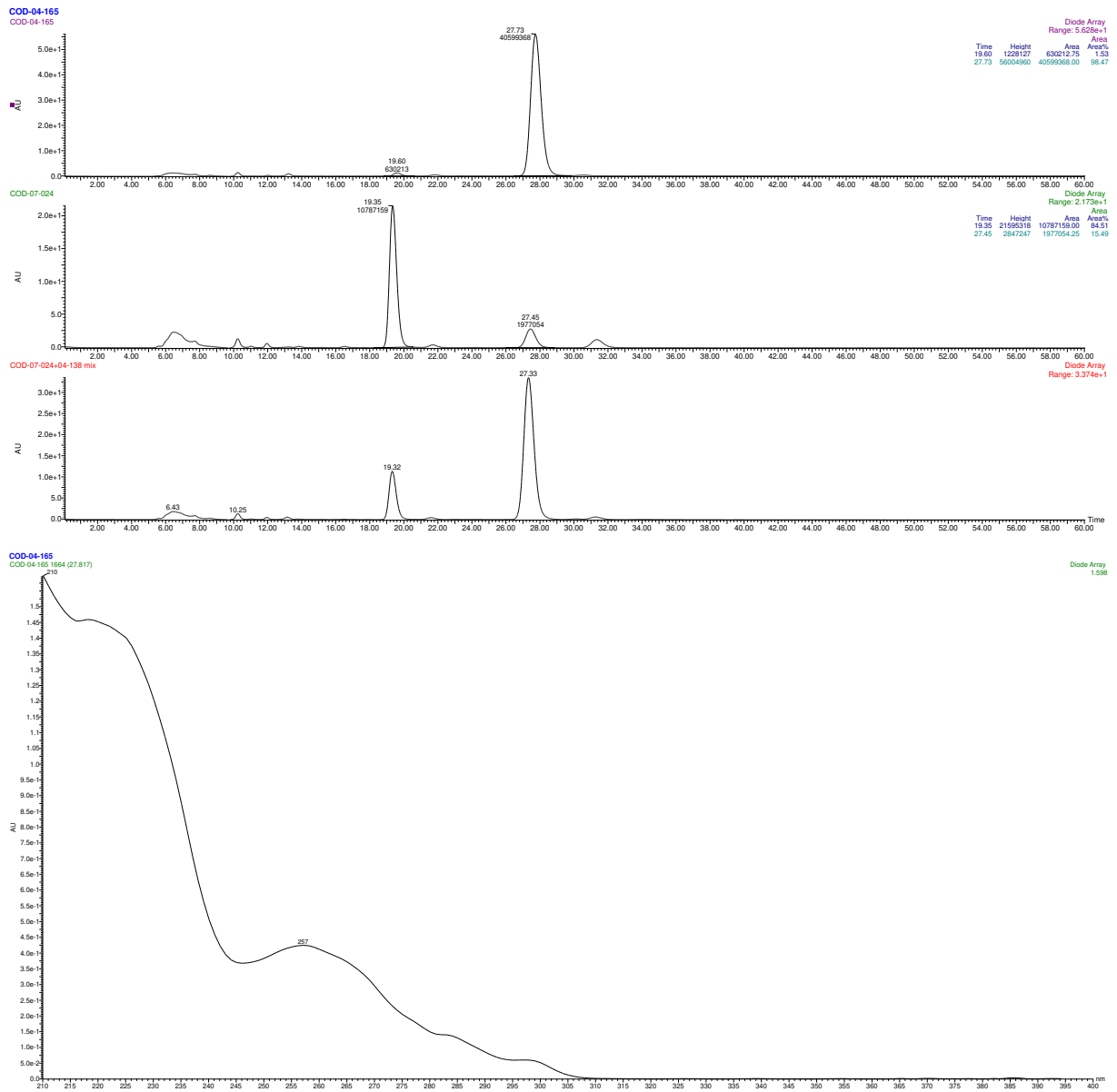
NMR and HPLC

Copy of ^1H , $^{13}\text{C}\{^1\text{H}\}$ spectra of 3-222



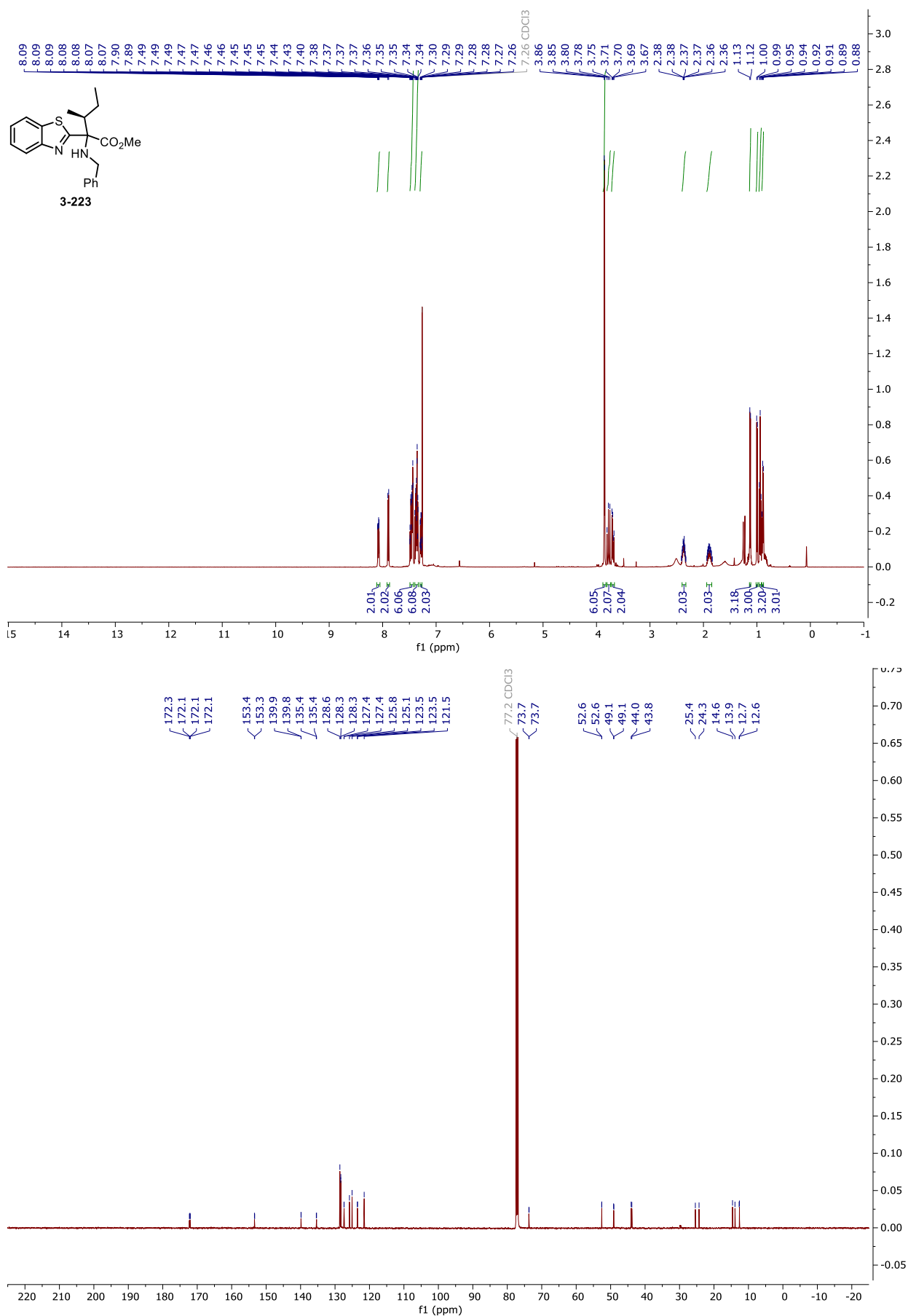
NMR and HPLC

HPLC chromatograms of 3-222



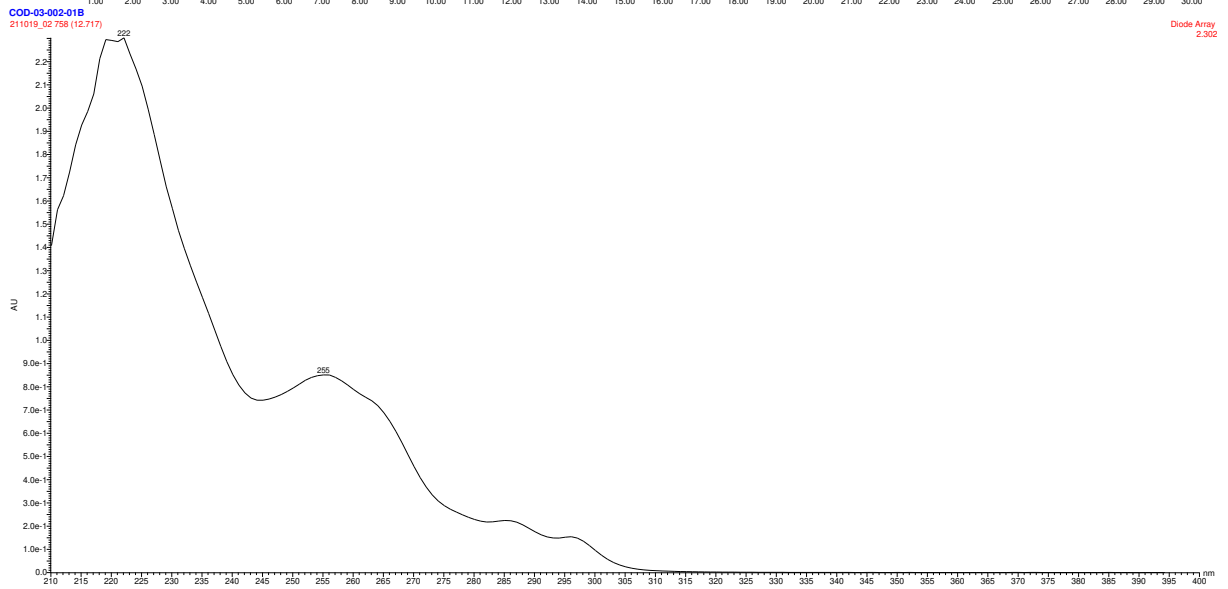
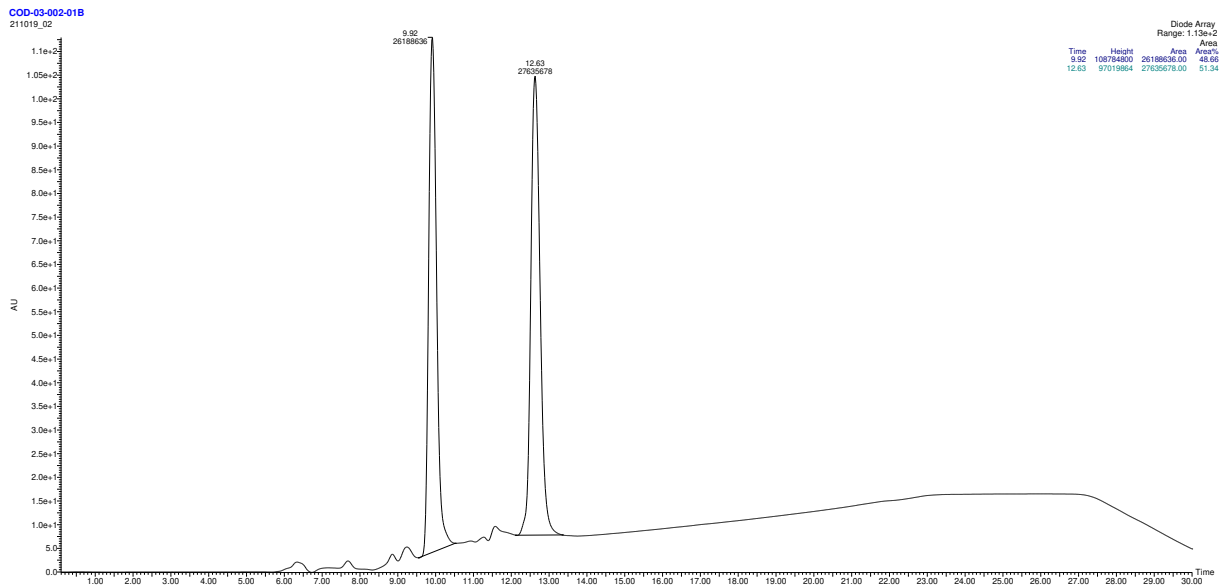
NMR and HPLC

Copy of ^1H , $^{13}\text{C}\{^1\text{H}\}$ spectra of 3-223



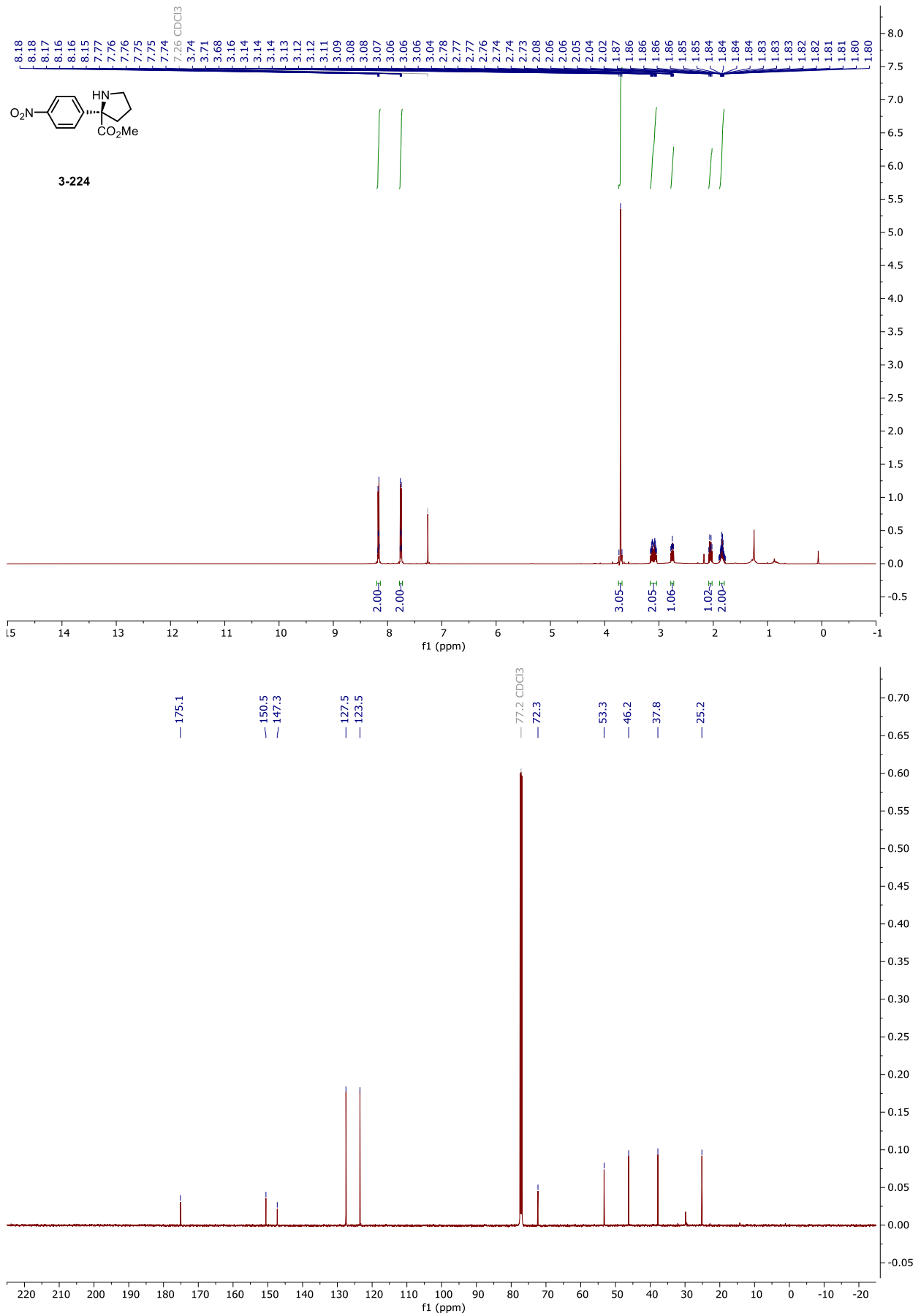
NMR and HPLC

HPLC chromatograms of 3-223



NMR and HPLC

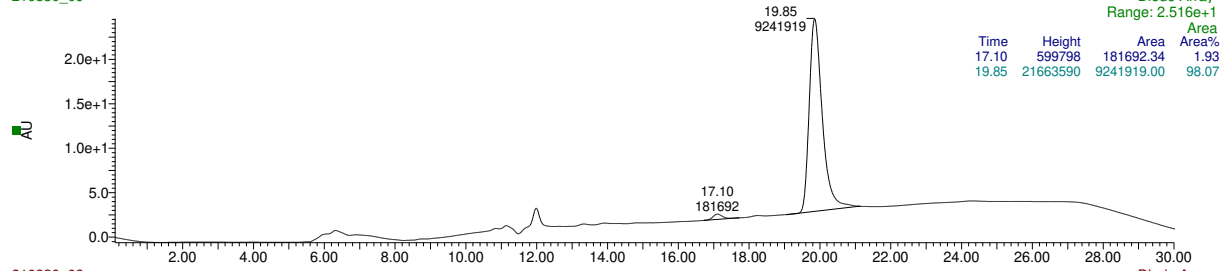
Copy of ^1H , $^{13}\text{C}\{^1\text{H}\}$ spectra of 3-224



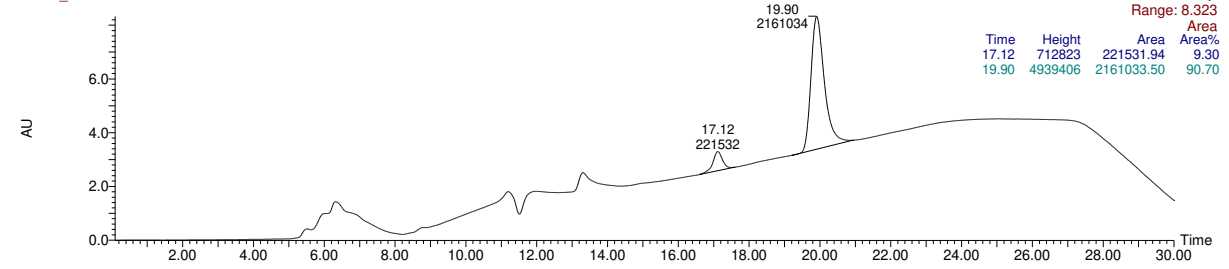
NMR and HPLC

HPLC chromatograms of 3-224

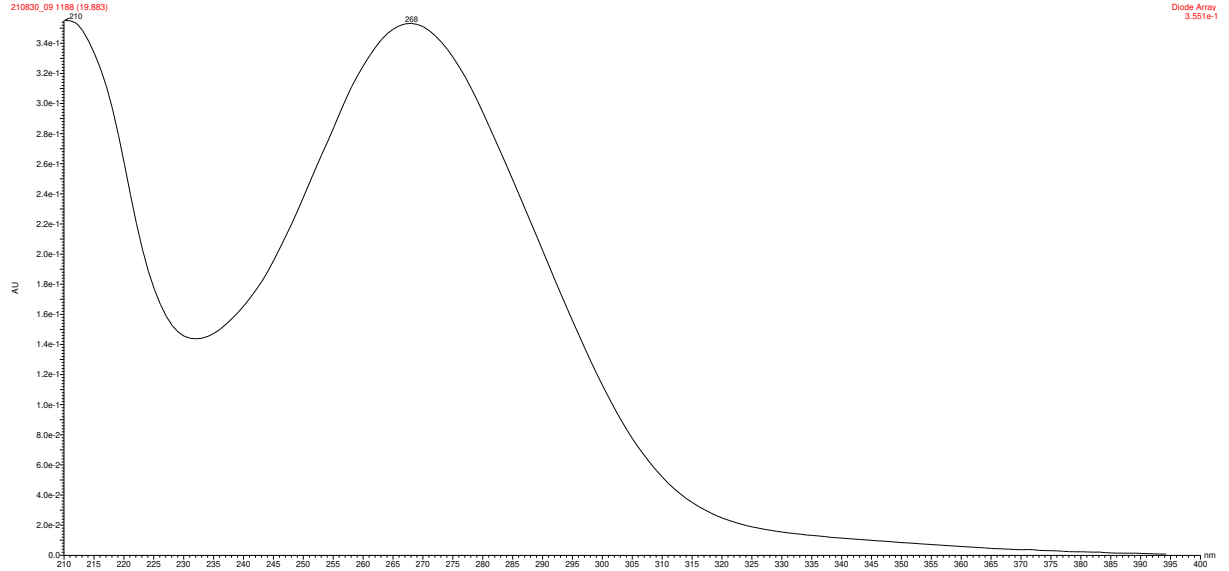
COD-02-159-00
210830_09



210830_08



COD-02-159-00
210830_09 1108 (19.883)



Cite this: *Org. Biomol. Chem.*, 2022, **20**, 3154Received 18th February 2022,
Accepted 21st March 2022DOI: [10.1039/d2ob00345g](https://doi.org/10.1039/d2ob00345g)rsc.li/obc

Heteroaryl sulfonamide synthesis: scope and limitations†

Roman O. Iakovenko,^a Daniel Chrenko,^{a,b} Jozef Kristek,^{b,c} Eline Desmedt,^d František Zálešák,^c Freija De Vleeschouwer^d and Jiří Pospíšil^{*,a,b,c}

Heteroaryl sulfonamides are important structural motifs in the medicinal and agrochemical industries. However, their synthesis often relies on the use of heteroaryl sulfonyl chlorides, which are unstable and toxic reagents. Herein, we report a protocol that allows direct oxidative coupling of heteroaryl thiols and primary amines, readily available and inexpensive commodity chemicals. The transformation proceeds under mild reaction conditions and yields the desired *N*-alkylated sulfonamides in good yields. *N*-alkyl heteroaryl sulfonamides can be further transformed using a microwave-promoted Fukuyama–Mitsunobu reaction to *N,N*-dialkyl heteroaryl sulfonamides. The developed protocols thus enable the preparation of previously difficult to prepare sulfonamides (toxic reagents, harsh conditions, and low yields) under mild conditions.

Introduction

Although the structural motif of sulfonamide is rather rare in nature,¹ it occupies a privileged position in the medicinal and agrochemical areas of research and applications.^{2–4} In fact, its metabolic stability⁵ and carboxyl group isosterism⁶ are presumably responsible for the high levels of biological activity that compounds with the sulfonamide group possess. The classical approach to their synthesis is based on the reunion of sulfonyl chlorides with amines (Fig. 1A).^{7,8} This widely used method suffers from the toxicity and instability of sulfonyl chloride reagents that must, in addition, be prepared using strong oxidizing and chlorinating agents.^{9–15} To overcome such a drawback, one-pot approaches^{16,17} and, more recently, the copper-catalysed arylboronic acid and DABSO-based approach¹⁸ were developed (Fig. 1B). Direct electrochemical oxidative coupling of thiols and amines was recently developed as a non-toxic alternative to the commonly used sulfonyl chloride route (Fig. 1C).^{19,20} Despite all the tremendous progress, polyheteroatomic heteroaryl sulfonamides still remain a challenging target when their synthesis is attempted. In the case of

heteroaryl sulfonamide synthesis, commonly used methods suffer from low stability of the required sulfonyl chlorides²¹ or low conversion of sulfenamide to sulfonamide during the oxidation step.^{19,22}

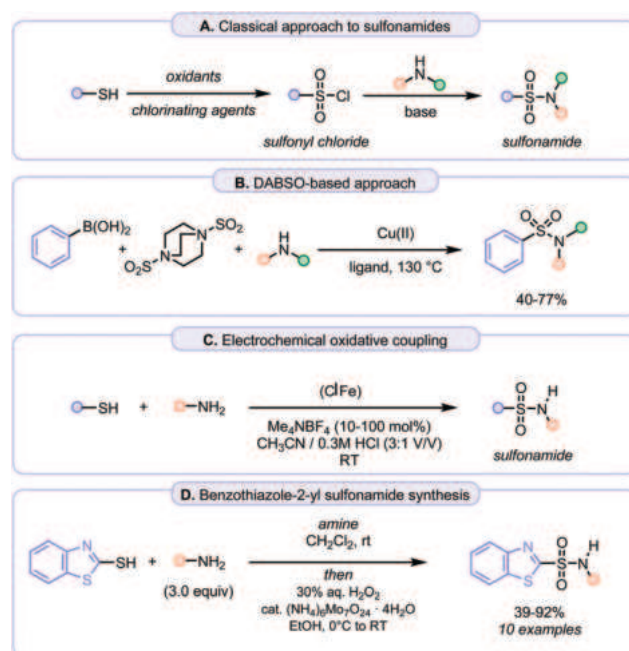


Fig. 1 Previous approaches to sulfonamides. (A) Commonly used route to sulfonamides via the corresponding sulfonyl chloride. (B) DABSO-based approach to sulfonamides starting from aryl boronic acids. (C) Electrochemical synthesis of *N*-alkyl sulfonamide. (D) Our previously developed approach to benzothiazole sulfonamides.

^aLaboratory of Growth Regulators, Institute of Experimental Botany of the Czech Academy of Sciences, and Faculty of Science, Palacky University, Štechtitelů 27, Olomouc CZ-78371, Czech Republic. E-mail: j.pospisil@upol.cz

^bDepartment of Chemical Biology, Faculty of Science, Palacky University, Štechtitelů 27, Olomouc CZ-78371, Czech Republic

^cDepartment of Organic Chemistry, Faculty of Science, Palacky University, tř. 17. listopadu 1192/12, Olomouc CZ-771 46, Czech Republic

^dEenheid Algemene Chemie (ALGC), Vrije Universiteit Brussel (VUB), Pleinlaan 2, 1050 Brussels, Belgium

† Electronic supplementary information (ESI) available. See DOI: <https://doi.org/10.1039/d2ob00345g>

Our interest in heteroaryl sulfonamide synthesis led us recently to develop a unified approach to *N*-substituted and *N,N*-disubstituted benzothiazole-2-yl sulfonamides from benzo[*d*]thiazole-2-thiol and alkyl amines, readily available bulk chemicals (Fig. 1D).²³ Simplicity of the developed protocol hand-in-hand with a quasi-nonexistent general method that would allow the synthesis of, for example, (benzo[*d*]oxazole-2-yl sulfonamides¹⁹ led us to the idea of extending this method to other heterocyclic thiols.

Results and discussion

Preliminary results

Before extension of our oxidative coupling method to other heteroaromatic thiols, the electrophilicity of the C_α sulfona-

mid carbon in representative (hetero)aromatic thiols (**1a–10a**, Fig. 2A) was evaluated *in silico*. Previous observations and data obtained during our research in the field of benzothiazole-2-yl sulfones and sulfonamides showed that sulfone/sulfonamide-bearing C_α carbon in the heterocycle is prone to nucleophilic attack.^{24–26} We exploited this behaviour, for example, in amine synthesis;²³ however, it also caused the instability of sulfones and sulfonamides on silica gel.^{24,27,28} For those reasons we wondered if the quasi-nonexistence of several classes of heteroaryl sulfonamides in the literature¹⁹ might be caused by their instability. To shed some light on the C_α atom electrophilicity in *N*-benzylated sulfonamides (Fig. 2A), the local electrophilicity index values ($\omega_{C_{\alpha}}^{+}$)^{29,30} were calculated for two optimized conformations, linear and sandwich-like (Fig. 2B, the latter being more stable).³¹ Computational data suggested that newly prepared heteroaryl sulfonamides **2a–10a** should not suffer from the C_α nucleophilic attack (similarly to known aryl sulfonamides **1**), since their $\omega_{C_{\alpha}}^{+}$ values are not exceeding those of sulfonamides **1a–c**. On the other hand, the stability of **2a–10a** in the presence of Lewis or Brønsted acid was still questionable.³² Based on the calculations, benzoxazole sulfonamide **7a**, in its protonated form, is very prone for a nucleophilic attack at C_α and, therefore, it was selected as the target substrate for reaction development.³²

The optimization of the reaction started by reacting benzoxazole-2-thiol with benzylamine under previously developed reaction conditions for 2-mercaptobenzothiazol (Fig. 2C, entry 1).²³ Only traces of product **7a** were observed. Detailed investigation and optimization of the reaction steps (sulfenamide formation (entry 2) and its oxidation to sulfonamide (entry 3)) and the isolation and purification of product **7a** allowed us to prepare the desired sulfonamide in a reasonable 35% isolated yield (entry 4).³² The low isolated yield is caused by the isolation process of **7a** (NMR-based yield is higher (68–69%), entries 3 and 4). In our hands, crystallization proved to be the only way of purification that allowed us to obtain pure sulfonamide **7a**.

Scope and limitations

Having identified optimal reaction conditions of the oxidative coupling, the scope and limitations were established (Fig. 3). It was observed that the applicability of the method is broad and that most of the heteroaryl sulfonamides can be generated in good yields using our two-step process. However, in many cases, generated *N*-substituted sulfonamides were unstable in solution and degraded during the purification process. Once obtained in pure form, if solid, they proved to be bench-stable over the period of 3 months. The observed instability was especially significant in the case of (benzo)oxazole sulfonamides **7** and **8**, heteroaryl sulfonamides substituted with electron-donating group ((–)-**9f**) or heteroaryl sulfonamides containing four nitrogens within the heterocycle (**6b** and **16**).³²

The reaction sequence proved to be futile when secondary amines, aromatic amines, cyanamide, or ammonium chloride were used as the reaction partner. In such cases, the first step, the formation of sulfenamide, failed. The only exception to

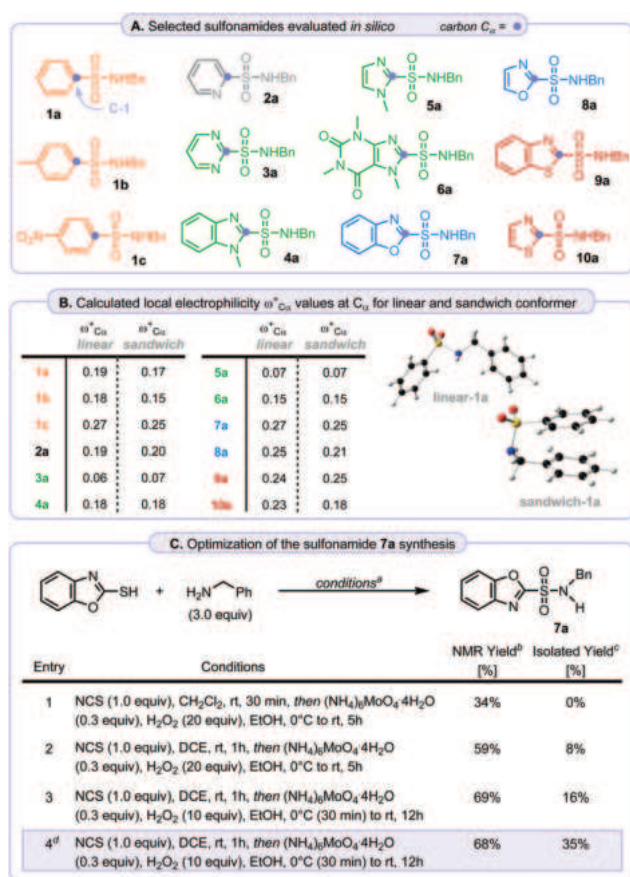


Fig. 2 *In silico* evaluation of the optimization of the reaction of sulfonamides **1a–10a** and sulfonamide **7a**. (A) Evaluated structures. (B) Calculated values of local electrophilicity $\omega_{C_{\alpha}}^{+}$ at carbon C_α for the two most stable conformers found during geometry optimization. (C) Representative examples of optimization of the synthesis reaction of sulfonamide **7a**. ^a Reactions were performed on the benzo[*d*]oxazole-2-thiol (1 mmol) and benzylamine (3 mmol) scale. ^b NMR yield determined using dimethylsulfone as the internal standard. ^c Obtained via crystallization. ^d Reaction carried out on benzo[*d*]oxazole-2-thiol (5 mmol) and benzylamine (15 mmol) scale.

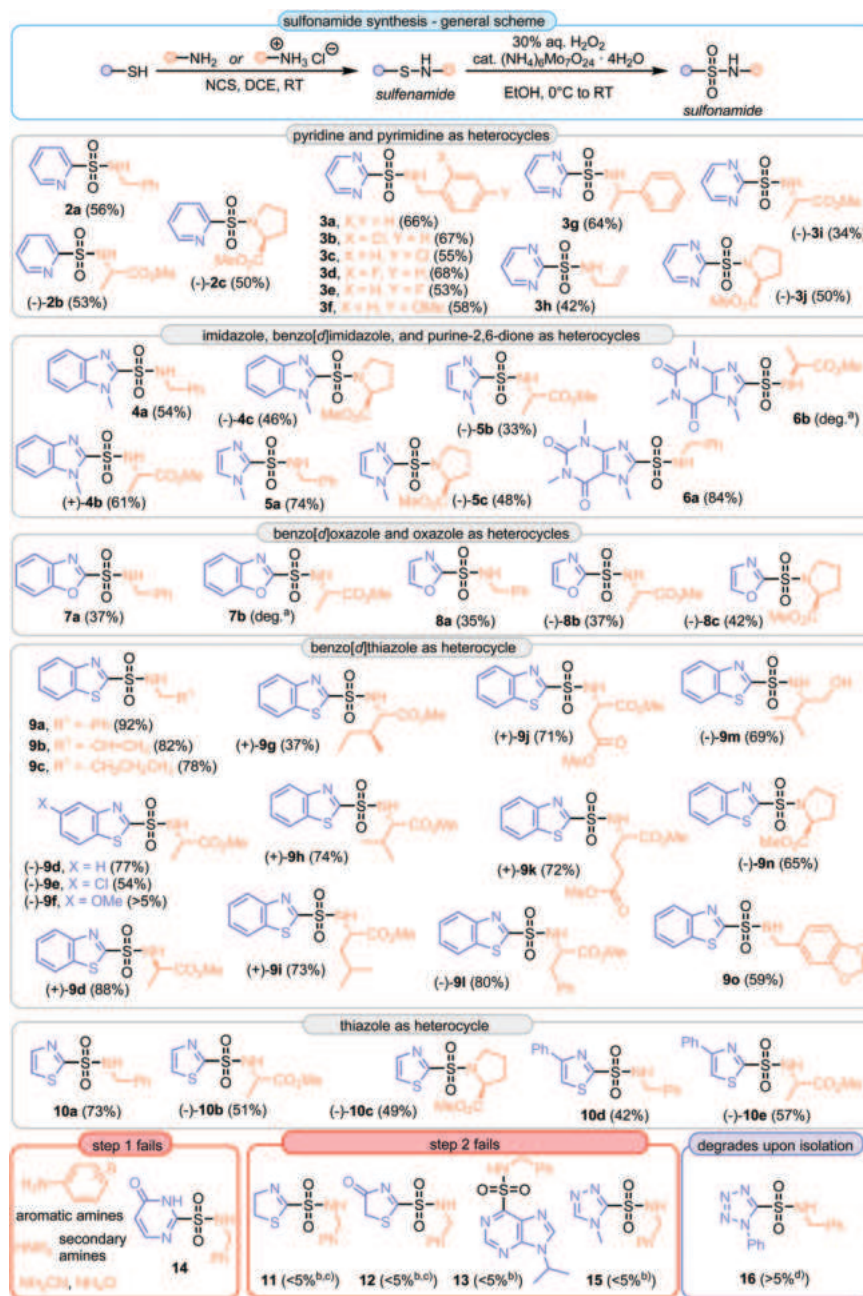


Fig. 3 Scope and limitations of the oxidative coupling between heteroaryl thiols and amines. Yields refer to pure isolated compounds after two steps. All reactions were typically performed on a 5 mmol scale of the corresponding heteroaryl thiol. ^a Sulfonamide detected by ¹H NMR; however, all attempts to isolate it failed. ^b No product formation was observed. Only intermediate sulfenamide was detected. ^c The oxidative opening of the heterocycle occurred during the oxidation step. Only side products were formed (see Scheme S3†). ^d Desired product **16** isolated only as a mixture of **16** with phenyl tetrazole **S9** (**16** : **S9** = 1 : 5). All attempts to purify compound **16** failed due to compound **16** decomposition.

this tendency was observed for proline esters (secondary amines observation exception). In such a case, the desired sulfonamides (**-2c**, (**-3j**), (**-4c**), (**-5c**), (**-8c**), (**-9n**) and (**-10c**) were isolated in good yields (42 to 62%). The reason behind this observation remains unclear. In the case of partially saturated heteroaryl sulfonamides (**11** and **12**), the formation of sulfenamide proceeded well; however, the oxidation step (from sulfenamide to sulfonamide) failed, and no traces

of the desired sulfonamides were detected. The oxidative decomposition of the intermediate sulfenamide is presumably occurring.³³ The same situation was observed when the synthesis of sulfonamides **13** and **15** was attempted. However, in those cases, no identifiable products of oxidative decomposition were observed. In the case of heterocycle **14**, however, even the first step of the sequence failed presumably due to the presence of N–H bond on the heterocycle.

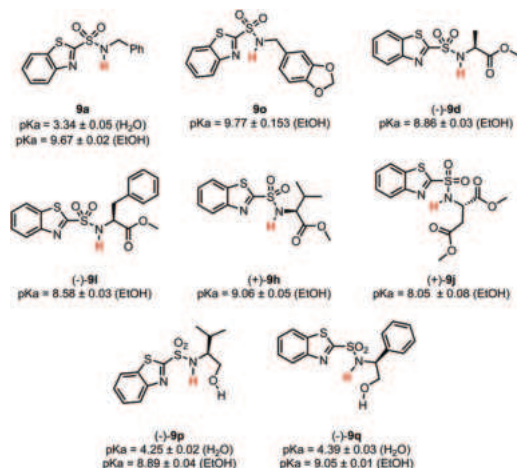


Fig. 4 Determined pK_a values of selected sulfonamides in H_2O and $EtOH$. Due to the low solubility of some of the sulfonamides in water, the pK_a values for all selected compounds were determined in $EtOH$.^{32,34}

N,N-Disubstituted heteroaryl sulfonamide synthesis

At this stage, we reasoned that the observed instability of several *N*-substituted sulfonamides **2–10** might be caused by the acidity of the sulfonamide *N*-hydrogen. To shed some light on the acidity and to evaluate the possible H-bond donor ability of the targeted sulfonamides, the pK_a value of the selected sulfonamides was determined (Fig. 4). The pK_a values of the simple benzylated sulfonamides **9a** and **9o** were observed to be slightly greater than 9.5 (for comparative reasons,³⁴ all values were determined in $EtOH$ due to a low solubility of several sulfonamides in H_2O). However, the pK_a values of amino acid-derived sulfonamides (sulfonamides **(-)-9d, i** and **(+)-9h**) were substantially lower ($pK_{a(EtOH)} \sim 8.6$ to 9 vs. 9.6–9.7).

Such an observation suggested that if an additional substitution of the sulfonamide nitrogen atom were introduced, the overall stability of the heteroaryl sulfonamides might increase.

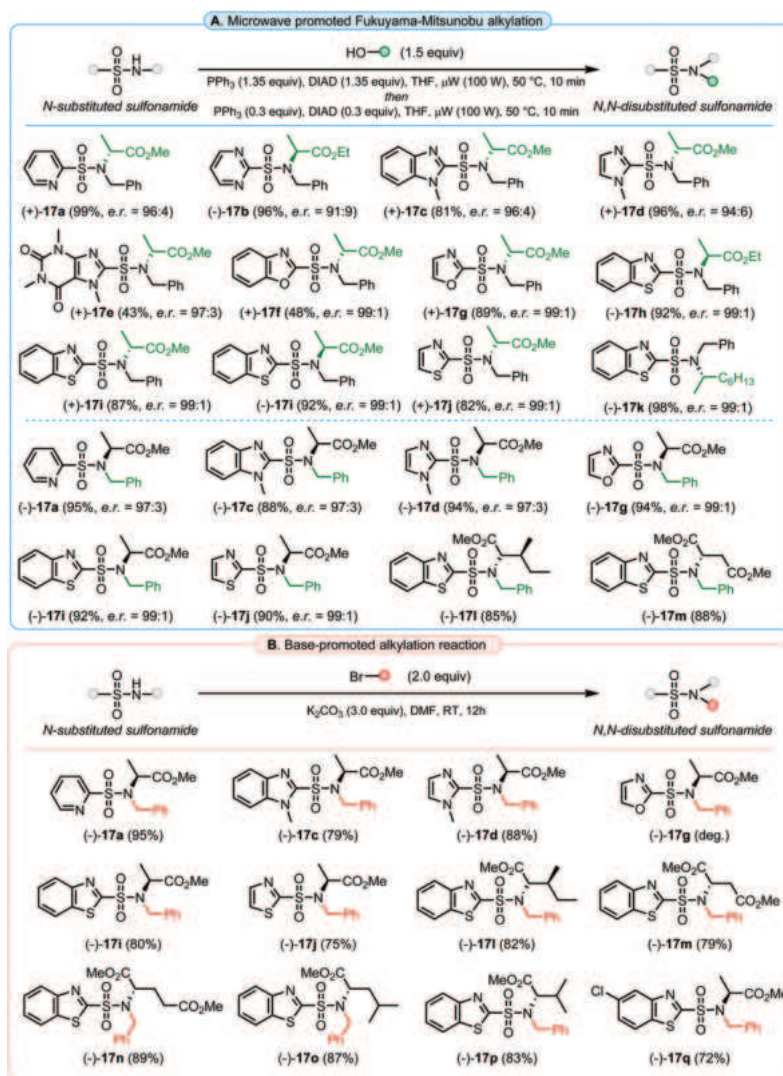


Fig. 5 Synthesis of *N,N*-disubstituted sulfonamide **17**. (A) Scope of the microwave-promoted Fukuyama–Mitsunobu alkylation reaction. (B) Scope of the base-mediated alkylation reaction.

Furthermore, proline-derived sulfonamides (–)-**2c**, (–)-**3j**, (–)-**4c**, (–)-**5c**, (–)-**8c**, (–)-**9n**, and (–)-**10c** proved to be reasonably stable and their lower isolated yields were mostly related to incomplete intermediate sulfenamide formation due to competitive disulfide formation during the first step of the sequence. Taking into account the low pK_a values of *N*-hydrogens in evaluated sulfonamides, two alkylation methods for preparation of *N,N*-disubstituted sulfonamides were designed (Fig. 5). In the first, *N*-alkyl sulfonamides reacted under our recently developed microwave-promoted Fukuyama–Mitsunobu alkylation conditions (Fig. 5A). The simple alkylation of amino acid-containing sulfonamides with benzyl bromide in the presence of base was also examined (Fig. 5B).

Due to the previously mentioned instability of (benzo)oxazole sulfonamides **7a**, compound **7a** was used as a model substrate for the development of alkylating conditions. After some evaluation, a slight modification of our recently developed microwave-promoted Fukuyama–Mitsunobu alkylation³² conditions was found to be suitable (Fig. 5A).^{23,35,36} Using such conditions, sulfonamide **7a** was transformed into *N,N*-dialkylated benzoxazole sulfonamide (+)-**17f** with a 48% yield. Pure (+)-**17f** was found to be shelf stable for at least 3 months. Using the same protocol, various *N,N*-dialkylated sulfonamides **17** (Fig. 5A) were prepared in good to excellent yields. Having easy access to *N*-benzylated sulfonamides (compounds **2a–10a**) and to the sulfonamides generated from *L*-alanine ((–)-**2b**, (–)-**3i**, (+)-**4b**, (–)-**5b**, (–)-**8b**, (–)-**9b**, and (–)-**10b**), synthesis of both enantiomeric forms of the corresponding sulfonamides **17a,c,d,g** and **i** could be accomplished. It was observed that *N*-alkylated sulfonamides can readily be benzylated with benzyl bromide in the presence of a base (Fig. 5B). The only exception were derivatives of (benz)oxazole sulfonamides **7a**, **8a**, and (–)-**8b** that degraded under the applied reaction conditions.

Conclusions

A short and efficient synthetic route to previously unreported *N*-alkylated heteroaryl sulfonamides based on the bulk chemicals (heteroaryl thiols and primary amines including α -amino esters) was developed. Prepared *N*-alkylated sulfonamides then served as a nucleophile in the microwave-promoted Fukuyama–Mitsunobu alkylation reaction and generated stereoselectively the desired *N,N*-disubstituted heteroaryl sulfonamides in good (benzoxazole sulfonamides) to excellent yields (other tested heterocycles).

Having demonstrated that various types of heteroaryl sulfonamide building blocks might be readily available starting from simple, inexpensive, and bulk chemicals, we expect that it will boost their use in the field of medicinal chemistry.

Author contributions

R. O. I. performed most of the experiments and analysed the experimental data. D. C., J. K., and F. Z. carried out the experi-

ments and analyzed the experimental data. R. O. I. optimized the Fukuyama–Mitsunobu reaction. D. C. optimized the alkylation reaction. J. K. performed the pK_a determination. R. O. I. and D. C. partially designed the experimental plans. E. D. and F. D. V. carried out the DFT calculations and analysed the obtained results. J. P. initiated the project, led the project team, designed the experiments, and analysed the results. R. O. I. and J. P. co-wrote the paper with input from all authors. All authors have approved the final version of the manuscript.

Conflicts of interest

There are no conflicts to declare.

Acknowledgements

The financial support from the Palacky University Internal Grant Agency (IGA_PrF_2021_011, IGA_PrF_2021_024, IGA_PrF_2022_012, IGA_PrF_2022_016, IGA_PrF_2022_022) and from the Czech Academy of Sciences (Mobility Plus Project, MPP-FWO-21-01) is gratefully acknowledged. E. D. thanks the Fund for Scientific Research-Flanders (FWO-11E0321N) for a predoctoral fellowship. FDV wishes to thank the VUB for a Strategic Research Program awarded to the ALGC research group. The Tier 2 computational resources and services were provided by the Shared ICT Services Center funded by the Vrije Universiteit Brussel, the Flemish Supercomputer Center (VSC), and FWO. JP is grateful for support from the European Regional Development Fund-Project ‘Centre for Experimental Plant Biology’ (no. CZ.02.1.01/0.0/0.0/16_019/0000738), and to Prof. M. Strnad and Prof. J. Hlaváč (Palacky University) for their continuous support. JP thanks Hana Omámiková (Department of Chemical Biology – performing HRMS measurement and semi-prep-HPLC separations) and Adam Příbylka (Department of Organic Chemistry – pK_a determination technical guide) for their technical assistance.

Notes and references

- 1 J. J. Petkowski, W. Bains and S. Seager, *J. Nat. Prod.*, 2018, **81**, 423–446.
- 2 M. Feng, B. Tang, S. H. Liang and X. Jiang, *Curr. Top. Med. Chem.*, 2016, **16**, 1200–1216.
- 3 K. P. Rakesh, S.-M. Wang, J. Leng, L. Ravindar, A. M. Asiri, H. M. Marwani and H.-L. Qin, *Anticancer. Agents Med. Chem.*, 2018, **18**, 488–505.
- 4 İ. Gulçin and P. Taslimi, *Expert Opin. Ther. Pat.*, 2018, **28**, 541–549.
- 5 E. Berrino, B. Michelet, A. Martin-Mingot, F. Carta, C. T. Supuran and S. Thibaudeau, *Angew. Chem., Int. Ed.*, 2021, **60**, 23068–23082.

- 6 P. K. Chinthakindi, T. Naicker, N. Thota, T. Govender, H. G. Kruger and P. I. Arvidsson, *Angew. Chem., Int. Ed.*, 2017, **56**, 4100–4109.
- 7 W. Autenriet and J. Koburger, *Ber. Dtsch. Chem. Ges.*, 1903, **36**, 3626–3634.
- 8 M. O. Forster and E. Kunz, *J. Chem. Soc. Trans.*, 1914, **105**, 1718–1733.
- 9 Y. Wang and F. S. Guziec, *J. Org. Chem.*, 2001, **66**, 8293–8296.
- 10 F. Serpier, J.-L. Brayer, B. Folléas and S. Darses, *Org. Lett.*, 2015, **17**, 5496–5499.
- 11 J. Matsuoka, H. Kumagai, S. Inuki, S. Oishi and H. Ohno, *J. Org. Chem.*, 2019, **84**, 9358–9363.
- 12 M. V. Dorogov, S. I. Filimonov, D. B. Kobylinsky, S. A. Ivanovsky, P. V. Korikov, M. Y. Soloviev, M. Y. Khahina, E. E. Shalygina, D. V. Kravchenko and A. V. Ivachtchenko, *Synthesis*, 2004, 2999–3004.
- 13 Z. Nie, C. Perretta, J. Lu, Y. Su, S. Margosiak, K. S. Gajiwala, J. Cortez, V. Nikulin, K. M. Yager, K. Appelt and S. Chu, *J. Med. Chem.*, 2005, **48**, 1596–1609.
- 14 M. R. Mallireddigari, V. R. Pallela, E. P. Reddy and M. V. R. Reddy, *Synthesis*, 2005, 3639–3643.
- 15 R. M. Kellogg, J. W. Nieuwenhuijzen, K. Pouwer, T. R. Vries, Q. B. Broxterman, R. F. P. Grimbergen, B. Kaptein, R. M. La Crois, E. de Wever, K. Zwaagstra and A. C. van der Laan, *Synthesis*, 2003, 1626–1638.
- 16 S. Sohrabnezhad, K. Bahrami and F. Hakimpoor, *J. Sulfur Chem.*, 2019, **40**, 256–264.
- 17 Y. Cao, S. Abdolmohammadi, R. Ahmadi, A. Issakhov, A. G. Ebadi and E. Vessally, *RSC Adv.*, 2021, **11**, 32394–32407.
- 18 Y. Chen, P. R. D. Murray, A. T. Davies and M. C. Willis, *J. Am. Chem. Soc.*, 2018, **140**, 8781–8787.
- 19 To the best of our knowledge, no reported method of oxazol-2-yl sulfonamide was published in the literature. First approach to benzo[d]oxazole-2-yl sulfonamides (3 examples) was reported only recently, see N. Youseflouei, S. Alizadeh, M. Masoudi-Khoram, D. Nematollahi and H. Alizadeh, *Electrochim. Acta*, 2020, **353**, 136451.
- 20 G. Laudadio, E. Barmpoutsis, C. Schotten, L. Struik, S. Govaerts, D. L. Browne and T. Noël, *J. Am. Chem. Soc.*, 2019, **141**, 5664–5668.
- 21 S. W. Wright and K. N. Hallstrom, *J. Org. Chem.*, 2006, **71**, 1080–1084.
- 22 J.-B. Feng and X.-F. Wu, *Org. Biomol. Chem.*, 2016, **14**, 6951–6954.
- 23 F. Zálešák, O. Kováč, E. Lachetová, N. Št'astná and J. Pospíšil, *J. Org. Chem.*, 2021, **86**, 11291–11309.
- 24 J. Pospíšil and H. Sato, *J. Org. Chem.*, 2011, **76**, 2269–2272.
- 25 D. J.-Y. D. Bon, O. Kováč, V. Ferugová, F. Zálešák and J. Pospíšil, *J. Org. Chem.*, 2018, **83**, 4990–5001.
- 26 O. Kováč, F. Zálešák, D. J.-Y. D. Bon, L. Roiser, L. V. Baar, M. Waser and J. Pospíšil, *J. Org. Chem.*, 2020, **85**, 7192–7206.
- 27 J. Pospíšil, R. Robiette, H. Sato and K. Debrus, *Org. Biomol. Chem.*, 2012, **10**, 1225–1234.
- 28 T. Zweifel, M. Nielsen, J. Overgaard, C. B. Jacobsen and K. A. Jørgensen, *Eur. J. Org. Chem.*, 2011, **2011**, 47–52.
- 29 P. Perez, A. Toro-Labbe, A. Aizman and R. Contreras, *J. Org. Chem.*, 2002, **67**, 4747–4752.
- 30 P. K. Chattaraj, B. Maiti and U. Sarkar, *J. Phys. Chem. A*, 2003, **107**, 4973–4975.
- 31 All calculations were performed using Gaussian 16 (Gaussian, Inc., Wallingford CT, 2016). Geometry optimizations and frequency calculations have been carried out at the B3LYP-D3(BJ)/cc-pVDZ level of theory using the SMD solvation model. Global and local electrophilicity index values were obtained at the same level of theory and for the latter, NBO analysis was applied. See ESI† for full details.
- 32 See ESI† for more details.
- 33 Only nonidentifiable complex mixtures of degradation products were detected in such cases. Only in case sulfur-containing heterocycles, some side products were characterized. For more details, see ESI.†
- 34 E. Rossini, A. D. Bochevarov and E. W. Knapp, *ACS Omega*, 2018, **3**, 1653–1662.
- 35 E. Marsault, K. Benakli, S. Beaubien, C. Saint-Louis, R. Déziel and G. Fraser, *Bioorg. Med. Chem. Lett.*, 2007, **17**, 4187–4190.
- 36 E. Marsault, H. R. Hoveyda, R. Gagnon, M. L. Peterson, M. Vézina, C. Saint-Louis, A. Landry, J.-F. Pinault, L. Ouellet, S. Beauchemin, S. Beaubien, A. Mathieu, K. Benakli, Z. Wang, M. Brassard, D. Lonergan, F. Bilodeau, M. Ramaseshan, N. Fortin, R. Lan, S. Li, F. Galaud, V. Plourde, M. Champagne, A. Doucet, P. Bhérer, M. Gauthier, G. Olsen, G. Villeneuve, S. Bhat, L. Foucher, D. Fortin, X. Peng, S. Bernard, A. Drouin, R. Déziel, G. Berthiaume, Y. L. Dory, G. L. Fraser and P. Deslongchamps, *Bioorg. Med. Chem. Lett.*, 2008, **18**, 4731–4735.

Julia-Kocienski-Like Connective C–C and C=C Bond-Forming Reaction

David J.-Y. D. Bon,^{+a} Daniel Chrenko,^{+c} Ondřej Kováč,^{+a} Vendula Ferugová,^a Pavel Lasák,^b Markéta Fuksová,^{b, c} František Zálešák,^a and Jiří Pospíšil^{a, b, c,*}

^a Department of Organic Chemistry
Faculty of Science, Palacky University
tř. 17. listopadu 1192/12, CZ-771 46 Olomouc, Czech Republic
Tel: +420 585 634 784

E-mail: j.pospisil@upol.cz

^b Laboratory of Growth Regulators
Palacký University & Institute of Experimental Botany AS CR
Šlechtitelů 27, 783 71 Olomouc, Czech Republic Affiliation

^c Department of Chemical Biology
Faculty of Science, Palacky University
Šlechtitelů 27, 783 71 Olomouc, Czech Republic

⁺ D. J. Y. D. B., D. C. and O. K. contributed equally (co-first authors). Names are in alphabetic order.


Manuscript received: September 18, 2023; Revised manuscript received: December 20, 2023;

Version of record online: January 7, 2024

Dedicated in memory of professor István E. Markó.



Supporting information for this article is available on the WWW under <https://doi.org/10.1002/adsc.202301054>

 This is an open access article under the terms of the Creative Commons Attribution Non-Commercial NoDerivs License, which permits use and distribution in any medium, provided the original work is properly cited, the use is non-commercial and no modifications or adaptations are made.

Abstract: In this paper, we present a one-pot protocol that enables a straightforward and selective transformation of alkyl benzothiazol-2-yl and phenyltetrazol-2-yl sulfones and acyl chlorides into ketones, E-olefins, Z-olefins, and even pyrroles. The final product of the reaction depends on the proper choice of the reaction workup. Notably, the protocol designed for olefin formation allows a switch between E- and Z-olefin formation by the correct choice of the reaction workup. These developed protocols facilitate the formation of all compounds under mild reaction conditions, as evidenced by the synthesis of (nitro)-fatty acids, and the concept can be extended to other product formations, as demonstrated by the synthesis of pyrroles.

Keywords: coupling reaction; olefination method; fatty acid synthesis; divergence in synthesis; stereoselectivity

Introduction

Carbon-carbon bond-forming reactions are the key connective reactions in organic synthetic chemistry. Among these, the stereoselective formation of unsaturated bonds, specifically olefins, holds fundamental significance due to their involvement in the synthesis of natural products, bioactive compounds, and materials. Presently, two commonly used methods for

achieving stereoselective connective olefination are olefin cross-metathesis^[1] and coupling of anion-stabilized reagents with aldehydes or ketones^[2] (Figure 1). These methods generally operate under mild reaction conditions, exhibit good tolerance towards functional groups, and yield predominantly (*E*)-configured olefins. However, there are limited methods that address the selective formation of (*Z*)-olefins. In such cases, specific catalysts (e. g., cross-metathesis)^[3] or modified

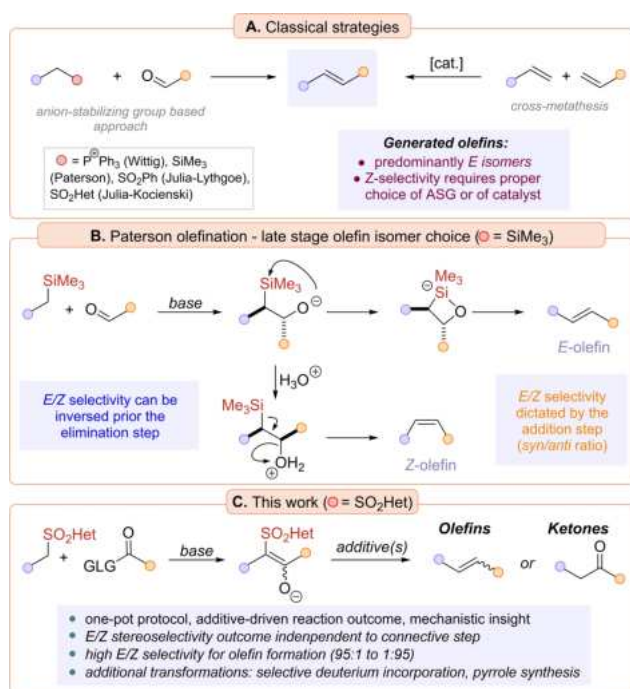


Figure 1. Connective olefination methods.

anion stabilizing groups (e.g., Still-Gennari modification of Horner-Wadsworth-Emmons olefination)^[4] are utilized. The Peterson olefination,^[2g,h] on the other hand, allows for the stereoselective formation of either (*E*) or (*Z*)-olefins from the same starting material by a simple alteration in the reaction work-up (acidic vs. basic).^[5] However, even in this case, the stereoselectivity of the *in situ* generated adduct (*syn/anti*) is reflected in the final stereochemical outcome of the olefination.

The objective of our study was to devise an olefination method capable of selectively producing either (*E*)- or (*Z*)-olefins from identical starting materials. We considered whether in our group the extensively developed Julia-Kocienski olefination reaction^[6] could be modified to meet these specific requirements. In previous endeavors, both our group^[6b,c] and others^[7] attempted to influence the stereochemical outcome of the Julia-Kocienski reaction using different approaches. However, the outcomes of such attempts proved to be highly substrate dependent.^[8]

To overcome these limitations, we speculated that introducing the *syn/anti* configuration independently after the connective C–C bond-forming reaction could potentially achieve two objectives: (1) increase the *E/Z* selectivity, and (2) selectively generate (*E*) or (*Z*) olefins. Moreover, we considered that the utilization of *in situ* generated C–C bond intermediates might be extended to additional transformations, making this connective approach advantageous for a wide range of

synthetic endeavors. Below, we summarize our findings from the aforementioned research efforts.

Results and Discussion

Preliminary Results

Our development of the novel connective Julia-Kocienski-type protocol began with identifying two key steps (C–C bond formation/stereochemistry introduction) that were later conducted in a one-pot manner. In our plan, the reaction between heteroaryl sulfone **1** and acyl halide **2** seemed the most suitable approach, as the *in situ* generated enolate **4** could likely be readily transformed to the β -keto sulfone **5** by an external proton source (Figure 2A). Subsequently, mild reducing agents like NaBH₄ were expected to facilitate the reduction of **5** to β -alkoxy sulfone **6**, which, through intramolecular Smiles rearrangement and further *anti*-elimination, would yield the desired olefin **3**.

The optimization of the reaction sequence began with the reaction of BT-sulfone **1a** with acyl chloride **2a** under previously described conditions (Figure 2B, entry 1).^[9] The *in situ* generated adduct **4a** was then protonated with an excess of AcOH, and to test the hypothesis that adduct **4a** can be transformed into ketone **5** and the BT-sulfone group can be removed *in situ*, a reducing metal, Zn dust (10 equiv.), was added.^[10] Encouragingly, the desired ketone **8a** was obtained in 73% yield.^[11]

After validating the feasibility of *in situ* protonation/sulfone reduction of adduct **4a**, the second step of the sequence, the stereoselective reduction of β -hydroxy sulfone **5a**, was attempted (Figure 2B). After some reaction condition optimization,^[11,12] it was observed that the addition of MeOH to the reaction mixture after the formation of adduct **4a**, followed by an excess of NaBH₄ (20 equiv.), generated the desired (*Z*)-**3a** olefin in 72% yield and with a 2:98 *E/Z*-selectivity (Figure 2B, entry 2). On the other hand, when *i*PrOH, followed by ZnCl₂ and NaBH₄, was added, olefin (*E*)-**3a** was obtained with a yield of 69% and a 98:2 *E/Z*-selectivity (Figure 2B, entry 3). Similar results were obtained when sulfone **1b** (Het = PT) was used as a starting material, although the desired products were isolated in somewhat lower yields (entries 4 to 6). It was also demonstrated that Zn(BH₄)₂^[13] could be used as the reducing agent in the case of *E*-selective olefin formation protocol (entry 7).

Based on the obtained data^[11] and in agreement with the work of Jørgensen *et al.*,^[12] we believe that the stereochemistry of the olefin formation is governed by the stereoselective reduction of intermediate **5**. In the case of the (*Z*)-olefin, the reduction of intermediate **5** occurs via the Felkin-Ahn-like transition state, driving the formation of the (*Z*)-olefin (Figure 2C). The subsequent transformation of *syn* β -hydroxy

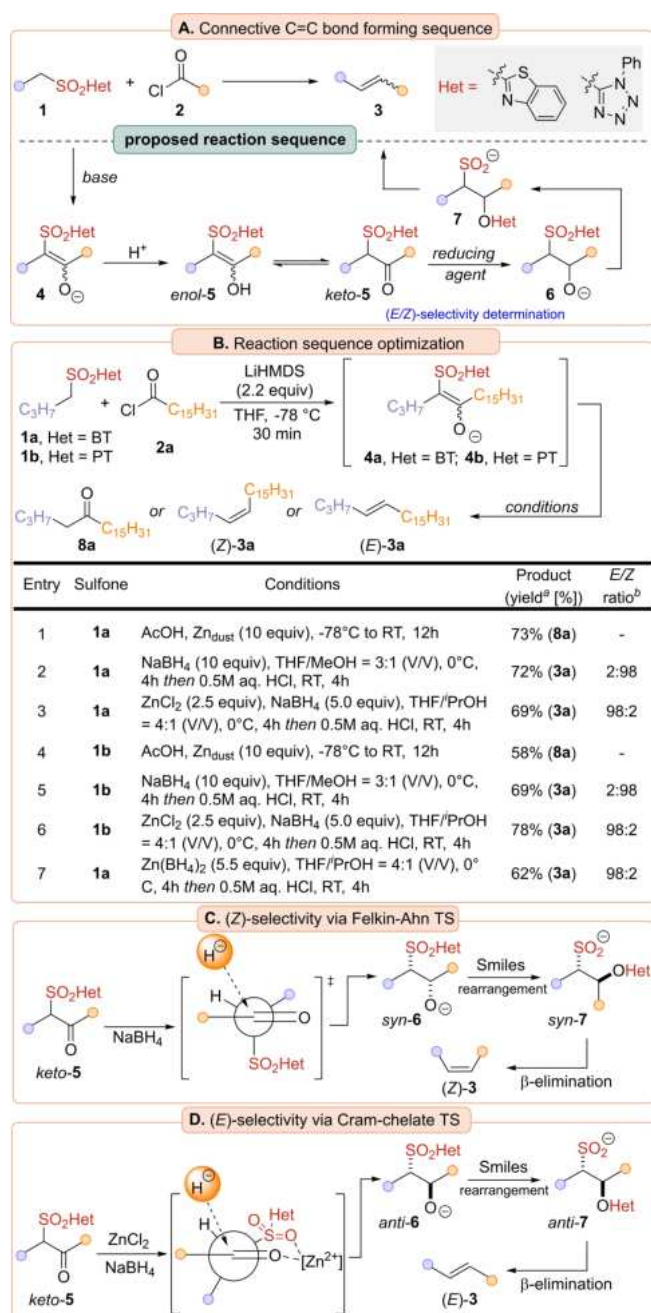


Figure 2. (A) Connective reaction sequence featuring olefin formation. (B) Reaction protocol optimization – selected representative examples. (C) Felkin-Ahn-based reaction mechanism presumably operating during the (*Z*)-olefin formation. (D) Cram-chelate-based reaction mechanism presumably operating during the (*E*)-olefin formation.

sulfone *syn*-6, involving Smiles rearrangement and β -anti-elimination processes, leads to the observed (*Z*)-olefin **3**.

In the case of (*E*)-olefin formation, the reduction of intermediate **5** proceeds via the Cram-chelate transition state, leading to the *anti* β -hydroxy sulfone *anti*-6.

Subsequently, the Smiles rearrangement and β -anti-elimination reactions complete the formation of the (*E*)-olefin **3**.

Scope and Limitations

With suitable reaction conditions in hands, the scope and limitations of the transformations could be established (Figure 3). It was observed that various substituted acyl and aryl chlorides were readily transformed to the corresponding ketones **8 a–i** in good to very good yields (Figure 3A). When succinyl dichloride was reacted with an excess of the corresponding sulfone **1** (2 equiv. of sulfone and 4.4 equiv. of LiHMDS were used), generated diketones **8 j** and **k** were isolated as the only products of the reaction. In all evaluated cases, transformations using PT-containing sulfones **1** yielded the desired ketones **8** in lower isolated yield when compared to BT-substituted sulfones **1**. The condensation reaction and the formation of ketone **8** failed when oxalyl mono and dichlorides, α -chloro acetyl chloride, monochloro fumarate ester, or TFAA were used as acylating reagents (Figure 3D).

In the case of olefination reactions, it was observed that the (*Z*)-selective transformations (Figure 3B) proceed in high *Z*-selectivity (*E/Z* from 2:98 to 20:80) when alkyl sulfones **1** were reacted with acyl or benzoyl chlorides **2**. The *Z*-selectivity decreased when benzyl sulfones **1** were used as substrates (*E/Z* from 27:73 to 46:54). The special case was the use of 4-methoxybenzoyl chloride as a substrate for the reaction. In this case, only *E*-olefins **3 f** and **3 g** were formed as the main products (*E/Z* = 90:10 to 93:7). It is expected that this observation is caused by the competitive *syn* elimination of the generated *syn*-6 adduct (*synperiplanar* elimination from *cisoid* conformation of intermediate *syn*-7) as previously described for such type of adducts containing the electron-donating group on the aromatic ring.^[6a,11] When the *E*-selective protocol was evaluated (Figure 3C), the desired *E*-olefins **3** were generated as the main products of the reaction in *E/Z* ratios ranging from 98:2 to 81:19. In all of the evaluated cases, reactions carried out with PT-sulfones generated the desired product in somewhat lower reaction yields than those that occurred with the corresponding BT-sulfone.

Subsequently, we explored further extensions of the developed methods (Figure 4). First, the selective incorporation of the deuterium atom into the newly generated olefin **3** was evaluated (Figure 4A). Based on the proposed reaction mechanism, the use of NaBD₄ instead of NaBH₄ should lead to selective **3-d** olefin formation (Figures 2C and 2D). In all evaluated cases, the assumption proved to be correct, however, the deuterium incorporation into generated olefins **3 a–d**, **h–d** and **i–d** was ranging between 88 to 92%.^[11] From the *E/Z* selectivity point of view the results were in

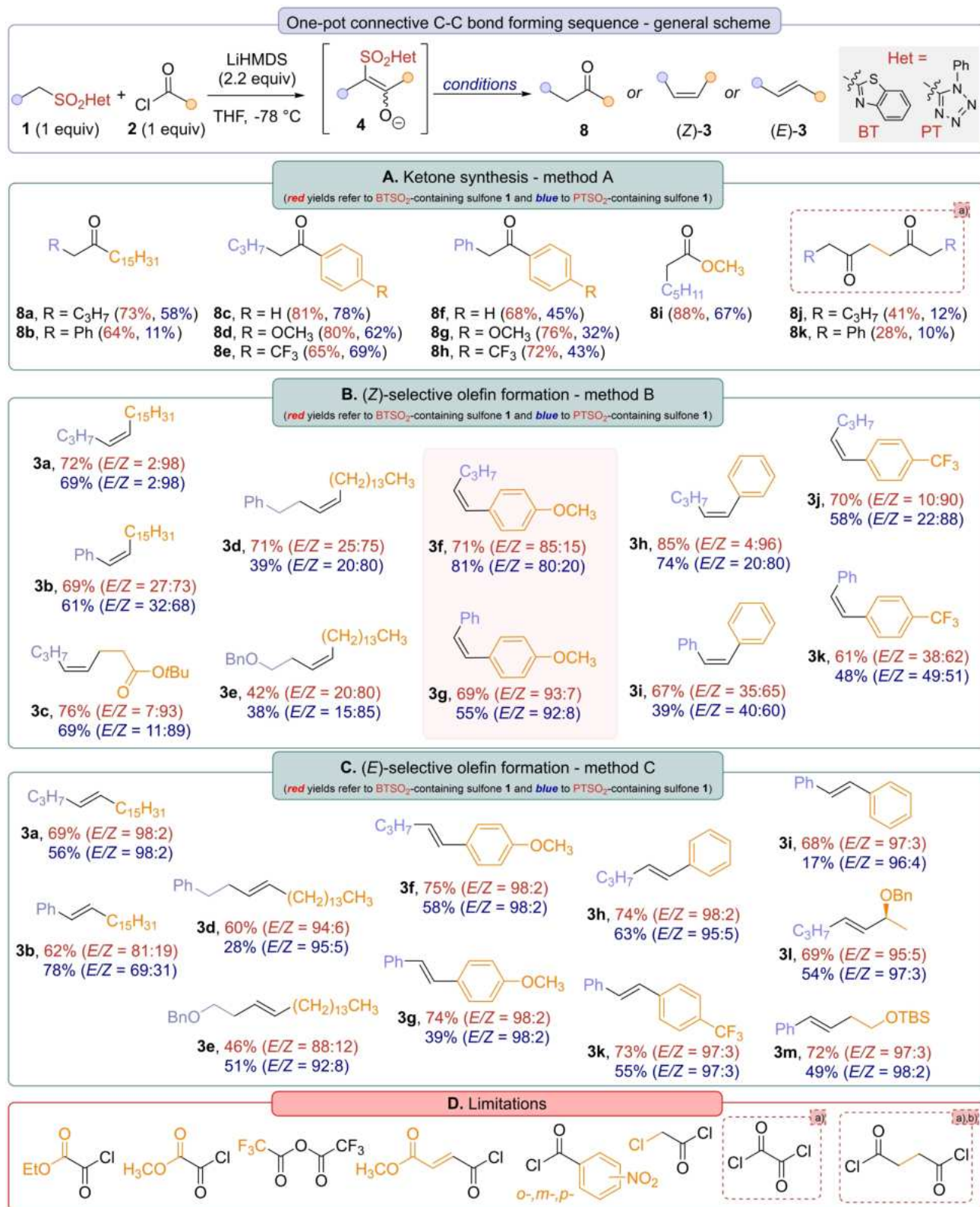


Figure 3. Scope and limitations of the connective method developed. (A) Scope of ketone formation. (B) Scope of the selective (*Z*)-olefin formation. The *E/Z* ratio is based on the ¹H NMR spectra of the crude reaction mixture analysis. (C) Scope of selective (*E*)-olefin formation. The *E/Z* ratio is based on the ¹H NMR spectra of the crude reaction mixture analysis. (D) Substrates that failed to yield any olefine or ketone under the investigated reaction conditions. **Conditions.** Method A: AcOH, Zn_{dust} (10 equiv.), -78 °C to RT, 12 h; Method B: NaBH₄ (10 equiv.), THF/MeOH = 3:1 (V/V), 0 °C, 4 h then 0.5 M aq. HCl, RT, 4 h; Method C: ZnCl₂ (2.5 equiv.), NaBH₄ (5.0 equiv.), THF/*i*PrOH = 4:1 (V/V), 0 °C, 4 h then 0.5 M aq. HCl, RT.

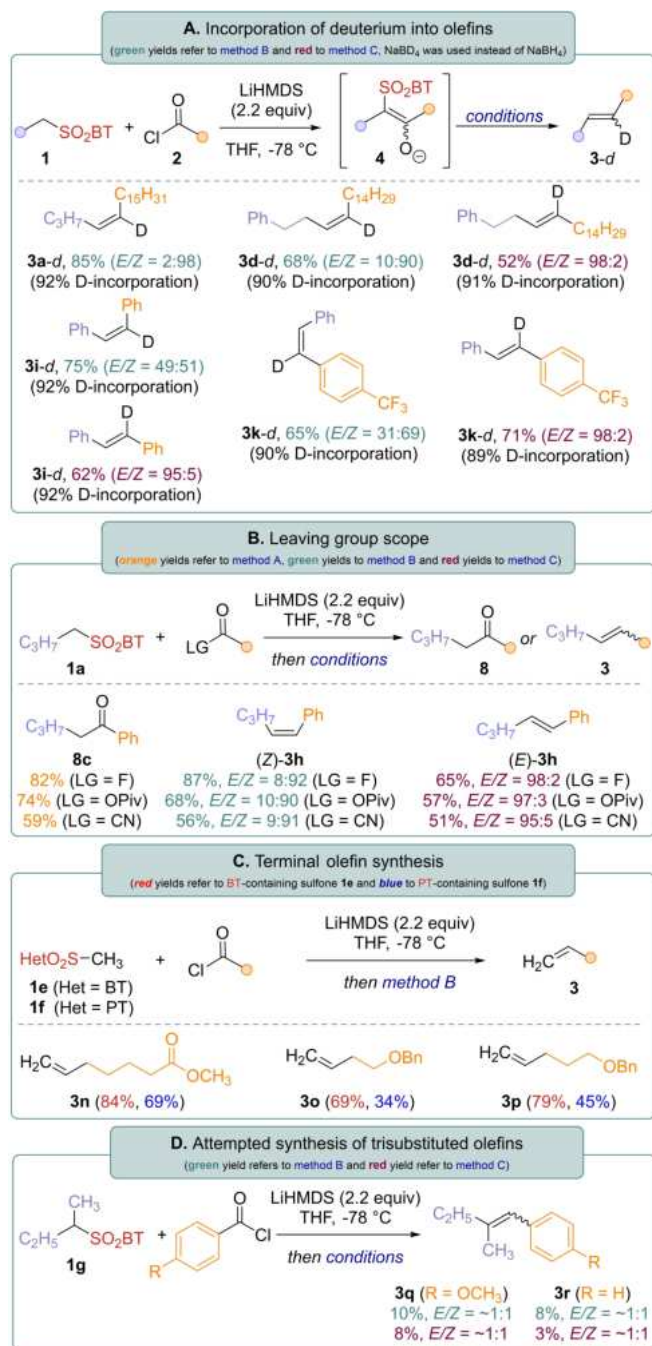


Figure 4. (A) Generation of deuterium-containing olefins **3**. Deuterium incorporation based on the ¹H-NMR spectra analysis. (B) Evaluation of the influence of the ability of the leaving group on the reaction sequence outcome. (C) One-pot protocol for the terminal olefin formation. (D) Attempt to apply our olefination method to the stereoselective trisubstituted olefin formation. **Conditions.** Method A: AcOH, Zn_{dust} (10 equiv.), -78 °C to RT, 12 h; Method B: NaBH₄ (10 equiv.), THF/MeOH=3:1 (V/V), 0 °C, 4 h then 0.5 M aq. HCl, RT, 4 h; Method C: ZnCl₂ (2.5 equiv.), NaBH₄ (5.0 equiv.), THF/*i*PrOH=4:1 (V/V), 0 °C, 4 h then 0.5 M aq. HCl, RT, 4 h.

agreement with the previously observed trends. The only exception was the formation of stilbene **3i-d** via the *Z*-selective method B. In such a case, the generated olefin **3i-d** was formed in a 49:51 *E/Z* ratio. We speculate that the observed selectivity is caused by the competitive *syn*-elimination of the intermediate **7**.^[6a]

To broaden the applicability of our methods, the influence of the three additional leaving groups on the acyl reagents, fluoride, pivaoylate and cyanide, were evaluated (Figure 4B). Gratifyingly, it was observed that all three leaving groups can be successfully used as chloride anion equivalents without any significant impact on the reaction yield and the *E/Z* selectivity.

Finally, olefin protocols were also evaluated in terms of terminal (Figure 4C) and trisubstituted (Figure 4D) olefin formation. In the first case, both the methyl heteroaryl sulfones **1e** (Het=BT) and **1f** (Het=PT) reacted smoothly and generated olefins **3n–p** with good to very good yields. Again, sulfone **1e** yielded the desired olefins in slightly better yields than the corresponding sulfone **1f**. In the case of the attempted stereoselective trisubstituted olefin **3q** formation (Figure 4D), the desired olefin was formed only in low reaction yields (11–17%) and selectivity (45:55 for the *Z*-selective protocol, and 63:37 for the *E* selective protocol).

Pyrrole Synthesis

Having easy access to 1,4-diketones (Figure 3A, compounds **8j** and **k**), a one-pot synthesis of the corresponding pyrroles **9** was attempted (Figure 5). After intensive reaction conditions optimization,^[10] the optimal reaction conditions under which aniline and benzylamine could be used to generate the desired pyrrole **9a** (from aniline), **9b** (from benzyl amine), and **9c** (from *n*-butyl amine) in one-pot manner and isolated yields of 28%, 37%, and 21%, respectively.

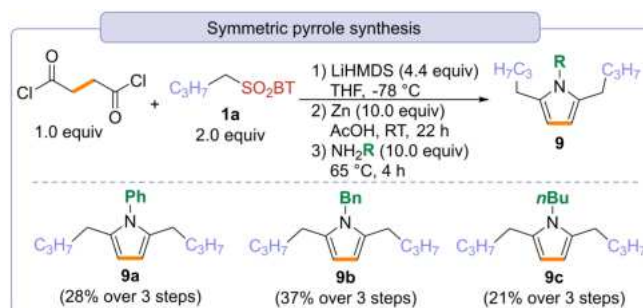


Figure 5. Three-step, one-pot protocol for symmetrically substituted pyrrole synthesis. BT = benzo[*d*]thiazole-2-yl.

Fatty Acid Synthesis

Finally, (*Z*)-olefination method (Method B) was also used to prepare selected (nitro)-fatty acids (Figure 6) in a short and efficient way. Indeed, starting from the readily available building blocks the synthesis of Oleic acid (**14**, 3 steps, 52% overall yield), Linoleic acid (**19**, 6 steps, 26% overall yield) and 10-NO₂-Linoleic acid (**24**, 7 steps, 8% overall yield) could be readily achieved.

Conclusion

We have developed a one-pot protocol that enables the generation of ketones, as well as *E* and *Z*-olefins, using commercially available starting materials. The remarkable aspect of this protocol is that the final product obtained is not influenced by the initial reaction conditions. Instead, the choice between the product being a ketone, *E*-olefin, or *Z*-olefin is determined during the reaction work-up process. It is important to emphasize that this olefination protocol allows for the independent synthesis of *E* and *Z* olefins from the same starting material. This selectivity adds to the versatility of the method. Thus, the described olefination sequence is equivalent to the well-known Petersen olefination, but allows the further extension of it to e. g. ketone synthesis.

Furthermore, we have demonstrated that the identified reaction conditions can be extended to other transformations. For example, we successfully applied the one-pot protocol to pyrrole synthesis, showcasing its potential for diverse applications in organic synthesis. Developed protocols can be applied in natural product synthesis, as demonstrated in the case of (nitro)-fatty acids. These findings underscore the significance of our protocol, which not only offers a versatile and efficient approach to ketone and olefin synthesis but also holds promise for various other synthetic endeavors and applications in the field of organic chemistry.

Experimental Section

General Procedure for Carbonyl Compound **8** Synthesis (Method A)

Sulfone **1** (1 mmol, 1.0 equiv.) was dissolved in dry THF (0.1 M) and cooled to -78°C (acetone/dry ice). After 5 minutes, LiHMDS (2.2 mmol, 2.2 equiv., 1.0 M solution in THF) was added dropwise, and the reaction mixture immediately turned light orange. Subsequently, acyl chloride **2** (1.1 mmol, 1.1 equiv.) was added over 5 minutes. The resulting reaction mixture was allowed to stir at -78°C for 30 minutes. Glacial AcOH (5 mL, 0.2 M) was added and the reaction mixture stirred at -78°C for additional 5 minutes. To this mixture Zn powder (5 mmol, 5.0 equiv.) was added and the cooling bath was removed. The resulting reaction mixture was allowed to warm

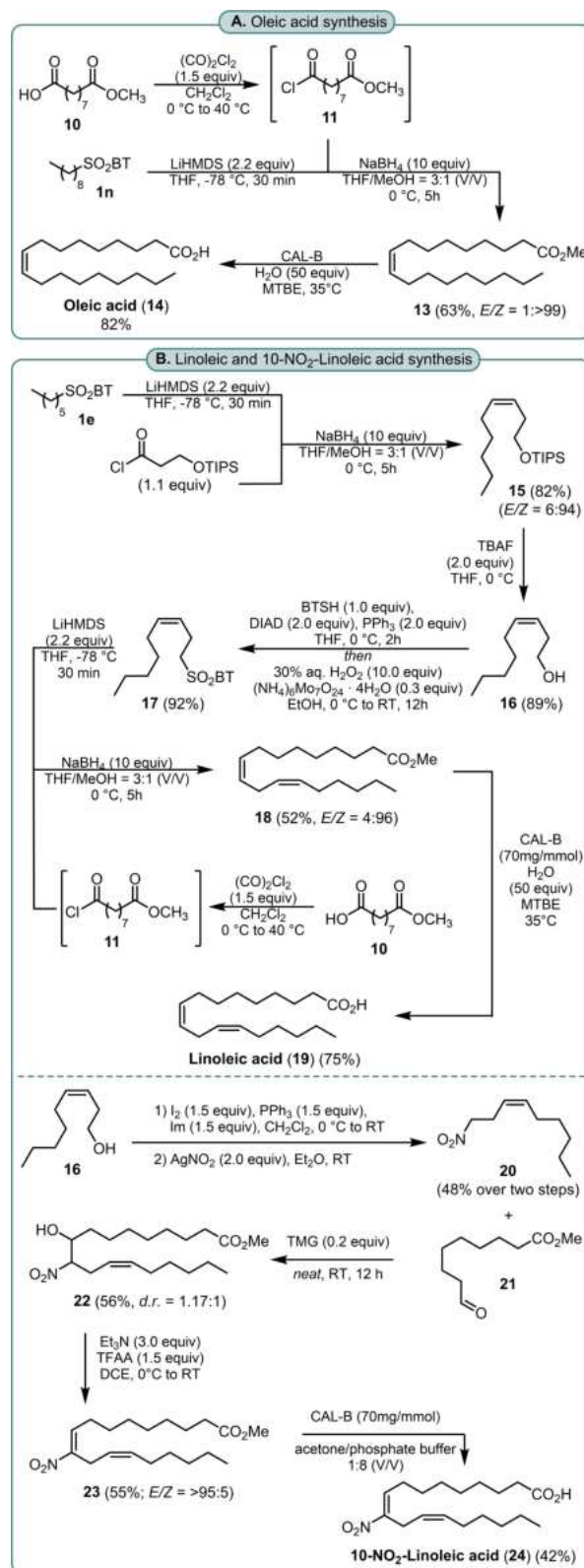


Figure 6. (A) Oleic acid synthesis based on the (*Z*)-selective Method B. (B) linoleic and 10-NO₂-Linoleic acid synthesis. TMG = 1,1,3,3-Tetramethylguanidine, CAL-B = *Candida antarctica* Lipase B, Im = imidazole.

spontaneously to RT, then stirred for 9 hours. Reaction was quenched with the addition of EtOAc (20 mL) and the whole solution was filtered through a pad of Celite®. The filter cake was washed with EtOAc (3×15 mL) and the combined filtrates were washed with saturated aqueous Na₂CO₃ (20 mL), brine (25 mL), dried over anhydrous Na₂SO₄ and solvents removed under reduce pressure to yield crude product. The crude product was purified by flash column chromatography on silica gel eluting with *n*-hexane/EtOAc to afford pure product **8**.

General Procedure for (Z)-Olefin 3 Synthesis (Method B)

Sulfone **1** (1 mmol, 1.0 equiv.) was dissolved in dry THF (10 mL, 0.1 M) and cooled to -78°C (acetone/dry ice, external). After 5 minutes, LiHMDS (2.2 mmol; 2.2 equiv.; 1.0 M solution in THF) was added dropwise. The reaction mixture turned light orange upon its addition. Acyl chloride **2** (1.1 mmol, 1.1 equiv.) was added slowly over 5 minutes. The resulting reaction mixture was allowed to stir at -78°C for 30 minutes before the cooling bath was removed. The reaction mixture was allowed to stir at RT for 20 min before MeOH (3.3 mL, THF/MeOH = 3:1 (V/V)) was added. The mixture was cooled to 0°C and stirred for an additional 5 minutes, before NaBH₄ (10 mmol, 10 equiv.) was added at 0°C . The resulting reaction mixture was stirred at 0°C for an additional 4 h, before being quenched with 2 M aq. HCl (20 mL). The resulting mixture was stirred at RT for 4 h. Resulting phases were separated, and the aqueous phase was extracted with EtOAc (3×20 mL). Organic layers were combined and washed with water (10 mL), brine (15 mL), dried over Na₂SO₄, filtered and solvents were removed under reduce pressure to provide the crude product. The crude product was purified by flash column chromatography on silica gel eluting with *n*-hexane/EtOAc to afford pure product **3**.

General Procedure for (E)-Olefin 3 Synthesis (Method C)

Sulfone **1** (1 mmol, 1.0 equiv.) was dissolved in dry THF (0.1 M) and cooled to -78°C (acetone/dry ice, external). After 5 minutes, LiHMDS (2.2 mmol, 2.2 equiv., 1.0 M solution in THF) was added dropwise. The reaction mixture turned light orange upon its addition. Acyl chloride **2** (1.1 mmol, 1.1 equiv.) was added slowly over 5 minutes. The resulting reaction mixture was allowed to stir at -78°C for 30 minutes before the cooling bath was removed. The reaction mixture was allowed to stir at RT for 20 min before 2-propanol (2.5 mL, THF/2-propanol = 4:1 (V/V)) was added. The mixture was stirred at RT for an additional 5 minutes, before adding anhydrous ZnCl₂ (2.5 mmol, 2.5 equiv.) was added. The resulting suspension was cooled to 0°C and stirred for an additional 5 minutes before NaBH₄ (5 mmol, 5 equiv.) was added. The resulting reaction mixture was then stirred at 0°C for an additional 4 h, before being quenched with 2 M aq. HCl (20 mL). The resulting mixture was stirred at RT for 4 h. Resulting phases were separated, and the aqueous phase was extracted with EtOAc (3×20 mL). Organic layers were combined and washed with water (10 mL), brine (15 mL), dried over Na₂SO₄, filtered, and solvents were removed under reduce pressure to provide the

crude product. The crude product was purified by flash column chromatography on silica gel eluting with *n*-hexane/EtOAc to afford pure product **3**.

Experimental procedures and characterization data for sulfones **1 a–n**, olefins **3 a–r**, ketones **8 a–k**, pyrroles **9 a–c**, oleic acid **13**, linoleic acid **19**, and 10-nitro-linoleic acid **24** preparation, as well as copy of ¹H and ¹³C{¹H} NMR spectra of prepared compounds are included in the supporting information.

Author Contributions

D. J.-Y. B., D. C., O. K., and J. P. carried out most of the experiments. V. F. carried out all experiments connected with the PT-sulfones. F. Z., P. L. and M. F. contributed to the olefination protocol and validated developed protocols. O. K. carried out all pyrrole-linked experiments. D. C. carried out all fatty acid synthesis related experiments. J. P. wrote the original draft based on the data obtained from all coauthors. J. P. designed the project, was responsible for the acquisition of funding and led the project. All coauthors read the original draft and collaborated on its corrections/modifications/changes.

Acknowledgements

The financial support by the Internal Grant Agency of Palacky University (IGA PrF 2023 031 and IGA PrF 2023 20) is gratefully acknowledged. D. C. and J. P. are grateful for the support from the Grant Agency of The Czech Republic (no. 23-06051S). J. P. and M. F. are grateful for the support from the European Regional Development Fund-Project "Centre for Experimental Plant Biology" (no. CZ.02.1.01/0.0/0.0/16 019/0000738). The authors thank Hana Omámiková (Department of Chemical Biology, performing HRMS measurement and semiprep-HPLC separations) for her technical assistance.



References

- [1] a) T. M. Trnka, R. H. Grubbs, *Acc. Chem. Res.* **2001**, *34*, 18–29; b) C. Samojłowicz, K. Grela, *Chem. Rev.* **2009**, *109*, 3708–3742.
- [2] For Wittig reaction see a) R. Schobert, C. Hölzel, B. Barnickel, *Sci. Synth.* **2010**, *47*, 9–84; b) G. Wittig, U. Schöllkopf, *Chem. Ber.* **1954**, *87*, 1318–1330; for Julia reaction see: c) I. E. Markó, J. Pospíšil, *Sci. Synth.* **2010**, *47*, 105–160; d) C. Aïssa, *Eur. J. Org. Chem.* **2009**, *2009*, 1831–1844; for alkenylation with metal carbenes see: e) N. A. Petasis, *Sci. Synth.* **2010**, *47*, 161–246; f) N. A. Petasis, E. I. Bzowej, *J. Am. Chem. Soc.* **1990**, *112*, 6392–6394; for Peterson olefination see: g) D. J. Peterson, *J. Org. Chem.* **1968**, *33*, 780–784; h) D. J. Ager, *Sci. Synth.* **2010**, *47*, 85–104.
- [3] a) G. C. Vougioukalakis, R. H. Grubbs, *Chem. Rev.* **2010**, *110*, 1746–1787; b) B. K. Keitz, K. Endo, P. R. Patel, M. B. Herbert, R. H. Grubbs, *J. Am. Chem. Soc.* **2012**,

- 134, 693–699; c) M. J. Koh, T. T. Nguyen, J. K. Lam, S. Torker, J. Hyvl, R. R. Schrock, A. H. Hoveyda, *Nature* **2017**, *542*, 80–85.
- [4] a) W. C. Still, C. Gennari, *Tetrahedron Lett.* **1983**, *24*, 4405–4408; b) I. Janicki, P. Kielbasiński, *Adv. Synth. Catal.* **2020**, *362*, 2552–2596; c) J. Clayden, S. Warren, *Angew. Chem. Int. Ed.* **1996**, *35*, 241–270.
- [5] L. F. van Staden, D. Gravestock, D. J. Ager, *Chem. Soc. Rev.* **2002**, *31*, 195–200.
- [6] a) R. Robiette, J. Pospíšil, *Eur. J. Org. Chem.* **2013**, *2013*, 836–840; b) F. Billard, R. Robiette, J. Pospíšil, *J. Org. Chem.* **2012**, *77*, 6358–6364; c) J. Pospíšil, *Tetrahedron Lett.* **2011**, *52*, 2348–2352.
- [7] a) P. R. Blakemore, *J. Chem. Soc. Perkin Trans. 1* **2002**, 2563–2585; b) B. Chatterjee, S. Bera, D. Mondal, *Tetrahedron: Asymmetry* **2014**, *25*, 1–55; c) P. R. Blakemore, W. J. Cole, P. J. Kocienski, A. Morley, *Synlett* **1998**, 26–28; d) A. B. Charette, H. Lebel, *J. Am. Chem. Soc.* **1996**, *118*, 10327–10328; e) P. Liu, E. N. Jacobsen, *J. Am. Chem. Soc.* **2001**, *123*, 10772–10773.
- [8] For excellent review handling the selectivity issues in Julia-Kocienski olefination see: G. Sakaine, Z. Leitis, R. Ločmele, G. Smits, *Eur. J. Org. Chem.* **2023**, *26(7)*, e2022012.
- [9] a) J. Pospíšil, H. Sato, *J. Org. Chem.* **2011**, *76*, 2269–2272; b) J. Pospíšil, R. Robiette, H. Sato, K. Debrus, *Org. Biomol. Chem.* **2012**, *10*, 1225–1234.
- [10] a) D. J.-Y. D. Bon, O. Kováč, V. Ferugová, F. Zálešák, J. Pospíšil, *J. Org. Chem.* **2018**, *83*, 4990–5001; b) B. R. Rani, M. Ubukata, H. Osada, *Bull. Chem. Soc. Jpn.* **1995**, *68*, 282–284.
- [11] For more information see SI.
- [12] During our stereoselective reduction reaction conditions optimization we took an inspiration in the work of Jørgensen et al. who demonstrated that β -keto- α -fluor-heteroaryl sulfones can be stereoselectively transformed into either *syn* or *anti* β -hydroxy- α -fluor-heteroaryl sulfones if suitable reducing agent and reaction conditions are used. See, C. B. Jacobsen, M. Nielsen, D. Worgull, T. Zweifel, E. Fisker, K. A. Jørgensen, *J. Am. Chem. Soc.* **2011**, *133*, 7398–7404.
- [13] D. C. Sarkar, A. R. Das, B. C. Ranu, *J. Org. Chem.* **1990**, *55*, 5799–5801.

Review

Latest Developments of the Julia–Kocienski Olefination Reaction: Mechanistic Considerations

 Daniel Chrenko¹  and Jiří Pospíšil^{1,2,3,*} 
¹ Department of Chemical Biology, Faculty of Science, Palacky University, Šlechtitelů 27, 779 00 Olomouc, Czech Republic; daniel.chrenko01@upol.cz

² Department of Organic Chemistry, Faculty of Science, Palacky University, 17. Listopadu, 779 00 Olomouc, Czech Republic

³ Laboratory of Growth Regulators, Palacky University & Institute of Experimental Botany AS CR, Šlechtitelů 27, 779 00 Olomouc, Czech Republic

* Correspondence: j.pospisil@upol.cz; Tel.: +420-585-634-784

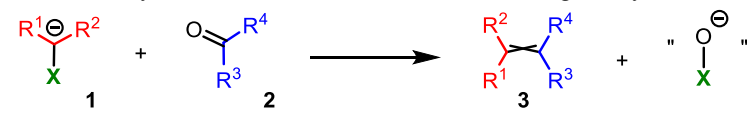
Abstract: Since its discovery, the Julia–Kocienski olefination reaction has over past 30 years become one of the key C–C connective methods that is used in late-stage natural product synthesis. The reaction proceeds under mild reaction conditions, with a wide substrate scope and functional group tolerance range and with high (*E*) selectivity. In this focused review, we discuss the reaction from a mechanistic point of view and disclose key features that play an important role in reaction selectivity. Finally, the mechanistic aspects of the newly developed modification of the Julia–Kocienski reaction, which allows the formation of both (*E*) and (*Z*) olefins from the same reaction partners, are discussed.

Keywords: Julia–Kocienski reaction; olefination; reaction selectivity; reaction mechanism

1. Introduction

Alkenes belong to a chemical functional group that is omnipresent in literally all natural products. Interestingly, since the early times when organic synthesis slowly became a ‘useful’ scientific discipline, many synthetic strategies have focused on the stereoselective synthesis of these structural motives. In particular, methods that allow for the connective stereoselective introduction of the olefin moiety have become very valuable tools for this goal. Over the past 100 years, many different connective olefination methods have been developed, although many of them follow the same retrosynthetic pathway [1]; they are based on the reunion of α -negative charge-stabilizing reagents **1** with aldehydes or ketones **2** (Table 1).

Table 1. Common carbonyl-based olefination methods used in organic synthesis.



Activating Unit X	Olefination Method	Litt. Reference
PhSO ₂	Julia–Lythgoe	Ref. [1]
ActSO ₂	Julia–Kocienski	Ref. [1]
PhSO(NMe)	Johnson	Ref. [2]
R ₃ P ⁺	Wittig	Ref. [3]
R ₂ P(=O)	Wittig–Horner	Ref. [3]
(RO) ₂ P(=O)	Horner–Wadsworth–Emmons (HWE)	Ref. [4]
R ₃ Si	Peterson	Ref. [5]
R ₂ B	Boron–Wittig	Ref. [6]



Citation: Chrenko, D.; Pospíšil, J. Latest Developments of the Julia–Kocienski Olefination Reaction: Mechanistic Considerations. *Molecules* **2024**, *29*, 2719. <https://doi.org/10.3390/molecules29122719>

Academic Editor: Georg Manolikakes

Received: 10 May 2024

Revised: 30 May 2024

Accepted: 3 June 2024

Published: 7 June 2024



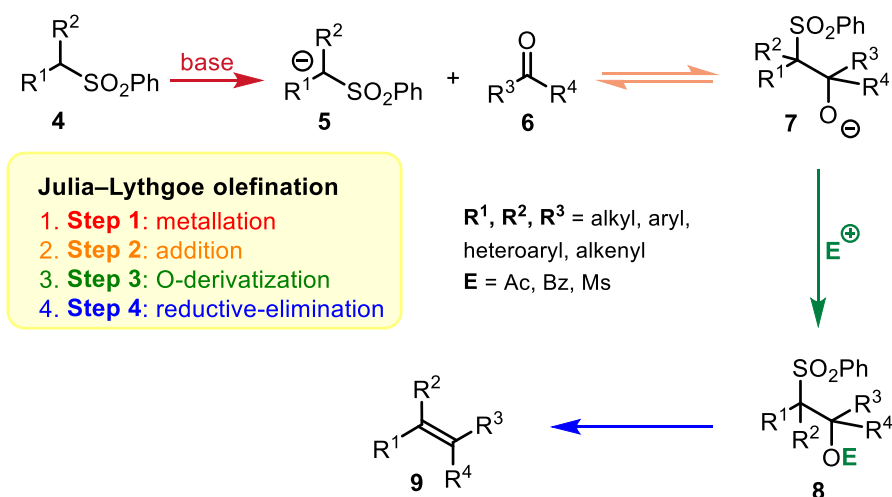
Copyright: © 2024 by the authors. Licensee MDPI, Basel, Switzerland. This article is an open access article distributed under the terms and conditions of the Creative Commons Attribution (CC BY) license (<https://creativecommons.org/licenses/by/4.0/>).

Since the introduction of the Wittig reaction [7,8] in the late 1950s of the twentieth century, the Wittig [3], Horner–Wadsworth–Emmons [4], Johnson [2], Peterson [5], and Julia olefination [1] methods have established themselves as the most widely used olefination protocols. Each of these methods has its advantages and drawbacks, which have changed over time because each of the methods has gone through a long and interesting development process since its original disclosure. In this personalized, focused review, we wish to discuss the mechanism of the so-called modified Julia reaction [1,9–16], also known as the Julia one-pot, Silvestre–Julia, or Julia–Kocienski olefination reaction, as well as its development in terms of the reaction mechanism and selectivity. The last part of the review will focus on the recently developed modification of the Julia–Kocienski olefination transformation that allows selective formation of (*E*) or (*Z*) olefins by a simple change in the reaction workup, and its scope and limitations will be compared with the Petersen and Zweifel olefination methods; protocols that also allow selective (*E*) or (*Z*) olefin formation by simple change in the reaction workup.

2. Origins and Mechanism of the Julia–Kocienski Olefination Reaction

2.1. Julia–Lythgoe Olefination vs. Julia–Kocienski Olefination: A Comparison

Classical Julia olefination, also known as Julia–Lythgoe olefination, was described for the first time in 1973 by (Mark) Julia and Paris [17] and was later developed by Kocienski and Lythgoe [18]. The original protocol was soon expanded for the beneficial *O*-derivatization step, consisting of four distinct stages carried out commonly in the two-pot protocol (Scheme 1): (1) the metalation of an alkylarylsulfone **4**; (2) the addition of the resulting carbanion species **5** to an aldehyde or ketone **6**; (3) the *O*-acylation (sulfonylation) of the adduct **7**; (4) the elimination of the β-acyl (sulfonyl) oxysulfone **8** intermediate. The addition of **5** to **6** typically yields product **7** as a mixture of all possible diastereoisomers; however, this is not of consequence because the stereochemical information encoded in **7** (or **8**) is lost during the elimination step. A common feature of Julia–Lythgoe olefination is its high (*E*)-stereoselectivity [1]—a consequence of the various radical mechanisms that operate in the final stage of reductive elimination [19].



Scheme 1. The Julia–Lythgoe olefination protocol.

The main drawbacks of Julia–Lythgoe olefination, namely the steric requirement-driven (*E/Z*) selectivity and the two-pot protocol, were in 1993 overcome by Silvestre Julia [20,21] (brother of Mark Julia). Their modification of the standard Julia–Lythgoe olefination protocol was based on the replacement of the phenylsulfonyl group with the benzo[*d*]thiazol-2-ylsulfonyl (BT) group (Scheme 2) [22–24]. The common features of the new transformation of the Julia–Lythgoe olefination reaction are the first two steps: (1) metalation; (2) the addition of metalated sulfone **11** to aldehyde **12**. Since in this case the aryl group in the alkyl aryl sulfone is an electron acceptor, the initially generated β-alkoxy

Table 2. Comparison of the Julia–Lythgoe and Julia–Kocienski olefination reactions—general features.

Key Features	Julia–Lythgoe	Julia–Kocienski
Practical Difference Origin of Stereoselectivity	Two-pot protocol Reductive elimination Step	One-pot protocol Addition step
Scope of olefin formation		
Terminal	✓	✓
1,2-disubstituted	✓	✓
Trisubstituted	✓	≈
Tetrasubstituted	≈	X
Scope of (E)-Stereoselectivity		
1,2-disubstituted	✓	✓
Trisubstituted	≈	X
Tetrasubstituted	≈	X
Scope of (Z)-Stereoselectivity		
1,2-disubstituted	X	✓ if the TBT-activating group is used;
Trisubstituted	X	X
Tetrasubstituted	X	X

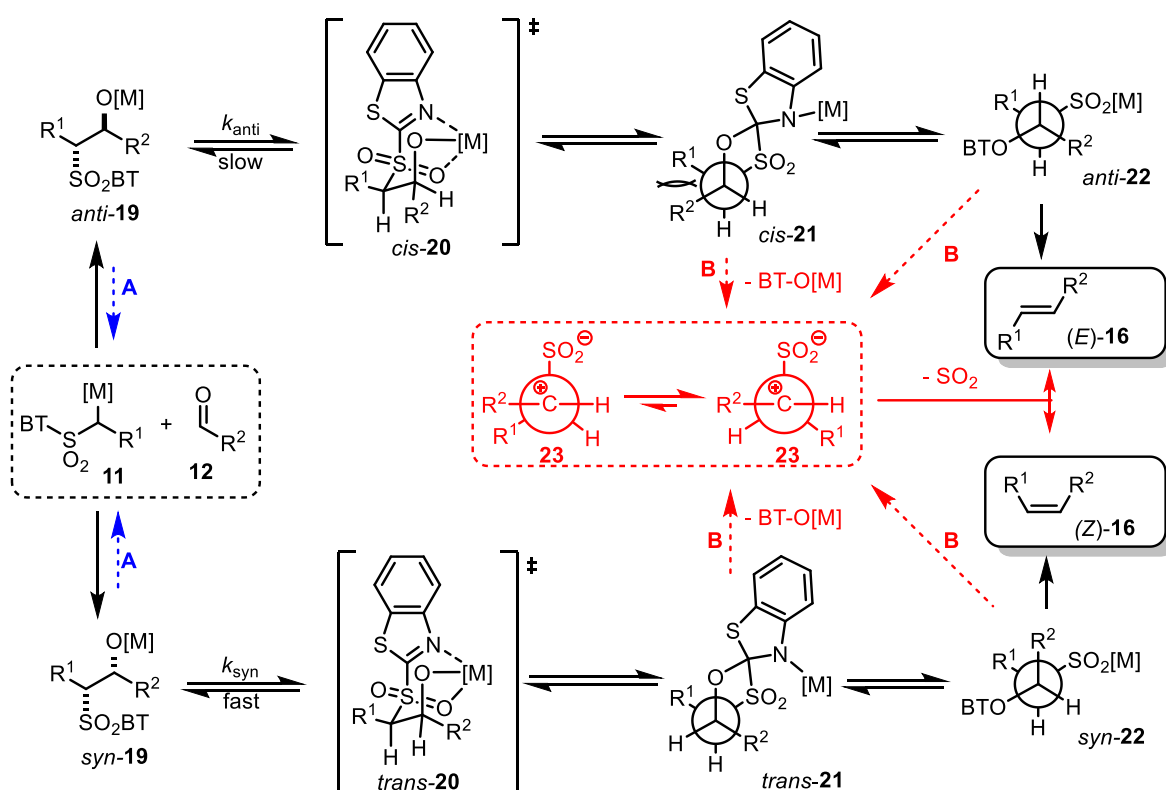
Note: ✓—good to excellent; ≈—acceptable; X—unsatisfactory result(s).

2.2. Reaction Mechanism and Its Impact on the Selectivity of Julia–Kocienski Olefination

The Julia–Kocienski reaction mechanism was intensively studied by Silvestre Julia [20,21], and their studies were further extended by Kocienski and Blackmore [11–13,26]. Based on these excellent mechanistic studies, the reaction mechanism can be established with respect to the stereochemical outcomes of the reaction (Scheme 3). There are three key features of this mechanism that deserve a brief comment.

- (1) The addition of metalated sulfone **11** to aldehyde **12** can provide *anti*-adduct *anti*-**19** via **TS1** or the *syn*-adduct *syn*-**19** via **TS2** (Figure 2). The selectivity in this step is extremely important, since all subsequent transformations of intermediate **19**, the Smiles rearrangement, and the β -elimination process are stereospecific. Thus, the *syn/anti*-selectivity of the addition step determines the final (*E/Z*) olefin ratio. Therefore, in theory, the (*E/Z*) selectivity of the reaction can be swapped from (*E*) to (*Z*) if proper reaction conditions are applied.
- (2) When stabilized metalated sulfonyl anions **11** ($R^1 = \text{Ph}$, alkenyl, etc.) are used, the addition of **11** to **12** becomes reversible (Scheme 3, path A). In this case, the original kinetically driven *syn/anti*-ratio of adduct **19** becomes less important in comparison with the Smiles rearrangement reaction rates (transformation of **19** to **22**). In such cases, the rearrangement of *anti*-**19** adduct leading to (*E*) olefin **16** is slower compared to the rearrangement of *syn*-**19** to olefin (*Z*)-**16** due to repulsive 1,2-interactions in the transition state (see *cis*-**20**).
- (3) For the elimination step, two borderline mechanisms are generally accepted. In the first, which is the most common, the rearranged intermediate **22** undergoes β -elimination. The elimination is stereospecific, and the *syn*-**19** adduct-rearranged intermediate *syn*-**22** furnishes the (*Z*) olefin and the *anti*-**19** adduct-rearranged intermediate, the compound *trans*-**22** (*trans* refers to the arrangement of R^1 and R^2 within the intermediate cycle), yields the (*E*) olefin. Alternatively, when (hetero)aryl aldehydes **12** ($R^2 = \text{(hetero)aryl}$) are used, an alternative elimination pathway (path B) is postulated to occur. In this case, the elimination pathway should proceed through the formation of an intermediate carbocation **23**. The steric requirements of R^1 and R^2 then play a crucial role in the final (*E/Z*) selectivity of the reaction. Path B was used

to explain the unexpected (*E*) selectivity of the coupling reactions carried out using (hetero)aryl aldehydes **12** as substrates.



Scheme 3. Detailed reaction mechanism of the Julia–Kocienski reaction. **A** refers to the retroaddition process that occurs for sulfones **11** with R^1 = (hetero)aryl, alken, alkyn (see point 2 below). **B** refers to previously proposed elimination process that was based on the cation **23** formation (see point 3 below). ‡ indicates the transition state.

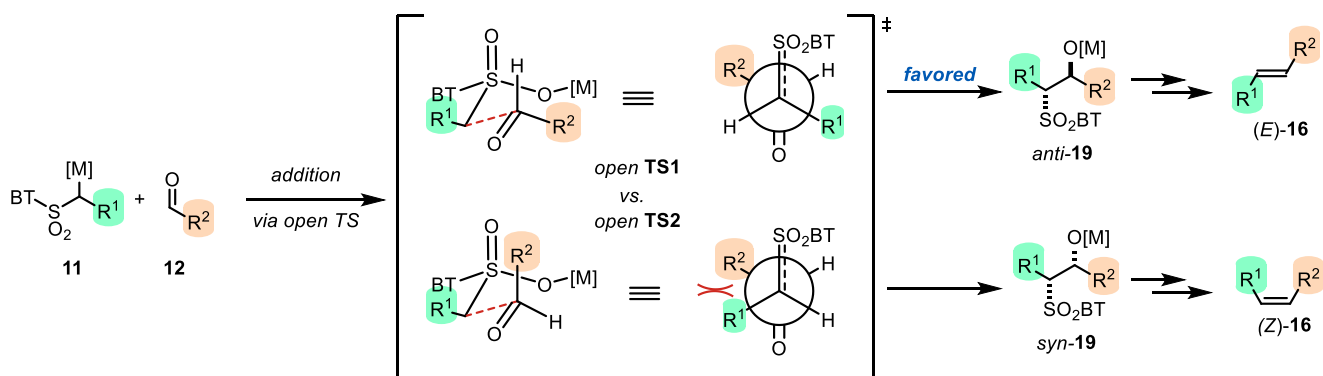
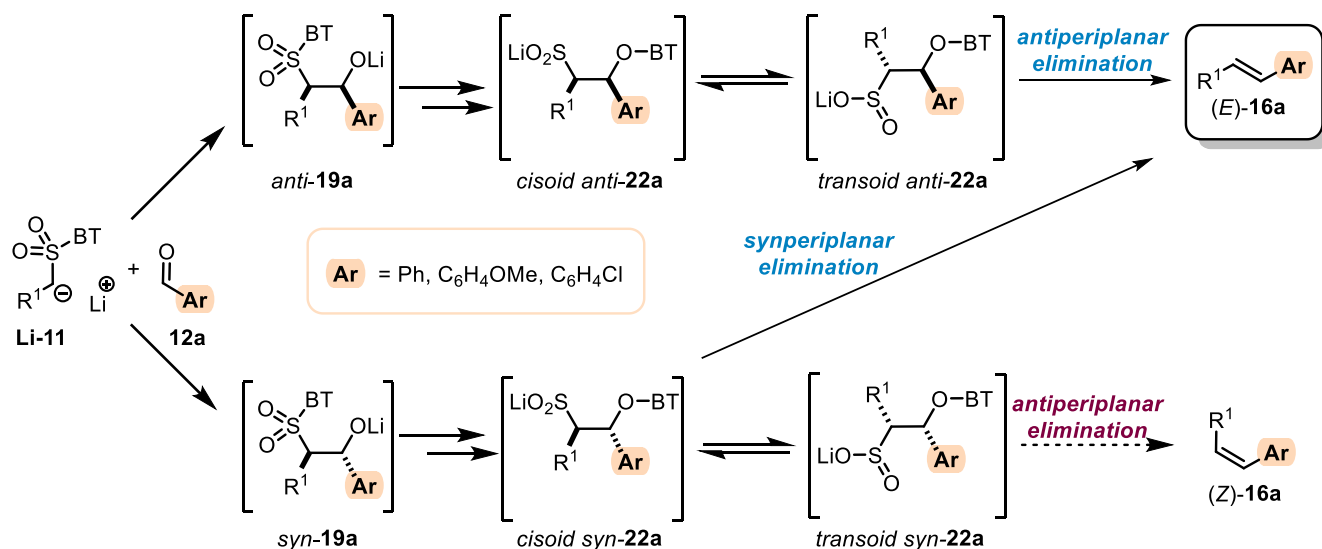


Figure 2. Addition of the metalated sulfone **11** to aldehyde **12**. Mechanistic rationale. ‡ indicates the transition state.

Recently, our group, in collaboration with Robiette's group, proposed an alternative explanation for the observed (*E*) selectivity of these reactions. Our explanation is based on a combined experimental and theoretical study that revealed that the key role in the elimination step is played by the rearrangement product **22a** (Scheme 4) [14]. In general, both the *anti*- and *syn*-**22a** intermediates can adopt the *cisoid* and *transoid* conformations. The conformational equilibrium is strongly influenced by the steric requirements of the R^1 and Ar groups, and in the case of the *anti*-**22a** intermediate, the *transoid* is preferred, while

in the case of *syn*-22a, the *cisoid* is preferred. Advanced experimental and theoretical studies have suggested that in the case of a *cisoid* conformation, competitive *syn* elimination can occur [14], explaining the almost exclusive formation of (*E*) olefins observed in the general structure 16a.

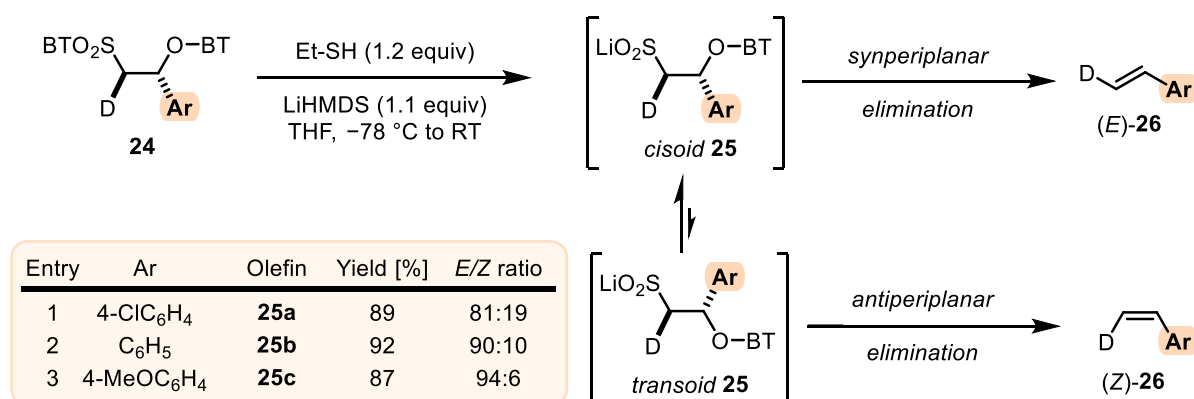


Scheme 4. The rationale for the observed high (*E*) selectivity in the Julia–Kocienski olefination of aromatic aldehydes.

Theoretical studies have also suggested that the *syn* elimination process should be more favored when the aryl substituent R² has electron-donating substituents and disfavored when an electron-deficient substituent is present. The postulated prediction was then evaluated using a stereodefined intermediate 24, which was selectively transformed in situ to the corresponding lithiated anion 25, which itself was allowed to undergo an elimination process (Scheme 5). With this approach, the generated anion cannot undergo the retroaddition process (it is an intermediate after the rearrangement step), and the nucleophile generated in situ (thiolate anion) is not basic enough to trigger the epimerization process of any of the two epimerizable stereogenic centers. Therefore, only (*Z*) olefin (*Z*)-26 should be produced as the main product of the transformation. If the reaction proceeds through the carbocation-type intermediate of 23 (see Scheme 3), an approximately 50:50 ratio of the (*E*/*Z*) isomeric mixture can be expected. In all tested cases, the (*E*)-isomer (*E*)-26, the product of the *synperiplanar* elimination process, was produced as the main product of the reaction, strongly suggesting that the *syn* elimination process is the main process that operates during the Julia–Kocienski olefination reaction of alkyl sulfones with aryl aldehydes. The observed stronger preference for electron-donating group-containing intermediates to undergo preferentially *synperiplanar* elimination was also in agreement with the DFT-calculation-based prediction.

2.3. Recent Reaction Selectivity Improvements

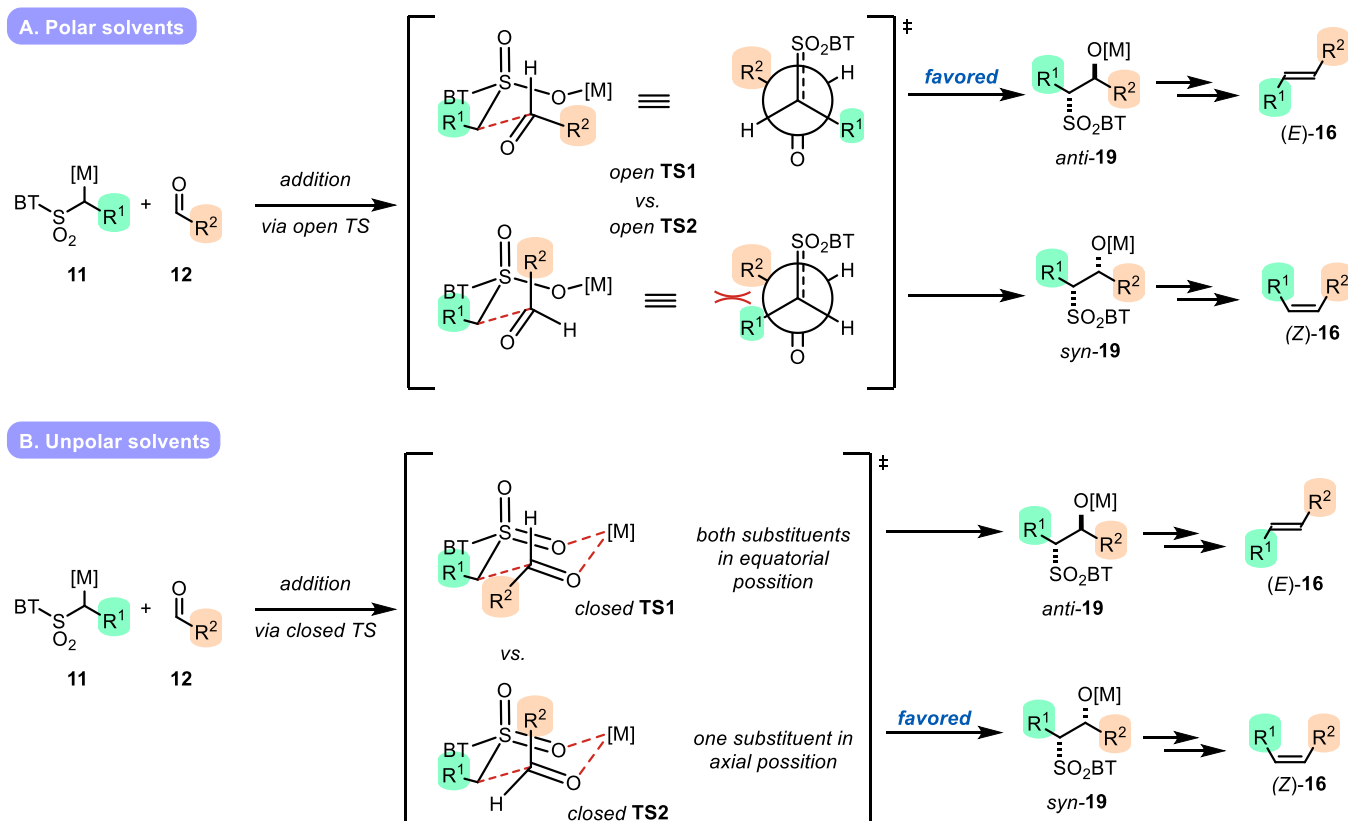
The reaction mechanism proposed by Julia and Kocienski, which was later confirmed by our own studies, implies that the reaction selectivity is directly linked with the initial *syn*/*anti*-selectivity of the addition step. The adduct ration further directly influences the selectivity (*E*/*Z*) of the overall reaction, regardless of whether the reaction proceeds through the *antiperiplanar* elimination (for R¹ and R² = alkyl) or mixed *antiperiplanar* and *synperiplanar* (for R¹ or R² = (hetero)aryl) elimination in the final step. Unsurprisingly, most of the methods developed to influence the reaction selectivity in favor of one of the two isomers focus on the key addition step.



Scheme 5. Stereoselectivity in the elimination step—a competition between the *synperiplanar* and *antiperiplanar* elimination processes.

2.3.1. Solvent Effect

The most important and straightforward way to influence the *syn/anti*-selectivity of the addition step is to choose the right solvent for the transformation. When polar solvents such as THF, DME, or DMF are used, *anti*-adduct *anti-19* is the preferred addition product due to its solvent stabilization potential (Scheme 6A). On the contrary, when nonpolar solvents such as toluene are used, the reaction proceeds via a closed transition state (Scheme 6B) and *syn*-adduct *syn-19* is preferred.

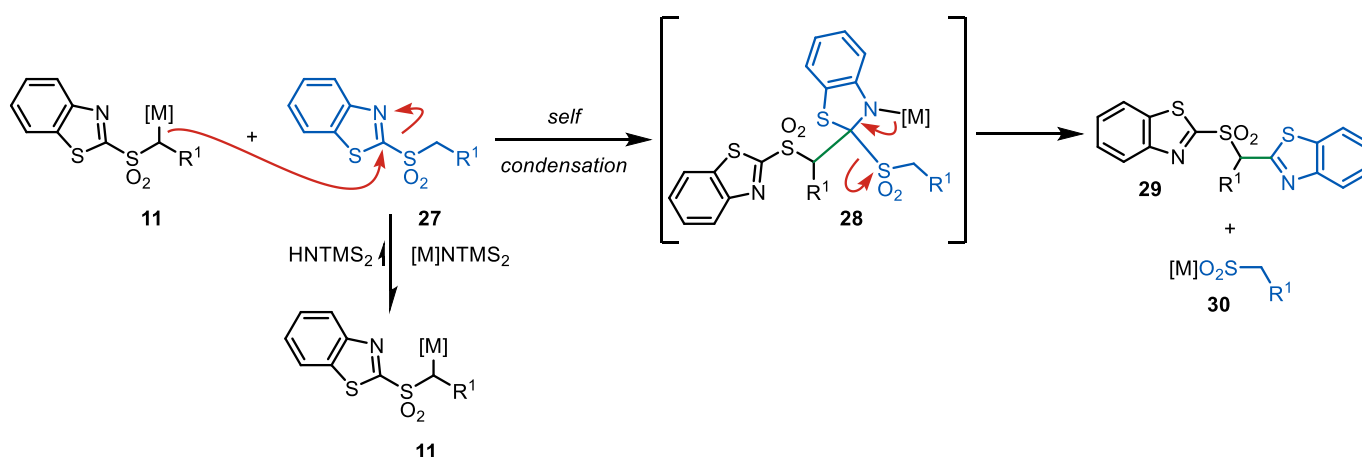


Scheme 6. The impact of the solvent's polarity on the stereochemical outcome of the Julia–Kocienski reaction. ‡ indicates the transition state.

It should be noted that although such an approach is generally applicable and correct, the role of the solvent might be further influenced by metal salts and additional cosolvents.

- Metal cation

The metal cation, which is always present in the reaction mixture as a ‘residue’ after the deprotonation step, has a key influence on the selectivity of the reaction. In general, cations with the character of a hard Lewis acid, such as Li^+ , favor the formation of the (*E*) olefins. It is assumed that the observed (*E*) selectivity is caused by better stabilization of the generated anion **11**, which can be further added due to its lower reactivity to aldehyde **12**, which has better selectivity and favors the *anti*-adduct *anti*-**19**. On the contrary, when a large cation is used, such as K^+ , the reaction can proceed preferentially either via closed TS or the solvent can increase the dissociation of the cation from **11**, thereby increasing the reactivity. The first case is typical for nonpolar solvents (e.g., toluene) because the solvent does not provide additional stabilization to the reagents or reaction intermediates. In the latter case, the dissociation of the cation from reagent **11** increases the reactivity of the anion and leads to faster production of the kinetic product of the addition step, *anti*-isomer *anti*-**19**. However, it should also be noted that an increase in anion **11**’s reactivity can also inevitably lead to the undesired self-condensation of reagent **11** (Scheme 7); thus, a compromise between selectivity and reactivity has to be reached.



Scheme 7. The self-condensation reaction that accompanies the reaction of anion **11**.

- Cosolvents

The addition of the cosolvents to the reaction mixture can also be beneficial when (*E*) selectivity is desired. It was observed that the addition of cosolvents such as DMPU or HMPA to reaction mixtures carried out in THF or DMF led to an increase in the (*E*) olefin selectivity of the desired product. It is believed that the cosolvent’s role is in metal cation scavenging, with an impact similar to that described in the previous section (increased reactivity that favors *anti*-adduct formation).

2.3.2. Additives

Another way to increase the selectivity (*E*/*Z*) of the Julia–Kocienski reaction is by adding additives to the reaction mixture. Over the years, many different additives have been used for such purposes; however, only a few of them have had a significant effect. The relevant ones are listed below.

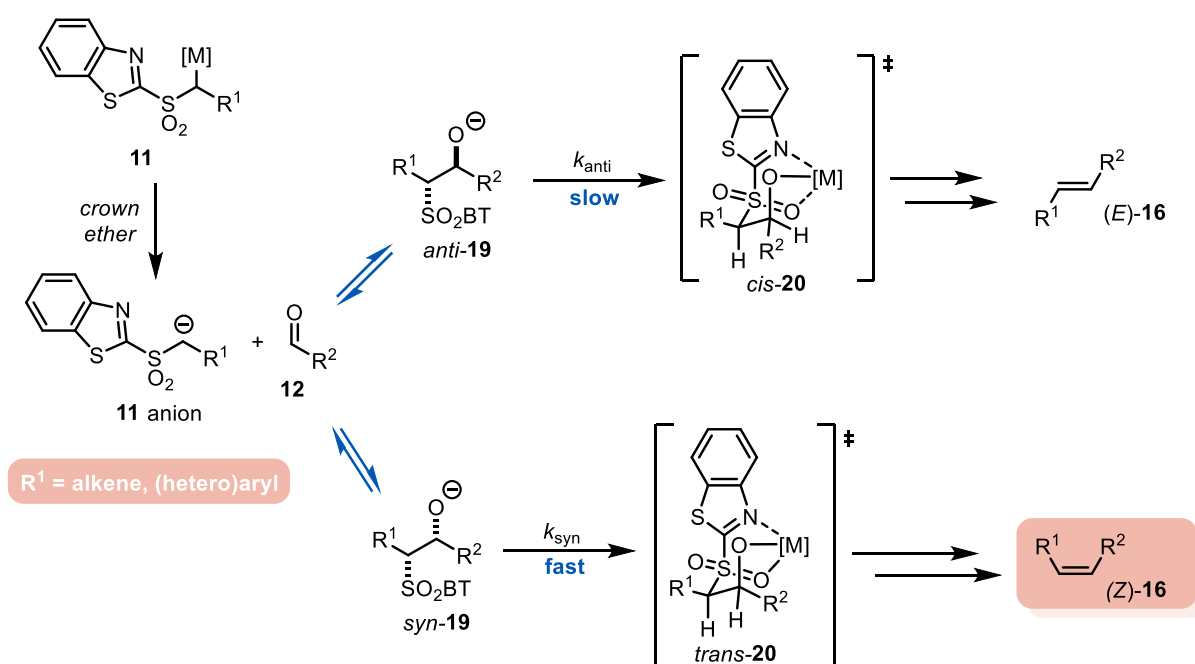
- Crown ethers

As mentioned in the previous section, the role of the (co-)solvent was shown to have a tremendous effect on the reaction yield and selectivity. As a modus operandi, it was postulated that polar solvents increase the reactivity of anion **11** due to a cation–anion separation (reaction kinetic) that leads to the preferential formation of *anti*-adducts (polar solvents) or *syn*-adducts (nonpolar solvents). As a disadvantage, the self-condensation of metalated sulfone **11** (Scheme 7) was observed. The use of specific cation-chelating

cosolvents such as HMPA or DMPU showed only limited success, even though in several cases it led to the diminished formation of self-condensation products and an increase in (*E*) selectivity.

Based on the same logic, to increase the reactivity of metalated sulfone **11** and increase the formation of the *anti*-adduct (kinetic product), an excess of crown ethers (18-crown-6 for K^+ , 12-crown-6 for Li^+) [29] can be used during the reaction, as demonstrated in several recent total syntheses of natural products (e.g., zeaenol [30], paecilomycins E and F [31], amphidinolide E [32], and salarins A and C [33]).

However, it should be noted that if metalated sulfone **11** is used with a group in the lateral chain (R^1) that is capable of stabilizing the generated anion, the addition of generated anion **11** to aldehyde **12** is reversible (Scheme 8). Consequently, the *syn/anti* ratio of adducts **19** is in equilibrium and (*Z*) olefin (*Z*-**16**) is formed preferentially due to a faster ($k_{anti} < k_{syn}$) Smiles rearrangement step [34].



Scheme 8. Role of crown ethers in the Julia–Kocienski reaction. High (*Z*) selectivity in the case of stabilized metalated sulfones. ‡ indicates the transition state.

- Ammonium salts

The use of ammonium salts proved to also be beneficial, and in several cases of highly complex molecular scaffolds led to increases in the observed reaction yield and (*E*) selectivity [35,36]. It is believed that the role of ammonium salts is in the activation of aldehyde **12**, where due to its steric requirements it increases the *anti*-selectivity of the addition step. Note also that the role of the counter-anion of the ammonium salt is not innocent. The best (*E*) selectivity was observed when potassium-containing metalated sulfone **11** was reacted in the presence of TBAB (tetrabutylammonium bromide) and lithium-containing metalated sulfone **11** was reacted in the presence of TBAC (tetrabutylammonium chloride). Such observations suggest the beneficial formation of KBr and LiCl salts during the reaction.

- Chelating salts

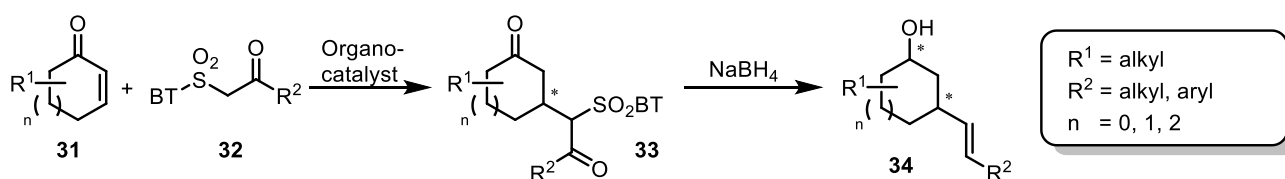
Similarly, metal cations (e.g., $CeCl_3$ [37,38], $MgCl_2$ [39], $ZnCl_2$, and $LiBr$) can be used to activate aldehyde **12** during the reaction. The addition of such a salt generally results in an increase in the reaction yield of the transformation. The (*E/Z*) selectivity of the transformation is influenced only if aldehydes bearing α -alkoxy substituents [39] are used

in the presence of an excess of MgCl_2 or ZnCl_2 (addition via the Cram chelate transition state) [40].

3. Julia–Kocienski Olefination—Extension to Carboxylic Acid Derivatives

All of the olefination methods mentioned above are based on the reunion of the metalated sulfone **11**-type intermediate and a carbonyl-containing intermediate **12** (Scheme 2). The overall transformation can, thus, be regarded as an addition–rearrangement–elimination sequence, where the final (*E/Z*) selectivity of the newly olefinic bond is determined by the addition step. Therefore, the stereoselectivity is dictated by the reaction kinetic of the addition step (kinetic conditions) or by the kinetic of the rearrangement step (as the addition step is in equilibrium) (Scheme 3). Gueyrard’s group also demonstrated that in some cases lactones can also be used as reaction partners in the Julia–Kocienski reaction and that the subsequent addition–rearrangement–elimination step then yields the corresponding enol ethers [16].

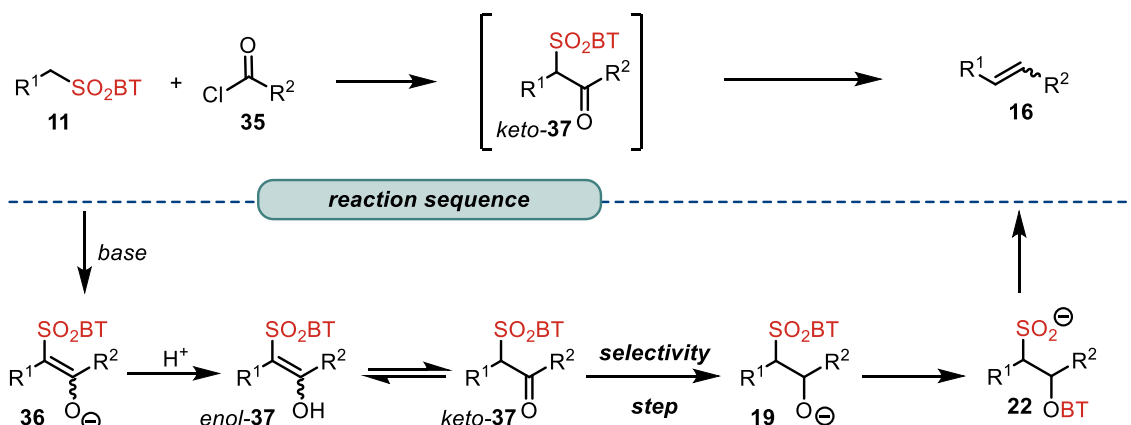
However, recently this paradigm changed, since we introduced the ‘reaction work-up-driven selectivity’ approach for the Julia–Kocienski reaction [41]. Analogous to the famous Peterson olefination reaction [5], we designed and optimized the new Julia–Kocienski protocol, which allows selective (*E*) or (*Z*) olefin formation via a simple change in the reaction work-up procedure. Our protocol is based on the seminal work by Jørgensen et al. [42,43], which demonstrated that β -keto BT sulfones **33** can be successfully transformed into the corresponding olefins **34** in high yields and with (*E*) stereoselectivity (Scheme 9).



Scheme 9. The seminal work by Jørgensen et al. [42,43] demonstrated the possibility of the stereoselective transformation of β -keto sulfones into the corresponding (*E*) olefins **34**. * refers to the stereogenic center.

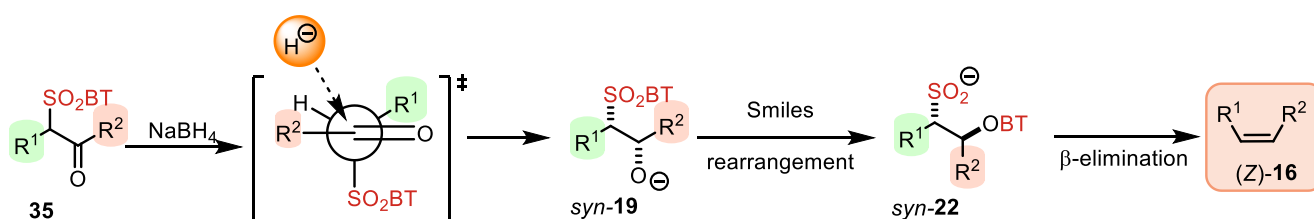
Based on these results, we designed a novel type of Julia–Kocienski reaction that allows the synthesis of the desired olefins **16**, starting from the metalated sulfone **11** and the acyl halides **35** (Scheme 10). In this sequence, the reunion of the two reagents (compounds **11** and **35**) is carried out using a previously described protocol [44,45]. The generated adduct **36** is then quenched in situ with the external source of the proton (the protic solvent, e.g., MeOH) and the β -keto sulfone **37** is formed. Compound **37** is present in the reaction mixture as a dynamic mixture of its keto and enol derivatives. When an external mild reducing agent (e.g., NaBH_4) is added, the keto form of *keto*-**37** is selectively reduced, and the nucleophilic hydride approach is directed according to the Felkin–Ahn model [46] (Scheme 11). Carbonyl reduction preferentially generates a *syn* derivative of β -hydroxy sulfone *syn*-**19**, and compound *syn*-**19** is further converted via the Smiles rearrangement– β -elimination sequence of the Julia–Kocienski olefination reaction to olefin (*Z*)-**16**. However, if chelating salts such as ZnCl_2 are added to the reaction mixture prior to NaBH_4 , the reduction proceeds through the Cram chelate model and the *anti*- β -hydroxy sulfone *anti*-**19** is formed. Consequently, compound *anti*-**19** then generates, after the Smiles rearrangement– β -elimination sequence, desired (*E*) olefin (*E*)-**16**.

Modified Julia–Kocienski Olefination reaction

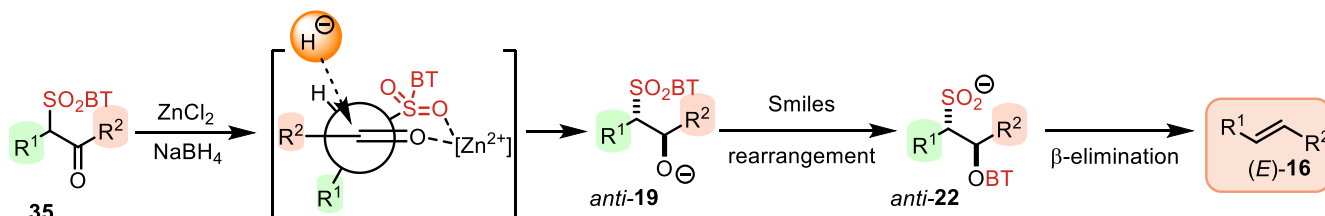


Scheme 10. Proposed reaction sequence for the modified Julia–Kocienski olefination reaction, where the stereoselectivity of the generated olefin is not determined in the addition step.

(Z)-selectivity via Felkin–Ahn TS



(E)-selectivity via Cram–chelate TS

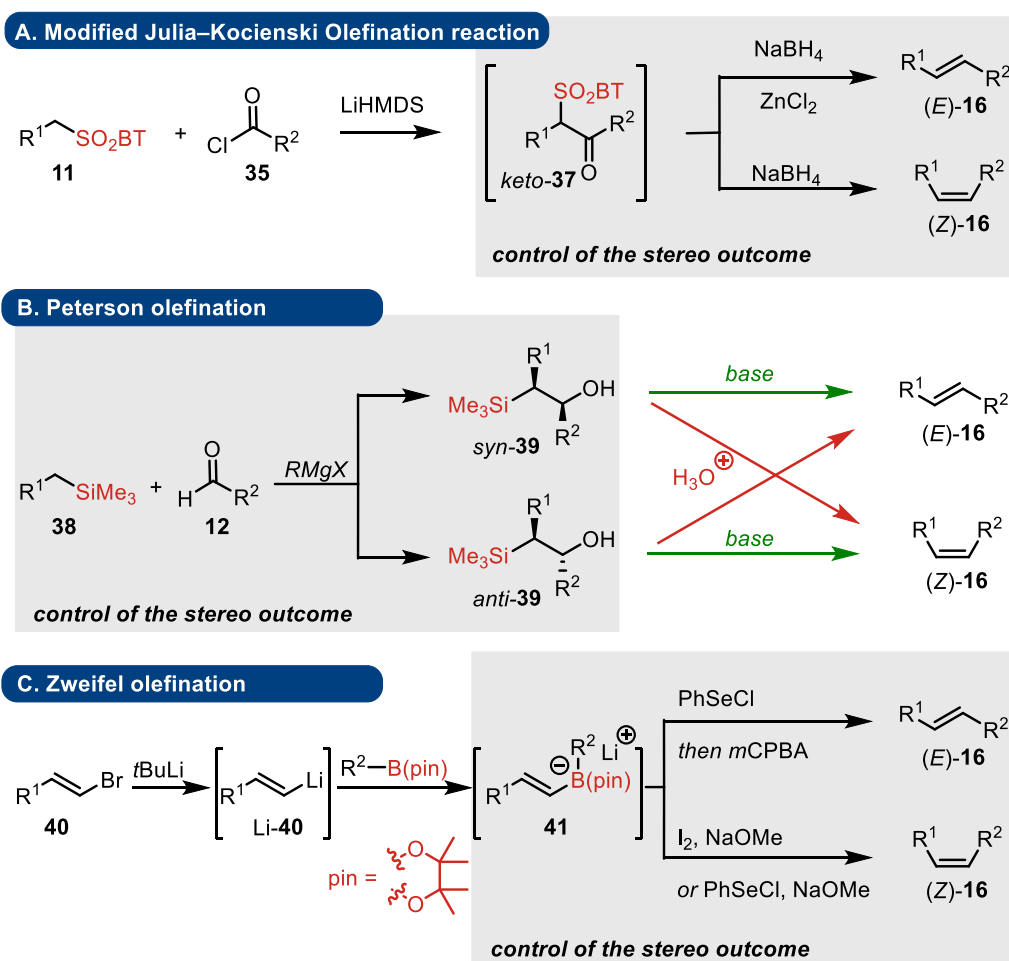


Scheme 11. The rational design behind the stereoselective modified Julia–Kocienski olefination reaction. † indicates the transition state.

Although only the preliminary scope and limitations of the transformation were established (28 examples), the method was successfully applied in the context of (nitro)fatty acid synthesis [41].

4. Julia–Kocienski, Peterson, and Zweifel Olefination Reactions: A Brief Comparison

In the previous chapter, we reviewed the modified Julia–Kocienski olefination reaction and disclosed its preliminary scope and limitations. In this chapter, we discuss this type of reaction in the context of the two presumably most used coupling methods that allow the generation of (*E*) or (*Z*) olefins stereoselectively during the reaction work-up—Peterson olefination [5,47] and Zweifel [48,49] olefination. Scheme 12 highlights three general schemes of the three mentioned methods. Each of the methods will now be discussed from the substrate and stereo outcome control viewpoints.



Scheme 12. Modified Julia–Kocienski, Peterson, and Zweifel olefination reactions. Three different transition-metal-free types of connective coupling reactions that allow selective (*E*) and (*Z*) olefin formation.

4.1. Modified Julia–Kocienski Reaction

- Substrates

Modified Julia–Kocienski olefination in general reunites two type substrates, sulfone **11** and acyl halide **35**. Sulfone **11** is generally obtained from the corresponding alcohol in the two-step Mitsunobu reaction [50]–oxidation protocol. Both steps generally proceed under very mild reaction conditions, since the second oxidation step is generally performed using H_2O_2 in the presence of molybdenum or tungsten-based catalysts [51].

- Elimination step

The mechanism of the elimination step that occurs after the decisive step controlling the stereo outcome of the reaction—the reduction of the carbonyl—was discussed in detail in the previous chapter. For the carbonyl reduction step, it should be noted that its result is strongly influenced by the steric encumbrance of the substituents on the acyl chloride **35**. Furthermore, if the R^1 and R^2 groups are aryl, a competitive *syn* elimination process will occur to further hammer the stereoselectivity of the reaction (see Section 2.2 for more details).

- Presence of stereogenic centers

At the present time, there are no sufficient experimental data that would experimentally address the question of the tolerance of the method toward the stereogenic center's

stability. However, one could conclude that stereogenic centers that are base- and acid-sensitive in the α position of acyl halide **35** should not be tolerated. Similarly, base-sensitive centers in and further on positions in sulfone **11** or acyl halide **35** might also undergo epimerization under the applied reaction conditions.

4.2. Peterson Olefination

Peterson olefination is seemingly ‘the most classical’ olefination transformation of the three methods discussed. It explores one of the ‘classical’ precursors of the olefination coupling, aldehyde, and the ratio (*E/Z*) of the formed olefin is determined in the first addition step [5,47]. However, there are also two characteristics that separate this type of connective method from the others: (1) the stability of the organosilicon compounds allows for further pre- or post-addition step transformations of β -hydroxy silanes that allow the stereoselective formation of enamines [52,53] or vinyl sulfones [54]; (2) due to the commercial availability of the TMS-CH₂-MgCl reagent, Peterson olefination is commonly used to generate vinyl olefins from sterically hindered or perfluorinated ketones [55]. However, both trends are beyond the scope of this focused review and will not be discussed.

- Substrates

The transformation is based on the reunion of the two substrates, aldehyde **12** and silane **38** (Scheme 12). While the synthesis of the aldehyde **12** coupling partner is well documented and can be achieved via various means, under very mild reaction conditions, and on rather complex substrates, the formation of the silicon-containing partner **38** was for decades rather tricky. However, recent (past two decades) developments, especially in the field of transition-metal-mediated hydrosilylation reactions, have made available even complex silanes **38** [56,57].

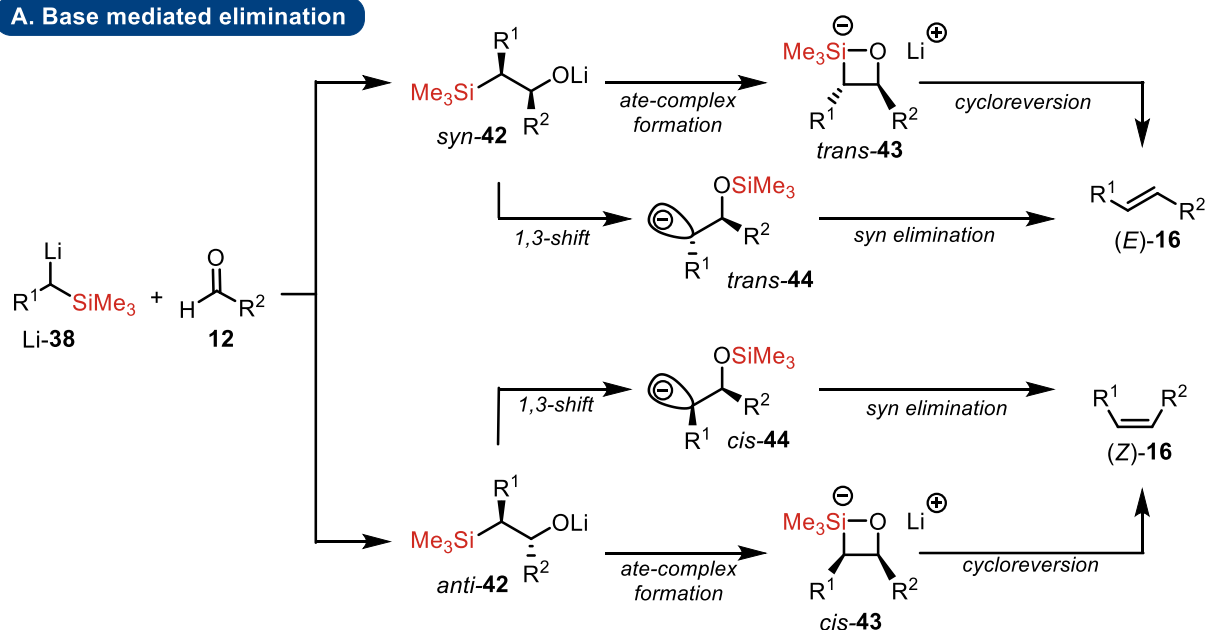
As mentioned previously, the stereoselectivity outcome of the reaction is determined in the first addition step of the reaction. The addition of an anion generated from **38** to aldehyde **12** generally proceeds with reasonably good diastereoselectivity, and the influence of (co)solvents and ions is similar to those observed for the Julia–Kocienski olefination reaction (see Scheme 6). The generated adducts, anion *syn*-**42** and *anti*-**42**, then spontaneously undergo elimination via the pentacoordinate 1,2-oxasiletanide intermediate, which subsequently undergoes cycloreversion (see the elimination step below). However, when using the α -silyl organomagnesium reagent Mg-**38**, due to a strong magnesium–oxygen bond, the corresponding adduct **42** is generally sufficiently stable and can be trapped in the form of β -hydroxy silane **39** (Scheme 12B). Both generated diastereoisomers, *syn*- and *anti*-**39**, can be further separated and submitted to the stereoselective elimination step (vide infra).

- Elimination step

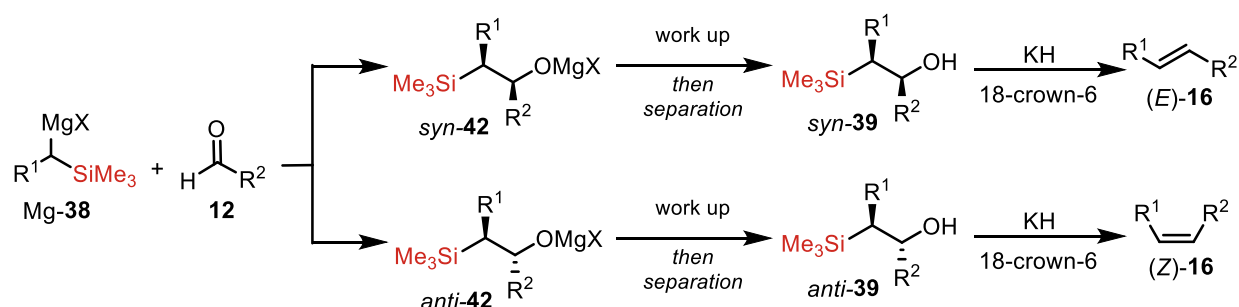
As mentioned above, the elimination step in Peterson olefination generally proceeds spontaneously immediately after the addition step (Scheme 13A). In such cases, it is generally accepted that the reaction proceeds through the formation of the 1,2-oxasiletanide intermediate through the addition–cycloreversion mechanism or through the 1,3 migration–*syn*periplanar β -elimination mechanism. The reaction is stereoselective and the configuration of adduct **42** is reflected in the final *E/Z* ratio of the olefinic product **16**, since the *syn*-**42** adduct yields (*E*) olefin (*E*)-**16** and the *anti*-**42** adduct yields (*Z*) olefin (*Z*)-**16**.

Pure (*E*) or (*Z*) olefins can be obtained if interrupted Peterson olefination is performed. In such a case, the intermediate β -hydroxy silane **39** is isolated and the two diastereoisomers are separated. In this case, if submitted to basic conditions, the same olefin type (*E/Z* configuration) as in the one-pot protocol is obtained (Scheme 13B). However, if the intermediates *syn*- and *anti*-**39** are submitted to Brønsted or Lewis acid reaction conditions, the reaction proceeds through the *antiperiplanar* β -elimination process and the stereochemical result of the reaction is the opposite of that from base-mediated elimination. The *syn*-**39** isomer then produces (*Z*) olefin (*Z*)-**16** and the *anti*-**39** yields (*E*) olefin (*E*)-**16** (Scheme 13C).

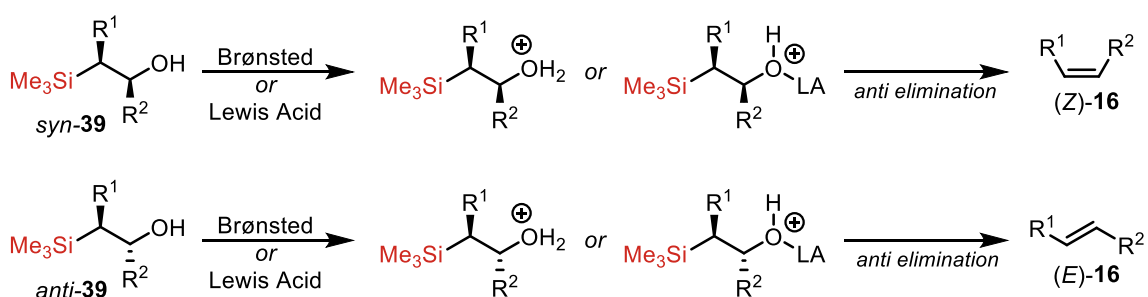
A. Base mediated elimination



B. Base mediated elimination of β -hydroxy intermediate



C. (Lewis) acid mediated elimination of β -hydroxy intermediate



Scheme 13. (A) The mechanism of Peterson olefination carried out in a one-pot manner. The mechanism of base-mediated elimination is depicted. (B) The Peterson olefination sequence carried out as a two-step protocol. The elimination of the β -hydroxy intermediate proceeds under basic conditions. (C) The second step of the Peterson olefination reaction, in which the elimination of the β -hydroxy intermediate proceeds under Brønsted or Lewis acid conditions.

- Presence of stereogenic centers

Similarly to Julia–Kocienski olefination, the substrates used as starting materials in the Peterson olefination reaction have stereogenic centers in the α position that are base- and acid-sensitive to the carbonyl group in $\mathbf{12}$. Similarly, the base-sensitive centers

in β and in positions close to the silicon group in silane **38** or aldehyde **12** could also undergo epimerization.

4.3. Zweifel Olefination

The Zweifel olefination protocol differs from the Julia–Kocienski and Peterson olefination reactions in many ways. Firstly, the olefinic bond found in the final product is already present in one of the two starting substrates, normally in the vinyl halide **40** (Scheme 12C). In its original form, Zweifel olefination is ‘nothing more’ than the Suzuki–Miyaura coupling-like reaction while being free of transition metals, which proceeds with the inversion of the stereochemistry when it comes to the double-bond geometry [48]. This statement is oversimplified, especially when the stereo outcome of the reaction is considered, although still states the point that the reaction is not stereodivergent, as is the case of the two previously discussed reactions. However, the situation has changed less than a decade ago, when Aggarwal and co-workers introduced a new PhSeCl-based reaction work-up protocol [58], which in combination with a base (NaOMe) or oxidant (*m*CPBA) was able to selectively produce (*E*) or (*Z*) olefins starting from the same vinyl boronic ester starting material. The difference between the newly developed reaction and the previous Zweifel olefination protocol is rather important; therefore, one could consider renaming the Zweifel stereodivergent olefination protocol as Zweifel–Aggarwal olefination.

- Substrates

The typical substrates in the Zweifel stereodivergent reaction are vinyl halide **40**, which is further transformed in situ to the corresponding lithiated species Li-**40**, and a boronic ester (normally pinacol alkyl borane). The synthesis of any of the two substrates need not to be discussed in detail, since many methods can be employed. However, what should be highlighted is that the boronic ester substrates can be readily prepared in an enantioenriched form (a stereogenic center to a boronic ester), and that the stereogenic center is due to boron migration properties conserved during the reaction (*vide infra*).

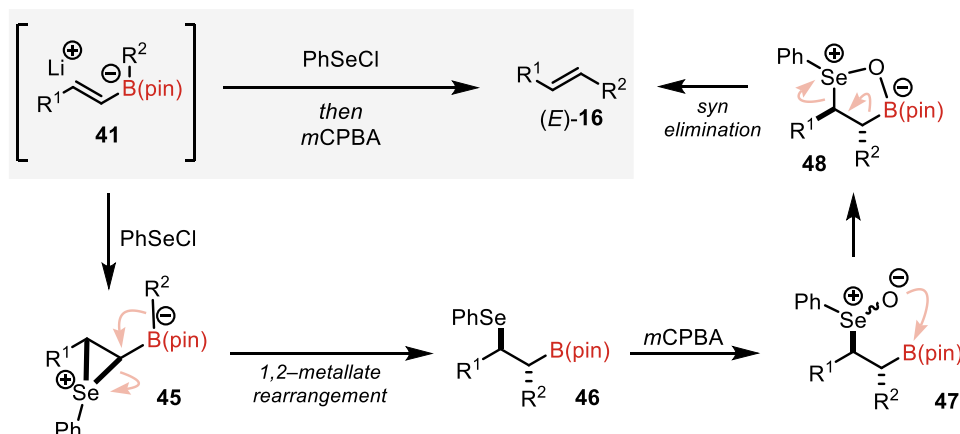
- Elimination step

Similarly to the previous two olefination methods, the stereodivergence of the Zweifel–Aggarwal olefination reaction is introduced in the elimination step. The common intermediate of the reaction is the borate complex **41** (shown for the (*E*) isomer), which is then reacted with the PhSeCl reagent to form intermediate **45** (Scheme 14). Intermediate **45** is highly reactive and initiates the spontaneous stereospecific 1,2-metallated migration of the alkyl group R² from the boron atom. Intermediate **46** is then treated with *m*CPBA (Scheme 14A) or MeONa (Scheme 14B). In the first case, *m*CPBA oxidizes phenyl selenium to selenium oxide **47** and the generated selenium oxide **47** undergoes an intramolecular *syn* elimination process that proceeds through the cyclic intermediate **48**. In this case, the transformation proceeds with the preservation of the configuration if the original configuration of the vinyl boronate intermediate **41** is considered.

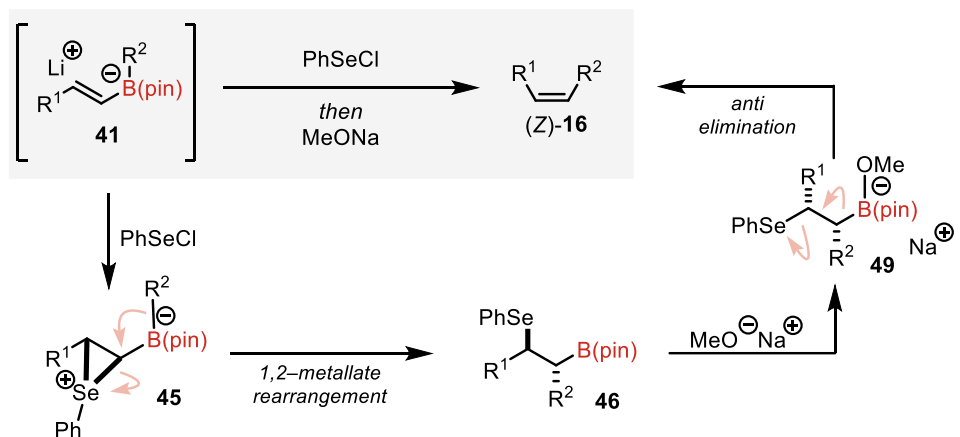
In the second case (Scheme 14B), the addition of the methanolate anion generates complex **49**. Complex **49** then spontaneously releases the phenyl selenium anion as a good leaving group via the *anti*-elimination process. In this case, a complete transformation takes place, with a formal inversion of the configuration compared to the original configuration on the vinyl boronate intermediate **41**.

Overall, starting from the same readily available 1-halide-2-alkyl/aryl olefin, both (*E*) and (*Z*) olefins **16** can be readily and stereoselectively generated.

A. Retention of the vinyl boronic ester configuration



B. Inversion of the vinyl boronic ester configuration



Scheme 14. Stereodivergent Zweifel olefination reaction mechanisms (A) for the transformation that preserves the original vinyl boronic ester configuration and (B) the transformation that inverts the original vinyl boronic ester configuration.

- Presence of stereogenic centers

The Zweifel–Aggarwal olefination method has an advantage over the Julia–Kocienski and Peterson olefination methods, which results from the structure of the starting reagents; namely, it does not contain labile stereogenic centers in the α -position to the aldehyde or acyl halide. Stereogenic centers in the α -position to the boron atom or in the allylic position in the case of the second reacting partner are generally very stable under the standard reaction conditions, and in the case of boron-containing reagents, they are also readily available using various synthetic methods. From a mechanistic point of view, the 1,2-metallated rearrangement proceeds while the configuration is preserved [59], meaning this method is highly suitable for 1,2-disubstituted olefins with a stereogenic center in the allylic position. This strategy has already been exploited several times in the context of natural product synthesis [60].

5. Conclusions

Since its first dissemination in 1993, the reaction sequence that is now referred to as the Julia–Kocienski reaction has become a very popular late-stage connective method in natural product synthesis because it combines highly efficient (reaction yield) and selective (predominantly (E)-selective) connective methods that proceed in a one-pot protocol under mild reaction conditions and with broad substrate and functional group tolerances. The past

30 years of reaction development have also identified key mechanistic properties that allow for better control of the reaction selectivity. Moreover, we have recently introduced a novel modification of the Julia–Kocienski reaction that not only increases the starting material scope (since it allows for the use of previously inaccessible carboxylic acid derivatives as substrates) but also allows for selective (*E*) or (*Z*) olefin formation. In addition, this method allows for the first time the development of the Julia–Kocienski olefination reaction for the independent formation of (*E*) or (*Z*) olefins, starting from the same starting materials and using simple reaction work-up protocol alternation.

Within this focused review, we wished to shed some light on the Julia–Kocienski reaction’s development and highlight the latest evolution, which resulted in the transition of the Julia–Kocienski olefination reaction into a stereodivergent method. In this context, the modified Julia–Kocienski olefination reaction was compared with the two other methods that allow the ‘workup-based’ stereodivergent formation of (*E*) and (*Z*) olefins, the Peterson olefination and modified Zweifel olefination methods (we propose naming the latter Zweifel–Aggarwal olefination to distinguish it from the original Zweifel olefination method).

Author Contributions: Conceptualization and methodology, D.C. and J.P.; writing—preparation, review, and editing of the original draft, D.C. and J.P. All authors have read and agreed to the published version of the manuscript.

Funding: This research was funded by the Internal Grant Agency of Palacky University, grant numbers IGA_PrF_2024_007 and IGA_PrF_2024_028.

Institutional Review Board Statement: Not applicable.

Informed Consent Statement: Not applicable.

Data Availability Statement: Not applicable.

Conflicts of Interest: The authors declare no conflicts of interest.

References

1. Markó, I.E.; Pospíšil, J. Julia, Julia–Kocienski, and Related Sulfur-Based Alkenations. In *Science of Synthesis*; de Meijere, A., Ed.; Georg Thieme Verlag: Stuttgart, Germany, 2010; Volume 47, pp. 105–160.
2. Johnson, C.R.; Shanklin, J.R.; Kirchhoff, R.A. Olefin Synthesis by Reductive Elimination of β -Hydroxysulfoximines. Methylenation of Carbonyl Compounds. *J. Am. Chem. Soc.* **1973**, *95*, 6462–6463. [[CrossRef](#)]
3. Maryanoff, B.E.; Reitz, A.B. The Wittig Olefination Reaction and Modifications Involving Phosphoryl-Stabilized Carbanions. Stereochemistry, Mechanism, and Selected Synthetic Aspects. *Chem. Rev.* **1989**, *89*, 863–927. [[CrossRef](#)]
4. Bisceglia, J.A.; Orelli, L.R. Recent Progress in the Horner–Wadsworth–Emmons Reaction. *Curr. Org. Chem.* **2015**, *19*, 744–775. [[CrossRef](#)]
5. Van Staden, L.F.; Gravestock, D.; Ager, D.J. New Developments in the Peterson Olefination Reaction. *Chem. Soc. Rev.* **2002**, *31*, 195–200. [[CrossRef](#)] [[PubMed](#)]
6. Coombs, J.R.; Zhang, L.; Morken, J.P. Synthesis of Vinyl Boronates from Aldehydes by a Practical Boron–Wittig Reaction. *Org. Lett.* **2015**, *17*, 1708–1711. [[CrossRef](#)] [[PubMed](#)]
7. Wittig, G.; Geissler, G. Zur Reaktionsweise Des Pentaphenyl-phosphors Und Einiger Derivate. *Justus Liebigs Ann. Chem.* **1953**, *580*, 44–57. [[CrossRef](#)]
8. Wittig, G.; Schöllkopf, U. Über Triphenyl-phosphin-methylene Als Olefinbildende Reagenzien. *Chem. Berichte* **1954**, *87*, 1318–1330. [[CrossRef](#)]
9. Chatterjee, B.; Bera, S.; Mondal, D. Julia–Kocienski Olefination: A Key Reaction for the Synthesis of Macrolides. *Tetrahedron Asymmetry* **2014**, *25*, 1–55. [[CrossRef](#)]
10. Legnani, L.; Porta, A.; Caramella, P.; Toma, L.; Zaroni, G.; Vidari, G. Computational Mechanistic Study of the Julia–Kocienski Reaction. *J. Org. Chem.* **2015**, *80*, 3092–3100. [[CrossRef](#)]
11. Aïssa, C. Mechanistic Manifold and New Developments of the Julia–Kocienski Reaction. *Eur. J. Org. Chem.* **2009**, *2009*, 1831–1844. [[CrossRef](#)]
12. Blakemore, P.R. The Modified Julia Olefination: Alkene Synthesis via the Condensation of Metallated Heteroarylalkylsulfones with Carbonyl Compounds. *J. Chem. Soc. Perkin 1* **2002**, *2*, 2563–2585. [[CrossRef](#)]
13. Blakemore, P.R.; Cole, W.J.; Kocienski, P.J.; Morley, A. A Stereoselective Synthesis of Trans-1,2-Disubstituted Alkenes Based on the Condensation of Aldehydes with Metallated 1-Phenyl-1 H -Tetrazol-5-Yl Sulfones. *Synlett* **1998**, *1998*, 26–28. [[CrossRef](#)]

14. Robiette, R.; Pospíšil, J. On the Origin of E/Z Selectivity in the Modified Julia Olefination—Importance of the Elimination Step. *Eur. J. Org. Chem.* **2013**, 836–840. [[CrossRef](#)]
15. Baudin, J.B.; Hareau, G.; Julia, S.A.; Ruel, O. A Direct Synthesis of Olefins by Reaction of Carbonyl Compounds with Lithio Derivatives of 2-[Alkyl- or (2'-Alkenyl)- or Benzyl-Sulfonyl]-Benzothiazoles. *Tetrahedron Lett.* **1991**, 32, 1175–1178. [[CrossRef](#)]
16. Gueyrard, D. Extension of the Modified Julia Olefination on Carboxylic Acid Derivatives: Scope and Applications. *Synlett* **2018**, 29, 34–45. [[CrossRef](#)]
17. Julia, M.; Paris, J.M. Synthèses à l'aide de Sulfones v(+)- Méthode de Synthèse Générale de Doubles Liaisons. *Tetrahedron Lett.* **1973**, 14, 4833–4836. [[CrossRef](#)]
18. Kocienski, P.J.; Lythgoe, B.; Ruston, S. Scope and Stereochemistry of an Olefin Synthesis from β -Hydroxysulphones. *J. Chem. Soc. Perkin 1* **1978**, 829–834. [[CrossRef](#)]
19. Keck, G.E.; Savin, K.A.; Weglarz, M.A. Use of Samarium Diiodide as an Alternative to Sodium/Mercury Amalgam in the Julia-Lythgoe Olefination. *J. Org. Chem.* **1995**, 60, 3194–3204. [[CrossRef](#)]
20. Baudin, J.B.; Hareau, G.; Julia, S.A.; Lorne, R.; Ruel, O. Stereochemistry of Direct Olefin Formation from Carbonyl Compounds and Lithiated Heterocyclic Sulfones. *Bull. Soc. Chim. Fr.* **1993**, 130, 856–878.
21. Baudin, J.B.; Hareau, G.; Julia, S.A.; Ruel, O. Stereochemistry of the Olefin Formation from Anti and Syn Heterocyclic β -Hydroxy-Sulfones. *Bull. Soc. Chim. Fr.* **1993**, 130, 336–357.
22. Sakaine, G.; Leitis, Z.; Ločmele, R.; Smits, G. Julia-Kocienski Olefination: A Tutorial Review. *Eur. J. Org. Chem.* **2023**, 26, e202201217. [[CrossRef](#)]
23. Ouzounthanasis, K.A.; Rizos, S.R.; Koumbis, A.E. Julia-Kocienski Olefination in the Synthesis of Trisubstituted Alkenes: Recent Progress. *Eur. J. Org. Chem.* **2023**, 26, e202300626. [[CrossRef](#)]
24. Rinu, P.X.T.; Radhika, S.; Anilkumar, G. Recent Applications and Trends in the Julia-Kocienski Olefination. *ChemistrySelect* **2022**, 7, e202200760. [[CrossRef](#)]
25. Charette, A.B.; Berthelette, C.; St-Martin, D. An Expedient Approach to E, Z-Dienes Using the Julia Olefination. *Tetrahedron Lett.* **2001**, 42, 5149–5153. [[CrossRef](#)]
26. Kocienski, P.J.; Bell, A.; Blakemore, P.R. 1- Tert -Butyl-1 H -Tetrazol-5-Yl Sulfones in the Modified Julia Olefination. *Synlett* **2000**, 2000, 365–366. [[CrossRef](#)]
27. Alonso, D.A.; Fuensanta, M.; Nájera, C.; Varea, M. 3,5-Bis(Trifluoromethyl)Phenyl Sulfones in the Direct Julia–Kocienski Olefination. *J. Org. Chem.* **2005**, 70, 6404–6416. [[CrossRef](#)] [[PubMed](#)]
28. Małosza, M.; Bujok, R. Synthesis of Benzylidenecyclopropanes from γ -Halopropyl Pentachlorophenyl Sulfones Using a Julia-Kocienski Olefination. *Synlett* **2008**, 2008, 586–588. [[CrossRef](#)]
29. Pospíšil, J. Simple Protocol for Enhanced (E)-Selectivity in Julia–Kocienski Reaction. *Tetrahedron Lett.* **2011**, 52, 2348–2352. [[CrossRef](#)]
30. Jana, N.; Nanda, S. Asymmetric Total Syntheses of Cochliomycin A and Zeaenol. *Eur. J. Org. Chem.* **2012**, 2012, 4313–4320. [[CrossRef](#)]
31. Mohapatra, D.K.; Reddy, D.S.; Mallampudi, N.A.; Yadav, J.S. Stereoselective Total Syntheses of Paecilomycins e and F through a Protecting Group Directed Diastereoselective Intermolecular Nozaki-Hiyama-Kishi (NHK) Reaction. *Eur. J. Org. Chem.* **2014**, 2014, 5023–5032. [[CrossRef](#)]
32. Sánchez, D.; Andreou, T.; Costa, A.M.; Meyer, K.G.; Williams, D.R.; Barasoain, I.; Díaz, J.F.; Lucena-Agell, D.; Vilarrasa, J. Total Synthesis of Amphidinolide K, a Macrolide That Stabilizes F-Actin. *J. Org. Chem.* **2016**, 80, 8511–8519. [[CrossRef](#)] [[PubMed](#)]
33. Wilson, D.M.; Britton, R. Enantioselective Total Synthesis of the Marine Macrolides Salarins A and C. *J. Am. Chem. Soc.* **2024**, 146, 8456–8463. [[CrossRef](#)] [[PubMed](#)]
34. Billard, F.; Robiette, R.; Pospíšil, J. Julia-Kocienski Reaction-Based 1,3-Diene Synthesis: Aldehyde-Dependent (E, E/E, Z)-Selectivity. *J. Org. Chem.* **2012**, 77, 6358–6364. [[CrossRef](#)] [[PubMed](#)]
35. Rehman, M.; Surendran, S.; Siddavatam, N.; Rajendar, G. The Influence of α -Coordinating Groups of Aldehydes on E/Z-Selectivity and the Use of Quaternary Ammonium Counter Ions for Enhanced E-Selectivity in the Julia–Kocienski Reaction. *Org. Biomol. Chem.* **2022**, 20, 329–333. [[CrossRef](#)] [[PubMed](#)]
36. Rajendar, G.; Corey, E.J. A Systematic Study of Functionalized Oxiranes as Initiating Groups for Cationic Polycyclization Reactions. *J. Am. Chem. Soc.* **2015**, 137, 5837–5844. [[CrossRef](#)]
37. Tsubone, K.; Hashizume, K.; Fuwa, H.; Sasaki, M. Studies toward the Total Synthesis of Gambieric Acids: Convergent Synthesis of the GHIJ-Ring Fragment Having a Side Chain. *Tetrahedron Lett.* **2011**, 52, 548–551. [[CrossRef](#)]
38. Tsubone, K.; Hashizume, K.; Fuwa, H.; Sasaki, M. Studies toward the Total Synthesis of Gambieric Acids, Potent Antifungal Polycyclic Ethers: Convergent Synthesis of a Fully Elaborated GHIJ-Ring Fragment. *Tetrahedron* **2011**, 67, 6600–6615. [[CrossRef](#)]
39. Rej, R.K.; Kumar, R.; Nanda, S. Asymmetric Synthesis of Cytospolides C and D through Successful Exploration of Stereoselective Julia-Kocienski Olefination and Suzuki Reaction Followed by Macrolactonization. *Tetrahedron* **2015**, 71, 3185–3194. [[CrossRef](#)]
40. Eliel, E.L.; Frye, S.V.; Hortelano, E.R.; Chen, X.; Bai, X. Asymmetric Synthesis and Cram's (Chelate) Rule. *Pure Appl. Chem.* **1991**, 63, 1591–1598. [[CrossRef](#)]
41. Bon, D.J.-Y.D.; Chrenko, D.; Kováč, O.; Ferugová, V.; Lasák, P.; Fuksová, M.; Zálešák, F.; Pospíšil, J. Julia-Kocienski-Like Connective C–C and C=C Bond-Forming Reaction. *Adv. Synth. Catal.* **2024**, 366, 480–487. [[CrossRef](#)]

42. Nielsen, M.; Jacobsen, C.B.; Paixão, M.W.; Holub, N.; Jørgensen, K.A. Asymmetric Organocatalytic Formal Alkynylation and Alkenylation of α,β -Unsaturated Aldehydes. *J. Am. Chem. Soc.* **2009**, *131*, 10581–10586. [[CrossRef](#)]
43. Jacobsen, C.B.; Nielsen, M.; Worgull, D.; Zweifel, T.; Fisker, E.; Jørgensen, K.A. Asymmetric Organocatalytic Monofluorovinylations. *J. Am. Chem. Soc.* **2011**, *133*, 7398–7404. [[CrossRef](#)] [[PubMed](#)]
44. Pospíšil, J.; Sato, H. Practical Synthesis of β -Acyl and β -Alkoxy carbonyl Heterocyclic Sulfones. *J. Org. Chem.* **2011**, *76*, 2269–2272. [[CrossRef](#)]
45. Pospíšil, J.; Robiette, R.; Sato, H.; Debrus, K. Practical Synthesis of β -Oxo Benzo[d]Thiazolyl Sulfones: Scope and Limitations. *Org. Biomol. Chem.* **2012**, *10*, 1225–1234. [[CrossRef](#)]
46. Bettens, T.; Alonso, M.; Geerlings, P.; De Proft, F. Mechanochemical Felkin–Anh Model: Achieving Forbidden Reaction Outcomes with Mechanical Force. *J. Org. Chem.* **2023**, *88*, 2046–2056. [[CrossRef](#)] [[PubMed](#)]
47. Ager, D.J. Peterson Alkenation. In *Science of Synthesis: Houben-Weyl Methods of Molecular Transformations Vol. 47a: Alkenes*; Georg Thieme Verlag: Stuttgart, Germany, 2014; p. 85.
48. Armstrong, R.; Aggarwal, V. 50 Years of Zweifel Olefination: A Transition-Metal-Free Coupling. *Synthesis* **2017**, *49*, 3323–3336. [[CrossRef](#)]
49. Li, X.; Song, Q. Recent Progress on the Zweifel Olefination: An Update. *Synthesis* **2023**. [[CrossRef](#)]
50. Fletcher, S. The Mitsunobu Reaction in the 21st Century. *Org. Chem. Front.* **2015**, *2*, 739–752. [[CrossRef](#)]
51. Dickman, M.H.; Pope, M.T. Peroxo and Superoxo Complexes of Chromium, Molybdenum, and Tungsten. *Chem. Rev.* **1994**, *94*, 569–584. [[CrossRef](#)]
52. Adam, W.; Ortega-Schulte, C.M. An Effective Synthesis of α -Cyanoenamines by Peterson Olefination. *Synlett* **2003**, *2003*, 414–416. [[CrossRef](#)]
53. Fürstner, A.; Brehm, C.; Cancho-Grande, Y. Stereoselective Synthesis of Enamides by a Peterson Reaction Manifold. *Org. Lett.* **2001**, *3*, 3955–3957. [[CrossRef](#)]
54. Ando, K.; Wada, T.; Okumura, M.; Sumida, H. Stereoselective Synthesis of Z- α,β -Unsaturated Sulfones Using Peterson Reagents. *Org. Lett.* **2015**, *17*, 6026–6029. [[CrossRef](#)] [[PubMed](#)]
55. Hamlin, T.A.; Kelly, C.B.; Cywar, R.M.; Leadbeater, N.E. Methylenation of Perfluoroalkyl Ketones Using a Peterson Olefination Approach. *J. Org. Chem.* **2014**, *79*, 1145–1155. [[CrossRef](#)] [[PubMed](#)]
56. Marciniak, B. Hydrosilylation of Carbon–Carbon Multiple Bonds in Organic Synthesis. In *Hydrosilylation: A Comprehensive Review on Recent Advances*; Marciniak, B., Ed.; Springer: Dordrecht, The Netherlands, 2009; pp. 87–123, ISBN 978-1-4020-8172-9.
57. Marciniak, B. Hydrosilylation of Alkenes and Their Derivatives. In *Hydrosilylation: A Comprehensive Review on Recent Advances*; Marciniak, B., Ed.; Springer: Dordrecht, The Netherlands, 2009; pp. 3–51, ISBN 978-1-4020-8172-9.
58. Armstrong, R.J.; García-Ruiz, C.; Myers, E.L.; Aggarwal, V.K. Stereodivergent Olefination of Enantioenriched Boronic Esters. *Angew. Chem. Int. Ed.* **2017**, *129*, 804–808. [[CrossRef](#)]
59. Linne, Y.; Lohrberg, D.; Struwe, H.; Linne, E.; Stohwasser, A.; Kalesse, M. 1,2-Metallate Rearrangement as a Toolbox for the Synthesis of Allylic Alcohols. *J. Org. Chem.* **2023**, *88*, 12623–12629. [[CrossRef](#)]
60. Yeung, K.; Mykura, R.C.; Aggarwal, V.K. Lithiation–Borylation Methodology in the Total Synthesis of Natural Products. *Nat. Synth.* **2022**, *1*, 117–126. [[CrossRef](#)]

Disclaimer/Publisher’s Note: The statements, opinions and data contained in all publications are solely those of the individual author(s) and contributor(s) and not of MDPI and/or the editor(s). MDPI and/or the editor(s) disclaim responsibility for any injury to people or property resulting from any ideas, methods, instructions or products referred to in the content.